

DOE/ID/12839-12  
(DE94005526)

CHARACTERIZATION OF OIL AND GAS  
RESERVOIR HETEROGENEITY

Final Report

By  
G.D. Sharma

July 1994

Performed Under Contract No. DE-FG07-90ID12839

University of Alaska Fairbanks  
Petroleum Development Laboratory  
Fairbanks, Alaska



**Bartlesville Project Office**  
**U. S. DEPARTMENT OF ENERGY**  
**Bartlesville, Oklahoma**

## **DISCLAIMER**

This report was prepared as an account of work sponsored by an agency of the United States Government. Neither the United States Government nor any agency thereof, nor any of their employees, makes any warranty, expressed or implied, or assumes any legal liability or responsibility for the accuracy, completeness, or usefulness of any information, apparatus, product, or process disclosed, or represents that its use would not infringe privately owned rights. Reference herein to any specific commercial product, process, or service by trade name, trademark, manufacturer, or otherwise does not necessarily constitute or imply its endorsement, recommendation, or favoring by the United States Government or any agency thereof. The views and opinions of authors expressed herein do not necessarily state or reflect those of the United States Government or any agency thereof.

**This report has been reproduced directly from the best available copy.**

**Available to DOE and DOE contractors from the Office of Scientific and Technical Information, P.O. Box 62, Oak Ridge, TN 37831; prices available from (615) 576-8401.**

**Available to the public from the National Technical Information Service, U.S. Department of Commerce, 5285 Port Royal Rd., Springfield VA 22161**

Characterization of Oil and Gas  
Reservoir Heterogeneity

Final Report  
by

G.D. Sharma

July 1994

Work Performed Under Contract No. DE-FG07-90ID12839

Prepared for  
U.S. Department of Energy  
Assistant Secretary for Fossil Energy

Leonard Keay, Project Manager  
Idaho Field Office  
785 DOE Place  
Idaho Falls, ID 83401-1562

R. Michael Ray, Project Manager  
Bartlesville Project Office  
P.O. Box 1398  
Bartlesville, OK 74005

Prepared by  
University of Alaska  
Petroleum Development Laboratory  
P.O. Box 75580  
Fairbanks, AK 99775-5880



# TABLE OF CONTENTS

	<u>Page</u>
<b>LIST OF FIGURES</b> .....	viii
<b>LIST OF TABLES</b> .....	xxi
<b>ACKNOWLEDGMENT</b> .....	xxvii
<b>ABSTRACT</b> .....	xxviii
<b>EXECUTIVE SUMMARY</b> .....	xxx
<b>CHAPTER I: INTRODUCTION</b> .....	I-1
A. Background .....	I-1
B. Exploration History .....	I-1
C. Oil and Gas Resources of North Slope Alaska .....	I-3
<b>CHAPTER II: WEST SAK RESERVOIR</b> .....	II-1
A. Introduction .....	II-1
B. Geological Overview .....	II-2
C. Reservoir Description Procedure .....	II-5
D. Log-Derived Petrophysical Parameters .....	II-6
E. Reservoir Description .....	II-10
E1. Sand Thickness Variation .....	II-13
E2. Spatial Distribution of Petrophysical Properties .....	II-16
E3. Sand Quality .....	II-20
<b>CHAPTER III: LOWER UG NU RESERVOIR</b> .....	III-1
A. Geological Overview .....	III-1
B. Reservoir Description Procedure .....	III-2
C. Log-Derived Petrophysical Properties .....	III-2
D. Reservoir Description .....	III-6
D1. Sand Bed Distribution .....	III-6
D2. Spatial Distribution of the Petrophysical Properties .....	III-11
D3. Sand Quality .....	III-11
D4. West Sak Versus Lower Ugnu Reservoir Quality .....	III-11

<b>CHAPTER IV: PETROGRAPHIC CHARACTERISTICS OF SELECTED STRATIGRAPHIC HORIZONS: UGNU SWPT #1 AND WEST SAK SWPT #1.....</b>	<b>IV-1</b>
A. Introduction.....	IV-1
B. Petrographic Analyses.....	IV-1
C. Sample Descriptions.....	IV-2
C1. Ugnu SWPT #1 Samples.....	IV-3
C1(a) Ugnu SWPT #1, 3532' (below West Sak Zone).....	IV-3
C1(b) Ugnu SWPT #1, 3526' (West Sak Sands).....	IV-4
C1(c) Ugnu SWPT #1, 3507' (West Sak Zone).....	IV-5
C1(d) Ugnu SWPT #1, 3497' (West Sak Zone).....	IV-6
C1(e) Ugnu SWPT #1, 3493' (West Sak Zone).....	IV-7
C1(f) Ugnu SWPT #1, 3457' (West Sak Zone).....	IV-8
C1(g) Ugnu SWPT #1, 3452' (West Sak Zone).....	IV-9
C1(h) Ugnu SWPT #1, 3425' (West Sak Zone).....	IV-10
C1(i) Ugnu SWPT #1, 3422' (West Sak Zone).....	IV-11
C1(j) Ugnu SWPT #1, 3412' (above West Sak Zone).....	IV-12
C1(k) Ugnu SWPT #1, 3264' (Lower Ugnu (?) Zone).....	IV-13
C1(l) Ugnu SWPT #1, 3241' (Lower Ugnu (?) Zone).....	IV-14
C1(m) Ugnu SWPT #1, 3235' (Lower Ugnu (?) Zone).....	IV-15
C1(n) Ugnu SWPT #1, 3174' (Lower Ugnu (?) Zone).....	IV-16
C1(o) Ugnu SWPT #1, 3128' (Lower Ugnu (?) Zone).....	IV-17
C1(p) Ugnu SWPT #1, 3112' (Lower Ugnu (?) Zone).....	IV-18
C1(q) Ugnu SWPT #1, 3059' (Lower Ugnu Zone).....	IV-19
C1(r) Ugnu SWPT #1, 2996' (Upper Ugnu Zone).....	IV-20
C2. West Sak SWPT #1 Samples.....	IV-21
C2(a) West Sak SWPT #1, 3960' (below West Sak Zone).....	IV-21
C2(b) West Sak SWPT #1, 3923' (below West Sak Zone).....	IV-22
C2(c) West Sak SWPT #1, 3917' (below West Sak Zone).....	IV-23
C2(d) West Sak SWPT #1, 3953' (below West Sak Zone).....	IV-24
C2(e) West Sak SWPT #1, 3812' (West Sak Zone).....	IV-25
C2(f) West Sak SWPT #1, 3804' (West Sak Zone).....	IV-26
C2(g) West Sak SWPT #1, 3780' (West Sak Zone).....	IV-27
C2(h) West Sak SWPT #1, 3769' (West Sak Zone).....	IV-28
C2(i) West Sak SWPT #1, 3761' (West Sak Zone).....	IV-29
C2(j) West Sak SWPT #1, 3723' (West Sak Zone).....	IV-30
C2(k) West Sak SWPT #1, 3715' (above West Sak Zone).....	IV-31
<b>CHAPTER V: ENDICOTT FIELD.....</b>	<b>V-1</b>
A. Overview and Geology of Endicott Field.....	V-1
B. Endicott Reservoir Description Procedure.....	V-7
C. Endicott Reservoir Description.....	V-10
C1. Structural Analysis.....	V-10
C2. Log-Derived Petrophysical Properties.....	V-13
D. Nomenclature.....	V-39
<b>CHAPTER VI: MILNE POINT - KUPARUK INTERVAL.....</b>	<b>VI-1</b>
A. Abstract.....	VI-1
B. Field History.....	VI-1

C.	Milne Point Geology .....	VI-5
D.	Faulting at Milne Point .....	VI-10
E.	Milne Point Sand Continuity .....	VI-16
F.	Milne Point Structure .....	VI-16
G.	Discussion of Milne Point Petrophysical Properties .....	VI-24

**CHAPTER VII, PART I: RESERVOIR CHARACTERIZATION OF KUPARUK FIELD .....** VII-1

A.	Introduction .....	VII-1
B.	Well Log Analysis .....	VII-1
C.	Discussion of Results .....	VII-29
C1.	Structure and Isopach Maps .....	VII-29
C2.	Cross Sections .....	VII-36
C3.	Porosity Determination .....	VII-36
C4.	Water Saturation Determination .....	VII-43
C5.	Sand Quality .....	VII-46

**CHAPTER VII, PART II: SUMMARY OF THE DEPOSITIONAL ENVIRONMENT AND RESERVOIR QUALITY OF THE KUPARUK RIVER FORMATION SANDS..** VII-55

A.	Introduction .....	VII-55
B.	Lower Sand Stratigraphy and Deposition .....	VII-55
C.	Upper Sand Stratigraphy and Deposition .....	VII-58
D.	Structure of the Kuparuk Formation at Kuparuk Field .....	VII-59
E.	Reservoir Quality of the Lower Sand .....	VII-67
F.	Reservoir Quality of the Upper Sand .....	VII-69
G.	Production Performance .....	VII-69

**CHAPTER VIII: RESERVOIR CHARACTERIZATION OF PRUDHOE BAY FIELD NORTH SLOPE, ALASKA .....** VIII-1

A.	Introduction .....	VIII-1
B.	Well Log Analysis .....	VIII-1
C.	Discussion of Results .....	VIII-10
C1.	Structure and Isopach Maps .....	VIII-10
C2.	Cross Sections .....	VIII-29
C3.	Porosity .....	VIII-33
C4.	Saturation .....	VIII-33
C5.	Sand Quality .....	VIII-38

**CHAPTER IX: NONPRODUCING FIELDS, NORTH SLOPE, ALASKA .....** IX-1

A.	Lisburne Field .....	IX-1
B.	Point McIntyre Field .....	IX-4
C.	Point Thomson Field .....	IX-8
D.	Gwydyr Bay Field .....	IX-10
E.	Niakuk Field .....	IX-13
F.	Seal Island/Northstar Fields .....	IX-18

<b>CHAPTER X: EXPERIMENTAL STUDY OF ASPHALTENE PRECIPITATION FOR ENRICHED GASES, CO<sub>2</sub> AND WEST SAK CRUDE SYSTEM.....</b>	<b>X-1</b>
A. Introduction .....	X-1
B. Literature Review .....	X-2
B1. Nature of Asphaltenes and Resins .....	X-2
B2. Causes of Asphaltene Flocculation .....	X-4
C. Experimental Results .....	X-6
C1. Asphaltene Precipitation Tests with Tank Oils .....	X-6
C2. Effect of Solvent/Oil Dilution Ratio .....	X-6
C3. Alteration of Crude Oil Composition Due to Precipitation .....	X-20
C4. Asphaltene Precipitation Tests for Recombined Oils .....	X-20
C5. Effect of CO <sub>2</sub> /Oil Ratio and Effect of Pressure .....	X-23
D. Conclusions .....	X-23
 <b>CHAPTER XI, PART I: MODELING OF ASPHALTENE EQUILIBRIA, HOMOGENEOUS MOLECULAR THERMODYNAMIC MODEL.....</b>	 <b>XI-1</b>
A. Introduction .....	XI-1
B. Review of Asphaltene Equilibria Modeling.....	XI-1
B1. Thermodynamic Molecular (Solubility) Approach.....	XI-1
B2. Thermodynamic Colloidal Approach.....	XI-2
C. Theoretical Basis.....	XI-3
D. Liquid-Liquid Polymer Solution Theory .....	XI-3
E. Vapor-Liquid Equilibria Calculations.....	XI-4
F. Model Performance .....	XI-7
G. Conclusions .....	XI-16
H. Nomenclature .....	XI-17
 <b>CHAPTER XI, PART II: MODELING OF ASPHALTENE EQUILIBRIA, POLYDISPERSED MOLECULAR THERMODYNAMIC MODEL.....</b>	 <b>XI-19</b>
A. Introduction .....	XI-19
B. Description of Multicomponent Asphaltene Model.....	XI-19
B1. Discretization of Continuous Asphaltene Molecular Weight Distribution Function .....	XI-21
B2. Asphaltene Pseudocomponent Property Estimation .....	XI-23
B3. Asphaltene Solid-Liquid Equilibria .....	XI-24
B4. Vapor-Liquid Equilibria.....	XI-25
B5. Stepwise Model Calculations and Regression of Experimental Data .....	XI-25
B6. Model Features, Advantages and Limitations.....	XI-27
C. Application of Model to West Sak Oil-Solvent Mixtures.....	XI-28
D. Conclusions .....	XI-33

<b>CHAPTER XII: EFFECT OF ASPHALTENE DEPOSITION ON ROCK-FLUID PROPERTIES .....</b>	<b>XII-1</b>
A. Introduction .....	XII-1
B. Experimental Program .....	XII-1
B1. Experimental Set-Up and Materials .....	XII-1
B2. Experimental Procedures .....	XII-4
C. Results and Discussion.....	XII-6
C1. Effect on Absolute Permeability .....	XII-6
C2. Effect on Displacement Performance .....	XII-14
C3. Effect on Pressure Drop .....	XII-15
C4. Effect on Oil-Water Relative Permeabilities and Fractional Flow .....	XII-18
D. Conclusions.....	XII-30
<b>CHAPTER XIII: FLUID PROPERTIES.....</b>	<b>XIII-1</b>
A. Introduction.....	XIII-1
B. Sadlerochit Group .....	XIII-1
C. Kuparuk River Field.....	XIII-28
D. Endicott Field .....	XIII-28
E. West Sak Field .....	XIII-28
F. Nomenclature .....	XIII-43
<b>CHAPTER XIV: RESERVOIR HETEROGENEITY CLASSIFICATION SYSTEM FOR TORIS AND TORIS DATABASE .....</b>	<b>XIV-1</b>
A. Objective and Introduction.....	XIV-1
B. North Slope Alaska, Oil Reservoirs .....	XIV-1
C. Cook Inlet Basin Alaska, Reservoirs .....	XIV-2
<b>CHAPTER XV: REFERENCES .....</b>	<b>XV-1</b>
<b>APPENDIX A .....</b>	<b>A-1</b>

# LIST OF FIGURES

<b>CHAPTER I:</b>	<u>Page</u>	
Figure I-1.	Map of Northern Alaska Showing Major Geographic Features and Locations of National Petroleum Reserve Alaska, Arctic National Wildlife Refuge, and the Trans-Alaskan Pipeline System (Thomas et al., 1991).....	I-5
Figure I-2.	Generalized Structural Features and Geologic Framework of Onshore and Offshore Northern Alaska (Thomas et al., 1991). .....	I-6
Figure I-3.	Generalized Columnar Section for the North Slope Showing Stratigraphic Relations, Age, Lithology, and Positions of Known Oil and Gas Accumulations (Thomas et al., 1991). .....	I-7
Figure I-4.	Known Oil and Gas Accumulations, Selected Dry Holes and Suspended Wells, and NPRA-ANWR Boundaries, North Slope, Alaska (Thomas et al., 1991). .....	I-8
<b>CHAPTER II:</b>		
Figure II-1.	Location Map of Major Fields in the Alaskan North Slope.....	II-2
Figure II-2.	Generalized North Slope Stratigraphic Column (adapted from Bird, 1987). .....	II-3
Figure II-3.	North Slope Index Map Showing Major Structural Elements (Jamison et al., 1980). .....	II-4
Figure II-4.	North-South Cross Section from Brooks Range to the Prudhoe Bay Complex (Jamison et al., 1980). .....	II-4
Figure II-5.	West Sak Sands Distribution Along the SE-NW Stratigraphic Cross Section BB'.....	II-11
Figure II-6.	West Sak Sands Distribution Along the SW-NE Stratigraphic Cross Section AA'.....	II-11
Figure II-7.	Contour Map Showing Depths to the Top of West Sak Upper Sand 1 (AA': SW-NE Cross Section, BB' NW-SE Cross Section). .....	II-12
Figure II-8.	Isopach Map of West Sak Upper Sand 1. ....	II-13
Figure II-9.	Isopach Map of West Sak Upper Sand 2. ....	II-14
Figure II-10.	Isopach Map of West Sak Lower Sand 1. ....	II-14
Figure II-11.	Isopach Map of West Sak Lower Sand 2. ....	II-15
Figure II-12.	Isopach Map of West Sak Lower Sand 3. ....	II-15
Figure II-13.	3-D Plot Showing the Distribution of Porosity in West Sak Sands. ....	II-16
Figure II-14.	Porosity Map of West Sak Sands. ....	II-17
Figure II-15.	Water Saturation Map of West Sak Sands. ....	II-17
Figure II-16.	3-D Plot Showing the Water Saturation Distribution in West Sak Sands. ....	II-18
Figure II-17.	Contour Map Showing Porosity Distribution in West Sak Upper Sand 1.....	II-19
Figure II-18.	Contour Map Showing Water Saturation Distribution in West Sak Upper Sand 1.....	II-19
Figure II-19.	Contour Map Showing Porosity Distribution in West Sak Upper Sand 2.....	II-20

Figure II-20.	Sand Quality Distribution in West Sak Sands Depicted by the Contour Map of Hydrocarbon Capacity.....	II-21
Figure II-21.	3-D Plot Showing the Sand Quality of West Sak Sands (viewed from southwest).....	II-21

**CHAPTER III:**

Figure III-1.	Lower Ugnu Sands Distribution Along the SW-NE Stratigraphic Cross Section CC'.....	III-8
Figure III-2.	Isopach Map of Lower Ugnu Sand 1. ....	III-9
Figure III-3.	Isopach Map of Lower Ugnu Sand 3. ....	III-10
Figure III-4.	Isopach Map of Lower Ugnu Sand 4. ....	III-10
Figure III-5.	Porosity Contour Map of Lower Ugnu Sands.....	III-12
Figure III-6.	3-D Plot Showing the Distribution of Porosity in Lower Ugnu Sands (viewed from the southeast). ....	III-12
Figure III-7.	Water Saturation Map of Lower Ugnu Sands.....	III-13
Figure III-8.	3-D Plot Showing the Water Saturation Distribution in Lower Ugnu Sands (viewed from the southeast). ....	III-13
Figure III-9.	Contour Map Showing Porosity Distribution in Lower Ugnu Sand 1.....	III-14
Figure III-10.	Contour Map Showing Water Saturation Distribution in Lower Ugnu Sand 1.....	III-14
Figure III-11.	Sand Quality Distribution in the Lower Ugnu Sands, Depicted by the Contour Map of Hydrocarbon Pore Volume (10 <sup>3</sup> bbl/acre-ft)....	III-15
Figure III-12.	3-D Plot Showing the Sand Quality of Lower Ugnu Sands (viewed from the southeast). ....	III-15

**CHAPTER IV:**

Figure IV-1.	Ugnu SWPT #1, 3532' (50 x PL).....	IV-3
Figure IV-2.	Ugnu SWPT #1, 3526' (50 x PL).....	IV-4
Figure IV-3.	Ugnu SWPT #1, 3507' (50 x PL).....	IV-5
Figure IV-4.	Ugnu SWPT #1, 3497' (50 x PL).....	IV-6
Figure IV-5.	Ugnu SWPT #1, 3493' (50 x PL).....	IV-7
Figure IV-6.	Ugnu SWPT #1, 3457' (50 x PL).....	IV-8
Figure IV-7.	Ugnu SWPT #1, 3452' (50 x PL).....	IV-9
Figure IV-8.	Ugnu SWPT #1, 3425' (50 x PL).....	IV-10
Figure IV-9.	Ugnu SWPT #1, 3422' (50 X PL).....	IV-11
Figure IV-10.	Ugnu SWPT #1, 3412' (50 X PL).....	IV-12
Figure IV-11.	Ugnu SWPT #1, 3264' (50 X PL).....	IV-13
Figure IV-12.	Ugnu SWPT #1, 3241' (50 X PL).....	IV-14
Figure IV-13.	Ugnu SWPT #1, 3235' (50 x PL).....	IV-15
Figure IV-14.	Ugnu SWPT #1, 3174' (50 x PL).....	IV-16
Figure IV-15.	Ugnu SWPT #1, 3128' (50 x PL).....	IV-17
Figure IV-16.	Ugnu SWPT #1, 3112' (50 X PL).....	IV-18
Figure IV-17.	Ugnu SWPT #1, 3059' (50 x PL).....	IV-19
Figure IV-18.	Ugnu SWPT #1, 2996' (50 x PL).....	IV-20
Figure IV-19.	West Sak SWPT #1, 3960' (50 x PL).....	IV-21
Figure IV-20.	West Sak SWPT #1, 3923' (50 x PL).....	IV-22
Figure IV-21.	West Sak SWPT #1, 3917' (50 x PL).....	IV-23
Figure IV-22.	West Sak SWPT #1, 3953' (50 x PL).....	IV-24

Figure IV-23.	West Sak SWPT #1, 3812' (50 x PL).....	IV-25
Figure IV-24.	West Sak SWPT #1, 3804' (50 x PL).....	IV-26
Figure IV-25.	West Sak SWPT #1, 3780' (50 x PL).....	IV-27
Figure IV-26.	West Sak SWPT #1, 3769' (50 x PL).....	IV-28
Figure IV-27.	West Sak SWPT #1, 3761' (50 x PL).....	IV-29
Figure IV-28.	West Sak SWPT #1, 3723' A (50 X PL) B (50 X xsPL).....	IV-30
Figure IV-29.	West Sak SWPT #1, 3715' (50 x PL).....	IV-31

## CHAPTER V:

Figure V-1.	Alaska North Slope Fields, Including Endicott. ....	V-2
Figure V-2.	Endicott Delineation Wells and Faulting (adapted from Woidneck et al., 1987). ....	V-2
Figure V-3.	Generalized North Slope Stratigraphic Column (adapted from Bird, 1987). ....	V-3
Figure V-4.	Endicott Group Stratigraphic Position and Lithologic Description (Woidneck et al., 1987). ....	V-6
Figure V-5.	Endicott Field Well Location Map (Woidneck et al., 1987). ....	V-9
Figure V-6.	Endicott Wells Analyzed in This Study with Cross Sections A-A' and B-B' Plotted. ....	V-9
Figure V-7.	Endicott East-West Cross Section A-A'.....	V-11
Figure V-8.	Endicott North-South Cross Section B-B'.....	V-12
Figure V-9.	Top Zone 2A Structure Contour Map C.I.50'.....	V-21
Figure V-10.	Zone 2A Porosity Contour Map C.I.2%.....	V-21
Figure V-11.	Zone 2A Water Saturation Contour Map C.I.10%.....	V-22
Figure V-12.	Zone 2A 3-D Porosity Isopach.....	V-23
Figure V-13.	Zone 2A 3-D Water Saturation Isopach.....	V-24
Figure V-14.	Zone 2B Structure Contour Map C.I.50'.....	V-26
Figure V-15.	Zone 2B Porosity Contour Map C.I.2%.....	V-26
Figure V-16.	Zone 2B Water Saturation Contour Map C.I.20%.....	V-27
Figure V-17.	Zone 2B 3-D Porosity Isopach.....	V-27
Figure V-18.	Zone 2B 3-D Water Saturation Isopach.....	V-28
Figure V-19.	Porosity - Sw: Zone 2B.....	V-28
Figure V-20.	Porosity - Sw: Zone 2A.....	V-29
Figure V-21.	Top Zone 3A Structure Contour Map C.I.50'.....	V-29
Figure V-22.	Zone 3A Porosity Contour Map C.I.2%.....	V-30
Figure V-23.	Zone 3A Water Saturation Contour Map C.I.10%.....	V-30
Figure V-24.	Zone 3A 3-D Porosity Isopach.....	V-31
Figure V-25.	Zone 3A 3-D Water Saturation Isopach.....	V-31
Figure V-26.	Top Zone 3B Structure Contour Map C.I.50'.....	V-33
Figure V-27.	Zone 3B Porosity Contour Map C.I.2%.....	V-33
Figure V-28.	Zone 3B Water Saturation Contour Map C.I.10%.....	V-34
Figure V-29.	Top Zone 3C Structure Contour Map C.I.50'.....	V-35
Figure V-30.	Zone 3C Porosity Contour Map C.I.2%.....	V-35
Figure V-31.	Zone 3C Water Saturation Contour Map C.I.10%.....	V-36
Figure V-32.	Zone 2A 3-D Net Pay Isopach.....	V-37
Figure V-33.	Zone 2B 3-D Net Pay Isopach.....	V-37
Figure V-34.	Zone 3A 3-D Net Pay Isopach.....	V-38
Figure V-35.	Zone 3B 3-D Net Pay Isopach.....	V-38

**CHAPTER VI:**

Figure VI-1.	Location Map of Major Fields (including Milne Point) on the Alaskan North Slope. ....	VI-2
Figure VI-2.	Base Map of Milne Point Wells Analyzed. ....	VI-3
Figure VI-3.	Generalized Stratigraphic Column of North Slope Formations, with Kuparuk Formation Highlighted. ....	VI-4
Figure VI-4.	Location Map Showing Milne Point Unit Adjacent to Kuparuk River Unit (Bird, 1987). ....	VI-6
Figure VI-5.	Kuparuk Formation in Relation to Overlying and Underlying Shales (Werner, 1987). ....	VI-7
Figure VI-6.	Log Plot of the B-3 Well. ....	VI-8
Figure VI-7.	Lower Kuparuk Formation Gamma Ray and SP Traces from Milne Point Well D-2. Trace Character Suggests Regressive Depositional Environment Between 7360' and 7400' (true vertical depth). ....	VI-9
Figure VI-8.	Arctic Slope Oil Fields (Alaska Division of Oil and Gas). ....	VI-11
Figure VI-9.	Milne Point Field Cross Section A-A' ....	VI-12
Figure VI-10.	Milne Point Base Map Showing Locations of Cross Sections. ....	VI-13
Figure VI-11.	Cross Section B-B' Indicating Possible Faulting Between C-3 and C-4 Wells. ....	VI-14
Figure VI-12.	Cross Section C-C'. The B-10 May Lie Within a Localized Horst. ....	VI-15
Figure VI-13a.	Southeast Portion of Cross Section D-D' Showing Milne Point Structural Crest at the C-6 Well. ....	VI-17
Figure VI-13b.	Northwest Portion of Cross Section D-D' Showing Milne Point Structural Crest at the C-6 Well. ....	VI-18
Figure VI-14.	Structure Top of Milne Point Upper Kuparuk Formation. ....	VI-19
Figure VI-15.	3-D View of Top Middle Kuparuk Formation (viewed from the southwest). ....	VI-20
Figure VI-16.	East-West Cross Section E-E', the Northern Part of the Field. ....	VI-21
Figure VI-17.	Structure Top of Milne Point Lower Kuparuk Formation. ....	VI-22
Figure VI-18.	3-D Structure Top of Milne Point Lower Kuparuk Formation (viewed from the southwest). ....	VI-23
Figure VI-19.	East-West Cross Section F-F' Across the Southcentral Portion of Milne Point Field. ....	VI-25
Figure VI-20.	East-West Cross Section G-G' Across the Southern Portion of Milne Point Field. ....	VI-26
Figure VI-21.	Isopach Contour Map of Upper Lobe of Milne Point Middle Kuparuk Formation. ....	VI-27
Figure VI-22.	3-D Isopach View of Upper Lobe of Milne Point Middle Kuparuk Formation (viewed from the southwest). ....	VI-28
Figure VI-23.	Isopach Contour Map of Lower Lobe of Milne Point Middle Kuparuk Formation. ....	VI-29
Figure VI-24.	3-D Isopach View of Lower Lobe of Milne Point Middle Kuparuk Formation (viewed from the southwest). ....	VI-30
Figure VI-25.	Isopach Contour Map of Upper Lobe of Milne Point Lower Kuparuk Formation. ....	VI-31
Figure VI-26.	3-D Isopach View of Upper Lobe of Milne Point Lower Kuparuk Formation (viewed from the southwest). ....	VI-32
Figure VI-27.	Isopach Contour Map of Lower Lobe of Milne Point Lower Kuparuk Formation. ....	VI-33
Figure VI-28.	3-D Isopach View of Lower Lobe of Milne Point Lower Kuparuk Formation (viewed from the southwest). ....	VI-34

Figure VI-29.	Net Reservoir Porosity Map of Lower Lobe of Milne Point Middle Kuparuk Formation. ....	VI-35
Figure VI-30.	3-D Net Reservoir Porosity Map of Lower Lobe of Milne Point Middle Kuparuk Formation (viewed from the southwest). ....	VI-36
Figure VI-31.	Net Reservoir Porosity Map of Upper Lobe of Milne Point Lower Kuparuk Formation. ....	VI-37
Figure VI-32.	3-D Net Reservoir Porosity Map of Upper Lobe of Milne Point Lower Kuparuk Formation (viewed from the southwest). ....	VI-38
Figure VI-33.	Net Reservoir Porosity Map of Lower Lobe of Milne Point Lower Kuparuk Formation. ....	VI-39
Figure VI-34.	3-D Net Reservoir Porosity Map of Lower Lobe of Milne Point Lower Kuparuk Formation (viewed from the southwest). ....	VI-40
Figure VI-35.	Net Reservoir Porosity Map of Upper Lobe of Milne Point Middle Kuparuk Formation. ....	VI-41
Figure VI-36.	3-D Net Reservoir Porosity Map of Upper Lobe of Milne Point Middle Kuparuk Formation (viewed from the southwest). ....	VI-42
Figure VI-37.	Net Reservoir Water Saturation Map of Upper Lobe of Milne Point Middle Kuparuk Formation. ....	VI-43
Figure VI-38.	3-D Net Reservoir Water Saturation Map of Upper Lobe of Milne Point Middle Kuparuk Formation (viewed from the southwest). ....	VI-44
Figure VI-39.	Net Reservoir Water Saturation Map of Lower Lobe of Milne Point Middle Kuparuk Formation. ....	VI-45
Figure VI-40.	3-D Net Reservoir Water Saturation Map of Lower Lobe of Milne Point Middle Kuparuk Formation (viewed from the southwest). ....	VI-46
Figure VI-41.	Net Reservoir Water Saturation Map of Upper Lobe of Milne Point Upper Kuparuk Formation. ....	VI-47
Figure VI-42.	3-D Net Reservoir Water Saturation Map of Upper Lobe of Milne Point Lower Kuparuk Formation (viewed from the southwest). ....	VI-48
Figure VI-43.	Net Reservoir Water Saturation Map of Lower Lobe of Milne Point Lower Kuparuk Formation. ....	VI-49
Figure VI-44.	3-D Net Reservoir Water Saturation Map of Lower Lobe of Milne Point Lower Kuparuk Formation (viewed from the southwest). ....	VI-50

**CHAPTER VII:**

Figure VII-1.	Location of Kuparuk River Field (Gaynor and Scheihing, 1989). ....	VII-2
Figure VII-2.	Western North Slope Stratigraphic Column with Kuparuk River Interval Highlighted (Bird, 1987). ....	VII-3
Figure VII-3.	Lower Cretaceous Unconformity (LCU) Cutting Across the Kuparuk River Formation (Gaynor and Scheihing, 1989). ....	VII-4
Figure VII-4.	Analysis Result Plot of Well 1d6 from Kuparuk River Field with Comparison of Sw from Three Different Models (Sw1: Archie, Sw2: Laminar Simondoux, Sw3: Dual Water). ....	VII-6
Figure VII-5.	Analysis Result Plot of Well 1q15 from Kuparuk River Field with Comparison of Sw from Three Different Models (Sw1: Archie, Sw2: Laminar Simondoux, Sw3: Dual Water). ....	VII-7
Figure VII-6.	Kuparuk River Field Base Map Showing Well Locations and Cross Sections. ....	VII-20

Figure VII-7.	Stratigraphic Cross Section A-A' in Kuparuk River Field Showing Distributions of Kuparuk River Upper and Lower Sands. ....	VII-21
Figure VII-8.	Stratigraphic Cross Section B-B' in Kuparuk River Field Showing Distributions of Kuparuk River Upper and Lower Sands. ....	VII-22
Figure VII-9.	Stratigraphic Cross Section C-C' in Kuparuk River Field Showing Distributions of Kuparuk River Upper and Lower Sands. ....	VII-23
Figure VII-10.	Stratigraphic Cross Section D-D' in Kuparuk River Field Showing Distributions of Kuparuk River Upper and Lower Sands. ....	VII-24
Figure VII-11.	Stratigraphic Cross Section E-E' in Kuparuk River Field Showing Distributions of Kuparuk River Upper and Lower Sands. ....	VII-25
Figure VII-12.	Stratigraphic Cross Section F-F' in Kuparuk River Field Showing Distributions of Kuparuk River Upper and Lower Sands. ....	VII-26
Figure VII-13.	Stratigraphic Cross Section G-G' in Kuparuk River Field Showing Distributions of Kuparuk River Upper and Lower Sands. ....	VII-27
Figure VII-14.	Stratigraphic Cross Section H-H' in Kuparuk River Field Showing Distributions of Kuparuk River Upper and Lower Sands. ....	VII-28
Figure VII-15.	Structure Contour Map Showing Top of Kuparuk River Formation Upper Sand. ....	VII-30
Figure VII-16.	Structure Contour Map Showing Top of Kuparuk River Formation Upper Sand (without faults). ....	VII-31
Figure VII-17.	Structure Contour Map Showing Top of Kuparuk River Formation Lower Sand. ....	VII-32
Figure VII-18.	Structure Contour Map Showing Top of Kuparuk River Formation Lower Sand (without faults). ....	VII-33
Figure VII-19.	3-D Structural View on Top of Kuparuk River Formation Upper Sand. ....	VII-34
Figure VII-20.	3-D Structural View on Top of Kuparuk River Formation Lower Sand. ....	VII-35
Figure VII-21.	Net Pay Porosity Distribution in Kuparuk River Formation Upper Sand. ....	VII-37
Figure VII-22.	Net Pay Porosity Distribution (shown in color) in Kuparuk River Formation Upper Sand. ....	VII-38
Figure VII-23.	Net Pay Porosity Distribution in Kuparuk River Formation Lower Sand. ....	VII-39
Figure VII-24.	Net Pay Porosity Distribution (shown in color) in Kuparuk River Formation Lower Sand. ....	VII-40
Figure VII-25.	3-D View of Kuparuk River Formation Upper Sand Net Pay Porosity. ....	VII-41
Figure VII-26.	3-D View of Kuparuk River Formation Lower Sand Net Pay Porosity. ....	VII-42
Figure VII-27.	Plots of Sw from Well Log Analysis Using Three Models (Sw1: Archie, Sw2: Laminar Simondoux, Sw3: Dual Water), Applied to Kuparuk Field Well 1g13. ....	VII-44
Figure VII-28.	Plots of Sw from Well Log Analysis Using Three Models (Sw1: Archie, Sw2: Laminar Simondoux, Sw3: Dual Water) Applied to Kuparuk Field Well 2z15. ....	VII-45
Figure VII-29.	Net Pay Water Saturation Distribution in Kuparuk River Field Upper Sand. ....	VII-47

Figure VII-30.	Net Pay Water Saturation Distribution in Kuparuk River Field Lower Sand. ....	VII-48
Figure VII-31.	Net Pay Water Saturation Distribution (shown in color) in Kuparuk River Formation Upper Sand. ....	VII-49
Figure VII-32.	Net Pay Water Saturation Distribution (shown in color) in Kuparuk River Formation Lower Sand. ....	VII-50
Figure VII-33.	Net Pay Hydrocarbon Pore Volume Distribution in Kuparuk River Upper Sand. ....	VII-51
Figure VII-34.	3-D View of Kuparuk River Formation Net Pay Hydrocarbon Pore Volume. ....	VII-52
Figure VII-35.	Net Pay Hydrocarbon Pore Volume Distribution in Kuparuk River Lower Sand. ....	VII-53
Figure VII-36.	3-D View of Kuparuk River Formation Lower Sand Net Pay Hydrocarbon Pore Volume. ....	VII-54
Figure VII-37.	Cross Section I-I' Showing Coarsening Upward in the Lower Sand of Kuparuk River Formation in Kuparuk River Field. ....	VII-56
Figure VII-38.	Stratigraphic Cross Section J-J' Showing Progradational Thickening of the Kuparuk River Formation Upper Sand. ....	VII-60
Figure VII-39.	Cross Section K-K' Showing Kuparuk River Formation Upper Sand Thickening on the Downthrown Side of Faulting. ....	VII-61
Figure VII-40.	Cross Section K-K' Showing Kuparuk River Formation Upper Sand Thickening on the Downthrown Side of Faulting (faulting omitted). ....	VII-62
Figure VII-41.	Cross Section L-L' Also Showing Kuparuk River Formation Upper Sand Thickening on the Downthrown Side of Faulting. ....	VII-63
Figure VII-42.	Cross Section L-L' Also Showing Kuparuk River Formation Upper Sand Thickening on the Downthrown Side of Faulting (faulting omitted). ....	VII-64
Figure VII-43.	Cross Section M-M' Showing Anomalous Dip Between Kuparuk River Field Wells 2x2-2w2. ....	VII-65
Figure VII-44.	Base Map Showing Kuparuk River Field Cross Sections I-I' Through M-M'. ....	VII-66
Figure VII-45.	Possible Faulting at Kuparuk River Field Well 2w2. ....	VII-68

### CHAPTER VIII:

Figure VIII-1.	Location Map of North Slope Fields, Including Prudhoe Bay Field (Werner, 1987). ....	VIII-2
Figure VIII-2.	North Slope Stratigraphic Column Showing Location of Sadlerochit Group (Bird, 1987). ....	VIII-3
Figure VIII-3.	Analysis Result Plot of A-15 Well from Prudhoe Bay Field, Including Comparison of Sw from Different Models (Sw-1-Laminar Simondoux, Sw-2-Indonesian, Sw-3-Dual Water). ....	VIII-5
Figure VIII-4.	Prudhoe Bay Structure Top Contour Map on Sadlerochit Group. ....	VIII-7
Figure VIII-5.	Prudhoe Bay Structure Top Color-Filled Contour Map on Sadlerochit Group. ....	VIII-8
Figure VIII-6.	3-D View of Structure Top on Sadlerochit Group. ....	VIII-9
Figure VIII-7.	Base Map of Prudhoe Bay Showing Locations of Cross Sections. ....	VIII-11
Figure VIII-8.	Cross Section Along Line A-A' in Prudhoe Bay Field. ....	VIII-12
Figure VIII-9.	Cross Section Along Line B-B' in Prudhoe Bay Field. ....	VIII-13
Figure VIII-10.	Cross Section Along Line C-C' in Prudhoe Bay Field. ....	VIII-14
Figure VIII-11.	Cross Section Along Line D-D' in Prudhoe Bay Field. ....	VIII-15

Figure VIII-12.	Cross Section Along Line E-E' in Prudhoe Bay Field. ....	VIII-16
Figure VIII-13.	Cross Section Along Line F-F' in Prudhoe Bay Field. ....	VIII-17
Figure VIII-14.	Cross Section Along Line G-G' in Prudhoe Bay Field. ....	VIII-18
Figure VIII-15.	Cross Section Along Line H-H' in Prudhoe Bay Field. ....	VIII-19
Figure VIII-16.	Cross Section Along Line I-I' in Prudhoe Bay Field. ....	VIII-20
Figure VIII-17.	Cross Section Along Line J-J' in Prudhoe Bay Field. ....	VIII-21
Figure VIII-18.	Cross Section Along Line K-K' in Prudhoe Bay Field. ....	VIII-22
Figure VIII-19.	Net Pay Porosity Map on Sadlerochit Group. ....	VIII-23
Figure VIII-20.	Color-Fill Net Pay Porosity Map on Sadlerochit Group. ....	VIII-24
Figure VIII-21.	3-D Porosity Map on Sadlerochit Group. ....	VIII-25
Figure VIII-22.	Net Pay Water Saturation Map on Sadlerochit Top. ....	VIII-26
Figure VIII-23.	Color-Fill Net Pay Water Saturation Map on Sadlerochit Group. ....	VIII-27
Figure VIII-24.	3-D Net Pay Water Saturation Map on Sadlerochit Group. ....	VIII-28
Figure VIII-25.	Location of Colville and Prudhoe Structural Highs (Bowsher, 1987). ....	VIII-30
Figure VIII-26.	Prudhoe Bay Field Net Pay True Vertical Thickness Map on Sadlerochit Group. ....	VIII-31
Figure VIII-27.	Prudhoe Bay Field 3-D Net Pay True Vertical Thickness Map on Sadlerochit Group. ....	VIII-32
Figure VIII-28.	Sadlerochit Group Net Pay Oil Saturation Contour Map. ....	VIII-35
Figure VIII-29.	Sadlerochit Group Net Pay Oil Saturation Color-Filled Contour Map. ....	VIII-36
Figure VIII-30.	Sadlerochit Group Net Pay Oil Saturation (3-D view). ....	VIII-37
Figure VIII-31.	Net Pay Hydrocarbon Pore Volume Contour Map on Sadlerochit Group. ....	VIII-39
Figure VIII-32.	3-D View of Net Pay Hydrocarbon Pore Volume on Sadlerochit Group. ....	VIII-40

## CHAPTER IX:

Figure IX-1.	North Slope Fields, Including Lisburne Field (adapted from Werner, 1985). ....	IX-2
Figure IX-2.	Log Plot of the Lisburne Field L4-15 Well with Lisburne Group and Its Subdivisions (formations). ....	IX-3
Figure IX-3.	Stratigraphic Cross Section Across Lisburne Field. ....	IX-5
Figure IX-4.	Base Map Showing Surface Well and Cross Section A-A' Locations in Lisburne Field (Thomas et al., 1993). ....	IX-6
Figure IX-5.	Point McIntyre Base Map with Bottom Hole Locations (Thomas et al., 1993). ....	IX-7
Figure IX-6.	Point Thomson Unit Base Map with Well Locations (Thomas et al., 1993). ....	IX-9
Figure IX-7.	North Slope Stratigraphic Column Showing Late Cretaceous Flaxman Island Field (Bird, 1987). ....	IX-9
Figure IX-8.	Log Plot of the Point Thomson #4 with Thomson Formation Log Picks. ....	IX-11
Figure IX-9.	Gwydyr Bay Base Map Showing Cross Section B-B' (adapted from Thomas et al., 1993). ....	IX-12
Figure IX-10.	Sadlerochit Reserves at Gwydyr Bay (Thomas et al., 1993). ....	IX-14
Figure IX-11.	Kuparuk Reserves at Gwydyr Bay (Thomas et al., 1993). ....	IX-15
Figure IX-12.	Cross Section Across Gwydyr Bay Illustrating Possible Oil-Trapping Structure (Thomas et al., 1993). ....	IX-15
Figure IX-13.	Cross Section B-B' Across Gwydyr Bay Field. ....	IX-16

Figure IX-14.	Base Map Showing Niakuk Field Location (from Thomas et al., 1993). .....	IX-17
Figure IX-15.	Niakuk Field Well Locations with Cross Section C-C' Highlighted (adapted from Thomas et al., 1993). .....	IX-17
Figure IX-16.	Niakuk Field Cross Section C-C' (measured depths). .....	IX-19
Figure IX-17.	Base Map of Seal and Northstar Islands with Well Locations (Thomas et al., 1993). .....	IX-22

## CHAPTER X:

Figure X-1.	Effect of Ethane/Oil Ratio on Amount of Asphaltene Precipitation. ....	X-11
Figure X-2.	Effect of CO <sub>2</sub> /Oil Ratio on Amount of Asphaltene Precipitation. ....	X-12
Figure X-3.	Effect of Propane/Oil Ratio on Amount of Asphaltene Precipitation. ....	X-13
Figure X-4.	Effect of N-Butane/Oil Ratio on Amount of Asphaltene Precipitation. ....	X-14
Figure X-5.	Effect of N-Pentane/Oil Ratio on Amount of Asphaltene Precipitation. ....	X-15
Figure X-6.	Effect of N-Heptane/Oil Ratio on Amount of Asphaltene Precipitation. ....	X-16
Figure X-7.	Effect of NGL/Oil Ratio on Amount of Asphaltene Precipitation. ....	X-17
Figure X-8.	Effect of PBG/Oil Ratio on Amount of Asphaltene Precipitation. ....	X-18
Figure X-9.	Effect of Solvent Molecular Weight on Amount of Asphaltene Precipitation at Highest Solvent/Oil Ratio. ....	X-19
Figure X-10.	Schematic of Experimental Apparatus for Asphaltene Precipitation Studies. ....	X-22

## CHAPTER XI:

Figure XI-1.	Comparison of Experimental and Predicted Amounts of Asphaltene Precipitation for Ethane - West Sak Tank Oil Mixtures. ....	XI-12
Figure XI-2.	Comparison of Experimental and Predicted Amounts of Asphaltene Precipitation for CO <sub>2</sub> - West Sak Tank Oil Mixtures. ....	XI-12
Figure XI-3.	Comparison of Experimental and Predicted Amounts of Asphaltene Precipitation for Propane - West Sak Tank Oil Mixtures. ....	XI-13
Figure XI-4.	Comparison of Experimental and Predicted Amounts of Asphaltene Precipitation for n-Butane - West Sak Tank Oil Mixtures. ....	XI-13
Figure XI-5.	Comparison of Experimental and Predicted Amounts of Asphaltene Precipitation for n-Heptane - West Sak Tank Oil Mixtures. ....	XI-14
Figure XI-6.	Comparison of Experimental and Predicted Amounts of Asphaltene Precipitation for NGL - West Sak Tank Oil Mixtures. ....	XI-14
Figure XI-7.	Comparison of Experimental and Predicted Amounts of Asphaltene Precipitation for PBG - West Sak Tank Oil Mixtures. ....	XI-15
Figure XI-8.	Schematic Representation of Various Fractions and Phases of Oil and Oil-Solvent Mixtures. ....	XI-20
Figure XI-9.	Discretization of a Continuous Normal Distribution Function of Asphaltenes Fractions. ....	XI-22
Figure XI-10.	Relation Between Molar Distribution as a Function of Molecular Weight of Asphaltenes for N-Pentane -- West Sak Tank Oil Ratio = 2.0. ....	XI-30

Figure XI-11.	Relation Between Molar Distribution as a Function of Molecular Weight of Asphaltene for N-Pentane -- West Sak Tank Oil Ratio = 7.0. ....	XI-31
Figure XI-12.	Relation Between Molar Distribution as a Function of Molecular Weight of Asphaltenes for N-Pentane -- West Sak Tank Oil Ratio = 12.5. ....	XI-31
Figure XI-13.	Relation Between Molar Distribution as a Function of Molecular Weight of Asphaltenes for N-Pentane -- West Sak Tank Oil Ratio = 20.2. ....	XI-32

## CHAPTER XII:

Figure XII-1.	Experiment Set-Up Used for Study of Effect of Asphaltene Deposition on Rock Fluid Properties. ....	XII-2
Figure XII-2.	Comparison of Experimental Oil Production Data with Regression Results. ....	XII-7
Figure XII-3.	Comparison of Experimental Relative Injectivity ( $I_r$ ) with Regression Results. ....	XII-7
Figure XII-4.	The Effect of Asphaltene Deposition on the Ratio of Absolute Permeability After Asphaltene Deposition to the Original Absolute Permeability ( $K_j/K_0$ ). ....	XII-14
Figure XII-5.	Cumulative Fractional Oil Recovery (PV) Versus Cumulative Water Injected (PV) for Various Degrees of Asphaltene Deposition (core 1). ....	XII-15
Figure XII-6.	Cumulative Fractional Oil Recovery (PV) Versus Cumulative Water Injected (PV) for Various Degrees of Asphaltene Deposition (core 2). ....	XII-16
Figure XII-7.	Cumulative Fractional Oil Recovery (PV) Versus Cumulative Water Injected (PV) for Various Degrees of Asphaltene Deposition (core 3). ....	XII-16
Figure XII-8.	Pressure Drop Across Core Versus Cumulative Water Injected (PV) for Various Degrees of Asphaltene Deposition (core 1). ....	XII-17
Figure XII-9.	Pressure Drop Across Core Versus Cumulative Water Injected (PV) for Various Degrees of Asphaltene Deposition (core 2). ....	XII-17
Figure XII-10.	Pressure Drop Across Core Versus Cumulative Water Injected (PV) for Various Degrees of Asphaltene Deposition (core 3). ....	XII-18
Figure XII-11.	Ratio of Oil Relative Permeability to Water Relative Permeability ( $K_{ro}/K_{rw}$ ) Versus $S_w$ (core 1). ....	XII-25
Figure XII-12.	Ratio of Oil Relative Permeability to Water Relative Permeability ( $K_{ro}/K_{rw}$ ) Versus $S_w$ (core 2). ....	XII-25
Figure XII-13.	Ratio of Oil Relative Permeability to Water Relative Permeability ( $K_{ro}/K_{rw}$ ) Versus $S_w$ (core 3). ....	XII-26
Figure XII-14.	Effect of Asphaltene Deposition on Fractional Flow Curves (core 1). ....	XII-26
Figure XII-15.	Effect of Asphaltene Deposition on Fractional Flow Curves (core 2). ....	XII-27
Figure XII-16.	Effect of Asphaltene Deposition on Fractional Flow Curves (core 3). ....	XII-27
Figure XII-17.	Effect of Asphaltene Deposition on Oil-Water Relative Permeability Curves (core 1). ....	XII-28
Figure XII-18.	Effect of Asphaltene Deposition on Oil-Water Relative Permeability Curves (core 2). ....	XII-29

Figure XII-19. Effect of Asphaltene Deposition on Oil-Water Relative Permeability Curves (core 3).....	XII-29
--	--------

**CHAPTER XIII:**

Figure XIII-1. Oil Relative Permeability Curve for Sadlerochit: Rock Region 1. ....	XIII-2
Figure XIII-2. Oil Relative Permeability Curve for Sadlerochit: Rock Region 2. ....	XIII-3
Figure XIII-3. Water Relative Permeability Curve for Sadlerochit. ....	XIII-4
Figure XIII-4. Gas Relative Permeability Curve for Sadlerochit. ....	XIII-5
Figure XIII-5. Oil-Water Capillary Pressure Curve for Sadlerochit. ....	XIII-6
Figure XIII-6. Oil Formation Volume Factor for Sadlerochit: Depth Interval 1 (8580 to 8653 ft). Mid-Interval Bubble Point = 4344 psi. ....	XIII-7
Figure XIII-7. Oil Formation Volume Factor for Sadlerochit: Depth Interval 2 (8653 to 8727 ft). Mid-Interval Bubble Point = 4366 psi. ....	XIII-8
Figure XIII-8. Oil Formation Volume Factor for Sadlerochit: Depth Interval 3 (8727 to 8800 ft). Mid-Interval Bubble Point = 4389 psi. ....	XIII-9
Figure XIII-9. Oil Formation Volume Factor for Sadlerochit: Depth Interval 4 (8800 to 8873 ft). Mid-Interval Bubble Point = 4412 psi. ....	XIII-10
Figure XIII-10. Oil Formation Volume Factor for Sadlerochit: Depth Interval 5 (8873 to 8946 ft). Mid-Interval Bubble Point = 4435 psi. ....	XIII-11
Figure XIII-11. Oil Formation Volume Factor for Sadlerochit : Depth Interval 6 (8946 to 9020 ft). Mid-Interval Bubble Point = 4458 psi. ....	XIII-12
Figure XIII-12. Solution Gas-Oil Ratio for Sadlerochit: Depth Interval 1 (8580 to 8653 ft). ....	XIII-13
Figure XIII-13. Solution Gas-Oil Ratio for Sadlerochit: Depth Interval 2 (8653 to 8727 ft). ....	XIII-14
Figure XIII-14. Solution Gas-Oil Ratio for Sadlerochit: Depth Interval 3 (8727 to 8800 ft). ....	XIII-15
Figure XIII-15. Solution Gas-Oil Ratio for Sadlerochit: Depth Interval 4 (8800 to 8873 ft). ....	XIII-16
Figure XIII-16. Solution Gas-Oil Ratio for Sadlerochit: Depth Interval 5 (8873 to 8946 ft). ....	XIII-17
Figure XIII-17. Solution Gas-Oil Ratio for Sadlerochit: Depth Interval 6 (8946 to 9020 ft). ....	XIII-18
Figure XIII-18. Oil Viscosity for Sadlerochit: Depth Interval 1 (8580 to 8653 ft). ....	XIII-19
Figure XIII-19. Oil Viscosity for Sadlerochit: Depth Interval 2 (8653 to 8727 ft). ....	XIII-20
Figure XIII-20. Oil Viscosity for Sadlerochit: Depth Interval 3 (8727 to 8800 ft). ....	XIII-21
Figure XIII-21. Oil Viscosity for Sadlerochit: Depth Interval 4 (8800 to 8873 ft). ....	XIII-22
Figure XIII-22. Oil Viscosity for Sadlerochit: Depth Interval 5 (8873 to 8946 ft). ....	XIII-23
Figure XIII-23. Oil Viscosity for Sadlerochit: Depth Interval 6 (8946 to 9020 ft). ....	XIII-24
Figure XIII-24. Gas Formation Volume Factor for Sadlerochit. ....	XIII-25
Figure XIII-25. Gas Viscosity for Sadlerochit. ....	XIII-26
Figure XIII-26. Water Formation Volume Factor for Sadlerochit. ....	XIII-27
Figure XIII-27. Oil Formation Volume Factor for Kuparuk River Formation.....	XIII-29
Figure XIII-28. Solution Gas-Oil Ratio for Kuparuk River Formation.....	XIII-30

Figure XIII-29. Normalized Oil Viscosity Versus Normalized Pressure for Kuparuk River Formation. ....	XIII-31
Figure XIII-30. Variation of Bubble Point Oil Viscosity with Depth for Kuparuk River Formation. ....	XIII-32
Figure XIII-31. Oil Formation Volume Factor for Endicott Field. ....	XIII-33
Figure XIII-32. Solution Gas-Oil Ratio for Endicott Field. ....	XIII-34
Figure XIII-33. Oil Viscosity for Endicott Field. ....	XIII-35
Figure XIII-34. Gas Viscosity for Endicott Field. ....	XIII-36
Figure XIII-35. Gas Specific Gravity for Endicott Field. ....	XIII-37
Figure XIII-36. Oil Formation Volume Factor for West Sak Field. ....	XIII-38
Figure XIII-37. Solution Gas-Oil Ratio for West Sak Field. ....	XIII-39
Figure XIII-38. Oil Density for West Sak Field. ....	XIII-40
Figure XIII-39. Oil Viscosity for West Sak Field. ....	XIII-41
Figure XIII-40. Gas Formation Volume Factor for West Sak Field. ....	XIII-42

**CHAPTER XIV:**

Figure XIV-1. Monthly Oil and Gas Production Data (Prudhoe Bay). ....	XIV-10
Figure XIV-2. Monthly Oil and Gas Injection Data (Prudhoe Bay). ....	XIV-11
Figure XIV-3. Monthly Oil and Gas Production Data (Lisburne). ....	XIV-15
Figure XIV-4. Monthly Oil and Gas Injection Data (Lisburne). ....	XIV-16
Figure XIV-5. Monthly Oil and Gas Production Data (Endicott - Ivishak). ....	XIV-20
Figure XIV-6. Monthly Oil and Gas Injection Data (Endicott - Ivishak). ....	XIV-21
Figure XIV-7. Monthly Oil and Gas Production Data (Endicott - Endicott). ....	XIV-22
Figure XIV-8. Monthly Oil and Gas Injection Data (Endicott - Endicott). ....	XIV-23
Figure XIV-9. Monthly Oil and Gas Production Data (Kuparuk River - Kuparuk River). ....	XIV-30
Figure XIV-10. Monthly Oil and Gas Injection Data (Kuparuk River - Kuparuk River). ....	XIV-31
Figure XIV-11. Monthly Oil and Gas Production Data (Kuparuk River - West Sak). ....	XIV-32
Figure XIV-12. Monthly Oil and Gas Injection Data (Kuparuk River - West Sak). ....	XIV-33
Figure XIV-13. Monthly Oil and Gas Production Data (Milne Point - Kuparuk River). ....	XIV-40
Figure XIV-14. Monthly Oil and Gas Injection Data (Milne Point - Kuparuk River). ....	XIV-41
Figure XIV-15. Monthly Oil and Gas Production Data (Milne Point - Schrader Bluff). ....	XIV-42
Figure XIV-16. Monthly Oil and Gas Injection Data (Milne Point - Schrader Bluff). ....	XIV-43
Figure XIV-17. Monthly Oil and Gas Production Data (Trading Bay - Middle Kenai B). ....	XIV-77
Figure XIV-18. Monthly Oil and Gas Production Data (Trading Bay - Middle Kenai C). ....	XIV-78
Figure XIV-19. Monthly Oil and Gas Injection Data (Trading Bay - Middle Kenai C). ....	XIV-79
Figure XIV-20. Monthly Oil and Gas Production Data (Trading Bay - Middle Kenai D). ....	XIV-80
Figure XIV-21. Monthly Oil and Gas Injection Data (Trading Bay - Middle Kenai D). ....	XIV-81
Figure XIV-22. Monthly Oil and Gas Production Data (Trading Bay - Middle Kenai E). ....	XIV-82

Figure XIV-23. Monthly Oil and Gas Production Data (Trading Bay - Hemlock)....	XIV-83
Figure XIV-24. Monthly Oil and Gas Production Data (Trading Bay - Undefined).....	XIV-84
Figure XIV-25. Monthly Oil and Gas Production Data (Trading Bay, G - NE/Hemlock - NE).....	XIV-91
Figure XIV-26. Monthly Oil and Gas Injection Data (Trading Bay, G - NE/Hemlock - NE).....	XIV-92
Figure XIV-27. Monthly Oil and Gas Production Data (North Trading Bay - West Foreland).....	XIV-93
Figure XIV-28. Monthly Oil and Gas Production Data (McArthur River - Hemlock).....	XIV-103
Figure XIV-29. Monthly Oil and Gas Injection Data (McArthur River - Hemlock).....	XIV-104
Figure XIV-30. Monthly Oil and Gas Production Data (McArthur River - Middle Kenai G Zone).....	XIV-105
Figure XIV-31. Monthly Oil and Gas Injection Data (McArthur River - Middle Kenai G Zone).....	XIV-106
Figure XIV-32. Monthly Oil and Gas Production Data (McArthur River - West Foreland).....	XIV-107
Figure XIV-33. Monthly Oil and Gas Injection Data (McArthur River - West Foreland).....	XIV-108
Figure XIV-34. Monthly Oil and Gas Production Data (Granite Point).....	XIV-112
Figure XIV-35. Monthly Oil and Gas Injection Data (Granite Point).....	XIV-113
Figure XIV-36. Monthly Oil and Gas Production Data (Swanson River).....	XIV-117
Figure XIV-37. Monthly Oil and Gas Injection Data (Swanson River).....	XIV-118
Figure XIV-38. Monthly Oil and Gas Production Data (Middle Ground Shoal - A Pool).....	XIV-128
Figure XIV-39. Monthly Oil and Gas Injection Data (Middle Ground Shoal - A Pool).....	XIV-129
Figure XIV-40. Monthly Oil and Gas Production Data (Middle Ground Shoal - B, C, & D Pool).....	XIV-130
Figure XIV-41. Monthly Oil and Gas Injection Data (Middle Ground Shoal - B, C, & D Pool).....	XIV-131
Figure XIV-42. Monthly Oil and Gas Production Data (Middle Ground Shoal - E, F, & G Pool).....	XIV-132
Figure XIV-43. Monthly Oil and Gas Injection Data (Middle Ground Shoal - E, F, & G Pool).....	XIV-133
Figure XIV-44. Monthly Oil and Gas Injection Data (Middle Ground Shoal - Undefined).....	XIV-134
Figure XIV-45. Monthly Oil and Gas Production Data (Beaver Creek).....	XIV-138
Figure XIV-46. Oil and Gas Projection Data for State of Alaska (1959-1991).....	XIV-139

# LIST OF TABLES

---

		<u>Page</u>
<b>CHAPTER I:</b>		
Table I-1:	North Slope Oil and Gas Producing Fields (as of January 1, 1990) (Thomas et al., 1991). .....	I-9
Table I-2:	North Slope Undeveloped Oil and Gas Accumulations (as of January 1, 1990) (Thomas et al., 1991). .....	I-10
 <b>CHAPTER II:</b>		
Table II-1:	Petrophysical Parameters of West Sak Upper Sands. ....	II-7
Table II-2:	Petrophysical Parameters of West Sak Lower Sand 1. ....	II-8
Table II-3:	Petrophysical Parameters of West Sak Lower Sand 2. ....	II-8
Table II-4:	Petrophysical Parameters of West Sak Lower Sand 3. ....	II-9
Table II-5:	Petrophysical Parameters of West Sak Lower Sand 4. ....	II-9
Table II-6:	Log-Derived Data for Selected Wells in the West Sak Sands. ....	II-10
 <b>CHAPTER III:</b>		
Table III-1:	Petrophysical Parameters of Lower Ugnu Sand 1. ....	III-3
Table III-2:	Petrophysical Parameters of Lower Ugnu Sand 2. ....	III-3
Table III-3:	Petrophysical Parameters of Lower Ugnu Sand 3. ....	III-4
Table III-4:	Petrophysical Parameters of Lower Ugnu Sand 4. ....	III-4
Table III-5:	Petrophysical Parameters of Lower Ugnu Sand 5. ....	III-5
Table III-6:	Log-Derived Data for Selected Wells in the Lower Ugnu Sands. ....	III-5
Table III-7:	Log-Derived Data for Selected Wells in the West Sak Sands. ....	III-7
 <b>CHAPTER V:</b>		
Table V-1:	Endicott Lithostratigraphic Zones and Subzones (Woidneck, et al., 1987). .....	V-5
Table V-2:	Endicott Wells Utilized in Well Log Analysis to Date. ....	V-8
Table V-3:	Zone 1 Tops at Endicott Field. ....	V-14
Table V-4:	Petrophysical Properties of Endicott Zone 2A. ....	V-15
Table V-5:	Petrophysical Properties of Endicott Zone 2B. ....	V-16
Table V-6:	Petrophysical Properties of Endicott Zone 3A. ....	V-17
Table V-7:	Petrophysical Properties of Endicott Zone 3B. ....	V-18
Table V-8:	Petrophysical Properties of Endicott Zone 3C. ....	V-19
Table V-9:	Weighted Zone Averages of Porosity and Water Saturation at Endicott Field. ....	V-20
 <b>CHAPTER VI:</b>		
Table VI-1:	Field-Wide Log-Derived Petrophysical Properties. ....	VI-51
Table VI-2:	Log-Derived Petrophysical Properties from Wells Within the Center of the Field. ....	VI-52

## CHAPTER VII:

Table VII-1:	Average Petrophysical Properties of Kuparuk River Upper Sand (6% porosity, 40% shale, 40% Sw cutoffs). .....	VII-8
Table VII-2:	Average Petrophysical Properties of Kuparuk River Upper Sand (6% porosity, 40% shale, 60% Sw cutoffs). .....	VII-10
Table VII-3:	Average Petrophysical Properties of Kuparuk River Upper Sand (6% porosity, 40% shale, 80% Sw cutoffs). .....	VII-12
Table VII-4:	Average Petrophysical Properties of Kuparuk River Lower Sand (6% porosity, 40% shale, 40% Sw cutoffs). .....	VII-14
Table VII-5:	Average Petrophysical Properties of Kuparuk River Lower Sand (6% porosity, 40% shale, 60% Sw cutoffs). .....	VII-16
Table VII-6:	Average Petrophysical Properties of Kuparuk River Lower Sand (6% porosity, 40% shale, 80% Sw cutoffs). .....	VII-18
Table VII-7:	Comparison of Porosities from Neutron and Density Tools in Kuparuk River Formation. ....	VII-36

## CHAPTER VIII:

Table VIII-1:	Log Derived Petrophysical Properties of Prudhoe Bay Wells (cutoffs: $\phi$ - 6%, Sh - 40%, Sw - 80%). .....	VIII-6
---------------	---	--------

## CHAPTER IX:

Table IX-1:	Petrophysical Properties of Reservoir Rocks in Niakuk Field. ....	IX-20
-------------	---	-------

## CHAPTER X:

Table X-1:	Compositional Analysis (Mol %) of West Sak Tank Oil. ....	X-7
Table X-2:	Compositional Analysis (Mol %) of Live (recombined) Oil-A, Prudhoe Bay Natural Gas (PBG) and Natural Gas Liquids (NGL). .....	X-8
Table X-3:	Asphalt/Asphaltene Precipitation Test Results for West Sak (Tank) Oil-A. ....	X-9
Table X-4:	Asphalt/Asphaltene Precipitation Test Results for West Sak (Tank) Oil-B. ....	X-10
Table X-5:	Compositional Changes (Mol %) and Density Changes in West Sak Crude (Tank Oil-A) After Asphaltene Precipitation by N-Pentane and N-Butane. ....	X-21
Table X-6:	Effect of CO <sub>2</sub> Addition to Recombined West Sak Oil A on the Asphaltene Precipitation (at 1705 psia, 80°F). ....	X-24
Table X-7:	Effect of Pressure on Amount of Asphaltene Precipitation 30 Mol % CO <sub>2</sub> - 70 Mol % West Sak Crude A (recombined at 1705 psia and 80°F). ....	X-24
Table X-8:	Effect of Pressure on Amount of Asphaltene Precipitation 50 Mol % CO <sub>2</sub> - 50 Mol % West Sak Crude A (recombined at 1705 psia and 80°F). ....	X-24

**CHAPTER XI:**

Table XI-1:	Comparison of Experimental and Predicted Amounts of Asphaltene Precipitation for Ethane - West Sak Tank Oil A Mixtures. ....	XI-8
Table XI-2:	Comparison of Experimental and Predicted Amounts of Asphaltene Precipitation for CO <sub>2</sub> - West Sak Tank Oil A Mixtures. ....	XI-8
Table XI-3:	Comparison of Experimental and Predicted Amounts of Asphaltene Precipitation for Propane - West Sak Tank Oil A Mixtures. ....	XI-9
Table XI-4:	Comparison of Experimental and Predicted Amounts of Asphaltene Precipitation for n-Butane - West Sak Tank Oil A Mixtures. ...	XI-9
Table XI-5:	Comparison of Experimental and Predicted Amounts of Asphaltene Precipitation for n-Pentane - West Sak Tank Oil A Mix- tures. ....	XI-10
Table XI-6:	Comparison of Experimental and Predicted Amounts of Asphaltene Precipitation for n-Heptane - West Sak Tank Oil A Mix- tures. ....	XI-10
Table XI-7:	Comparison of Experimental and Predicted Amounts of Asphaltene Precipitation for NGL - West Sak Tank Oil A Mixtures. ....	XI-11
Table XI-8:	Comparison of Experimental and Predicted Amounts of Asphaltene Precipitation for PBG - West Sak Tank Oil A Mixtures. ....	XI-11
Table XI-9:	Optimized Values of Asphaltene Solubility Parameter, Asphaltene Molar Volume and Asphaltene Molecular Weight for Various Solvents (West Sak Tank Oil A). ....	XI-16
Table XI-10:	Comparison of Experimental and Predicted Amounts of Asphaltene Precipitation for Various Solvents - West Sak Tank Oil A Mixtures. ....	XI-29
Table XI-11:	Optimized Model Parameters for West Sak Oil -- Solvent Mix- tures. ....	XI-30
Table XI-12:	Comparison of Experimental Results and Model Predictions for CO <sub>2</sub> -- West Sak Oil Mixtures at Higher Pressures. ....	XI-33

**CHAPTER XII:**

Table XII-1:	Properties of Cores Used in the Study. ....	XII-3
Table XII-2:	Sand Grain Size Distribution (weight %) for Unconsolidated Cores. ....	XII-4
Table XII-3:	Unsteady State Displacement Data for Core No. 1 and Run No. 1. ....	XII-8
Table XII-4:	Unsteady State Displacement Data for Core No. 1 and Run No. 2. ....	XII-8
Table XII-5:	Unsteady State Displacement Data for Core No. 1 and Run No. 3. ....	XII-9
Table XII-6:	Unsteady State Displacement Data for Core No. 1 and Run No. 4. ....	XII-9
Table XII-7:	Unsteady State Displacement Data for Core No. 2 and Run No. 1. ....	XII-10
Table XII-8:	Unsteady State Displacement Data for Core No. 2 and Run No. 2. ....	XII-10
Table XII-9:	Unsteady State Displacement Data for Core No. 2 and Run No. 3. ....	XII-11
Table XII-10:	Unsteady State Displacement Data for Core No. 2 and Run No. 4. ....	XII-11

Table XII-11:	Unsteady State Displacement Data for Core No. 3 and Run No. 1.....	XII-12
Table XII-12:	Unsteady State Displacement Data for Core No. 3 and Run No. 2.....	XII-12
Table XII-13:	Unsteady State Displacement Data for Core No. 3 and Run No. 3.....	XII-13
Table XII-14:	Unsteady State Displacement Data for Core No. 3 and Run No. 4.....	XII-13
Table XII-15:	Calculated Results for Core No. 1 and Run No. 1.....	XII-19
Table XII-16:	Calculated Results for Core No. 1 and Run No. 2.....	XII-19
Table XII-17:	Calculated Results for Core No. 1 and Run No. 3.....	XII-20
Table XII-18:	Calculated Results for Core No. 1 and Run No. 4.....	XII-20
Table XII-19:	Calculated Results for Core No. 2 and Run No. 1.....	XII-21
Table XII-20:	Calculated Results for Core No. 2 and Run No. 2.....	XII-21
Table XII-21:	Calculated Results for Core No. 2 and Run No. 3.....	XII-22
Table XII-22:	Calculated Results for Core No. 2 and Run No. 4.....	XII-22
Table XII-23:	Calculated Results for Core No. 3 and Run No. 1.....	XII-23
Table XII-24:	Calculated Results for Core No. 3 and Run No. 2.....	XII-23
Table XII-25:	Calculated Results for Core No. 3 and Run No. 3.....	XII-24
Table XII-26:	Calculated Results for Core No. 3 and Run No. 4.....	XII-24

**CHAPTER XIV:**

Table XIV-1:	Reservoir Heterogeneity Classification System for TORIS (Prudhoe Bay Sadlerochit Reservoir).....	XIV-4
Table XIV-2:	TORIS Data Base (Prudhoe Bay, Ivishak).....	XIV-5
Table XIV-3:	Reservoir Heterogeneity Classification System for TORIS (Prudhoe Bay Sadlerochit Reservoir).....	XIV-7
Table XIV-4:	TORIS Data Base (Prudhoe Bay, Sadlerochit).....	XIV-8
Table XIV-5:	Reservoir Heterogeneity Classification System for TORIS (Lisburne Field).....	XIV-12
Table XIV-6:	TORIS Data Base (Lisburne Field).....	XIV-13
Table XIV-7:	Reservoir Heterogeneity Classification System for TORIS (Endicott Field).....	XIV-17
Table XIV-8:	TORIS Data Base (Endicott Field).....	XIV-18
Table XIV-9:	Reservoir Heterogeneity Classification System for TORIS (Kuparuk River - Kuparuk River).....	XIV-24
Table XIV-10:	TORIS Data Base (Kuparuk River).....	XIV-25
Table XIV-11:	Reservoir Heterogeneity Classification System for TORIS (Prudhoe Bay - Kuparuk River).....	XIV-27
Table XIV-12:	TORIS Data Base (Prudhoe Bay - Kuparuk River).....	XIV-28
Table XIV-13:	Reservoir Heterogeneity Classification System for TORIS (Milne Point - Kuparuk).....	XIV-34
Table XIV-14:	TORIS Data Base (Milne Point - Kuparuk).....	XIV-35
Table XIV-15:	Reservoir Heterogeneity Classification System for TORIS (Milne Point - Schrader Bluff).....	XIV-37
Table XIV-16:	TORIS Data Base (Milne Point - Schrader Bluff).....	XIV-38
Table XIV-17:	Reservoir Heterogeneity Classification System for TORIS (West Sak).....	XIV-44
Table XIV-18:	TORIS Data Base (West Sak).....	XIV-45
Table XIV-19:	Reservoir Heterogeneity Classification System for TORIS (Upper Ugnu - Ugnu).....	XIV-47
Table XIV-20:	TORIS Data Base (Upper Ugnu - Ugnu).....	XIV-48

Table XIV-21:	Reservoir Heterogeneity Classification System for TORIS (Kuparuk - Lower Ugnu). .....	XIV-50
Table XIV-22:	TORIS Data Base (Kuparuk - Lower Ugnu). .....	XIV-51
Table XIV-23:	Reservoir Heterogeneity Classification System for TORIS (Trading Bay - Middle Kenai B). .....	XIV-53
Table XIV-24:	TORIS Data Base (Trading Bay - Middle Kenai B). .....	XIV-54
Table XIV-25:	Reservoir Heterogeneity Classification System for TORIS (Trading Bay - Middle Kenai C). .....	XIV-56
Table XIV-26:	TORIS Data Base (Trading Bay - Middle Kenai C). .....	XIV-57
Table XIV-27:	Reservoir Heterogeneity Classification System for TORIS (Trading Bay - Middle Kenai D). .....	XIV-59
Table XIV-28:	TORIS Data Base (Trading Bay - Middle Kenai D). .....	XIV-60
Table XIV-29:	Reservoir Heterogeneity Classification System for TORIS (Trading Bay - Middle Kenai E). .....	XIV-62
Table XIV-30:	TORIS Data Base (Trading Bay - Middle Kenai E). .....	XIV-63
Table XIV-31:	Reservoir Heterogeneity Classification System for TORIS (Trading Bay - Hemlock). .....	XIV-65
Table XIV-32:	TORIS Data Base (Trading Bay - Hemlock). .....	XIV-66
Table XIV-33:	Reservoir Heterogeneity Classification System for TORIS (Trading Bay ('G' & Hemlock NE Commingle)). .....	XIV-68
Table XIV-34:	TORIS Data Base (Trading Bay ('G' & Hemlock NE Commingle)). .....	XIV-69
Table XIV-35:	Reservoir Heterogeneity Classification System for TORIS (Trading Bay - Undefined). .....	XIV-71
Table XIV-36:	TORIS Data Base (Trading Bay - Undefined). .....	XIV-72
Table XIV-37:	Reservoir Heterogeneity Classification System for TORIS (Trading Bay - West Foreland). .....	XIV-74
Table XIV-38:	TORIS Data Base (Trading Bay - West Foreland). .....	XIV-75
Table XIV-39:	Reservoir Heterogeneity Classification System for TORIS (North Trading Bay). .....	XIV-85
Table XIV-40:	TORIS Data Base (North Trading Bay). .....	XIV-86
Table XIV-41:	Reservoir Heterogeneity Classification System for TORIS (North Trading Bay). .....	XIV-88
Table XIV-42:	TORIS Data Base (North Trading Bay). .....	XIV-89
Table XIV-43:	Reservoir Heterogeneity Classification System for TORIS (McArthur River - Hemlock). .....	XIV-94
Table XIV-44:	TORIS Data Base (McArthur River - Hemlock). .....	XIV-95
Table XIV-45:	Reservoir Heterogeneity Classification System for TORIS (McArthur River - Tyonek Middle Kenai G Zone). .....	XIV-97
Table XIV-46:	TORIS Data Base (McArthur River - Tyonek Middle Kenai G Zone). .....	XIV-98
Table XIV-47:	Reservoir Heterogeneity Classification System for TORIS (McArthur River - West Foreland). .....	XIV-100
Table XIV-48:	TORIS Data Base (McArthur River - West Foreland). .....	XIV-101
Table XIV-49:	Reservoir Heterogeneity Classification System for TORIS (Granite Point). .....	XIV-109
Table XIV-50:	TORIS Data Base (Granite Point). .....	XIV-110
Table XIV-51:	Reservoir Heterogeneity Classification System for TORIS (Swanson River). .....	XIV-114
Table XIV-52:	TORIS Data Base (Swanson River). .....	XIV-115
Table XIV-53:	Reservoir Heterogeneity Classification System for TORIS (Middle Ground Shoal - A Pool). .....	XIV-119
Table XIV-54:	TORIS Data Base (Middle Ground Shoal - A Pool). .....	XIV-120

Table XIV-55:	Reservoir Heterogeneity Classification System for TORIS (Middle Ground Shoal - B, C & D Pool). .....	XIV-122
Table XIV-56:	TORIS Data Base (Middle Ground Shoal - B, C & D Pool). .....	XIV-123
Table XIV-57:	Reservoir Heterogeneity Classification System for TORIS (Middle Ground Shoal). .....	XIV-125
Table XIV-58:	TORIS Data Base (Middle Ground Shoal). .....	XIV-126
Table XIV-59:	Reservoir Heterogeneity Classification System for TORIS (Beaver Creek). .....	XIV-135
Table XIV-60:	TORIS Data Base (Beaver Creek). .....	XIV-136

## ACKNOWLEDGMENT

---

This report was prepared for the U.S. Department of Energy under the Cooperative Agreement No. DE-FG07-90ID12839. The financial support of the U.S. Department of Energy, Idaho field office, is gratefully acknowledged. The matching support was provided by the Petroleum Development Laboratory, University of Alaska Fairbanks. The research work described herein was made possible by the cooperation and assistance of Alaska Oil and Gas Conservation Commission who provided well log data; and North Slope Operators who provided natural gas and crude oil samples. This report is a result of the work performed by co-investigators Mr. Shirish L. Patil, Mr. Walter C. Munly, Dr. Vidyadhar A. Kamath, Dr. Dimitrios Hatzignatiou, Dr. David O. Ogbe and Dr. Santanu Khataniar, and graduate students, Ansar Ali, Maruti Inaganti, Zhaowu Huang, Yuan Wang, Samuel Atta-Darkwah, Guangming Ti, Jinchun Jiang, Milind Kakade, Jiede Yang, Vivek Mehta, and Liao Yang. This report was compiled by Mr. Shirish L. Patil and was typed by Ms. Vickie L. Ivester.

## ABSTRACT

---

The Alaskan North Slope comprises one of the Nation's and the world's most prolific oil province. Original oil in place (OOIP) is estimated at nearly 70 BBL (Kamath and Sharma, 1986). Generalized reservoir descriptions have been completed by the University of Alaska's Petroleum Development Laboratory over North Slope's major fields. These fields include West Sak (20 BBL OOIP), Ugnu (15 BBL OOIP), Prudhoe Bay (23 BBL OOIP), Kuparuk (5.5 BBL OOIP), Milne Point (3 BBL OOIP), and Endicott (1 BBL OOIP). Reservoir description has included the acquisition of open hole log data from the Alaska Oil and Gas Conservation Commission (AOGCC), computerized well log analysis using state-of-the-art computers, and integration of geologic and logging data.

West Sak oil occurs in relatively shallow Late Cretaceous to Early Tertiary marine shelf and deltaic sands at depths from 2000 to 4500 feet subsea. Low oil gravities (12 to 22 degree API) have resulted in the field's being classified marginally economic by its operator (Arco Alaska Inc.). Ugnu reservoir sands directly overlie West Sak sands. Being shallower, they yield even lower oil gravities (3 to 12 degree API). However, Ugnu clay volumes are less than 5% (compared to between 5% and 30% in West Sak) and Ugnu sands are slightly coarser than West Sak sands.

Endicott production occurs from the Mississippian Kekiktuk formation at depths below 9500 feet subsea. Fluvial sandstones and conglomerates deposited in braided stream and point bar environment comprise the majority of these producing units. Faulting plays a major role in trapping Endicott oil. Close proximity to production and transport facilities make the field economic.

Milne Point Unit deep oil-bearing rocks are found in the Lower Cretaceous Kuparuk River formation. This is the same formation from which the Kuparuk River field produces. However, production at Kuparuk River field occurs at slightly shallower depths than at Milne Point (from below about 6000 feet subsea at Kuparuk River field versus 6800 feet subsea at Milne Point). Structural and stratigraphic elements have combined in allowing oil to accumulate at both fields. Faulting at both fields is abundant and best evaluated seismically. Kuparuk formation sand lobes thin and pinch out across both fields. Kuparuk field is by far the larger of the two fields, with production at Milne Point currently resumed.

Although Prudhoe Bay is the North Slope's largest producing field, it has recently experienced production declines. Production occurs primarily from the Permo-Triassic

Sadlerochit group, with additional production occurring from the Triassic Shublik and Sag River formations. The field lies structurally in an anticline, but faulting and truncations provide additional trapping mechanisms. Oil saturations are consistently high, and porosities range from 20% to over 30%. Most production occurs between 8200 and 9400 feet subsea.

Lisburne field is the only North Slope field to produce from carbonate rocks. Lying within, and adjacent to, the Prudhoe Bay Unit, it has produced 90 MMBO through 1992 from fractured, low-permeability shallow marine limestones and dolomites.

Non-producing fields on the North Slope include Point McIntyre, Point Thomson, Gwydyr Bay, Niakuk, and Seal Island/Northstar units. Test wells have produced from various formations, and at various rates, with maximum rates exceeding 5400 BOPD. The most promising unit is Point McIntyre, with estimated recoverable reserves of 300 MMBO.

The studies pertaining to fluid characterization described in this report include: experimental study of asphaltene precipitation for enriched gases, CO<sup>2</sup> and West Sak crude system, modeling of asphaltene equilibria including homogeneous as well as polydispersed thermodynamic models, effect of asphaltene deposition on rock-fluid properties, fluid properties of some Alaskan north slope reservoirs. Finally, the last chapter summarizes the reservoir heterogeneity classification system for TORIS and TORIS database.

## EXECUTIVE SUMMARY

---

West Sak reservoir, with 20 BBL OOIP, rivals Prudhoe Bay field, immediately to the west, in terms of production potential. The West Sak reservoir directly overlies another major producing horizon, the Kuparuk River. Thick permafrost and resulting low reservoir temperatures, combined with degradation of shallow crudes, make West Sak crude viscous (12 to 22 degree API). With current oil prices remaining relatively low, West Sak remains marginally economic.

Late Cretaceous to Early Tertiary sands make up the West Sak Reservoir. They were deposited as part of a shallow deltaic and shelf complex, and lie between 2000 and 4500 feet subsea. These sands are subdivided into two upper sand members and four lower sand members. The entire sand package averages 300 feet in thickness in the area of greatest productive potential. Sands tend to be fine-to-medium grained. Upper sand porosities range between 15% and 40%, and water saturations vary from 9% to 46%. Lower sand porosities are similar, but water saturations are higher, ranging up to 80%. Overall, the upper sands exhibit the best reservoir properties at West Sak. This can be attributed, in major part, to differing depositional environments. Shallow marine and delta front environments corresponding to the upper sands produced relatively clean thick sands. Shelf deposition of lower sands resulted in thinner sands and generally less well developed sand quality.

Concordantly overlying West Sak reservoir are the Ugnu sands, also Late Cretaceous to Early Tertiary in age. Although generally fine-to-medium grained, the Ugnu sands exhibit a slightly coarser grained character as compared to the West Sak sands. They are also cleaner, with clay volumes being less than 5% (versus 5 to 30% in West Sak). However, due to their closer proximity to overlying permafrost, gravities of crude within these sands are very low, ranging between 3 and 12 degree API.

Analysis at Ugnu focused on the package of five Lower Ugnu sands due to availability of core data. Petrophysical analysis indicates three of the lower sands to be potentially productive. The uppermost lower sand (Sand 1) exhibits the highest porosities, lowest water saturations, and thickest net pay zones. Overall, the Lower Ugnu sands are characterized by better porosities, water saturations, and net pay thicknesses than the West Sak sands. However, because West Sak crude is warmer and less viscous, it presents a more attractive target for development.

Endicott field, located offshore from the Sagavanirktok River delta, is the first Arctic offshore field to be developed. Production occurs from the Mississippian Kekiktuk formation, and is classified in terms of three fluvial lithostratigraphic units. These units are labeled from bottom to top as Zones 1, 2, and 3. Each zone is further subdivided individually into subzones A, B, and C. Zone 1 was deposited in a low energy, swampy environment. Zone 2 is characterized predominately by high energy, braided stream deposits. Zone 3 consists of point bar deposits within a meandering stream system.

A combination of structure and stratigraphy form the trap for Endicott hydrocarbon accumulation. Bounding faults define three sides of the field, and southwest dip combined with truncation against shales directly above the regional Lower Cretaceous Unconformity (LCU), to seal the reservoir. Production occurs, generally below 9500 feet subsea, and is mostly from Zones 2 and 3. Porosities in Zones 2 and 3 vary from a low of 11% to a high of 36%. Water saturations vary widely, ranging between 9% and 100%. Zone 3A exhibits the highest average porosity (28%) and lowest average water saturation (39%).

Milne Point field is estimated to hold 3 BBL OOIP at the Kuparuk level. Two main sand members, labeled the Middle Kuparuk and Lower Kuparuk, occur at Milne Point. Each member is composed of two individual sand lobes. Lower lobes of each Kuparuk member are discontinuous across the field. Although production can occur from any of the four lobes, it rarely occurs from more than two lobes in any given well.

Milne Point is likely bounded by northwest-to-southeast trending faults. This faulting may define Milne Point as an uplifted and tilted fault block. Stratigraphically, the Middle Kuparuk thickens southeastward. This contrasts with the Lower Kuparuk, which shows relatively uniform thicknesses toward the southeast. Both the Middle and Lower Kuparuk were deposited on a marine shelf. Well log trace character indicates a regressive marine environment was in control at Milne Point during Kuparuk time.

Porosities as high as 30% occur at Milne Point. Lower Kuparuk porosities are generally higher than those in the Upper Kuparuk. Water saturations in both members are highest toward the southeast, with lowest saturations commonly occurring in the middle of the field. Analysis of seismic data to better delineate faulting would facilitate reservoir description at Milne Point.

Kuparuk field, also producing from the Kuparuk River formation, lies approximately ten miles west and southwest of Milne Point field. Most, if not all, of the Kuparuk River formation has been eroded by the Lower Cretaceous Unconformity in the field area. The

formation is composed of two easily distinguishable sands (labeled upper and lower sands), and one intermittent, thin sand which lies between these. The sands exhibit structural crest in the middle of the field, with steepest dip occurring on the field's north side. Lower sand thicknesses are relatively consistent, but upper sand thickness vary across the field.

Average porosities at Kuparuk range from a low of 11% to a high of 34% in analyzed wells. Average water saturations are relatively low, even when the maximum allowable water saturation in net pay calculations is raised to 80%. No well yielded water saturations of 100%.

Kuparuk upper and lower sands represent two distinct cyclic sequences, responding to differing environments of deposition. Lower sand deposition was episodic and storm related, resulting in coarsening upward clastic sequences. Reservoir quality of this sand was controlled by depositional processes. In contrast, post-depositional, diagenetic features, primarily siderite cementation and dissolution controlled reservoir quality of the lower sand. Grain size distribution in the lower sand is also a major controlling component of reservoir quality in this sand. Production rates vary from up to 5000 barrels of oil per day in the upper sand to 1300 barrels per day in the lower sand.

Prudhoe Bay, located approximately 250 miles north of the Arctic Circle, is estimated to have held 23 BBL OOIP, of which approximately 12 BBL are recoverable. The principal hydrocarbon reservoir is the Permo-Triassic Ivishak formation of the Sadlerochit group. Other hydrocarbon-bearing formations at Prudhoe Bay include the Triassic Shublik and Sag River formations, both of which overlie the Sadlerochit group.

The hydrocarbon accumulation at Prudhoe Bay is both structurally and stratigraphically controlled. Faulting defines the north and west limits of the producing area, while truncation delineates field limits to the east. Southerly dip, combined with the oil-water contact determines the southern limits of the field.

The Ivishak sandstone ranges from 350 feet to nearly 700 feet in thickness. It was deposited as part of a northerly-sourced fluvial deltaic complex. Ivishak thinning occurs from southwest to northeast, and is attributed to pre-Shublik erosion. At Prudhoe Bay, the Ivishak consists primarily of two fine-to-medium grained sandstones separated by massive conglomerates.

Well log data from 27 wells uniformly spread across Prudhoe Bay field were utilized in petrophysical analysis and reservoir description. The top of the Ivishak in these wells

ranges from 8200 feet to 9400 feet subsea, and dips at 1 to 2 degrees. Net pay ranges from 76 feet to over 400 feet. Average porosities vary from 20% to 31% but are generally in the low-to-mid 20% range. Calculated average water saturations are low, especially in view of the 80% water saturation cutoff used to calculate average values.

Lisburne field is the only field to produce from carbonates on the North Slope. The field is located within and adjacent to Prudhoe Bay field. Shallow marine limestones and dolomites of the Lisburne group, subdivided into the Mississippian Alapah and overlying Pennsylvanian Wahoo formations, make up the reservoir. A gas cap occurs above 8600 feet subsea and the oil column extends to approximately 9300 feet subsea. Porosity in the Lisburne averages 10%, but permeabilities are low, averaging only 1 md. Fractures have contributed significantly to Lisburne production. Cumulative oil production through 1992 was nearly 90 MMBO and 1992's annual production totaled 12.5 MMBO.

Point McIntyre is one of the more recent exploration discoveries on the North Slope, testing oil in both the Lower Cretaceous Kuparuk River and Late Cretaceous Seabee formations. Based on high test flow rates (over 5400 BOPD) and geologic analysis, the field's operator (Arco Alaska Inc.) estimates recoverable reserves to be 300 MMBO.

Point Thomson, located 50 miles southeast of Prudhoe Bay, has tested oil in both the Lower Tertiary Canning formation and the Lower Cretaceous Thomson sand. Maximum test production rates of over 2500 BOPD have been recorded. Data from wells drilled to date and a recently shot 3-D seismic survey will determine Point Thomson's economic viability.

Gwydyr Bay reservoir, located adjacent to, and north of Prudhoe Bay has tested oil in the Sadlerochit and Kuparuk River formations. Faulting may play an important role in the accumulation of oil here. Recoverable oil totals are expected to be about 70 MMBO.

Niakuk reservoir, located beneath a gravel island in waters northeast of Prudhoe Bay, has tested oil at rates of over 4700 BOPD from the Kuparuk River formation. Uncertainties currently exist as to whether or not the field's operator (British Petroleum Alaska) has elected to expand production capabilities at Niakuk.

Seal Island/Northstar reservoir is located in offshore waters of the Beaufort Sea. Test rates from this reservoir have exceeded 4700 BOPD. Additional seismic acquisition and reservoir engineering studies are planned prior to determining whether expanded production investments are warranted at Seal Island/Northstar.

The rest of the report describes studies pertaining to fluid characterization studies. In this study, experimental data on the amount of asphalt and asphaltene precipitation due to the addition of solvents to West Sak crude were obtained. The first set of tests were conducted for two types of West Sak stock tank oils. Solvents used include: ethane, carbon dioxide, propane, n-butane, n-pentane, n-heptane, Prudhoe Bay natural gas (PBG) and natural gas liquids (NGL). The effect of solvent to oil dilution ratio on the amount of precipitation was studied. Compositional changes in crude oil as a result of asphalt precipitation were measured using gas-liquid chromatography. A second set of experiments was conducted to measure asphaltene precipitation due to the addition of CO<sub>2</sub> to live (recombined) West Sak crude. Effects of pressure and amount CO<sub>2</sub> in CO<sub>2</sub>/oil mixture on the degree of asphaltene precipitation were studied.

Two asphaltene equilibria models were developed: The first model is a thermodynamic model based on the coupled Equation of State model and Flory-Huggins theory for polymer solutions. The model parameters such as solubility-parameter of asphaltenes, molecular weight of asphaltenes, and molar volume of asphaltenes were obtained by fitting the model to experimental data gathered. Although the model results show excellent agreement with the experimental data, it was determined that the model is not suitable for the prediction of asphaltene precipitation at high pressures. Further work is in progress to develop a generalized model on asphaltenes that will include heterogeneous characteristics of asphaltenes within crude oil.

The second model, a molecular thermodynamic model was developed to represent asphaltene equilibria and to predict the amount of asphaltene precipitation that would occur from a reservoir oil under influence of a miscible solvent or immiscible gas. The model treats the asphaltenes to exist in the crude in a large range of molecular weights represented by a normal distribution function. The properties of each asphaltene pseudo-component such as solubility parameter and molar volume are obtained based on their molecular weights at given pressure and temperature. Scott-Magat theory along with binary interaction parameter between asphaltene free liquid phase (solvent) and asphaltenes are used to represent asphaltene solid-liquid equilibria and to predict the degree of asphaltene precipitation, the molar distribution of asphaltene pseudo-components in equilibrium solid and liquid phases at various pressures, temperatures and solvent-oil compositions. The model is coupled with Peng-Robinson equation of state for vapor-liquid equilibria calculations. The model uses an iterative Newton-Raphson scheme to obtain solution. Four parameters in the model are determined by fitting the model to experimental asphaltene precipitation data for tank West Sak

oil-solvent mixtures. The model is used to predict asphaltene precipitation for CO<sub>2</sub>-West Sak oil mixtures at various pressures.

The flocculation and deposition of asphaltenes in porous media and their interactions with rock and fluids represent complex phenomena which need to be investigated under dynamic flowing conditions. Experimental results are provided to determine the effect of asphaltene deposition on the dynamic displacements of heavy oil by water in consolidated as well as unconsolidated porous media. Dynamic method was used for in-situ asphaltene precipitation in the porous media. Several dynamic displacement experiments were conducted to understand the displacement of heavy oil by water at various degrees of asphaltene deposition.

Fluid properties in Alaskan petroleum reservoirs can be widely variable. Chapter XIII presents a collection of fluid property data for Sadlerochit and Kuparuk formations of the Prudhoe Bay field, the West Sak field and the Endicott field. The fluid properties shown include formation volume factor, solution gas-oil ratio, density, viscosity and bubble point pressure. Oil, water and gas relative permeabilities and capillary pressures also are shown for Sadlerochit formation.

Finally, Chapter XIV summarizes the TORIS database. Data for the reservoir heterogeneity classification system for TORIS includes information regarding depositional system, diagenetic overprint, structural compartmentalization, reservoir heterogeneity ternary diagram, trap type, etc. All the data collected for the TORIS database are included on a floppy disk which accompanies this report.



## **CHAPTER I: INTRODUCTION**

---

### **A. BACKGROUND**

Petroleum resources in Alaska constitute a substantial portion of the total estimated resource base of the Nation. For the past decade and a half, Alaska has produced almost 660 million barrels of oil per year, or about 25% of the U.S. total production. It is estimated that Alaska will also provide more than 25% of the undiscovered recoverable oil and 18% of recoverable gas of the Nation's future supply. A clear understanding of the current oil and natural gas reserves and the future potential resources in Alaska is vital for the U.S.'s future domestic energy supply and energy strategy planning.

Production in the last two years has begun to decline and shall continue to decline. The major decline in production is attributed to super-giant Prudhoe Bay oil field. It is projected that over the next decade the decline on the average will be about 10% per year. The impact of this magnitude of decline on the Nation's economy and energy security, however, can be minimized by developing known undeveloped and many marginal fields on the North Slope. These fields contain large reserves and far exceed those estimated and potential reserves in the Lower 48 states. In spite of known reserves, oil and gas exploration and development in Alaska are in decline. This is attributed to political and regulatory considerations rather than economics. The recovery from these fields, however, will require development of new and advanced technology.

### **B. EXPLORATION HISTORY**

Oil in Alaska was first discovered at Katalla, on the southeast coast of the Gulf of Alaska in 1902. The field was developed and a small refinery was built to provide fuel for a nearby copper mine. The field was abandoned in 1933 after the cumulative production reached 154,000 barrels. The primary reason for abandonment was a fire at the mine and its subsequent closure.

The modern oil era dawned in Alaska in August 1957 with the discovery of oil on the Kenai Peninsula in Swanson River Unit 1 well drilled by the Richfield Oil Corporation. This set the stage for a period of intense exploration throughout Alaska.

One area included in this exploration was the North Slope, an area which already had a history of minor oil and gas discoveries. The earliest North Slope geological account of potential oil-bearing formations, written in 1919 by Leffingwell of the U.S. Geological Survey, described the Canning River region. Then, in 1923, the 23-million acre Naval Petroleum Reserve No. 4 (NPR-4) was established north and west of the Colville River, and extended from the Beaufort Sea on the north to the foothills of the Brooks Range on the south. From 1944 to 1953, both the Navy and the USGS explored NPR-4, drilling a number of test wells and shallow core holes. Three oil accumulations and six gas accumulations were found, although none were commercial.

In 1958, with the Swanson River discovery, the Bureau of Land Management (BLM) opened up nearly 15 million acres of North Slope lands for leasing, exploration, drilling, and development under conditions similar to those established in the western Lower 48 states. Intensive exploration of the North Slope was undertaken by industry during the next ten years. However, no North Slope discoveries were made during this time. Discoveries were made in the Cook Inlet region, leading to the establishment of commercial oil and gas production in this region. Commercial recoverable reserves from the Cook Inlet area are estimated to be 1.173 BBO and 7.607 TCF of gas.

With the 1960 establishment of the Arctic National Wildlife Range (ANWR), about 9 million acres from the Canning River to the Canadian Border and from the Beaufort Sea to the Brooks Range became off limits to exploration and development. This restricted industry to the area between the Colville and Canning rivers, and to an area west and south of NPR-4. In addition, in 1964, the State of Alaska, under the Statehood Act, selected 1.6 million acres between the Colville and Canning rivers for sales which were subsequently held in 1965, 1966, and 1967.

Between 1958 and 1968, industry drilled ten dry holes on the North Slope. Discouraged by the dry holes, industry-wide exploration and drilling activity ceased by 1968, except for activity carried on by Arco Alaska Inc. and Humble (now Exxon USA). And it was the Arco-Humble Prudhoe Bay State No. 1, announced as a discovery in January 1968 and completed the following April, that proved to be the most important discovery in Alaska. Prudhoe Bay field, established from this discovery well and the Sag River State 1 confirmation well, has recoverable reserves of between 11.5 and 12.9 BBO and 28.5 TCF of gas. The field is the largest oil field discovered in North America.

The Prudhoe Bay discovery led industry to drill 33 exploratory wells in 1969. The September 1969 State competitive lease sale in the Prudhoe Bay area drew \$900 million in bonus bids. However, because of legal and environmental obstacles placed in the way of exploration, no more sales were held on the North Slope until 1979, when the State and Federal governments held a joint sale.

Despite these obstacles, industry did manage to drill over 100 North Slope wells between 1968 and 1979. This drilling activity resulted in 19 discoveries and 12 significant accumulations. In 1974, NPR-4 was renamed the National Petroleum Reserve-Alaska (NPRA), and the Federal government initiated a second major exploration effort there. Although 27 exploratory wells were drilled, only two minor gas fields were discovered. NPRA was then opened for industry leasing through BLM competitive sales, but interest was low, with only one well (a dry hole) being drilled there by industry.

After 1979, the Federal government held three offshore OCS lease sales and the State held 17 sales on both onshore uplands and offshore State waters. Since 1979, nine accumulations have been discovered. Two of these (Niakuk with reserves of 58 MMBO and Point McIntyre with reserves of 300 MMBO) are planned to be developed using the Prudhoe Bay infrastructure.

In 1980, the Arctic National Wildlife Range was enlarged from 9 million acres to 19 million acres and renamed the Arctic National Wildlife Refuge (ANWR). Congress restricted industry exploration in ANWR to surface geological and geophysical work, with no drilling permitted. During the summers of 1983 through 1985, 15 oil companies performed surface geological work in ANWR. A helicopter survey was completed in 1983. Over 1300 miles of seismic data were acquired during the winters of 1983/84 and 1984/85. In 1987, Secretary of the Interior Hodel recommended to Congress that oil and gas leasing be conducted in ANWR, but Congress has made no final decision on this recommendation. In 1986, an exploratory well was drilled adjacent to ANWR by Chevron Inc. and British Petroleum Alaska (BP), but all results remain confidential. Future ANWR and North Slope exploration and development will likely depend as much on political and regulatory considerations as on economic factors.

### **C. OIL AND GAS RESOURCES OF NORTH SLOPE ALASKA**

The North Slope, a narrow east-west oriented strip between Point Barrow and the Canadian Border extends northward of the northern foothills of the Brooks Range and the

shallow Beaufort Shelf. The onshore area consists of about 65,000 square miles, including 23-million acre National Petroleum Reserves in the West and the 19-million acre Arctic National Wildlife Refuge in the East (Figure I-1).

The region is composed of a broad continental platform, on which carbonate rocks were deposited during the Late Paleozoic Era with a northerly sediment source. During the Late Mesozoic Era the compression of the Colville Geosyncline and rise of the Brooks Range provided the clastic sediments for this shallow platform.

The North Slope consists of three major structural elements: the highly folded and thrustured Brooks Range, the Colville Trough, a foredeep basin lying north of and parallel to the range, and the east-west broad Barrow Arch along the coast. The 375-mile arch plunges to the east. The vast majority of North Slope oil and gas accumulations occur either along the southern flank of, or close to, the Barrow Arch (Figure I-2).

Oil and gas accumulations on the North Slope are so prolific that they are found virtually throughout the entire stratigraphic section (Figure I-3). With the exception of the carbonate reservoir deposited during Upper Paleozoic time, most reservoir rocks are clastic sandstones.

The first discovery of commercial accumulation in northern Alaska was established by the discovery of Prudhoe Bay field in 1968. Endicott field, discovered in 1978, and with a total recovery estimated at 393 MMBO, is the only offshore producing field in the Arctic Ocean. The Nation's second ranking producing field after Prudhoe Bay field is the North Slope's Kuparuk River field, discovered in 1969. It is only a few miles from Prudhoe Bay field. The smallest economic field on the North Slope is Milne Point field, with reserves estimated at 51 MMBO. To date, 32 oil and gas fields have been discovered and eight fields have been on production. The known oil and gas accumulations on the North Slope are shown in Figure I-4.

The production data and reserves of the producing fields are listed in Table I-1 and the estimated hydrocarbons in the undeveloped fields are listed in Table I-2.

It is anticipated that both Niakuk and Point McIntyre should begin production some time soon.

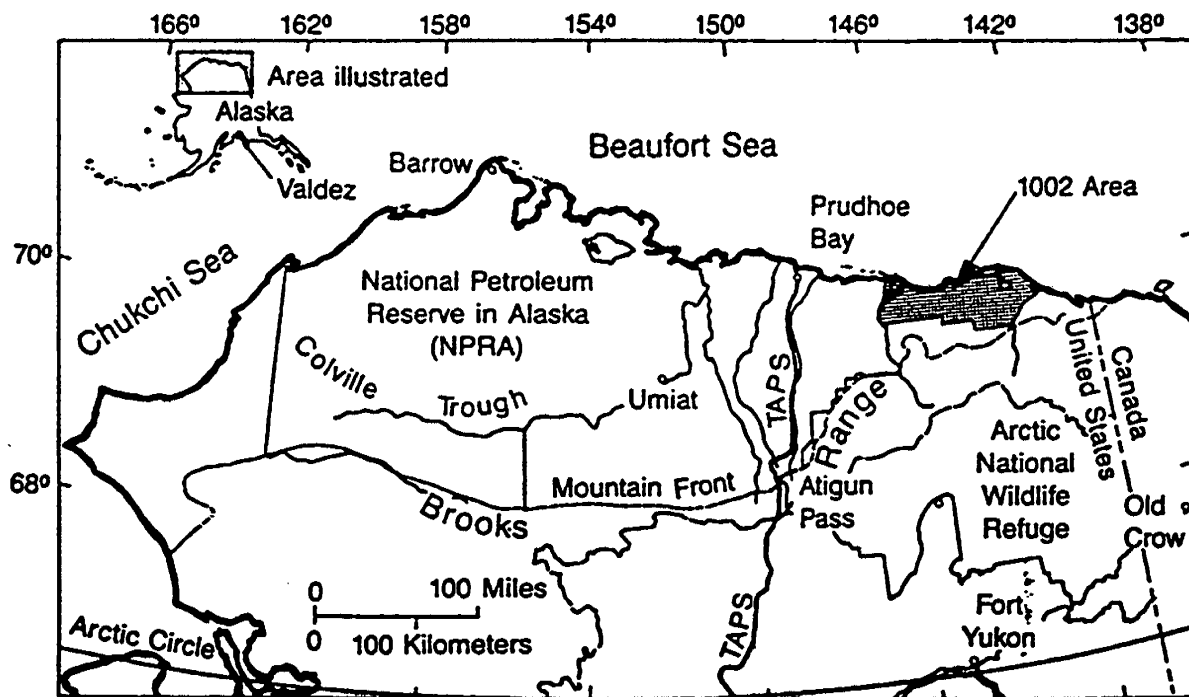


Figure I-1. Map of Northern Alaska Showing Major Geographic Features and Locations of National Petroleum Reserve Alaska, Arctic National Wildlife Refuge, and the Trans-Alaskan Pipeline System (Thomas et al., 1991).

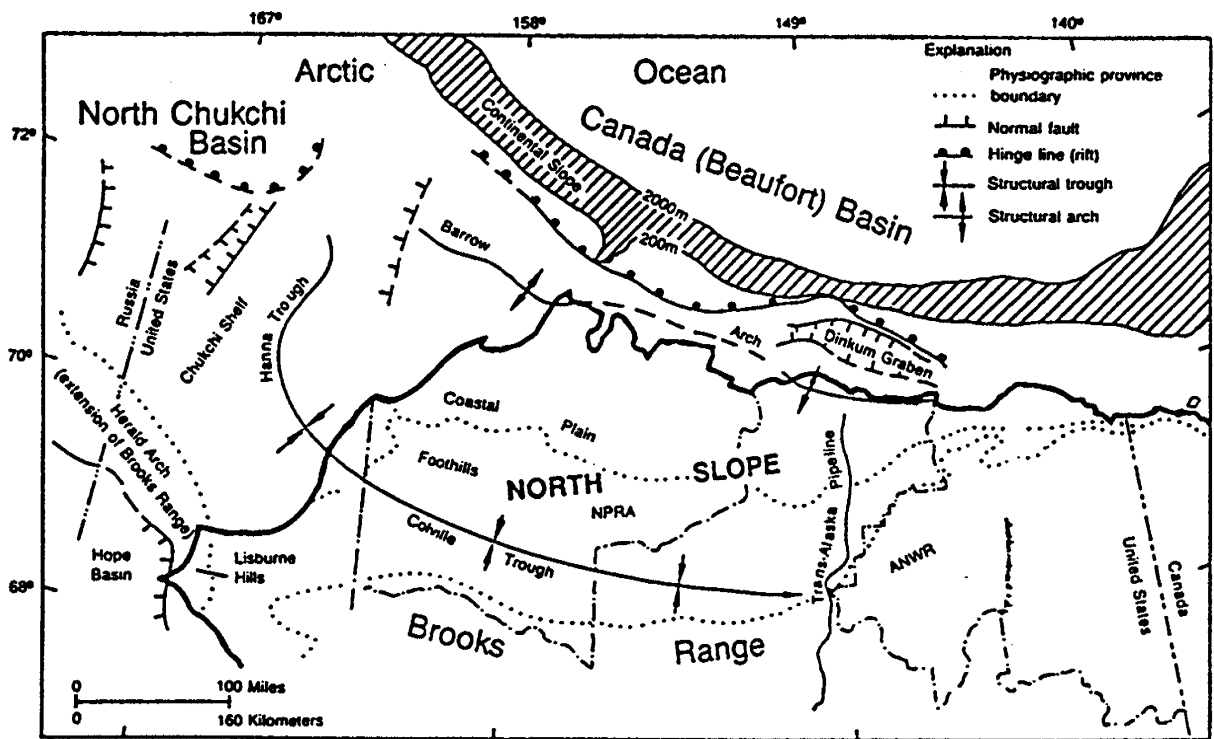
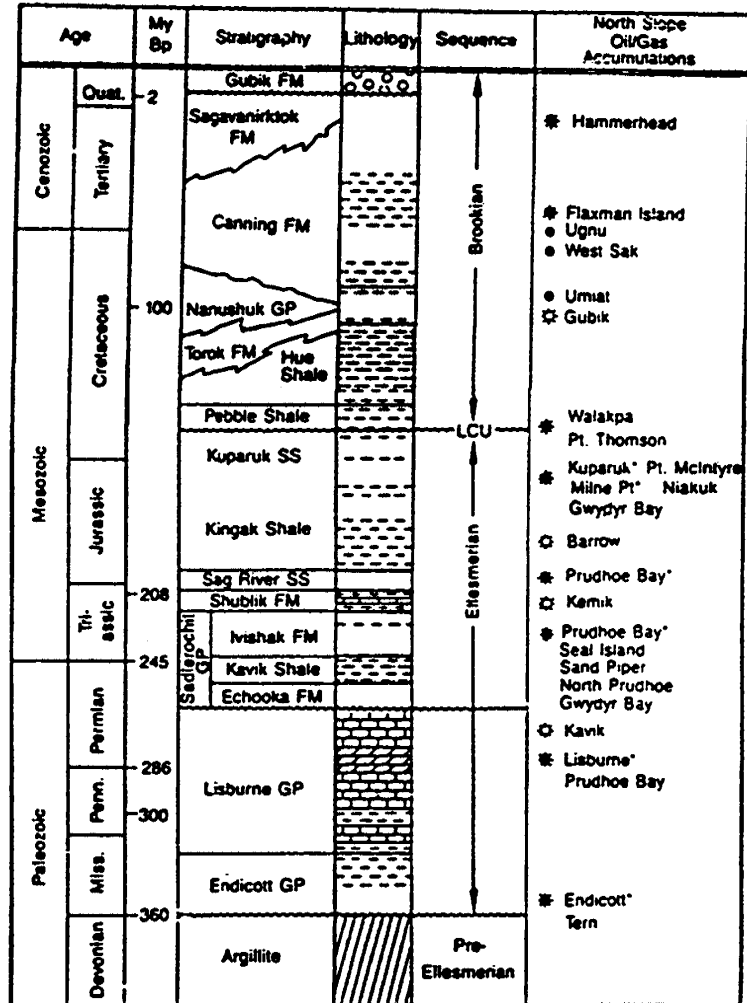


Figure I-2. Generalized Structural Features and Geologic Framework of Onshore and Offshore Northern Alaska (Thomas et al., 1991).

**NORTH SLOPE  
GENERALIZED STRATIGRAPHIC  
COLUMN**



Explanation

6-4770

- LCU: Lower Cretaceous Unc.
- |                |               |                            |
|----------------|---------------|----------------------------|
| □ Sandstone    | ▨ Siltstone   | ● Oil Accumulation         |
| ⊙ Conglomerate | ▩ Dolomite    | ⊙ Gas Accumulation         |
| ▨ Shale        | ▨ Metamorphic | ⊙ Oil and Gas Accumulation |
| ▨ Limestone    |               | * Currently Producing      |

Figure I-3. Generalized Columnar Section for the North Slope Showing Stratigraphic Relations, Age, Lithology, and Positions of Known Oil and Gas Accumulations (Thomas et al., 1991).

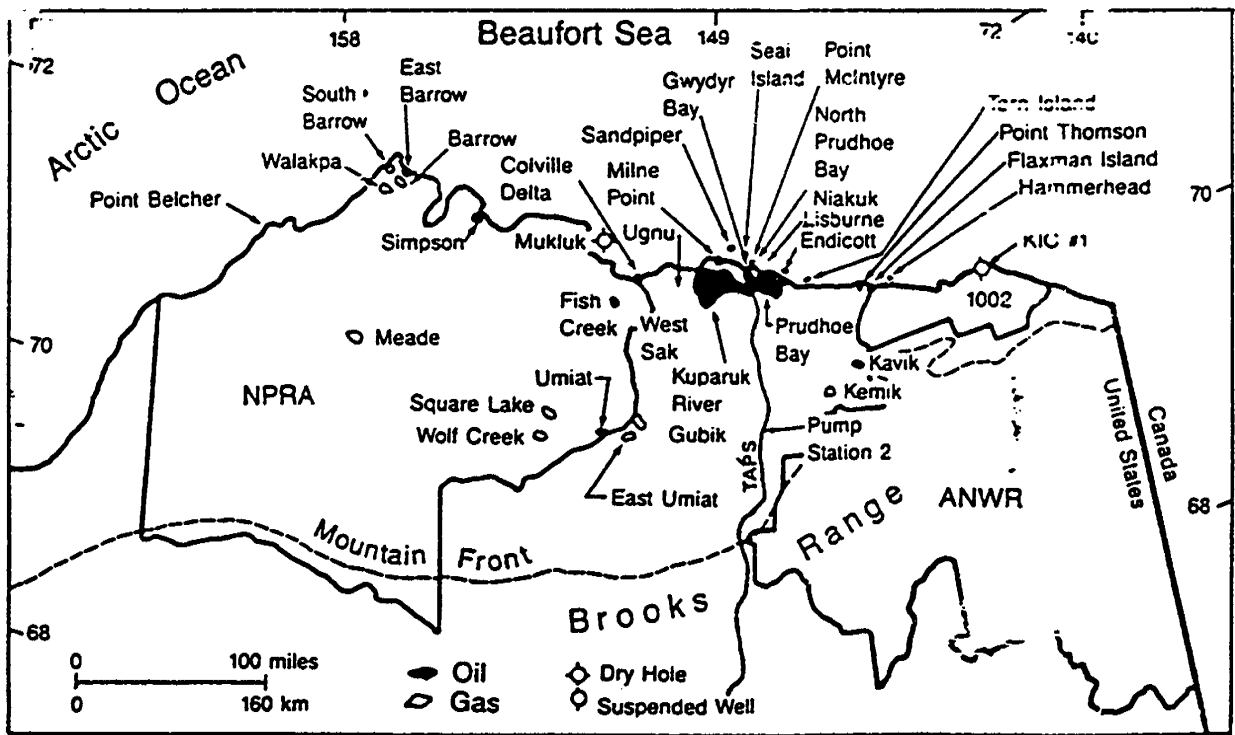


Figure I-4. Known Oil and Gas Accumulations, Selected Dry Holes and Suspended Wells, and NPRA-ANWR Boundaries, North Slope, Alaska (Thomas et al., 1991).

Table I-1. North Slope Oil and Gas Producing Fields<sup>a</sup>  
(as of January 1, 1990) (Thomas et al., 1991).

Field Name	Discovery Date	Estimated Original Recoverable Reserves	Production Start-up Date	Cumulative Production	Remaining <sup>b</sup> Reserves/Resource	Estimated Current Total Recoverable Reserves <sup>b</sup>
Prudhoe Bay	4/68	28,500 BCF 9,590 MMBO	10/69 (Tests) 7/77 (Pipeline)	1,211 BCF <sup>c</sup> 6,605 MMBO <sup>d</sup>	27,290 BCF 6,266 MMBO <sup>d</sup>	28,500 BCF 12,900 MMBO
Kuparuk River	4/69	640 BCF 1,600 MMBO	12/81 -----	697 BCF <sup>e</sup> 615 MMBO	520 BCF 1,509 MMBO	> 640 BCF 2,124 MMBO
Prudhoe Bay (Lisburne Pool)	4/68	635 BCF 400 MMBO	11/83 (Tests) 3/85	275 BCF <sup>e</sup> 49 MMBO	888 BCF 157 MMBO	> 888 BCF 206 MMBO
Milne Point	10/69	0 100 MMBO	5/85-1/87 4/90	2.9 BCF <sup>e</sup> 9 MMBO	0 51 MMBO	0 BCF 60 MMBO
Endicott	3/78	731 BCF 375 MMBO	1987 -----	85 BCF <sup>e</sup> 82 MMBO	782 BCF 311 MMBO	782 BCF 393 MMBO
S. Barrow	4/49	25.2 BCF	8/49	20.2 BCF	5 BCF	25.2 BCF
E. Barrow	5/74	12.4 BCF	12/83	5.4 BCF	7 BCF	12.4 BCF
<b>TOTALS</b>		<b>30,544 BCF 12,065 MMBO</b>		<b>2,296 BCF<sup>e</sup> 7,360 MMBO<sup>d</sup></b>	<b>29,492 BCF 8,294 MMBO<sup>d</sup></b>	<b>&gt; 30,847 BCF 15,683 MMBO</b>

<sup>a</sup>After Alaska Department of Natural Resources.

<sup>b</sup>A resource is changed to reserves when a field is developed for production and a transportation system is under development or in-place to move the product to market. The only gas volumes currently considered reserves are the volumes used as Fuel Gas for North Slope operations. Current gas reserves are not given in this table.

<sup>c</sup>Production less reinjection.

<sup>d</sup>Excludes NGL.

<sup>e</sup>Portions of gas reinjected.

**Table I-2. North Slope Undeveloped Oil and Gas Accumulations  
(as of January 1, 1990) (Thomas et al., 1991).**

<b>DISCOVERED RESOURCES</b>		
<b>LOCATION</b>	<b>YEAR</b>	<b>AMOUNT</b>
Umiat	1946	70 MMBO
Fish Creek	1949	Oil
Simpson	1950	12 MMBO
Meade	1950	20 BCF
Wolf Creek	1951	Gas
Gubik	1951	600 BCF
Square Lake	1952	58 BCF
E. Umiat	1963	4 BCF
Kavik	1969	Gas
West Sak	1969	0-1200 MMBO <sup>a</sup>
Ugnu	1969	Heavy Oil
Gwydyr Bay	1969	30-60 MMBO
No. Prudhoe	1970	75 (?) MMBO
Kemik	1972	Gas
Flaxman Island	1975	Oil
Point Thomson	1977	300 MMBO <sup>b</sup> , 5000 BCF
Walakpa	1980	Gas
Niakuk	1981	58 MMBO, 30 BCF
Tern Island	1982	Oil
Seal Island	1984	150 MMBO
Hammerhead	1985	Oil
Colville Delta	1985	Oil
Sandpiper	1986	Oil
Barrow	1988	Gas
Point McIntyre	1988	300 MMBO

<sup>a</sup>Heavy Oil

<sup>b</sup>Condensate

## CHAPTER II: WEST SAK RESERVOIR

---

### A. INTRODUCTION

West Sak reservoir, with 20 billion barrels of oil (BBO) and Ugnu reservoir, containing 15 BBO, are among the largest oil fields in North America. West Sak's 20 BBO is nearly as large as Prudhoe Bay's 23 billion barrels of original oil in place (OOIP). Both West Sak and Ugnu are located west of, and adjacent to Prudhoe Bay, with Ugnu lying just north of West Sak (Figure II-1). The West Sak formation predominately overlies the Kuparuk River formation in the Kuparuk River Unit. The sheer size of these fields makes them prime candidates for commercial development. With production declines now occurring at Prudhoe Bay, and oil prices on the rise, greater consideration will be given to developing these two giant fields.

Because oil gravities are low within both West Sak and Ugnu reservoirs (12 to 22 API in West Sak and 3 to 12 API within Ugnu), production at recently lower oil prices was determined to be only marginally economic by Arco Alaska Inc., the fields' operator. This determination was based on the response of West Sak to waterflooding. Subsequently, Arco Alaska Inc. has intensified its effort to arrive at an alternative means of development, including immiscible or miscible gas injection. The University of Alaska's Petroleum Development Laboratory is also working on alternative development or enhanced oil recovery (EOR) methods.

Assessing the potential of any EOR method for low gravity reservoirs with complex rock and fluid properties must include comprehensive geological and petrophysical descriptions of the reservoirs. Geological well-to-well correlation of reservoir zones and adjacent facies is the first step in the analysis. In addition, determination of numerical values of porosity and permeability is required in order to quantify reservoir characteristics used in EOR simulation programs.

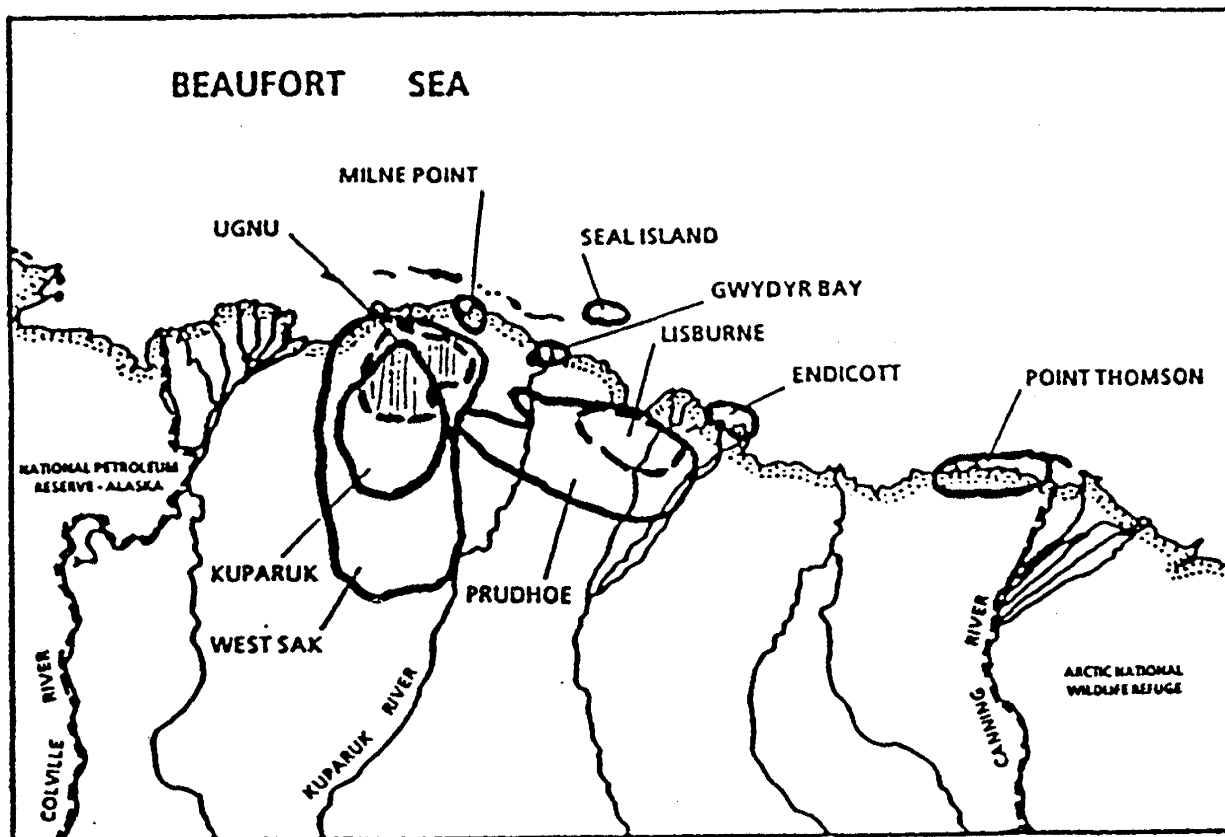


Figure II-1. Location Map of Major Fields in the Alaskan North Slope.

## B. GEOLOGICAL OVERVIEW

Both West Sak and overlying Ugnu sands are Late Cretaceous to Early Tertiary shallow sands (Figure II-2) that were deposited in a shallow marine and deltaic complex. Although several other stratigraphic horizons locally contain heavy oil, West Sak and Ugnu are the most laterally extensive oil-bearing sands. As such, they have the greatest commercial potential (Werner, 1985). The oil-bearing portions of these zones are primarily within the Kuparuk River Unit and Milne Point Unit, where they range in depth between 2,000 and 4,500 ft (1,141 m to 1,231 m) subsea.

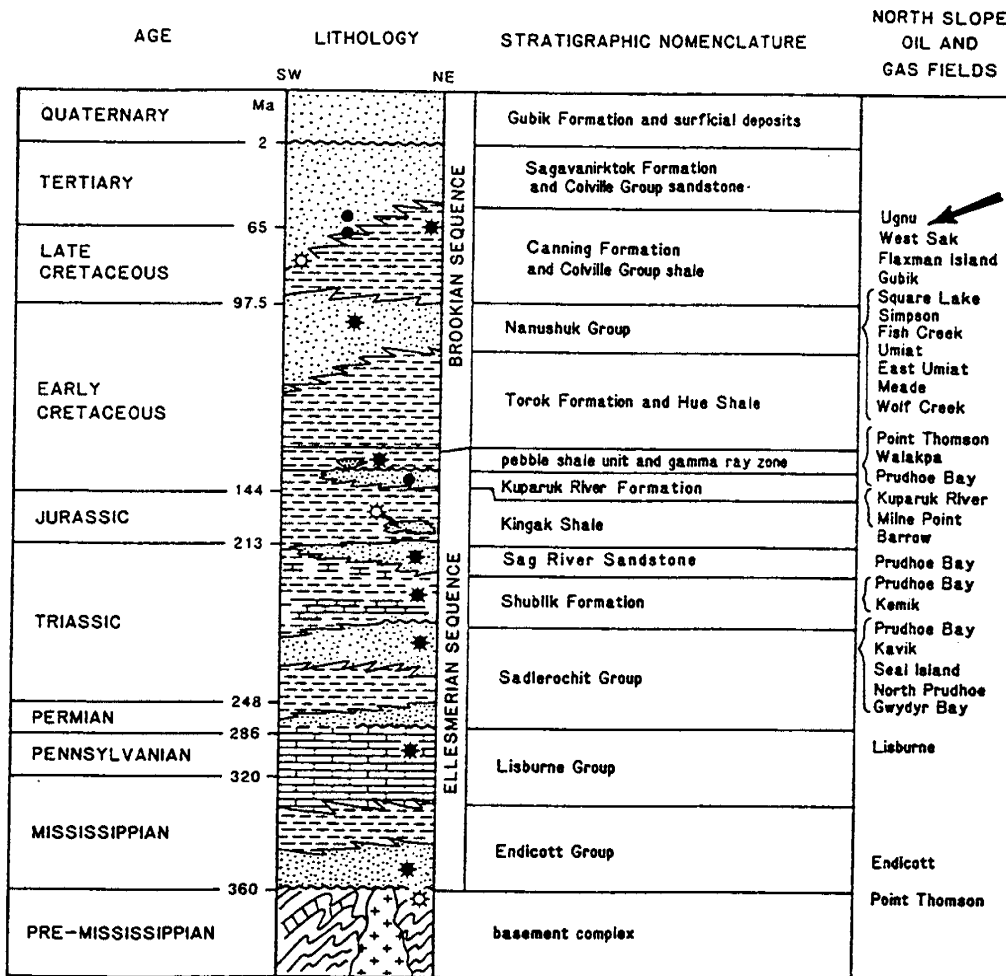


Figure II-2. Generalized North Slope Stratigraphic Column (adapted from Bird, 1987).

West Sak and Ugnu sands were deposited during the Early Cretaceous of the Brookian depositional sequence. Brookian sediments, derived from the ancestral Brooks Range to the south, prograded north and northeast during Late Cretaceous time and buried the remnants of the west-to-east trending Barrow Arch. The Barrow Arch, and the subparallel Colville Trough to the south (Figure II-3), comprise the principal subsurface geological structures along the North Slope of Alaska. The Barrow Arch had, by this time, probably been deformed by large scale rifting which was also responsible for the opening of the Canadian Basin. The geologic setting involving major North Slope features is illustrated in Figure II-4.

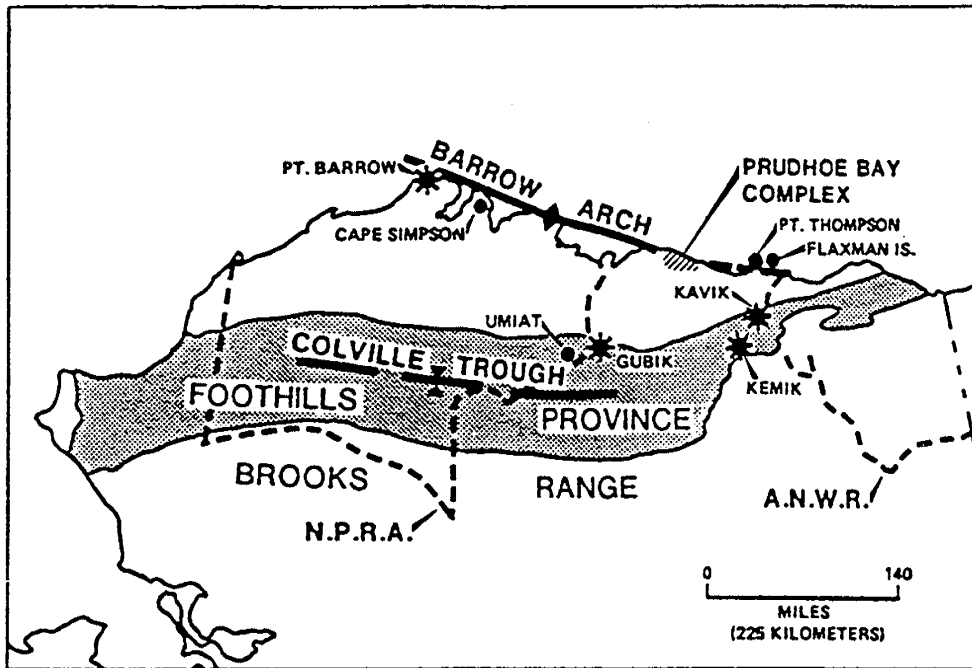


Figure II-3. North Slope Index Map Showing Major Structural Elements (Jamison et al., 1980).

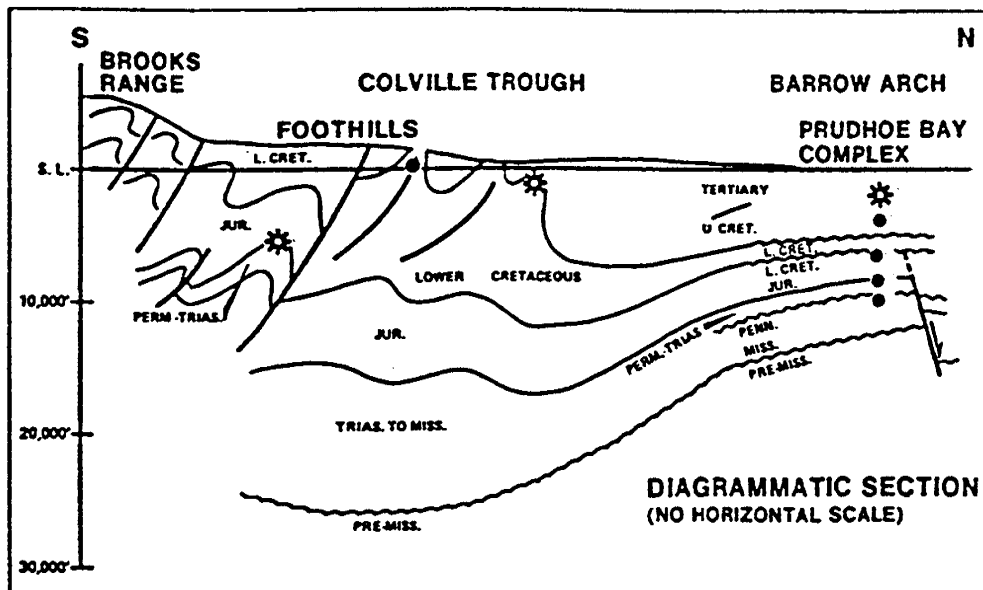


Figure II-4. North-South Cross Section from Brooks Range to the Prudhoe Bay Complex (Jamison et al., 1980).

West Sak sands average about 300 ft (91 m) thick in the area of greatest productive potential (Kuparuk River and Milne Point Units). These sands have been divided into an upper and lower member. Werner (1985) describes the lower member as consisting of thin bedded sands characterized by ripple bedding and hummocky cross stratification with interbedded bioturbated siltstone and mudstone. Individual sand beds vary in thickness from 0.2 to 5 ft (6 cm to 1.5 m). Some of these sands are laterally continuous for three to five miles. Bioturbation is common. The Upper West Sak member is further subdivided into two distinct and laterally continuous sand units by Werner (1985). Each unit is 25 to 40 ft (8 to 12 m) thick. Main sedimentary features within these units include massive beds with planar bedding, and low angle cross-bedding. Bioturbation is common. This member represents shallow marine or delta front deposition whereas the lower member represents an inner shelf depositional environment.

Analysis of logs and core descriptions by Zhang (1990) indicates that West Sak is comprised of six individual sands. Two of these sands make up the upper member and the remaining four sands comprise the lower member. These sands are labeled from top to bottom as follows:

1. Upper West Sak Sand Member
  - Sand 1
  - Sand 2
2. Lower West Sak Sand Member
  - Sand 1
  - Sand 2
  - Sand 3
  - Sand 4

### **C. RESERVOIR DESCRIPTION PROCEDURE**

A detailed reservoir description of West Sak was completed, in part, by means of computerized well log analysis. Core descriptions were incorporated into the analysis in order to better correlate stratigraphic markers. The computer programs utilized in the analy-

sis are titled *LOGCALC* and *LOGCALC II*, and were written by Scientific Software-Intercomp, Inc., Denver, Colorado. These programs provide an efficient and rapid method of determining petrophysical parameters at intervals as thin as 0.5 ft. *LOGCALC* also provides log plotting capabilities for both Measured While Drilling (MWD) and true vertical depth (TVD) logs. A graphics package written by the Kansas State Geological Survey titled *SURF II* was used in converting log-derived data into two-dimensional and three-dimensional plots.

#### **D. LOG-DERIVED PETROPHYSICAL PARAMETERS**

Petrophysical parameters corresponding to the six West Sak sand units were calculated using data from thirteen wells. These values are listed in Tables II-1 through II-6. The Upper West Sak sand porosities range from a low of 15% in the West Sak No. 17 to a high of 40% in the Kugaruk No 3B-14. Water saturations range from a low of 9% in the West Sak No. 2 to a high of 46% in the East Ugnu No. 1. Net pay thickness varies from just one foot in the West Sak No. 5 to 37 ft in the West Sak No. 2.

The porosity values of lower sands 1 and 2 are similar to those of the upper two sands, but water saturations are noticeably higher. Even higher water saturations (up to 80%) occur in lower sand 3. Also, net pay is thinner in the lower sands, being in many cases less than 10 feet. Lower sand 4 appears to be discontinuous throughout this area, and it is absent in four of the thirteen wells analyzed.

These petrophysical data indicate that upper sands 1 and 2 contain West Sak's best reservoir qualities. The difference in petrophysical values between the upper and lower sands reflects their differing depositional histories. The shallow marine and delta front environments corresponding to the upper sands should result in cleaner and generally thicker sands, as compared to the shelf depositional environment corresponding to the lower sands.

**Table II-1: Petrophysical Parameters of West Sak Upper Sands.**

<b>SAND 1</b>				
<b>Well Name</b>	<b>Interval (ft)</b>	<b>Average <math>\phi</math> (%)</b>	<b>Average <math>S_w</math> (%)</b>	<b>Net Pay (ft)</b>
West Sak No. 1	3746-3784	33	26	32
West Sak No. 2	3304-3334	29	9	30
West Sak No. 3	2628-2672	30	28	18
West Sak No. 5	3332-3374	27	18	10
West Sak No. 9	2678-2716	37	43	33
West Sak No. B-10	2695-2747	35	38	7
West Sak No. 11	2324-2364	28	44	17
West Sak No. 17	3516-3558	18	28	4
West Sak No. 18	No log data available			
East Ugnu No. 1	3386-3424	34	43	8
Kuparuk No. 1G-7	3408-3455	28	37	23
Kuparuk No. 3B-14	2538-2559	40	37	21
Milne Pt. No. N-1B	3555-3570	21	32	10
<b>SAND 2</b>				
<b>Well Name</b>	<b>Interval (ft)</b>	<b>Average <math>\phi</math> (%)</b>	<b>Average <math>S_w</math> (%)</b>	<b>Net Pay (ft)</b>
West Sak No. 1	3810-3844	35	33	34
West Sak No. 2	3364-3404	29	14	37
West Sak No. 3	2706-2734	25	37	10
West Sak No. 5	3410-3428	25	18	1
West Sak No. 9	2770-2786	34	40	9
West Sak No. B-10	2804-2860	38	40	12
West Sak No. 11	2402-2432	31	45	9
West Sak No. 17	3597-3620	15	34	8
West Sak No. 18	No log data available			
East Ugnu No. 1	3459-3490	32	46	14
Kuparuk No. 1G-7	3477-3512	22	31	27
Kuparuk No. 3B-14	2575-2613	39	43	36
Milne Pt. No. N-1B	3582-3617	33	19	20

**Table II-2: Petrophysical Parameters of West Sak Lower Sand 1.**

Well Name	Interval (ft)	Average $\phi$ (%)	Average $S_w$ (%)	Net Pay (ft)
West Sak No. 1	3860-3874	36	39	11
West Sak No. 2	3428-3434	28	17	5
West Sak No. 3	2753-2772	0	50	0
West Sak No. 5	No log data available			
West Sak No. 9	2852-2860	34	41	6
West Sak No. B-10	2934-2945	34	45	3
West Sak No. 11	2566-2575	24	59	0
West Sak No. 17	3714-3722	17	80	0
West Sak No. 18	2526-2536	36	35	4
East Ugnu No. 1	3511-3530	34	42	5
Kuparuk No. 1G-7	3533-3540	21	46	2
Kuparuk No. 3B-14	2698-2740	40	41	37
Milne Pt. No. N-1B	3677-3684	17	37	4

**Table II-3: Petrophysical Parameters of West Sak Lower Sand 2.**

Well Name	Interval (ft)	Average $\phi$ (%)	Average $S_w$ (%)	Net Pay (ft)
West Sak No. 1	3930-3940	37	33	9
West Sak No. 2	3456-3460	32	18	4
West Sak No. 3	2796-2806	32	38	4
West Sak No. 5	No log data available			
West Sak No. 9	2892-2904	35	48	2
West Sak No. B-10	3048-3076	38	41	20
West Sak No. 11	2630-2638	21	68	0
West Sak No. 17	3770-3790	17	80	0
West Sak No. 18	2612-2618	36	42	3
East Ugnu No. 1	3622-3654	32	48	2
Kuparuk No. 1G-7	3588-3605	27	38	5
Kuparuk No. 3B-14	2774-2807	40	43	29
Milne Pt. No. N-1B	3719-3750	17	26	12

**Table II-4: Petrophysical Parameters of West Sak Lower Sand 3.**

Well Name	Interval (ft)	Average $\phi$ (%)	Average $S_w$ (%)	Net Pay (ft)
West Sak No. 1	3972-3984	39	42	6
West Sak No. 2	3472-3476	29	20	4
West Sak No. 3	2815-2824	30	46	1
West Sak No. 5	No log data available			
West Sak No. 9	2918-2930	31	45	1
West Sak No. B-10	3112-3132	38	46	11
West Sak No. 11	2688-2694	28	48	2
West Sak No. 17	3836-3844	18	80	0
West Sak No. 18	2692-2720	37	39	6
East Ugnu No. 1	-	-	-	-
Kuparuk No. 1G-7	3637-3658	25	36	8
Kuparuk No. 3B-14	2898-2907	27	50	2
Milne Pt. No. N-1B	3786-3806	21	26	11

**Table II-5: Petrophysical Parameters of West Sak Lower Sand 4.**

Well Name	Interval (ft)	Average $\phi$ (%)	Average $S_w$ (%)	Net Pay (ft)
West Sak No. 1	4032-4044	28	46	4
West Sak No. 2	3524-3530	30	15	4
West Sak No. 3	2872-2882	31	41	8
West Sak No. 5	No log data available			
West Sak No. 9	-	-	-	-
West Sak No. B-10	3167-3174	45	44	4
West Sak No. 11	2726-2730	19	67	0
West Sak No. 17	3969-3974	13	91	0
West Sak No. 18	-	-	-	-
East Ugnu No. 1	-	-	-	-
Kuparuk No. 1G-7	-	-	-	-
Kuparuk No. 3B-14*	2941-2969	27	43	6
Milne Pt. No. N-1B	3888-3905	10	71	0

\* Only this well has sand #5 in the interval 3007-3026 ft with net pay of 6 ft, average porosity of 25% and average water saturation of 35.9%.

**Table II-6: Log-Derived Data for Selected Wells in the West Sak Sands.**

Well Name	Interval* (ft)	Weighted Mean Effective Porosity (%) $\phi$	Weighted Mean Water Saturation (%) $S_w$	Net Pay Thickness (ft) $h$	Hydrocarbon Pore Volume ( $10^3$ bbl/acre-ft)
West Sak No. 1	3746-4044	35	33	116	173.8
West Sak No. 2	3304-3530	29	19	84	151.4
West Sak No. 3	2628-2882	30	34	41	63.2
West Sak No. 5	3332-3428	27	18	12	17.9
West Sak No. 9	2678-2930	36	42	50	79.5
West Sak No. B-10	2695-3174	38	42	55	93.2
West Sak No. 11	2324-2694	29	44	27	33.4
West Sak No. 17	3516-3620	16	31	12	10.1
West Sak No. 18	2526-2720	36	38	13	22.6
East Ugnu No. 1	3386-3654	33	44	27	38.1
Kuparuk No. 1G-7	3408-3638	25	35	64	80.5
Kuparuk No. 3B-14	2538-3025	38	41	136	238.4
Milne Pt. No. N-1B	3555-3806	24	24	56	79.4

\* Represents interval that is potentially hydrocarbon bearing. Properties of individual West Sak sand members are listed in Tables II-1 through II-5.

## E. RESERVOIR DESCRIPTION

Reservoir characteristics of West Sak observed are presented in three parts: sand thickness variation, spatial distribution of petrophysical properties, and sand quality evaluation. Contour maps, cross sections, and three-dimensional plots are used to describe various units.

Figures II-5 and II-6 present NW-SE and SW-NE cross sections of the West Sak interval. Locations of wells used for these sections are shown in Figure II-7. This figure also depicts the top of the West Sak upper sand 1, with depths representing a northeast monoclinial dip. Northeast dip may have resulted from regional tilting in response to sedimentary loading as the Brookian deltaic depocenter shifted northeast (Werner, 1985). Although each of the sand units generally exhibits the same strike, the magnitude of the dip varies. This dip variation may be due, in part, both to shift in depocenter and to subsequent post-depositional faulting and burial.

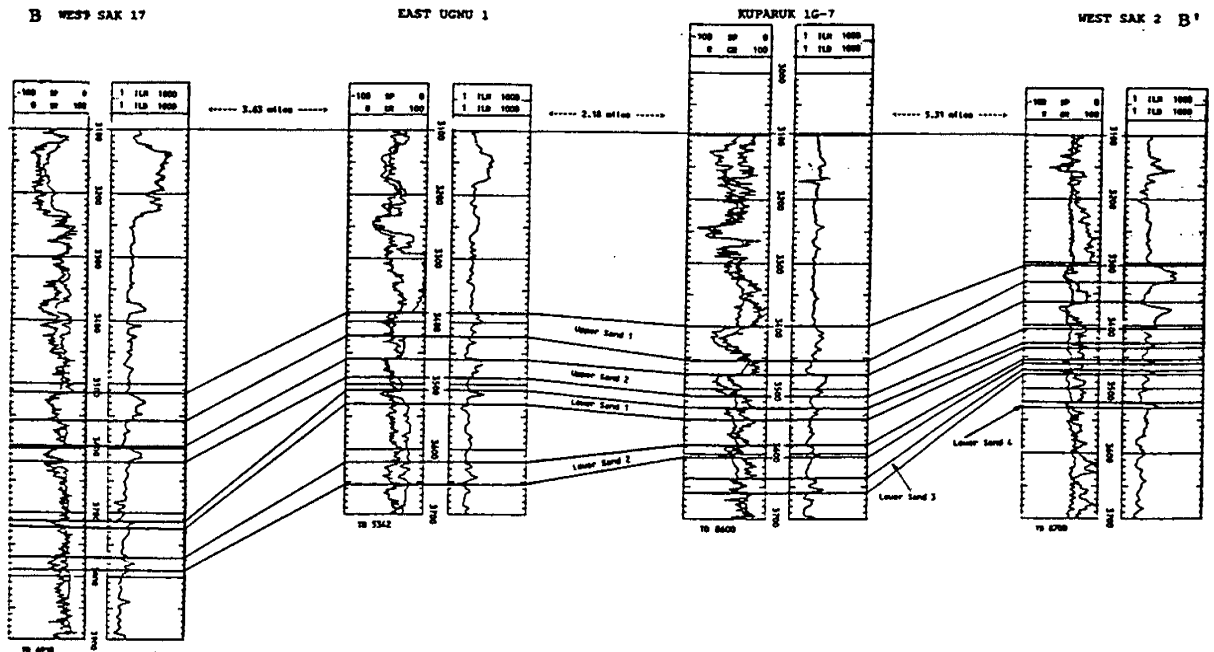


Figure II-5. West Sak Sands Distribution Along the SE-NW Stratigraphic Cross Section BB'.

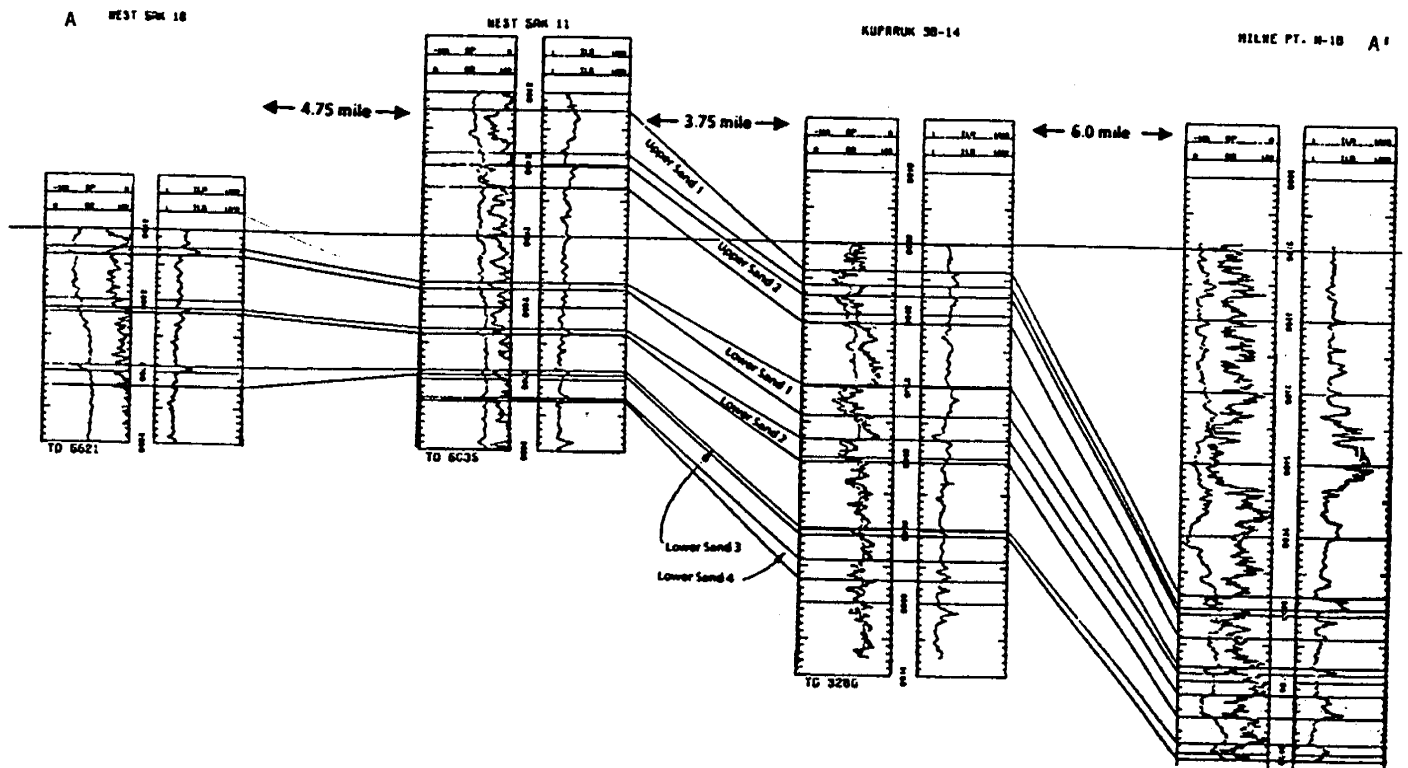


Figure II-6. West Sak Sands Distribution Along the SW-NE Stratigraphic Cross Section AA'.

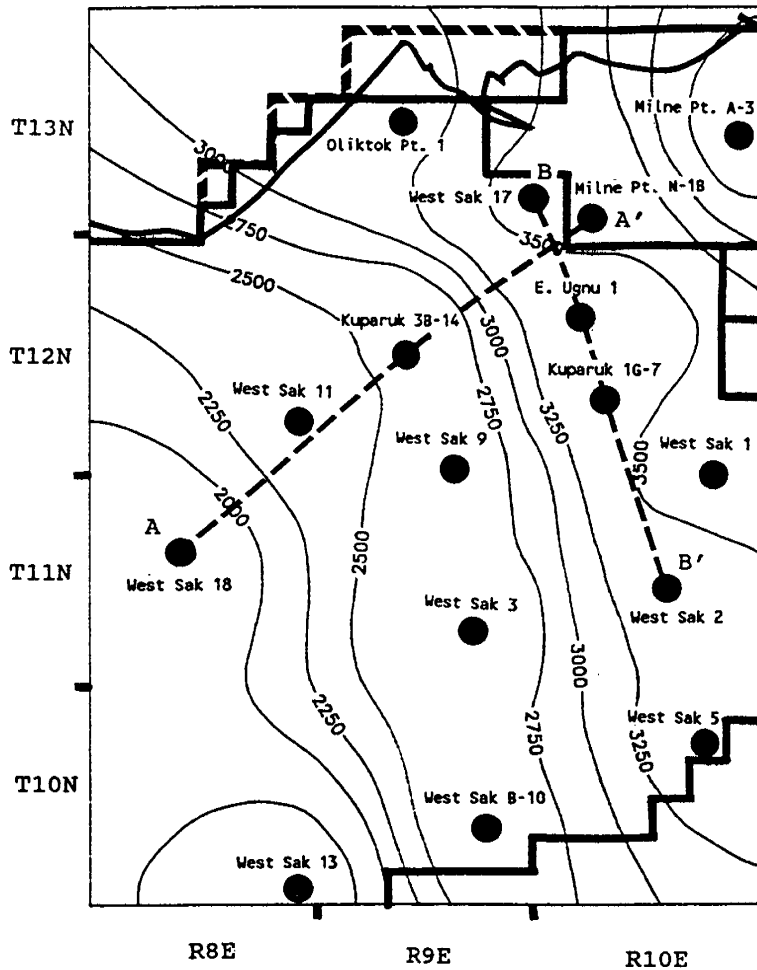


Figure II-7. Contour Map Showing Depths to the Top of West Sak Upper Sand 1 (AA': SW-NE Cross Section, BB' NW-SE Cross Section).

The origin of the shallow faults in the West Sak/Ugnu sands is not known. The fault trends are north-south, and throws are down to the east. This pattern of faulting may be due to sedimentary loading as the Brookian deltaic center shifted northeast of the present day shoreline during burial and compaction of West Sak/Ugnu sediments (Carmen and Hardwick, 1983). Although dewatering and compaction of shales may have induced faulting, Werner (1985) states that there is no evidence of major growth faults in the shallow zones in the Kuparuk Unit. Growth faults are common in deltaic deposits.

## E1. Sand Thickness Variation

The spatial thickness variation of each West Sak sand is shown as isopach maps in Figures II-8 through II-12. Figure II-8 shows upper sand 1 is thicker in the area around the Kuparuk 1G-7 and West Sak 3 than in the northern border area of the Kuparuk River Unit. On the other hand, upper sand 2 is thicker in the Kuparuk 3B-14, as compared to upper sand 1. If thicknesses of sands can be attributed to depocenters, then Figures II-8 and II-9 may indicate that the depocenters retreated slightly to the south during the deposition of upper sand 2 and upper sand 1. The lower sand units generally show limited lateral continuity, while other sands are absent in some wells. Thickness variations associated with these sands are most extreme within lower sand 1. The remaining lower sands exhibit minor variations in spatial thicknesses.

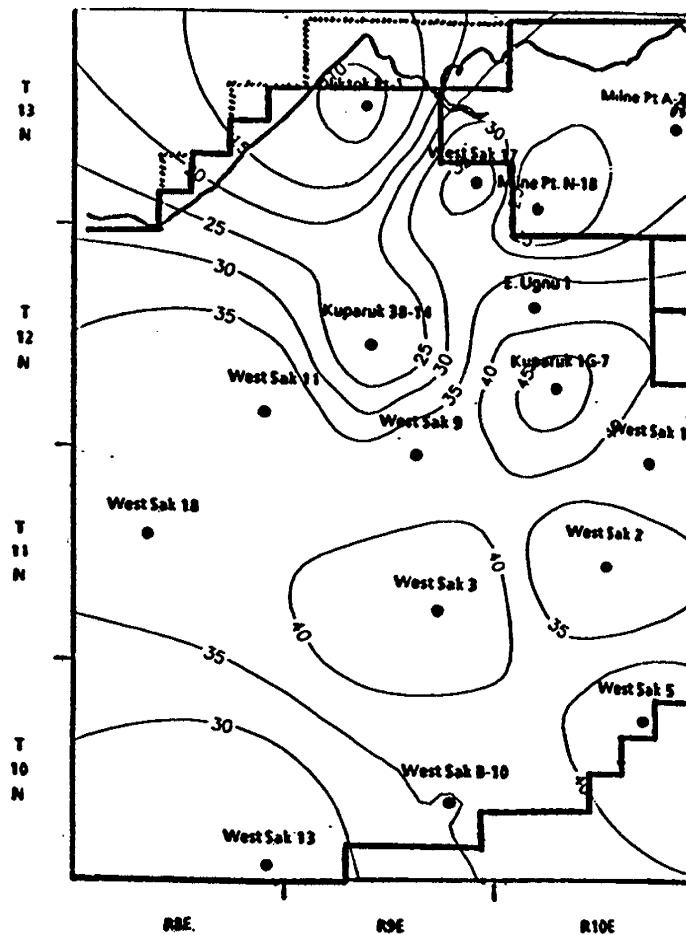


Figure II-8. Isopach Map of West Sak Upper Sand 1.

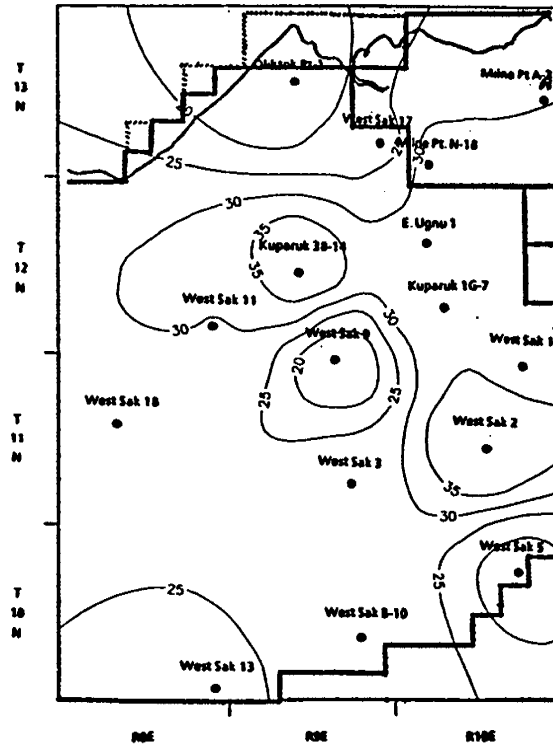


Figure II-9. Isopach Map of West Sak Upper Sand 2.

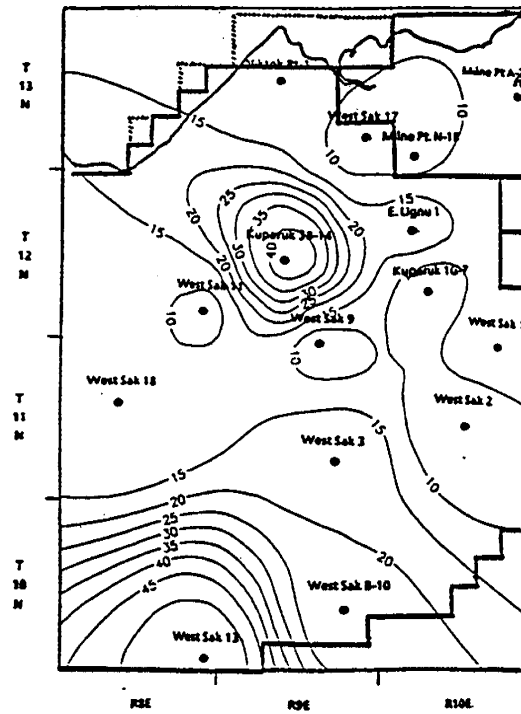


Figure II-10. Isopach Map of West Sak Lower Sand 1.

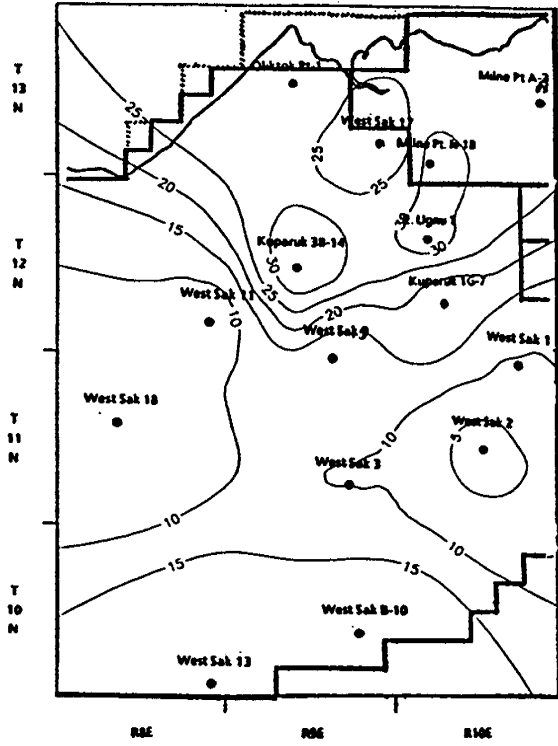


Figure II-11. Isopach Map of West Sak Lower Sand 2.

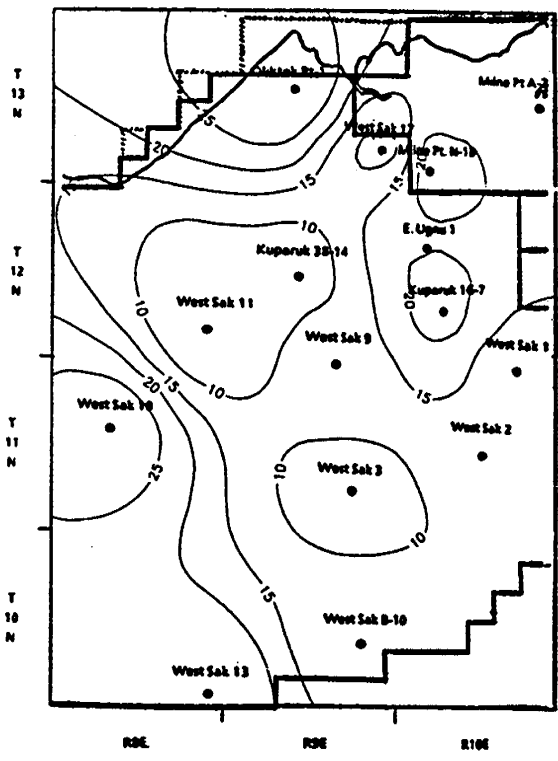


Figure II-12. Isopach Map of West Sak Lower Sand 3.

## E2. Spatial Distribution of Petrophysical Properties

Distributions of petrophysical properties (porosities and water saturations) of West Sak sands are shown in Figures II-13 through II-16. These maps and plots indicate very high porosity in the region near the Kuparuk 3B-14 and West Sak B-10. Porosity values in the northeast region are lowest. Water saturation contour maps show several local highs, particularly in the middle and northeast sections.

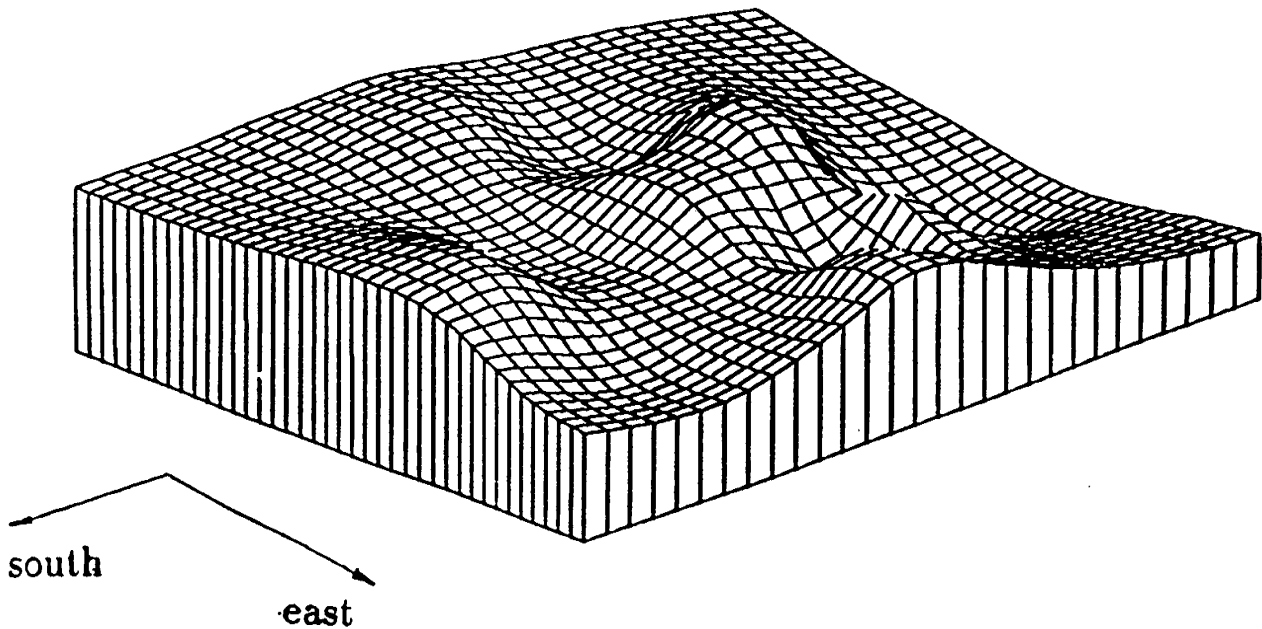


Figure II-13. 3-D Plot Showing the Distribution of Porosity in West Sak Sands.

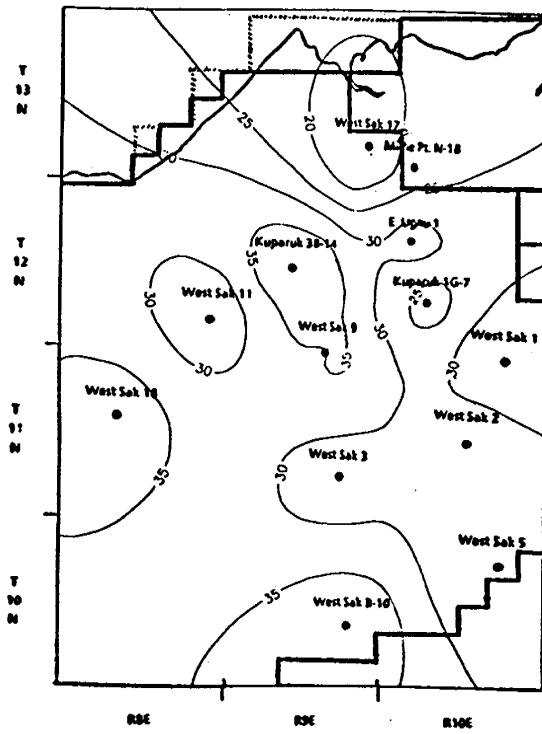


Figure II-14. Porosity Map of West Sak Sands.

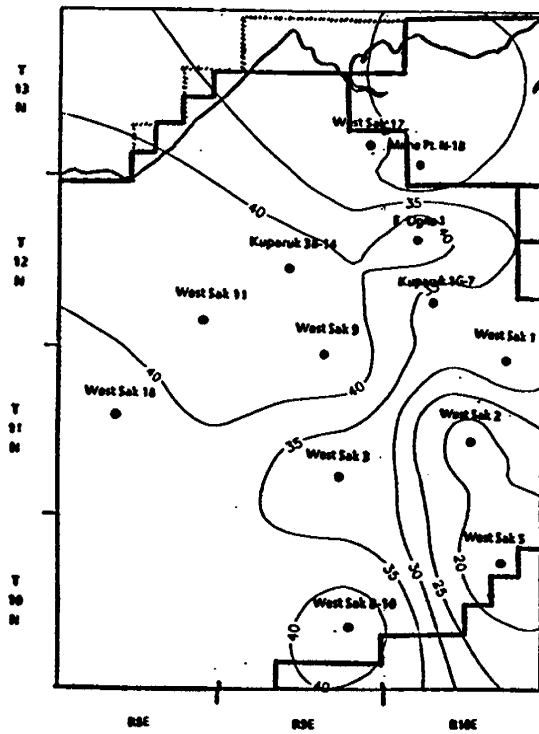


Figure II-15. Water Saturation Map of West Sak Sands.

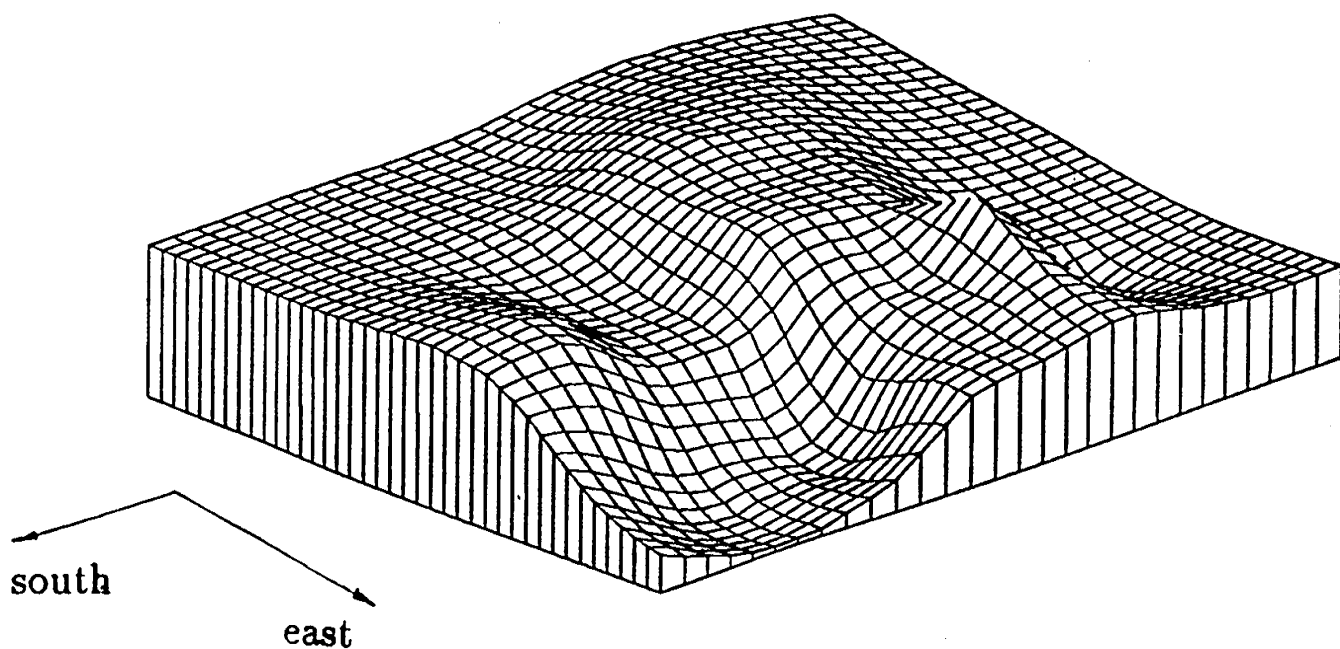


Figure II-16. 3-D Plot Showing the Water Saturation Distribution in West Sak Sands.

Because the two upper sands show the best lateral continuity and greater net pay zone thicknesses, individual plots of porosity and water saturation corresponding to these sands are also presented (Figures II-17 through II-19). These plots show that the upper sands exhibit generally similar porosity and water saturation trends. The data represented by these plots are being directly applied to reservoir simulation studies.

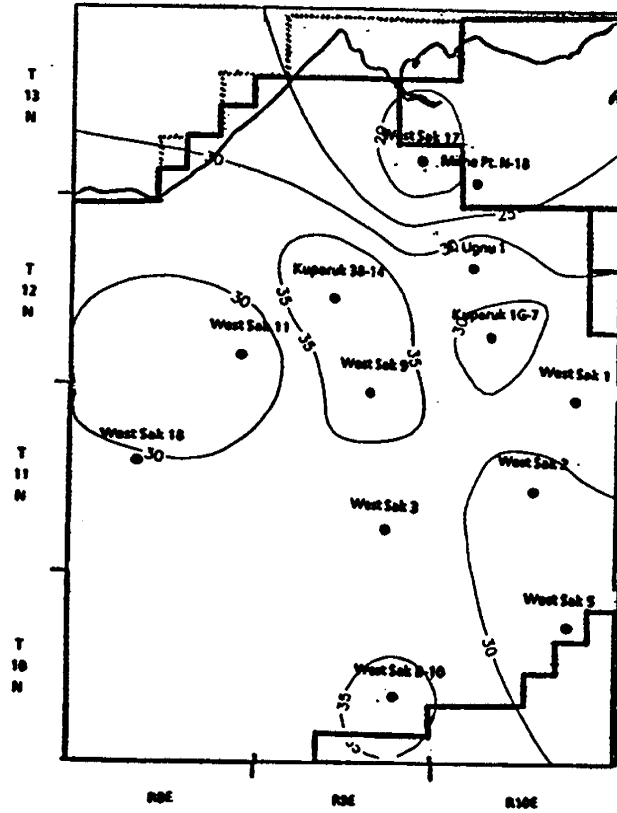


Figure II-17. Contour Map Showing Porosity Distribution in West Sak Upper Sand 1.

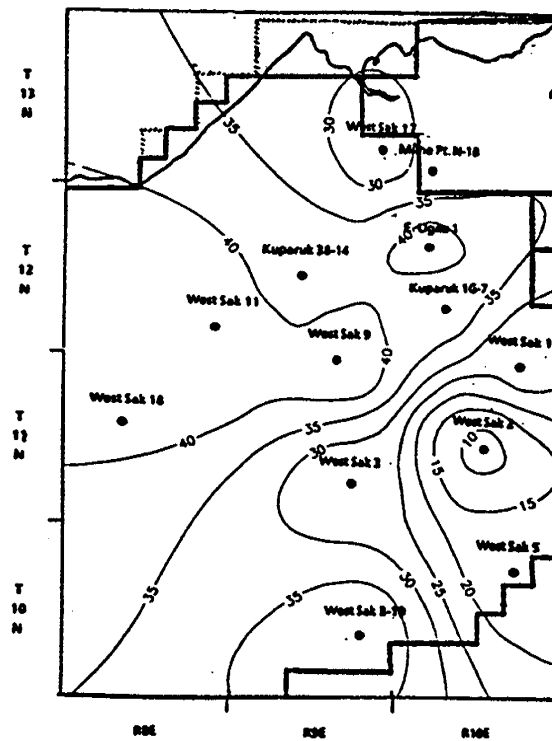


Figure II-18. Contour Map Showing Water Saturation Distribution in West Sak Upper Sand 1.

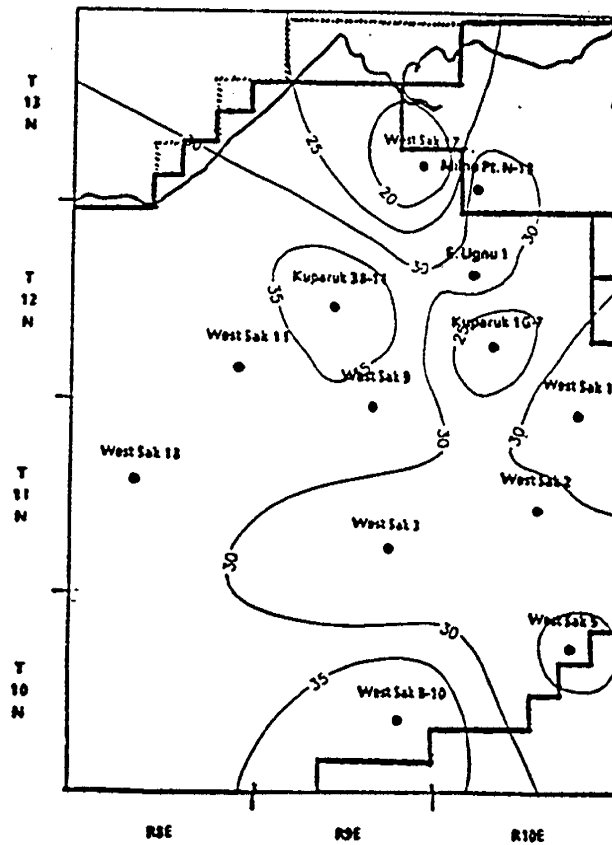


Figure II-19. Contour Map Showing Porosity Distribution in West Sak Upper Sand 2.

### E3. Sand Quality

The computed values of hydrocarbon pore volume (barrels/acre-ft) listed in Table II-6 were used to generate a related contour map (Figure II-20). Hydrocarbon pore volume is a measure of formation storage capacity and transmissivity. It is a function of net pay zone thickness, porosity, and water saturation. Sand intervals with water saturations greater than 50%, effective porosities less than 6%, or shale volumes greater than 40% are not considered as net pay. Figure II-21 indicates that the most productive sands occur in the central and eastern regions. Thinner pay zones in the west and southeast correspondingly have lower hydrocarbon capacities.

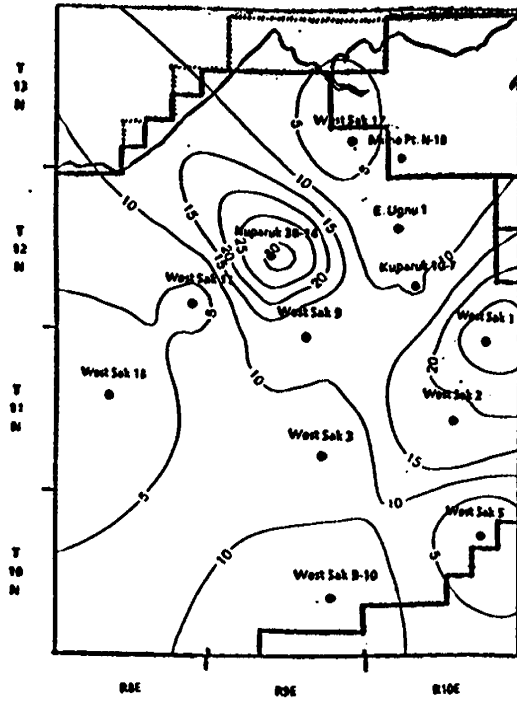


Figure II-20. Sand Quality Distribution in West Sak Sands Depicted by the Contour Map of Hydrocarbon Capacity.

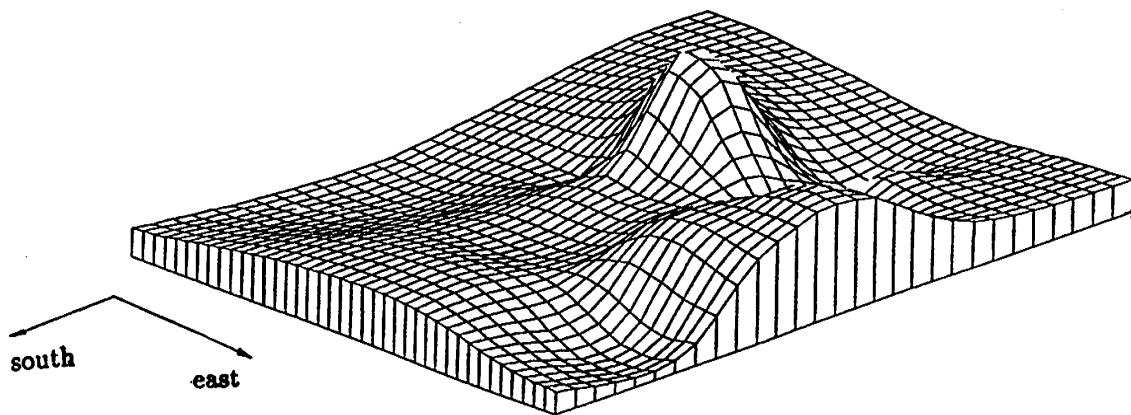


Figure II-21. 3-D Plot Showing the Sand Quality of West Sak Sands (viewed from southwest).



## CHAPTER III: LOWER UGNU RESERVOIR

---

### A. GEOLOGICAL OVERVIEW

The Ugnu sands overlie West Sak sands concordantly. These sands can be further subdivided into lower and upper members. Oil accumulations in both formations occur in traps which are a combination of both structural and stratigraphic features. Trapping in Lower Ugnu may be entirely a function of facies changes and stratigraphic features associated with a delta plain environment (Werner, 1985). The Ugnu sands are fine-to-medium grained, but are slightly coarser-grained than West Sak sands. Clay concentrations are less than 5%, as compared to concentrations between 5% and 30% within the West Sak sands. Porosities are slightly higher within the Ugnu sands.

Interbedded siltstones, mudstones, and coal seams separate the various Ugnu sands from one another. Core data indicate that the uppermost Lower Ugnu sands are massive, with infrequent low-to-moderate angle cross-bedding and ripple bedding (Werner, 1985). Basal Ugnu contacts are generally sharp and occasionally marked by shale rip-ups and thin zones of pebbly chert. These sands and their associated mudstones and coals are believed to be deposited in delta plain and fluvial environments.

As with West Sak, the identification of the Lower Ugnu interval was the initial step in the well log analysis. Five Lower Ugnu sands have been identified as potentially oil-bearing, although two of these are considered to contain poor pay zones. The five units are termed from top to bottom as follows:

- Sand 1
- Sand 2
- Sand 3
- Sand 4
- Sand 5

## **B. RESERVOIR DESCRIPTION PROCEDURE**

The reservoir description procedure used is the same as that applied to West Sak. LOGCALC, SURF II, and visual inspection of plotted logs were the primary means of data analysis. Petrophysical properties have been derived and plotted in the same manner as at West Sak, and cross sections were generated in order to better evaluate structural trends. Core sample reports were also utilized to correlate various sand units.

The uppermost Lower Ugnu sands have the most areal extension of all the Ugnu sands. They also show the greatest potential for further petroleum production (Werner, 1985). It must be stated, however, that the investigation of Upper Ugnu sands was constrained due of the lack of available core data. As such, we have concentrated Ugnu reservoir analysis primarily on the Lower Ugnu sands.

## **C. LOG-DERIVED PETROPHYSICAL PROPERTIES**

A complete analysis was conducted for each lower sand unit. Average porosities, water saturations, and net pay thicknesses are listed in Tables III-1 through III-6. Porosity in sand 1 is high, typically ranging between 23% and 40% (Table III-1). Average water saturations range between 14% and 45%, but most are below 25%. The net pay thickness of this sand exceeds 20 ft in most of the wells analyzed.

Sand 3 and sand 4 also have high porosities (Tables III-3 and III-4). Compared to sand 1, net pay is small, but areal extension is better. Water saturations are high, ranging between 30% and 50% in most wells. Sand 3 and sand 4 yield water saturations greater than 50% at three wells (Kuparuk 1H-7, Kuparuk 2C-4, and Oliktok Pt. 1). Because of the high water saturations, these sands are not considered to be of pay zone quality at these wells.

Sand 5 was found in nine of the thirteen wells that were analyzed, and sand 2 was found in only four wells, indicating that these sands have poor lateral continuity. Porosities are high in these two sands, but water saturations are also high, leading to low values of net pay. As such, sand 1, sand 3, and sand 4 are the three potentially productive sand units in the Lower Ugnu reservoir. They all have significant pay zones, but sand 1, with high porosity, thick pay zone, and low water saturation, is the most promising.

**Table III-1: Petrophysical Parameters of Lower Ugnu Sand 1.**

Well Name	Interval (ft)	Average $\phi$ (%)	Average $S_w$ (%)	Net Pay (ft)
West Sak No. 17	3122-3237	38	19	111
East Ugnu No. 1	3007-3060	35	22	52
Kuparuk No. 1B-2	3314-3338	38	40	16
Kuparuk No. 1H-3	3278-3370	26	14	75
Kuparuk No. 1H-7	3304-3386	38	19	49
Kuparuk No. 1G-7	3381-3428	40	22	24
Kuparuk No. 1G-8	3040-3080	23	23	6
Kuparuk No. 1G-13	3469-3505	35	46	19
Kuparuk No. 1C-4	3760-3799	28	27	21
Kuparuk No. 3B-14	2286-2328	42	23	43
Oliktok Pt. No. 1	3035-3096	27	36	3
Milne Pt. No. N-1B	3356-3389	31	15	28
Milne Pt. No. A-3	4266-4312	31	31	23

**Table III-2: Petrophysical Parameters of Lower Ugnu Sand 2.**

Well Name	Interval (ft)	Average $\phi$ (%)	Average $S_w$ (%)	Net Pay (ft)
West Sak No. 17	3266-3280	16	74	0
East Ugnu No. 1	-	-	-	-
Kuparuk No. 1B-2	3356-3388	40	40	23
Kuparuk No. 1H-3	3378-3410	36	20	25
Kuparuk No. 1H-7	3470-3490	16	71	0
Kuparuk No. 1G-7	3465-3514	36	42	29
Kuparuk No. 1G-8	-	-	-	-
Kuparuk No. 1G-13	3535-3619	36	47	46
Kuparuk No. 1C-4	-	-	-	-
Kuparuk No. 3B-14	-	-	-	-
Oliktok Pt. No. 1	-	-	-	-
Milne Pt. No. N-1B	-	-	-	-
Milne Pt. No. A-3	-	-	-	-

**Table III-3: Petrophysical Parameters of Lower Ugnu Sand 3.**

Well Name	Interval (ft)	Average $\phi$ (%)	Average $S_w$ (%)	Net Pay (ft)
West Sak No. 17	3368-3390	38	34	14
East Ugnu No. 1	3130-3180	33	26	45
Kuparuk No. 1B-2	3479-3531	33	40	32
Kuparuk No. 1H-3	3456-3510	38	43	45
Kuparuk No. 1H-7	3482-3486	21	62	0
Kuparuk No. 1G-7	3610-3620	25	34	4
Kuparuk No. 1G-8	3126-3140	30	4	7
Kuparuk No. 1G-13	3707-3732	26	48	2
Kuparuk No. 1C-4	3826-3902	28	65	0
Kuparuk No. 3B-14	2340-2370	38	35	30
Oliktok Pt. No. 1	3114-3137	36	94	0
Milne Pt. No. N-1B	3396-3464	38	9	62
Milne Pt. No. A-3	4336-4388	30	32	9

**Table III-4: Petrophysical Parameters of Lower Ugnu Sand 4.**

Well Name	Interval (ft)	Average $\phi$ (%)	Average $S_w$ (%)	Net Pay (ft)
West Sak No. 17	3404-3412	25	45	2
East Ugnu No. 1	3233-3292	33	44	46
Kuparuk No. 1B-2	3560-3632	34	42	42
Kuparuk No. 1H-3	3568-3592	39	47	14
Kuparuk No. 1H-7	3518-3564	37	54	0
Kuparuk No. 1G-7	3715-3748	38	45	17
Kuparuk No. 1G-8	3194-3212	26	15	10
Kuparuk No. 1G-13	3834-3854	39	48	3
Kuparuk No. 1C-4	3988-4023	9	71	0
Kuparuk No. 3B-14	2436-2464	38	41	29
Oliktok Pt. No. 1	3174-3193	26	97	0
Milne Pt. No. N-1B	3514-3570	18	30	20
Milne Pt. No. A-3	4430-4460	11	100	0

**Table III-5: Petrophysical Parameters of Lower Ugnu Sand 5.**

Well Name	Interval (ft)	Average $\phi$ (%)	Average $S_w$ (%)	Net Pay (ft)
West Sak No. 17	3422-3462	25	74	0
East Ugnu No. 1	-	-	-	-
Kuparuk No. 1B-2	3707-3728	30	39	12
Kuparuk No. 1H-3	3610-3630	41	50	1
Kuparuk No. 1H-7	3636-3662	36	59	0
Kuparuk No. 1G-7	3755-3790	32	48	4
Kuparuk No. 1G-8	-	-	-	-
Kuparuk No. 1G-13	3878-3901	34	47	2
Kuparuk No. 1C-4	-	-	-	-
Kuparuk No. 3B-14	2470-2490	41	34	20
Oliktok Pt. No. 1	3309-3318	24	100	0
Milne Pt. No. N-1B	-	-	-	-
Milne Pt. No. A-3	4504-4514	15	25	3

**Table III-6: Log-Derived Data for Selected Wells in the Lower Ugnu Sands.**

Well Name	Interval* (ft)	Weighted Mean Effective Porosity (%) $\phi$	Weighted Mean Water Saturation (%) $S_w$	Net Pay Thickness (ft) $h$	Hydrocarbon Pore Volume ( $10^3$ bbl/acre-ft)
West Sak No. 17	3122-3462	37	21	127	294.3
East Ugnu No. 1	3007-3292	34	30	142	260.4
Kuparuk No. 1B-2	3314-3728	35	41	128	206.5
Kuparuk No. 1H-3	3278-3630	32	26	161	289.1
Kuparuk No. 1H-7	3304-3662	38	19	49	115.4
Kuparuk No. 1G-7	3381-3790	37	36	77	384.5
Kuparuk No. 1G-8	3040-3212	26	14	22	38.1
Kuparuk No. 1G-13	3469-3901	36	46	71	354.6
Kuparuk No. 1C-4	3760-4023	28	27	21	33.0
Kuparuk No. 3B-14	2286-2490	40	32	121	255.3
Oliktok Pt. No. 1	3035-3318	27	36	3	4.3
Milne Pt. No. N-1B	3356-3570	32	14	110	236.0
Milne Pt. No. A-3	4266-4514	30	31	35	55.2

\* Measured Depth

Weighted average porosities of the Lower Ugnu sands are listed in Table III-6. The average porosity and water saturation among the sands range from 27% to 38% and 14% to 46%, respectively. Net pay in most wells exceeds 50 ft. A comparison of the data in Table III-6 with West Sak data in Table III-7 suggests that the Lower Ugnu sands have generally higher porosities, lower water saturations, and greater net pay thicknesses.

#### **D. RESERVOIR DESCRIPTION**

Lower Ugnu reservoir can be subdivided and characterized in terms of bed thickness variations, spatial distribution of petrophysical properties, and sand quality. The various log traces were input into LOGCALC and the results were used to generate cross-sectional plots, contour maps, isopach maps, and three-dimensional plots. This procedure is the same as that used in the West Sak reservoir analysis.

##### **D1. Sand Bed Distribution**

Cross section CC' (Figure III-1) shows that the Lower Ugnu sands dip toward the northeast at an angle of between 1° and 2°. Down-to-the-east faults most likely cut the Ugnu sands along this cross section. Tables III-1 through III-6 illustrate that sand 2 and sand 5 units of Ugnu have the poorest hydrocarbon-bearing prospects, due to poor lateral continuity, low net pay thicknesses, and high water saturations. For this reason, isopach maps were not generated for these two sands.

As shown in Figure III-2, sand 1 varies considerably in thickness, with maximum thickness in West Sak well No. 17. Overall, this sand is thicker than any other Lower Ugnu sand units. Figures III-3 and III-4 indicate that sand 3 thickens toward the northeast and southeast while sand 4 is locally thicker in the region of the Kuparuk 1B-2 and 1H-3. Visual inspection of the isopach maps corresponding to sand 1, sand 2, and sand 3, indicate little similarity in thickness patterns.

**Table III-7: Log-Derived Data for Selected Wells in the West Sak Sands.**

Well Name	Interval* (ft)	Weighted Mean Effective Porosity (%) $\phi$	Weighted Mean Water Saturation (%) $S_w$	Net Pay Thickness (ft) $h$	Hydrocarbon Pore Volume ( $10^3$ bbl/acre-ft)
West Sak No. 1	3746-4044	35	33	116	173.8
West Sak No. 2	3304-3530	29	19	84	151.4
West Sak No. 3	2628-2882	30	34	41	63.2
West Sak No. 5	3332-3428	27	18	12	17.9
West Sak No. 9	2678-2930	36	42	50	79.5
West Sak No. B-10	2695-3174	38	42	55	93.2
West Sak No. 11	2324-2694	29	44	27	33.4
West Sak No. 17	3516-3620	16	31	12	10.1
West Sak No. 18	2526-2720	36	38	13	22.6
East Ugnu No. 1	3386-3654	33	44	27	38.1
Kuparuk No. 1G-7	3408-3638	25	35	64	80.5
Kuparuk No. 3B-14	2538-3025	38	41	136	238.4
Milne Pt. No. N-1B	3555-3806	24	24	56	79.4

\* Represents interval that is potentially hydrocarbon bearing.

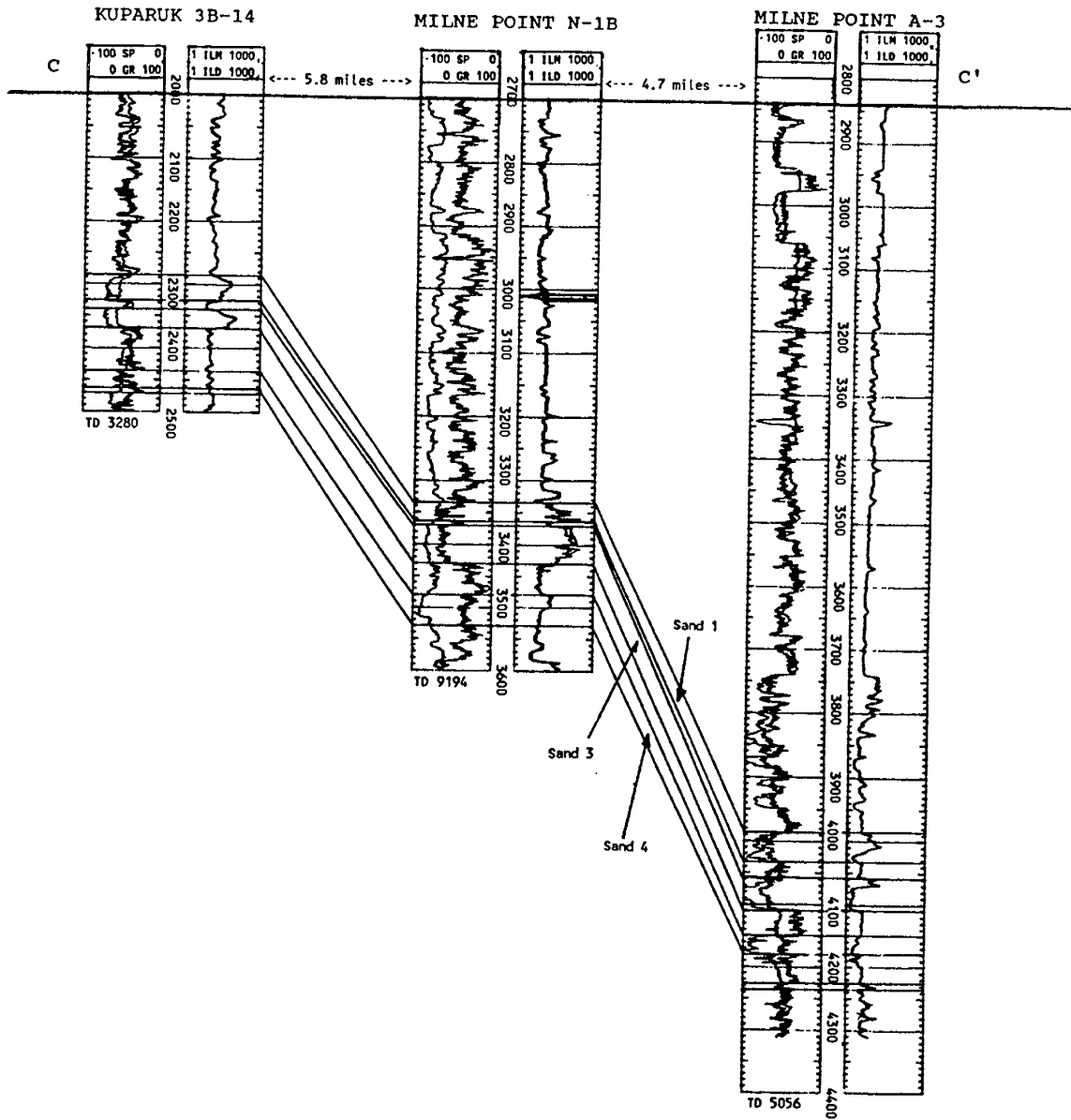


Figure III-1. Lower Ugnu Sands Distribution Along the SW-NE Stratigraphic Cross Section CC'.

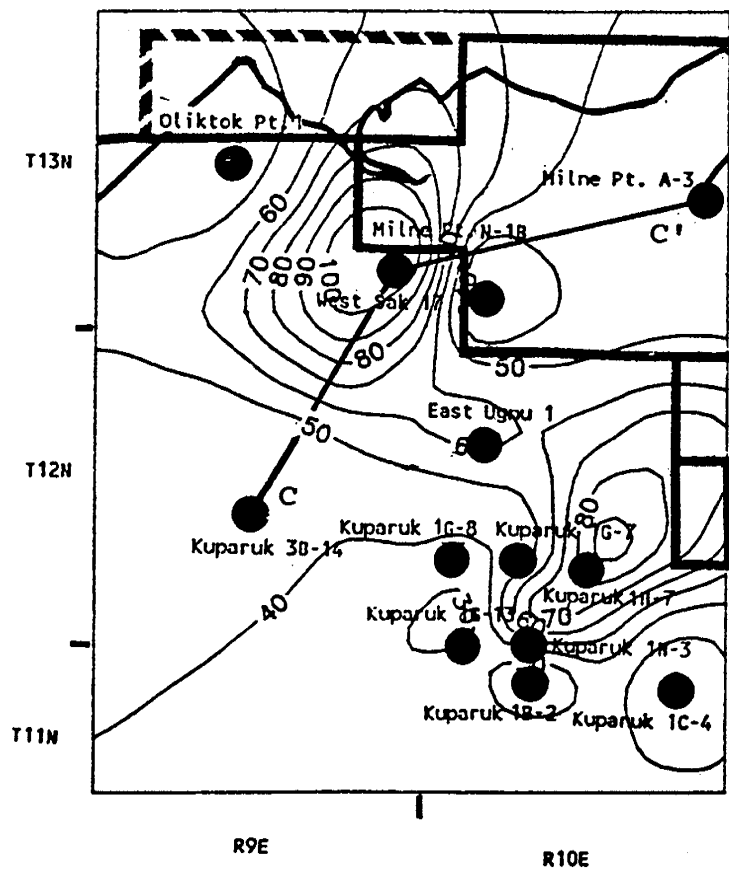


Figure III-2. Isopach Map of Lower Ugnu Sand 1.

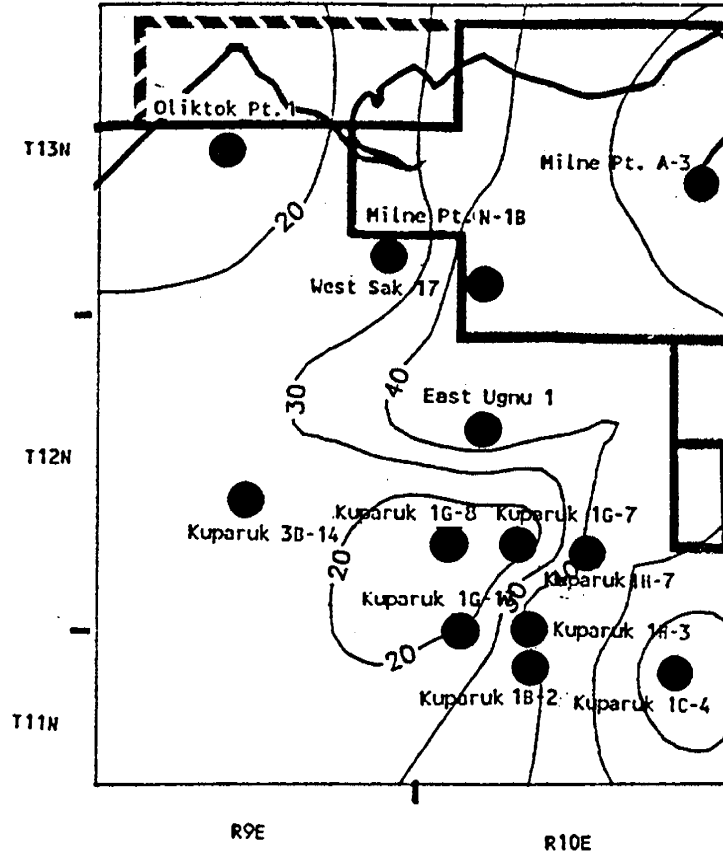


Figure III-3. Isopach Map of Lower Ugnu Sand 3.

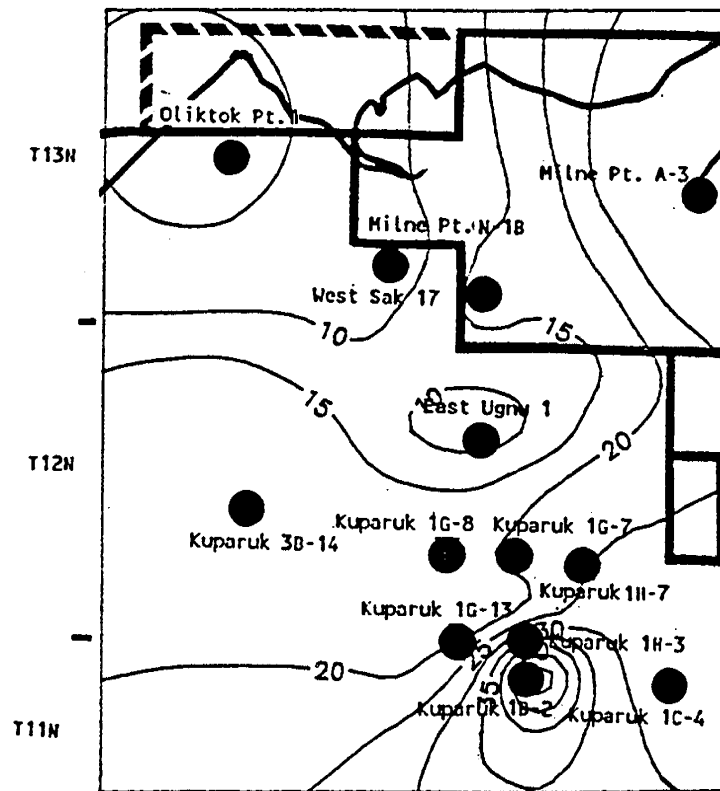


Figure III-4. Isopach Map of Lower Ugnu Sand 4.

## **D2. Spatial Distribution of the Petrophysical Properties**

The average Lower Ugnu porosities and water saturations shown in Table III-6 were used to generate corresponding porosity and water saturation maps and three-dimensional plots. Porosity in Lower Ugnu sands varies between 29% and 38% (Figures III-5 and III-6). High porosities are in the Kuparuk 3B-14 and Kuparuk 1H-7, but a large zone of low porosity extends to the south between these wells. Water saturations show general increases toward the northwest and adjacent to the Kuparuk 1G-13, as indicated by Figures III-7 and III-8.

Contour maps of porosity and water saturation corresponding to sand 1 are shown in Figures III-9 and III-10. They indicate that sand 1 porosities are generally 30% or greater in most of the study area. Also, sand 1 water saturations are less than 25%. These values, combined with thicknesses consistently greater than 20 ft, show that this sand presents the best Ugnu oil potential.

## **D3. Sand Quality**

Hydrocarbon capacity in terms of hydrocarbon pore volume (barrels/acre-ft) was evaluated and the results are listed in Table III-6. Cutoff values for the Lower Ugnu are the same as those applied to the West Sak sands (porosity less than 6%, water saturation greater than 50%, and shale volume greater than 40%). Figures III-11, and III-12 indicate that the best Lower Ugnu sand quality occurs in the northeastern portion of the Kuparuk River Unit and in the adjacent western portion of the Milne Point Unit. In this region, hydrocarbon pore volumes range between 200,000 and 250,000 barrels/acre-ft. The Kuparuk 1G-13 shows a localized high of 300,000 barrels/acre-ft. Lower porosities, coupled with thinner pay zones in the southeastern portion of the area, result in poorer sand qualities in that area.

## **D4. West Sak Versus Lower Ugnu Reservoir Quality**

Overall, the Lower Ugnu sands are characterized by better porosities, lower water saturations, and higher net pay zone thicknesses than the West Sak sands. On this basis, Ugnu reservoir rock is of better quality than that of West Sak. Reservoir temperature, however, is also an important consideration with these low gravity, high viscosity sands. Oil column reservoir temperatures range from 45° to 100° F (7° to 38°C), depending on proximity to the overlying permafrost (Werner, 1985). Because West Sak oil, in being deeper than Ugnu oil, is warmer, it has presented a more attractive target for development and exploitation.

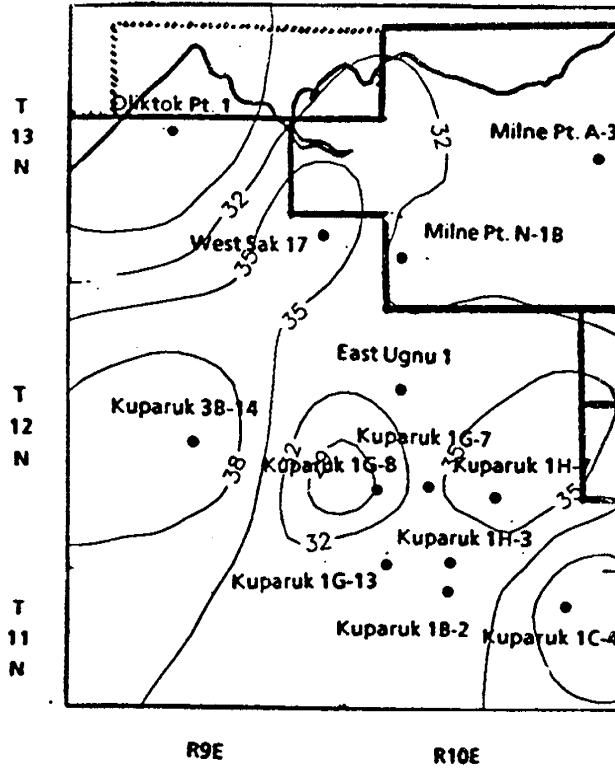


Figure III-5. Porosity Contour Map of Lower Ugnu Sands.

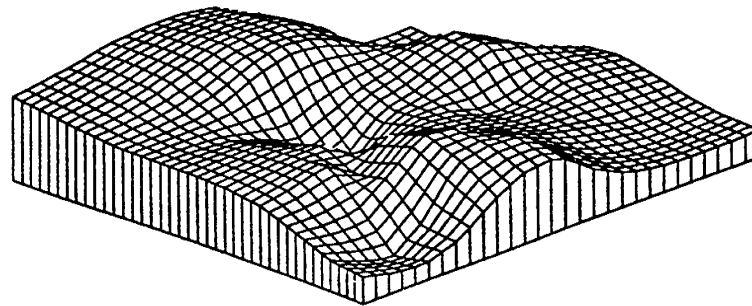


Figure III-6. 3-D Plot Showing the Distribution of Porosity in Lower Ugnu Sands (viewed from the southeast).

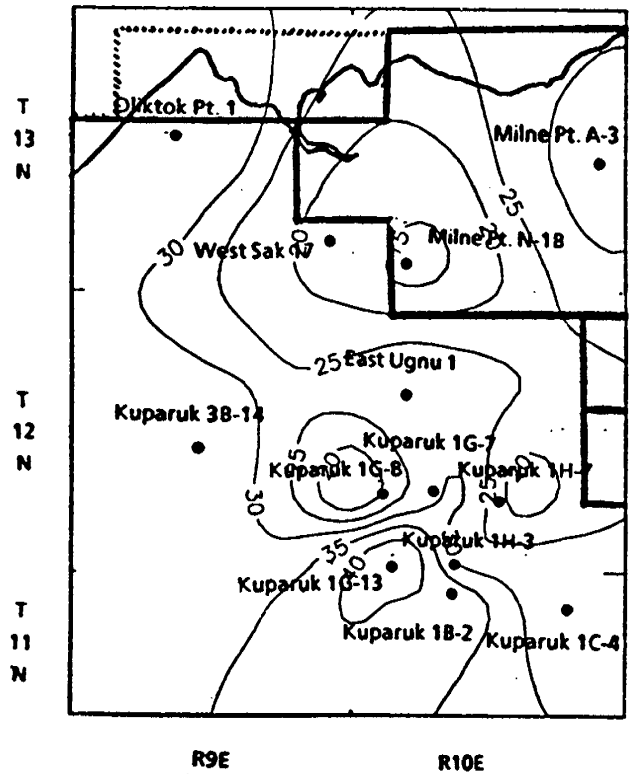


Figure III-7. Water Saturation Map of Lower Ugnu Sands.

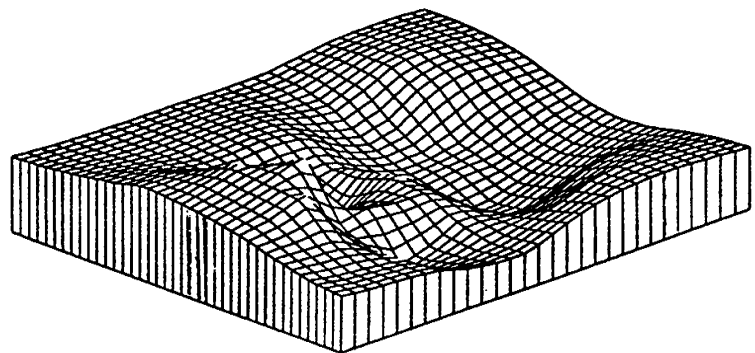


Figure III-8. 3-D Plot Showing the Water Saturation Distribution in Lower Ugnu Sands (viewed from the southeast).

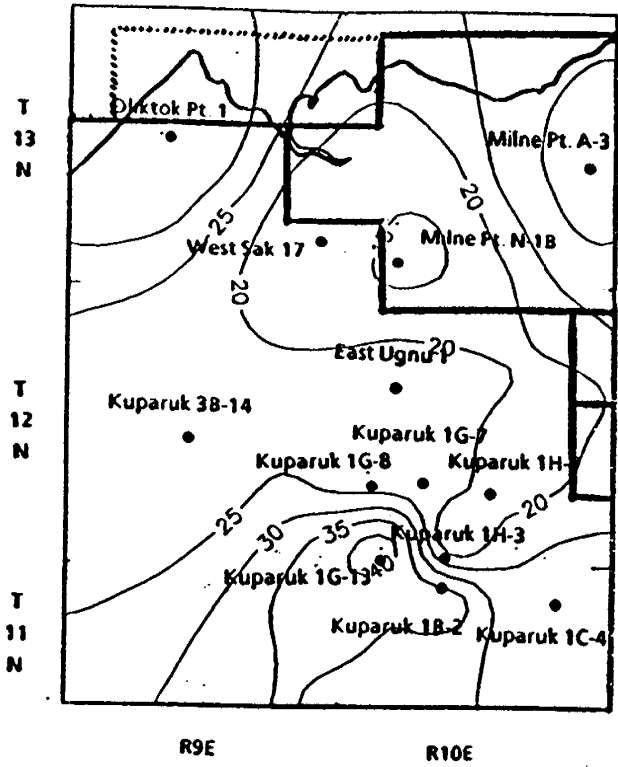


Figure III-9. Contour Map Showing Porosity Distribution in Lower Ugnu Sand 1.

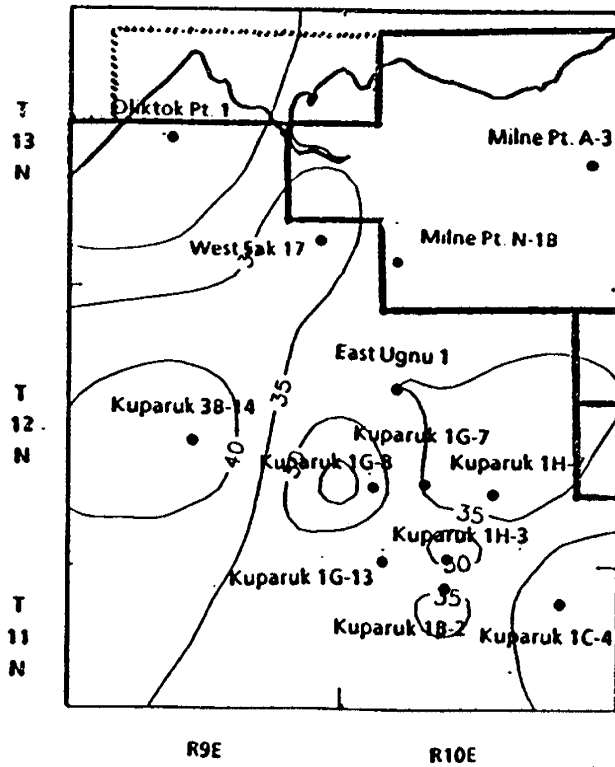


Figure III-10. Contour Map Showing Water Saturation Distribution in Lower Ugnu Sand 1.

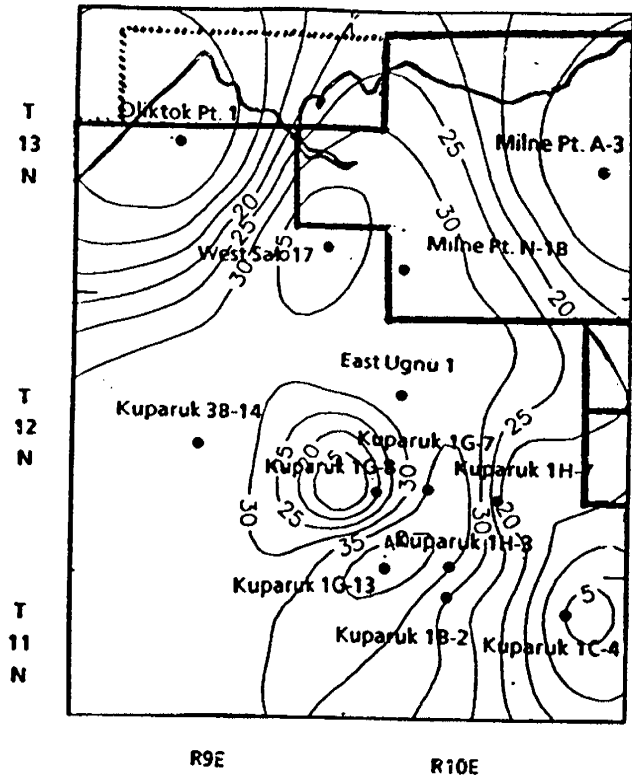


Figure III-11. Sand Quality Distribution in the Lower Ugnu Sands, Depicted by the Contour Map of Hydrocarbon Pore Volume ( $10^3$  bbl/acre-ft).

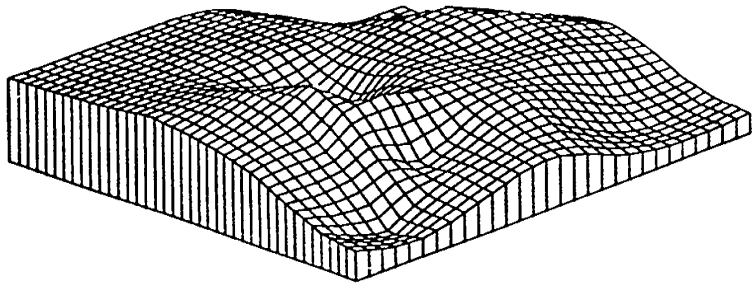


Figure III-12. 3-D Plot Showing the Sand Quality of Lower Ugnu Sands (viewed from the southeast).



# CHAPTER IV: PETROGRAPHIC CHARACTERISTICS OF SELECTED STRATIGRAPHIC HORIZONS

## UGNU SWPT #1 AND WEST SAK SWPT #1

---

---

### A. INTRODUCTION

This petrographic work is part of the reservoir characterization project carried out under the aegis of the Petroleum Development Laboratory, University of Alaska Fairbanks, to obtain increased understanding of the West Sak and Ugnu (Brookian) petroleum reservoirs of northern Alaska. It is viewed as a key aspect of PDL's reservoir characterization effort, since it is intended to provide direct, substantive physical characterization, i.e. mineralogy, textural features/relationships of the rocks.

This chapter provides petrographic analyses of thirty samples of core material from selected stratigraphic horizons representing the West Sak and the Ugnu intervals in the Arco Alaska Inc. Ugnu Single-Well Production Test (SWPT) #1 and West Sak SWPT #1 wells, Northern Alaska. These samples represent the spectrum of lithologies, and attendant apparent petrophysical characteristics, i.e. reservoir/seal qualities, observed megascopically. Wireline logs also were used to guide sample selection.

A technical paper representing a preliminary synthesis of this analysis was presented at the Annual Meeting of the American Association of Petroleum Geologists in Dallas, Texas in April, 1991. A copy of the abstract of this paper (Mowatt, Ogbe, Kamath and Sharma, 1991) is included as Appendix A.

### B. PETROGRAPHIC ANALYSES

Quantitative petrographic analysis was carried out on each of 20 thin-sections. Since many of the samples were, at best, semi-consolidated—cemented by viscous hydrocarbon material in situ, several problems are inherent here. Sample integrity, especially in terms of textural relationships, becomes a serious concern. This involves the entire series of events from initial perturbation of in situ materials during drilling through sample recovery, handling, transportation, and ultimately preparation as petrographic thin-sections. Thus, though the resultant observed mineralogic compositions likely at least somewhat closely resemble those originally extant in situ, textural relationships are an entirely different matter. Some-

what surprisingly, however, serious disruptions were not apparent in many instances in the present work, particularly in those samples of inherently low reservoir quality, i.e. the more coherent and/or finer-grained samples. For those samples of apparently better reservoir quality with higher porosities, less proportions of finer-grained constitutions, etc., varying amounts of disruptions of original textures were all too evident in thin-section. However, with these caveats, and an awareness of certain limitations, appreciable potentially useful information remains to be gleaned from petrographic study of these materials.

The present focus has been on the West Sak and Ugnu SWPT wells, and immediately adjacent horizons in terms of reservoir characterization. Similar investigations of other wells should lead to increased understanding of areal relationships which will be fundamental to effective recovery of hydrocarbons as a development geology-engineering concern.

### **C. SAMPLE DESCRIPTIONS**

The following pages contain descriptions of 30 samples analyzed petrographically. First, the 18 samples obtained from Ugnu SWPT #1 are described. Second, the 12 samples from the West Sak SWPT #1 are described. Additional photomicrographs of each sample are on file at PDL.

**C1. Ugnu SWPT #1 Samples**

**C1(a) Ugnu SWPT #1, 3532' (below West Sak Zone).**

Description:

Lithic Wacke. Framework grains (33%) : predominately very fine-fine sand-sized, with trace amounts of medium sand-sized materials, poorly-moderately sorted, angular/subangular/subrounded, consisting of quartz (48%), feldspars (4%, plagioclase and potassium feldspars), lithic fragments (44%) and other minor-trace constituents, including micas, chlorite, glauconite, organic materials.

Detrital matrix (46%) as patches-streaks-layers-clasts of silt/clay-rich material. Rock exhibits sedimentary layering and is also moderately burrowed.

Visible porosity (shown in blue) estimated as 19%, principally as semi-pervasive intergranular (associated especially with burrows); moderately-highly effective.

Some microporosity, associated with silt-clay. Cement not apparent, but trace amounts of pyrite are present.

This sample has undergone slight apparent compaction.

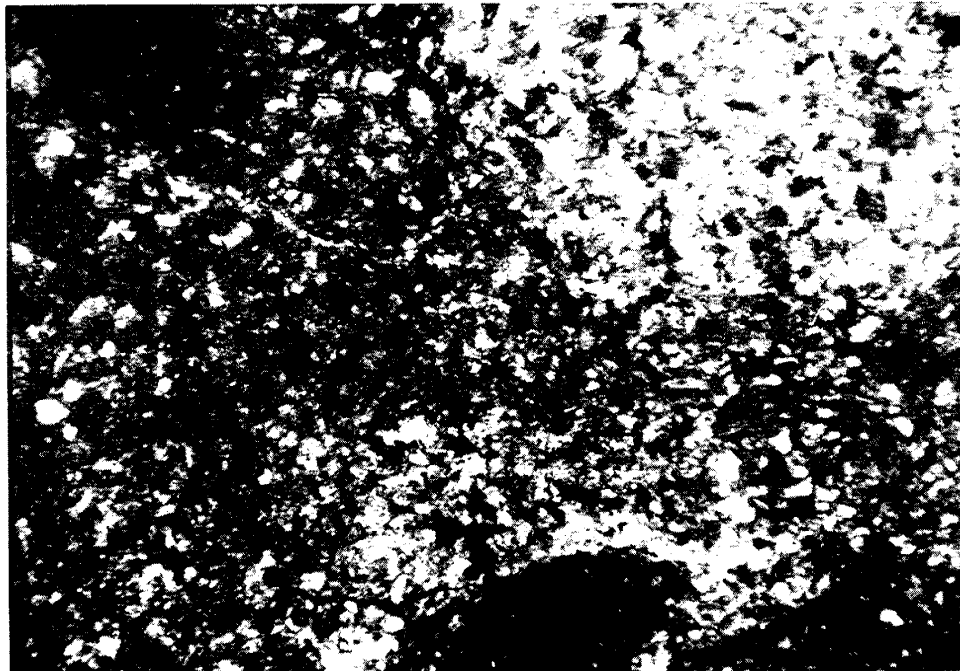


Figure IV-1: Ugnu SWPT #1, 3532' (50 x PL).

**C1(b) Ugnu SWPT #1, 3526' (West Sak Sands).**

Description:

Lithic Wacke. Framework grains (48%): predominately very fine sand-sized, with minor amounts of fine sand-sized materials, poorly-moderately sorted, angular/subangular, consisting of quartz (40%), feldspar (3%; plagioclase and potassium feldspar), lithic fragments (53%), and other minor-trace constituents, including micas, chlorite, glauconite, iron-oxide opaque minerals, and organic materials.

Detrital matrix (33%) as patches-streaks of silt-clay rich material. Rock exhibits sedimentary layering, and is slightly-moderately burrowed.

Visible porosity (shown in blue) estimated as 18%, principally as semi-pervasive intergranular; highly effective. Some (?) of this may be an artifact of thin-section preparation.

Some microporosity, associated with silt-clay. Cement not apparent, but some of the iron-oxide material may be diagenetic (?).

This sample has undergone slight apparent compaction.

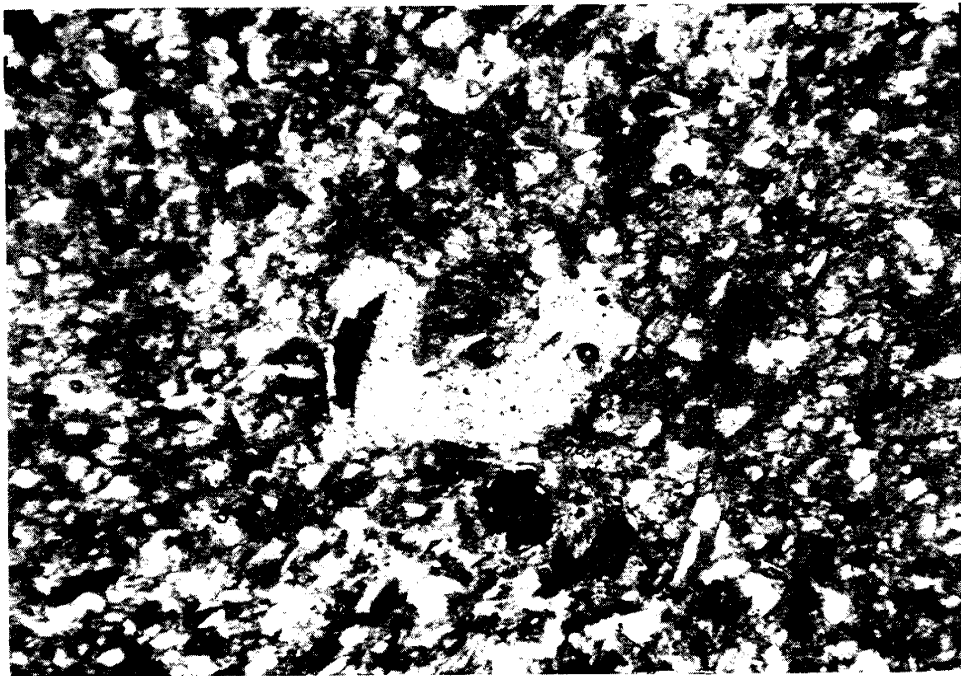


Figure IV-2: Ugnu SWPT #1, 3526' (50 x PL).

**C1(c) Ugnu SWPT #1, 3507' (West Sak Zone).**

Description:

Lithic Wacke. Framework grains (43%): range from very coarse to fine sand-sized, with subordinate amounts of granule-pebble-sized fossil materials, very poorly sorted, angular/subangular/subrounded, consisting of quartz (39%), feldspars (3%, plagioclase and potassium feldspars.), lithic fragments (56%), and other minor-trace constituents, including micas, chlorite, glauconite, opaque iron-oxide minerals, and organic materials.

Detrital matrix ("54%") difficult to elucidate; could also include clay cements. It does include residential hydrocarbon material in this analysis and thus, is at least in part equivalent to "porosity." The relative amounts of matrix versus porosity are not rigorously determinable in this thin-section.

Some, at least, is microporosity, associated with clays. Cement as such is not apparent, although the hydrocarbon material as well as perhaps at least some of the "matrix" clays could represent cement in this sample. Most likely, at least an appreciable proportion of the "matrix/porosity" here represents effective intergranular pore space.

This sample has undergone slight apparent compaction. The rock fabric is indeterminate due to specimen disaggregation, but appears to have been massive.

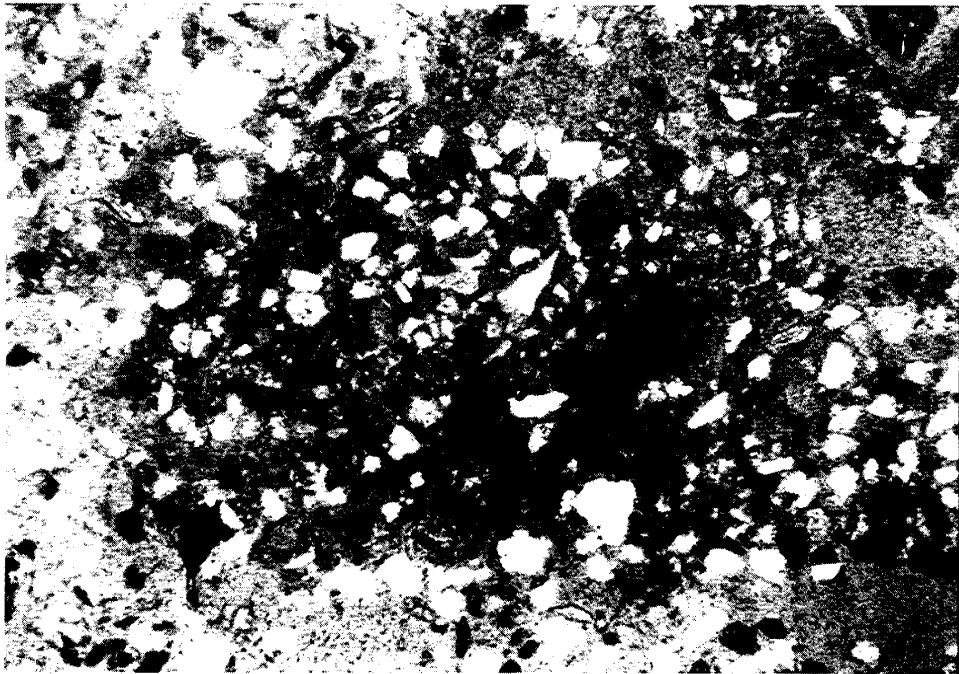


Figure IV-3: Ugnu SWPT #1, 3507' (50 x PL).

**C1(d) Ugnu SWPT #1, 3497' (West Sak Zone).**

Description:

Lithic Wacke/Siltstone. Framework grains (30%): predominately very fine sand-sized, with subordinate amounts of fine sand-sized materials, poorly-moderately sorted, angular/subangular/subrounded, consisting of quartz (40%), feldspars (3%; plagioclase and potassium feldspars), lithic fragments (50%), and other minor-trace constituents, including micas, chlorite, glauconite, opaque iron-oxide minerals, and organic materials.

Detrital matrix (56%) as lenses-patches-streaks of silt-clay materials. Rock is strongly burrowed with coarser grains filling burrows.

Visible porosity (shown in blue) estimated as 9%, principally as intergranular, and associated in large part with burrow-filling grains. It may be only moderately effective, thus, although on the order of 30% within the burrows.

Also sample shows is some microporosity associated with silt-clay. Cement not apparent, although some of the iron-oxides may be diagenetic. This sample has undergone slight apparent compaction.

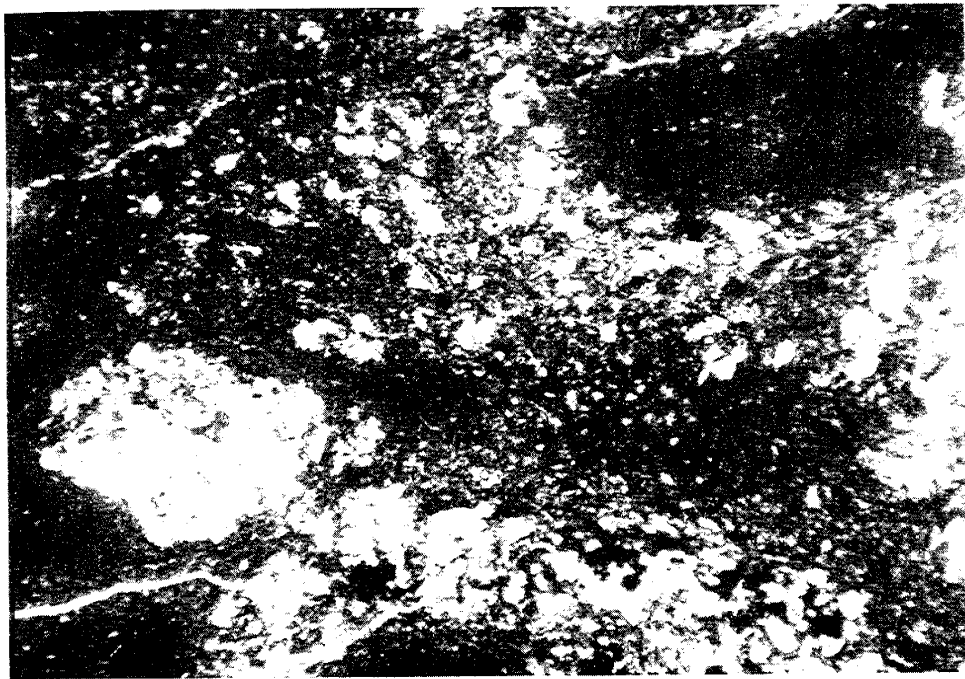


Figure IV-4: Ugnu SWPT #1, 3497' (50 x PL).

**C1(e) Ugnu SWPT #1, 3493' (West Sak Zone).**

Description:

Litharenite. Framework grains (66%): predominately very fine sand-sized, with trace amounts of fine sand-sized materials, well-very well sorted, angular/sub-angular/subrounded, consisting of quartz (30%) feldspars (3%; plagioclase and potassium feldspars), lithic fragments (64%), and other minor-trace constituents, including micas, chlorite, glauconite, opaque iron-oxide minerals, and organic materials.

Detrital matrix (16%) as vague patchy areas/layers of clay materials. At least some may (?) represent, rather, diagenetic clay cement.

Visible porosity (shown in blue) estimated as 17%, principally as pervasive intergranular; highly effective. A moderate amount of microporosity, associated with clays. Cement not apparent, although at least a portion of "matrix" clay material may well be rather diagenetic clay cement.

This sample has undergone slight apparent compaction.

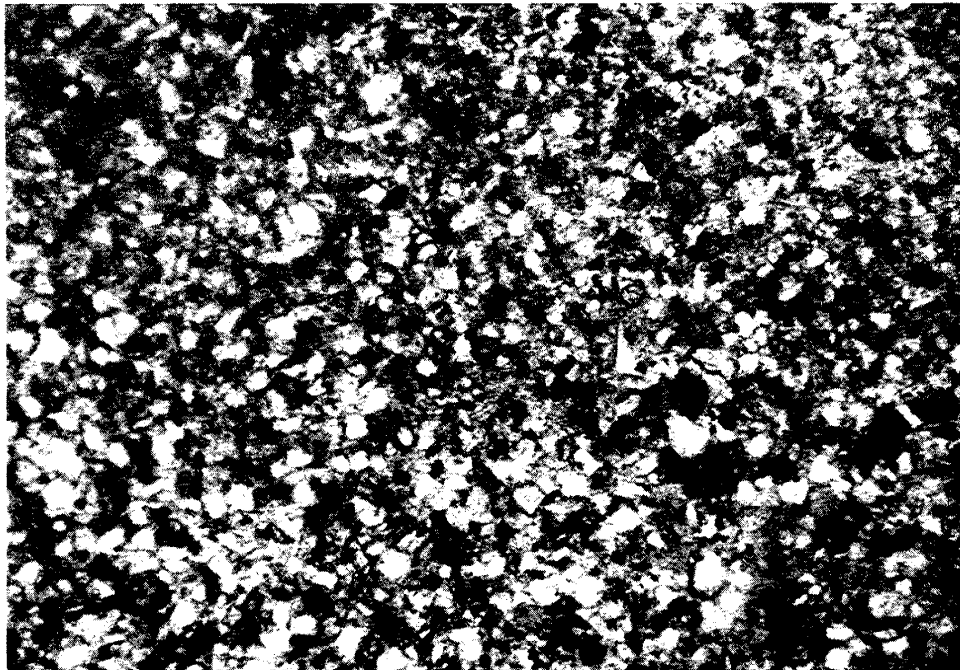


Figure IV-5: Ugnu SWPT #1, 3493' (50 x PL).

**C1(f) Ugnu SWPT #1, 3457' (West Sak Zone).**

Description:

Lithic Wacke/Siltstone. Framework grains (38%): predominantly very fine sand-sized, with subordinate amounts of fine and medium sand-sized materials, poorly-moderately sorted, angular/subangular/subrounded, consisting of quartz (40%), feldspars (6%; plagioclase and potassium feldspars), lithic fragments (50%), and other minor-trace constituents, including micas, chlorite, glauconite, and organic materials.

Detrital matrix (55%) as patchy areas of silt-clay. Rock is moderately burrowed.

Visible porosity (shown in blue) estimated as 5%, principally as intergranular, patchy; moderately-poorly effective. Some microporosity, associated with clay. Cement not apparent, although some of the "matrix" clay may represent diagenetic material. Minor pyrite, with euhedral crystal faces, is authigenic-diagenetic.

This sample has undergone slight apparent compaction.

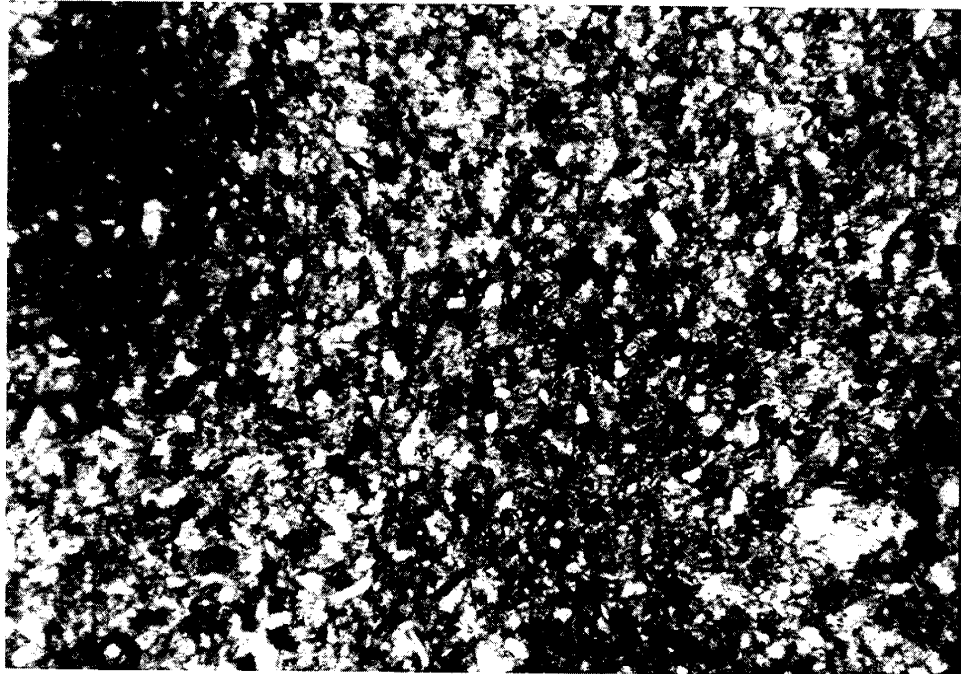


Figure IV-6: Ugnu SWPT #1, 3457' (50 x PL).

**C1(g) Ugnu SWPT #1, 3452' (West Sak Zone).**

Description:

Litharenite. Framework grains (63%): predominantly fine sand-sized, with trace amounts of medium and coarse sand-sized materials, well-very well sorted, angular/subangular/subrounded, consisting of quartz (37%), feldspars (4%; plagioclase and potassium feldspars), lithic fragments (56%), and other minor-trace constituents, including micas, chlorite, glauconite, and organic materials.

Detrital matrix (11%) as vague patches among framework grains. Some, at least, may, rather, represent intergranular clay "cement." Vague sedimentary layering.

Visible porosity (shown in blue) estimated as 26%, principally as pervasive intergranular; highly effective. Some microporosity, associated with clays. Cement not apparent, although at least some of the clays present may well represent diagenetic "cement." Minor pyrite present, appears to be of authigenic-diagenetic origin.

This sample has undergone slight apparent compaction.

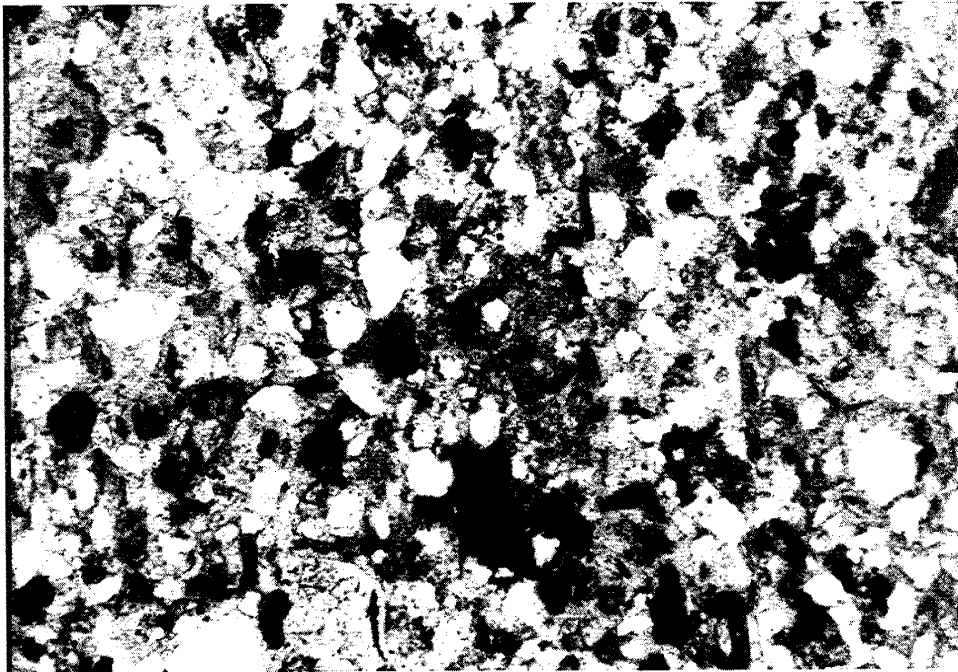


Figure IV-7: Ugnu SWPT #1, 3452' (50 x PL).

**C1(h) Ugnu SWPT #1, 3425' (West Sak Zone).**

Description:

Litharenite. Framework grains (70%): predominantly very fine sand-sized, with subordinate-trace amounts of fine, medium, and coarse sand-sized materials, well-very well sorted, angular/subangular/subrounded, consisting of quartz (30%), feldspars (3%; plagioclase and potassium feldspars), lithic fragments (65%), and other minor-trace constituents, including micas, chlorite, glauconite, and organic materials.

Detrital matrix (6%) as vague layers-zones containing clay materials. Vague sedimentary layering.

Visible porosity (shown in blue) estimated as 23%, principally as pervasive intergranular; highly effective.

Some microporosity, associated with clays. Cement not apparent. At least some of the clays may represent diagenetic "cement." Minor pyrite, of authigenic-diagenetic origin.

This sample has undergone slight apparent compaction.

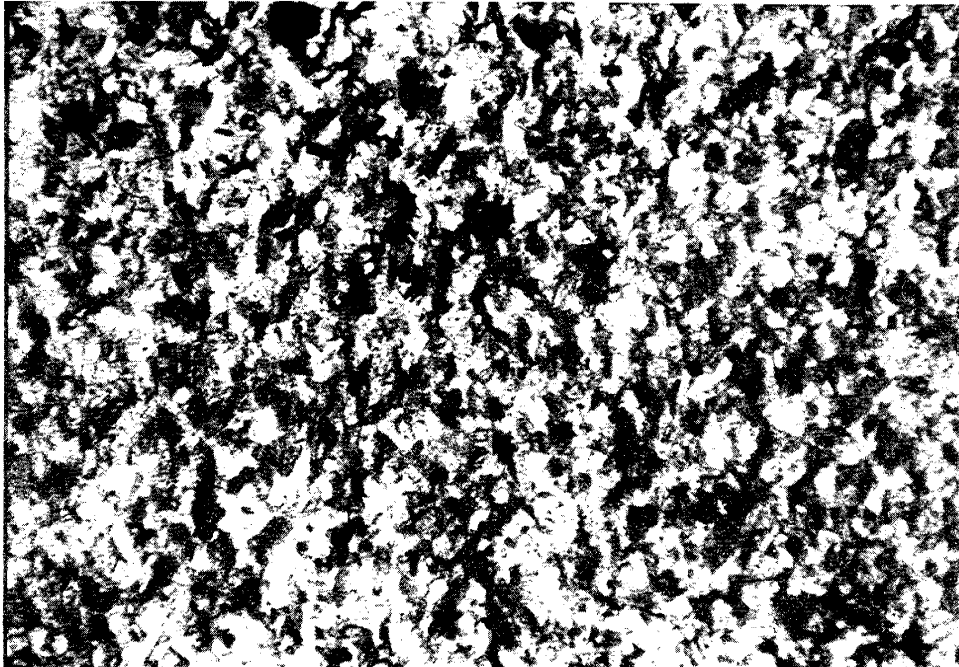


Figure IV-8: Ugnu SWPT #1, 3425' (50 x PL).

**C1(i) Ugnu SWPT #1, 3422' (West Sak Zone).**

Description:

Litharenite (or Lithic Wacke?). Framework grains (66%): predominantly fine sand-sized, with trace amounts of medium and coarse sand-sized materials, well (poorly?) sorted, angular/subangular/ subrounded, consisting of quartz (40%), feldspars (5%; plagioclase and potassium feldspars), lithic fragments (50%), and other minor-trace constituents, including micas, chlorite, glauconite, opaque iron-oxide minerals, and organic materials.

Detrital matrix (a minimum of 18%) as clays intergranular to framework grains, associated with residual hydrocarbon material. These clays may, rather, be diagenetic in origin. Alternatively, they might represent thorough mixing due to burrowing of organisms. Vague sedimentary layering.

Visible porosity (shown in blue) estimated as up to 15%, principally as intergranular; probably moderately-highly (?) effective.

Moderate amount of microporosity, associated with clays. Cement not apparent, although at least a portion of the "matrix" clays might, rather, represent "cement" of diagenetic origin.

This sample has undergone slight apparent compaction.

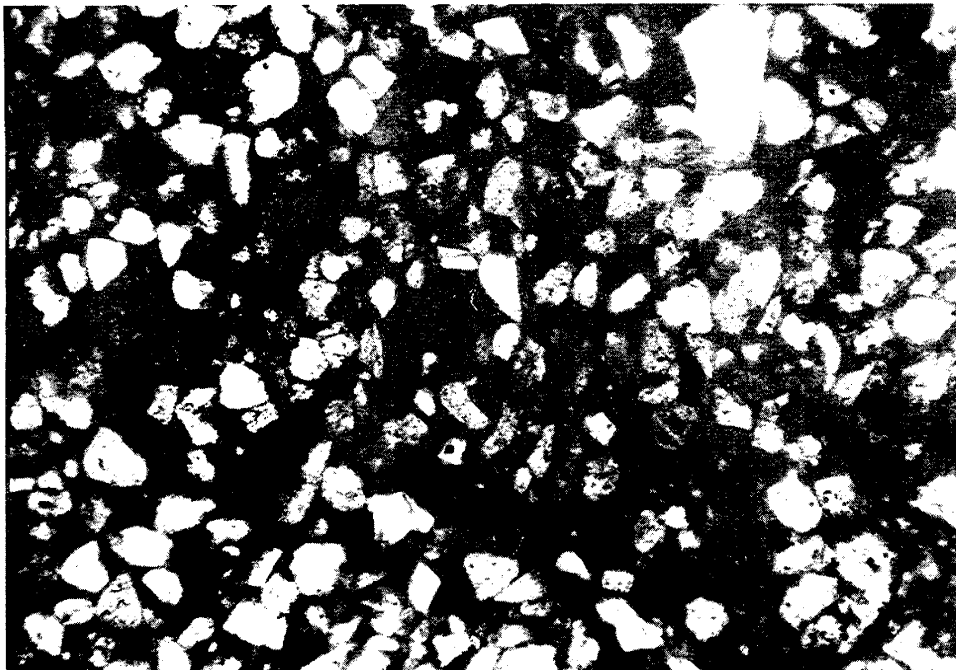


Figure IV-9: Ugnu SWPT #1, 3422' (50 X PL).

**C1(j) Ugnu SWPT #1, 3412' (above West Sak Zone).**

Description:

Sandy Siltstone. Sand-size grains (27%): predominantly very fine sand-sized; rock is poorly-very poorly sorted, angular/subangular, consisting of quartz (45%), feldspars (5%; plagioclase and potassium feldspars), lithic fragments (46%), and other minor-trace constituents, including micas, chlorite, glauconite, opaque iron-oxide minerals, and organic materials.

Detrital matrix (66%) in silt-clay-rich layers-patches. Moderately burrowed.

Visible porosity (shown in blue) estimated as 7%, principally as intergranular to burrow-filling grains; burrowed areas are patchy; porosity of poor effectiveness.

Some microporosity, associated with clays. Cement not apparent.

This sample has undergone slight apparent compaction.



Figure IV-10: Ugnu SWPT #1, 3412' (50 X PL).

**C1(k) Ugnu SWPT #1, 3264' (Lower Ugnu (?) Zone).**

Description:

Lithic Wacke. Framework grains (59%): predominantly fine and very fine sand-sized, with trace amounts of medium and coarse sand-sized materials, poorly-very poorly sorted, angular/subangular/subrounded, consisting of quartz (32%), feldspars (4%; plagioclase and potassium feldspars), lithic fragments (60%), and other minor-trace constituents, including micas, chlorite, glauconite, opaque iron-oxide minerals, and organic materials (flakes, some recognizable plant fragments)

Detrital matrix (28%) of silt-clay, patchy. Fair sedimentary layering. Moderately burrowed.

Visible porosity (shown in blue) estimated as 13%, principally as intergranular, particularly in burrowed areas. Effectiveness: fair-poor.

Appreciable microporosity, associated with clays. Cement not apparent, although some of the clays might represent diagenetic clay "cement."

This sample has undergone slight apparent compaction.

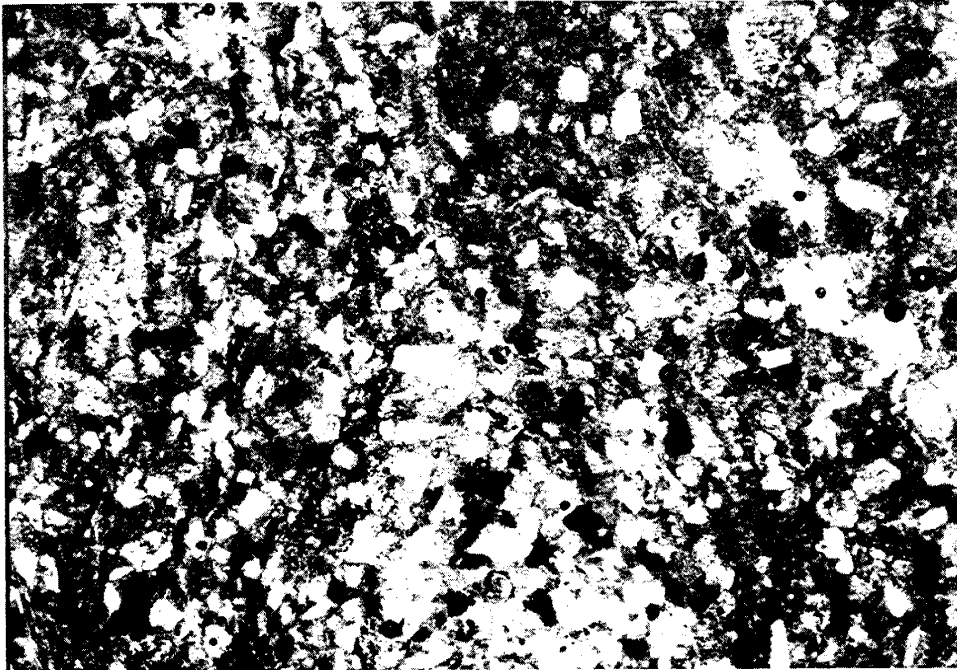


Figure IV-11: Ugnu SWPT #1, 3264' (50 X PL).

**C1(1) Ugnu SWPT #1, 3241' (Lower Ugnu (?) Zone).**

Description:

Siltstone. Sand-sized grains (14%): predominantly very fine; fine, and medium sand-sized, poorly-very poorly sorted, angular/subangular/subrounded, consisting of quartz (50%), feldspars (2%; plagioclase and potassium feldspars), lithic fragments (44%), and other minor-trace constituents, including micas, chlorite, glauconite (in burrow), opaque iron-oxide minerals, and organic materials (including recognizable plant fragments)

Detrital matrix (75%) of silt-clay, semi-pervasive, streaky-patchy with sedimentary layering. Moderately burrowed.

Visible porosity (shown in blue) estimated as 11%, principally as intergranular to burrow-filling grains (coarser).

Effectiveness: poor-fair parallel to layering, poor perpendicular to layering.

Appreciable microporosity, associated with clays. Cement not apparent, some iron-oxide could be authigenic/diagenetic.

This sample has undergone slight apparent compaction.

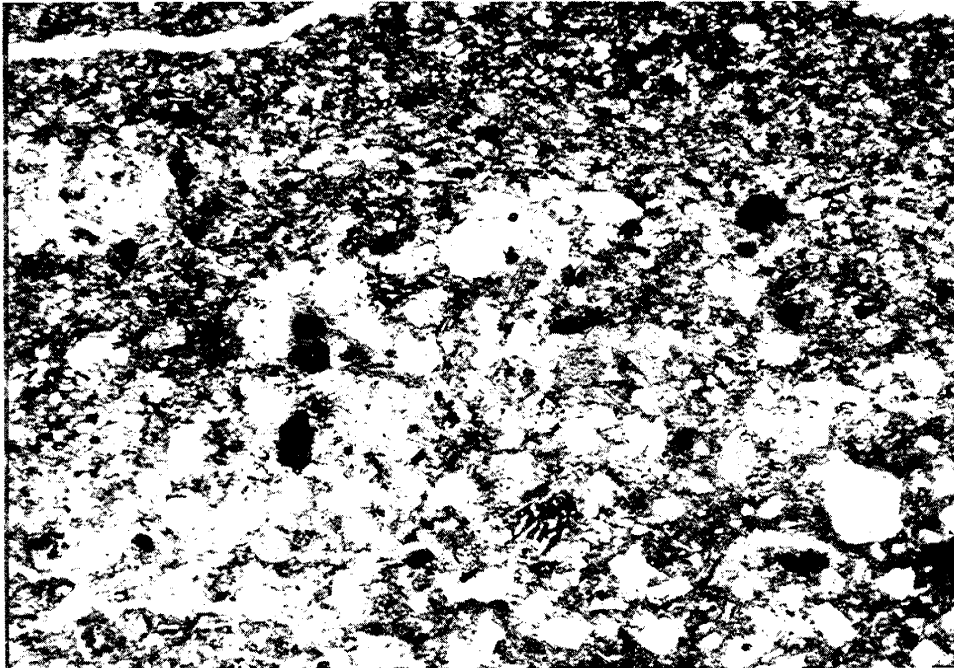


Figure IV-12: Ugnu SWPT #1, 3241' (50 X PL).

**C1(m) Ugnu SWPT #1, 3235' (Lower Ugnu (?) Zone).**

Description:

Sandy Siltstone. Sand-size grains (31%): predominantly very fine, fine, and medium sand-sized, with trace amounts of coarse sand-sized materials, very poorly (bimodally?) sorted, angular/subangular/subrounded, consisting of quartz (30%), feldspars (10%; plagioclase and potassium feldspars), lithic fragments (38%), and other minor constituents, including micas, chlorite, glauconite, epidote, opaque iron-oxide minerals (4%), and organic materials (15%; including recognizable plant fragments).

Detrital matrix (57%) of silt-clay, semi-pervasive/lense-like/ patchy-fair sedimentary layering. Moderately burrowed.

Visible porosity (shown in blue) estimated as 12%, principally as intergranular, particularly associated with burrow-filling grains of coarser material. Effectiveness: fair-poor.

Fair amount of microporosity, associated with clays. Cement not apparent.

This sample has undergone slight apparent compaction.

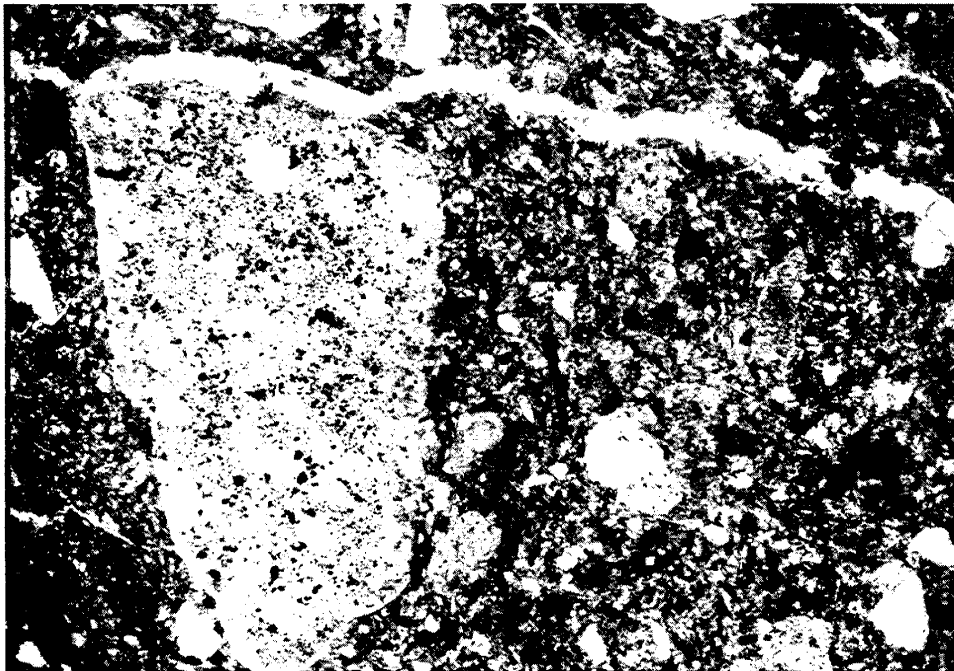


Figure IV-13: Ugnu SWPT #1, 3235' (50 x PL).

**C1(n) Ugnu SWPT #1, 3174' (Lower Ugnu (?) Zone).**

Description:

Lithic Wacke. Framework grains (47%): predominantly coarse sand-sized, with subordinate amounts of medium sand-sized materials, (rock is bimodally sorted), angular/subangular/subrounded, consisting of quartz (23%), feldspars (14%; plagioclase and potassium feldspars), lithic fragments (62%), and other minor-trace constituents, including micas, chlorite, glauconite, opaque iron-oxide minerals, and organic materials.

Detrital matrix (41%) of semi-pervasive silt-clay among framework grains.

Visible porosity (shown in blue) estimated as 13%, principally as intergranular, with an appreciable proportion as microporosity, associated with clays. Effectiveness: low.

Moderate microporosity, associated with clays. Cement consists of traces of quartz overgrowths on some framework grains; some of the "matrix" clays might, rather, represent diagenetic clay "cement."

This sample has undergone slight apparent compaction.

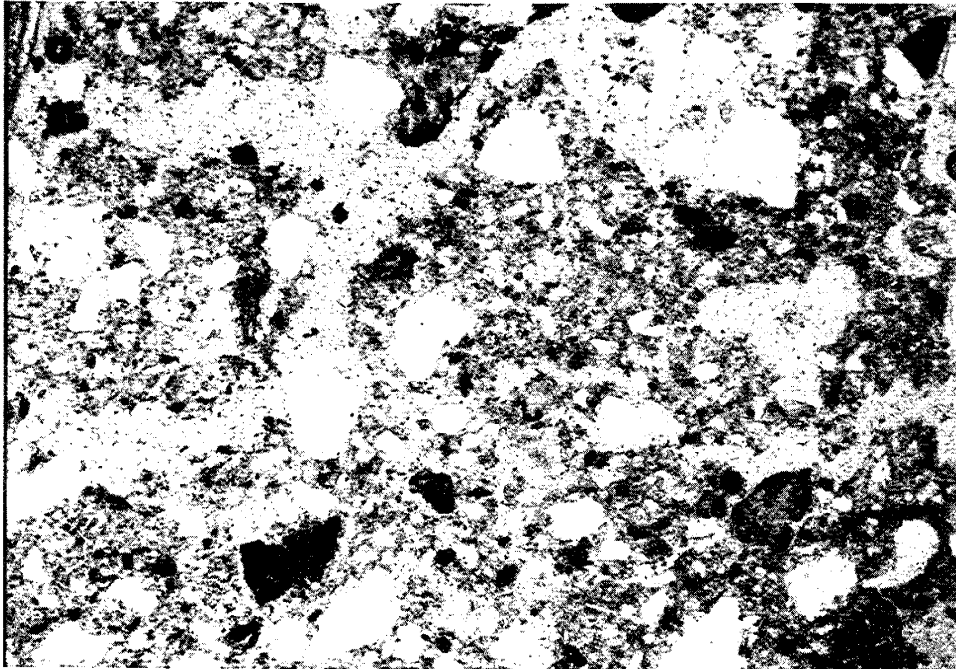


Figure IV-14: Ugnu SWPT #1, 3174' (50 x PL).

**C1(o) Ugnu SWPT #1, 3128' (Lower Ugnu (?) Zone)**

Description:

Siltstone. Sand-size grains (10%): predominantly very fine sand-sized, moderately sorted, angular/subangular, consisting of quartz (59%), feldspars (18%; plagioclase and potassium feldspars), lithic fragments (4%), and other minor-trace constituents, including micas, chlorite, glauconite, opaque iron-oxide (10%) minerals, organic (7%) materials and patches of residual hydrocarbons.

Detrital matrix (79%) principally of silt, with subordinate clay. Vague sedimentary layering.

Visible porosity (shown in blue) estimated as 11%, principally as microporosity, with intergranular porosity as well. Effectiveness: marginal-fair(?). Cement not apparent.

This sample has undergone slight apparent compaction.

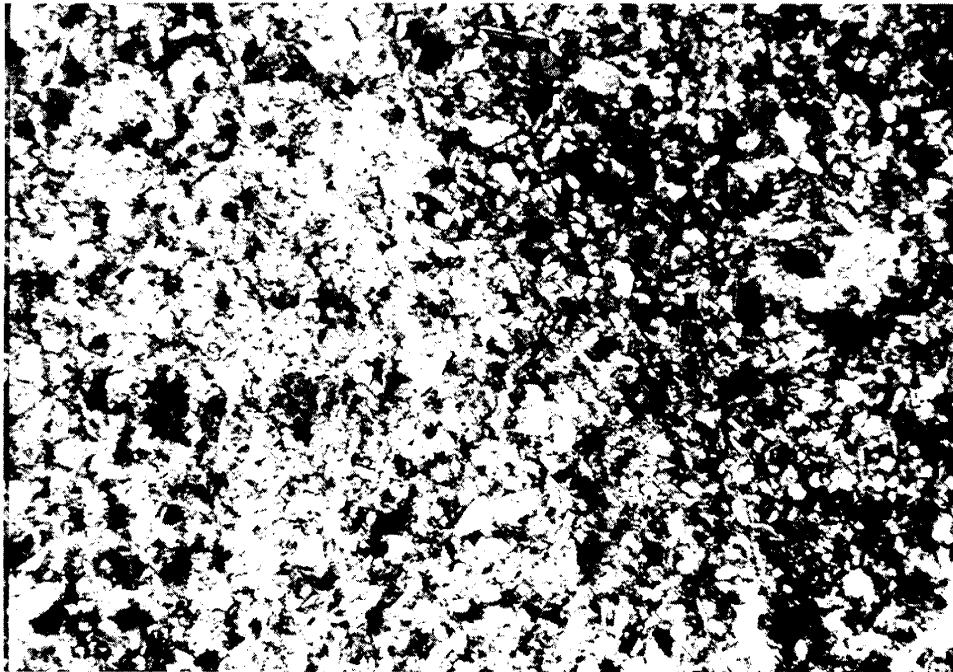


Figure IV-15: Ugnu SWPT #1, 3128' (50 x PL).

**C1(p) Ugnu SWPT #1, 3112' (Lower Ugnu (?) Zone).**

Description:

Lithic Wacke. Framework grains (51%): predominantly fine sand-sized, with subordinate amounts of medium and coarse sand-sized materials, moderately sorted, angular/subangular/subrounded, consisting of quartz (38%), feldspars (13%; plagioclase and potassium feldspars), lithic fragments (45%), and other minor-trace constituents, including micas, chlorite, glauconite(?), opaque iron-oxide minerals, and organic materials (3%).

Detrital matrix (26%) intergranular to framework grains, and as layers enriched in silt clay.

Visible porosity (shown in blue) estimated as 24%, principally as intergranular, with an appreciable component of microporosity as well.

Effectiveness: good-fair. Cement not apparent. However, an appreciable proportion of the "matrix" clays might well, rather, represent diagenetic "cement."

This sample has undergone slight apparent compaction.

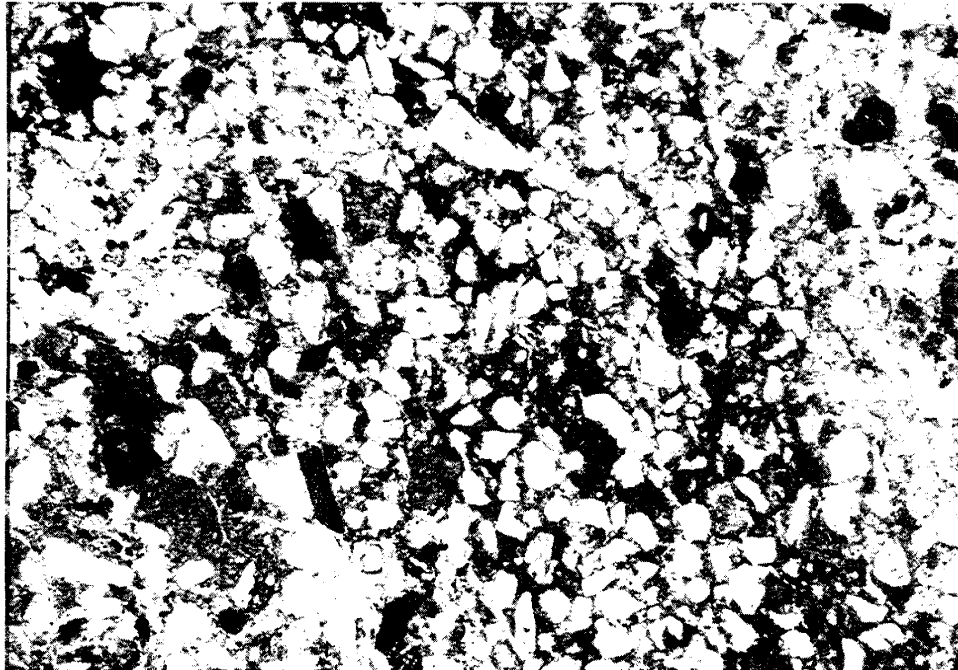


Figure IV-16: Ugnu SWPT #1, 3112' (50 X PL).

C1(q) Ugnu SWPT #1, 3059' (Lower Ugnu Zone).

Description:

Litharenite. Framework grains (54%): predominantly coarse sand-sized, with trace amounts of very fine-sized materials, (rock is well/bimodally(?) sorted), angular/subangular/subrounded, consisting of quartz (18%), feldspars (4%; plagioclase and potassium feldspars), lithic fragments (77%), and other minor-trace constituents, including micas, glauconite and epidote. There is appreciable residual hydrocarbon material as well.

Detrital matrix (46%) questionable/optically indeterminate; much of this may, rather, represent hydrocarbon-occupied pore space(?). Some clay material is recognizable.

Visible porosity is optically indeterminate, but could be on the order of as much as 30+% of the specimen. Such porosity would be principally intergranular, with some associated minor microporosity. Effectiveness: good-fair. Cement not apparent, although some/much of the "matrix" clays which are present may well represent diagenetic "cement."

This sample has undergone slight apparent compaction.

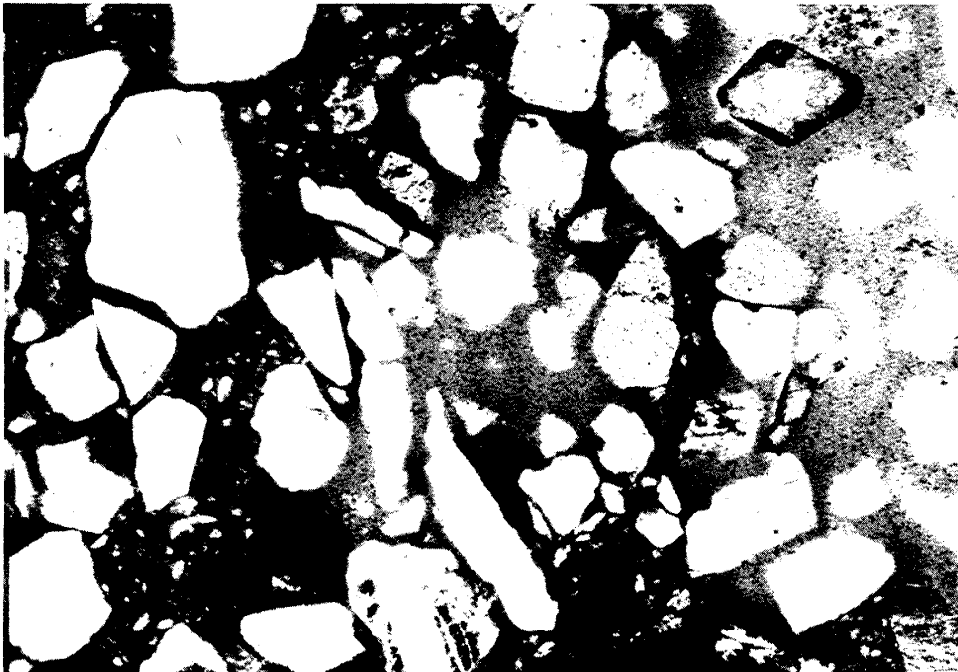


Figure IV-17: Ugnu SWPT #1, 3059' (50 x PL).

**C1(r) Ugnu SWPT #1, 2996' (Upper Ugnu Zone).**

Description:

Litharenite. Framework grains (64%): predominantly very fine sand-sized, with trace amounts of fine and medium sand-sized materials, well sorted, angular/sub-angular/subrounded, consisting of quartz (50%), feldspars (2%; plagioclase and potassium feldspars), lithic fragments (47%), and other minor-trace constituents, including micas, chlorite, glauconite(?). Also appreciable residual hydrocarbons.

Detrital matrix (37%?) questionable/optically indeterminate, due to presence of hydrocarbon material. Some clay material is recognizable, but much of the "matrix" here may, rather, represent porosity, which thus could be on the order of as much as 30%, or greater. This would be principally intergranular, with some microporosity.

Effectiveness: good. Cement not apparent, although at least some of the intergranular clay as is actually present may well represent diagenetic clay "cement."

This sample has undergone slight apparent compaction.

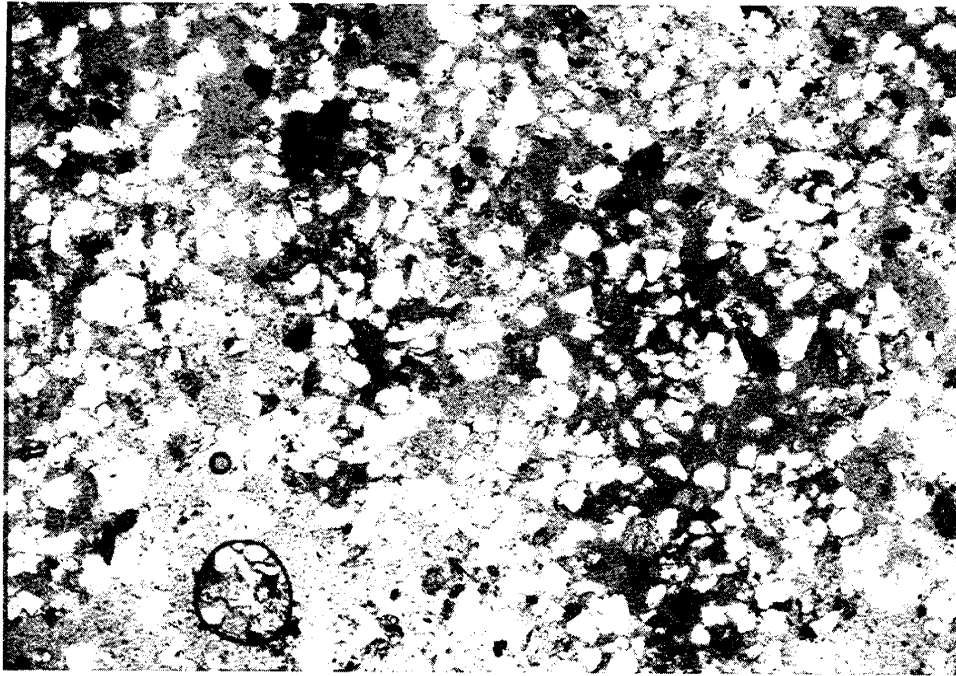


Figure IV-18: Ugnu SWPT #1, 2996' (50 x PL).

## C2. West Sak SWPT #1 Samples

The following are the results of the Petrographic analyses on the 11 Samples obtained from West Sak SWPT #1.

### C2(a) West Sak SWPT #1, 3960' (below West Sak Zone).

#### Description:

Litharenite. Framework grains (72%): predominantly very fine sand-sized, with subordinate amounts of fine sand-sized materials, well sorted, angular, consisting of quartz (30%), feldspars (3%; plagioclase and potassium feldspars), lithic fragments (64%), and other minor-trace constituents, including micas, opaque iron-oxide minerals, glauconite, and organic materials.

Detrital matrix (10%) as streaks-patches, richer in clays. Fair-good sedimentary layering.

Visible porosity (shown in blue) estimated as 15%, principally as semi-pervasive intergranular; moderately effective.

Moderate microporosity, associated with clays. Cement not apparent, although at least some of the clays might well represent diagenetic "cement."

This sample has undergone slight-moderate apparent compaction.

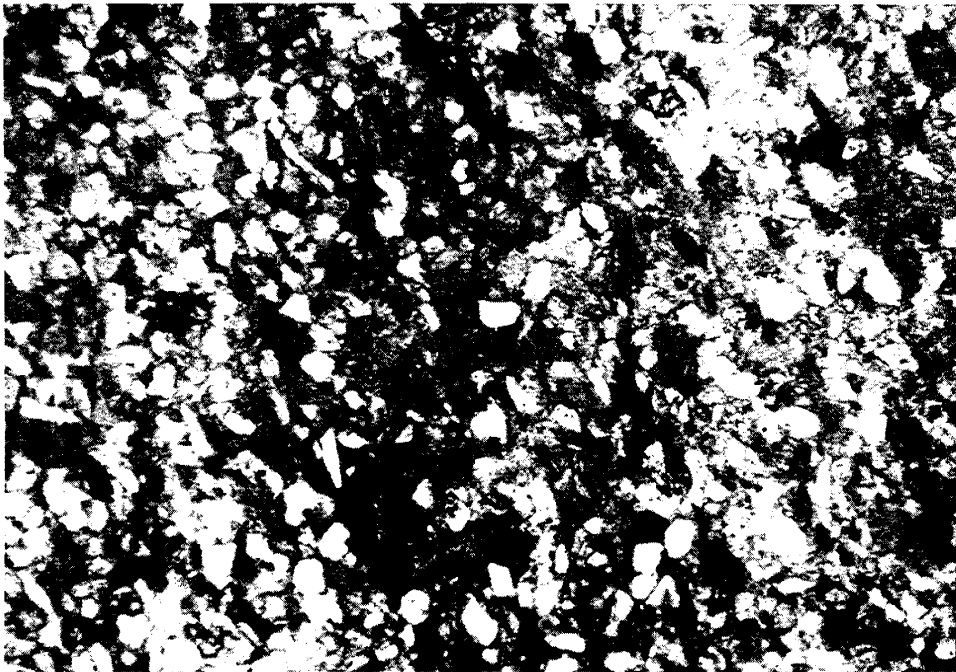


Figure IV-19: West Sak SWPT #1, 3960' (50 x PL).

**C2(b) West Sak SWPT #1, 3923' (below West Sak Zone).**

Description:

Lithic Wacke. Framework grains (58%): predominantly very fine sand-sized, with subordinate amounts of fine and medium sand-sized materials, moderately-poorly sorted, very angular/angular/subangular, consisting of quartz (40%), feldspars (5%; plagioclase and potassium feldspars), lithic fragments (50%), and other minor-trace constituents, including micas, chlorite, glauconite, and organic materials.

Detrital matrix (37%) as lenses-streaks-patches, richer in silt-clays. Fair sedimentary layering, with moderate burrowing.

Visible porosity (shown in blue) estimated as 5%, principally as patchy intergranular; poorly effective.

Moderate microporosity, associated with clays. Cement not apparent, although some of the clays might well represent diagenetic "cement." Irregular patches of iron-oxide minerals (after sulfides?) are scattered within rock.

This sample has undergone slight apparent compaction.

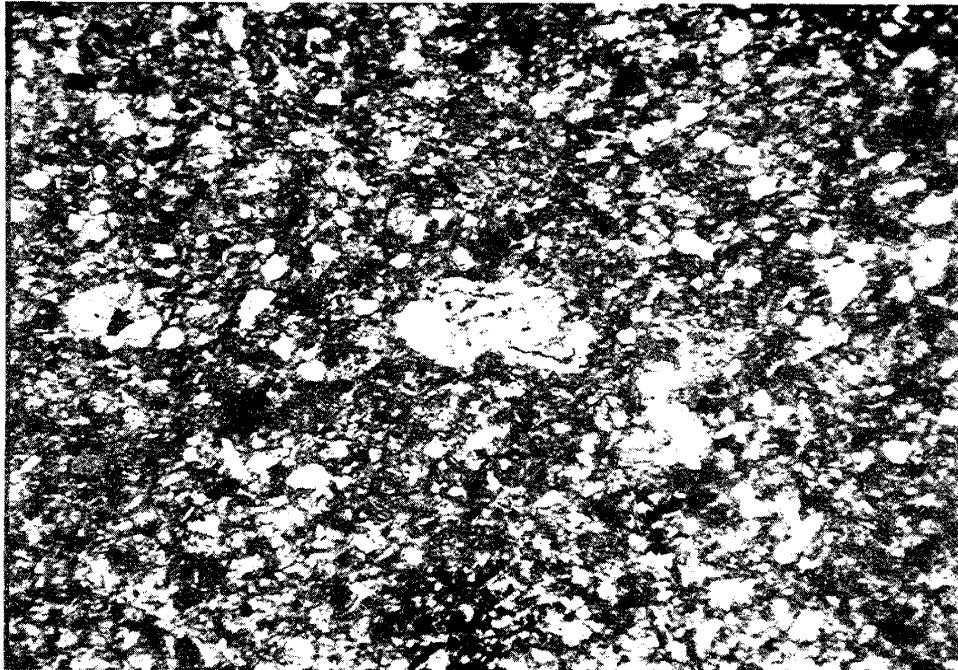


Figure IV-20: West Sak SWPT #1, 3923' (50 x PL).

**C2(c) West Sak SWPT #1, 3917' (below West Sak Zone).**

Description:

Siltstone. Sand-size grains (35%): predominantly fine and very fine sand-sized, with trace amounts of medium sand-sized materials, poorly sorted, angular/sub-angular, consisting of quartz (46%), feldspars (7%; plagioclase and potassium feldspars), lithic fragments (44%), and other minor-trace constituents, including micas, chlorite, glauconite, and organic materials.

Detrital matrix (59%) of silt and clays. Fair sedimentary layering, with streaks-patches of sand-size grains. Moderately burrowed.

Visible porosity estimated as 3%, principally as intergranular to sand-size grains in burrow fillings. Discontinuous-poorly effective.

Microporosity, associated with clays. Cement not apparent., although some of the clays might represent diagenetic "cement." Pyrite (3%) as framboids, aggregates, irregular masses, some in excess of 1.0 mm in size; of authigenic/diagenetic origin.

This sample has undergone slight apparent compaction.

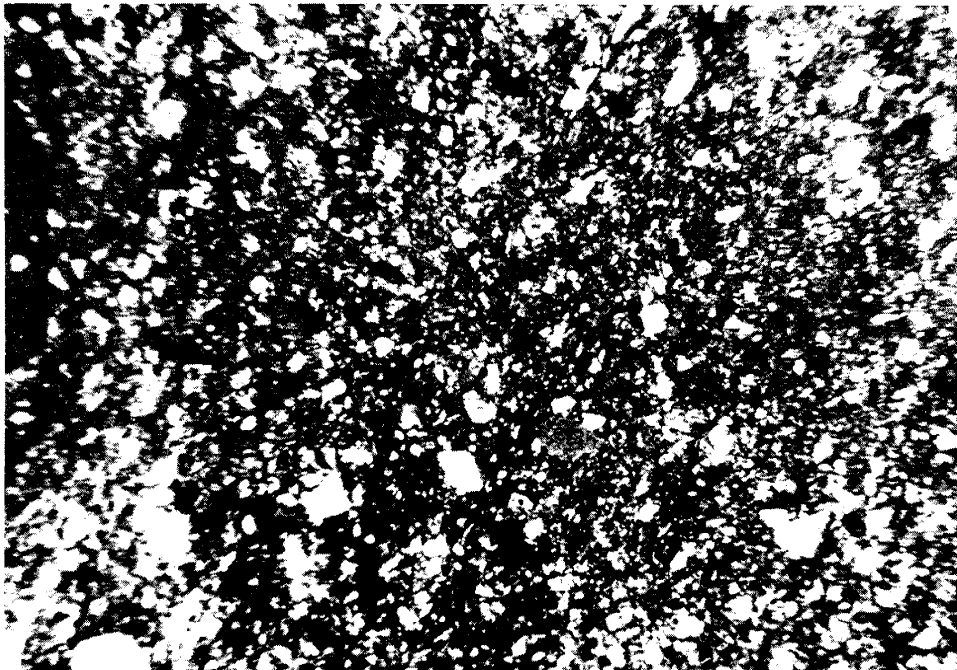


Figure IV-21: West Sak SWPT #1, 3917' (50 x PL).

**C2(d) West Sak SWPT #1, 3953' (below West Sak Zone).**

Description:

Lithic Wacke/Siltstone. Framework grains (43%): predominantly very fine sand-sized, with subordinate amounts of fine and medium sand-sized materials, poorly sorted; angular/subangular/subrounded, consisting of quartz (48%), feldspars (3%; plagioclase and potassium feldspars), lithic fragments (46%), and other minor-trace constituents, including micas, chlorite, glauconite, and organic materials (pervasive, evenly distributed; plant fragments, etc.).

Detrital matrix (46%) as streaks-patches of silt and clay-rich material. Fair sedimentary layering, moderately burrowed.

Visible porosity (shown in blue) estimated as 4%, principally as intergranular to sand-size grains in burrow fillings. Discontinuous, and poorly effective

Microporosity, associated with clays. Cement not apparent., although some of the clays might represent diagenetic "cement." Pyrite (3%) as authigenic/diagenetic aggregates; irregular/sub-euhedral; some as large as 2.5 mm, some, at least, associated with burrows.

This sample has undergone slight apparent compaction.

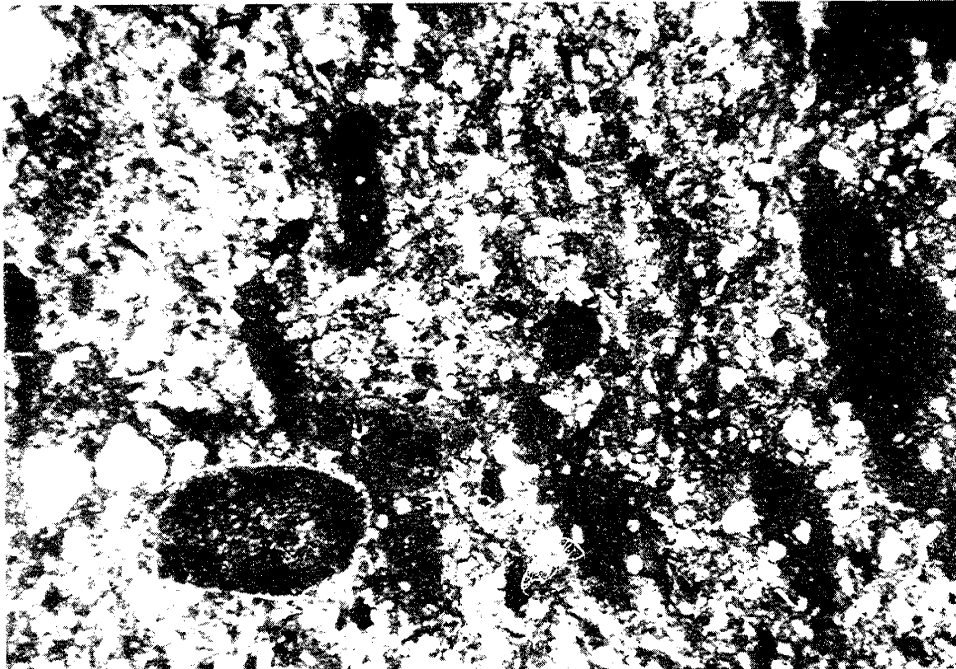


Figure IV-22: West Sak SWPT #1, 3953' (50 x PL).

C2(e) West Sak SWPT #1, 3812' (West Sak Zone).

Description:

Lithic Wacke. Framework grains (60%): predominantly very fine sand-sized, with trace amounts of fine sand-sized materials, poorly sorted, angular/subangular/sub-rounded, consisting of quartz (35%), feldspars (3%; plagioclase and potassium feldspars), lithic fragments (58%), and other minor-trace constituents, including micas, chlorite, glauconite, and organic materials (including recognizable plant fragments).

Detrital matrix (33%) pervasive. Fair sedimentary layering. Moderately burrowed.

Visible porosity (shown in blue) estimated as 6%, principally as patchy areas, intergranular; some, at least, associated with burrows; poorly effective.

Microporosity, associated with clays. Cement not apparent, some clay might represent diagenetic "cement."

This sample has undergone slight apparent compaction.

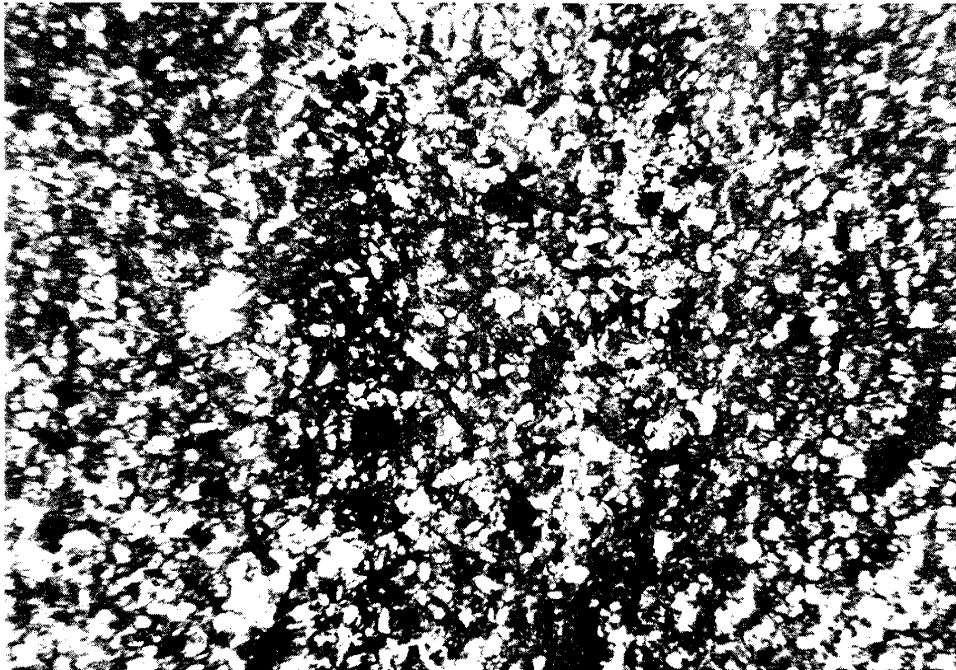


Figure IV-23: West Sak SWPT #1, 3812' (50 x PL).

C2(f) West Sak SWPT #1, 3804' (West Sak Zone).

Description:

Lithic Wacke. Framework grains (70%): predominantly very fine sand-sized, with subordinate amounts of fine sand-sized materials, poorly-moderately sorted, angular/subangular/subrounded, consisting of quartz (38%), feldspars (5%; plagioclase and potassium feldspars), lithic fragments (54%), and other minor-trace constituents, including micas, chlorite, glauconite, and organic materials.

Detrital matrix (19%) as patches richer in silt and clays. Fair sedimentary layering. Moderately burrowed.

Visible porosity (shown in blue) estimated as 11%, principally as semi-pervasive intergranular; moderately effective. Somewhat patchy/discontinuous.

Moderate microporosity, associated with clays. Cement not apparent, some clay might represent diagenetic "cement." Some speculative amount of the carbonate minerals present might represent intergranular cement (?).

This sample has undergone slight apparent compaction.

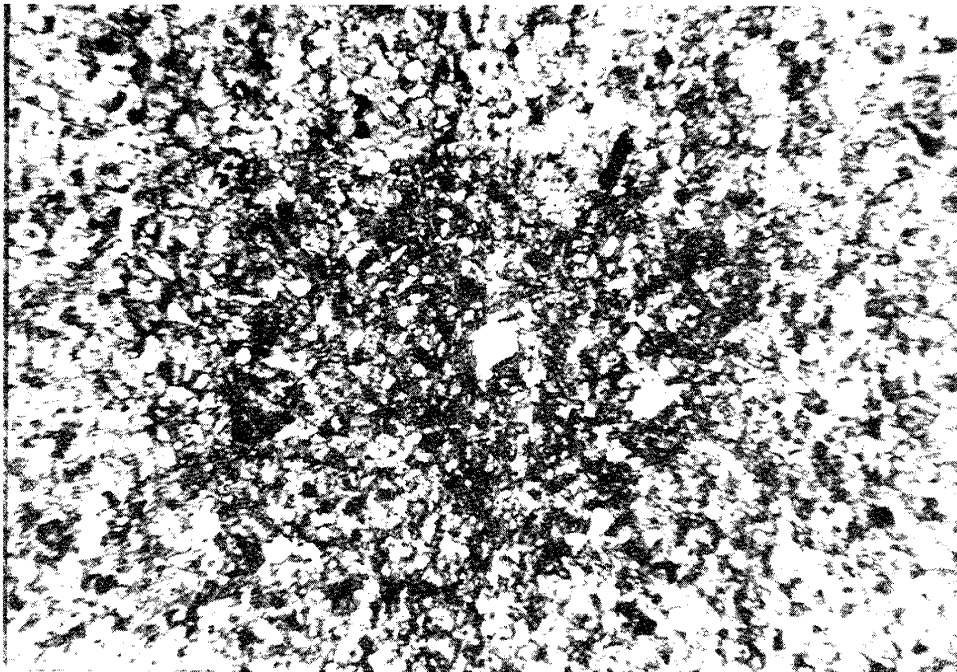


Figure IV-24: West Sak SWPT #1, 3804' (50 x PL).

**C2(g) West Sak SWPT #1, 3780' (West Sak Zone).**

Description:

Litharenite. Framework grains (68%): predominantly fine sand-sized, with subordinate amounts of very fine sand-sized materials, moderately well sorted, angular/subangular/subrounded, consisting of quartz (42%), feldspars (3%; plagioclase and potassium feldspars), lithic fragments (52%), and other minor-trace constituents, including micas, chlorite, opaque iron-oxide minerals, glauconite, and organic materials (some recognizable plant fragments).

Detrital matrix (10%) evenly disseminated, silt-clay. Faint indication of sedimentary layering.

Visible porosity (shown in blue) estimated as 13%, principally as intergranular, pervasive; moderately-highly effective.

Trace of microporosity, associated with clays. Cement not apparent, although at least some of the "matrix" clays might well represent diagenetic clay "cement." Some irregular patches of iron-oxide minerals may be reprecipitated of precursorial pyrite.

This sample has undergone slight apparent compaction.

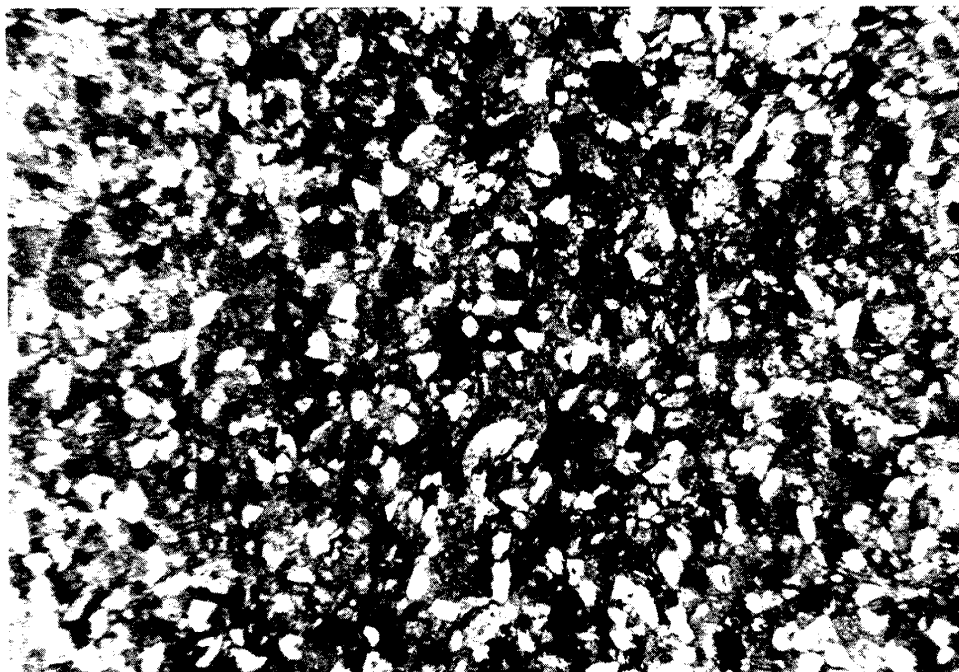


Figure IV-25: West Sak SWPT #1, 3780' (50 x PL).

**C2(h) West Sak SWPT #1, 3769' (West Sak Zone).**

Description:

Siltstone. Sand-size grains (21%): predominantly very fine sand-sized, with trace amounts of fine and medium sand-sized materials, poorly-very poorly sorted, angular/subangular/subrounded, consisting of quartz (69%), feldspars (9%; plagioclase and potassium feldspars), lithic fragments (20%), and other minor-trace constituents, including micas, chlorite, and organic materials.

Detrital matrix (76%) semi-pervasive; fair sedimentary layering. Somewhat burrowed.

Visible porosity (shown in blue) estimated as <3%, principally as intergranular, discontinuous, associated with burrow fillings; poorly effective.

Some microporosity, associated with clays.

Cement not apparent, although some of the clays might represent diagenetic "cement." Pyrite (<3%) as extremely fine-grained (framboids?) some with euhedral faces on margins. Some (<3%) iron-oxide minerals (red- and black-colored), up to 0.5 mm in size, side-by-side with pyrite particles.

This sample has undergone slight apparent compaction.

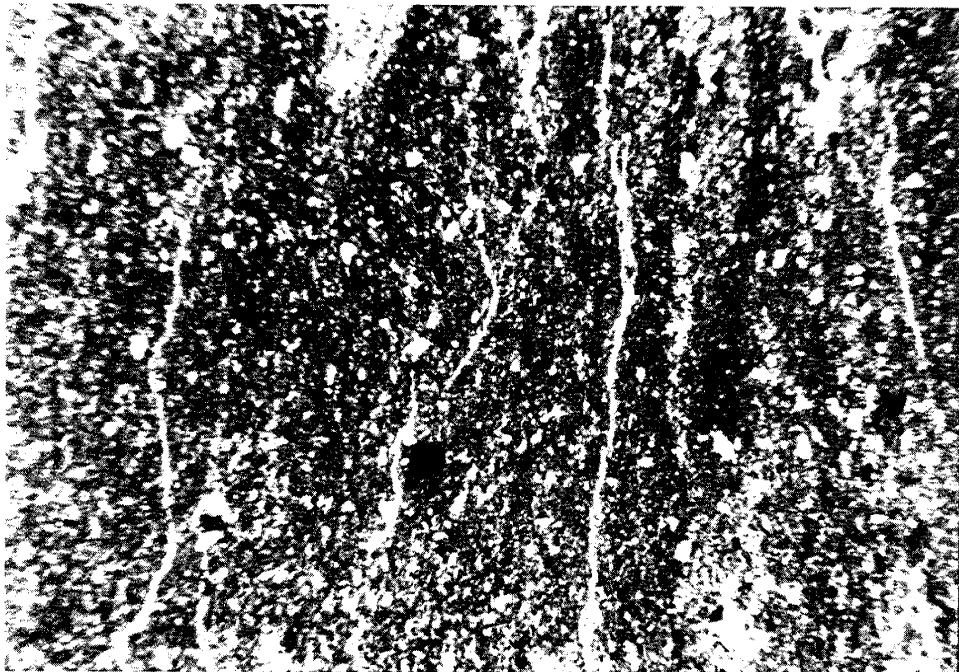


Figure IV-26: West Sak SWPT #1, 3769' (50 x PL).

**C2(i) West Sak SWPT #1, 3761' (West Sak Zone).**

Description:

Siltstone. Sand-size grains (25%): predominantly very fine sand-sized, with trace amounts of fine sand-sized materials, poorly sorted, angular/subangular/sub-rounded, consisting of quartz (44%), feldspars (8%; plagioclase and potassium feldspars), lithic fragments (40%), and other minor-trace constituents, including organic materials (5%), micas, chlorite, and glauconite (?).

Detrital matrix (69%) semi-pervasive; fair sedimentary layering, somewhat streaky-patchy. Somewhat burrowed.

Visible porosity (shown in blue) estimated as 2%, principally as intergranular to burrow-filling grains; poorly effective.

Some microporosity, associated with clays. Cement not apparent, Pyrite (4%) as irregular patches up to 1.0 mm in size; also as framboids (?) with euhedral faces projecting from margins; some with red-colored margins (hematite/goethite?).

This sample has undergone slight apparent compaction.

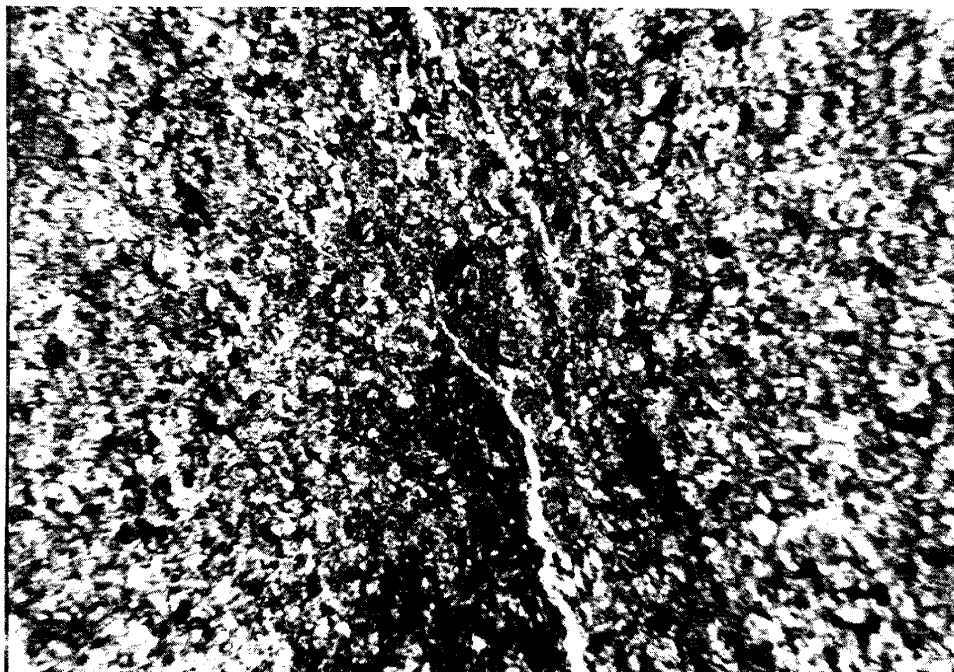


Figure IV-27: West Sak SWPT #1, 3761' (50 x PL).

C2(j) West Sak SWPT #1, 3723' (West Sak Zone).

Description:

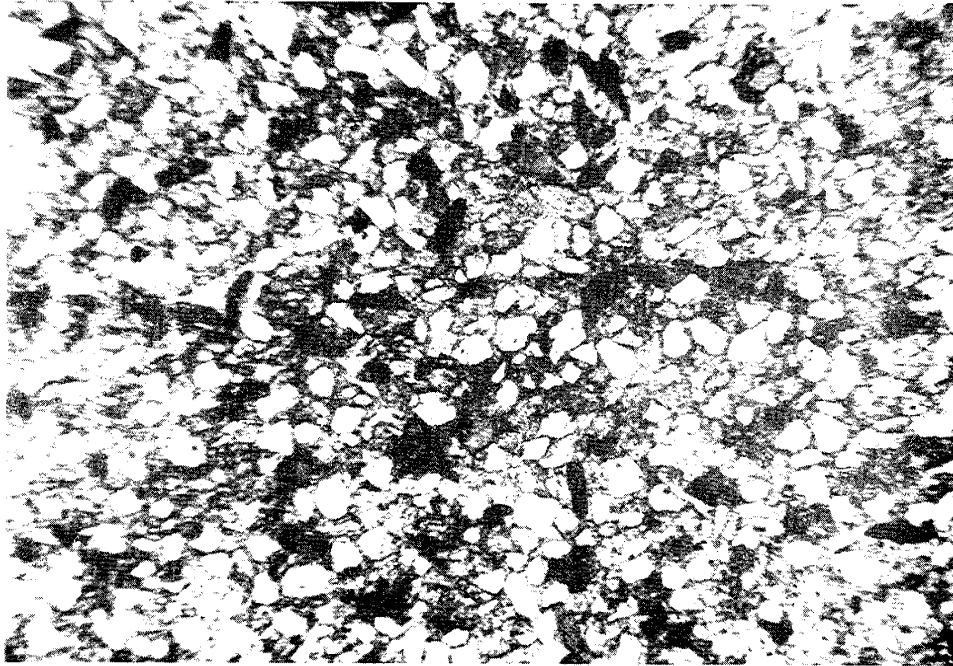
Litharenite. Framework grains (66%): predominantly fine sand-sized materials, well-very well sorted, angular/subangular/subrounded/rounded, consisting of quartz (44%), feldspars (5%; plagioclase and potassium feldspars), lithic fragments (49%), and other trace constituents, including organic materials and glauconite.

Detrital matrix essentially nil.

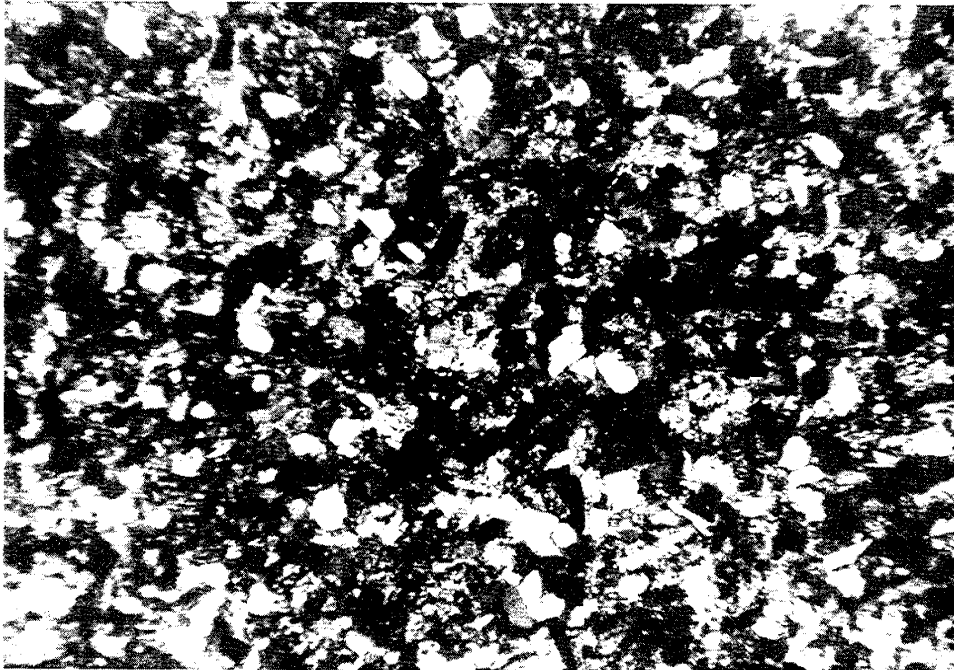
Visible porosity (shown in blue) estimated as essentially nil.

Cement (34% of sample) consists of intergranular carbonate (calcite?) mineral(s).

This sample has undergone slight apparent compaction.



A (50 X PL)



B (50 X xsPL)

Figure IV-28: West Sak SWPT #1, 3723' A (50 X PL) B (50 X xsPL).

**C2(k) West Sak SWPT #1, 3715' (above West Sak Zone).**

Description:

Siltstone. Sand-size grains (40%): predominantly fine and very fine sand-sized materials, poorly-very poorly sorted; angular/subangular/subrounded, consisting of quartz (34%), feldspars (9%; plagioclase and potassium feldspars), lithic fragments (49%), and other minor-trace constituents, including micas, chlorite, glauconite, and organic materials (5%).

Detrital matrix (55%) patchy-streaky/semi-pervasive; fair sedimentary layering, somewhat burrowed.

Visible porosity (shown in blue) estimated as 4%, principally as discontinuous patches of intergranular, associated with burrow-filling grains. Poorly effective.

Some microporosity, associated with clays. Cement not apparent, Pyrite (2%) as irregular patches up to 0.6 mm in size; some with euhedral faces on margins, representing authigenic/diagenetic materials.

This sample has undergone slight apparent compaction.

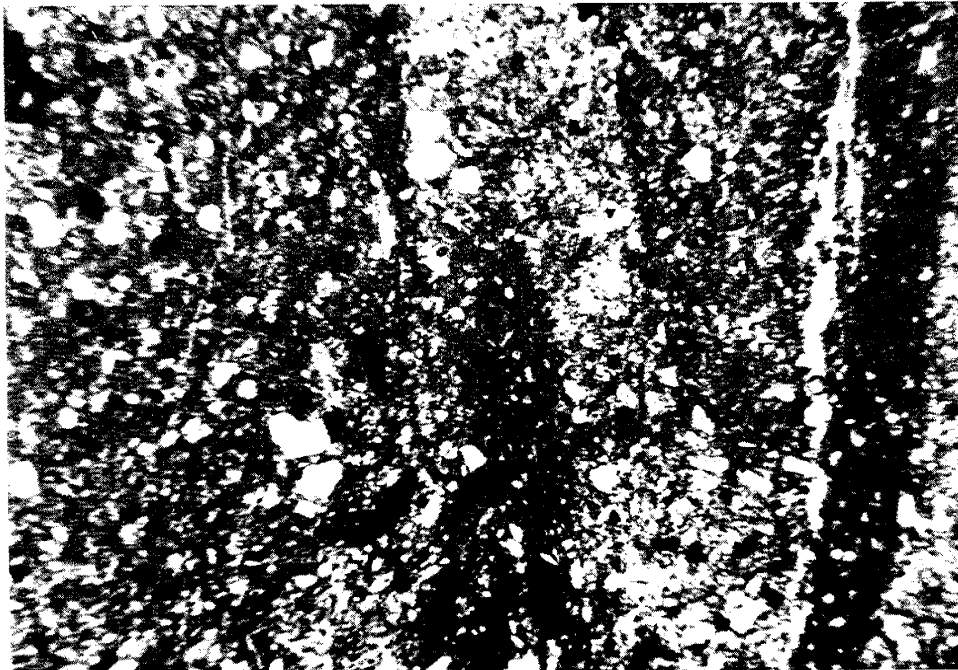


Figure IV-29: West Sak SWPT #1, 3715' (50 x PL).



## CHAPTER V: ENDICOTT FIELD

---

### A. OVERVIEW AND GEOLOGY OF ENDICOTT FIELD

Endicott field is located in the Beaufort Sea, approximately eight miles east of Prudhoe Bay and one to four miles offshore from the Sagavanirktok River delta (Figures V-1 and V-2). It is the first Arctic offshore field to be developed, and is being produced from artificial gravel islands. Original oil-in-place was estimated at one billion stock tank barrels and original gas reserves were estimated to be three-quarters of a trillion cubic feet (Woidneck et al., 1987).

Production is from Mississippian Kekiktuk formation, within the Endicott group (Figure V-3), where it is positioned on a major North Slope structural feature aligned from northwest to southeast beneath Alaska's Arctic shoreline. The northern most extent of the Endicott group (including Kekiktuk) reaches to the Barrow Arch along only its most southeastern extent. It is in this area that Endicott field is found.

Woidneck et al., (1987) have described the Kekiktuk formation at Endicott in terms of three fluvial lithostratigraphic units, labeled from bottom to top as Zones 1, 2, and 3. Zone 1, Early Viséan in time, is shaly but includes interbedded coal and sandstone layers. It was depositionally located within a slowly-subsiding intermontaine basin that was being buried by fine-grained terrigenous and coal-forming deposits. As such, it is comprised primarily of swampy, low energy deposits. Sediment influx was from low-lying source areas surrounding the basin. As expected from this depositional environment, Zone 1 is not the predominant hydrocarbon bearing zone at Endicott.

Relative uplift of a sedimentary source area northeast of Endicott field during mid-Viséan time allowed for development of a braided-stream system proximal to the source area and a distal meandering stream system. It was this environment that resulted in Zone 2 braided stream deposition. The major area of braided stream sand deposition formed southeast of Endicott field, but a secondary axis of deposition developed concurrently near the Endicott field. Down-to-the-southwest syndepositional faulting during Zone 2 time is evidenced by local Zone 2 thickening adjacent to the downthrown side of northwest striking faults.

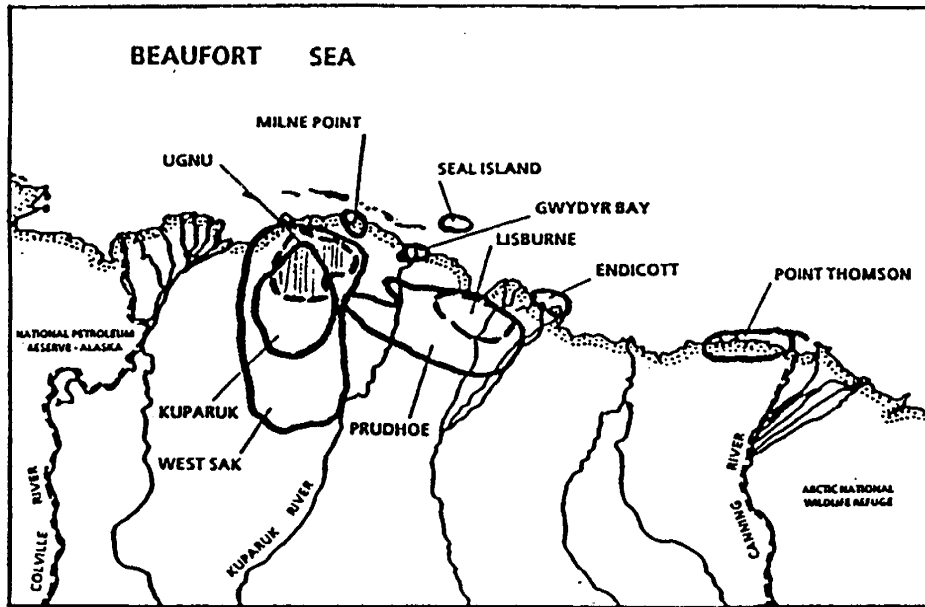


Figure V-1. Alaska North Slope Fields, Including Endicott.

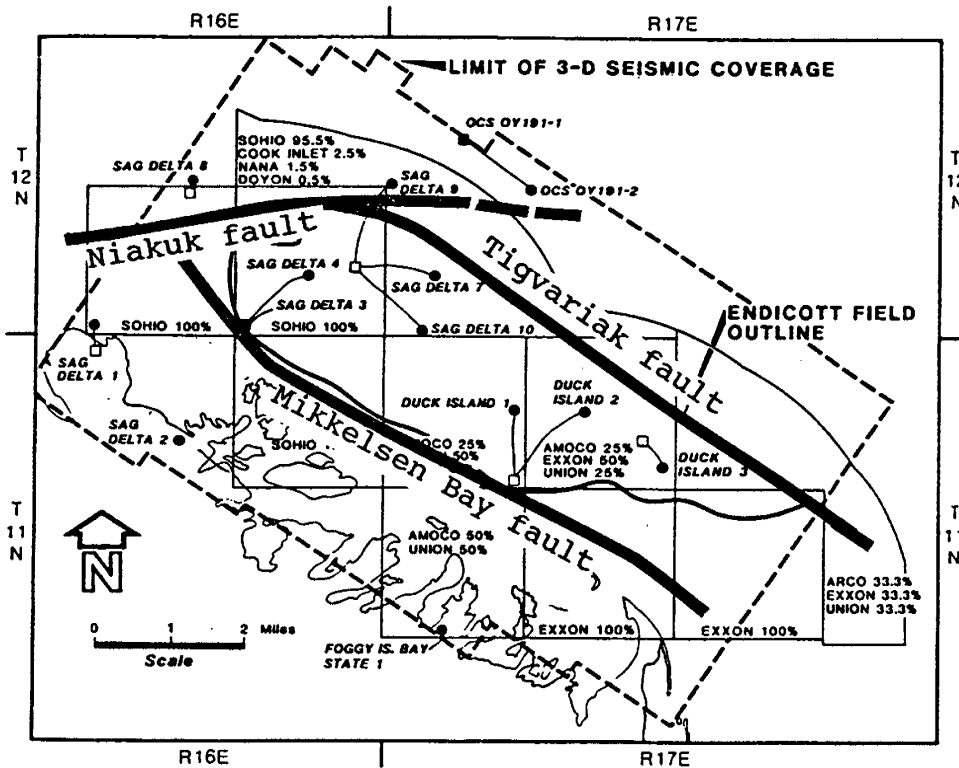


Figure V-2. Endicott Delineation Wells and Faulting (adapted from Woidneck et al., 1987).

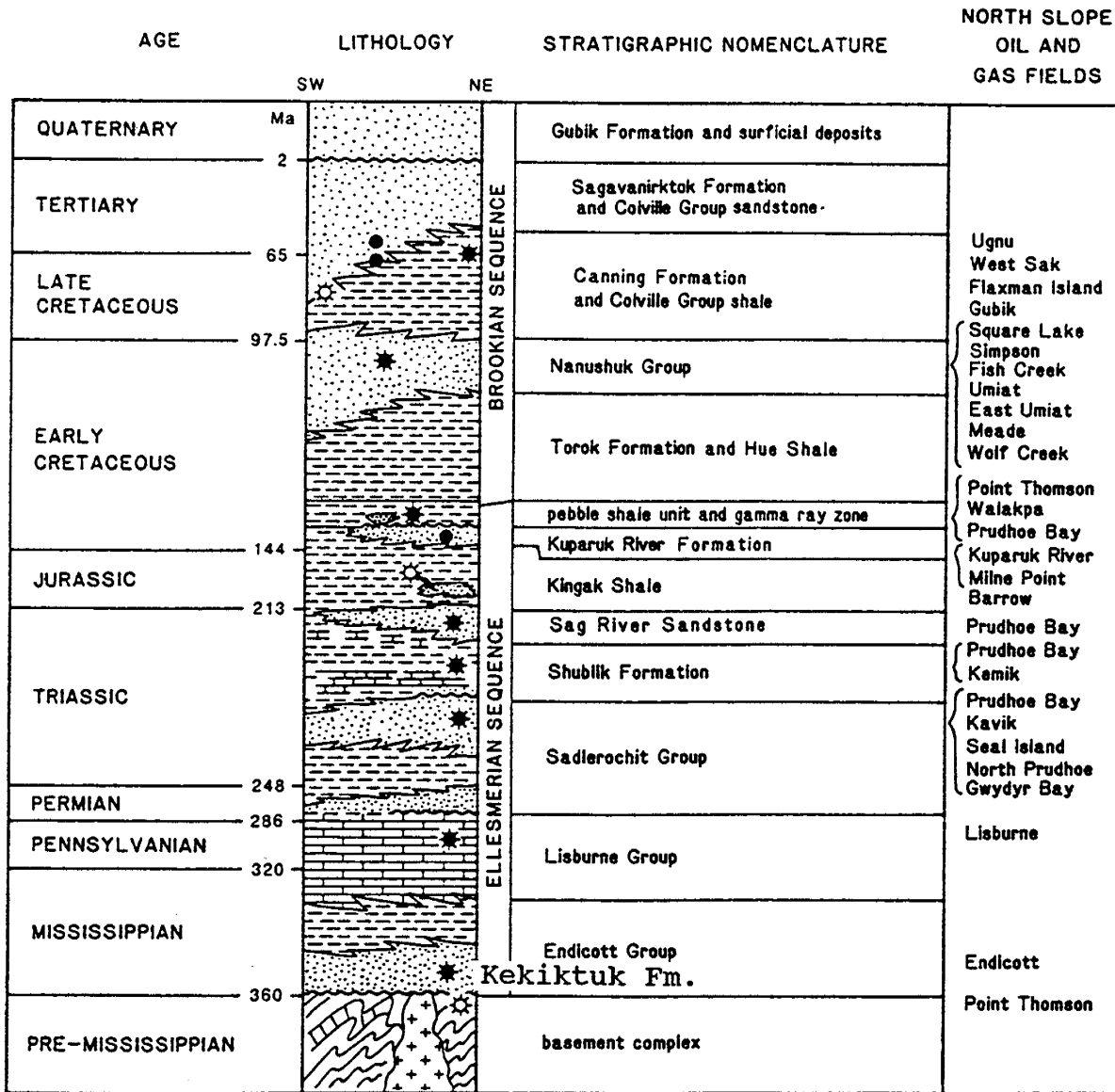


Figure V-3. Generalized North Slope Stratigraphic Column (adapted from Bird, 1987).

Although generally composed of high-energy, unconsolidated braided river deposits, Zone 2 also includes both permanent and ephemeral lake deposits. The braided streams led to medium-to-coarse grained multi-layered sandstone bedsets while lake deposition resulted in shales. Minor conglomerate and coal zones also occur in Zone 2. Commonly occurring upward-fining sand bodies near the top of this zone are interpreted as amalgamated point bar deposits and probably represent an increase in stream sinuosity. Woidneck et al. (1987) have determined overall sand proportions in Zone 2 to be greater than 60%. Such a high proportion of sand is believed to be a result of overlapping sand bodies coalescing to form sheet-like deposits.

The top of Zone 2 is frequently indicated by a barrel or blocky shaped gamma ray profile, and is often 50 to 100 feet beneath a major correlatable coal bed in Zone 3. However, in contrast to the identifiable boundary separating Zone 2 from Zone 1, the transition from Zone 2 to Zone 3 is gradual, resulting in some degree of uncertainty in pinpointing the top of Zone 2. This zone is subdivided into Zones 2A and 2B by a shale interval near its center. Zones 2 and 3 are the major Endicott producing intervals.

Zone 3 is interpreted by Melvin (1987) as consisting of point bar deposits within the meandering stream system. This is consistent with a changing Late-Visean depositional environment at Endicott. Although syndepositional faulting continued, the energy of the fluvial system diminished due to lowered source terrain relief (in response to erosion), or displacement of tectonic activity and associated high energy activity northwestward. Sandstones with lesser amounts of conglomerate and coal make up this zone. Evidence of point bar deposition is found in the abundance of stacked, upward-fining sequences with basal conglomerates. Interbedded floodplain mudstones and fine-grained sandstones deposited within interchannels of the floodplain also occur. Zone 3 is subdivided into three subzones (A, B, and C from bottom to top). Zones 3A and 3C are sand prone and separated by a major shaly interval (Zone 3B). The top of Zone 3 is gradational and difficult to determine exactly.

Table V-1 summarizes Kekiktuk lithostratigraphic zones as defined above for the Endicott locality. To the west and south, Zone 3 grades laterally into the overlying Kayak shale, and Zone 2 pinches out. Zone 1 onlaps basement just west of the Prudhoe Bay State well No. 1 (Woidneck et al., 1987). As such, the zonal definitions in Table V-1 are limited primarily to the Endicott area.

**Table V-1: Endicott Lithostratigraphic Zones and Subzones (Woidneck et al., 1987).**

<b>Kekiktuk Interval</b>	<b>Zone</b>	<b>Subzone</b>
Upper	3	3C 3B 3A
Middle	2	2B 2A
Lower	1	--

The Kekiktuk formation at Endicott makes up a northwest trending elongate depocenter which thickens southeastward beyond the field limits. Net sandstone thickness also follows this trend. Despite thinner Kekiktuk isopachs within Endicott, high primary porosity combined with porosity enhancement by dissolution of framework grains and cement led to better reservoir conditions here. Low primary porosity south and west of Endicott is partly due to decreased grain size. In addition, Woidneck et al. (1987) believe that lower permeability associated with smaller grain size may have led to greater cementation and suppressed development of secondary porosity in these areas.

A combination of structure and stratigraphy form the trap in which Endicott hydrocarbon accumulations occur. Woidneck et al. (1987) have determined that this trap formed partly in response to tilting of an antiformal fault block which dips four to six degrees southwest. The crestal portion of the trap is truncated by a major unconformity (the Lower Cretaceous Unconformity or LCU) which dips gently to the southeast. Seal-forming marine shales of the Lower Cretaceous "Highly Radioactive Zone" (HRZ) overlie the LCU.

Major normal faults define three sides of the field (Figure V-2). The northwest striking Mikkelsen Bay and Tigvariak faults enclose the western and eastern sides, respectively. Both faults have a down-to-the-west sense of movement. The northern limit of the field occurs along the west striking, down-to-the-north Niakuk fault zone. Shales of the Itkilyariak formation form a barrier to upward hydrocarbon migration over the untruncated portion of the structure. Figure V-4 describes the stratigraphic relationship of these formations.

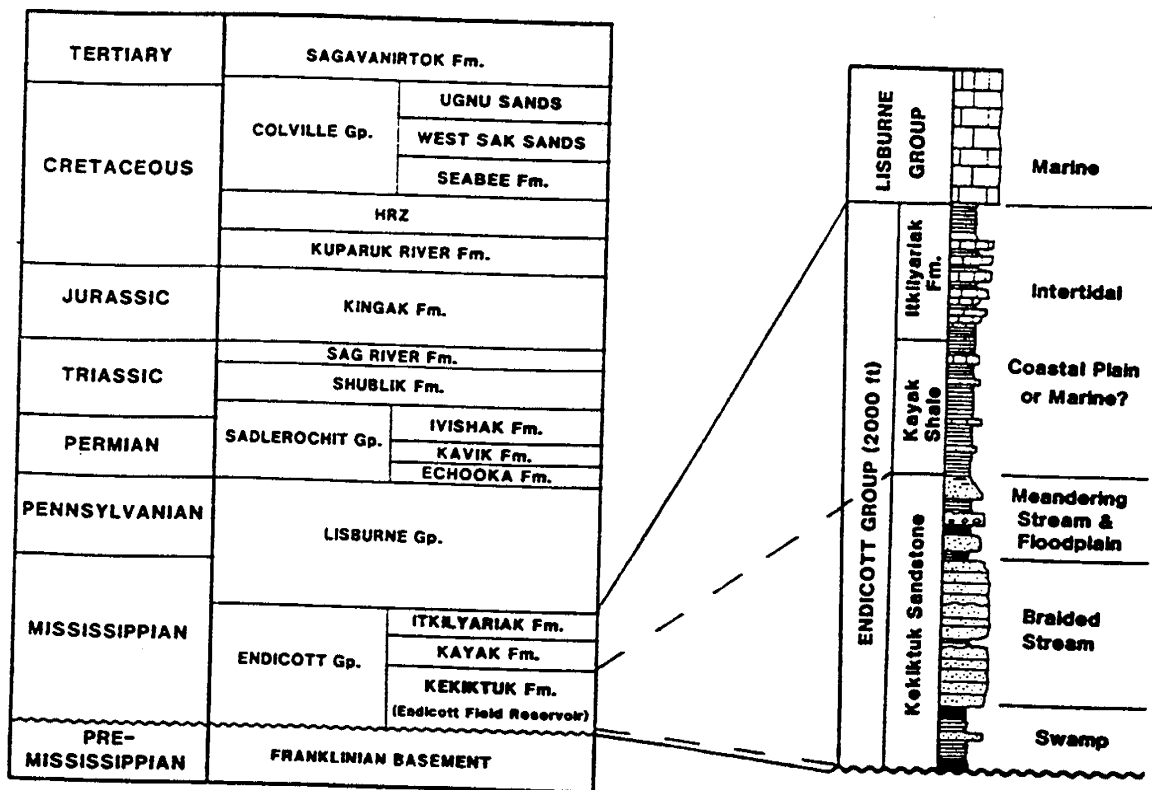


Figure V-4. Endicott Group Stratigraphic Position and Lithologic Description (Woidneck et al., 1987).

Seismic data indicate that Endicott faults can be categorized into one group which was active synchronous with and after LCU time, and into another group which was not. The Niakuk fault zone falls in the former category. The Mikkelsen Bay and Tigvariak faults fall in the latter, as the LCU is unbroken by these faults. They were active during Late Mississippian time, having affected Kekiktuk and Kayak deposition. Seismic and geologic analysis of offsets of several Kekiktuk coal markers across the Mikkelsen Bay fault indicate this fault to be a growth fault during Kekiktuk time with greatest sediment accumulation on the downthrown side. Because growth does not occur in the shallower Itkilyariak formation, syndepositional fault movement within the Endicott group is constrained to pre-Itkilyariak time. The Niakuk fault zone offsets the LCU, indicating post-Lower Cretaceous movement on this fault. Greater amounts of offset associated with pre-LCU horizons indicate pre-LCU movement also occurred across the Niakuk fault.

## **B. ENDICOTT RESERVOIR DESCRIPTION PROCEDURE**

Following a review of the literature discussing Endicott field, the Endicott zones were identified at key wells and correlated throughout the wells in the field. Correlation entailed visual inspection and comparison of well log traces from neighboring wells. Occasionally, the correlation process was aided by listings of zone tops in well completion reports obtained from AOGCC. The computer programs developed by Scientific-Software Intercomp, LOGCALC, were then used in the conversion of data from measured well depths (MWD) to true vertical depths (TVD), in generation of cross sections, and in the detailed well log analysis. Surf II, a contouring program written by the Kansas Geological Survey, was utilized in generation of contour plots.

The comprehensive article by Woidneck et al. (1987) provided values of input parameters for log analysis, including reservoir salinity, formation temperature, and the tortuosity and cementation exponents. The primary objective of Endicott well log analysis to date has been to determine the petrophysical properties of each zone as defined in the literature. In general, the Endicott field presents a complicated combination of faulting, structure, and lateral stratigraphic variation. As such, reservoir zones may not represent time stratigraphic units, but rather, as Woidneck et al. (1987) stated, lithostratigraphic units composed of rocks with similar reservoir properties. Although rocks within defined zones may transgress time lines from well-to-well, they possess common reservoir properties unique to each zone which are identifiable for correlation and well log analysis. For brevity, individual well names have been abbreviated in this report and are listed in Table V-2. A map of all

wells at Endicott is shown in Figure V-5. Figure V-6 shows the Endicott wells which have been analyzed in this report and the locations of cross sections A-A' and B-B'.

**Table V-2: Endicott Wells Utilized in Well Log Analysis to Date.**

	<b>Full Well Name</b>	<b>Abbreviated Well Name</b>
1.	Duck Island 1	Duck 1
2.	Duck Island 2	Duck 2
3.	Duck Island 3	Duck 3
4.	Sag Delta 4	SD-4
5.	Sag Delta 7	SD-7
6.	Sag Delta 10	SD-10
7.	MPI 2-4/M-19	M-19
8.	MPI 1-29/M-25	M-25
9.	MPI 2-14/O 16	O-16
10.	MPI 1-5/O 20	O-20
11.	MPI 2-34/P-14	P-14
12.	MPI 2-62/Q-17	Q-17
13.	SDI 3-33/K-37	K-37
14.	SDI 4-20/M-35	M-35
15.	SDI 4-28/P-27	P-27
16.	MPI 2-8/K-16	K-16
17.	SDI 4-42/P-38	P-38
18.	MPI 1-55/R-25	R-25
19.	MPI 2-52/S-14	S-14
20.	SDI 3-45/M-39	M-39

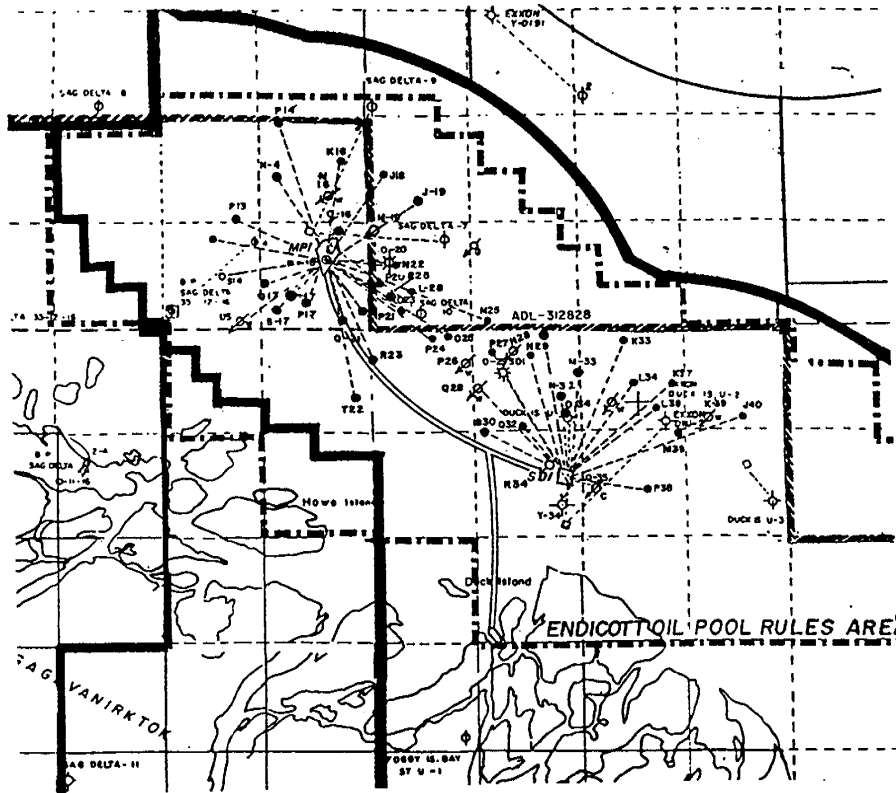


Figure V-5. Endicott Field Well Location Map (Woidneck et al., 1987).

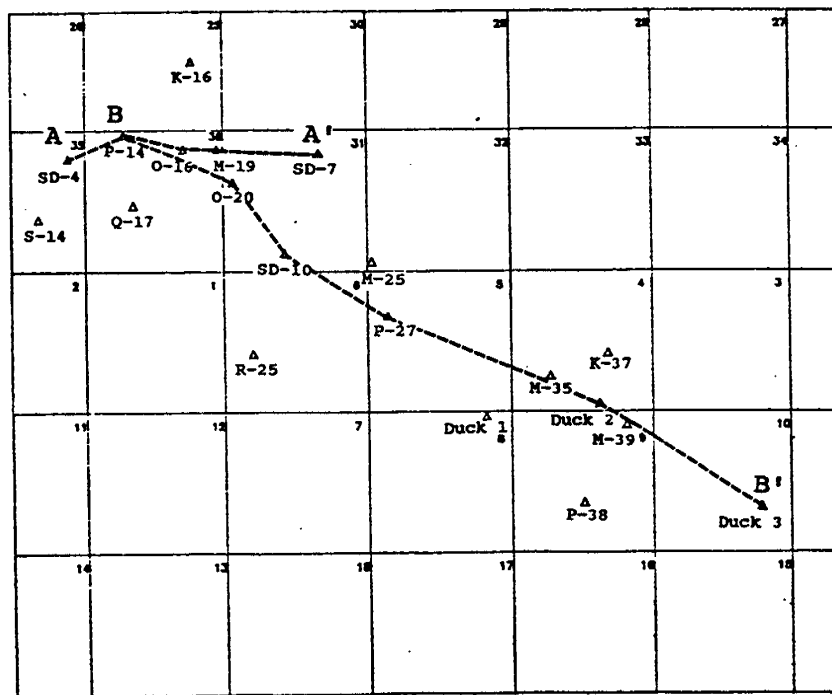


Figure V-6. Endicott Wells Analyzed in This Study with Cross Sections A-A' and B-B' Plotted.

## **C. ENDICOTT RESERVOIR DESCRIPTION**

### **C1. Structural Analysis**

Cross sections A-A' and B-B' (Figures V-7 and V-8) provide evidence of the structural component at Endicott, with dips to the south and west. Since true dip is southwest at 4 to 6 degrees, these cross sections illustrate west and south components of dip only. The Lower Cretaceous Unconformity (LCU) truncates the Kekiktuk formation throughout much of the field area. Exceptions include western portions of the field, such as the region surrounding Sag Delta 4. The LCU lies at approximately 9425 feet subsea at this well, while the top Kekiktuk formation lies at 9792 ft subsea.

Cross section A-A' illustrates the impact of the LCU on the Kekiktuk formation as it truncates into progressively older rocks to the east. While the LCU exhibits only slight (1 to 2 degree) easterly dip, the Kekiktuk formation exhibits readily observable westward dip. Were the distances between wells scaled to true distances, the dips would appear less exaggerated between Sag Delta 4 and O-16. Similarly, eastward dip at the level of the LCU would also be less pronounced. Faulting may exist between these two wells, however, and, as such, a fault has been dashed in on the cross section.

Kekiktuk formation structure crest is evident along cross section B-B' at well O-20. The LCU appears relatively flat in the vicinity of this well, but develops slight dip along the southeast portion of the cross section. The analysis does not contradict the possibility of faulting between Duck Island 2 and Duck Island 3; hence a fault is dashed between these wells.

Well P-14 and K-16 are in close proximity to the LCU-cutting Niakuk fault zone. Endicott production ends at the edge of this fault system, approximately one-half mile to the north of the P-14, but continues down-dip and south of the P-14 for several miles to include the major portion of Endicott field (Figure V-2).

Well-to-well correlations along the cross sections reflect a relatively consistent pattern of correlatable sands and shales. However, shales tend to be less continuous in the northwestern portion of the field, resulting in increased difficulty in determining subzone tops in this area. Relatively continuous coal markers with consistently high resistivities, low bulk densities, and high interval transit times aided in correlating where shales were less consistent.

A  
WEST

A'  
EAST

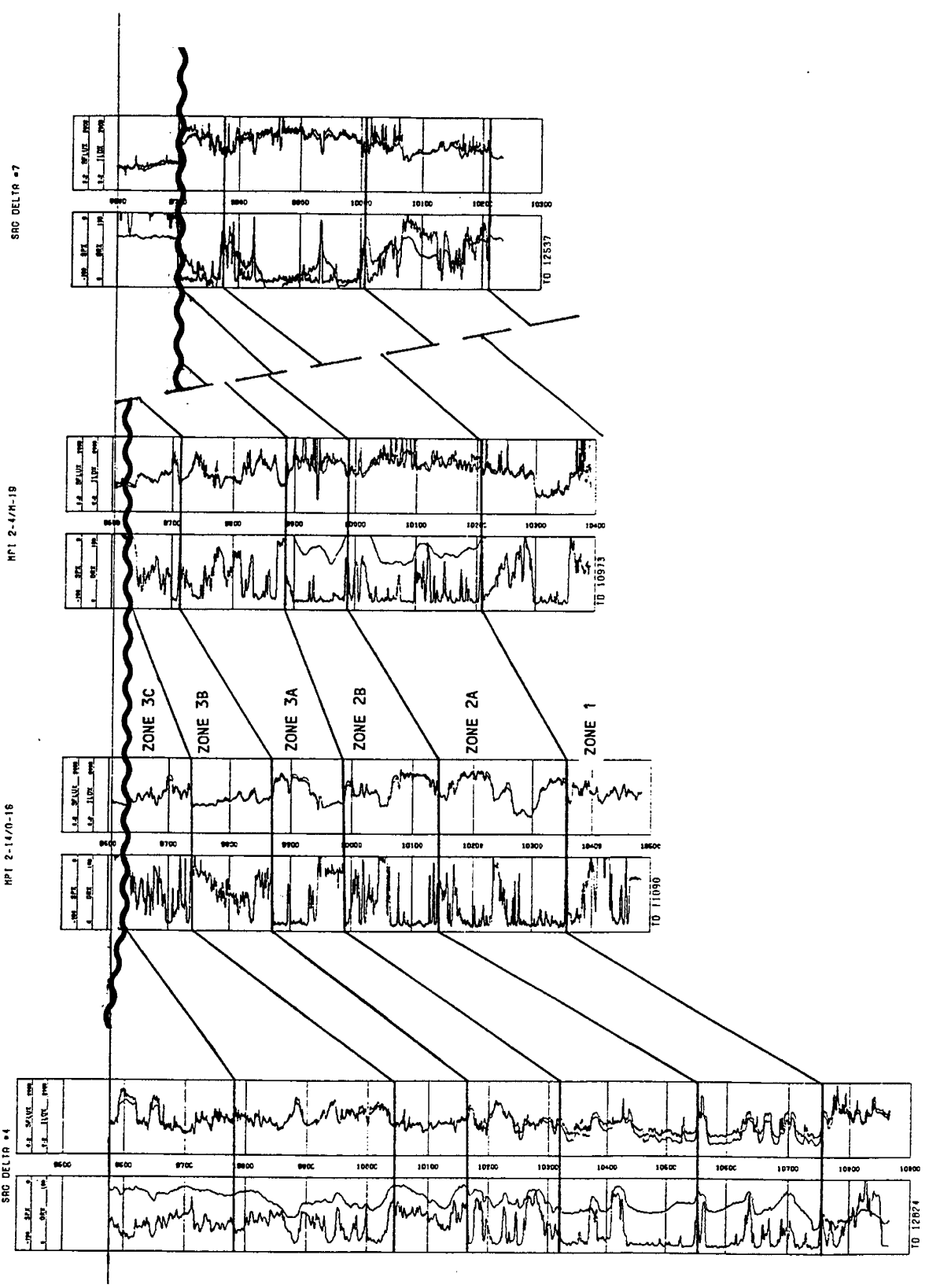


Figure V-7. Endicott East-West Cross Section A-A'.

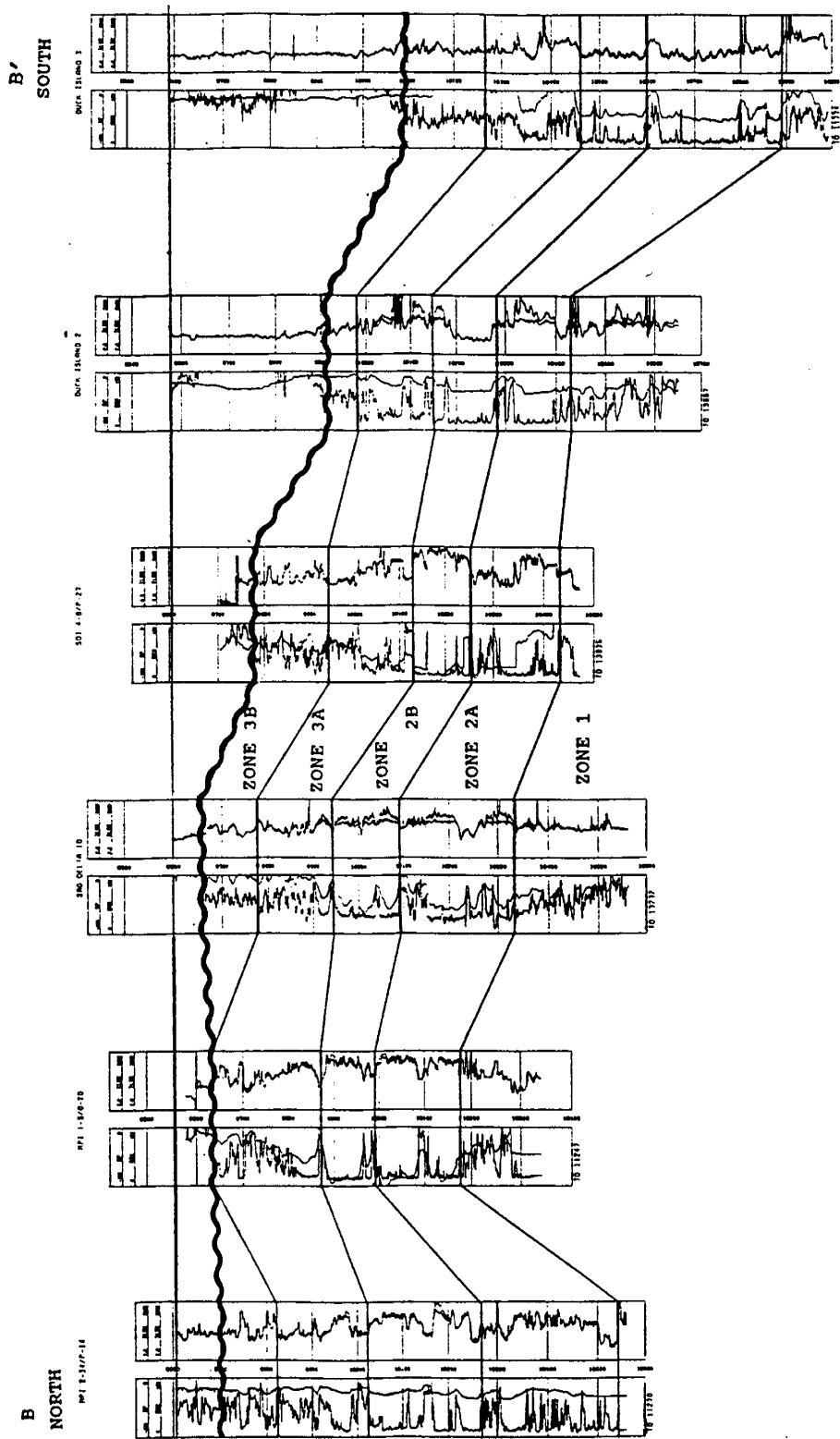


Figure V-8. Endicott North-South Cross Section B-B'.

Because gradational transitions from one zone to another do occur at Endicott field, several of the zonal picks taken from well logs carry a fair degree of uncertainty. Particular difficulty occurred in locating Zone 3B and 2B tops in the P-38, R-25, and S-14 wells. In addition, picks corresponding to the tops of Zone 2A were made with difficulty at the S-14 and M-39 wells. The top of Zone 3C was difficult to precisely determine at the K-16. Finally, the top of Zone 1 was estimated at the K-16, S-14 and M-39 wells, based on log trace character and picks taken from adjacent wells. While these picks carry the greatest uncertainty, determination of picks at other wells occasionally presented some difficulty, although to a lesser degree.

## **C2. Log-Derived Petrophysical Properties**

Effective porosity, water saturation, and net and gross thicknesses are listed in Tables V-3 through V-8. Table V-9 lists weighted averages of porosity and water saturation for each zone. Cut-off values for net pay calculations are 6% for effective porosity, and 40% for water saturation and shale volume. Analysis was performed at one-half foot intervals. In addition to data tabulation, structural contour maps and isopach maps of porosity and water saturation have been generated. Three-dimensional plots are also provided and will be utilized with the contour and isopach maps in future enhanced oil recovery modeling at PDL.

Excluding Zone 1 geologic correlations and picks (listed in Table V-3), data corresponding to Zone 1 have not been tabulated for two reasons. First, Zone 1 is not a major producer at Endicott field; only two out of the nearly 100 wells produce from this zone. This fits with the low energy, swampy depositional environment characteristic of this zone. Shales and coals are abundant, and sandstones, when present, tend to be fine-grained with low porosities. Second, most wells do not completely penetrate this zone, so that petrophysical analyses, including isopachs and single-valued zonal results cannot be generated.

Overlying Zone 1 is Zone 2, which is subdivided into Zones 2A and 2B by a shale interval. This shale is visible on both cross sections, thinning toward the west of cross section A-A' (Figure V-7). On the north-south cross section B-B' (Figure V-8), the shale interval becomes less distinct toward the north, as thin sand stringers tend to interfinger in and out from well to well. Despite this interfingering, the shale remains distinct enough to be employed as a marker bed.

**Table V-3: Zone 1 Tops at Endicott Field.**

<b>Well</b>	<b>Subsea Depth to Top (ft)</b>	<b>Measured Depth to Top (ft)</b>
Duck 1	-10711	12137
Duck 2	-10475	13529
Duck 3	-10850	11468
SD-4	-10752	12694
SD-7	-9947	12170
SD-10	-10277	12878
M-19	-10242	10798
M-25	-10192	13870
O-16	-10300	10875
O-20	-10121	11019
P-14	-10487	11196
Q-17	NDE	NDE
K-37	-10251	13210
M-35	-10437	12142
P-27	-10373	13703
K-16	-10316	12331 (EST)
P-38	NDE	NDE
R-25	NDE	NDE
S-14	-10867	12825 (EST)
M-39	-10519	12810 (EST)

NDE = Not Deep Enough  
 EST = Estimated

**Table V-4: Petrophysical Properties of Endicott Zone 2A.**

Well	Subsea Depth to Zone 2A (ft)	Measured Depth to Zone 2A (ft)	Thickness (ft)	Net Pay (ft)	Avg. Ø (%)	Avg. Sw (%)
Duck 1	-10515	10900	196	10	20	80
Duck 2	-10250	13283	225	75	23	62
Duck 3	-10554	11147	296	16	19	87
SD-4	-10520	12403	232	19	20	80
SD-7	-9721	11874	226	32	21	67
SD-10	-10041	12567	236	133	21	51
M-19	-9929	10460	313	153	26	46
M-25	-9984	13620	208	85	25	51
O-16	-10091	10586	209	139	24	31
O-20	-9927	10800	194	0	--	--
P-14	-10211	10897	276	171	21	21
Q-17	-10470	10748	99	14	24	68
K-37	-10061	12950	190	140	23	17
M-35	-10277	11934	160	115	21	34
P-27	-10197	13485	176	83	20	48
K-16	-10120	12067	196	69	22	52
P-38	NDE	NDE	--	--	--	--
R-25	NDE	NDE	--	--	--	--
S-14	-10639	12578	232	0	--	100
M-39	-10373	12653	177	27	18	68

NDE = Not Deep Enough

**Table V-5: Petrophysical Properties of Endicott Zone 2B.**

Well	Subsea Depth to Zone 2B (ft)	Measured Depth to Zone 2B (ft)	Thickness (ft)	Net Pay (ft)	Avg. Ø (%)	Avg. Sw (%)
Duck 1	-10315	11694	164	36	22	73
Duck 2	-10123	13142	127	21	22	85
Duck 3	-10416	10999	138	--	18	100
SD-4	-10292	12116	228	10	19	88
SD-7	-9651	11793	70	1	20	85
SD-10	-9894	12377	147	104	22	43
M-19	-9832	10356	97	51	25	53
M-25	-9863	13472	121	76	26	47
O-16	-9933	10372	158	118	26	14
O-20	-9824	10683	103	0	--	100
P-14	-9971	10634	240	189	24	21
Q-17	-10240	10510	230	91	24	58
K-37	-9910	12752	151	147	24	9
M-35	-10131	11746	146	64	25	50
P-27	-10057	13311	140	117	26	9
K-16	-10030	11944	90	79	23	17
P-38	-10513	11820 (EST)	NDE	--	--	--
R-25	NDE	NDE	--	--	--	--
S-14	-10445	12364	194	0	21	98
M-39	-10239	12499	134	77	19	51

NDE = Not Deep Enough  
 EST = Estimated

**Table V-6: Petrophysical Properties of Endicott Zone 3A.**

Well	Subsea Depth to Zone 3A (ft)	Thickness (ft)	Net Pay (ft)	Avg. Ø (%)	Avg. Sw (%)
Duck 1	-10157	194	94	27	38
Duck 2	-9951	172	81	30	44
Duck 3	-10229	187	43	31	45
SD-4	-10161	131	36	18	50
SD-7	NP	--	--	--	--
SD-10	-9727	167	55	25	43
M-19	-9622	210	45	24	63
M-25	09718	145	46	34	50
O-16	-9816	117	71	22	19
O-20	-9618	206	12	22	58
P-14	-9885	86	49	22	18
Q-17	-10034	206	90	22	24
K-37	NP	--	--	--	--
M-35	-9999	132	110	33	16
P-27	-9896	161	78	33	13
K-16	-9947	83	49	23	15
P-38	-10398	115	25	31	42
R-25	-10269	NDE	--	--	--
S-14	-10298	147	0	20	84
M-39	-10039	200	100	31	10

NP = Not Present  
 NDE = Not Deep Enough

**Table V-7: Petrophysical Properties of Endicott Zone 3B.**

Well	Subsea Depth to Zone 3B (ft)	Gross Thickness (ft)	Net Pay (ft)	Avg. Ø (%)	Avg. Sw (%)
Duck 1	-9978	179	5	15	45
Duck 2	-9878	73	0	18	100
Duck 3	-10053	176	22	36	51
SD-4	-10000	161	10	14	44
SD-7	NP	--	--	--	--
SD-10	-9631	96	16	12	75
M-19	-9587	35	0	13	99
M-25	NP	NP	--	--	--
O-16	-9681	135	7	11	62
O-20	-9580	38	14	18	57
P-14	-9767	118	15	13	51
Q-17	-9964	70	--	--	100
K-37	NP	--	--	--	--
M-35	-9850	149	61	20	49
P-27	-9724	172	35	14	47
K-16	-9838	109	5	17	40
P-38	-10173	225	4	15	72
R-25	-10123	146	0	--	100
S-14	-10160	138	0	12	72
M-39	-9943	96	11	15	33

NP = Not Present

**Table V-8: Petrophysical Properties of Endicott Zone 3C.**

Well	Subsea Depth to Zone 3C (ft)	Gross Thickness (ft)	Net Pay (ft)	Avg. Ø (%)	Avg. Sw (%)
Duck 1	-9791	187	--	13	42
Duck 2	NP	--	--	--	--
Duck 3	NP	--	--	--	--
SD-4	-9792	208	107	18	22
SD-7	NP	--	--	--	--
SD-10	NP	--	--	--	--
M-19	NP	--	--	--	--
M-25	NP	--	--	--	--
O-16	-9545	136	51	17	33
O-20	NP	--	--	--	--
P-14	-9662	105	41	16	31
Q-17	-9752	212	84	18	33
K-37	NP	--	--	--	--
M-35	NP	--	--	--	--
P-27	NP	--	--	--	--
K-16	-9677	161	115	22	25
P-38	-9919	254	36	14	46
R-25	-9895	228	5	20	70
S-14	-9931 (EST)	229	28	16	48
M-39	NP	--	--	--	--

NP = Not Present  
 EST = Estimated

**Table V-9: Weighted Zone Averages of Porosity and Water Saturation at Endicott Field.**

<b>Zone</b>	<b>Average Porosity (%)</b>	<b>Average Water Saturation (%)</b>
3C	17	41
3B	16	59
3A	28	39
2B	20	51
2A	23	50

Table V-4 lists calculated petrophysical values associated with Zone 2A. For the most part, Zone 2A thickness is well over 100 feet, and in one well (the M-19) it exceeds 300 feet. Average porosities vary from a low of 18% to a high of 26%, excluding the O-20 well, while water saturations range between 11% and 51%. The highest porosity value of 26% occurs in the M-19, where the calculated net pay is relatively large--153 ft. Weighted averages of porosity and water saturation given in Table V-9 are 23% and 50%, respectively.

Zone 2A structure is contoured in Figure V-9. The selected contouring option utilized in this report estimated grid nodal values as distance-weighted averaged of dips projected from nearby sample data points. The Surf II manual (Sampson, 1984) provides more details on its contouring routines. The surface of Zone 2A generally strikes northwest-southeast, and dips toward the southwest. The K-16 well is responsible for the development of a structural low which noses into Section 25 from southwest to interrupt the otherwise consistent patterns of strike and dip.

The contour plot of Zone 2A porosity (Figure V-10) shows highest values in the central and northwest portions of the mapped area, but the distribution of values shows a high degree of randomness. Water saturations also vary from well-to-well across the mapped southeast edge. Generally lower values are found in the northwest and central regions (Figure V-11). 3-D plots of porosity and water saturation (Figures V-12 and V-13) tend to reflect a poor correlation between high porosities and low water saturations.

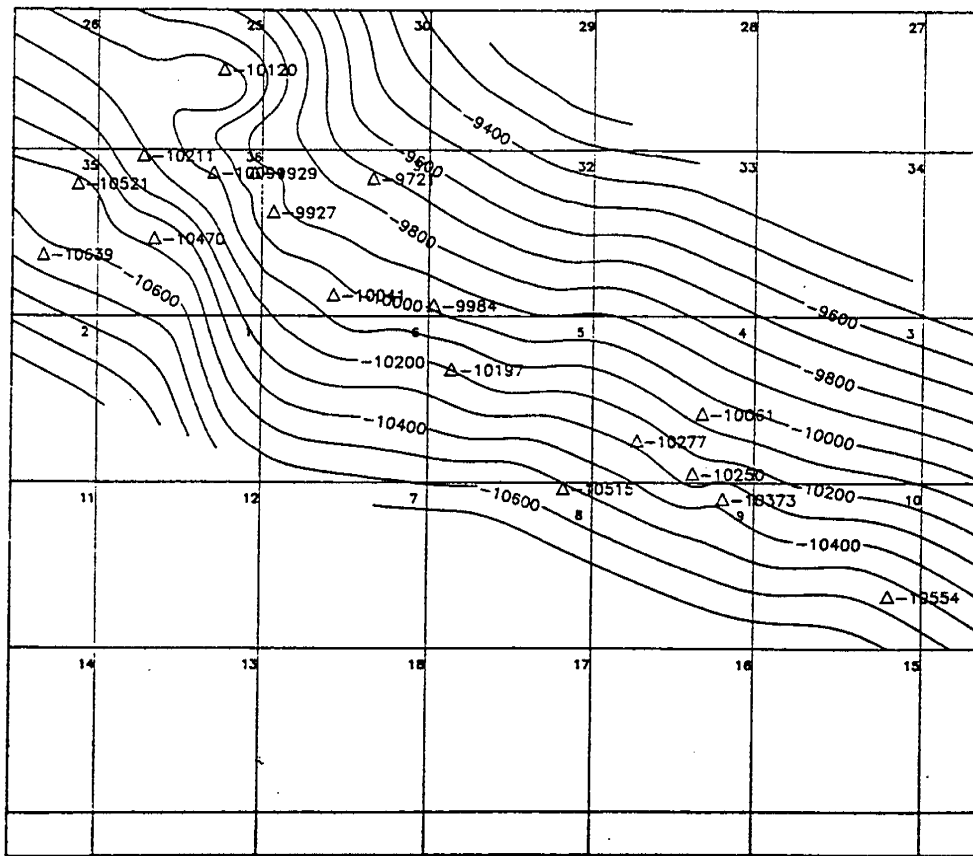


Figure V-9. Top Zone 2A Structure Contour Map C.I.50'.

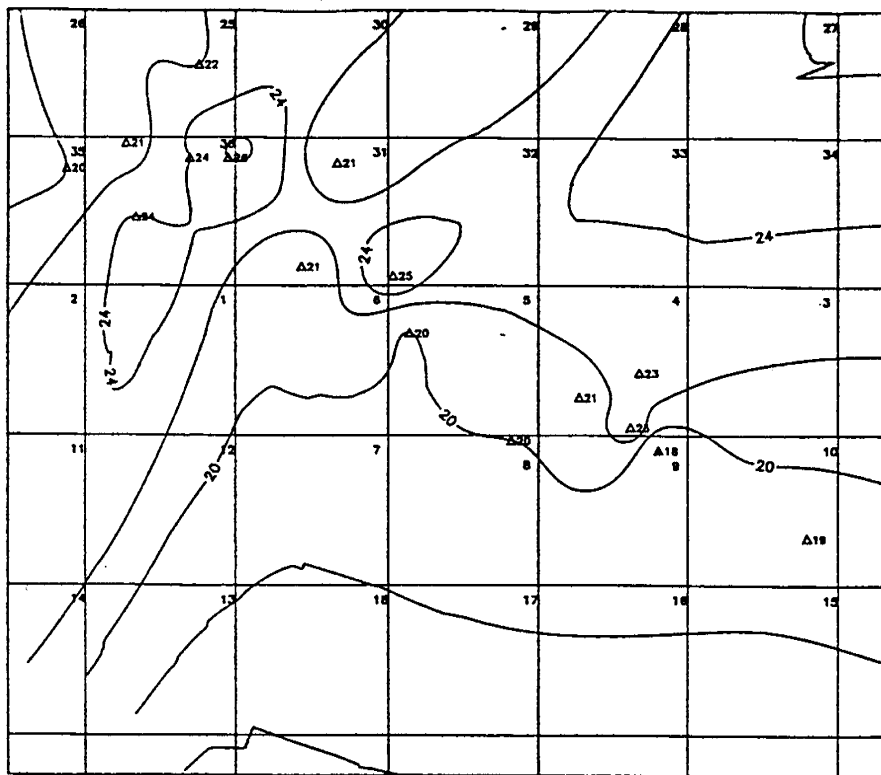


Figure V-10. Zone 2A Porosity Contour Map C.I.2%.

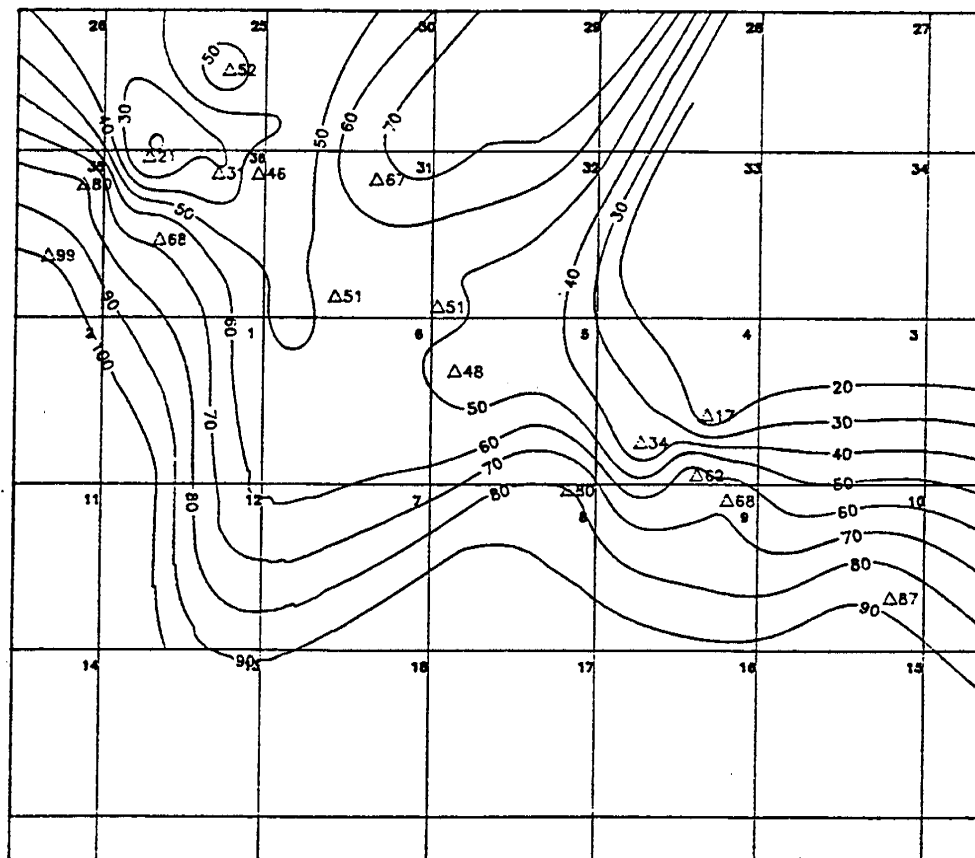


Figure V-11. Zone 2A Water Saturation Contour Map C.I.10%.

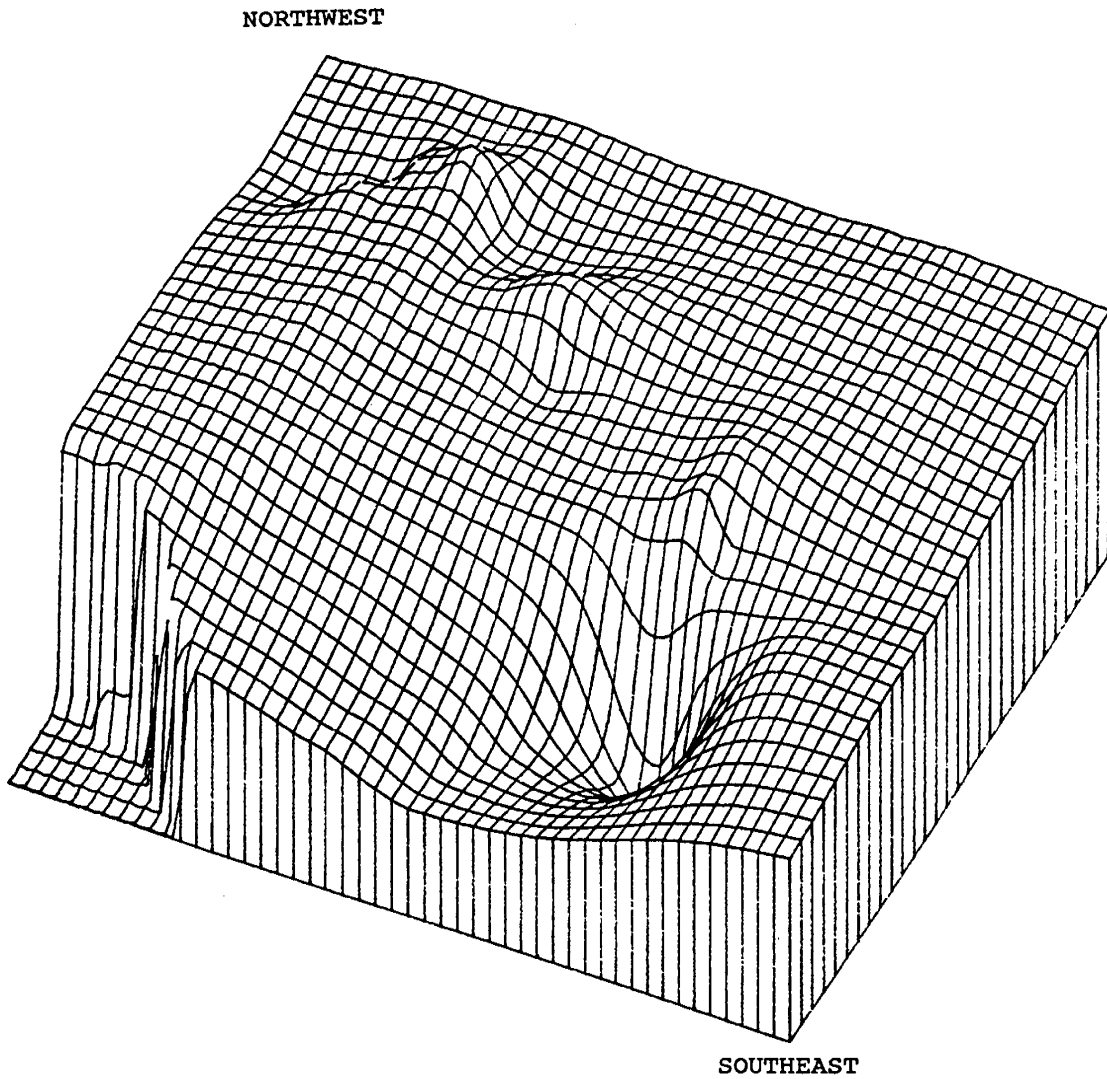


Figure V-12. Zone 2A 3-D Porosity Isopach.

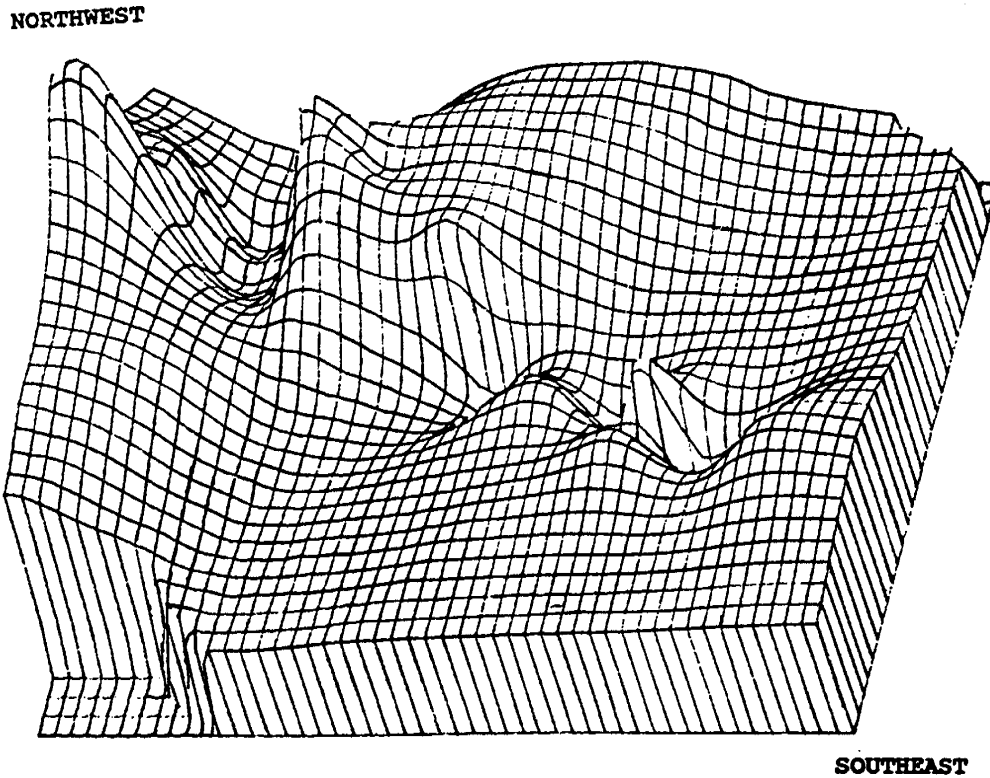


Figure V-13. Zone 2A 3-D Water Saturation Isopach.

Zoned 2B average porosity is somewhat lower than that corresponding to Zone 2A (20% versus 23%, respectively, as listed in Table V-9). Average water saturation remains essentially unchanged at 51%, compared to 50% for Zone 2A. Excluding the Duck Island well 3 and well O-20, the values of water saturation range from a low of 9% at the P-27 and K-37 wells to a high of 88% at the Sag Delta 4.

Contour maps depicting structure of Zone 2A and 2B (Figures V-9 and V-14) show strong similarities. These similarities are also reflected in their generally unchanging interval thicknesses on cross sections A-A' and B-B' (Figures V-7 and V-8). Interval thicknesses do vary enough, however, to result in slightly less dip at the level of Zone 2B, as compared with Zone 2A. In contrast to Zone 2A, a reasonably good correlation exists between Zone 2B higher porosities and low water saturations. Zone 2B porosity and water saturation contour maps show this, as do corresponding 3-D plots (Figures V-15 through V-18). The bar graphs of Zone 2B porosity and water saturation (Figure V-19) also highlight the relatively good correlation between lower porosity and higher water saturation associated with this zone. The corresponding bar graph for Zone 2A (Figure V-20) reflects the poor correlation between lower porosities and high water saturations.

Zone 3 is derived from a more mature environment of deposition as compared to Zone 2. Meandering stream sand sequences predominate in the former zone as compared to sheet-like geometries associated with braided stream deposits in the latter (Woidneck et al., 1987). Overlapping point bars with good interconnectivity exist in Zone 3, and help to explain why the highest Endicott porosities are found in this zone. The structural contour map of the top of Zone 3A (shown in Figure V-21) strongly resembles the structural contour maps of Zones 2A and 2B. The zone shallows toward the northwest as is expected, and dips south and west away from the M-19 and O-20 wells. Also, this map shows a continuation of the trend toward progressively shallower dips up section through the Kekiktuk zones.

Zone 3A porosities range from a low of 18% in the Sag Delta 4 to a high of 34% in the M-25 (Table V-6). The thickness-weighted average porosity for this zone is 28% and is the highest of any of the zones (Table V-9). Figure V-22 shows the trend of higher porosities toward the central region of the map area with lowest values occurring in the northwest. A region of very similar porosities (around 22%) exists in the northwest but consistently higher porosities occur toward the southeast (Figure V-22).

In contrast, water saturations vary widely across the area but show highest values in the northwest and southeast (Figure V-23). They range from a minimum of 13% at the P-27 to a high of 84% at the S-14. These porosity and water saturation patterns can also be seen in 3-D plots of Zone 3A porosity and water saturation (Figures V-24 and V-25). Because several wells exhibit a combination of relatively high porosities and low water saturations in Zone 3A, it is potentially the most prolific hydrocarbon-producing zone in Endicott field.

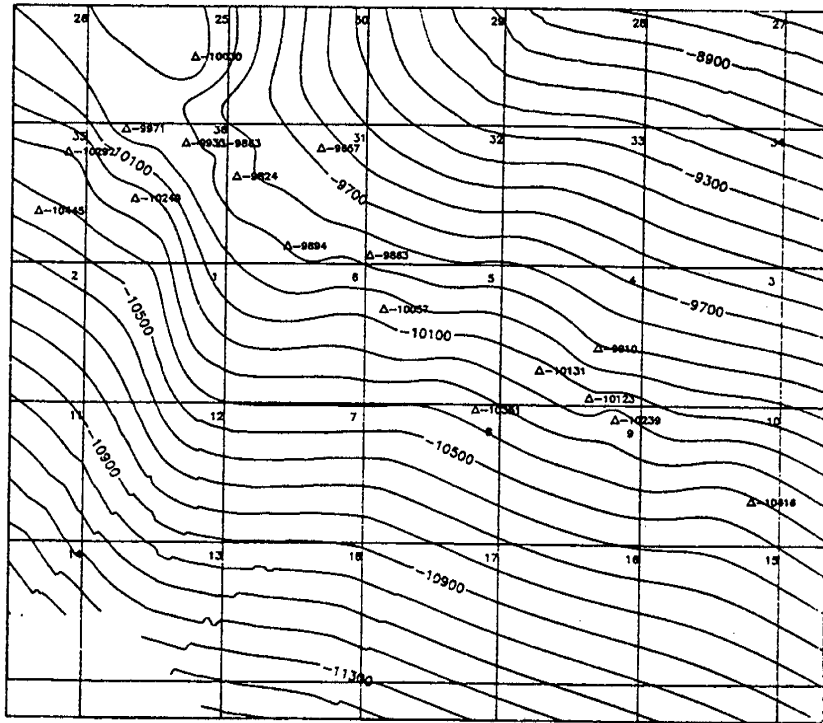


Figure V-14. Zone 2B Structure Contour Map C.I.50'.

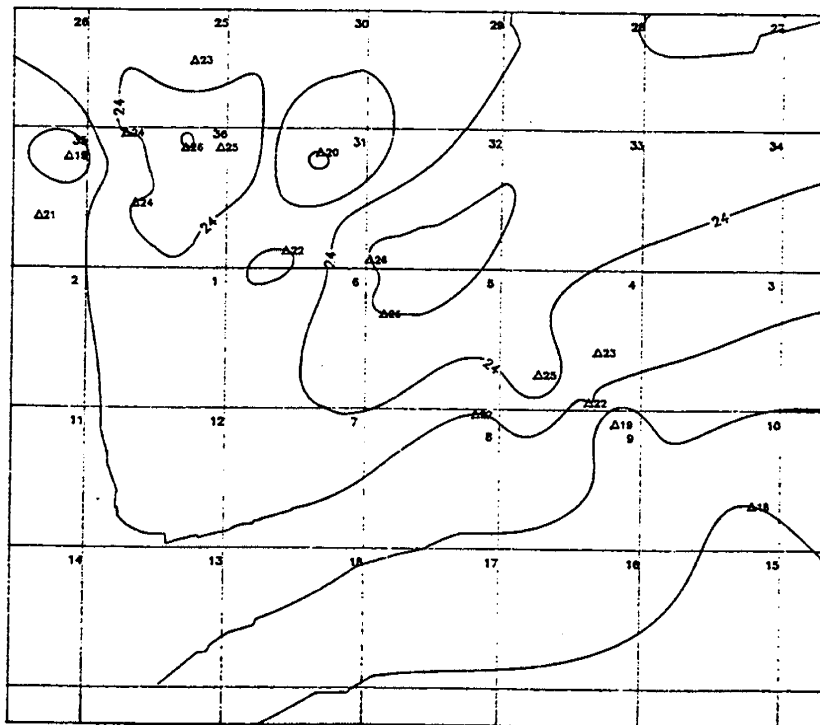


Figure V-15. Zone 2B Porosity Contour Map C.I.2%.

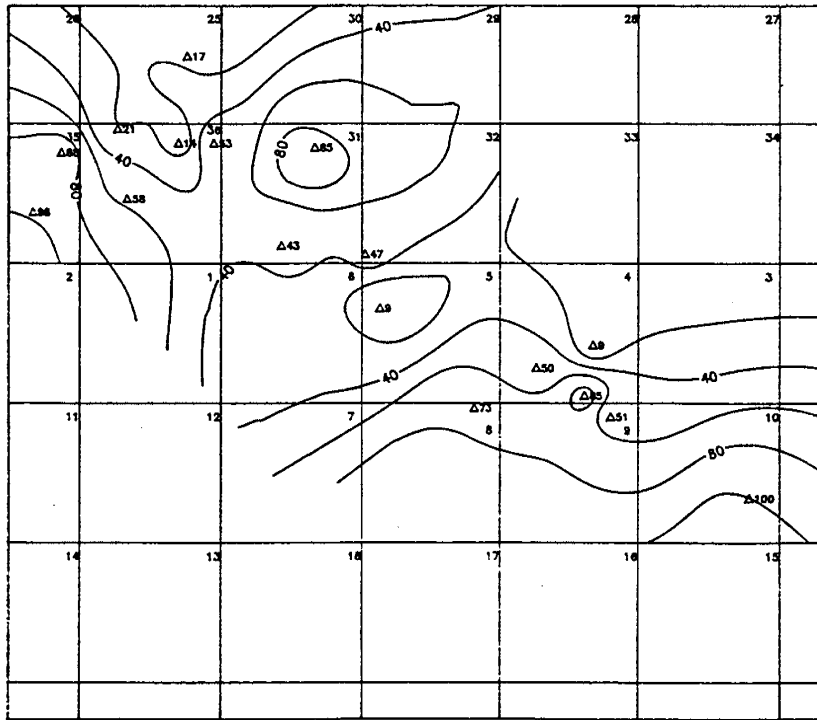


Figure V-16. Zone 2B Water Saturation Contour Map C.I.20%.

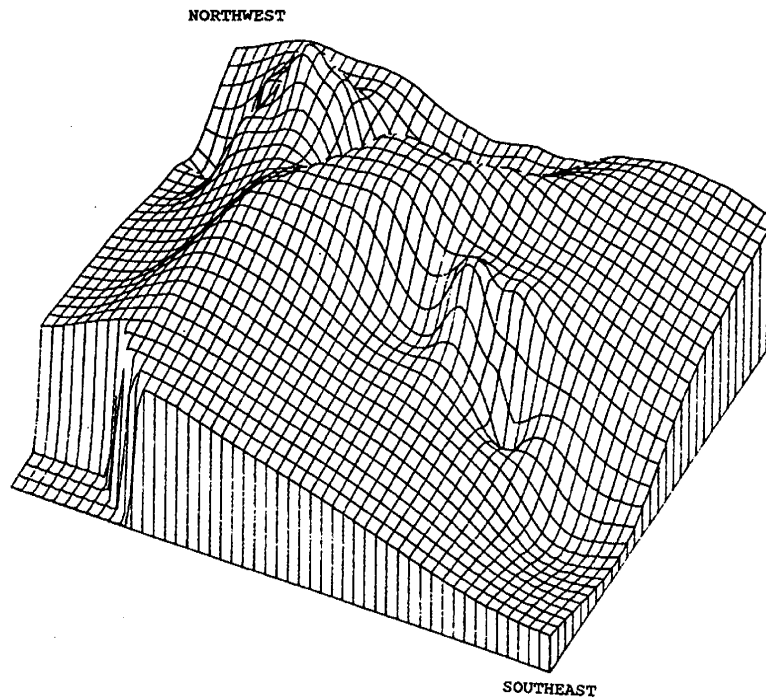


Figure V-17. Zone 2B 3-D Porosity Isopach.

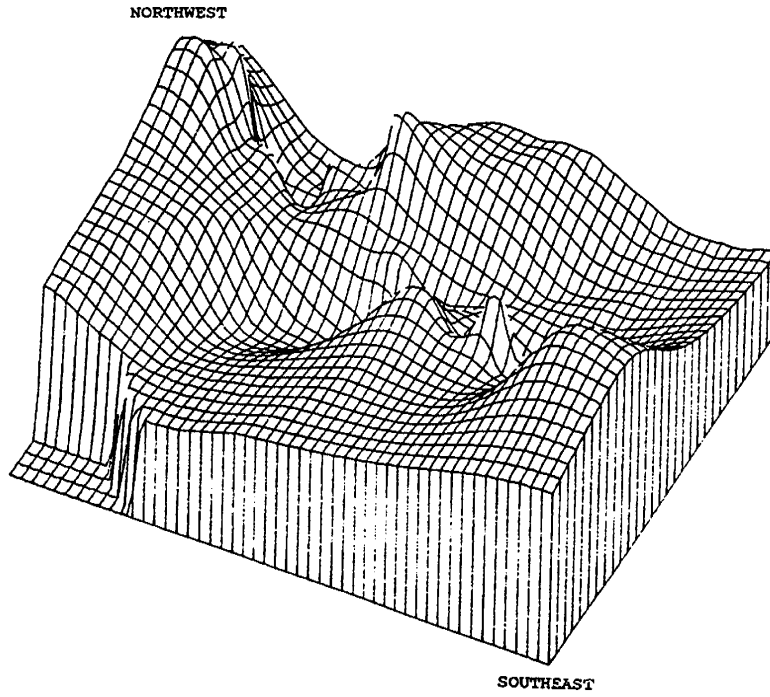


Figure V-18. Zone 2B 3-D Water Saturation Isopach.

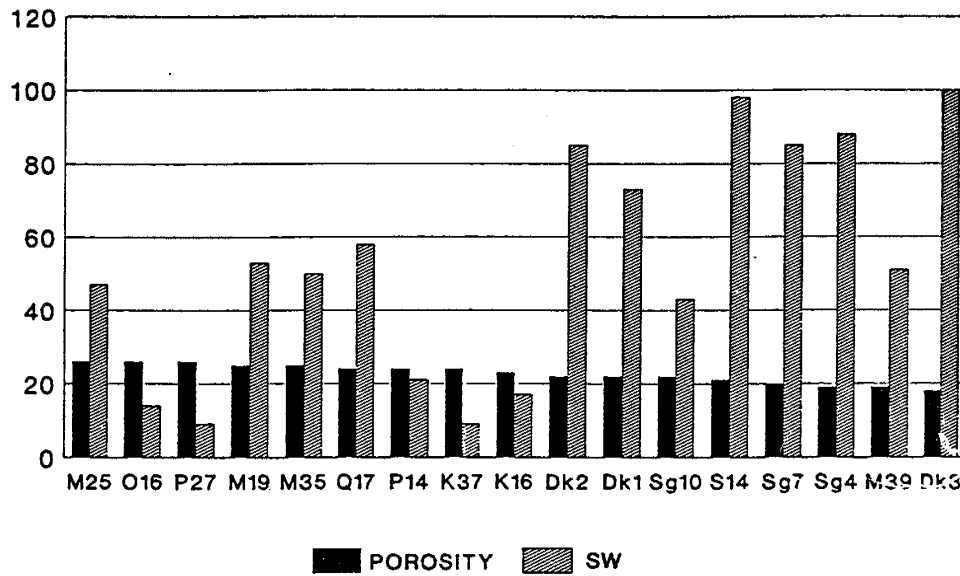


Figure V-19. Porosity - Sw: Zone 2B.



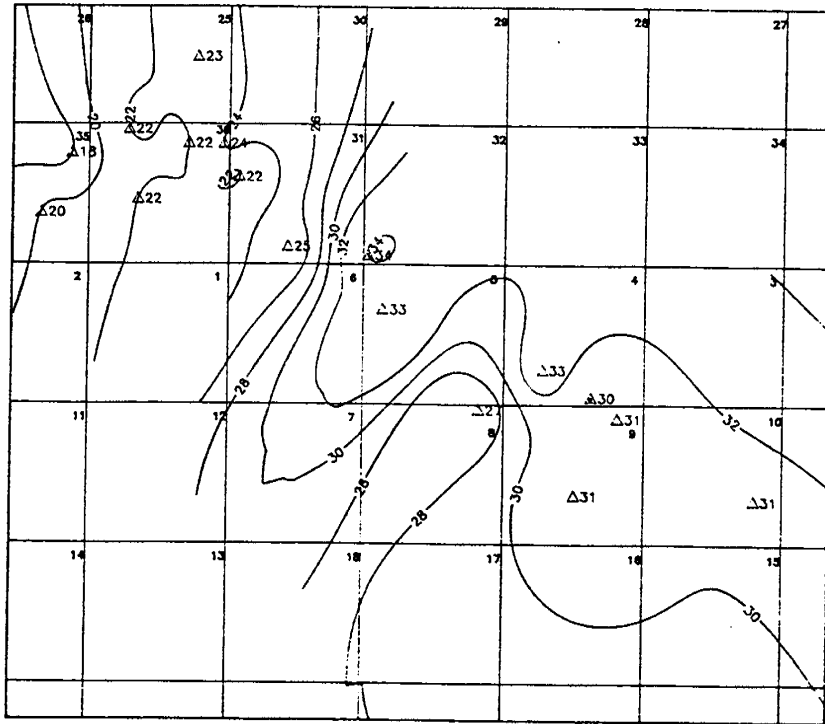


Figure V-22. Zone 3A Porosity Contour Map C.I.2%.

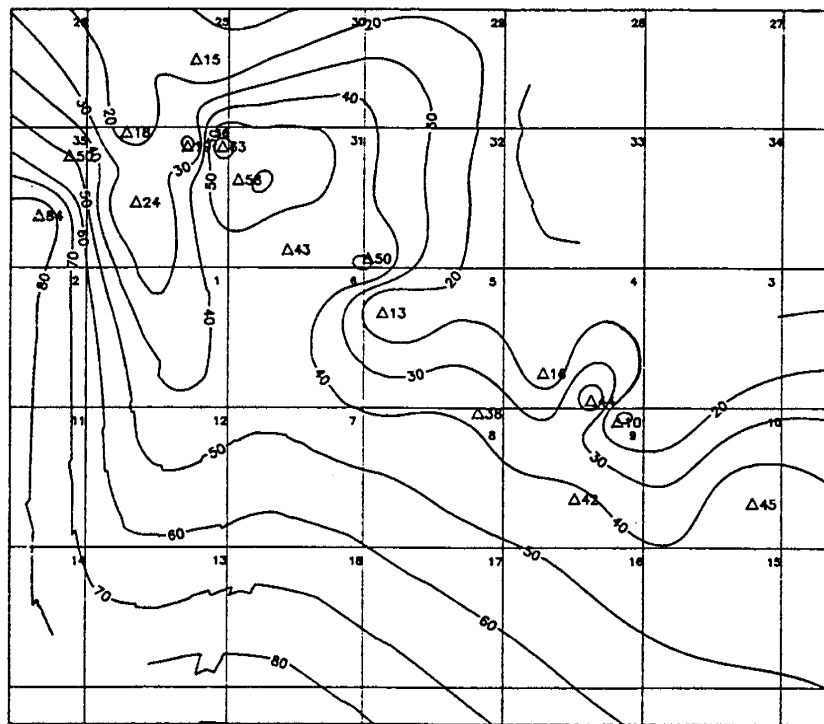


Figure V-23. Zone 3A Water Saturation Contour Map C.I.10%.

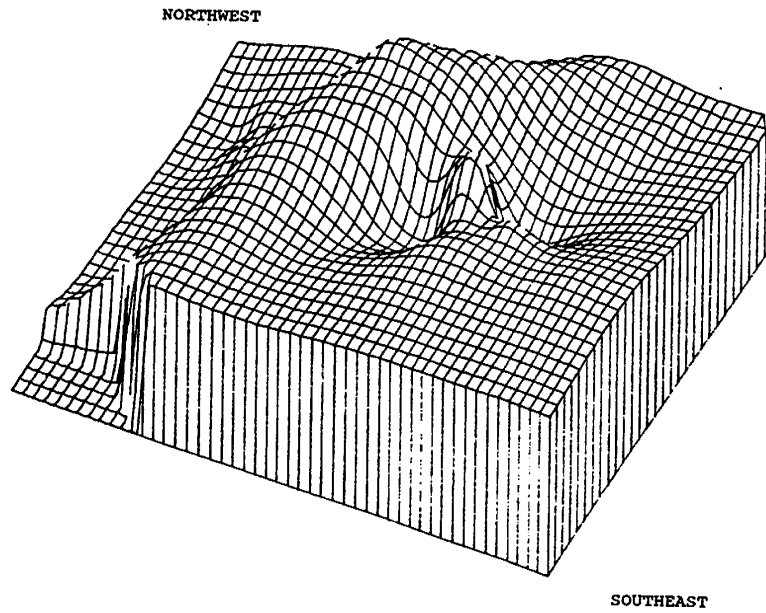


Figure V-24. Zone 3A 3-D Porosity Isopach.

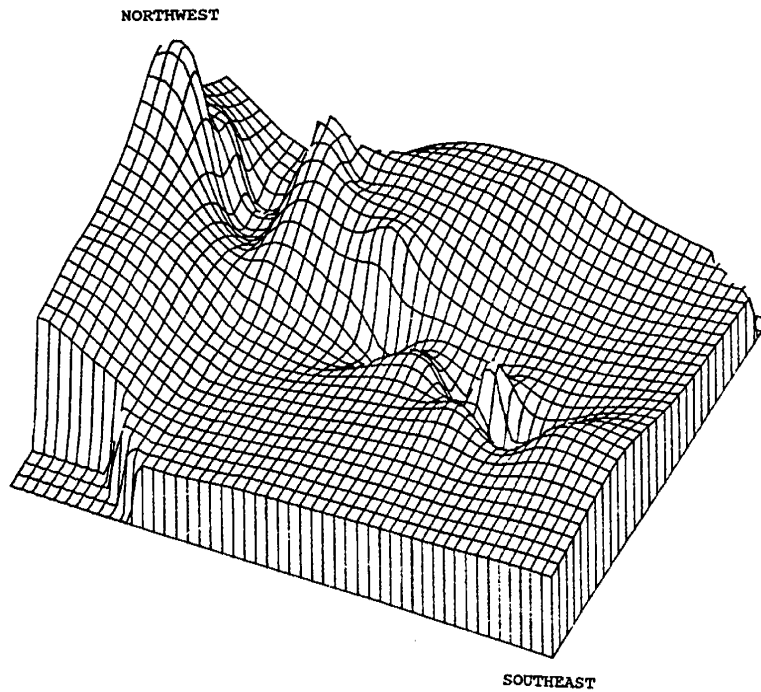


Figure V-25. Zone 3A 3-D Water Saturation Isopach.

Zone 3B, being shaly in most of the mapped area, yields comparatively low values of net pay, ranging from 7 to 61 feet (Table V-7). Porosities within non-shaly intervals are similar to those in Zone 2. The highest porosity (36%) occurs in Duck Island 3 while the lowest value (11%) is found in the O-16. The average porosity in Zone 3B is 16% versus 28% in Zone 3A. Water saturations in Zone 3B are considerably higher than in Zone 3A. The average water saturation in Zone 3B is 59%, considerably higher than the 39% calculated for Zone 3A.

No Zone 3B net pay is observed in four wells: Duck Island 2, M-19, R-25, and S-14. This is due to the high shale volumes at these wells. At those depth points where shale volumes are greater than the cut-off limit, LOGCALC sets the porosities to 0% and then excludes these points from net pay calculations. LOGCALC also sets water saturation to 100% at such points. A visual inspection of Zone 3B log traces confirms overwhelming shale content in the Duck Island 2 and Q-17 wells. At the M-19, R-25 and S-14, Zone 2B also consists primarily of shale, but some shaly sands are present.

The structure of Zone 3B shown in Figure V-26 conforms to the general structural trend of the underlying Kekiktuk zones. Comparison of structure contour maps (Figures V-9, V-14, V-21, and V-26) shows that dip on the Kekiktuk horizons gradually lessens up section. Figure V-27 shows that porosities are generally constant from northwest to southeast, and decrease toward the southwest. The most notable exception to this pattern occurs at the Duck Island 3, where a high porosity of 36% produces a contoured porosity high in its vicinity. Water saturations (Figure V-28) vary dramatically across the area and show no similar directional trend of consistent values. Between the Duck Island 2 and Duck Island 3, porosities double from 18% to 36%. Values of water saturation vary substantially over short distances, especially near Duck Island 2 and the Q-17 wells. Overall, Zone 3B is of poorer reservoir quality than the other zones, which is predictable considering its higher shale content. Production from Zone 3B does occur in about 15% of the Endicott wells, although no well produces entirely from this zone.

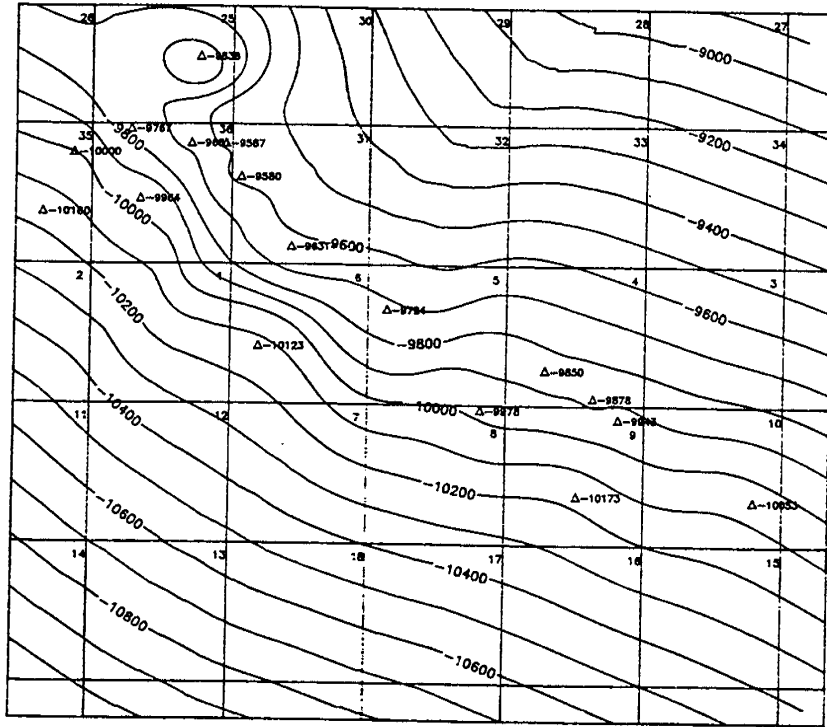


Figure V-26. Top Zone 3B Structure Contour Map C.I.50'.

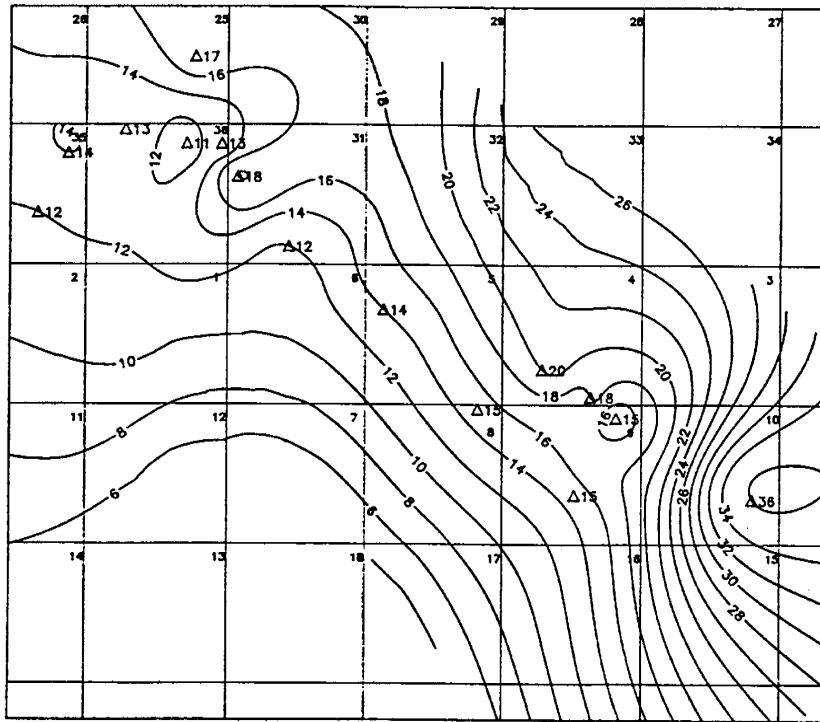


Figure V-27. Zone 3B Porosity Contour Map C.I.2%.

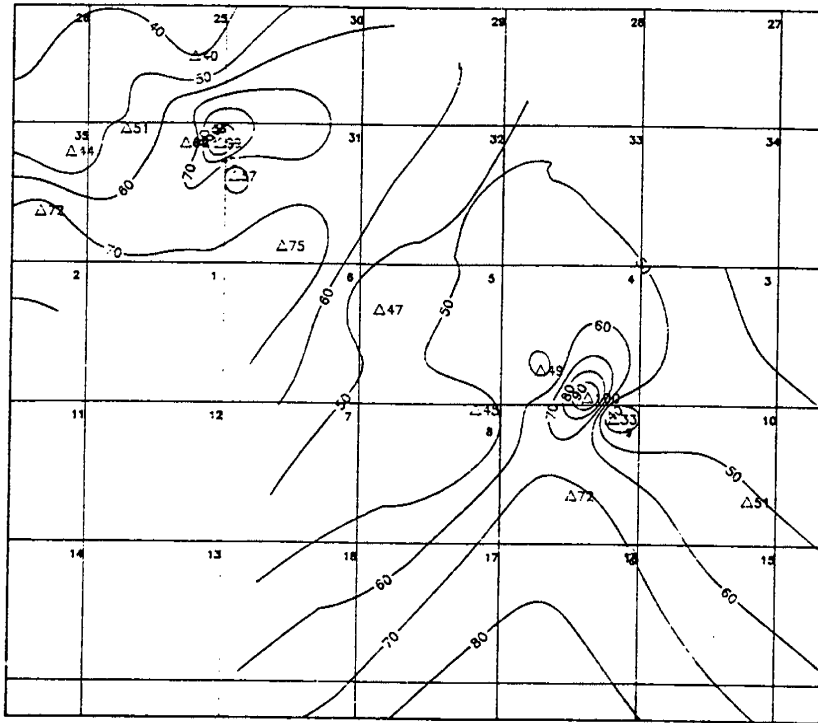


Figure V-28. Zone 3B Water Saturation Contour Map C.I.10%.

Zone 3C provides only a limited number of wells for analysis, as it is truncated by the LCU along the north-south axis of the reservoir. The structural contour map of the top of Zone 3C (Figure V-29) indicates southwest dip. The production from this zone is derived primarily from 28 wells located along the western, or down dip, flank of the field. Additional production occurs from two wells within the Niakuk fault zone, but on the upthrown side of the northernmost Niakuk fault. Porosity and water saturation are shown in Figures V-30 and V-31 and they illustrate increasing porosity combined with increasing water saturation southwestward with best values in the northwest.

Notwithstanding the relatively limited amount of data associated with this horizon, average values of porosity and water saturation are computed to be 17% and 41%, respectively. Both porosity and water saturation are generally lower than in other zones. Highest porosity is 22% and is found in the K-16 and the Sag Delta 4 (Table V-8). The lowest value of porosity is 13% and is found in the Duck Island 1. Water saturation ranges from a high of 48% in the S-14 to a low of 22% in Sag Delta 4. Analysis of additional down dip wells would probably yield higher porosities assuming the effects of upward fining sands in Zone 3C to be less predominant lower down the section.

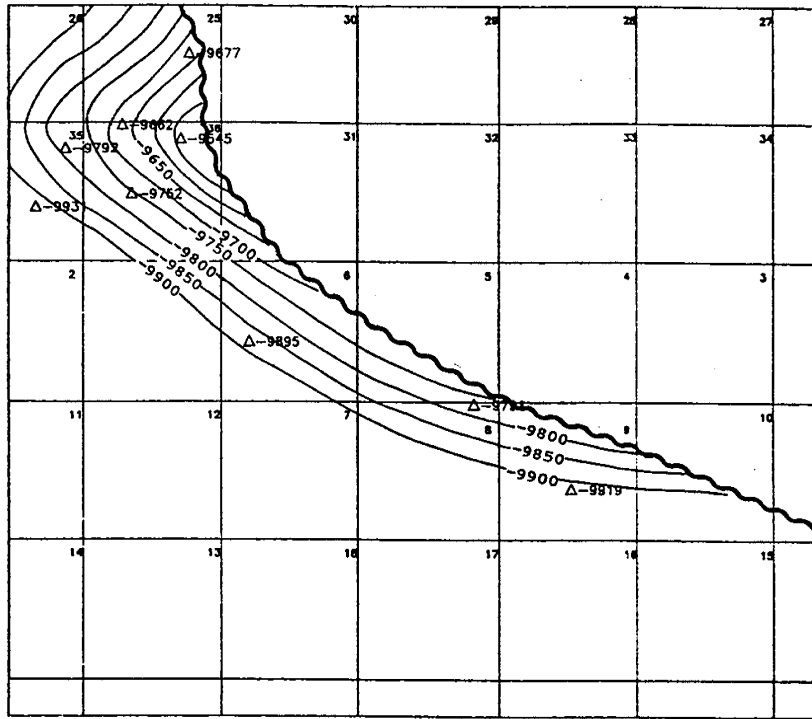


Figure V-29. Top Zone 3C Structure Contour Map C.I.50'

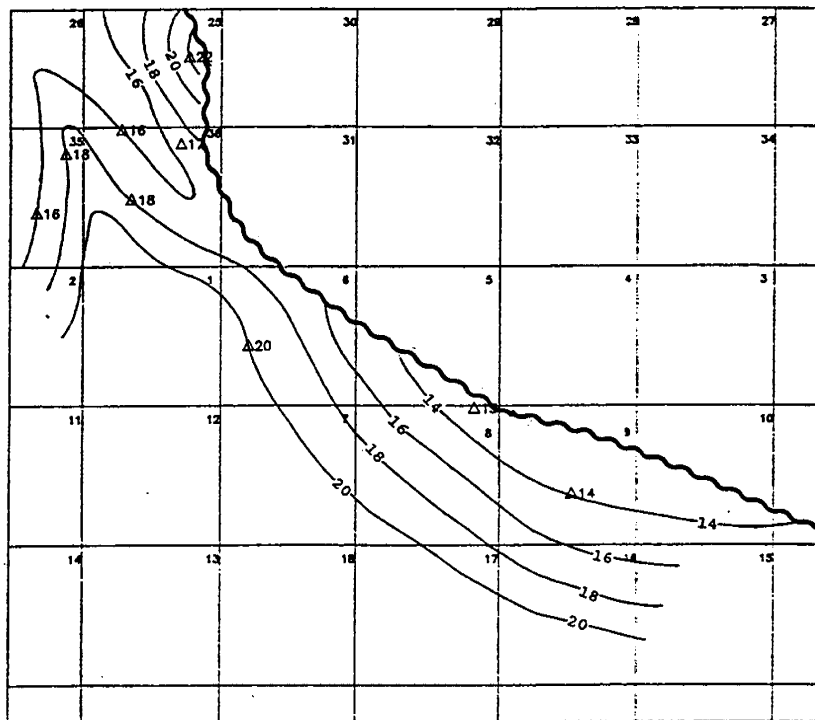


Figure V-30. Zone 3C Porosity Contour Map C.I.2%

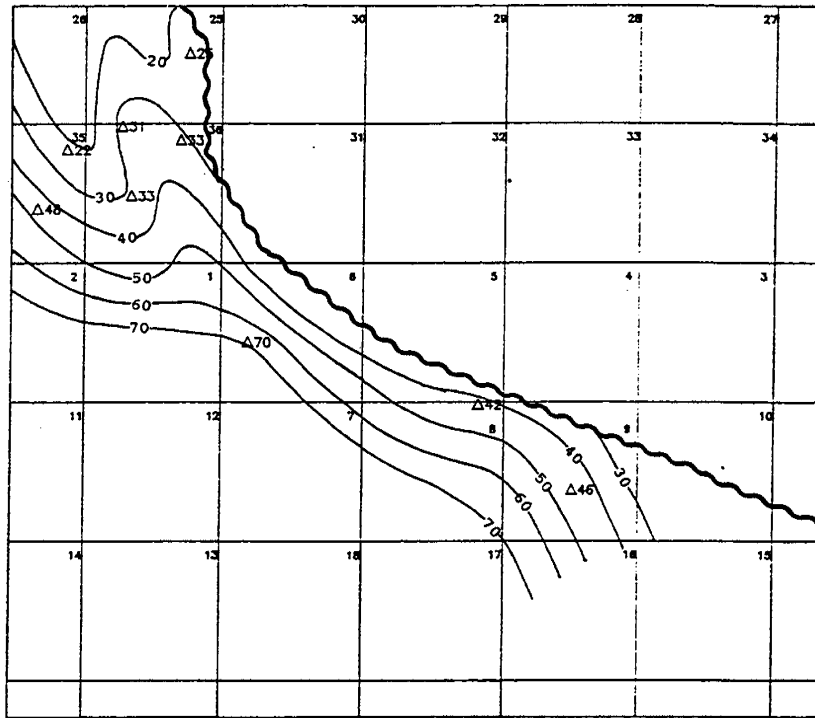


Figure V-31. Zone 3C Water Saturation Contour Map C.I.10%.

Figures V-33 through V-35, show the 3-D plots of net pay thicknesses corresponding to the formation subzones. Zones 2A and 2B (Figures V-32 and V-33) indicate net pay to generally increase from southeast to northwest. Considerable differences exist between net pay thicknesses of wells P-14 and Sag Delta 4, as indicated most dramatically in Figure V-33. Zone 2B in net pay in well P-14 is 189 feet but diminishes to just 10 feet at Sag Delta 4. Such a rapid change in sand thickness over a short distance is possible in a braided stream environment. For example, depositionally, reverse eddies from active channels can carry silt and clay into connected, but abandoned older channels and then dump it as velocities rapidly drop. This results in silt and clay traps juxtaposed against sand deposits (Selley, 1978).

Net pay trends in Zone 3 (Figures V-34 and V-35) show a reversal of the trend in Zone 2. Generally, higher values of net pay occur in Zone 3 in the southeast, contrasting with lower Zone 2 values there, while thicknesses decrease toward the northwest. A region of consistently high net pay occurs from west to east but migrates northward in Zone 3B as compared to Zone 3A. This may be representative of lateral migration of a meandering stream channel and associated deposition over time.

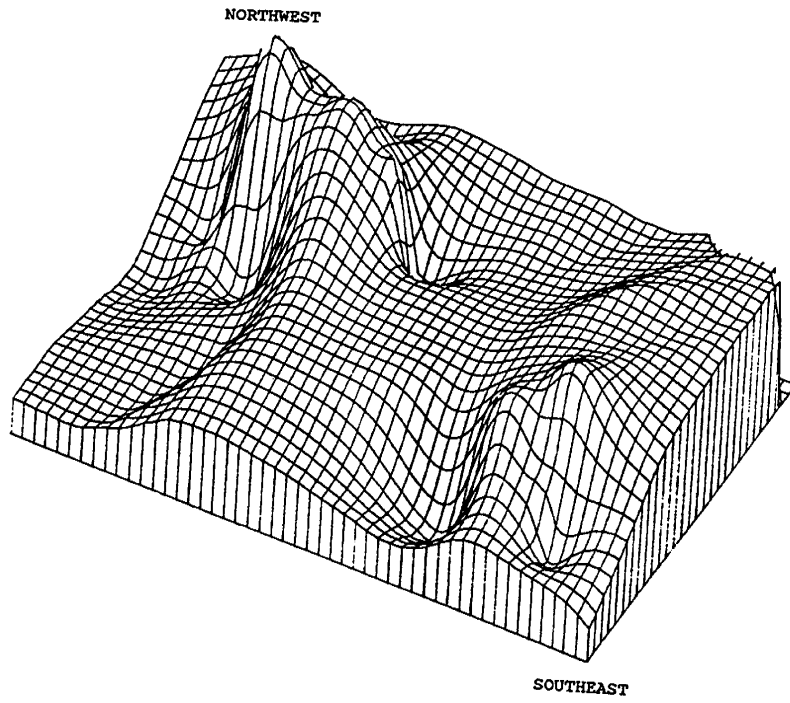


Figure V-32. Zone 2A 3-D Net Pay Isopach.

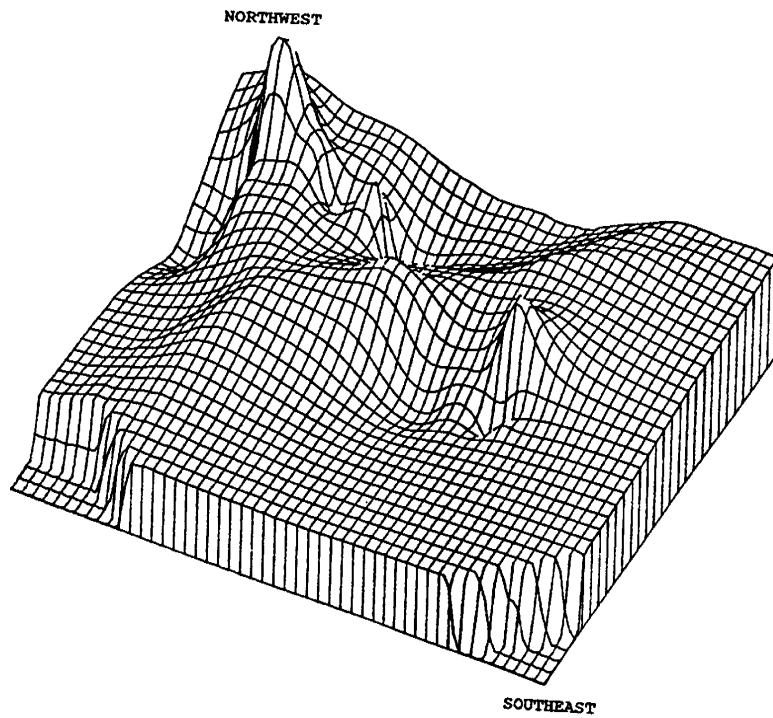


Figure V-33. Zone 2B 3-D Net Pay Isopach.

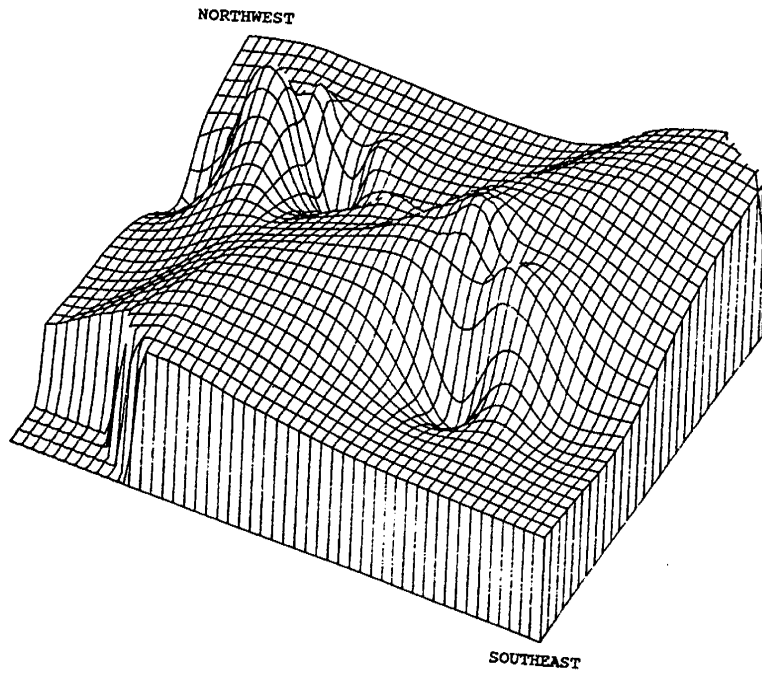


Figure V-34. Zone 3A 3-D Net Pay Isopach.

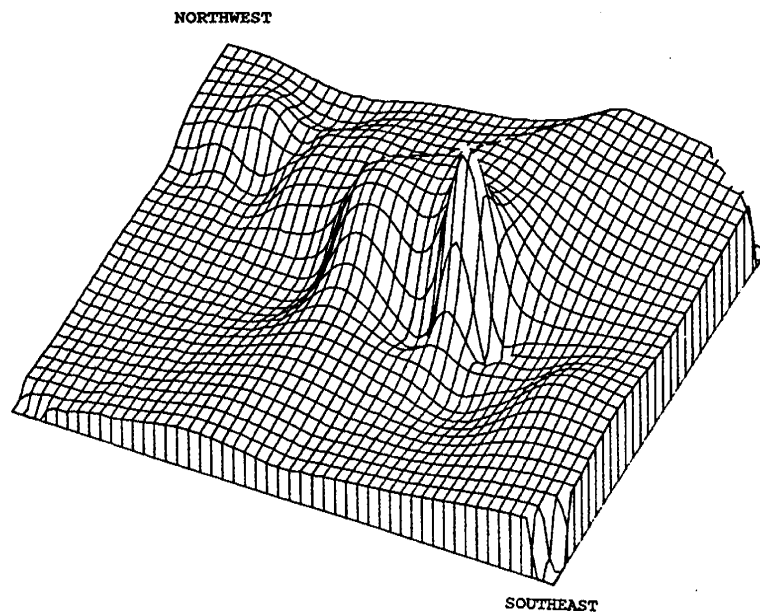


Figure V-35. Zone 3B 3-D Net Pay Isopach.

## **D. NOMENCLATURE**

AOGCC	=	Alaska Oil and Gas Conservation Commission
HRZ	=	Highly Radioactive Zone
LCU	=	Lower Cretaceous Unconformity
MWD	=	Measured Well Depth
NDE	=	Not Deep Enough
NP	=	Not Present
TVD	=	True Vertical Depth



## **CHAPTER VI: MILNE POINT - KUPARUK INTERVAL**

---

### **A. ABSTRACT**

Milne Point field is located on Alaska's North Slope, thirty miles northwest of Prudhoe Bay (Figure VI-1). An expanded base map of Milne Point shows those wells petrophysically analyzed by PDL to date (Figure VI-2). The field is relatively small in size, with less than 70 to 100 million barrels of oil in place. It is operated by Conoco Inc. and produces from the Cretaceous Kuparuk River formation at approximately 6950 to 7000 feet subsea. Figure VI-3, a stratigraphic column from Bird (1987) highlights the Kuparuk River formation. Milne Point is economically viable as a satellite field at acceptably high oil prices through use of production facilities originally intended for the larger North Slope fields.

### **B. FIELD HISTORY**

Exploration history at Milne Point began with the 1969 drilling by Chevron of two Sadlerochit sand group exploratory wells, the 32-14 and 32-14a. They tested wet at the Sadlerochit group but tested oil at both the Kuparuk and West Sak levels. Conoco Inc. then drilled the 18-1 in 1970, the deepest exploratory well on the North Slope at that time. It tested wet at the Sadlerochit group but again, oil was found in the Cretaceous Kuparuk and West Sak sands.

In 1979 and 1980 Conoco Inc. drilled two more exploratory wells. Twenty-two seismic lines were then shot between 1981 and 1984. Conoco Inc. also traded 2-D seismic for Arco Alaska Inc. 3-D seismic. Integrating the 3-D seismic into their analysis, Conoco Inc. drilled nineteen additional wells between 1981 and 1984. Chevron Inc. also drilled six wells to the west and Arco Alaska Inc. drilled the West Sak 25 during this time. These wells proved the West Sak to be of good quality, oil-bearing reservoir rock. They also continued to test oil in the Kuparuk sands. To date, Conoco Inc. has drilled over 63 wells in and around the Milne Point Unit.

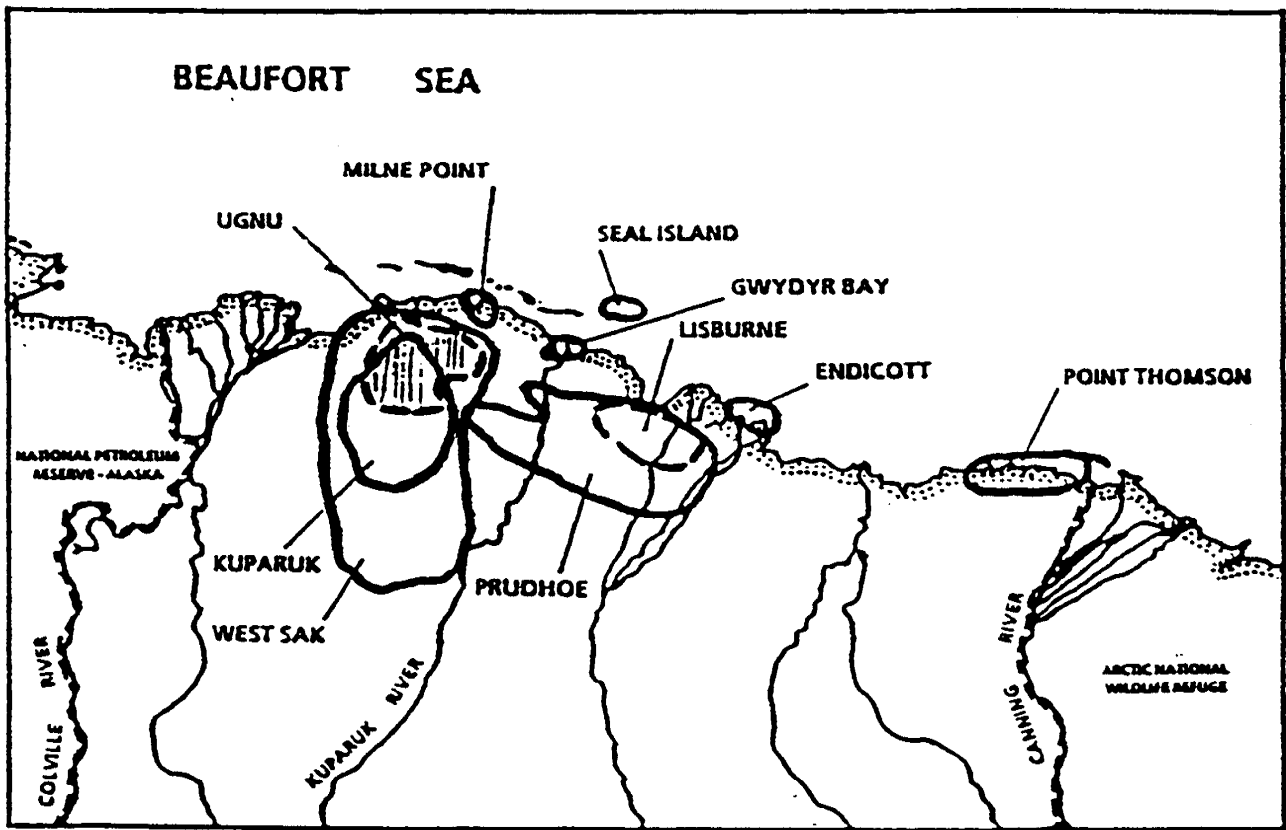


Figure VI-1. Location Map of Major Fields (including Milne Point) on the Alaskan North Slope.

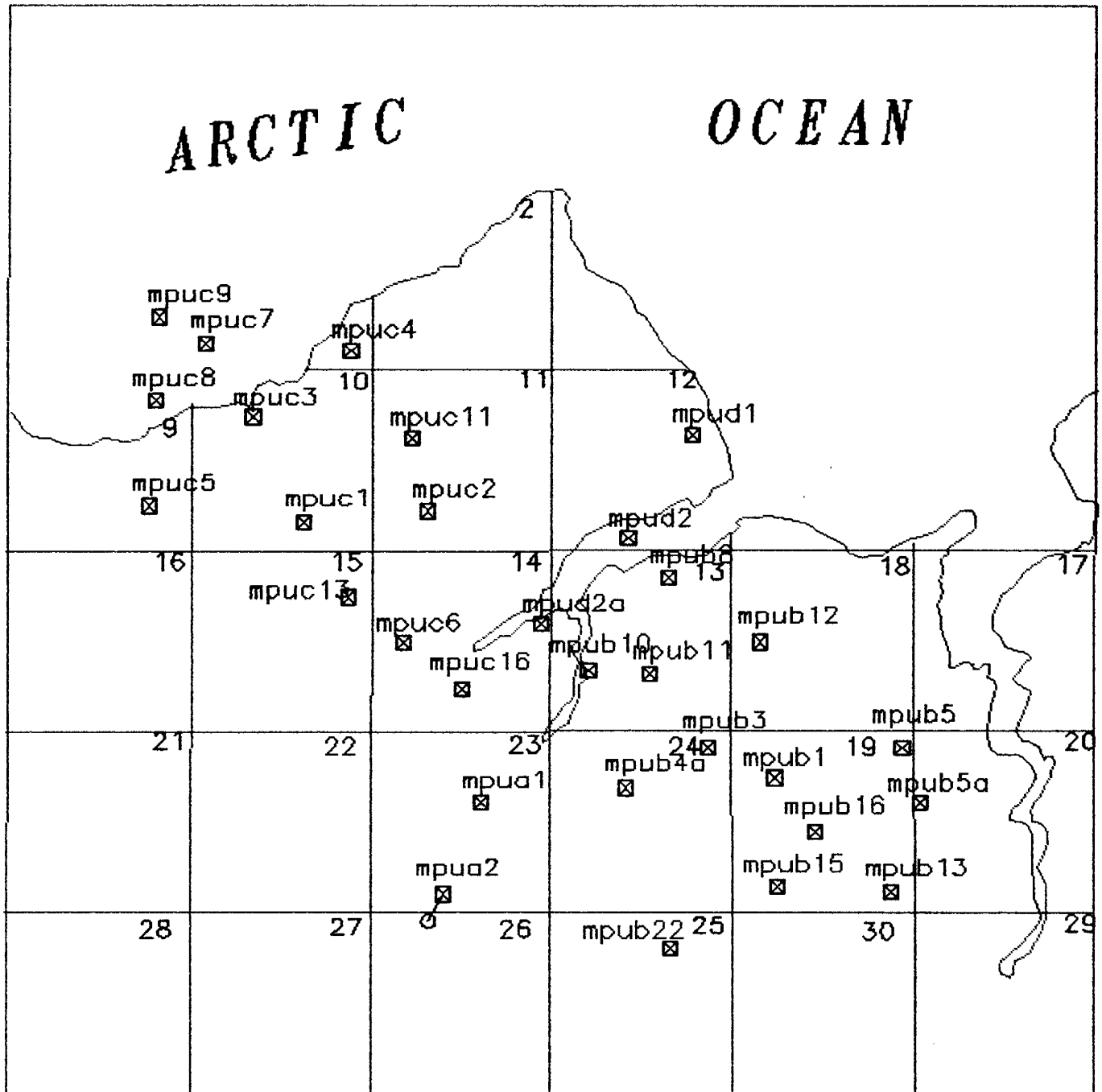
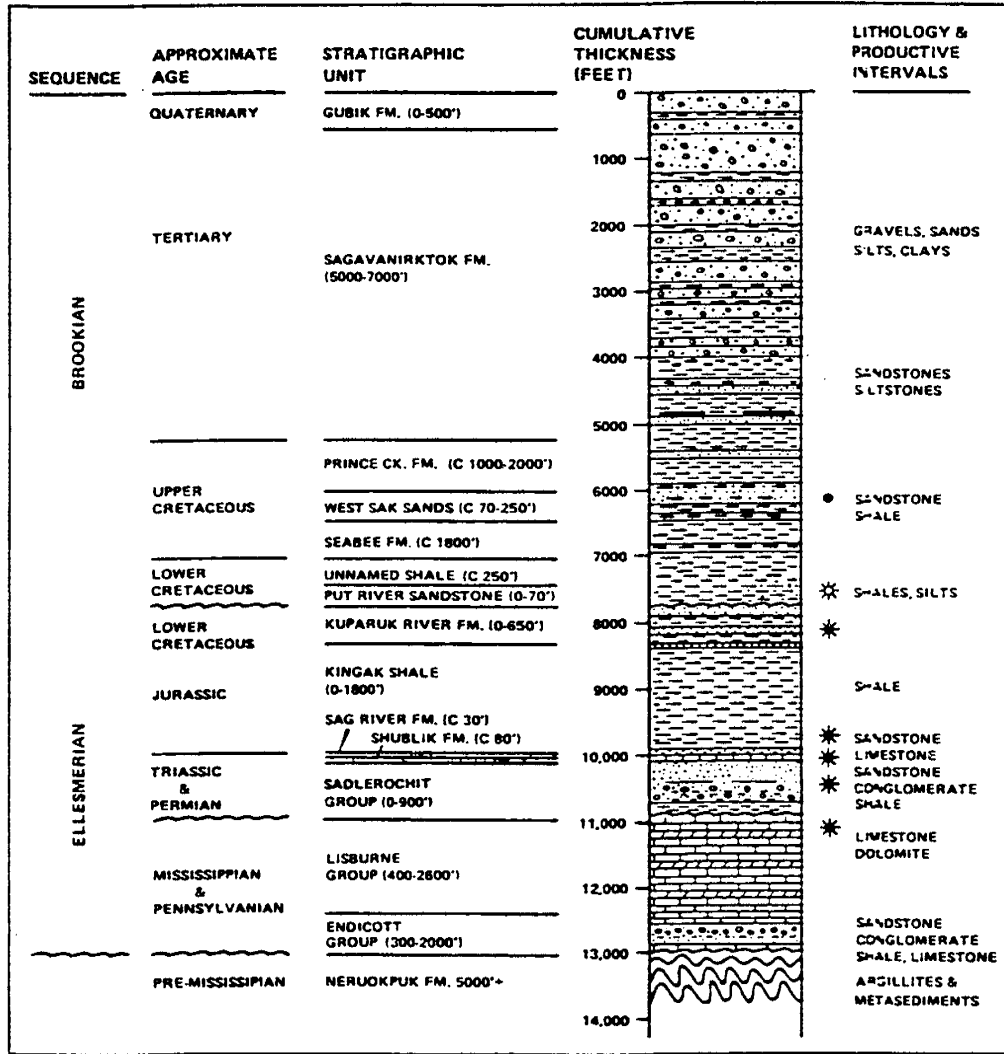


Figure VI-2. Base Map of Milne Point Wells Analyzed.



EXPLANATION:  GAS     GAS AND OIL     OIL

Figure VI-3. Generalized Stratigraphic Column of North Slope Formations, with Kuparuk Formation Highlighted.

## C. MILNE POINT GEOLOGY

Milne Point field lies on the edge of the Kuparuk River Unit (Figure VI-4). The Kuparuk River formation, which is the main producing formation at Milne Point field, is distributed throughout most of northern Alaska (Gaynor and Scheihing, 1989). The sediments were deposited during the Jurassic and Lower Cretaceous rifting episode in the Arctic. Silts and shales of the Jurassic Kingat formation and overlying Miluveach and Kuparuk formations make up the synrift sequence (Figure VI-5).

The Kingat shales were derived from a northerly location and deposited on a shelf and slope environment. The Miluveach shales and Kuparuk sandstones were derived from the adjacent Barrow Arch. The clastics of the Kuparuk formation consist of deltaic-fluvial dominated shelf deposits. Facies include channel sandstones, shelf shales, and siltstones.

Well completion reports define the Kuparuk at Milne Point field in terms of two main members. These members are labeled the Middle Kuparuk formation and Lower Kuparuk formation. At the top of each of these members are two sandy lobes. Production can occur from any of these lobes, although it rarely occurs from more than two lobes in any given well. Artificial fracturing of the Lower Kuparuk lobes by the operator (Conoco Inc.) has been a common practice in attempting to increase production. A plot of well log traces taken from a typical well at Milne Point (the B-3) is shown in Figure VI-6. Lower lobes of both the Middle and Lower Kuparuk formations are not present in several wells, with the Lower Kuparuk formation exhibiting a greater degree of missing section. Preliminary geologic evaluation indicates that abundant faulting exists within, and adjacent to, the producing areas. Several well logs, including those corresponding to the D-2 well (Figure VI-7), indicate that a regressive marine environment of deposition may have predominated during Kuparuk (Neocomian) time.

The formation nomenclature selected at Milne Point by Conoco Inc. differs from that used at the larger Kuparuk field, notwithstanding the fact that the Kuparuk formation consists of two main sand members at both locations. In contrast to Milne Point field, the producing zones at Kuparuk field are defined as occurring within the Upper and Lower Kuparuk formations, rather than within the Lower and Middle Kuparuk formations. However, at both Kuparuk field and Milne Point field, these zones are divided into units, being labeled A through D. Kuparuk units A and C are further subdivided into units A-1 through A-6 and C-1 through C-4, respectively (Masterson and Paris, 1987).

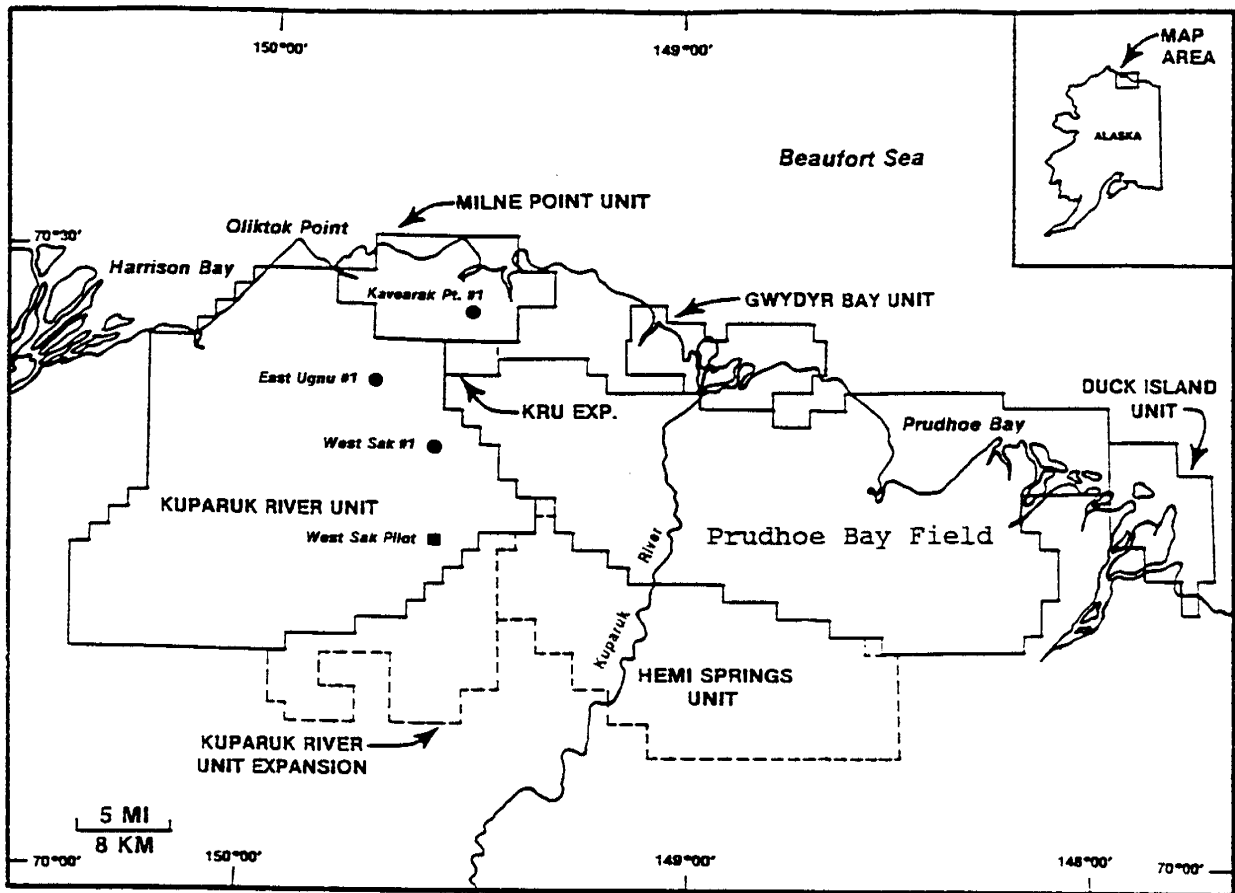


Figure VI-4. Location Map Showing Milne Point Unit Adjacent to Kuparuk River Unit (Bird, 1987).

ERA	SYSTEM	SERIES	GROUP	FORMATIONS Members	HEAVY OIL ZONES KUPARUK AREA	
CENOZOIC	QUAT.	HOLOCENE / PLEISTOCENE		GUBIK FM.		
	TERTIARY	PLIOCENE		SAGAVANIRKTOK FORMATION		
		MIOCENE				
		OLIGOCENE				
		EOCENE				
	PALEOCENE	Sagwon Mbr. (2)	Upper Ugnu Sands			
MESOZOIC	CRETACEOUS	UPPER	COLVILLE GROUP (1)	PRINCE CREEK FM.	Lower Ugnu Sands	
				SCHRADER BLUFF FM.	West Sak Sands	
				SEABEE FORMATION		
				HRZ Unit		
	LOWER	UGNURAVIK GROUP (3)	KALUBIK FM.	← SHALE		
			KUPARUK FM.			
			MILUVEACH FM.	← SHALE		
JURASSIC				KINGAK SHALES		

Figure VI-5. Kuparuk Formation in Relation to Overlying and Underlying Shales (Werner, 1987).

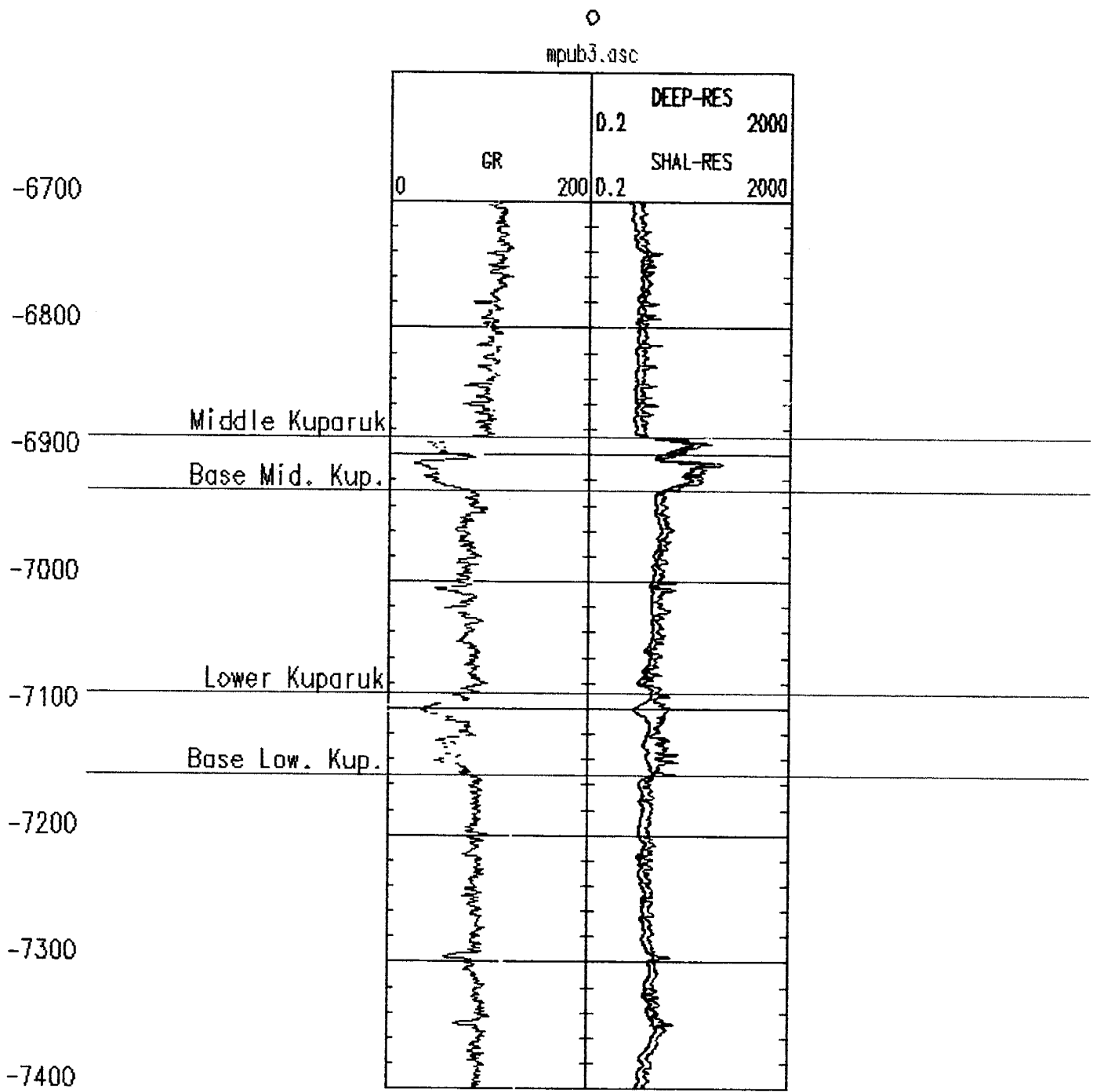


Figure VI-6. Log Plot of the B-3 Well.

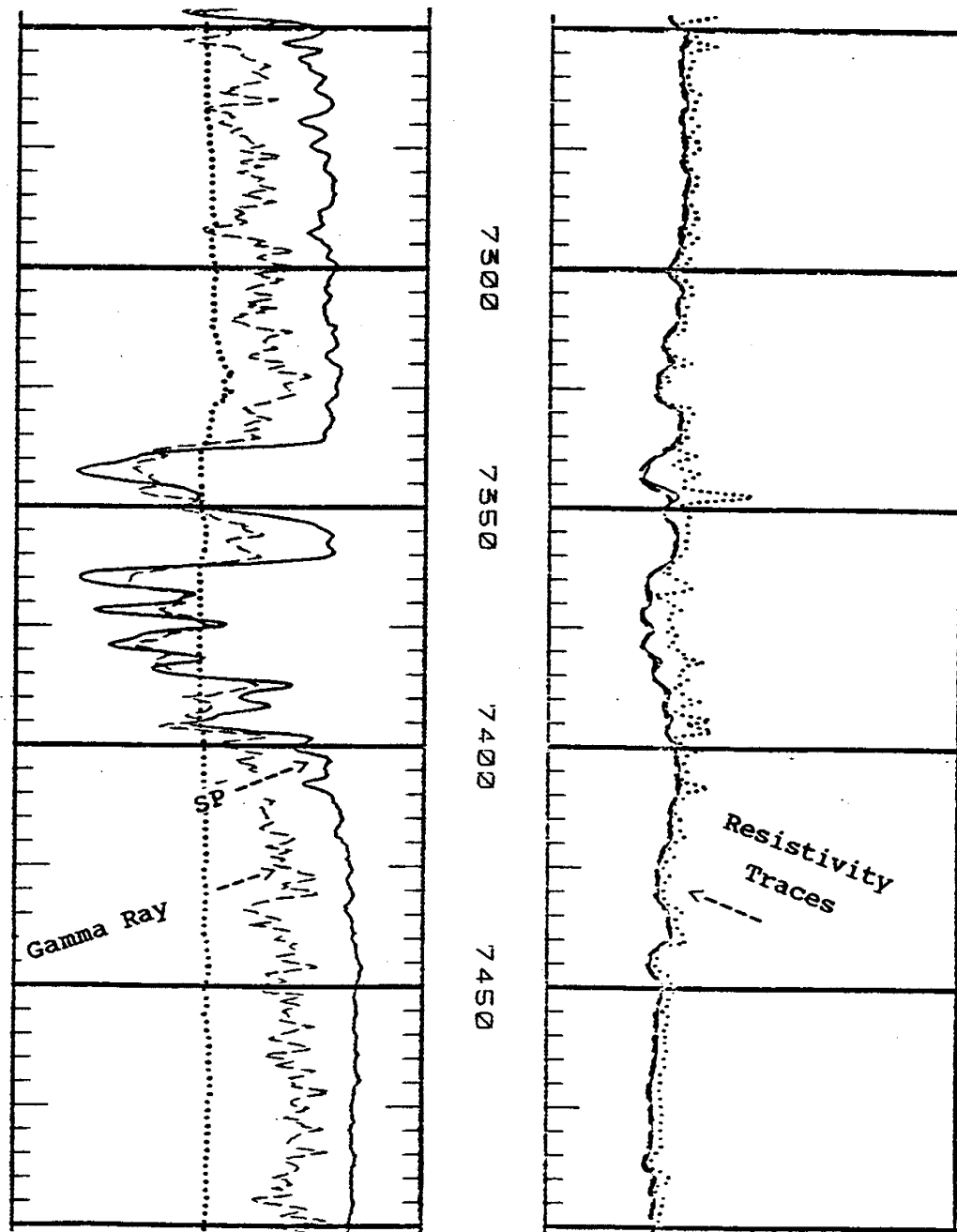


Figure VI-7. Lower Kuparuk Formation Gamma Ray and SP Traces from Milne Point Well D-2. Trace Character Suggests Regressive Depositional Environment Between 7360' and 7400' (true vertical depth).

The difference in nomenclature is likely attributable to nondeposition of the Upper Kuparuk formation in Milne Point field. Figure VI-8, relating North Slope field locations to producing formations, indeed indicates that the Upper Kuparuk formation was not deposited at Milne Point field. This, combined with possible preferential depositional development of Middle Kuparuk sand in Milne Point field vis-a-vis Kuparuk field, would provide, in part, a geological explanation for the difference in nomenclature.

#### **D. FAULTING AT MILNE POINT**

Major faults trending northwest-southeast likely occur on either side of the main field. Such faults could have provided the major structural impetus to the concentration of oil in Milne Point field, in that an uplifted and tilted block with limits defined by these faults may have developed there. Analysis of well test and pressure data may provide insight as to whether any such existing faults are sealing or not. Faulting of this type occurs elsewhere on the North Slope, and was instrumental in the development of reservoirs at Endicott and Prudhoe Bay fields.

PDL analysis provides strong evidence of faulting in Milne Point field, especially between the C-8 and C-3 wells. Cross section AA' (Figure VI-9) shows the C-3 to be down-thrown approximately 150 feet with respect to the C-8. In addition, the completion report for the C-8 indicates that a fault cuts this well approximately 45 feet above the top of the Middle Kuparuk formation. This fault, in all probability, cuts across the Kuparuk formation in the C-3 well (Figure VI-10 shows the locations of cross sections).

Additional faulting is undoubtedly present in Milne Point field as the literature reports the existence of a great number of normal faults in and around the Kuparuk field (Masterson and Paris, 1987). The top of the Middle Kuparuk formation in the C-4 well is considerably lower than in the C-3, and is probably due to faulting (Figure VI-11). Normal faults appear to exist on either side of the B-10 well, as the top of the Middle Kuparuk formation is approximately 40 feet shallower in this well than in the surrounding D-2A and B-3 wells (Figure VI-12). This suggests that the B-10 may lie within a small graben.

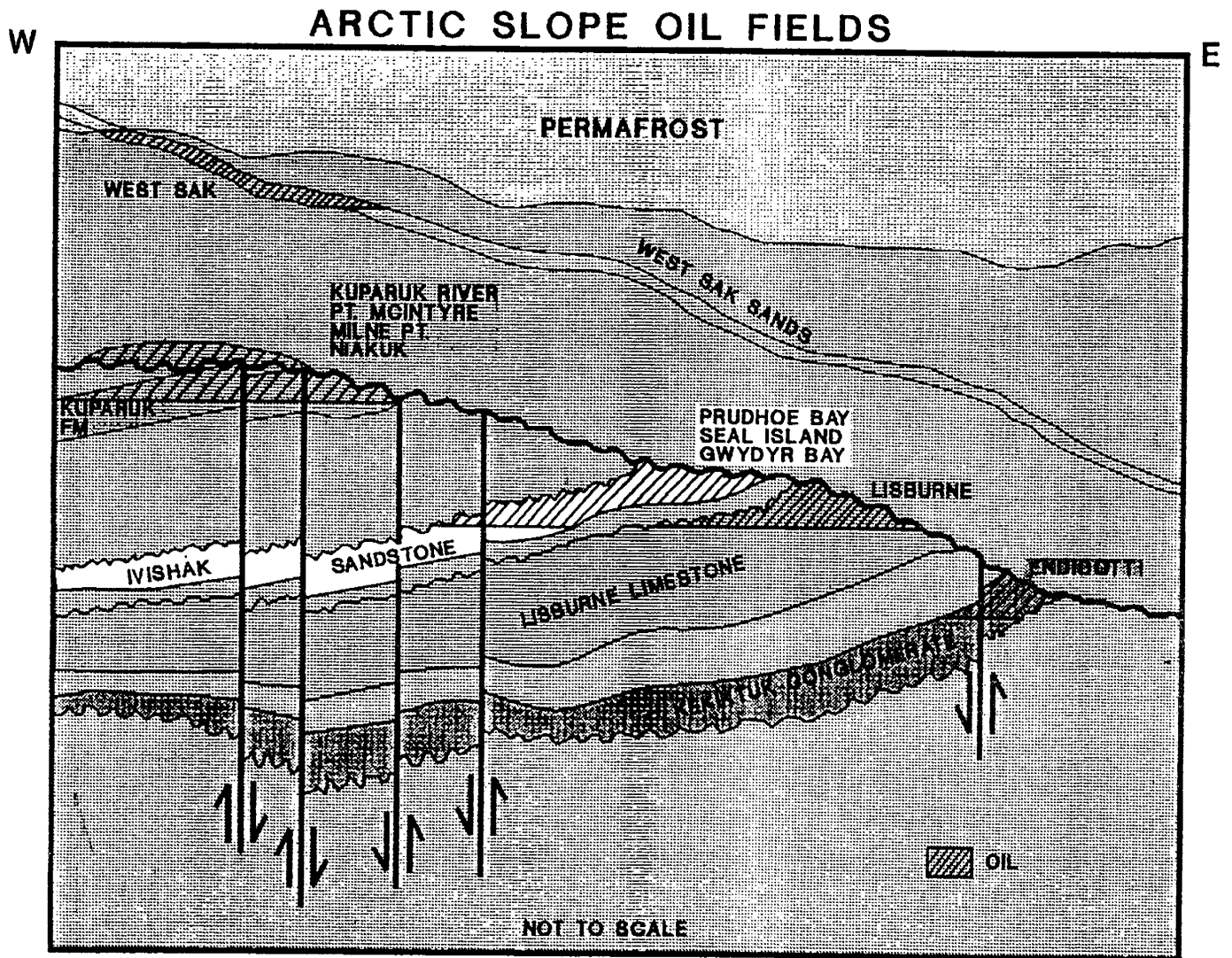


Figure VI-8. Arctic Slope Oil Fields (Alaska Division of Oil and Gas).

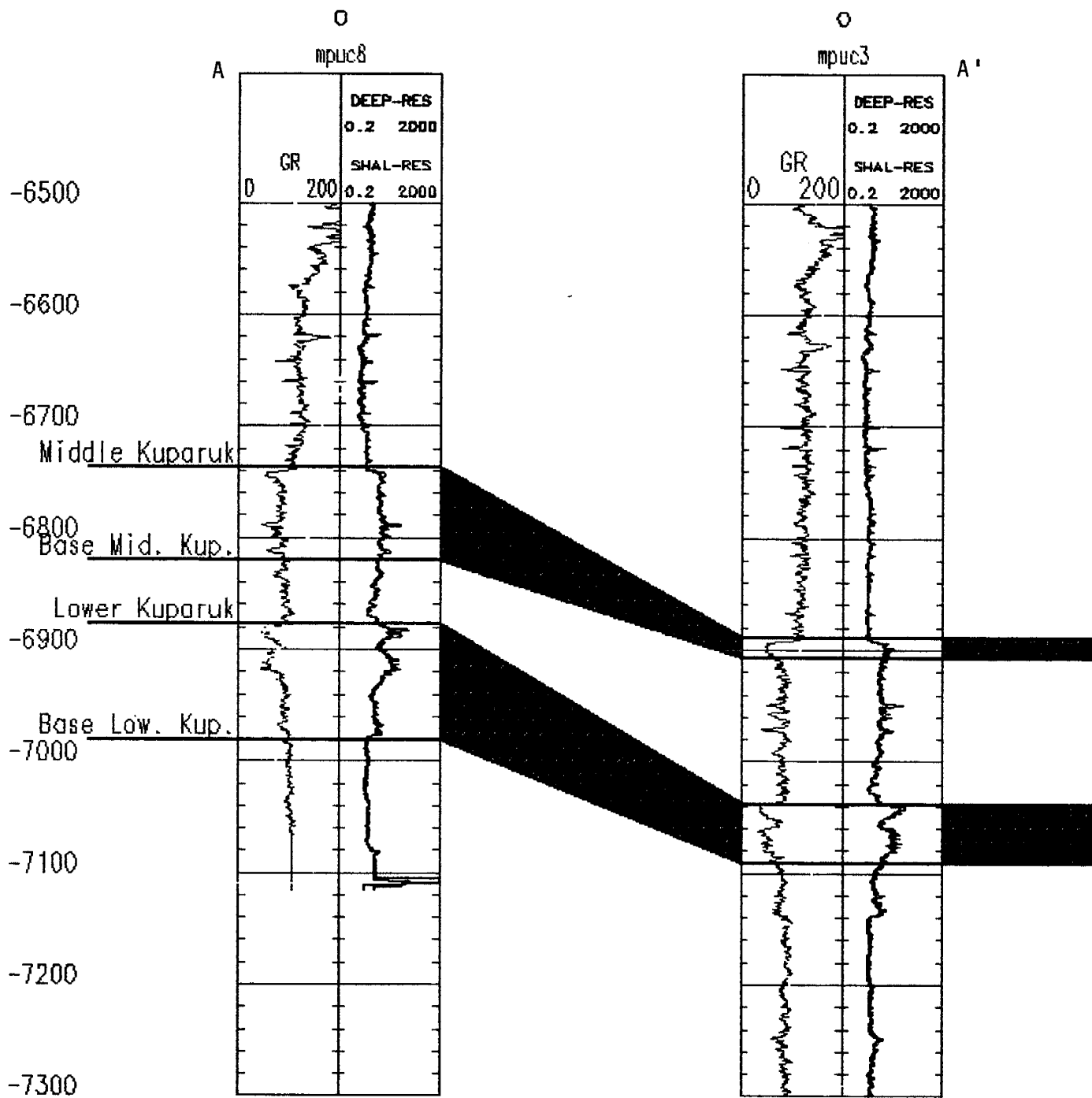


Figure VI-9. Milne Point Field Cross Section A-A'.

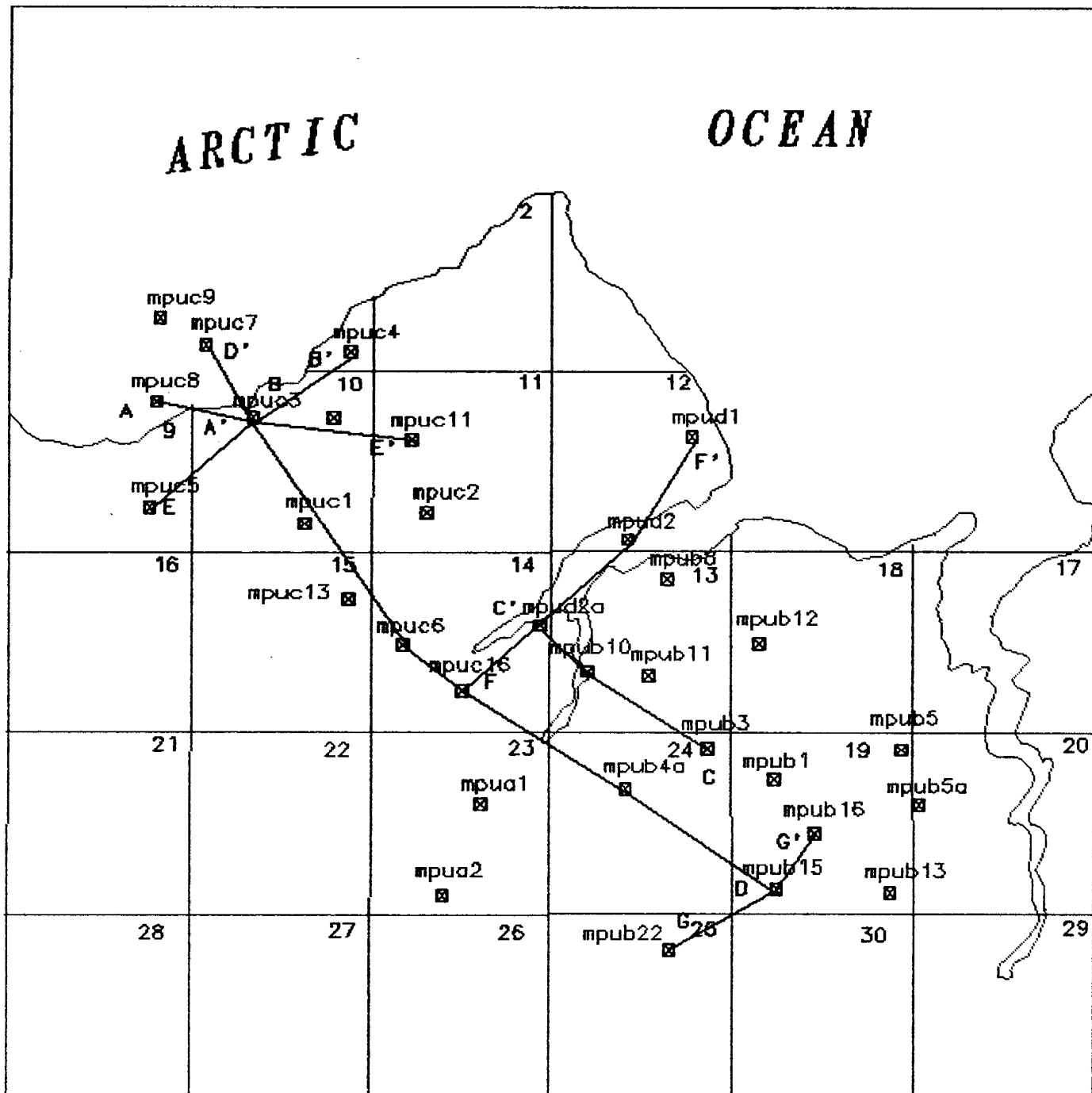


Figure VI-10. Milne Point Base Map Showing Locations of Cross Sections.

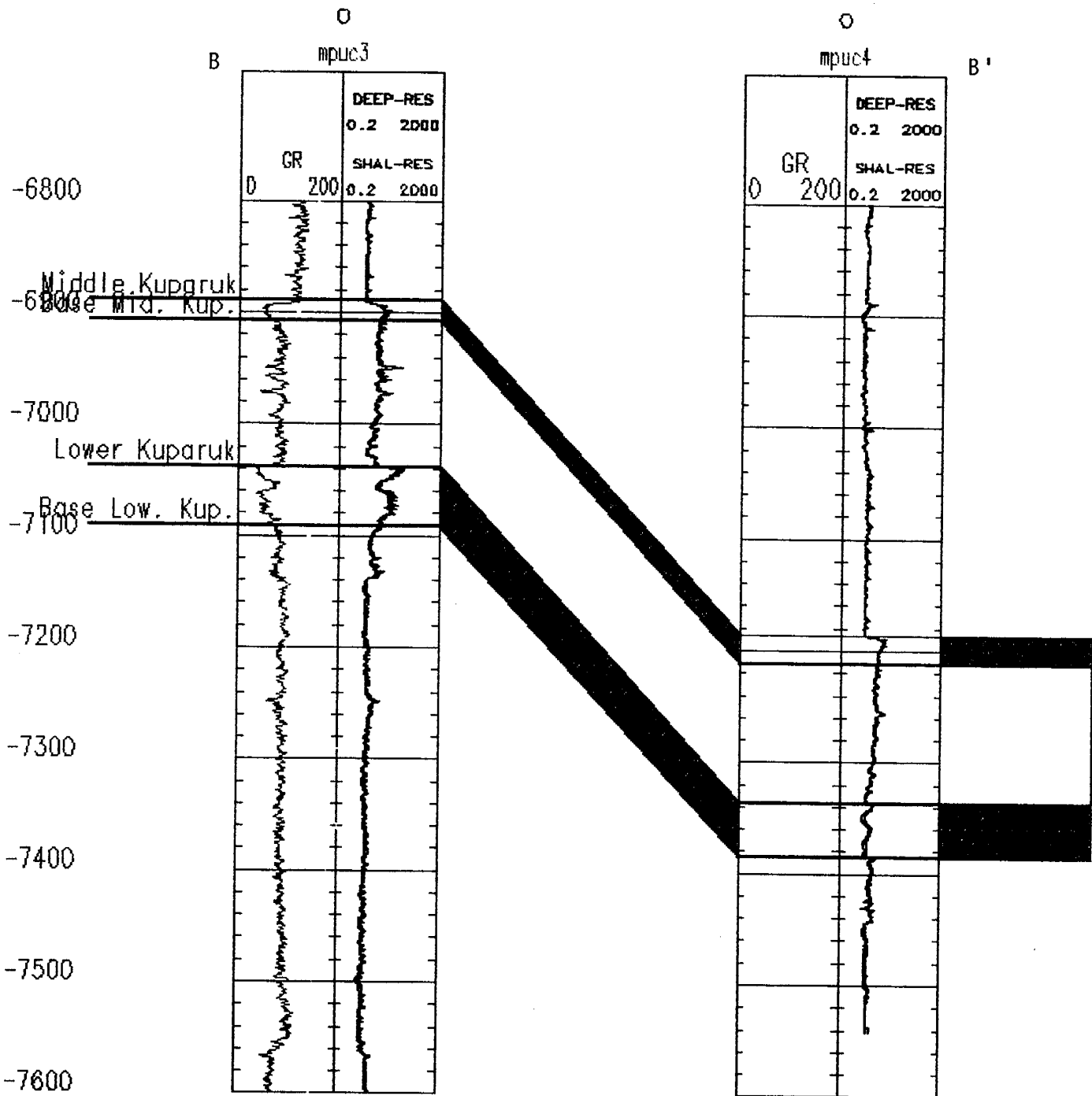


Figure VI-11. Cross Section B-B' Indicating Possible Faulting Between C-3 and C-4 Wells.

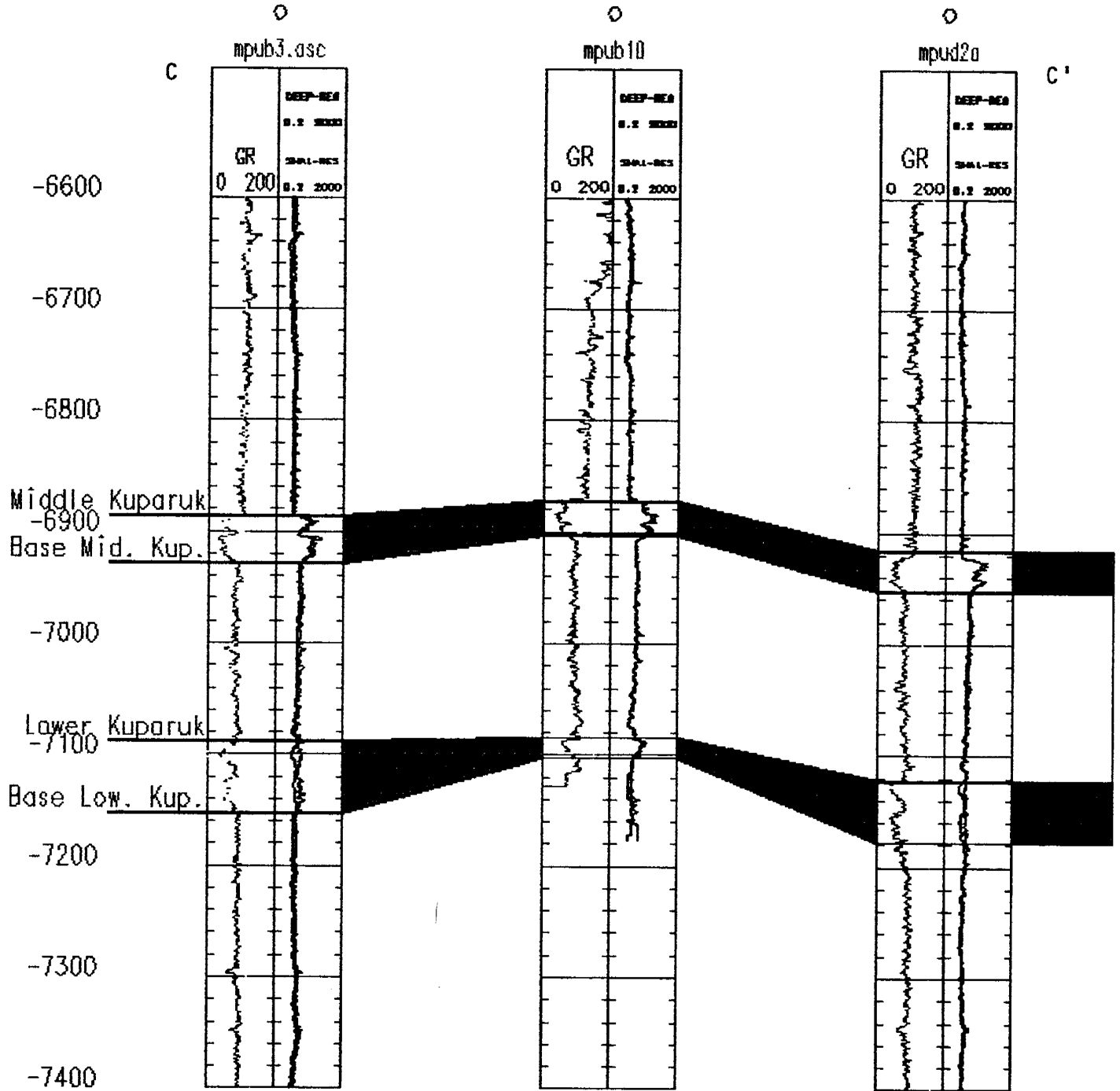


Figure VI-12. Cross Section C-C'. The B-10 May Lie Within a Localized Horst.

## **E. MILNE POINT SAND CONTINUITY**

Stratigraphically, the Middle Kuparuk formation generally thickens towards the southeast, with this thickening first becoming evident in the D-2A well. The lower lobe of the Middle Kuparuk formation may not be present in this well, as the "double-lobed" nature of the Middle Kuparuk formation is not readily apparent north of the D-2A. Southwest-to-northeast cross section D-D' (Figures VI-13a and VI-13b) also shows replacement of two lobes by one upon approaching the C-6 well from the southwest. (The C-6 well is adjacent to the D-2A in Figure VI-10.) The Middle Kuparuk formation's lower lobe most likely thins northward toward these wells, with this thinning therefore being responsible for the overall northward thinning of this entire interval.

The Lower Kuparuk formation, in contrast, shows no general thickening toward the south. Both Lower Kuparuk formation lobes are relatively well developed in all the analyzed wells. Although all four of the Middle and Lower Kuparuk formation sand lobes were deposited on a marine shelf (as is the case with the Kuparuk formation sand lobes at Kuparuk field), the absence of the Middle Kuparuk formation's lower lobe in the northern part of the field represents a differing depositional environment in this area during Middle Kuparuk time, barring erosion. Sands may have been deposited elsewhere during this time or depositional starvation may have occurred.

## **F. MILNE POINT STRUCTURE**

The top Middle Kuparuk formation structure map at Milne Point (Figures VI-14 and VI-15) suggests a northwest oriented anticlinal structure with strong northeasterly dip and a prominent saddle at the crest. The anticline also has a slight plunge toward the northwest. Cross section E-E' (Figure VI-16) indicates the northern part of the field at all Kuparuk formation levels to be structurally pronounced, with the Kuparuk formation in the C-3 well being much shallower than in surrounding wells. Figures VI-17 and VI-18 show Lower Kuparuk formation structure to closely mimic the structure on the Middle Kuparuk formation.

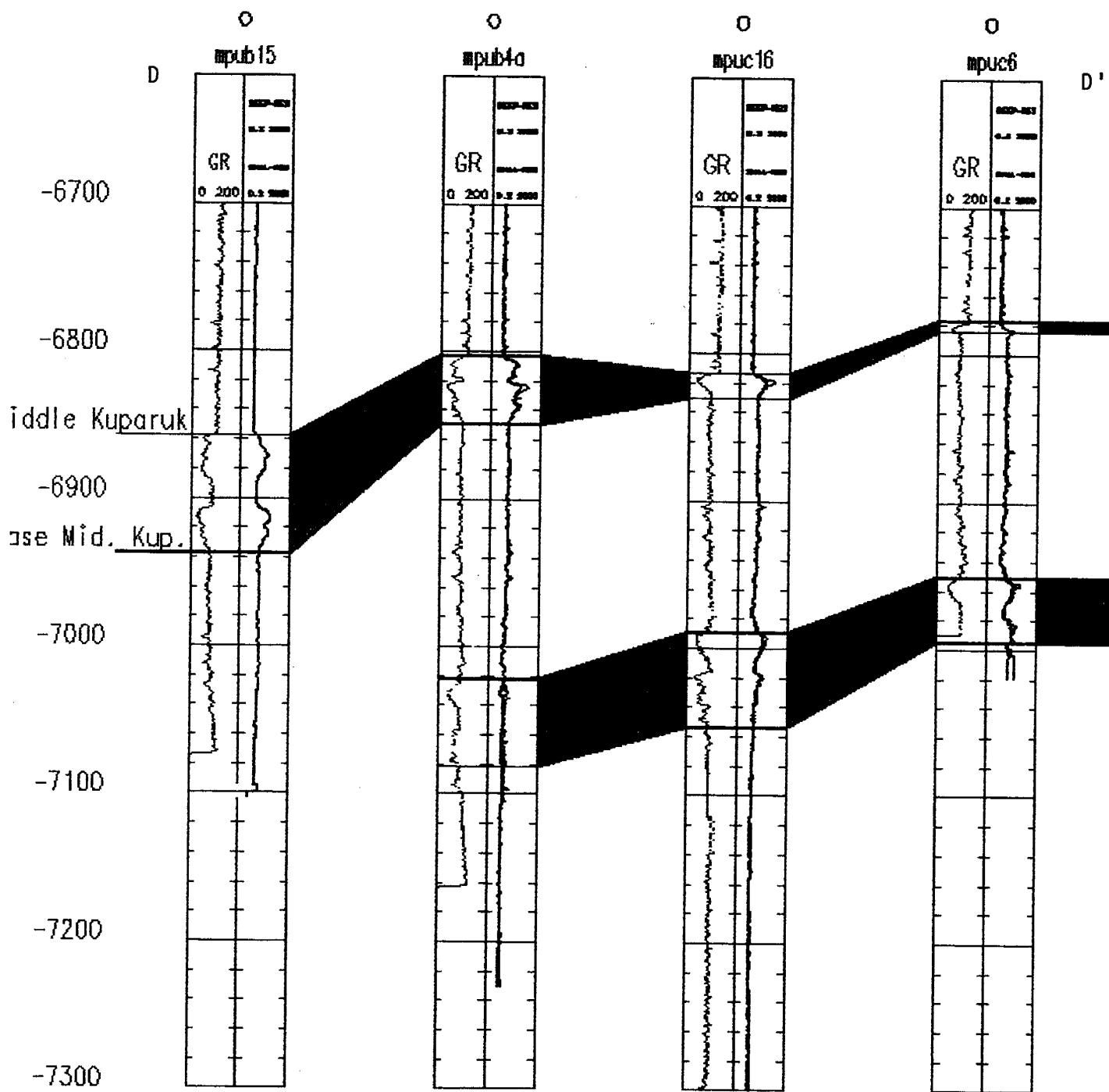


Figure VI-13a. Southeast Portion of Cross Section D-D' Showing Milne Point Structural Crest at the C-6 Well.

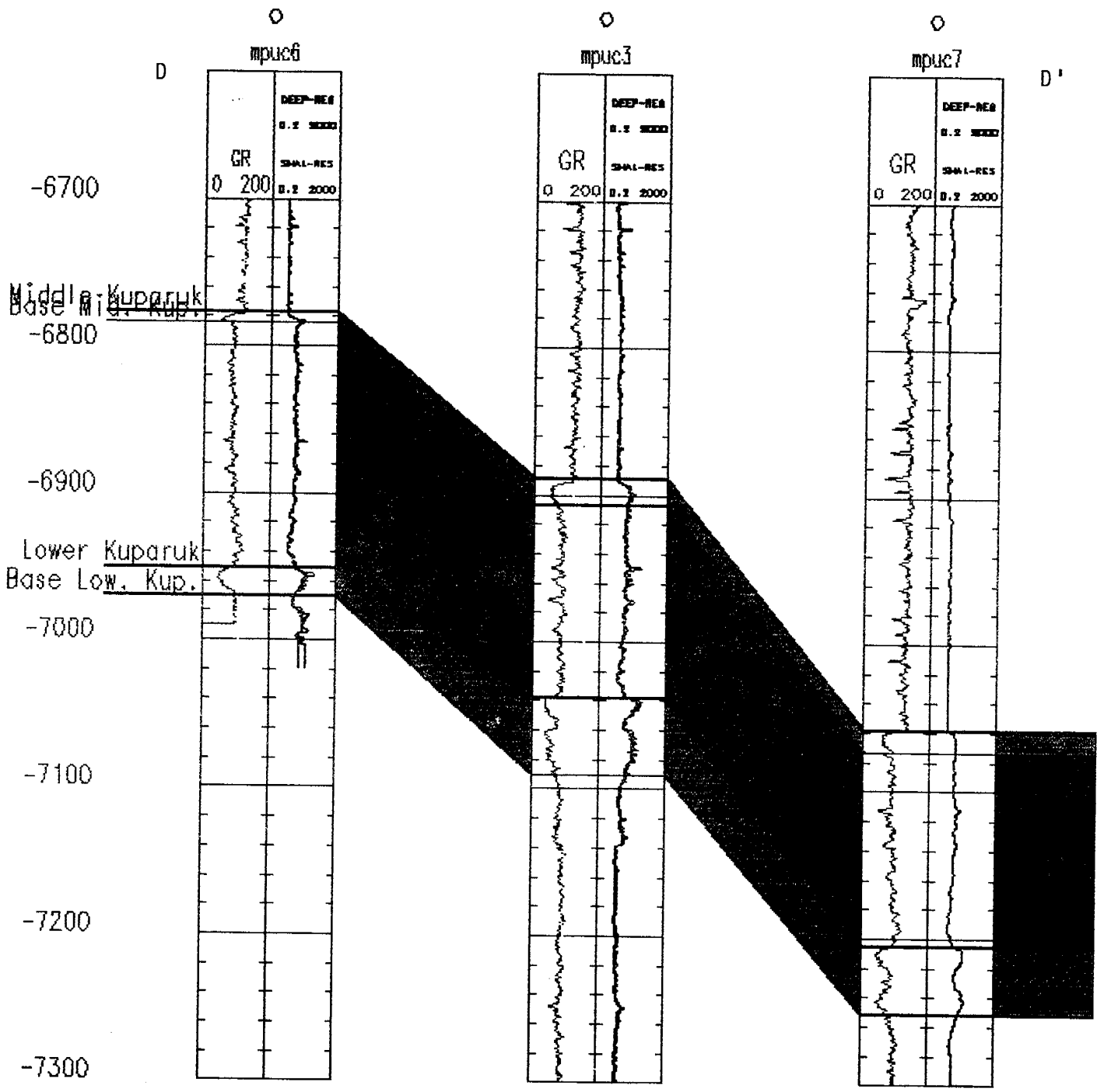


Figure VI-13b. Northwest Portion of Cross Section D-D' Showing Milne Point Structural Crest at the C-6 Well.

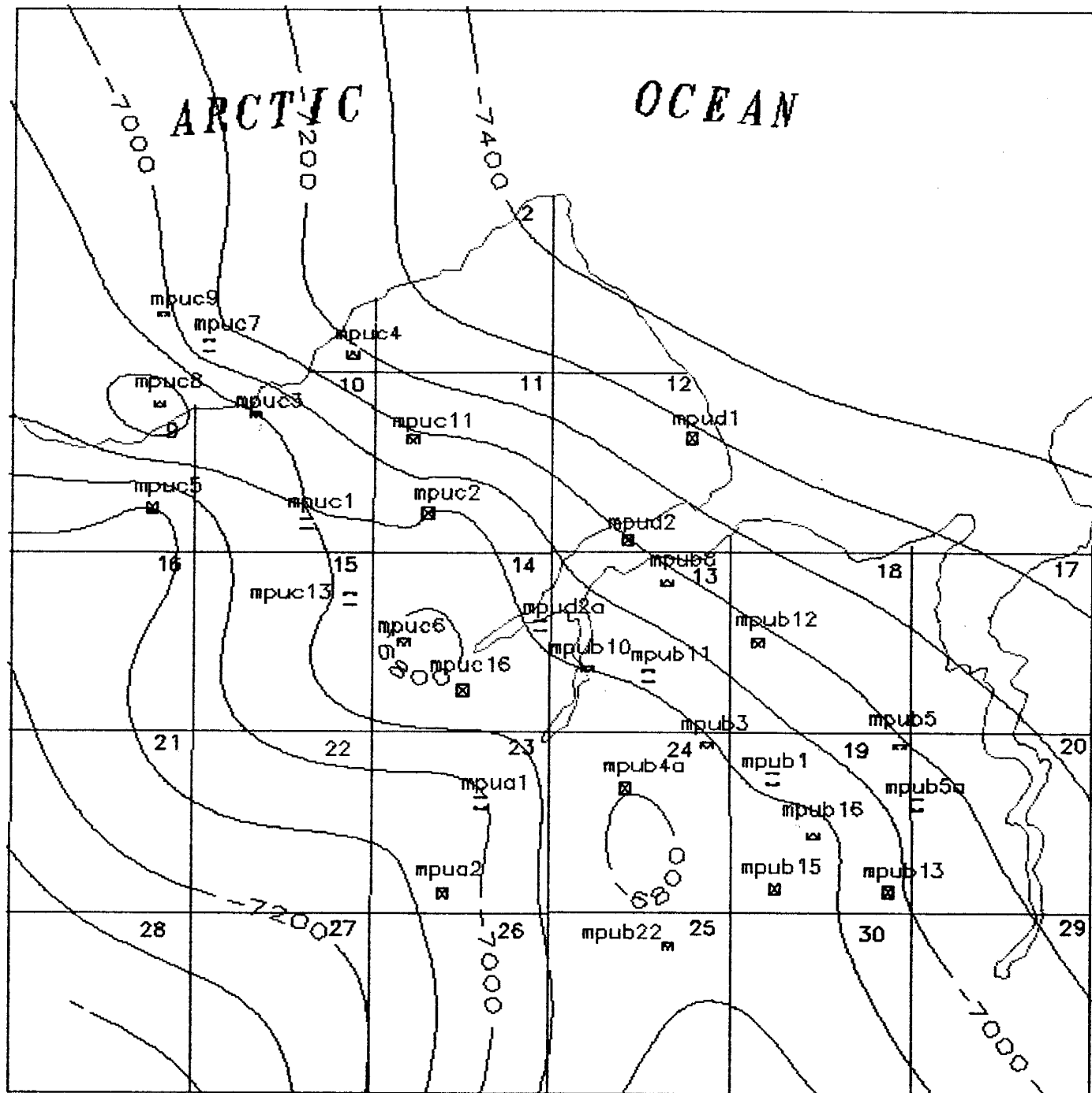


Figure VI-14. Structure Top of Milne Point Upper Kuparuk Formation.

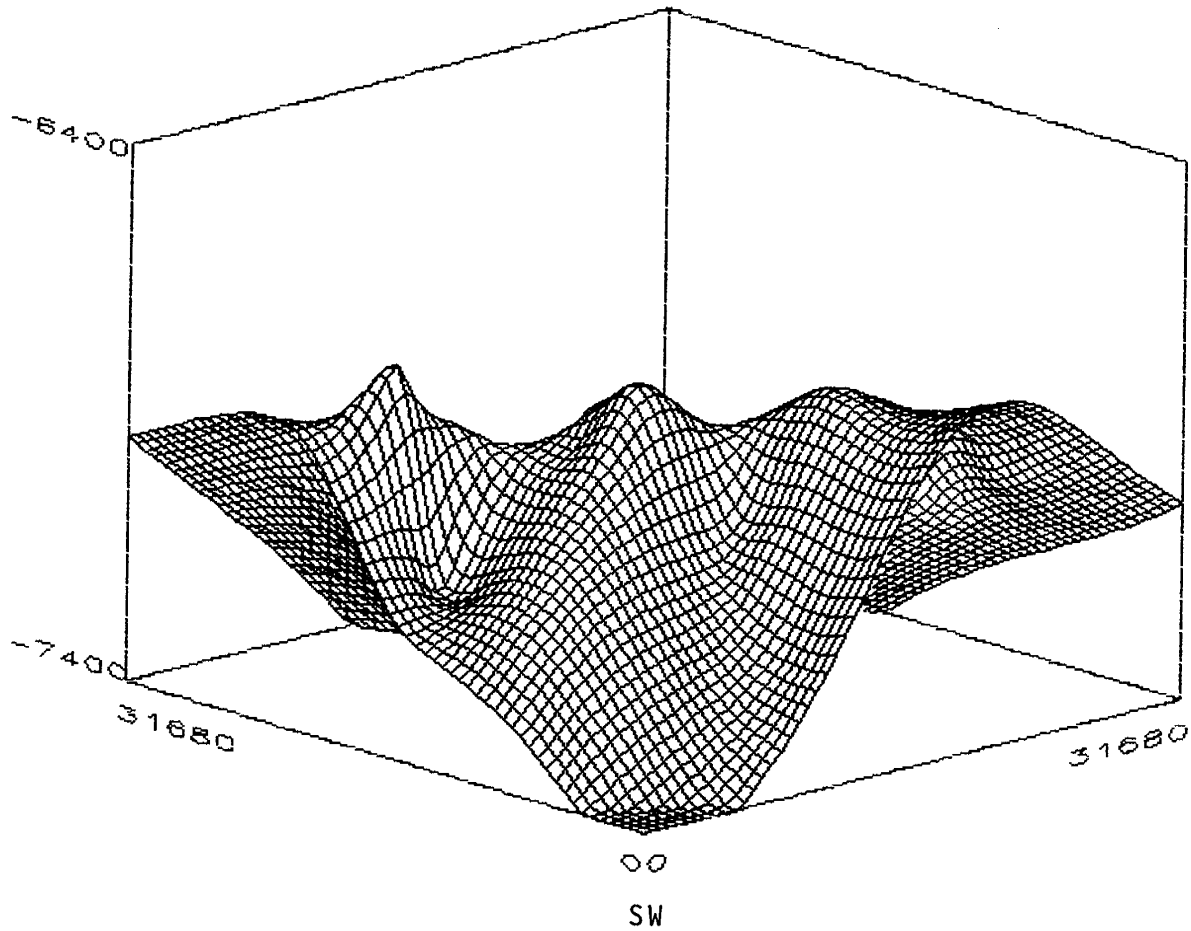


Figure VI-15. 3-D View of Top Middle Kuparuk Formation (viewed from the southwest).

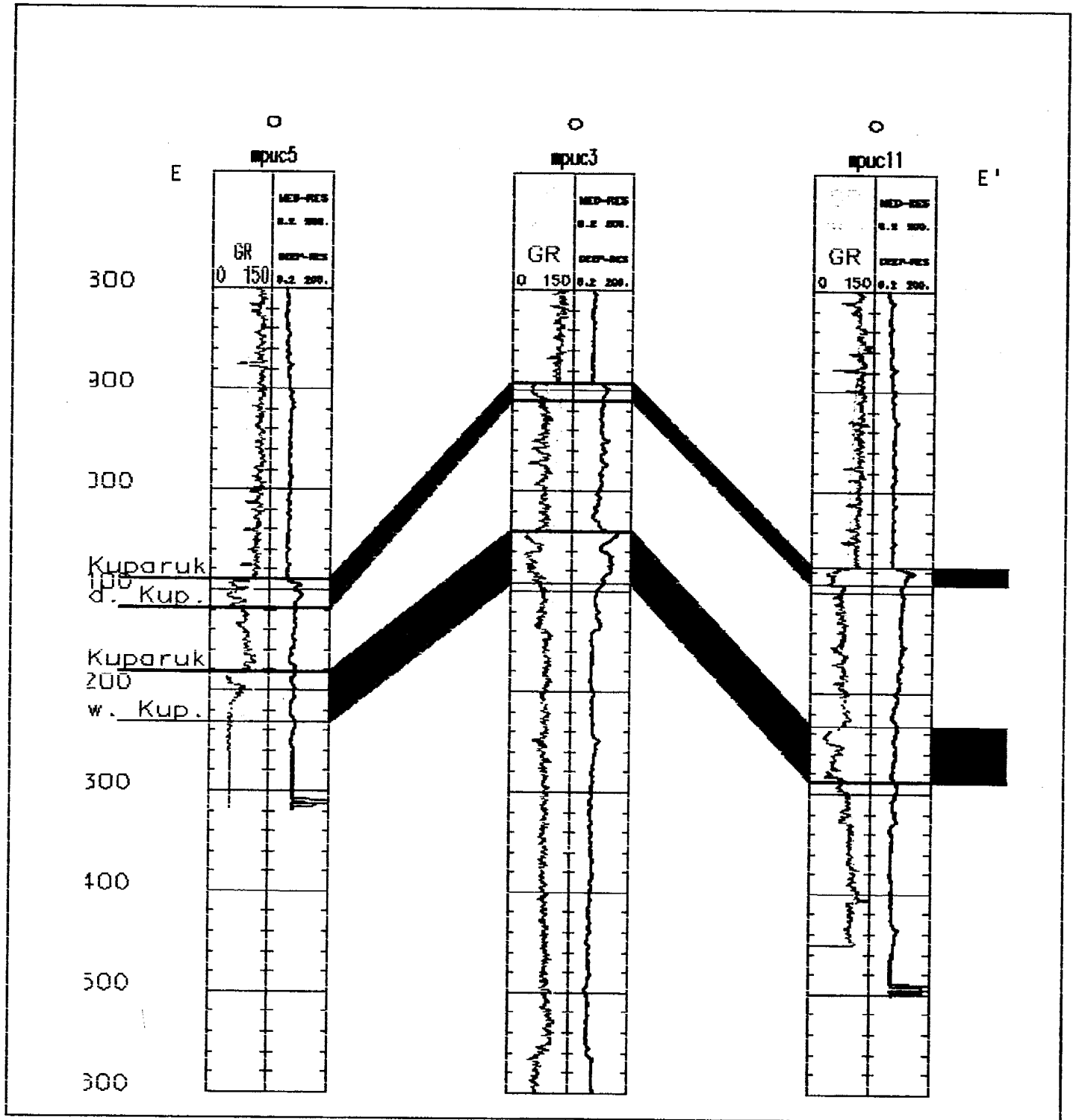


Figure VI-16. East-West Cross Section E-E', the Northern Part of the Field.

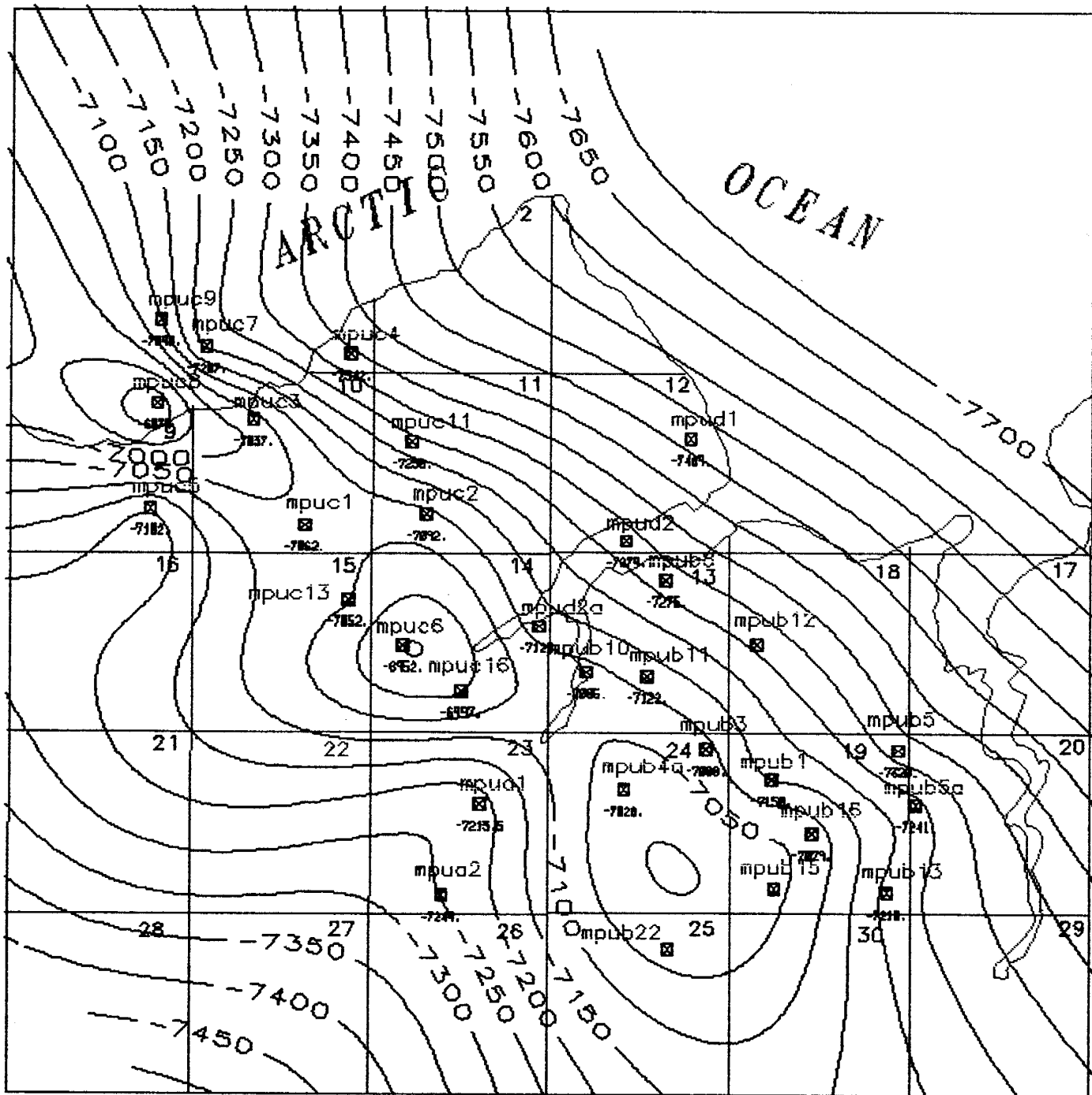


Figure VI-17. Structure Top of Milne Point Lower Kuparuk Formation.

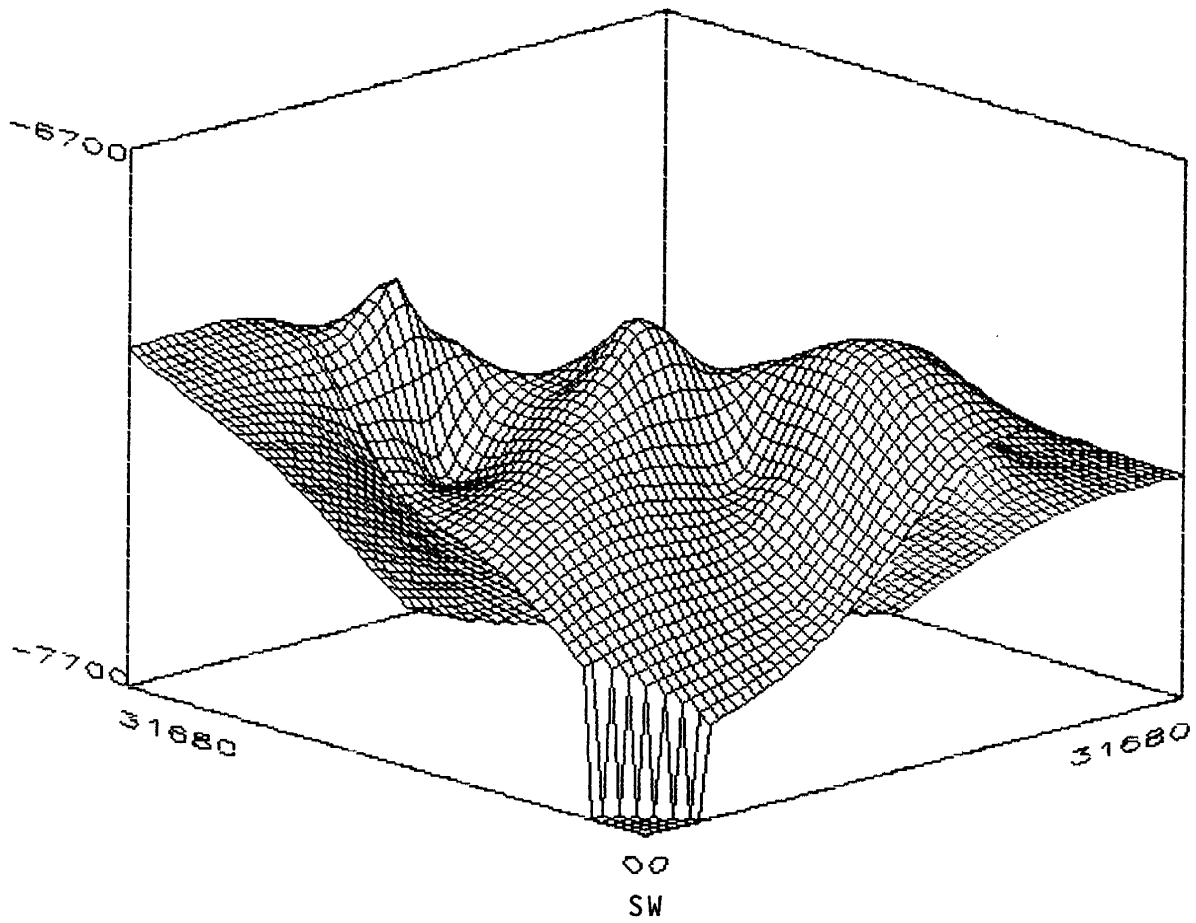


Figure VI-18. 3-D Structure Top of Milne Point Lower Kuparuk Formation (viewed from the southwest).

Cross sections F-F' and G-G' (Figures VI-19 and VI-20) are sub-parallel to cross section E-E', but lie across the southern portion of the field. They show lessening structural relief southward but also show the thickening and strengthening character of the Middle Kuparuk formation's lower lobe southward. In general, both Middle Kuparuk formation lobes shallow and steepen northward. They are broader and lower toward the southeast.

## **G. DISCUSSION OF MILNE POINT PETROPHYSICAL PROPERTIES**

Isopach contour maps and 3-D plots of Middle and Lower Kuparuk formation upper and lower lobes are presented in Figures VI-21 through VI-28. The isopach contour map on the Upper Kuparuk formation's upper lobe generally mimics the structure on the top of the Middle Kuparuk formation (Figures VI-21 and VI-22). However, as is evident in Figures VI-23 through VI-28, thickness patterns corresponding to the remaining Kuparuk formation sand lobes vary greatly across the field. Thicknesses in the center of the field average 15 to 25 feet, with lower lobes of both Middle and Lower Kuparuk formations exhibiting the greatest thicknesses.

Porosity maps of the Middle and Lower Kuparuk formations at Milne Point Unit lobes are presented in Figures VI-29 through VI-36. In the case of the Upper Kuparuk formation, highest porosities (30%) exist locally in the case of the B-15 well. Although porosities in the Lower Kuparuk formation do not range quite as high as those in the Upper Kuparuk formation, they are higher over a wider area of the field. This, in turn, makes the Lower Kuparuk formation more promising as a reservoir.

Finally, water saturation maps for the Middle and Lower Kuparuk formations are presented in Figures VI-37 through VI-44. In all cases, water saturations are highest in the southeast portion of the field, ranging from 80 to 100%. In the case of the lower lobe of the Middle Kuparuk formation, they lessen to 50% on the northwest side of the field. The same pattern generally holds for the lower lobe of the Lower Kuparuk formation. In the case of the upper lobes of both Middle and Lower Kuparuk formations, water saturations are lower in the center of the field and increase in all directions away from the center.

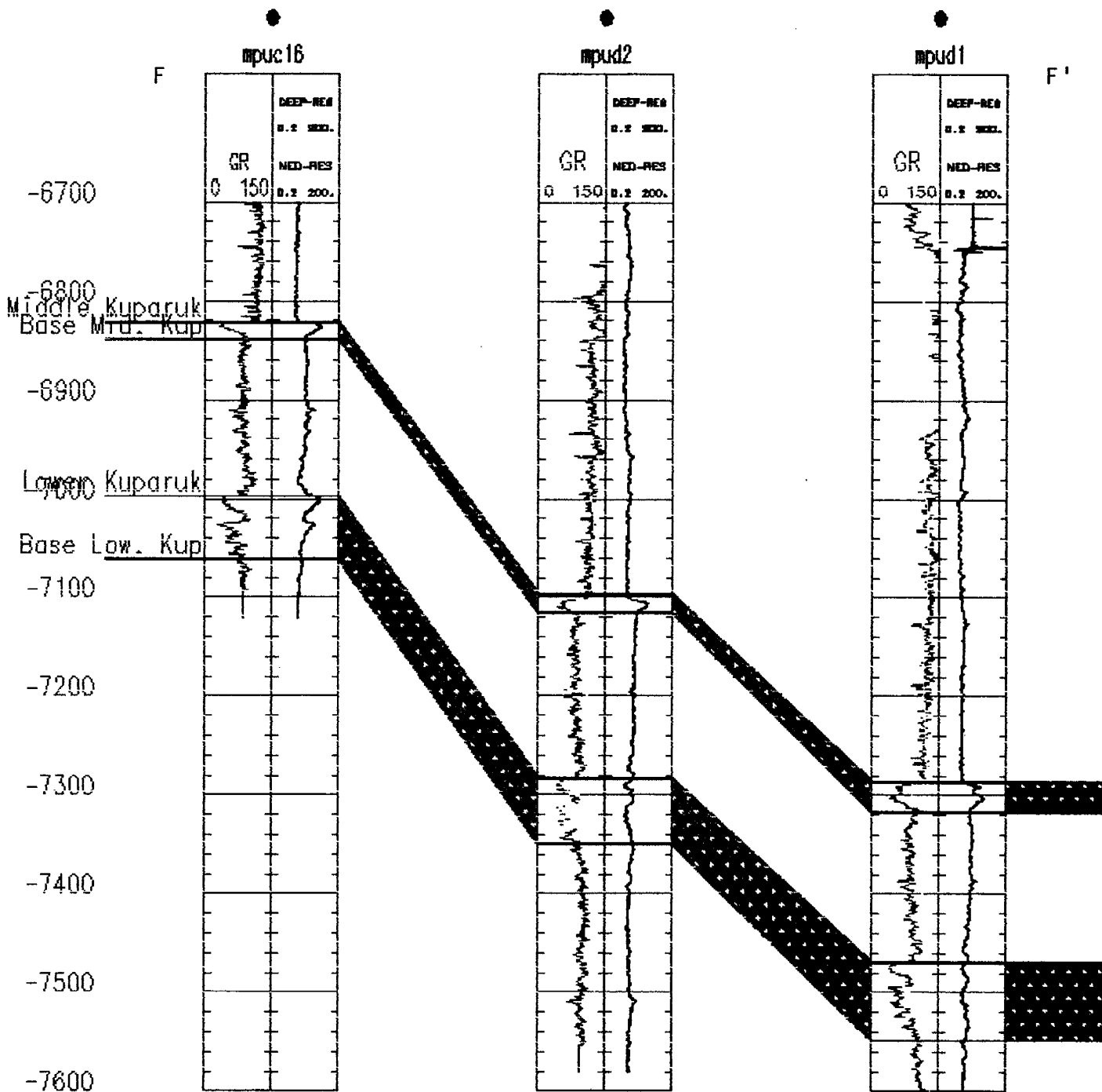


Figure VI-19. East-West Cross Section F-F' Across the Southcentral Portion of Milne Point Field.

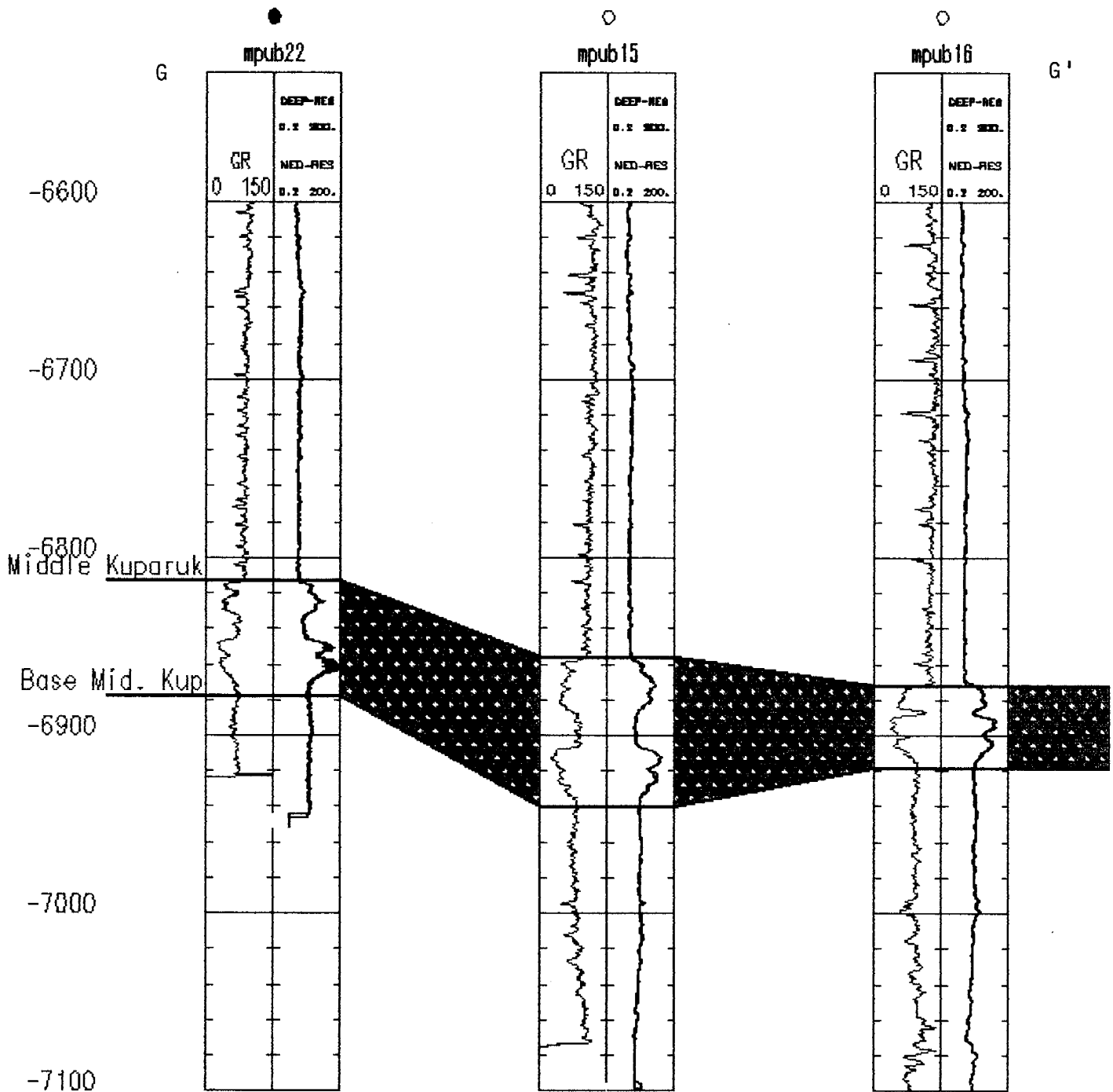


Figure VI-20. East-West Cross Section G-G' Across the Southern Portion of Milne Point Field.

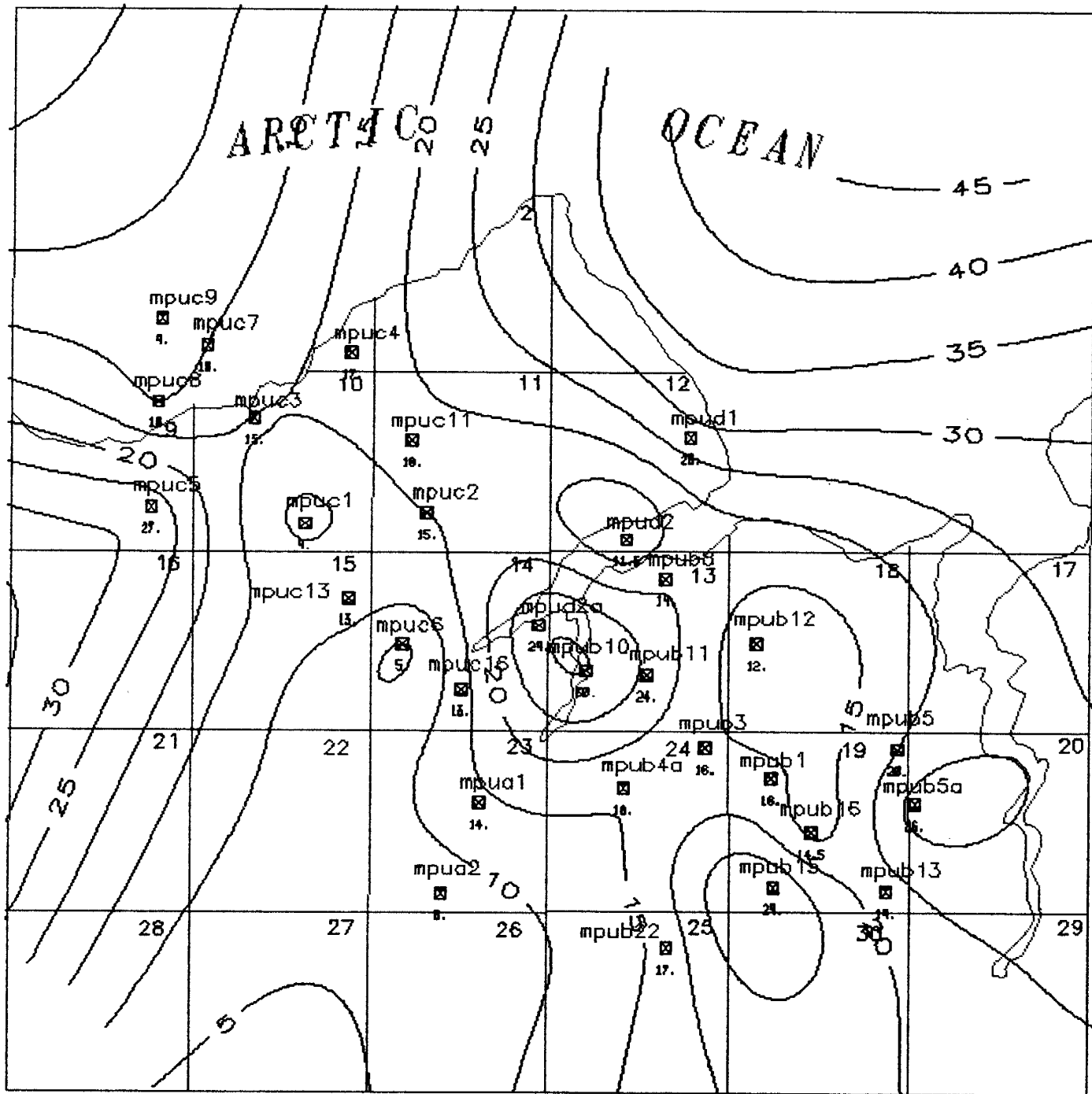


Figure VI-21. Isopach Contour Map of Upper Lobe of Milne Point Middle Kuparuk Formation.

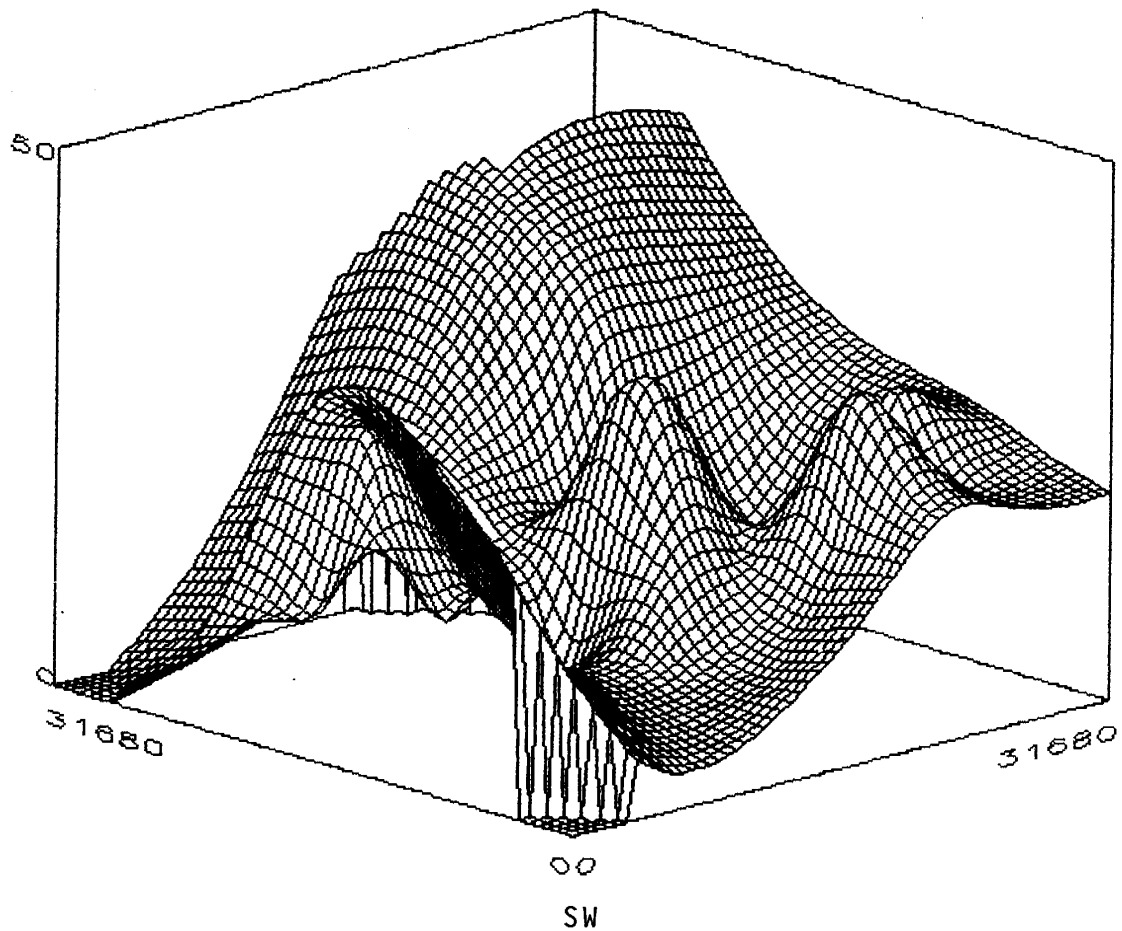


Figure VI-22. 3-D Isopach View of Upper Lobe of Milne Point Middle Kuparuk Formation (viewed from the southwest).

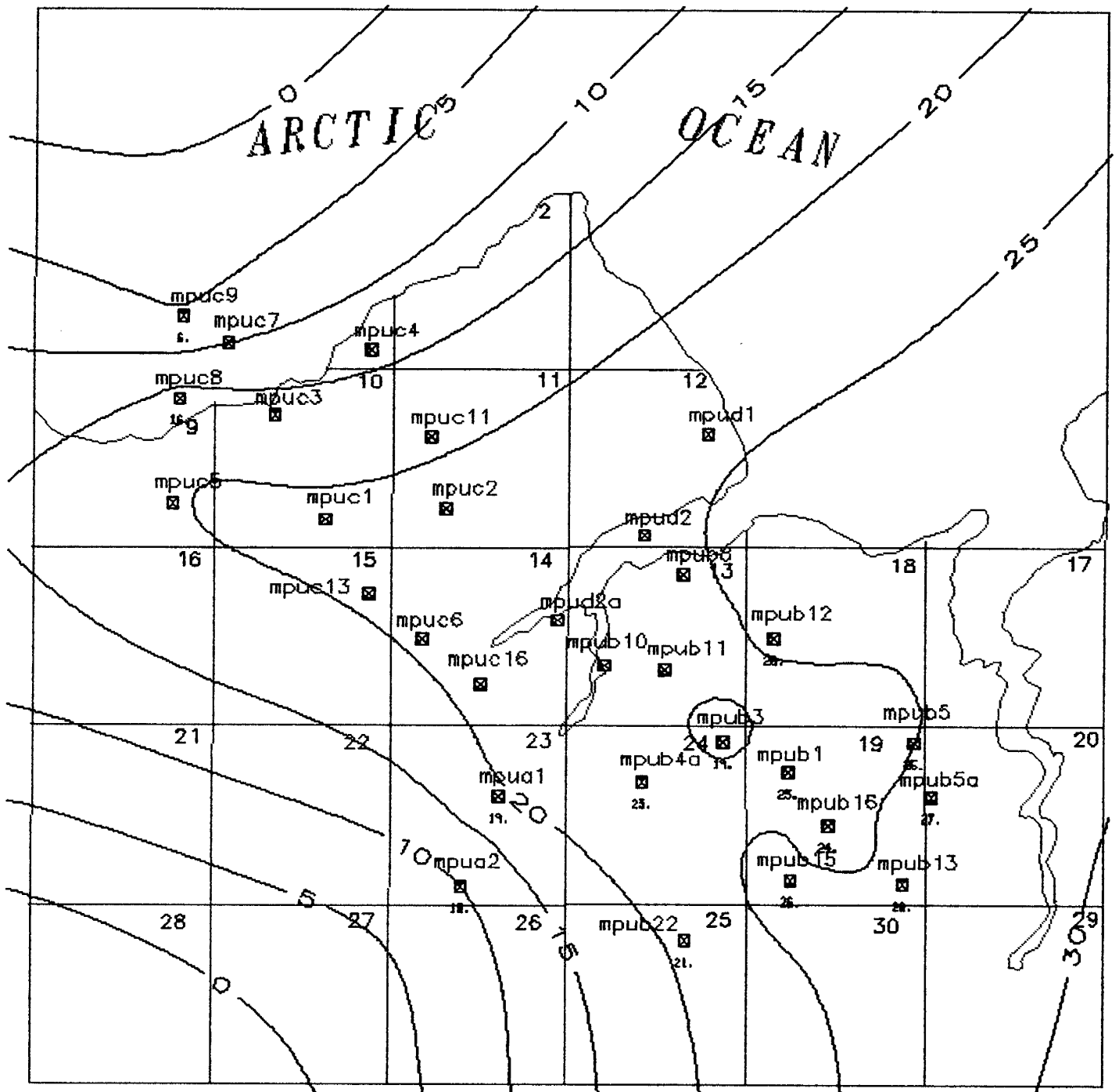


Figure VI-23. Isopach Contour Map of Lower Lobe of Milne Point Middle Kuparuk Formation.

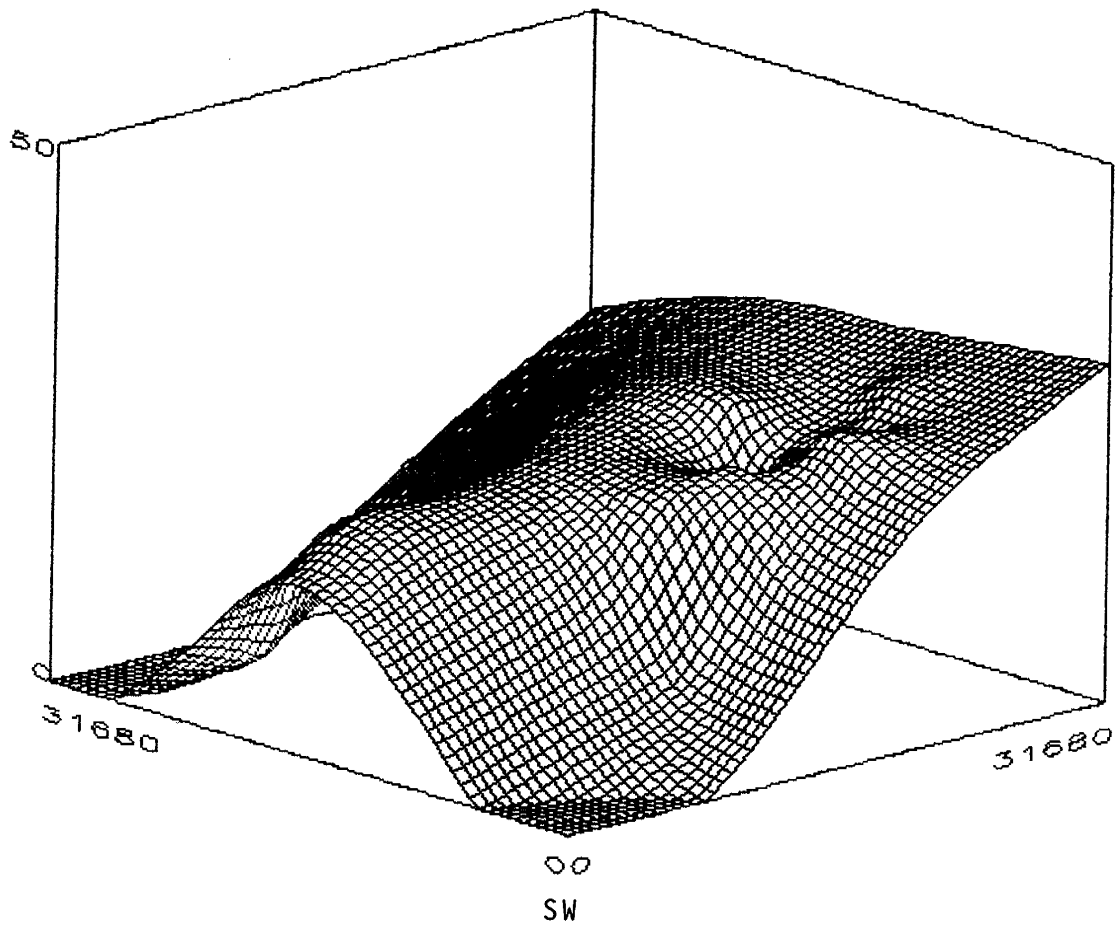


Figure VI-24. 3-D Isopach View of Lower Lobe of Milne Point Middle Kuparuk Formation (viewed from the southwest).

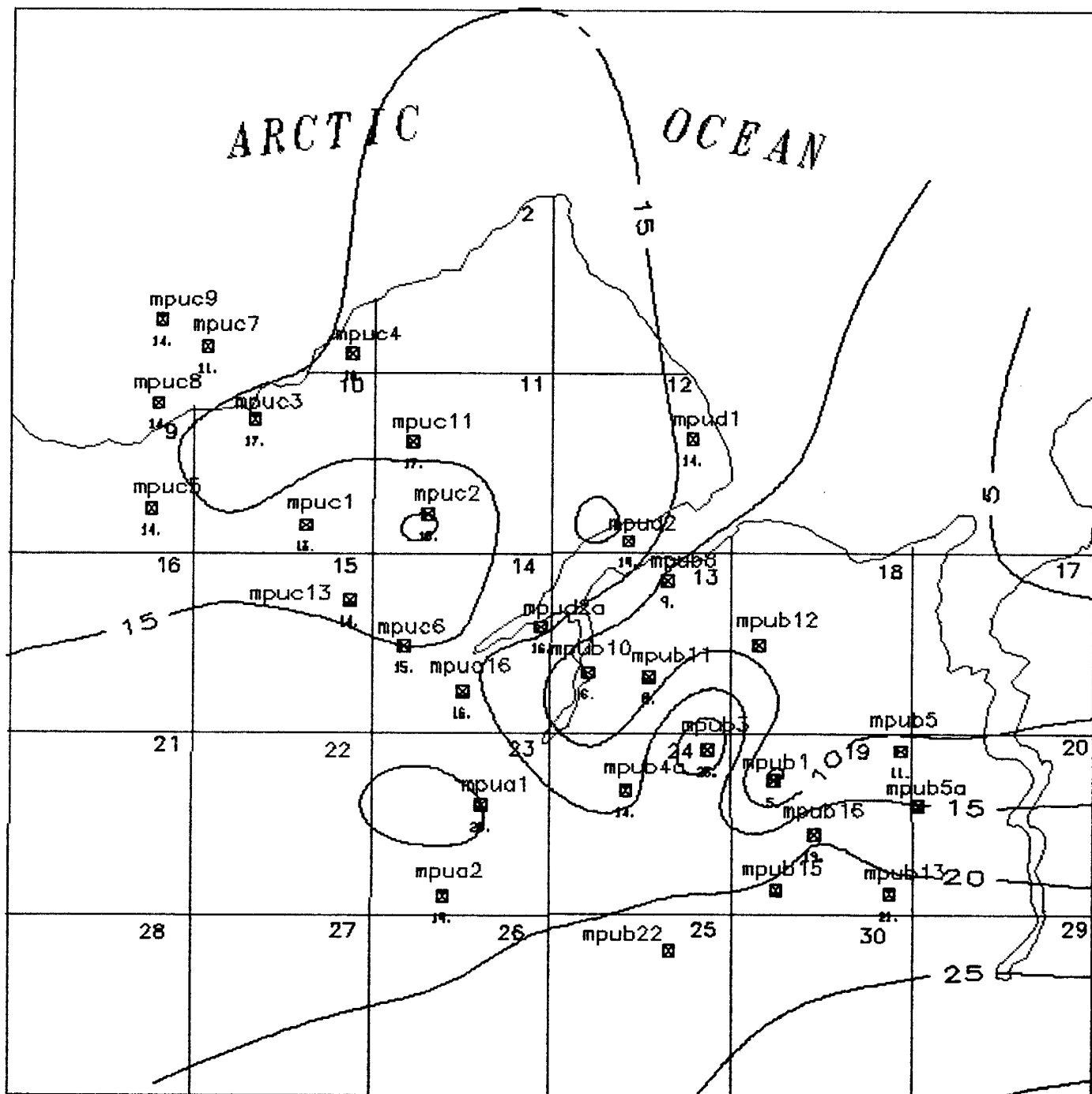


Figure VI-25. Isopach Contour Map of Upper Lobe of Milne Point Lower Kuparuk Formation.

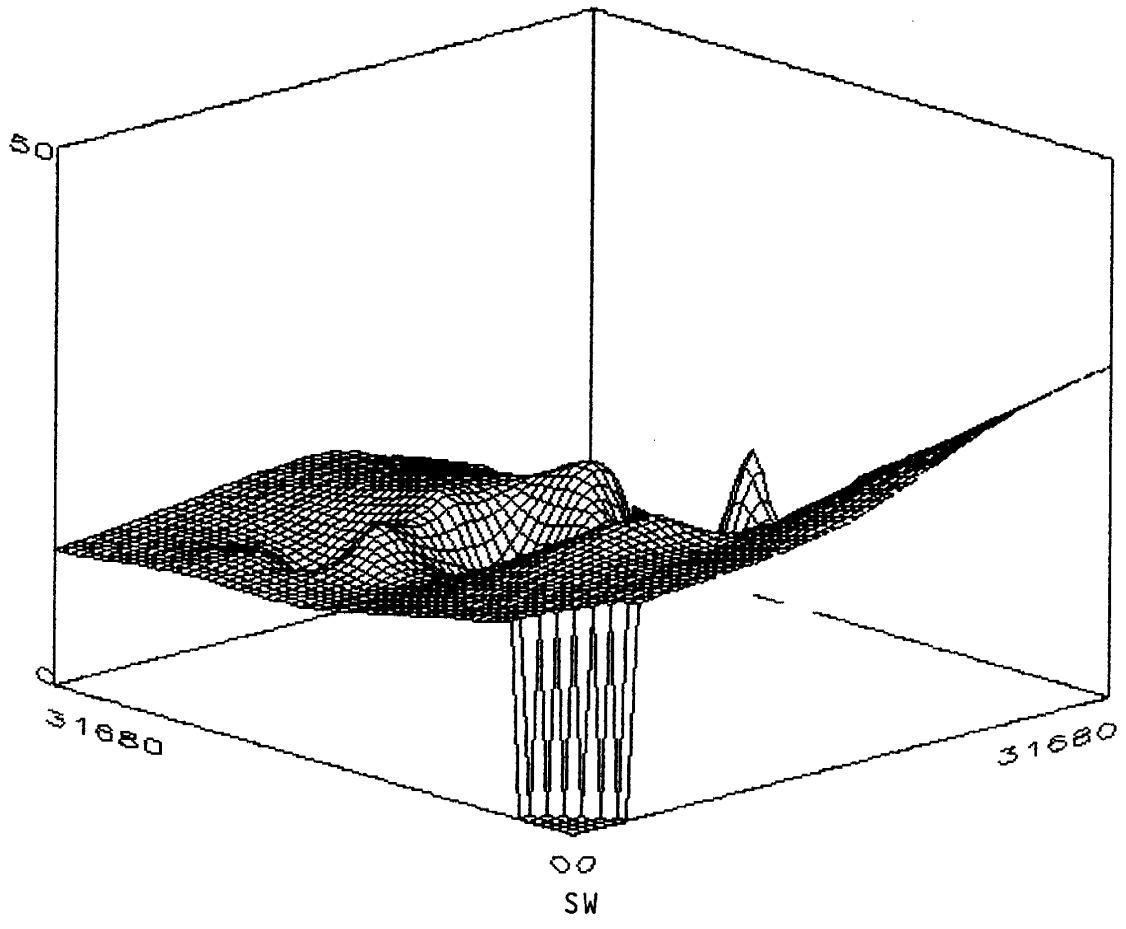


Figure VI-26. 3-D Isopach View of Upper Lobe of Milne Point Lower Kuparuk Formation (viewed from the southwest).

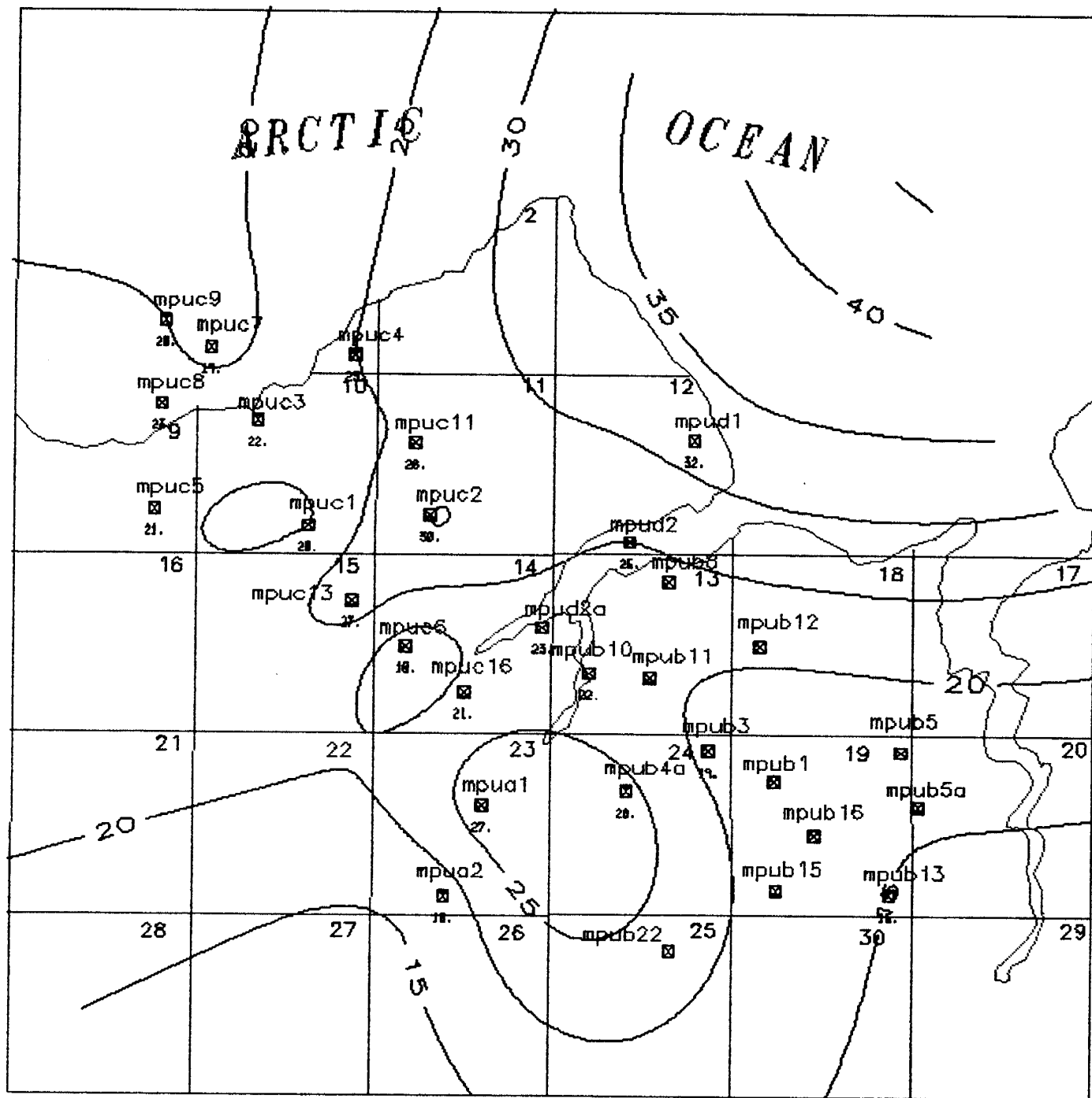


Figure VI-27. Isopach Contour Map of Lower Lobe of Milne Point Lower Kuparuk Formation.

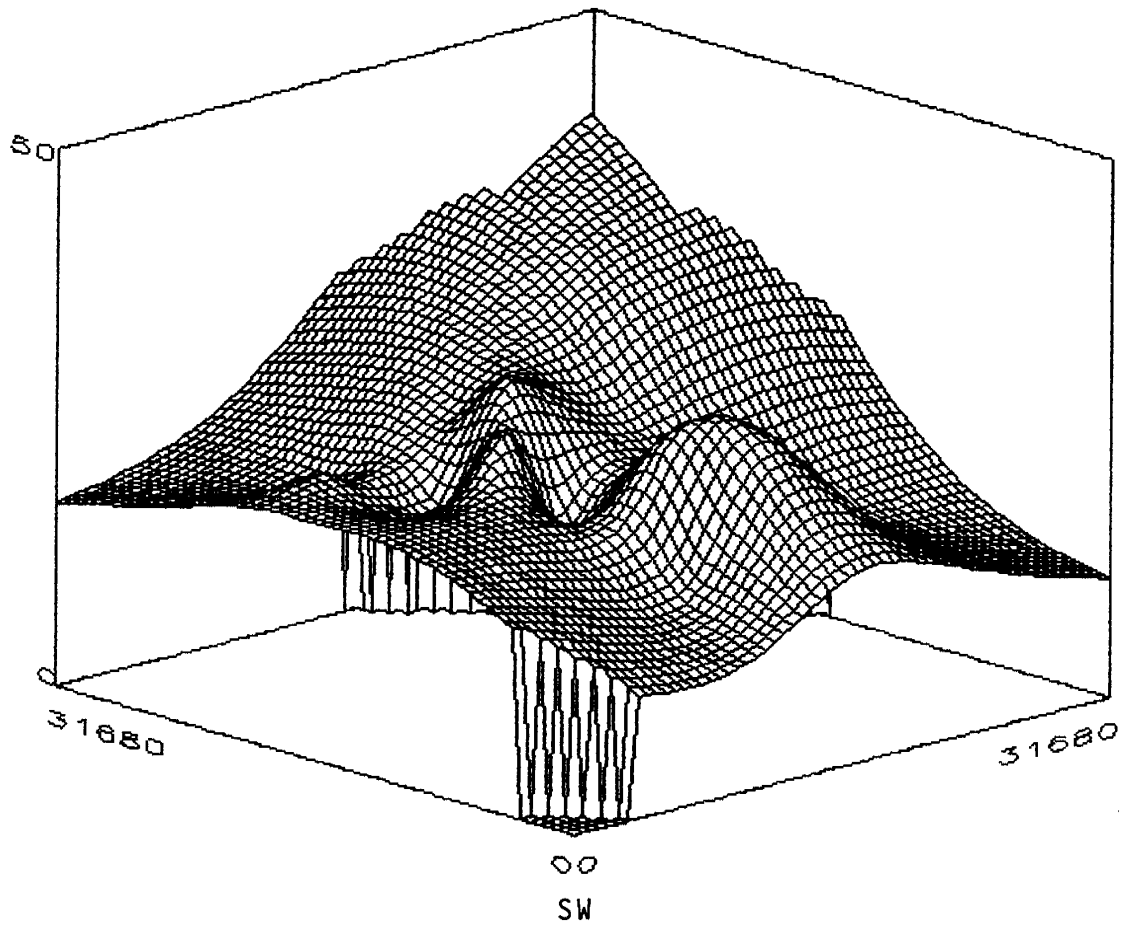


Figure VI-28. 3-D Isopach View of Lower Lobe of Milne Point Lower Kuparuk Formation (viewed from the southwest).

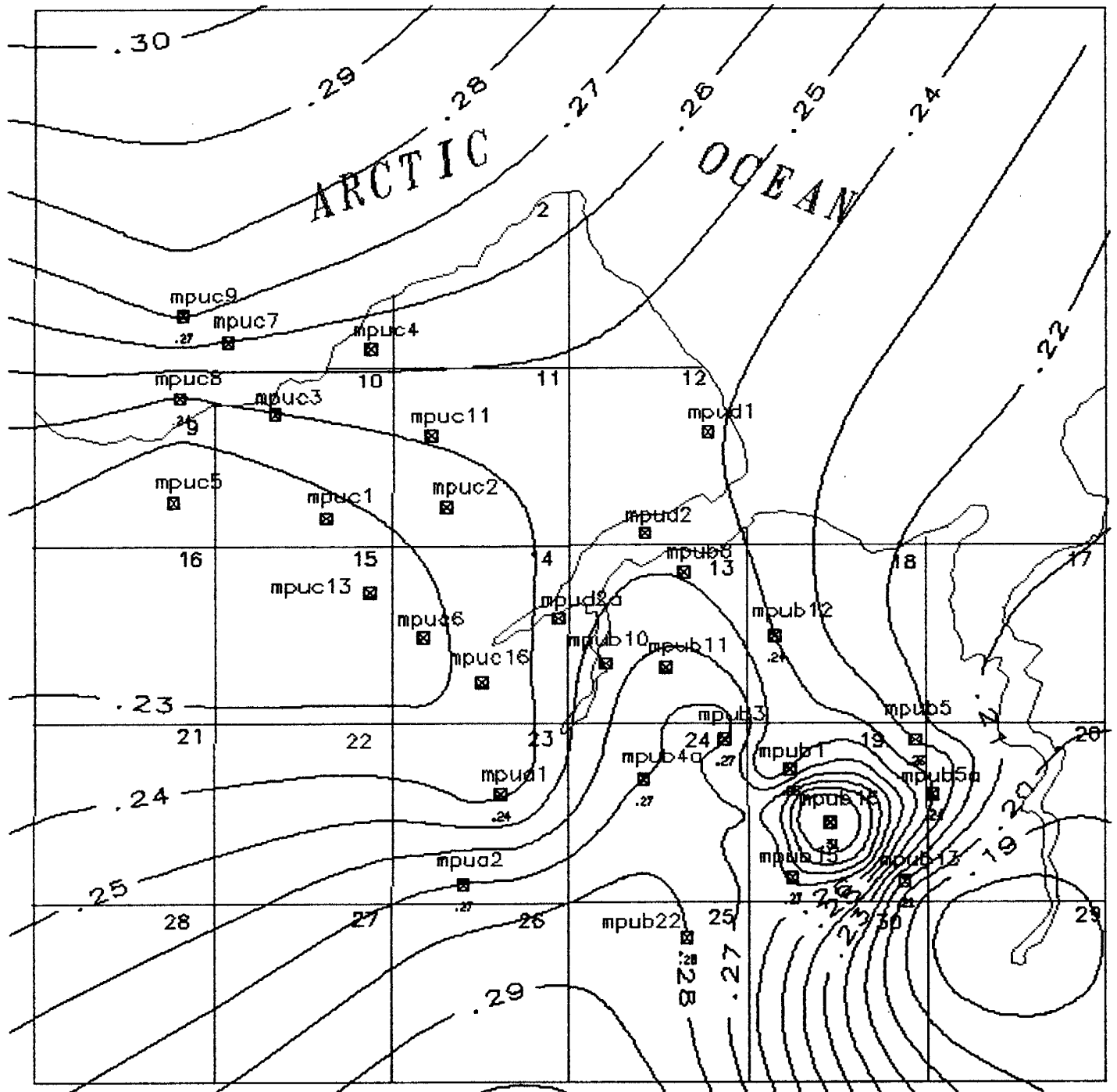


Figure VI-29. Net Reservoir Porosity Map of Lower Lobe of Milne Point Middle Kupařuk Formation.

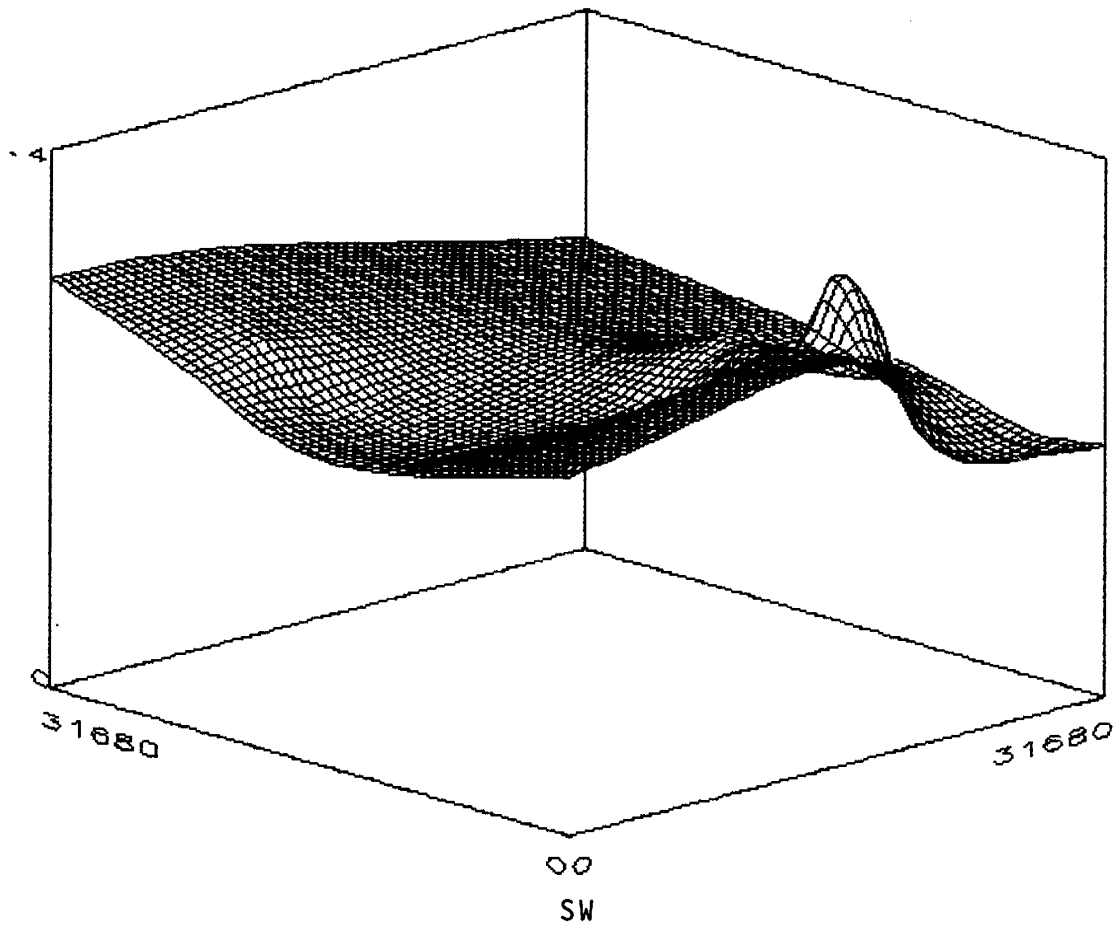


Figure VI-30. 3-D Net Reservoir Porosity Map of Lower Lobe of Milne Point Middle Kuparuk Formation (viewed from the southwest).

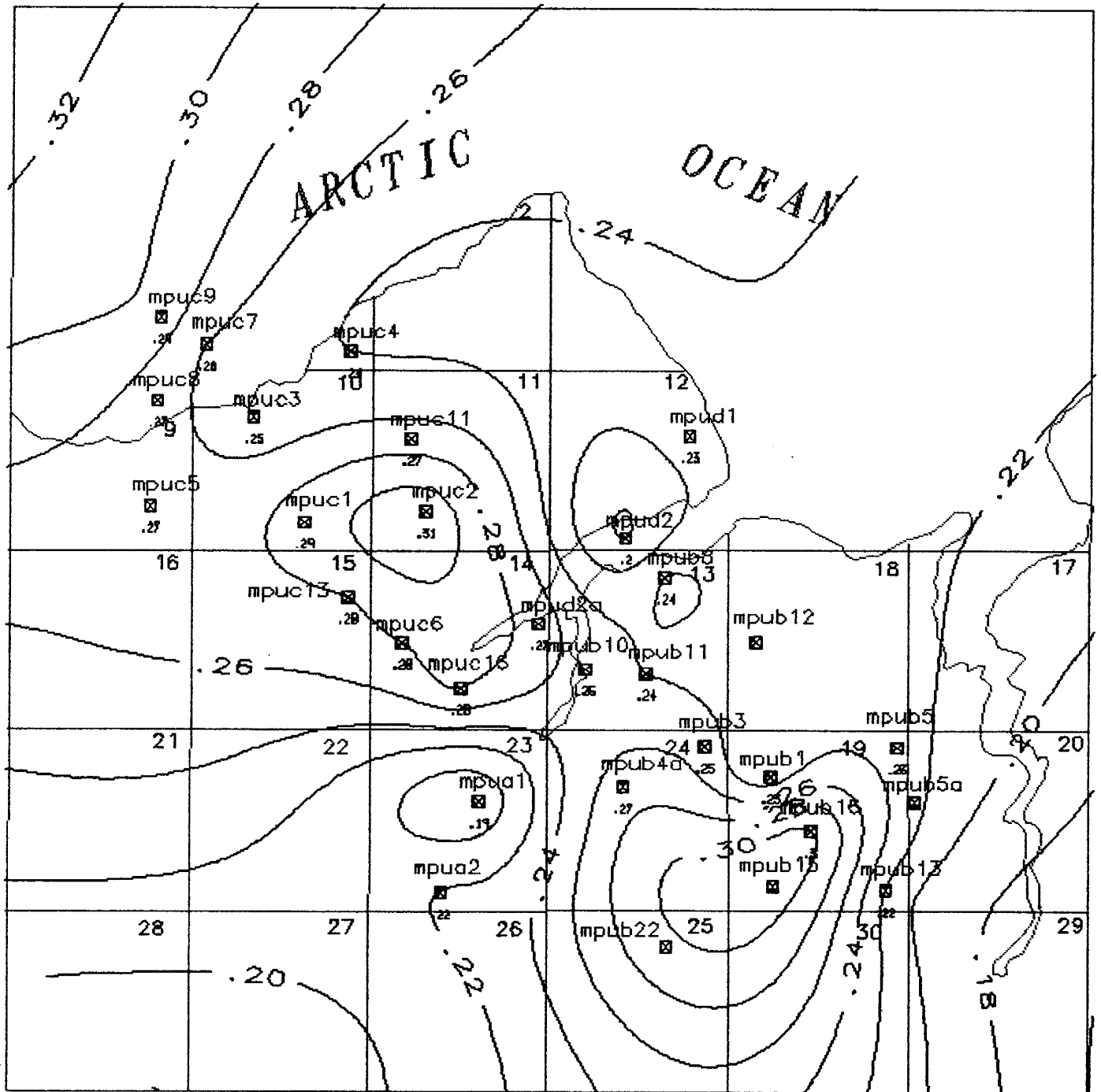


Figure VI-31. Net Reservoir Porosity Map of Upper Lobe of Milne Point Lower Kuparuk Formation.

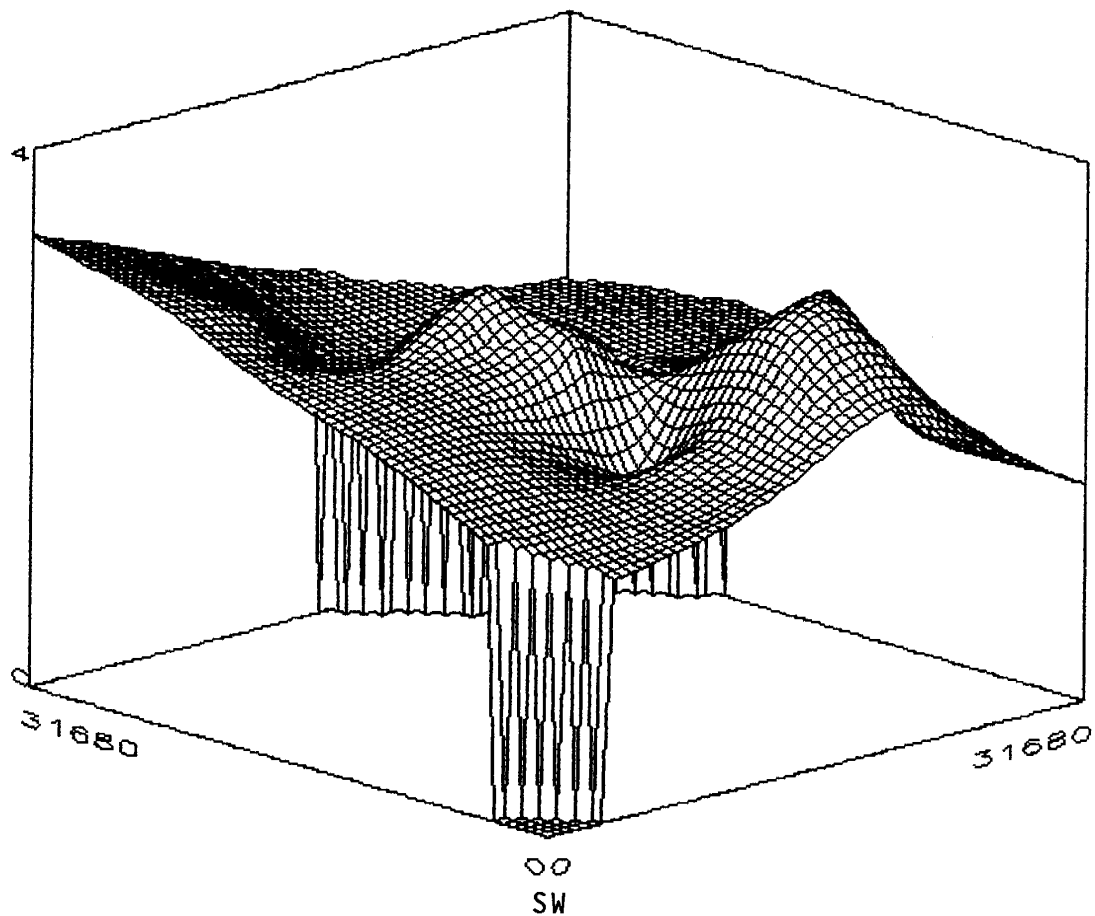


Figure VI-32. 3-D Net Reservoir Porosity Map of Upper Lobe of Milne Point Lower Kuparuk Formation (viewed from the southwest).

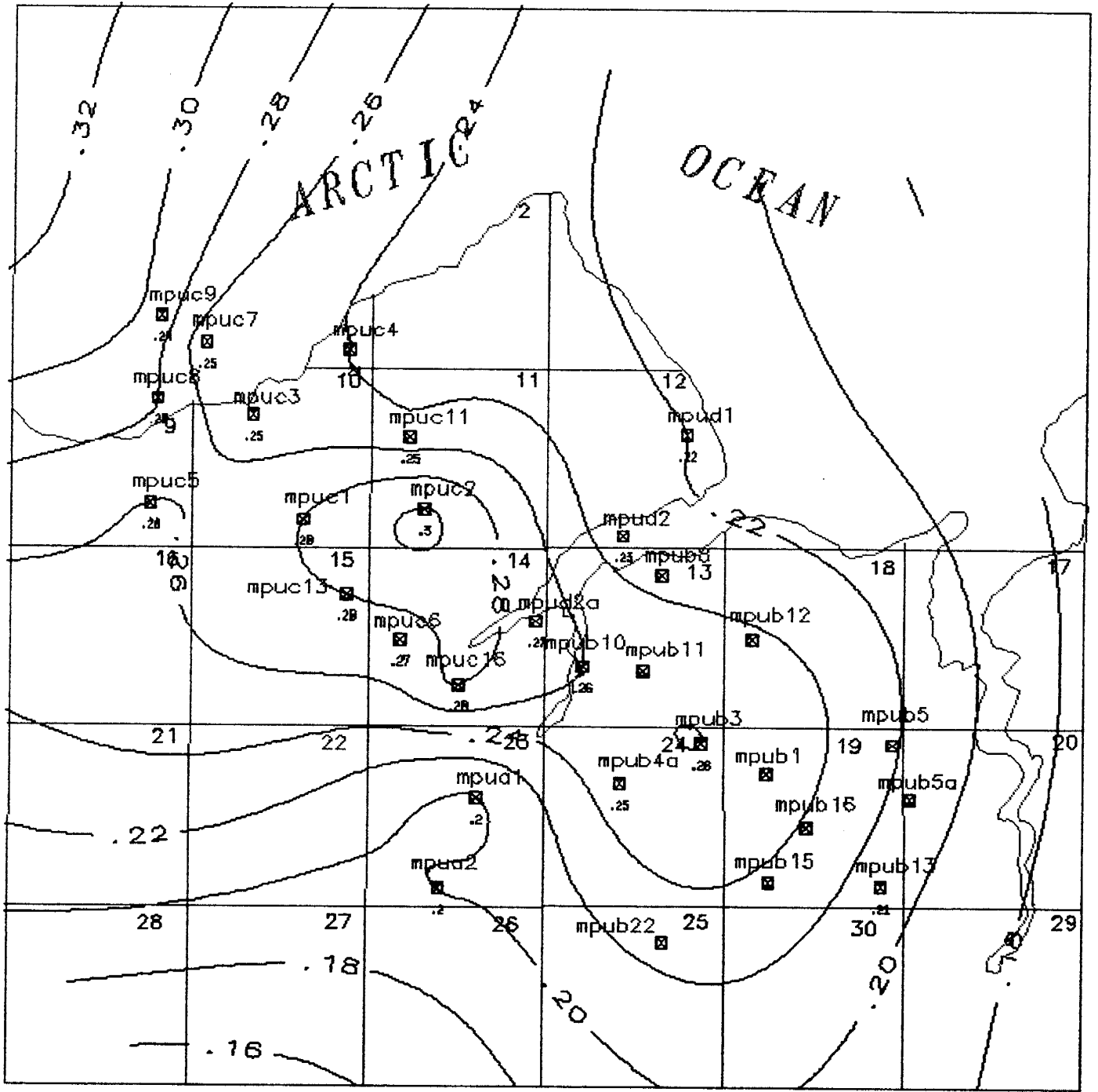


Figure VI-33. Net Reservoir Porosity Map of Lower Lobe of Milne Point Lower Kuparuk Formation.

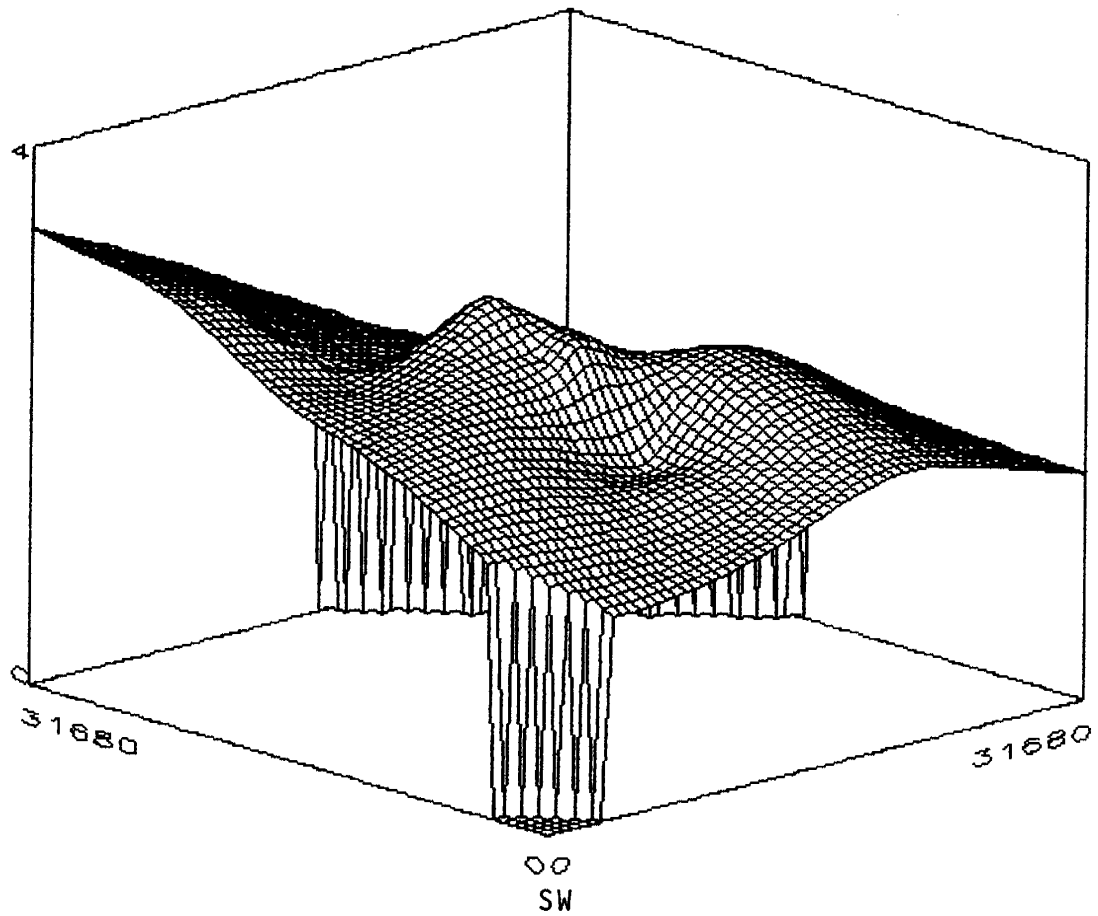


Figure VI-34. 3-D Net Reservoir Porosity Map of Lower Lobe of Milne Point Lower Kuparuk Formation (viewed from the southwest).

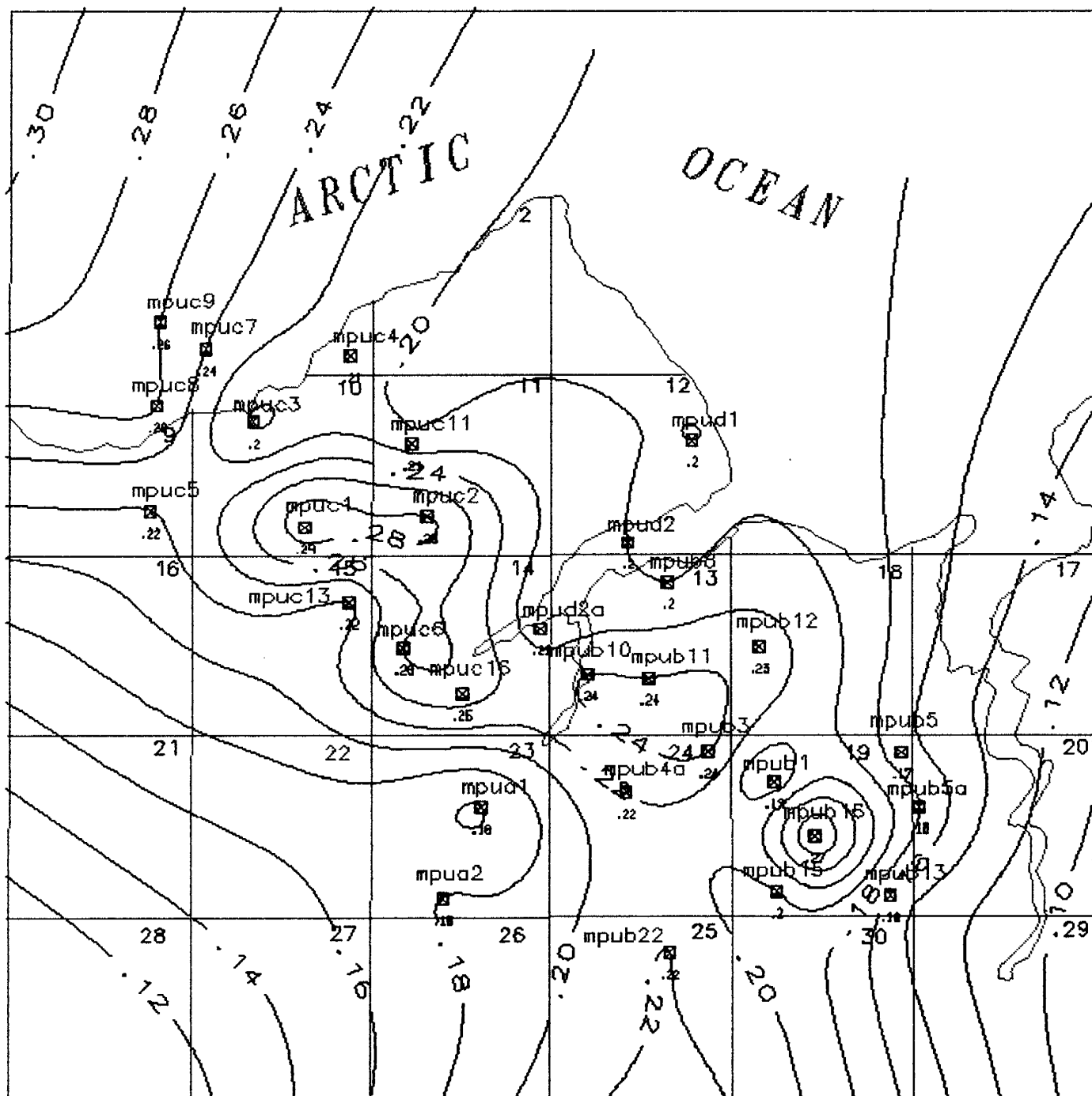


Figure VI-35. Net Reservoir Porosity Map of Upper Lobe of Milne Point Middle Kugaruk Formation.

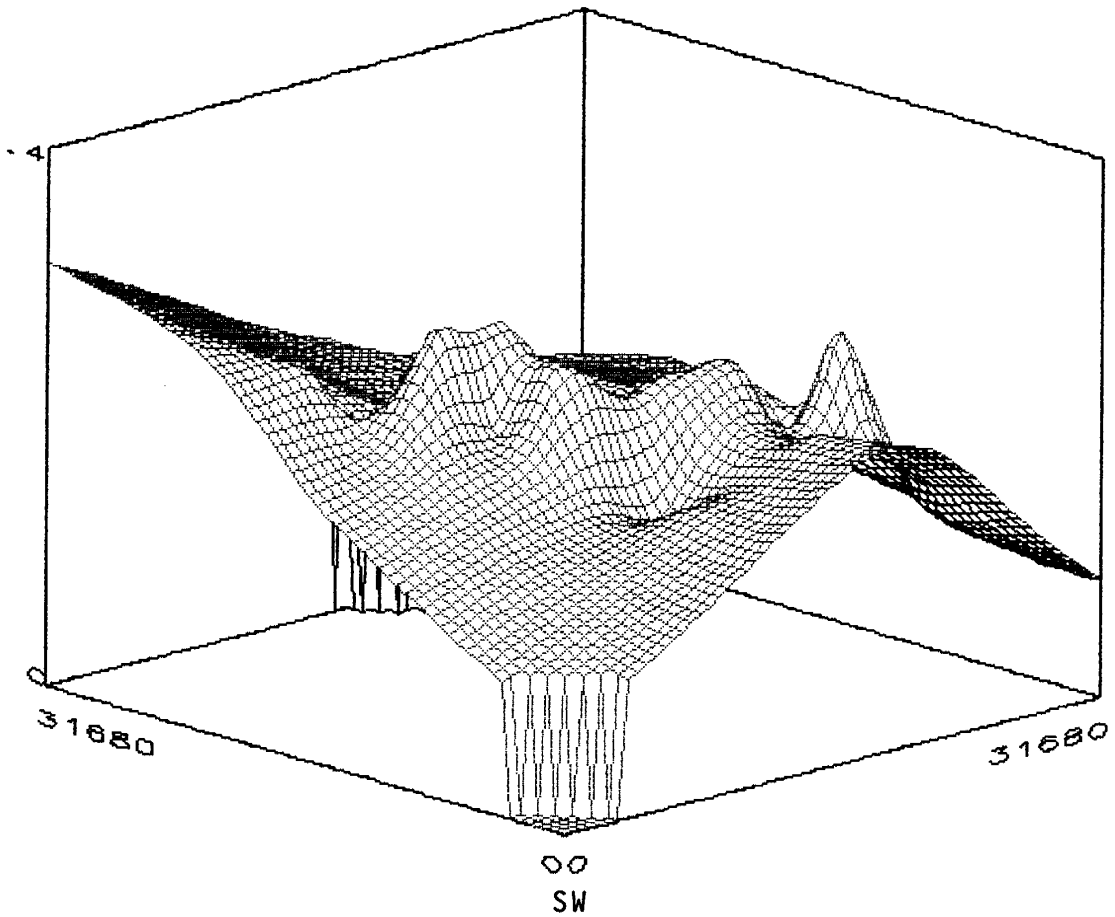


Figure VI-36. 3-D Net Reservoir Porosity Map of Upper Lobe of Milre Point Middle Kuparuk Formation (viewed from the southwest).



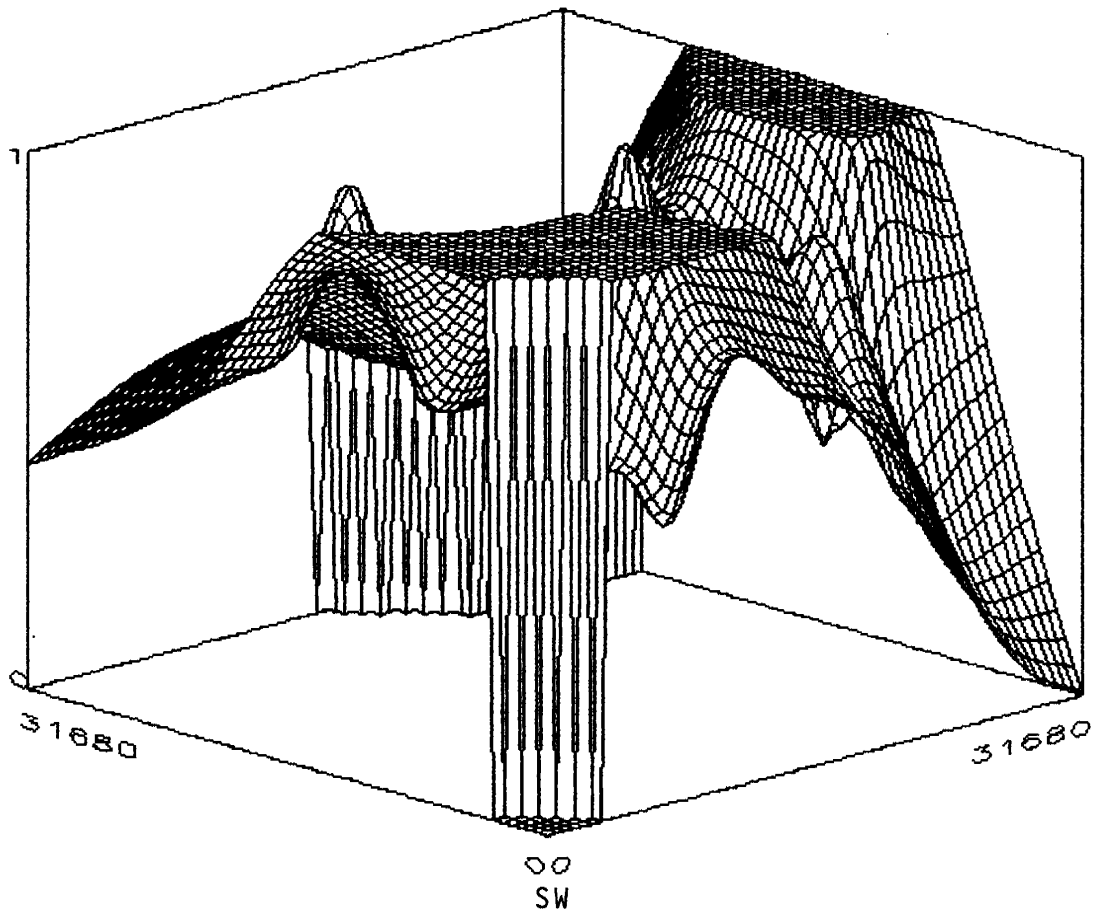


Figure VI-38. 3-D Net Reservoir Water Saturation Map of Upper Lobe of Milne Point Middle Kuparuk Formation (viewed from the southwest).

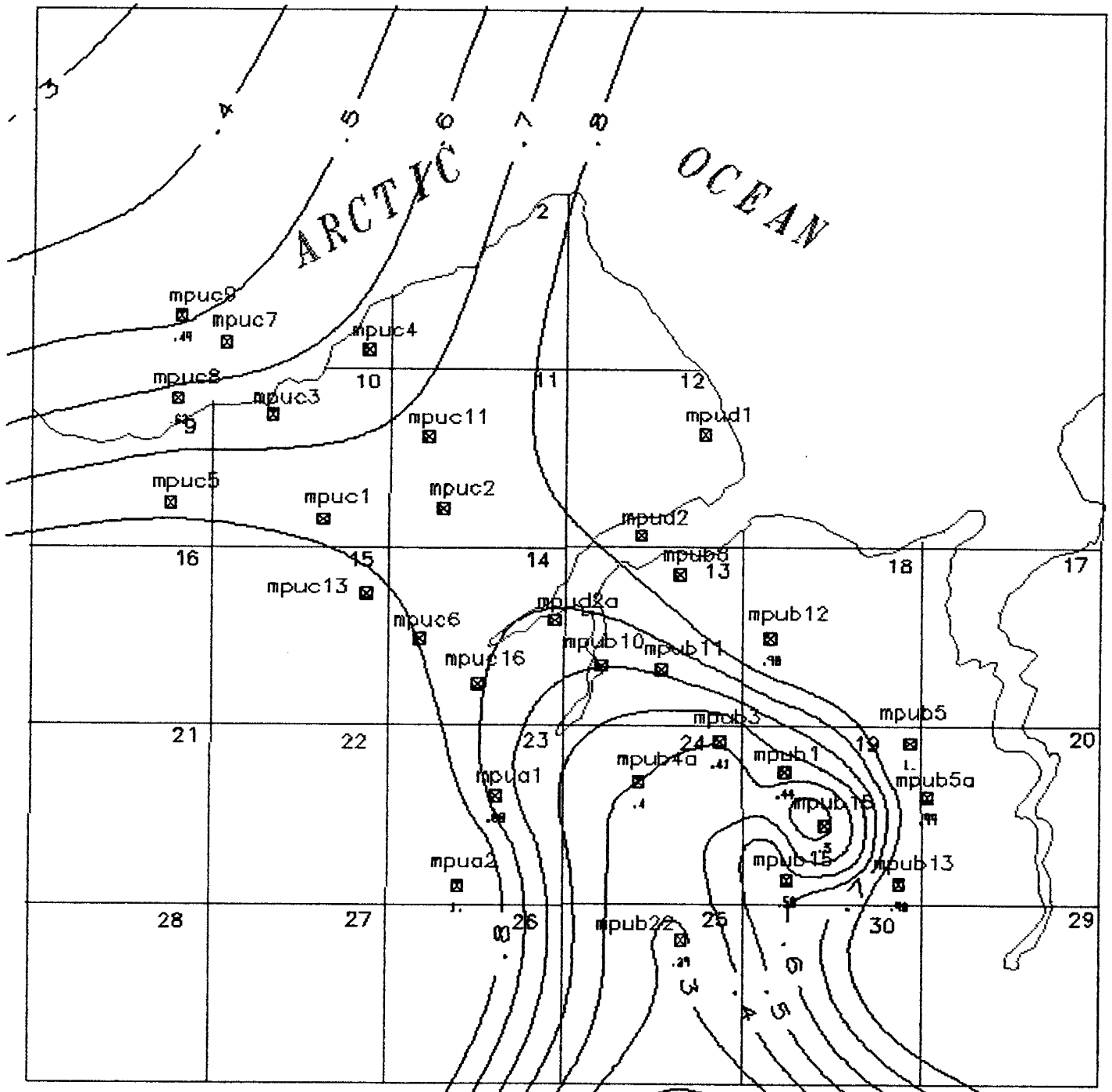


Figure VI-39. Net Reservoir Water Saturation Map of Lower Lobe of Milne Point Middle Kuparuk Formation.

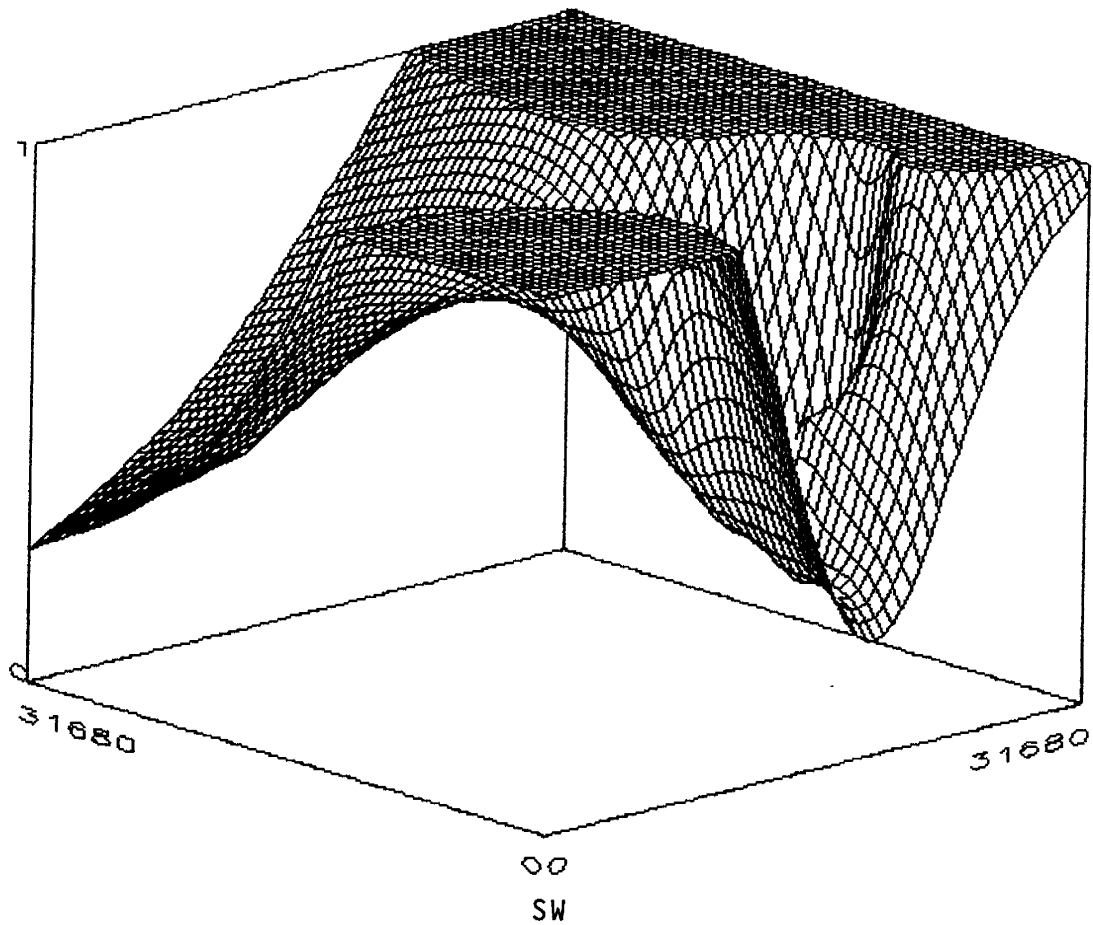


Figure VI-40. 3-D Net Reservoir Water Saturation Map of Lower Lobe of Milne Point Middle Kuparuk Formation (viewed from the southwest).

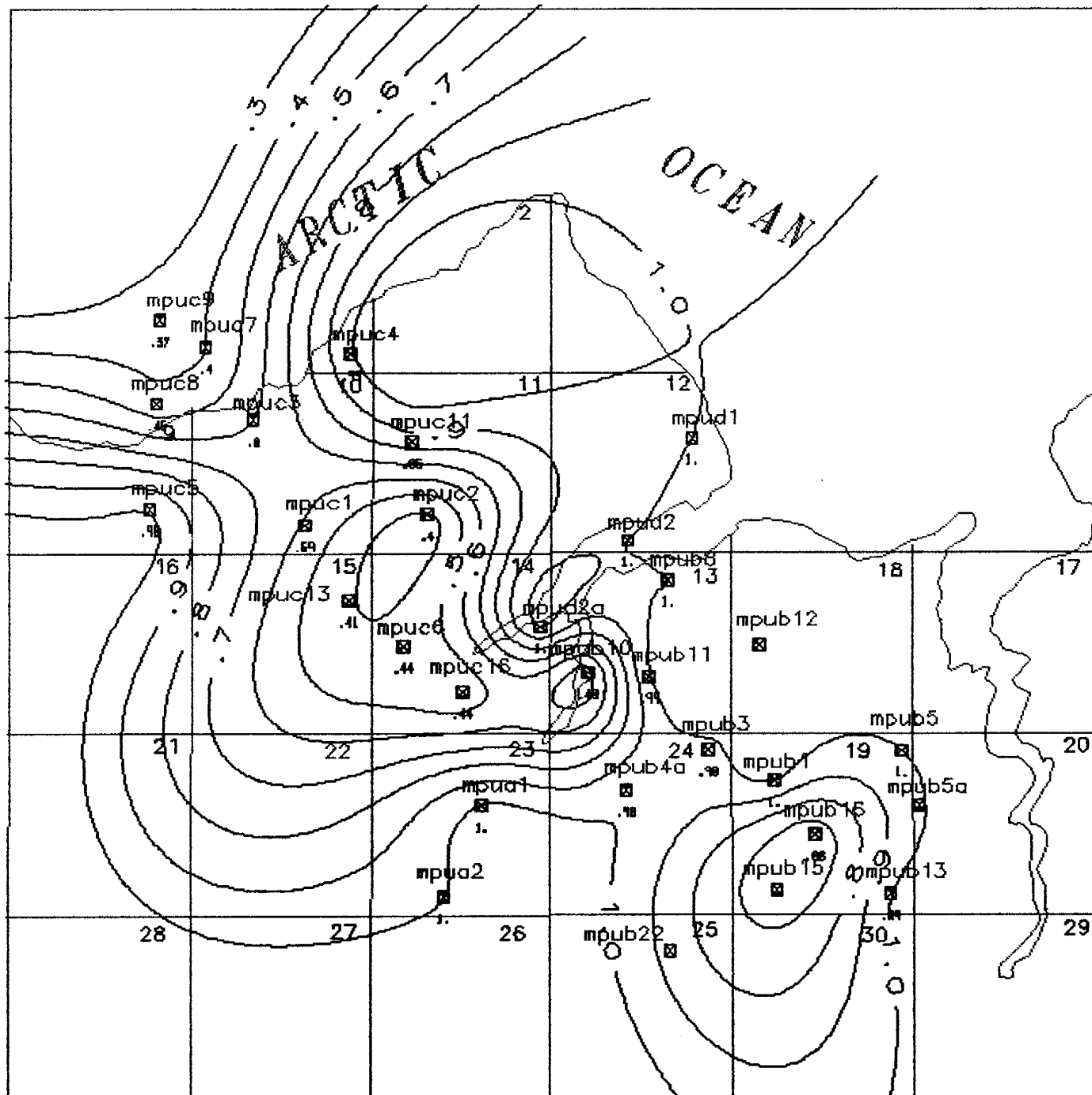


Figure VI-41. Net Reservoir Water Saturation Map of Upper Lobe of Milne Point Upper Kuparuk Formation.

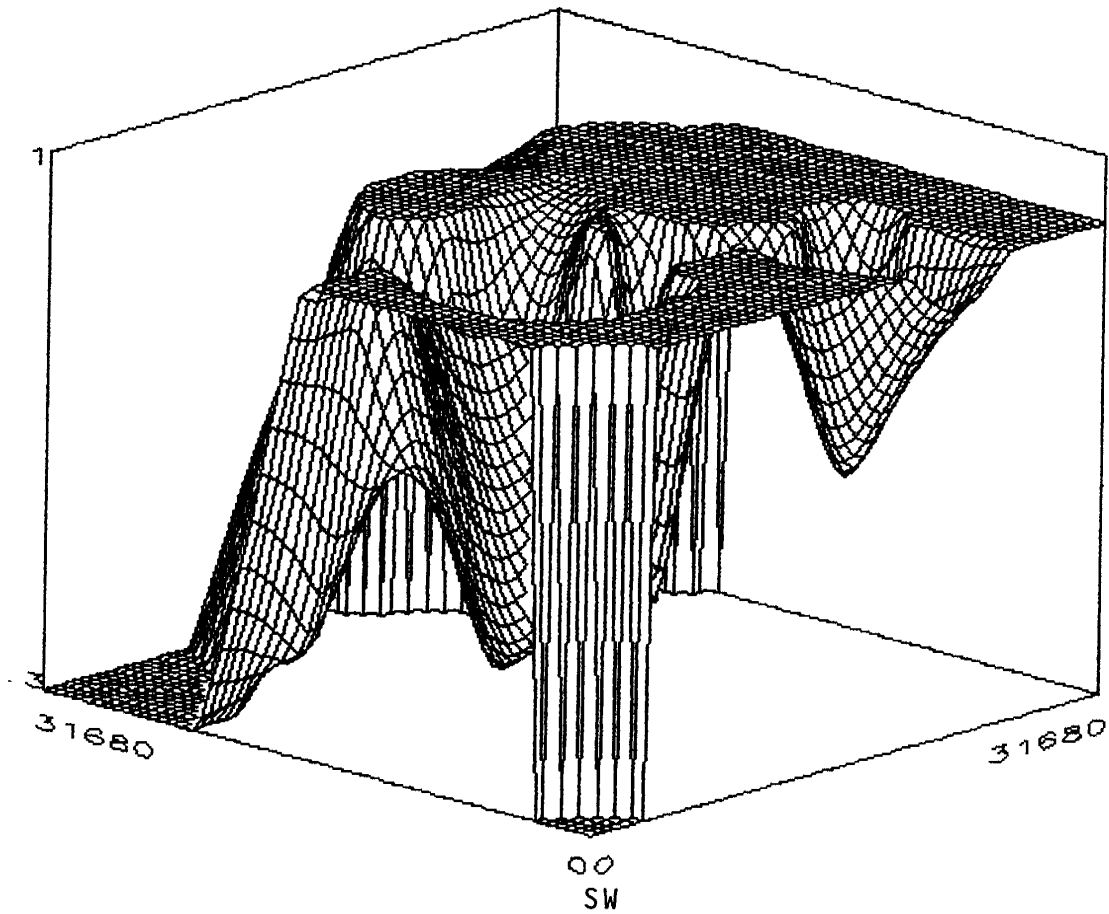


Figure VI-42. 3-D Net Reservoir Water Saturation Map of Upper Lobe of Milne Point Lower Kuparuk Formation (viewed from the southwest).

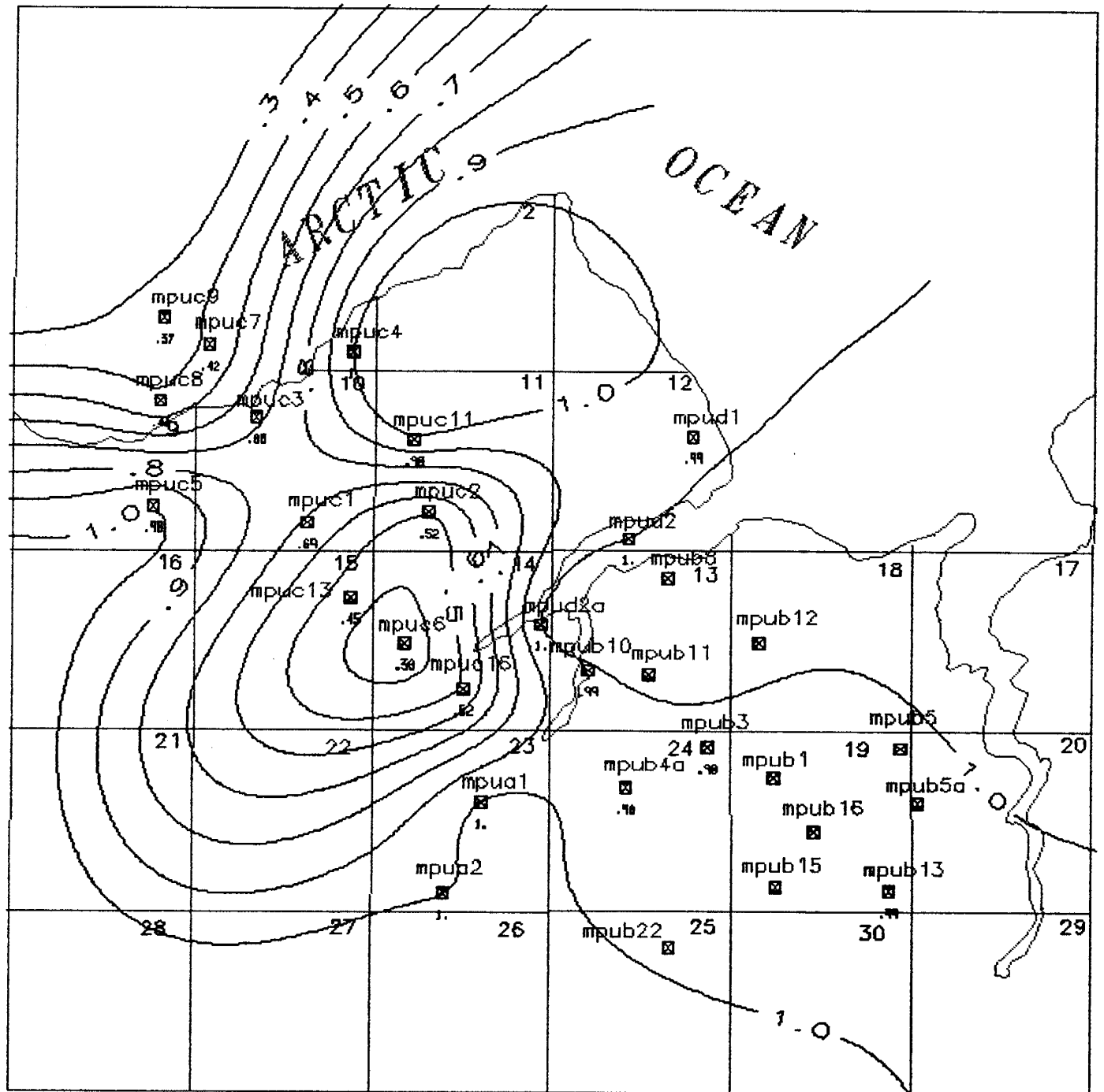


Figure VI-43. Net Reservoir Water Saturation Map of Lower Lobe of Milne Point Lower Kuparuk Formation.

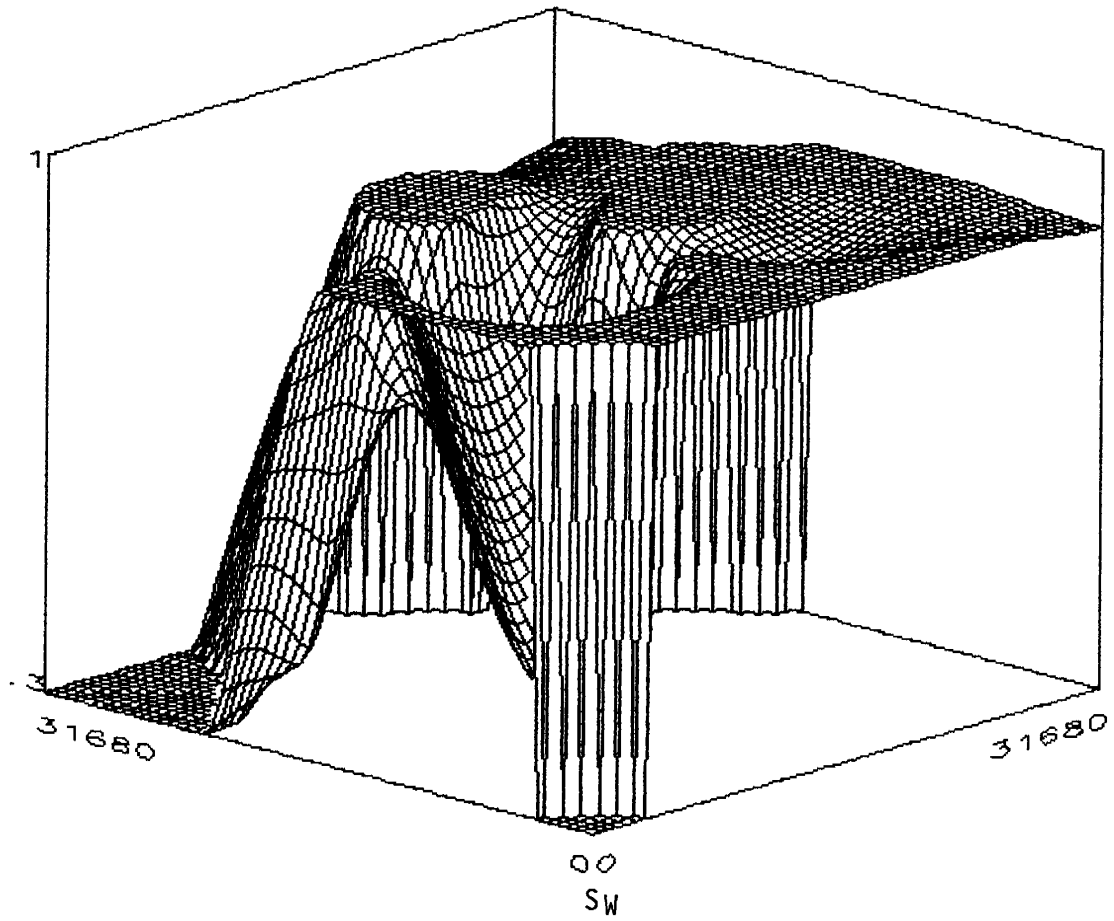


Figure VI-44. 3-D Net Reservoir Water Saturation Map of Lower Lobe of Milne Point Lower Kuparuk Formation (viewed from the southwest).

Petrophysical properties of the Milne Point Unit derived from well logs have been tabulated for the 30 analyzed wells. Calculated field-wide average water saturations in Table VI-1 are higher than those measured within the main producing region of the field (Table VI-2). Also, field-wide average porosities listed in Table VI-1 are lower than those taken from wells within the main producing region of the field. In these wells, Middle Kuparuk formation production occurs between 6741 ft and 7146 ft subsea. Production from the Lower Kuparuk formation occurs between 6879 ft and 7525 ft subsea.

These calculated values for water saturation are arguably higher than actual values. A more in-depth analysis of water saturation, including analysis of core data, is needed in order to better estimate the correct water saturation model to be used in saturation calculations. In addition, analysis of seismic data in order to better determine fault patterns across Milne Point field is necessary for a more complete reservoir description.

**Table VI-1: Field-Wide Log-Derived Petrophysical Properties.**

Zone	Lobes	Subsea Interval Depth (ft)	Average Gross Thickness (ft)	Net Pay (ft)	Average Porosity (%)	Average Water Saturation (%)
Middle Kuparuk	Upper Lobe	-6741 to -7313	17	9	22	66
Middle Kuparuk	Lower Lobe	-6785 to -7146	21 <sup>1</sup>	12 <sup>1</sup>	25	67
Lower Kuparuk	Upper Lobe	-6879 to -7483	14 <sup>2</sup>	6	25	78
Lower Kuparuk	Lower Lobe	-6900 to -7525	23 <sup>3</sup>	9	25	79

<sup>1</sup>Present in 47% of wells analyzed.

<sup>2</sup>Present in 87% of wells analyzed.

<sup>3</sup>Present in 70% of wells analyzed.

**Table VI-2: Log-Derived Petrophysical Properties  
from Wells Within the Center of the Field**

<b>Zone</b>	<b>Lobes</b>	<b>Subsea Interval Depth (ft)</b>	<b>Average Gross Thickness (ft)</b>	<b>Net Pay (ft)</b>	<b>Average Porosity (%)</b>	<b>Average Water Saturation (%)</b>
Middle Kuparuk	Upper Lobe	-6902 to -6919	17	5	23	43
Middle Kuparuk	Lower Lobe	-6920 to -6940	20	9	27	41
Lower Kuparuk	Upper Lobe	-7086 to -7103	17	3	28	49
Lower Kuparuk	Lower Lobe	-7111 to -7134	23	6	28	46

## **CHAPTER VII, PART I: RESERVOIR CHARACTERIZATION OF KUPARUK FIELD**

---

### **A. INTRODUCTION**

Kuparuk field is located on the North Slope, Alaska, approximately 32 miles west of Prudhoe Bay field (Figure VII-1). The Kuparuk River formation, which contains the producing interval of Kuparuk field, is either Late Jurassic or Early Cretaceous in age and overlies the Kingkak shale, which was deposited during Jurassic time (Figure VII-2). All or part of the Kuparuk River formation in Kuparuk field appears to have been eroded, resulting in a major unconformity (Figure VII-3). Kuparuk formation includes shale, siltstone and poorly sorted sandstone. The field is characterized by numerous northwest-southeast trending faults. The initial oil in place in Kuparuk is estimated at 5.5 billion stock tank barrels.

The objective of this study was to characterize the upper and lower sands in the Kuparuk River formation. This characterization includes study of petrophysical properties, depositional environment, truncation of sands, and geological trends, and is based on Kuparuk field well log data.

### **B. WELL LOG ANALYSIS**

A total of more than 50 Kuparuk field wells across the field were selected for analysis, and the wells are chosen in such a manner to represent the entire field.

For well log analysis and for generating different maps and cross sections, the WorkBench software from Scientific Software, Inc., was used for this study. WorkBench is an integrated software program consisting of separate modules for reservoir description, reservoir simulation, well test analysis, etc. For the purpose of this study, only the reservoir description module of WorkBench has been used extensively.

At the beginning of the study, the base map of Kuparuk field was digitized into WorkBench. Locations of wells selected for analysis were imported into the map database, also by digitization. Raw log data from magnetic tapes were transferred to WorkBench and loaded against corresponding wells. Once log trace data were loaded into the database, additional well information, including logged intervals, bit size, mud properties, bottom hole temperature, etc., were fed in.

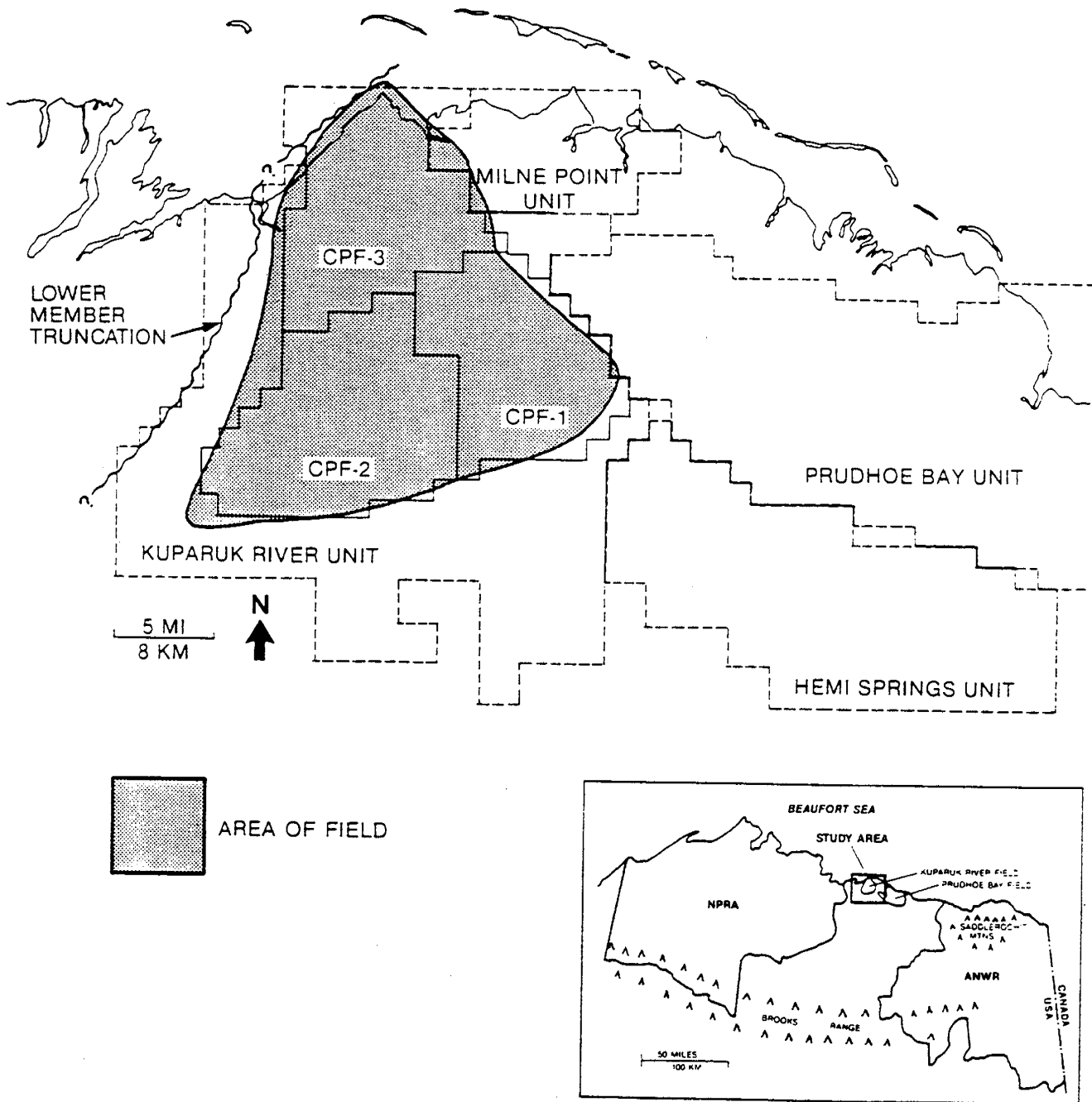


Figure VII-1. Location of Kuperuk River Field (Gaynor and Scheihing, 1989).

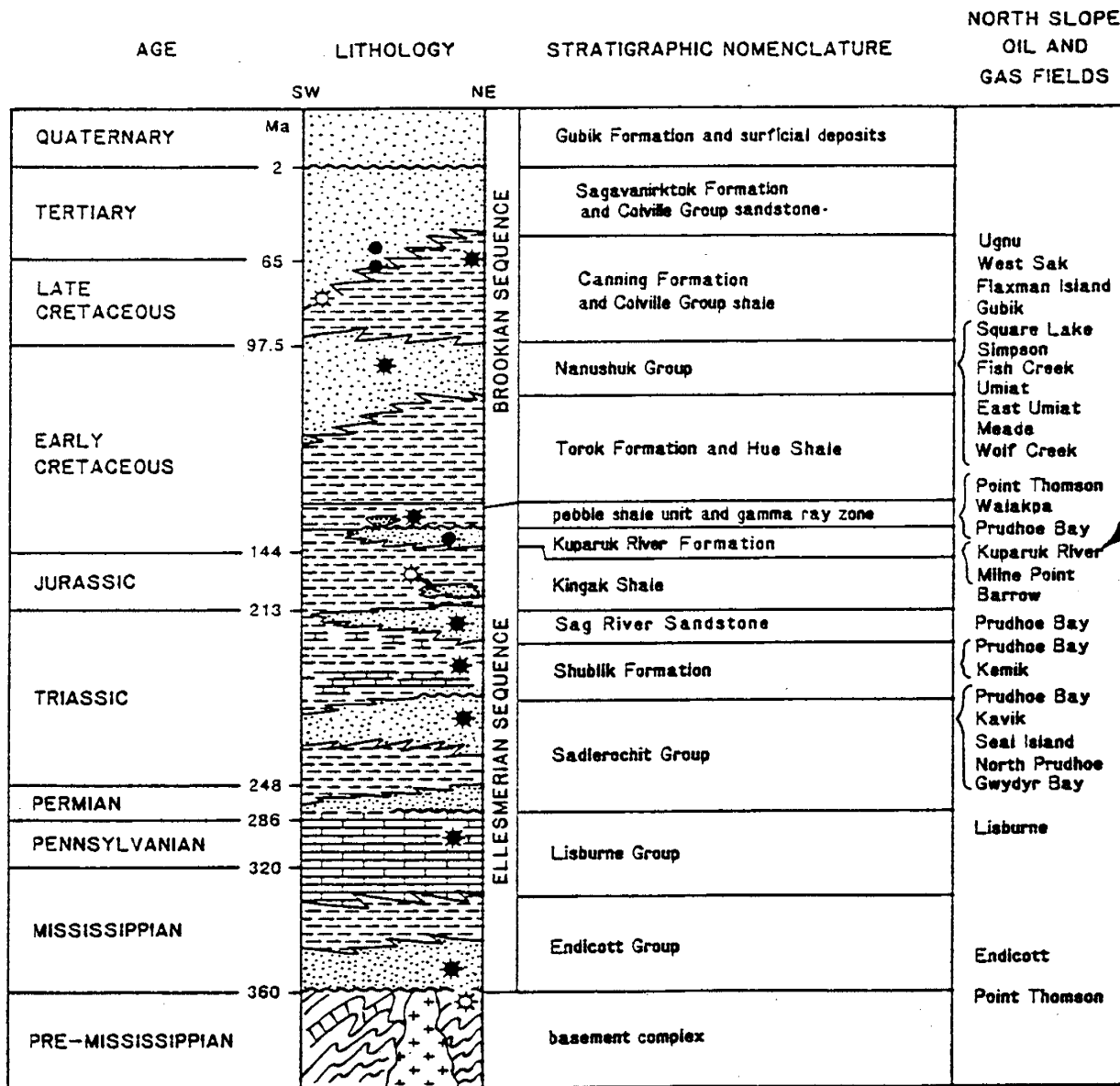


Figure VII-2. Western North Slope Stratigraphic Column with Kuparuk River Interval Highlighted (Bird, 1987).

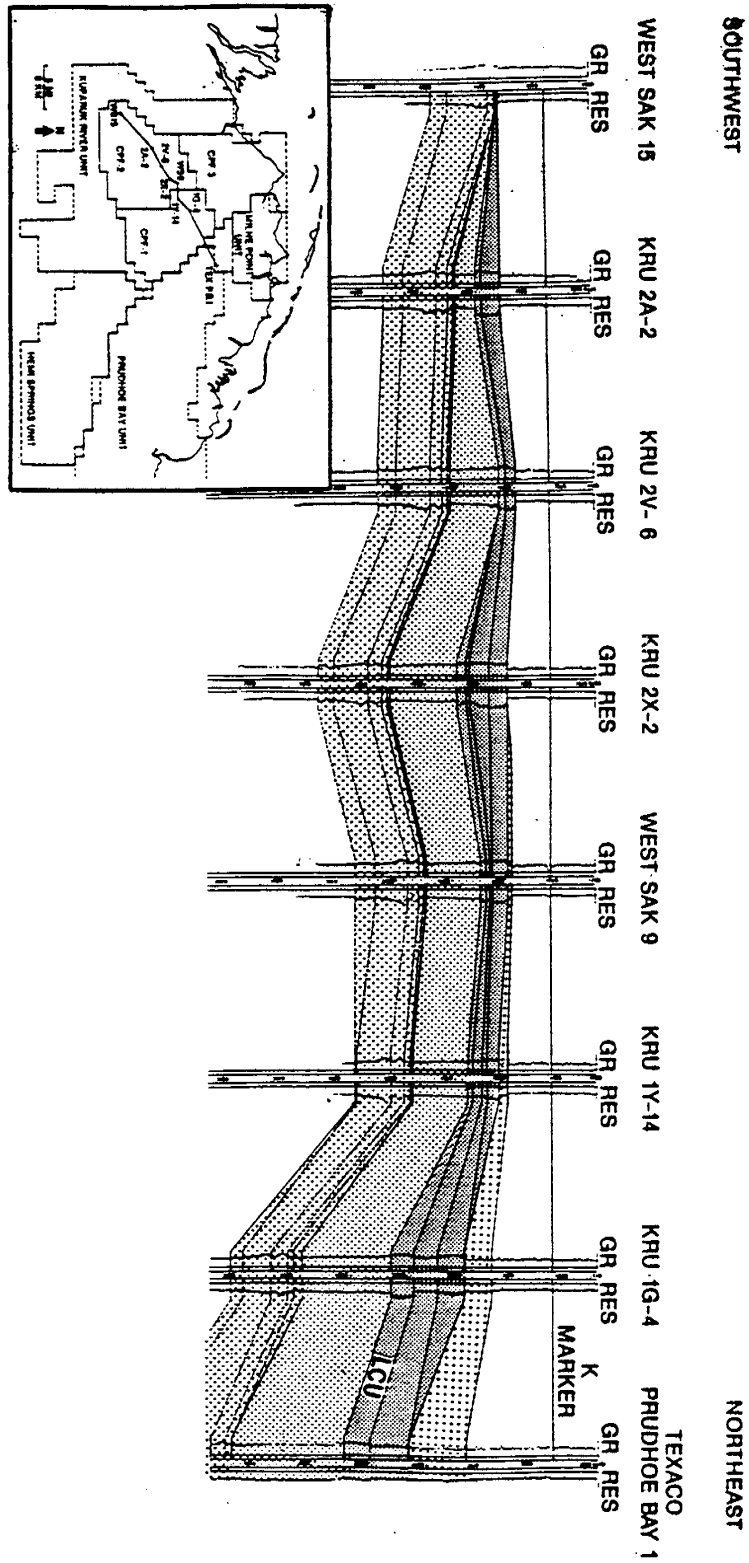


Figure VII-3. Lower Cretaceous Unconformity (LCU) Cutting Across the Kuparuk River Formation (Gaynor and Scheiing, 1989).

After editing or shifting the curves as necessary, they were further adjusted for environmental corrections. Then geologic zones or markers were identified and sand tops and bases were picked. For most of the wells, all geologic zone or marker information was obtained from well reports provided by the Alaska Oil and Gas Conservation Commission (AOGCC).

After defining a parameter interval (PI), or geologic interval, on which the log analysis would be run, and fixing clean sand and shale lines on frequency versus GR and frequency versus SP plots, final log analysis was run. A log analysis "results" plot was then generated showing lithology, fluid saturations, etc. Analysis plots of some wells are shown in Figures VII-4 and VII-5.

The log analyses for all the wells were run utilizing the Indonesian model for Sw calculations. Sw calculations were then validated or compared with those from three other models, including Archie, Laminar-Simondoux and Dual Water model. Finally, summations were run for each sand to obtain average petrophysical properties viz; gross pay, net pay, Sw, So, porosity, shale volume, etc.

For summations, different cutoff values for shale, porosity, and water saturation were selected. For all the summations, shale and porosity cutoffs were kept constant at 40% and 6%, respectively, but water saturation cutoff values were varied from 40% to 60%, and finally to 80%. Specifically, any sample point with a shale volume greater than 40%, on a porosity less than 6%, was excluded in calculation of net pay, average water saturation, hydrocarbon test, etc. All points with water saturations greater than 40%, 50% or 60%, depending on run, were similarly excluded. The summation results for each sand for different cutoff values are tabulated in Tables VII-1 through VII-6.

For the purpose of the geologic study, a large number of north-south and east-west cross sections were generated across the entire Kuparuk field. Faults, when encountered, were incorporated in these cross sections. Stratigraphic cross sections were also generated by hanging the Kuparuk formation from the upper sand. Figure VII-6 shows locations of cross sections, and cross sections are shown in Figures VII-7 through VII-14.

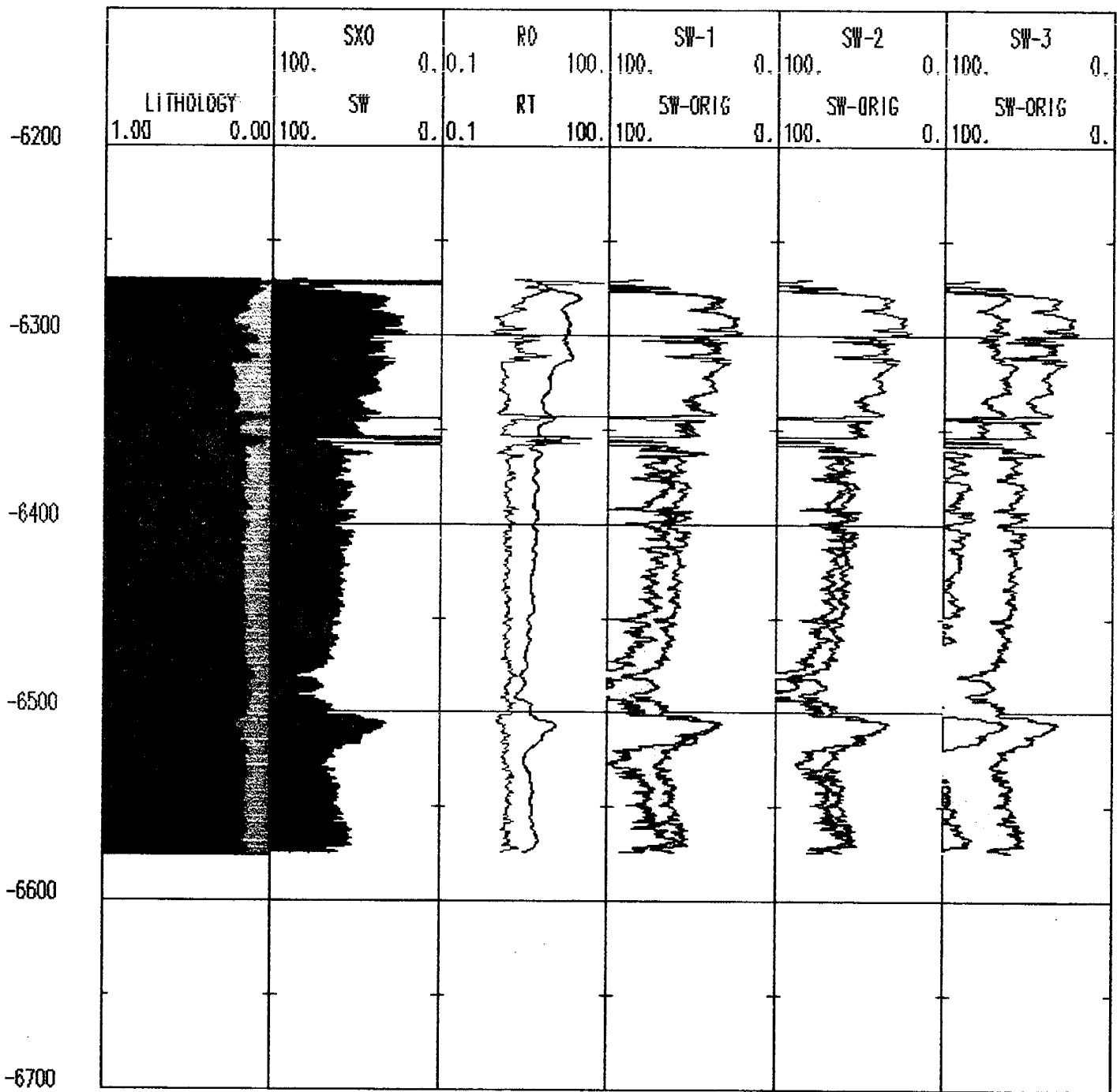


Figure VII-4. Analysis Result Plot of Well 1d6 from Kuparuk River Field with Comparison of Sw from Three Different Models (Sw1: Archie, Sw2: Laminar Simondoux, Sw3: Dual Water).

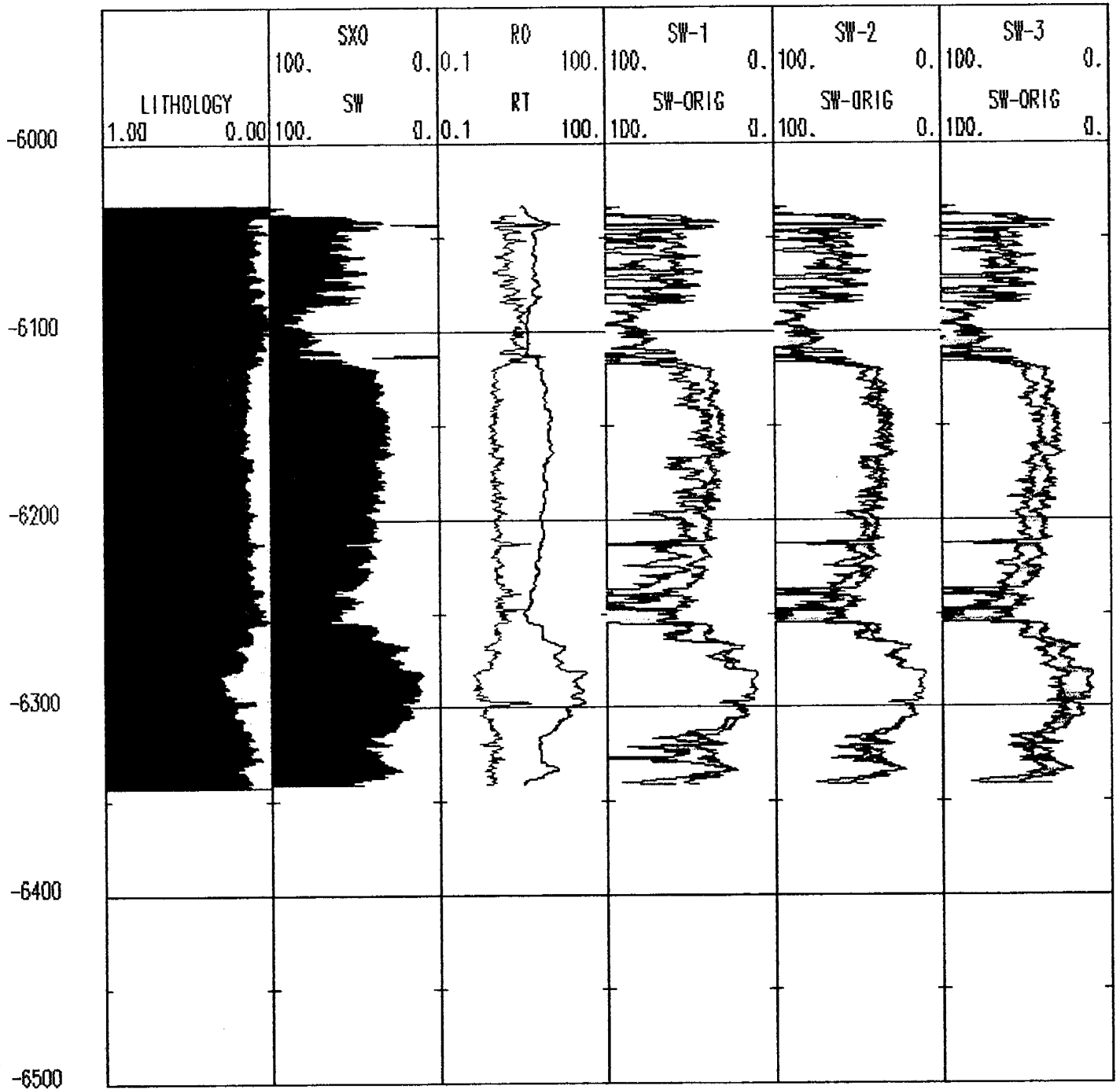


Figure VII-5. Analysis Result Plot of Well 1q15 from Kugaruk River Field with Comparison of Sw from Three Different Models (Sw1: Archie, Sw2: Laminar Simondoux, Sw3: Dual Water).

**Table VII-1: Average Petrophysical Properties of Kuparuk River Upper Sand  
(6% porosity, 40% shale, 40% Sw cutoffs).**

No.	Well Name	Interval (ft)	Thickness Gross (ft)	Thickness Net (ft)	Shale Volume (%)	Porosity (%)	Saturation Water (%)	Saturation Oil (%)	Hydrocarbon Feet hO (1-Sw)
1	1A-11	8877.5-8920.5	28.90	15.36	0.81	20.38	28.22	71.78	2.248
2	1b7	6294.0-6374.0	80.00	2.50	11.96	27.73	38.28	61.72	0.429
3	1c2	6437.5-6492.5	55.00	45.00	7.07	24.14	24.74	75.26	8.174
4	1c5	7043.0-7113.0	58.37	39.30	12.16	24.41	23.83	76.17	7.306
5	1c6	9409.0-9497.0	57.90	32.89	8.55	26.01	28.09	71.91	6.152
6	1d2	6446.5-6495.5	49.00	35.50	5.74	26.50	26.36	73.64	6.881
7	1d4	6458.5-6582.0	123.50	21.50	15.06	24.64	31.70	68.30	3.618
8	1d6	8041.0-8155.0	97.84	45.03	4.61	21.78	33.08	66.92	6.565
9	1G-13	7538.0-7646.5	90.38	38.03	23.08	16.52	25.67	74.33	4.671
10	1g7	6352.0-6448.0	93.50	22.00	0.00	20.66	19.73	80.27	3.649
11	1i8	7301.5-7370.0	60.30	12.60	9.04	12.75	27.35	72.65	1.167
12	1q15	6125.0-6190.0	65.00	2.50	13.69	17.79	35.66	64.34	0.286
13	1r-1	8070.0-8120.0	38.86	24.08	15.76	19.13	17.11	82.89	3.818
14	1q11	5872.0-5960.0	85.00	53.5	3.58	23.14	28.85	71.15	8.808
15	1y3	6019.5-6118.5	99.00	41.50	5.27	19.85	29.95	70.05	5.771
16	2a5	5893.5-5925.5	29.00	14.50	1.19	23.18	31.51	68.49	2.302
17	2A-8	8076.5-8143.5	51.41	24.24	4.70	13.98	26.74	63.26	2.484
18	2c6	5829.5-5853.5	24.00	10.50	25.72	14.95	26.35	63.65	1.156
19	2d12	8182.0-8295.5	69.46	4.97	9.12	24.65	35.96	64.04	0.785
20	2f2	5939.0-6012.0	73.00	8.00	5.41	26.27	31.65	68.35	1.437
21	2h15	5977.0-6005.5	28.00	0.50	34.43	17.06	33.59	66.01	0.057
22	2h4	6386.0-6405.0	15.88	0.42	12.29	15.98	36.17	63.83	0.043
23	2t10	7847.5-7902.5	37.11	1.35	11.45	16.41	34.75	65.25	0.144
24	2u-1	6853.0-6934.5	62.12	15.62	1.68	16.06	29.72	70.28	1.763
25	2u11	5747.5-5761.0	13.50	3.00	12.55	23.66	26.14	73.86	0.524

Table VII-1: (Continued) Average Petrophysical Properties of Kuparuk River Upper Sand  
(6% porosity, 40% shale, 40% Sw cutoffs).

No.	Well Name	Interval (ft)	Thickness Gross (ft)	Thickness Net (ft)	Shale Volume (%)	Porosity (%)	Saturation Water (%)	Saturation Oil (%)	Hydrocarbon Feet hØ (1-Sw)
26	2v14	5810.0-5857.5	47.50	32.00	3.89	19.44	21.35	78.65	4.893
27	2v8a	8584.5-8607.5	23.00	18.00	18.27	23.13	17.83	82.17	3.422
28	2w2	6412.0-6448.0	28.97	15.69	4.33	22.16	29.88	70.12	2.438
29	2z15	5895.0-5976.5	81.50	21.00	1.41	26.19	28.14	71.86	3.952
30	2z7	5874.0-5927.5	53.50	38.50	4.80	25.55	19.40	80.60	7.930
31	3a-3	7784.5-7858.5	56.13	31.85	0.00	24.74	28.29	71.71	5.650
32	3a-6	7128.0-7313.0	131.55	39.67	9.32	19.60	23.06	76.94	5.982
33	3A-8	6582.0-6728.0	100.87	11.82	6.87	19.11	31.83	68.17	1.540
34	3a-9	5988.5-6068.5	80.00	1.50	1.45	19.45	37.19	62.81	0.183
35	3b14	6021.5-6046.0	24.50	9.50	2.97	26.95	25.19	74.81	1.915
36	3b-2	7774.5-7796.0	15.42	11.12	0.00	22.60	26.43	73.57	1.849
37	3b-7	6073.5-6094.0	20.50	1.50	30.43	15.63	33.33	66.67	0.156
38	3c-16	6395.0-6419.0	23.02	15.35	14.74	19.87	17.90	82.10	2.503
39	3c-8	9741.0-9785.0	28.19	5.51	34.91	13.56	22.28	77.72	0.580
40	3f14	6416.0-6445.0	22.50	8.15	16.87	19.31	27.35	72.65	1.143
41	3H-11	6057.5-6089.5	32.00	3.00	11.82	34.13	35.74	64.26	0.658
42	3k3	8400.0-8421.5	15.93	7.41	23.78	15.56	34.65	65.35	0.753
43	3N-12	7685.5-7718.0	27.03	6.66	18.76	20.65	23.63	76.37	1.051
44	3N-13	7470.5-7508.5	29.01	9.55	27.63	16.71	34.45	65.55	1.046

**Table VII-2: Average Petrophysical Properties of Kuparuk River Upper Sand  
(6% porosity, 40% shale, 60% Sw cutoffs).**

No.	Well Name	Interval (ft)	Thickness Gross (ft)	Thickness Net (ft)	Shale Volume (%)	Porosity (%)	Saturation Water (%)	Saturation Oil (%)	Hydrocarbon Feet hO (1-Sw)
1	1A-11	8877.5-8920.5	28.90	23.49	1.87	19.50	35.75	64.25	2.944
2	1b7	6294.0-6374.0	80.00	45.50	14.69	23.43	69.68	50.32	5.364
3	1c2	6437.5-6492.5	55.00	52.00	8.54	23.17	26.57	73.43	8.847
4	1c5	7043.0-7113.0	58.37	54.19	13.83	23.23	28.65	71.35	8.982
5	1c6	9409.0-9497.0	57.90	46.59	10.04	24.51	32.74	67.26	7.681
6	1d2	6446.5-6495.5	49.00	46.50	6.83	25.09	30.73	69.27	8.081
7	1d4	6458.5-6582.0	123.50	61.00	21.30	20.69	42.77	57.23	7.224
8	1d6	8041.0-8155.0	97.84	81.10	6.49	20.54	39.47	60.52	10.08
9	1G-13	7538.0-7646.5	99.38	48.57	25.19	15.86	29.68	70.32	5.417
10	1g7	6352.0-6448.0	93.50	58.00	0.00	20.65	38.26	61.74	7.394
11	1h6	6445.0-6474.0	29.00	1.50	0.00	20.19	51.70	48.30	0.146
12	1i8	7301.5-7370.0	60.30	16.65	6.49	11.46	30.42	69.58	1.328
13	1q15	6125.0-6190.0	65.00	31.00	23.67	12.95	50.07	49.93	2.005
14	1r-1	8070.0-8120.0	38.86	25.24	15.75	18.59	17.66	82.34	3.863
15	1q11	5872.0-5960.0	85.00	53.50	7.81	20.34	33.92	66.08	7.191
16	1y3	6019.5-6118.5	99.00	56.00	8.71	18.45	34.23	65.77	6.795
17	2a5	5893.5-5925.5	29.00	22.50	1.82	21.18	36.41	63.59	3.031
18	2A-8	8076.5-8143.5	51.41	36.12	5.42	12.48	31.28	68.72	3.100
19	2c6	5829.5-5853.5	24.00	15.50	24.03	15.57	33.36	66.64	1.609
20	2d12	8182.0-8295.5	69.46	13.92	17.76	20.66	44.42	55.58	1.587
21	2f2	5939.0-6012.0	73.00	24.00	11.19	23.80	45.38	54.62	3.120
22	2h15	5977.0-6005.5	28.00	17.50	24.03	16.39	51.80	48.20	1.382
23	2h4	6386.0-6405.0	15.88	4.60	21.07	13.49	51.51	48.49	0.301
24	2t10	7847.5-7902.5	37.11	12.47	11.47	13.29	48.15	51.85	0.860
25	2u-1	6853.0-6934.5	62.12	37.35	6.87	13.91	39.66	60.34	3.135

Table VII-2: (Continued) Average Petrophysical Properties of Kuparuk River Upper Sand  
(6% porosity, 40% shale, 60% Sw cutoffs).

No.	Well Name	Interval (ft)	Thickness Gross (ft)	Thickness Net (ft)	Shale Volume (%)	Porosity (%)	Saturation Water (%)	Saturation Oil (%)	Hydrocarbon Feet hO (1-Sw)
26	2u11	5747.5-5761.0	13.50	6.00	13.29	18.36	33.83	66.17	0.737
27	2v14	5810.0-5857.5	47.50	43.50	5.54	17.68	26.38	73.62	5.663
28	2v8a	8584.5-8607.5	23.00	18.00	18.27	23.13	17.83	82.17	3.422
29	2w2	6412.0-6448.0	28.97	20.52	5.90	20.44	32.62	67.38	2.826
30	2x2	6285.0-6386.5	96.05	19.11	14.69	17.11	53.60	46.40	1.517
31	2z15	5895.0-5976.5	81.50	53.50	12.42	21.61	40.00	60.00	6.936
32	2z7	5874.0-5927.5	53.50	49.50	5.57	24.39	24.13	75.87	9.159
33	3a-3	7784.5-7858.5	56.13	42.85	0.00	23.61	32.96	67.04	6.783
34	3a-6	7128.0-7313.0	131.55	66.86	14.68	17.58	31.16	68.84	8.094
35	3A-8	6582.0-6728.0	100.87	31.88	19.13	15.03	40.70	59.30	2.842
36	3a-9	5988.5-6068.5	80.00	55.50	13.97	19.09	48.43	51.57	5.464
37	3b-10	5991.5-6045.0	53.50	10.50	11.91	20.28	55.56	44.44	0.946
38	3b14	6021.5-6046.0	24.50	13.00	8.33	23.54	29.18	70.82	2.167
39	3b-2	7774.5-7796.0	15.42	14.34	0.00	21.26	29.99	70.01	2.135
40	3b-7	6073.5-6094.0	20.50	5.00	29.60	11.35	43.26	56.74	0.322
41	3c-16	6395.0-6419.0	23.02	16.31	15.77	19.30	18.88	81.12	2.553
42	3c-8	9741.0-9785.0	28.19	5.51	34.91	13.56	22.28	77.72	0.580
43	3f14	6416.0-6445.0	22.50	16.68	21.00	17.47	36.47	63.53	1.851
44	3H-11	6057.5-6089.5	32.00	19.00	12.70	32.10	47.09	52.91	3.226
45	3i1	8648.5-8686.0	27.47	15.38	20.57	17.68	48.44	51.56	1.402
46	3i5	7604.5-7625.0	17.51	2.99	26.87	13.60	54.13	45.87	0.186
47	3k3	8400.0-8421.5	15.93	8.89	25.68	15.16	35.71	64.29	0.867
48	3N-12	7685.5-7718.0	27.03	10.82	21.68	17.65	30.19	59.81	1.333
49	3N-13	7470.5-7508.5	29.01	16.04	27.26	15.76	39.94	60.06	1.519

**Table VII-3: Average Petrophysical Properties of Kuparuk River Upper Sand  
(6% porosity, 40% shale, 80% Sw cutoffs).**

No.	Well Name	Interval (ft)	Thickness Gross (ft)	Thickness Net (ft)	Shale Volume (%)	Porosity (%)	Saturation Water (%)	Saturation Oil (%)	Hydrocarbon Feet hO (1-Sw)
1	1A-11	8877.5-8920.5	28.90	27.21	2.28	18.77	38.83	61.17	3.124
2	1b7	6294.0-6374.0	80.00	76.00	19.25	20.75	55.77	44.23	6.977
3	1c2	6437.5-6492.5	55.00	53.00	8.53	22.92	26.91	73.09	8.877
4	1c5	7043.0-7113.0	58.37	54.60	13.82	23.16	28.83	71.17	9.001
5	1c6	9409.0-9497.0	57.90	52.76	10.79	23.21	35.23	64.77	7.932
6	1d2	6446.5-6495.5	49.00	49.00	6.93	24.54	31.77	68.23	8.202
7	1d4	6458.5-6582.0	123.50	68.00	22.75	19.98	44.27	55.73	7.572
8	1d6	8041.0-8155.0	97.84	88.40	7.01	19.92	40.94	59.06	10.402
9	1G-13	7538.0-7646.5	99.38	56.81	26.90	15.09	33.47	66.53	5.703
10	1g7	6352.0-6448.0	93.50	89.00	0.00	19.58	47.65	52.35	9.124
11	1h6	6445.0-6474.0	29.00	7.50	0.00	21.13	68.12	31.88	0.505
12	1i8	7301.5-7370.0	60.30	16.65	9.49	11.46	30.42	69.58	1.328
13	1q15	6125.0-6190.0	65.00	41.00	24.66	11.87	52.72	47.28	2.300
14	1r-1	8070.0-8120.0	38.86	25.24	15.75	18.59	17.66	82.34	3.863
15	1q11	5872.0-5960.0	53.00	53.00	8.67	19.5	35.42	64.58	6.674
16	1y3	6019.5-6118.5	99.00	68.50	12.81	17.21	38.72	61.28	7.226
17	2a5	5893.5-5925.5	29.00	24.00	3.09	20.87	37.79	62.21	3.116
18	2A-8	8076.5-8143.5	51.41	41.89	7.26	12.42	36.66	63.34	3.298
19	2c6	5829.5-5853.5	24.00	16.50	23.03	16.21	37.66	42.34	1.668
20	2d12	8182.0-8295.5	69.46	27.87	23.99	18.35	57.15	42.85	2.157
21	2f2	5939.0-6012.0	73.00	70.00	16.65	20.89	58.93	41.07	6.007
22	2h15	5977.0-6005.5	28.00	24.50	24.63	15.56	55.04	44.96	1.714
23	2h4	6386.0-6405.0	15.88	8.78	19.79	12.72	58.09	41.94	6.468
24	2t10	7847.5-7902.5	37.11	19.56	16.71	12.66	55.79	44.21	1.095
25	2u-1	6853.0-6934.5	62.12	47.26	8.30	13.26	44.27	55.73	3.492

**Table VII-3: (Continued) Average Petrophysical Properties of Kuparuk River Upper Sand  
(6% porosity, 40% shale, 80% Sw cutoffs).**

No.	Well Name	Interval (ft)	Thickness Gross (ft)	Thickness Net (ft)	Shale Volume (%)	Porosity (%)	Saturation Water (%)	Saturation Oil (%)	Hydrocarbon Feet h <sub>0</sub> (J.Sw)
26	2u11	5747.5-5761.0	13.50	6.50	12.52	17.71	35.08	64.92	0.747
27	2v14	5810.0-5857.5	47.50	44.00	5.68	17.69	26.79	73.21	5.700
28	2v8a	8584.5-8607.5	23.00	18.00	18.27	23.13	17.83	82.17	3.422
29	2w2	6412.0-6448.0	28.97	22.53	6.48	19.36	34.09	65.91	2.874
30	2x2	6285.0-6386.5	96.05	40.68	13.91	15.65	61.43	38.57	2.456
31	2z15	5895.0-5976.5	81.50	67.50	15.65	19.75	43.34	56.66	7.554
32	2z7	5874.0-5927.5	53.50	53.50	6.47	24.08	26.65	73.35	9.450
33	3a-3	7784.5-7858.5	56.13	48.54	0.00	22.92	36.25	63.75	7.090
34	3a-6	7128.0-7313.0	131.55	77.20	15.99	16.99	34.90	65.10	8.543
35	3A-8	6582.0-6728.0	100.87	38.71	19.04	14.09	44.49	55.51	3.027
36	3a-9	5988.5-6068.5	80.00	74.00	15.60	17.99	52.12	47.88	6.375
37	3b-10	5991.5-6045.0	53.50	23.00	15.05	17.93	62.36	37.64	1.552
38	3b14	6021.5-6046.0	24.50	18.00	13.37	19.77	34.88	65.12	2.317
39	3b-2	7774.5-7796.0	15.42	15.06	0.00	20.87	31.11	68.89	2.166
40	3b-7	6073.5-6094.0	20.50	5.50	30.36	10.96	45.17	54.83	0.331
41	3c-16	6395.0-6419.0	23.02	16.78	16.21	18.93	19.43	80.57	2.560
42	3c-8	9741.0-9785.0	28.19	5.51	34.91	13.56	22.28	77.72	0.580
43	3f14	6416.0-6445.0	22.50	18.23	20.77	16.73	37.84	62.16	1.896
44	3H-11	6057.5-6089.5	32.00	26.00	13.35	30.76	52.08	47.92	3.832
45	3i1	8648.5-8686.0	27.47	21.61	20.44	16.55	53.03	46.97	1.680
46	3i5	7604.5-7625.0	17.51	9.40	28.22	11.21	61.52	38.48	0.405
47	3N-12	7685.5-7718.0	27.03	11.65	22.38	17.01	31.74	68.26	1.354
48	3N-13	7470.5-7508.5	29.01	22.14	25.92	15.04	45.64	54.36	1.810
49	2d11	7354.0-7407.0	44.59	6.72	29.99	15.11	76.61	23.39	0.238
50	3k3	8400.0-8421.5	15.93	8.89	25.68	15.16	35.71	64.29	0.867

**Table VII-4: Average Petrophysical Properties of Kuparuk River Lower Sand  
(6% porosity, 40% shale, 40% Sw cutoffs).**

No.	Well Name	Interval (ft)	Thickness Gross (ft)	Thickness Net (ft)	Shale Volume (%)	Porosity (%)	Saturation Water (%)	Saturation Oil (%)	Hydrocarbon Feet hO (1-Sw)
1	1A-11	6080.5-9224.5	102.81	22.92	0.00	26.27	29.66	70.34	4.235
2	1b7	6508.0-6560.5	52.50	20.00	6.16	26.40	30.81	69.19	3.653
3	1c2	6712.0-6738.5	26.00	1.00	0.00	28.18	38.40	61.60	0.174
4	1c6	9844.5-9948.5	73.39	0.36	39.87	32.58	38.29	61.71	0.0172
5	1d6	8295.5-8394.5	85.19	6.02	6.28	23.26	36.01	63.99	6.897
6	1G-13	7784.0-7889.0	96.09	16.93	29.49	19.23	27.41	72.59	2.363
7	1g7	6574.5-6690.0	113.00	51.00	0.00	24.80	27.89	72.11	9.121
8	1i8	7482.5-7569.5	79.71	2.73	30.34	18.75	26.70	73.30	0.375
9	1q15	6348.5-6421.5	73.00	59.00	16.16	21.46	21.09	78.91	9.992
10	1r-1	8196.0-8304.5	84.98	41.49	21.56	18.91	21.67	78.34	0.167
11	1y3	6234.5-6347.5	83.50	30.50	12.35	23.88	26.44	73.56	5.359
12	2a5	5945.0-6059.0	114.00	10.50	4.36	25.96	34.62	65.38	1.782
13	1q11	6041.0-6164.0	119.50	40.50	13.24	25.56	24.08	75.92	7.859
14	2A-8	8155.5-8294.0	108.42	13.18	6.15	25.07	28.03	71.97	2.378
15	2c6	5933.5-6040.5	107.00	11.50	10.30	24.20	31.99	68.01	1.893
16	2d11	7424.0-7511.5	74.39	22.92	4.96	25.96	32.59	67.41	4.010
17	2d12	8313.0-8373.5	45.97	19.00	6.66	26.51	32.63	67.37	3.393
18	2f1	5931.0-6044.5	113.50	22.00	12.70	25.35	31.51	68.49	3.820
19	2f2	6026.0-6111.5	85.50	28.50	4.10	28.29	25.73	74.27	5.988
20	2g6	8173.5-8315.5	114.15	2.42	0.00	28.31	34.51	65.49	0.448
21	2h15	6013.0-6127.0	114.00	51.50	9.56	23.37	26.09	73.91	8.896
22	2h4	6467.5-6584.0	97.43	25.53	9.14	22.26	29.63	70.37	3.999
23	2i10	7949.0-8041.0	63.87	9.39	1.96	28.64	31.13	68.97	1.852
24	2u-1	7054.0-7210.0	119.07	16.02	5.27	27.14	29.71	70.29	3.055
25	2u11	5817.0-5925.0	108.00	21.50	10.28	23.19	24.56	75.44	3.761

Table VII-4: (Continued) Average Petrophysical Properties of Kuparuk River Lower Sand  
(6% porosity, 40% shale, 40% Sw cutoffs).

No.	Well Name	Interval (ft)	Thickness Gross (ft)	Thickness Net (ft)	Shale Volume (%)	Porosity (%)	Saturation Water (%)	Saturation Oil (%)	Hydrocarbon Feet hO (1-Sw)
26	2v14	5916.5-6043.0	126.50	33.00	3.46	26.10	26.60	73.40	6.322
27	2v8a	8627.0-8742.0	115.00	29.00	12.86	23.59	16.57	83.43	5.708
28	2w2	6577.5-6723.0	115.50	31.37	10.47	25.35	25.60	74.40	5.915
29	2z15	6083.0-6194.5	111.00	14.00	26.69	22.19	33.04	66.96	2.080
30	2z7	6005.5-6110.5	105.00	22.00	4.47	28.09	30.91	69.09	4.269
31	3a-3	7995.0-8159.5	125.36	18.31	0.00	27.72	34.10	65.90	3.345
32	3a-6	7329.0-7475.0	111.36	28.73	21.94	21.32	26.87	73.13	4.480
33	3A-8	6748.5-6900.5	109.85	36.90	16.88	21.82	23.98	76.02	6.112
34	3a-9	6084.5-6200.0	107.50	50.50	6.03	24.17	29.81	70.19	8.569
35	3b-10	6176.5-6273.5	97.00	21.00	4.45	27.15	25.22	74.78	4.264
36	3b14	6151.5-6277.0	122.50	19.00	9.50	27.44	25.24	74.76	3.898
37	3b-2	7941.5-8067.5	85.64	64.39	6.65	22.08	26.37	73.63	10.466
38	3b-7	6204.5-6314.5	110.00	21.50	28.49	20.84	19.23	80.77	3.620
39	3c-16	6563.5-6678.5	110.80	46.24	23.77	18.84	22.43	77.57	6.757
40	3c-8	9890.5-1003.0	73.86	19.05	22.75	19.00	10.01	89.99	3.257
41	3f14	6573.0-6681.0	83.69	21.31	10.71	23.87	30.67	69.33	3.526
42	3i1	8724.0-8826.5	75.09	45.42	14.93	22.04	30.78	69.22	6.929
43	3i5	7642.0-7764.5	104.71	60.26	14.26	22.16	28.16	71.84	9.595
44	3k3	8512.5-8676.5	124.07	61.18	22.21	20.69	22.74	77.26	9.764
45	3N-12	7795.0-7935.5	117.46	48.05	16.20	21.55	24.53	75.47	7.813
46	3N-13	7543.5-7688.0	108.40	66.80	22.55	21.17	22.98	77.02	10.891

**Table VII-5: Average Petrophysical Properties of Kuparuk River Lower Sand  
(6% porosity, 40% shale, 60% Sw cutoffs).**

No.	Well Name	Interval (ft)	Thickness Gross (ft)	Thickness Net (ft)	Shale Volume (%)	Porosity (%)	Saturation Water (%)	Saturation Oil (%)	Hydrocarbon Feet h <sub>0</sub> (1-Sw)
1	1A-11	6080.5-9224.5	102.81	44.29	0.20	24.73	38.44	61.56	6.744
2	1b7	6508.0-6560.5	52.50	39.00	15.82	22.88	38.45	61.55	5.491
3	1c2	6712.0-6738.5	26.00	23.00	17.37	21.10	46.46	53.54	2.599
4	1c5	7442.5-7496.5	44.44	2.06	24.23	21.57	59.26	40.76	0.181
5	1c6	9844.5-9948.5	73.39	4.66	17.60	28.28	53.50	46.50	0.613
6	1d2	6658.5-6690.0	31.50	18.00	14.57	23.66	53.81	46.19	1.967
7	1d6	8295.5-8394.5	85.19	36.57	16.63	19.30	49.83	50.17	3.541
8	1G-13	7784.0-7889.0	96.09	21.05	30.66	18.05	30.36	69.54	2.645
9	1g7	6574.5-6690.0	113.00	108.00	1.75	22.81	38.48	61.52	15.159
10	1i8	7482.5-7569.5	79.71	2.73	30.34	18.75	26.70	73.30	0.375
11	1q15	6348.5-6421.5	73.00	65.50	18.08	20.59	22.42	77.58	10.462
12	1r-1	8196.0-8304.5	84.98	43.45	22.25	18.57	22.31	77.69	6.271
13	1y3	6234.5-6347.5	83.50	49.00	20.08	20.26	32.33	67.67	6.719
14	2a5	5945.0-6059.0	114.00	32.00	7.25	22.81	43.48	56.52	4.126
15	1q11	6041.0-6164.0	119.50	40.50	16.85	23.75	26.87	73.13	7.034
16	2A-8	8155.5-8294.0	108.42	36.18	12.85	20.88	42.39	57.61	4.350
17	2c6	5933.5-6040.5	107.00	31.00	20.36	20.41	39.45	60.55	3.832
18	2d11	7424.0-7511.5	74.39	45.87	12.77	22.64	39.89	60.11	6.243
19	2d12	8313.0-8373.5	45.97	35.34	15.83	23.02	39.88	60.12	4.891
20	2f1	5931.0-6044.5	113.50	30.50	15.46	23.86	35.52	64.48	4.691
21	2f2	6026.0-6111.5	85.50	50.50	9.47	25.46	35.30	64.70	8.317
22	2g6	8173.5-8315.5	114.15	22.17	7.30	24.20	46.28	53.72	2.882
23	2h15	6013.0-6127.0	114.00	105.00	14.71	20.50	35.48	64.52	13.887
24	2h4	6467.5-6584.0	97.43	66.08	18.10	18.60	40.82	59.18	7.274
25	2t10	7949.0-8041.0	63.87	32.63	13.76	23.13	43.33	56.67	4.276

Table VII-5: (Continued) Average Petrophysical Properties of Kuparuk River Lower Sand  
(6% porosity, 40% shale, 60% Sw cutoffs).

No.	Well Name	Interval (ft)	Thickness Gross (ft)	Thickness Net (ft)	Shale Volume (%)	Porosity (%)	Saturation Water (%)	Saturation Oil (%)	Hydrocarbon Feet hO (1.Sw)
26	2u-1	7054.0-7210.0	119.07	41.94	14.80	23.41	41.42	58.58	5.751
27	2u11	5817.0-5925.0	108.00	26.00	13.75	21.81	26.75	73.25	4.153
28	2v14	5916.5-6043.0	126.50	81.50	8.72	22.60	40.39	59.61	10.981
29	2v8a	8627.0-8742.0	115.00	30.50	13.26	23.13	17.55	82.45	5.817
30	2w2	6577.5-6723.0	115.50	77.39	20.09	19.86	38.04	61.96	9.522
31	2z15	6083.0-6194.5	111.00	27.00	29.29	20.13	39.69	60.31	3.278
32	2z7	6005.5-6110.5	105.00	50.50	9.84	25.27	41.13	58.87	7.512
33	3a-3	7995.0-8159.5	125.36	48.46	1.27	26.21	42.71	57.29	7.276
34	3a-6	7329.0-7475.0	111.36	30.66	22.74	21.02	27.66	72.34	4.662
35	3A-8	6748.5-6900.5	109.85	45.95	20.06	20.37	26.82	73.18	6.838
36	3a-9	6084.5-6200.0	107.50	98.00	11.41	21.50	38.45	61.55	12.968
37	3b-10	6176.5-6273.5	97.00	64.00	14.91	21.96	39.93	60.07	8.443
38	3b14	6151.5-6277.0	122.50	30.00	18.25	23.93	30.72	69.28	4.973
39	3b-2	7941.5-8067.5	85.64	83.53	7.01	21.79	30.30	69.70	12.690
40	3b-7	6204.5-6314.5	110.00	23.50	29.30	20.06	20.52	79.48	3.746
41	3c-16	6563.5-6678.5	110.80	53.47	25.35	18.06	24.77	75.23	7.263
42	3c-8	9890.5-1003.0	73.86	19.05	22.75	19.00	10.01	80.89	3.257
43	3f14	6573.0-6681.0	83.69	55.41	23.48	18.47	39.47	60.53	6.194
44	3H-11	6130.5-6233.0	102.50	13.50	9.31	28.93	51.14	48.86	1.906
45	3i1	8724.0-8826.5	75.09	66.67	18.15	20.65	34.65	65.35	8.999
46	3i5	7642.0-7764.5	104.71	98.30	20.67	19.52	34.32	65.68	12.602
47	3j9	6466.0-6547.0	81.00	5.00	27.43	21.32	56.36	43.64	0.465
48	3k3	8512.5-8676.5	124.07	66.42	22.49	20.30	23.97	76.03	10.239
49	3N-12	7795.0-7935.5	117.46	74.79	19.89	19.43	31.25	68.75	9.990
50	3N-13	7543.5-7688.0	108.40	79.02	24.09	20.26	25.66	74.34	11.901

**Table VII-6: Average Petrophysical Properties of Kuparuk River Lower Sand  
(6% porosity, 40% shale, 80% Sw cutoffs).**

No.	Well Name	Interval (ft)	Thickness Gross (ft)	Thickness Net (ft)	Shale Volume (%)	Porosity (%)	Saturation Water (%)	Saturation Oil (%)	Hydrocarbon Feet hØ (1-Sw)
1	1A-11	6080.5-9224.5	102.81	92.81	1.15	23.10	53.68	46.32	9.933
2	1b7	6508.0-6560.5	52.50	45.00	16.88	21.57	40.78	59.22	5.749
3	1c2	6712.0-6738.5	26.00	25.00	15.98	20.36	47.79	52.21	2.685
4	1c5	7442.5-7496.5	44.44	30.45	14.61	24.25	65.75	34.25	2.529
5	1c6	9844.5-9948.5	73.39	28.95	12.84	27.36	64.75	35.25	2.791
6	1d2	6658.5-6690.0	31.50	22.00	17.46	22.10	55.06	44.94	2.185
7	1d4	6697.5-6729.5	32.00	8.00	29.36	19.10	71.49	28.51	0.436
8	1d6	8295.5-8394.5	85.19	83.04	19.15	17.81	58.12	42.88	6.193
9	1G-13	7784.0-7889.0	96.09	21.96	30.91	17.72	31.25	68.75	2.675
10	1g7	6574.5-6690.0	113.00	113.00	1.85	22.66	39.37	60.63	15.526
11	1i8	7482.5-7569.5	79.71	2.73	30.34	18.75	26.70	73.30	0.375
12	1q15	6348.5-6421.5	73.00	65.50	18.08	20.59	22.42	77.58	10.462
13	1r-1	8196.0-8304.5	84.98	43.45	22.25	18.57	22.31	77.69	6.271
14	1y3	6234.5-6347.5	83.50	49.00	20.08	20.26	32.33	67.67	6.719
15	2a5	5945.0-6059.0	114.00	65.00	13.47	19.61	55.54	44.46	5.668
16	1q11	6041.0-6164.0	119.5	40.5	16.85	23.75	26.87	73.13	7.034
17	2A-8	8155.5-8294.0	108.42	99.37	20.67	18.08	57.39	42.61	7.650
18	2c6	5933.5-6040.5	107.00	33.50	20.16	20.07	41.05	58.95	3.963
19	2d12	8313.0-8373.5	45.97	40.27	17.95	22.17	41.95	58.05	5.183
20	2f1	5931.0-6044.5	113.50	34.50	16.34	23.24	38.40	61.60	4.939
21	2f2	6026.0-6111.5	85.50	85.00	13.85	23.22	46.00	54.00	10.660
22	2q6	8173.5-8315.5	114.15	33.36	9.14	22.14	53.00	47.00	3.519
23	2h15	6013.0-6127.0	114.00	114.00	15.30	20.24	37.42	62.58	14.441
24	2h4	6467.5-6584.0	97.43	92.42	21.48	17.19	46.18	53.82	8.552
25	2t10	7949.0-8041.0	63.87	51.10	19.42	20.53	50.32	49.68	5.210
26	2u-1	7054.0-7210.0	119.07	61.79	20.36	21.55	48.12	51.88	6.907

**Table VII-6: (Continued) Average Petrophysical Properties of Kuparuk River Lower Sand  
(6% porosity, 40% shale, 80% Sw cutoffs).**

No.	Well Name	Interval (ft)	Thickness Gross (ft)	Thickness Net (ft)	Shale Volume (%)	Porosity (%)	Saturation Water (%)	Saturation Oil (%)	Hydrocarbon Feet h <sub>0</sub> (1-Sw)
27	2u11	5817.0-5925.0	108.00	26.00	13.75	21.81	26.75	73.25	4.153
28	2v14	5916.5-6043.0	126.50	121.50	11.46	21.17	48.33	51.67	13.288
29	2v8a	8627.0-8742.0	115.00	31.00	13.33	22.94	17.99	82.01	5.832
30	2w2	6577.5-6723.0	115.50	89.30	21.53	19.00	40.55	59.45	10.087
31	2x2	6512.0-6638.0	122.47	2.45	9.10	25.32	77.74	23.26	0.138
32	2z15	6083.0-6194.5	111.00	32.50	29.53	19.15	43.23	56.77	3.532
33	2z7	6005.5-6110.5	105.00	103.00	16.19	23.52	54.15	45.85	11.105
34	3a-3	7995.0-8159.5	125.36	76.70	2.26	25.13	52.14	47.86	9.222
35	3a-6	7329.0-7475.0	111.36	31.42	23.13	20.82	28.39	71.61	4.683
36	3A-8	6748.5-6900.5	109.85	46.68	20.24	20.22	27.10	72.90	6.868
37	3a-9	6084.5-6200.0	107.50	106.00	12.22	21.16	40.06	59.94	13.442
38	3b-10	6176.5-6273.5	97.00	95.00	20.08	19.74	46.84	53.16	9.971
39	3b14	6151.5-6277.0	122.50	30.00	18.25	23.93	30.72	69.28	4.973
40	3b-2	7941.5-8067.5	85.64	85.29	7.62	21.62	30.76	69.24	12.768
41	3b-7	6204.5-6314.5	110.00	23.50	29.30	20.06	20.52	79.48	3.746
42	3c-16	6563.5-6678.5	110.80	53.47	25.35	18.06	24.77	75.23	7.263
43	3c-8	9890.5-1003.0	73.86	19.05	22.75	19.00	10.01	89.99	3.257
44	3f14	6573.0-6681.0	83.69	60.06	24.25	18.07	40.94	59.06	6.411
45	3H-11	6130.5-6233.0	102.50	23.50	12.31	27.51	58.68	41.32	2.671
46	3i1	8724.0-8826.5	75.09	67.03	18.27	20.62	34.76	65.24	9.020
47	3i5	7642.0-7764.5	104.71	100.86	21.08	19.33	34.79	65.21	12.716
48	3j9	6466.0-6547.0	81.00	13.00	29.18	18.39	62.36	37.64	0.900
49	3N-12	7795.0-7935.5	117.46	76.88	19.97	19.25	31.93	68.07	10.071
50	3N-13	7543.5-7688.0	108.40	79.40	24.11	20.23	25.79	74.21	11.923
51	3d11	7424.0-7511.5	74.39	63.33	17.59	20.65	45.43	54.57	7.132
52	3k3	8512.5-8676.5	124.07	66.42	22.49	20.30	23.97	76.03	10.239



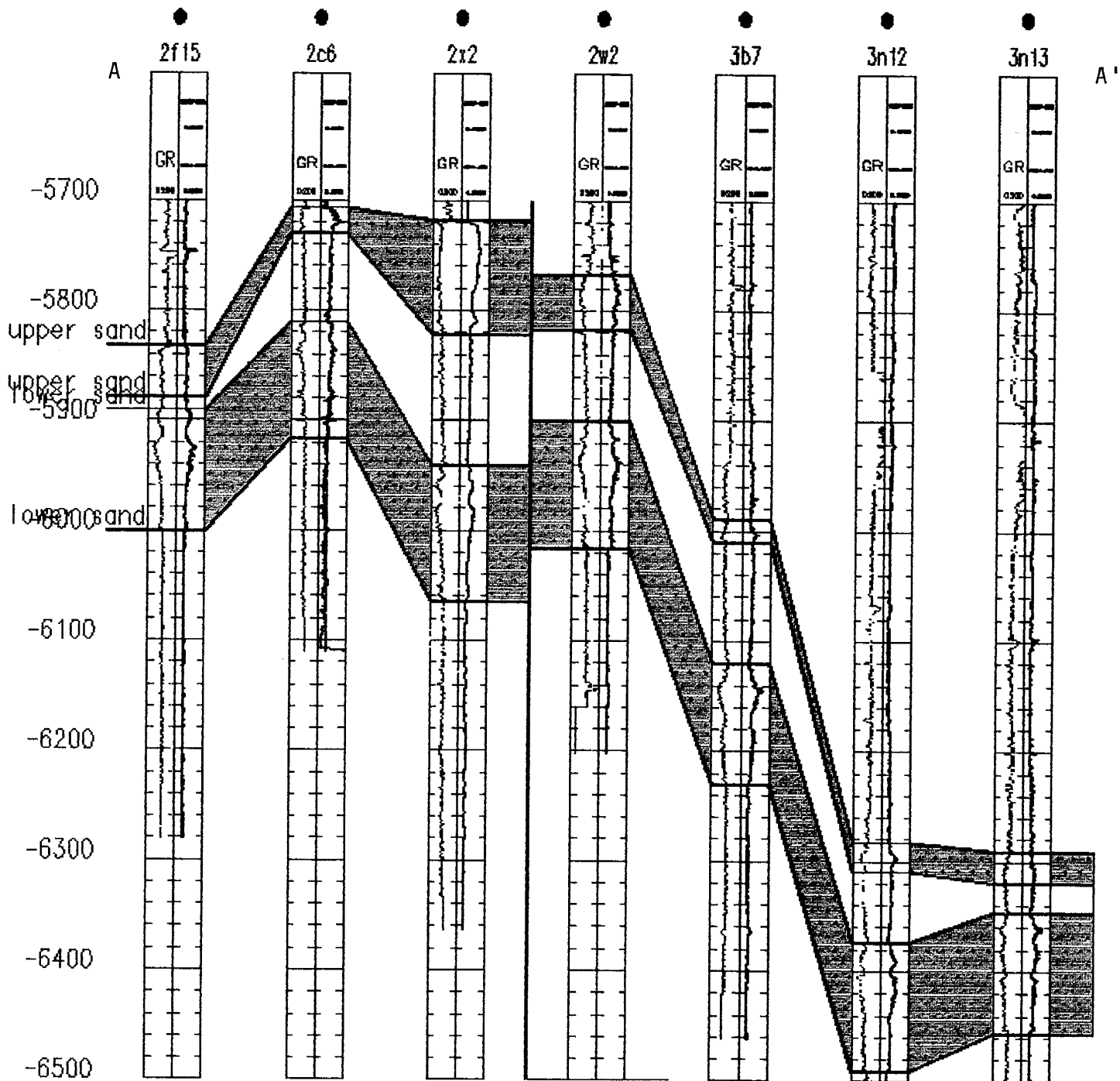


Figure VII-7. Stratigraphic Cross Section A-A' in Kuparuk River Field Showing Distributions of Kuparuk River Upper and Lower Sands.

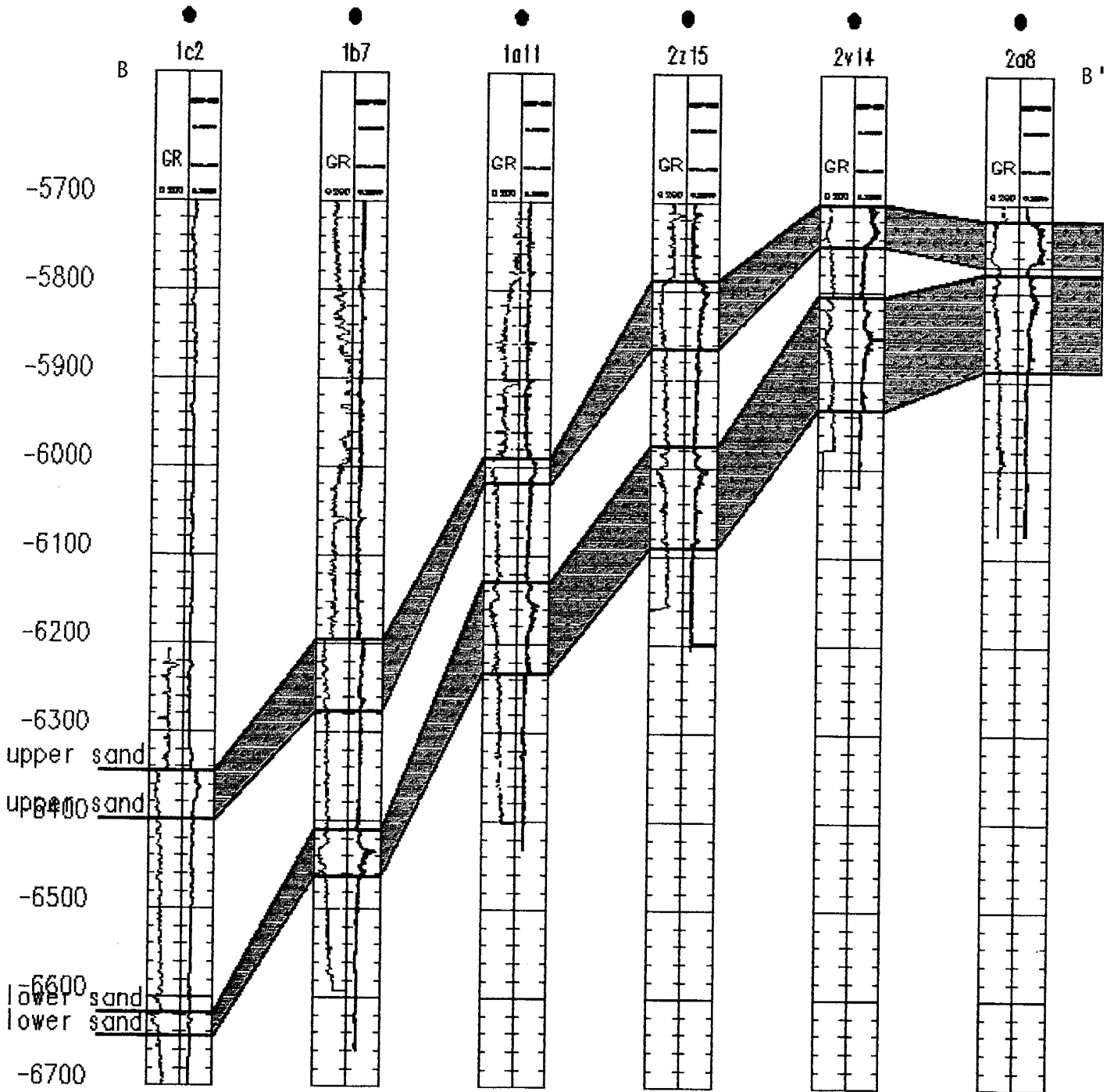


Figure VII-8. Stratigraphic Cross Section B-B' in Kugaruk River Field Showing Distributions of Kugaruk River Upper and Lower Sands.

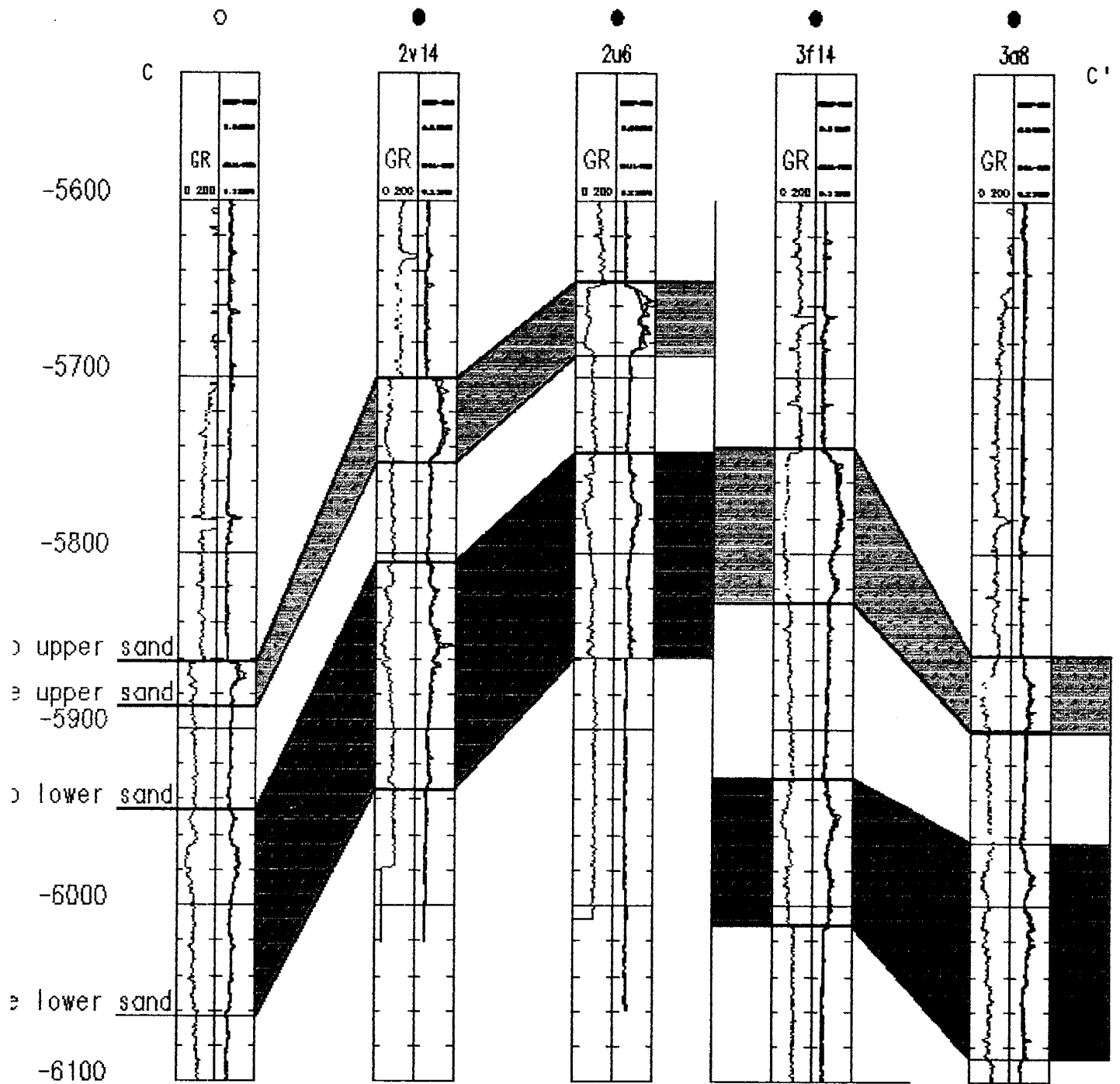


Figure VII-9. Stratigraphic Cross Section C-C' in Kuparuk River Field Showing Distributions of Kupa-ruk River Upper and Lower Sands.

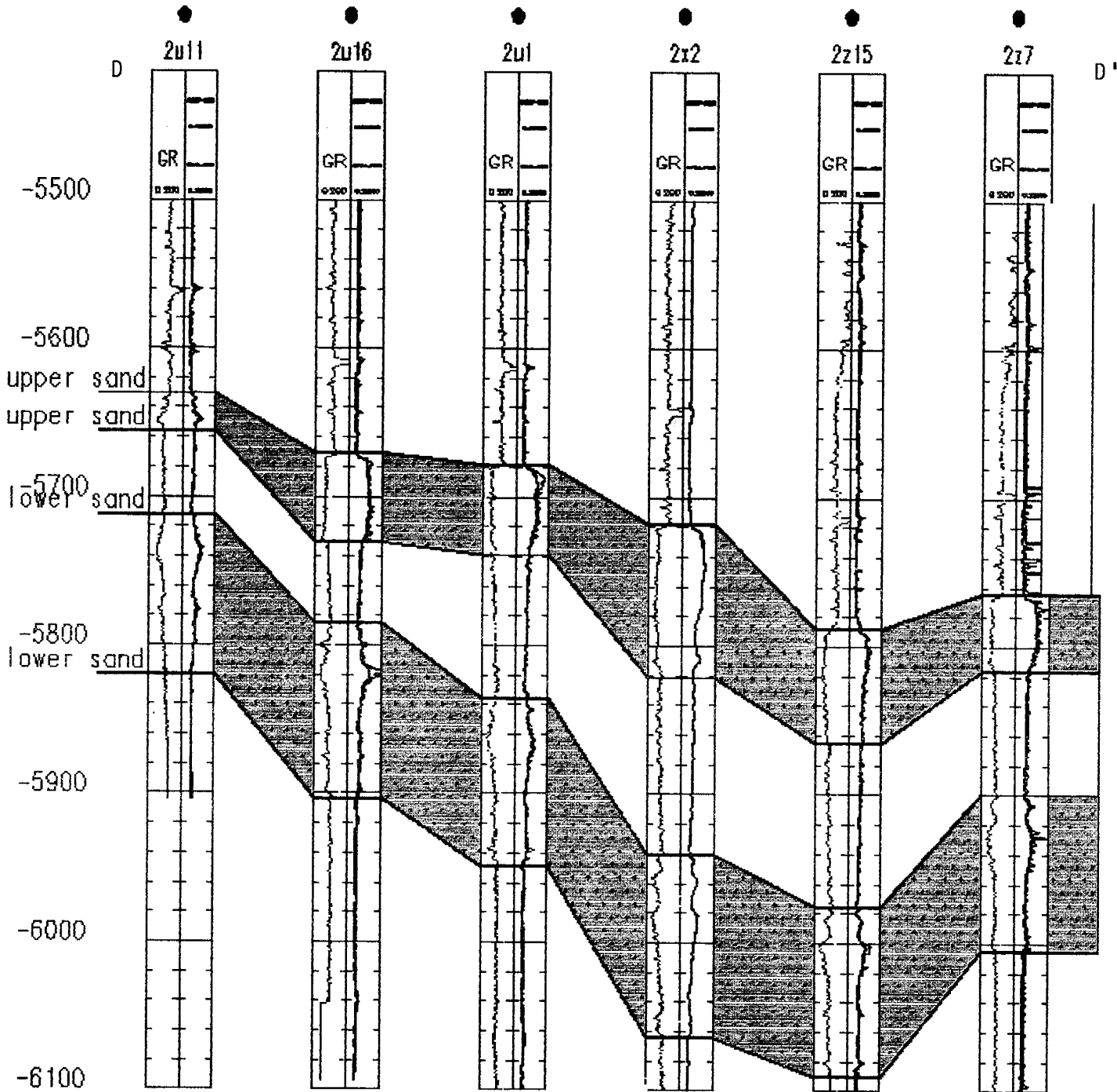


Figure VII-10. Stratigraphic Cross Section D-D' in Kuparuk River Field Showing Distributions of Kuparuk River Upper and Lower Sands.

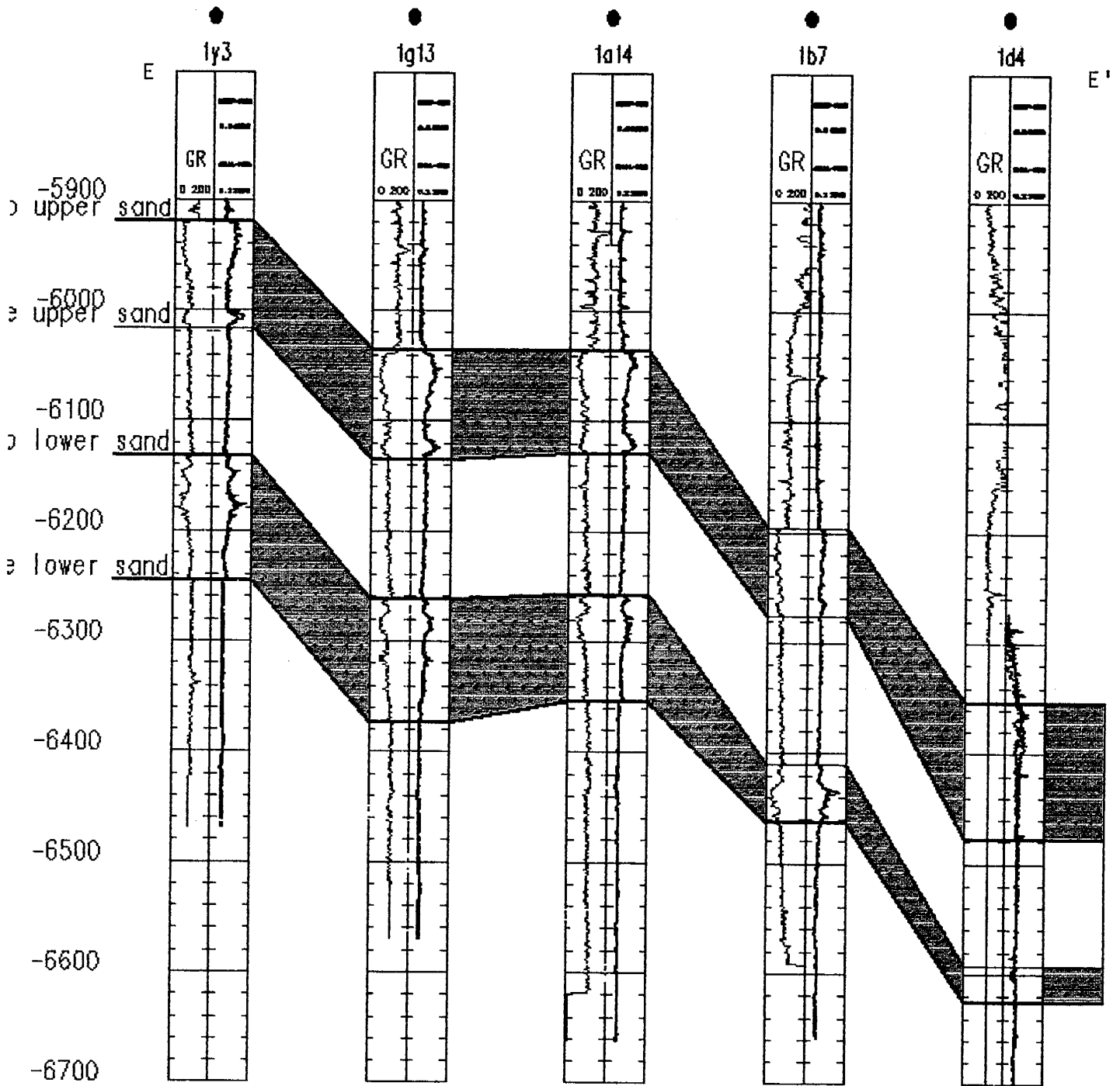


Figure VII-11. Stratigraphic Cross Section E-E' in Kuparuk River Field Showing Distributions of Kuparuk River Upper and Lower Sands.

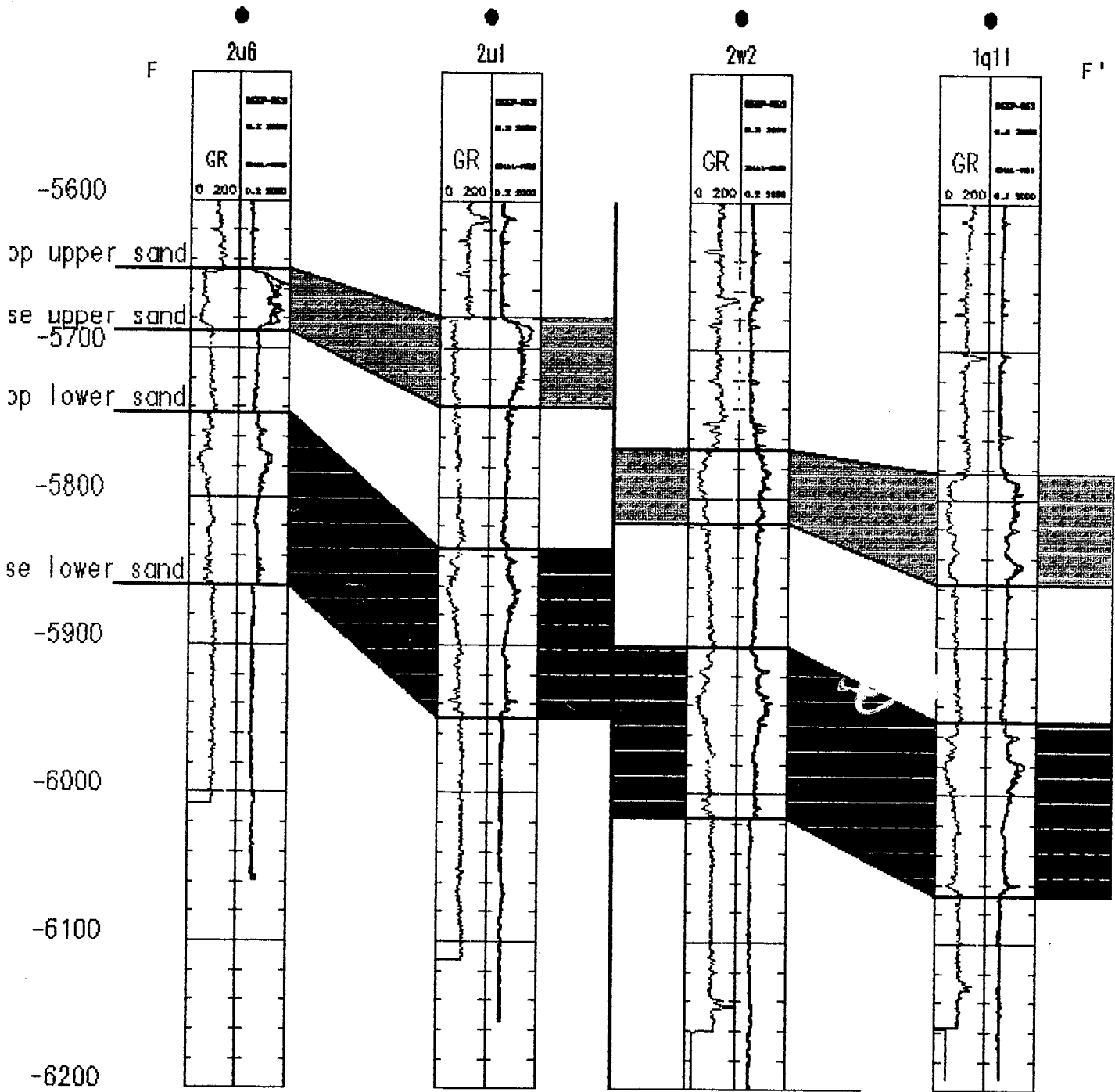


Figure VII-12. Stratigraphic Cross Section F-F' in Kuparuk River Field Showing Distributions of Kuparuk River Upper and Lower Sands.

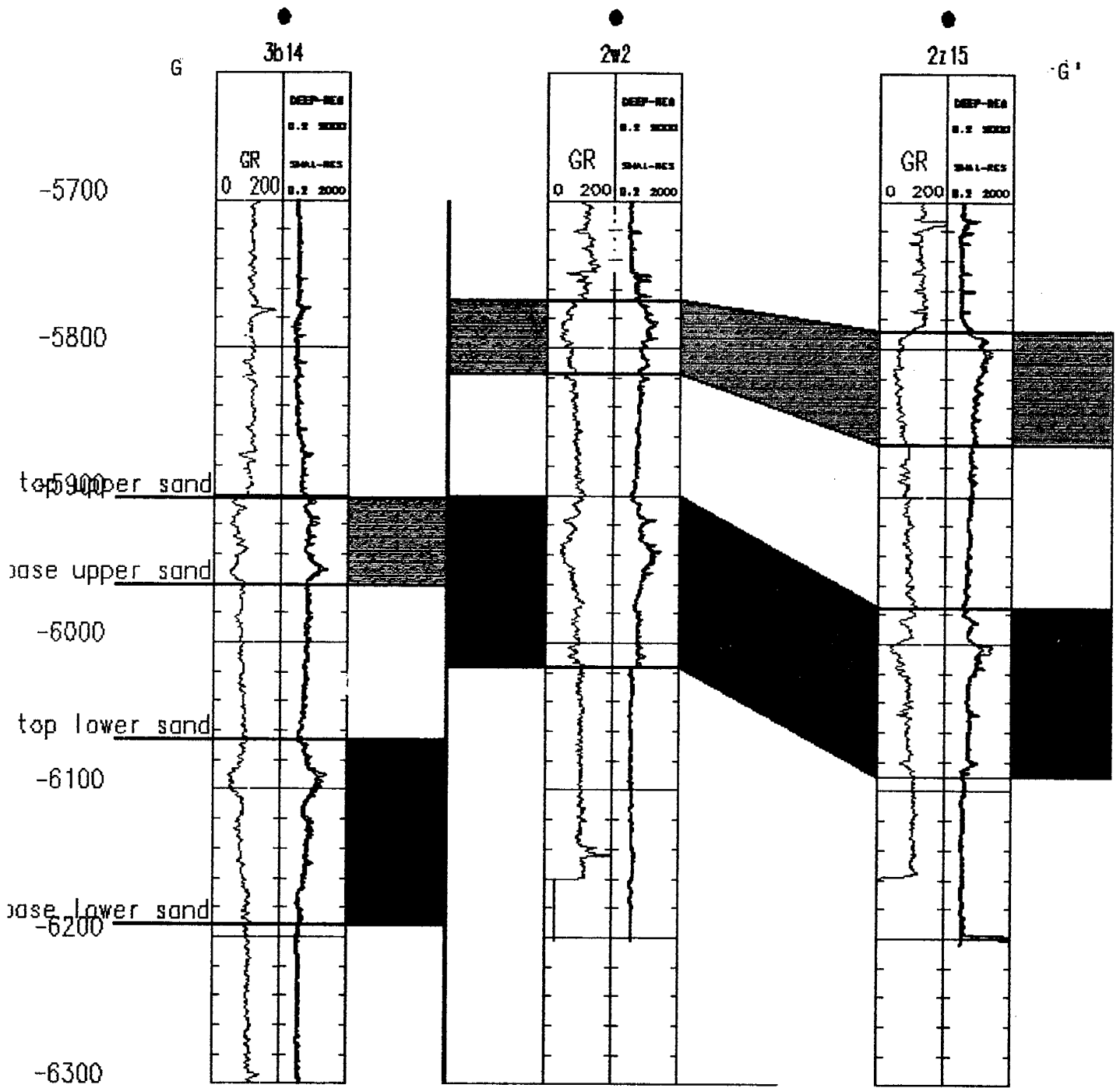


Figure VII-13. Stratigraphic Cross Section G-G' in Kuparuk River Field Showing Distributions of Kuparuk River Upper and Lower Sands.

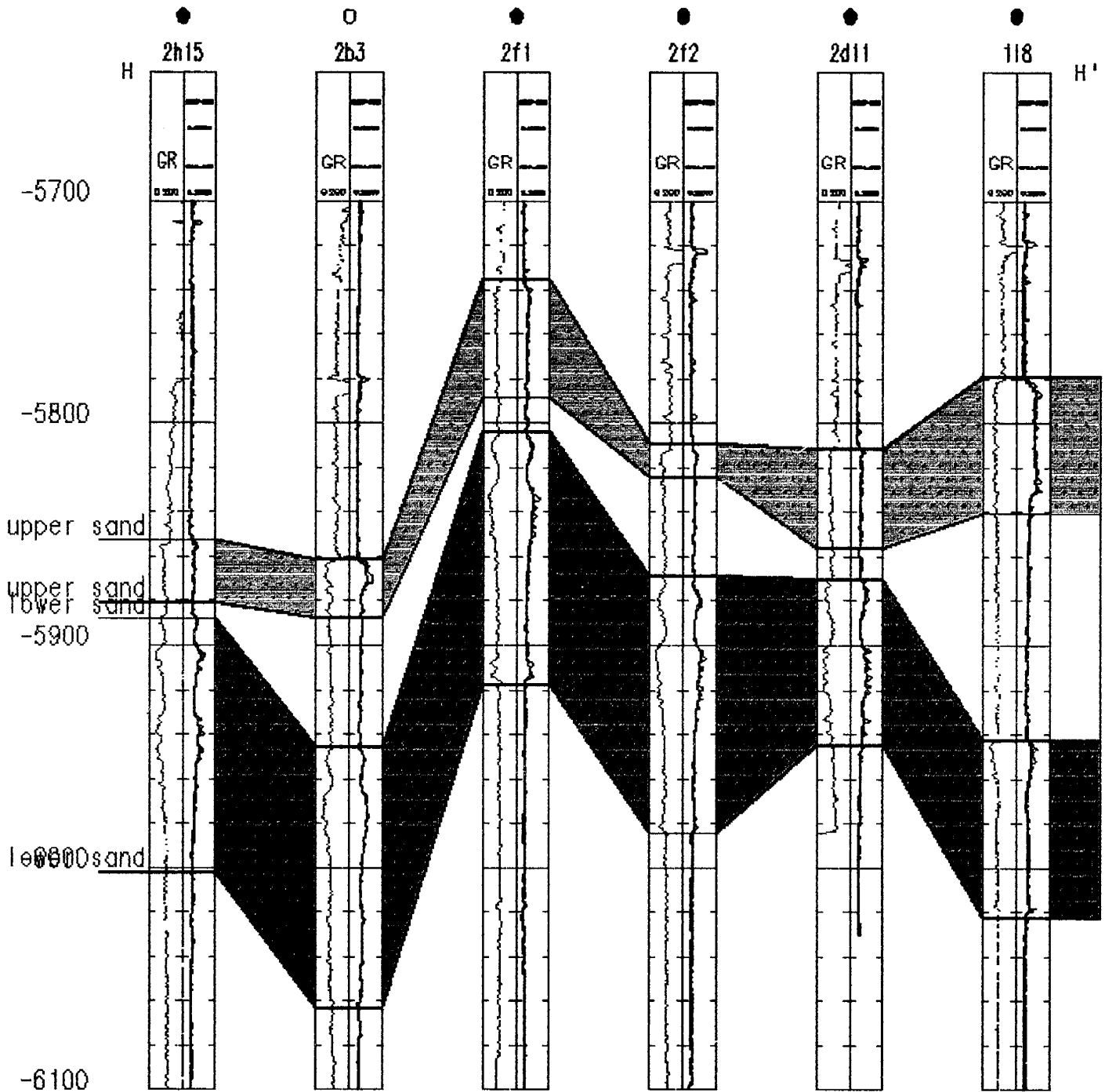


Figure VII-14. Stratigraphic Cross Section H-H' in Kuparuk River Field Showing Distributions of Kuparuk River Upper and Lower Sands.

Structure top contour maps were generated both with and without major faults. This was done, in part, to assess the ability of the WorkBench program to contour with faults. Faulting provides a noticeable degree of difficulty for Workbench's contouring routine, as is evident in Figures VII-15 and VII-17. (Corresponding contour maps without faulting are shown in Figures VII-16 and VII-18.) However, both sets of contour maps present a general trend of northwest-to-southeast trending strike with northeast dip. Unfaulted 3-D structural views of the Kuparuk River upper and lower sands are presented in Figures VII-19 and VII-20.

In order to study the distribution of sand thicknesses, porosity, water saturation, oil saturation, etc., across the field, several maps of these properties were generated. Additional property maps were also generated with color filled contours, as a means of better visualizing distribution of properties across the field. Three-dimensional views of the above-mentioned properties were also generated and are discussed below.

## **C. DISCUSSION OF RESULTS**

### **C1. Structure and Isopach Maps**

Based on geologic marker information obtained from well reports, the Kuparuk River formation has been divided into two sand members, the upper and lower sands. In some published literature (Van Poolen, et al.) there is mention of a "middle" sand between upper and lower sands, which could not be identified as a separate sand in the wells selected for this study. The geologic marker information of this middle sand was also not available from well reports. However, based upon log characteristic, a thin sand member was identified in some of the wells analyzed, which appears to coalesce with the upper sand across the field. This thin sand member, which was treated as the bottom portion of the upper sand in this study, is probably the middle sand.

Several maps have been prepared to delineate the structure on the top of each zone. From net pay thickness maps, it can be observed that maximum net sand values in the upper sand occur in the center of the field and range from 40 to 80 feet. Net thicknesses decrease, between 20 and 40 feet, on both north and south sides of the field. Lower sand maximum thicknesses extend from the center through the northern side of the field.

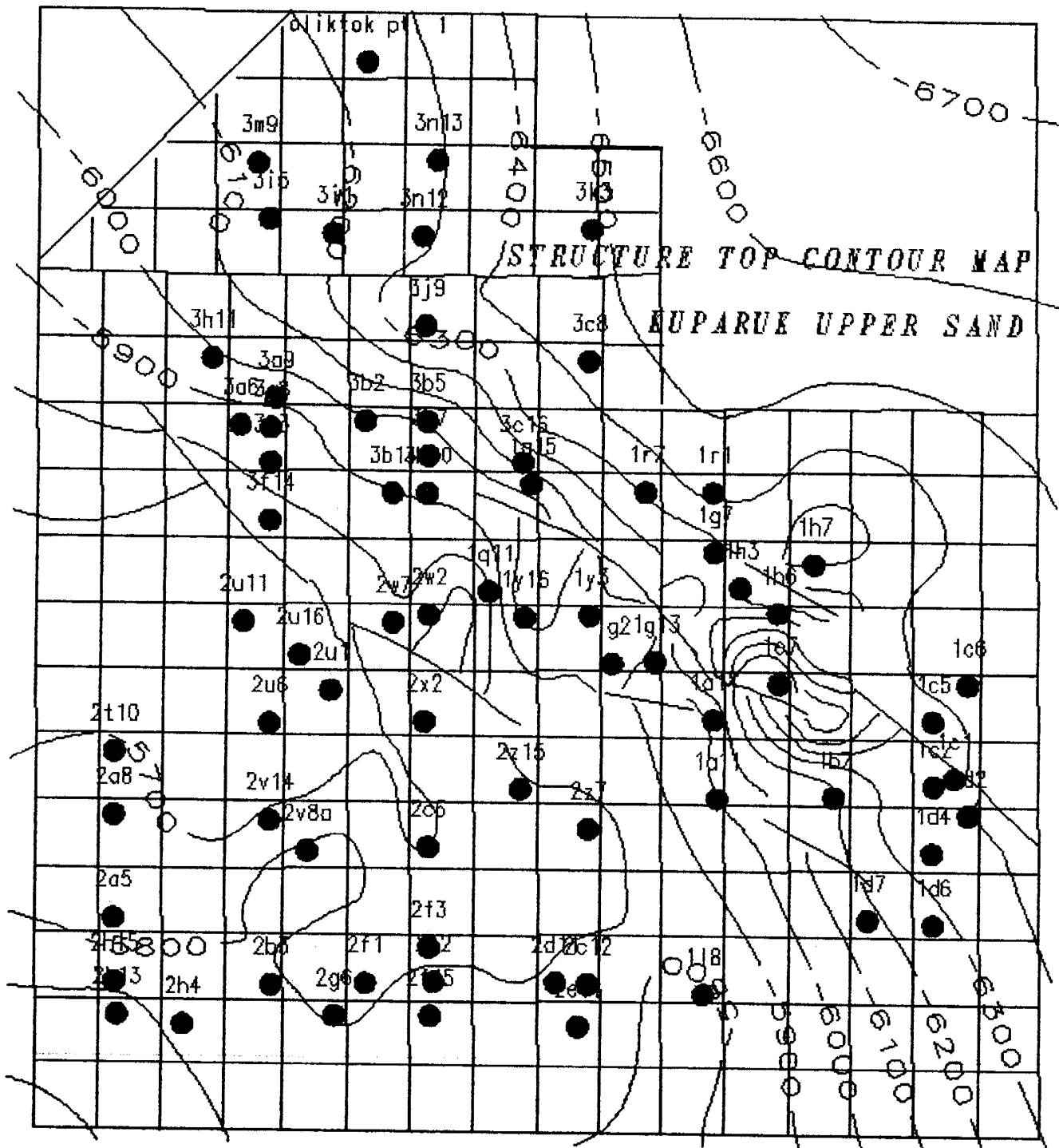


Figure VII-15. Structure Contour Map Showing Top of Kuparuk River Formation Upper Sand.

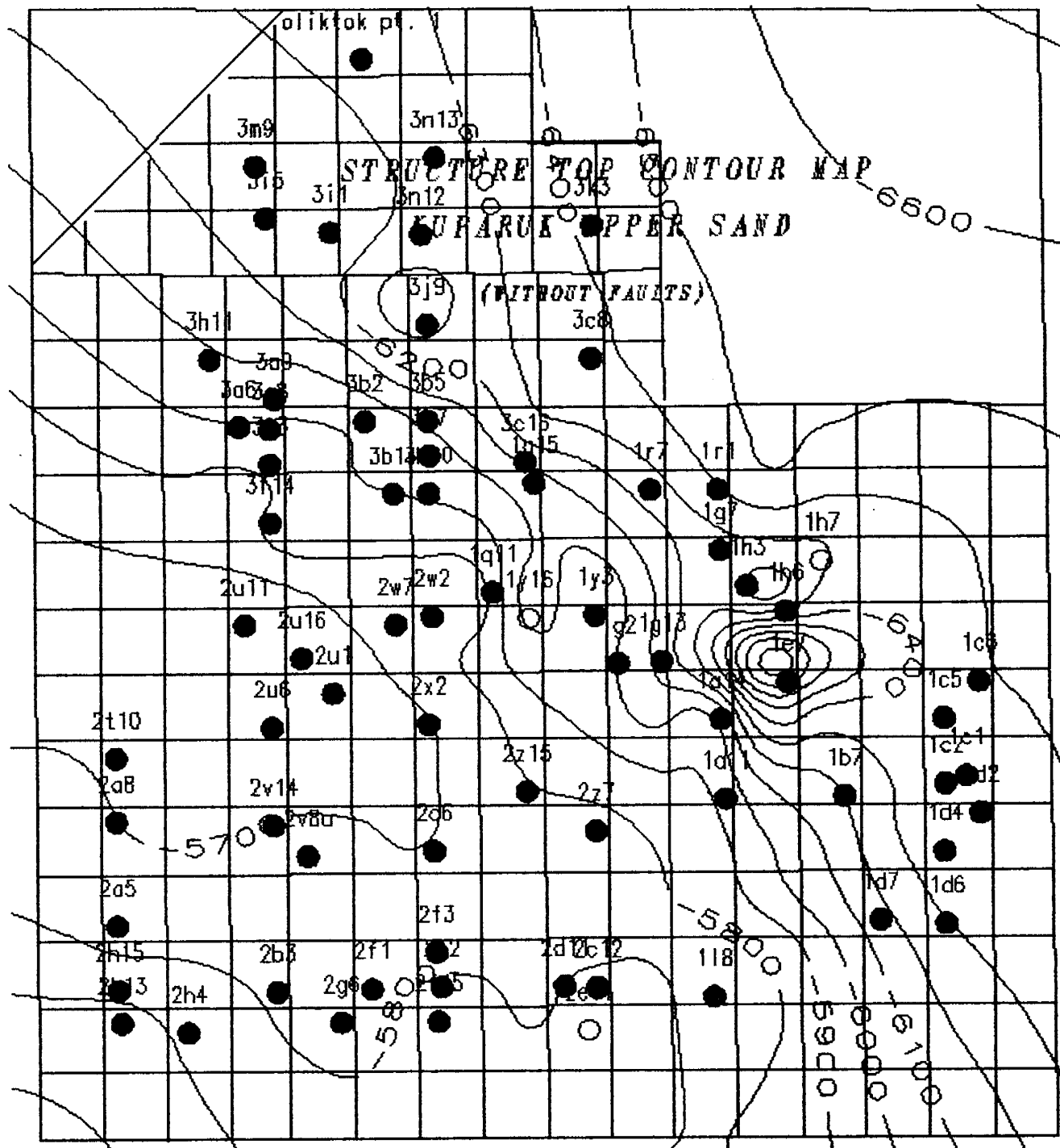


Figure VII-16. Structure Contour Map Showing Top of Kuparuk River Formation Upper Sand (without faults).

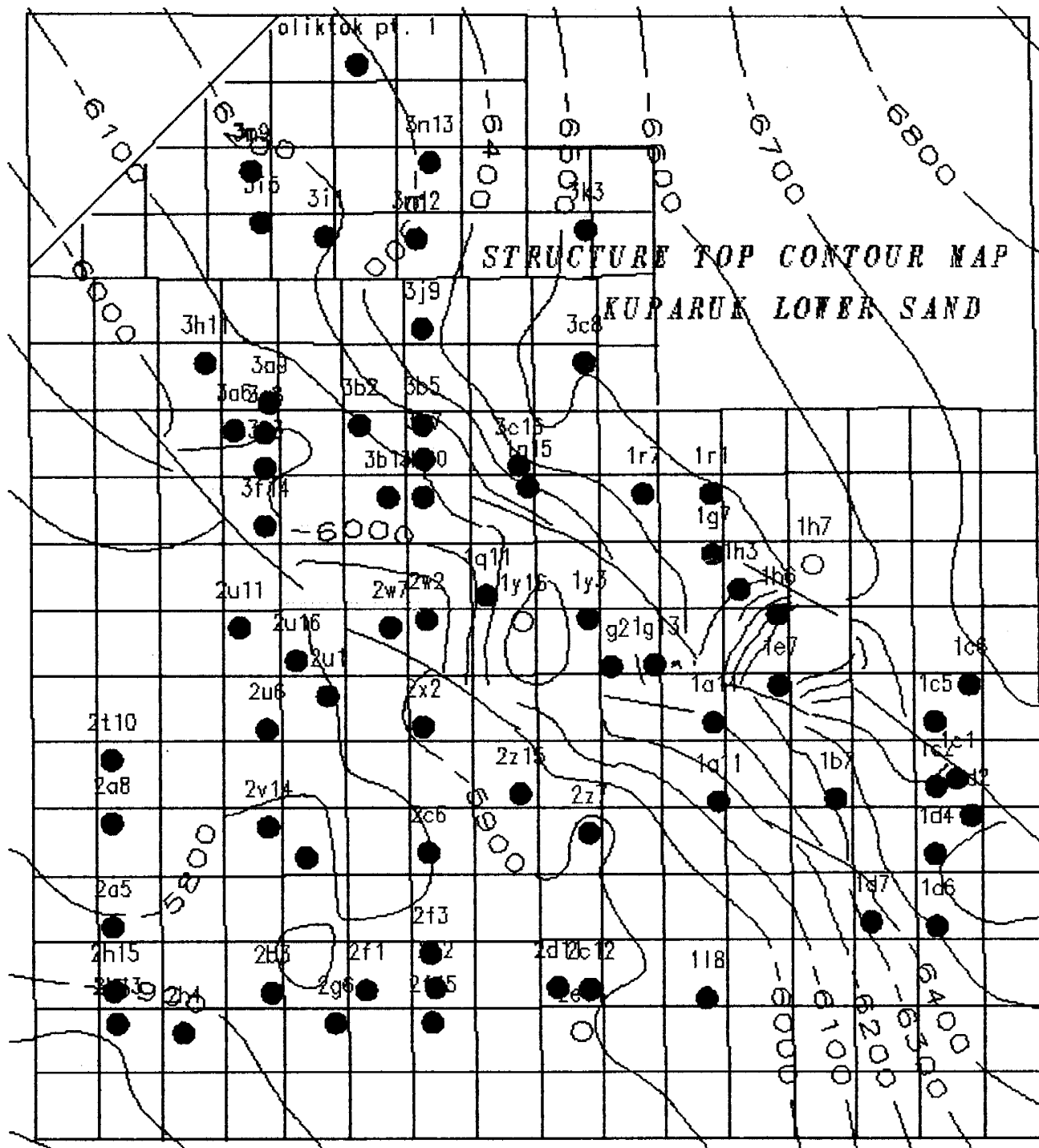


Figure VII-17. Structure Contour Map Showing Top of Kuparuk River Formation Lower Sand.



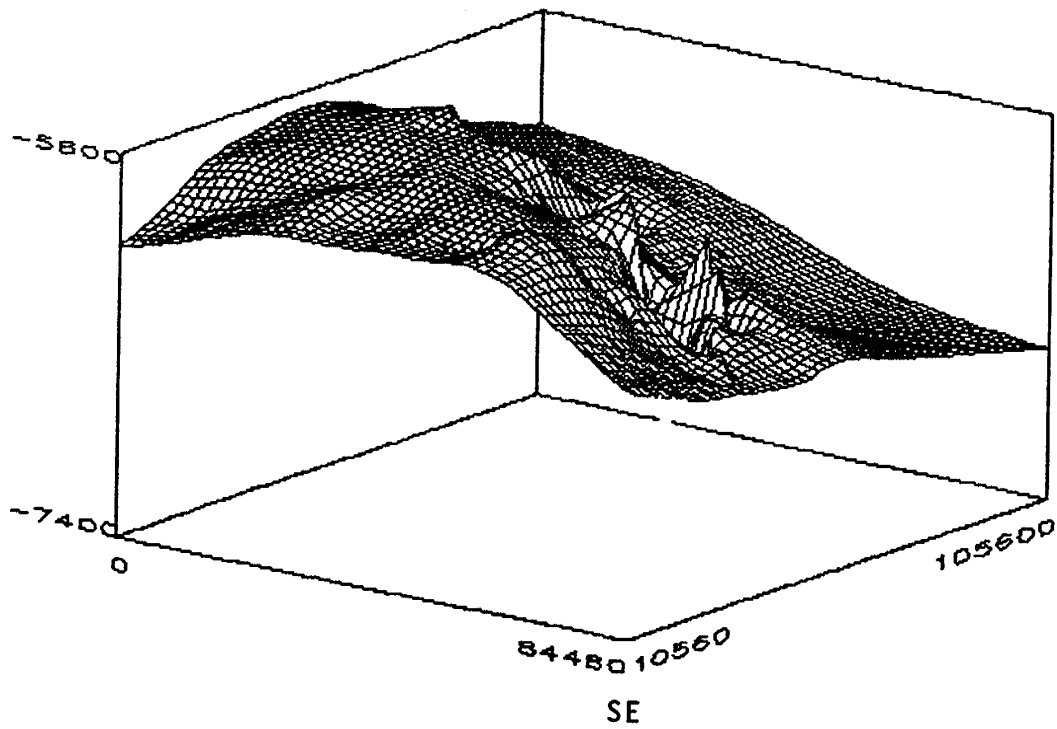


Figure VII-19. 3-D Structural View on Top of Kuparuk River Formation Upper Sand.

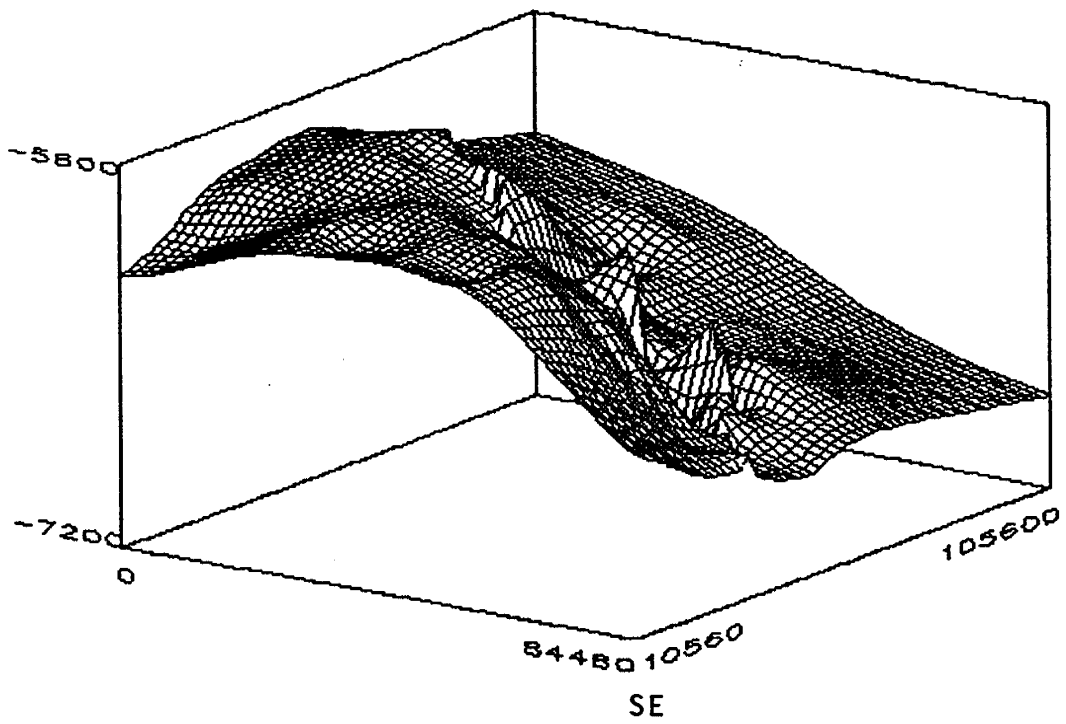


Figure VII-20. 3-D Structural View on Top of Kuparuk River Formation Lower Sand.

## C2. Cross Sections

Cross section A-A', comprised of 7 wells, was created from the southern end to the northern end of the field (Figure VII-6). As seen in this cross section, both upper and lower sands exhibit structural crest in the middle of the field (wells 2c6, 2x2) with steepest dip on the northern side. From both north-south and east-west cross sections, it can be seen that the thickness of lower sand between the wells is more or less consistent across the field, but the upper sand thickness varies from well-to-well. Major northwest striking faults were incorporated in the cross sections where they were encountered.

## C3. Porosity Determination

The porosities were calculated from neutron and density porosity logs using the cross-plot method. Some controversy exists regarding the use of neutron logs in porosity determination, because in some cases the density porosity alone correlates well with core data (Van Poolen et al., 1978). Due to this controversy, porosities were recalculated for some of the wells using only density logs. Comparisons between the two porosities are shown in Table VII-7.

In order to evaluate the distribution pattern of porosity across the field, porosity maps and 3-D views were generated (Figures VII-21 through VII-26) for both upper and lower sands. From these maps it was hard to establish any typical pattern of porosity distribution, except that the eastern side of the field has good porosity, with values ranging from 18 to 24 percent. In other parts of the field, the porosity is more or less randomly distributed.

**Table VII-7: Comparison of Porosities from Neutron and Density Tools in Kugaruk River Formation.**

Well Name	Upper Sand		Lower Sand	
	Neutron-Density	Density	Neutron-Density	Density
1A11	18.77	12.48	23.10	18.06
1G13	15.09	19.09	17.72	18.83
1G7	19.58	16.61	22.66	17.86
2C6	16.21	11.88	20.07	18.13
2d12	18.35	19.82	22.17	21.65
2U11	17.71	18.99	21.85	18.55
2Z15	19.75	17.65	19.15	19.44
3B7	10.96	11.03	20.06	21.32
3N13	15.04	10.92	20.23	18.63
average	*	*	*	*



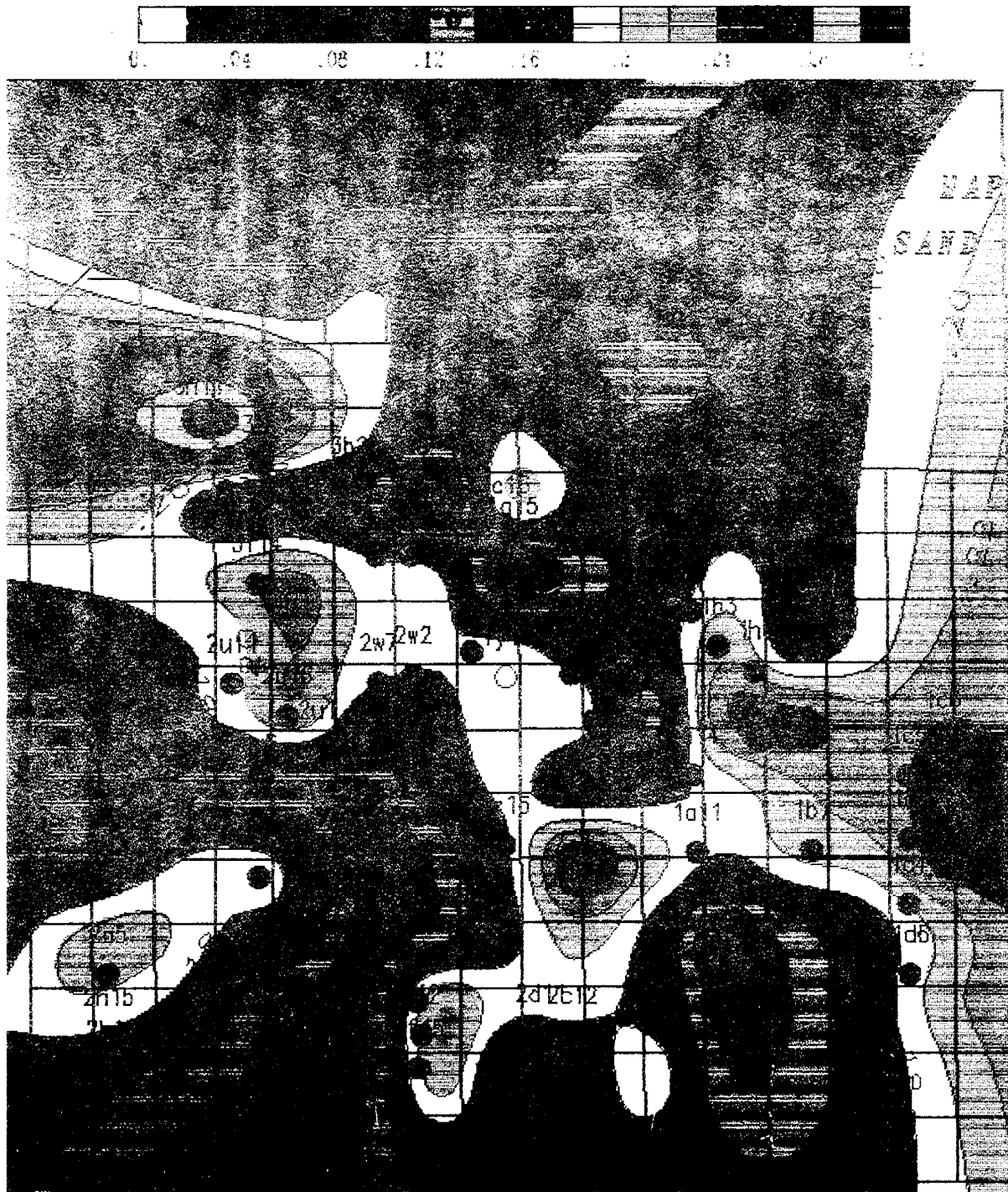


Figure VII-22. Net Pay Porosity Distribution (shown in color) in Kuparuk River Formation Upper Sand.

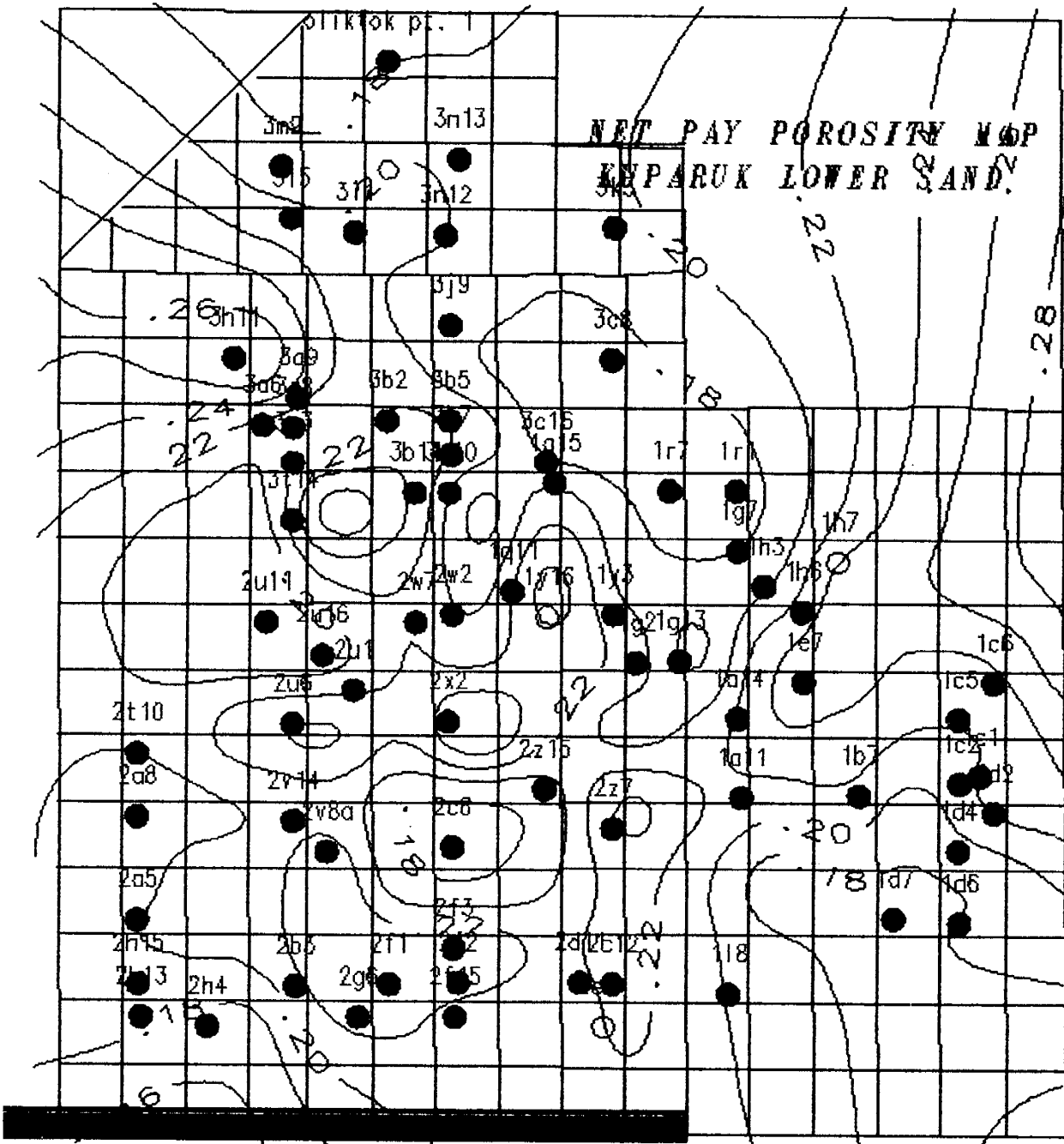


Figure VII-23. Net Pay Porosity Distribution in Kuparuk River Formation Lower Sand.

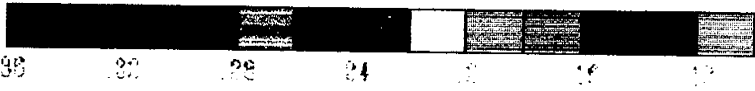
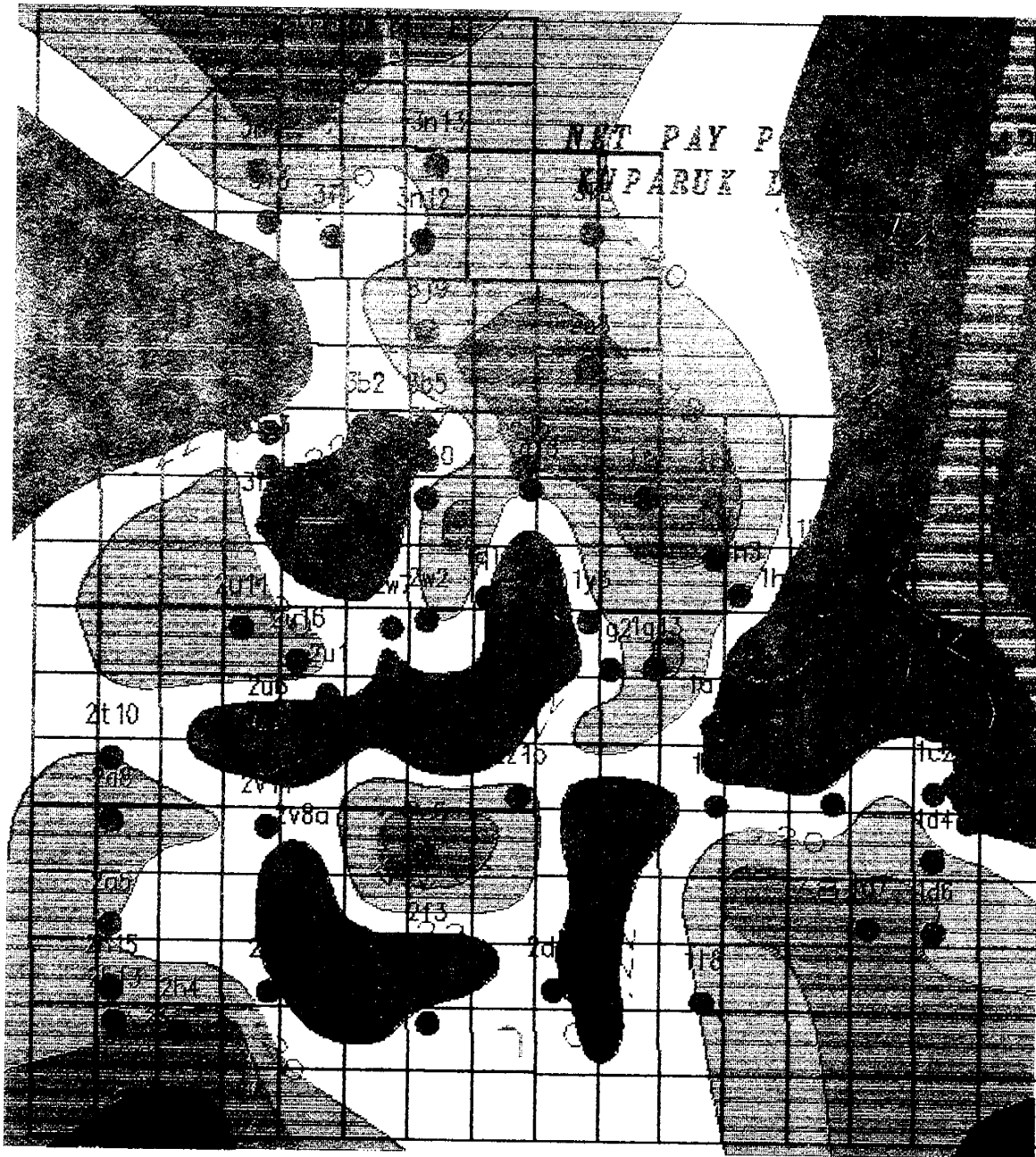


Figure VII-24. Net Pay Porosity Distribution (shown in color) in Kuperuk River Formation Lower Sand.

*3-D VIEW*  
*UPPER SAND NET PAY POROSITY*

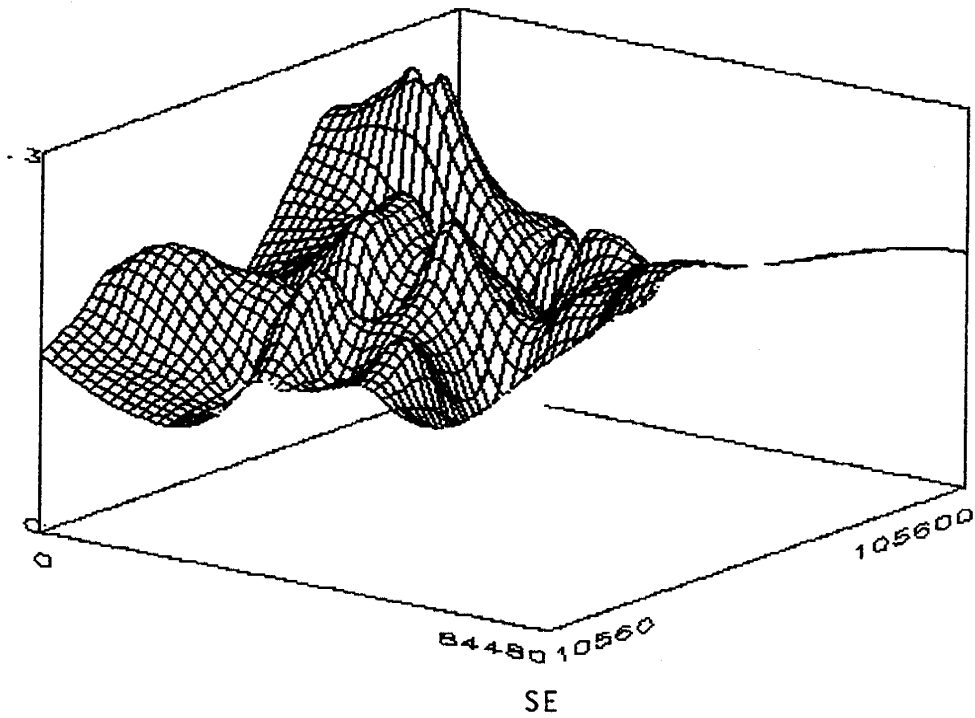


Figure VII-25. 3-D View of Kuparuk River Formation Upper Sand Net Pay Porosity.

*3-D VIEW*  
*NET PAY POROSITY MAP*  
*KUPARUK LOWER SAND*

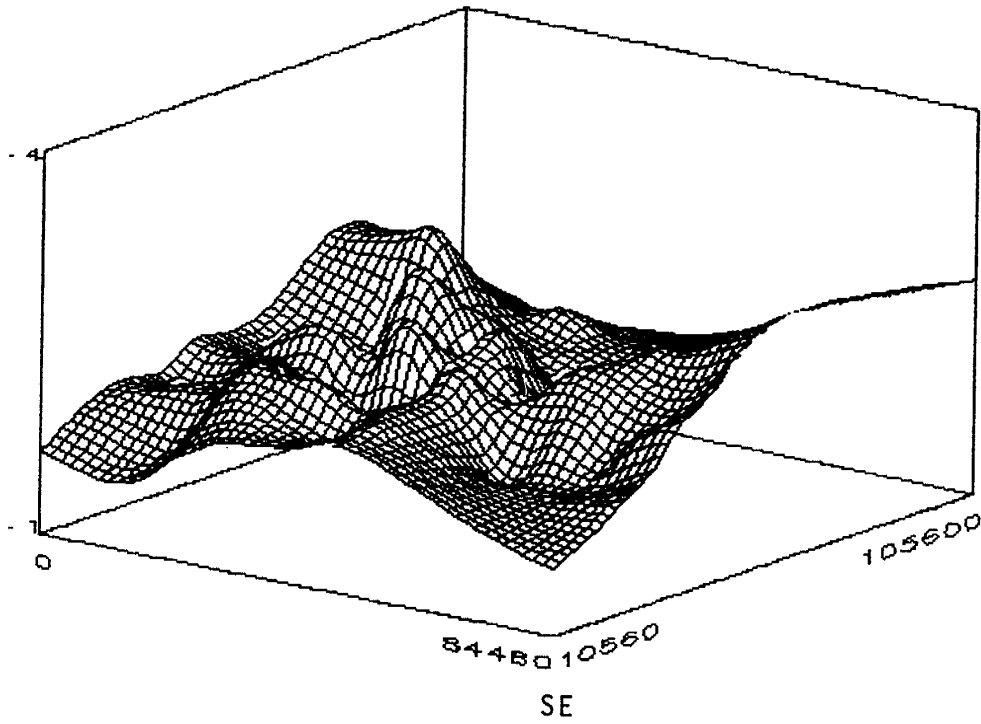


Figure VII-26. 3-D View of Kuparuk River Formation Lower Sand Net Pay Porosity.

The average porosity for each zone in each well was calculated in WorkBench using the summation module. Any intervals with porosity less than 6% were ignored and treated as non-pay.

#### **C4. Water Saturation Determination**

Eight different water saturation equations are available in WorkBench. Due to unavailability of water saturation data from core analysis, sensitivity studies could not be carried out to determine which equation yields most reasonable results for calculated value of water saturation. However, as per Schlumberger's recommendation (personal communication with DeWayne Schnorr, Schlumberger, Anchorage), the Indonesian equation was used in this study to calculate water saturation. After calculating water saturation with Indonesian equation, it was validated by comparison with three other equations (Archie, Laminar-Simondoux and Dual water), and comparisons are shown in analysis result plots (Figures VII-27 and VII-28).

Again, due to lack of core data, the cementation exponent  $m$  and saturation exponent  $n$  could not be tuned and typical values of 2 for both  $m$  and  $n$  were used in this study. Also, a typical value of 1 was used for tortuosity exponent  $a$ . The formation water resistivity used was 0.17 ohm-m. The deep resistivity was environmentally corrected to yield the true resistivity ( $R_t$ ).  $R_t$  was then used to calculate water saturation.

For the purpose of this study, the cementation exponent, saturation exponent, tortuosity exponent and water resistivity at reservoir temperature were considered to be constant for all the analyzed wells.

The arithmetic average water saturation was determined for upper and lower sands using summation method, whereby non-pay saturation-feet values were excluded in the summation of saturation times vertical feet. Any water saturation greater than the cutoff value was treated as non-pay. After deduction for the non-pay, the resultant net summation of saturation-feet was divided by the net vertical thickness to obtain the average water saturation. Tables 1 through 6 include the water saturation values of each well analyzed and for each cutoff value.

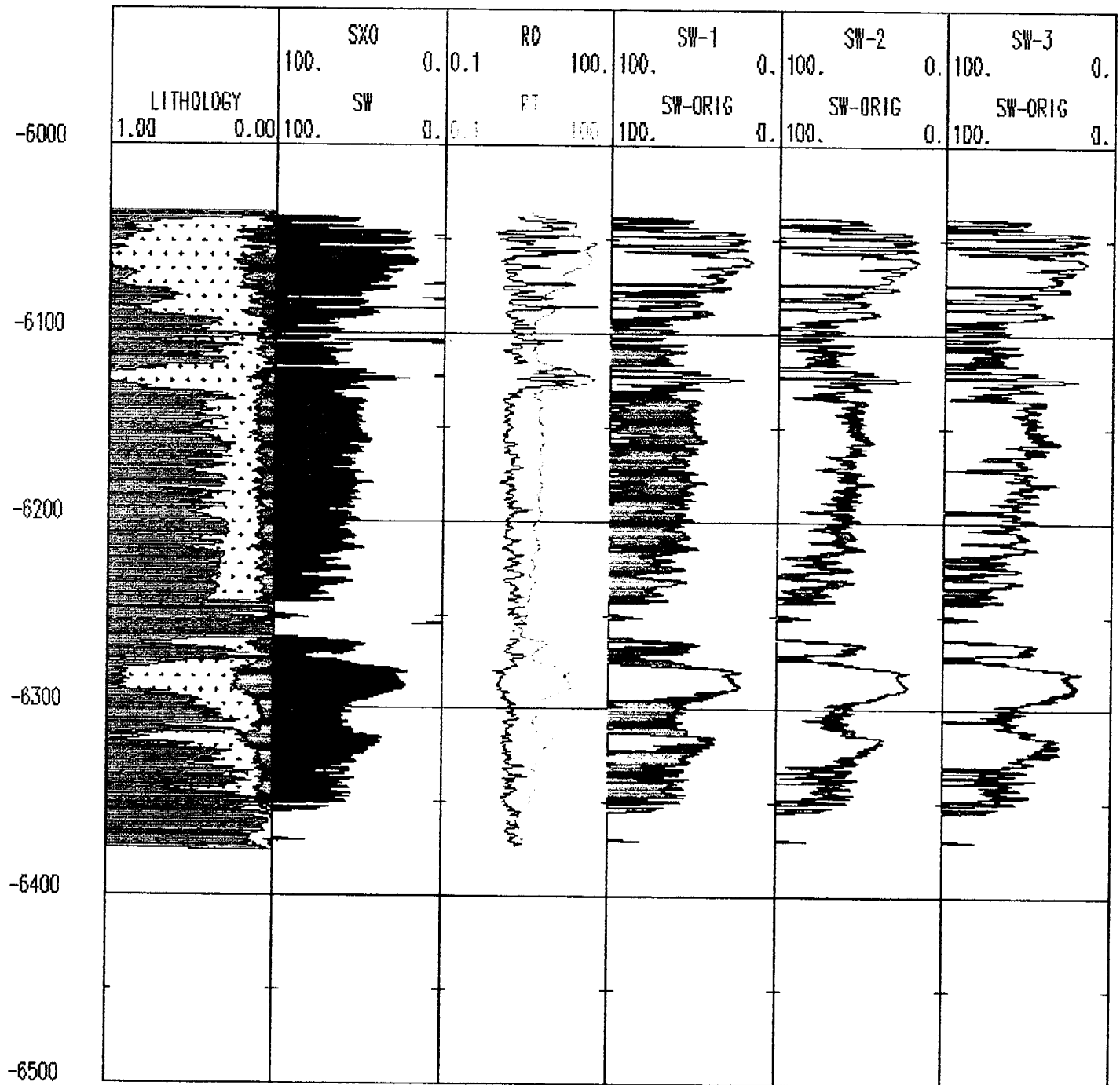


Figure VII-27. Plots of Sw from Well Log Analysis Using Three Models (Sw1: Archie, Sw2: Laminar Simondoux, Sw3: Dual Water), Applied to Kuparuk Field Well 1g13.

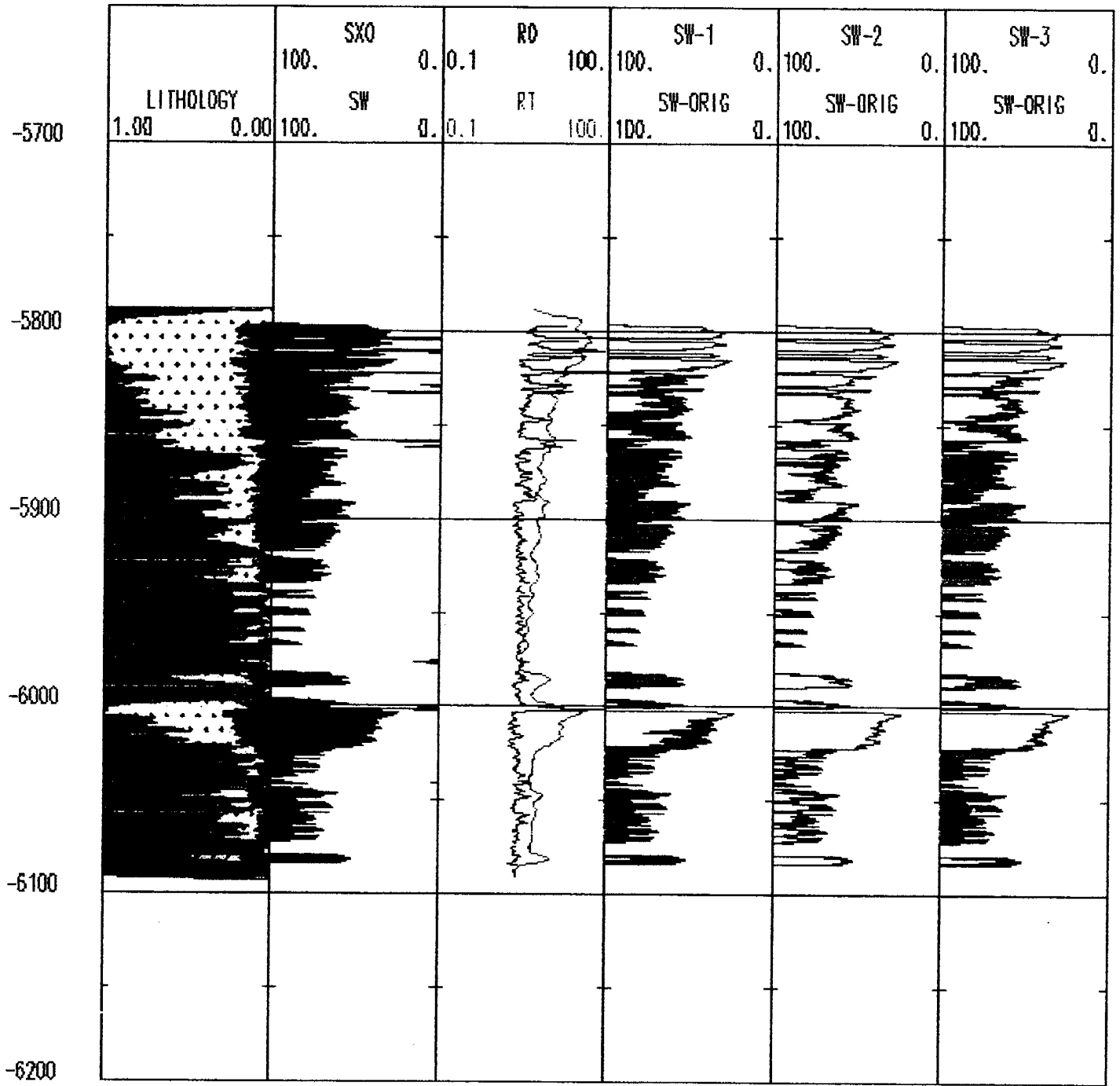


Figure VII-28. Plots of Sw from Well Log Analysis Using Three Models (Sw1: Archie, Sw2: Laminar Simondoux, Sw3: Dual Water) Applied to Kuparuk Field Well 2z15.

Net pay water saturation contour maps were generated for both upper and lower sand using 80% water saturation cutoff value (Figures VII-29 and VII-30). For better visual illustrations, color filled contour maps with water saturation were also generated. From these maps as shown in Figures VII-31 and VII-32, the water saturation distribution across the field for both the sands can easily be traced. For the upper sand, the average saturation varies from 20 to 80 percent. Most of the north, the center and the southeast side of the upper sand have saturations ranging from 40 to 50 percent. However, portions of the northeast exhibit more favorable saturations, ranging from 20 to 30 percent. The southwest part of the upper sand, in the vicinity of 2h13, 2h4, 2b3, 2g6 and 2f15 wells, yields field-wide water saturation maximums of 60 to 80 percent. The higher water saturations at the southwest corner of the upper sand might be due to a nearby aquifer, which in the future may affect the production performance of southerly located wells by means of water coning or early water breakthrough.

In the case of lower sand, the water saturation varies from 30 to 50 percent. The northern half of the field has 30 to 40 percent saturation values, whereas the southern half maintains a consistent distribution of 50 percent water saturation with some scattered 40 percent water saturation values.

In general, it may be concluded from the water saturation distribution pattern that in terms of hydrocarbon volume, the Kuparuk River lower sand has more favorable characteristics than the upper sand.

## **C5. Sand Quality**

In order to evaluate sand quality, the net hydrocarbon feet,  $\emptyset h (1-S_w)$ , was calculated and included in Tables 1 through 6 for each analyzed well. The parameter 'h' is the net pay thickness, which was determined by subtracting non-pay intervals from gross thickness according to respective cutoff values. For better visual illustration, contour maps and 3D maps were also created with hydrocarbon feet values. These maps are shown in Figures VII-33 through VII-36.

The reservoir parameter distribution maps indicate that the productive horizons in the upper sand occur in the southeast, and in the lower sand in the northwest of the Kuparuk River field. Highest values of hydrocarbon-feet were yielded by the Kuparuk River lower sand. On an individual well-by-well basis, the maximum lower sand value of 14.441 hydrocarbon feet (at well 2h15) represents a 39% improvement over the maximum upper sand value of 10.402 hydrocarbon-feet (at well 2h15).

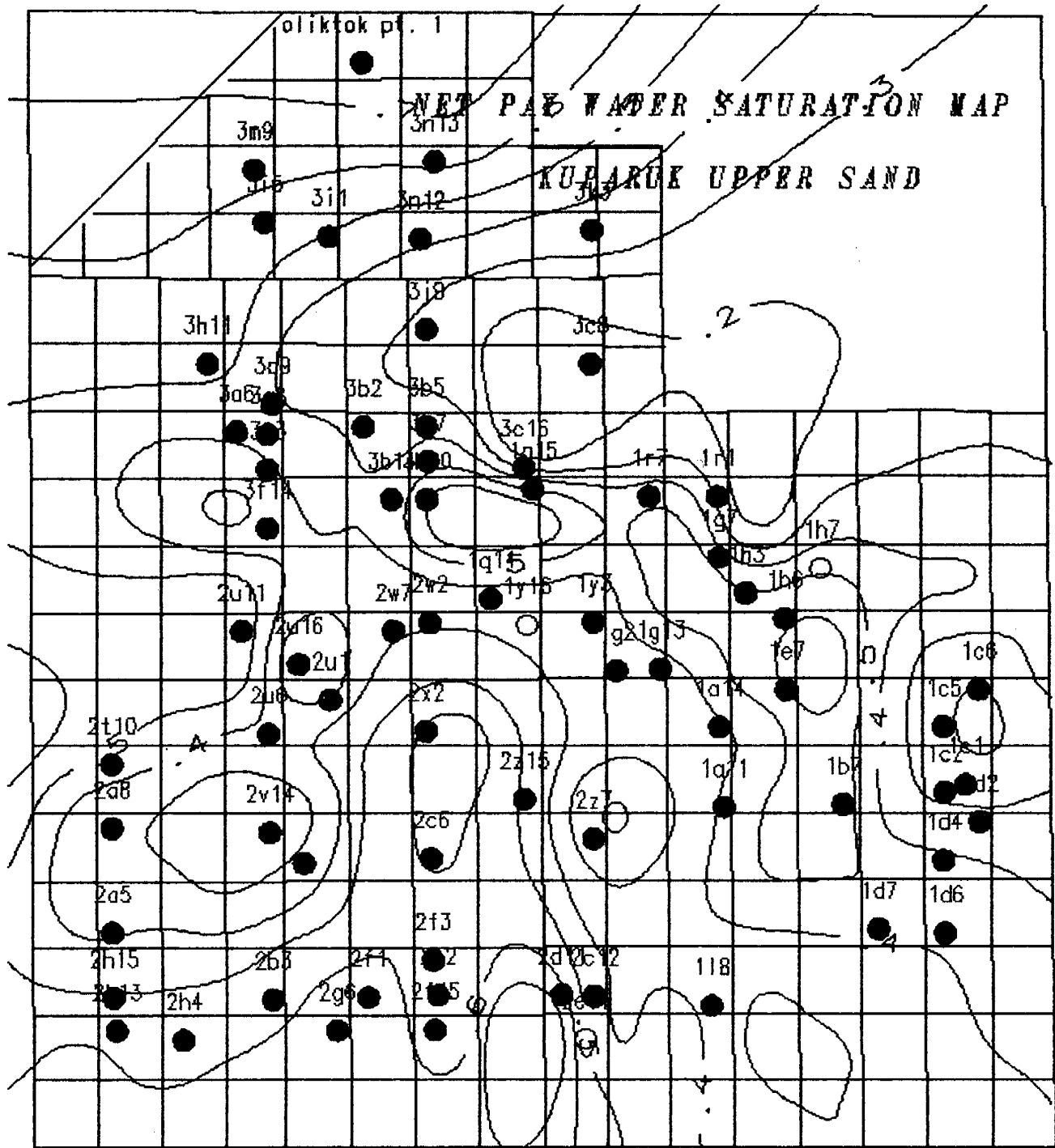


Figure VII-29. Net Pay Water Saturation Distribution in Kuparuk River Field Upper Sand.

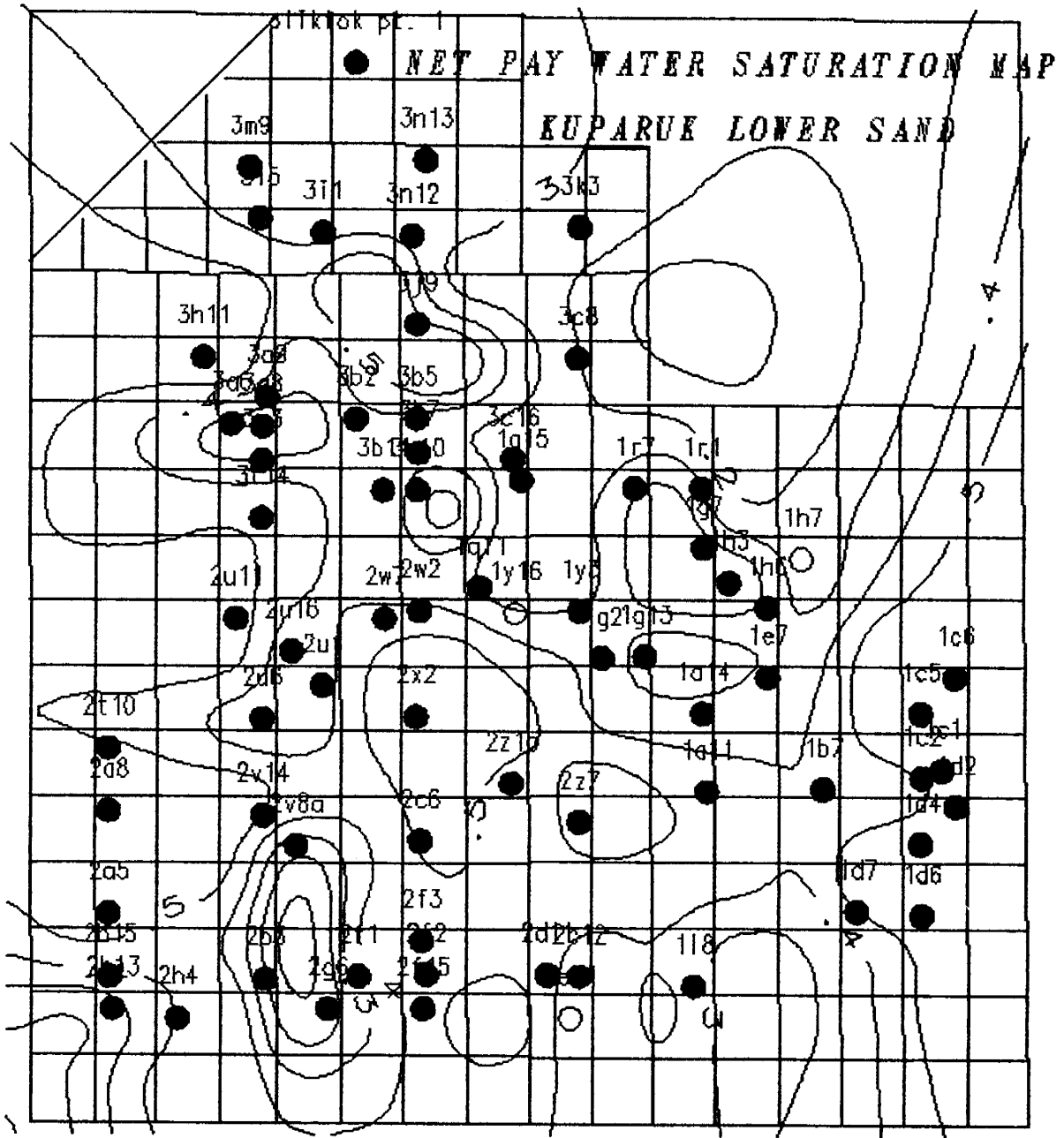


Figure VII-30. Net Pay Water Saturation Distribution in Kuparuk River Field Lower Sand.

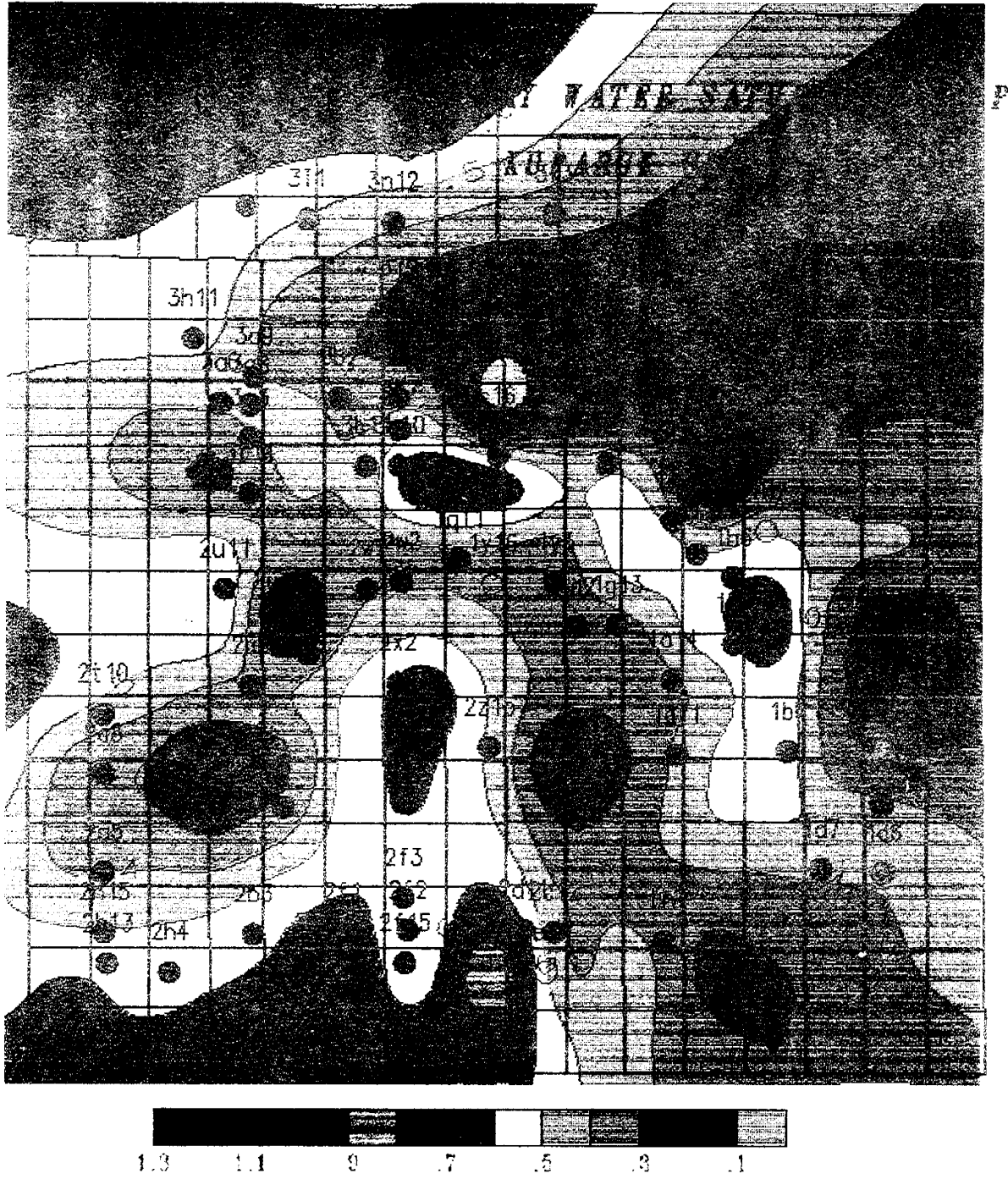
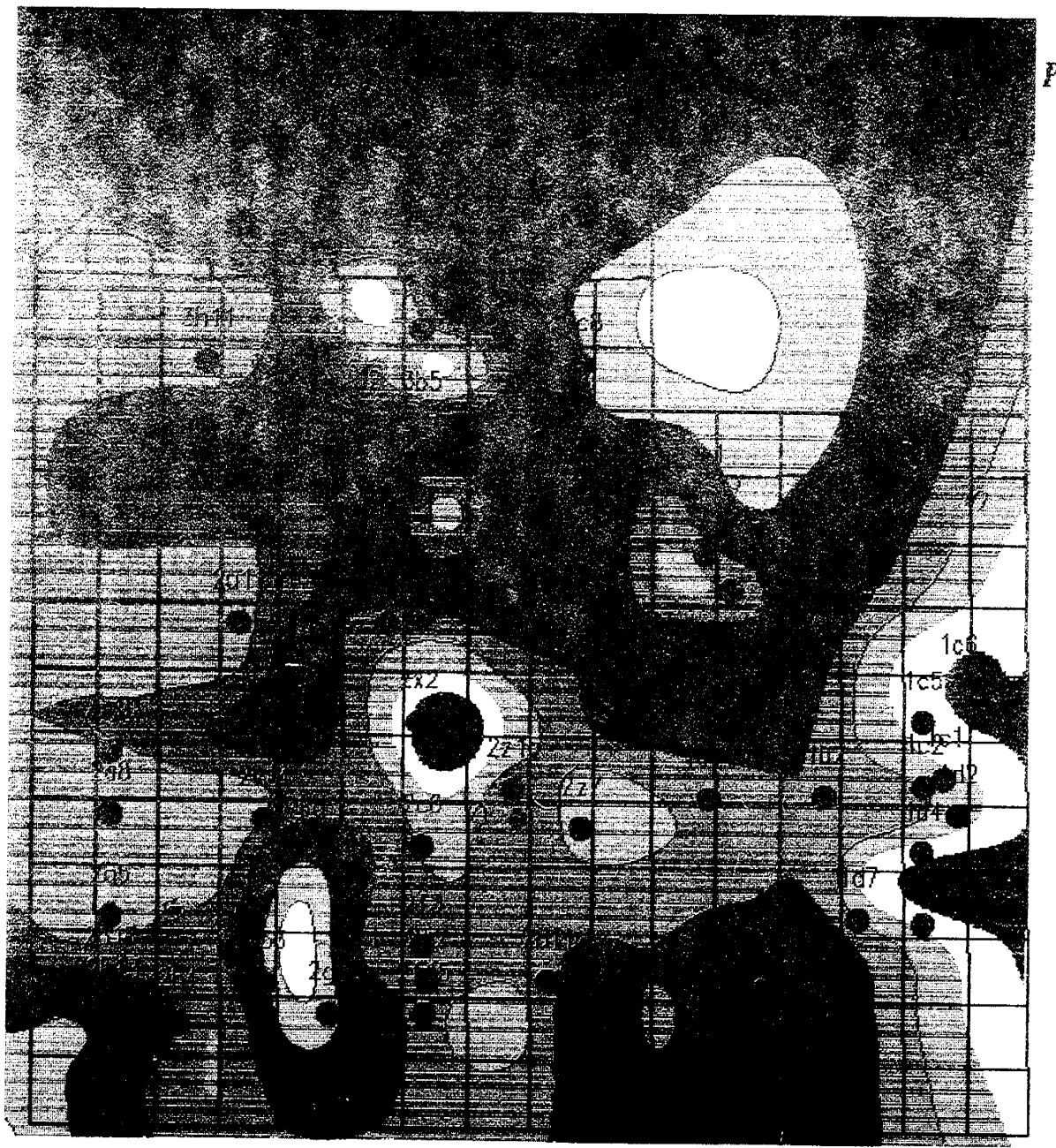


Figure VII-31. Net Pay Water Saturation Distribution (shown in color) in Kuparuk River Formation Upper Sand.



P



Figure VII-32. Net Pay Water Saturation Distribution (shown in color) in Kuparuk River Formation Lower Sand.

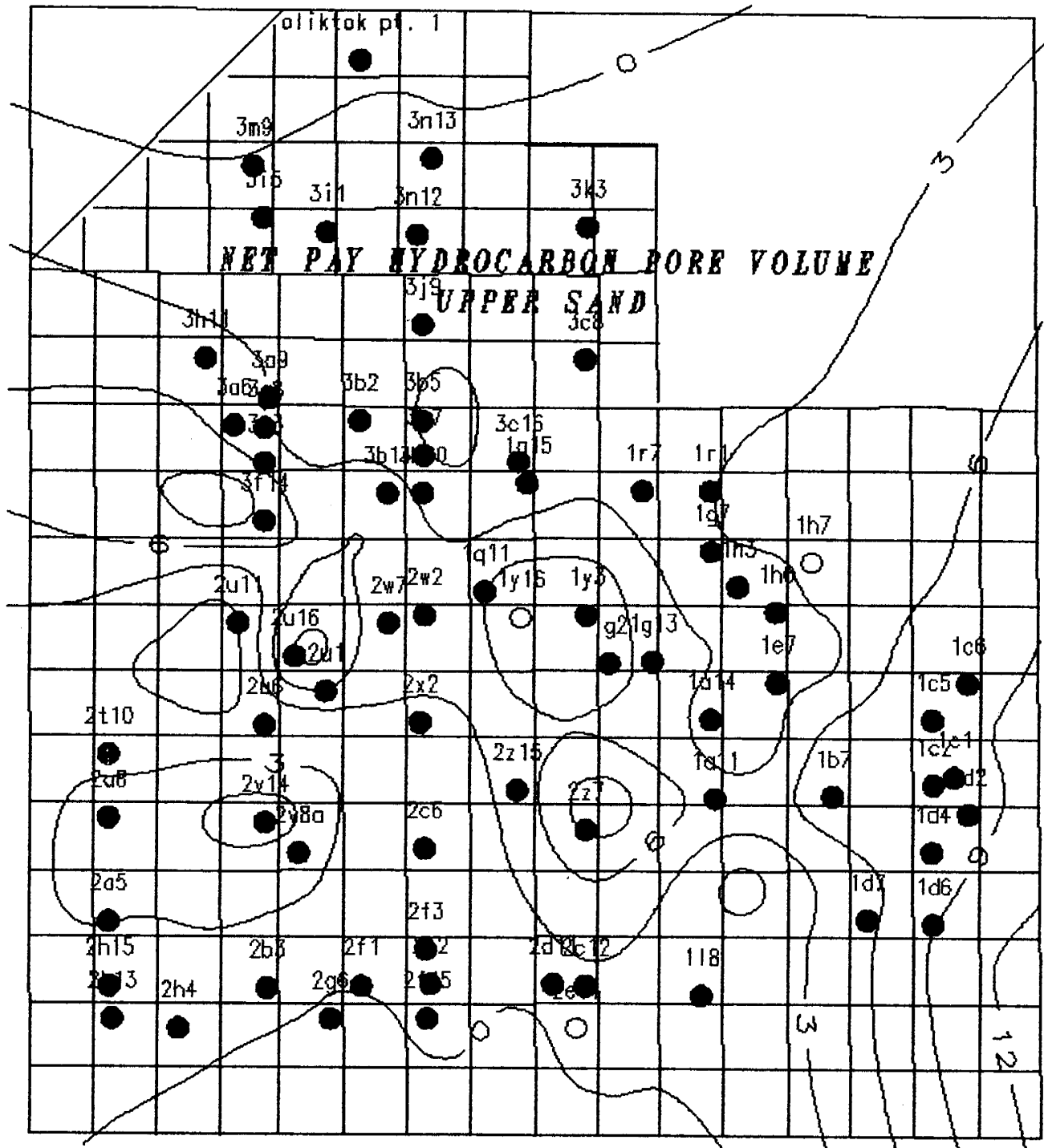


Figure VII-33. Net Pay Hydrocarbon Pore Volume Distribution in Kuparuk River Upper Sand.

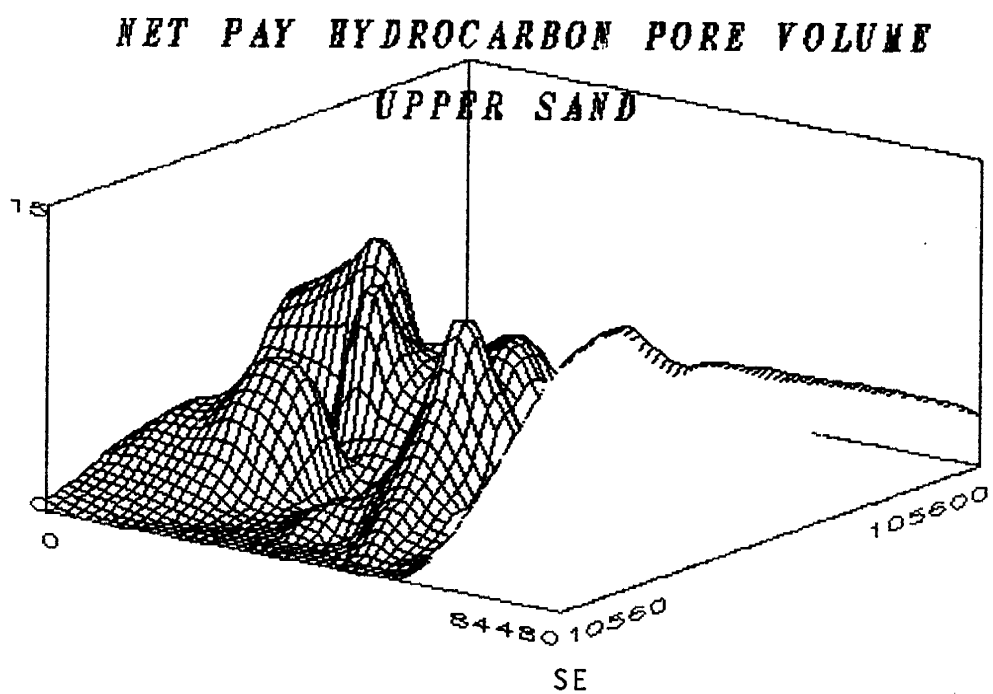


Figure VII-34. 3-D View of Kuparuk River Formation Net Pay Hydrocarbon Pore Volume.

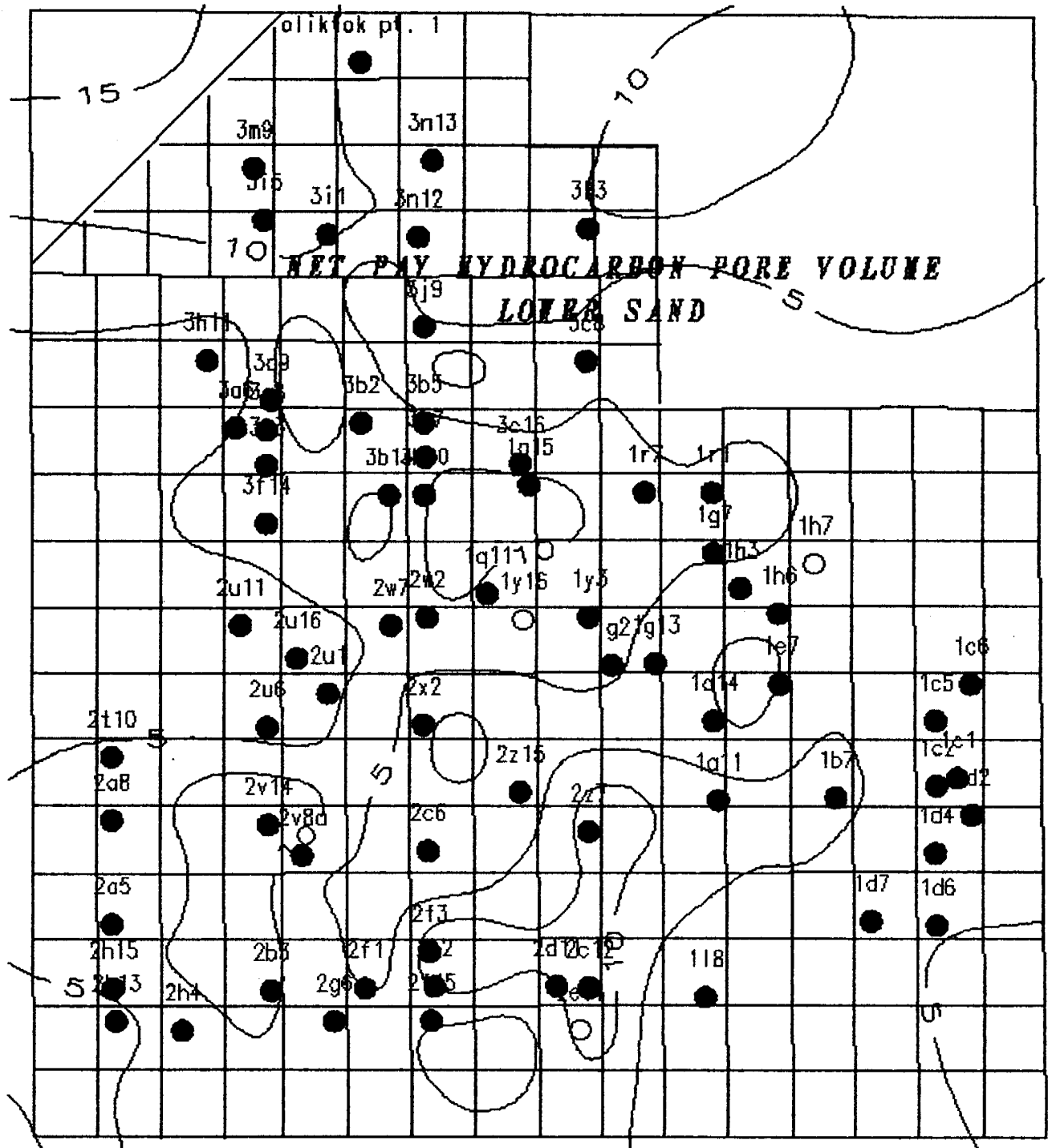


Figure VII-35. Net Pay Hydrocarbon Pore Volume Distribution in Kuparuk River Lower Sand.

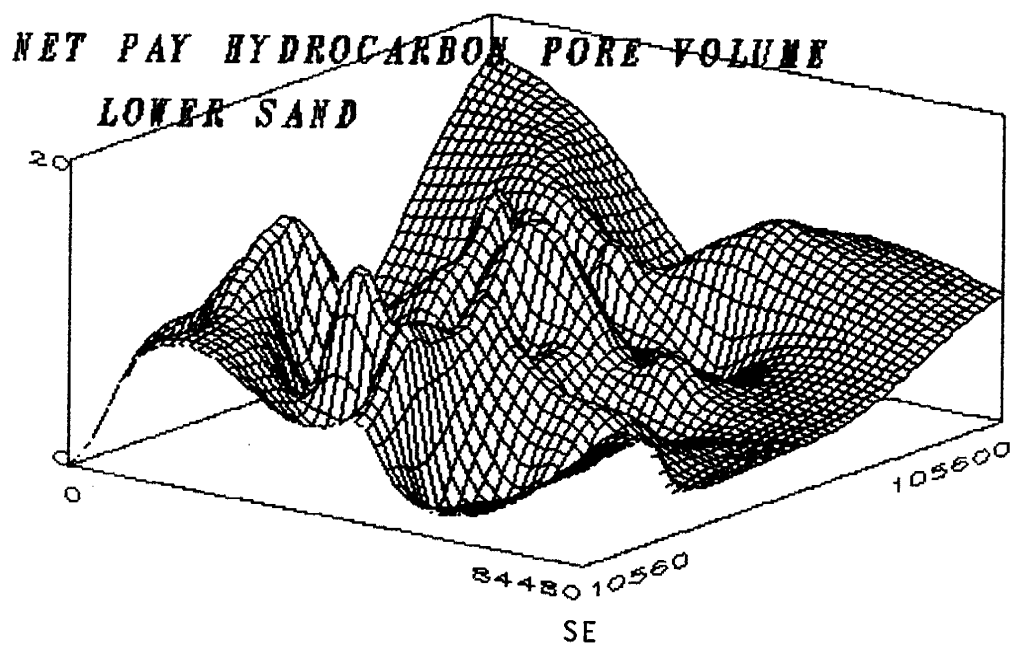


Figure VII-36. 3-D View of Kuparuk River Formation Lower Sand Net Pay Hydrocarbon Pore Volume.

## **CHAPTER VII, PART II: SUMMARY OF THE DEPOSITIONAL ENVIRONMENT AND RESERVOIR QUALITY OF THE KUPARUK RIVER FORMATION SANDS**

---

### **A. INTRODUCTION**

This discussion of the Kuparuk sands is taken from Gaynor and Scheihing (1989), and Masterson and Paris (1987). The Lower Cretaceous Kuparuk River formation is characterized by two distinct cyclic sequences that are separated by the regional Lower Cretaceous Unconformity (LCU). Reservoir quality and heterogeneity of the lower sequence, labeled the lower sand, were controlled by depositional processes. In contrast, reservoir quality of the upper sand sequence was controlled by post-depositional, diagenetic features, primarily siderite cementation and dissolution. Both sands, being shelf sandstones, show that shelf environments can be just as prolific oil producers as their continental, strand line, or deep water counterparts.

### **B. LOWER SAND STRATIGRAPHY AND DEPOSITION**

The lower sand downlaps onto the underlying Miluveal shale. Based on core analysis, the stratigraphic contact is probably paraconformable (Gaynor and Scheihing, 1989). The Miluveal shale was deposited in deep water as part of a broad, regional muddy shelf that dipped southward. It is characterized by a lack of wave generated sedimentary structures and sparse trace fossil assemblages. This and other evidence indicates that the shale was deposited from suspension.

Cyclical upward coarsening, clastic sequences characterize the bottom portion of the lower sand (Figure VII-37). These sequences begin as lenticular-bedded silty mudstones and grade into flaser-bedded and hummocky, cross-stratified, very fine-grained sandstones. The lenticular, silty mudstones are believed to be a result of deposition from suspension by marine currents. The absence of reworking in these beds indicates their deposition occurred below storm-wave base. Subsequent lower sand deposition was storm related to and occurred in a shallow marine shelf environment. Palynology indicates deposition was close to a strand line or delta front, as only terrestrial spores and pollen have been found in core samples (Masterson and Paris, 1987).

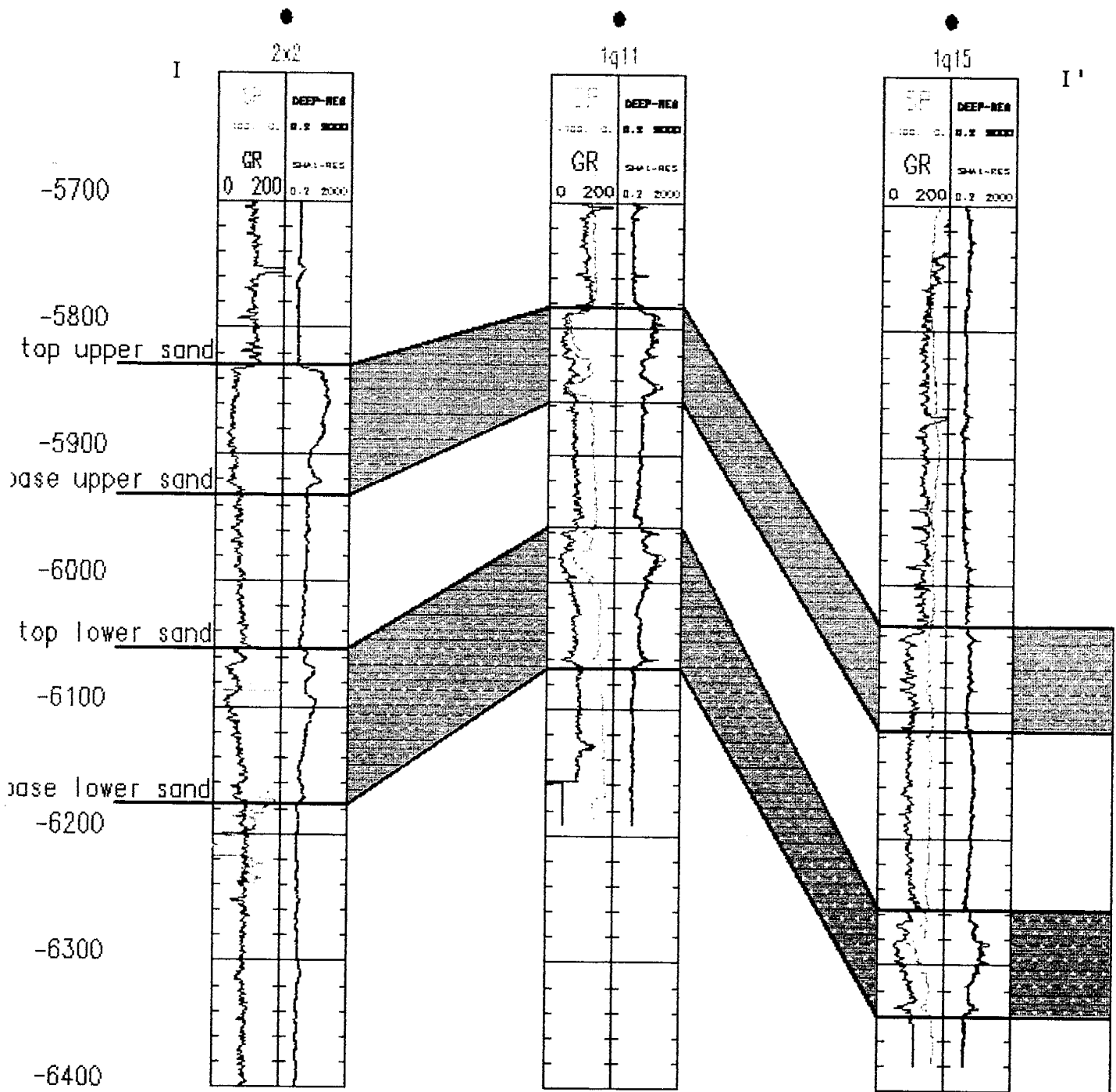


Figure VII-37. Cross Section I-I' Showing Coarsening Upward in the Lower Sand of Kugaruk River Formation in Kugaruk River Field.

The overlying hummocky beds are ripple and parallel laminated, and were probably deposited above storm-wave base, also out of suspension. They were molded by oscillatory wave motion on the shelf bottom. Above these beds, and completing the cycle, are massive, sheet-like sandstones. They are interpreted as being dumped onto the shelf bottom out of storm generated, high-energy transport. The rate of deposition was too high to allow reworking of these sands into hummocks.

Northwest-to-southeast moving storm-generated currents carried the sands alongshore to obliquely offshore. Sedimentation occurred from storm currents as they encountered shelf widening or deepening. Over geologic time, sea level regression increased landward erosion. Subsequent sand/silt deposition from storm currents into deeper, seaward water on the southeast side of the shelf became more frequent. The result is a series of sand sheets that converge landward (northwestward) and diverge seaward (southeastward). The size and geometry of these sand sheets are functions of storm intensity. The northeast trend of the sheets was controlled by shelf topography and direction of storm currents.

The LCU is believed to truncate the upper portion of the lower sand, based on correlation sections traced across the field using wireline logs. Over 300 feet of relief is present on this unconformity at Kuparuk River field, based on analysis of well log data (Gaynor and Scheihing, 1989). Textural evidence indicates that the lower sand may have been partially lithified prior to deposition of the upper sand. For example, lower sand trace fossil morphologies are subvertical in profile and demonstrate a cross-cutting relationship to the lower sand. Borings in the lower sand are filled with glauconitic sandstone from directly above the LCU contact. In addition to large amounts of erosion, the presence of borings indicates that this unconformity occurred during a major sea level fall. Because of the lack of evidence for subaerial exposure, such as soil or root mottles, erosion is believed to have been primarily submarine in nature.

The interval separating the lower and upper sands not only shows the effects of the LCU, but also shows major changes in depositional environments throughout the region during Upper Jurassic and Lower Cretaceous time. The depocenter responsible for prior sand deposition shifted northeast, thus allowing only for distal storm deposits to accumulate. Subsequently, the nearby tectonic activity initiated deposition of coarse, glauconitic sands, and eventually led to the depositional environment responsible for upper sand development.

Vail and others (1984) propose that, tectonically, the movement of lower sands onto the shelf was caused by the Berriasian global sea level drop and the Valanginian lowstand.

Also, the cyclic presence of mudstones in the lower sand is due either to cyclical decreases in storm intensity and frequency, sea level rises, or shifting source rock locations. However, each succeeding resumption in sand deposition was located seaward (southeast) of the previous zone of deposition. This overall depositional environment resulted in a regressive shelf record and coarsening upward lower sand cycles.

### **C. UPPER SAND STRATIGRAPHY AND DEPOSITION**

Overall, the upper sand is a bioturbated, glauconitic combination of sandstones and siltstones that unconformably overlie the lower sand unit. The bottom-most portion of the basal zone consists of medium-to-coarse grained sandstones. Primary sedimentary structures within the zone have been obliterated by burrowing. The zone also contains wood fragments. Bottom-most pebble lags of eroded sedimentary rocks and a lack of fine silts are a result of higher energy winnowing and reworking. The presence of glauconite indicates deposition occurred in a marine, probably shelf, setting.

The basal layer grades into finer-grained massive, bioturbated sands. These, in turn, grade upward into muddy siltstones and clays, and represent deposition in increasingly deeper waters. They also reflect a period of maximum sediment starvation in association with the deeper water environment. Subsequent shallowing is indicated by coarsening upward textures of sands overlying the clays. These sands are bioturbated and contain wood fragments, and the presence of glauconite is believed to indicate a relatively slow rate of sediment input.

An unconformity associated with falling sea level truncated this portion of the upper sand zone across all the Kuparuk field area. In the west-central portion of Kuparuk field, erosion, combined with non-deposition, resulted in this zone's absence. Resumption of rise in sea level, accompanied by low sediment supply, then allowed for reworking of previously deposited material to form the medium-to-very coarse-grained quartz sand and abundant glauconite deposits that lie above the unconformity. These sands comprise the uppermost portion of the Kuparuk River formation upper sand member. The presence of glauconite is again believed to indicate a lack of detritus during that time. Subsequent siderite cementation occluded much of the primary porosity. However, local dissolution yielded areas of secondary porosity and associated friable sands.

In contrast to the storm-related, pulse-like nature of deposition associated with the lower sand, tectonism and/or eustatic sea level changes are believed to have been the main cause of upper sand deposition. However, although transgression was dominant during upper sand time, minor regressions did occur. Basinward progradational thickening is evident in cross section J-J' in Figure VII-38. While depositional processes controlled reservoir quality of lower sand units, post-depositional, diagenetic factors, primarily siderite cementation and dissolution, were mostly responsible for reservoir quality in the upper sand.

#### **D. STRUCTURE OF THE KUPARUK FORMATION AT KUPARUK FIELD**

Kuparuk River field is located on an anticline that plunges 0.8 degrees to the southeast. Oil emplacement on the northeast side of the anticline is structurally controlled. However, stratigraphy controls the western and southern limits of the field. To the west, the upper sand pinches out and the lower sands are truncated by the Lower Cretaceous Unconformity. To the south, both upper and lower sands pinch out or grade into mudstones.

Faulting in Kuparuk River field is abundant and normal faulting is the only style of faulting present. Northwest striking faults were active during deposition of the upper sand. Evidence for this includes upper sand thickening along downthrown sides of these faults and lower sand thinning due to erosion (Figures VII-39 through VII-42). Seismic evidence indicates no displacement exists at the top of the Kuparuk River formation along many of these faults. From this it is concluded these faults were probably inactive by the end of upper member deposition. Northeast dipping normal faults are also present but occurred after deposition of the Kuparuk formation. They do not affect Kuparuk River formation sand thicknesses.

The abundance of faulting has likely resulted in wells cutting faults. This may be the case in well 2x2 in Figure VII-43. Comparison of the cross section in this figure with those in Figures VII-7 and VII-8 shows lower sand dip to be similar across all three cross sections (Figure VII-44 shows locations of cross sections). Also, thinning of the lower sand is apparent at this well, indicating erosion removed some of the lower sand after faulting. This fits the pattern of uplift and erosion of the lower sand in adjacent wells. However, apparent dip on the upper sand in Figure VII-43 is opposite of that in Figures VII-39 and VII-41. Also, the upper sand in well 2w2 is much thinner than in any of the adjacent wells.

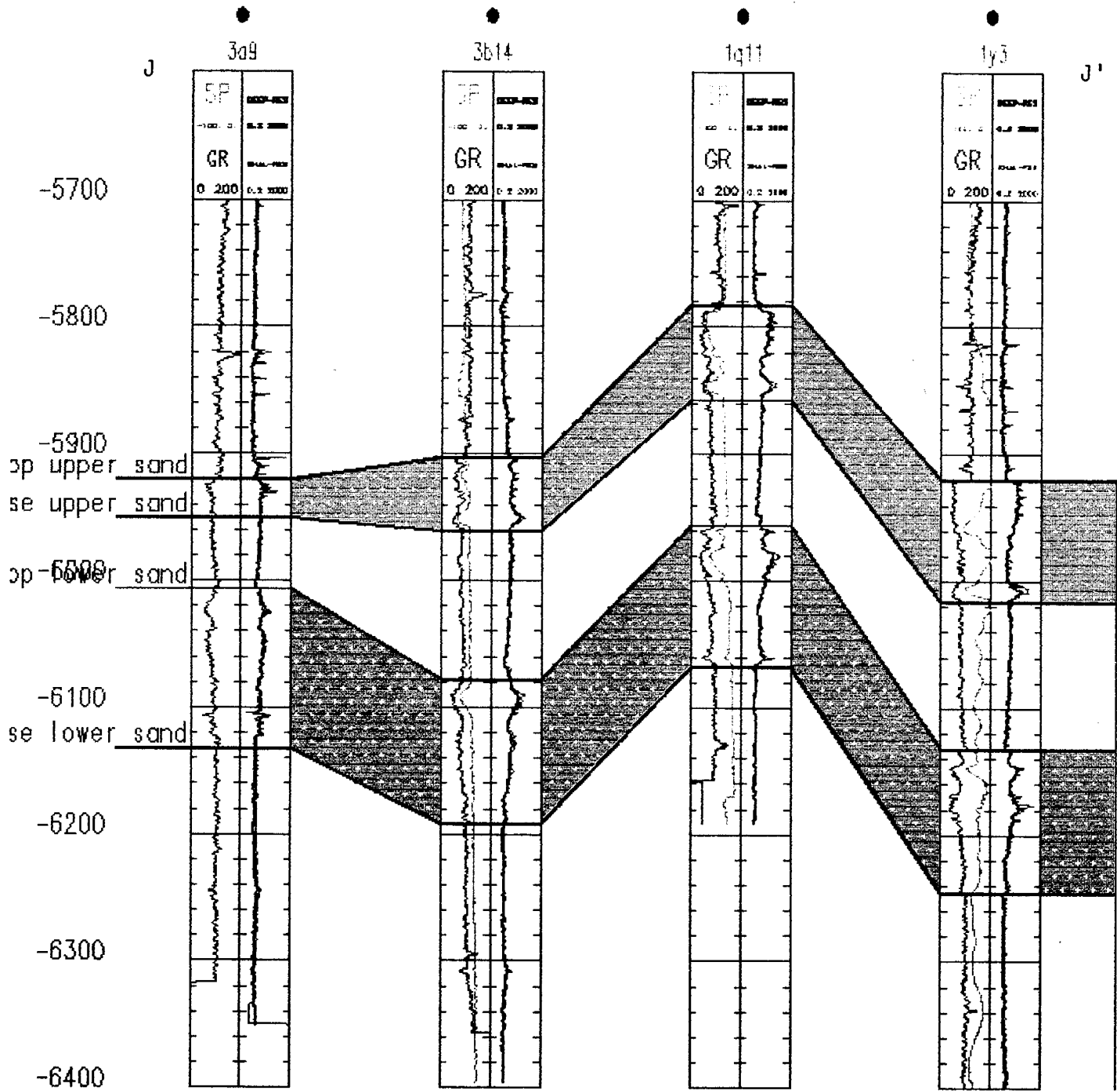


Figure VII-38. Stratigraphic Cross Section J-J' Showing Progradational Thickening of the Kuparuk River Formation Upper Sand.

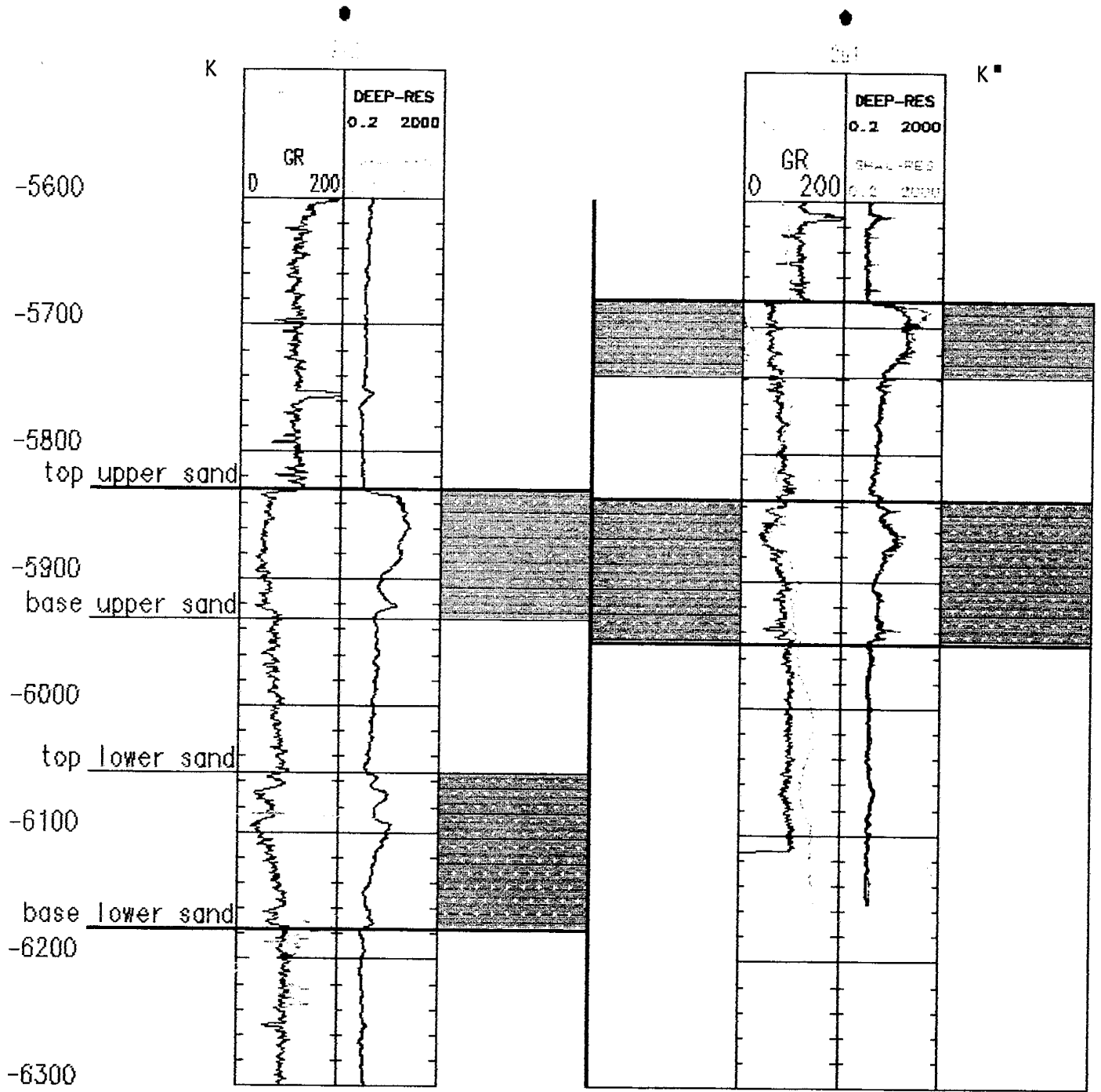


Figure VII-39. Cross Section K-K' Showing KUPARUK RIVER FORMATION Upper Sand Thickening on the Downthrown Side of Faulting.

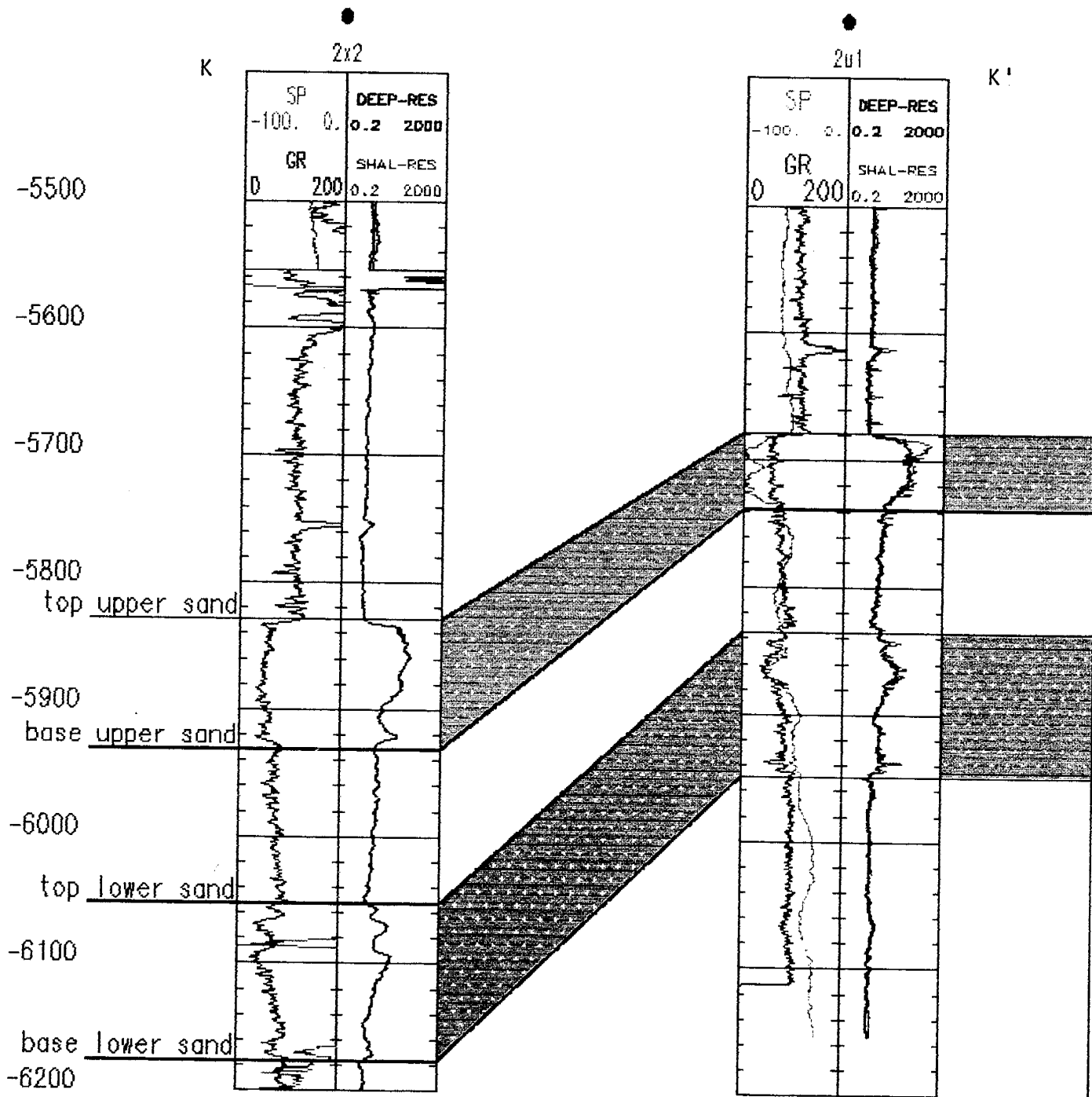


Figure VII-40. Cross Section K-K' Showing Kuparuk River Formation Upper Sand Thickening on the Downthrown Side of Faulting (faulting omitted).

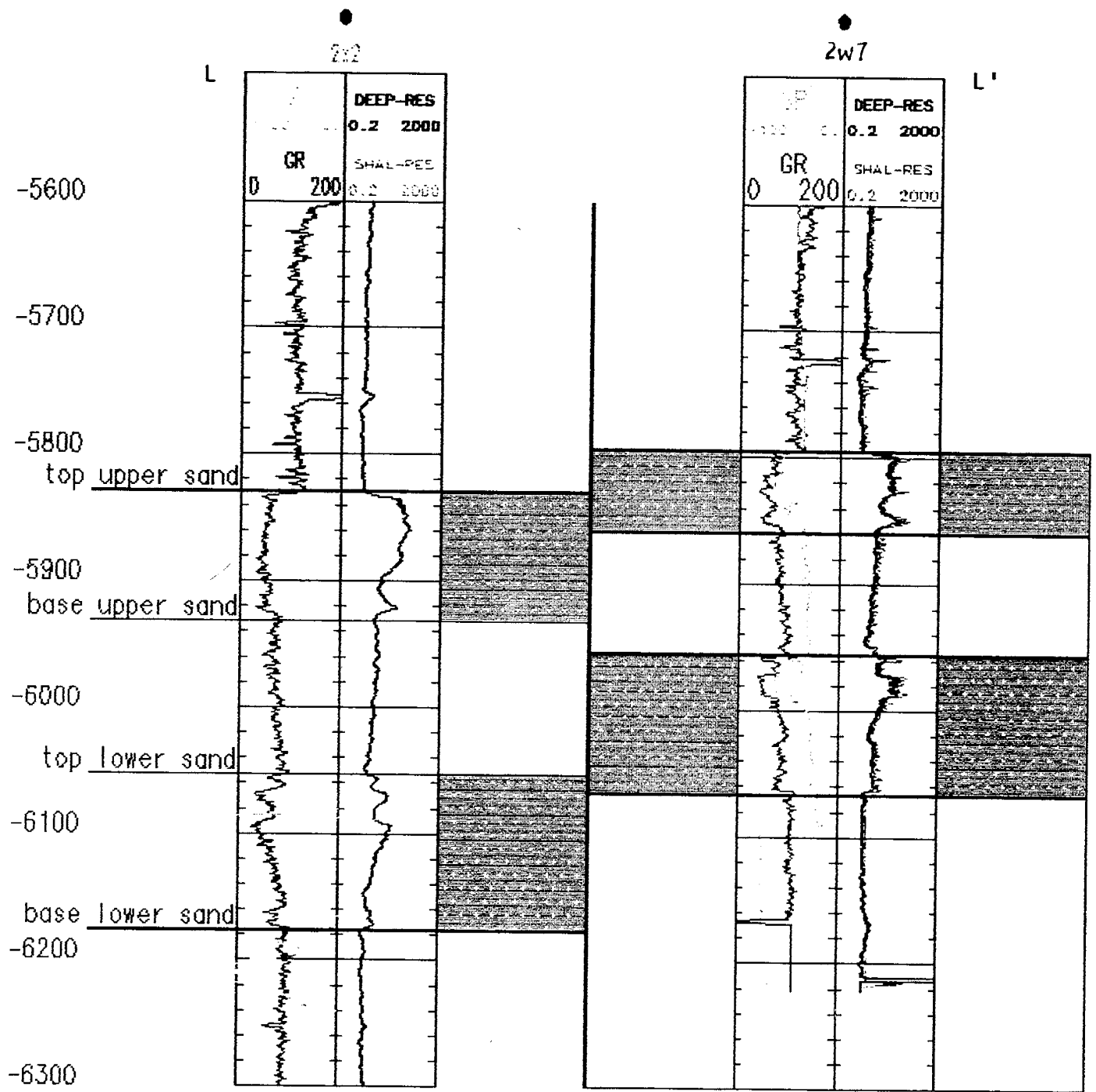


Figure VII-41. Cross Section L-L' Also Showing Kuparuk River Formation Upper Sand Thickening on the Downthrown Side of Faulting.

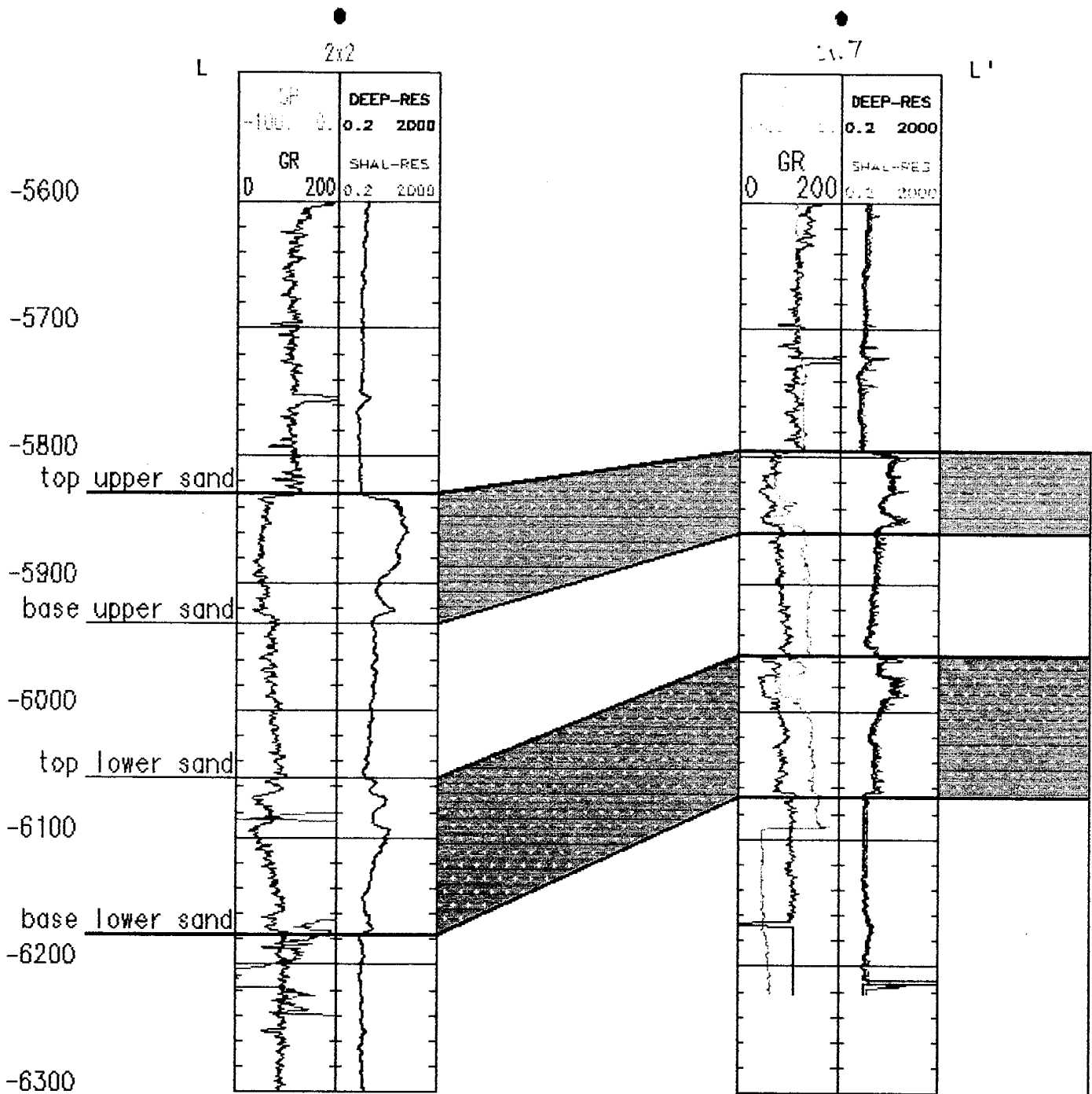


Figure VII-42. Cross Section L-L' Also Showing Kuparuk River Formation Upper Sand Thickening on the Downthrown Side of Faulting (faulting omitted).

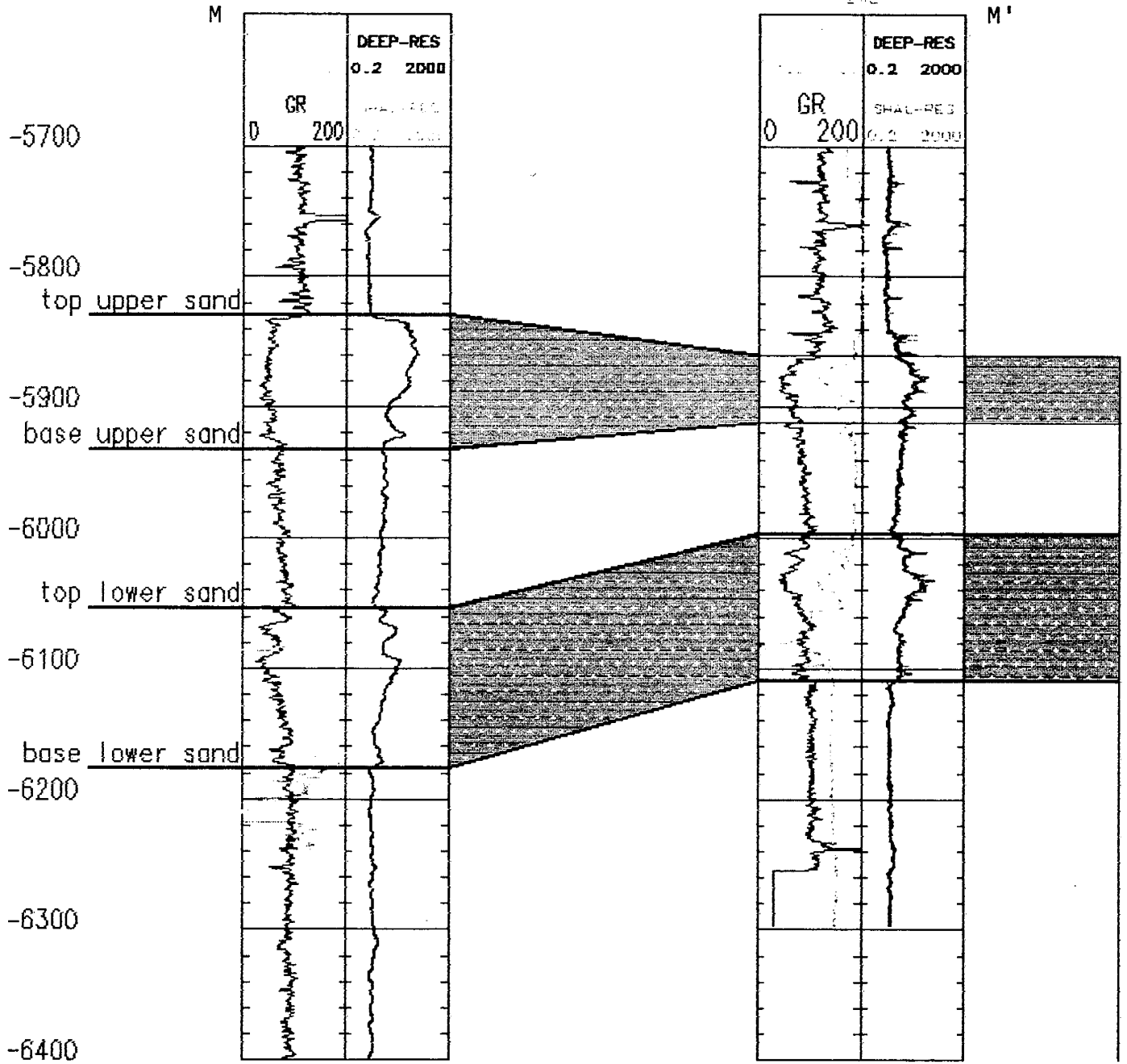


Figure VII-43. Cross Section M-M' Showing Anomalous Dip Between Kuparuk River Field Wells 2x2-2w2.

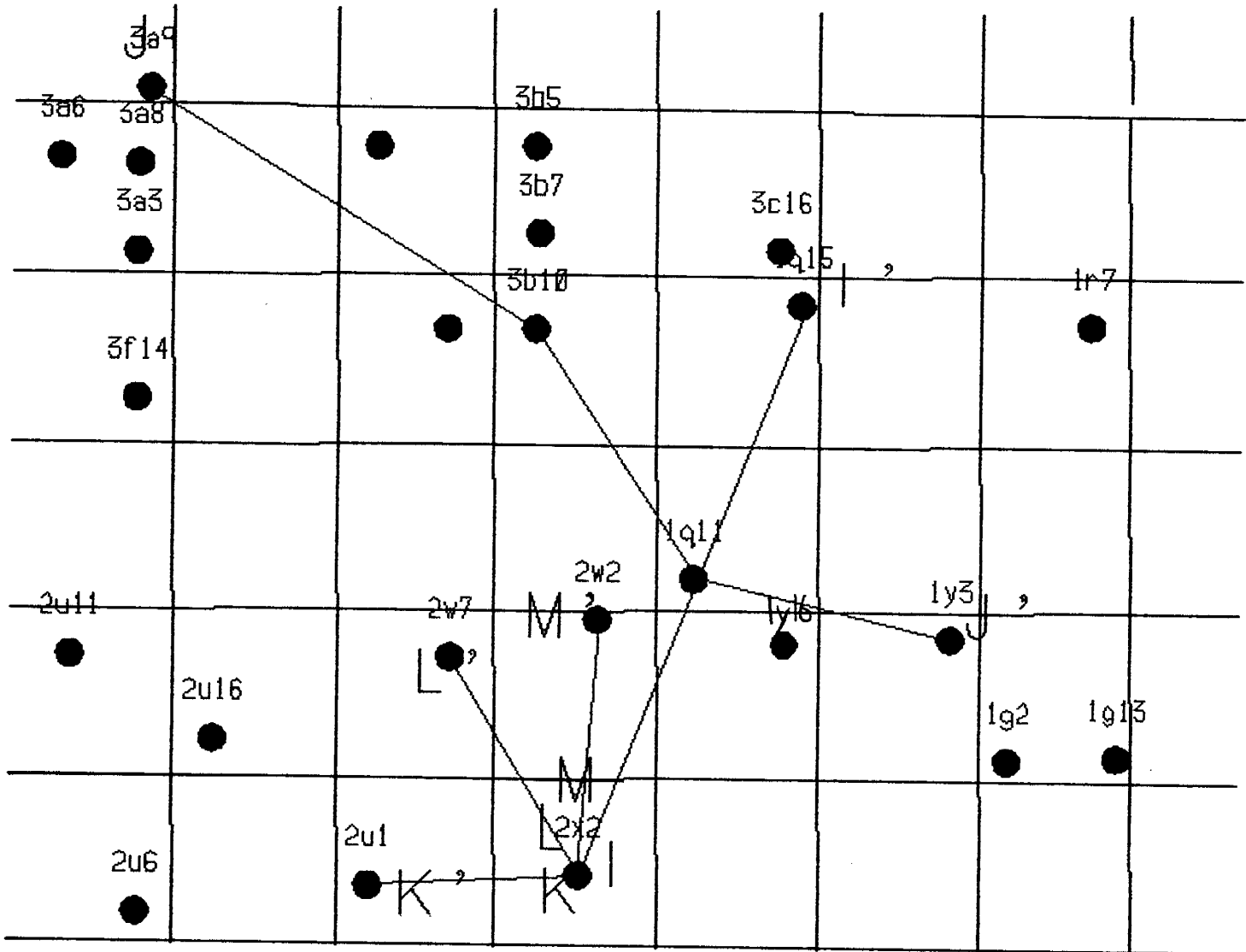


Figure VII-44. Base Map Showing Kuparuk River Field Cross Sections I-I' Through M-M'.

Possibly well 2w2, drilled towards the northeast, encountered the fault plane of a northwest striking, down-to-the-northeast fault, and drilled down and within the fault. In doing so, the well would miss the upper portion of the upper sand but would drill out of the fault in time to cut through the lower sand (Figure VII-45). This would explain the abruptly shorter section and deeper top of the upper sand in the 2w2, but allow for the up-dip location of the lower sand in this well as compared to the 2x2.

#### **E. RESERVOIR QUALITY OF THE LOWER SAND**

The porosity and permeability distributions in this sand are a direct function of a sand lithofacies deposited in a shallow high energy environment and thus the reservoir quality improves with corresponding increases in the energy of deposition. Grain size and sorting directly influences both horizontal and vertical permeability. Zones possessing the best sorted and largest grains also possess the highest percentage of pore throats and greatest permeability. In general, these zones consist of parallel-laminated sandstones and hummocky cross-stratified sandstones. Good porosity and permeability may also be found in wave rippled sandstones but which include clay flasers and mud drapes.

Zones with poorly sorted sands are characterized by smaller grains and have low permeability. Silt and clay laminae are common in these zones. Poor permeability also occurs in sands with silt and clay in intergranular pore spaces.

Lateral continuity, and hence better producibility, of the lower sand is a function of bed thickness. Only the amalgamated, hummocky, and cross-stratified sandstone units maintain good reservoir quality over significant lateral distances. Vertical permeability barriers exist and are of two main types: ankerite cemented sandstones and mudstone-rich units. Of these two, the mudstone-rich units are a very effective barrier against vertical flow. Overall, the lower sand exhibits better horizontal permeability than vertical permeability.

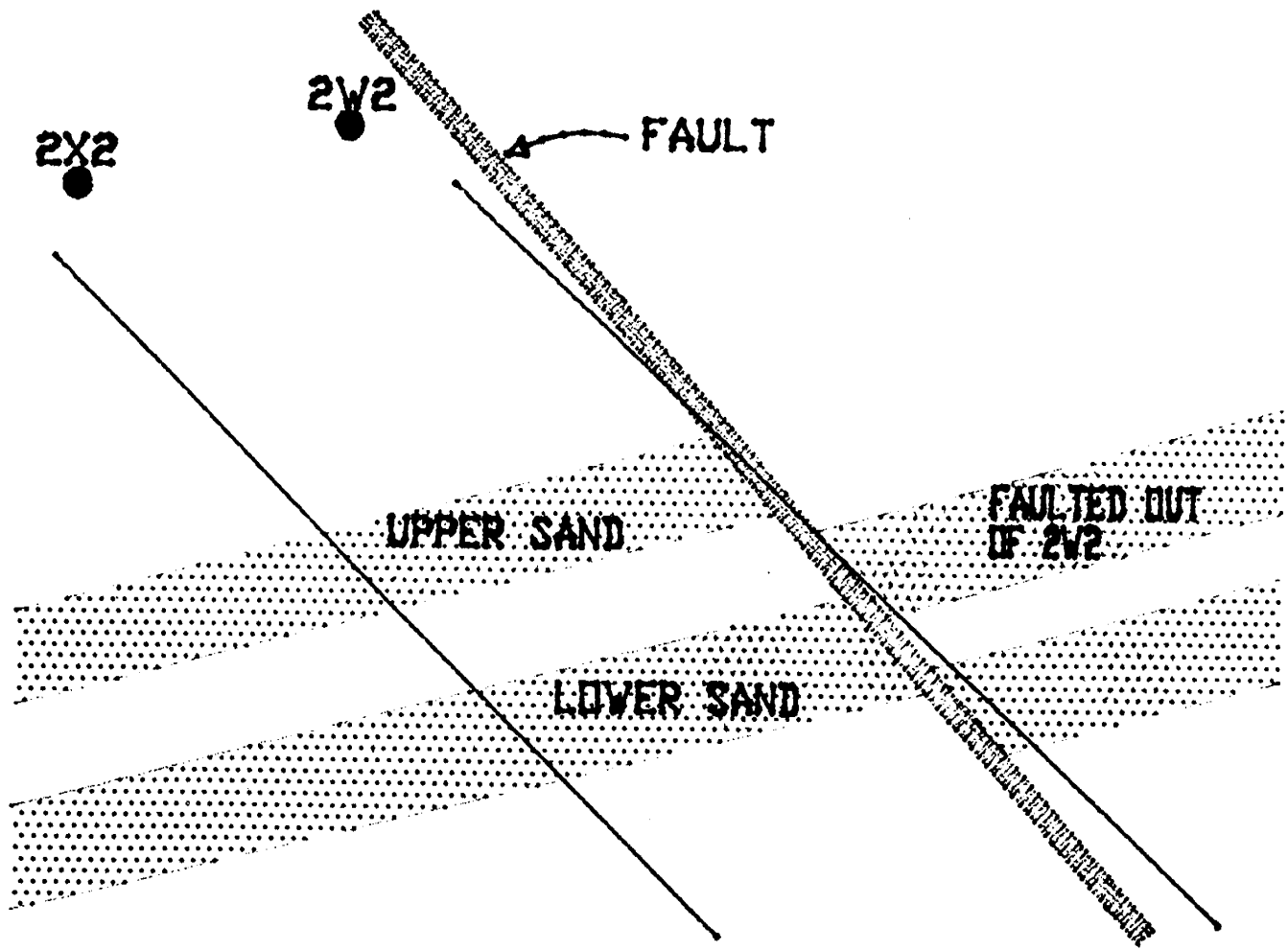


Figure VII-45. Possible Faulting at Kuparuk River Field Well 2w2.

## **F. RESERVOIR QUALITY OF THE UPPER SAND**

In contrast to the lower sand, bioturbation and diagenesis have removed preexisting relationships between porosity and permeability in the upper sand. Original sediment characteristics are significantly modified in the upper sand. In this sand the major controls on permeability and porosity are grain size distribution, combined with siderite cementation and dissolution. Core samples show good porosities and permeabilities where sideritization has not completely cemented sand units. But where a zone has been completely sideritized, porosity and permeability are drastically reduced. Bioturbation has led to isotropic permeability in the upper sand. Burrowing removed any directional component to permeability by destroying sedimentary structures or local permeability barriers.

Lateral continuity of reservoir-quality upper sands is controlled by topography on the LCU, and by an erosional truncation within the upper sand itself. Syndepositional faulting may have formed topographic lows in which thick pebbly sandstones were deposited. Permeability-inhibiting shale barriers are much less abundant in the upper sand as compared to the lower sand because of winnowing and reworking, as well as bioturbation.

## **G. PRODUCTION PERFORMANCE**

Upper sands are capable of higher production rates (up to 5000 barrels of oil per day) than lower sands (1300 barrels of oil per day). When both sand units are simultaneously open to production through a single completion, the upper sand can outperform the lower sand by a ratio of 9-to-1. Waterflood studies indicate that successful recovery from the upper sand requires that it be isolated from the lower sand. While porosities in the upper and lower members are similar, permeabilities are generally greater in the upper member. Maximum permeability in the upper sand is over 2000 millidarcies greater than in the lower sand. These and other data make it clear that the upper sand is the better producer of the two.



# **CHAPTER VIII: RESERVOIR CHARACTERIZATION OF PRUDHOE BAY FIELD NORTH SLOPE, ALASKA**

---

## **A. INTRODUCTION**

Prudhoe Bay field, the largest oil field in North America, was discovered in 1968 on the North Slope of Alaska. It is situated about 250 miles north of the Arctic Circle. The location of Prudhoe Bay and other North Slope fields is shown in Figure VIII-1. The estimated initial oil-in-place is 23 billion barrels, of which 12 billion are recoverable. The production at Prudhoe Bay began in 1977, after completion of the Trans-Alaska Pipeline System. The field is jointly operated by British Petroleum Alaska (BP Alaska) and Atlantic Richfield Co. (ARCO) as a unit.

The principal hydrocarbon reservoir in Prudhoe Bay field is the Permo-Triassic Ivishak formation of the Sadlerochit group (Figure VIII-2). Other hydrocarbon bearing zones are Shublik and Sag River formations, which overlie the Sadlerochit group. The Prudhoe Bay structure is an anticline with a gentle dipping south flank and a highly faulted northern flank. The hydrocarbon trap mechanism in the Prudhoe Bay field is a combination of structural and stratigraphic traps. Hydrocarbons in the trap are retained by faults to the north and west, truncation of the sand to the east, and the oil-water contact to the south. The principal hydrocarbon accumulation occurs in an area called the Main Area, which is confined by several northwest-southeast trending faults. Immediately west of the Main Area is the Eileen Area, which is a smaller hydrocarbon accumulation connected to the Main Area.

The objective of this study is to describe the reservoir and characterize the Sadlerochit group of Prudhoe Bay field based on well log analysis. The study includes determination of petrophysical properties of the sand, generation of various property maps to delineate the distribution pattern of the sand thickness, porosity, water and oil saturation, etc., across the field. It also includes well-to-well correlation and plots of cross sections of the field.

## **B. WELL LOG ANALYSIS**

A total of 27 wells were analyzed to date in this study. These wells were selected from the entire field in order to develop a field-wide understanding of reservoir properties. For the purpose of this study, an integrated well log analysis software package called Petroleum WorkBench developed by Scientific Software Inc. was used.

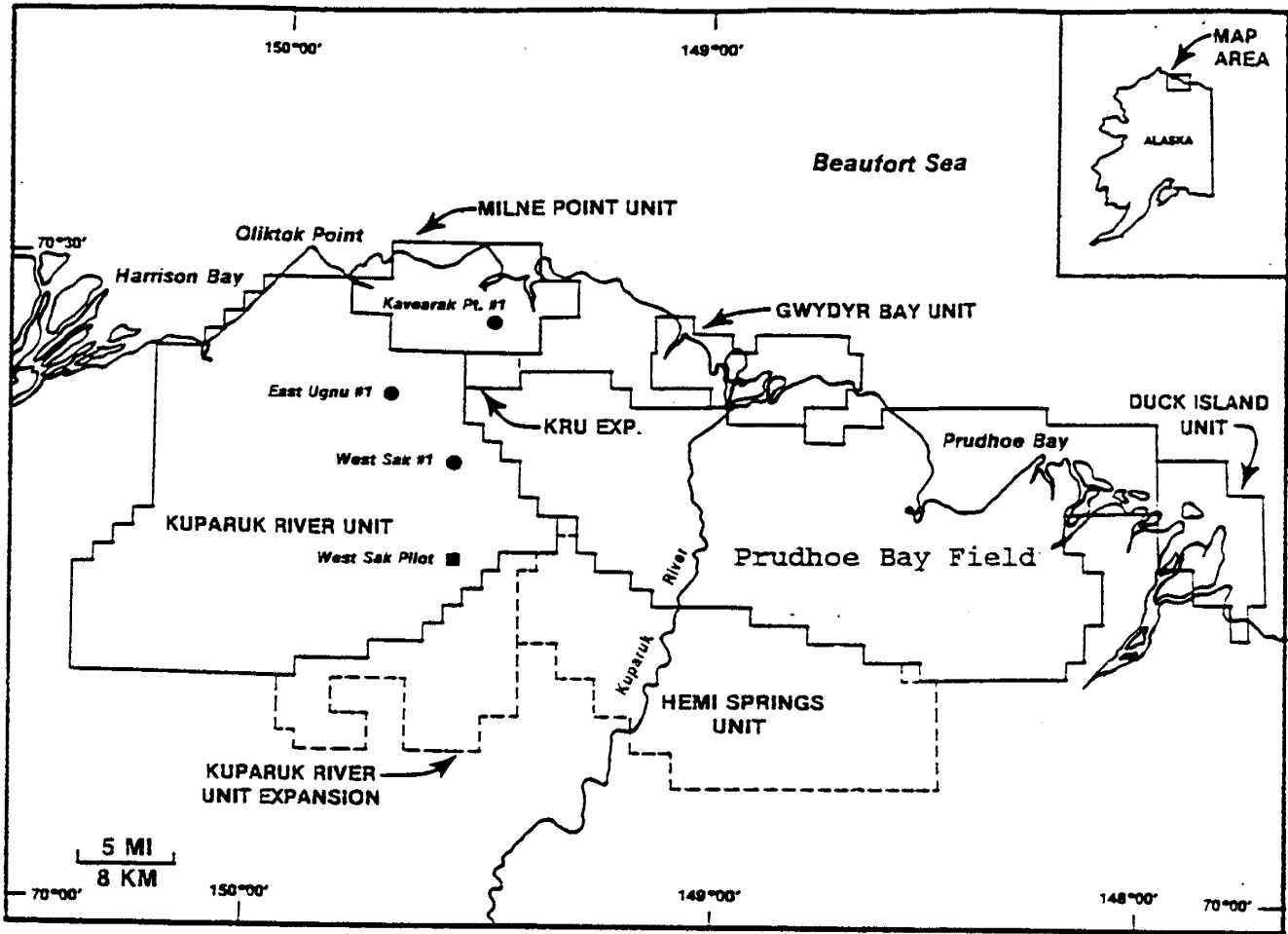


Figure VIII-1. Location Map of North Slope Fields, Including Prudhoe Bay Field (Werner, 1987).

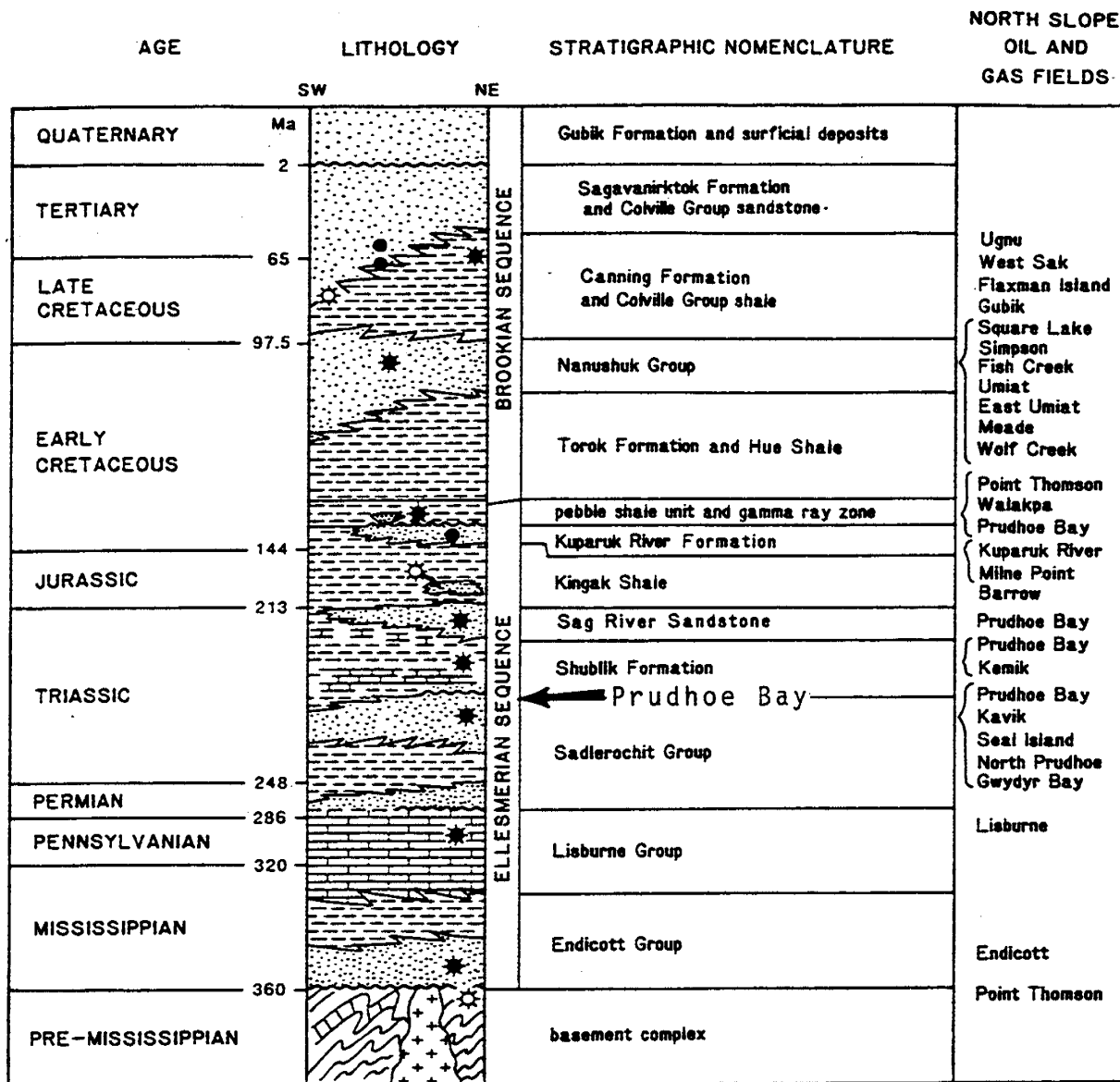


Figure VIII-2. North Slope Stratigraphic Column Showing Location of Sadlerochit Group (Bird, 1987).

Raw log traces in measured depth were loaded against corresponding wells. Then deviation data for each well were imported, and the traces were converted to true vertical depth (TVD). After loading log traces into database, additional well information including logged intervals, mud properties, bottom-hole temperature, and bit size, etc., were loaded. In the next step environmental corrections to log traces were made and top and base of Ivishak formation were picked for each well. A parameter interval (PI) was defined on which the log analysis would be run, and clean sand and shale lines were picked on frequency versus SP and frequency versus GR plots. Then the log analysis was run for individual wells.

In well log analysis, the Archie equation was used for water saturation ( $S_w$ ) calculation. Calculated  $S_w$  values were then compared with those from three other equations, including Laminar-Simondoux, Indonesian, and Dual-Water. The comparison of  $S_w$  from different equations for a well is shown in Figure VIII-3. This figure also predicts lithology and fluid saturation.

Average petrophysical properties including gross pay, net pay, porosity, water saturation, oil saturation, and hydrocarbon-porosity thickness of Sadlerochit formation for all the wells were determined by utilizing the following cutoff values:

Shale Volume.....	40%,
Porosity .....	6%,
Water Saturation .....	80%.

These cutoffs determine net pay thickness as described below.

Any sample point with shale volume higher than 40%, porosity less than 6%, and water saturation higher than 80% was excluded in net pay determination. Points included in net pay determination are arithmetically averaged to yield average porosity,  $S_w$ , and oil saturation. They are also included in net pay and hydrocarbon porosity thickness calculations. The petrophysical properties of all the wells for Sadlerochit group are shown in Table VIII-1.

Structure top and net pay true vertical thickness (TVT) maps on Sadlerochit group were generated to evaluate the overall structure of the Sadlerochit group and distribution of thicknesses. Color-filled contour and 3-D view of these maps were also made as a means of better visual illustration. These maps are shown in Figures VIII-4 through VIII-6.

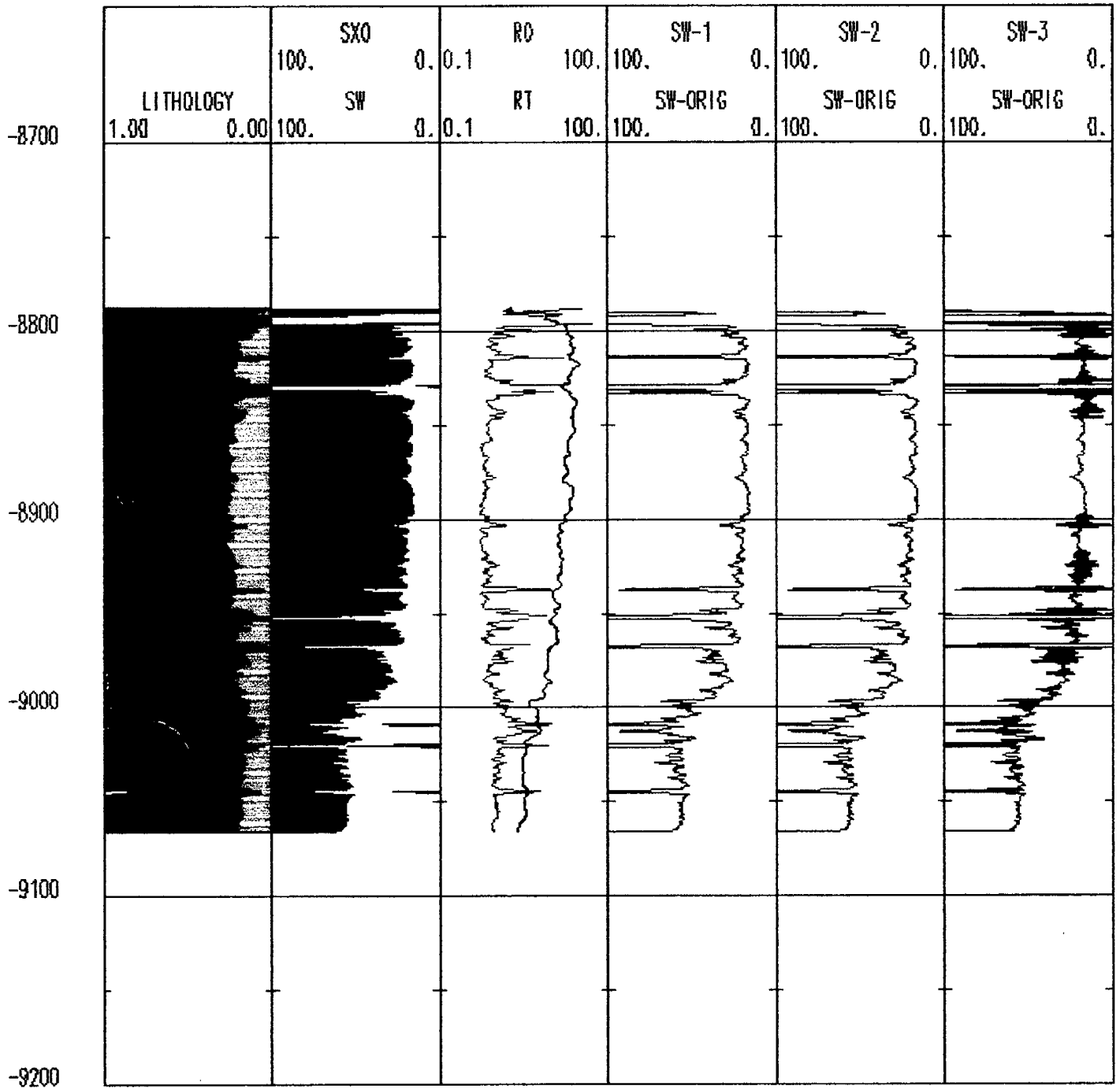


Figure VIII-3. Analysis Result Plot of A-15 Well from Prudhoe Bay Field, Including Comparison of Sw from Different Models (Sw-1-Laminar Simondoux, Sw-2-Indonesian, Sw-3-Dual Water).

Table VIII-1: Log Derived Petrophysical Properties of Prudhoe Bay Wells (cutoffs:  $\phi$  - 6%, Sh - 40%, Sw - 80%).

SL No.	Well Name	Analyzed Interval (ft) Top-Bottom	Gross Thickness (ft)	Net Pay (ft)	Porosity (%)	Water Saturation (%)	Oil Saturation (%)	Hydrocarbon Porosity-Thickness (ft)
1.	A-15	10769-10986.5	182	164	22.7	21.3	78.7	29.4
2.	A-21	11349-11529	144	127	24.6	31.25	68.75	21.5
3.	A-28	11792-12063	199	183	24.4	16	84	37.4
4.	D-9	9826-10374	442	411	20.9	17.7	82.3	70.9
5.	D-10	10533-11083	441	426	22.96	17.9	82.1	80.4
6.	DS 2-13	9215-9672	410	394	24.6	11.9	88.1	85.4
7.	DS 2-19	8991-9265	264	229	23.94	22.8	77.2	42.3
8.	DS 6-16	9440-9848	350	311	24.04	38.5	61.5	46
9.	DS 7-24	10759-11190	363	297	25.22	38.7	61.3	46
10.	DS 12-13	9852-10045	183	150	25.77	40.5	59.5	23
11.	DS 14-31	9342-9710	368	343	27.3	15.85	84.15	78.9
12.	DS 15-2	10208-10589	292	277	24.1	38.5	61.5	41
13.	DS 15-3	8708-9258	549	432	27.35	43.4	56.6	67
14.	DS 15-16	10902-11807	460	398	23.7	7	93	87.7
15.	D-17	9642-10040	347	237	21.88	56.6	43.4	22.5
16.	DS 16-9	10786-10936	113	107	21.83	29.17	70.83	16.5
17.	DS 16-14	9826-9956	114	76	23.3	56.8	43.2	7.7
18.	E-8	9721-9937	196	191	20.1	14.7	85.3	32.8
19.	E-16	8842-9091	248	198	23.65	51.3	48.7	22.9
20.	F-24	12072-12280	153	121	24.11	44.73	55.27	16
21.	G-18	9813-10151	313	251	22.91	51.52	48.48	27.9
22.	J-12	9473-9788	275	255	20.11	19.44	80.56	41.3
23.	M-15	9003-9278	248	228	22	19.86	80.14	40.3
24.	N-11-A	10035-10375	265	98	31	66.25	33.75	10.2
25.	N-12	9417-9808	351	331	21.51	23.7	76.3	54.4
26.	N-13	9393-9773	332	307	20.03	40.28	59.72	36.7
27.	Y-3	9185-9347	161	141	23.32	38.86	61.14	20.15

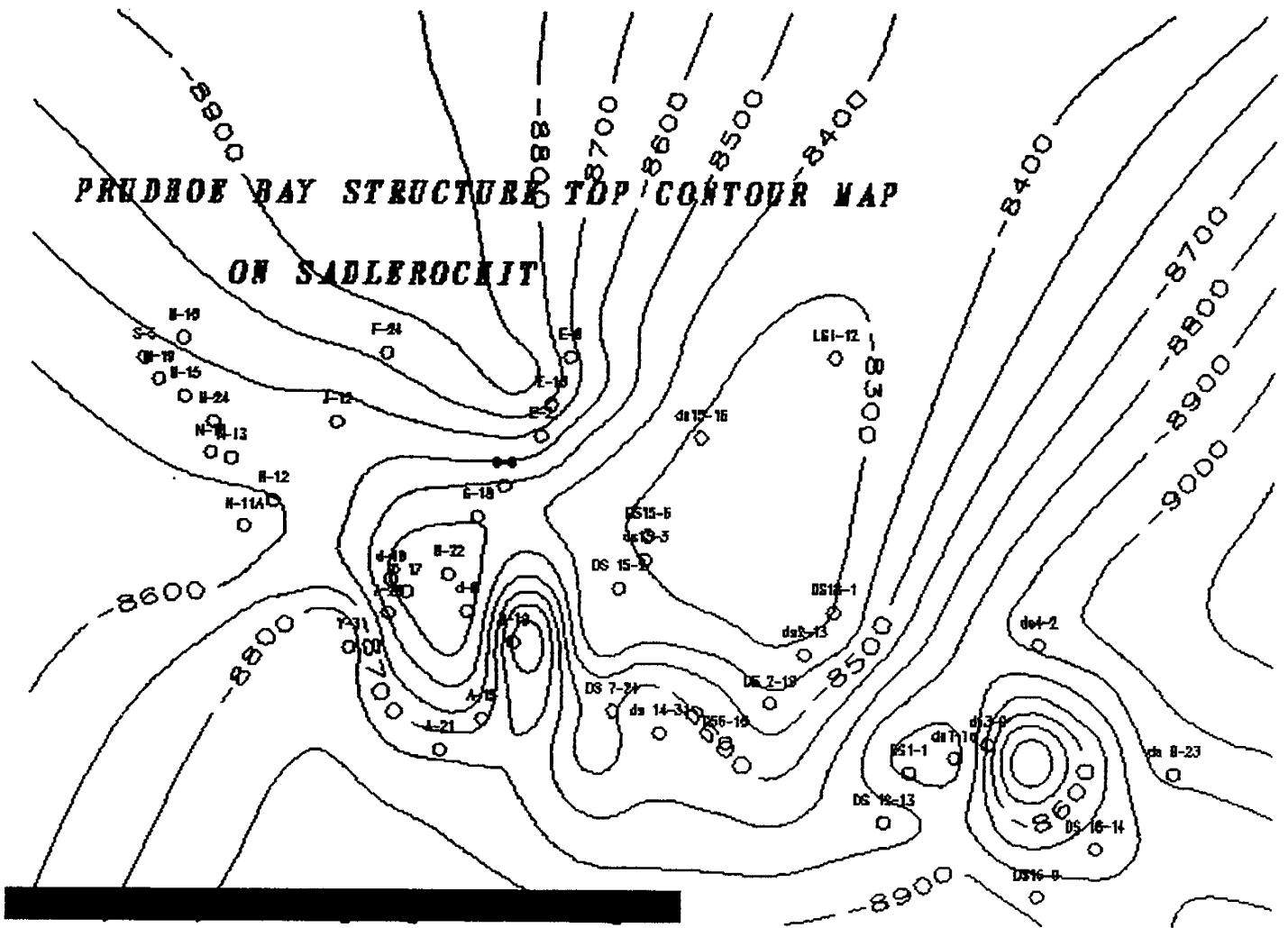


Figure VIII-4. Prudhoe Bay Structure Top Contour Map on Sadlerochit Group.

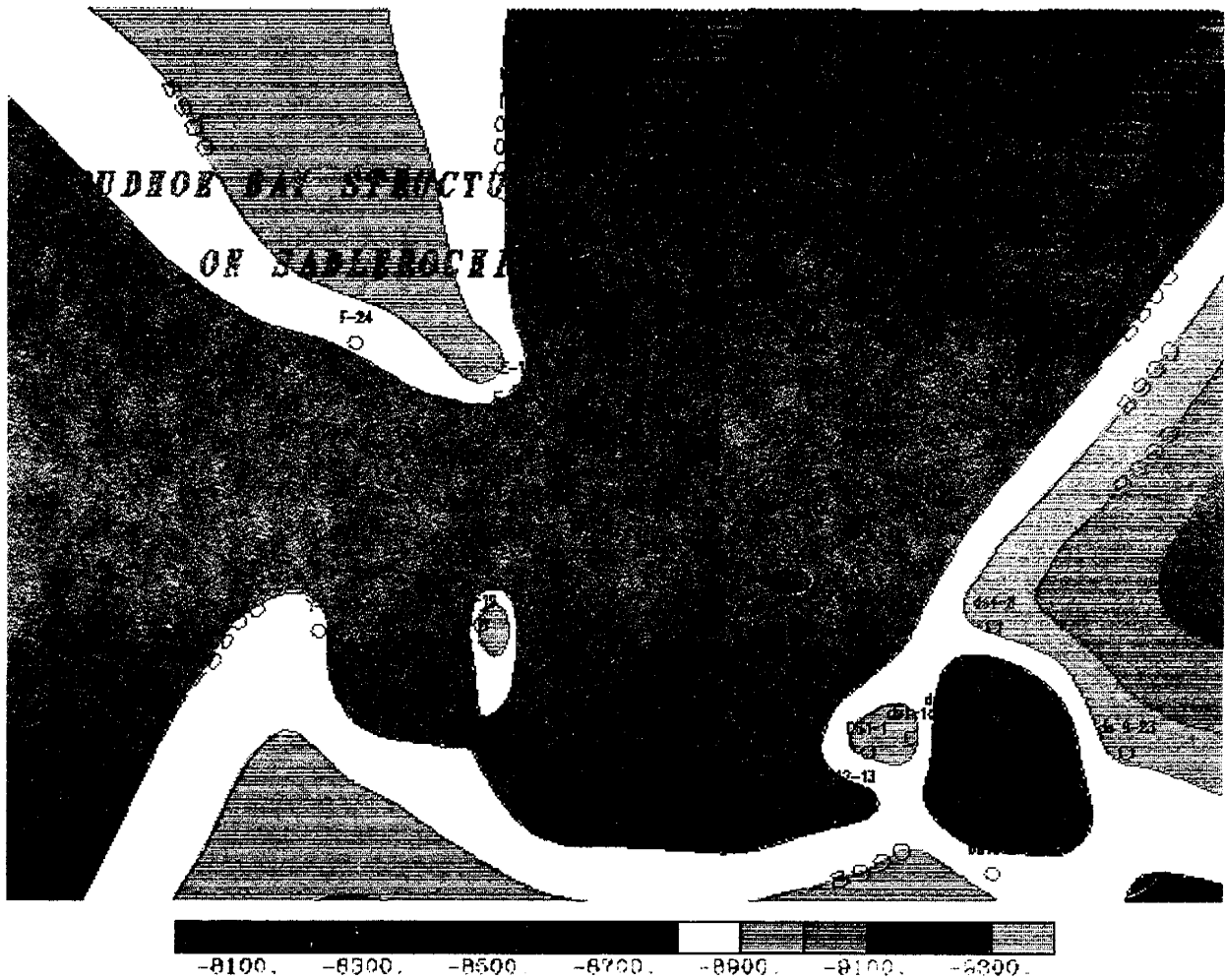


Figure VIII-5. Prudhoe Bay Structure Top Color-Filled Contour Map on Sadlerochit Group.

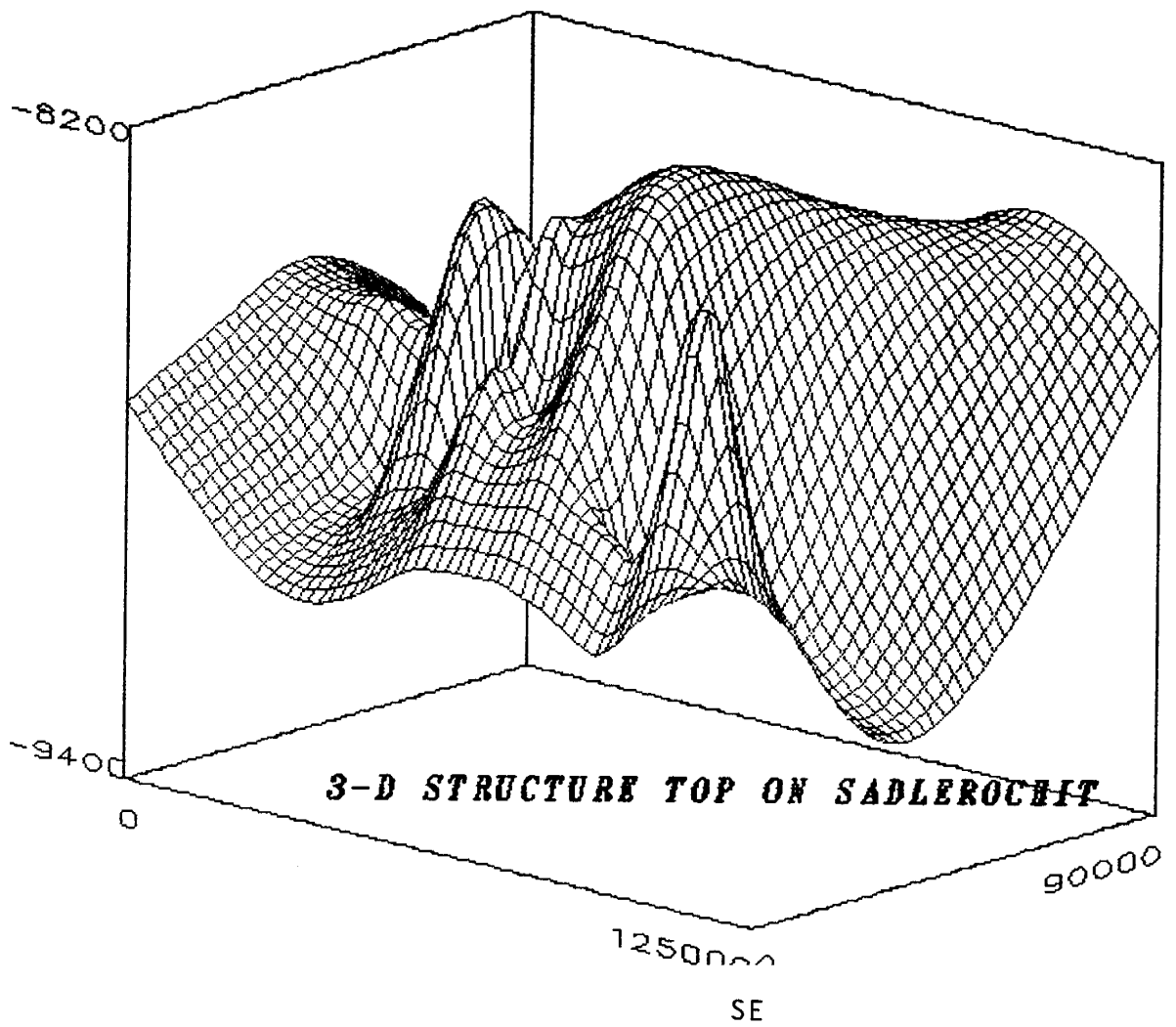


Figure VIII-6. 3-D View of Structure Top on Sadlerochit Group.

Several southwest-northeast and southeast-northwest cross sections were plotted to study the thickening and thinning of the sand across the field. Almost all the analyzed wells were incorporated in the cross section study. Figure VIII-7 provides a base map of cross section locations. Cross sections are shown in Figures VIII-8 through VIII-18.

Property maps including porosity, water saturation and oil saturation were generated to study the distribution pattern of these properties across the field. Some of these property maps were also plotted with color-filled contour and 3-D views. These maps are shown in Figures VIII-19 through VIII-24.

## **C. DISCUSSION OF RESULTS**

### **C1. Structure and Isopach Maps**

The Prudhoe Bay field lies on the southern flank of the subsurface Barrow Arch, a major uplift which generally parallels the Arctic coastline and plunges to the southeast. The structural contour map of the field (Figure VIII-4) illustrates that the top of the Ivishak formation ranges in subsea depth from 8200 ft to 9400 ft and dips away from structural crest at approximately 1-2°. The color-filled contour map and 3-D view of the structural contour map (Figures VIII-4 and VIII-5) again show the Prudhoe Bay structural crest trending northeast to southwest. The Ivishak reservoir is bounded to the north by normal faults; on the east by the Lower Cretaceous Unconformity (LCU); on the south by the oil/water contact; and on the west by another series of normal faults.

The sandstones in the Ivishak formation range from 350 to nearly 700 ft in thickness in Prudhoe Bay field. Various authors have suggested that the Ivishak formation was deposited as part of a northerly-sourced fluvio-deltaic complex (Jamison et al., 1980). Thickness decreases from more than 650 ft in the south and southwestern part of the Prudhoe Bay field to less than 350 ft in the northeast. Jones and Speers (1976) attributed much of the northwest thinning to Middle Jurassic erosion, prior to deposition of the Shublik formation.



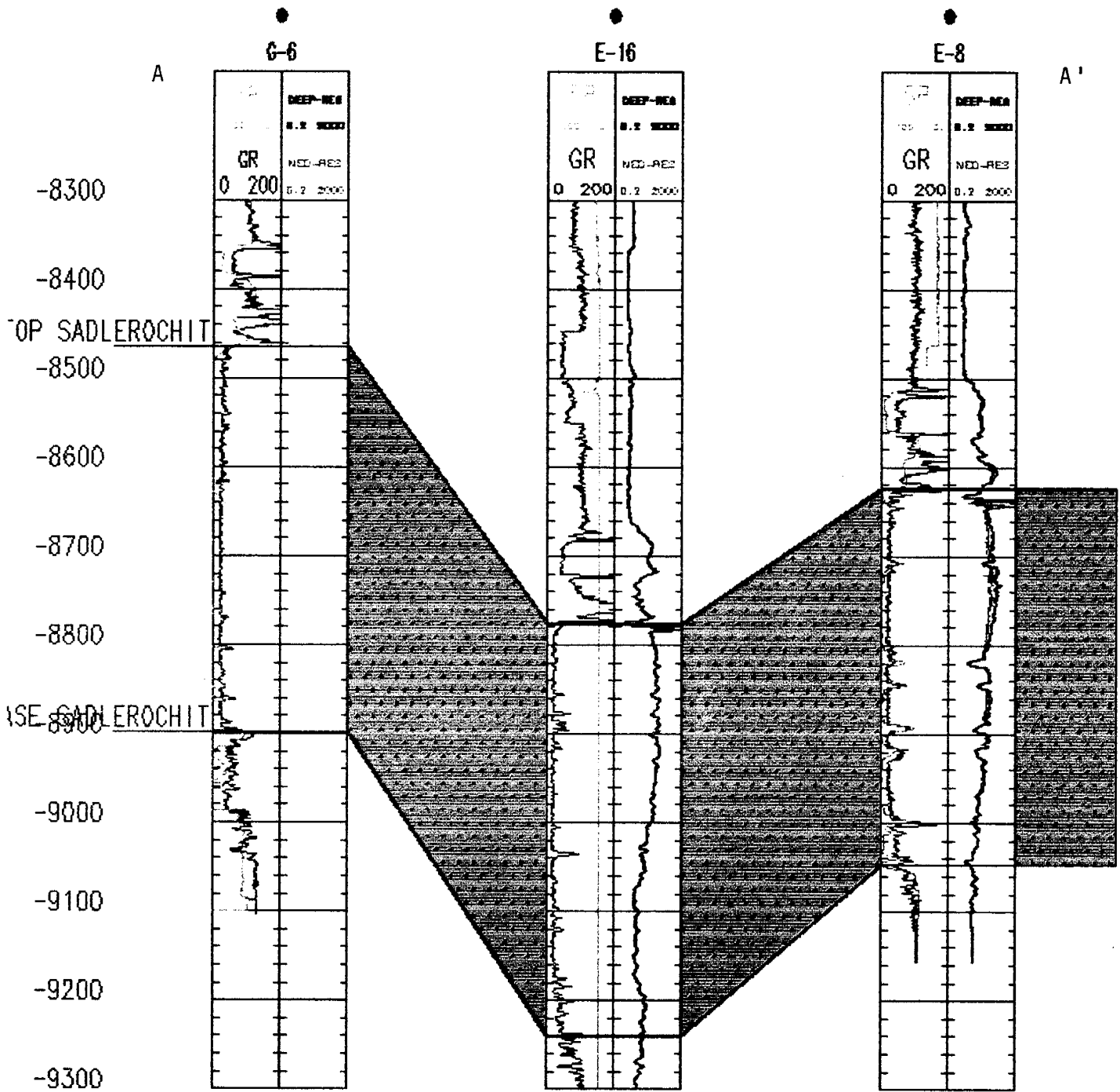


Figure VIII-8. Cross Section Along Line A-A' in Prudhoe Bay Field.

prudhoe: B-B' / TVDSS

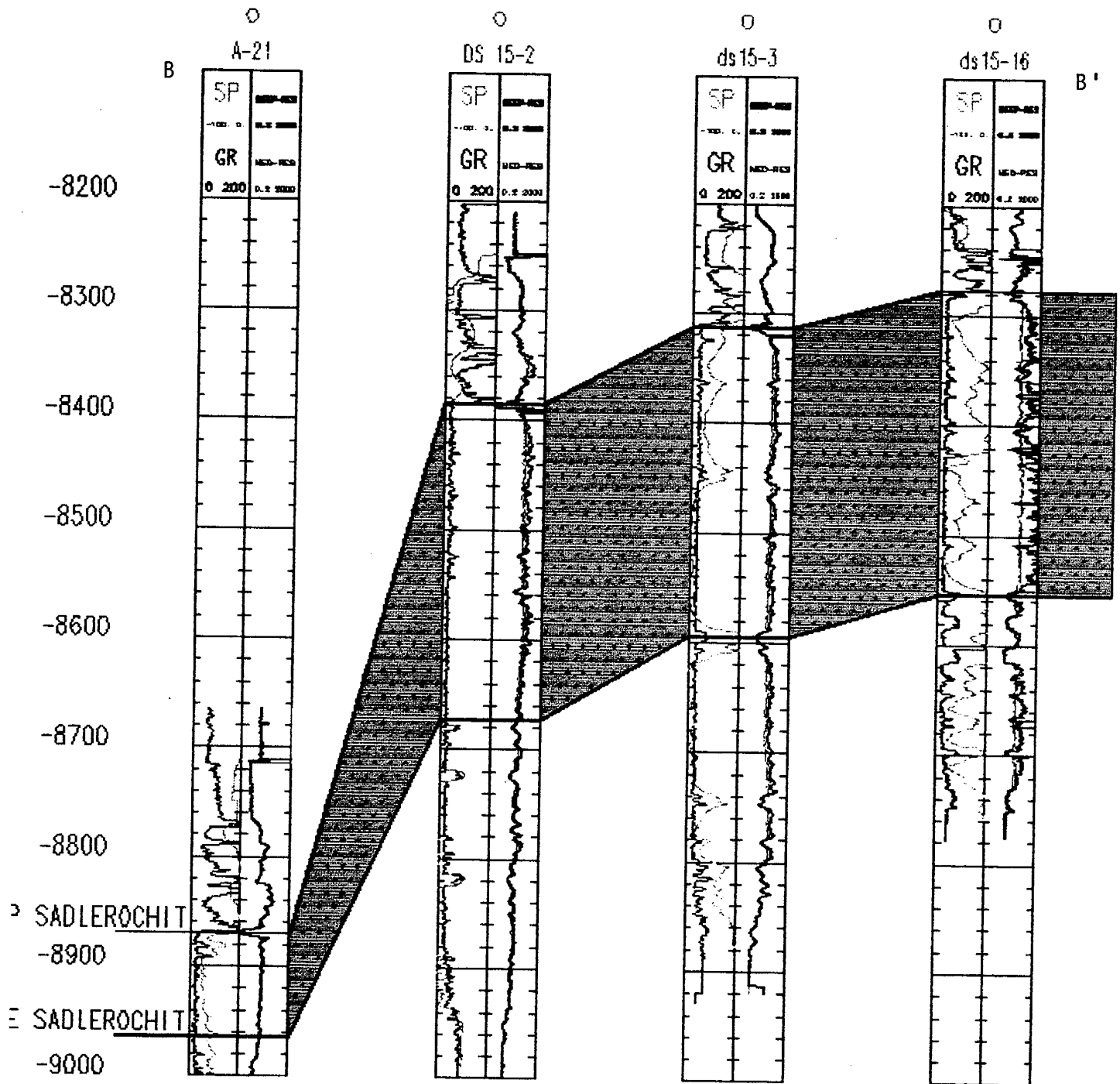


Figure VIII-9. Cross Section Along Line B-B' in Prudhoe Bay Field.

prudhoe: C-C'/TVOSS

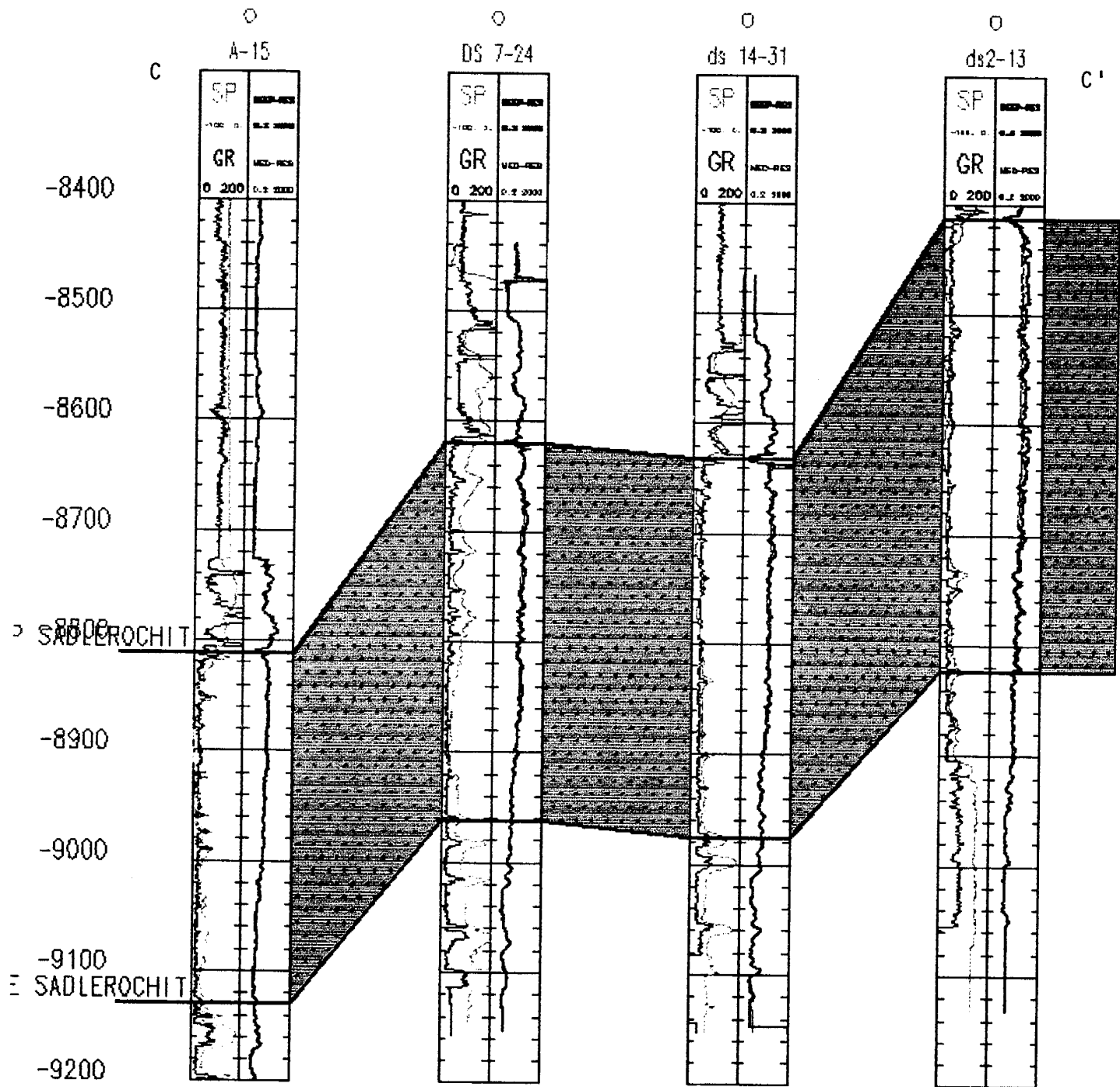


Figure VIII-10. Cross Section Along Line C-C' in Prudhoe Bay Field.

prudhoe: D-D' / TVOSS

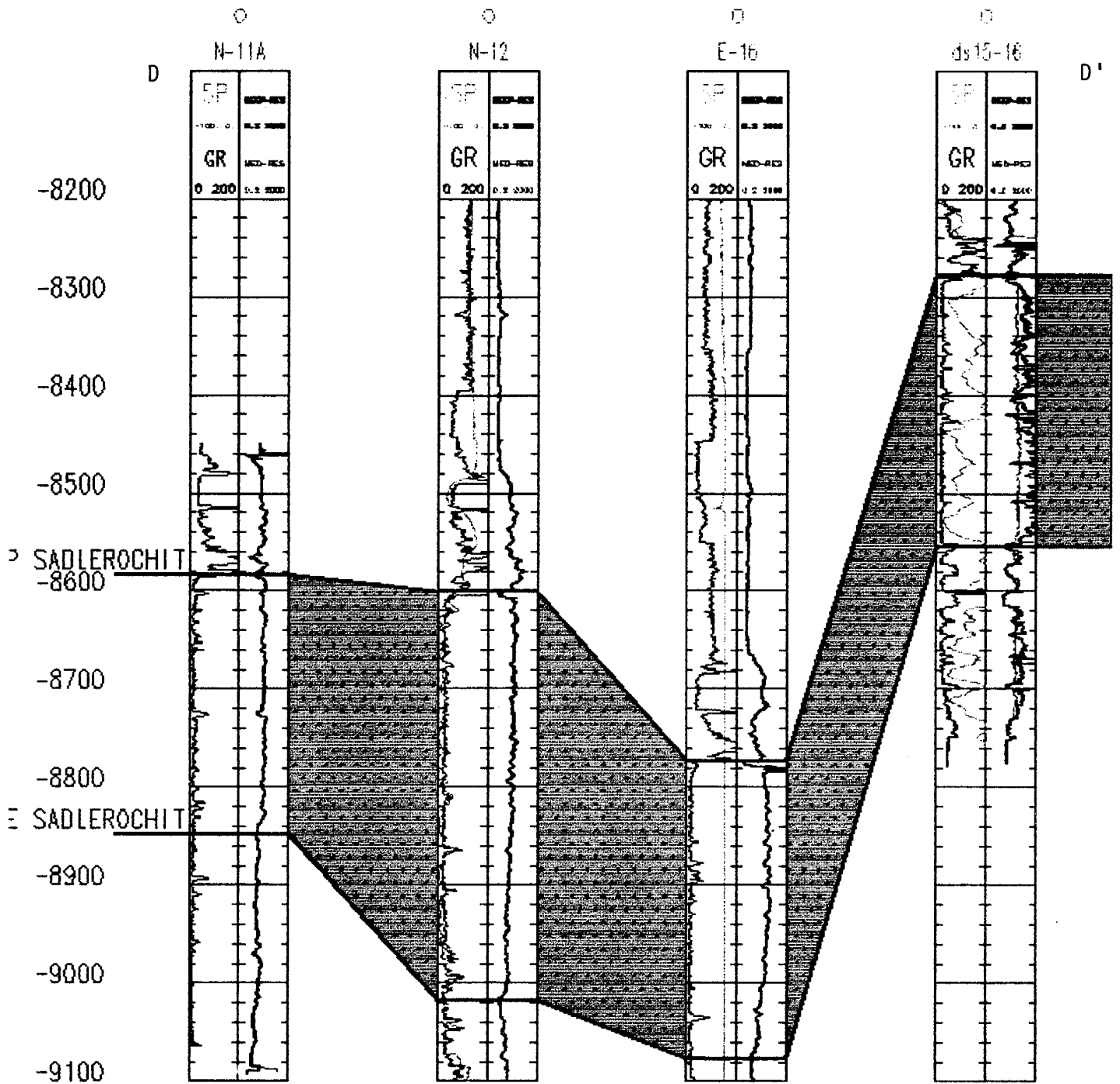


Figure VIII-11. Cross Section Along Line D-D' in Prudhoe Bay Field.

prudhoe: E-E' / TVDSS

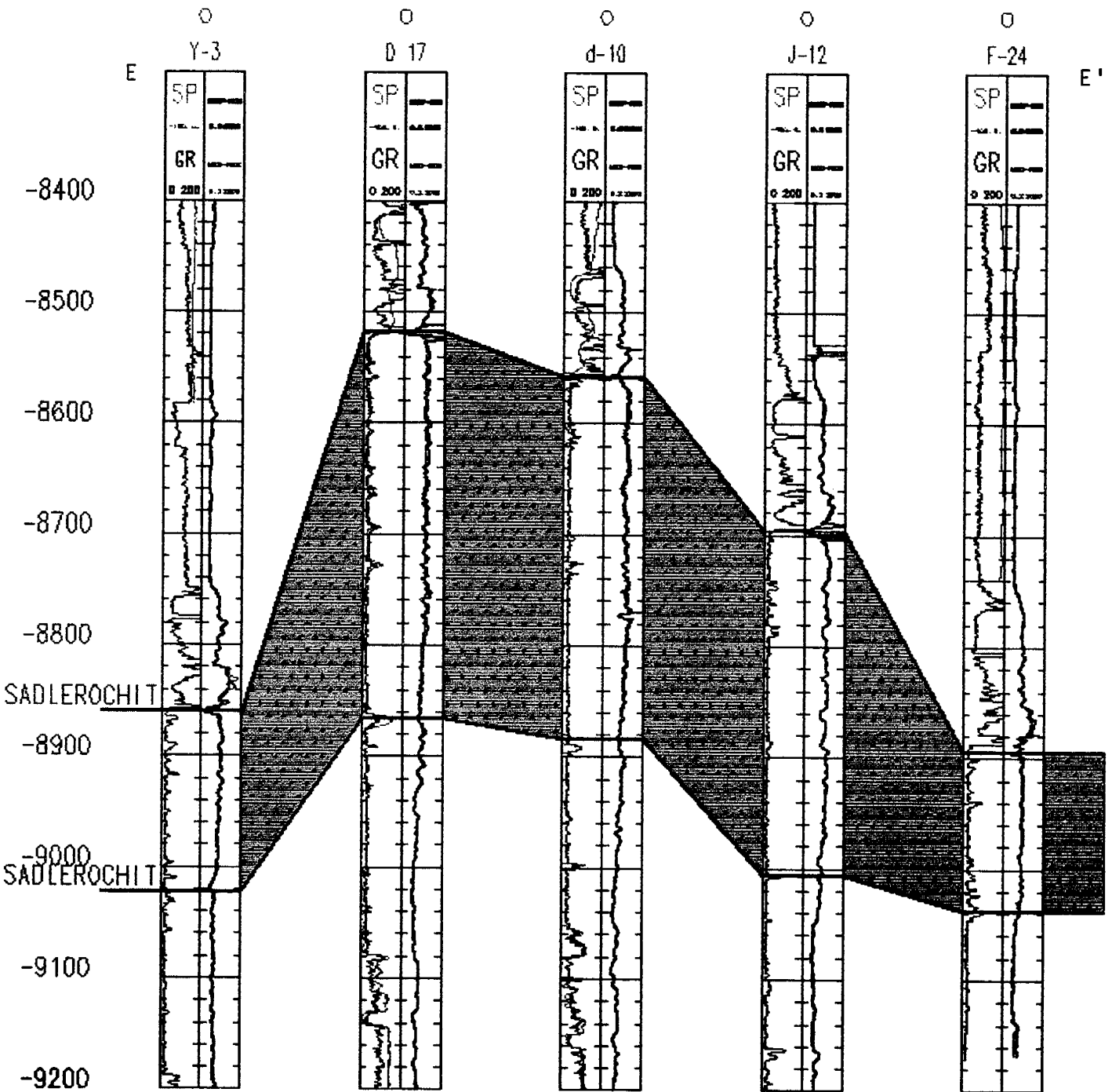


Figure VIII-12. Cross Section Along Line E-E' in Prudhoe Bay Field.

prudhoe: F-F' / TVDSS

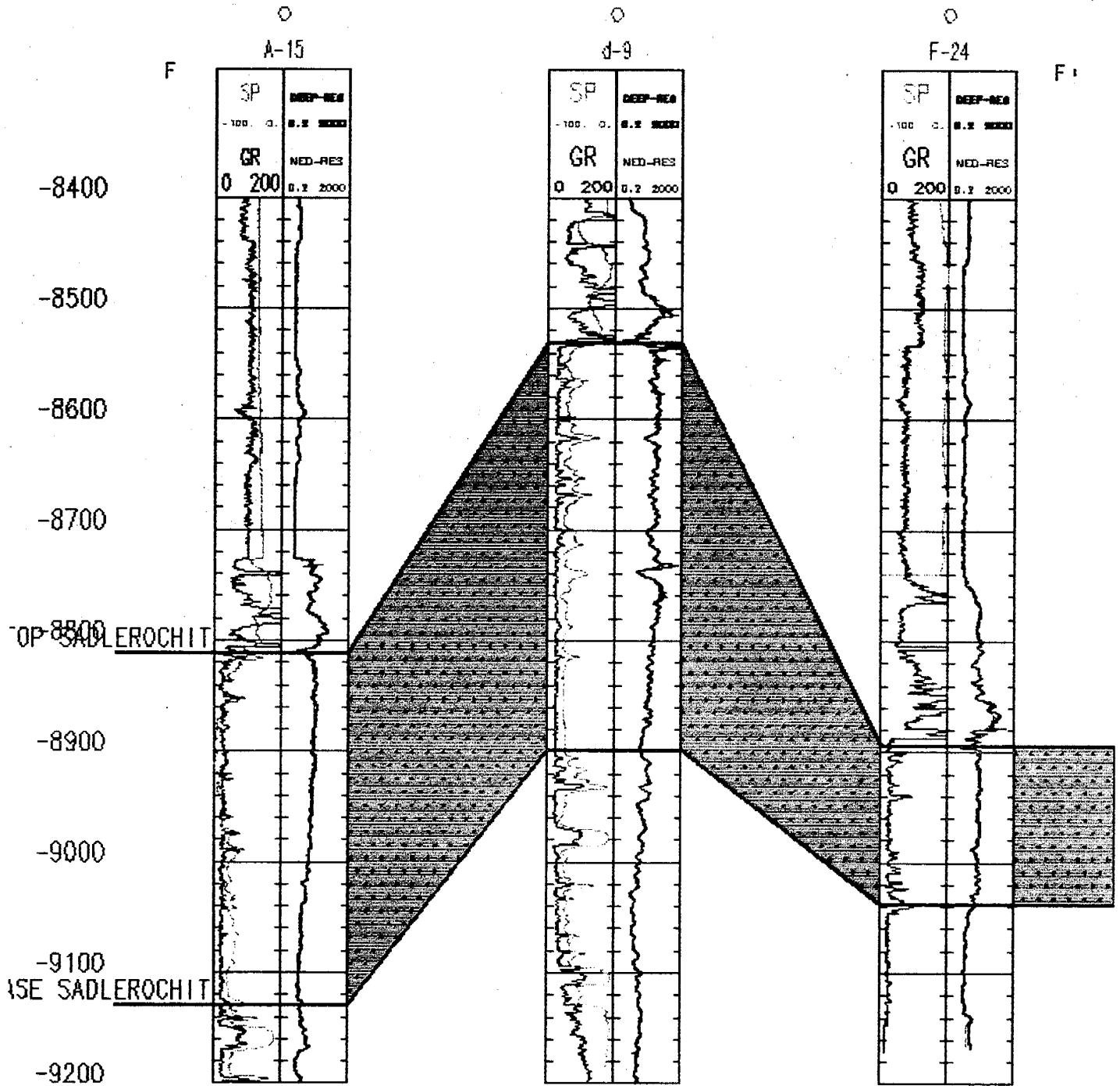


Figure VIII-13. Cross Section Along Line F-F' in Prudhoe Bay Field.

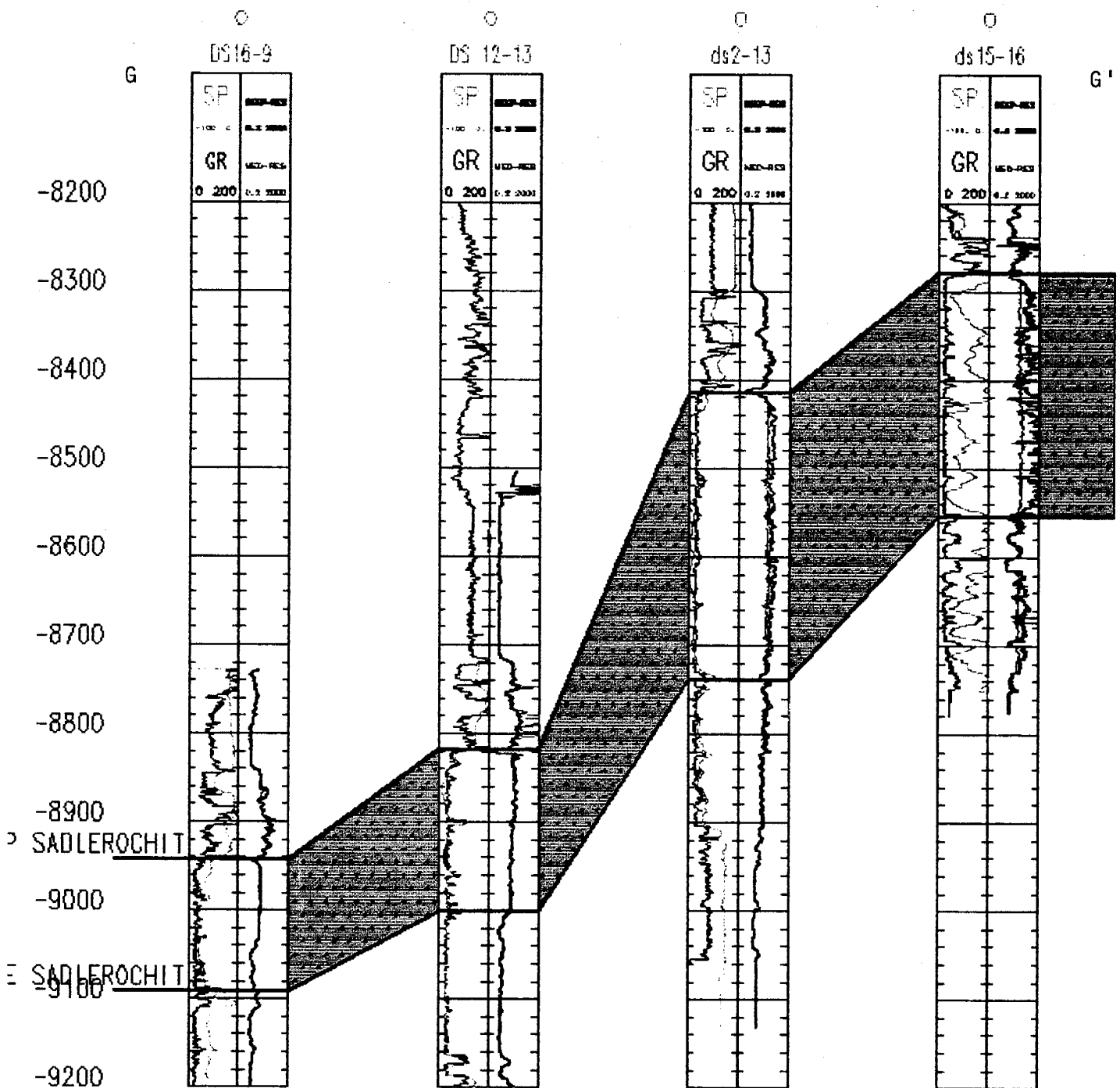


Figure VIII-14. Cross Section Along Line G-G' in Prudhoe Bay Field.

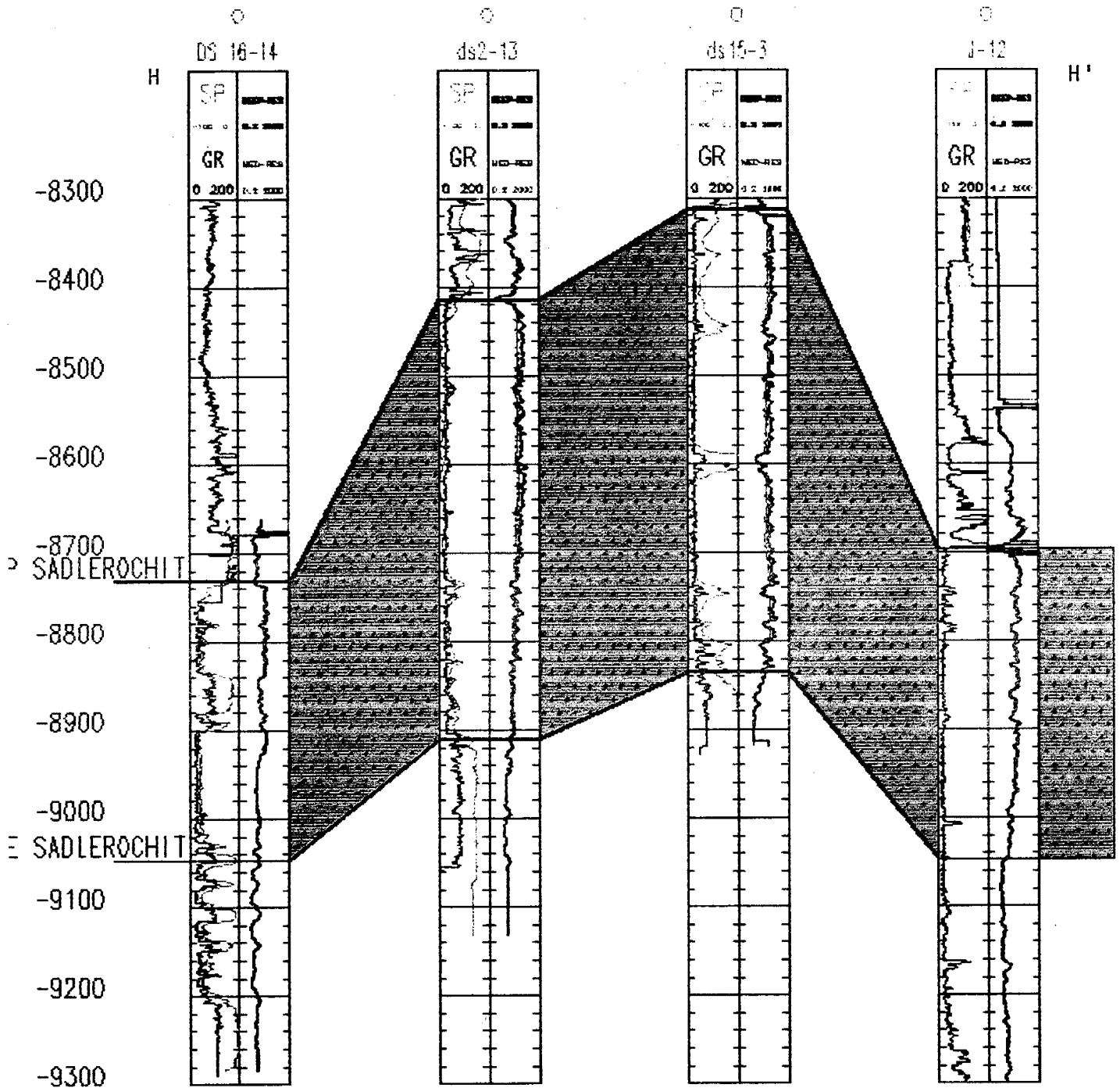


Figure VIII-15. Cross Section Along Line H-H' in Prudhoe Bay Field.

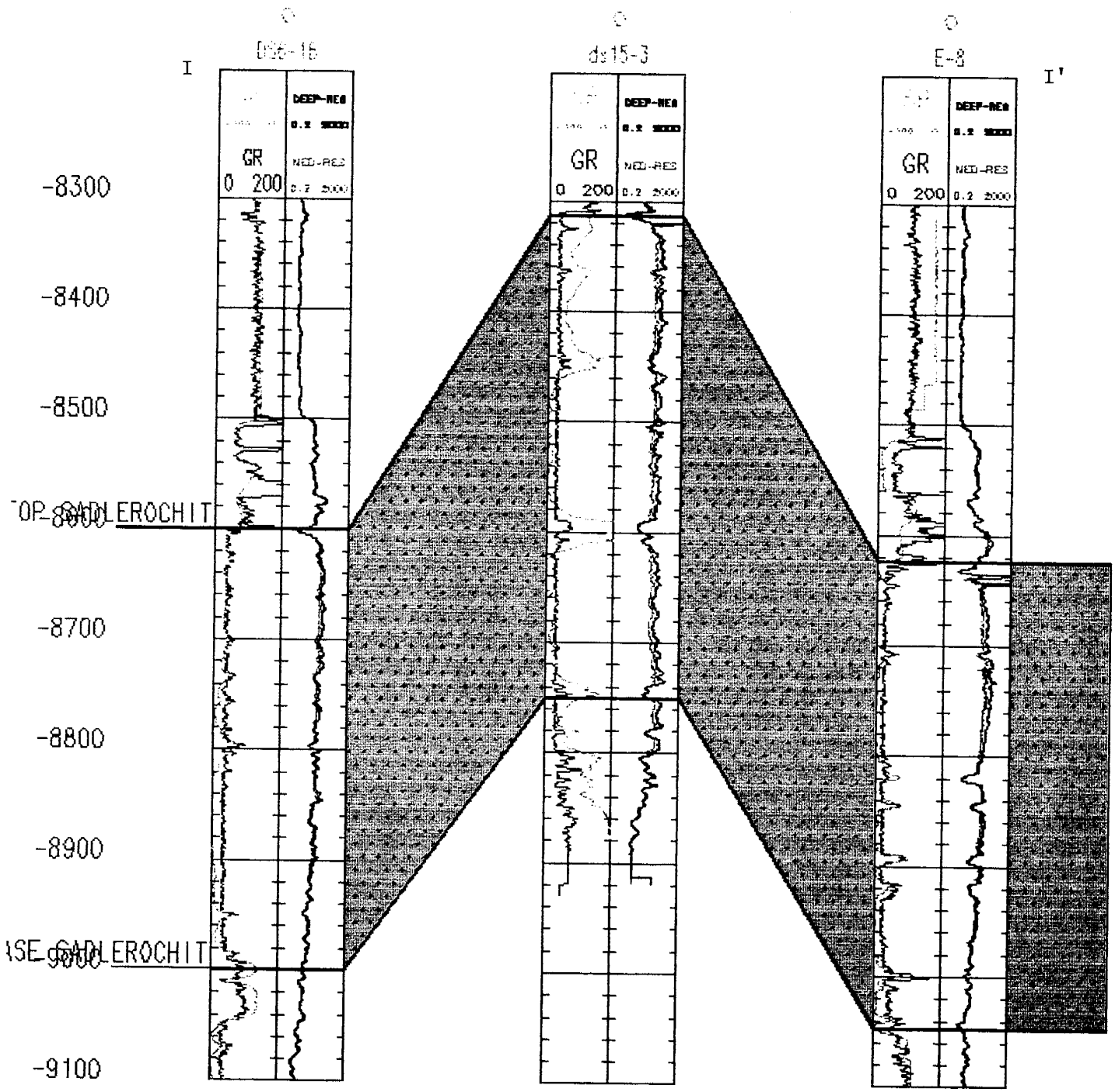


Figure VIII-16. Cross Section Along Line I-I' in Prudhoe Bay Field.

prudhoe: J-J' / TVDSS

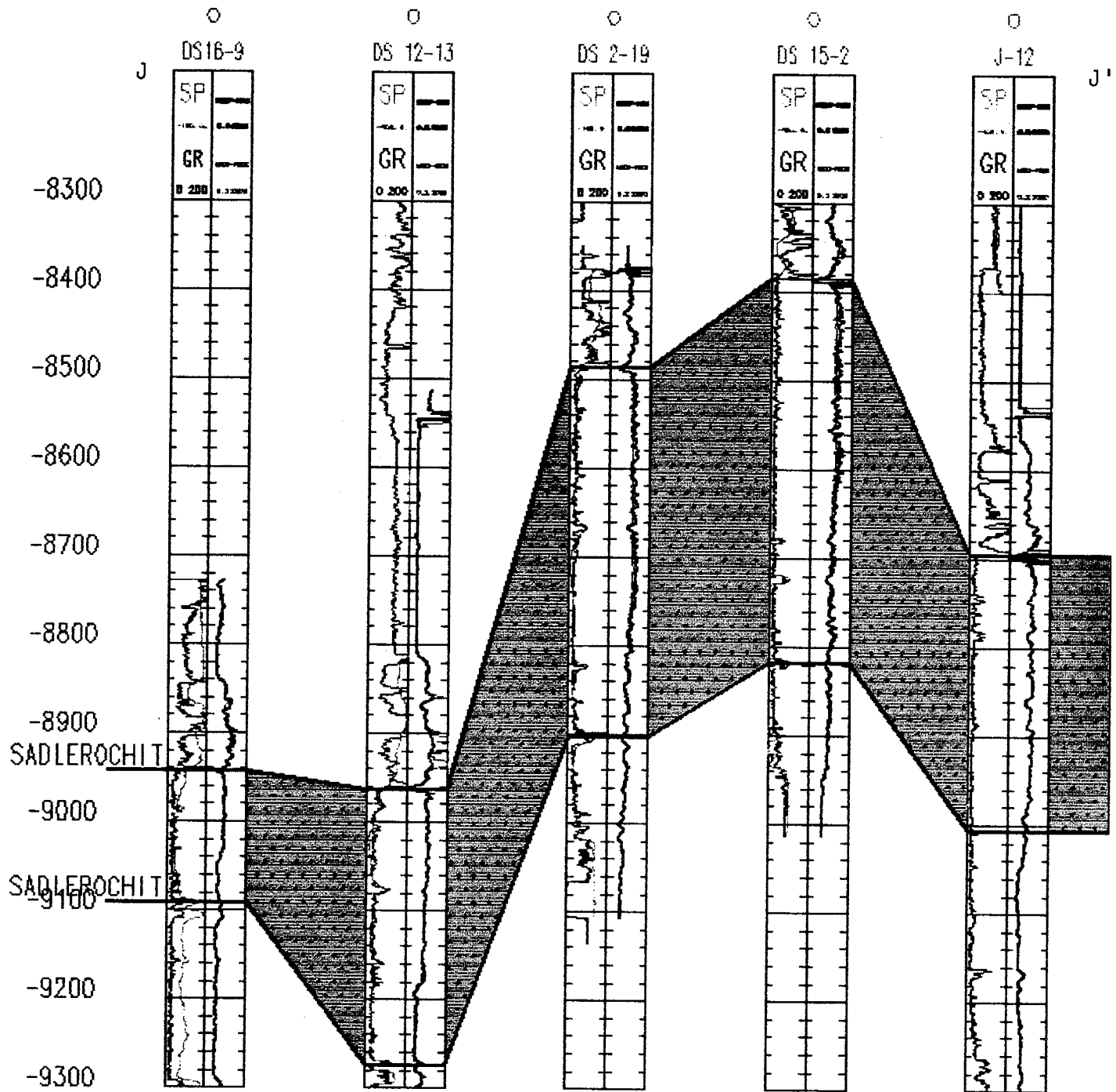


Figure VIII-17. Cross Section Along Line J-J' in Prudhoe Bay Field.

prudhoe: K-K' / TVDSS

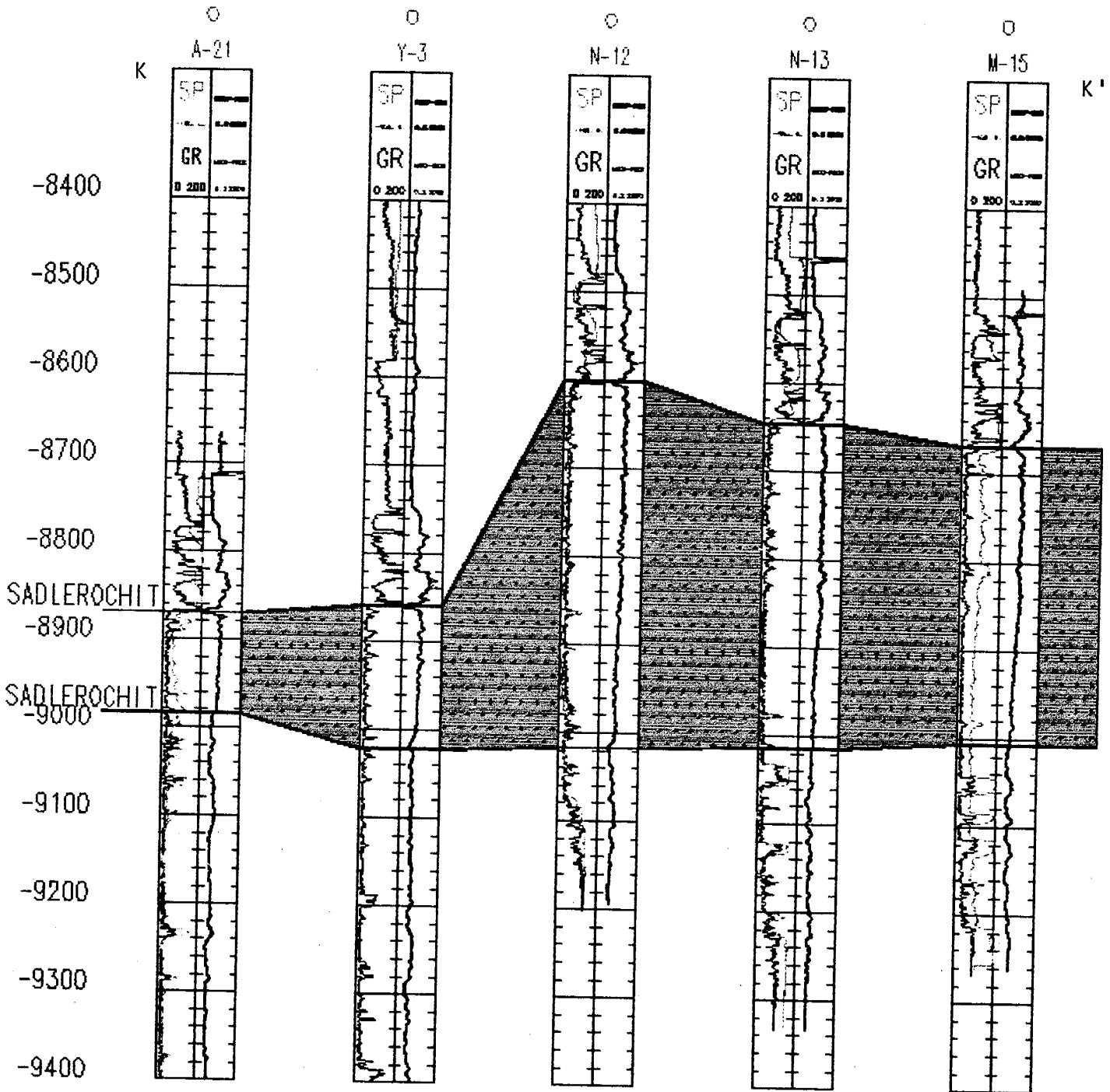


Figure VIII-18. Cross Section Along Line K-K' in Prudhoe Bay Field.

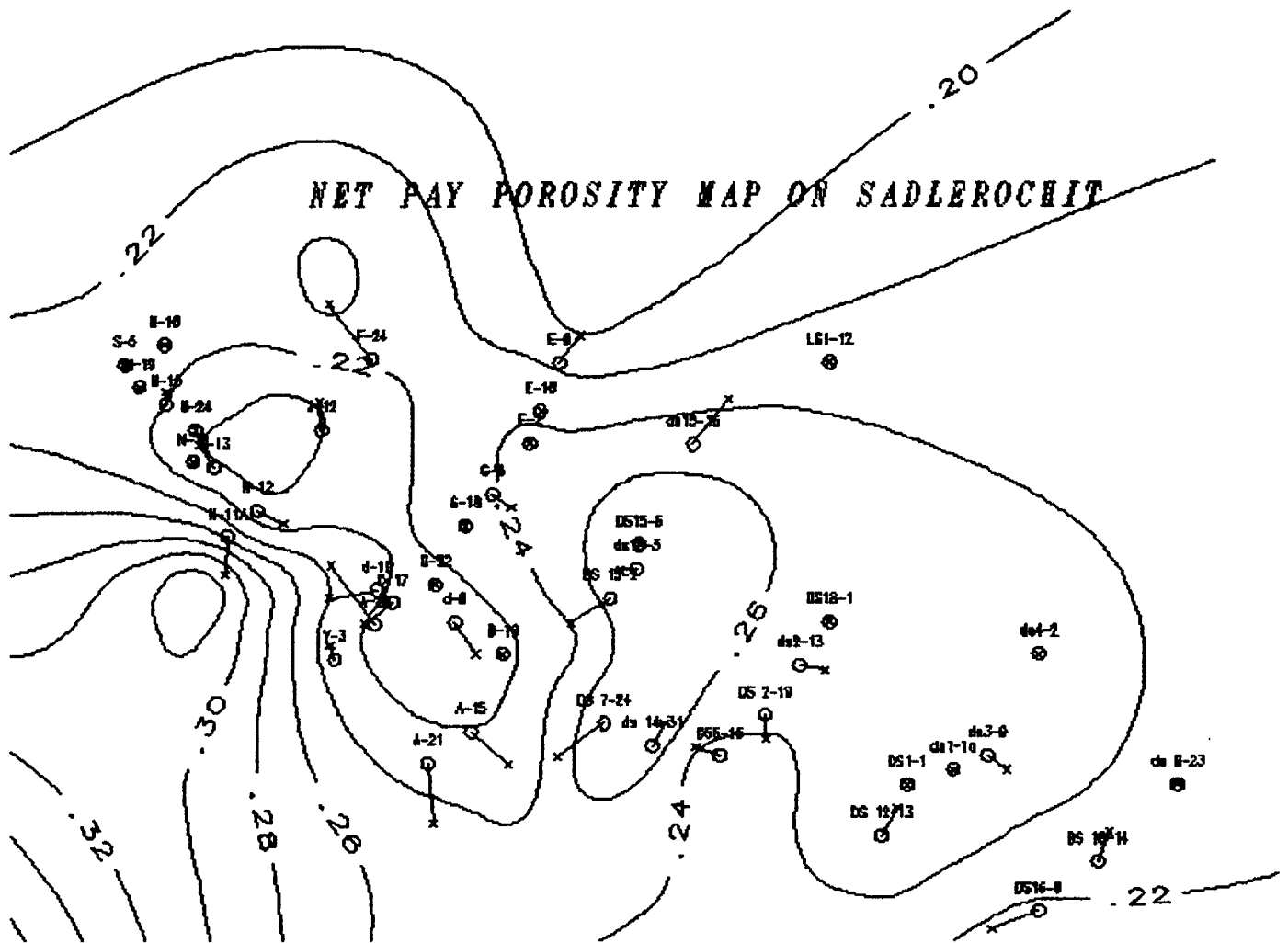


Figure VIII-19. Net Pay Porosity Map on Sadlerochit Group.

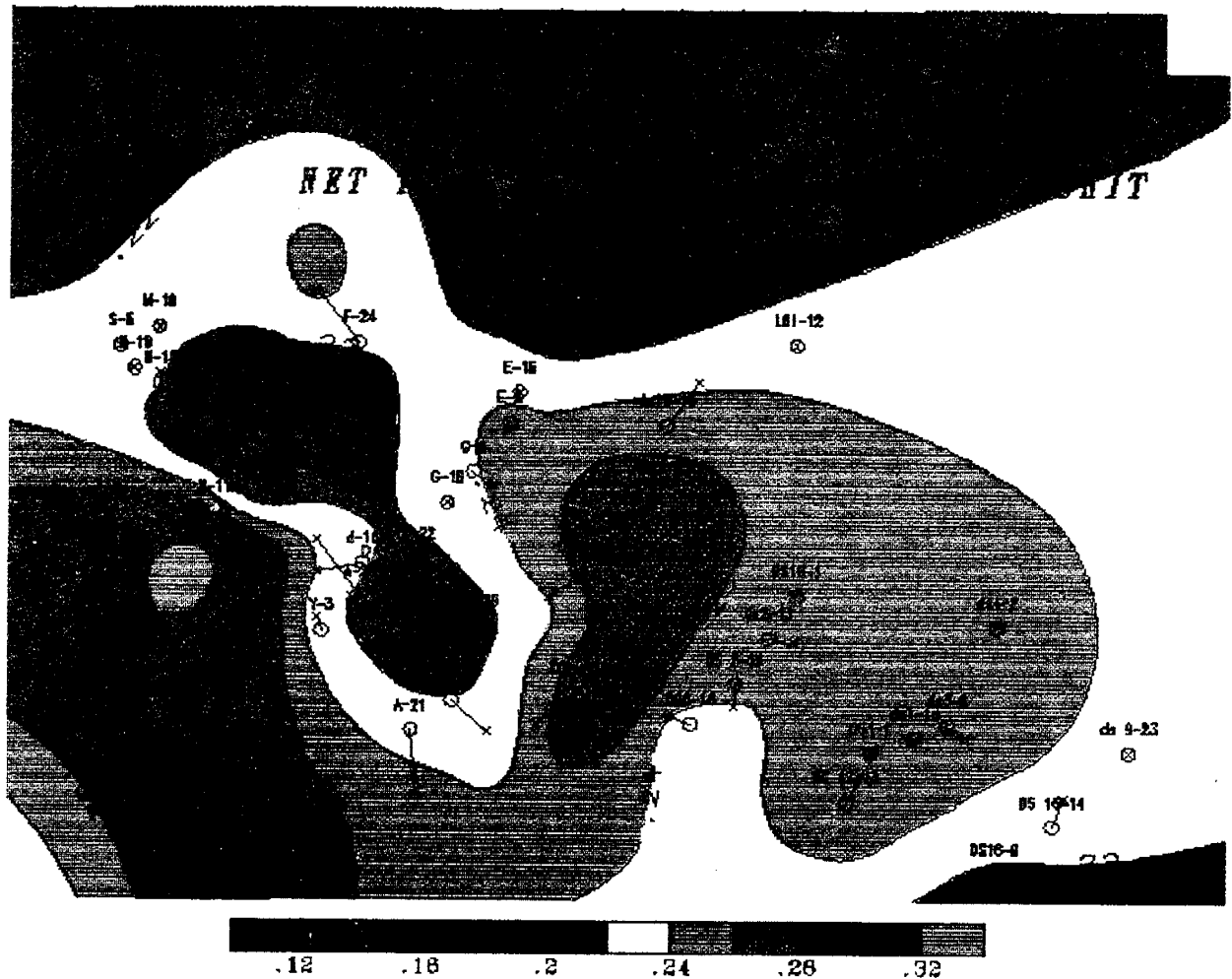


Figure VIII-20. Color-Fill Net Pay Porosity Map on Sadlerochit Group.

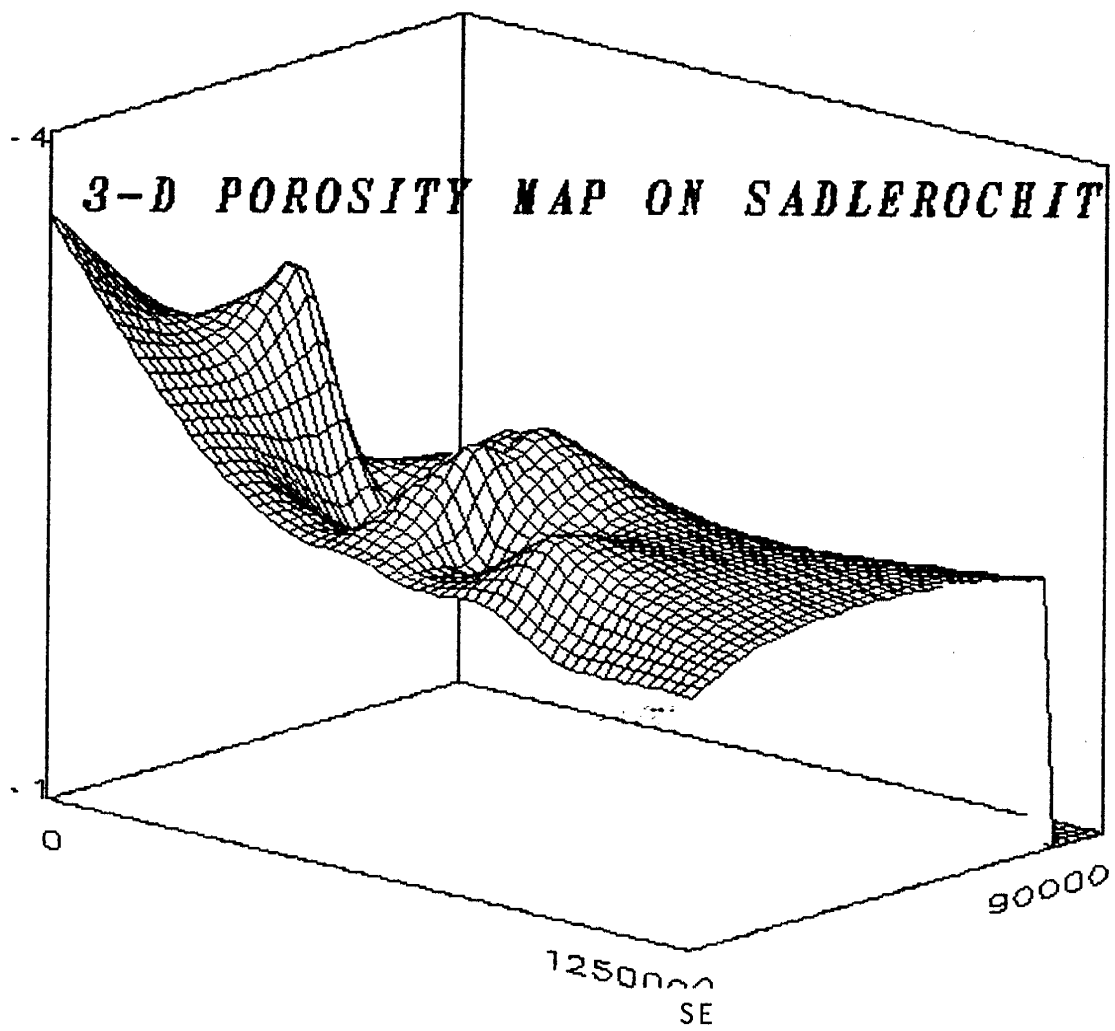


Figure VIII-21. 3-D Porosity Map on Sadlerochit Group.

NET PAY WATER SATURATION MAP  
ON SADLEROCHIT

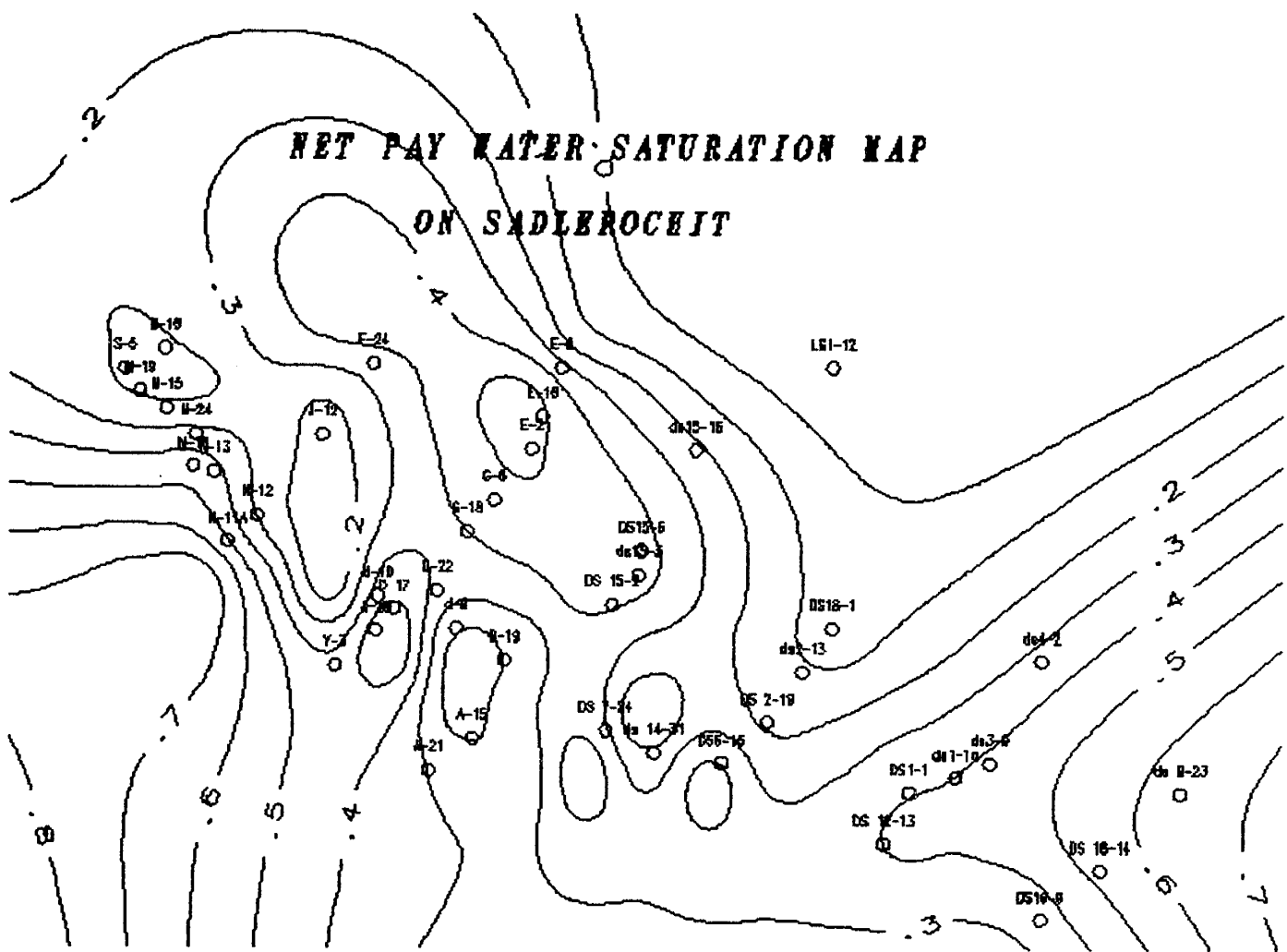


Figure VIII-22. Net Pay Water Saturation Map on Sadlerochit Top.

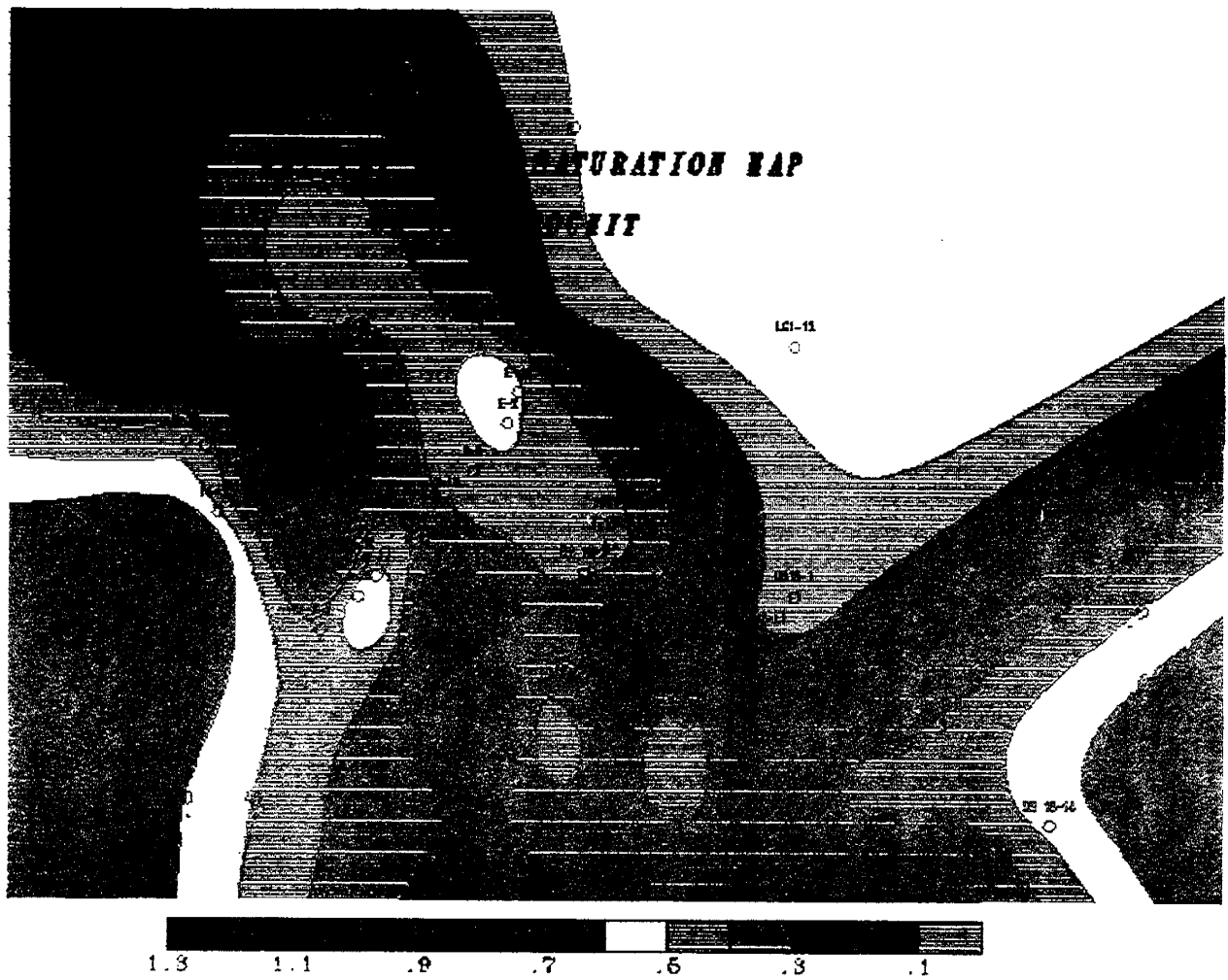


Figure VIII-23. Color-Fill Net Pay Water Saturation Map on Sadlerochit Group.

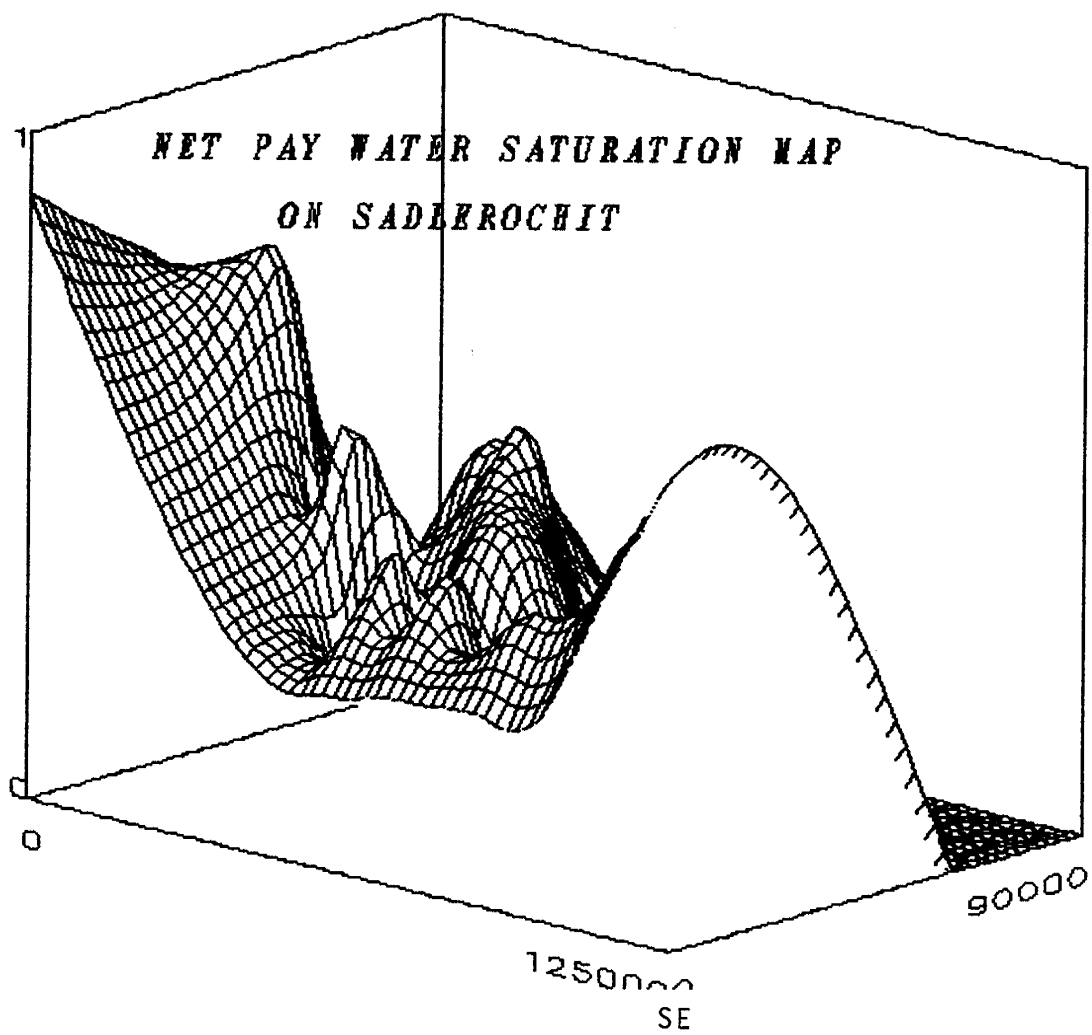


Figure VIII-24. 3-D Net Pay Water Saturation Map on Sadlerochit Group.

Regionally the structure on top of the Ivishak sandstone in the Prudhoe Bay field is expressed as an east to southeast anticlinal trend containing two prominent highs, one at Prudhoe Bay, called "Prudhoe High," and one in Colville River delta area, called "Colville High" (Figure VIII-25). Preliminary exploration in the region, correctly indicated the Prudhoe High to be more promising than the Colville High, because the arrangement of tilting was believed to have led to a migration of hydrocarbons eastward toward the Prudhoe High (Bowsher, 1987).

In the Prudhoe Bay field the Ivishak sandstone consists primarily of two fine-grained to medium-grained sandstone sequences separated by an interval of massive conglomerates. The top of the Ivishak sandstone is commonly placed at the base of a thin conglomerate that is overlain by calcareous mudstones of the Shublik formation. Sandstones of the lower sequences are separated by major shale interbeds. The sandstones are clean, massive, occasionally conglomeratic, and grade downward into finer grained sandstones interbedded with siltstone and shale that overlie the Kavik shale.

The net-pay true vertical thickness contour map on Ivishak formation, and the corresponding 3-D view (Figures VIII-26 and VIII-27, respectively), show the net-pay thickness distribution of Ivishak sandstone across the field to trend in the same manner as structural crest, from northwest to southeast.

## **C2. Cross Sections**

It can be observed from cross sections that the crest of the Prudhoe Bay anticline is lying in a northeast-southwest direction with a gentle dipping south flank and a highly faulted northern flank. The average dip from the crest is about 1-2°. Wells DS 16-14, DS 2-13, DS 15-16, DS 15-2, DS 15-3, D-10 and D-9 etc., lying on the northern flank of the anticline, are situated near structural crest as indicated by the cross sections (Figures VIII-8 and VIII-9). Wells A-15, A-21, DS 16-9, DS 12-13, N-11A etc., situated on the south flank of the anticline, exhibit dip from the crest (Figures VIII-8, VIII-9, and VIII-13). Wells F-24, E-8, and E-16 situated on the northern flank of the anticline also exhibit gentle dip (Figures VIII-7, VIII-11, and VIII-15). However, due to the highly faulted nature of the northern flank, some wells exhibit unusually steep dip, especially compared with wells on the southern flank.

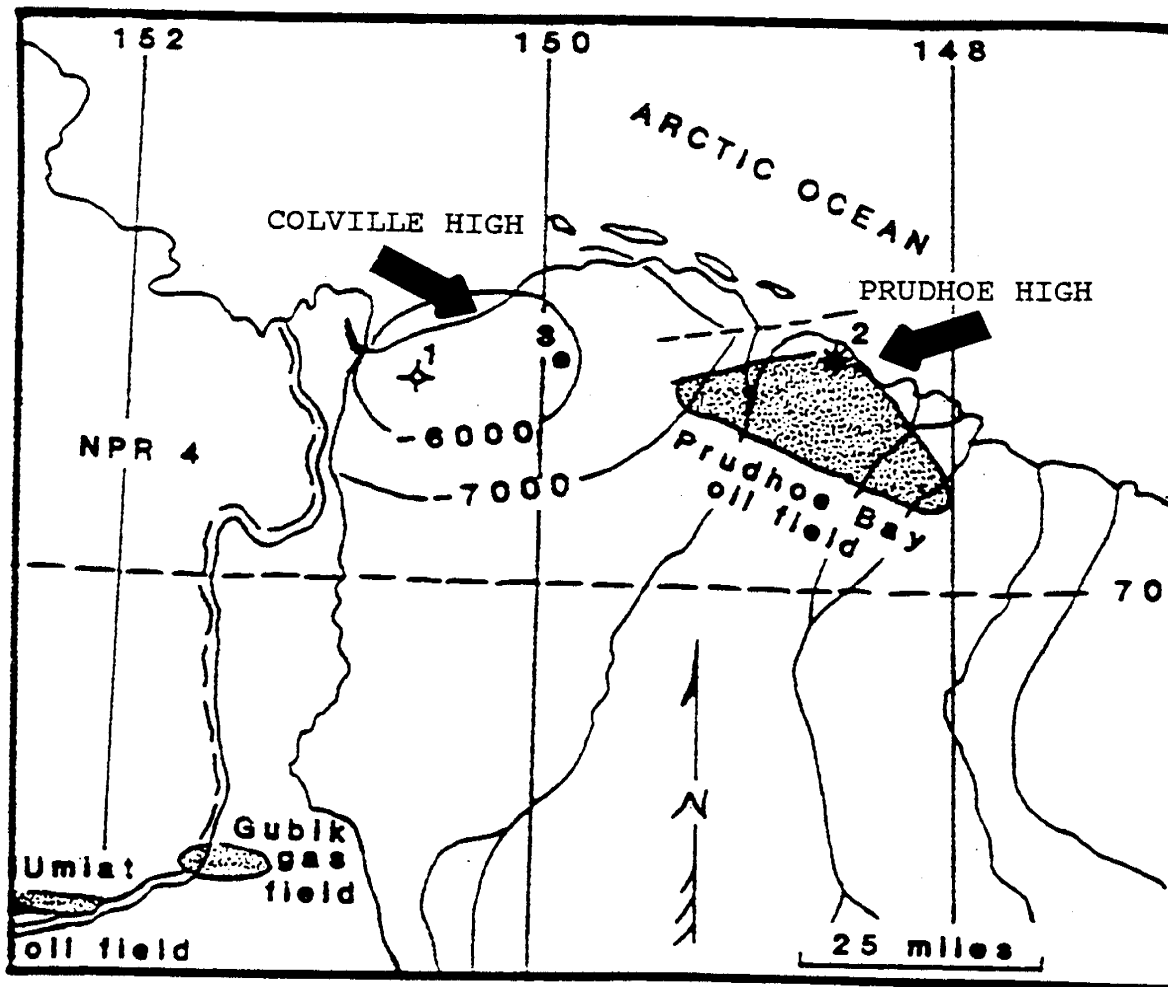


Figure VIII-25. Location of Colville and Prudhoe Structural Highs (Bowsher, 1987).

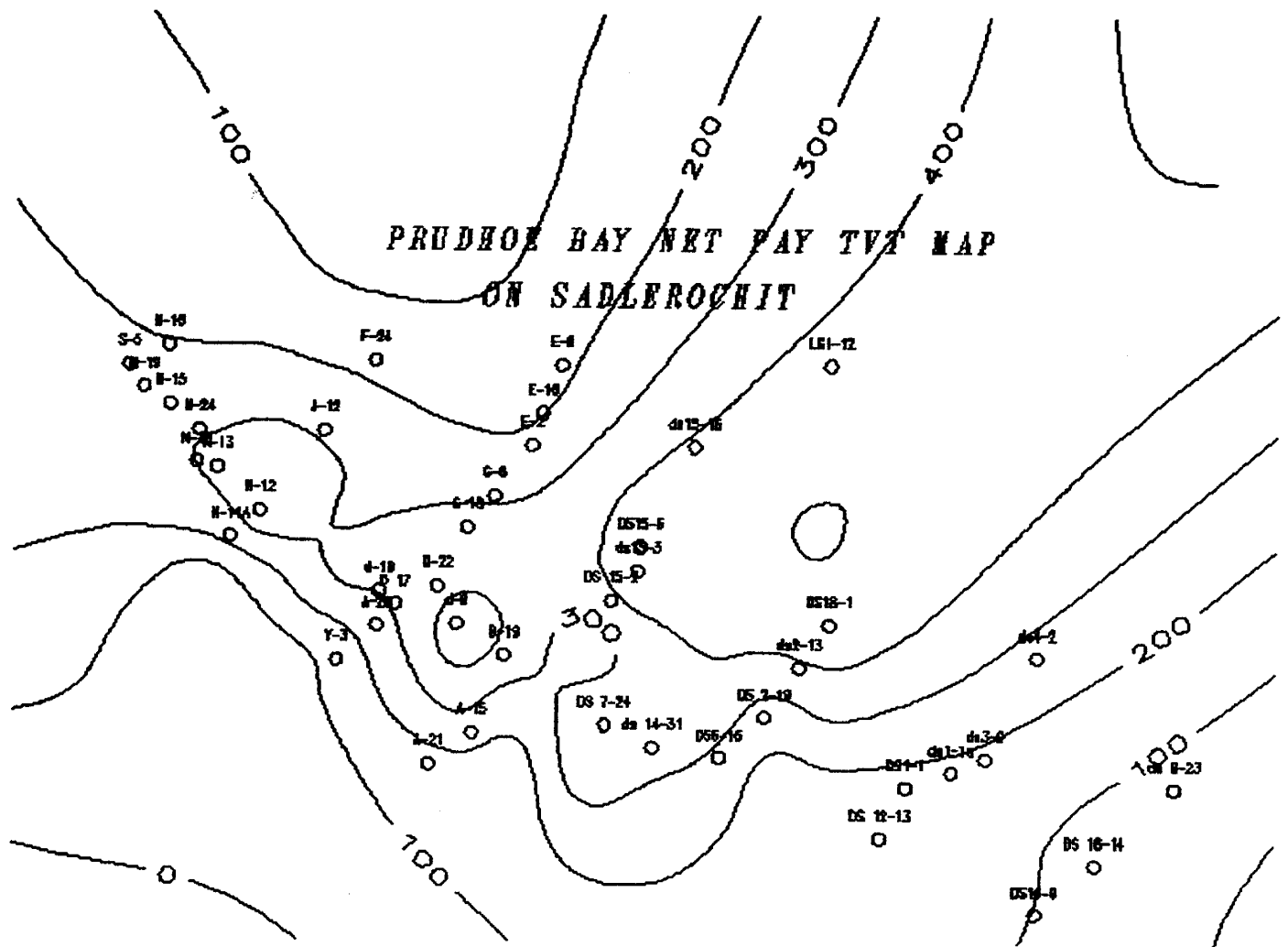


Figure VIII-26. Prudhoe Bay Field Net Pay True Vertical Thickness Map on Sadlerochit Group.

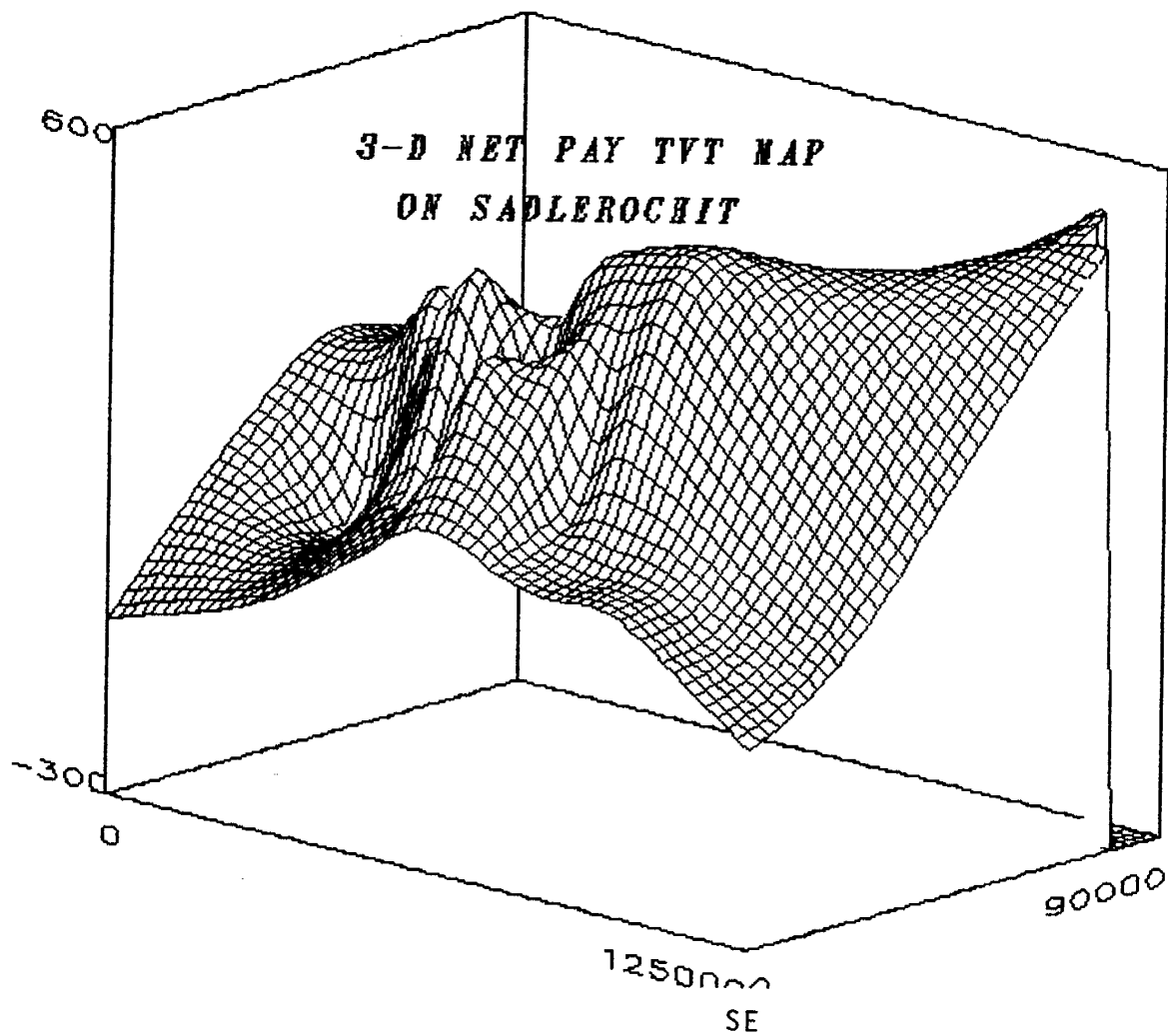


Figure VIII-27. Prudhoe Bay Field 3-D Net Pay True Vertical Thickness Map on Sadlerochit Group.

There is no abrupt change in Ivishak formation sand thickness from well to well, although changes in sand thickness can be seen in distant wells. Picking the base of the Ivishak formation is difficult in several wells. As such, gross thickness maps may be subjected to some interpretation and future adjustments. However, log analysis was performed on the oil bearing zone only, in order to better evaluate the oil bearing rock in terms of porosity,  $S_w$ , etc.

### **C3. Porosity**

Porosity was calculated from neutron and density porosity logs using the cross plot method. Porosity was determined in each well at half feet interval. Average porosity of the sand for each well is shown in Table VIII-1.

The net pay porosity contour map was generated and is shown in Figure VIII-19. Color-filled contour and 3-D view of net-pay porosity map were also generated and are shown in Figures VIII-20 and VIII-21, respectively. From all these maps, the distribution pattern of porosity across the field is evident. A minimum porosity value of 20% was found in J-12 well near the crest in the western portion of the structure, whereas a maximum of 31% porosity was found in N-11A well on the southern flank of the structure. The entire structure along the crest is characterized by good porosity, ranging from 22% to 28%, except for a small area on the western side of the field where porosities range from 18% to 20%.

As mentioned earlier, the Ivishak formation sandstone consists primarily of two fine-to-medium grained sandstone sequences separated by an interval dominated by massive conglomerates (Jamison et al., 1980). The lower sequence is about 300 ft thick and the porosity averages 20%, whereas the upper sandstone sequence is more than 200 ft thick with average porosity ranging from 25% to 30%. The conglomerates are more than 140 ft thick in the north-eastern part of Prudhoe Bay field and thin to less than 40 ft to the east, west, and south with porosities ranging from 10% to 20%.

### **C4. Saturation**

Archie's equation was used to calculate water saturation in this study. Tortuosity ( $a$ ), cementation ( $m$ ), and saturation exponent ( $n$ ), values of 1, 1.73 and 2 were used respectively to calculate water saturation in all the wells. Water saturation was also calculated using three other equations, including Laminar-Simondoux, Indonesian, and Dual-water. Results were compared with Archie's values. The comparison of water saturations are shown in analysis result plot (Figure VIII-3). Both the Laminar-Simondoux and Indonesian results compare

favorably with Archie's results. Significant differences are evident between the Dual-Water and Archie's values, most notably in shaly zones. These differences warrant further research.

Any sample point with more than 80% water saturation was excluded in net pay determination. After deduction for the non-pay, the resultant net summation of saturation-feet was divided by the net vertical thickness to obtain the average water saturation. Table VIII-1 summarizes the average water saturation of the sand for each well.

A net pay water saturation contour map was generated and is shown in Figure VIII-22. Color-filled contour and 3-D of this map were also generated for better visual illustration and are shown in Figures VIII-23 and VIII-24, respectively. These maps show the lateral distribution of water saturation across the field. Maximum water saturation is concentrated in the southeast and southwest corners of the field with values ranging from 60 to 80%. In contrast, the entire northern flank is characterized by low water saturations ranging from 20 to 30%. A maximum of 66% water saturation was observed in the southwest at well N-11A and a minimum of 7% was observed in the northern flank at well DS 15-16. All along the crest of the structure, water saturation varies from 30 to 40%, with the exception of 20% in some scattered areas. From these data, it is apparent that the northern flank of the field represents the best production potential.

The Sadlerochit group oil-water contact is irregular and slightly tilted, ranging from slightly above 8,950 ft subsea in the Eileen Area to subsea depths of between 8,990 and 9,050 ft within the Main Area (Wadman et al., 1979). In the Main area, the contact is deepest along an approximate northwest-southeast trending line. This line generally corresponds to the occurrence of the thickest heavy-oil/tar interval immediately above the contact. The Sadlerochit group aquifer is quite extensive, covering about 10,000 sq. miles, but the effective volume is much smaller due to low permeability, resulting in limited expected influx.

A contour map of oil saturation and corresponding color-filled contour and 3-D views were also generated and are shown in Figures VIII-28 through VIII-30. These plots corroborate the tabular data in showing that the best hydrocarbon potential exists in the northern portion of the field.

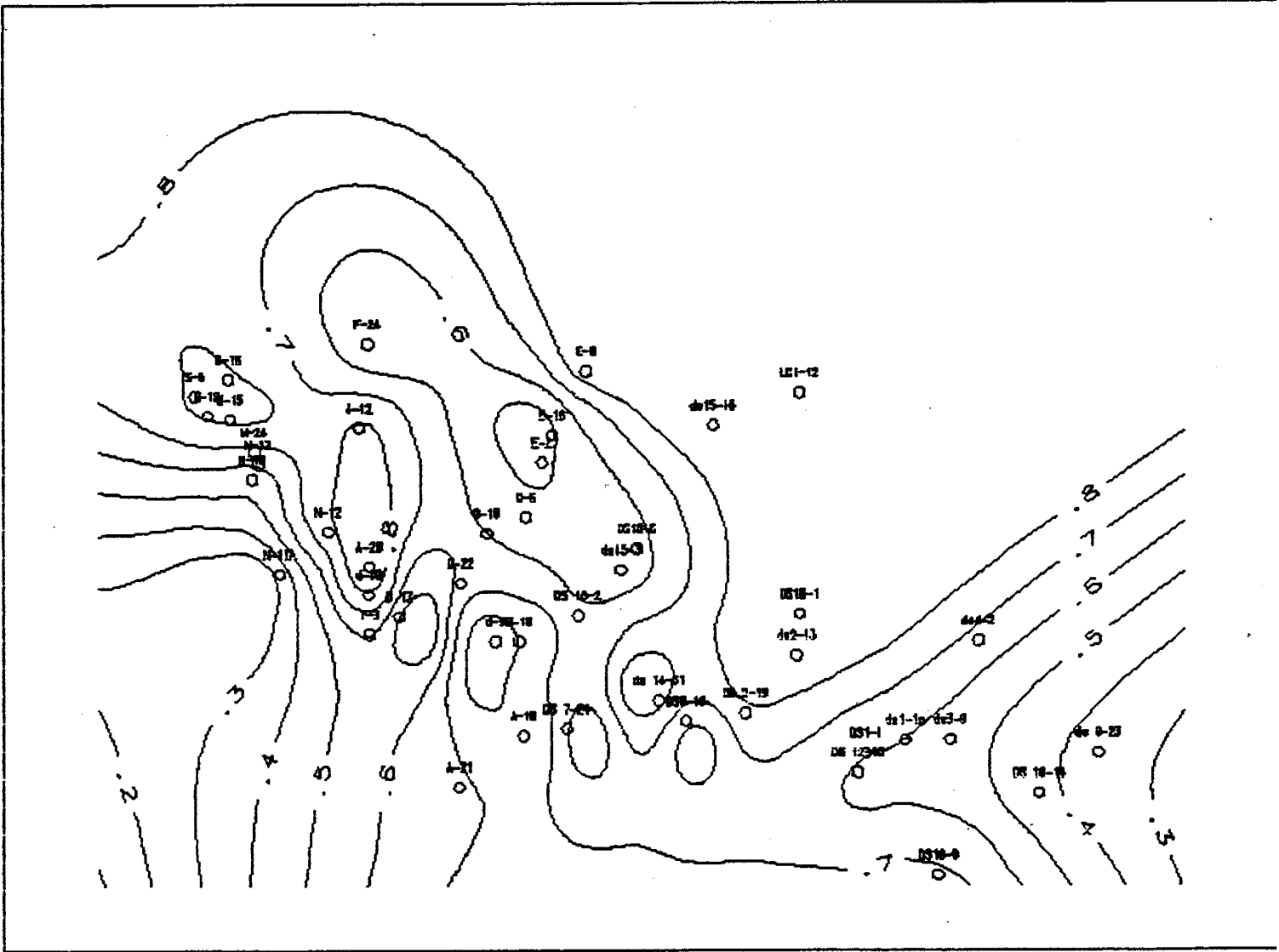


Figure VIII-28. Sadlerochit Group Net Pay Oil Saturation Contour Map.

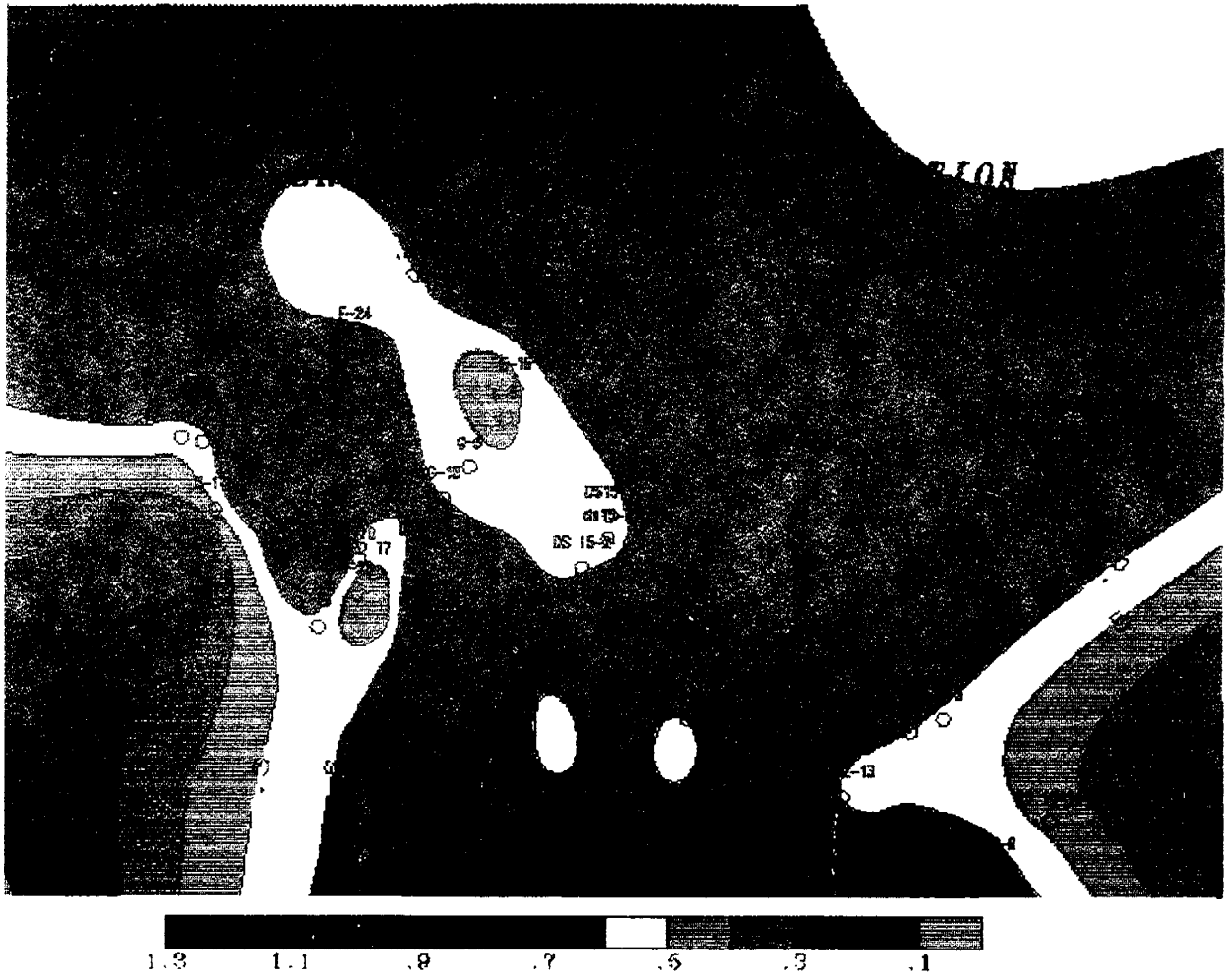


Figure VIII-29. Sadlerochit Group Net Pay Oil Saturation Color-Filled Contour Map.

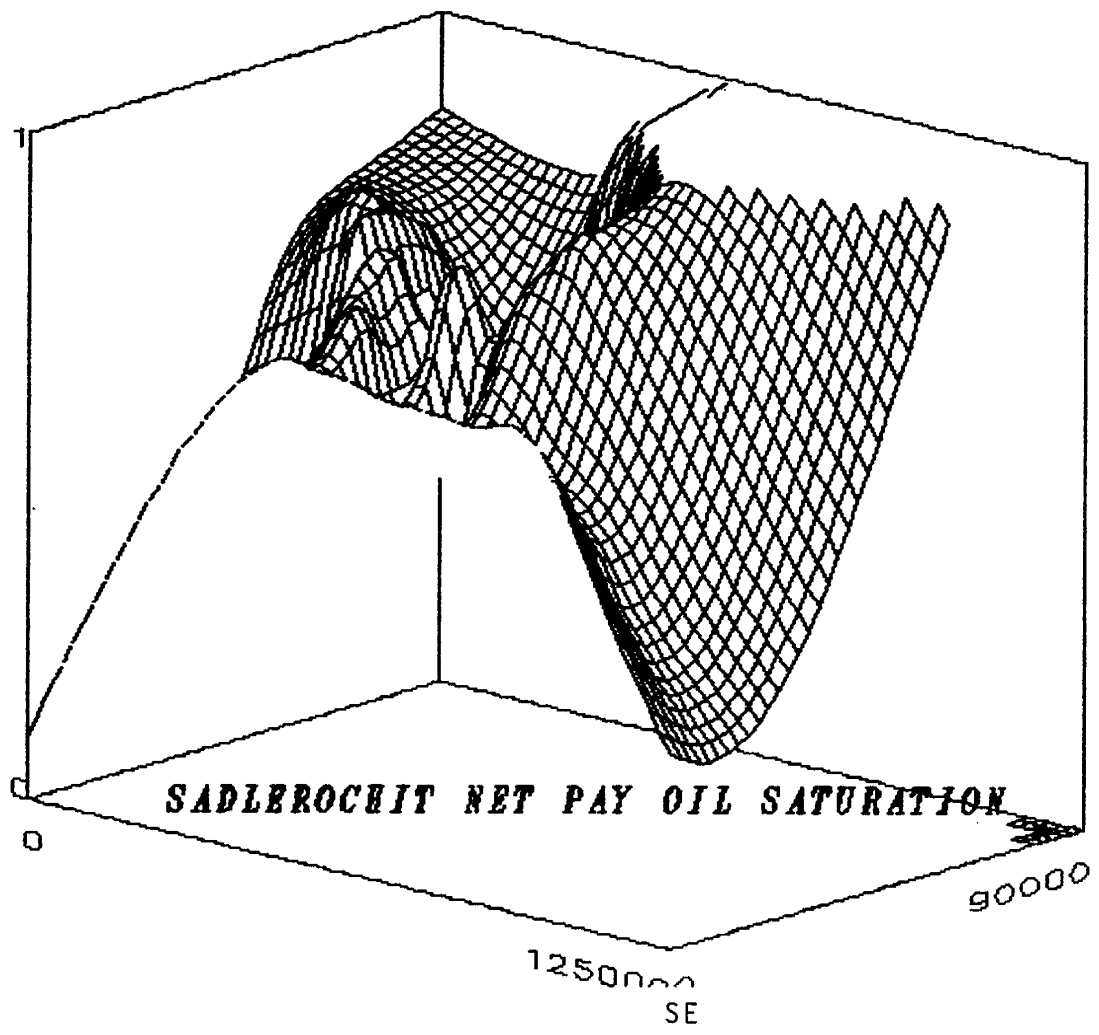


Figure VIII-30. Sadlerochit Group Net Pay Oil Saturation (3-D view).

### C5. Sand Quality

Sand quality was evaluated by calculating the net hydrocarbon feet values,  $h \times (1-S_w) \times \emptyset$ , for each well which are shown in Table VIII-1, where,

- h = Net thickness,
- S<sub>w</sub> = Water saturation, and
- ∅ = Porosity.

Contour and 3-D view maps were also generated with hydrocarbon feet volume and are shown in Figures VIII-31 and VIII-32, respectively.

The 3-D view map shows that the best sand in terms of hydrocarbon pore volume occurs all along the crest line of the structure in northwest-southeast direction. It implies that the principal hydrocarbon accumulation in Prudhoe Bay field lies near the crest. The data of Table VIII-1 also show that the well D-9, D-10, DS 2-13 and DS 15-16 have the best sand quality with more than 80 feet of hydrocarbon feet values, whereas well DS 16-14 and N-11A have comparatively lower hydrocarbon feet values, 7.7 ft and 10.2 ft, respectively. These two wells with lower hydrocarbon feet values are located in the southern flank of the structure in close proximity to the oil-water contact. The corresponding higher average water saturations around these wells resulted in lower hydrocarbon feet values.

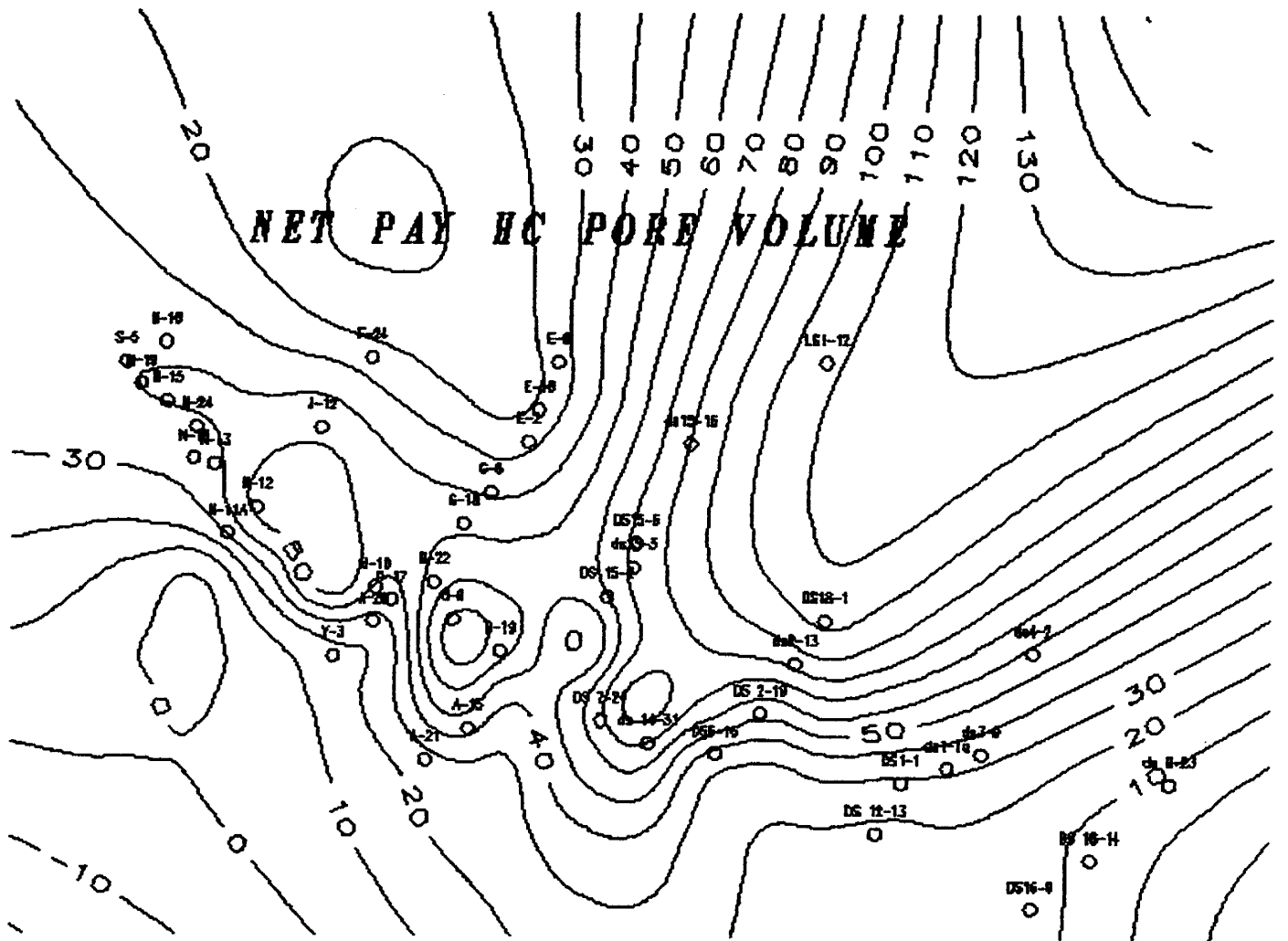


Figure VIII-31. Net Pay Hydrocarbon Pore Volume Contour Map on Sadlerochit Group.

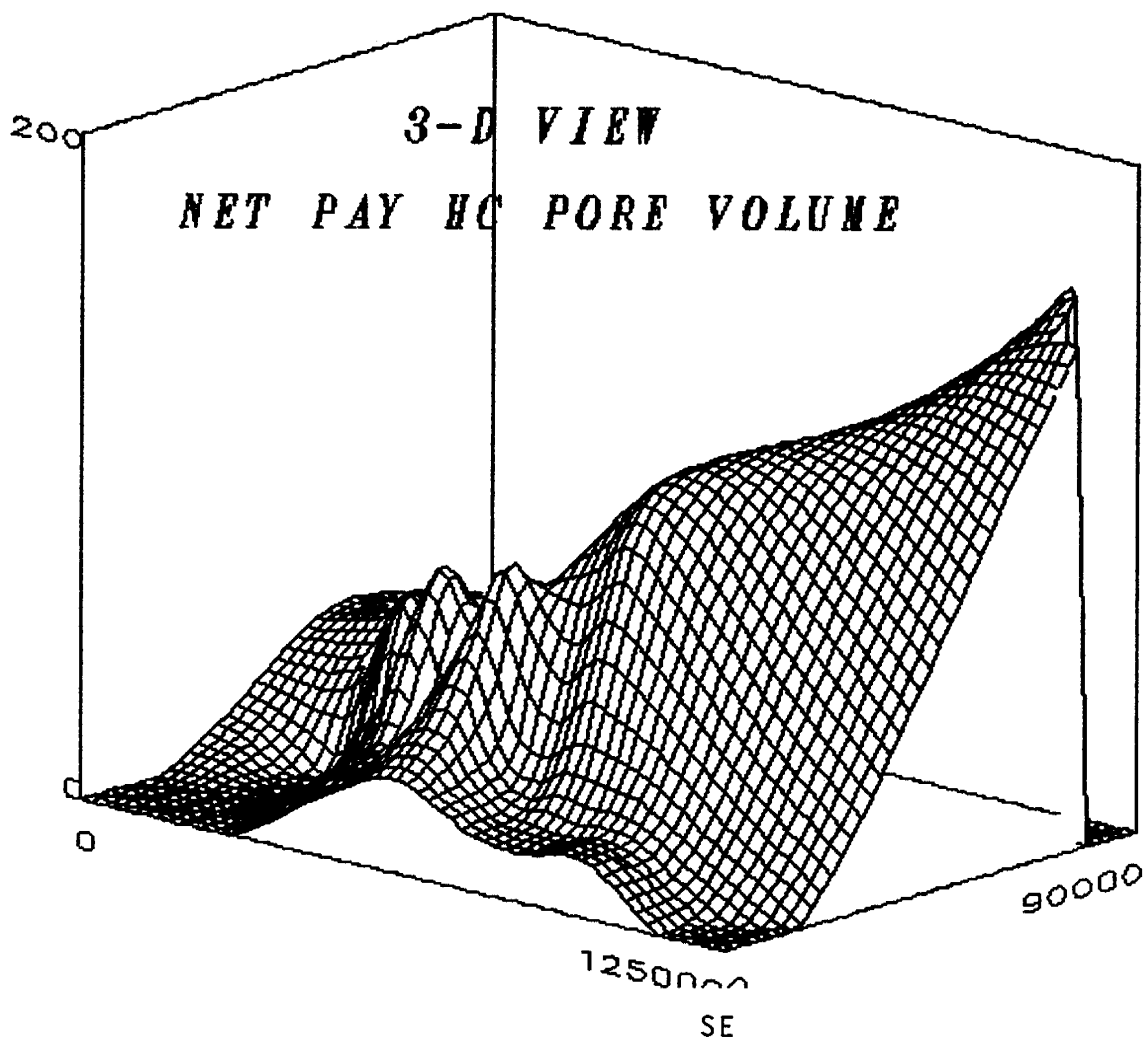


Figure VIII-32. 3-D View of Net Pay Hydrocarbon Pore Volume on Sadlerochit Group.

## CHAPTER IX: NONPRODUCING FIELDS, NORTH SLOPE, ALASKA

---

### A. LISBURNE FIELD

Lisburne field, the North Slope's only carbonate producer, is located within and adjacent to Prudhoe Bay (Figure IX-1). The field was discovered in 1968 in the Arco Alaska Inc./Humble (Exxon USA) Prudhoe Bay State well No. 1. This well was also the Prudhoe Bay discovery well. Initial test rates ranged from 434 to 1150 BOPD and 1.3 to 22 MMCFPD. Mississippian and Pennsylvania carbonates of the Lisburne group comprise the producing zones. Development of Lisburne field was delayed due to the emphasis that was placed on the shallower, more productive Ivishak sandstones of the Prudhoe Bay field (Thomas et al., 1993).

The production from Lisburne field was formally approved by the state in 1986, with most drilling occurring since that time. Arco Alaska Inc. was designated as operator. Approximately 80 wells have been drilled to date. Production from Lisburne field has yielded to date 95 MMBO and 726 BCF of gas. Little-to-no recent oil production has occurred from Lisburne field, but gas production does continue, with 11.3 BCF reported for May of this year.

Geologically, the Lisburne group is dominated by shallow marine carbonates (including both limestones and dolomites). Minor interbeds of clastics, cherts, and thin evaporites are also found. The group is subdivided into the Mississippian Alapah formation, and overlying Pennsylvanian Wahoo formation. A typical well log with the Lisburne group between 8,720 and 10,000 ft is shown in Figure IX-2. The Lisburne group averages 1,800 feet in thickness.

Porosity in the Lisburne group averages 10%, but permeabilities are low, averaging only 1 md. Porosity is predominately secondary, and is a function of facies distributions, dolomitization, and leaching (Thomas et al., 1993). Occasional vuggy dolomitic porosities up to 20% can be found. Vertical fracturing is common, but it is generally partially or entirely cemented with calcite. However, fractures are believed to have contributed significantly to Lisburne group production rates.

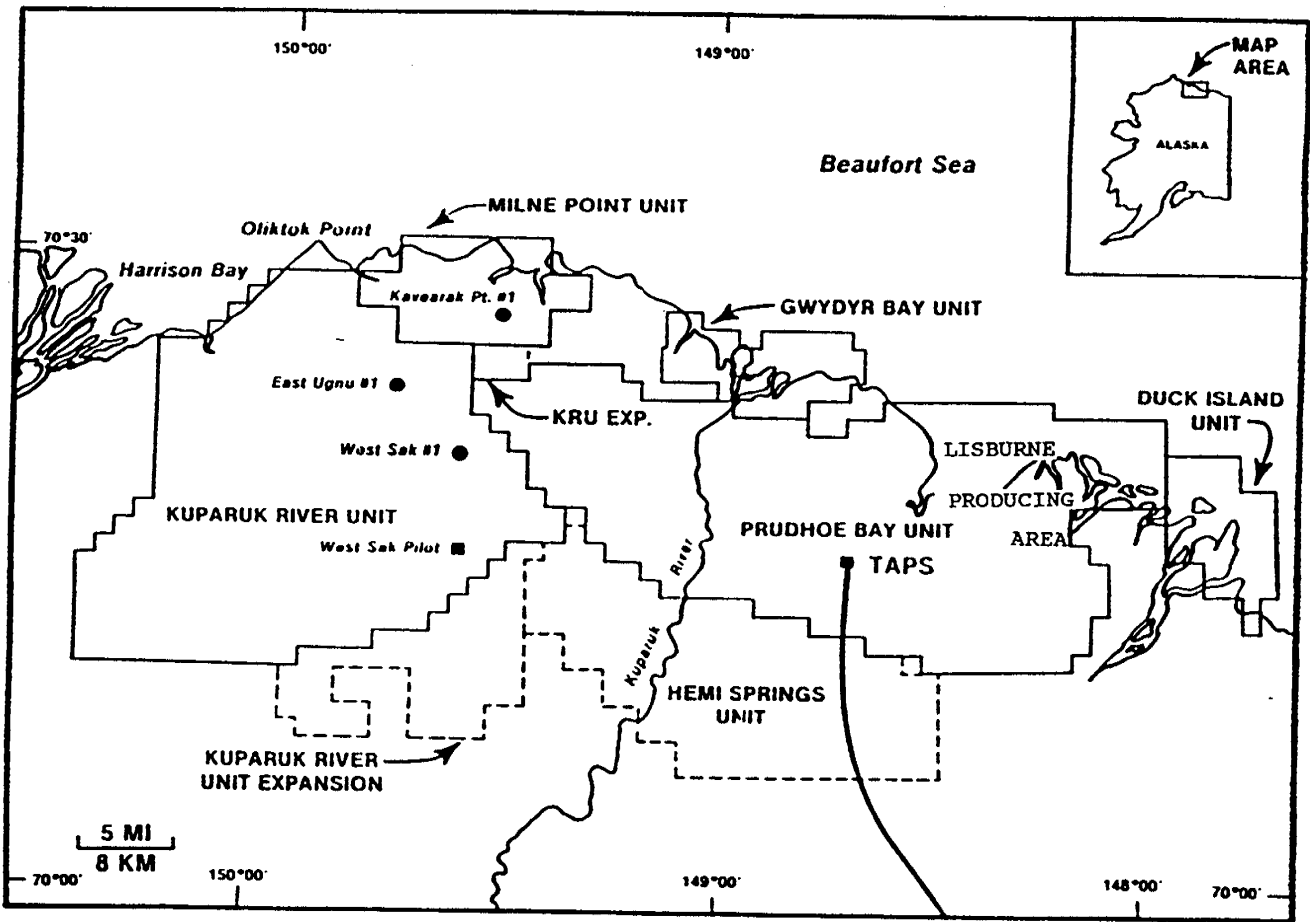


Figure IX-1. North Slope Fields, Including Lisburne Field (adapted from Werner, 1985).

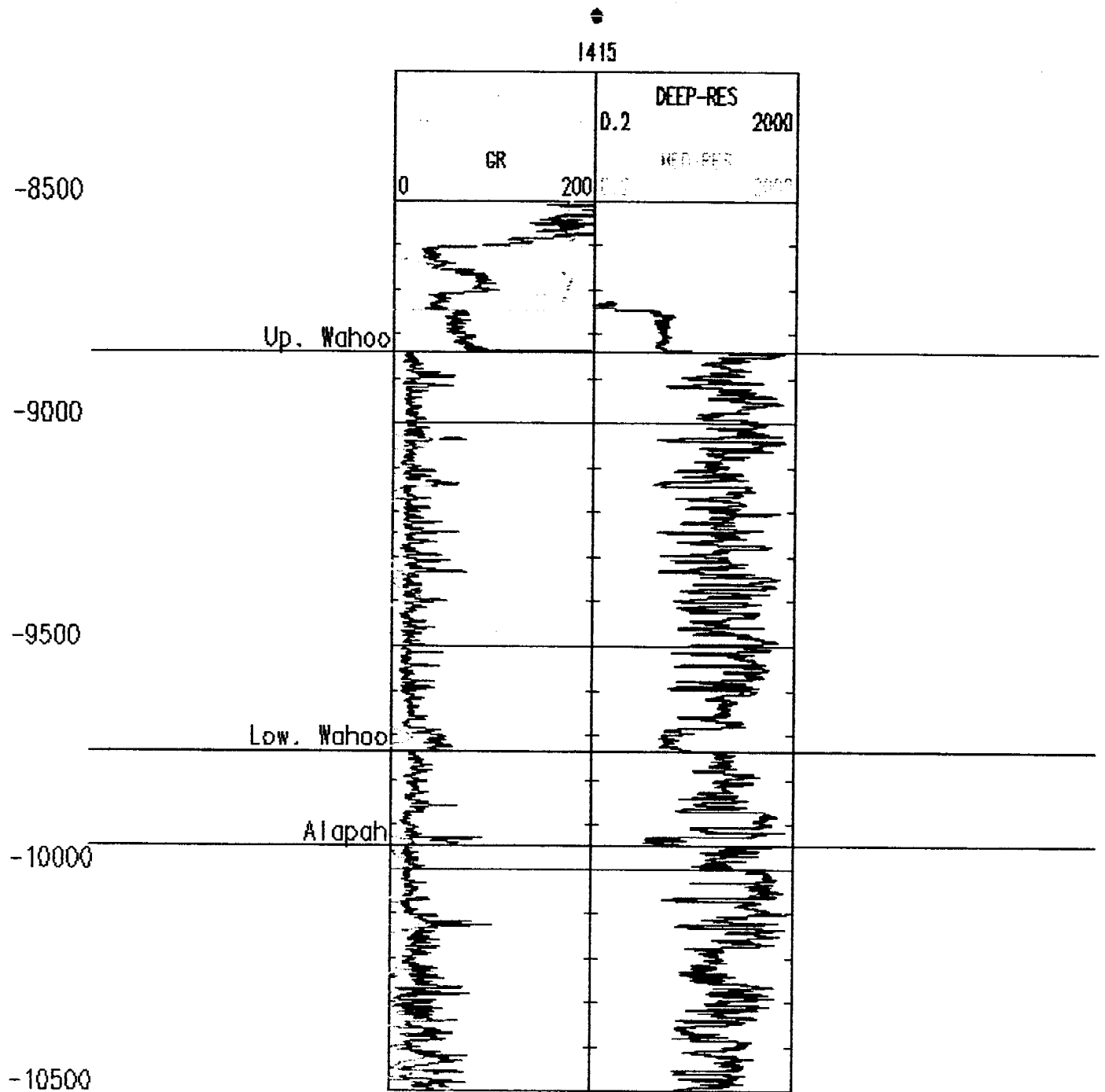


Figure IX-2. Log Plot of the Lisburne Field L4-15 Well with Lisburne Group and Its Subdivisions (formations).

Structurally, the top of the Lisburne group dips gently southward off an east-west trending anticline. Faulting on the north side of the field terminates the field while the east and southeast sides of the field are truncated by the Lower Cretaceous Unconformity. A gas cap is present above 8600 feet subsea, and the oil column extends to approximately 9300 feet subsea. Oil staining exists below this depth.

Figure IX-3 displays stratigraphic cross section A-A' across Lisburne field. Well locations are shown on the Lisburne field base map (Figure IX-4). The distinctive low gamma and high resistivity log characteristics are evident in this cross section. High gamma ray kicks may represent terrigenous clays or shales.

Initial petrophysical analysis completed by PDL on the L4-15 yielded an average Lisburne group porosity of 9.5%. Average shale content was calculated to be 7%. Computed water saturation was quite low (32.5%). This suggests a more in-depth analysis of log-analysis input parameters may be required in order to better assess water saturation. In particular, values of "a," "m," and "n" utilized by Archie's equation may need additional fine tuning prior to future analysis.

## **B . POINT MCINTYRE FIELD**

Point McIntyre field, one of the most recent exploration discoveries on the North Slope, lies mostly offshore in Prudhoe Bay, Alaska (Figure IX-5). Arco Alaska Inc., Exxon USA and British Petroleum Alaska jointly announced the discovery in 1989. The Arco Alaska Inc./Exxon USA Point McIntyre well No. 3 tested at almost 2500 BOPD. The first delineation well tested at a maximum rate of 5350 BOPD and the second delineation well tested up to 5400 BOPD (Thomas et al., 1993). Based in part on these flow rates, Arco Alaska Inc. has estimated recoverable reserves of 300 MMBO.

Both the K-10 or Cretaceous Seabee and Lower Cretaceous Kuparuk River formations tested oil at Point McIntyre field. In the Point McIntyre well No. 3, the Seabee flowed 1016 BOPD of 28° API gravity oil and 772 MCFPD of gas from a zone lying between 8480 and 8890 measured feet below surface. But the Lower Cretaceous Kuparuk River Sand, flowing 2442 BOPD of 28° API gravity oil and 1917 MCFPD of gas in this well, is the main productive horizon. Two additional wells (the Point McIntyre wells Nos. 4 and 5) flowed at average respective rates of 5349 BOPD and 5415 BOPD from the Kuparuk River formation. These wells also produced between one and three MMCFPD of gas. A total of ten delineation wells have been drilled at Point McIntyre field. Figure IX-5 shows bottom hole well locations.

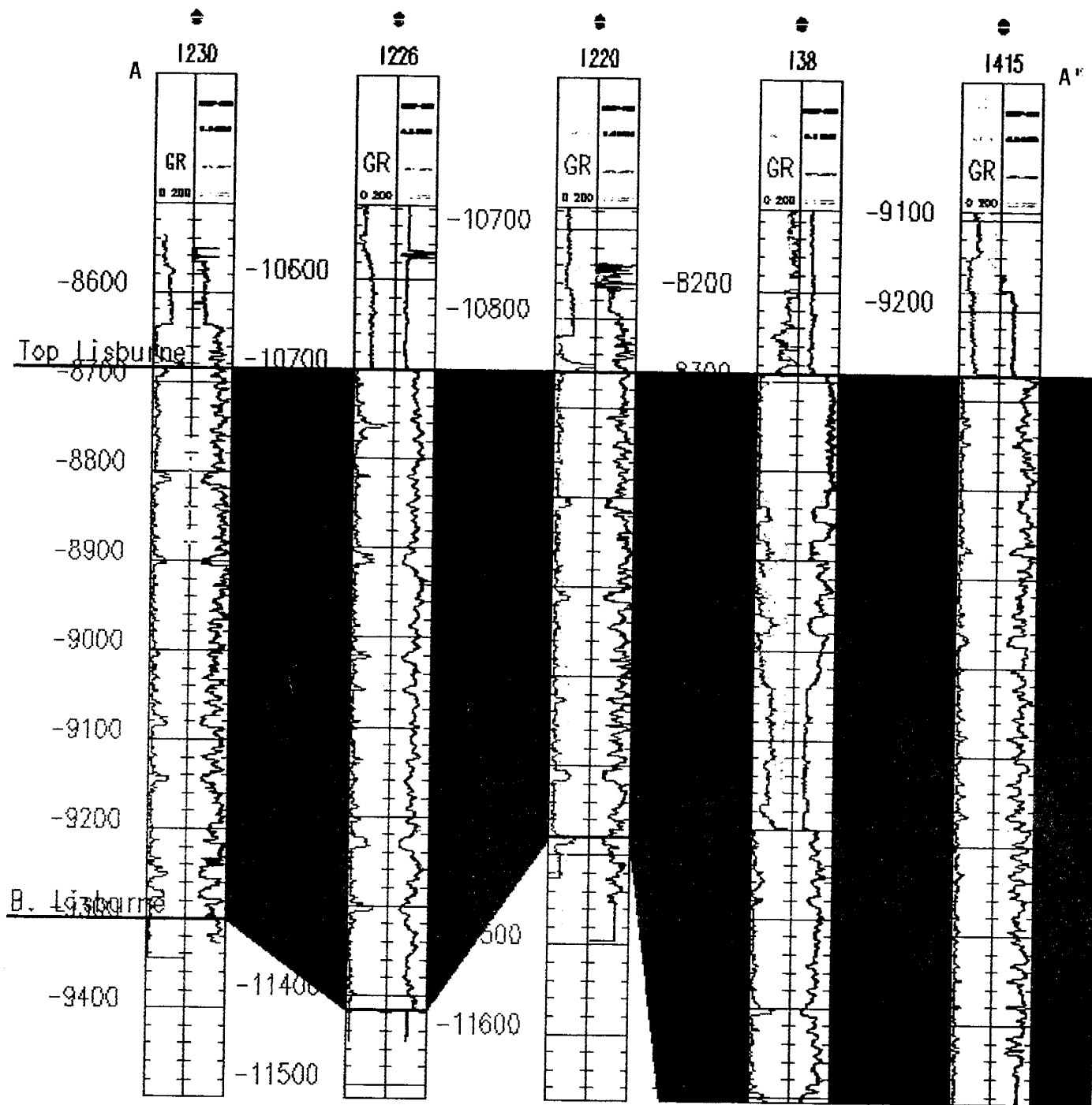


Figure IX-3. Stratigraphic Cross Section Across Lisburne Field.

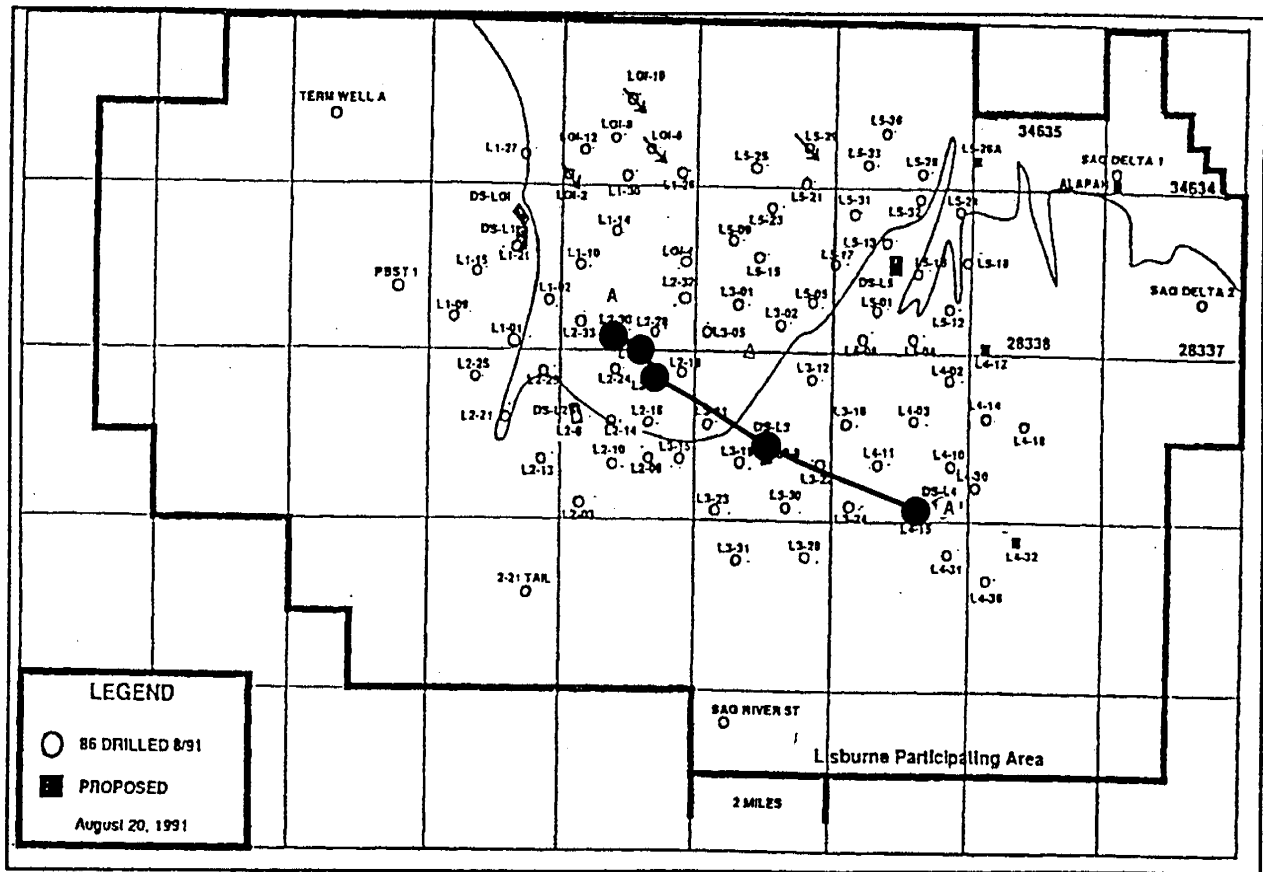


Figure IX-4. Base Map Showing Surface Well and Cross Section A-A' Locations in Lisburne Field (Thomas et al., 1993).

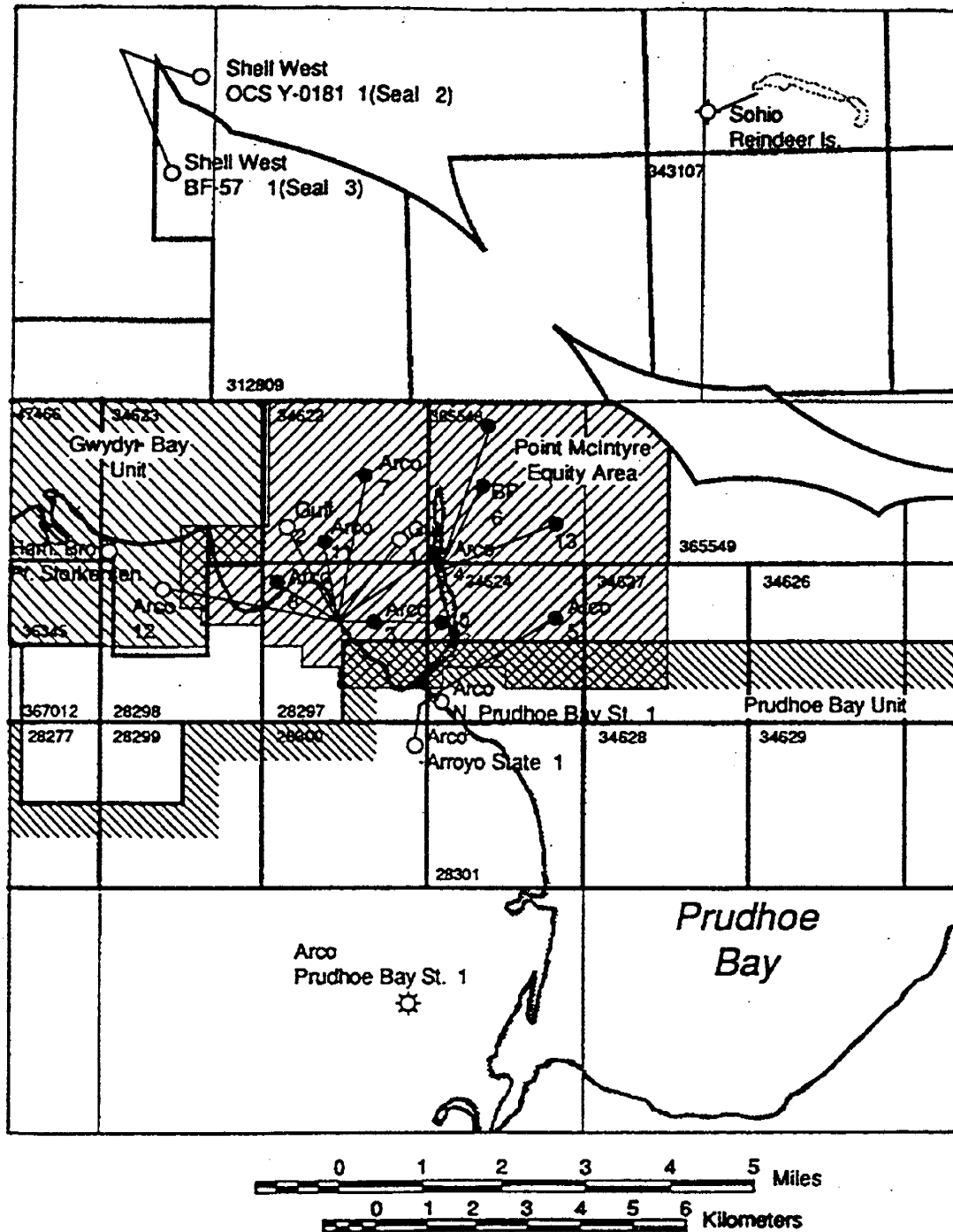


Figure IX-5. Point McIntyre Base Map with Bottom Hole Locations (Thomas et al., 1993).

A 3-D seismic survey shot in 1990 by the working interest owners, combined with core and log data, should provide enough information for detailed mapping and analysis across Point McIntyre field. Initial production is targeted for 1994. Based on areal extent and 80-acre spacing, 84 wells will be required to develop Point McIntyre field. PDL is currently acquiring Point McIntyre field well log data. Future plans include log analysis and reservoir characterization for this field.

### **C. POINT THOMSON FIELD**

The Point Thomson field unit lies 50 miles southeast of Prudhoe Bay along the Beaufort Sea coast. Potential reserves are estimated at 750 MMB condensate and 5 TCF of gas. A base map of the Point Thomson Unit and wells are shown in Figure IX-6.

The Exxon USA Alaska State well A-1, testing 23° API gravity oil at a rate of 2507 BOPD and 2.2 MMCFPD of gas in 1975, was Point Thomson field's discovery well. The oil-bearing zone initially tested in this well is in the Lower Tertiary (Canning formation) Flaxman Sand (Figure IX-7). Following this discovery, the Point Thomson Unit (PTU) was formed. In 1977 the PTU well No. 1 was flow-tested from the Lower Cretaceous (Neocomian) Point Thomson sand to yield an average flow rate of 2283 BOPD. The depth interval tested was between 12,963 and 13,050 feet. In addition, between 12,834 and 12,874 feet, the well tested 3,860 MMCFPD of gas and 170 BPD condensate. This then became the prime reservoir discovery in Point Thomson Unit, and resulted in initial recoverable reserves of 5 TCF of gas and 350 MMB condensate.

During the next several years, additional drilling led to discovery of two additional hydrocarbon reservoirs. Oil from a local sand in the Canning formation of Tertiary age (11,580 to 11,678 feet) flowed 248 BOPD and 124 MCFPD of gas from the PTU No. 2 well in 1978. This sand coarsens northward in the unit area, changing from fine-grained and dolomitic in the south to conglomeratic in the north (Thomas et al., 1993). Porosities average 16% and permeabilities vary from 10 to over 1000 md. And in 1982, the Exxon USA Alaska State well F-1 flowed 2.97 MMCFPD of gas and 152 BOPD in a pre-Late Metasedimentary sequence otherwise known as "Pre-Miss." Porosities in the Pre-Miss are quite low, averaging less than 5%, and average permeabilities are less than 1 md.

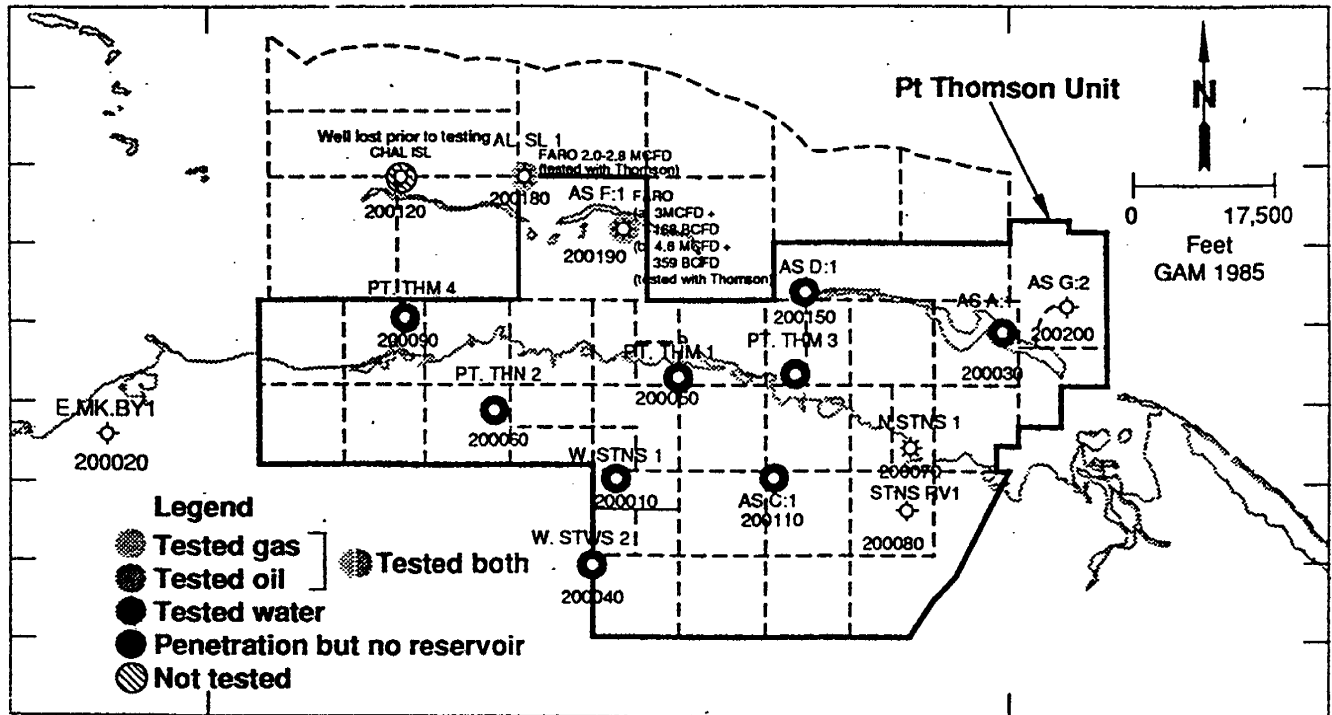


Figure IX-6. Point Thomson Unit Base Map with Well Locations (Thomas et al., 1993).

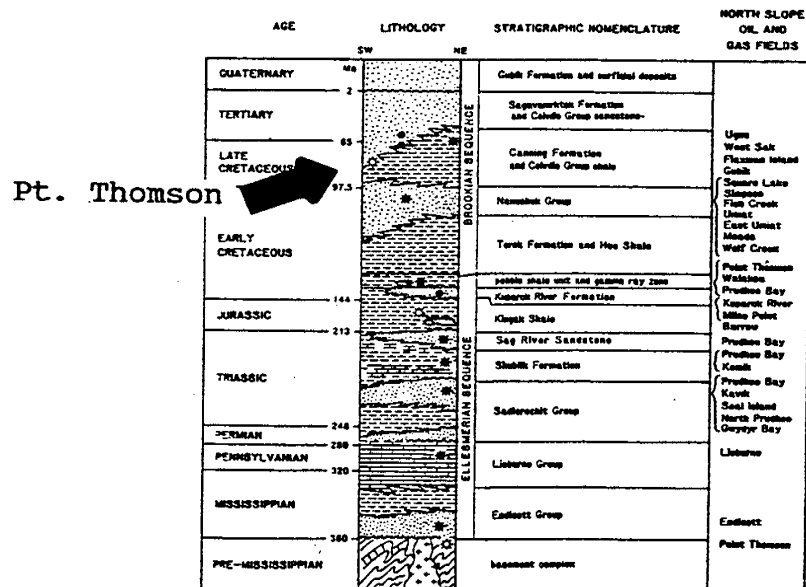


Figure IX-7. North Slope Stratigraphic Column Showing Late Cretaceous Flaxman Island Field (Bird, 1987).

To this date, approximately 15 wells have been drilled within or near the Point Thomson Unit. Also, a 3-D seismic survey has been conducted over the area. The number of wells drilled in Point Thomson Unit, combined with the 3-D seismic survey, should provide the unit's operator (Exxon USA) with the ability to make an economic assessment of developmental potential.

Figure IX-8 provides a measured depth log plot of the Point Thomson Unit well No. 4 with the Thomson formation tops marked. This well is a non-producer, as it lacks reservoir-quality rock. As can be seen in Figure IX-6, a number of other wells do not contain reservoir-quality rock. The relatively large number of wells showing no potential has probably played a large role in the "off-again, on-again" history of lease acquisition and contraction that has occurred at Point Thomson Unit. However, more recently, several leases have been reacquired by Exxon USA in the Point Thomson Unit. Also, during October 1993, production from Point Thomson has been initiated at a rate of 75,000 BOPD.

#### **D. GWYDYR BAY FIELD**

The Gwydyr Bay Unit is located adjacent to, and north of, the Prudhoe Bay Unit (Figure IX-9). The discovery well was the Hamilton Brothers Point Storkerson well No. 1, which tested 5.5 MMCFPD of gas and 381 BOPD from the Sadlerochit group. Prior to unitization in 1979, four more wells were drilled, with the Mobil Gwydyr Bay South well No. 1 being the most successful. It tested 2263 BOPD, and was the first Gwydyr Bay field well to be certified by the state as a producer (Thomas et al., 1993). Of these five wells, four tested hydrocarbons in the Sadlerochit group or the Kuparuk River formation, with the Sadlerochit group being the most promising.

Subsequent to unitization, five additional wells were drilled, with only one (the Conoco Inc. Gwydyr Bay State well No. 2A) striking hydrocarbons. The level of interest in the area remained high enough to support a 3-D seismic program in 1990. An additional 2-D seismic program was conducted by Arco Alaska Inc. in 1992 (Thomas et al., 1993).

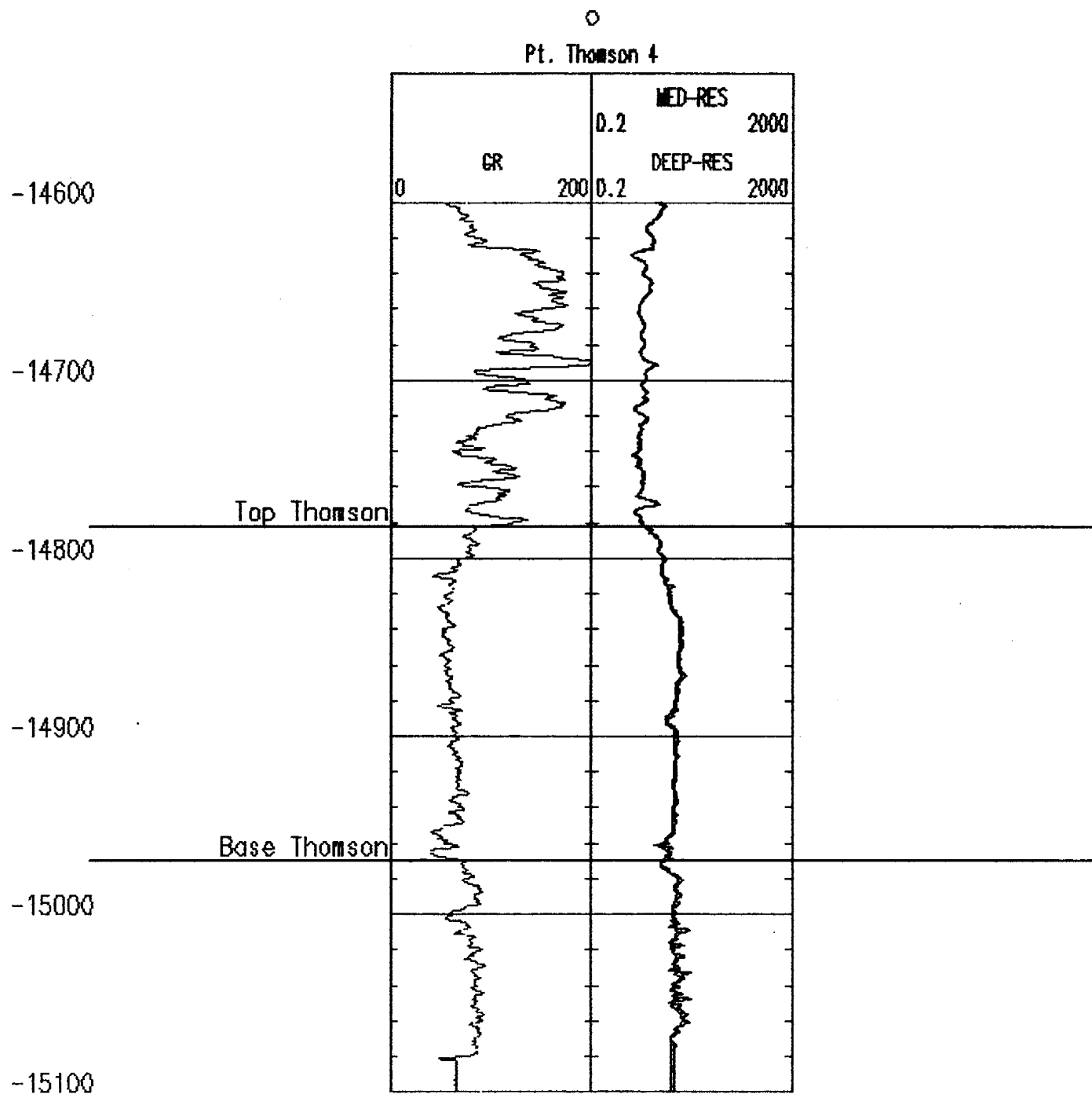


Figure IX-8. Log Plot of the Point Thomson #4 with Thomson Formation Log Picks.



Gwydyr Bay oil potential is derived from two probable accumulations (Thomas et al., 1993). A 3 MMB Sadlerochit group recoverable oil accumulation is expected from the Mobil Gwydyr Bay South well No. 1. It is believed that this well is located along a fault block. Presumably, the nature of the faulting is responsible for the oil accumulation. An even larger potential Sadlerochit group accumulation of 30 to 40 MMB is believed to exist north of the Mobil well (Figure IX-10). In addition, a potential 15-30 MMB Kuparuk River formation accumulation updip from the Mobil well may exist (Figure IX-11). The structural cross section in Figure IX-12 provides a possible explanation for the Sadlerochit group accumulations.

Structural cross section B-B' in Figure IX-13 (with location shown in Figure IX-9) shows the Sadlerochit group in Gwydyr Bay field to be thinner and less well developed as compared to Prudhoe Bay field. The resistivity response curves are maximum toward the bottom of the Sadlerochit group, indicating that the oil accumulation may also be at the bottom. Also, the gamma ray curve shows a probable shaly interval immediately above the location of highest resistivities. If this is true, then this shale may serve as a seal to trap hydrocarbons underneath. Initial petrophysical analysis of the Gwydyr Bay State No. 2 well indicates a possible 60 feet of net pay. The pay zone has a porosity of 18%, water saturation of 56%, and an average of 10% shale.

Before Gwydyr Bay field can be proven to be economically viable, additional exploration must be completed. Sadlerochit group reserve potentials to the north of the Mobil Gwydyr Bay South well No. 1 must be confirmed. Similar confirmation of the updip Kuparuk River formation potential is required. Nearby production and transport facilities would increase the viability of Gwydyr Bay field development once the reserves are proven.

## **E. NIAKUK FIELD**

Niakuk field is located on and around the Niakuk well No. 4 gravel island in state offshore waters northeast of Prudhoe Bay field (Figure IX-14). The field first showed promise with the drilling of the Niakuk well No. 2-A in 1977 (Figure IX-15 shows Niakuk well locations). This well flowed 674 BOPD of 42.7° API gravity oil from the Triassic/Jurassic Sag River sandstone at a drill depth below 12,200 feet (Thomas et al., 1993).

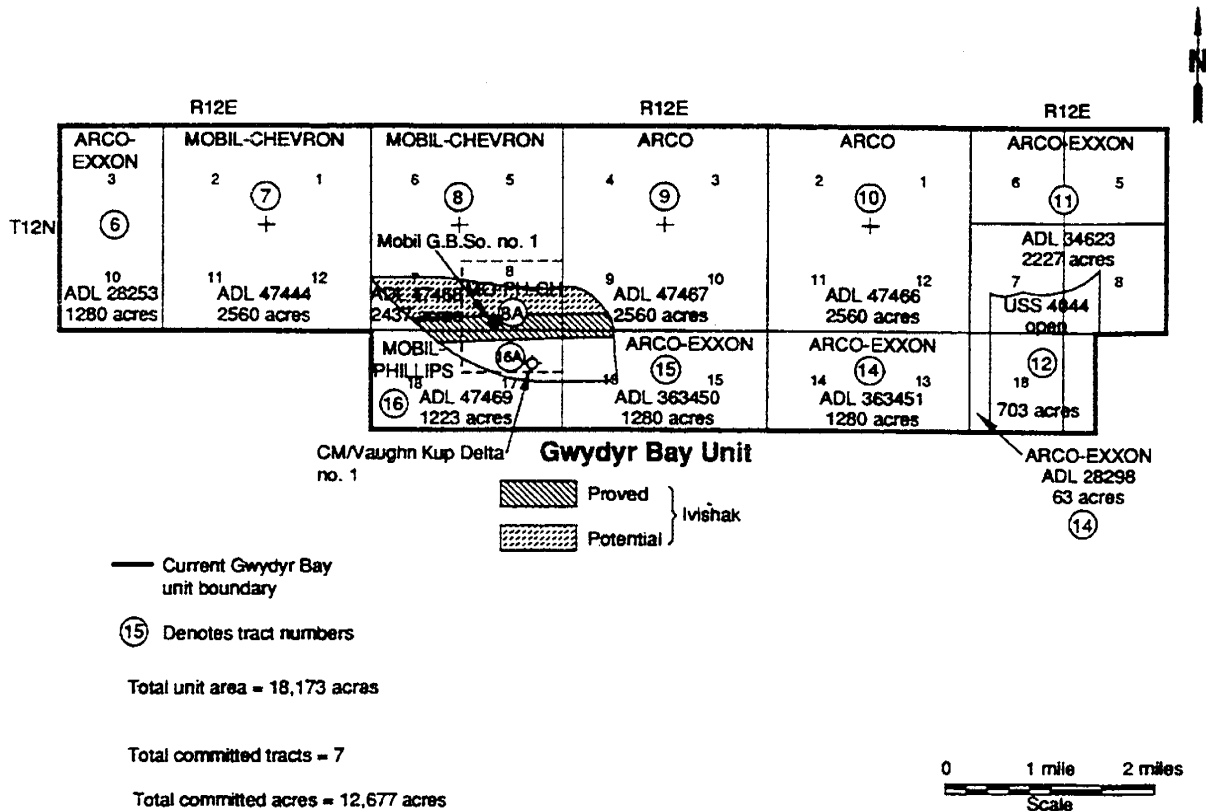


Figure IX-10. Sadlerochit Reserves at Gwydyr Bay (Thomas et al., 1993).

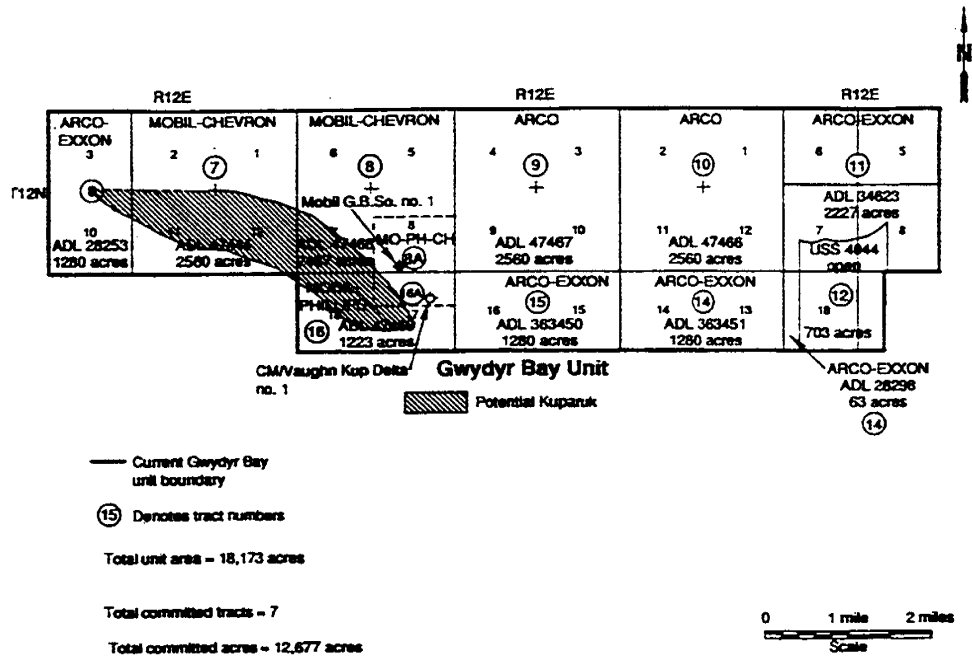


Figure IX-11. Kuparuk Reserves at Gwydyr Bay (Thomas et al., 1993).

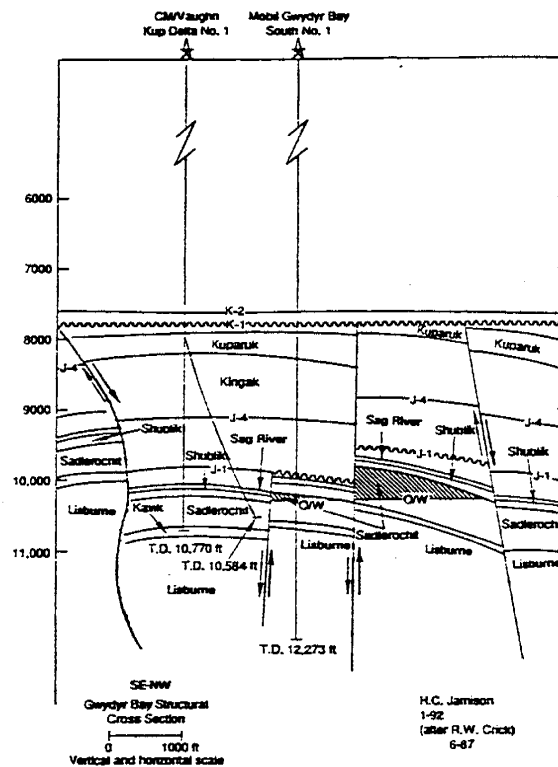


Figure IX-12. Cross Section Across Gwydyr Bay Illustrating Possible Oil-Trapping Structure (Thomas et al., 1993).

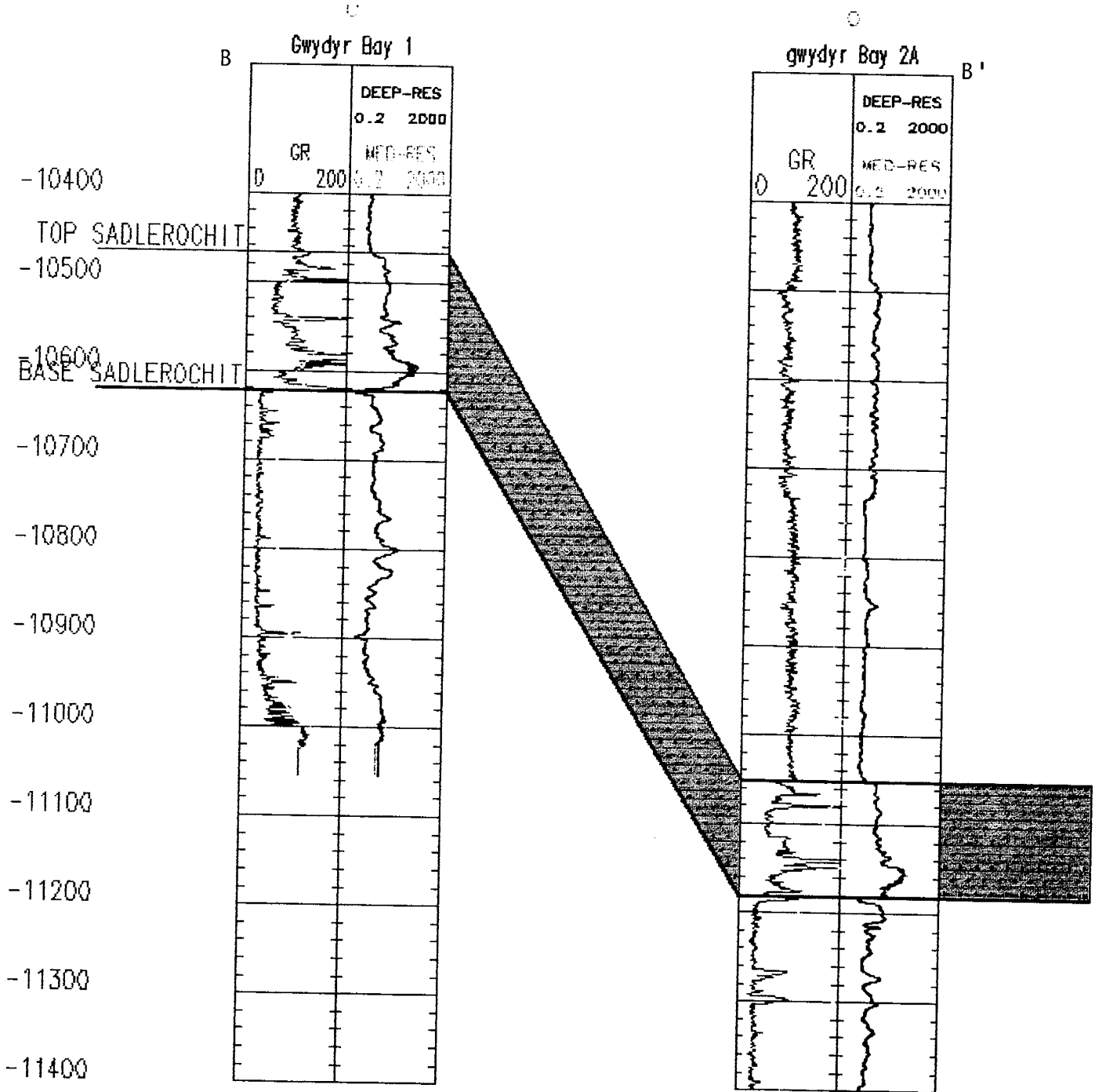


Figure IX-13. Cross Section B-B' Across Gwydyr Bay Field.

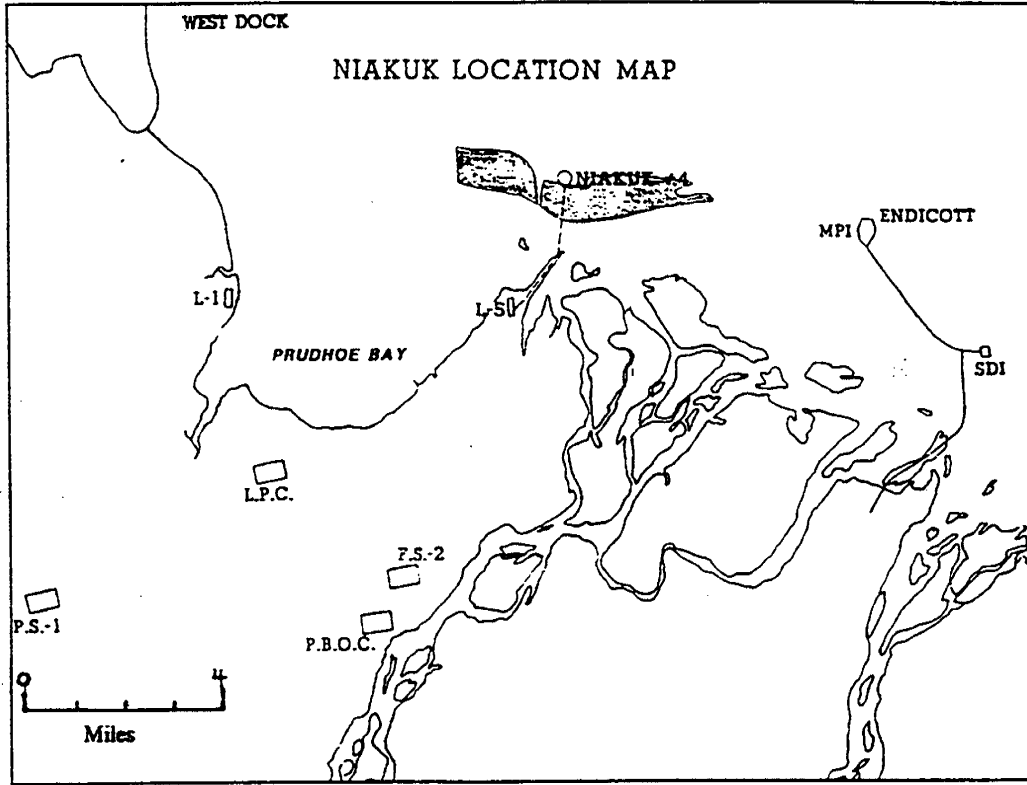


Figure IX-14. Base Map Showing Niakuk Field Location (from Thomas et al., 1993).

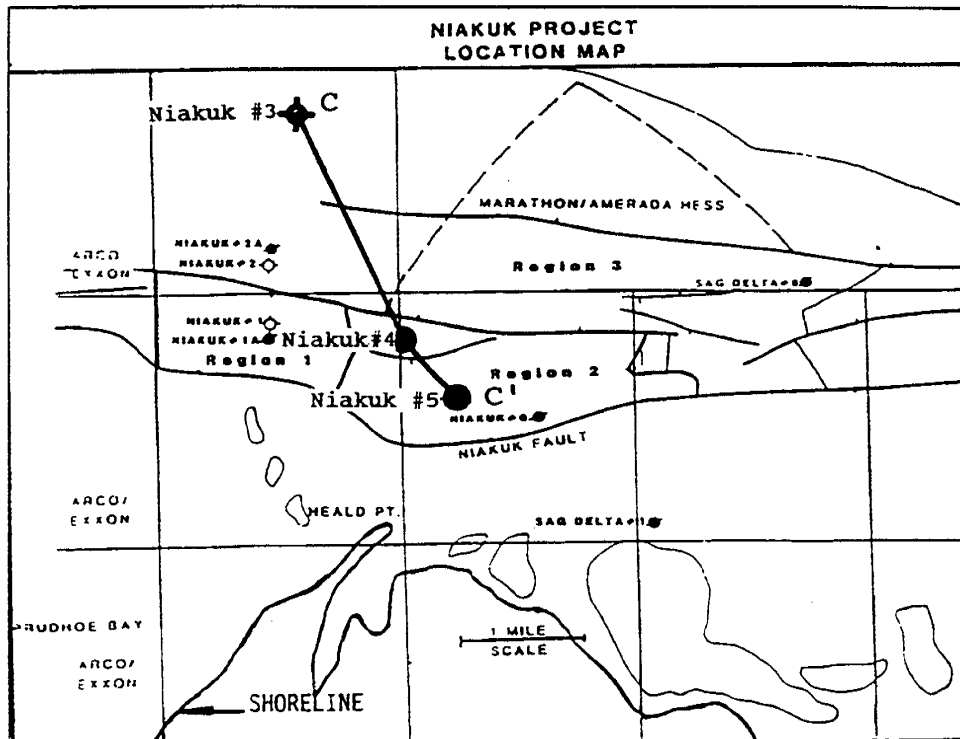


Figure IX-15. Niakuk Field Well Locations with Cross Section C-C' Highlighted (adapted from Thomas et al., 1993).

The drilling in 1985 of the Niakuk well No. 5 from the gravel island proved to be the true discovery well for this field, as it yielded an average flow rate of 4521 BOPD of 25.3 API gravity oil. Production was from the Kuparuk River formation interval between the depths of 10,016 and 10,038 feet. The success of this well led to British Petroleum Alaska's drilling of the Niakuk well No. 6 from the same island. This well produced an average of 4737 BOPD of 26° API gravity oil and 3.12 MMCFPD of gas at a subsea depth approximately 9500 ft subsea (Thomas et al., 1993). With these successes, British Petroleum Alaska initially planned to expand the Niakuk well No. 4 gravel island but later elected to forego this expansion.

Little geological information has been released relative to Niakuk field. A 3-D seismic survey was conducted in 1985 but results or interpretation from the survey have similarly not been released, although the areal extent of Niakuk field has been reported to be about 5000 acres (Thomas et al., 1993). Besides the main Kuparuk River reserve development, an additional smaller Kuparuk River formation prospect further offshore is under study. And a small Lisburne group (Alapah formation) accumulation is also being considered for evaluation.

Structural cross section C-C' (Figure IX-16) provides tentative picks on Kuparuk River formation, Sadlerochit group, and Lisburne group. (The location of the cross section is shown in Figure IX-15.) Picks are especially difficult to make in the Niakuk well No. 4, as typical Kuparuk River formation log characteristics are absent in this well. This may be due to possible adjacent faulting. Both the Sadlerochit group and Kuparuk River formation are structurally higher in the Niakuk well No. 4, as compared to the Niakuk wells Nos. 3 and 5. The Niakuk well No. 4 may have drilled into a horst block where faulting and Kuparuk River formation erosion occurred simultaneously. Table IX-1 lists preliminary petrophysical log analysis results for several Niakuk field wells based on our initial log picks.

## **F. SEAL ISLAND/NORTHSTAR FIELDS**

The Seal Island field, with its reservoir in Sadlerochit group, is located in offshore waters of the Beaufort Sea. Seal Island was constructed by Shell Oil Company in 1982. Of four wells drilled from Seal Island, two were certified producers, another encountered hydrocarbons, and one was a dry hole. The first well drilled, the BF-47 well No. 1, tested 4750 BOPD from the Ivishak formation of the Sadlerochit group (Thomas et al., 1993).

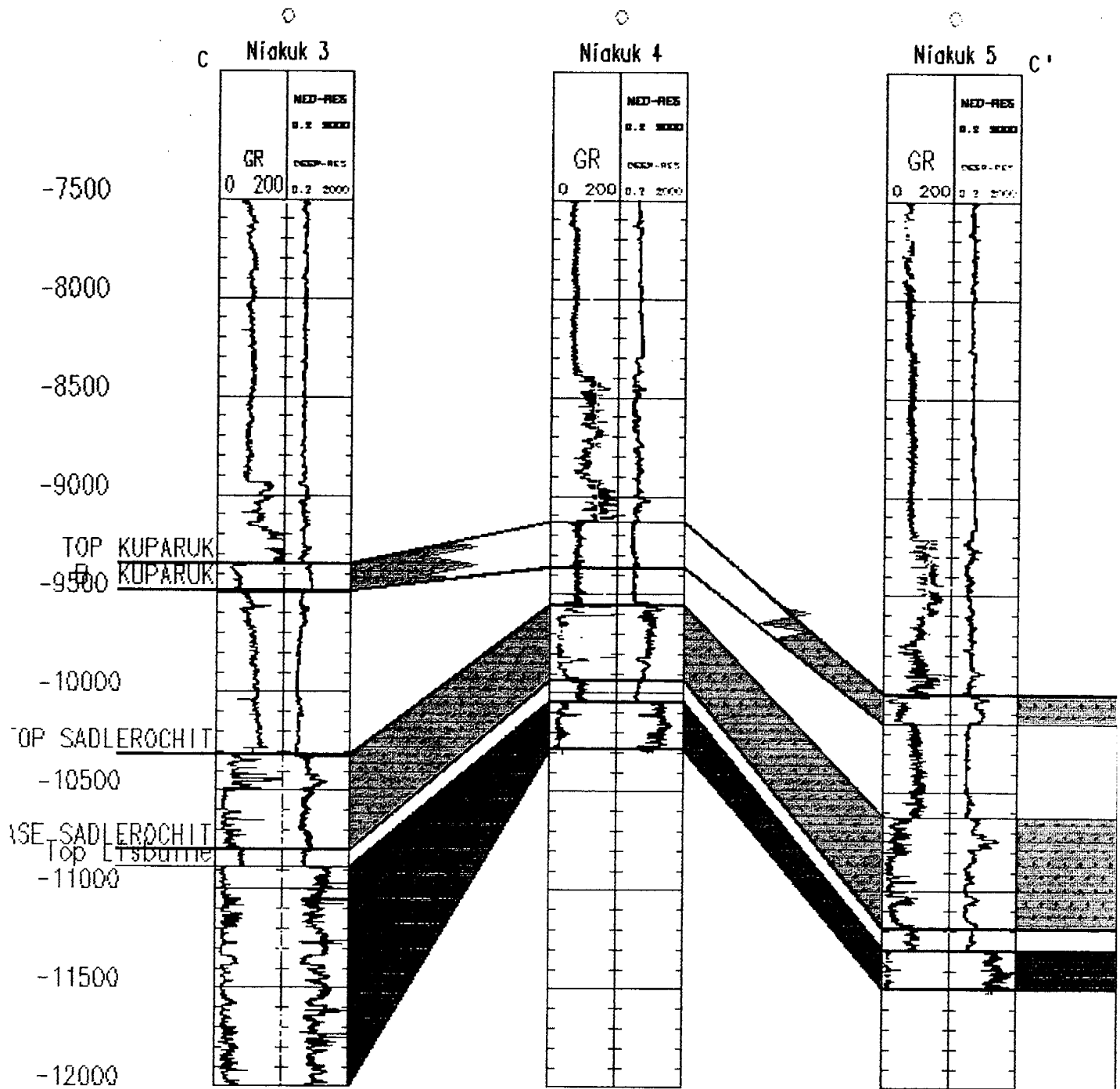


Figure IX-16. Niakuk Field Cross Section C-C' (measured depths).

**Table IX-1: Petrophysical Properties of Reservoir Rocks in Niakuk Field.**

WELL NAME	Formation	Groups and Formations	Gross Thickness (ft)	Net Thickness (ft)	Volume of Shale	Effective Porosity	S <sub>w</sub>	S <sub>o</sub>	HC Pore Thickness (ft)
Niakuk 1	Kuparuk-----	NP							
	Sadlerochit---	NP							
	Lisburne-----	10854.5-11596.5	742	137	8.628	9.60	20.20	79.80	10.50
Niakuk 3	Kuparuk-----	9345-9487.5	142.5	67.5	22.815	14.34	53.63	46.37	4.49
	Sadlerochit---	10311-10499	188	75	12.14	17.53	46.6	53.4	5.198
	Lisburne-----	10887-							
Niakuk 4	Kuparuk-----	9117.5-9347.5	230	126.5	30.93	23.47	40.38	59.62	17.7
	Sadlerochit---	9557.5-9820	262.5	203.5	4.93	19.67	50.86	49.14	19.67
	Lisburne-----	10037.5-							
Niakuk 5	Kuparuk-----	10014-10143	129	82.5	16.33	16.11	47.95	52.04	6.92
	Sadlerochit---	10626.5-10790	163.5	80.5	17.56	15.12	43.0	57.0	6.81
	Lisburne-----	11300.5-							

In 1985 Amerada Hess Oil Company constructed Northstar Island in a location 4 1/2 miles northwest of Seal Island and drilled the BF46 well No. 1. This well tested at an average rate of 3500 BOPD (the well location map of Seal and Northstar Islands is shown in Figure IX-17). With these successful wells, the Northstar Unit was formed. Plans for petrophysical/petrographic studies, seismic acquisition and interpretation, and reservoir engineering studies were included as part of the unit formation.

To date, the petrophysical/petrographic program has been completed and seismic analysis is underway. Although technical data available to the public is limited, the State of Alaska reserve estimates for the Beaufort Sea range between 180 to 225 MMBO (Thomas et al., 1993). Presumably, these reserve estimates pertain primarily to the Seal Island/Northstar oil accumulation. However, due to this unit's offshore location and attendant difficulties related to development of production facilities, the operators are electing at this time to delay development.



# CHAPTER X: EXPERIMENTAL STUDY OF ASPHALTENE PRECIPITATION FOR ENRICHED GASES, CO<sub>2</sub> AND WEST SAK CRUDE SYSTEM

---

---

## A. INTRODUCTION

Many field cases and laboratory studies have reported precipitation and deposition of asphaltenes in porous media during enhanced recovery of asphaltic crude oils by immiscible and miscible flooding operations (Danesh et al., 1988; Monger and Trujillo, 1988; Kokal et al., 1991; Hansen, 1977).

The precipitation of asphaltenes in petroleum reservoirs, wells and surface separation-upgrading facilities pose technical problems and increase the cost of production and processing of crudes. Precipitation of asphaltenes can also occur as a result of natural depletion, caustic flooding, acid stimulation and gas-lift operations. On many occasions, problems relating to the asphaltene precipitation and subsequent deposition have threatened the recovery of oil economically or has increased considerably the production cost. Such cases were reported in the Princess field, Greece (Adialalis, 1982), the Mata-Acema field, Venezuela (Lichaa, 1977), the Hassi-Messaud field, Algeria (Haskett and Tartera, 1965), and the Ventura field, California (Tuttle, 1983). In most of these fields, asphaltene precipitation problems were not foreseen either during production or even during subsequent developmental stages. As a result, the operating company became aware of the problem only after having spent a large capital expenditure, thus making it difficult to abandon a huge investment project. Therefore, it is important to evaluate any potential asphaltene problems and its economic implications prior to development of the field.

In miscible flooding, enriched hydrocarbon gases, LPG's or CO<sub>2</sub> (termed as solvents) are injected into the reservoir to reduce oil viscosity and interfacial tension, to provide more efficient drive mechanism, and to achieve (dynamic or direct contact) miscibility with the reservoir oil, thus resulting in very high displacement efficiency and ultimate oil recovery. In such processes, however, the miscible solvents may cause precipitation of asphaltenes by altering the ratio of "heavy" to "light" components and "polar" to "non-polar" components (or resin to asphaltene ratio) in the crude. The asphaltene precipitation problem is particularly important in miscible flooding since it can reduce permeability, affect well injectivities and productivities, alter rock wettability characteristics, and even may result in plugging of producing wells (Danesh et al., 1988; Stalkup, 1983). The amount of asphaltene precipitation depends upon

the oil composition (the original asphaltene and resin content of the crude), the solvent composition, the pressure and temperature conditions, and the phase behavior of solvent-oil mixtures. Asphaltene deposition in the reservoir is an even more complex phenomenon since several processes such as solvent mixing, fingering, mass transfer between oil and solvent in a multi-contact process, and adsorption of asphaltenes on preferential rock sites occur simultaneously. Detailed understanding of asphaltene precipitation in crudes has been impeded by limited availability of experimental data and the lack of accurate and reliable laboratory methods to measure asphaltene precipitation.

The State of Alaska is the largest oil producing state in the nation and currently contributes nearly 24% of the nation's oil production. It is estimated that Alaska also has nearly 20% of the total U.S. proven oil reserves. The key to sustaining the long-term oil production in Alaska to help meet the nation's oil demand is to improve recovery efficiencies from the giant fields such as Prudhoe Bay, Kuparuk River, and Endicott under production and develop marginally economic fields such as the West Sak heavy oil reservoir. The need to study the problem of asphaltene deposition in reservoirs is particularly important to Alaska due to the nature of enhanced oil recovery projects planned or currently underway. For example, production from a part of the Prudhoe Bay field is derived by enriched gas miscible flood project and asphaltene deposition has been observed. Similar miscible floods are also planned for Kuparuk River and Endicott fields. Miscible flooding is also considered as one of the methods for recovery of heavy oil from super-giant West Sak reservoir. In this project, the experimental data on the amount of asphaltene precipitation during addition of solvents to West Sak oil were obtained. This data will be useful in understanding the effects of asphaltene precipitation on the miscible displacement process. Similar experimental data can be easily obtained for other North Slope crudes.

## **B. LITERATURE REVIEW**

### **B1. Nature of Asphaltenes and Resins**

Asphaltenes were originally described by Boussingault (1837) as alcohol insoluble but turpentine soluble solids obtained from distillation residue of asphalt. Later, several investigators determined asphaltenes to be the low molecular weight n-paraffin insoluble and benzene soluble fraction of crude oil (Long, 1981; McKay et al., 1978; Speight, 1981; Chilingar and Yen, 1978; Yen, 1982). In general, asphaltenes can be classified as polar, aromatic-based, high molecular weight hydrocarbons of amorphous structure which exist in crude oils partly in the form of colloiddally dispersed fine particles and partly as dissolved compounds. Corbett and

Petrossi (1978) showed that asphaltenes must be classified by the particular precipitating solvent since different solvents cause different amounts of precipitation of asphaltenes of different molecular weight. Although, the exact chemical structure of asphaltenes is unknown and will be the function of the type of crude, their chemical structure consists of aromatic ring structures with oxygen, nitrogen, and sulphur present in heterocyclic side chains, and oxygen in alkyl side chains. Speight and Moschopedis (1981) showed that elemental compositions of asphaltene fractions precipitated by different solvents from various crudes are different. According to Long (1981), asphaltenes exist in a broad range of size distributions, polarities and molecular weights.

For practical purposes, the asphaltene fraction of an oil is defined as the part precipitated by the addition of n-heptane using the IP-143 test. This definition is used in this study. The asphaltene fraction generally consists of condensed aromatic and naphthenic molecules of molecular weights in the range of 1,000 to 500,000. They contain larger carbon to hydrogen ratios than those prevalent in crude oils. Thus, addition of low molecular weight n-paraffinic solvents which have lower carbon to hydrogen ratio than crude oils, cause precipitation of the asphaltene colloids. This is accompanied by the removal (dissolution and desorption) of maltenes which are n-heptane soluble fraction of oil. Apart from n-paraffins, CO<sub>2</sub>, water and acids also cause precipitation of asphaltenes. In addition to a reduction in the solubility of asphaltenes in oil, CO<sub>2</sub> causes rigid asphaltene film formation on the interfaces due to its effect on the pH value of the water present. Measurement of surface tension indicates that there exists a critical micelle concentration (CMC) for the dilute solution of asphaltenes in toluene (Rogacheva et al., 1980). Below CMC, asphaltenes in the solution are in a molecular state, but above CMC, they tend to associate and agglomerate.

Resins are also polycyclic aromatic-based compounds, somewhat lower in molecular weight (250 - 1000) than asphaltenes. They are non-polar compared to polar asphaltenes. Resins are easily adsorbed in common adsorbents like clay or silica gel. Resins are defined as the fraction of crude oil insoluble in ethyl acetate but soluble in n-heptane. There may be a close relationship between asphaltenes and resins coexisting in a crude. Resins are the primary cause of keeping asphaltene particles from coagulation and agglomeration. The heavy polycyclic aromatic compounds during oxidation form neutral resins, while asphaltenes form as a result of subsequent oxidation of resins. Asphalt is used as a general term to designate the mixture that flocculates out of oil and contains asphaltene particles surrounded by resins, oil and other liquid components in oil that are trapped in the flocculated mass.

## **B 2. Causes of Asphaltene Flocculation**

Asphaltene deposition as a result of flocculation of finer asphaltene particles is a complex phenomenon and not well understood. Some of the recent studies (Leontaritis and Mansoori, 1987; Hirshberg et al., 1984) provide a more comprehensive description on the causes of asphaltene deposition.

Asphaltenes are lyophobic with respect to low molecular weight paraffinic hydrocarbons and lyophilic with respect to aromatics and resins. That is why resin molecules are adsorbed on the surface of asphaltene particles or micelle (onion skin model). As a result, when asphaltene particles are completely surrounded by resin molecules, they remain in fine colloidal suspension and do not agglomerate or precipitate. This process is known as "peptization". The degree of dispersion of asphaltenes in crude oils depends upon the chemical composition of crude. In heavy, highly aromatic crudes, asphaltenes are well dispersed, but in presence of paraffinic hydrocarbons, they flocculate and precipitate. Also, in crudes with high resin contents the degree of asphaltene precipitation is less.

McKay et al. (1978) suggested that the ratios of "polar to non-polar" and "heavy to light" molecules in a crude are particularly important in keeping mutual solubility of the compounds in the crude. By the addition of a solvent to the crude, this ratio is altered. The heavy and polar (asphaltene) molecules separate from the mixture either in the form of another liquid phase or as a solid precipitate. Hydrogen bonding and the sulfur (and/or nitrogen) containing segments of the separated (asphaltene) molecules start to aggregate (or polymerize) and as a result, produce the asphaltene deposits which are insoluble in solvents.

In general, any action of chemical, mechanical, or electrical nature which depeptizes the asphaltene micelle can lead to precipitation of the asphaltenes from the crude oil-asphaltene suspension. The amount of resins adsorbed on the surface of the asphaltenes is essentially a function of the concentration of the resin in the liquid phase of the oil. Processes which depletes or dilutes the resin concentration in the oil may lead to asphaltene precipitation. For example, when miscible solvents (CO<sub>2</sub> or lighter hydrocarbons) are added to asphaltene containing crudes, the resin concentration may be so depleted that the entire surfaces of the asphaltene micelles cannot be covered. The result is flocculation of the asphaltenes and sludging or precipitation.

Asphaltene deposition problems upon natural depletion (primary recovery) have been encountered in the well tubing of the Hassi-Messahoud field in Algeria (Haskett and Tartera, 1965) and the Ventura field in California (Tuttle, 1983). In both fields the crude was strongly

undersaturated with respect to gas. At Hassi-Messahoud, heavy asphaltene precipitation took place in a 450m region of the tubing located just below the level at which bubble point was reached. Furthermore, upon gas injection, a reduced injectivity (factor of two) was experienced due to asphaltene deposition. In the Ventura field, severe asphaltene plugging was experienced in the first period of field development until 1970. However, once the reservoir pressure reached the bubble point, the wells produced without asphaltene related problems.

Reduction in well injectivity or productivity by a factor of 2 to 3 during several CO<sub>2</sub> flood field projects (Stalkup, 1978) and water alternating gas drives (Dyes, 1972; Harvey et al., 1977) have been caused by asphaltene deposition. The asphaltene deposition problems have also been reported for the Little Creek CO<sub>2</sub> injection EOR pilot in Mississippi (Tuttle, 1983).

Asphaltenes have an electrical charge and thus their precipitation is possible by the application of electric field. Stream potential experiments conducted by Prekshot (1954) demonstrated that crude oil flowing through sand produces a potential, and this appears to be responsible for the formation of precipitated asphaltenes in the flow of crude oil through porous reservoir rock. This same phenomenon is thought to be responsible for asphaltene deposition in the slotted liners of low gravity wells in California.

Asphaltene deposition also occurs during release of low molecular weight hydrocarbons from the crude below its bubble point. There appears to be controversy over the issue whether asphaltene precipitation is a reversible or irreversible mechanism, especially due to the lack of sufficient experimental evidence. Hirshberg et al. (1984) provides some proof as to reversibility in asphaltene deposition. It makes sense to consider the asphaltene precipitation phenomenon as reversible because adsorption of resins on asphaltene micelle follows reversible Langmuir type phenomenon. It is not quite clear, however, if the asphaltene deposition caused by the flow of crude through porous media (rather than caused by chemical alteration of resin concentrations in the oil phase) is reversible or not.

Use of hydrochloric acid as a well stimulation fluid can cause severe damage in wells containing asphaltenic crude. In such cases, a rigid asphaltene film gets deposited in the porous media around the wellbore.

## **C. EXPERIMENTAL RESULTS**

### **C1. Asphaltene Precipitation Tests with Tank Oils**

Asphaltene/asphalt precipitation tests were conducted for two different types of West Sak (tank ) oils using eight different solvents. Compositions of Oil A and Oil B which represent oils from two different horizons of the West Sak reservoir are given in Table X-1. Solvents used include: carbon dioxide, ethane, propane, n-butane, n-pentane, n-heptane, Prudhoe Bay natural gas (PBG) and natural gas liquids (NGL). The compositions of PBG and NGL are given in Table X-2.

The following procedure was used to measure asphalt and asphaltene precipitation. Initially, a known amount of tank oil was taken in a visual cell. In case of liquid solvents such as n-pentane and n-heptane, a predetermined amount of solvent was added directly to the tank oil in the cell. In case of volatile solvents such as ethane, propane, n-butane, CO<sub>2</sub> and NGL, the solvents were first condensed to a liquid state and then a known amount of the solvent was added to the tank oil in the cell. After preparation of a solvent-oil mixture in the cell, the mixture was continuously agitated with a rocking mechanism for several hours at room temperature. The mixture was then flashed, and precipitated solids were separated through filtration. The solid precipitates were then thoroughly dried and weighed. In case of n-heptane, the solids precipitated represent asphaltenes. For all other solvents, the solids precipitated represent asphalts. Additional n-heptane was then added to the asphalts to redissolve resins leaving behind only asphaltenes. Here again, asphaltenes after thorough drying were then weighed. These experiments were repeated for each solvent at varying solvent/oil ratio.

### **C2. Effect of Solvent/Oil Dilution Ratio**

The amounts of asphalts and asphaltenes precipitated from various solvents are summarized in Table X-3 (for Oil A) and Table X-4 (for Oil B). Figures X-1 through X-8 show that, in general, with increasing solvent/oil ratio there is a rapid increase in the amount of asphaltene precipitation which soon levels off after certain solvent/oil ratio. The addition of solvent to oil reduces the concentration of resins (which acts as a peptizing agent for asphaltenes) in the oil, resulting in asphaltene precipitation. Figure X-9 shows that for normal paraffinic solvents, the amount of asphalts precipitated (at maximum solvent/oil ratio) increase with a decrease in molecular weight of solvents while the amount of asphaltenes precipitated remains relatively the same. The mutual solubility of resins (which are part of asphalts) in oil decreases with a decrease in the molecular weight of the solvent added. The variation of the amount of asphaltenes precipitated for each solvent is probably due to differences in the range of asphaltene components that were precipitated by each solvent.

**Table X-1: Compositional Analysis (Mol %) of West Sak Tank Oil.**

COMPONENT	TANK OIL-A	TANK OIL-B
C <sub>1</sub> -C <sub>6</sub>	-	-
C <sub>7</sub>	1.27	0.08
C <sub>8</sub>	1.05	0.01
C <sub>9</sub>	1.35	0.03
C <sub>10</sub>	1.47	0.16
C <sub>11</sub>	1.94	1.83
C <sub>12</sub>	1.97	0.83
C <sub>13</sub>	2.49	0.99
C <sub>14</sub>	2.67	1.23
C <sub>15</sub>	2.30	1.35
C <sub>16</sub>	2.35	0.96
C <sub>17</sub>	2.80	1.61
C <sub>18</sub>	2.55	1.84
C <sub>19</sub>	2.44	1.02
C <sub>20</sub>	1.90	1.10
C <sub>21</sub>	2.43	1.26
C <sub>22</sub>	1.98	1.49
C <sub>23</sub>	1.87	1.10
C <sub>24</sub>	1.22	0.70
C <sub>25</sub>	1.75	1.03
C <sub>26</sub>	1.60	1.03
C <sub>27</sub>	1.25	1.18
C <sub>28</sub>	1.23	0.92
C <sub>29</sub>	1.55	0.60
C <sub>30</sub>	0.69	0.46
C <sub>31</sub>	2.11	0.85
C <sub>32</sub>	2.11	2.13
C <sub>33</sub>	2.52	1.60
C <sub>34</sub>	1.45	1.49
C <sub>35</sub>	2.63	1.78
C <sub>36</sub>	4.14	2.50
C <sub>37</sub> <sup>+</sup>	40.41	66.84

**Table X-2: Compositional Analysis (Mol %) of Live (recombined) Oil-A, Prudhoe Bay Natural Gas (PBG) and Natural Gas Liquids (NGL).**

COMPONENT	LIVE OIL-A	PBG	NGL
N <sub>2</sub>	0.03	trace	0.02
CO <sub>2</sub>	0.02	12.73	trace
C <sub>1</sub>	38.33	72.80	trace
C <sub>2</sub>	0.86	7.44	trace
C <sub>3</sub>	0.36	3.94	1.50
C <sub>4</sub>	0.18	2.29	50.50
C <sub>5</sub>	0.06	0.80	29.13
C <sub>6</sub>	0.20		18.85 (C <sub>6</sub> <sup>+</sup> )
C <sub>7</sub>	0.02		
C <sub>8</sub>	0.01		
C <sub>9</sub>	0.82		
C <sub>10</sub>	1.50		
C <sub>11</sub>	1.72		
C <sub>12</sub>	1.35		
C <sub>13</sub>	1.50		
C <sub>14</sub>	1.80		
C <sub>15</sub>	1.94		
C <sub>16</sub>	1.80		
C <sub>17</sub>	1.57		
C <sub>18</sub>	1.80		
C <sub>19</sub>	2.47		
C <sub>20</sub>	2.84		
C <sub>21</sub> <sup>+</sup>	38.82		
Mol. Wt. of Plus Fraction	455		96

**Table X-3: Asphalt/Asphaltene Precipitation Test Results  
for West Sak (Tank) Oil-A.**

SOLVENT USED	SOLVENT/OIL RATIO BY WEIGHT	WT% SOLID (ASPHALTS) PRECIPITATED	WT% SOLID ASPHALTENES
Ethane	3.0	*	5.14
	13.0	*	5.28
	*	45.60	*
CO <sub>2</sub>	3.6	*	5.56
	6.0	36.80	*
	13.6	*	5.80
	15.3	*	5.89
Propane	4.7	32.07	8.87
	7.8	34.40	8.60
	16.3	38.90	9.07
N-Butane	2.0	28.16	6.22
	8.1	25.98	6.36
	18.3	24.55	6.45
N-Pentane	2.0	13.42	1.79
	7.0	16.30	6.20
	12.5	13.60	6.30
	20.2	16.48	6.69
N-Heptane	2.0	3.83	3.83
	7.3	5.34	5.34
	13.5	7.50	7.50
	20.1	7.32	7.32
NGL	3.2	17.50	5.73
	7.6	22.80	8.80
	9.9	23.85	8.88
Prudhoe Bay Gas	1.6	*	5.49
	1.7	29.80	7.40
	5.8	*	8.15
	10.4	*	8.08

\* Values not measured

**Table X-4: Asphalt/Asphaltene Precipitation Test Results  
for West Sak (Tank) Oil-B.**

<b>SOLVENT USED</b>	<b>SOLVENT/OIL RATIO BY WEIGHT</b>	<b>WT% SOLID (ASPHALTS) PRECIPITATED</b>	<b>WT% SOLID ASPHALTENES</b>
Ethane	2.93	36.60	2.90
	7.34	42.91	4.96
	21.00	43.92	5.44
CO <sub>2</sub>	2.09	*	4.20
	2.69	36.00	4.70
	19.33	*	4.85
	20.93	42.50	5.50
Propane	2.44	24.00	8.00
	6.85	33.71	9.79
	21.15	41.68	9.00
Prudhoe Bay Gas	1.99	33.00	7.00
	17.26	30.75	8.32
N-Butane	2.08	24.80	11.38
	4.34	24.40	11.40
	10.49	18.50	11.68
N-Pentane	2.50	6.60	3.00
	12.52	12.80	5.30
	20.00	9.90	6.70
N-Heptane	2.00	5.10	5.10
	10.00	6.54	6.54
	20.00	5.70	5.70
NGL	1.95	18.47	6.82
	7.99	16.97	6.84
	11.04	17.32	6.79

\* Values not measured

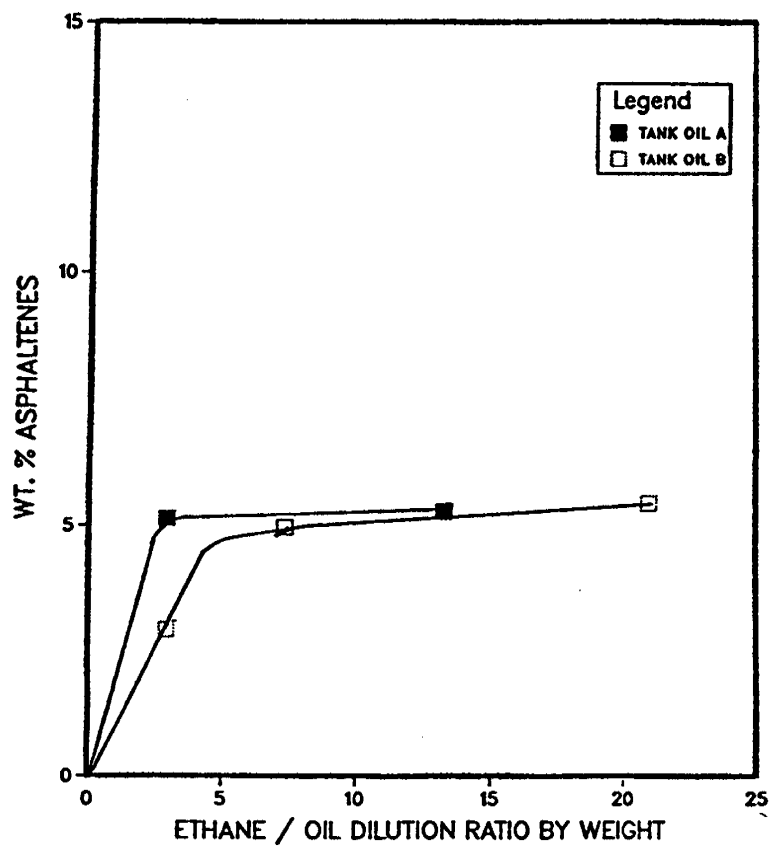


Figure X-1. Effect of Ethane/Oil Ratio on Amount of Asphaltene Precipitation.

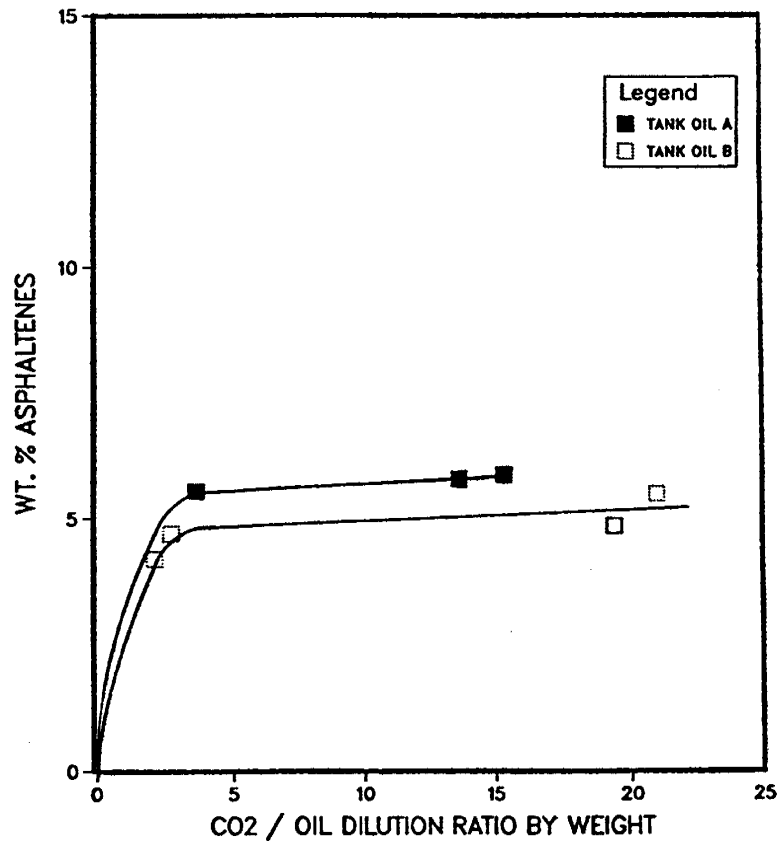


Figure X-2. Effect of CO<sub>2</sub>/Oil Ratio on Amount of Asphaltene Precipitation.

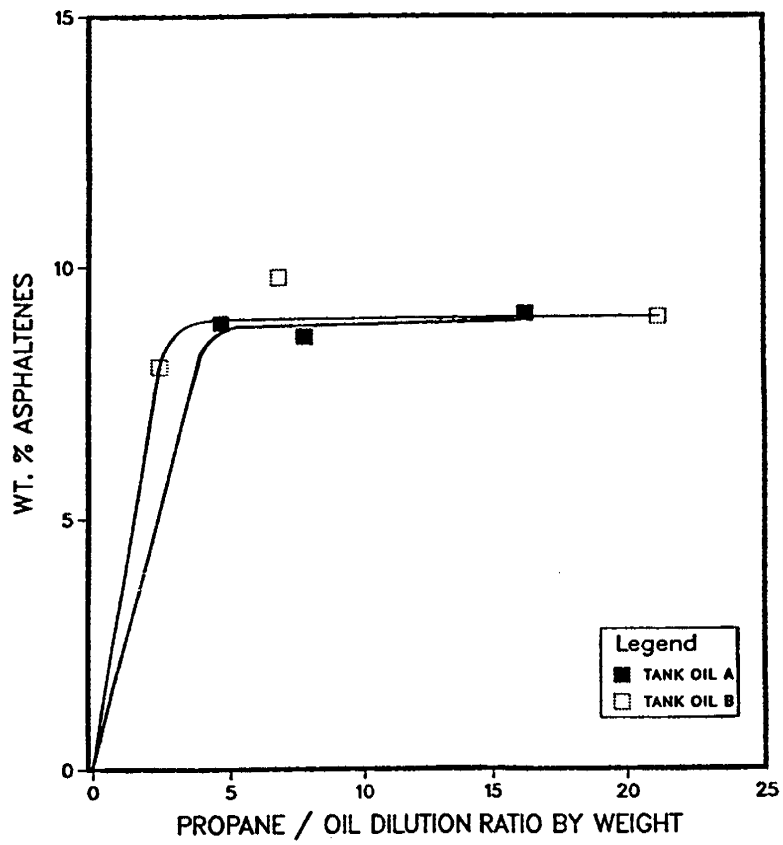


Figure X-3. Effect of Propane/Oil Ratio on Amount of Asphaltene Precipitation.

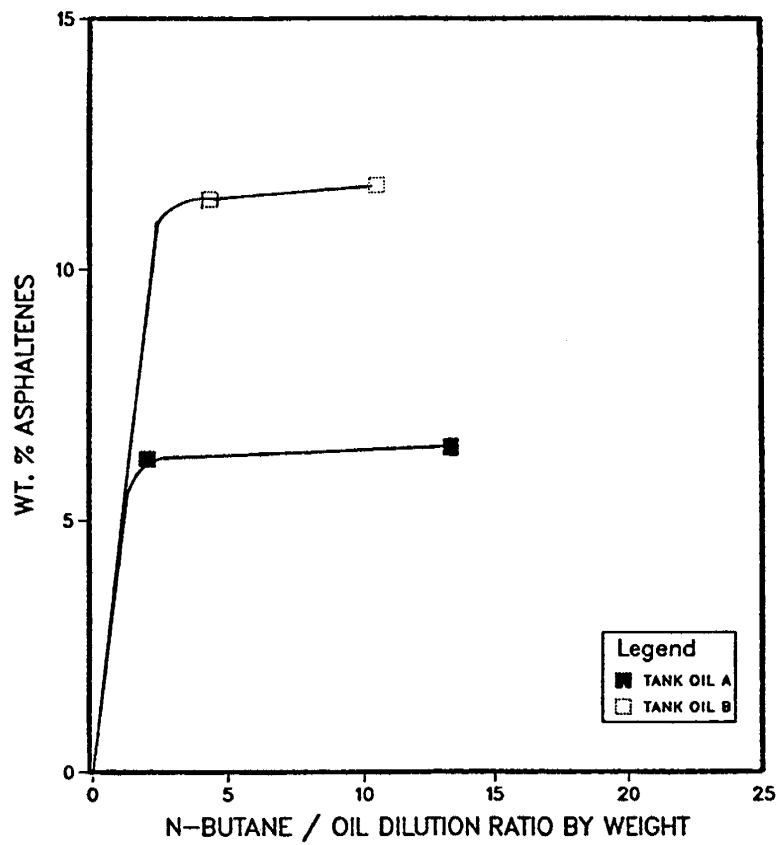


Figure X-4. Effect of N-Butane/Oil Ratio on Amount of Asphaltene Precipitation.

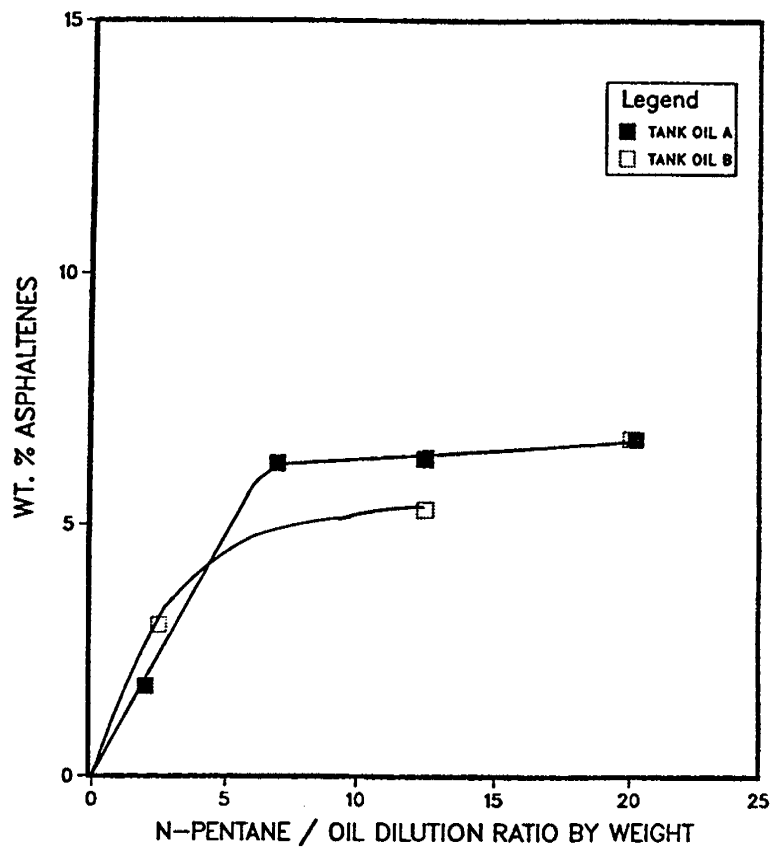


Figure X-5. Effect of N-Pentane/Oil Ratio on Amount of Asphaltene Precipitation.

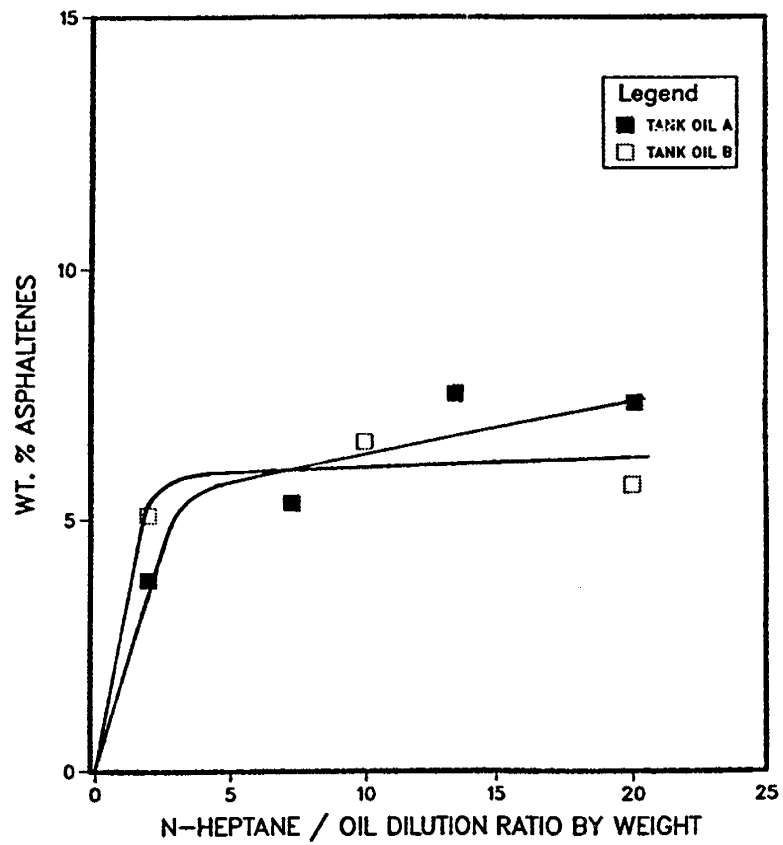


Figure X-6. Effect of N-Heptane/Oil Ratio on Amount of Asphaltene Precipitation.

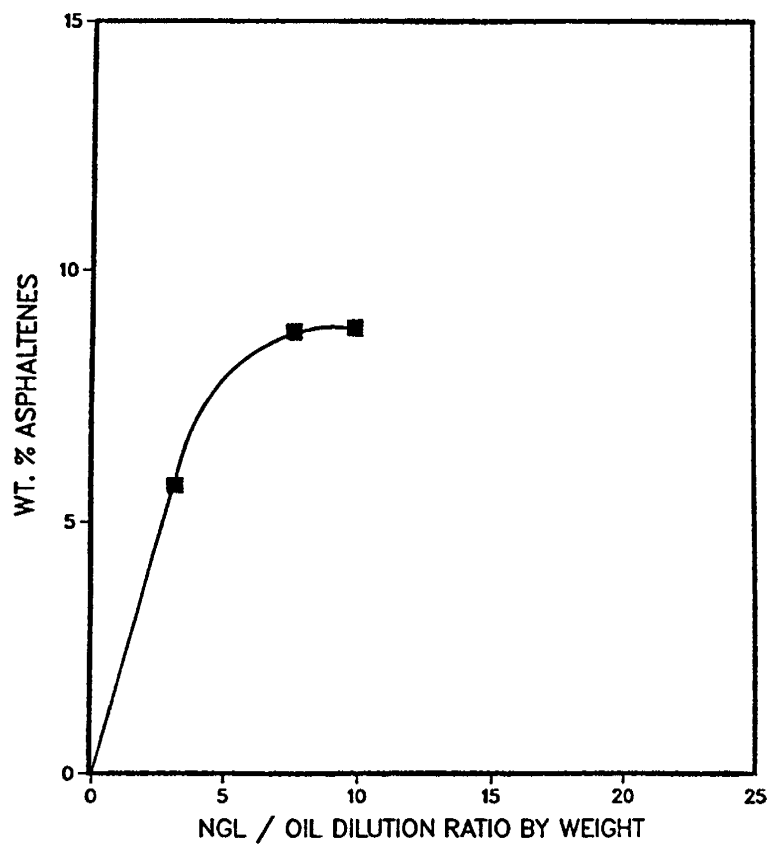


Figure X-7. Effect of NGL/Oil Ratio on Amount of Asphaltene Precipitation.

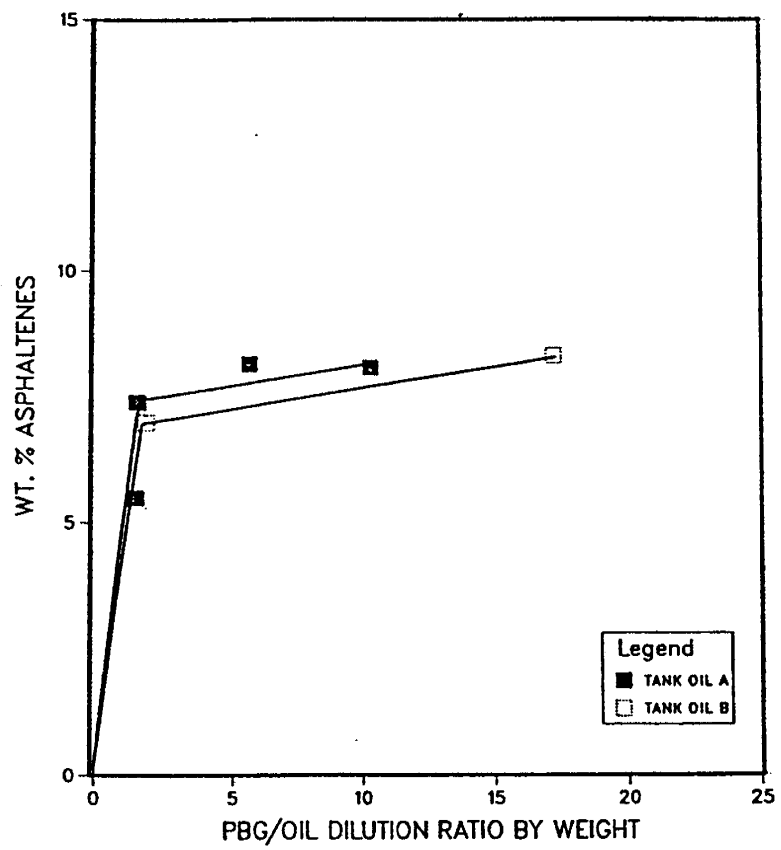


Figure X-8. Effect of PBG/Oil Ratio on Amount of Asphaltene Precipitation.

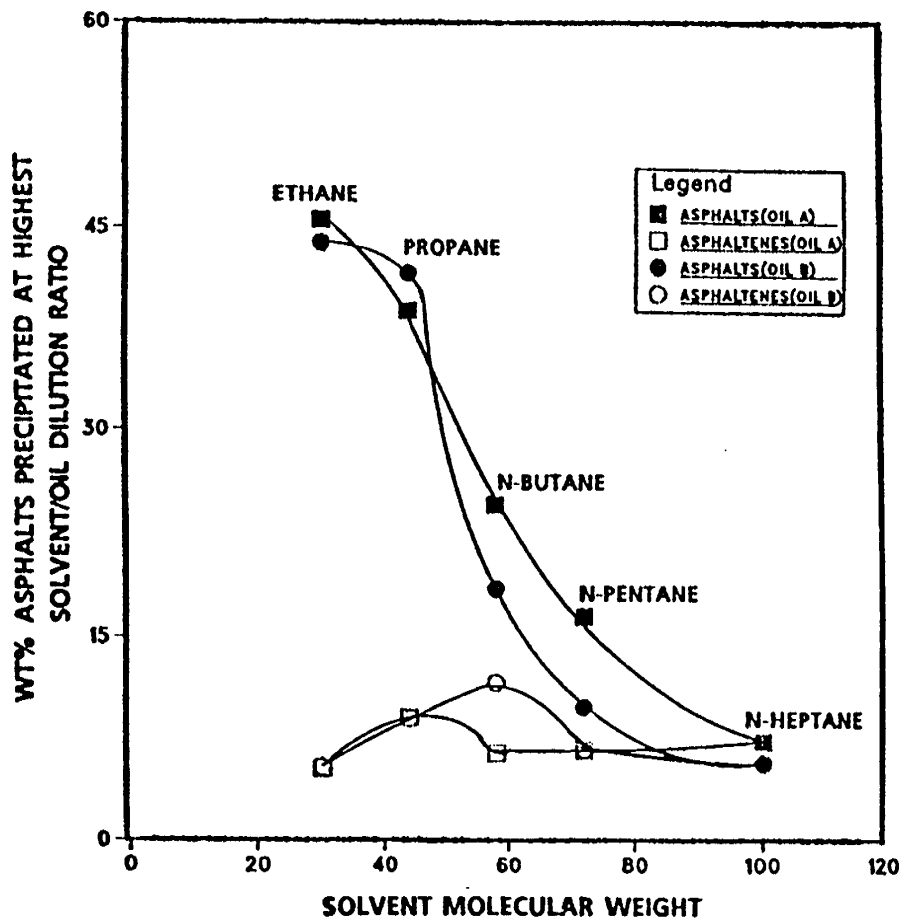


Figure X-9. Effect of Solvent Molecular Weight on Amount of Asphaltene Precipitation at Highest Solvent/Oil Ratio.

### **C3. Alteration of Crude Oil Composition Due to Precipitation**

In two of the precipitation tests, the asphalts were first precipitated by the addition of n-butane and n-pentane to the tank Oil-A. After separation of asphalts from the crude, the deasphalted crude was analyzed by gas-liquid chromatography. In this case, the original oil composition is considerably altered by asphalt precipitation (Table X-5). The amount of heavier ends in the deasphalted crude is less than in the original crude. Also, n-butane removed greater amounts of heavier fraction ( $C_{37}^+$ ) than n-pentane. Furthermore, the deasphalted crude has lower density than original crude. This indicates that in a miscible process, asphaltene precipitation can alter the composition of crude oil which needs to be accounted for in the prediction of solvent-oil phase behavior, compositional path, and miscibility conditions for solvent-oil systems.

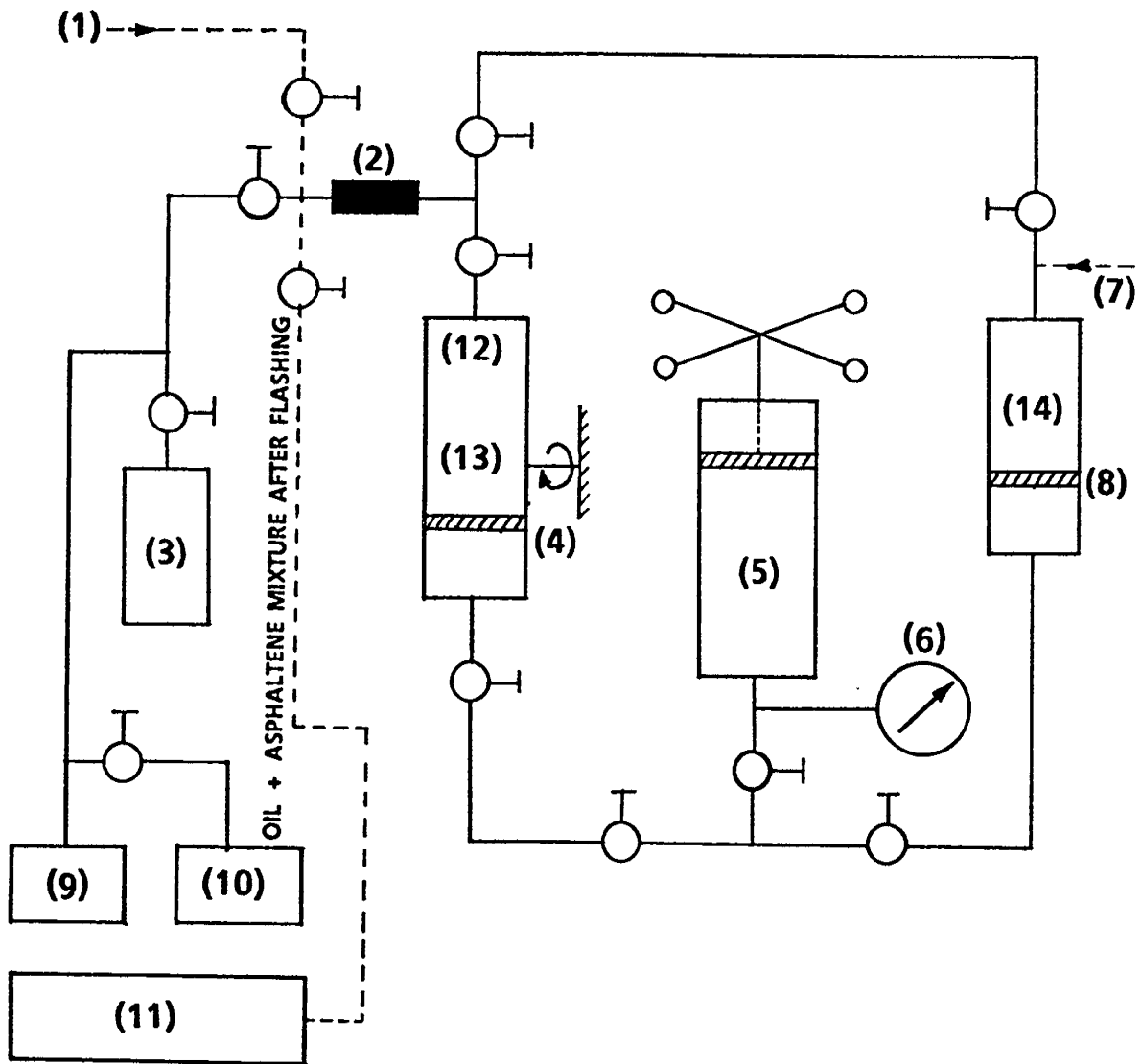
### **C4. Asphaltene Precipitation Tests for Recombined Oils**

An experimental set-up was assembled to study both the asphaltene precipitation from live oil systems at reservoir conditions and the effect of pressure on the amount of asphaltene precipitation. A schematic diagram of the experimental set-up is shown in Figure X-10. The major components of the set up include: 1) JEFRI positive displacement pump, 2) recombination cell, 3) solvent transfer (piston) cell, 4) stainless steel (60 micron) in-line filter, 5) air bath equipped with temperature controller and rocking mechanism. The positive displacement pump was used either to inject gas during recombination of oil or to inject  $CO_2$  at constant pressure into recombination cell to obtain the desired  $CO_2$ -recombined oil mixture.

Initially, a known amount of tank Oil-A was taken into the recombination cell. The dead oil was recombined with methane at 1705 psia and 80°F. The composition of the live oil is given in Table X-2 (page X-8). The solvent ( $CO_2$ ) was then injected from the transfer cell into the recombination cell (which also acted as an asphaltene cell) at constant pressure. The amount of  $CO_2$  injected was monitored from the pump reading. The resulting  $CO_2$ -oil mixture was rocked for several hours to achieve thorough mixing. The mixture was then passed through a high pressure stainless steel in-line filter to separate and recover the precipitated solids. The deasphalted crude was then flashed into a oil-gas separator. The amount of asphaltenes in the filter and oil were then measured using the same procedure as previously described.

**Table X-5: Compositional Changes (Mol %) and Density Changes in West Sak Crude (Tank Oil-A) After Asphaltene Precipitation by N-Pentane and N-Butane.**

<b>COMPONENT</b>	<b>ORIGINAL DEAD OIL</b>	<b>AFTER PREC. WITH N-BUTANE</b>	<b>AFTER PREC. WITH N-PENTANE</b>
C <sub>1</sub> -C <sub>6</sub>	-	-	-
C <sub>7</sub>	1.27	1.19	0.16
C <sub>8</sub>	1.05	2.01	0.28
C <sub>9</sub>	1.35	2.03	0.75
C <sub>10</sub>	1.47	2.11	1.41
C <sub>11</sub>	1.94	2.74	1.94
C <sub>12</sub>	1.97	3.27	2.85
C <sub>13</sub>	2.49	3.45	3.28
C <sub>14</sub>	2.67	3.49	3.53
C <sub>15</sub>	2.30	3.20	3.42
C <sub>16</sub>	2.35	3.29	3.64
C <sub>17</sub>	2.80	3.74	4.28
C <sub>18</sub>	2.55	3.34	3.89
C <sub>19</sub>	2.44	3.10	3.54
C <sub>20</sub>	1.90	2.38	2.68
C <sub>21</sub>	2.43	2.55	2.79
C <sub>22</sub>	1.98	2.75	2.87
C <sub>23</sub>	1.87	1.73	2.13
C <sub>24</sub>	1.22	1.67	1.39
C <sub>25</sub>	1.75	2.06	0.96
C <sub>26</sub>	1.60	1.84	1.58
C <sub>27</sub>	1.25	1.46	1.52
C <sub>28</sub>	1.23	1.59	0.72
C <sub>29</sub>	1.55	1.21	0.91
C <sub>30</sub>	0.69	1.17	0.90
C <sub>31</sub>	2.11	1.38	1.10
C <sub>32</sub>	2.11	3.02	2.55
C <sub>33</sub>	2.52	2.70	2.33
C <sub>34</sub>	1.45	3.22	2.12
C <sub>35</sub>	2.63	1.14	1.90
C <sub>36</sub>	4.14	3.62	2.72
C <sub>37</sub> <sup>+</sup>	40.41	27.01	35.86
	100.00	100.00	100.00
Sp. gravity	0.9390	0.9125	0.9242



- |                        |                           |
|------------------------|---------------------------|
| (1) DEAD OIL VESSEL    | (8) SOLVENT VESSEL        |
| (2) INLINE FILTER      | (9) GAS CHROMATOGRAPH     |
| (3) FLASHED GAS VESSEL | (10) GASOMETER            |
| (4) RECOMBINATION CELL | (11) LIQUID CHROMATOGRAPH |
| (5) DISPLACEMENT PUMP  | (12) GAS                  |
| (6) PRESSURE GAUGE     | (13) CRUDE OIL            |
| (7) GAS CYLINDER       | (14) SOLVENT              |

Figure X-10. Schematic of Experimental Apparatus for Asphaltene Precipitation Studies.

## **C5. Effect of CO<sub>2</sub>/Oil Ratio and Effect of Pressure**

In the first set of experiments, the amount of asphaltenes precipitated by adding CO<sub>2</sub> to oil A in various proportions at 1705 psia (bubble point pressure of oil A) and 80°F was measured. Addition of CO<sub>2</sub> in CO<sub>2</sub>-oil mixture resulted in an increased amount of asphaltene precipitation (Table X-6).

In the second set of experiments, the effect of pressure on asphaltene precipitation from a mixture with constant CO<sub>2</sub>-oil ratio was studied. The results for a mixture containing 30 mol% CO<sub>2</sub> - 70 mol% Oil A, and the results for a mixture containing 50 mol% CO<sub>2</sub> - 50 mol% Oil A are shown in Tables X-7 and X-8, respectively. These data suggest that asphaltene precipitation is highest at the bubble point pressure, and decreases with an increase in the pressure above the bubble point pressure and with decrease in pressure below the bubble point pressure.

## **D. CONCLUSIONS**

Experimental work was undertaken to obtain data on asphaltene precipitation during the addition of various hydrocarbon gases and liquids and CO<sub>2</sub> to two types of tank oils. The experimental results indicate:

1. The amount of asphalt (asphaltene+resin) precipitation from crudes with maximum solvent to oil ratio increases with a decrease in molecular weight of normal paraffinic solvents.
2. Initially an increase in the solvent/oil ratio results in an increase in asphaltene precipitation. However, after a certain point, further increase in solvent/oil ratio results in an insignificant increase in precipitation.

The high pressure asphaltene precipitation tests with CO<sub>2</sub>-live oil mixtures indicate that the effect of pressure on asphaltene precipitation is closely related to the effect of pressure on the solubility of gas in oil which results in changes in oil density and oil-solvent mixture solubility parameter. In general, highest asphaltene precipitation occurs at bubble point pressure and decreases as pressure is increased or decreased below the bubble point pressure.

**Table X-6: Effect of CO<sub>2</sub> Addition to Recombined West Sak Oil A on the Asphaltene Precipitation (at 1705 psia, 80°F).**

MOL% CO <sub>2</sub> IN CO <sub>2</sub> /OIL MIXTURE	WT% ASPHALTENES
0	3.14
20	3.23
40	3.99
60	4.79
80	5.89

**Table X-7: Effect of Pressure on Amount of Asphaltene Precipitation 30 Mol % CO<sub>2</sub> - 70 Mol % West Sak Crude A (recombined at 1705 psia and 80°F).**

PRESSURE (PSIA)	WT% ASPHALTENES IN THE IN-LINE FILTER	WT% ASPHALTENES IN THE OIL
900	0.177	4.472
1300	0.183	4.631
1705	0.197	4.833
2500	0.151	4.569
3000	0.179	4.963
3500	0.183	3.817
4000	0.212	3.389

**Table X-8: Effect of Pressure on Amount of Asphaltene Precipitation 50 Mol % CO<sub>2</sub> - 50 Mol % West Sak Crude A (recombined at 1705 psia and 80°F).**

PRESSURE (PSIA)	WT% ASPHALTENES IN THE IN-LINE FILTER	WT% ASPHALTENES IN THE OIL
1000	0.140	4.170
1705	0.192	6.430
3000	0.156	4.750
4000	0.108	4.510

# CHAPTER XI, PART I: MODELING OF ASPHALTENE EQUILIBRIA, HOMOGENEOUS MOLECULAR THERMODYNAMIC MODEL

---

---

## A. INTRODUCTION

A thermodynamic model based on the coupled Equation of State model and Flory-Huggins theory for polymer solutions was developed. The model parameters such as solubility-parameter of asphaltenes, molecular weight of asphaltenes, and molar volume of asphaltenes were obtained by fitting the model to experimental data gathered. Although the model results show excellent agreement with the experimental data, it was determined that the model is not suitable for the prediction of asphaltene precipitation at high pressures. Further work is in progress to develop a generalized model on asphaltenes that will include heterogeneous characteristics of asphaltenes within crude oil.

## B. REVIEW OF ASPHALTENE EQUILIBRIA MODELING

Two distinct approaches have emerged in formulating asphaltene precipitation thermodynamic model. These are: 1) thermodynamic molecular approach, and 2) thermodynamic colloidal approach. In the first approach (molecular), asphaltene molecules are considered to be dissolved in oil in a true liquid state and may precipitate as a result of changing thermodynamic conditions such as temperature, pressure and composition. Thus, asphaltene precipitation is considered to be thermodynamically reversible. The dissolution of asphaltenes in oil takes longer time than precipitation. The complete dissolution of some asphaltenes in organic solvents like toluene and benzene supports this assumption. In the second approach (colloidal), asphaltenes are considered to colloiddally suspended in crude oil which are stabilized by the adsorbed resin molecules. When the adsorbed resins are dissolved into solution, the asphaltene particles may aggregate mechanically or by electrostatic attraction.

### B1. Thermodynamic Molecular (Solubility) Approach

The different asphaltene equilibria models emerged within the thermodynamic molecular (solubility) approach type, can be classified under two categories based on the treatment of asphaltenes as: i) monodispersed (homogeneous or single component) poly-

meric molecules and, ii) polydispersed (or heterogeneous or multi-component) polymeric molecules.

Models presented by Fussel (1979), Hirschberg et al. (1983), Burke et al. (1988) and Kamath et al. (1991) fall under the monodispersed type. These models are based on the treatment of asphaltenes as a single pseudo component having an average molecular weight, molar volume and solubility parameter. With some modifications these models combine the Flory-Huggins polymer solution theory with the equation of state vapor/liquid equilibria calculations to predict the solubility parameter and molar volume of the asphaltene free-liquid phase and the amount of asphaltene precipitation. Kamath et al. applied the homogeneous model to predict the degree of asphaltene precipitation for various solvent-West Sak oil mixtures and found that homogeneous models have several limitations. These include: 1) insufficient representation of asphaltenes within oil by a single component and 2) limited range of application of the model since molar volume and solubility parameter of asphaltenes treated as independent of pressure and temperature. Recently, Novasad and Costain (1990) adopted Hirschberg's molecular solubility model, but introduced association parameter to represent resin-asphaltene interaction. They were able to successfully correlate the model with the experimental asphaltene precipitation data, but recommended that asphaltenes be described as continuous (polydispersed) phase to improve the accuracy of predictions.

Kawanaka et al. (1988) were the first researchers to represent asphaltenes as continuous polydispersed molecules having molecular weight distribution. Their model uses Scott-Magat theory (Scott and Magat, 1945) to represent asphaltene equilibria and represents an improvement over the homogeneous type models. The model developed in this paper also treats asphaltenes as multicomponent system, but differs from Kawanaka et al.'s model in many other ways.

## **B2. Thermodynamic Colloidal Approach**

This approach assumes that asphaltenes exist in the oil as solid particles in suspension, stabilized by resins (peptizing agents) adsorbed on their surface. Model development and results are discussed in part II of this chapter. The intermolecular repulsive forces between neutral aromatic resin molecules adsorbed on the polar asphaltene particles prevent them from flocculating. When the concentration of resins falls below the critical resin concentration (due to addition of paraffinic solvents), asphaltene particles may aggregate due to neutralization of their weak repulsive forces by mechanical (agitation) or electrical (opposing stream potential) means. Leontaritis and Mansoori (1987), considering the above factors,

developed a thermodynamic-colloidal model capable of predicting the onset of asphaltene flocculation. Their model contains two parts: a static model to determine the chemical potential of resin based on the Flory-Huggins theory and a dynamic model to determine the stream potential for asphaltene to precipitate.

### C. THEORETICAL BASIS

Asphaltenes in crude oil are large, bulky molecules which behave like polymer molecules. Thus, liquid-liquid polymer solution theories can be used to describe phase behavior of asphaltenes, where the remaining components of the crude can be considered as solvent phase in which asphaltenes are either dissolved or suspended. Inherent assumption in such modeling is that the process of asphaltene precipitation is reversible and asphaltenes behave like a non-associating liquid. To model the effect of pressure, temperature, oil composition, and solvent composition on the amount of precipitation, it is necessary to couple the liquid/liquid polymer solution theory to the vapor-liquid equilibria of oil-solvent mixtures.

Two approaches are available to describe asphaltene phase behavior. The first approach considers asphaltenes as a single homogeneous compound represented by an average molecular weight and other asphaltene properties. Such an approach has been used by Hirshberg et al. (1983) and Burke et al. (1988) and is used in this study as well. The second approach considers that asphaltene particles exist in wide ranges of sizes and molecular weights and treats asphaltenes as a polydispersed heterogeneous polymer. In such modelling it is necessary to treat asphaltenes by a continuous distribution function (Kawanaka et al., 1988). While the second approach is more generalized, it requires a large amount of extensive experimental data for fitting model parameters.

### D. LIQUID-LIQUID POLYMER SOLUTION THEORY

In order to apply Flory-Huggins polymer solution theory to asphaltene-crude oil solutions, it is necessary to treat the crude as a mixture of two liquid phases, the first phase being pure asphaltene liquid phase which acts as a solute, and the second phase consisting of the remaining components of crude oil which act as a solvent phase.

The volume fraction  $\phi_A$  of dissolved asphaltenes is given by following expression:

$$\phi_A = \exp\left[\frac{V_A}{V_L}\left(1 - \frac{V_L}{V_A} - \frac{V_L}{RT}(\delta_A - \delta_L)^2\right)\right] \quad (1)$$

where  $V_A$  = molar volume of asphaltenes  
 $V_L$  = molar volume of liquid phase  
 $\delta_A$  = solubility parameter of asphaltenes  
 $\delta_L$  = solubility parameter of liquid phase.

The solubility parameter is defined as a measure of cohesive energy density or the internal pressure that is exerted by the molecules within a solution. It is obtained from the following definition:

$$\delta_i = \left( \frac{\Delta U_i^v}{V_i} \right)^{\frac{1}{2}} \quad (2)$$

where  $\Delta U_i^v$  is the internal energy function and  $V_i$  is the molar volume of component  $i$ . The calculation of solubility parameters will be discussed later.

The value of the solubility parameter is characteristic of a specific molecule. When two liquids possessing considerably different solubility parameters are mixed together, the internal pressure exerted by the liquid with higher solubility parameters will basically squeeze the molecules of lower solubility parameter liquid out of solution matrix, resulting in immiscibility. When the solubility parameters of two liquids approach each other, the mutual solubility also increases.

## E. VAPOR-LIQUID EQUILIBRIA CALCULATIONS

In order to determine the solubility parameter ( $\delta_L$ ) and molar volume ( $V_L$ ) for solvent-oil mixtures at a given pressure and temperature, vapor-liquid equilibrium calculations are performed using Peng-Robinson Equation of State.

Prior to using the Peng-Robinson Equation of State for vapor-liquid equilibria calculations, the Equation of State parameters for each component must be tuned using PVT data for oil. Once the Equation of State has been tuned, the mixture of crude oil and solvent is flashed at desired pressure and temperature to determine the composition of liquid phase. Coat's PVT simulator (Coats, 1984) was used for this purpose. A separate Peng-Robinson Equation of State function program was written to determine the parameters  $\delta_L$  and  $V_L$ .

The first step is to determine parameters  $a_L$  and  $b_L$  as follows:

$$a_i(T_{c_i}) = \Omega_{A_i}^0 \frac{R^2 T_{c_i}^2}{P_{c_i}} \quad (3)$$

where  $R$  is universal gas constant,  $P_{c_i}$  and  $T_{c_i}$  are the critical pressure and the critical temperature of component  $i$ ,  $\Omega_{A_i}^0$  is a constant obtained from tuning of EOS.

At a given temperature  $T$ ,

$$a_i(T) = a_i(T_{c_i}) a_i(T_{r_i}, \omega_i) \quad (4)$$

where

$$a_i = \left[ 1 + K_i \left( 1 - \sqrt{T_{r_i}} \right) \right]^2 \quad (5)$$

where

$$T_{r_i} = \frac{T_{c_i}}{T} \quad (6)$$

and

$$K_i = 0.37464 + 1.54226 \omega_i - 0.26992 \omega_i^2 \quad (7)$$

The  $\omega_i$  is Pitzer accentric factor defined by

$$\omega_i = -\log_{10} \left( \frac{P}{P_{c_i}} \right) T_{r_i} = 0.7 \quad (8)$$

similarly;

$$b_i = \Omega_{B_i}^0 \frac{RT_{c_i}}{P_{c_i}} \quad (9)$$

The mixing rules are then used to calculate  $a_L$  and  $b_L$

$$a_L = \sum_{i=1}^N \sum_{j=1}^N x_i x_j a_{ij} \quad (10)$$

where

$$a_{ij} = (1 - \delta_{ij}) \sqrt{a_i a_j} \quad (11)$$

$x_i$  is mole fraction of component  $i$  in liquid phase and  $\delta_{ij}$  is the binary interaction parameter.

$$b_L = \sum_{i=1}^N x_i b_i \quad (12)$$

The cubic form of Peng-Robinson Equation of State is solved to determine  $Z_L$ , the compressibility factor for liquid phase.

$$Z^3 - (1 - B) Z^2 + (A - 3B^2 - 2B) Z - (AB - B^2 - B^3) = 0 \quad (13)$$

where

$$A = \frac{a_L}{(RT)^2} \quad (14)$$

$$B = \frac{b_L}{RT} \quad (15)$$

The molar volume  $V_L$  is then obtained using

$$V_L = \frac{Z_L RT}{P} \quad (16)$$

In order to obtain the internal energy function  $\Delta U_L^v$ , equation (10) is differentiated w.r.t. temperature to obtain

$$\frac{da_L}{dT} = \sum_i \sum_j x_i x_j (1 - \delta_{ij}) \left( a_i a_j T_{c_i} T_{c_j} \right)^{\frac{1}{2}} \left\{ \left[ 1 + K_j (1 - \sqrt{T_{r_j}}) \right] \left[ -\frac{K_i}{2} \sqrt{T_{r_i}} \right] + \left[ 1 + K_i (1 - \sqrt{T_{r_i}}) \right] \left[ -\frac{K_j}{2} \sqrt{T_{r_j}} \right] \right\} \quad (17)$$

Then

$$\Delta U_L^v = \left( \frac{a_L}{2\sqrt{2b_L}} - \frac{T}{2\sqrt{2b_L}} \frac{da_L}{dT} \right) \ln \left( \frac{V_L + 2.414b_L}{V_L - 0.414b_L} \right) \quad (18)$$

The solubility parameter  $\delta_L$  is then obtained by

$$\delta_L = \left( \frac{\Delta U_L^v}{V_L} \right)^{\frac{1}{2}} \quad (19)$$

## F. MODEL PERFORMANCE

Our model has three parameters, namely, ( $V_A$ ) the molar volume of asphaltenes, ( $\delta_A$ ) the solubility parameter of asphaltenes, and ( $M_A$ ) the molecular weight of asphaltenes. With the knowledge of these three parameters it is possible to predict the amount of asphaltene precipitation that will occur due to addition of a given amount of solvent to crude oil at any pressure and temperature.

To test the model performance, experimental data gathered with Tank Oil A (Table X-1 = Chapter X) were used to fit these 3 parameters. An optimization program was written to obtain the three parameters. For the initial guesses of the parameters  $V_A$  and  $\delta_A$  literature values (Hirshberg et al., 1983; Burke et al., 1988) were used. Method of steepest ascent was used to minimize the following objective function,  $F$ :

$$F = \frac{1}{N_{DATA}} \sqrt{\sum_{i=1}^{N_{DATA}} \left( 1 - \frac{(wt\% Asp)_{pred}}{(wt\% Asp)_{exp}} \right)^2} \quad (20)$$

where  $N_{DATA}$  is number of experimental data points,  $(wt\% Asp)_{exp}$  is experimental value of weight % asphaltenes precipitated and  $(wt\% Asp)_{pred}$  is the predicted value.

Tables XI-1 through XI-8 show the comparison between experimental and predicted amounts of asphaltene precipitation for various solvents such as ethane, CO<sub>2</sub>, propane, n-butane, n-pentane, n-heptane, NGL and PBG, respectively, after optimization of the three parameters. Figures XI-1 through XI-7 give plots of weight percent of asphaltenes (predicted by this model as well as experimentally determined amounts) versus solvent/oil ratio by weight for the same solvents, respectively. A good match can be seen between the experimental and predicted amounts of asphaltene precipitation. Also, the trend of initial increase in the weight percent of precipitated asphaltenes with solvent ratio can be seen which levels off after reaching a peak value. This trend is not seen obviously due to insufficient data points on the graphs.

**Table XI-1: Comparison of Experimental and Predicted Amounts of Asphaltene Precipitation for Ethane - West Sak Tank Oil A Mixtures.**

<b>SOLVENT/OIL RATIO BY WT.</b>	3.0	13.0
$V_L$ (FT <sup>3</sup> /LBMOLE)	6.20	6.24
$\delta_L$ (PSIA) <sup>0.5</sup>	196.41	196.54
$M_L$ (LB/LBMOLE)	363.4	366.6
<b>WT % ASP. (EXPERIMENTAL)</b>	5.14	5.28
<b>WT % ASP. (PREDICTION)</b>	5.14	5.28
<b>% ERROR</b>	0.00	0.00

**Table XI-2: Comparison of Experimental and Predicted Amounts of Asphaltene Precipitation for CO<sub>2</sub> - West Sak Tank Oil A Mixtures.**

<b>SOLVENT/OIL RATIO BY WT.</b>	3.60	13.60	15.30
$V_L$ (FT <sup>3</sup> /LBMOLE)	6.27	6.30	6.30
$\delta_L$ (PSIA) <sup>0.5</sup>	196.55	196.62	196.65
$M_L$ (LB/LBMOLE)	368.4	370.8	371.2
<b>WT % ASP. (EXPERIMENTAL)</b>	5.56	5.80	5.89
<b>WT % ASP. (PREDICTION)</b>	5.50	5.80	5.89
<b>% ERROR</b>	1.09	3.97	2.88

**Table XI-3: Comparison of Experimental and Predicted Amounts of Asphaltene Precipitation for Propane - West Sak Tank Oil A Mixtures.**

<b>SOLVENT/OIL RATIO BY WT.</b>	4.70	7.80	16.30
$V_L$ (FT <sup>3</sup> /LBMOLE)	5.84	5.85	5.87
$\delta_L$ (PSIA) <sup>0.5</sup>	196.05	196.07	196.13
$M_L$ (LB/LBMOLE)	340.5	341.2	342.9
<b>WT % ASP. (EXPERIMENTAL)</b>	8.87	8.60	9.07
<b>WT % ASP. (PREDICTION)</b>	8.34	9.05	9.14
<b>% ERROR</b>	6.03	5.02	0.82

**Table XI-4: Comparison of Experimental and Predicted Amounts of Asphaltene Precipitation for n-Butane - West Sak Tank Oil A Mixtures.**

<b>SOLVENT/OIL RATIO BY WT.</b>	2.00	8.13	13.30
$V_L$ (FT <sup>3</sup> /LBMOLE)	4.46	4.47	4.47
$\delta_L$ (PSIA) <sup>0.5</sup>	193.98	194.03	194.08
$M_L$ (LB/LBMOLE)	250.9	251.4	252.0
<b>WT % ASP. (EXPERIMENTAL)</b>	6.22	6.36	6.45
<b>WT % ASP. (PREDICTION)</b>	6.20	6.43	6.40
<b>% ERROR</b>	0.34	1.09	0.76

**Table XI-5: Comparison of Experimental and Predicted Amounts of Asphaltene Precipitation for n-Pentane - West Sak Tank Oil A Mixtures.**

<b>SOLVENT/OIL RATIO BY WT.</b>	2.00	7.00	12.50	20.20
$V_L$ <b>(FT<sup>3</sup>/LBMOLE)</b>	2.19	1.92	1.87	1.85
$\delta_L$ <b>(PSIA)<sup>0.5</sup></b>	182.44	178.27	177.28	176.70
$M_L$ <b>(LB/LBMOLE)</b>	98.56	80.20	76.71	74.99
<b>WT % ASP. (EXPERIMENTAL)</b>	1.79	6.20	6.30	6.69
<b>WT % ASP. (PREDICTION)</b>	-	6.47	5.37	7.38
<b>% ERROR</b>	-	4.39	14.78	10.37

**Table XI-6: Comparison of Experimental and Predicted Amounts of Asphaltene Precipitation for n-Heptane - West Sak Tank Oil A Mixtures.**

<b>SOLVENT/OIL RATIO BY WT.</b>	2.00	7.30	13.50	20.10
$V_L$ <b>(FT<sup>3</sup>/LBMOLE)</b>	2.85	2.53	2.47	2.45
$\delta_L$ <b>(PSIA)<sup>0.5</sup></b>	185.27	182.08	181.32	181.03
$M_L$ <b>(LB/LBMOLE)</b>	132.3	130.8	106.8	103.8
<b>WT % ASP. (EXPERIMENTAL)</b>	3.83	5.34	7.50	7.32
<b>WT % ASP. (PREDICTION)</b>	-	5.41	7.05	7.32
<b>% ERROR</b>	-	1.29	6.06	4.81

**Table XI-7: Comparison of Experimental and Predicted Amounts of Asphaltene Precipitation for NGL - West Sak Tank Oil A Mixtures.**

<b>SOLVENT/OIL RATIO BY WT.</b>	3.20	7.60	9.90
$V_L$ (FT <sup>3</sup> /LBMOLE)	2.33	2.12	2.08
$\delta_L$ (PSIA) <sup>0.5</sup>	183.07	179.87	179.23
$M_L$ (LB/LBMOLE)	105.3	91.1	88.4
<b>WT % ASP. (EXPERIMENTAL)</b>	5.73	8.80	8.88
<b>WT % ASP. (PREDICTION)</b>	-	8.80	8.88
<b>% ERROR</b>	-	0.00	0.00

**Table XI-8: Comparison of Experimental and Predicted Amounts of Asphaltene Precipitation for PBG - West Sak Tank Oil A Mixtures.**

<b>SOLVENT/OIL RATIO BY WT.</b>	1.59	1.70	5.85	10.42
$V_L$ (FT <sup>3</sup> /LBMOLE)	6.19	6.19	6.22	6.24
$\delta_L$ (PSIA) <sup>0.5</sup>	196.41	196.43	196.49	196.55
$M_L$ (LB/LBMOLE)	362.7	372.8	364.6	366.2
<b>WT % ASP. (EXPERIMENTAL)</b>	5.49	7.40	8.15	8.08
<b>WT % ASP. (PREDICTION)</b>	6.22	6.24	7.54	8.48
<b>% ERROR</b>	13.32	15.66	7.54	5.01

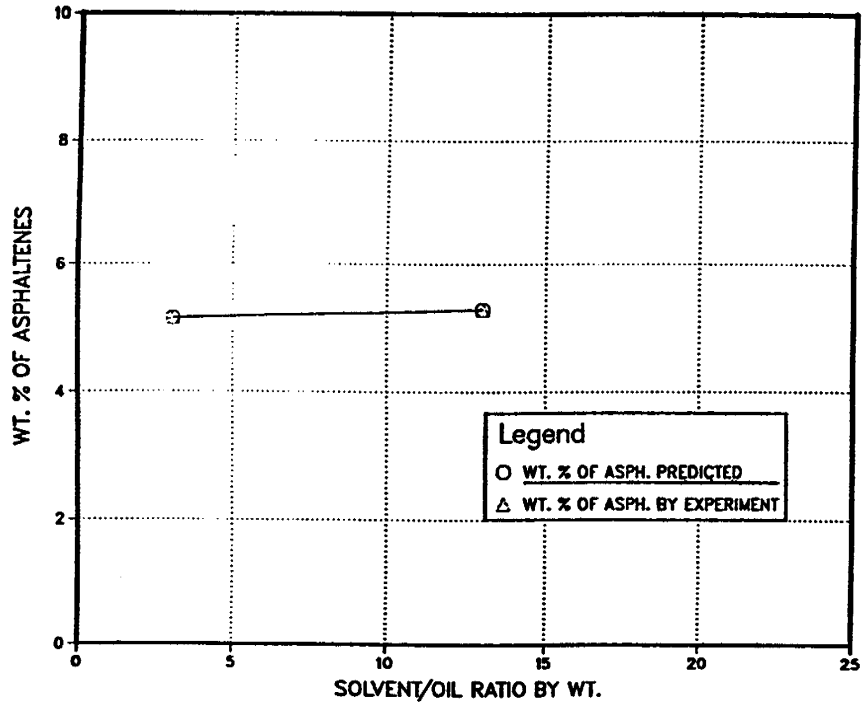


Figure XI-1. Comparison of Experimental and Predicted Amounts of Asphaltene Precipitation for Ethane - West Sak Tank Oil Mixtures.

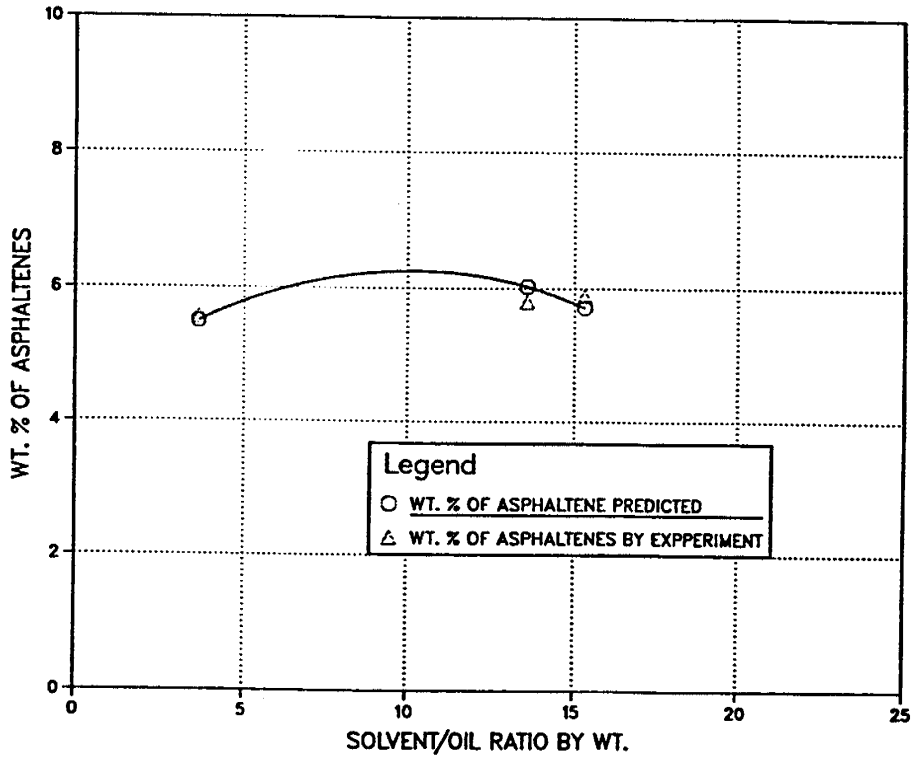


Figure XI-2. Comparison of Experimental and Predicted Amounts of Asphaltene Precipitation for CO<sub>2</sub> - West Sak Tank Oil Mixtures.

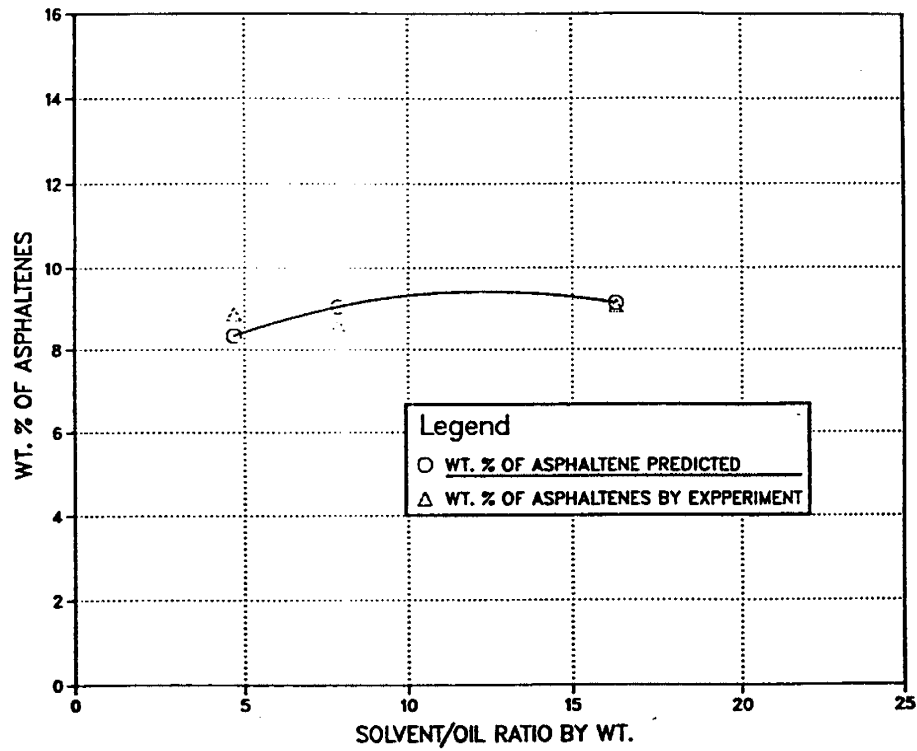


Figure XI-3. Comparison of Experimental and Predicted Amounts of Asphaltene Precipitation for Propane - West Sak Tank Oil Mixtures.

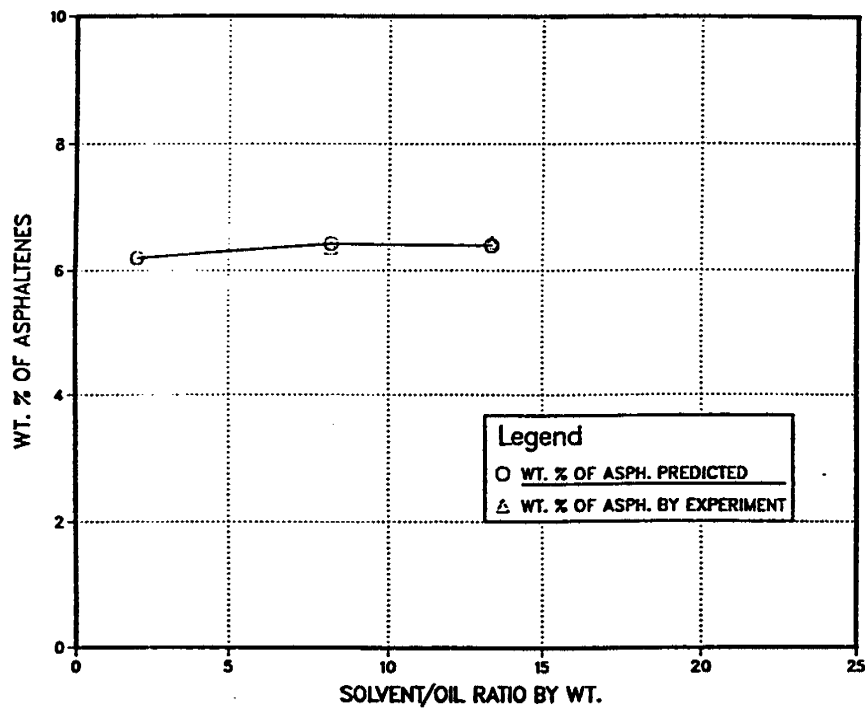


Figure XI-4. Comparison of Experimental and Predicted Amounts of Asphaltene Precipitation for n-Butane - West Sak Tank Oil Mixtures.

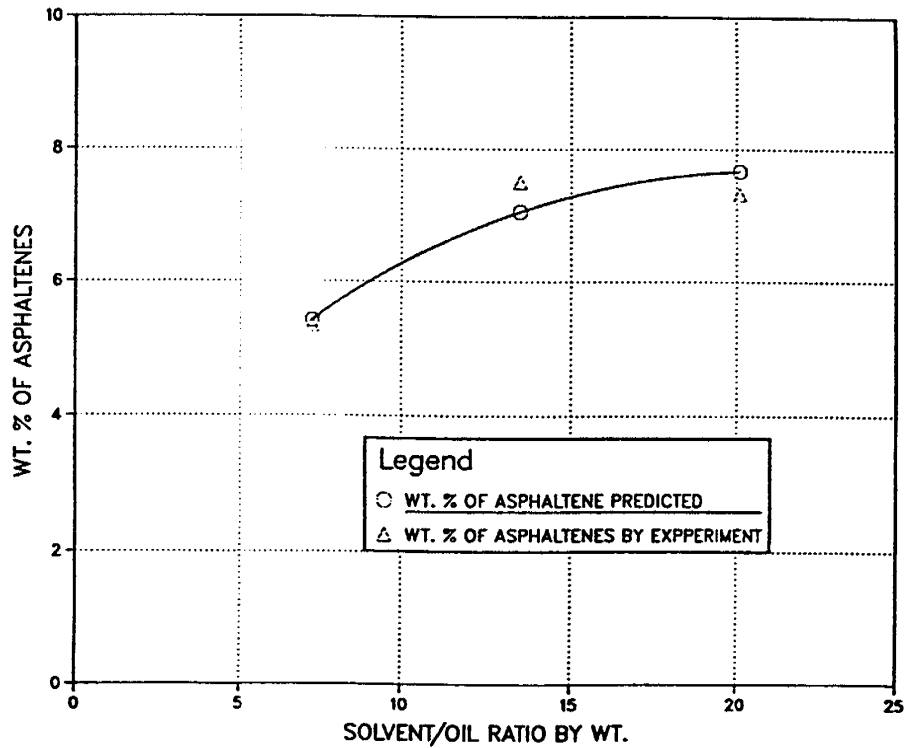


Figure XI-5. Comparison of Experimental and Predicted Amounts of Asphaltene Precipitation for n-Heptane - West Sak Tank Oil Mixtures.

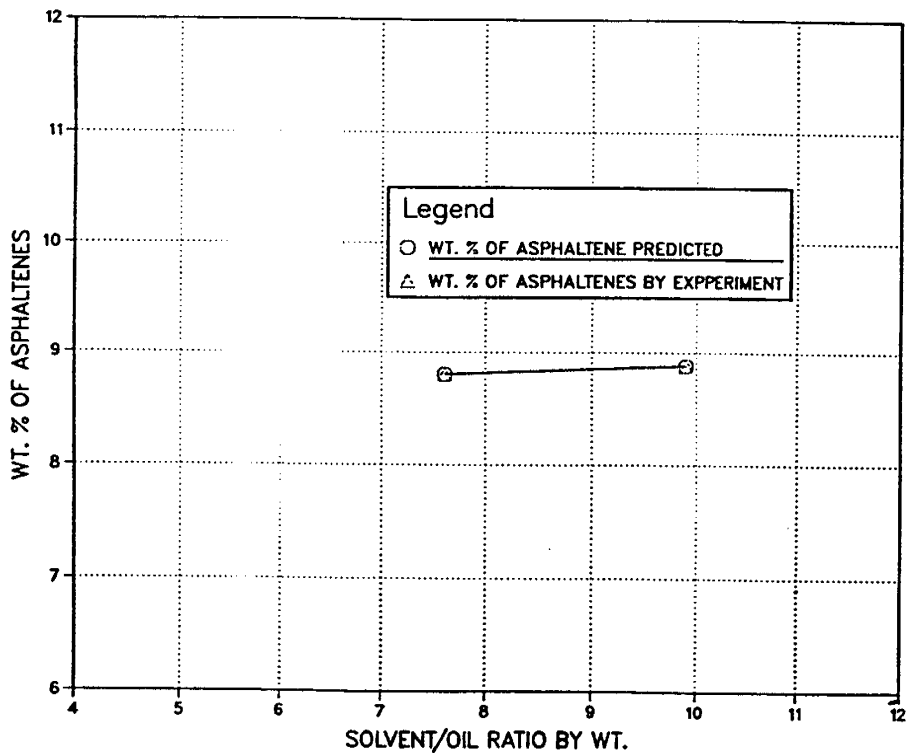


Figure XI-6. Comparison of Experimental and Predicted Amounts of Asphaltene Precipitation for NGL - West Sak Tank Oil Mixtures.

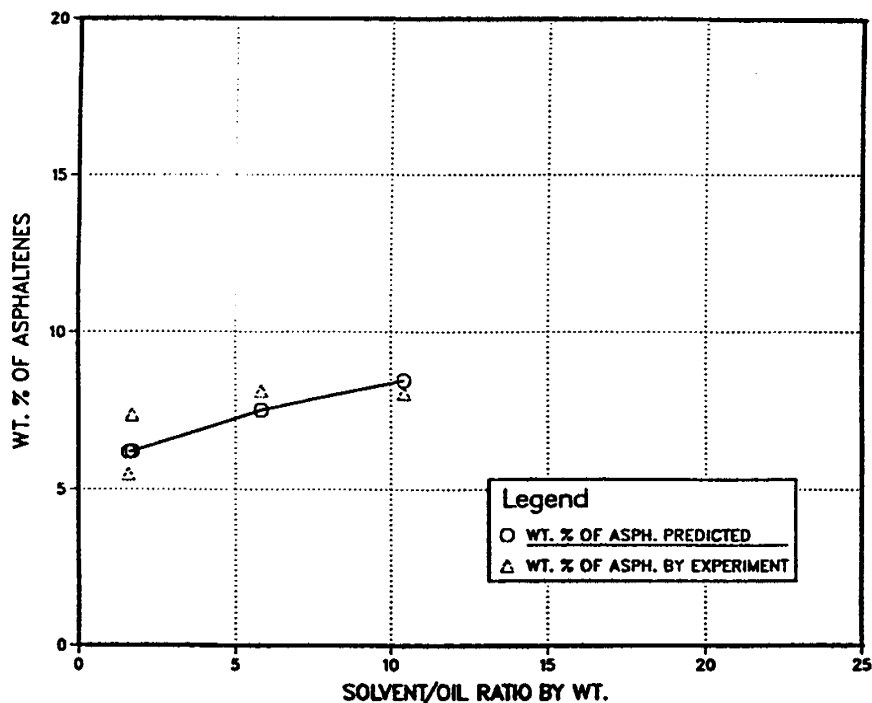


Figure XI-7. Comparison of Experimental and Predicted Amounts of Asphaltene Precipitation for PBG - West Sak Tank Oil Mixtures.

The values of optimized parameters for asphaltenes are given in Table XI-9. The model predictions in general are in close agreement with the experimental values of asphaltene precipitation. However, there are three problems with this model, i.e., equation (1). First, it was not possible to obtain one set of parameters for all solvent-oil mixtures. This is expected since each solvent may precipitate a different range of asphaltene fractions of the crude oil. Hence optimization was done to fit parameters for each solvent separately. The second problem is more important; the model is not capable of predicting asphaltene precipitation for those solvent-oil systems which have considerable variation in  $V_L$  and  $\delta_L$  parameters due to addition of solvent to oil. This is due to the exponential nature of equation (1). For example, in Tables XI-5 through XI-7 (i.e., for solvents n-pentane, n-heptane and NGL) the addition of solvent changes the  $V_L$  and  $\delta_L$  values for liquid phase, thus low solvent/oil dilution ratio's were not used in regression of asphaltene parameters. But for other solvents such as ethane to n-butane,  $\text{CO}_2$ , and PBG, the addition of solvents did not change  $V_L$  and  $\delta_L$  considerably and thus all solvent/oil dilution ratios could be used in regression of

parameters. The third problem observed with the model is that the parameters fitted with low pressure experimental data are not useful in predicting asphaltene precipitation at higher pressures. Again, this is due to alteration of  $V_L$  and  $\delta_L$  with pressure. Thus, model improvement is needed to account for the effect of pressure on the asphaltene precipitation.

**Table XI-9: Optimized Values of Asphaltene Solubility Parameter, Asphaltene Molar Volume and Asphaltene Molecular Weight for Various Solvents (West Sak Tank Oil A).**

SOLVENT	$\delta_A$ (PSIA) <sup>0.5</sup>	$V_A$ (FT <sup>3</sup> /LBMOLE)	$M_A$ (LB/LBMOLE)
Ethane	219.69	14.48	2491
Carbon Dioxide	219.71	14.48	1531
Propane	220.57	14.48	3080
N-Butane	208.06	5.17	1100
N-Pentane	216.84	3.76	1605
N-Heptane	219.89	6.68	2483
NGL	217.00	4.21	1468
PBG	202.70	6.37	1738

## G. CONCLUSIONS

A thermodynamic model based on Flory-Huggins polymer-solution theory was developed and coupled with Equation of State model to predict the amount of asphaltene precipitation. The model prediction shows close agreement with the experimental data after regression of asphaltene properties such as molar volume, solubility parameter and molecular weight. The model, however, fails to account for the effect of large changes in the solubility parameters of the oil-solvent mixtures.

## H. NOMENCLATURE

$a_i$	Variables defined by equations (3) and (4)
$a_L$	Equation of state constant defined by equation (10)
$A$	Equation of state parameter defined by equation (11)
$b_i$	Variables defined by equation (9)
$b_L$	Equation of state constant defined by equation (12)
$B$	Equation of state parameter defined by equation (15)
$F$	Objective function defined by equation (20)
$K_i$	Variable defined by equation (7)
$M_A$	Molecular weight of asphaltenes
$M_L$	Molecular weight of liquid phase
$N$	Number of components
$P$	Pressure
$P_{c_i}$	Critical pressure of component $i$
$R$	Universal gas constant
$T$	Temperature
$T_{c_i}$	Critical temperature of component $i$
$T_{r_i}$	Reduced temperature of component $i$
$V_A$	Molar volume of asphaltenes
$V_L$	Molar volume of liquid phase
$x_i$	Mole fraction of component $i$ in liquid phase

## H. NOMENCLATURE (Continued)

$z_L$  Compressibility factor for liquid phase

### Greek Symbols

$a_i$  Parameter defined by equation (5)

$\delta_A$  Solubility parameter of asphaltenes

$\delta_L$  Solubility parameter of liquid phase

$\delta_{ij}$  Binary interaction parameter in EOS

$\phi_A$  Vol. fraction of asphaltenes dissolved in liquid phase

$\Delta U_i^v$  Internal energy function in equation (2) for component  $i$

$\Omega_{A_i^o}$  Tuned constant for component  $i$

$\Omega_{B_i^o}$  Tuned constant for component  $i$

$\omega_i$  Accentric factor for component  $i$

## CHAPTER XI, PART II: MODELING OF ASPHALTENE EQUILIBRIA, POLYDISPERSED MOLECULAR THERMODYNAMIC MODEL

---

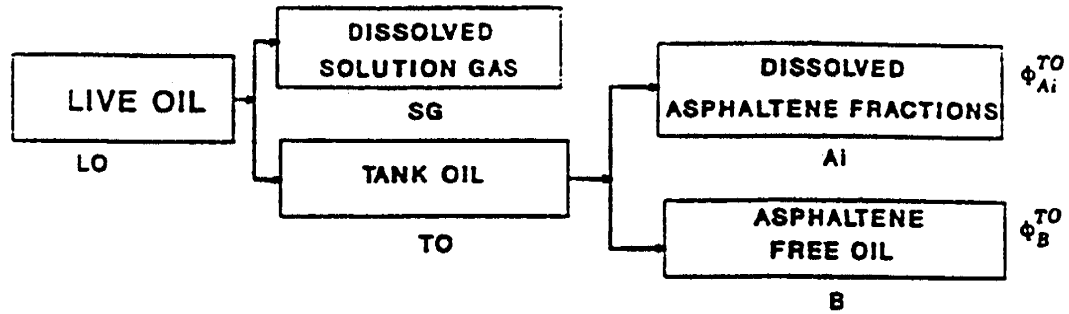
### A. INTRODUCTION

In this chapter, a molecular thermodynamic model was developed to represent asphaltene equilibria and to predict the amount of asphaltene precipitation that would occur from a reservoir oil under influence of a miscible solvent or immiscible gas. The model treats the asphaltenes to exist in the crude in a large range of molecular weights represented by a normal distribution function. The properties of each asphaltene pseudo-component such as solubility parameter and molar volume are obtained based on their molecular weights at given pressure and temperature. Scott-Magat theory along with binary interaction parameter between asphaltene free liquid phase (solvent) and asphaltenes are used represent asphaltene solid-liquid equilibria and to predict the degree of asphaltene precipitation, the molar distribution of asphaltene pseudo-components in equilibrium solid and liquid phases at various pressures, temperatures and solvent-oil compositions. The model is coupled with Peng-Robinson equation of state for vapor-liquid equilibria calculations. The model uses an iterative Newton-Raphson scheme to obtain solution. The model has four parameters which are determined by fitting the model to experimental asphaltene precipitation data for tank West Sak oil-solvent mixtures. The model is used to predict asphaltene precipitation for CO<sub>2</sub>-West Sak oil mixtures at various pressures.

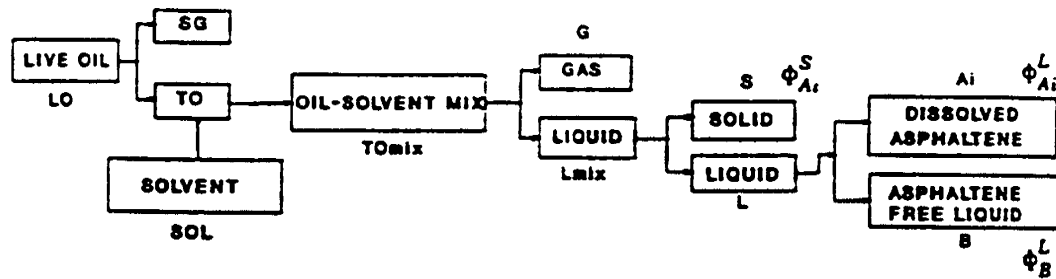
### B. DESCRIPTION OF MULTICOMPONENT ASPHALTENE MODEL

Since asphaltenes exist in crude oil in large range of molecular weights, for proper representation of asphaltene equilibria we considered multi-component asphaltene modeling approach. Figure XI-8 shows a schematic representation of various phases and fractions of oil and oil-solvent mixtures for three situations: a) asphaltenes in reservoir oil, b) asphaltenes precipitated by addition of solvents to tank oil, c) asphaltenes precipitated by addition of solvents to live oil. In case (a), the live oil (*LO*) is considered to be a mixture of  $N_T$  components of which,  $N_F$  are asphaltene free components and  $N_A$  are asphaltene pseudocomponents. The live oil is made up of solution gas (*SG*) which contains asphaltene free lighter hydrocarbons which are dissolved and tank oil (*TO*) which is further divided into asphaltene free oil (*B*) and dissolved asphaltene components ( $A_i, i=1, N_A$ ).

A. Asphaltenes in Live Reservoir Oil



B. Asphaltene Precipitation from Addition of Solvents to Tank Oil



C. Asphaltene Precipitation from Addition of Solvents to Live Oil

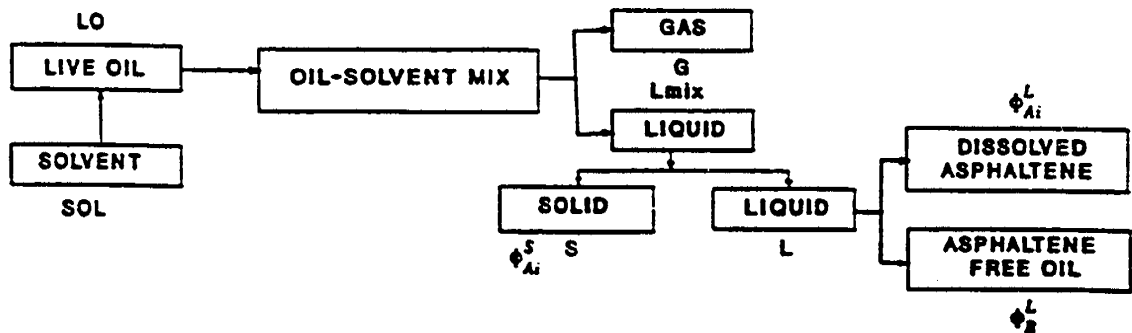


Figure XI-8. Schematic Representation of Various Fractions and Phases of Oil and Oil-Solvent Mixtures.

In case (b), upon addition of certain proportion of solvent (*SOL*) to the tank oil (*TO*), an overall oil-solvent mixture (*TO<sub>mix</sub>*) is formed which splits into vapor (*G*) and liquid (*L<sub>mix</sub>*) phases according to VLE calculations. The *L<sub>mix</sub>* phase instantaneously splits into an equilibrium solid (*S*) phase which contains only precipitated asphaltene components and an equilibrium liquid (*L*) phase according to solid-liquid equilibrium calculations. Finally, the *L* phase consists of asphaltene free liquid (*B*) phase and dissolved asphaltene fractions (*A<sub>i</sub>*). The case (c) is similar to case (b) except solvents are added to live oil (*LO*) rather than tank oil (*TO*).

### B1. Discretization of Continuous Asphaltene Molecular Weight Distribution Function

If we consider the asphaltenes in crude oil in a large range of molecular weights described a continuous normal distribution function,  $F(M_A)$  given by:

$$F(M_A) = \frac{1}{\sigma\sqrt{2\pi}} \exp\left(-\frac{\xi^2}{2}\right) \quad (1)$$

where,

$$\xi = \frac{M_A - \overline{M_A}}{\sigma} \quad (2)$$

$M_A$  is the molecular weight of asphaltenes treated as a continuous variable,  $\overline{M_A}$  is the average molecular weight of asphaltenes and  $\sigma$  is standard deviation of the normal distribution function.

If we discretize the continuous normal distribution function as shown in Figure XI-9 such that the area under the two curves are same, then the discretized distribution is characterized by  $N_A$  equal intervals of  $\Delta M_A$  and the initial value  $M_{AO}$  and the final value  $M_{AF}$ . Theoretically,  $M_{AO}$  tends to  $-\infty$  and  $M_{AF}$  tends to  $+\infty$ . But for practical purposes, it is sufficient to approximate the span of molecular weight to  $6\sigma$  since it causes only 0.26% error.

Therefore, 
$$M_{AO} = \overline{M_A} - 3\sigma \quad (3)$$

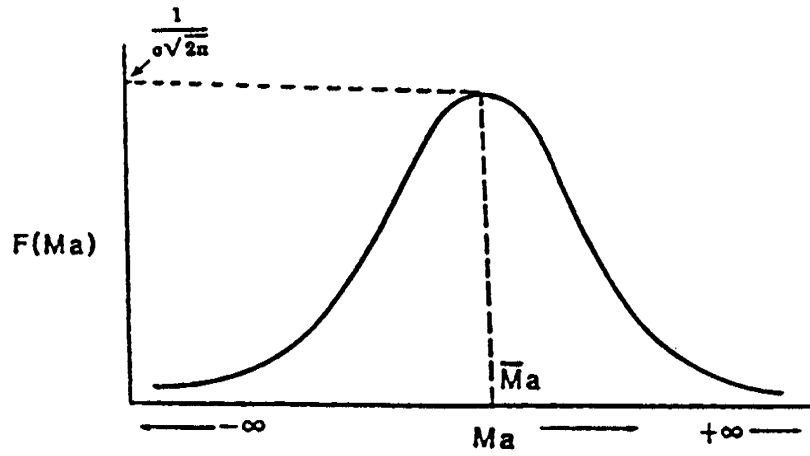
$$M_{AF} = \overline{M_A} + 3\sigma \quad (4)$$

$$\int_{-\infty}^{+\infty} F(M_A) dM_A = \sum_{i=1}^{N_A} F(M_{Ai}) \Delta M_A = 0.9974 \approx 1 \quad (5)$$

Thus, the molecular weight of *i*th component of asphaltenes is given by:

$$M_{Ai} = M_{AO} + \frac{3\sigma}{N_A} [2i - 1], \quad i = 1, N_A \quad (6)$$

CONTINUOUS



DISCRETIZED

$N_a$  Intervals

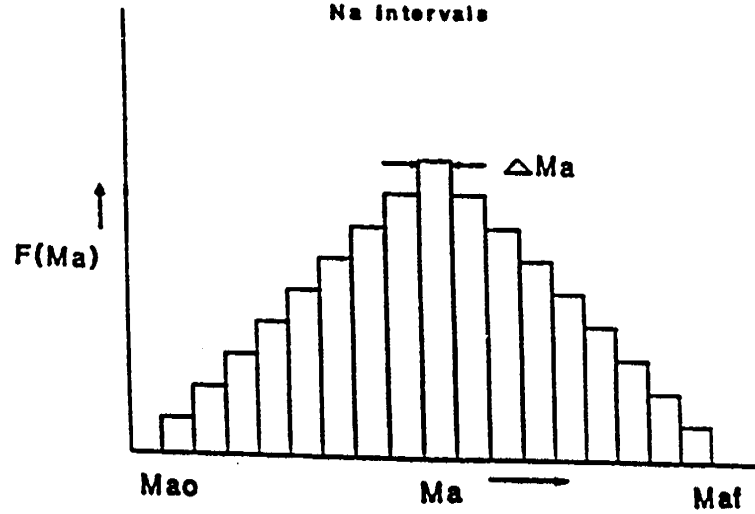


Figure XI-9. Discretization of a Continuous Normal Distribution Function of Asphaltenes Fractions.

Also, 
$$\xi_i = \frac{3}{N_A} [2i - 1 - N_A], \quad i = 1, N_A \quad (7)$$

If  $X_{AT}^{TO}$  is the total mole fractions of asphaltenes in the tank oil, then

$$X_{AT}^{TO} = \sum_{i=1}^{N_A} X_{Ai}^{TO} \quad (8)$$

and 
$$\overline{M}_A^{TO} = \frac{1}{X_{AT}^{TO}} \sum_{i=1}^{N_A} M_{Ai} X_{Ai}^{TO} \quad (9)$$

The mole fraction of *i*th asphaltene component is then obtained by

$$X_{Ai}^{TO} = \frac{3\sqrt{2}}{\sqrt{n}} \frac{X_{AT}^{TO}}{N_A} \exp(-0.5 \xi_i^2), \quad i = 1, N_A \quad (10)$$

## B2. Asphaltene Pseudocomponent Property Estimation

The molar volume of each asphaltene pseudocomponent is given by:

$$V_{Ai} = \frac{M_{Ai}}{\rho_A} \quad (11)$$

where  $\overline{\rho}_A$  is the average density of the asphaltenes.

Twu's critical property correlation (Twu, 1984) is used to compute critical temperature ( $T_{ci}$ ) and the normal boiling point ( $T_{bi}$ ) for *i*th asphaltene component based on the molecular weight,  $M_{Ai}$ . Kistyakowsky's equation (Gambill, 1957) is then used to compute the heat of vaporization given by:

$$(\Delta H_i)_T = (\Delta H_i)_{TB} \left( \frac{T_{Ci} - T}{T_{Ci} - T_{bi}} \right) \quad (12)$$

where 
$$(\Delta H_i)_{TB} = 1.014 [T_{bi} (8.75 + 4.571 \log (T_{bi}))] \quad (13)$$

where  $T_{Ci}$ ,  $T_{bi}$  and  $T$  are in ( $^{\circ}\text{K}$ ) and  $(\Delta H_i)_T$  is in (cal/gmole). The solubility parameter for each asphaltene component is then given by:

$$\delta_{Ai} = \left[ \frac{(\Delta H_i)_T - RT}{V_{Ai}} \right]^{0.5} \quad (14)$$

### B3. Asphaltene Solid-Liquid Equilibria

Using the Scott-Magat theory to represent solid-liquid equilibria for asphaltenes as proposed by Kawanaka et al. (1988), the solid-liquid equilibrium constant for the  $i$ th asphaltene component, ( $K_{Ai}$ ) is given by:

$$K_{Ai} = \frac{X_{Ai}^S}{X_{Ai}^L} = \frac{\phi_{Ai}^S}{\phi_{Ai}^L} \cdot \frac{V_A}{V_L} = \frac{V_A}{V_L} \exp \left[ \left( \frac{V_{Ai}}{V_A} - \frac{V_{Ai}}{V_B} \right) \phi_B + f \frac{V_{Ai}}{V_B} \phi_B^2 \right] \quad (15)$$

where superscripts  $S$  and  $L$  refer to equilibrium solid and liquid phases respectively,  $X_{Ai}$  is the mole fraction and  $\phi_{Ai}$  is the volume fraction of  $i$ th component of asphaltenes,  $V_A$  and  $V_B$  are the molar volumes of asphaltenes and asphaltene-free liquid phase, respectively, given by:

$$V_A = \sum_{i=1}^{N_A} \frac{(V_{Ai} X_{Ai}^{Lmix})}{X_{AT}^{Lmix}} \quad (16)$$

$$V_B = \frac{(V_{Lmix} - X_{AT}^{Lmix} \cdot V_A)}{(1 - X_{AT}^{Lmix})} \quad (17)$$

where  $V_{Lmix}$ ,  $X_{Ai}^{Lmix}$  and  $X_{AT}^{Lmix}$  are molar volume, mole fraction of  $i$ th asphalt component and total asphaltene mole fraction in  $Lmix$  phase respectively.  $V_L$  is the mole volume of equilibrium liquid phase.  $\phi_B$  is the volume fraction of asphaltene free components in  $Lmix$  phase which is obtained as:

$$\phi_B = 1 - \phi_A = 1 - \sum_{i=1}^{N_A} \phi_{Ai}^{Lmix} \quad (18)$$

and

$$\phi_{Ai}^{Lmix} = \frac{X_{Ai}^{Lmix} V_{Ai}}{V_{Lmix}} \quad (19)$$

The parameter  $f$  in equation (15) is defined as:

$$f = \frac{1}{r} + \frac{V_B}{RT} \left[ (\delta_A - \delta_B)^2 + 2K_{AB} \delta_A \delta_B \right] \quad (20)$$

where  $r$  is coordination number (between 3 and 4),  $K_{AB}$  is the binary interaction parameter between asphaltenes and asphaltene free components,  $\delta_A$  and  $\delta_B$  are the average solubility parameters for asphaltenes and asphaltene free components given by:

$$\delta_A = \frac{1}{\phi_A} \left[ \sum \phi_{Ai}^{Lmix} \delta_{Ai} \right] \quad (21)$$

$$\delta_B = \frac{(\delta_{Lmix} - \delta_A \phi_A)}{\phi_B} \quad (22)$$

In equation (20), the first term comes from entropy of mixing whereas the second term comes from the enthalpy of mixing.

The interaction parameter  $K_{AB}$  is treated as the linear function of the average molecular weight of asphaltene free components in the  $L_{mix}$  phase.

$$K_{AB} = a' + b' \overline{M_B^{Lmix}} \quad (23)$$

where  $a'$  and  $b'$  are parameters obtained by fitting experimental asphaltene precipitation data for tank oil-solvent mixtures. Thus, this interaction parameter incorporates effect of solvent/oil ratio and solvent molecular weight on the degree of asphaltene precipitation.

#### B4. Vapor-Liquid Equilibria

In order to determine the equilibrium  $L_{mix}$  phase composition ( $X_i^{Lmix}$ ), molar volume ( $V_{Lmix}$ ), and solubility parameter ( $\delta_{Lmix}$ ), vapor-liquid equilibria calculations for a given oil-solvent mixture ( $Z_i^{Lomix}$  or  $Z_i^{Tomix}$ ) at given pressure and temperature are performed using the Peng-Robinson equation of state as described in Kamath et al. (1991).

#### B5. Stepwise Model Calculations and Regression of Experimental Data

The model is capable of predicting the amount of asphaltene precipitation, the molar distribution of various asphaltene components in the equilibrium solid ( $S$ ) and liquid ( $L$ ) phases and the equilibrium constant for each asphaltene component ( $K_{Ai}$ ) for a given oil-solvent mixture at given pressure and temperatures. The input data to the model includes: the overall composition of the oil, composition of solvent, solvent to oil ratio, pressure, temperature and values for four model parameters namely:  $a'$ ,  $b'$ ,  $\sigma$  and  $\beta$  (the ratio of total mole fraction of asphaltenes to mole fraction of plus fraction in the tank oil). The model can be used in predictive mode or regression mode. In the regression mode, the experimental

asphaltene precipitation data for tank oil/solvent mixtures for various solvent/oil ratios are fitted to obtain the four model parameters. The stepwise procedure in predictive mode is given below:

- Step 1) The PVT data for the oil is initially used to tune the Equation of State parameters.
- Step 2) The VLE calculations are then performed at given  $P$ ,  $T$  and overall oil-solvent mixture composition to determine flashed equilibrium liquid phase properties ( $X_i^{Lmix}$ ,  $V_{Lmix}$  and  $\delta_{Lmix}$ )
- Step 3) The mole fractions ( $X_{Ai}^{TO}$  or  $X_{Ai}^{LO}$ ,  $X_{Ai}^{Lmix}$ ) and molecular weights ( $M_{Ai}$ ) of each asphaltene components in the tank oil (or live oil) and the oil-solvent mixture ( $L_{mix}$ ) are obtained using equations (1) through (10). Note that superscript  $TO$  can be replaced by  $LO$  or  $L_{mix}$  in equations (8-10). Also note that:

$$X_{AT}^j = \beta X_+^j \quad j = TO, LO \text{ or } Lmix \quad (24)$$

- Step 4) The molar volume ( $V_{Ai}$ ) and solubility parameter ( $\delta_{Ai}$ ) are calculated using equations (11) through (14). Also,  $V_A$ ,  $V_{\bar{B}}$ ,  $\phi_A$ ,  $\delta_A$ ,  $\delta_B$  are calculated using equations 16, 17, 18, 19, 21, and 22 respectively.
- Step 5) The ratio  $\frac{\phi_{Ai}^S}{\phi_{Ai}^L}$  and  $K_{Ai}$  are obtained using equations (23), (20) and (15) in that order.
- Step 6) Newton Raphson iterative technique is used to calculate molar volume of equilibrium liquid phase ( $V_L$ ) using  $V_L = 0.95 V_{Lmix}$  as initial guess. The function  $f(V_L)$  is defined and calculated as:

$$f(V_L) = V_A - \sum_{i=1}^{N_A} \frac{V_{Ai} X_{Ai}^{Lmix}}{\left[ \left( \frac{V_{Lmix} - V_A}{V_L - V_A} \right) + \left( \frac{V_L - V_{Lmix}}{V_L - V_A} \right) K_{Ai} \right]} \quad (25)$$

The new value of  $V_L$  is then obtained as:

$$V_L \text{ (new)} = V_L \text{ (old)} - \frac{f(V_L)}{f'(V_L)} \quad (26)$$

where  $f'(V_L)$  is the derivative of  $f(V_L)$  with respect to  $V_L$ . These calculations are repeated till the following convergence criteria is satisfied:

$$\left( \frac{f(V_L)}{f'(V_L)V_L} \right) \leq 0.001 \quad (27)$$

Step 7) By considering the material balance for each asphaltene component between  $L_{mix}$ ,  $L$  and  $S$  phases the following expressions are derived and used to calculate mole and volume fractions of each component of asphaltene in  $L$  phase and  $S$  phase respectively:

$$X_{Ai}^L = \frac{X_{Ai}^{Lmix}}{\left[ \left( \frac{V_{Lmix} - V_A}{V_L - V_A} \right) + \left( \frac{V_L - V_{Lmix}}{V_L - V_A} \right) K_{Ai} \right]} \quad (28)$$

$$X_{Ai}^S = K_{Ai} X_{Ai}^L \quad (29)$$

$$\phi_{Ai}^L = \frac{(X_{Ai}^L V_{Ai})}{V_L} \quad (30)$$

$$\phi_{Ai}^S = \frac{(X_{Ai}^S V_{Ai})}{V_A} \quad (31)$$

the average molecular weights of asphaltene in solid and liquid are then calculated.

Step 8) The weight fraction of asphaltene precipitated ( $W_{AD}$ , gm asphaltene precipitated/gm of tank or live oil) is then obtained as follows:

$$W_{AD} = \left( \frac{V_L - V_{Lmix}}{V_L - V_A} \right) \frac{\overline{M}_A^S}{\overline{M}_O} \left( \frac{X_{AT}^O}{X_{AT}^{Lmix}} \right) \quad O = LO \text{ or } TO \quad (32)$$

where  $\overline{M}_O$  is the average molecular weight of oil.

## B6. Model Features, Advantages and Limitations

This model has several advantages over the homogeneous model developed previously (Kamath et al., 1991). These are as follows:

1. The model is a more realistic representation of asphaltene existence in the crude oil, i.e., they exist in large range of molecular weight distributions. Thus the limitation of

using one average molecular weight to represent all asphaltene components within the crude oil are eliminated.

2. The model allows for effect of solvent molecular weight through the use of an interaction parameter between asphaltenes and asphaltene-free components.
3. The model allows for incorporation of effect of pressure and temperature on the asphaltene properties.
4. The model allows calculation of molar distribution of various asphaltene components in equilibrium solid(*S*), liquid (*L*), oil-solvent mixture ( $L_{mix}$ ) and oil phases.
5. The model allows calculation of solid-liquid equilibrium constants for each asphaltene component, which provide further insight into asphaltene deposition process.

The only limitation of the model is that it requires experimental data on asphaltene precipitation for tank oil-solvent mixtures to obtain model parameters which are needed for predictions at other pressure and temperature conditions.

### **C. APPLICATION OF MODEL TO WEST SAK OIL-SOLVENT MIXTURES**

Kamath et al. (1991) reported asphaltene precipitation experimental results for various mixtures of West Sak tank oil and solvents such as ethane, carbon dioxide, propane, n-butane, n-pentane, n-heptane, a natural gas liquid (NGL) and Prudhoe Bay natural gas (PBG) at various solvent to oil ratios. These data were used to fit the model parameters of this model. Table XI-10 shows a comparison of experimental amounts of asphaltene precipitated and predicted values. The average error between the experimental and predicted values is about  $\pm 5.3\%$ . Table XI-11 shows the optimized model parameters. Figures XI-10 through XI-13 show the molar distribution (moles) of various asphaltene components as a function of their molecular weight in tank oil, equilibrium liquid phase and equilibrium solid phase for West Sak tank oil-n-pentane mixtures at various solvent to oil ratios varying from 2 to 20.2. These results show that as more n-pentane is added to tank oil the Wt% asphaltene precipitation increases and then levels off. Also, the heavier asphaltenes (higher molecular weight) tend to precipitate first, and remain in solid phase whereas the lower molecular weight asphaltenes tend to dissolve and remain in equilibrium liquid phase. This means that the solid-liquid equilibrium constant increases with increase in molecular weight of asphaltenes.

**Table XI-10: Comparison of Experimental and Predicted Amounts of Asphaltene Precipitation for Various Solvents--West Sak Tank Oil Mixtures.**

<b>Solvent Used</b>	<b>Solvent/Oil Ratio by Weight</b>	<b>Wt % Asph. (Experimental)</b>	<b>Wt % Asph. (Predicted)</b>
Ethane	3.0	5.14	5.19
	13.0	5.28	5.22
CO <sub>2</sub>	3.6	5.56	5.73
	13.6	5.80	5.75
	15.3	5.89	5.76
Propane	4.7	8.87	8.88
	7.8	8.60	8.88
	16.3	9.07	8.89
N-Butane	2.0	6.22	6.05
	8.1	6.36	6.55
	13.3	6.45	6.55
N-Pentane	2.0	1.79	1.93
	7.0	6.20	6.25
	12.5	6.30	6.20
	20.2	6.69	6.20
N-Heptane	2.0	3.83	3.32
	7.3	5.34	6.56
	13.5	7.50	6.56
	20.1	7.32	6.56
NGL	3.2	5.73	5.66
	7.6	8.80	8.76
	9.9	8.88	8.78
PBG	1.59	5.49	4.32
	1.70	7.40	6.26
	5.85	8.15	8.12
	10.42	8.08	8.12

**Table XI-11: Optimized Model Parameters for West Sak Oil -- Solvent Mixtures.**

SOLVENT	$\beta$	$\sigma$	$a'$	$b'$
Ethane	0.01979	166.0	0.09995	-1.495E-07
Carbon Dioxide	0.02187	166.0	0.09975	-1.7066E-07
Propane	0.03387	166.0	0.10966	-1.5414E-07
PBG	0.031	166.1	0.61094	-0.006555
N-Butane	0.025	166.0	0.60979	-0.005767
N-Pentane	0.02365	166.0	0.60896	-0.005776
N-Heptane	0.025018	166.0	0.60963	-0.0044638
NGL	0.03344	166.0	0.60975	-0.0058807

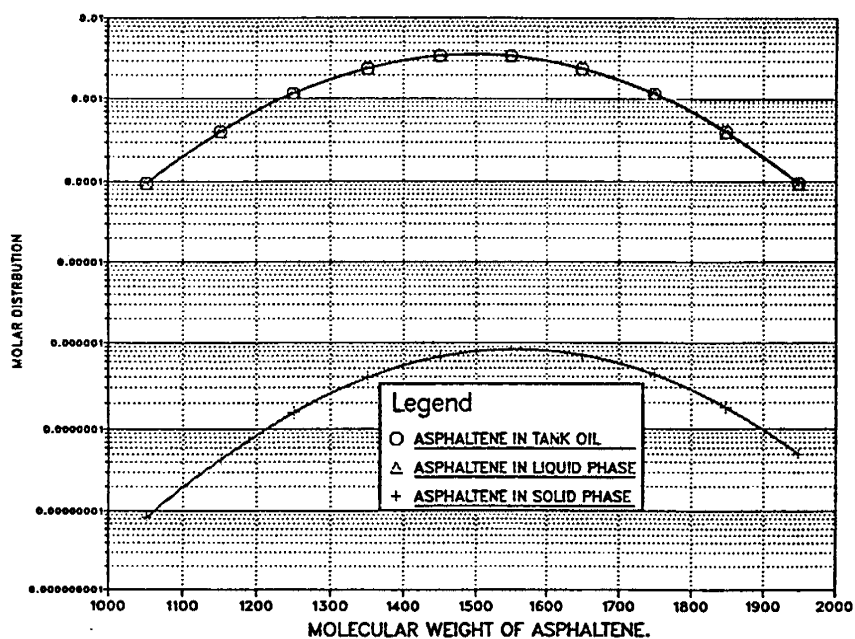


Figure XI-10. Relation Between Molar Distribution as a Function of Molecular Weight of Asphaltenes for N-Pentane -- West Sak Tank Oil Ratio = 2.0.

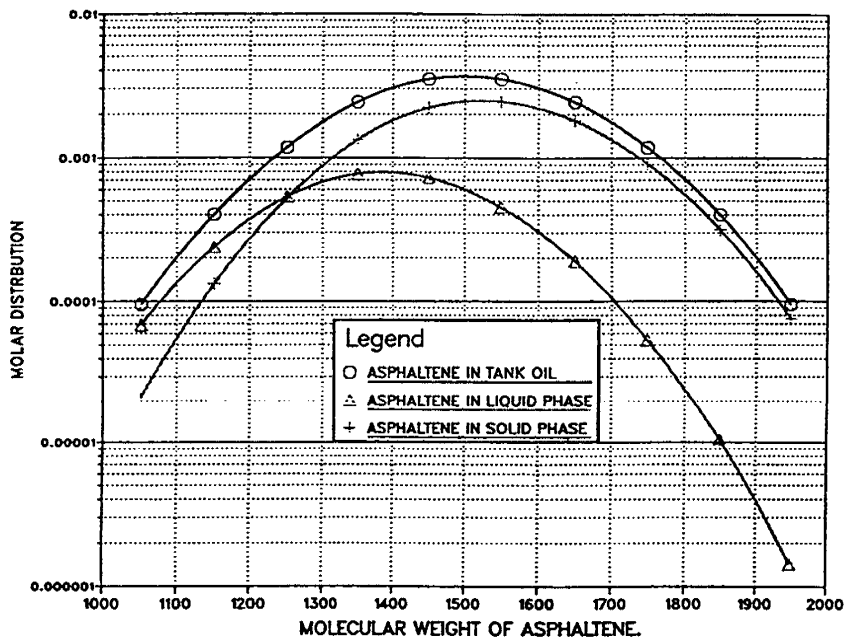


Figure XI-11. Relation Between Molar Distribution as a Function of Molecular Weight of Asphaltenes for N-Pentane -- West Sak Tank Oil Ratio = 7.0.

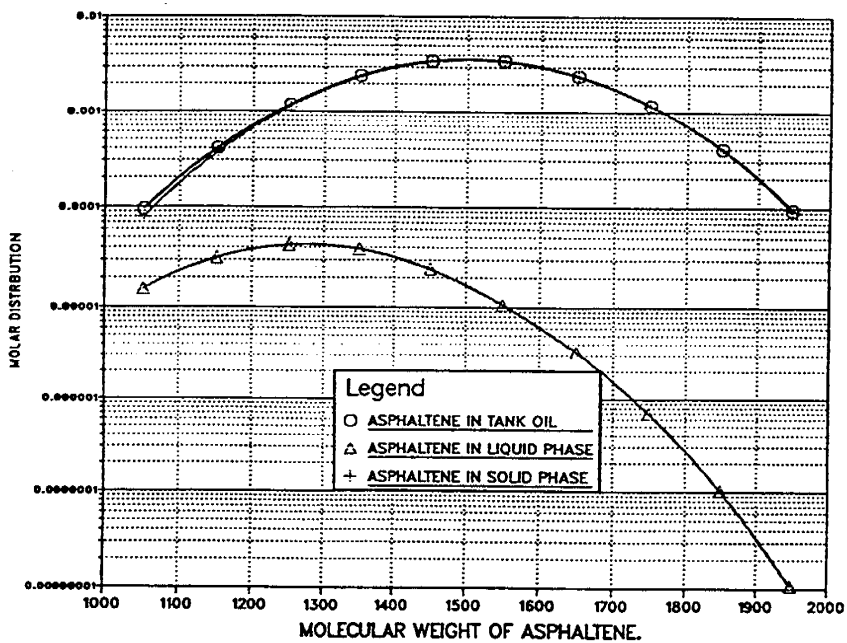


Figure XI-12. Relation Between Molar Distribution as a Function of Molecular Weight of Asphaltenes for N-Pentane -- West Sak Tank Oil Ratio = 12.5.

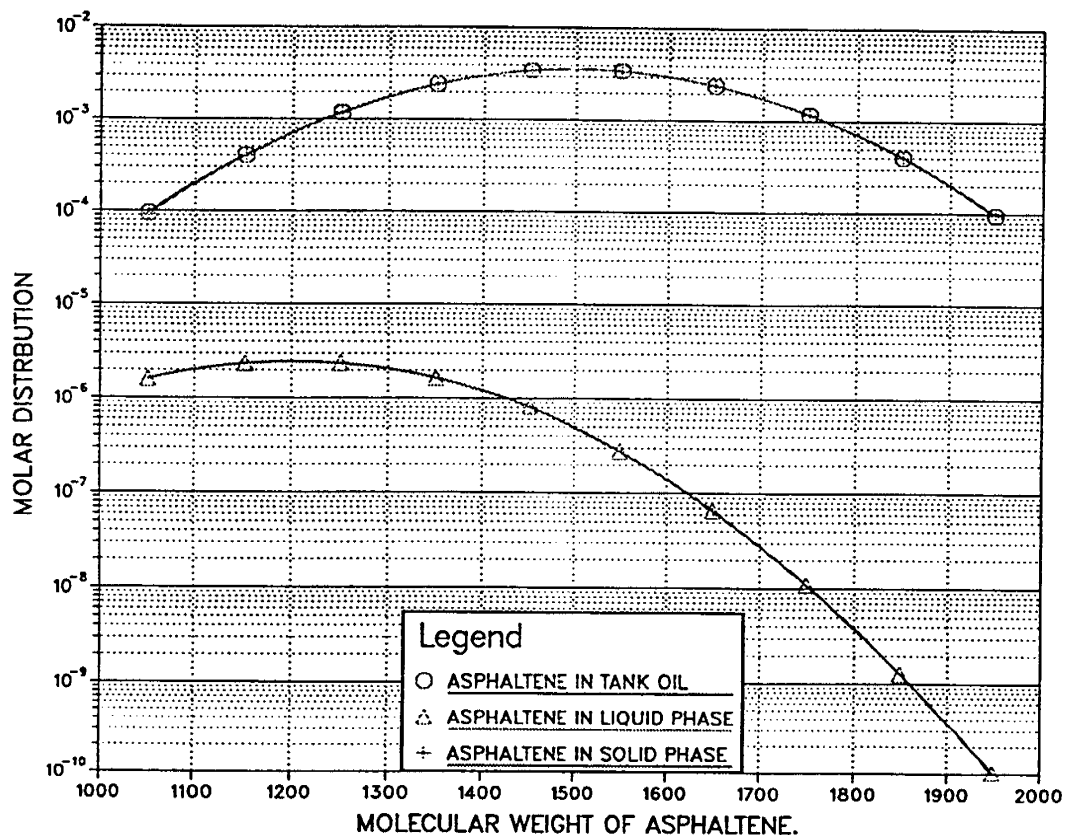


Figure XI-13. Relation Between Molar Distribution as a Function of Molecular Weight of Asphaltenes for N-Pentane -- West Sak Tank Oil Ratio = 20.2.

The model was also used to predict the amount of asphaltene precipitation for CO<sub>2</sub>-West Sak oil mixtures at pressures up to 4000 psia. The comparison of the predicted asphaltene precipitation amounts with the experimentally measured values is given in Table XI-12. The results in Table XI-12 show that both the experimental results and model predictions indicate considerably lower amounts of asphaltene precipitation at higher pressures than for CO<sub>2</sub>-tank oil mixtures.

**Table XI-12: Comparison of Experimental Results  
and Model Predictions for CO<sub>2</sub> -- West Sak Oil  
Mixtures at Higher Pressures.**

Mol % CO <sub>2</sub>	Pressure (Psia)	Wt % Asph. (Experimental)	Wt % Asph. (Predicted)
30	900	0.177	0.124
	1300	0.183	0.097
	1705	0.197	0.195
	2500	0.151	0.067
	3000	0.179	0.079
	3500	0.183	0.102
	4000	0.212	0.151
50	1000	0.140	0.149
	1705	0.192	0.062
	3000	0.156	0.156
	4000	0.108	0.206

**D. CONCLUSIONS**

1. A generalized multicomponent molecular thermodynamic model has been developed to represent asphaltene equilibria and to calculate solid-liquid equilibrium constants of asphaltene components, molar distribution of asphaltenes in equilibrium solid and liquid phases and to predict the amount of asphaltene precipitation from reservoir oil upon influence of a injected solvent for different pressure, temperature and compositions.
2. The heterogeneous models such as presented here are more realistic and provide insight into asphaltene precipitation phenomena than the homogeneous type models which treat asphaltenes by a single-pseudo component.
3. The model results show that the solid-liquid equilibrium constants increase with molecular weight of asphaltenes and the higher molecular weight asphaltenes precipitate out first where as the lower molecular weight asphaltenes tend to remain dissolved in liquid phase.



## **CHAPTER XII: EFFECT OF ASPHALTENE DEPOSITION ON ROCK-FLUID PROPERTIES**

---

### **A. INTRODUCTION**

Asphaltene precipitation in the reservoir is a complex and dynamic phenomenon since several processes such as fluid mixing, channeling, and adsorption of asphaltenes on rock surfaces occur simultaneously. Adsorption of asphaltenes on rock surfaces under static conditions has been well studied (Clementz, 1976; Collins and Melrose, 1983; Dubey and Waxman, 1989; Crocker and Marchin, 1988). Rock-fluid properties such as wettability and interfacial tension have been shown to be affected by asphaltene deposition (Kim et al., 1990). These properties in turn govern fluid distribution during displacement processes by controlling the relative permeabilities and end point saturations. However, very limited research has been done to evaluate the consequences of asphaltene precipitation under dynamic flow conditions. Danesh et al. (1988) reported impairment of absolute permeability due to asphaltene precipitation. Permeability reduction is believed to occur by two distinct mechanisms: 1) smaller pore throat blocking by larger asphaltene particles, and 2) adsorption of smaller size asphaltenes in larger pore throats, causing gradual reduction of the pore throat radii. While permeability impairment is generally detrimental to recovery, a possible beneficial effect may occur as a result of flow diversion. Flow diversion will occur if the high permeability streaks in the reservoir are blocked by asphaltene deposition, thereby forcing the fluid into low permeability regions and improving sweep efficiency. Thus, the effect of asphaltene precipitation on the overall flow behavior can be very complicated and warrants further investigation.

This chapter presents an experimental study of the effect of asphaltene deposition on rock-fluid properties under dynamic flow conditions. Displacement experiments using heavy oil were performed in several consolidated and unconsolidated porous media. Varying degrees of in-situ asphaltene precipitation were achieved and the effect of asphaltene precipitation on absolute permeability, relative permeabilities and oil recovery were studied.

### **B. EXPERIMENTAL PROGRAM**

#### **B1. Experimental Set-Up and Materials**

Figure XII-1 shows the schematic diagram of the experimental set-up used in this study to determine the effect of asphaltene deposition on dynamic displacement of heavy oil

by water. This set-up consisted of one positive displacement computer controlled dual cylinder fluid injection pump [FDS 220] along with pump data acquisition system, one TEMCO radial core holder (Model RCH-10-3), differential pressure transducer (Model DP-15) and carrier demodulators (Model CD-18) along with Fisher series 5000 strip chart recorder, a back pressure regulator (Model 91W Mity Mite Dome Type) and a fractional collector. The radial core holder, held a core through a viton sleeve with a size of one-inch diameter and ten-inch long. To prevent leakage or bypass of fluids around the core in experiments, a constant overburden pressure was applied around this sleeve by connecting it to a nitrogen bottle, which maintained a constant overburden pressure of 750 psi around the sleeve. The core holder had three inlet ports for two liquid injection and one gas injection and one outlet port for fluid production.

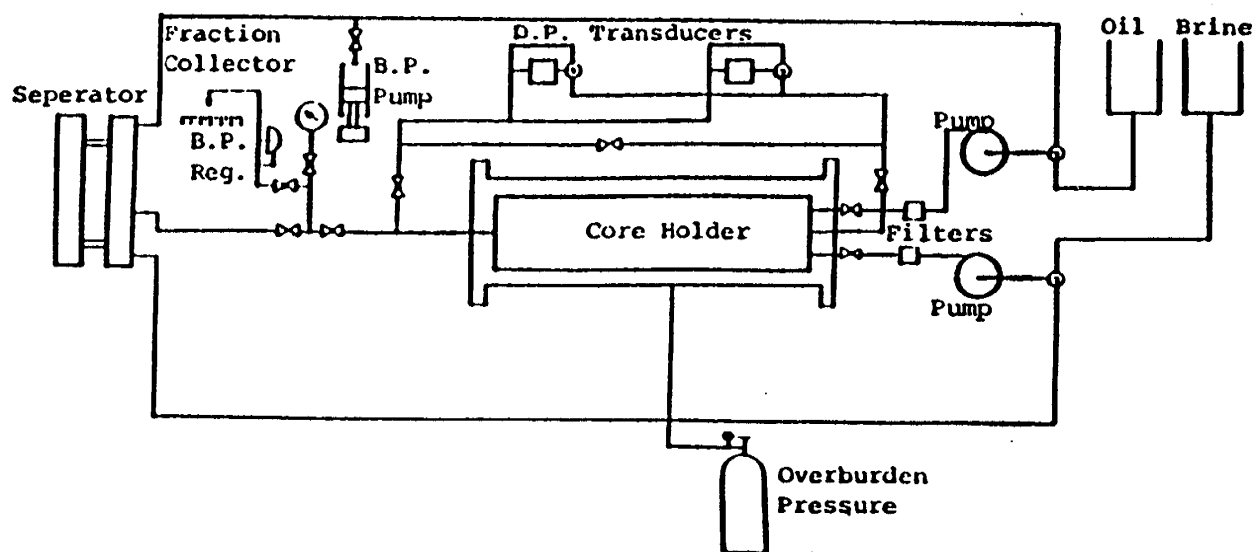


Figure XII-1. Experiment Set-Up Used for Study of Effect of Asphaltene Deposition on Rock Fluid Properties.

The inlet and outlet ports of the coreholder were connected to the differential pressure transducer which had 3 pressure drop ranges (0-80, 0-120 and 0-320 psi). The differential pressure transducers through demodulators converted pressure signals into voltage signals which were recorded on the strip chart recorders as differential pressures with 1% accuracy. The inlet ports of the coreholders were also connected to the displacement pump. One cylinder of the pump allowed injection of brine or solvents (toluene, n-heptane, and n-pentane), while other allowed injection of heavy oil. The pump was operated in constant rate mode without any pressure fluctuations and with an accuracy of 0.001 (cc/min). The outlet port of the coreholder was connected to the fraction collector through a back pressure regulator for collection of produced fluids from the core. The collector tubes were later centrifuged for accurate measurement of oil and water production.

Three core samples were used in this study. Core 1 was a consolidated Berea sandstone core, while the other two cores were unconsolidated sand packs (Ottawa Sand). The dimensions and properties of these cores are given in Table XII-1. The measured sand grain size distributions for the two unconsolidated sand packs are given in Table XII-2. Other materials used in these experiments included West Sak Oil-B with viscosity of 820 (cp), n-heptane and n-pentane as solvents for precipitating asphaltenes, toluene, and acetone for core cleaning, and brine (2% NaCl). The properties of West Sak oil and the measured amount of asphaltene precipitation for various solvent to oil ratios are given in Jiang et al. (1990).

**Table XII-1: Properties of Cores Used in the Study.**

	<b>Core No. 1</b>	<b>Core No. 2</b>	<b>Core No. 3</b>
<b>Condition</b>	consolidated	bigger sand	smaller sand
<b>Length (cm)</b>	25.2	25.38	27.07
<b>Diameter (cm)</b>	2.527	2.667	2.667
<b>Pore volume (cc)</b>	37.40	49.01	50.00
<b>Porosity (%)</b>	27.86	32.67	31.25
<b>Initial Swir</b>	0.1998	0.2480	0.1560
<b>Absolute Permeability (Darcy)</b>	0.236	2.38	1.52

**Table XII-2: Sand Grain Size Distribution (weight %) for Unconsolidated Cores.**

Mesh	Diameter (in)	Core No. 2	Core No. 3
16	0.039	0.00	0.00
20	0.0328	4.95	0.00
24	0.0276	42.66	0.00
32	0.0195	42.78	0.00
35	0.0164	7.32	0.00
42	0.0138	2.29	0.00
60	0.0097	0.00	1.94
65	0.0082	0.00	69.66
100	0.0058	0.00	22.86
115	0.0049	0.00	4.73
150	0.0041	0.00	0.93

## **B2. Experimental Procedures**

For each core, the experimental steps involved were as follows:

1. Core Preparation - This involved firing of core or sand at 352°C for 12 hours followed by cooling and packing of sand in the sleeve and mounting the core in the core holder. After measuring core porosity using helium porosimeter the core was then evacuated for 8 to 10 hours to about 200 micron level. CO<sub>2</sub> was then injected for several hours into core continuously at a low rate to displace the air from pores. The core was further evacuated to 200 microns for several hours.
2. Irreducible Water Saturation Measurement - Brine was then injected into core to displace any CO<sub>2</sub> left and to saturate the core completely at a rate of 1 (cc/min) under a back pressure of 500 psi until the pressure drop across the core stabilized. The total amount of water injected and produced were recorded. Oil was then injected into the at a rate of 0.019 (cc/min) to displace water until pressure drop was again stabilized and no more water could be displaced from the core. The irreducible water saturation was then determined from material balance.

3. Absolute Permeability Measurement - During the process of oil injection for complete saturation of the core with oil, the stabilized pressure drop was used to calculate absolute permeability using Darcy's law.
4. Relative Permeability Measurement - Once the core was fully saturated with oil at irreducible water saturation, the oil injection was stopped and water injection was started at a constant rate of 0.019 (cc/min) to displace oil out. During this unsteady state displacement of oil by water, pressure drop, oil and water production were measured continuously until water-oil ratio (WOR) reached about 12. The oil and water relative permeabilities were computed from the displacement data using technique described by Johnson et al. (1959), and data smoothing procedures described by Miller and Ramey (1983).
5. Deposition of Asphaltenes - After determining the original oil-water relative permeability curves, the core was ready for asphaltene deposition experiment. The core was again fully resaturated with oil as determined from pressure drop stabilization and no water production. The asphaltene precipitating solvent (n-pentane or n-heptane) was injected simultaneously, but separately along with oil injection. The solvent and oil only mixed at the core entrance resulting in asphaltene deposition inside the core. The ratios of solvent to oil injection rate were carefully chosen to obtain desired degree of asphaltene precipitation. The process of asphaltene deposition was continued for 5 days during which the pressure drops were recorded and showed sharp increase indicating asphaltene deposition. The process was stopped when the pressure drops were stabilized. The solvent injection was then stopped but oil injection was continued for additional 2 days until the pressure drops once again stabilized and the core was saturated fully with oil. This stabilized pressure drop was used to calculate the new absolute permeability of the core after asphaltene deposition.
6. Dynamic Displacements by Water - Step 4 was repeated to obtain effect of asphaltene deposition on dynamic displacement of oil by water and on oil-water relative permeability curves.
7. Cleaning - After each asphaltene deposition experiment followed by dynamic displacement by water, the core was flushed with toluene to dissolve deposited asphaltenes and to displace remaining oil and water. After injecting toluene continuously for 2 days at a rate of 2 (cc/min) the injection was stopped and the core was soaked with toluene for about half a day. The toluene was then injected for additional

2 pore volumes followed by 3 pore volumes of acetone. The core was then evacuated for one day to remove all acetone and toluene.

Oil and water relative permeabilities were computed from the displacement data by using the technique developed by Johnson et al. (1959). The method requires the determination of two derivatives. This was achieved by fitting smooth functional relationships through the observed data by the least square method and then differentiating these functions. This procedure was suggested by Miller and Ramey (1983). They suggested the following functional relationships.

$$Q_o = A_1 + A_2[\ln(Q_i)] + A_3[\ln(Q_i)]^2$$

$$\ln(Q_i I_r) = B_1 + B_2[\ln(Q_i)] + B_3[\ln(Q_i)]^2$$

where  $A_1, A_2, A_3, B_1, B_2$  &  $B_3$  are regression coefficients,  $I_r$  is relative injectivity,  $Q_i$  and  $Q_o$  are total water injected and total oil produced in pore volume, respectively. These equations fitted the experimental data of this study satisfactorily, as shown in Figures XII-2 and XII-3, respectively.

## C. RESULTS AND DISCUSSION

A total of 12 dynamic unsteady state displacement experiments were conducted for all 3 cores. This is equivalent to 4 runs for each core where the amount (wt %) of asphaltenes deposited was varied from 0% for run 1, 5.1% for run 2, 9.9% for run 3 to 12.8% for run 4. Pressure drops, water production, oil production were recorded for each experiment as a function of cumulative water injected and are given in Tables XII-3 through XII-14.

### C1. Effect on Absolute Permeability

Figure XII-4 shows the ratio of absolute permeability of the core after asphaltene deposition to the original absolute permeability of the core ( $K_i/K_o$ ) for all three cores at various degrees of asphaltene deposition. For Core 1 with lowest initial absolute permeability ( $K_o = 236$  md), the permeability reduction was highest (about 50% at 12.8% asphaltenes deposited), whereas for core 2 with highest initial absolute permeability ( $K_o = 2380$  md), the permeability reduction was lowest (about 26% at 12.8% asphaltenes deposited). Figure XII-4 also shows that the degree of permeability reduction increased with increase in the degree of asphaltene precipitation. Currently, further work is in progress to develop a theoretical model to predict the permeability impairment due to asphaltene deposition that incorporates the asphaltene particle size distribution in relation to pore size distribution, pore blocking phenomena and adsorption phenomena.

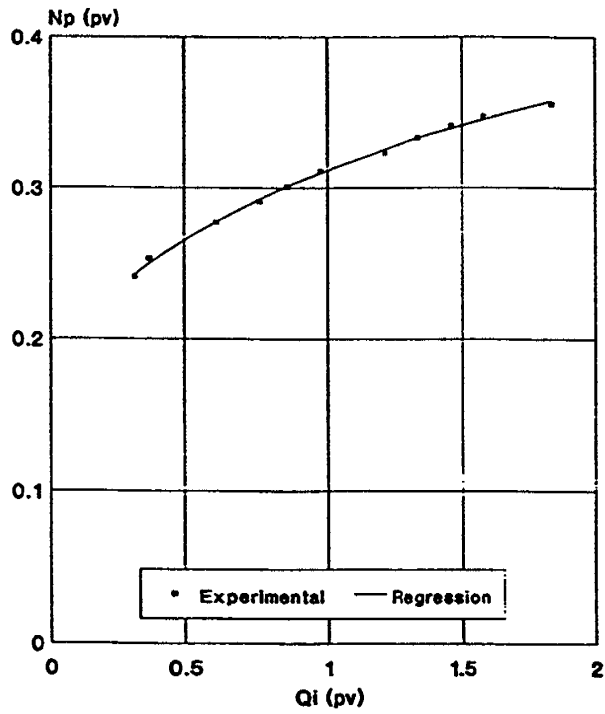


Figure XII-2. Comparison of Experimental Oil Production Data with Regression Results.

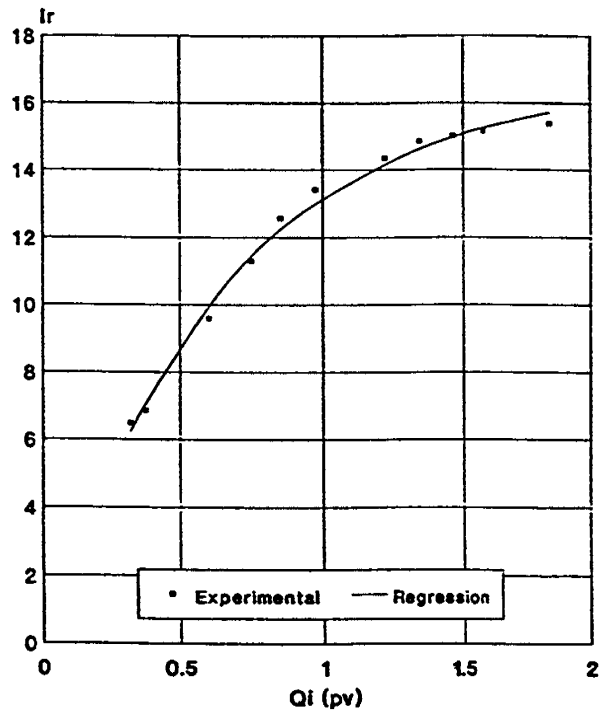


Figure XII-3. Comparison of Experimental Relative Injectivity ( $I_r$ ) with Regression Results.

**Table XII-3: Unsteady State Displacement Data for Core No. 1 and Run No. 1.**

Pressure Drop (psi)	Cum. Water Injected (cc)	Cum. Oil Produced (cc)
57.44	0.00	0.00
32.90	6.8	5.55
27.09	13.90	8.25
22.28	20.50	10.25
19.51	27.10	11.65
16.86	33.50	12.45
15.22	39.90	13.15
13.77	46.10	13.65
12.32	52.50	14.25
10.82	58.80	14.75
9.60	64.30	15.25
8.52	70.60	15.55
7.88	82.50	16.25
7.31	94.60	16.75
6.91	107.30	17.15

**Table XII-4: Unsteady State Displacement Data for Core No. 1 and Run No. 2.**

Pressure Drop (psi)	Cum. Water Injected (cc)	Cum. Oil Produced (cc)
94.22	0.00	0.00
48.38	2.00	1.95
24.93	7.40	7.34
18.88	10.80	10.24
14.55	16.30	12.04
13.73	18.90	12.64
9.84	30.20	13.84
8.34	37.60	14.54
7.50	42.70	15.04
7.03	48.70	15.54
6.57	60.70	16.14
6.35	67.00	16.64
6.28	73.10	17.04
6.22	78.90	17.34
6.13	91.90	17.74

**Table XII-5: Unsteady State Displacement Data for Core No. 1 and Run No. 3.**

Pressure Drop (psi)	Cum. Water Injected (cc)	Cum. Oil Produced (cc)
108.17	0.00	0.00
29.97	2.70	2.70
16.13	7.80	7.80
11.50	9.70	9.70
8.47	12.40	11.25
7.37	16.65	12.50
7.35	19.15	13.10
6.37	29.60	14.30
6.27	31.90	14.70
5.94	35.40	15.20
5.44	39.80	15.70
5.39	42.80	16.20
4.56	60.30	17.20
4.39	65.80	17.70
3.60	74.30	18.10
3.53	86.60	18.90

**Table XII-6: Unsteady State Displacement Data for Core No. 1 and Run No. 4.**

Pressure Drop (psi)	Cum. Water Injected (cc)	Cum. Oil Produced (cc)
134.09	0.00	0.00
26.36	2.90	2.90
15.63	7.70	7.70
10.45	9.80	9.80
9.02	11.50	11.10
8.20	14.20	12.40
7.20	17.20	13.50
6.50	18.90	14.10
6.45	19.40	14.30
5.78	25.00	16.40
4.80	31.50	18.40
3.77	42.00	19.20
3.49	48.60	19.60
3.29	55.10	20.10
3.18	61.00	20.40
2.85	73.90	20.80
2.74	84.20	21.30

**Table XII-7: Unsteady State Displacement Data for Core No. 2 and Run No. 1.**

Pressure Drop (psi)	Cum. Water Injected (cc)	Cum. Oil Produced (cc)
16.5	0.00	0.00
9.86	5.80	5.80
3.60	11.30	10.60
3.46	16.80	13.60
3.36	25.20	16.70
3.15	31.60	18.40
2.36	39.10	19.70
2.10	46.70	21.00
1172	54.00	21.80
1.61	62.80	22.90
1.36	71.30	23.70
1.26	83.00	24.70
0.86	93.80	25.20

**Table XII-8: Unsteady State Displacement Data for Core No. 2 and Run No. 2.**

Pressure Drop (psi)	Cum. Water Injected (cc)	Cum. Oil Produced (cc)
19.6	0.00	0.00
6.80	3.80	3.80
2.11	7.55	7.55
0.89	12.75	12.55
0.91	19.05	16.95
0.95	25.55	19.55
0.90	32.15	21.45
0.83	39.85	23.05
0.71	48.75	24.45
0.69	56.55	25.25
0.63	66.45	26.25
0.61	73.95	26.75
0.56	83.45	27.25
0.41	92.85	27.85
0.37	104.05	28.55
0.36	113.55	28.95

**Table XII-9: Unsteady State Displacement Data for Core No. 2 and Run No. 3.**

Pressure Drop (psi)	Cum. Water Injected (cc)	Cum. Oil Produced (cc)
21.2	0.00	0.00
6.39	3.70	3.70
1.12	8.40	8.40
1.06	12.80	12.63
1.29	18.50	16.33
1.36	25.00	19.33
1.31	32.10	21.73
1.23	40.40	23.93
1.07	48.40	25.63
0.91	58.10	27.43
0.86	68.60	29.23
0.81	79.70	30.53
0.92	91.40	31.63
1.06	102.80	32.53
0.61	115.20	33.33
0.51	128.20	34.33

**Table XII-10: Unsteady State Displacement Data for Core No. 2 and Run No. 4.**

Pressure Drop (psi)	Cum. Water Injected (cc)	Cum. Oil Produced (cc)
22.3	0.00	0.00
7.43	3.30	3.30
3.17	6.40	6.40
1.56	10.40	10.40
1.05	15.90	15.00
1.30	21.80	18.60
1.58	29.10	22.70
1.47	37.30	25.00
1.29	45.80	27.00
1.07	54.30	28.60
0.98	63.60	30.10
1.00	75.60	31.70
0.98	87.80	33.30
0.84	99.70	34.80
0.78	112.00	36.10
0.84	125.70	37.60
0.71	139.60	38.80

**Table XII-11: Unsteady State Displacement Data for Core No. 3 and Run No. 1.**

Pressure Drop (psi)	Cum. Water Injected (cc)	Cum. Oil Produced (cc)
54.50	0.00	0.00
23.00	3.40	3.40
17.00	8.70	8.40
12.00	14.20	11.60
9.50	19.60	14.00
8.00	27.10	16.80
6.50	36.30	19.50
6.00	43.70	21.90
7.00	51.60	24.10
5.00	62.40	26.30
4.00	80.60	28.70
5.00	93.80	30.00
3.50	109.60	32.00
3.00	120.60	33.20
4.00	133.10	34.40
3.50	142.60	35.30

**Table XII-12: Unsteady State Displacement Data for Core No. 3 and Run No. 2.**

Pressure Drop (psi)	Cum. Water Injected (cc)	Cum. Oil Produced (cc)
60.00	0.00	0.00
19.00	3.20	3.20
12.00	8.50	8.50
9.50	13.50	13.30
9.00	18.40	17.60
8.00	23.60	21.90
7.50	31.20	26.30
6.00	38.60	29.40
5.00	45.40	31.60
4.50	52.70	33.50
4.50	64.30	35.60
4.50	78.10	37.40
4.50	88.20	38.60
4.50	100.80	39.90
4.50	112.50	41.60

**Table XII-13: Unsteady State Displacement Data for Core No. 3 and Run No. 3.**

Pressure Drop (psi)	Cum. Water Injected (cc)	Cum. Oil Produced (cc)
80.00	0.00	0.00
21.00	3.20	3.20
14.00	8.50	8.50
11.50	14.40	14.40
9.00	21.30	20.30
8.00	28.50	26.00
7.50	35.10	29.00
6.00	42.50	32.30
5.00	51.60	34.60
4.50	59.20	36.60
4.00	67.50	38.00
4.00	76.80	39.10
4.00	87.10	40.50
4.00	97.40	41.70
4.00	106.80	43.20
4.00	112.90	44.10

**Table XII-14: Unsteady State Displacement Data for Core No. 3 and Run No. 4.**

Pressure Drop (psi)	Cum. Water Injected (cc)	Cum. Oil Produced (cc)
96	0.00	0.00
28	3.5	3.5
18	9.0	9.0
14.5	14.90	14.90
11	22.00	21.40
8.2	29.30	27.70
7.3	36.10	32.30
5.8	42.50	34.90
5.2	52.30	37.70
4.5	58.90	39.50
3.5	66.30	41.00
3.5	73.20	41.70
3.5	84.50	43.20
3.5	94.80	43.90
3.5	103.80	44.40

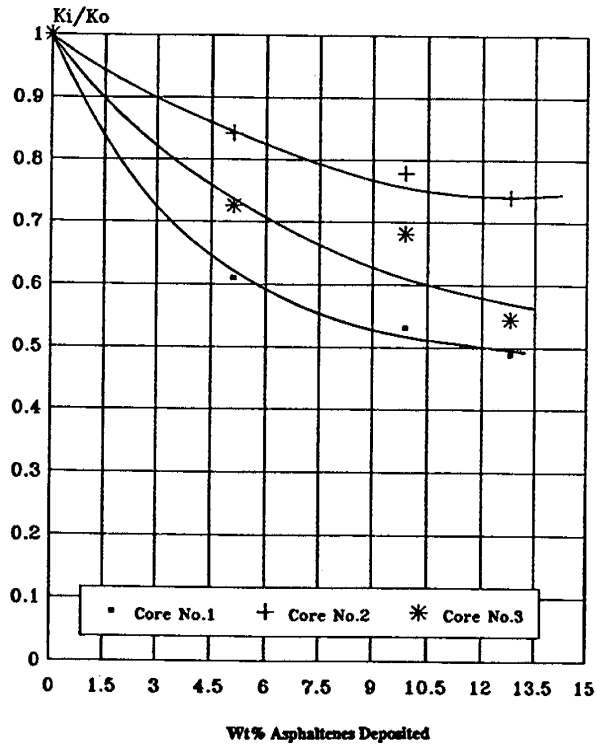


Figure XII-4. The Effect of Asphaltene Deposition on the Ratio of Absolute Permeability After Asphaltene Deposition to the Original Absolute Permeability ( $K_i/K_o$ ).

## C2. Effect on Displacement Performance

Figures XII-5, XII-6, and XII-7 show the cumulative fractional oil recovery ( $N_p$  in pore volumes) versus the cumulative pore volume of water injected ( $Q_i$ ) at various degrees of asphaltene deposition for Cores 1, 2 and 3 respectively. These figures show that: 1) the water breakthrough time increased with the increase in asphaltene deposition, and 2) the fractional oil recovery, and the fractional flow of oil increased with the increase in asphaltene deposition. The improvement in displacement performance due to asphaltene deposition could be contributed by several simultaneous mechanisms which include: 1) Alteration of wettability of rock surface from water-wet to oil-wet which may increase the irreducible oil saturation but also may cause drastic reduction in the irreducible water saturation (i.e. higher initial oil saturation in the core prior to displacement); 2) Improvement in the ratio of effective oil permeability to effective water permeability at a given saturation level resulting in

favorable oil fractional flow; 3) Improvement in sweep efficiency as a result of flow diverting effect of asphaltene deposition. It was not possible to identify the most dominating mechanism of improvement in oil recovery due to asphaltene deposition. Further work will be needed to identify this.

### C3. Effect on Pressure Drop

Figures XII-8, XII-9, and XII-10 show measured pressure drops versus pore volume of water injected at various degrees of asphaltene deposition for cores 1, 2, and 3 respectively. These figures show that although the initial pressure drops were higher due to asphaltene deposition compared to those for no asphaltene deposition, the subsequent pressure drops after water breakthrough were much lower in presence of asphaltene deposition compared to no asphaltene deposition. This indicates that asphaltene deposition process reduced the initial injectivity of water in the core but the injectivity improved after water breakthrough.

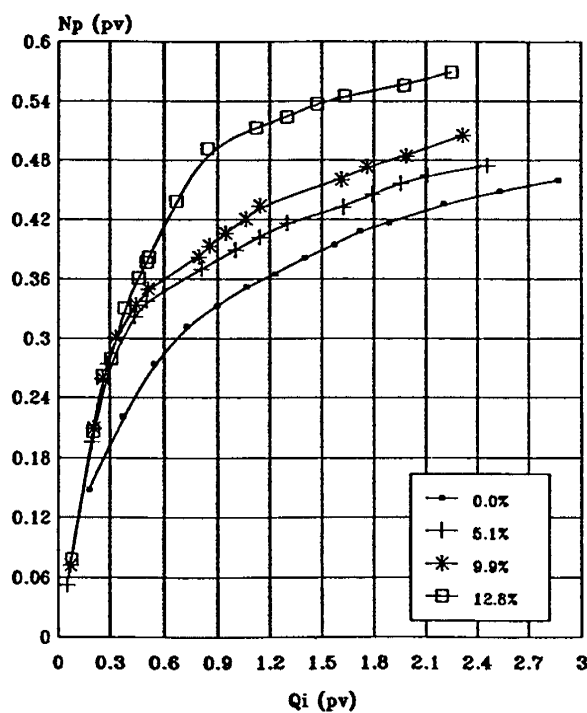


Figure XII-5. Cumulative Fractional Oil Recovery (PV) Versus Cumulative Water Injected (PV) for Various Degrees of Asphaltene Deposition (core 1).

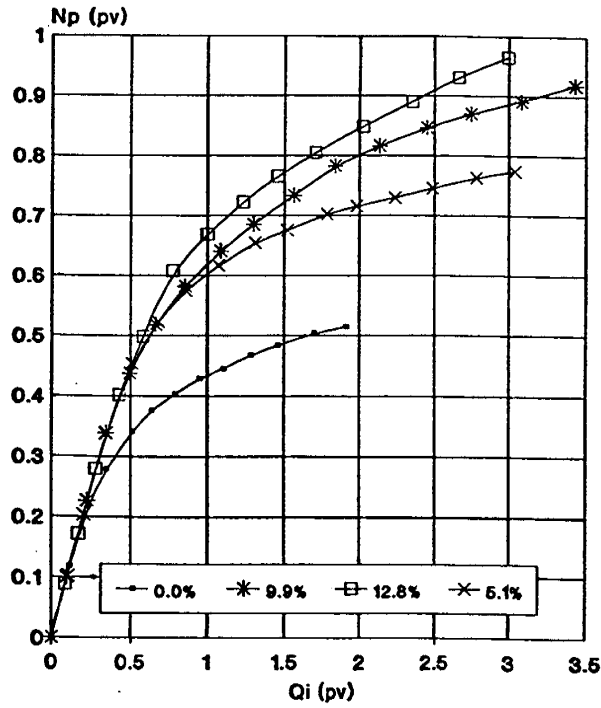


Figure XII-6. Cumulative Fractional Oil Recovery (PV) Versus Cumulative Water Injected (PV) for Various Degrees of Asphaltene Deposition (core 2).

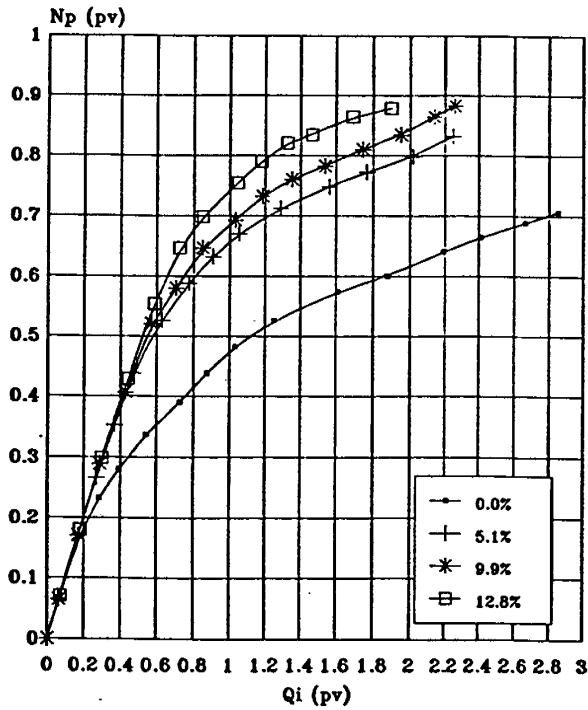


Figure XII-7. Cumulative Fractional Oil Recovery (PV) Versus Cumulative Water Injected (PV) for Various Degrees of Asphaltene Deposition (core 3).

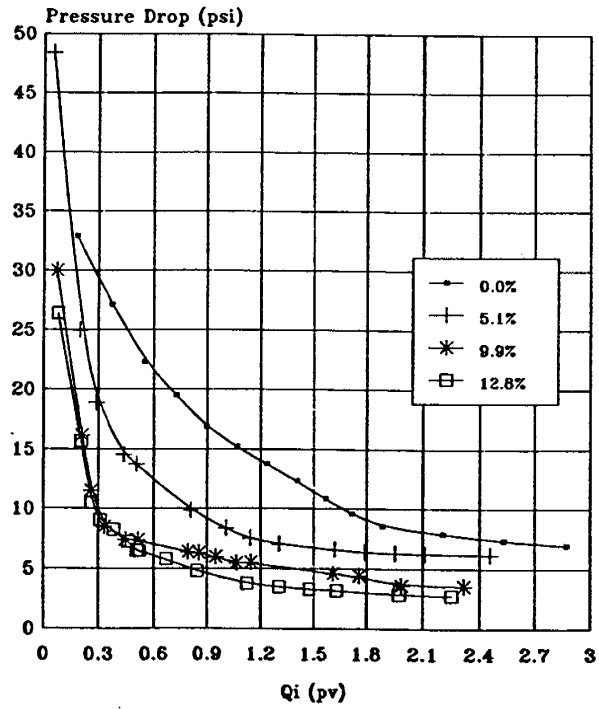


Figure XII-8. Pressure Drop Across Core Versus Cumulative Water Injected (PV) for Various Degrees of Asphaltene Deposition (core 1).

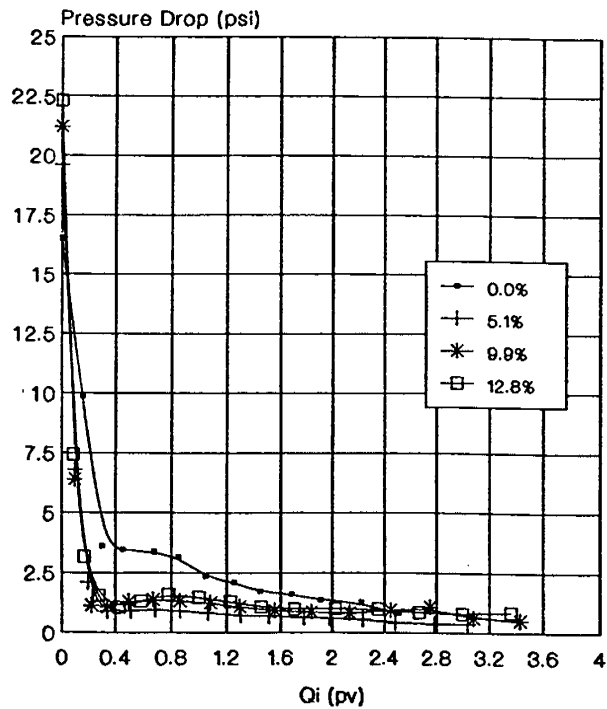


Figure XII-9. Pressure Drop Across Core Versus Cumulative Water Injected (PV) for Various Degrees of Asphaltene Deposition (core 2).

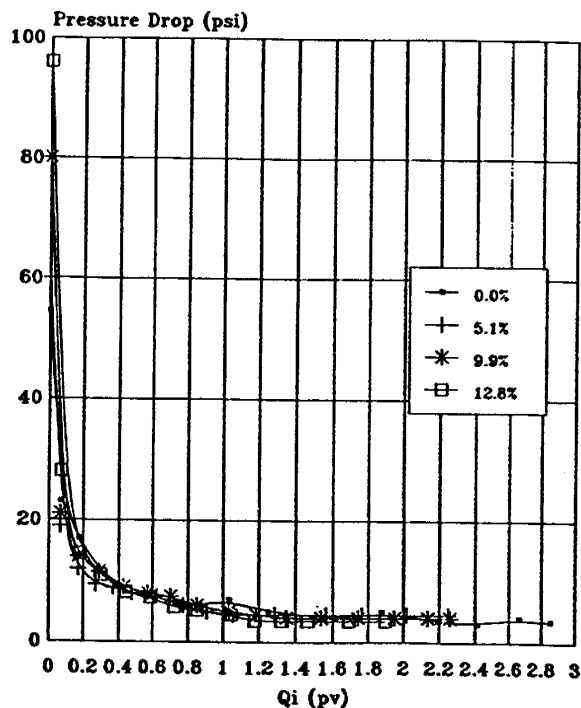


Figure XII-10. Pressure Drop Across Core Versus Cumulative Water Injected (PV) for Various Degrees of Asphaltene Deposition (core 3).

#### C4. Effect on Oil-Water Relative Permeabilities and Fractional Flow

The unsteady state displacement data for all runs were used to compute the relative permeabilities of oil and water and fractional flows of oil and water as a function of water-saturation. The calculated results for all the runs are given in Tables XII-15 through XII-26. The ratio of relative oil permeability to relative water permeability ( $K_{RO}/K_{RW}$ ) are plotted against water saturations ( $S_W$ ) in Figures XII-11, XII-12 and XII-13. From all these figures, it can be seen that, after asphaltene deposition, the ratio of oil relative permeability to water relative permeability increases with increase in asphaltene deposition. The water saturations ( $S_W$ ) were calculated based on the  $S_{wir}$  value in the core prior to asphaltene deposition. The water fractional flow curves ( $f_W$  vs.  $S_W$ ) are plotted in Figures XII-14 through XII-16 for three cores at different degrees of asphaltene deposition. Again, these figures show that at the same  $S_W$  (this  $S_W$  is calculated based on the  $S_{wir}$  from the original core without asphaltene deposition), outlet oil flow fraction increases with asphaltene deposition potential for all these three cores. This shows improvement in displacement performance due to asphaltene deposition.

**Table XII-15: Calculated Results for Core No. 1 and Run No. 1.**

$S_w^*$	$S_{wD}$	$K_{ro}$	$K_{rw}$	$f_o$	$f_w$
0.2791	0.1468	0.5679	0.0011	0.3803	0.6197
0.3078	0.2348	0.4677	0.0013	0.3030	0.6790
0.3576	0.2958	0.3945	0.0018	0.2121	0.7879
0.4207	0.3410	0.2336	0.0020	0.1250	0.8750
0.4347	0.3775	0.2469	0.0025	0.1094	0.8906
0.4654	0.4071	0.1887	0.0026	0.0806	0.9194
0.4492	0.4333	0.2224	0.0026	0.0938	0.9062
0.4694	0.4558	0.1837	0.0026	0.0794	0.9206
0.4513	0.4734	0.2188	0.0027	0.0909	0.9091
0.5257	0.4916	0.1326	0.0032	0.0476	0.9524
0.5045	0.5214	0.2743	0.0054	0.0588	0.9412
0.5431	0.5472	0.2017	0.0057	0.0413	0.9587
0.5680	0.5705	0.1758	0.0066	0.0315	0.9685

\* Based on irreducible water saturation when the core has no asphaltene deposition.

**Table XII-16: Calculated Results for Core No. 1 and Run No. 2.**

$S_w^*$	$S_{wD}$	$K_{ro}$	$K_{rw}$	$f_o$	$f_w$
0.3592	0.3877	0.1279	0.0003	0.3108	0.6892
0.4227	0.4625	0.1262	0.0006	0.2069	0.7 931
0.4457	0.4894	0.1243	0.0007	0.1787	0.8213
0.4800	0.5751	0.1144	0.0011	0.1124	0.8876
0.4972	0.6153	0.1080	0.0013	0.0905	0.9095
0.5096	0.6387	0.1039	0.0015	0.0798	0.9202
0.5230	0.6629	0.0994	0.0016	0.0700	0.9300
0.5410	0.7035	0.0915	0.0019	0.0563	0.9437
0.5508	0.7217	0.0879	0.0020	0.0511	0.9489
0.5623	0.7378	0.0846	0.0021	0.0469	0.9531
0.5711	0.7520	0.0817	0.0022	0.0434	0.9566
0.5835	0.7802	0.0760	0.0024	0.0374	0.9626

\* Based on irreducible water saturation when the core has no asphaltene deposition.

**Table XII-17: Calculated Results for Core No. 1 and Run No. 3.**

$S_w^*$	$S_{wD}$	$K_{ro}$	$K_{rw}$	$f_o$	$f_w$
0.3969	0.3977	0.5136	0.0016	0.2804	0.7196
0.4336	0.4448	0.3912	0.0017	0.2154	0.7846
0.4511	0.4677	0.3472	0.0018	0.1899	0.8101
0.4824	0.5413	0.2492	0.0021	0.1283	0.8717
0.4889	0.5543	0.2368	0.0021	0.1199	0.8801
0.5013	0.5725	0.2212	0.0022	0.1091	0.8909
0.5142	0.5933	0.2057	0.0023	0.0981	0.9019
0.5247	0.6063	0.1971	0.0024	0.0919	0.9081
0.5535	0.6691	0.1646	0.0028	0.0673	0.9327
0.5615	0.6854	0.1581	0.0029	0.0622	0.9378
0.5741	0.7083	0.1500	0.0031	0.0556	0.9444
0.5903	0.7377	0.1414	0.0034	0.0484	0.9516

\* Based on irreducible water saturation when the core has no asphaltene deposition.

**Table XII-18: Calculated Results for Core No. 1 and Run No. 4.**

$S_w^*$	$S_{wD}$	$K_{ro}$	$K_{rw}$	$f_o$	$f_w$
0.2663	0.0901	1.000	0.0004	0.7472	0.2528
0.3226	0.1966	0.8772	0.0009	0.5566	0.4434
0.3684	0.2878	0.7709	0.0013	0.4231	0.5769
0.3907	0.3307	0.7206	0.0015	0.3688	0.6312
0.3977	0.3424	0.7069	0.0016	0.3549	0.6451
0.4664	0.4506	0.5799	0.0022	0.2422	0.7578
0.5379	0.5413	0.4738	0.0029	0.1683	0.8317
0.6004	0.6434	0.3553	0.0037	0.1038	0.8962
0.6216	0.6907	0.3010	0.0042	0.0799	0.9201
0.6431	0.7289	0.2575	0.0047	0.0630	0.9370
0.6612	0.7582	0.2244	0.0050	0.0515	0.9485
0.6892	0.8095	0.1670	0.0058	0.0340	0.9660
0.7101	0.8413	0.1317	0.0063	0.02348	0.9752

\* Based on irreducible water saturation when the core has no asphaltene deposition.

**Table XII-19: Calculated Results for Core No. 2 and Run No. 1.**

$S_w^*$	$S_{wD}$	$K_{ro}$	$K_{rw}$	$f_o$	$f_w$
0.2909	0.0568	0.3558	0.0002	0.7130	0.2870
0.3644	0.1367	0.1603	0.0002	0.4553	0.5447
0.4342	0.2145	0.0875	0.0003	0.2870	0.7130
0.4777	0.2563	0.0676	0.0003	0.2215	0.7785
0.5116	0.2945	0.0555	0.0003	0.1734	0.8266
0.5396	0.3256	0.0487	0.0004	0.1413	0.8587
0.5620	0.3505	0.0448	0.0004	0.1194	0.8806
0.5846	0.3758	0.0419	0.0005	0.1002	0.8998
0.6052	0.3967	0.0402	0.0005	0.0864	0.9136
0.6279	0.4212	0.0390	0.0006	0.0724	0.9276
0.6640	0.4405	0.0386	0.0007	0.0627	0.9373

\* Based on irreducible water saturation when the core has no asphaltene deposition.

**Table XII-20: Calculated Results for Core No. 2 and Run No. 2.**

$S_w^*$	$S_{wD}$	$K_{ro}$	$K_{rw}$	$f_o$	$f_w$
0.3852	0.1561	0.9920	0.0006	0.5048	0.4952
0.4662	0.2352	0.5411	0.0012	0.3389	0.6611
0.5215	0.2928	0.3579	0.0013	0.2459	0.7541
0.5692	0.3432	0.2535	0.0014	0.1808	0.8192
0.6112	0.3876	0.1894	0.0015	0.1343	0.8657
0.6399	0.4185	0.1555	0.0016	0.1072	0.8928
0.6689	0.4502	0.1275	0.0017	0.08333	0.9167
0.6883	0.4702	0.1126	0.0018	0.0701	0.9299
0.7068	0.4919	0.0985	0.0020	0.0574	0.9426
0.7241	0.5102	0.0879	0.0021	0.0478	0.9522
0.7449	0.5288	0.0782	0.0023	0.0391	0.9609
0.7607	0.5424	0.0716	0.0025	0.0333	0.9667

\* Based on irreducible water saturation when the core has no asphaltene deposition.

**Table XII-21: Calculated Results for Core No. 2 and Run No. 3.**

$S_w^*$	$S_{wD}$	$K_{ro}$	$K_{rw}$	$f_o$	$f_w$
0.3674	0.1294	1.0000	0.0010	0.5512	0.4488
0.4355	0.1988	0.5740	0.0011	0.3972	0.6028
0.4907	0.2551	0.3863	0.0011	0.3025	0.6975
0.5398	0.3058	0.2812	0.0011	0.2353	0.7647
0.5787	0.3450	0.2257	0.0012	0.1931	0.8096
0.6175	0.3840	0.1854	0.0012	0.1581	0.8419
0.6557	0.4189	0.1583	0.0013	0.1318	0.8682
0.6886	0.4500	0.1396	0.0014	0.1117	0.8883
0.7144	0.4780	0.1262	0.0014	0.0961	0.9039
0.7352	0.5018	0.1169	0.0015	0.0845	0.9155
0.7542	0.5246	0.1096	0.0017	0.0745	0.9255
0.7739	0.5458	0.1039	0.0018	0.0662	0.9338

\* Based on irreducible water saturation when the core has no asphaltene deposition.

**Table XII-22: Calculated Results for Core No. 2 and Run No. 4.**

$S_w^*$	$S_{wD}$	$K_{ro}$	$K_{rw}$	$f_o$	$f_w$
0.3960	0.1586	0.9325	0.0011	0.5046	0.4936
0.4750	0.2264	0.5568	0.0011	0.3742	0.6258
0.5392	0.2839	0.3797	0.0011	0.2885	0.7115
0.5813	0.3310	0.2875	0.0012	0.2326	0.7674
0.6165	0.3696	0.2340	0.0012	0.1946	0.8054
0.6486	0.4053	0.1970	0.0012	0.1648	0.8352
0.6833	0.4440	0.1666	0.0013	0.1375	0.8625
0.7153	0.4772	0.1466	0.0013	0.1175	0.8825
0.7461	0.5052	0.1331	0.0014	0.1028	0.8972
0.7749	0.5308	0.1230	0.0015	0.0910	0.9090
0.8045	0.5559	0.1147	0.0016	0.0806	0.9194
0.8321	0.5787	0.1086	0.0017	0.0722	0.9278

\* Based on irreducible water saturation when the core has no asphaltene deposition.

**Table XII-23: Calculated Results for Core No. 3 and Run No. 1.**

$S_w^*$	$S_{wD}$	$K_{ro}$	$K_{rw}$	$f_o$	$f_w$
0.1795	0.0352	0.3834	0.0001	0.7807	0.2193
0.2297	0.1040	0.3818	0.0004	0.5515	0.4485
0.2652	0.1567	0.3734	0.0006	0.4344	0.5656
0.3045	0.2175	0.3598	0.0009	0.3396	0.6604
0.3475	0.2741	0.3441	0.0011	0.2706	0.7294
0.3830	0.3137	0.3327	0.0013	0.2338	0.7662
0.4208	0.3508	0.3217	0.0015	0.2048	0.7952
0.4596	0.3952	0.3084	0.0018	0.1758	0.8242
0.5017	0.4583	0.2895	0.0021	0.1428	0.8572
0.5230	0.4975	0.2779	0.0023	0.1262	0.8738
0.5502	0.5391	0.2659	0.0026	0.1110	0.8890
0.5719	0.5653	0.2584	0.0028	0.1026	0.8974
0.5923	0.5929	0.2507	0.0029	0.0945	0.9055
0.6070	0.6125	0.2452	0.0031	0.0892	0.9108

\* Based on irreducible water saturation when the core has no asphaltene deposition.

**Table XII-24: Calculated Results for Core No. 3 and Run No. 2.**

$S_w^*$	$S_{wD}$	$K_{ro}$	$K_{rw}$	$f_o$	$f_w$
0.1801	0.0399	0.9667	0.0001	0.8932	0.1068
0.2767	0.1545	0.8518	0.0006	0.6531	0.3469
0.3874	0.2761	0.7228	0.0010	0.4573	0.5427
0.4708	0.3638	0.6276	0.0014	0.3471	0.6529
0.5308	0.4279	0.5581	0.0017	0.2804	0.7169
0.5814	0.4845	0.4972	0.0020	0.2300	0.7700
0.6413	0.5568	0.4213	0.0024	0.1758	0.8242
0.6945	0.6239	0.3536	0.0028	0.1345	0.8655
0.7273	0.6641	0.3147	0.0030	0.1135	0.8865
0.7636	0.7065	0.2751	0.0032	0.0938	0.9062
0.8002	0.7402	0.2450	0.0034	0.0801	0.9199

\* Based on irreducible water saturation when the core has no asphaltene deposition.

**Table XII-25: Calculated Results for Core No. 3 and Run No. 3.**

$S_w^*$	$S_{wD}$	$K_{ro}$	$K_{rw}$	$f_o$	$f_w$
0.1978	0.0528	0.8858	0.0002	0.8548	0.1452
0.3282	0.1987	0.8418	0.0007	0.5840	0.4160
0.4247	0.2696	0.7908	0.0012	0.4424	0.5576
0.5042	0.3826	0.7324	0.0017	0.3412	0.6588
0.5796	0.4651	0.6645	0.0023	0.2608	0.7392
0.6299	0.5208	0.6128	0.0027	0.2149	0.7851
0.6764	0.5720	0.5618	0.0032	0.1780	0.8220
0.7142	0.6203	0.5110	0.0036	0.1475	0.8525
0.7516	0.6655	0.4616	0.0040	0.1223	0.8777
0.7876	0.7042	0.4185	0.0044	0.1032	0.8968
0.8223	0.7349	0.3838	0.0048	0.0895	0.9105
0.8489	0.7529	0.3633	0.0050	0.0820	0.9180

\* Based on irreducible water saturation when the core has no asphaltene deposition.

**Table XII-26: Calculated Results for Core No. 3 and Run No. 4.**

$S_w^*$	$S_{wD}$	$K_{ro}$	$K_{rw}$	$f_o$	$f_w$
0.2797	0.1489	1.0000	0.0005	0.7160	0.2840
0.4233	0.2934	0.9345	0.0011	0.5087	0.4913
0.5262	0.3983	0.8612	0.0017	0.3840	0.6160
0.6333	0.5212	0.7445	0.0026	0.2623	0.7377
0.6971	0.5864	0.6683	0.0031	0.2076	0.7924
0.7581	0.6475	0.5875	0.0037	0.1621	0.8379
0.8018	0.6958	0.5174	0.0042	0.1299	0.8701
0.8612	0.7610	0.4137	0.0050	0.0912	0.9088
0.9085	0.8093	0.3305	0.0057	0.0661	0.9339
0.9408	0.8448	0.2658	0.0062	0.0494	0.9506

\* Based on irreducible water saturation when the core has no asphaltene deposition.

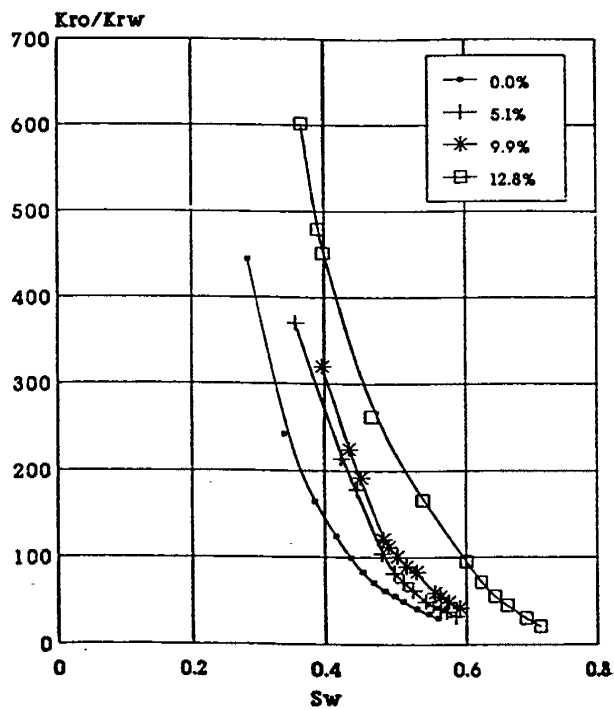


Figure XII-11. Ratio of Oil Relative Permeability to Water Relative Permeability ( $K_{ro}/K_{rw}$ ) Versus  $S_w$  (core 1).

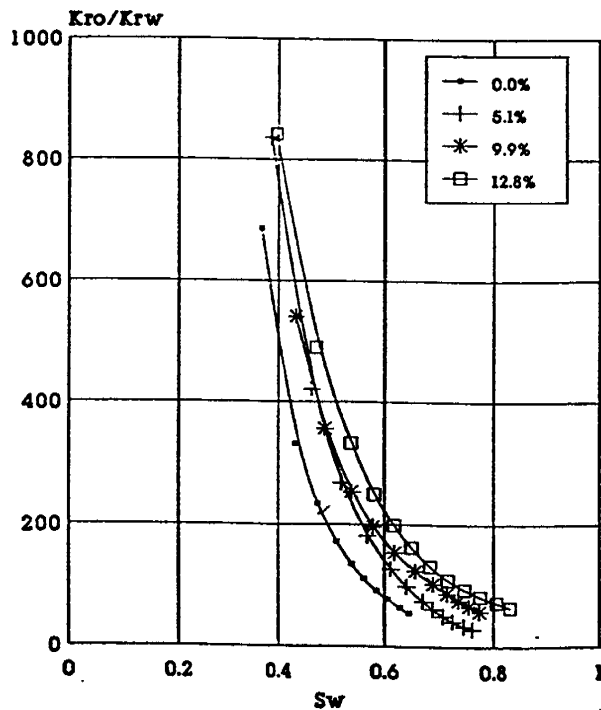


Figure XII-12. Ratio of Oil Relative Permeability to Water Relative Permeability ( $K_{ro}/K_{rw}$ ) Versus  $S_w$  (core 2).

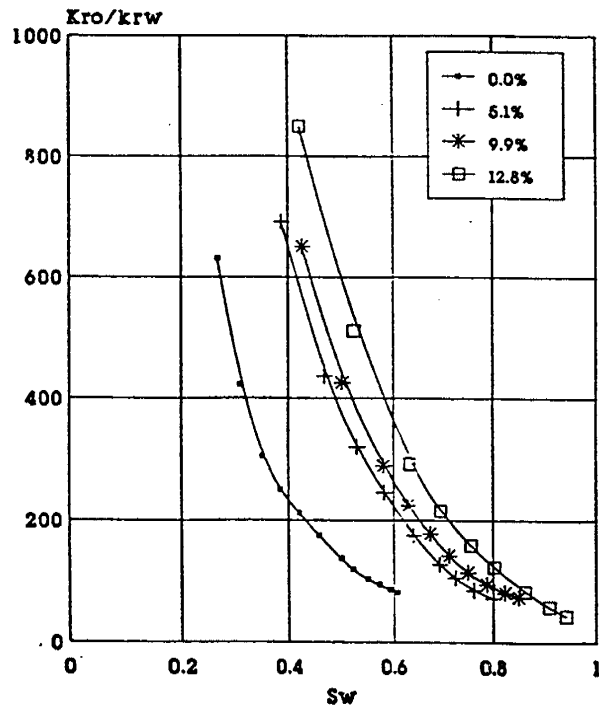


Figure XII-13. Ratio of Oil Relative Permeability to Water Relative Permeability ( $K_{ro}/K_{rw}$ ) Versus  $S_w$  (core 3).

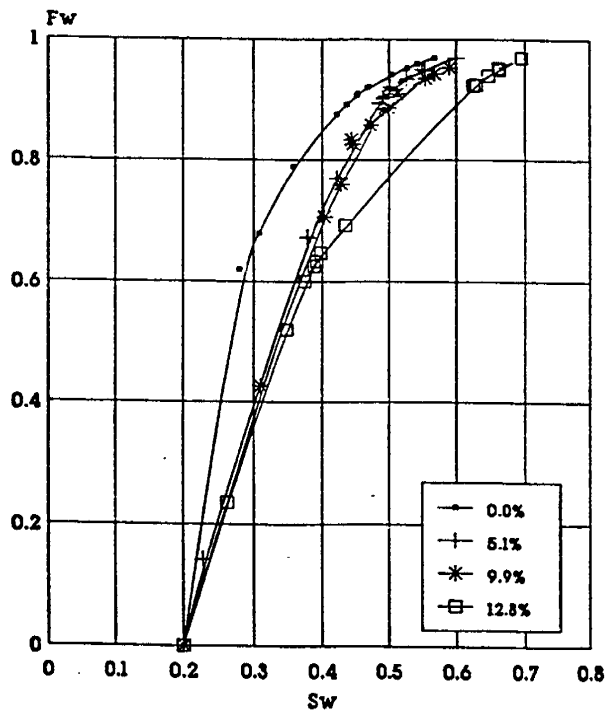


Figure XII-14. Effect of Asphaltene Deposition on Fractional Flow Curves (core 1).

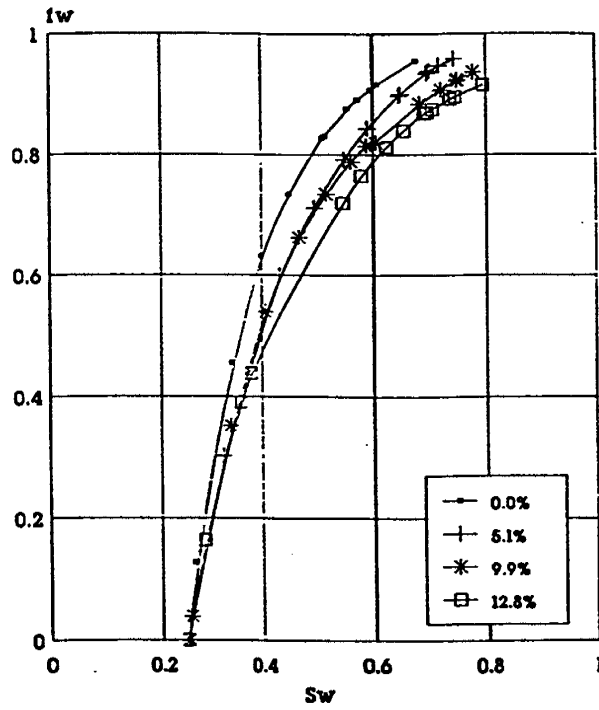


Figure XII-15. Effect of Asphaltene Deposition on Fractional Flow Curves (core 2).

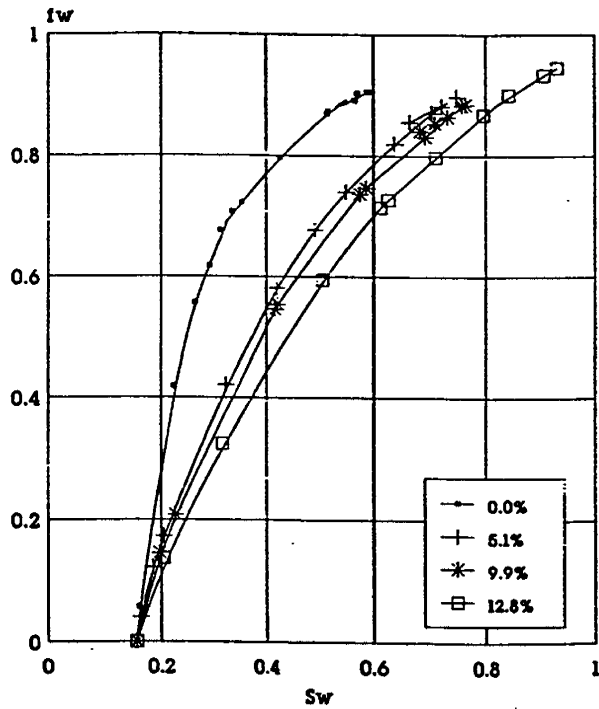


Figure XII-16. Effect of Asphaltene Deposition on Fractional Flow Curves (core 3).

Figures XII-17, XII-18, and XII-19 show the effect of asphaltene deposition on oil-water relative permeability curves for Cores 1, 2, and 3 respectively. In these figures the left y-axis represent oil relative permeability ( $K_{ro}$ ), the right y-axis represent water relative permeability ( $K_{rw}$ ) and x-axis represents dimensionless water saturation ( $S_{wd}$ ) defined as:

$$S_{wd} = \frac{S_w - S_{wir}}{1 - S_{or} - S_{wir}} \quad (1)$$

These results for all cores show that asphaltene deposition resulted in improved relative oil permeability which contributed to improved displacement performance.

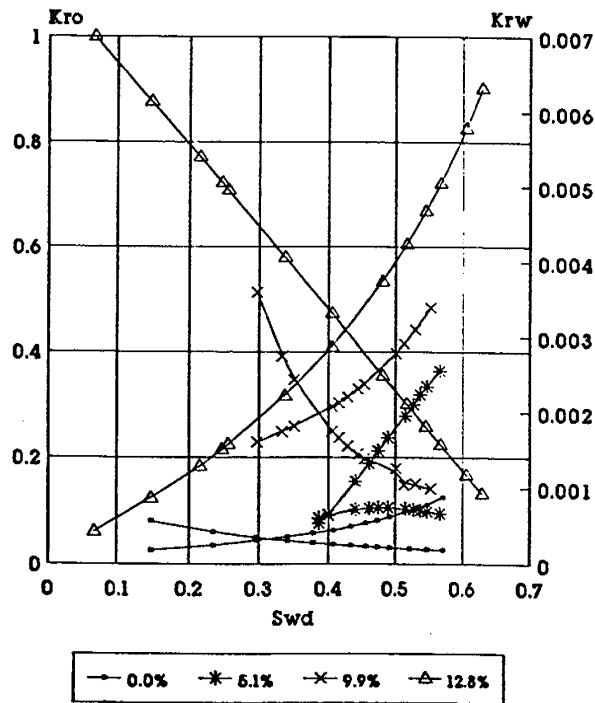


Figure XII-17. Effect of Asphaltene Deposition on Oil-Water Relative Permeability Curves (core 1).

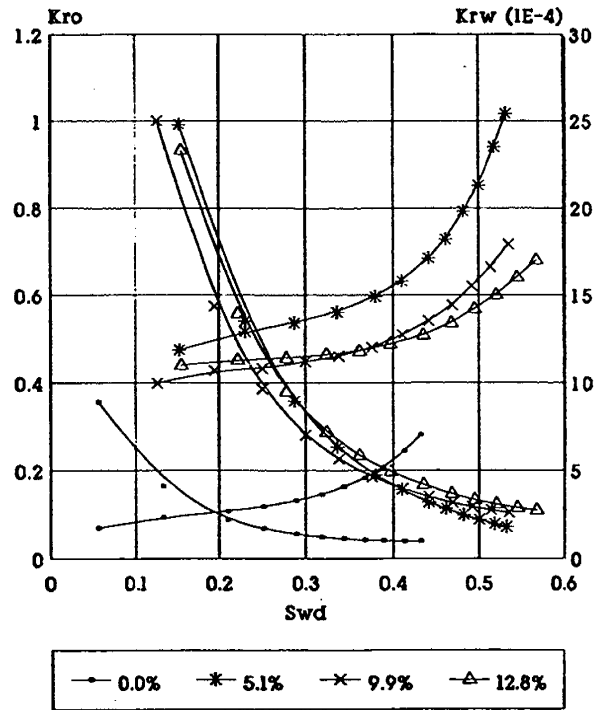


Figure XII-18. Effect of Asphaltene Deposition on Oil-Water Relative Permeability Curves (core 2).

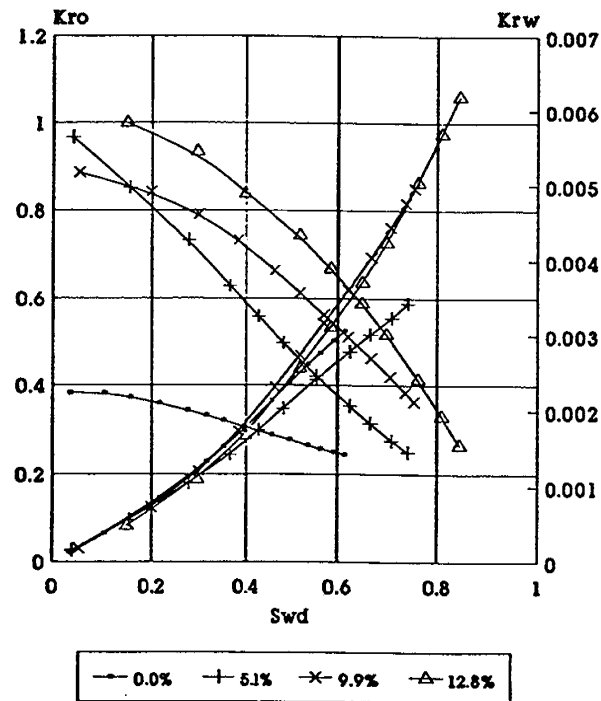


Figure XII-19. Effect of Asphaltene Deposition on Oil-Water Relative Permeability Curves (core 3).

## **D. CONCLUSIONS**

Experimental work was undertaken to determine the effect of asphaltene deposition on dynamic displacement of heavy oil by water and on rock-fluid properties for both consolidated and unconsolidated porous media. The following conclusions can be drawn from this study.

1. The increase in asphaltene deposition resulted in increased pore plugging of cores causing increased reduction in absolute permeability (50% reduction in one case). The permeability reduction effect was more pronounced in tighter porous media compared to high permeability porous media.
2. The displacement performance and the oil recovery during dynamic displacement of heavy oil by water improved significantly by asphaltene deposition. It is believed that the improvement in displacement performance may be partly due to improvement in relative oil permeability caused by end point saturation and wettability changes and partly also due to the flow diversion effect of asphaltene deposition.

## CHAPTER XIII: FLUID PROPERTIES

---

### A. INTRODUCTION

Fluid properties in Alaskan petroleum reservoirs can be widely variable. This chapter presents a collection of fluid property data for Sadlerochit group and Kuparuk River formation of the Prudhoe Bay, the West Sak and the Endicott fields. The fluid properties shown include formation volume factor, solution gas-oil ratio, density, viscosity and bubble point pressure. Oil, water and gas relative permeabilities and capillary pressures also are shown for Sadlerochit group. The following sections present the fluid properties for each reservoir in graphical form.

### B. SADLEROCHIT GROUP

The oil, water and gas relative permeability curves for Sadlerochit group are shown in Figures XIII-1 through XIII-4. For the oil relative permeability curve, the reservoir was divided into two rock regions: region 1 was near the gas-oil contact, and region 2 was near the oil-water contact. Based on core analysis, the residual oil saturations were determined to be 32% in the presence of water and gas (region 1), and 23% in the presence of water only (region 2). For water and gas relative permeabilities, single sets of curves are applicable to the entire reservoir (Figures XIII-3 and XIII-4). The average connate water saturation was determined to be 19% from log analysis. The critical gas saturation was estimated at 3%. The oil-water capillary pressure curve is shown in Figure XIII-5.

The oil bearing zone of Sadlerochit reservoir was divided into six depth intervals to describe the oil PVT properties. Figures XIII-6 through XIII-11 show the oil formation volume factor as a function of pressure in each of the six depth intervals. The oil bubble point pressure in each interval is indicated in the respective figures. Figures XIII-12 through XIII-17 show solution gas-oil ratio and Figures XIII-18 through XIII-23 show oil viscosity as functions of pressure in the six depth intervals. For water and gas PVT properties, however, single sets of data are applicable over the entire reservoir. Gas formation volume factor and viscosity versus pressure are shown in Figures XIII-24 and XIII-25, respectively, and water formation volume factor is shown in Figure XIII-26. The water viscosity at reservoir pressure and temperature is 0.32 cp and salinity, 19125 ppm.

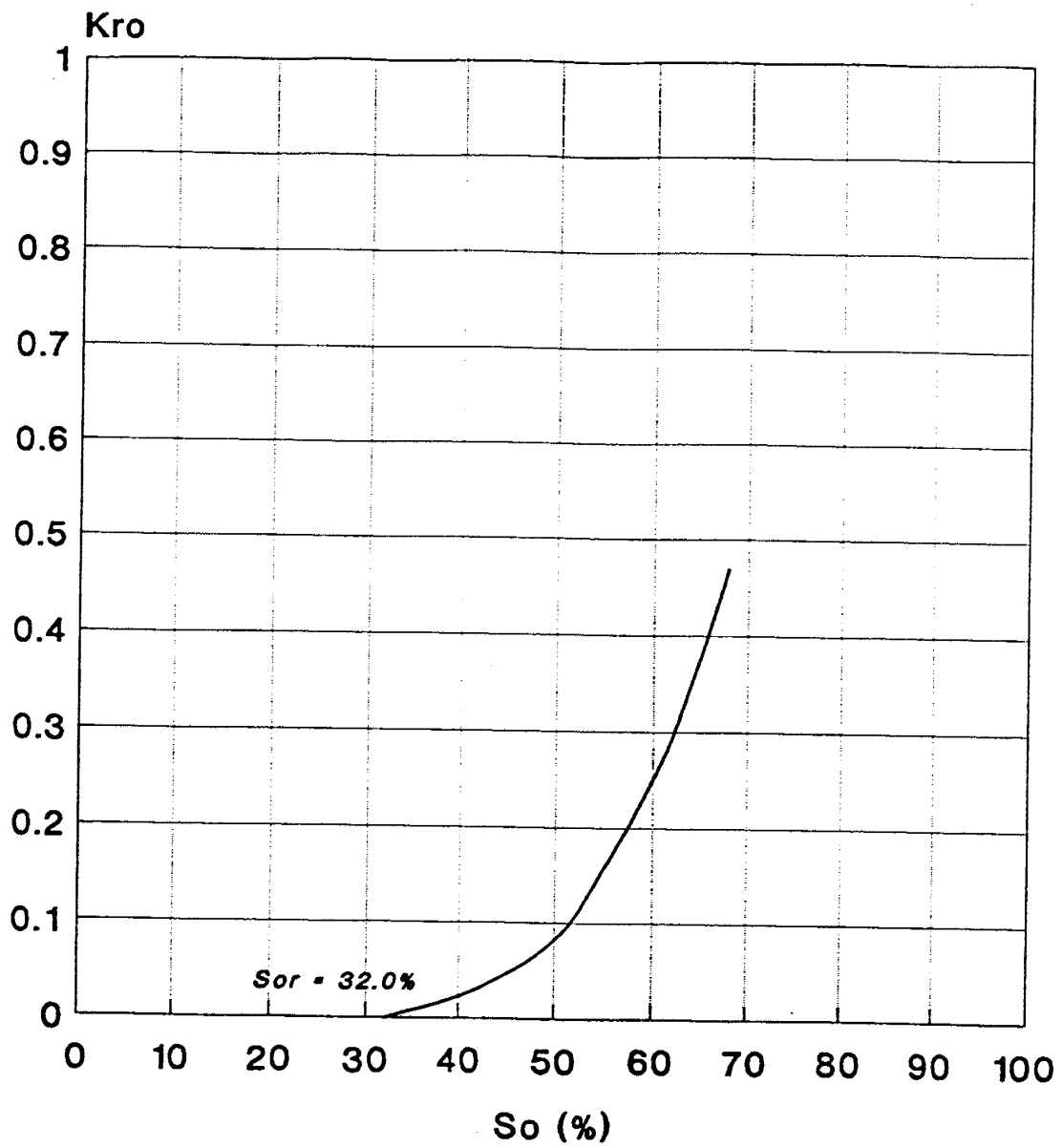


Figure XIII-1. Oil Relative Permeability Curve for Sadlerochit: Rock Region 1.

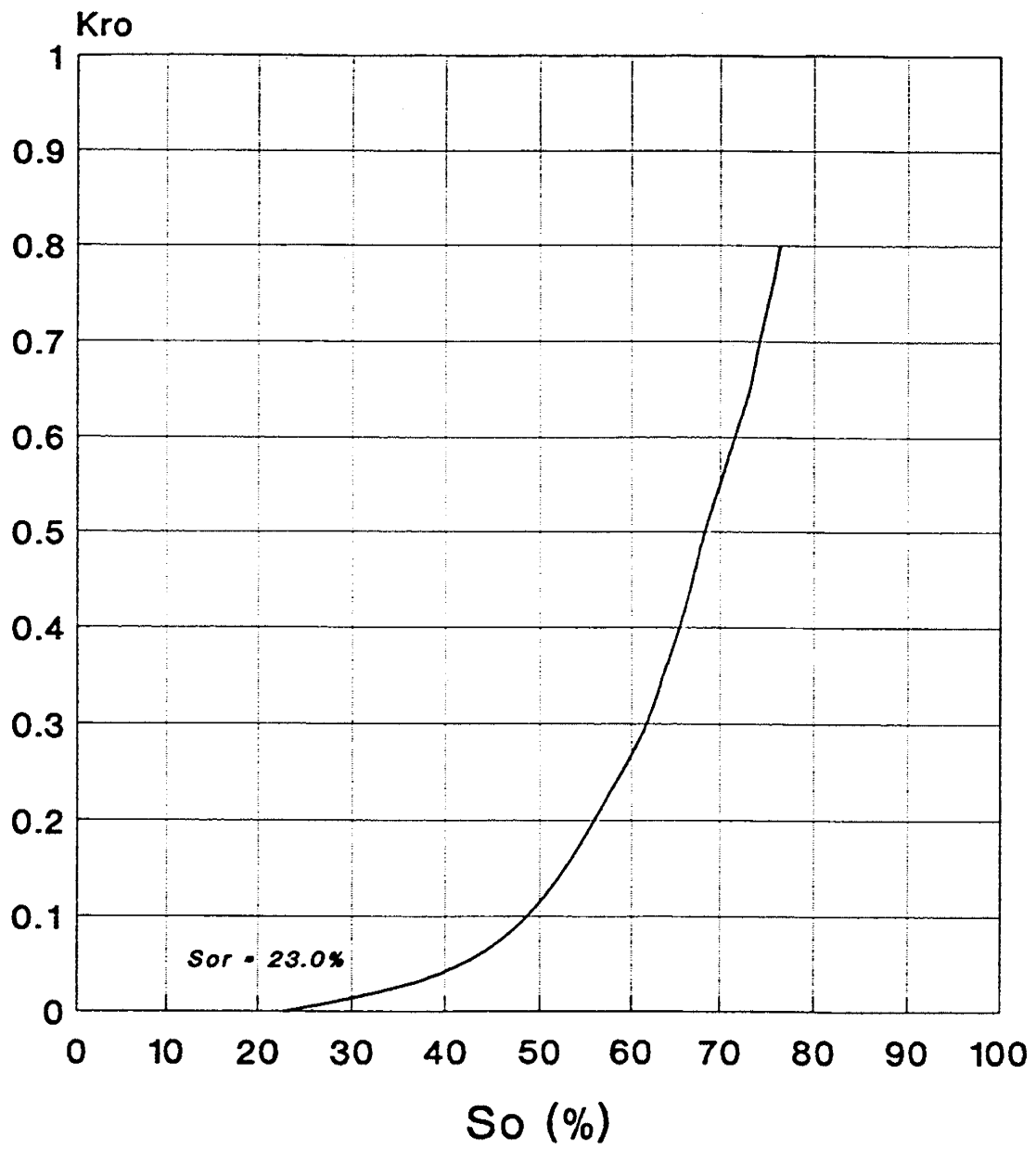


Figure XIII-2. Oil Relative Permeability Curve for Sadlerochit: Rock Region 2.

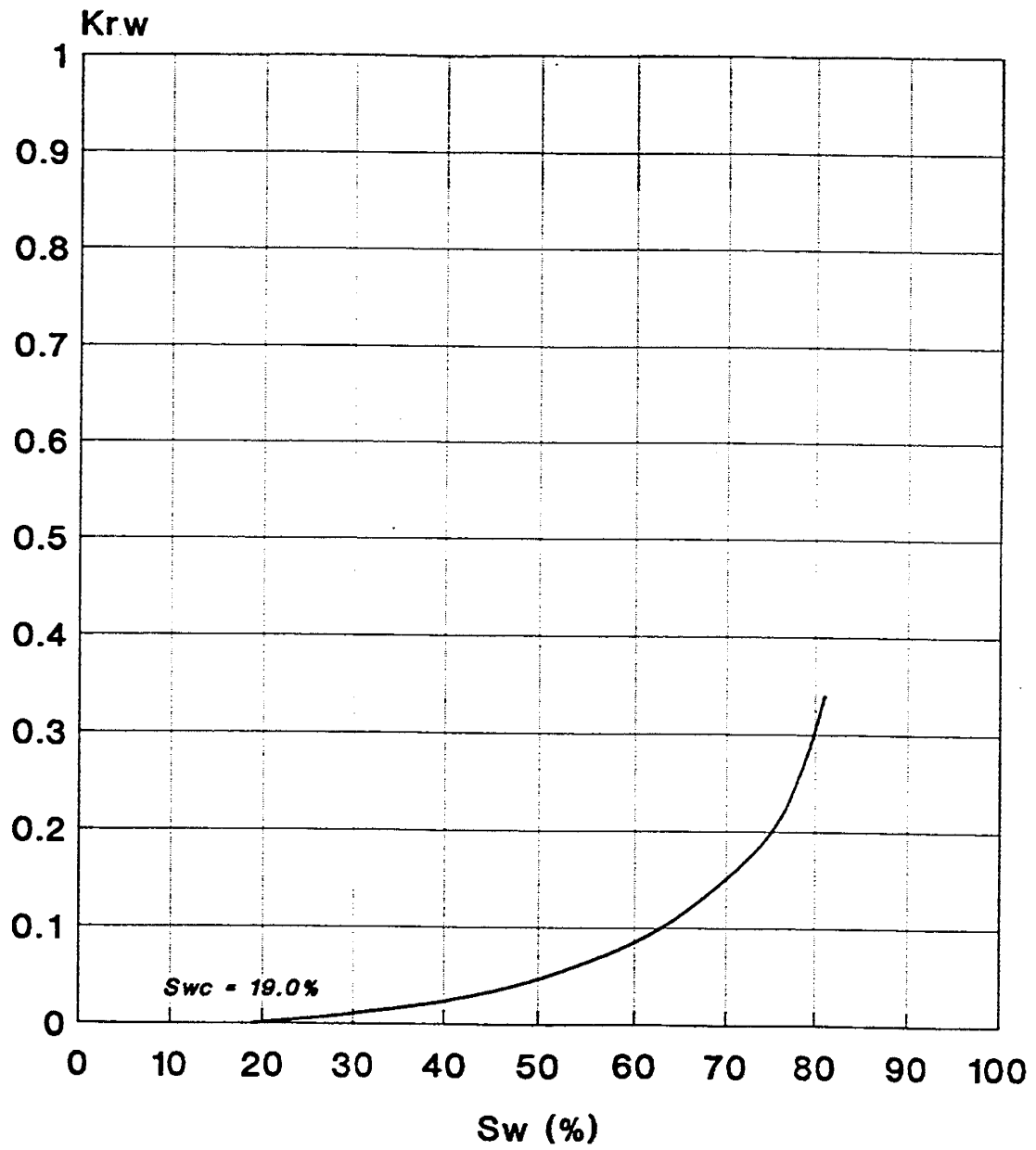


Figure XIII-3. Water Relative Permeability Curve for Sadlerochit.

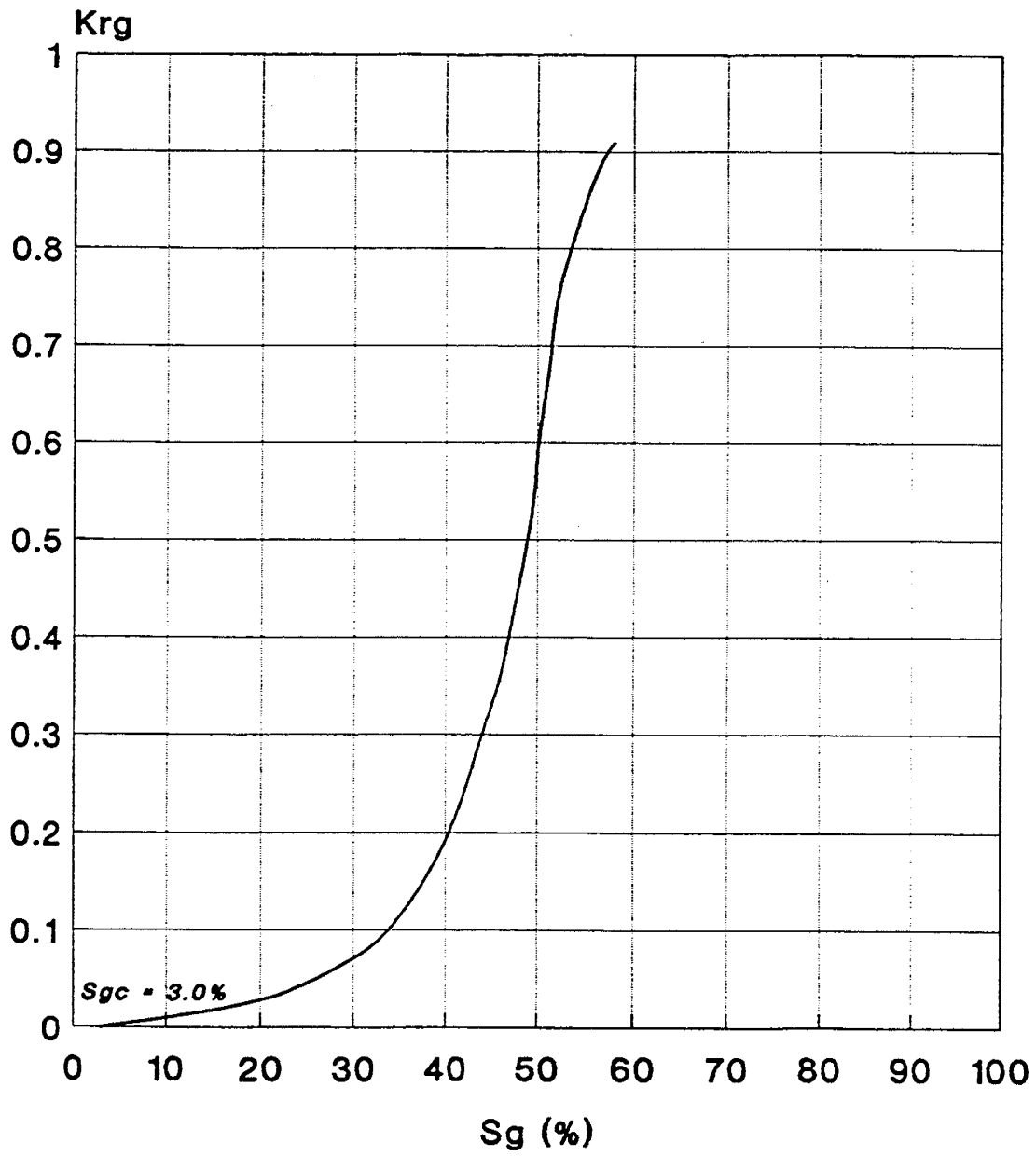


Figure XIII-4. Gas Relative Permeability Curve for Sadlerochit.

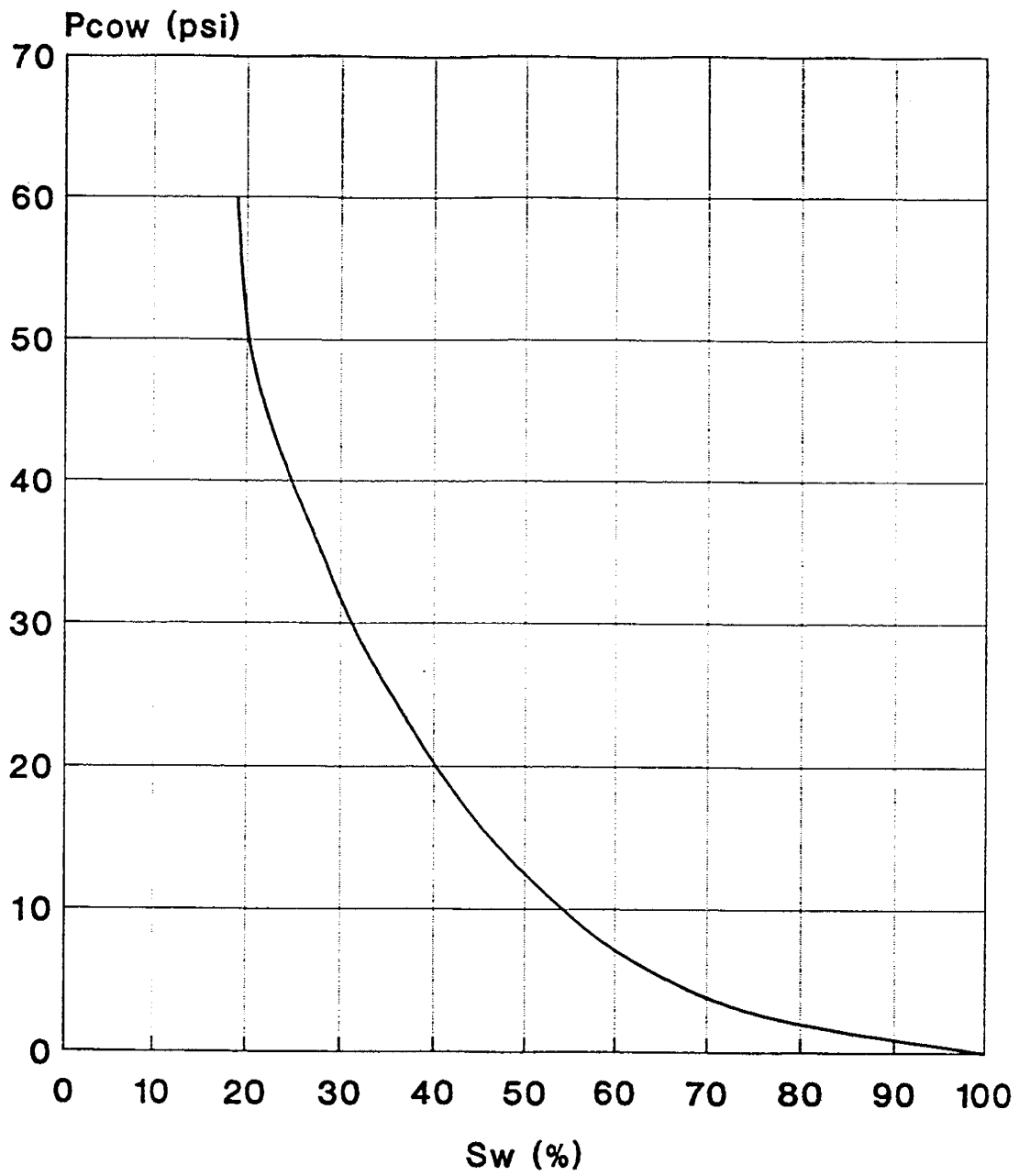


Figure XIII-5. Oil-Water Capillary Pressure Curve for Sadlerochit.

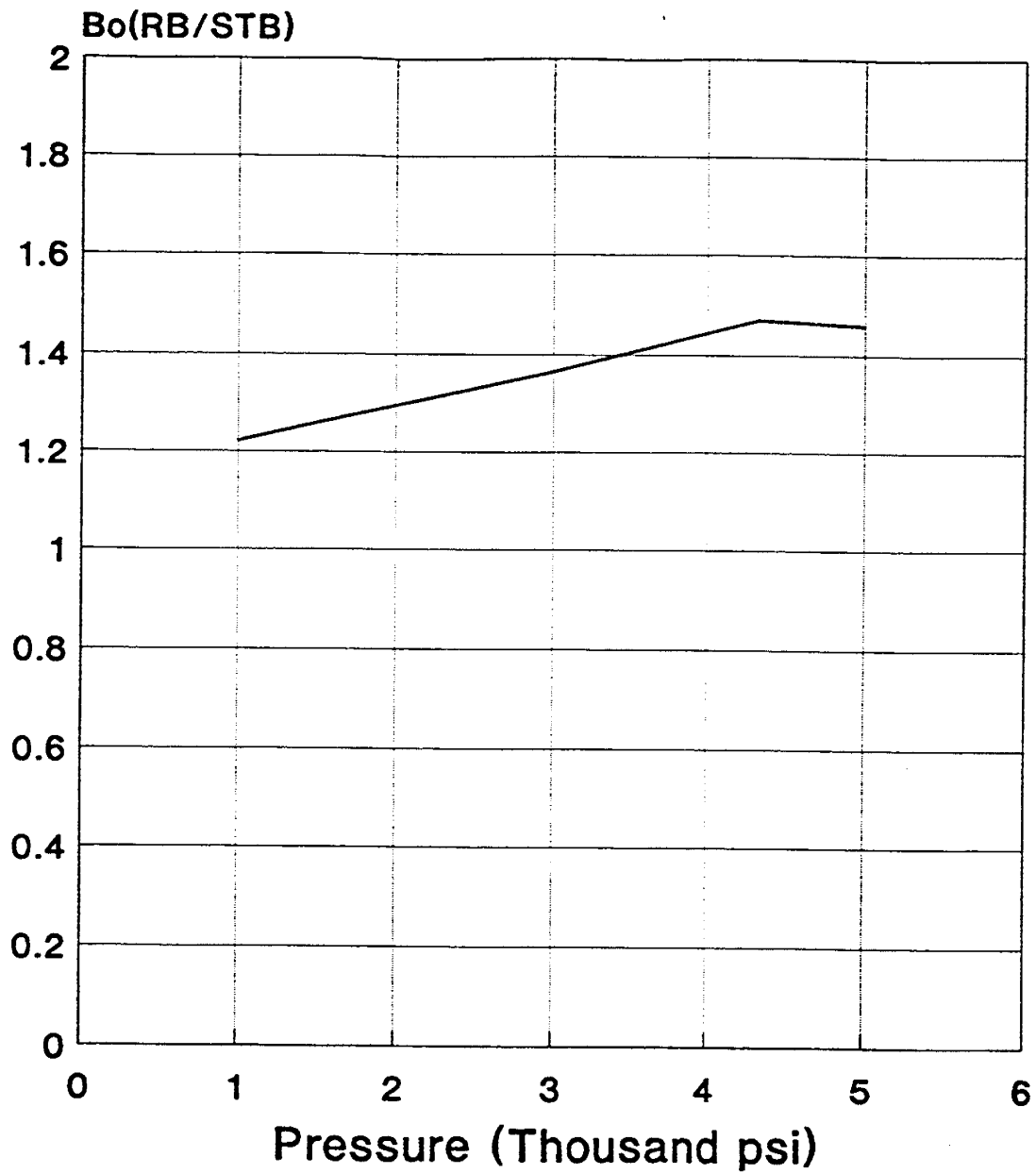


Figure XIII-6. Oil Formation Volume Factor for Sadlerochit: Depth Interval 1 (8580 to 8653 ft). Mid-Interval Bubble Point = 4344 psi.

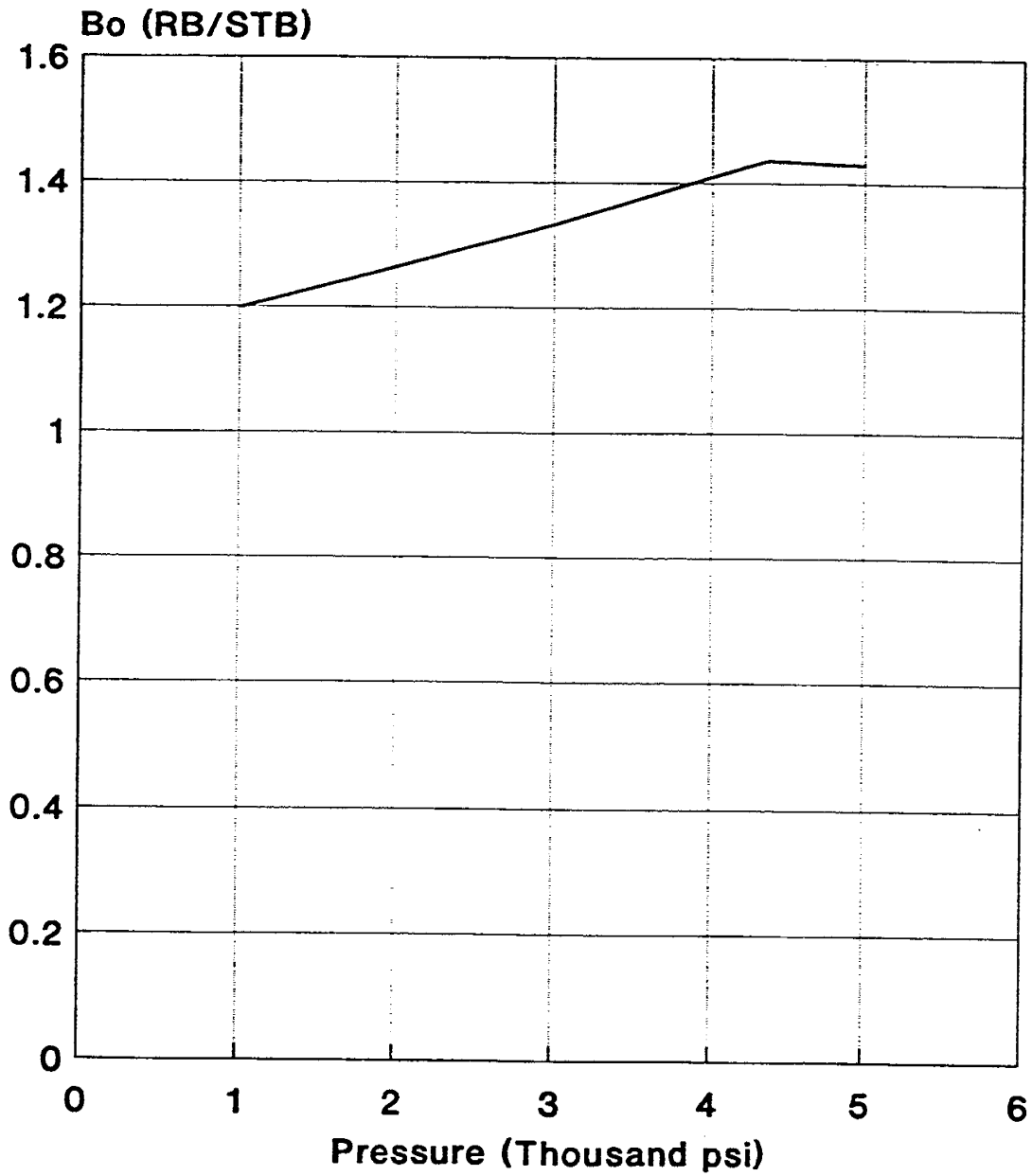


Figure XIII-7. Oil Formation Volume Factor for Sadlerochit: Depth Interval 2 (8653 to 8727 ft). Mid-Interval Bubble Point = 4366 psi.

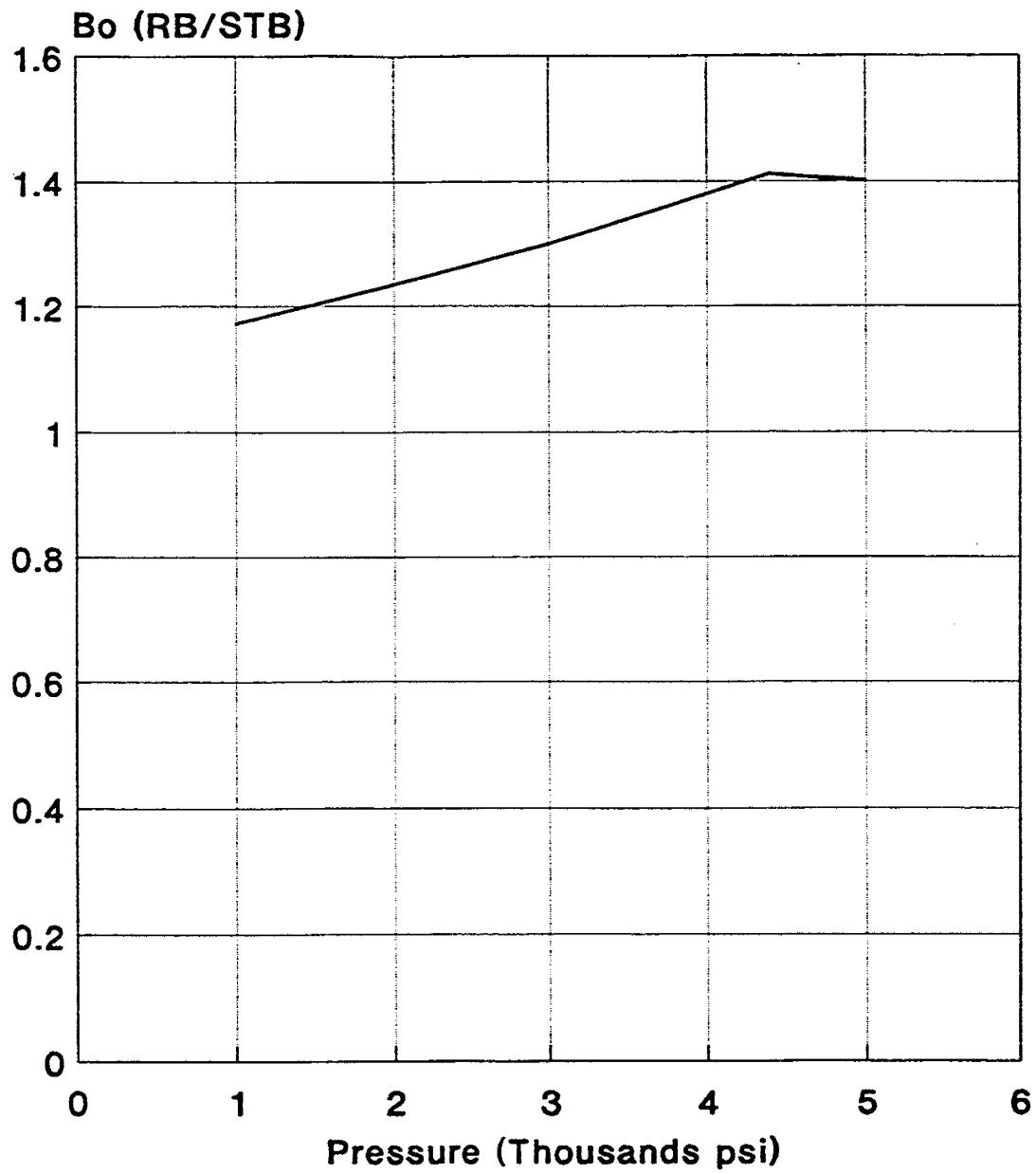


Figure XIII-8. Oil Formation Volume Factor for Sadlerochit: Depth Interval 3 (8727 to 8800 ft). Mid-Interval Bubble Point = 4389 psi.

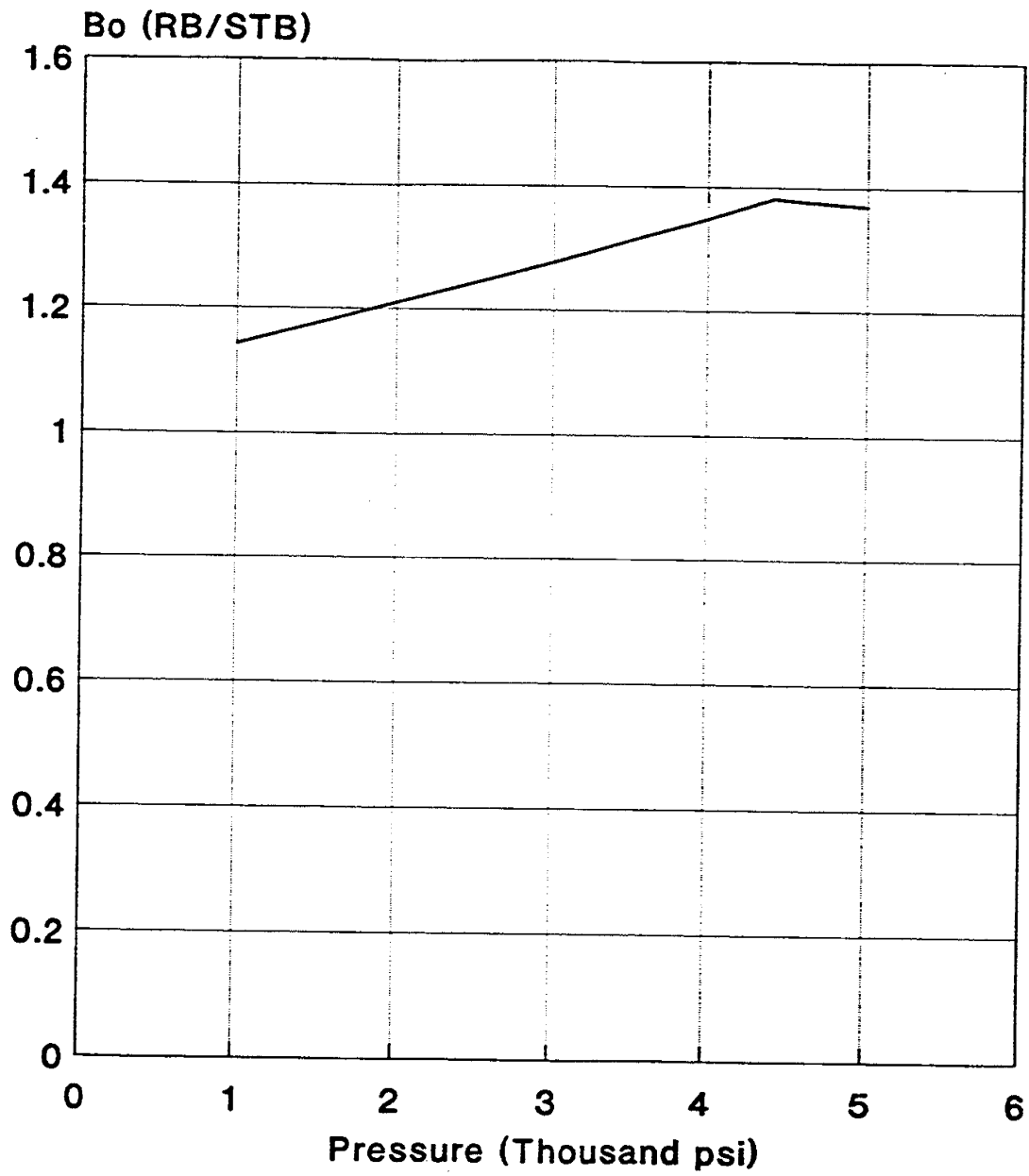


Figure XIII-9. Oil Formation Volume Factor for Sadlerochit: Depth Interval 4 (8800 to 8873 ft). Mid-Interval Bubble Point = 4412 psi.

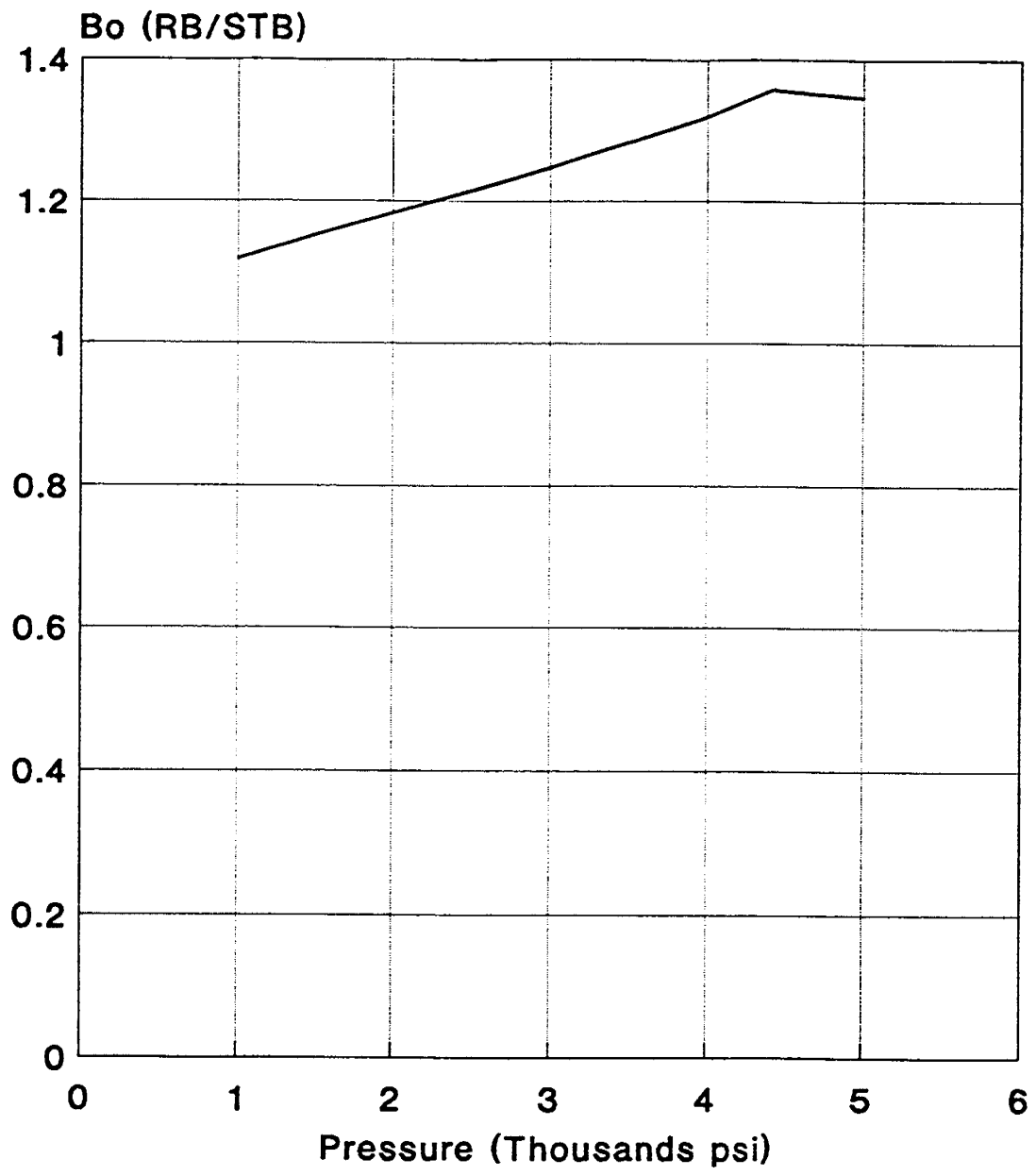


Figure XIII-10. Oil Formation Volume Factor for Sadlerochit: Depth Interval 5 (8873 to 8946 ft). Mid-Interval Bubble Point = 4435 psi.

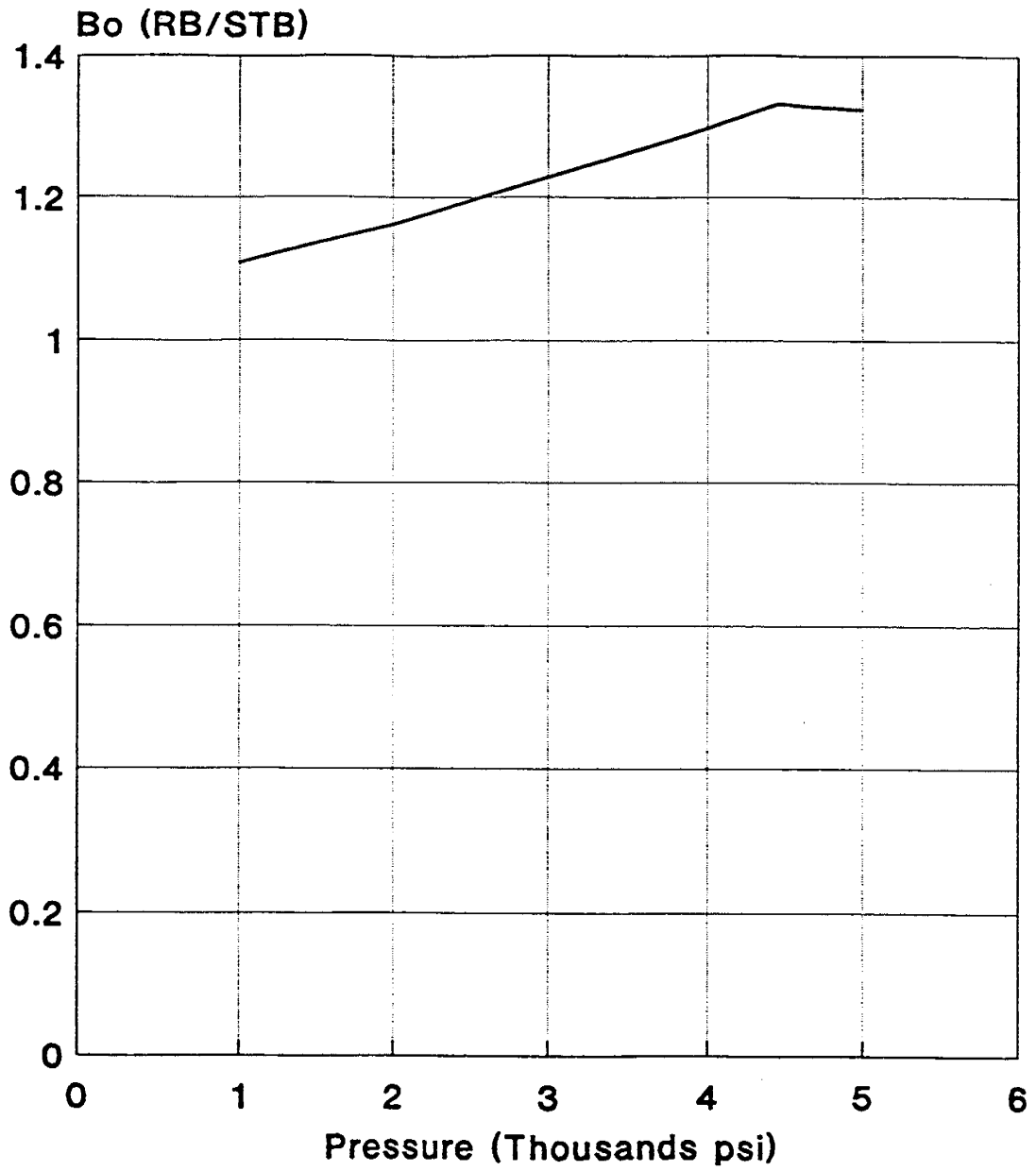


Figure XIII-11. Oil Formation Volume Factor for Sadlerochit: Depth Interval 6 (8946 to 9020 ft). Mid-Interval Bubble Point = 4458 psi.

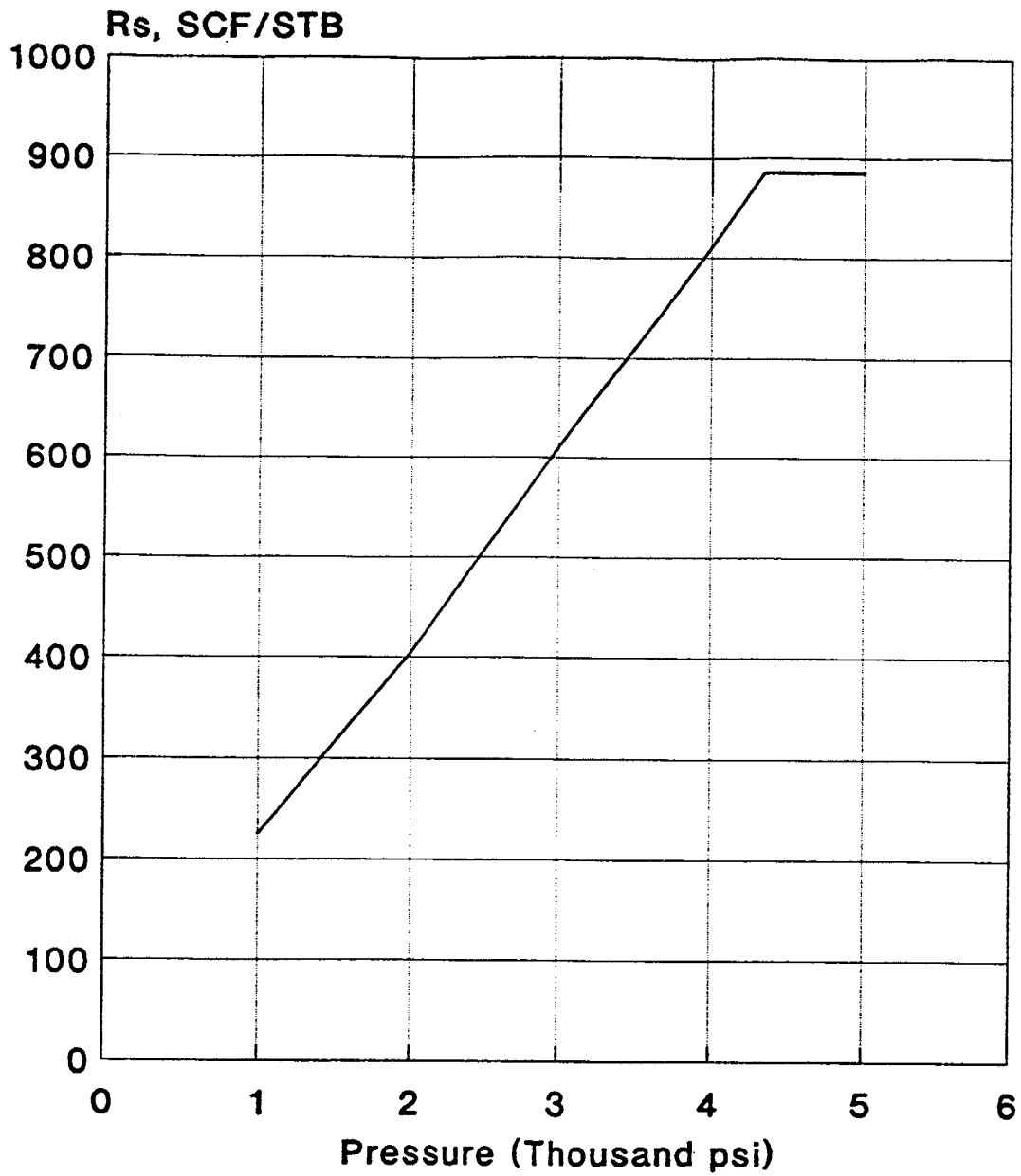


Figure XIII-12. Solution Gas-Oil Ratio for Sadlerochit: Depth Interval 1 (8580 to 8653 ft).

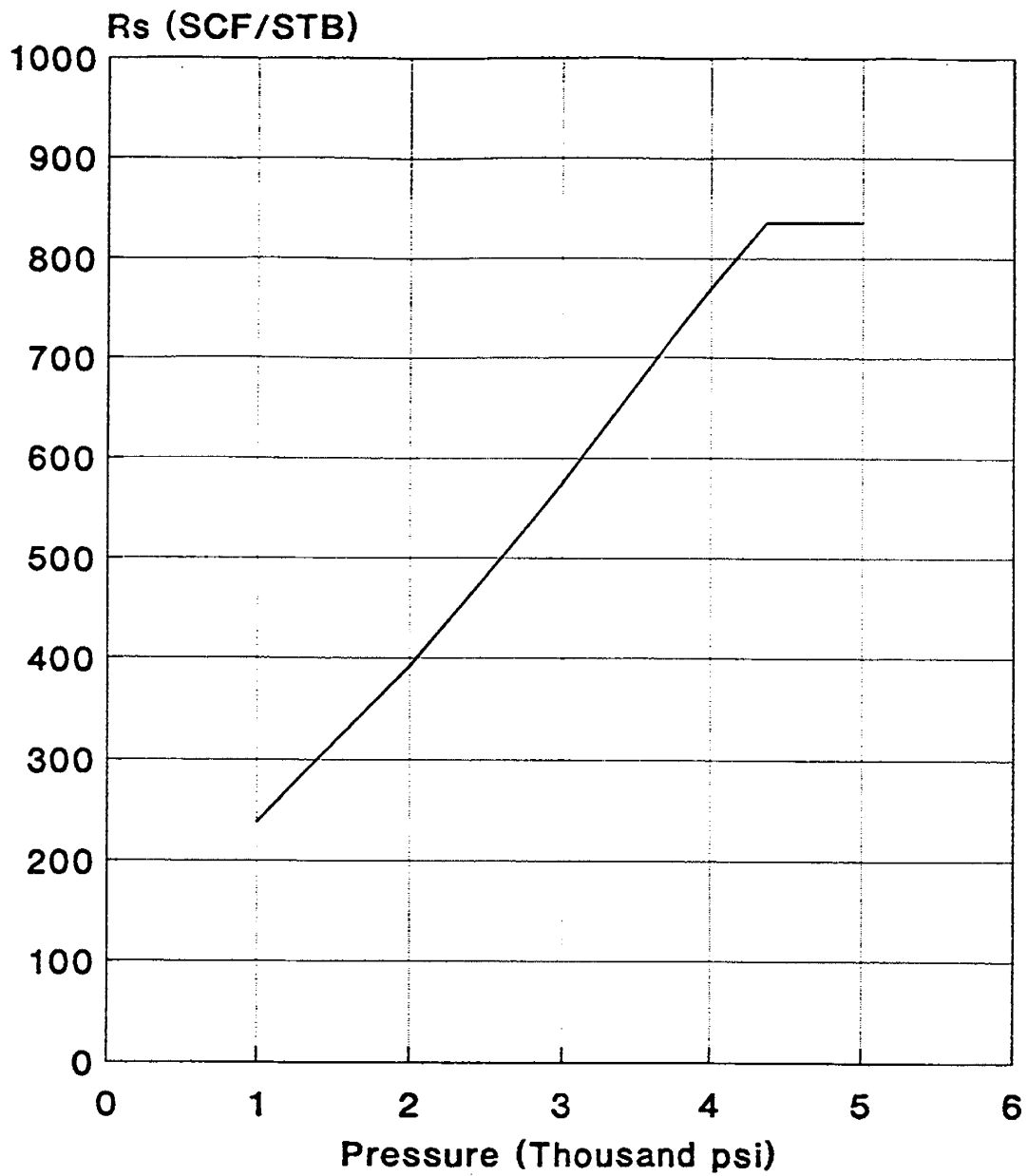


Figure XIII-13. Solution Gas-Oil Ratio for Sadlerochit: Depth Interval 2 (8653 to 8727 ft).

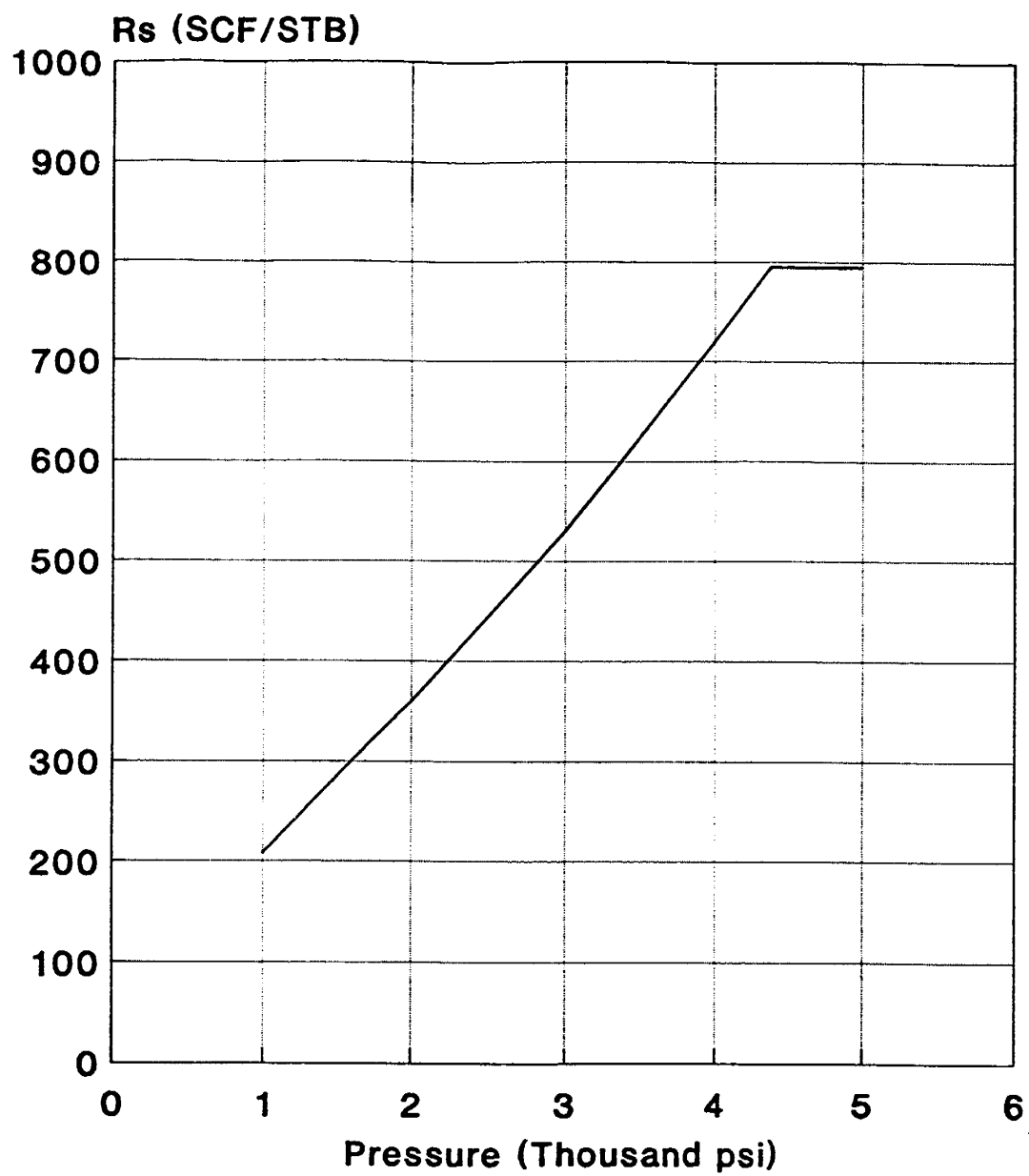


Figure XIII-14. Solution Gas-Oil Ratio for Sadlerochit: Depth Interval 3 (8727 to 8800 ft).

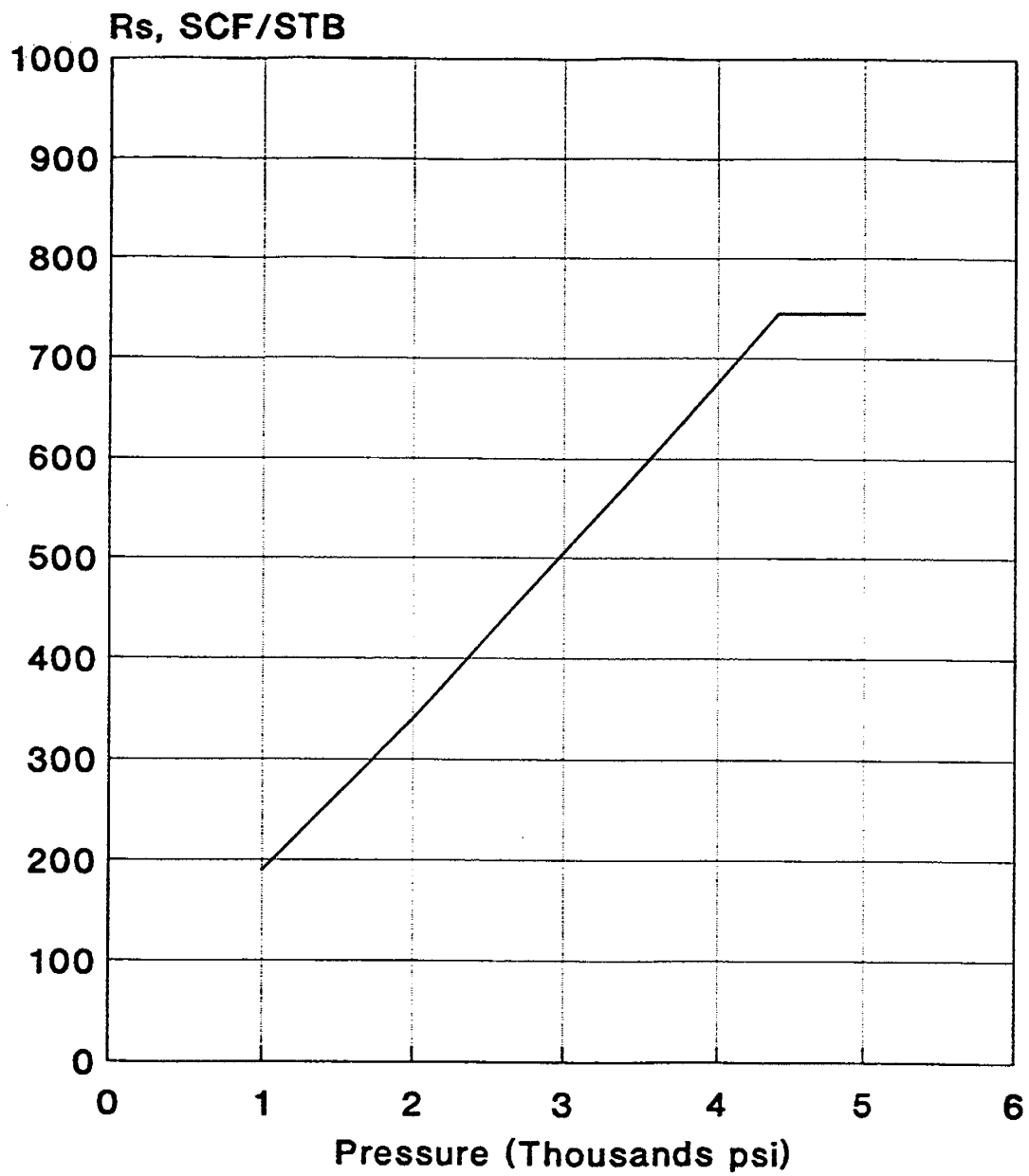


Figure XIII-15. Solution Gas-Oil Ratio for Sadlerochit: Depth Interval 4 (8800 to 8873 ft).

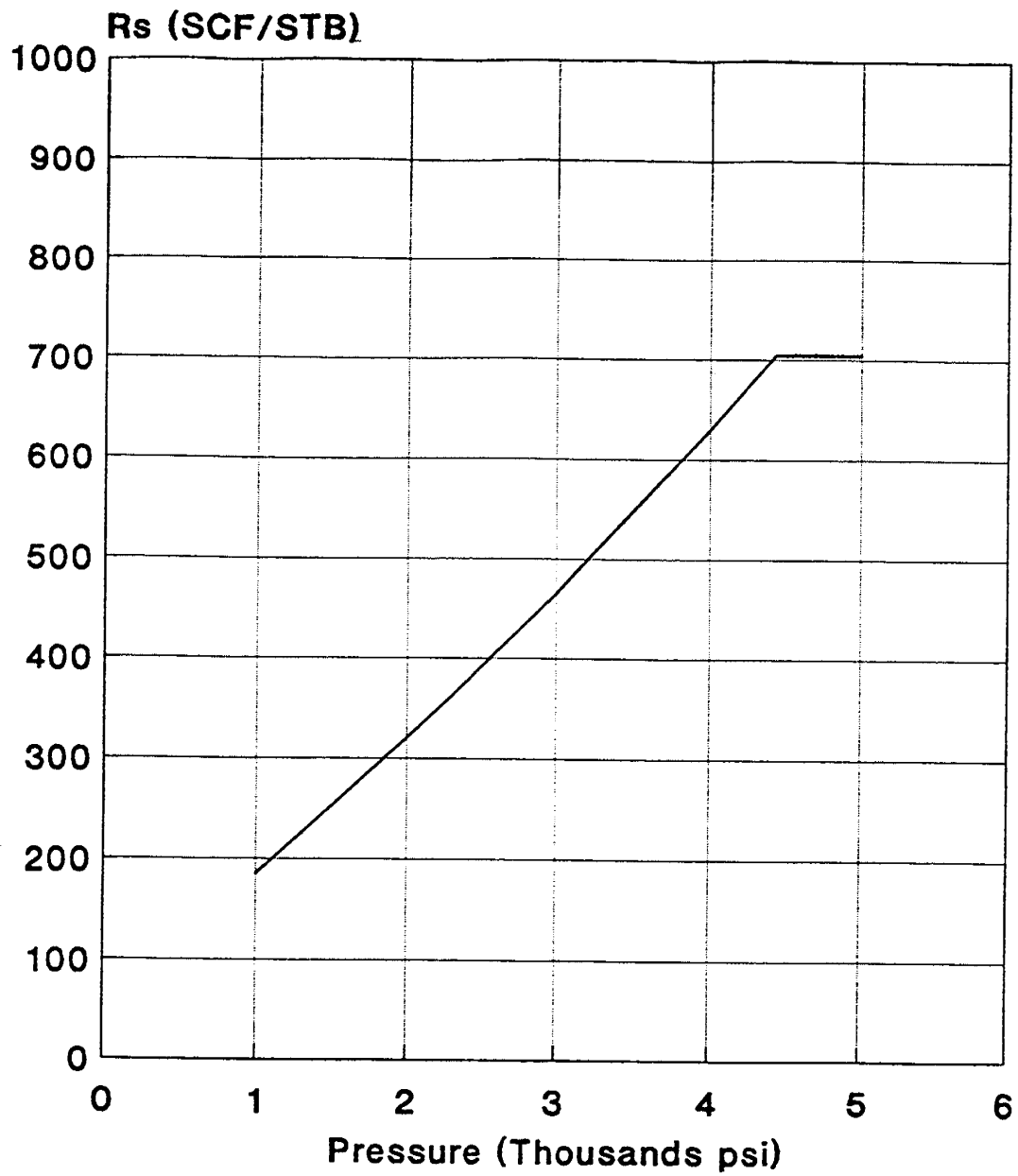


Figure XIII-16. Solution Gas-Oil Ratio for Sadlerochit: Depth Interval 5 (8873 to 8946 ft).

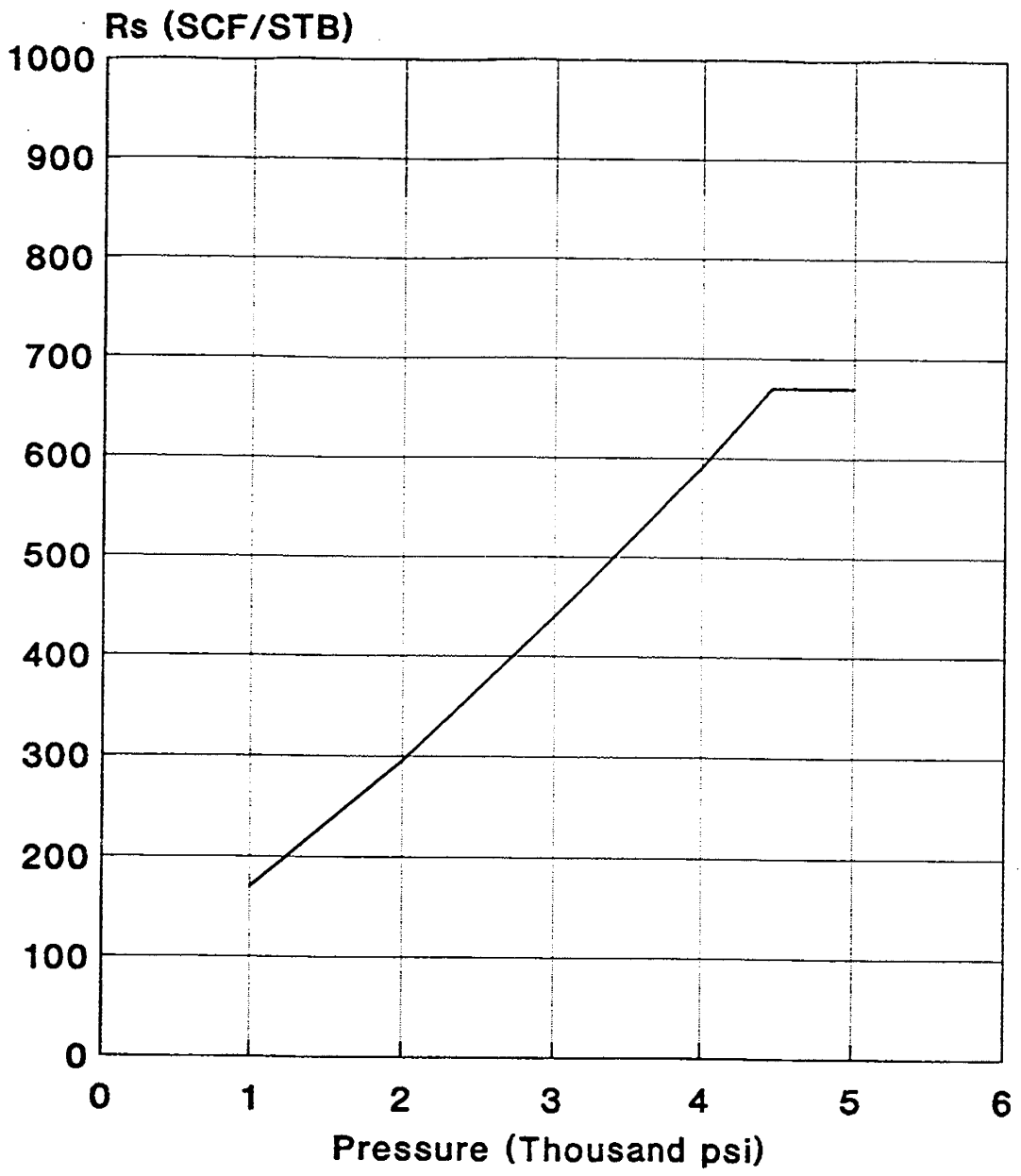


Figure XIII-17. Solution Gas-Oil Ratio for Sadlerochit: Depth Interval 6 (8946 to 9020 ft).

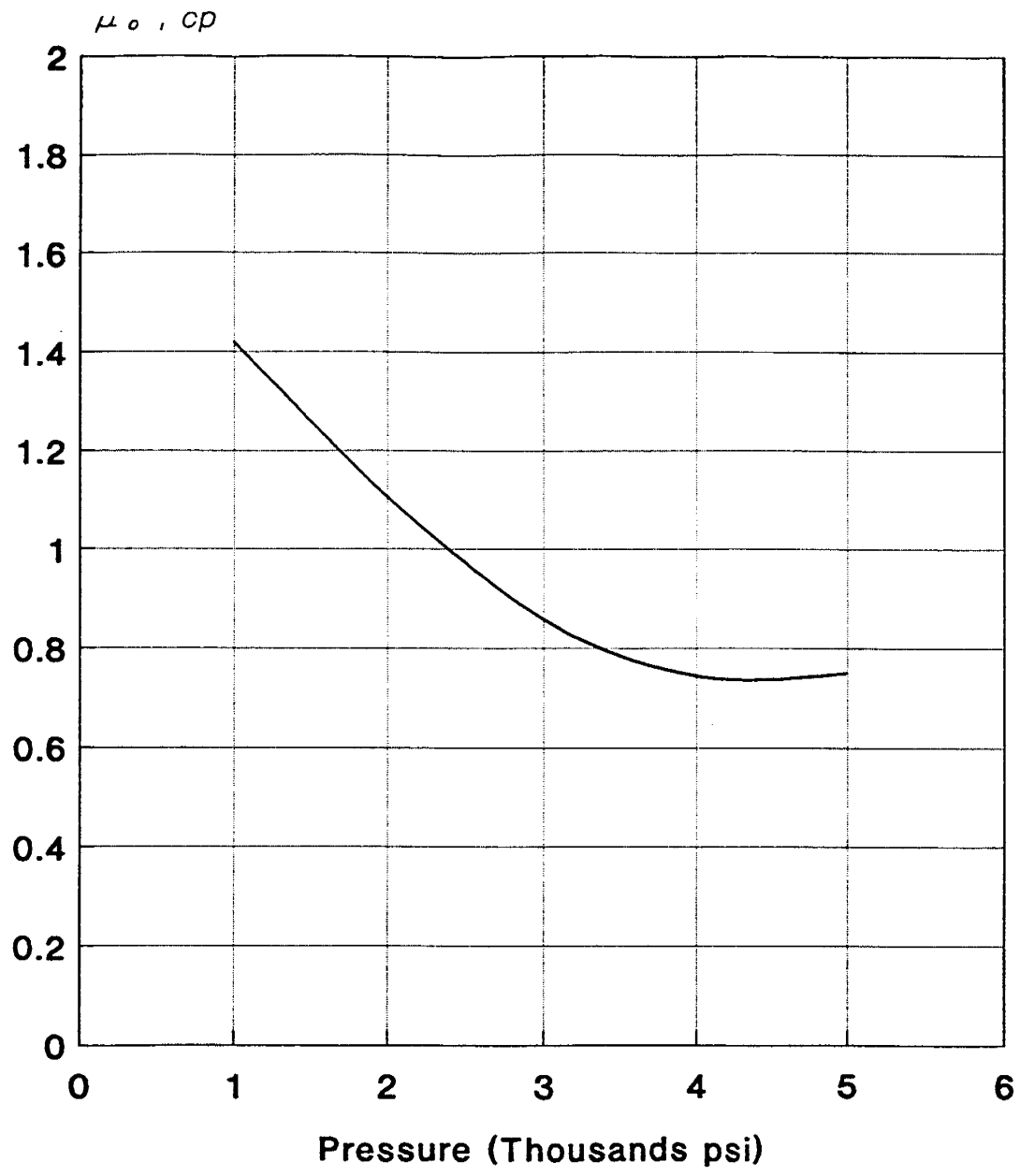


Figure XIII-18. Oil Viscosity for Sadlerochit: Depth Interval 1 (8580 to 8653 ft).

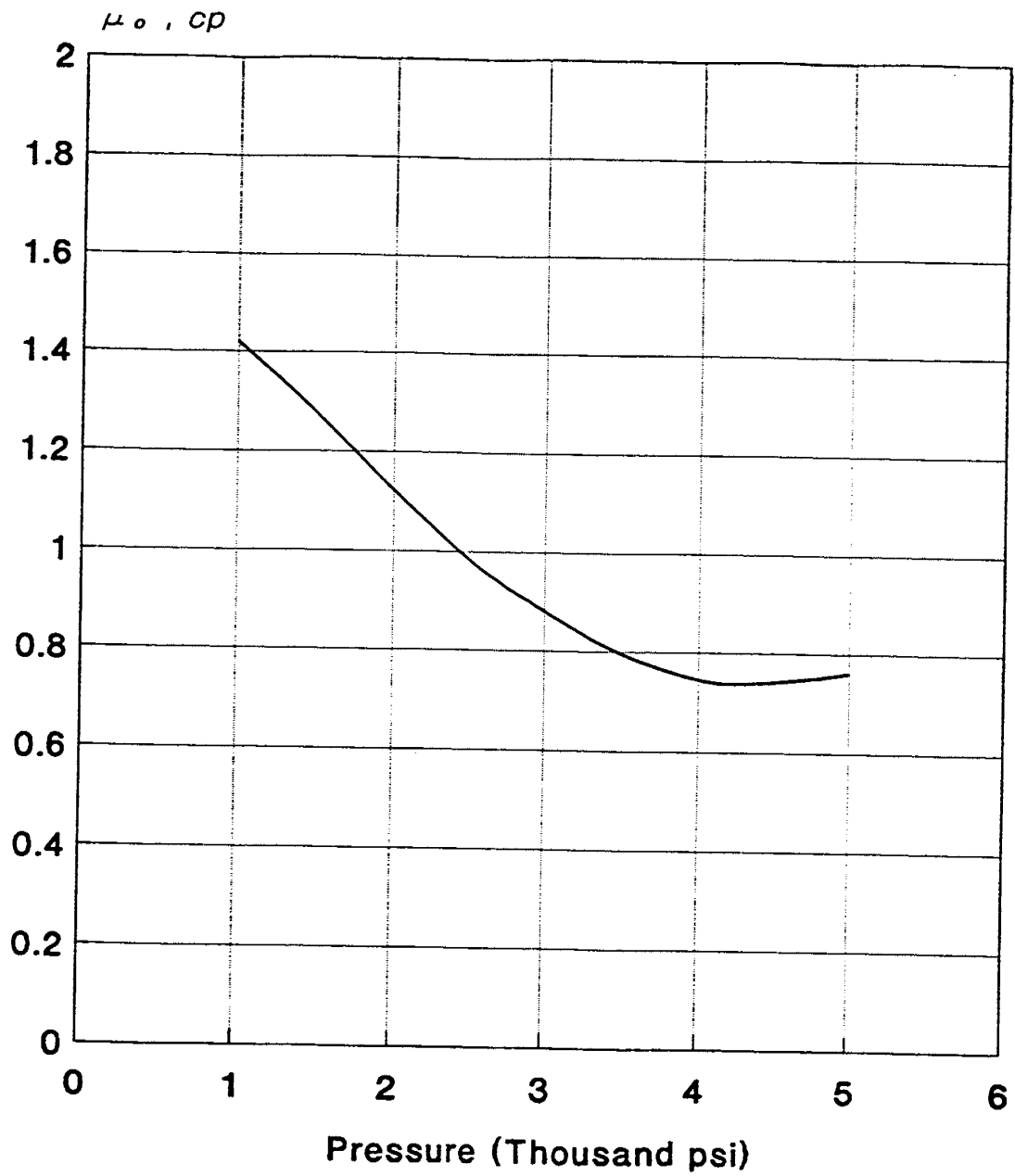


Figure XIII-19. Oil Viscosity for Sadlerochit: Depth Interval 2 (8653 to 8727 ft).

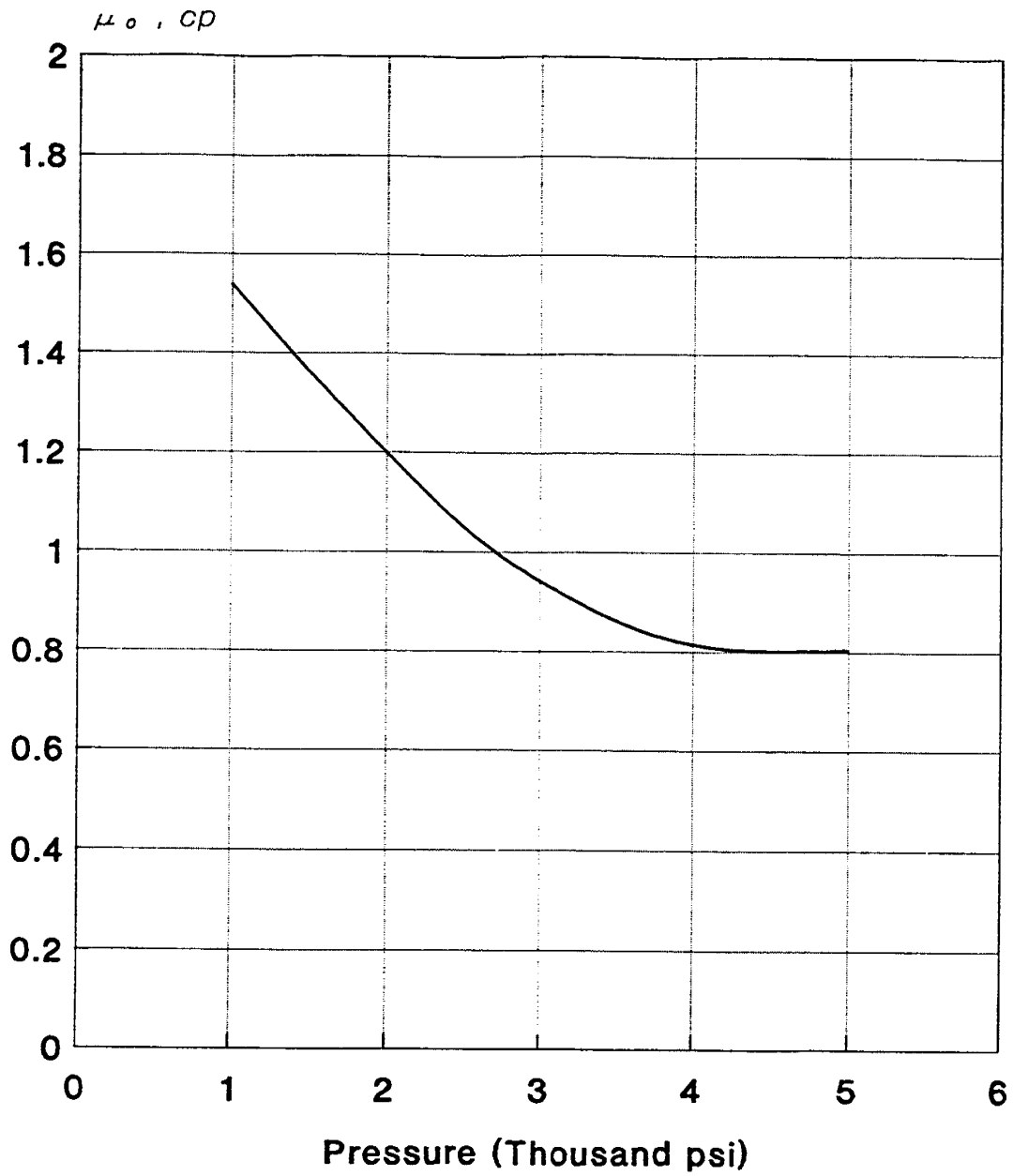


Figure XIII-20. Oil Viscosity for Sadlerochit: Depth Interval 3 (8727 to 8800 Ft).

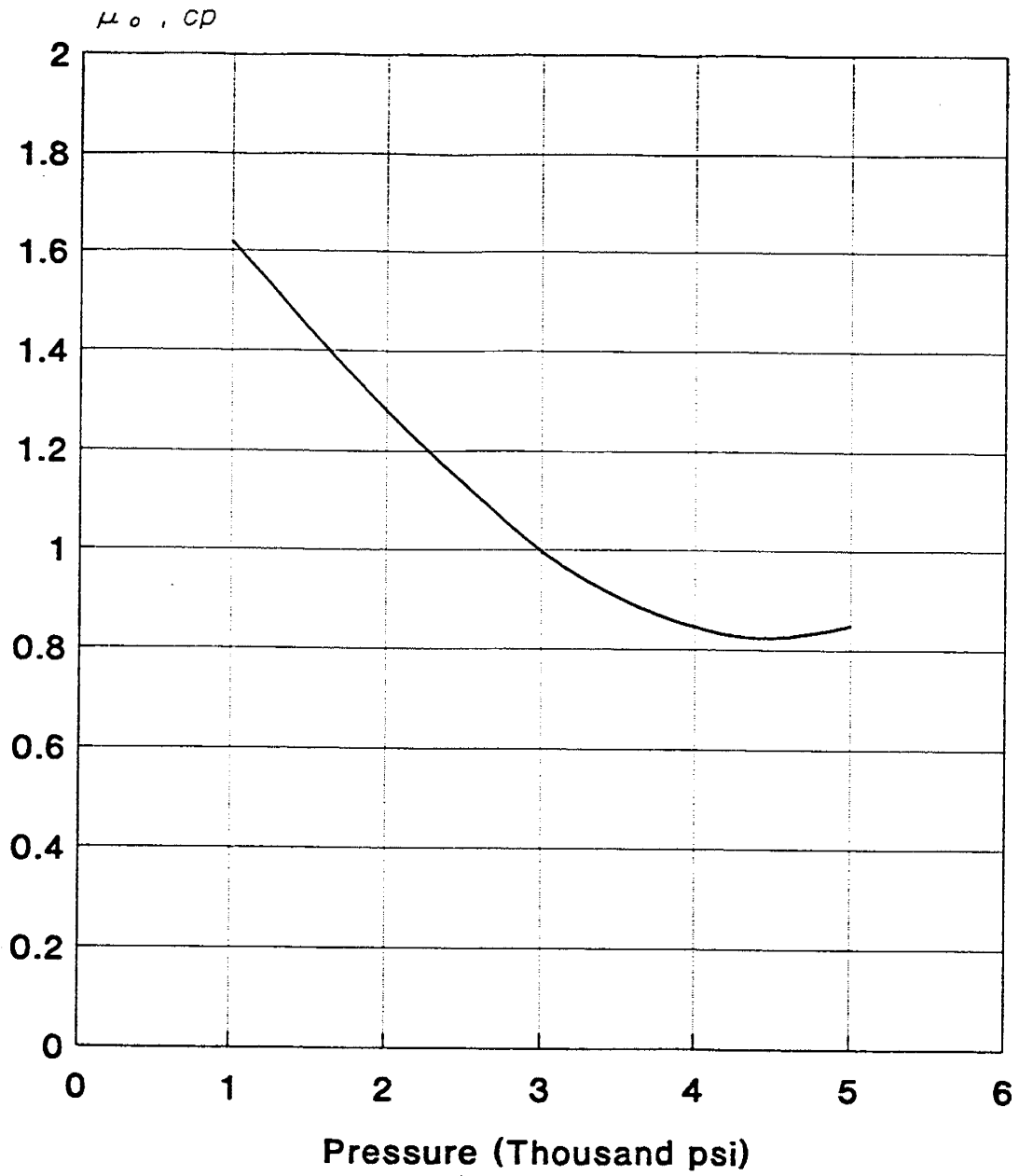


Figure XIII-21. Oil Viscosity for Sadlerochit: Depth Interval 4 (8800 to 8873 ft).

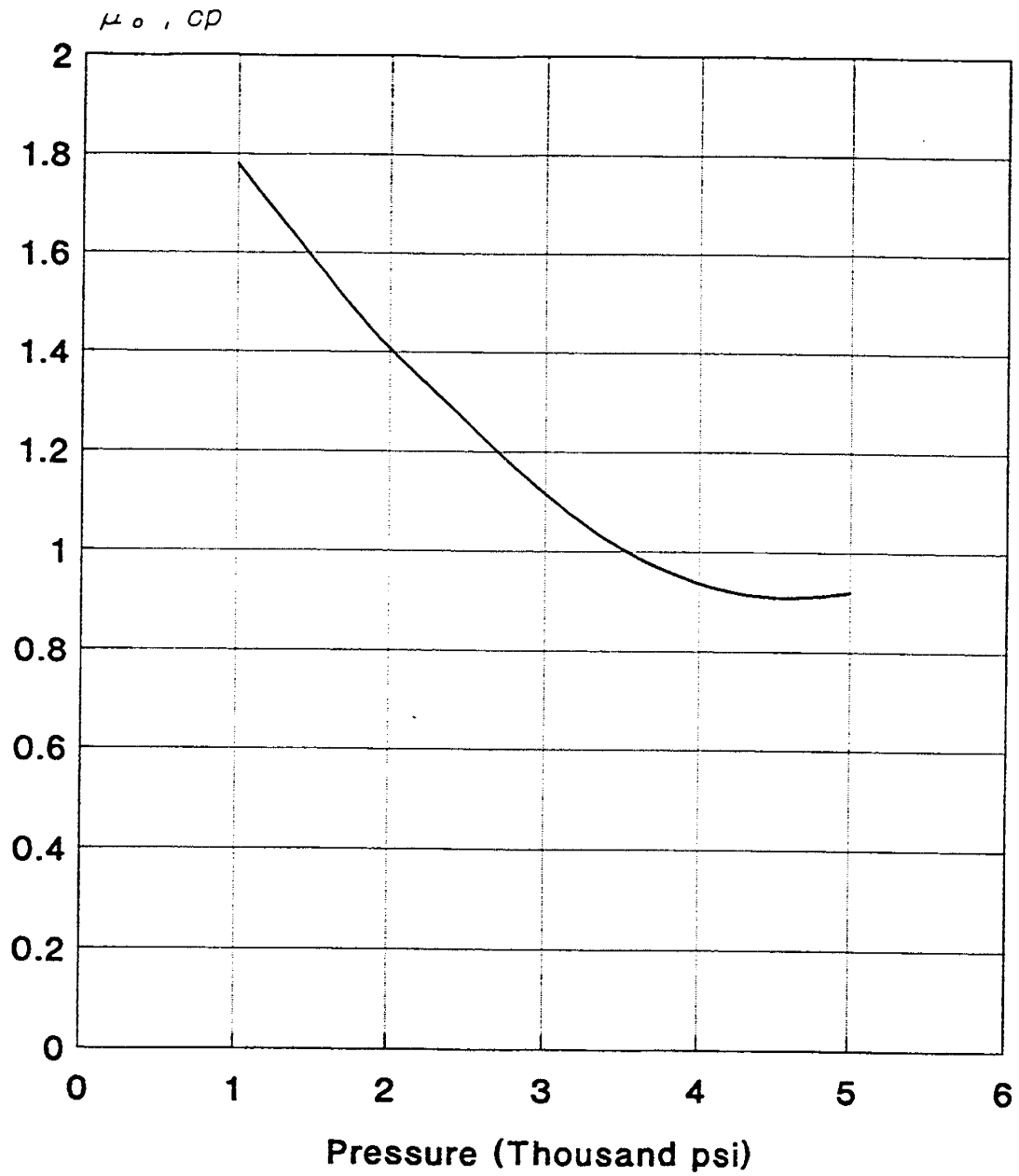


Figure XIII-22. Oil Viscosity for Sadlerochit: Depth Interval 5 (8873 to 8946 ft).

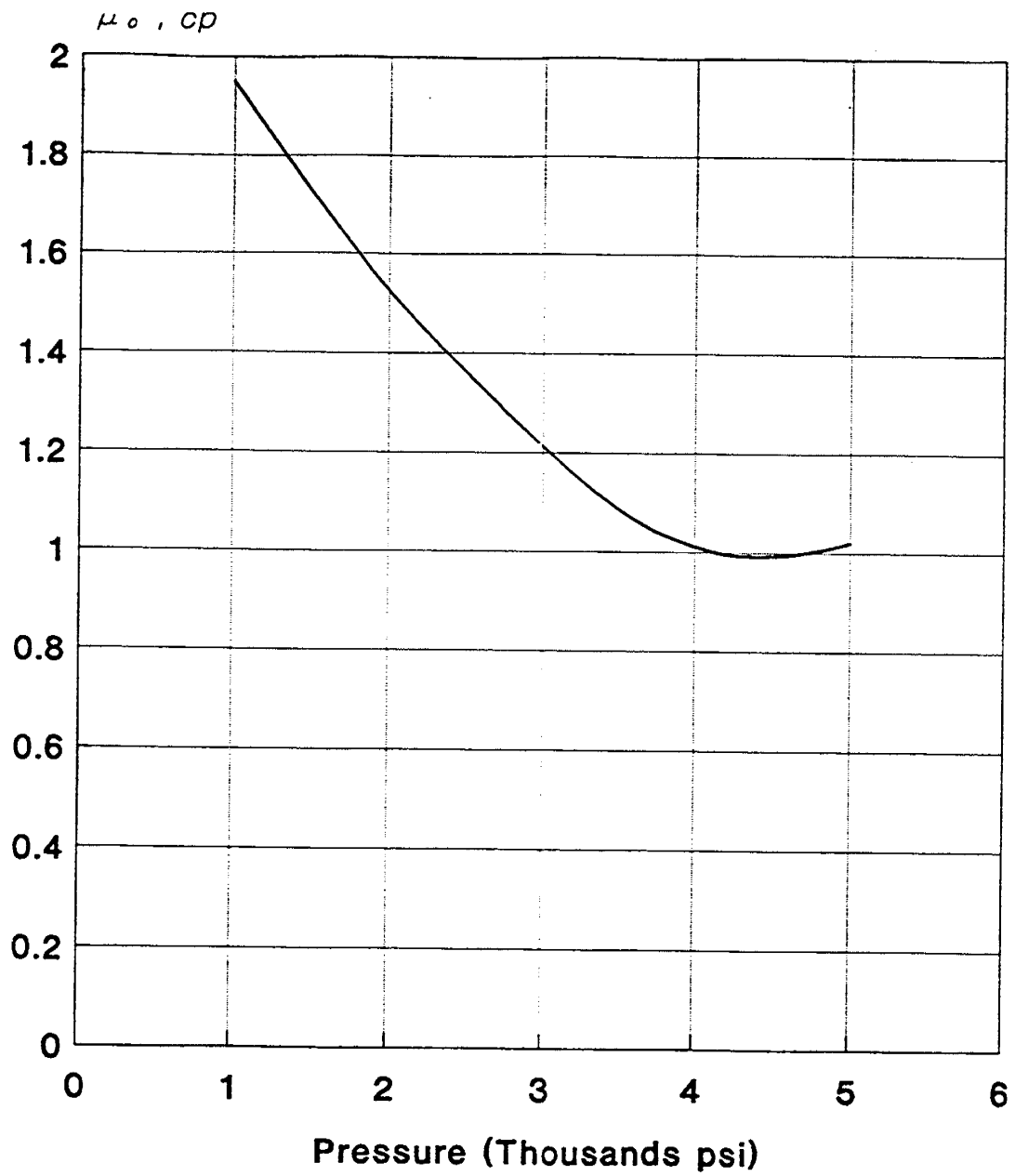


Figure XIII-23. Oil Viscosity for Sadlerochit: Depth Interval 6 (8946 to 9020 ft).

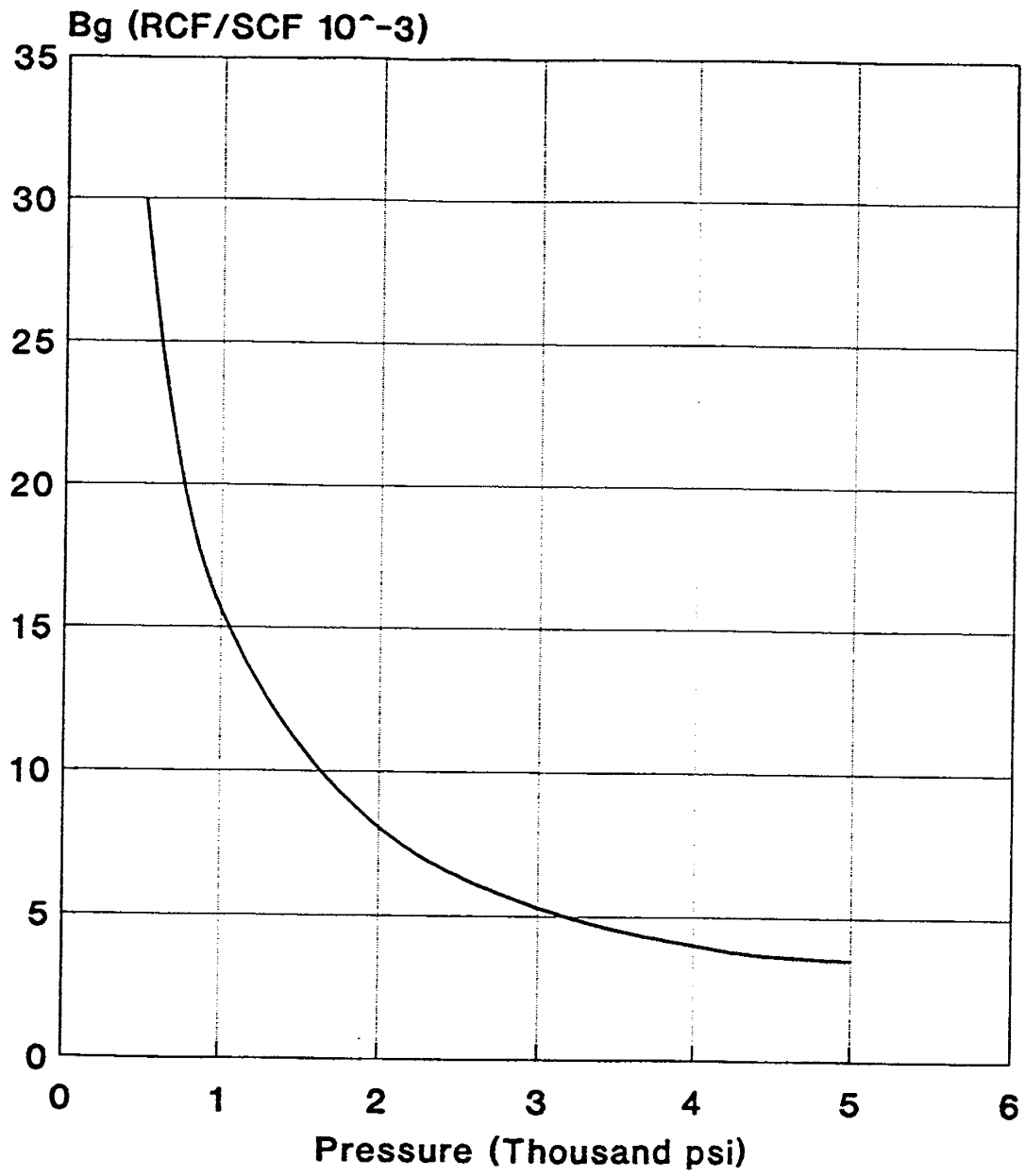


Figure XIII-24. Gas Formation Volume Factor for Sadlerochit.

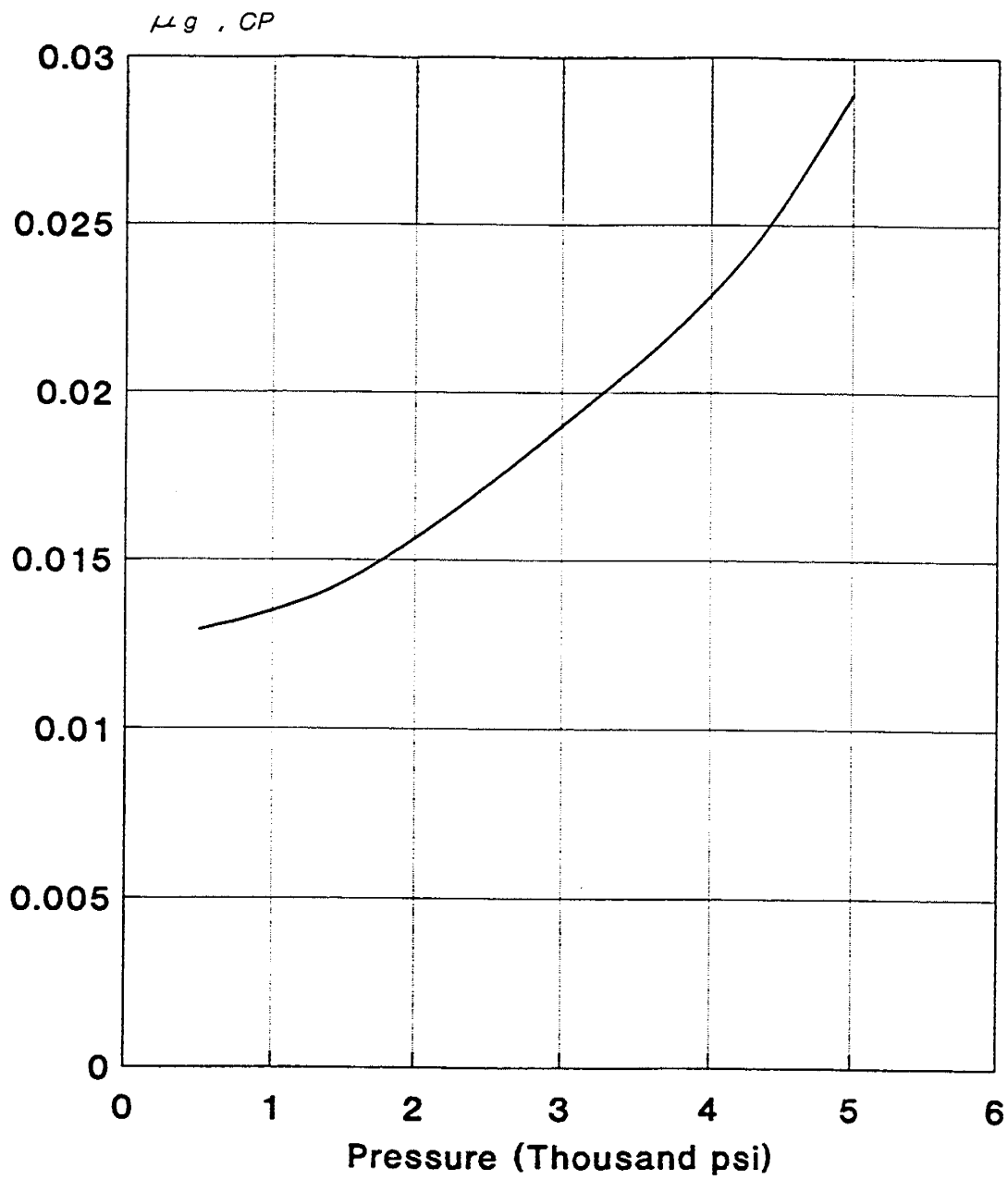


Figure XIII-25. Gas Viscosity for Sadlerochit.

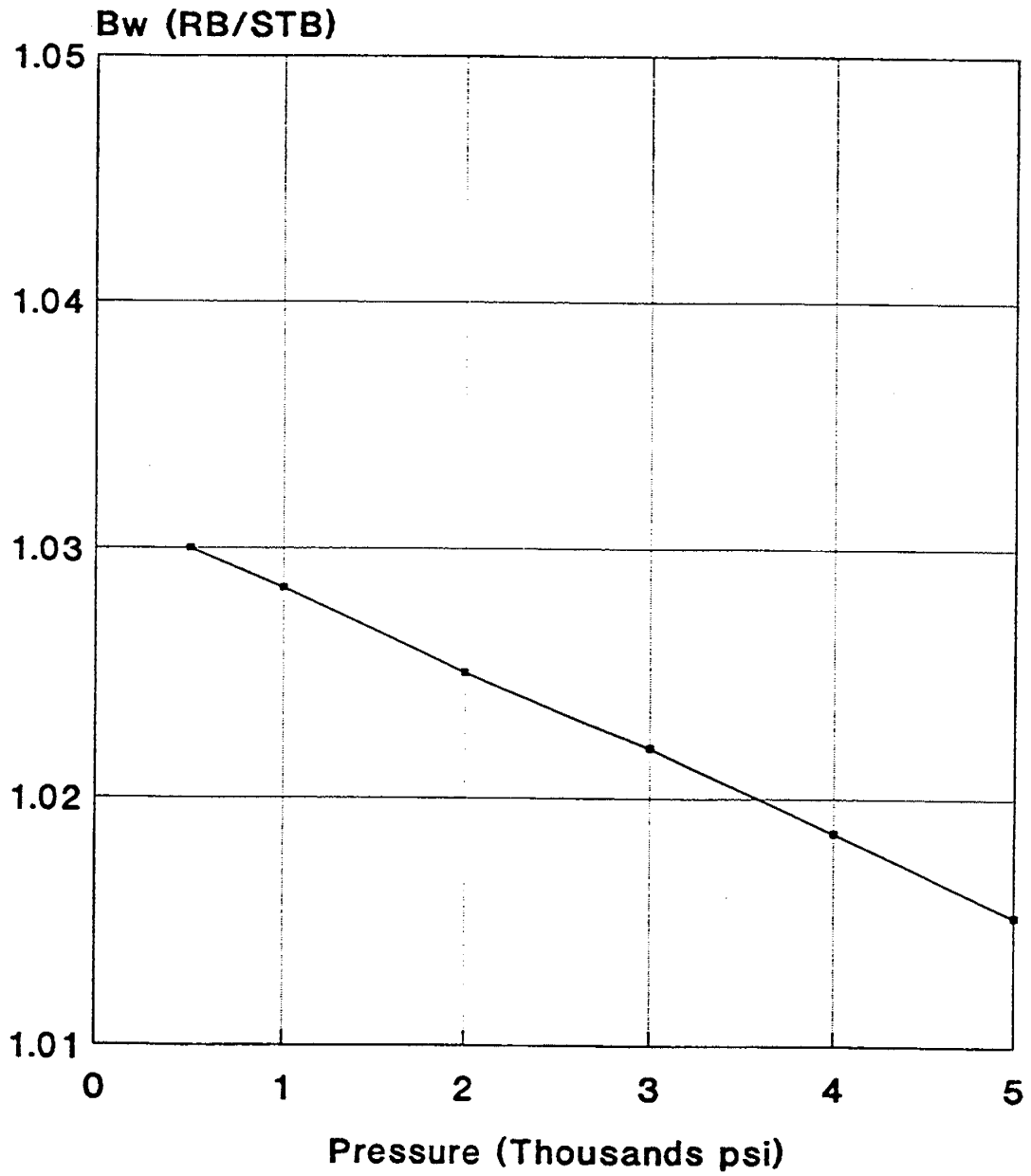


Figure XIII-26. Water Formation Volume Factor for Sadlerochit.

### C. KUPARUK RIVER FIELD

The properties of Kuparuk River oil are shown in Figures XIII-27 through XIII-30. Oil formation volume factor, and solution gas-oil ratio as functions of pressure are shown in Figures XIII-27 and XIII-28, respectively. The bubble point pressure of the oil is 2982 psi. The oil viscosity data (Figure XIII-29) are presented in a dimensionless form by plotting normalized oil viscosity versus normalized pressure. The viscosity and pressure are normalized as follows:

$$\mu_{on} = \frac{\mu_o}{\mu_{ob}}$$
$$P_n = \frac{P}{P_b}$$

Figure XIII-30 is a plot of oil viscosity at bubble point pressure of Kuparuk River oil as a function of subsea depth. Regression analysis was used to curve fit the observed data and the following equation was found to provide a very good fit (correlation coefficient = 0.84):

$$\mu_o = 1.7 \times 10^{-7} D^2 + 2.5 \times 10^{-4} D - 5.5$$

The fitted curve also is plotted in Figure XIII-30.

### D. ENDICOTT FIELD

The formation volume factor and solution gas-oil ratio of Endicott crude are shown in Figures XIII-31 and XIII-32, respectively. The bubble point pressure of the oil is 4619 psi. Figures XIII-33 and XIII-34 show oil and gas viscosities, respectively, as functions of pressure. Gas specific gravity (with air = 1) versus pressure is shown in Figure XIII-35.

### E. WEST SAK FIELD

Figures XIII-36 and XIII-37 show oil formation volume factor and solution gas-oil ratio of West Sak crude up to the bubble point pressure of 1690 psi. These properties could not be measured beyond the bubble point pressure due to experimental difficulties caused by the heavy nature of the crude oil. Oil density and viscosity as functions of pressure are shown in Figures XIII-38 and XIII-39, respectively. Figure XIII-40 shows gas formation volume factor as a function of pressure.

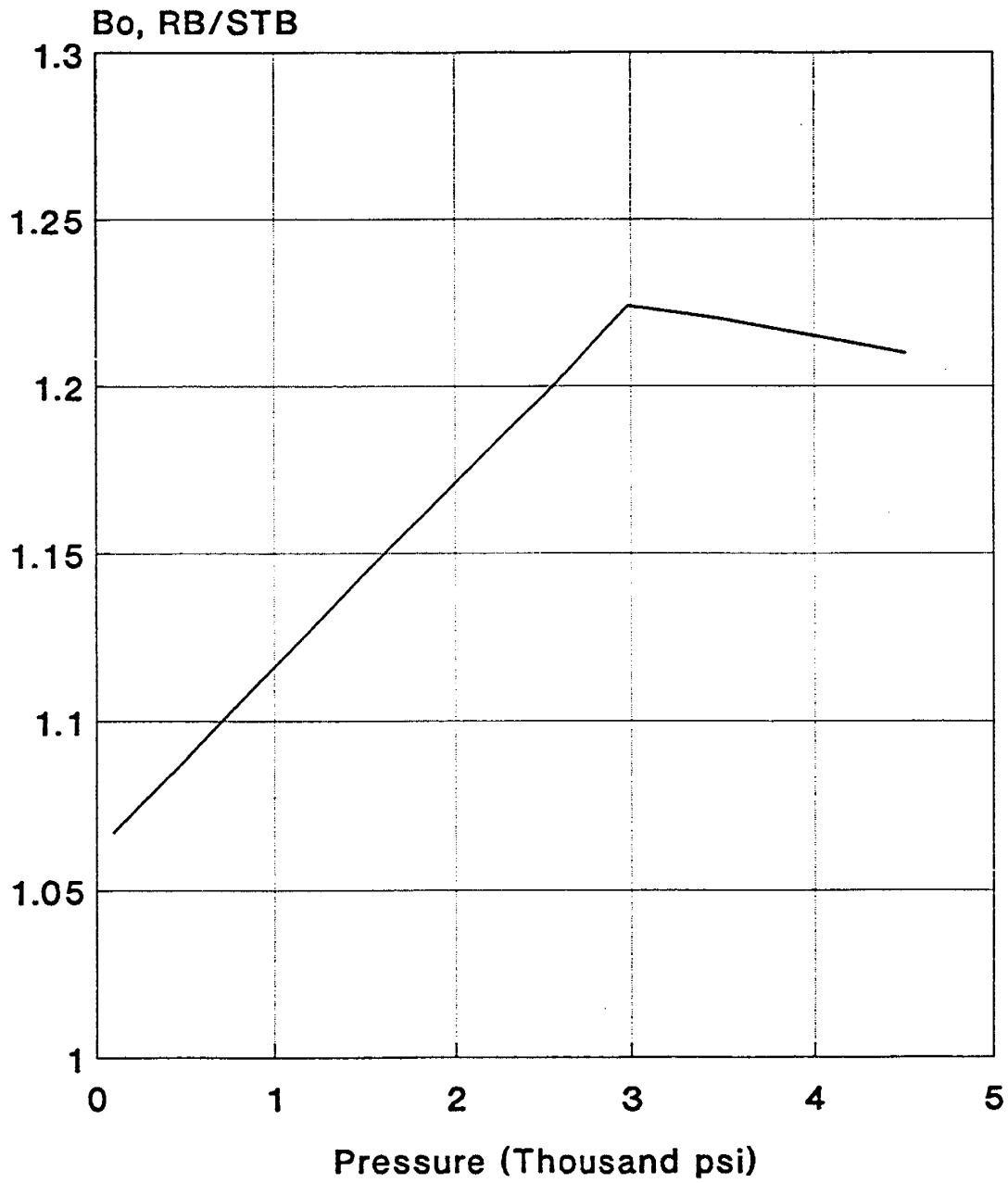


Figure XIII-27. Oil Formation Volume Factor for Kuparuk River Formation.

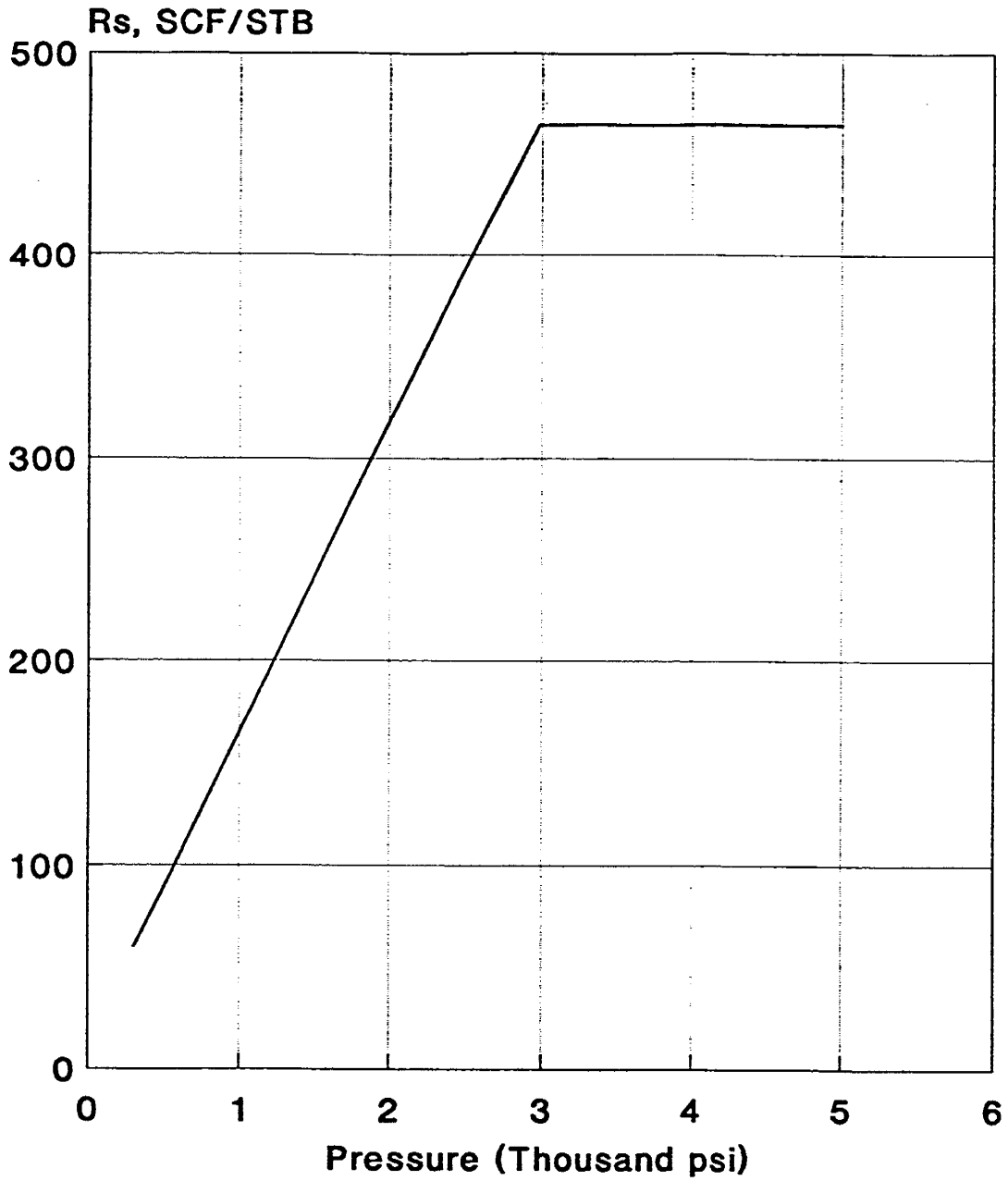


Figure XIII-28. Solution Gas-Oil Ratio for Kuperuk River Formation.

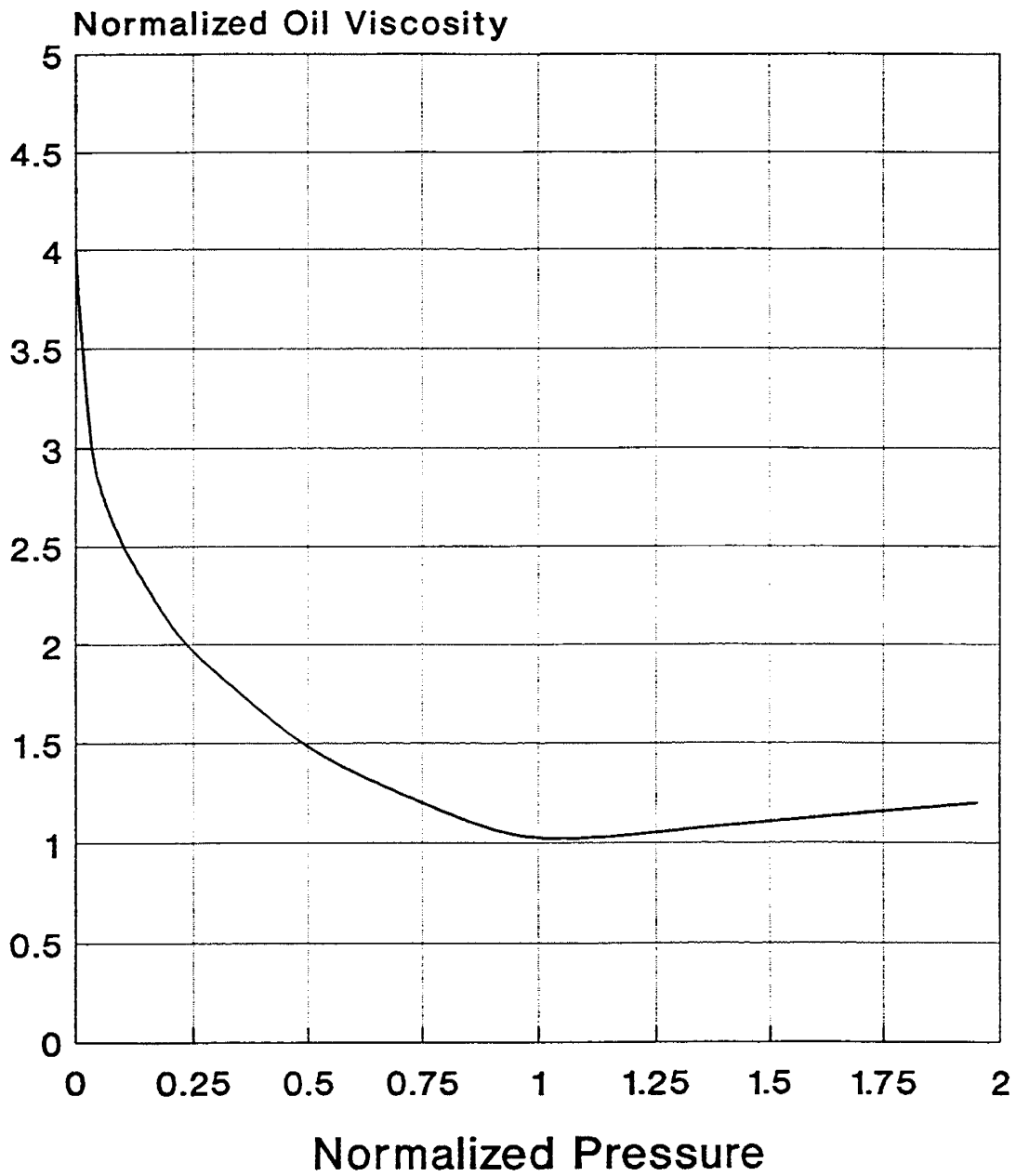
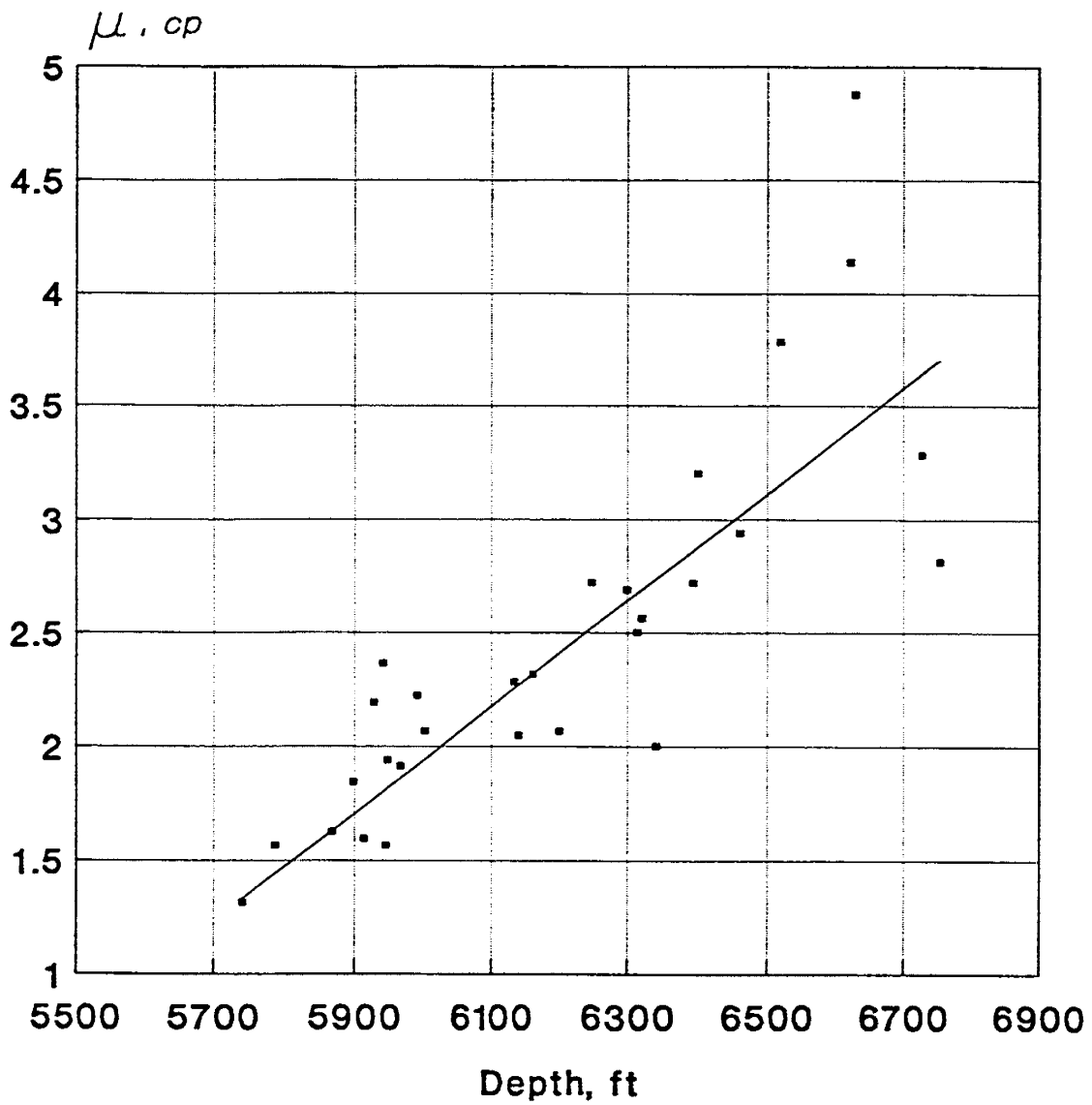


Figure XIII-29. Normalized Oil Viscosity Versus Normalized Pressure for Kuparuk River Formation.



▪ Real Values      — Correlated Values

Figure XIII-30. Variation of Bubble Point Oil Viscosity with Depth for Kuparuk River Formation.

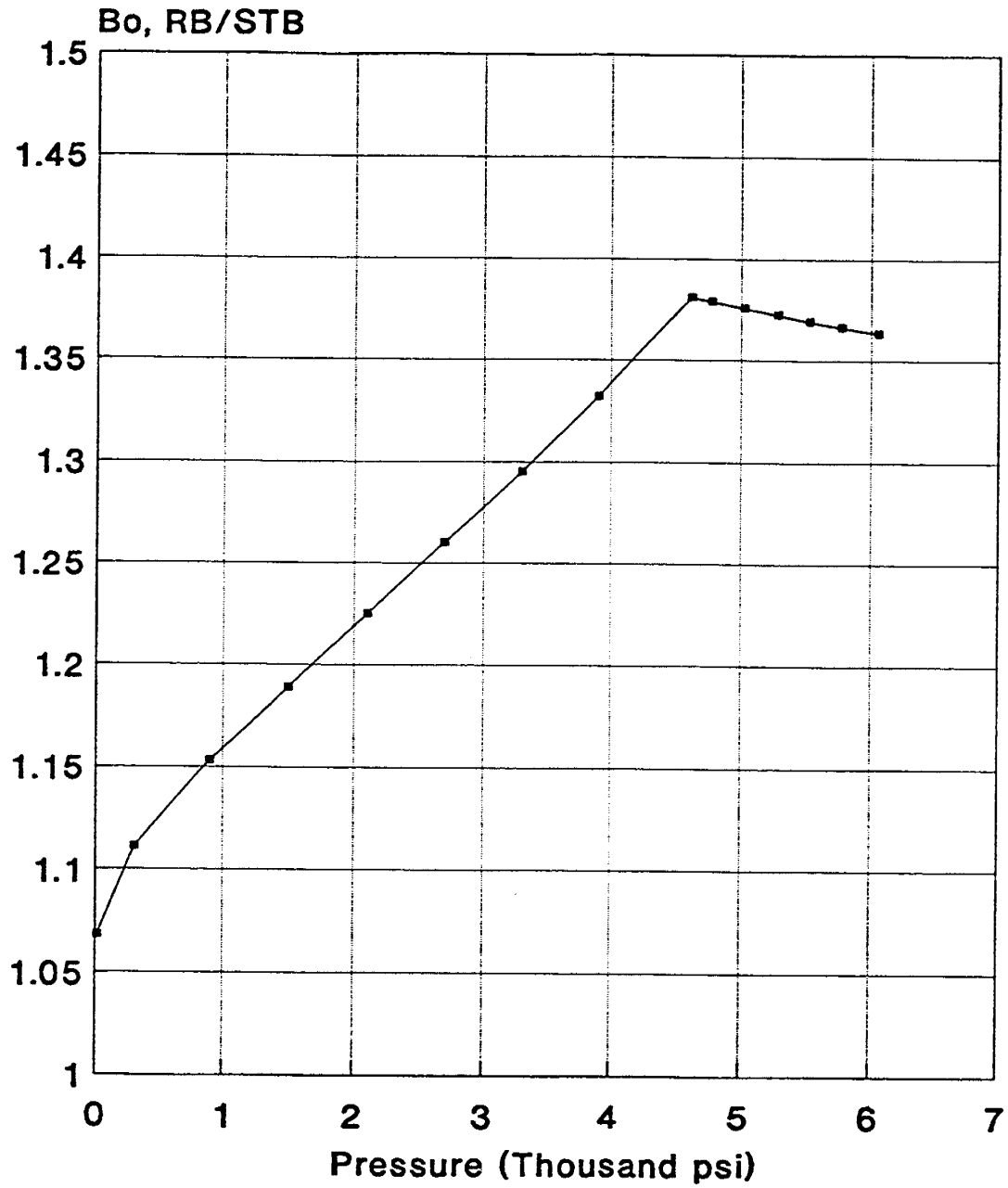


Figure XIII-31. Oil Formation Volume Factor for Endicott Field.

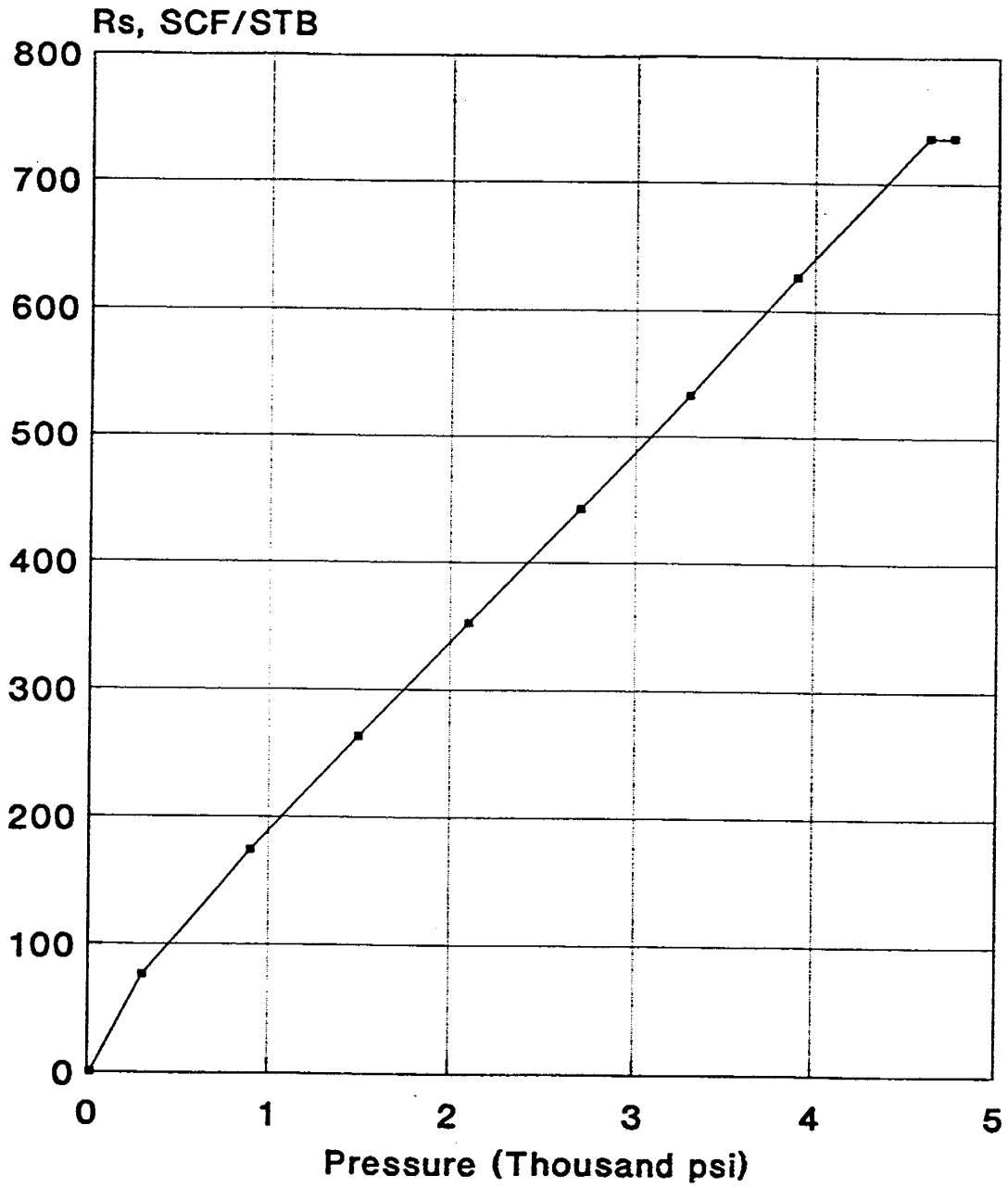


Figure XIII-32. Solution Gas-Oil Ratio for Endicott Field.

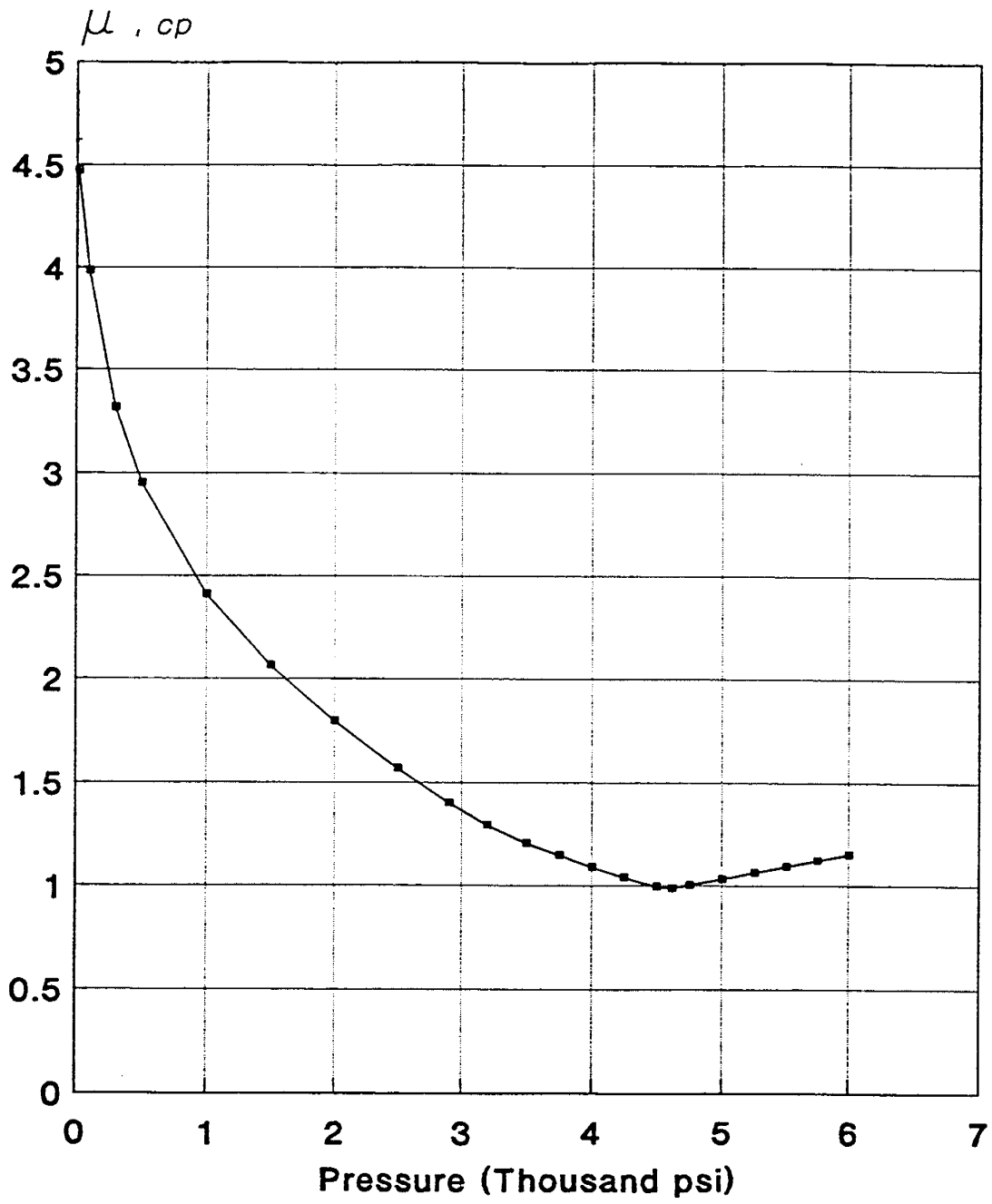


Figure XIII-33. Oil Viscosity for Endicott Field.

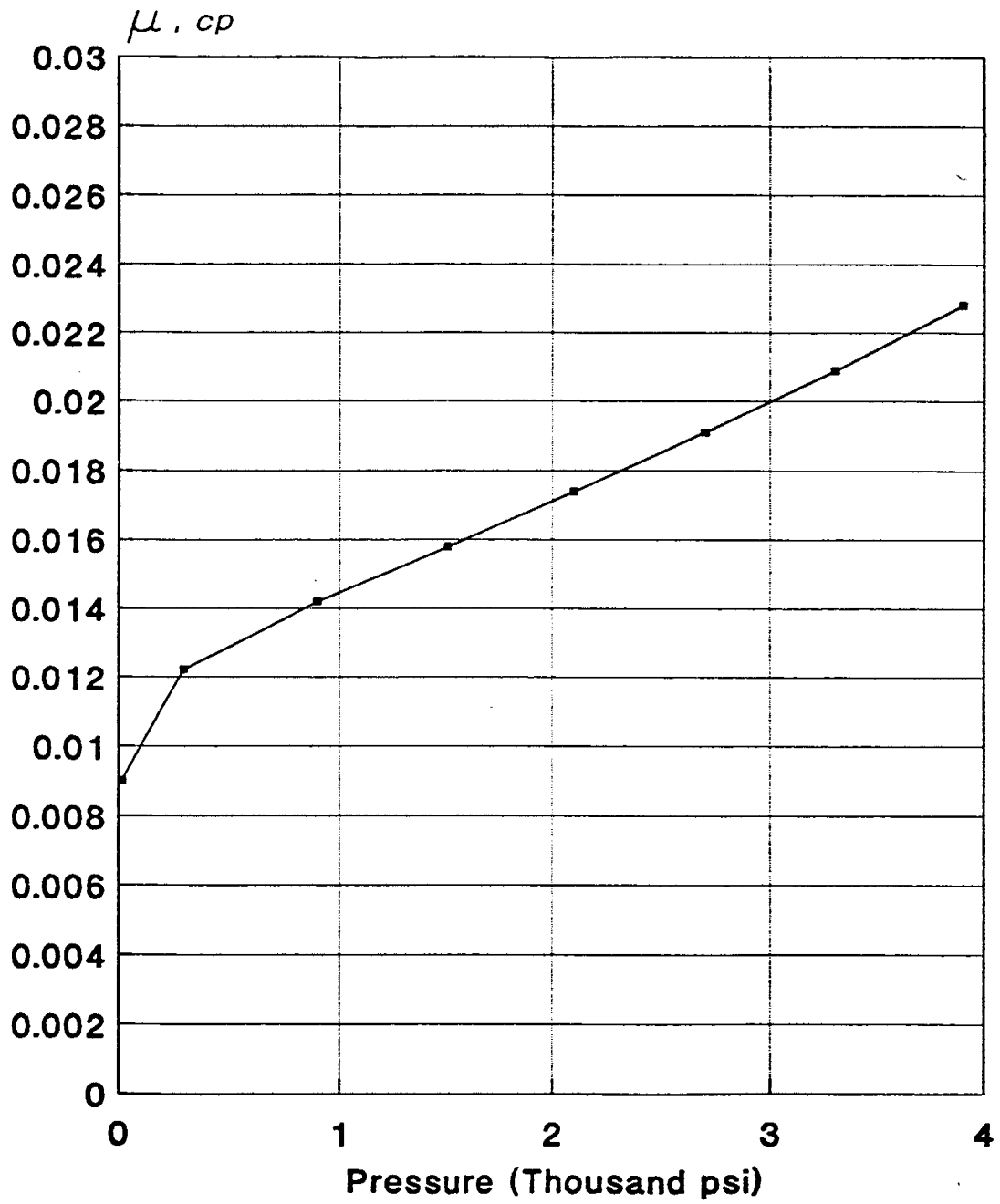


Figure XIII-34. Gas Viscosity for Endicott Field.

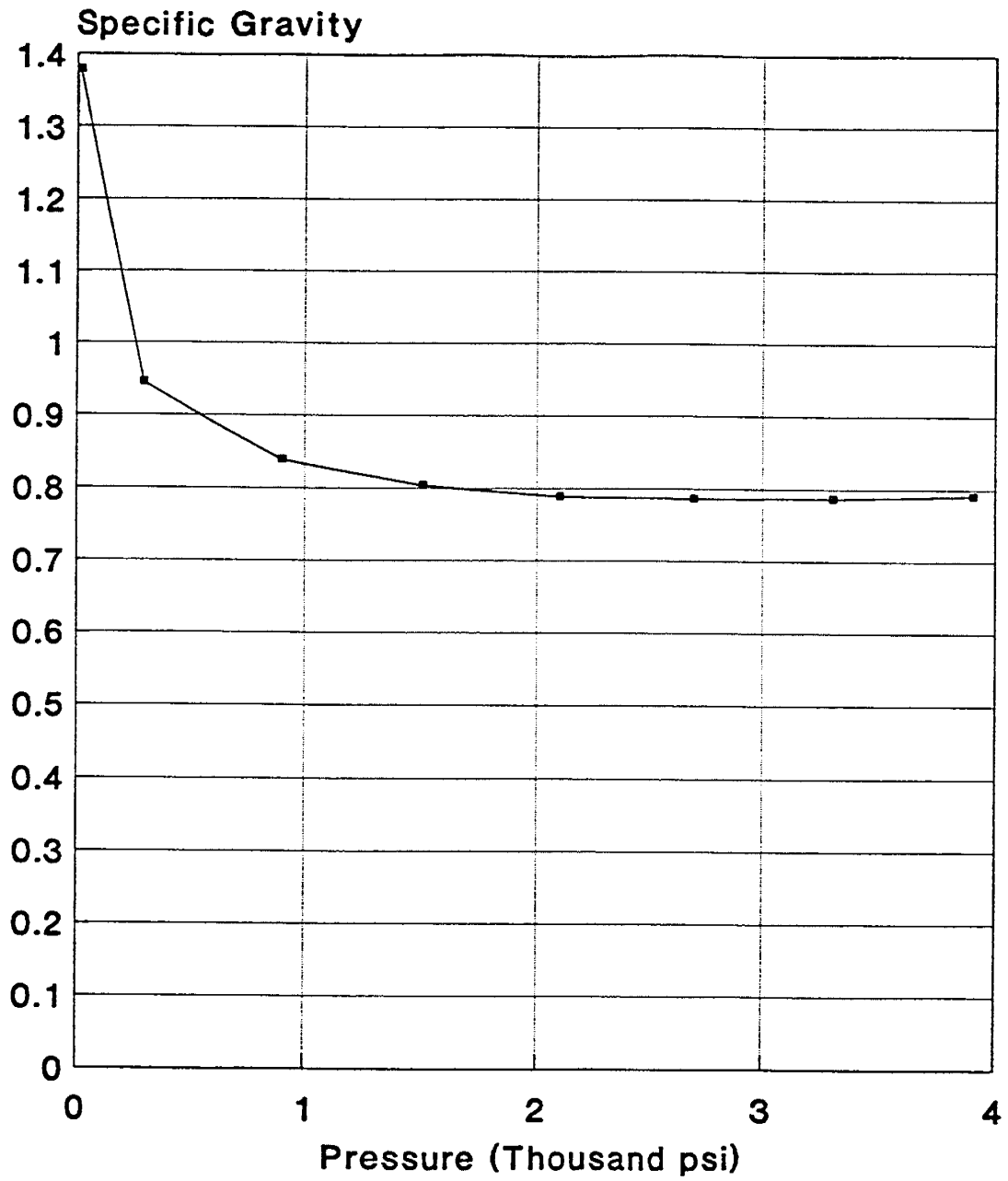


Figure XIII-35. Gas Specific Gravity for Endicott Field.

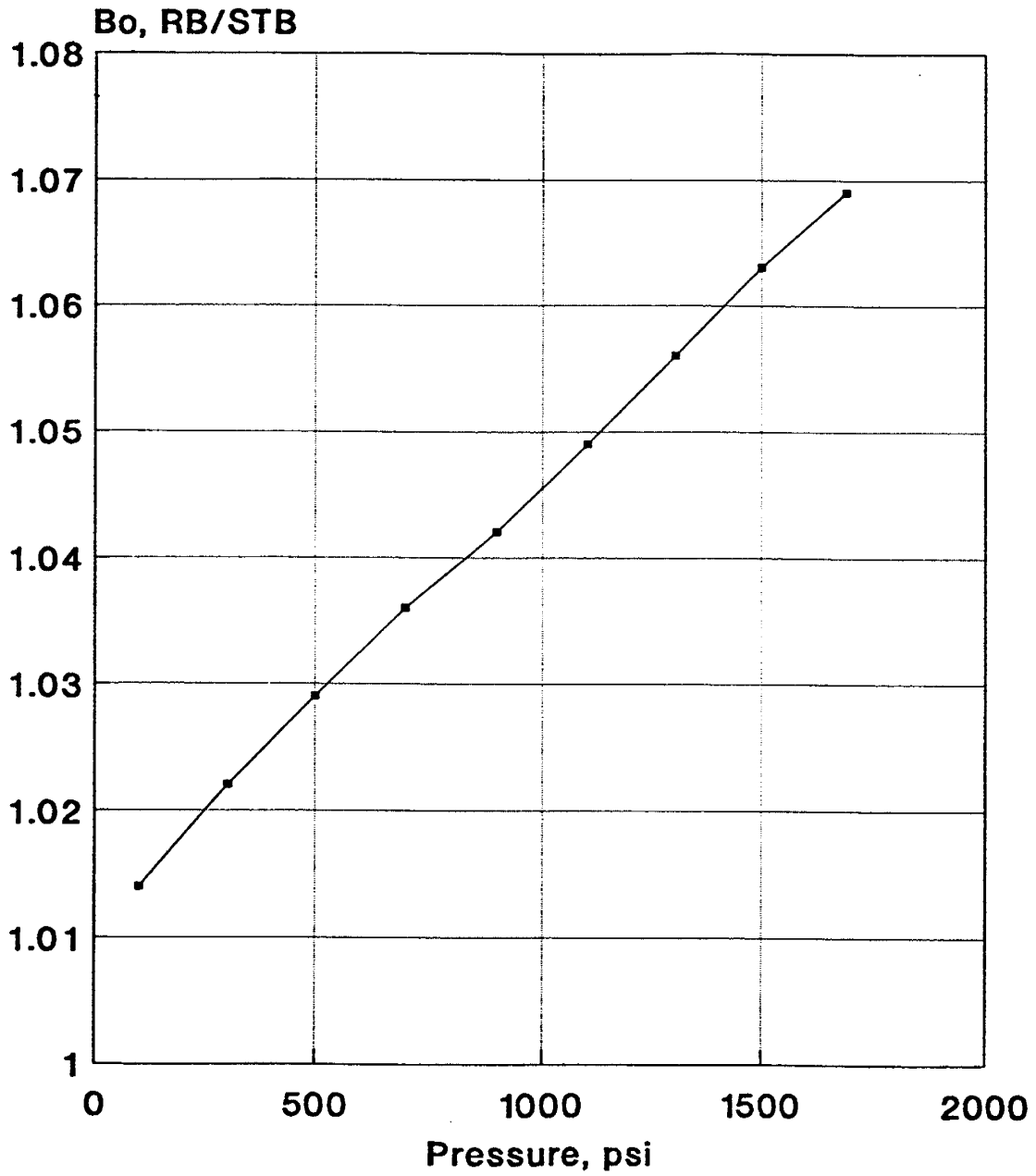


Figure XIII-36. Oil Formation Volume Factor for West Sak Field.

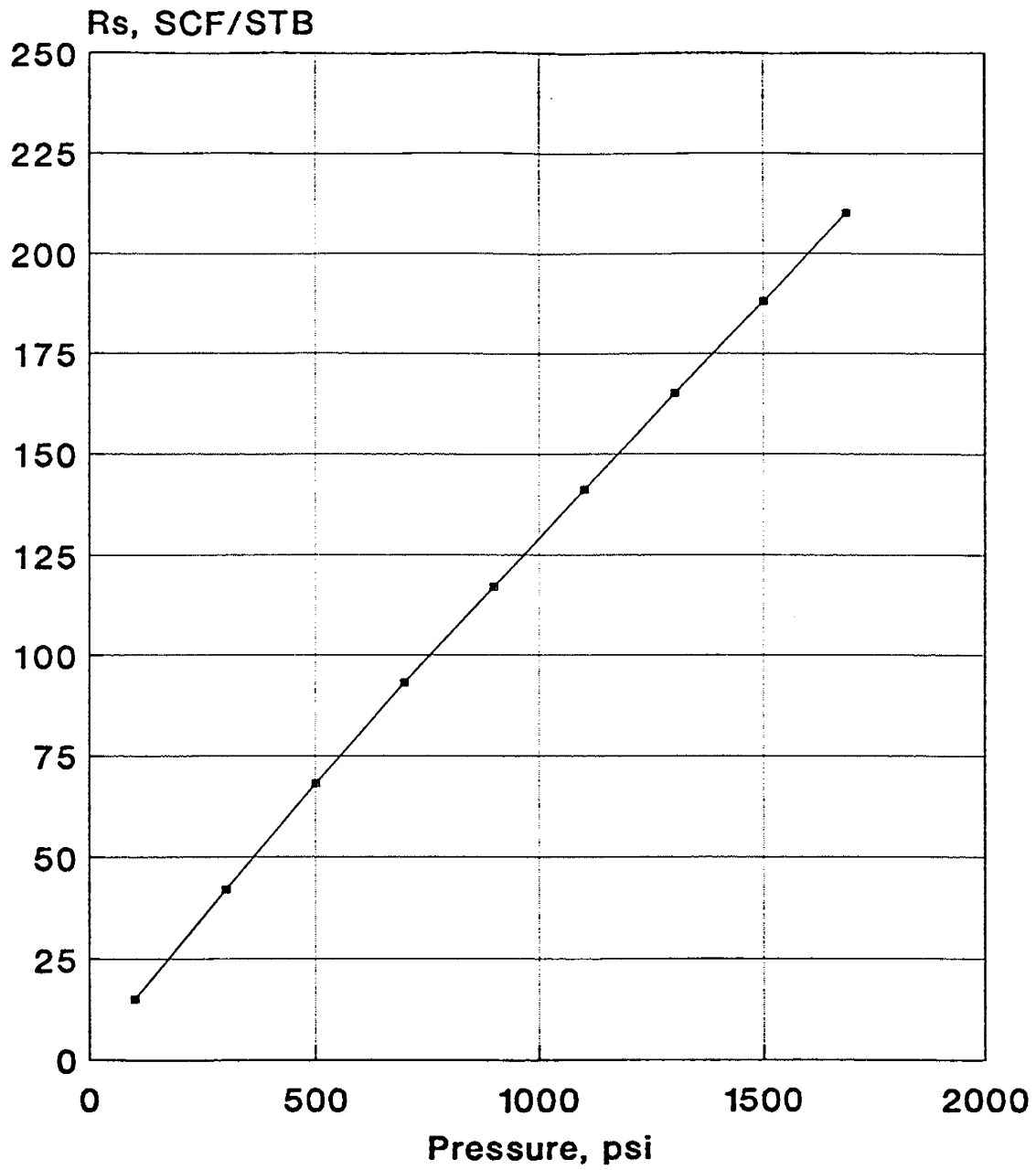


Figure XIII-37. Solution Gas-Oil Ratio for West Sak Field.

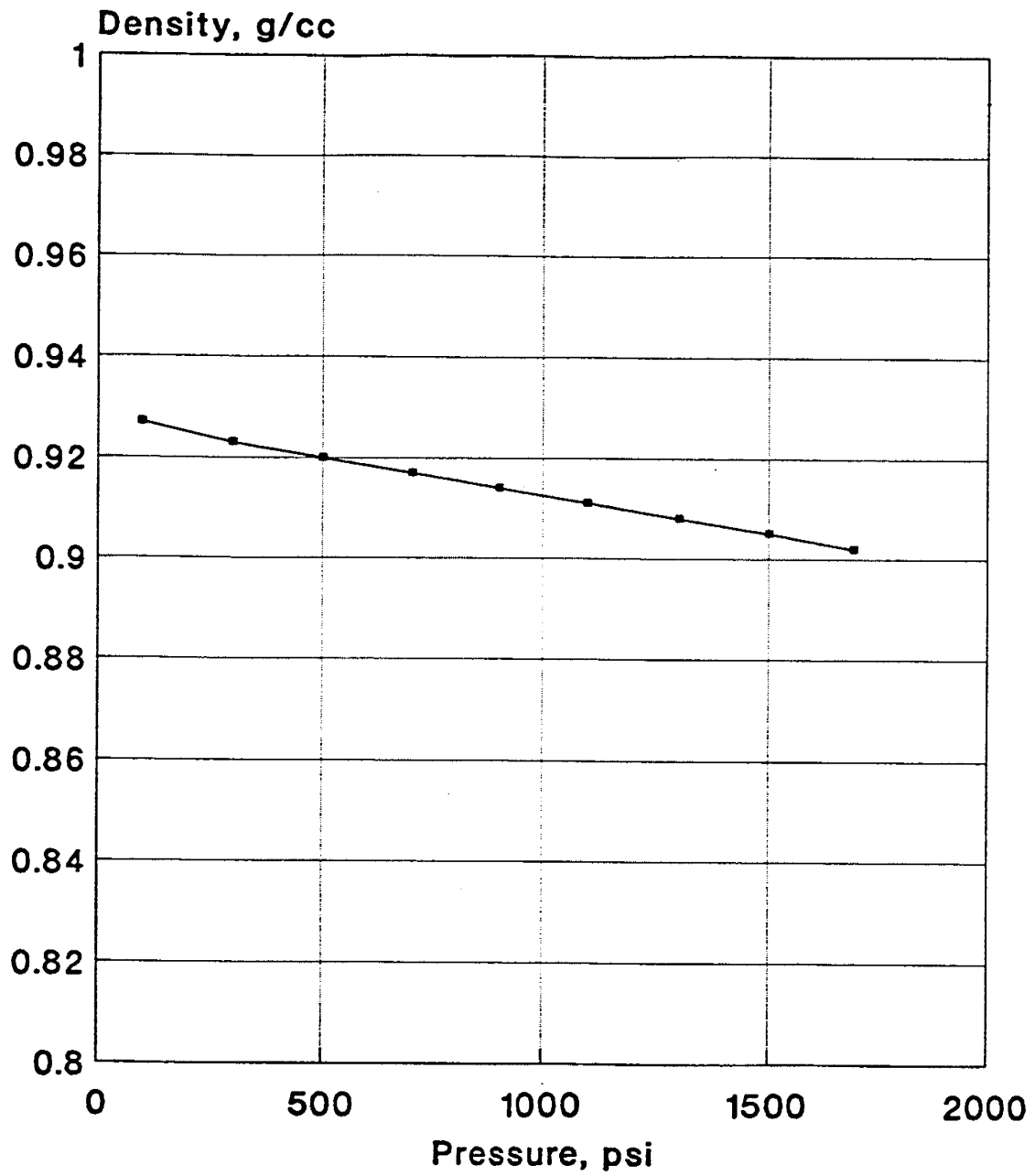


Figure XIII-38. Oil Density for West Sak Field.

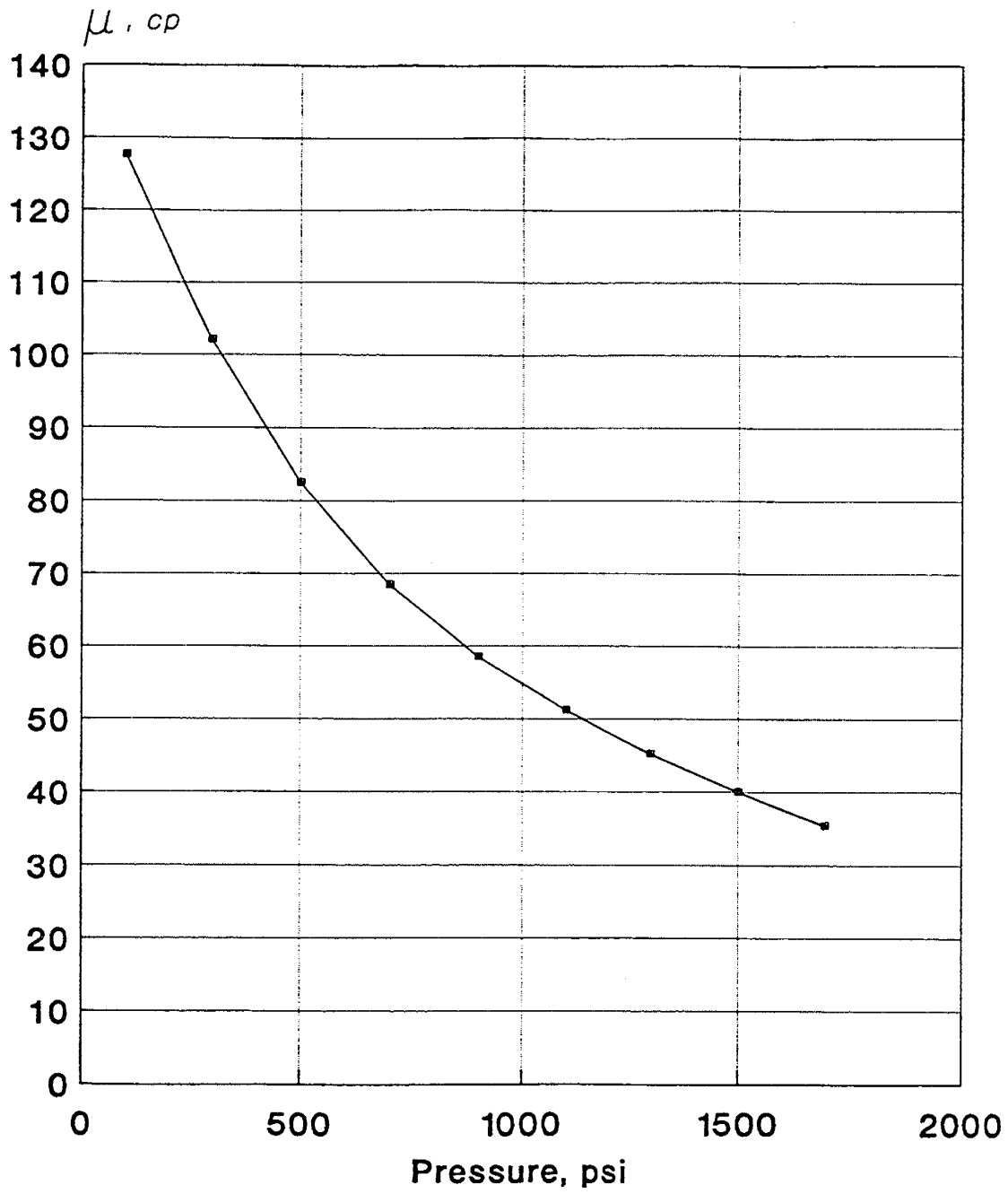


Figure XIII-39. Oil Viscosity for West Sak Field.

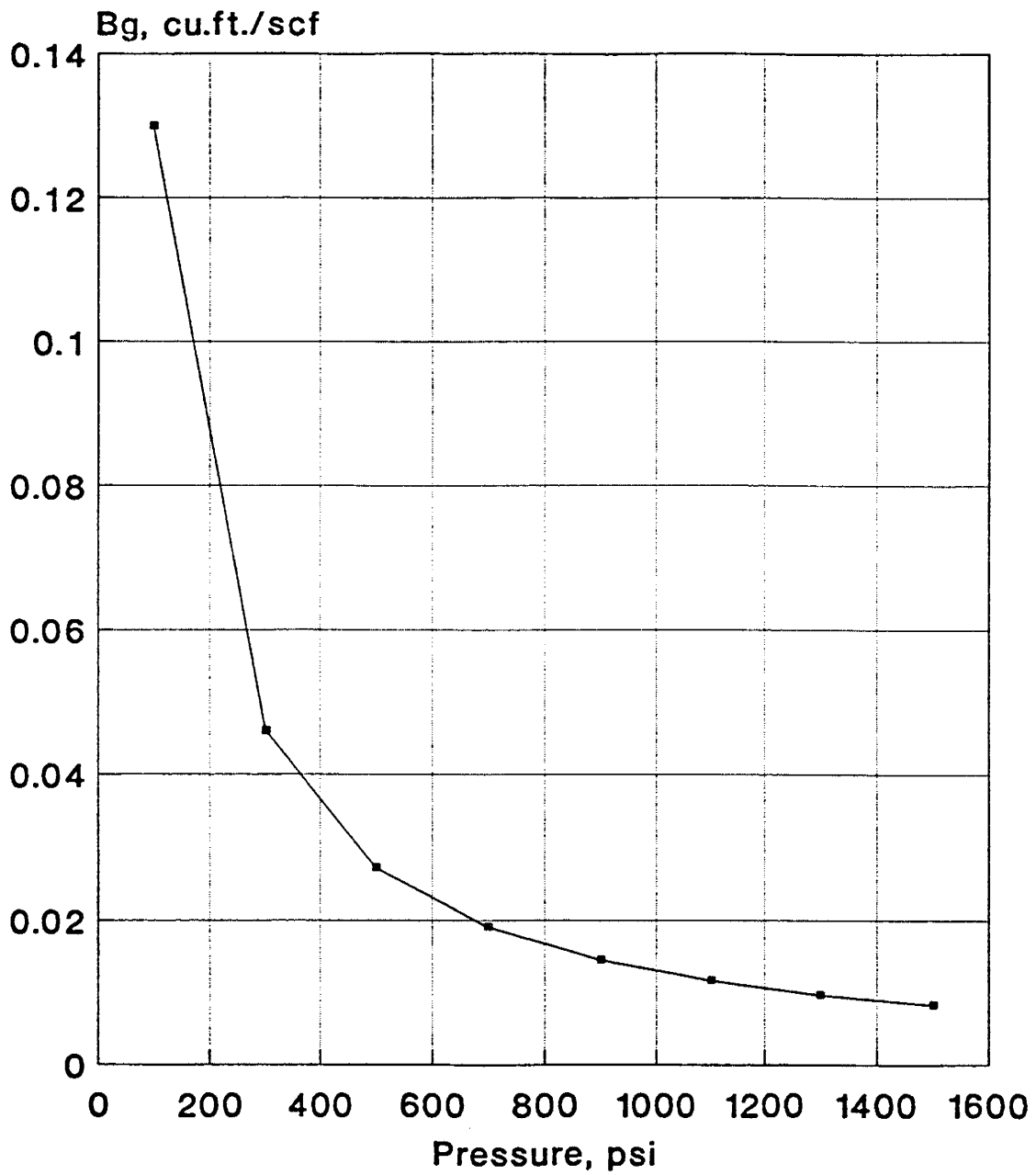


Figure XIII-40. Gas Formation Volume Factor for West Sak Field.

## F. NOMENCLATURE

$D$	=	subsea depth, ft
$P$	=	pressure, psi
$P_b$	=	bubble point pressure, psi
$P_n$	=	normalized pressure, dimensionless
$\mu_o$	=	oil viscosity, cp
$\mu_{ob}$	=	oil viscosity at bubble point pressure, cp
$\mu_{on}$	=	normalized oil viscosity, dimensionless



# CHAPTER XIV: RESERVOIR HETEROGENEITY CLASSIFICATION SYSTEM FOR TORIS AND TORIS DATABASE

---

---

## A. OBJECTIVE AND INTRODUCTION

The objective of this work was to collect and compile a database of geological, reservoir, production and injection data for the oil and gas reservoirs in the State of Alaska.

Alaskan oil reservoirs contribute approximately 25% of the domestic oil production. Therefore, addition of data pertaining to these reservoirs to the existing DOE TORIS database was of great interest. To accomplish this task, a cooperative study between the Petroleum Development Laboratory of the University of Alaska Fairbanks and the Department of Energy was initiated in 1989.

An extensive literature survey was first initiated to locate and collect relevant geological, reservoir, production and injection data available in the literature. Data for the reservoir heterogeneity classification system for TORIS included information regarding depositional system, diagenetic overprint, structural compartmentalization, reservoir heterogeneity ternary diagram, trap type, etc. It was found that the available data were sparced and scattered, and were sometimes conflicting. A preliminary data compilation was performed based on the data available in literature and missing information were requested from field operators.

The existing database was revised based on the responses received from field operators; production and injection data were provided by the Alaska Oil and Gas Conservation Commission. Difficulties in the data compilation were encountered due to (i) the variation of reservoir parameters within the formation and (ii) the lack of information.

In the following two sections the collected data for the Alaskan fields on the North Slope and Cook Inlet basin are presented.

## B. NORTH SLOPE ALASKA, OIL RESERVOIRS

Tables XIV-1 through XIV-4 provide the geological and reservoir data for the Prudhoe Bay Sadlerochit reservoir and Figures XIV-1 and XIV-2 show the monthly oil and gas production, and water and gas injection rates, respectively.

Tables XIV-5 and XIV-6 and Figures XIV-3 and XIV-4 display the geological, reservoir, oil and gas production, and water and gas injection rates for the Lisburne field.

Tables XIV-7 and XIV-8 and Figures XIV-5 through XIV-8 show the pertinent geological, reservoir, oil and gas production, and water and gas injection rates for the Endicott field.

Tables XIV-9 through XIV-12 and Figures XIV-9 through XIV-12 display the geological, reservoir, oil and gas production, and water and gas injection rates for the Kuparuk River field.

Tables XIV-13 through XIV-16 and Figures XIV-13 through XIV-16 refer to the geological, reservoir, oil and gas production, and water and gas injection data of the Milne Point field in the Kuparuk and Schrader Bluff reservoirs.

Finally, Tables XIV-17 through XIV-22 show the geological, and reservoir data for the West Sak, Upper and Lower Ugnu fields. Note that production or injection data for these fields do not exist because these fields are not under production.

### **C. COOK INLET BASIN ALASKA, RESERVOIRS**

Tables XIV-23 through XIV-38 and Figures XIV-17 through XIV-24 display the data for the reservoir heterogeneity classification system for TORIS database, and production and injection data of the Trading Bay field for the Middle Kenai B, C, D, E, Hemlock, Undefined, and West Foreland reservoirs.

Tables XIV-39 through XIV-42 and Figures XIV-25 through XIV-27 refer to the geological, reservoir, oil and gas production, and water and gas injection data of the North Trading Bay field for the G Zone/Hemlock and West Foreland reservoirs.

Tables XIV-49 and XIV-50 and Figures XIV-34 and XIV-35 display the data for the reservoir heterogeneity classification system for TORIS database, and production and injection data of the Granite Point field for the Middle Kenai reservoir.

Tables XIV-51 and XIV-52 and Figures XIV-36 and XIV-37 refer to the geological, reservoir, oil and gas production, and water and gas injection data of the Swanson River field for the Hemlock reservoir.

The geological, reservoir, oil and gas production, and water and gas injection data of the Middle Ground Shoal field for the A, B, C and D Pools, and Tyonek-Hemlock reservoirs are displayed on Tables XIV-53 through XIV-58 and Figures XIV-38 through XIV-44.

Tables XIV-59 and XIV-60 and Figure XIV-45 display the geological, reservoir, and production data for the Beaver Creek gas field.

Finally, Figure XIV-46 displays the oil and gas productions for the State of Alaska between 1959 and 1991.

All the data collected for the TORIS database are included on a floppy disk which accompanies this report.

The geological, reservoir, oil and gas production, and water and gas injection data of the McArthur River field for the Hemlock, Tyonek Middle Kenai G Zone and West Foreland reservoirs are displayed on Tables XIV-43 through XIV-48 and Figures XIV-28 through XIV-33.

Table XIV-1.

Reservoir Heterogeneity Classification System for TORIS			
<b>1. Reservoir Identification</b> Reservoir Play: _____			
Reservoir Name: <u>Sadlerochit</u>	Geologic Province: <u>Arctic Coastal Plain</u>	Date: <u>7/10/92</u>	
Field Name: <u>Prudhoe Bay</u>	Geologic Age: <u>Triassic/Lower</u>	Prepared By: <u>UAF/PDL</u>	
State: <u>AK</u>	Formation: <u>Ivishak</u>	Version: <u>1</u>	
<b>2. Depositional System</b> <input checked="" type="checkbox"/> 1 <input type="checkbox"/> 2 <input type="checkbox"/> 3    Degree of Confidence in Selection    (1=Highest, 3= Lowest)			
Carbonate Reservoirs		Clastic Reservoirs	
<input type="checkbox"/> Lacustrine <input type="checkbox"/> Peritidal ___ Supratidal ___ Intertidal ___ Subtidal <input type="checkbox"/> Shallow Shelf ___ Open Shelf ___ Restricted Shelf <input type="checkbox"/> Shelf Margin ___ Rimmed Shelf ___ Ramp	<input type="checkbox"/> Feeds ___ Pinnacle Reefs ___ Bioherms ___ Atolls <input type="checkbox"/> Slope/Basin ___ Carbonate Fans ___ Turbidite Fans ___ Voids <input type="checkbox"/> Basin ___ Drowned Shelf ___ Deep Basin	<input type="checkbox"/> Estuarine ___ Ergs ___ Coastal Dunes <input type="checkbox"/> Lacustrine ___ Basin Margin ___ Basin Center <input checked="" type="checkbox"/> Fluvial ___ Braided Streams ___ Meandering Streams <input type="checkbox"/> Alluvial Fan ___ Humid (Stream-Dominated) ___ Arid/Semi-Arid ___ Fan Deltas <input type="checkbox"/> Delta ___ Wave-Dominated ___ Fluvial-Dominated ___ Tide-Dominated	<input type="checkbox"/> Strandplain ___ Barrier Cores ___ Barrier Shorefaces ___ Back Barriers ___ Tidal Channels ___ Washover Fan/Tidal Deltas <input type="checkbox"/> Shelf (Accretionary Processes) ___ Sand Waves ___ Sand Ridges/Bars <input type="checkbox"/> Slope/Basin ___ Turbidite Fans ___ Carbonate Fans <input type="checkbox"/> Basin ___ Pelagic
<b>3. Diagenetic Overprint</b> <input checked="" type="checkbox"/> 1 <input type="checkbox"/> 2 <input type="checkbox"/> 3    Degree of Confidence in Selection    (1=Highest, 3= Lowest)			
Carbonate Reservoirs		Clastic Reservoirs	
<input type="checkbox"/> Compaction/Compaction <input type="checkbox"/> Grain Enhancement <input type="checkbox"/> Dolomitization <input type="checkbox"/> Diagenetic Cementation (Evaporites) <input type="checkbox"/> Massive Dissolution <input type="checkbox"/> Sulfidation		<input checked="" type="checkbox"/> Compaction/Compaction <input type="checkbox"/> Intergranular Dissolution <input type="checkbox"/> Authigenic Clay <input type="checkbox"/> Chertification	
<b>4. Structural Compartmentalization</b> <input checked="" type="checkbox"/> 1 <input type="checkbox"/> 2 <input type="checkbox"/> 3    Degree of Confidence in Selection    (1=Highest, 3= Lowest)			
<input type="checkbox"/> Natural Fracture Porosity <input type="checkbox"/> Unstructured		<input checked="" type="checkbox"/> Faulted ___ Normal Fault ___ Reverse Fault ___ Strike-Slip Fault	<input type="checkbox"/> Fault/Field <input type="checkbox"/> Folded ___ Normal Fault ___ Reverse Fault ___ Strike-Slip Fault
<b>5. Reservoir Heterogeneity Ternary Diagram</b>			
Predominant Element of Reservoir Heterogeneity: (Check Only One)		100% Depositional System	
<input type="checkbox"/> Depositional System <input type="checkbox"/> Diagenetic Overprint <input type="checkbox"/> Structural Compartmentalization			
<b>6. Trap Type</b> <input type="checkbox"/> Stratigraphic <input type="checkbox"/> Structural <input checked="" type="checkbox"/> Concretion			
<b>7. Optional Comments (References, Details on Above Selections, Etc.)</b>			
<u>"Joint Geologic/Engineering Analysis of the Sadlerochit Reservoir,</u> <u>Prudhoe Bay Field," JPT, July 1979, p. 933-940, D. H. Wadman et al</u>			

**Table XIV-2.**

**TORIS DATA BASE**  
**FIELD: PRUDHOE BAY (IVISHAK)**

Record 1:

Field Code .....	N/A
STATE Postal Code .....	AK
Lithology Code (-1, 0 = Unknown; 1 = SS, 2 = LS; 3 = Dolo.) .....	1
Geologic Age Code AAPG .....	237
Field Name .....	Prudhoe Bay
Reservoir Name .....	Sadlerochit
Reference Number .....	3189
Load Number .....	N/A
Formation Name .....	Ivishak

Record 2:

( 1) Field Acres (Acres) .....	135000
( 2) Proven Acres (Acres) .....	N/A
( 3) Well Spacing (Acres) .....	930
( 4) Total Wells (Number) .....	920
( 5) Net Pay (Feet) .....	0-444
( 6) Gross Pay (Feet) .....	350-630
( 7) Porosity (%) .....	22
( 8) Initial Oil Saturation (%) .....	65.00
( 9) Current Oil Saturation (%) .....	58.02
(10) Initial Water Saturation (%) .....	35
(11) Current Water Saturation (%) .....	41.98
(12) Initial Gas Saturation (%) .....	0.0
(13) Current Gas Saturation (%) .....	0.0
(14) Initial Oil FVF (Res bbl/STB) .....	1.4
(15) Current Oil FVF (Res bbl/STB) .....	1.35
(16) True Vertical Depth (Feet)----Mid-Perforation .....	8800
(17) Formation Temperature (°F) .....	200.00

Record 3:

(18) Current Formation Pressure (PSI) .....	3600
(19) Permeability (md) .....	265
(20) Geologic Age (AAPG) .....	237
(21) API Gravity (°API) .....	27-28
(22) Oil Viscosity (CP) :e Reservoir condition .....	0.81 (@ 4390 psi)
(23) Formation Salinity (ppm TDS) .....	23000.00
(24) OOIP (BBL) .....	22 x 10 <sup>9</sup>
(25) Primary Recovery Factor (Fraction of OOIP) .....	0.12 (1982)
(26) Cumulative Oil Production (BBL) .....	7.5 x 10 <sup>9</sup>

**Table XIV-2 (continued).**

(27)	Year For Cumulative Oil Production; EX/1986 .....	1991
(28)	Technical Availability Date (Year); Ex/1990 .....	N/A
(29)	Primary Recovery (BBL/AC.FT.) .....	0.12
(30)	Primary Recovery (BBL) .....	N/A
(31)	Year For Primary Recovery .....	N/A
(32)	Current Producing GOR (SCF/BBL) .....	1097 (1990)
(33)	Initial Producing GOR (SCF/BBL) .....	730

Record 4:

(34)	Reservoir Acreage (Acres) .....	135000
(35)	Initial Formation Pressure (PSI) .....	4390
(36)	Reservoir Dip (DEG) .....	1.0
(37)	Production Wells (Number) .....	778
(38)	Injection Wells (Number) .....	152
(39)	Swept Zone Oil Saturation (%) (Residual to Water) .....	28.48
(40)	Injection Water Salinity (ppm TDS) .....	20000.00
(41)	Clay Content (%) .....	0.11
(42)	Dykstra-Parsons Coefficient .....	N/A
(43)	Current Injection Rate (B/D/WELL) .....	17000.00
(44)	Fractured-Fault (Y,N) (N = 0, Y = 1) .....	1
(45)	Shale Break or Laminations (Y,N) (N = 0, Y = 1) .....	1
(46)	Major Gas Cap (Y,N) (N = 0, Y = 1) .....	1
(47)	Field Multiplier (Number) .....	1
(48)	RRC District .....	N/A
(49)	Production Rate (MBBL/D); For the Year shown in element 28 .....	1203
(50)	Recovery Efficiency-Waterflood (Factor) .....	N/A
(51)	Ultimate Recovery Factor (Fraction of OOIP) (Primary Plus Secondary) .....	0.43

Record 5:

(52)	Geologic Play Code (Table II) .....	-1
(53)	Depositional System Code (Table III) .....	131
(54)	Depositional System Degree of Confidence (1 = Highest, 2 = Moderate, 3 = Lowest) .....	1
(55)	Diagenetic Overprint Code (Table IV) .....	1
(56)	Diagenetic Overprint Degree of Confidence (1 = Highest, 2 = Moderate, 3 = Lowest) .....	1
(57)	Structural Compartmentalization (Table V) .....	30
(58)	Structural Compartmentalization Degree of Confidence (1 = Highest, 2 = Moderate, 3 = Lowest) .....	1
(59)	Predominant Element of Reservoir Heterogeneity (1 = Depositional System, 2 = Diagenetic Overprint, 3 = Structural Compartmentalization) .....	N/A
(60)	Trap Type (1 = Stratigraphic, 2 = Structural, 3 = Combination) .....	3
(61)	Geologic Province (Table VI) .....	058

Table XIV-3.

Reservoir Heterogeneity Classification System for TORIS		
<b>1. Reservoir Identification</b>		
Reservoir Play: _____		
Reservoir Name: <u>Sadlerochit</u>	Geologic Province: <u>Arctic Coastal Plain</u>	Date: <u>7/10/92</u>
Field Name: <u>Prudhoe Bay</u>	Geologic Age: <u>Permo Triassic/Upper</u>	Prepared By: <u>PDL/UAF</u>
State: <u>AK</u>	Formation: _____	Version: <u>1</u>
<b>2. Depositional System</b> <input checked="" type="checkbox"/> 1 <input type="checkbox"/> 2 <input type="checkbox"/> 3 Degree of Confidence in Selection (1=Highest, 3= Lowest)		
<p style="text-align: center;">Carbonate Reservoirs</p> <div style="display: flex; justify-content: space-between;"> <div style="width: 45%;"> <input type="checkbox"/> Lacustrine   <input type="checkbox"/> Peritidal  <div style="margin-left: 20px;"> <input type="checkbox"/> Supratidal  <input type="checkbox"/> Intertidal  <input type="checkbox"/> Subtidal                 </div> <input type="checkbox"/> Shallow Shelf  <div style="margin-left: 20px;"> <input type="checkbox"/> Open Shelf  <input type="checkbox"/> Restricted Shelf                 </div> <input type="checkbox"/> Shelf Margin  <div style="margin-left: 20px;"> <input type="checkbox"/> Rimmed Shelf  <input type="checkbox"/> Ramp                 </div> </div> <div style="width: 45%;"> <input type="checkbox"/> Reefs  <div style="margin-left: 20px;"> <input type="checkbox"/> Pinnacle Reefs  <input type="checkbox"/> Bioherms  <input type="checkbox"/> Atolls                 </div> <input type="checkbox"/> Slope/Basin  <div style="margin-left: 20px;"> <input type="checkbox"/> Debris Fans  <input type="checkbox"/> Turbidite Fans                 </div> <input type="checkbox"/> Basin  <div style="margin-left: 20px;"> <input type="checkbox"/> Mounds  <input type="checkbox"/> Crowned Shelf  <input type="checkbox"/> Deep Basin                 </div> </div> </div>	<p style="text-align: center;">Clastic Reservoirs</p> <div style="display: flex; justify-content: space-between;"> <div style="width: 45%;"> <input type="checkbox"/> Eolian  <div style="margin-left: 20px;"> <input type="checkbox"/> Ergs  <input type="checkbox"/> Coastal Dunes                 </div> <input type="checkbox"/> Lacustrine  <div style="margin-left: 20px;"> <input type="checkbox"/> Basin Margin  <input type="checkbox"/> Basin Center                 </div> <input type="checkbox"/> Fluvial  <div style="margin-left: 20px;"> <input type="checkbox"/> Braided Streams  <input type="checkbox"/> Meandering Streams                 </div> <input type="checkbox"/> Alluvial Fan  <div style="margin-left: 20px;"> <input type="checkbox"/> Humid (Stream-Dominated)  <input type="checkbox"/> Arid/Semi-Arid  <input type="checkbox"/> Fan Deltas                 </div> <input checked="" type="checkbox"/> Delta  <div style="margin-left: 20px;"> <input type="checkbox"/> Wave-Dominated  <input checked="" type="checkbox"/> Fluvial-Dominated  <input type="checkbox"/> Tide-Dominated                 </div> </div> <div style="width: 45%;"> <input type="checkbox"/> Strandplain  <div style="margin-left: 20px;"> <input type="checkbox"/> Barrier Cores  <input type="checkbox"/> Barrier Shorefaces  <input type="checkbox"/> Back Barriers  <input type="checkbox"/> Tidal Channels  <input type="checkbox"/> Washover Fan/Tidal Deltas                 </div> <input type="checkbox"/> Shelf (Accretionary Processes)  <div style="margin-left: 20px;"> <input type="checkbox"/> Sand Waves  <input type="checkbox"/> Sand Ridges/Bars                 </div> <input type="checkbox"/> Slope-Basin  <div style="margin-left: 20px;"> <input type="checkbox"/> Turbidite Fans  <input type="checkbox"/> Debris Fans                 </div> <input type="checkbox"/> Basin  <div style="margin-left: 20px;"> <input type="checkbox"/> Pelagic                 </div> </div> </div>	
<b>3. Diagenetic Overprint</b> <input type="checkbox"/> 1 <input type="checkbox"/> 2 <input type="checkbox"/> 3 Degree of Confidence in Selection (1=Highest, 3= Lowest)		
<p style="text-align: center;">Carbonate Reservoirs</p> <div style="display: flex; justify-content: space-between;"> <div style="width: 45%;"> <input type="checkbox"/> Compaction/Cementation  <input type="checkbox"/> Grain Enlargement  <input type="checkbox"/> Dolomitization                 </div> <div style="width: 45%;"> <input type="checkbox"/> Dolomitization (Evaporites)  <input type="checkbox"/> Massive Dissolution  <input type="checkbox"/> Silification                 </div> </div>	<p style="text-align: center;">Clastic Reservoirs</p> <div style="display: flex; justify-content: space-between;"> <div style="width: 45%;"> <input type="checkbox"/> Compaction/Cementation  <input type="checkbox"/> Intergranular Dissolution                 </div> <div style="width: 45%;"> <input type="checkbox"/> Authigenic Clay  <input type="checkbox"/> Chertification                 </div> </div>	
<b>4. Structural Compartmentalization</b> <input checked="" type="checkbox"/> 1 <input type="checkbox"/> 2 <input type="checkbox"/> 3 Degree of Confidence in Selection (1=Highest, 3= Lowest)		
<input type="checkbox"/> Natural Fracture Porosity  <input type="checkbox"/> Unstructured  <input checked="" type="checkbox"/> Faulted <div style="margin-left: 20px;"> <input checked="" type="checkbox"/> Normal Fault  <input type="checkbox"/> Reverse Fault  <input type="checkbox"/> Strike-Slip Fault                 </div>	<input type="checkbox"/> Fault/Fold  <input type="checkbox"/> Folded <div style="margin-left: 20px;"> <input type="checkbox"/> Normal Fault  <input type="checkbox"/> Reverse Fault  <input type="checkbox"/> Strike-Slip Fault                 </div>	
<b>5. Reservoir Heterogeneity Ternary Diagram</b>		
<p>Predominant Element of Reservoir Heterogeneity: (Check Only One)</p> <ul style="list-style-type: none"> <li>• Depositional System <input checked="" type="checkbox"/></li> <li>• Diagenetic Overprint <input type="checkbox"/></li> <li>• Structural Compartmentalization <input type="checkbox"/></li> </ul>		
<b>6. Trap Type</b> <input type="checkbox"/> Stratigraphic <input type="checkbox"/> Structural <input checked="" type="checkbox"/> Combination		
<b>7. Optional Comments (References, Details on Above Selections, Etc.)</b>		
<hr/> <hr/> <hr/> <hr/>		

**Table XIV-4.**

**TORIS DATA BASE**  
**FIELD: PRUDHOE BAY (SADLEROCHIT)**

**Record 1:**

Field Code .....	N/A
STATE Postal Code .....	AK
Lithology Code (-1, 0 = Unknown; 1 = SS, 2 = LS; 3 = Dolo.) .....	1
Geologic Age Code AAPG .....	231
Field Name .....	Prudhoe Bay
Reservoir Name .....	Sadlerochit
Reference Number .....	3189
Load Number .....	N/A
Formation Name .....	N/A

**Record 2:**

( 1) Field Acres (Acres) .....	250000
( 2) Proven Acres (Acres) .....	N/A
( 3) Well Spacing (Acres) .....	160
( 4) Total Wells (Number) .....	930
( 5) Net Pay (Feet) .....	0-444
( 6) Gross Pay (Feet) .....	350-630
( 7) Porosity (%) .....	22
( 8) Initial Oil Saturation (%) .....	65
( 9) Current Oil Saturation (%) .....	56.02
(10) Initial Water Saturation (%) .....	20.77
(11) Current Water Saturation (%) .....	43.92
(12) Initial Gas Saturation (%) .....	14.23
(13) Current Gas Saturation (%) .....	0.06
(14) Initial Oil FVF (Res bbl/STB) .....	1.40
(15) Current Oil FVF (Res bbl/STB) .....	1.35
(16) True Vertical Depth (Feet)---Mid-Perforation .....	8900.0
(17) Formation Temperature (°F) .....	200

**Record 3:**

(18) Current Formation Pressure (PSI) .....	3600.0
(19) Permeability (md) .....	265.0
(20) Geologic Age (AAPG) .....	231
(21) API Gravity (°API) .....	28.0
(22) Oil Viscosity (CP) :e Reservoir condition .....	0.81
(23) Formation Salinity (ppm TDS) .....	23000.0
(24) OOIP (BBL) .....	22.0 × 10 <sup>9</sup>
(25) Primary Recovery Factor (Fraction of OOIP) .....	0.12 (1982)
(26) Cumulative Oil Production (BBL) .....	70.26 × 10 <sup>8</sup>

**Table XIV-4 (continued).**

(27)	Year For Cumulative Oil Production; EX/1986 .....	1990
(28)	Technical Availability Date (Year); Ex/1990 .....	N/A
(29)	Primary Recovery (BBL/AC.FT.) .....	N/A
(30)	Primary Recovery (BBL) .....	2620.0 x 10 <sup>6</sup>
(31)	Year For Primary Recovery .....	1982
(32)	Current Producing GOR (SCF/BBL) .....	1097.0
(33)	Initial Producing GOR (SCF/BBL) .....	730.0

Record 4:

(34)	Reservoir Acreage (Acres) .....	135000.0
(35)	Initial Formation Pressure (PSI) .....	4390.0
(36)	Reservoir Dip (DEG) .....	1.0
(37)	Production Wells (Number) .....	778.0
(38)	Injection Wells (Number) .....	152.0
(39)	Swept Zone Oil Saturation (%) (Residual to Water) .....	30-60
(40)	Injection Water Salinity (ppm TDS) .....	20000
(41)	Clay Content (%) .....	11
(42)	Dykstra-Parsons Coefficient .....	0.5
(43)	Current Injection Rate (B/D/WELL) .....	17000 (1982)
(44)	Fractured-Fault (Y,N) (N = 0, Y = 1) .....	1
(45)	Shale Break or Laminations (Y,N) (N = 0, Y = 1) .....	1
(46)	Major Gas Cap (Y,N) (N = 0, Y = 1) .....	1
(47)	Field Multiplier (Number) .....	N/A
(48)	RRC District .....	N/A
(49)	Production Rate (MBBL/D); For the Year shown in element 28 .....	1200
(50)	Recovery Efficiency-Waterflood (Factor) .....	N/A
(51)	Ultimate Recovery Factor (Fraction of OOIP) (Primary Plus Secondary) .....	N/A

Record 5:

(52)	Geologic Play Code (Table II) .....	302
(53)	Depositional System Code (Table III) .....	152
(54)	Depositional System Degree of Confidence (1 = Highest, 2 = Moderate, 3 = Lowest) .....	2
(55)	Diagenetic Overprint Code (Table IV) .....	-1
(56)	Diagenetic Overprint Degree of Confidence (1 = Highest, 2 = Moderate, 3 = Lowest) .....	N/A
(57)	Structural Compartmentalization (Table V) .....	31
(58)	Structural Compartmentalization Degree of Confidence (1 = Highest, 2 = Moderate, 3 = Lowest) .....	1
(59)	Predominant Element of Reservoir Heterogeneity (1 = Depositional System, 2 = Diagenetic Overprint, 3 = Structural Compartmentalization) .....	1
(60)	Trap Type (1 = Stratigraphic, 2 = Structural, 3 = Combination) .....	3
(61)	Geologic Province (Table VI) .....	058

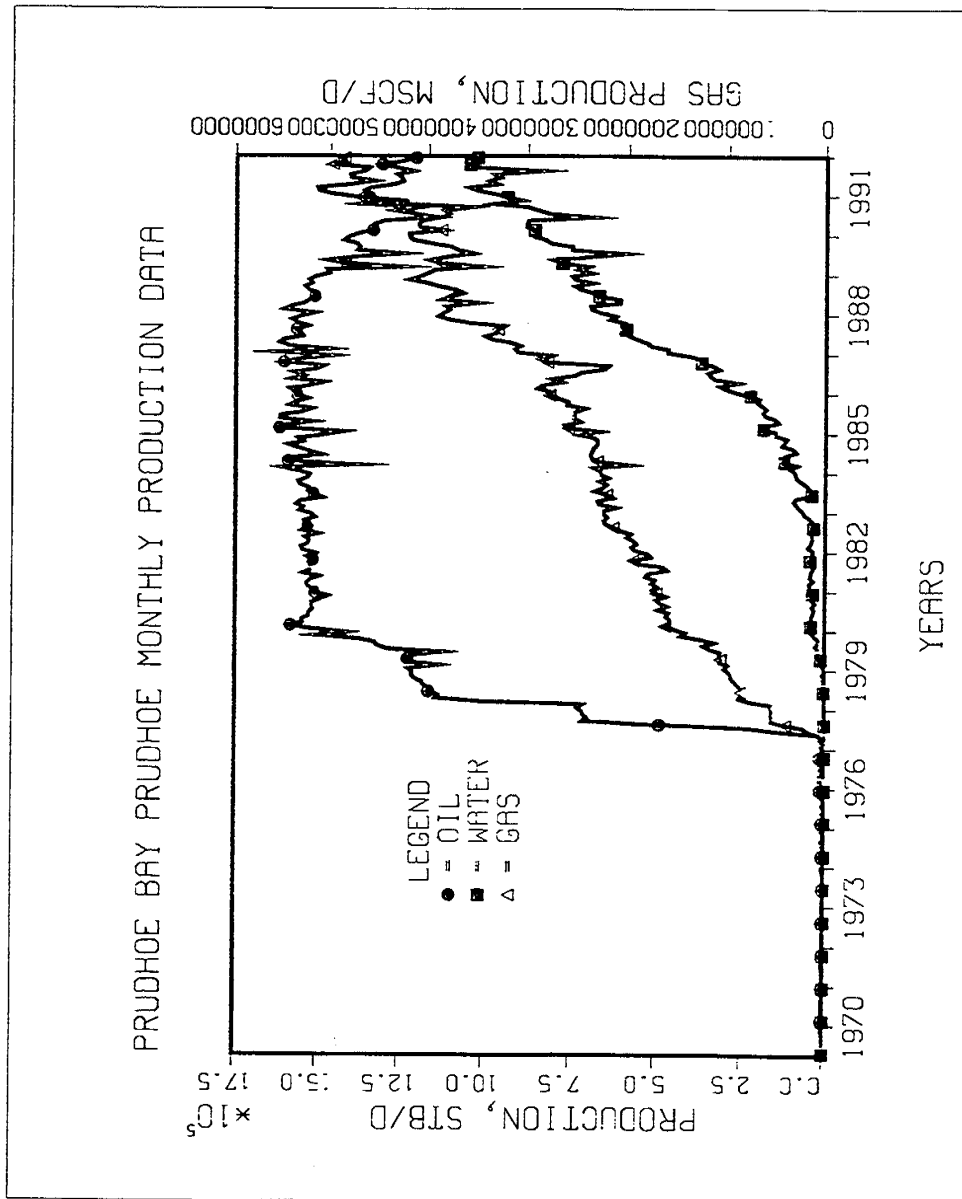


Figure XIV-1.

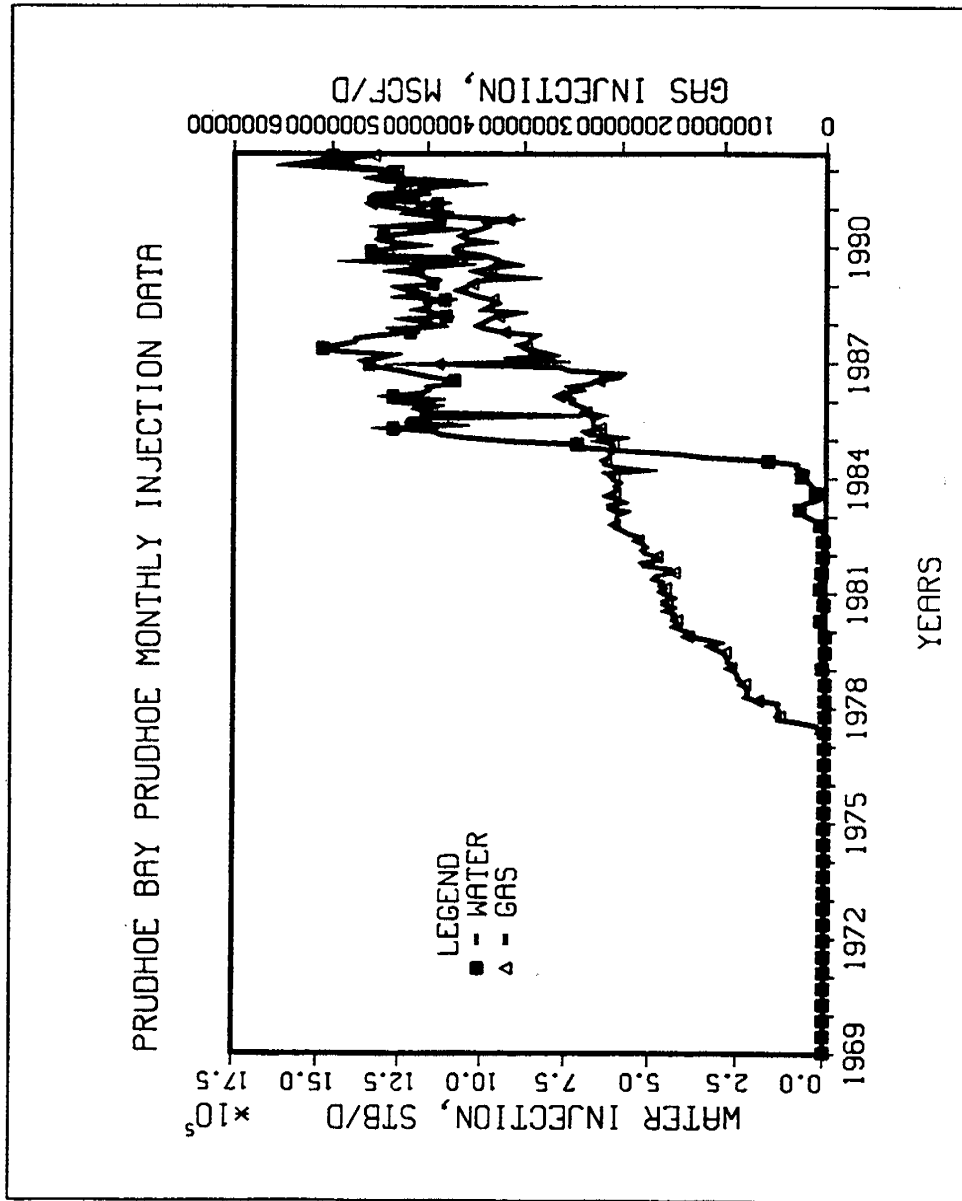


Figure XIV-2.



**Table XIV-6.**

**TORIS DATA BASE  
FIELD: LISBURNE**

Record 1:

Field Code .....	N/A
STATE Postal Code .....	AK
Lithology Code (-1, 0 = Unknown; 1 = SS, 2 = LS; 3 = Dolo.) .....	2
Geologic Age Code AAPG .....	330
Field Name .....	Lisburne
Reservoir Name .....	Lisburne
Reference Number .....	N/A
Load Number .....	N/A
Formation Name .....	Wahoo

Record 2:

( 1) Field Acres (Acres) .....	122880
( 2) Proven Acres (Acres) .....	N/A
( 3) Well Spacing (Acres) .....	160
( 4) Total Wells (Number) .....	75
( 5) Net Pay (Feet) .....	0-150
( 6) Gross Pay (Feet) .....	0-300
( 7) Porosity (%) .....	10
( 8) Initial Oil Saturation (%) .....	N/A
( 9) Current Oil Saturation (%) .....	N/A
(10) Initial Water Saturation (%) .....	20.0
(11) Current Water Saturation (%) .....	N/A
(12) Initial Gas Saturation (%) .....	N/A
(13) Current Gas Saturation (%) .....	N/A
(14) Initial Oil FVF (Res bbl/STB) .....	1.385
(15) Current Oil FVF (Res bbl/STB) .....	1.40 at 4335 psi
(16) True Vertical Depth (Feet)----Mid-Perforation .....	8900
(17) Formation Temperature (°F) .....	183

Record 3:

(18) Current Formation Pressure (PSI) .....	3364
(19) Permeability (md) .....	0.1-2.0
(20) Geologic Age (AAPG) .....	330
(21) API Gravity (°API) .....	27
(22) Oil Viscosity (CP) :e Reservoir condition .....	1.12
(23) Formation Salinity (ppm TDS) .....	N/A
(24) OOIP (BBL) .....	2.0 × 10 <sup>9</sup>
(25) Primary Recovery Factor (Fraction of OOIP) .....	0.062 (1982)
(26) Cumulative Oil Production (BBL) .....	82 × 10 <sup>6</sup>

**Table XIV-6 (continued).**

(27)	Year For Cumulative Oil Production; EX/1986 .....	1991
(28)	Technical Availability Date (Year); Ex/1990 .....	N/A
(29)	Primary Recovery (BBL/AC.FT.) .....	N/A
(30)	Primary Recovery (BBL) .....	300
(31)	Year For Primary Recovery .....	N/A
(32)	Current Producing GOR (SCF/BBL) .....	656
(33)	Initial Producing GOR (SCF/BBL) .....	830

Record 4:

(34)	Reservoir Acreage (Acres) .....	38400
(35)	Initial Formation Pressure (PSI) .....	4490
(36)	Reservoir Dip (DEG) .....	0
(37)	Production Wells (Number) .....	71
(38)	Injection Wells (Number) .....	4
(39)	Swept Zone Oil Saturation (%) (Residual to Water) .....	N/A
(40)	Injection Water Salinity (ppm TDS) .....	N/A
(41)	Clay Content (%) .....	N/A
(42)	Dykstra-Parsons Coefficient .....	N/A
(43)	Current Injection Rate (B/D/WELL) .....	N/A
(44)	Fractured-Fault (Y,N) (N = 0, Y = 1) .....	N/A
(45)	Shale Break or Laminations (Y,N) (N = 0, Y = 1) .....	1
(46)	Major Gas Cap (Y,N) (N = 0, Y = 1) .....	1
(47)	Field Multiplier (Number) .....	1
(48)	RRC District .....	N/A
(49)	Production Rate (MBBL/D); For the Year shown in element 28 .....	40.00
(50)	Recovery Efficiency-Waterflood (Factor) .....	0.16
(51)	Ultimate Recovery Factor (Fraction of OOIP) (Primary Plus Secondary) .....	N/A

Record 5:

(52)	Geologic Play Code (Table II) .....	-1
(53)	Depositional System Code (Table III) .....	230
(54)	Depositional System Degree of Confidence (1 = Highest, 2 = Moderate, 3 = Lowest) .....	1
(55)	Diagenetic Overprint Code (Table IV) .....	-1
(56)	Diagenetic Overprint Degree of Confidence (1 = Highest, 2 = Moderate, 3 = Lowest) .....	N/A
(57)	Structural Compartmentalization (Table V) .....	31
(58)	Structural Compartmentalization Degree of Confidence (1 = Highest, 2 = Moderate, 3 = Lowest) .....	1
(59)	Predominant Element of Reservoir Heterogeneity (1 = Depositional System, 2 = Diagenetic Overprint, 3 = Structural Compartmentalization) .....	N/A
(60)	Trap Type (1 = Stratigraphic, 2 = Structural, 3 = Combination) .....	3
(61)	Geologic Province (Table VI) .....	058

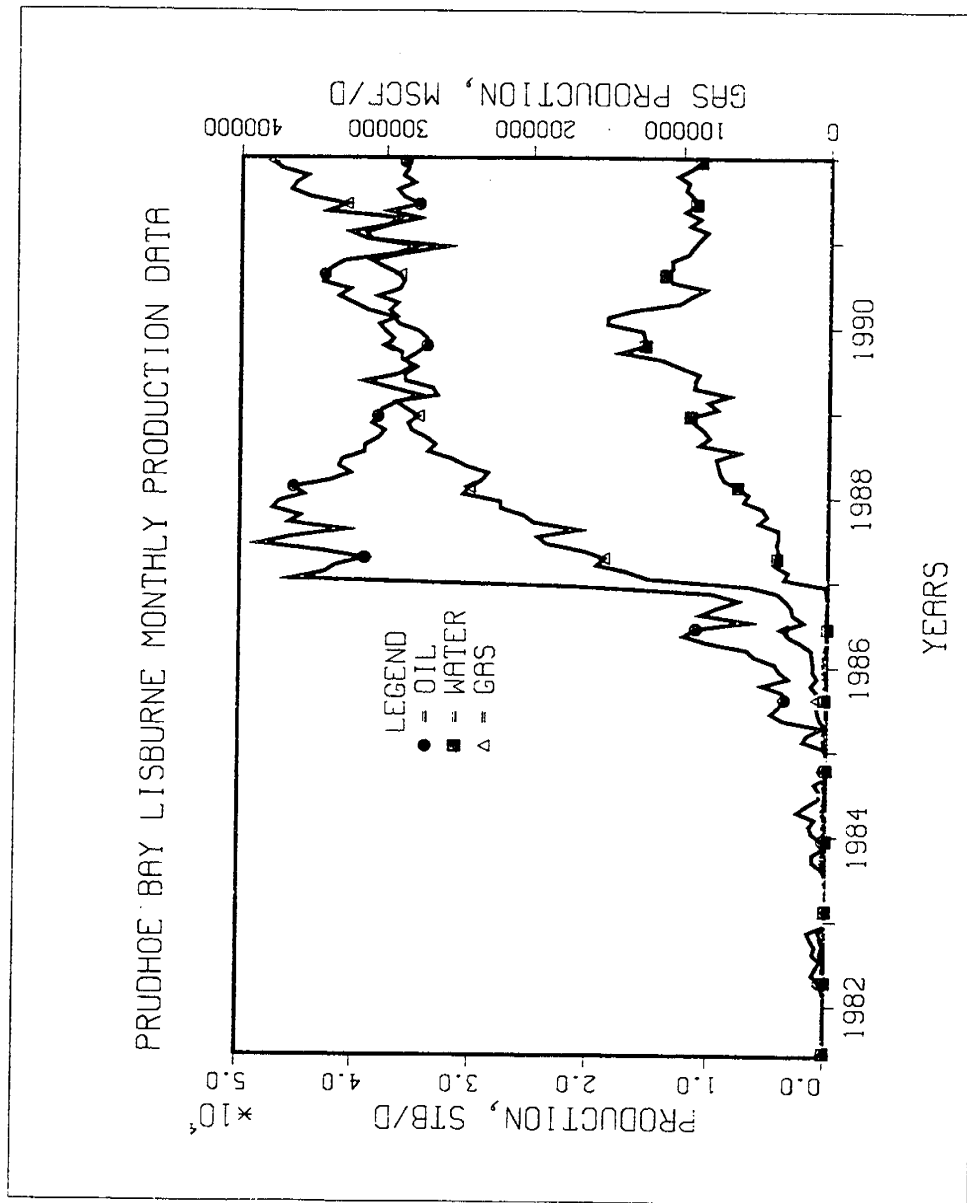


Figure XIV-3.

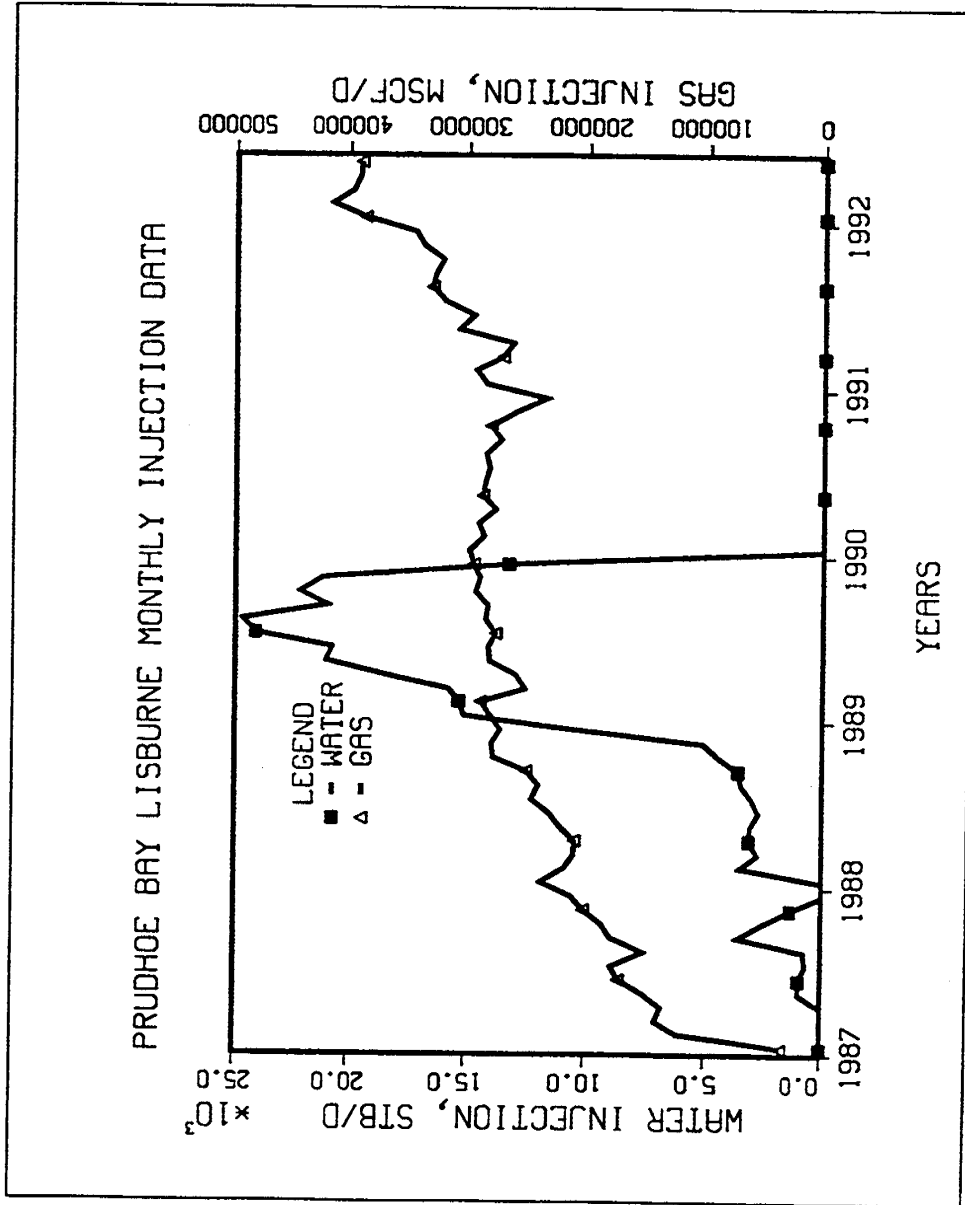


Figure XIV-4.



**Table XIV-8.**

**TORIS DATA BASE  
FIELD: ENDICOTT (KEKIKTUK)**

**Record 1:**

Field Code .....	N/A
STATE Postal Code .....	AK
Lithology Code (-1, 0 = Unknown; 1 = SS, 2 = LS; 3 = Dolo.) .....	1
Geologic Age Code AAPG .....	330
Field Name .....	Endicott
Reservoir Name .....	Endicott
Reference Number .....	N/A
Load Number .....	N/A
Formation Name .....	Kekiktuk

**Record 2:**

( 1) Field Acres (Acres) .....	8700
( 2) Proven Acres (Acres) .....	8700
( 3) Well Spacing (Acres) .....	160
( 4) Total Wells (Number) .....	80
( 5) Net Pay (Feet) .....	56
( 6) Gross Pay (Feet) .....	240 TVT
( 7) Porosity (%) .....	22.0
( 8) Initial Oil Saturation (%) .....	80-94%
( 9) Current Oil Saturation (%) .....	N/A
(10) Initial Water Saturation (%) .....	20-6%
(11) Current Water Saturation (%) .....	N/A
(12) Initial Gas Saturation (%) .....	N/A
(13) Current Gas Saturation (%) .....	N/A
(14) Initial Oil FVF (Res bbl/STB) .....	1.35
(15) Current Oil FVF (Res bbl/STB) .....	1.36
(16) True Vertical Depth (Feet)---Mid-Perforation .....	10000.0
(17) Formation Temperature (°F) .....	218.0

**Record 3:**

(18) Current Formation Pressure (PSI) .....	N/A
(19) Permeability (md) .....	847
(20) Geologic Age (AAPG) .....	330
(21) API Gravity (°API) .....	23
(22) Oil Viscosity (CP) :e Reservoir condition .....	1
(23) Formation Salinity (ppm TDS) .....	28000
(24) OOIP (BBL) .....	1.170 × 10 <sup>9</sup>
(25) Primary Recovery Factor (Fraction of OOIP) .....	10%
(26) Cumulative Oil Production (BBL) .....	11.82 × 10 <sup>7</sup>

**Table XIV-8 (continued).**

(27)	Year For Cumulative Oil Production; EX/1986	1990
(28)	Technical Availability Date (Year); Ex/1990	N/A
(29)	Primary Recovery (BBL/AC.FT.)	100
(30)	Primary Recovery (BBL)	115.5 x 10 <sup>6</sup>
(31)	Year For Primary Recovery	1982
(32)	Current Producing GOR (SCF/BBL)	1220.0
(33)	Initial Producing GOR (SCF/BBL)	763.0

Record 4:

(34)	Reservoir Acreage (Acres)	8700
(35)	Initial Formation Pressure (PSI)	4890 psi @ 10,000 TVDSS
(36)	Reservoir Dip (DEG)	5.5
(37)	Production Wells (Number)	61
(38)	Injection Wells (Number)	18
(39)	Swept Zone Oil Saturation (%) (Residual to Water)	N/A
(40)	Injection Water Salinity (ppm TDS)	N/A
(41)	Clay Content (%)	Trace - 5%
(42)	Dykstra-Parsons Coefficient	N/A
(43)	Current Injection Rate (B/D/WELL)	10,000
(44)	Fractured-Fault (Y,N) (N = 0, Y = 1)	1
(45)	Shale Break or Laminations (Y,N) (N = 0, Y = 1)	1
(46)	Major Gas Cap (Y,N) (N = 0, Y = 1)	1
(47)	Field Multiplier (Number)	N/A
(48)	RRC District	N/A
(49)	Production Rate (MBBL/D); For the Year shown in element 28	100.0
(50)	Recovery Efficiency-Waterflood (Factor)	67%
(51)	Ultimate Recovery Factor (Fraction of OOIP) (Primary Plus Secondary)	45%

Record 5:

(52)	Geologic Play Code (Table II)	-1
(53)	Depositional System Code (Table III)	130
(54)	Depositional System Degree of Confidence (1 = Highest, 2 = Moderate, 3 = Lowest)	1
(55)	Diagenetic Overprint Code (Table IV)	7
(56)	Diagenetic Overprint Degree of Confidence (1 = Highest, 2 = Moderate, 3 = Lowest)	1
(57)	Structural Compartmentalization (Table V)	41
(58)	Structural Compartmentalization Degree of Confidence (1 = Highest, 2 = Moderate, 3 = Lowest)	1
(59)	Predominant Element of Reservoir Heterogeneity (1 = Depositional System, 2 = Diagenetic Overprint, 3 = Structural Compartmentalization)	3
(60)	Trap Type (1 = Stratigraphic, 2 = Structural, 3 = Combination)	3
(61)	Geologic Province (Table VI)	058

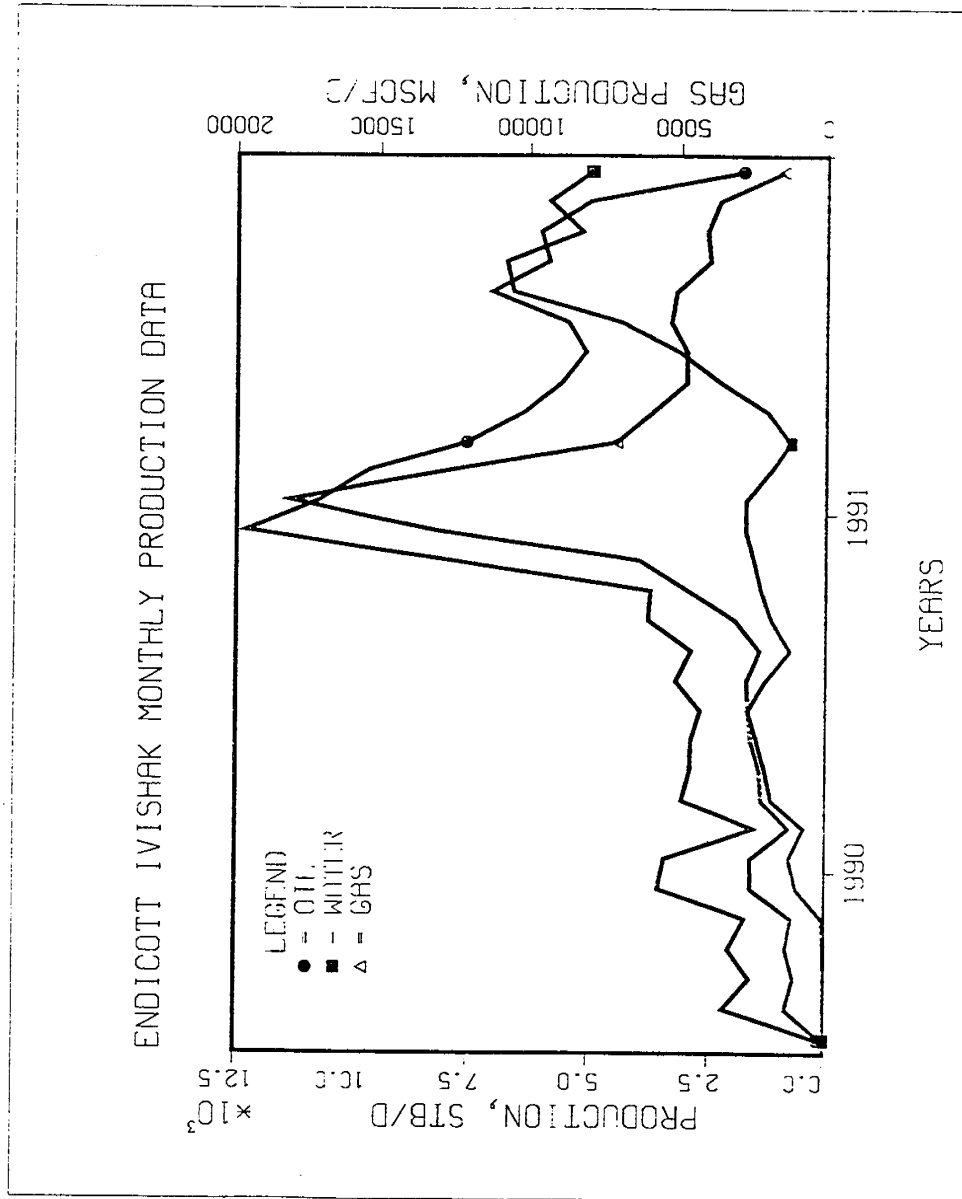


Figure XIV-5.

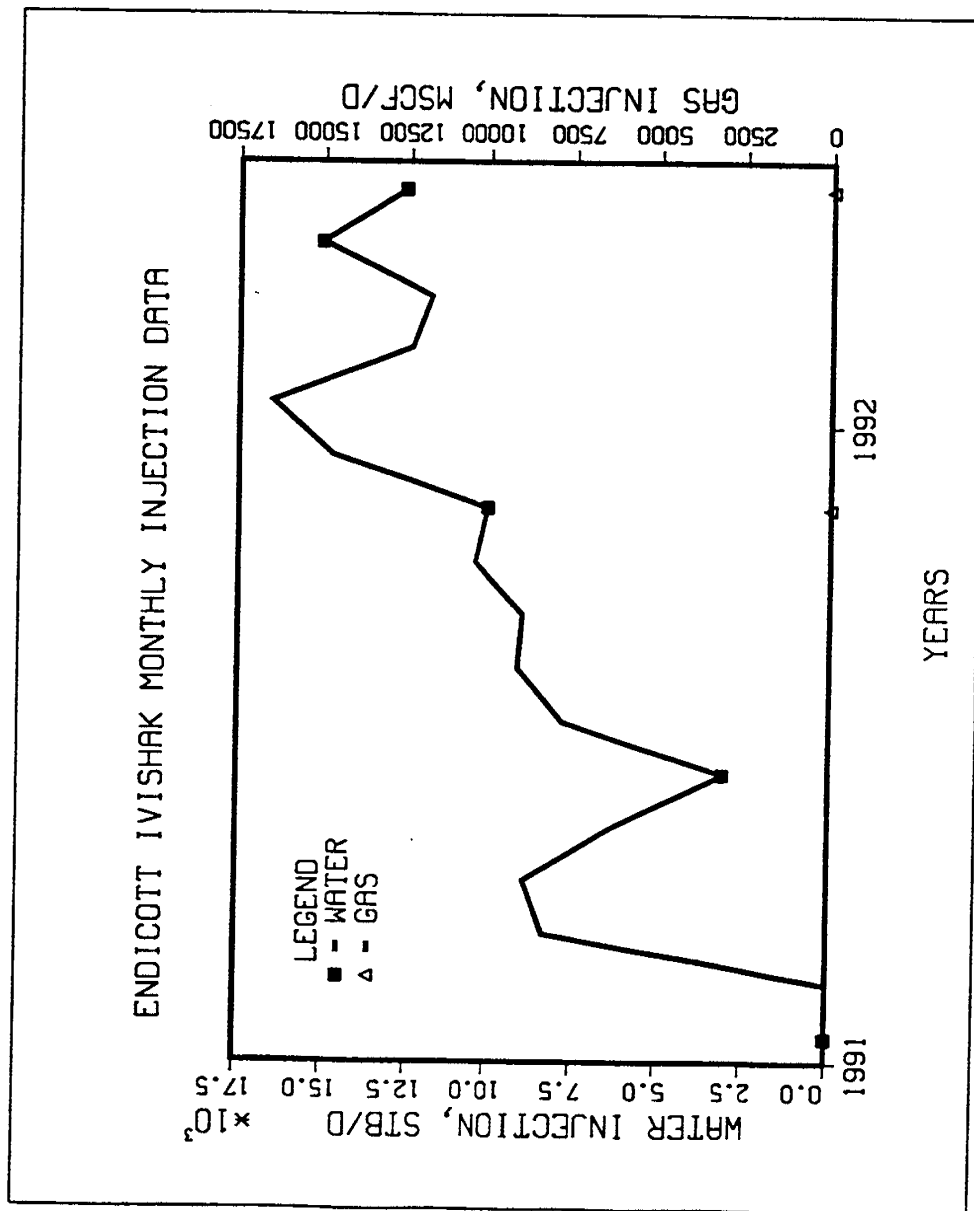


Figure XIV-6.

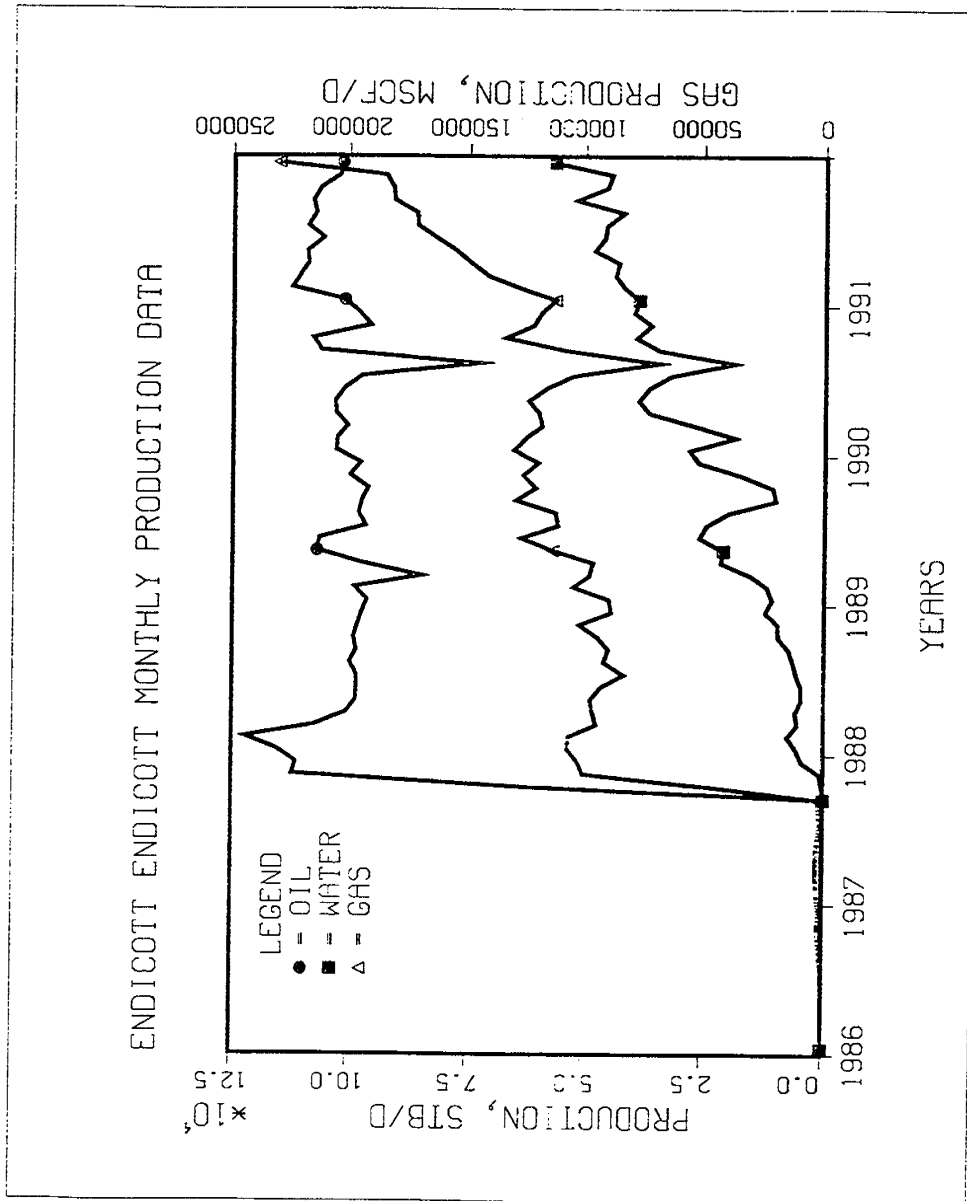


Figure XIV-7.

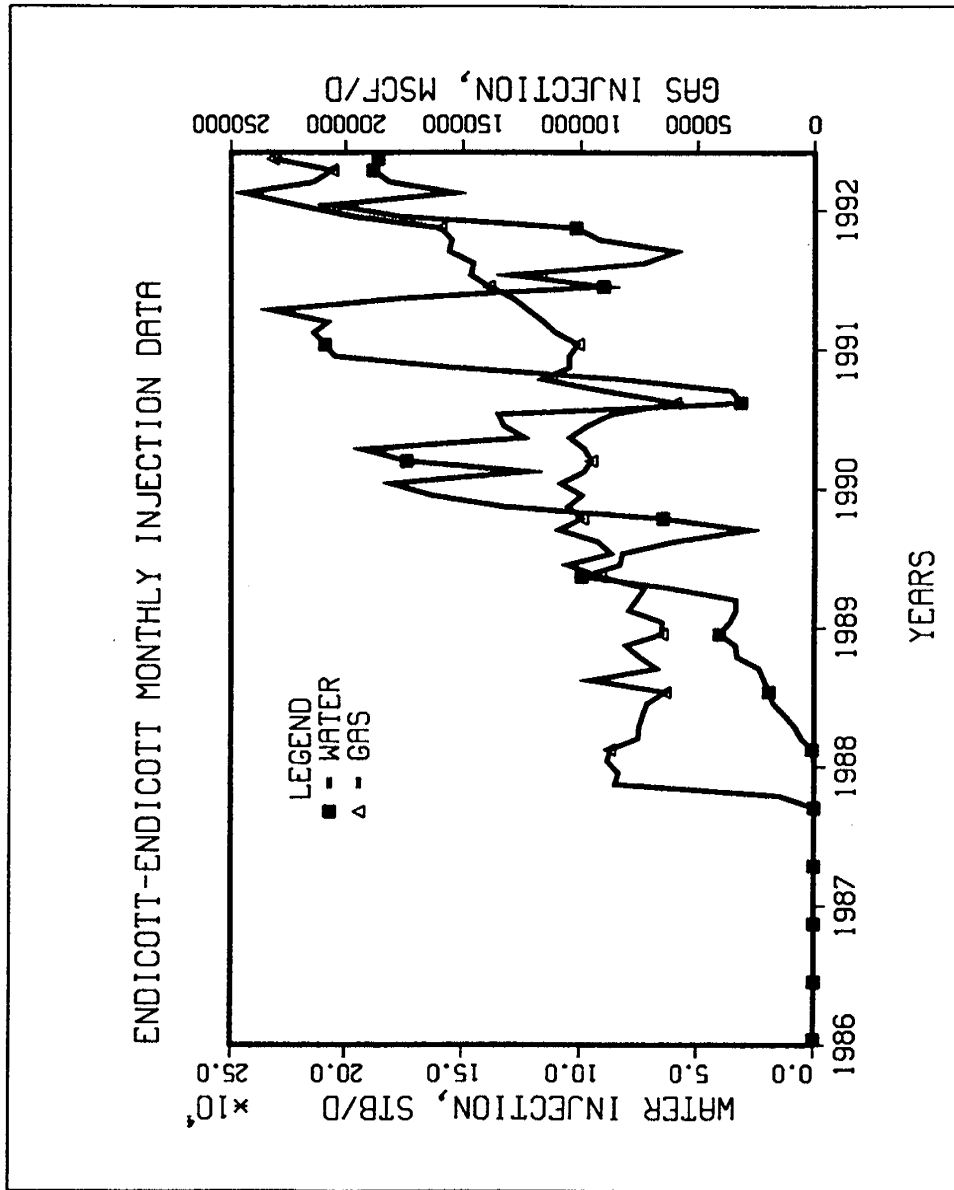


Figure XIV-8.

Table XIV-9.

Reservoir Heterogeneity Classification System for TORIS			
<b>1. Reservoir Identification</b> Reservoir Play: _____			
Reservoir Name: <u>Kuparuk River</u>	Geologic Province: <u>Arctic Coastal Plain</u>	Date: <u>7/10/92</u>	
Field Name: <u>Kuparuk River</u>	Geologic Age: <u>Cretaceous/Colorado</u>	Prepared By: <u>PDL/UAF</u>	
State: <u>AK</u>	Formation: <u>Kuparuk River</u>	Version: <u>1</u>	
<b>2. Depositional System</b> <input type="checkbox"/> 1 <input type="checkbox"/> 2 <input type="checkbox"/> 3    Degree of Confidence in Selection    (1=Highest, 3= Lowest)			
<b>Carbonate Reservoirs</b>		<b>Clastic Reservoirs</b>	
<input type="checkbox"/> Lacustrine <input type="checkbox"/> Peritidal ___ Supratidal ___ Intertidal ___ Subtidal <input checked="" type="checkbox"/> Shallow Shelf ___ Open Shelf ___ Restricted Shelf <input type="checkbox"/> Shelf Margin ___ Rimmed Shelf ___ Ramp	<input type="checkbox"/> Reefs ___ Pinnacle Reefs ___ Bioherms ___ Atolls <input type="checkbox"/> Slope/Basin ___ Cyclic Fans ___ Turbidite Fans ___ Mounds <input type="checkbox"/> Basin ___ Drowned Shelf ___ Deep Basin	<input type="checkbox"/> Estuarine ___ Ergs ___ Coastal Dunes <input type="checkbox"/> Lacustrine ___ Basin Margin ___ Basin Center <input type="checkbox"/> Fluvial ___ Braided Streams ___ Meandering Streams <input type="checkbox"/> Alluvial Fan ___ Humid (Stream-Dominated) ___ Arid/Semi-Arid ___ Fan Deltas <input type="checkbox"/> Delta ___ Wave-Dominated ___ Fluvial-Dominated ___ Tide-Dominated	<input type="checkbox"/> Strandplain ___ Barrier Cores ___ Barrier Shorefaces ___ Back Barriers ___ Tidal Channels ___ Washover Fan/Tidal Deltas <input type="checkbox"/> Shelf (Accretionary Processes) ___ Sand Waves ___ Sand Ridges/Bars <input type="checkbox"/> Slope-Basin ___ Turbidite Fans ___ Cyclic Fans <input type="checkbox"/> Basin ___ Pelagic
<b>3. Diagenetic Overprint</b> <input type="checkbox"/> 1 <input type="checkbox"/> 2 <input type="checkbox"/> 3    Degree of Confidence in Selection    (1=Highest, 3= Lowest)			
<b>Carbonate Reservoirs</b>		<b>Clastic Reservoirs</b>	
<input type="checkbox"/> Compaction/Cementation <input type="checkbox"/> Grad. Enhancement <input type="checkbox"/> Dolomitization	<input type="checkbox"/> Dolomitization (Evaporites) <input type="checkbox"/> Massive Dissolution <input type="checkbox"/> Silicification	<input type="checkbox"/> Compaction/Cementation <input checked="" type="checkbox"/> Intergranular Dissolution	<input type="checkbox"/> Authigenic Clay <input type="checkbox"/> Chertification
<b>4. Structural Compartmentalization</b> <input type="checkbox"/> 1 <input type="checkbox"/> 2 <input type="checkbox"/> 3    Degree of Confidence in Selection    (1=Highest, 3= Lowest)			
<input type="checkbox"/> Natural Fracture Permeability <input type="checkbox"/> Unstructured <input checked="" type="checkbox"/> Faulted <input type="checkbox"/> Fault/Fold <input type="checkbox"/> Folded			
___ Normal Fault      ___ Normal Fault ___ Reverse Fault     ___ Reverse Fault ___ Strike-Slip Fault   ___ Strike-Slip Fault			
<b>5. Reservoir Heterogeneity Ternary Diagram</b>			
Predominant Element of Reservoir Heterogeneity: (Check Only One)			
<ul style="list-style-type: none"> <li>• Depositional System      ___</li> <li>• Diagenetic Overprint     ___</li> <li>• Structural Compartmentalization    <input checked="" type="checkbox"/></li> </ul>			
<b>6. Trap Type</b> <input type="checkbox"/> Stratigraphic <input type="checkbox"/> Structural <input checked="" type="checkbox"/> Combination			
<b>7. Optional Comments (References, Details on Above Selections, Etc.)</b>			
_____ _____ _____ _____			

**Table XIV-10.**

**TORIS DATA BASE  
FIELD: KUPARUK RIVER**

Record 1:

Field Code .....	N/A
STATE Postal Code .....	AK
Lithology Code (-1, 0 = Unknown; 1 = SS, 2 = LS; 3 = Dolo.) .....	1
Geologic Age Code AAPG .....	217
Field Name .....	Kuparuk River
Reservoir Name .....	Kuparuk River
Reference Number .....	3190
Load Number .....	N/A
Formation Name .....	Kuparuk River

Record 2:

( 1) Field Acres (Acres) .....	240000.0
( 2) Proven Acres (Acres) .....	N/A
( 3) Well Spacing (Acres) .....	320
( 4) Total Wells (Number) .....	604
( 5) Net Pay (Feet) .....	50
( 6) Gross Pay (Feet) .....	150
( 7) Porosity (%) .....	21
( 8) Initial Oil Saturation (%) .....	68
( 9) Current Oil Saturation (%) .....	67
(10) Initial Water Saturation (%) .....	32
(11) Current Water Saturation (%) .....	32
(12) Initial Gas Saturation (%) .....	0
(13) Current Gas Saturation (%) .....	1
(14) Initial Oil FVF (Res bbl/STB) .....	1.22
(15) Current Oil FVF (Res bbl/STB) .....	1.25 (@ 3000 psi)
(16) True Vertical Depth (Feet)----Mid-Perforation .....	6300.0
(17) Formation Temperature (°F) .....	155

Record 3:

(18) Current Formation Pressure (PSI) .....	3120.0 (@ 6000 ft.)
(19) Permeability (md) .....	100
(20) Geologic Age (AAPG) .....	217
(21) API Gravity (°API) .....	22.9-29.0
(22) Oil Viscosity (CP) :e Reservoir condition .....	2.50
(23) Formation Salinity (ppm TDS) .....	22000.0
(24) OOIP (BBL) .....	4.4 × 10 <sup>9</sup>
(25) Primary Recovery Factor (Fraction of OOIP) .....	.07 (1982)
(26) Cumulative Oil Production (BBL) .....	72.27 × 10 <sup>7</sup>

**Table XIV-10 (continued).**

(27)	Year For Cumulative Oil Production; EX/1986 .....	1990
(28)	Technical Availability Date (Year); Ex/1990 .....	N/A
(29)	Primary Recovery (BBL/AC.FT.) .....	N/A
(30)	Primary Recovery (BBL) .....	308 x 10 <sup>6</sup>
(31)	Year For Primary Recovery .....	1982
(32)	Current Producing GOR (SCF/BBL) .....	1129
(33)	Initial Producing GOR (SCF/BBL) .....	228-413

Record 4:

(34)	Reservoir Acreage (Acres) .....	91623.0
(35)	Initial Formation Pressure (PSI) .....	3360
(36)	Reservoir Dip (DEG) .....	0.8
(37)	Production Wells (Number) .....	343
(38)	Injection Wells (Number) .....	261
(39)	Swept Zone Oil Saturation (%) (Residual to Water) .....	27
(40)	Injection Water Salinity (ppm TDS) .....	N/A
(41)	Clay Content (%) .....	0.25
(42)	Dykstra-Parsons Coefficient .....	0.72
(43)	Current Injection Rate (B/D/WELL) .....	N/A
(44)	Fractured-Fault (Y,N) (N = 0, Y = 1) .....	1
(45)	Shale Break or Laminations (Y,N) (N = 0, Y = 1) .....	1
(46)	Major Gas Cap (Y,N) (N = 0, Y = 1) .....	0
(47)	Field Multiplier (Number) .....	N/A
(48)	RRC District .....	N/A
(49)	Production Rate (MBBL/D); For the Year shown in element 28 .....	300
(50)	Recovery Efficiency-Waterflood (Factor) .....	N/A
(51)	Ultimate Recovery Factor (Fraction of OOIP) (Primary Plus Secondary) .....	N/A

Record 5:

(52)	Geologic Play Code (Table II) .....	-1
(53)	Depositional System Code (Table III) .....	230
(54)	Depositional System Degree of Confidence (1 = Highest, 2 = Moderate, 3 = Lowest) .....	N/A
(55)	Diagenetic Overprint Code (Table IV) .....	7
(56)	Diagenetic Overprint Degree of Confidence (1 = Highest, 2 = Moderate, 3 = Lowest) .....	N/A
(57)	Structural Compartmentalization (Table V) .....	31
(58)	Structural Compartmentalization Degree of Confidence (1 = Highest, 2 = Moderate, 3 = Lowest) .....	N/A
(59)	Predominant Element of Reservoir Heterogeneity (1 = Depositional System, 2 = Diagenetic Overprint, 3 = Structural Compartmentalization) .....	3
(60)	Trap Type (1 = Stratigraphic, 2 = Structural, 3 = Combination) .....	3
(61)	Geologic Province (Table VI) .....	058

Table XIV-11.

Reservoir Heterogeneity Classification System for TORIS		
<b>1. Reservoir Identification</b> Reservoir Play: _____ Reservoir Name: <u>Kuparuk River</u> Geologic Province: <u>Arctic Coastal Plain</u> Date: <u>7/10/92</u> Field Name: <u>Prudhoe Bay</u> Geologic Age: <u>Cretaceous/Lower</u> Prepared By: <u>UAF/PDL</u> State: <u>AK</u> Formation: <u>PB Kuparuk River</u> Version: <u>1</u>		
<b>2. Depositional System</b> <input checked="" type="checkbox"/> 1 <input type="checkbox"/> 2 <input type="checkbox"/> 3      Degree of Confidence in Selection (1=Highest, 3= Lowest)		
<b>Carbonate Reservoirs</b> <input type="checkbox"/> Lacustrine <input type="checkbox"/> Peritidal ___ Supratidal ___ Intertidal ___ Subtidal <input checked="" type="checkbox"/> Shallow Shelf ___ Open Shelf ___ Restricted Shelf <input type="checkbox"/> Shelf Margin ___ Rimmed Shelf ___ Ramp <input type="checkbox"/> Reefs ___ Pinnacle Reefs ___ Bioherms ___ Atolls <input type="checkbox"/> Slope/Basin ___ Debris Fans ___ Turbidite Fans ___ Mounds <input type="checkbox"/> Basin ___ Drowned Shelf ___ Deep Basin	<b>Clastic Reservoirs</b> <input type="checkbox"/> Eolian ___ Ergs ___ Coastal Dunes <input type="checkbox"/> Lacustrine ___ Basin Margin ___ Basin Center <input type="checkbox"/> Fluvial ___ Branched Streams ___ Meandering Streams <input type="checkbox"/> Alluvial Fan ___ Humid (Stream-Dominated) ___ Arid/Semi-Arid ___ Fan Deltas <input type="checkbox"/> Delta ___ Wave-Dominated ___ Fluvial-Dominated ___ Tide-Dominated <input type="checkbox"/> Strandplain ___ Barrier Cores ___ Barrier Shorefaces ___ Back Barriers ___ Tidal Channels ___ Washover Fan/Tidal Deltas <input type="checkbox"/> Shelf (Accretionary Processes) ___ Sand Waves ___ Sand Ridge/Bars <input type="checkbox"/> Slope/Basin ___ Turbidite Fans ___ Debris Fans <input type="checkbox"/> Basin ___ Pelagic	
<b>3. Diagenetic Overprint</b> <input type="checkbox"/> 1 <input type="checkbox"/> 2 <input type="checkbox"/> 3      Degree of Confidence in Selection (1=Highest, 3= Lowest)		
<b>Carbonate Reservoirs</b> <input type="checkbox"/> Compaction/Compensation <input type="checkbox"/> Grain Enhancement <input type="checkbox"/> Dolomitization <input type="checkbox"/> Dolomitization (Evaporites) <input type="checkbox"/> Massive Dissolution <input type="checkbox"/> Silicification	<b>Clastic Reservoirs</b> <input type="checkbox"/> Compaction/Compensation <input type="checkbox"/> Intergranular Dissolution <input type="checkbox"/> Authigenic Clay <input type="checkbox"/> Chertification	
<b>4. Structural Compartmentalization</b> <input checked="" type="checkbox"/> 1 <input type="checkbox"/> 2 <input type="checkbox"/> 3      Degree of Confidence in Selection (1=Highest, 3= Lowest)		
<input type="checkbox"/> Natural Fracture Porosity <input type="checkbox"/> Unstructures <input checked="" type="checkbox"/> Faulted <input type="checkbox"/> Fault/Fold <input type="checkbox"/> Folded ___ Normal Fault    ___ Reverse Fault    ___ Strike-Slip Fault    ___ Normal Fault    ___ Reverse Fault    ___ Strike-Slip Fault		
<b>5. Reservoir Heterogeneity Ternary Diagram</b> Predominant Element of Reservoir Heterogeneity: (Check Only One) <input checked="" type="checkbox"/> Depositional System <input type="checkbox"/> Diagenetic Overprint <input type="checkbox"/> Structural Compartmentalization		
<b>6. Trap Type</b> <input type="checkbox"/> Stratigraphic <input type="checkbox"/> Structural <input checked="" type="checkbox"/> Combination		
<b>7. Optional Comments (References, Details on Above Selections, Etc.)</b> <u>"Sandstone Petrology, Diagenesis and Reservoir Quality, Lower Cretaceous</u> <u>Kuparuk River Formation Kuparuk River Field, North Slope, Alaska."</u> <u>1985 AAPG/SEPM/SEG Pacific Section Meeting, Anchorage, AK, by</u> <u>J. Thomas Eggert.</u>		

**Table XIV-12.**

**TORIS DATA BASE**  
**FIELD: PRUDHOE BAY (KUPARUK)**

Record 1:

Field Code .....	N/A
STATE Postal Code .....	AK
Lithology Code (-1, 0 = Unknown; 1 = SS, 2 = LS; 3 = Dolo.) .....	1
Geologic Age Code AAPG .....	217
Field Name .....	Prudhoe Bay
Reservoir Name .....	Kuparuk River
Reference Number .....	N/A
Load Number .....	N/A
Formation Name .....	PB Kuparuk River

Record 2:

( 1) Field Acres (Acres) .....	N/A
( 2) Proven Acres (Acres) .....	N/A
( 3) Well Spacing (Acres) .....	N/A
( 4) Total Wells (Number) .....	0
( 5) Net Pay (Feet) .....	30-80
( 6) Gross Pay (Feet) .....	40-95
( 7) Porosity (%) .....	23
( 8) Initial Oil Saturation (%) .....	N/A
( 9) Current Oil Saturation (%) .....	N/A
(10) Initial Water Saturation (%) .....	37
(11) Current Water Saturation (%) .....	N/A
(12) Initial Gas Saturation (%) .....	N/A
(13) Current Gas Saturation (%) .....	N/A
(14) Initial Oil FVF (Res bbl/STB) .....	1.22
(15) Current Oil FVF (Res bbl/STB) .....	N/A
(16) True Vertical Depth (Feet)----Mid-Perforation .....	6200
(17) Formation Temperature (°F) .....	150

Record 3:

(18) Current Formation Pressure (PSI) .....	2980
(19) Permeability (md) .....	3-200
(20) Geologic Age (AAPG) .....	217
(21) API Gravity (°API) .....	23.0
(22) Oil Viscosity (CP) :e Reservoir condition .....	1.8-4.0 (@ 3210 psi)
(23) Formation Salinity (ppm TDS) .....	16000
(24) OOIP (BBL) .....	3.6 × 10 <sup>9</sup>
(25) Primary Recovery Factor (Fraction of OOIP) .....	0
(26) Cumulative Oil Production (BBL) .....	0

**Table XIV-12 (continued).**

(27)	Year For Cumulative Oil Production; EX/1986 .....	(1991)
(28)	Technical Availability Date (Year); Ex/1990 .....	N/A
(29)	Primary Recovery (BBL/AC.FT.) .....	0
(30)	Primary Recovery (BBL) .....	0
(31)	Year For Primary Recovery .....	0
(32)	Current Producing GOR (SCF/BBL) .....	N/A
(33)	Initial Producing GOR (SCF/BBL) .....	450

Record 4:

(34)	Reservoir Acreage (Acres) .....	N/A
(35)	Initial Formation Pressure (PSI) .....	3210
(36)	Reservoir Dip (DEG) .....	0
(37)	Production Wells (Number) .....	0
(38)	Injection Wells (Number) .....	0
(39)	Swept Zone Oil Saturation (%) (Residual to Water) .....	N/A
(40)	Injection Water Salinity (ppm TDS) .....	N/A
(41)	Clay Content (%) .....	N/A
(42)	Dykstra-Parsons Coefficient .....	N/A
(43)	Current Injection Rate (B/D/WELL) .....	0
(44)	Fractured-Fault (Y,N) (N = 0, Y = 1) .....	N/A
(45)	Shale Break or Laminations (Y,N) (N = 0, Y = 1) .....	1
(46)	Major Gas Cap (Y,N) (N = 0, Y = 1) .....	0
(47)	Field Multiplier (Number) .....	1
(48)	RRC District .....	N/A
(49)	Production Rate (MBBL/D); For the Year shown in element 28 .....	0
(50)	Recovery Efficiency-Waterflood (Factor) .....	0
(51)	Ultimate Recovery Factor (Fraction of OOIP) (Primary Plus Secondary) .....	0

Record 5:

(52)	Geologic Play Code (Table II) .....	-1
(53)	Depositional System Code (Table III) .....	230
(54)	Depositional System Degree of Confidence (1 = Highest, 2 = Moderate, 3 = Lowest) .....	1
(55)	Diagenetic Overprint Code (Table IV) .....	-1
(56)	Diagenetic Overprint Degree of Confidence (1 = Highest, 2 = Moderate, 3 = Lowest) .....	N/A
(57)	Structural Compartmentalization (Table V) .....	31
(58)	Structural Compartmentalization Degree of Confidence (1 = Highest, 2 = Moderate, 3 = Lowest) .....	1
(59)	Predominant Element of Reservoir Heterogeneity (1 = Depositional System, 2 = Diagenetic Overprint, 3 = Structural Compartmentalization) .....	N/A
(60)	Trap Type (1 = Stratigraphic, 2 = Structural, 3 = Combination) .....	3
(61)	Geologic Province (Table VI) .....	058

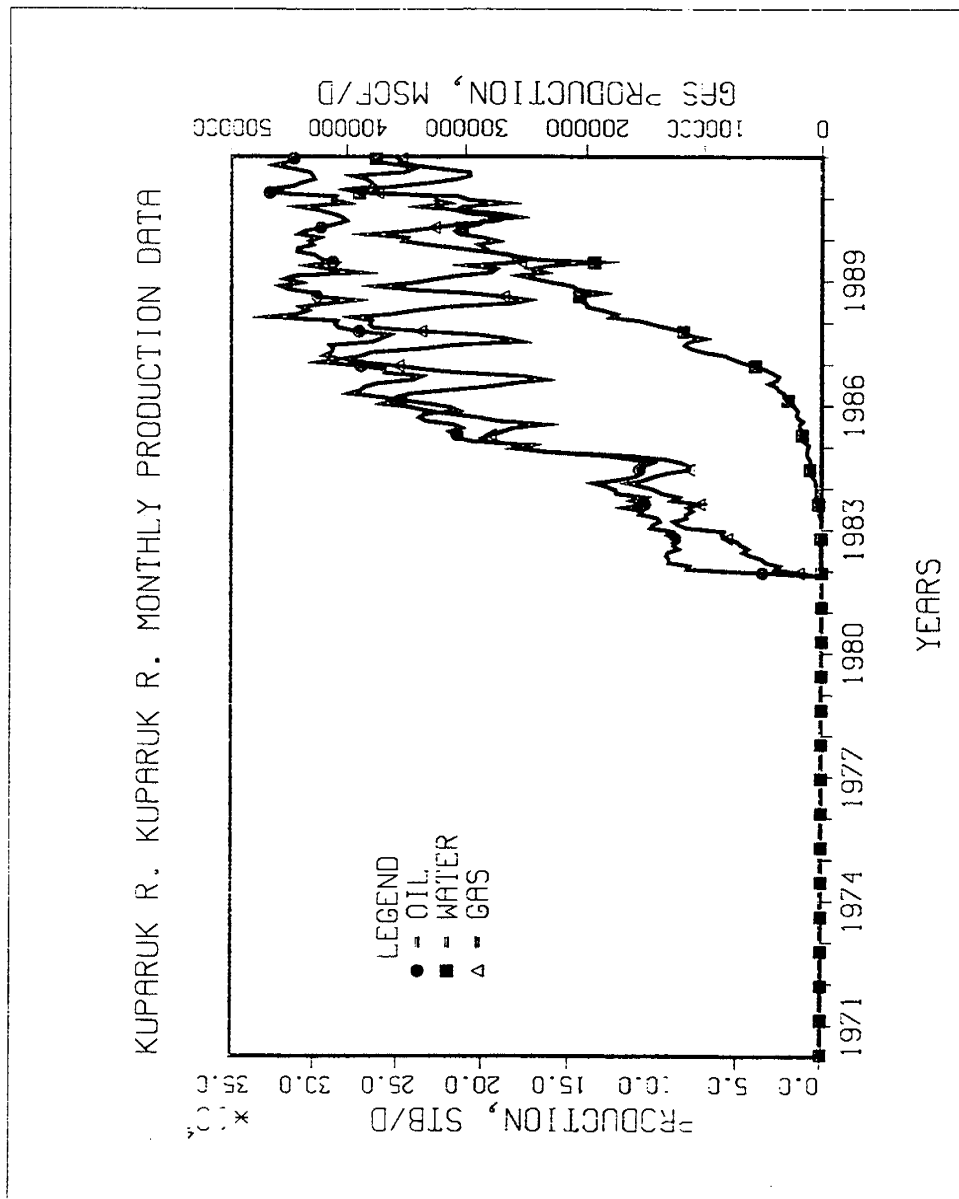


Figure XIV-9.

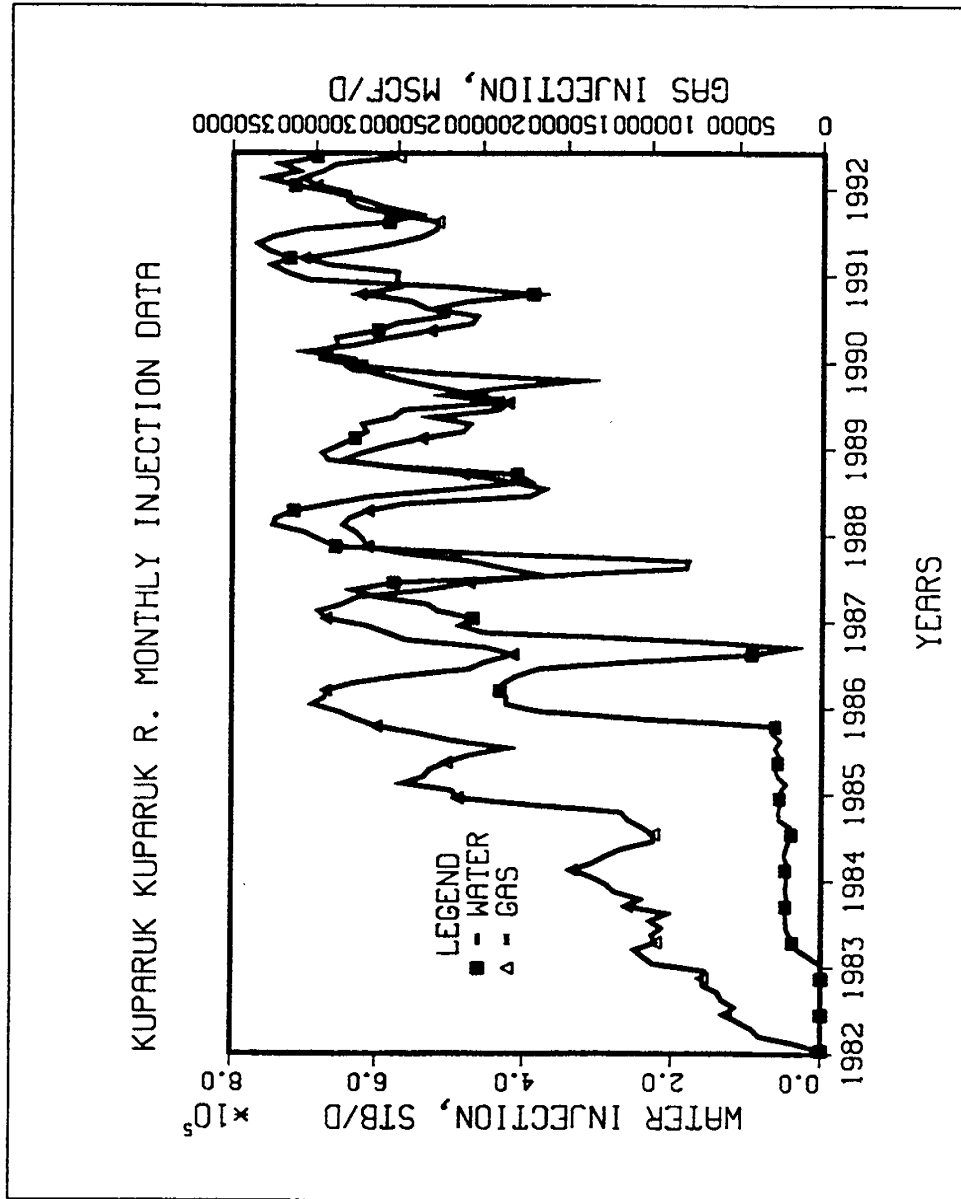


Figure XIV-10.

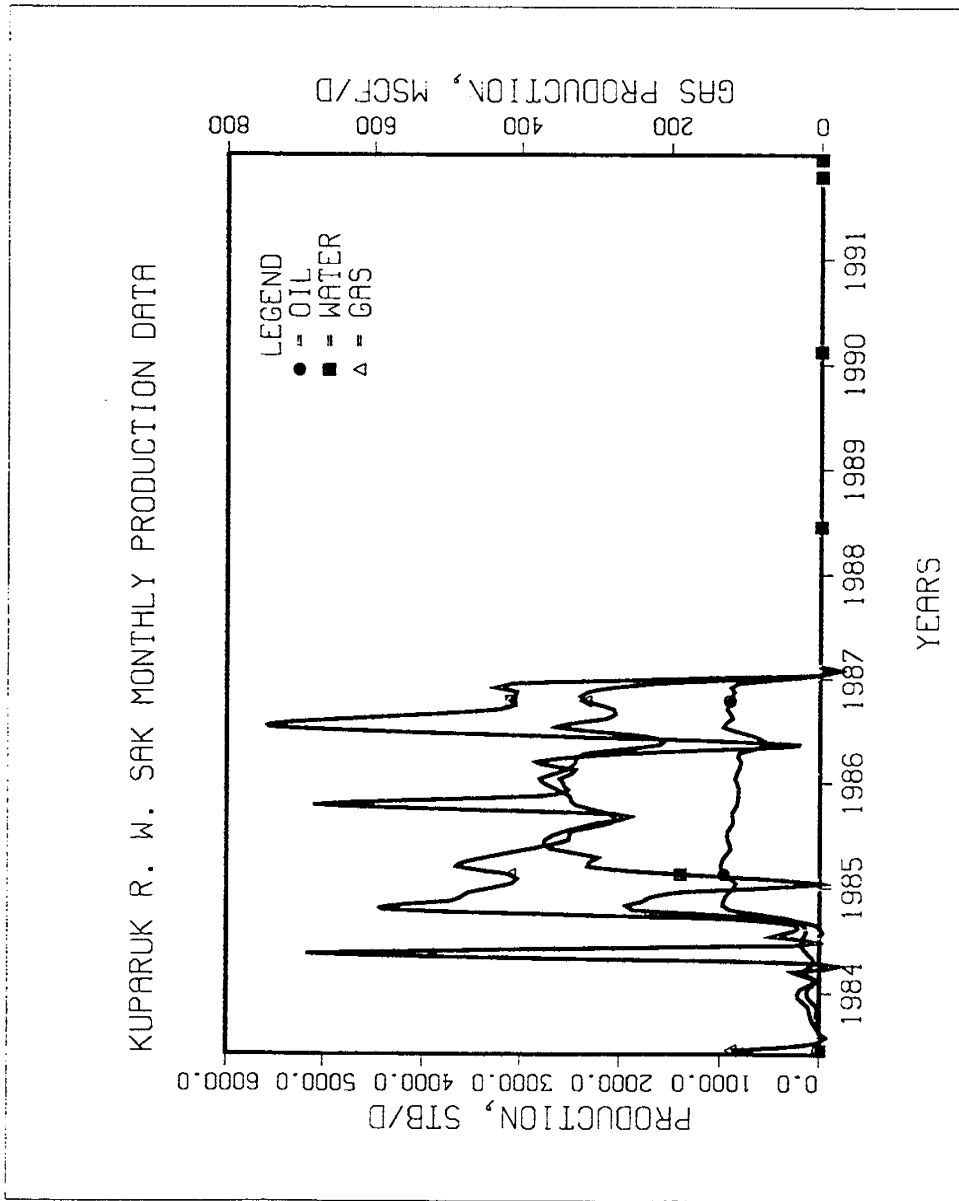


Figure XIV-11.

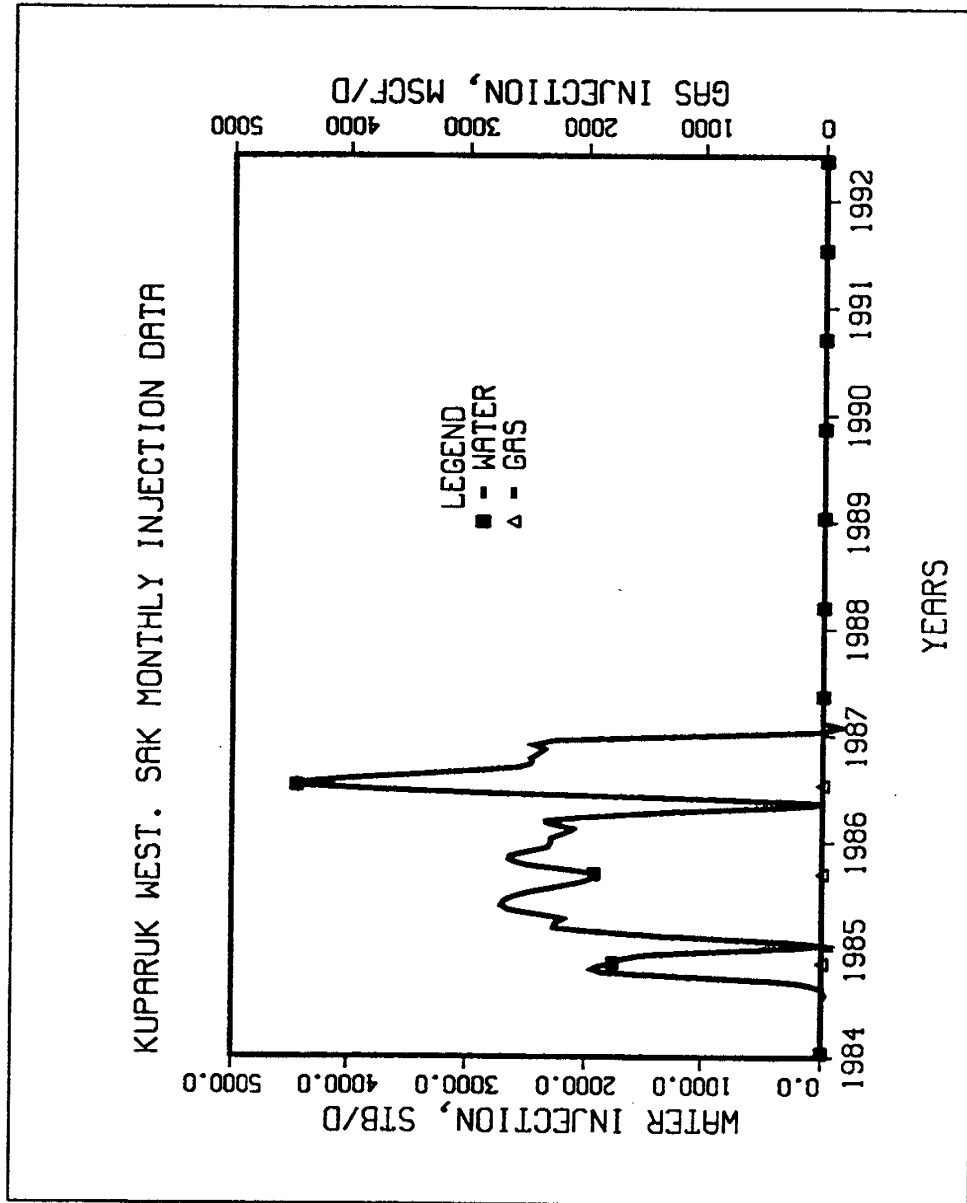


Figure XIV-12.

Table XIV-13.

Reservoir Heterogeneity Classification System for TORIS			
<b>1. Reservoir Identification</b>			
Reservoir Name: <u>Kuparuk</u>		Reservoir Play: _____	
Field Name: <u>Milne Point</u>		Geologic Province: <u>Central North Slope</u> Date: <u>9-10-92</u>	
State: <u>Alaska</u>		Geologic Age: <u>Cretaceous</u> Prepared By: _____	
		Formation: <u>Kuparuk</u> Version: _____	
<b>2. Depositional System</b> <input checked="" type="checkbox"/> 1 <input type="checkbox"/> 2 <input type="checkbox"/> 3 Degree of Confidence in Selection (1=Highest, 3= Lowest)			
<b>Carbonate Reservoirs</b> <input type="checkbox"/> Lacustrine <input type="checkbox"/> Peritidal ___ Supratidal ___ Intertidal ___ Subtidal <input type="checkbox"/> Shallow Shelf ___ Open Shelf ___ Restricted Shelf <input type="checkbox"/> Shelf Margin ___ Rimmed Shelf ___ Ramp <input type="checkbox"/> Reefs ___ Pinnacle Reefs ___ Bioherms ___ Atolls <input type="checkbox"/> Slope/Basin ___ Debris Fans ___ Turbidite Fans <input type="checkbox"/> Basin ___ Mounds ___ Drowned Shelf ___ Deep Basin		<b>Clastic Reservoirs</b> <input type="checkbox"/> Eolian ___ Ergs ___ Coastal Dunes <input type="checkbox"/> Lacustrine ___ Basin Margin ___ Basin Center <input type="checkbox"/> Fluvial ___ Braided Streams ___ Meandering Streams <input type="checkbox"/> Alluvial Fan ___ Humid (Stream-Dominated) ___ Arid/Semi-Arid ___ Fan Deltas <input type="checkbox"/> Delta ___ Wave-Dominated ___ Fluvial-Dominated ___ Tide-Dominated <input type="checkbox"/> Strandplain ___ Barrier Cores ___ Barrier Shoofaces ___ Back Barriers ___ Tidal Channels ___ Washover Fan/Tidal Deltas <input checked="" type="checkbox"/> Shell (Accretionary Processes) ___ Sand Waves ___ Sand Ridges/Bars <input type="checkbox"/> Slope/Basin ___ Turbidite Fans ___ Debris Fans <input type="checkbox"/> Basin ___ Pelagic	
<b>3. Diagenetic Overprint</b> <input type="checkbox"/> 1 <input checked="" type="checkbox"/> 2 <input type="checkbox"/> 3 Degree of Confidence in Selection (1=Highest, 3= Lowest)			
<b>Carbonate Reservoirs</b> <input type="checkbox"/> Compaction/Cementation <input type="checkbox"/> Grain Enhancement <input type="checkbox"/> Dolomitization <input type="checkbox"/> Dolomitization (Evaporites) <input type="checkbox"/> Massive Dissolution <input type="checkbox"/> Silicification		<b>Clastic Reservoirs</b> <input checked="" type="checkbox"/> Compaction/Cementation <input checked="" type="checkbox"/> Intergranular Dissolution <input type="checkbox"/> Authigenic Clay <input type="checkbox"/> Chertification	
<b>4. Structural Compartmentalization</b> <input checked="" type="checkbox"/> 1 <input type="checkbox"/> 2 <input type="checkbox"/> 3 Degree of Confidence in Selection (1=Highest, 3= Lowest)			
<input type="checkbox"/> Natural Fracture Porosity <input type="checkbox"/> Unstructured <input type="checkbox"/> Faulted ___ Normal Fault ___ Reverse Fault ___ Strike-Slip Fault		<input checked="" type="checkbox"/> Fault/Fold <input type="checkbox"/> Folded ___ Normal Fault ___ Reverse Fault ___ Strike-Slip Fault	
<b>5. Reservoir Heterogeneity Ternary Diagram</b>			
Predominant Element of Reservoir Heterogeneity: (Check Only One) • Depositional System _____ • Diagenetic Overprint _____ • Structural Compartmentalization <input checked="" type="checkbox"/>			
<b>6. Trap Type</b> <input type="checkbox"/> Stratigraphic <input checked="" type="checkbox"/> Structural <input type="checkbox"/> Combination			
<b>7. Optional Comments (References, Details on Above Selections, Etc.)</b>			
_____ _____ _____ _____			

**Table XIV-14.**

**TORIS DATA BASE  
FIELD: MILNE POINT (KUPARUK)**

Record 1:

Field Code .....	N/A
STATE Postal Code .....	AK
Lithology Code (-1, 0 = Unknown; 1 = SS, 2 = LS; 3 = Dolo.) .....	1
Geologic Age Code AAPG .....	210
Field Name .....	Milne Point Unit
Reservoir Name .....	Kuparuk MK-1, MK-2, LZ, LK-1, LK-2
Reference Number .....	N/A
Load Number .....	N/A
Formation Name .....	Kuparuk

Record 2:

( 1) Field Acres (Acres) .....	71152
( 2) Proven Acres (Acres) .....	13923
( 3) Well Spacing (Acres) .....	160
( 4) Total Wells (Number) .....	57
( 5) Net Pay (Feet) .....	70
( 6) Gross Pay (Feet) .....	120
( 7) Porosity (%) .....	22
( 8) Initial Oil Saturation (%) .....	70
( 9) Current Oil Saturation (%) .....	N/A
(10) Initial Water Saturation (%) .....	30
(11) Current Water Saturation (%) .....	N/A
(12) Initial Gas Saturation (%) .....	0
(13) Current Gas Saturation (%) .....	N/A
(14) Initial Oil FVF (Res bbl/STB) .....	1.165
(15) Current Oil FVF (Res bbl/STB) .....	N/A
(16) True Vertical Depth (Feet)---Mid-Perforation .....	7200
(17) Formation Temperature (°F) .....	178

Record 3:

(18) Current Formation Pressure (PSI) .....	1200-4400 PSIG
(19) Permeability (md) .....	160
(20) Geologic Age (AAPG) .....	210
(21) API Gravity (°API) .....	21
(22) Oil Viscosity (CP) :e Reservoir condition .....	3.8
(23) Formation Salinity (ppm TDS) .....	22000
(24) OOIP (BBL) .....	263600000
(25) Primary Recovery Factor (Fraction of OOIP) .....	15%
(26) Cumulative Oil Production (BBL) .....	26 x 10 <sup>6</sup>

**Table XIV-14 (continued).**

(27)	Year For Cumulative Oil Production; EX/1986 .....	1992
(28)	Technical Availability Date (Year); Ex/1990 .....	N/A
(29)	Primary Recovery (BBL/AC.FT.) .....	154
(30)	Primary Recovery (BBL) .....	39.5 MMBO (ultimate)
(31)	Year For Primary Recovery .....	N/A
(32)	Current Producing GOR (SCF/BBL) .....	490
(33)	Initial Producing GOR (SCF/BBL) .....	290

Record 4:

(34)	Reservoir Acreage (Acres) .....	11000
(35)	Initial Formation Pressure (PSI) .....	3500
(36)	Reservoir Dip (DEG) .....	2.7°
(37)	Production Wells (Number) .....	39
(38)	Injection Wells (Number) .....	18
(39)	Swept Zone Oil Saturation (%) (Residual to Water) .....	N/A
(40)	Injection Water Salinity (ppm TDS) .....	10000
(41)	Clay Content (%) .....	10
(42)	Dykstra-Parsons Coefficient .....	N/A
(43)	Current Injection Rate (B/D/WELL) .....	2250
(44)	Fractured-Fault (Y,N) (N = 0, Y = 1) .....	1
(45)	Shale Break or Laminations (Y,N) (N = 0, Y = 1) .....	1
(46)	Major Gas Cap (Y,N) (N = 0, Y = 1) .....	0
(47)	Field Multiplier (Number) .....	N/A
(48)	RRC District .....	N/A
(49)	Production Rate (MBBL/D); For the Year shown in element 28 .....	16.3
(50)	Recovery Efficiency-Waterflood (Factor) .....	25%
(51)	Ultimate Recovery Factor (Fraction of OOIP) (Primary Plus Secondary) .....	25%

Record 5:

(52)	Geologic Play Code (Table II) .....	-1
(53)	Depositional System Code (Table III) .....	170
(54)	Depositional System Degree of Confidence (1 = Highest, 2 = Moderate, 3 = Lowest) .....	1
(55)	Diagenetic Overprint Code (Table IV) .....	1
(56)	Diagenetic Overprint Degree of Confidence (1 = Highest, 2 = Moderate, 3 = Lowest) .....	2
(57)	Structural Compartmentalization (Table V) .....	31
(58)	Structural Compartmentalization Degree of Confidence (1 = Highest, 2 = Moderate, 3 = Lowest) .....	1
(59)	Predominant Element of Reservoir Heterogeneity (1 = Depositional System, 2 = Diagenetic Overprint, 3 = Structural Compartmentalization) .....	3
(60)	Trap Type (1 = Stratigraphic, 2 = Structural, 3 = Combination) .....	2
(61)	Geologic Province (Table VI) .....	058



**Table XIV-16.**

**TORIS DATA BASE**  
**FIELD: MILNE POINT (SCHRADER BLUFF)**

Record 1:

Field Code .....	N/A
STATE Postal Code .....	AK
Lithology Code (-1, 0 = Unknown; 1 = SS, 2 = LS; 3 = Dolo.) .....	1
Geologic Age Code AAPG .....	210
Field Name .....	Milne Point Unit (Kuparuk River Field)
Reservoir Name .....	Schrader Bluff Pool
Reference Number .....	N/A
Load Number .....	N/A
Formation Name .....	Schrader Bluff

Record 2:

( 1) Field Acres (Acres) .....	71152
( 2) Proven Acres (Acres) .....	16800
( 3) Well Spacing (Acres) .....	80
( 4) Total Wells (Number) .....	22
( 5) Net Pay (Feet) .....	80
( 6) Gross Pay (Feet) .....	250
( 7) Porosity (%) .....	26
( 8) Initial Oil Saturation (%) .....	65
( 9) Current Oil Saturation (%) .....	65
(10) Initial Water Saturation (%) .....	35
(11) Current Water Saturation (%) .....	35
(12) Initial Gas Saturation (%) .....	N/A
(13) Current Gas Saturation (%) .....	N/A
(14) Initial Oil FVF (Res bbl/STB) .....	1.06
(15) Current Oil FVF (Res bbl/STB) .....	1.06
(16) True Vertical Depth (Feet)----Mid-Perforation .....	4000
(17) Formation Temperature (°F) .....	82

Record 3:

(18) Current Formation Pressure (PSI) .....	1750
(19) Permeability (md) .....	300
(20) Geologic Age (AAPG) .....	210
(21) API Gravity (°API) .....	14-20
(22) Oil Viscosity (CP) :e Reservoir condition .....	305-25
(23) Formation Salinity (ppm TDS) .....	19000
(24) OOIP (BBL) .....	1800000000
(25) Primary Recovery Factor (Fraction of OOIP) .....	12% (estimated)
(26) Cumulative Oil Production (BBL) .....	1464065

**Table XIV-16 (continued).**

(27)	Year For Cumulative Oil Production; EX/1986 .....	1992
(28)	Technical Availability Date (Year); Ex/1990 .....	N/A
(29)	Primary Recovery (BBL/AC.FT.) .....	148
(30)	Primary Recovery (BBL) .....	192000000 ultimate (1464065 to date)
(31)	Year For Primary Recovery .....	ultimate
(32)	Current Producing GOR (SCF/BBL) .....	567
(33)	Initial Producing GOR (SCF/BBL) .....	191

Record 4:

(34)	Reservoir Acreage (Acres) .....	16800
(35)	Initial Formation Pressure (PSI) .....	1750
(36)	Reservoir Dip (DEG) .....	2-3°
(37)	Production Wells (Number) .....	15
(38)	Injection Wells (Number) .....	5
(39)	Swept Zone Oil Saturation (%) (Residual to Water) .....	35
(40)	Injection Water Salinity (ppm TDS) .....	10000
(41)	Clay Content (%) .....	N/A
(42)	Dykstra-Parsons Coefficient .....	N/A
(43)	Current Injection Rate (B/D/WELL) .....	700
(44)	Fractured-Fault (Y,N) (N = 0, Y = 1) .....	1
(45)	Shale Break or Laminations (Y,N) (N = 0, Y = 1) .....	1
(46)	Major Gas Cap (Y,N) (N = 0, Y = 1) .....	0
(47)	Field Multiplier (Number) .....	N/A
(48)	RRC District .....	N/A
(49)	Production Rate (MBBL/D); For the Year shown in element 28 .....	3
(50)	Recovery Efficiency-Waterflood (Factor) .....	21% (ultimate)
(51)	Ultimate Recovery Factor (Fraction of OOIP) (Primary Plus Secondary) .....	21% (ultimate)

Record 5:

(52)	Geologic Play Code (Table II) .....	-1
(53)	Depositional System Code (Table III) .....	172
(54)	Depositional System Degree of Confidence (1 = Highest, 2 = Moderate, 3 = Lowest) .....	2
(55)	Diagenetic Overprint Code (Table IV) .....	1
(56)	Diagenetic Overprint Degree of Confidence (1 = Highest, 2 = Moderate, 3 = Lowest) .....	1
(57)	Structural Compartmentalization (Table V) .....	30
(58)	Structural Compartmentalization Degree of Confidence (1 = Highest, 2 = Moderate, 3 = Lowest) .....	1
(59)	Predominant Element of Reservoir Heterogeneity (1 = Depositional System, 2 = Diagenetic Overprint, 3 = Structural Compartmentalization) .....	3
(60)	Trap Type (1 = Stratigraphic, 2 = Structural, 3 = Combination) .....	2
(61)	Geologic Province (Table VI) .....	058

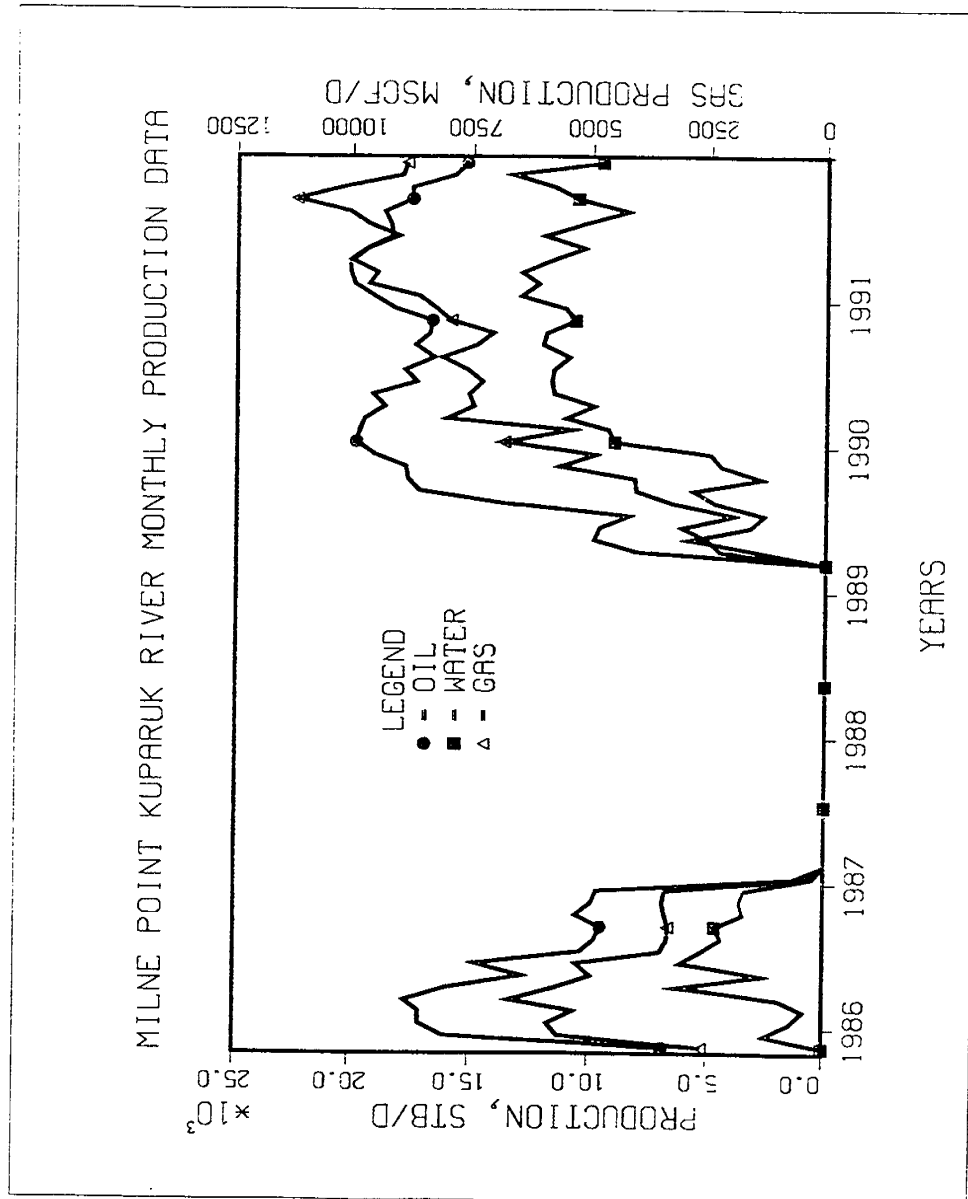


Figure XIV-13.

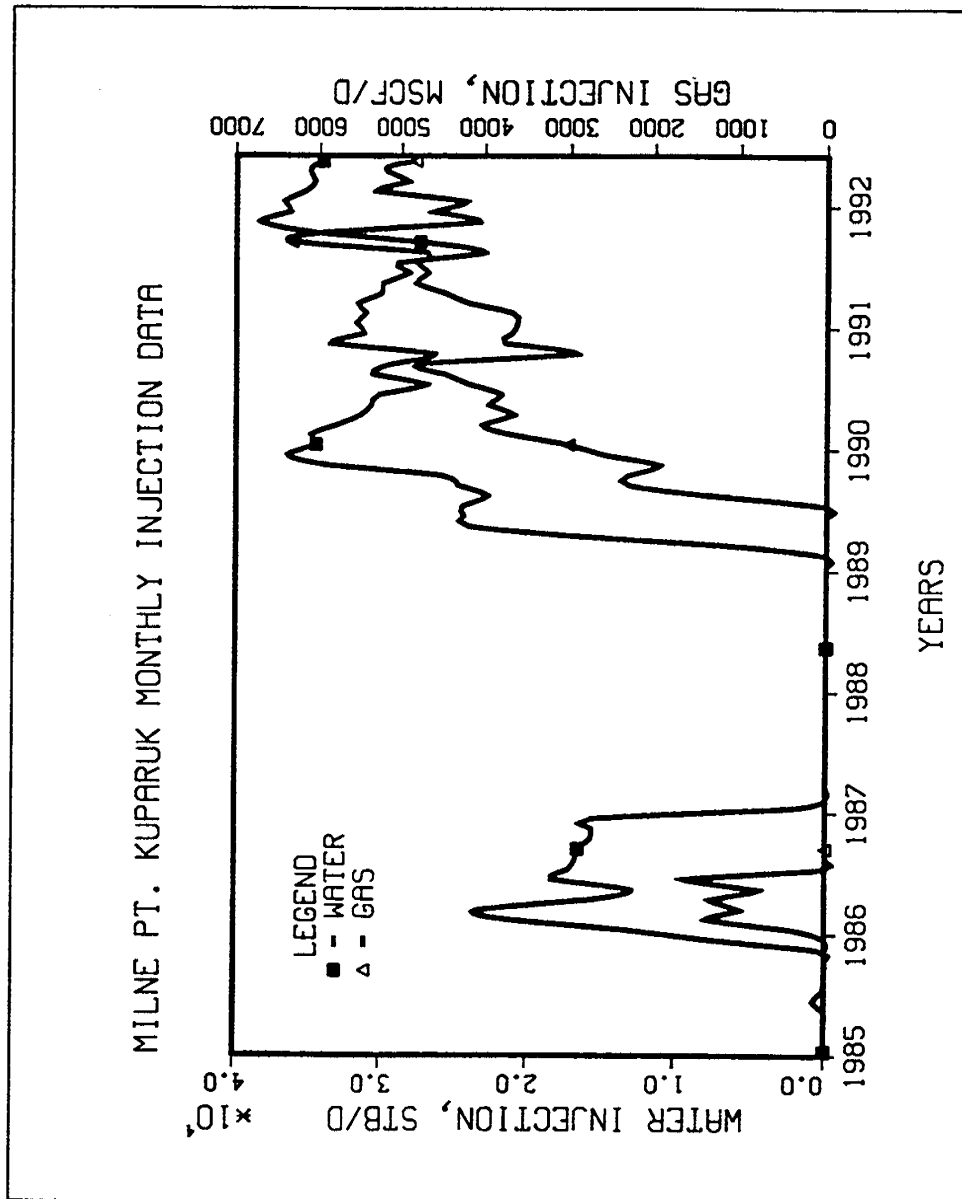


Figure XIV-14.

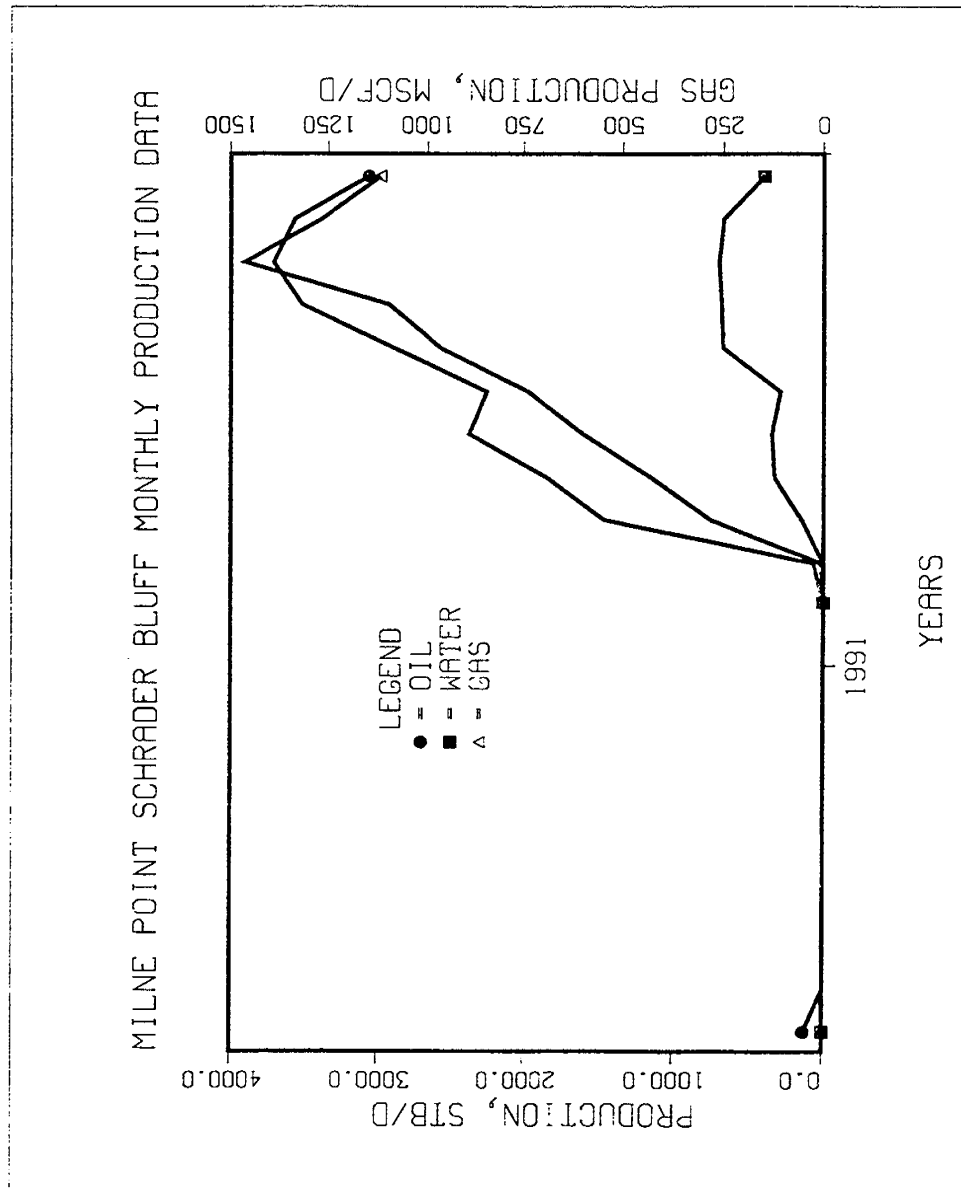


Figure XIV-15.

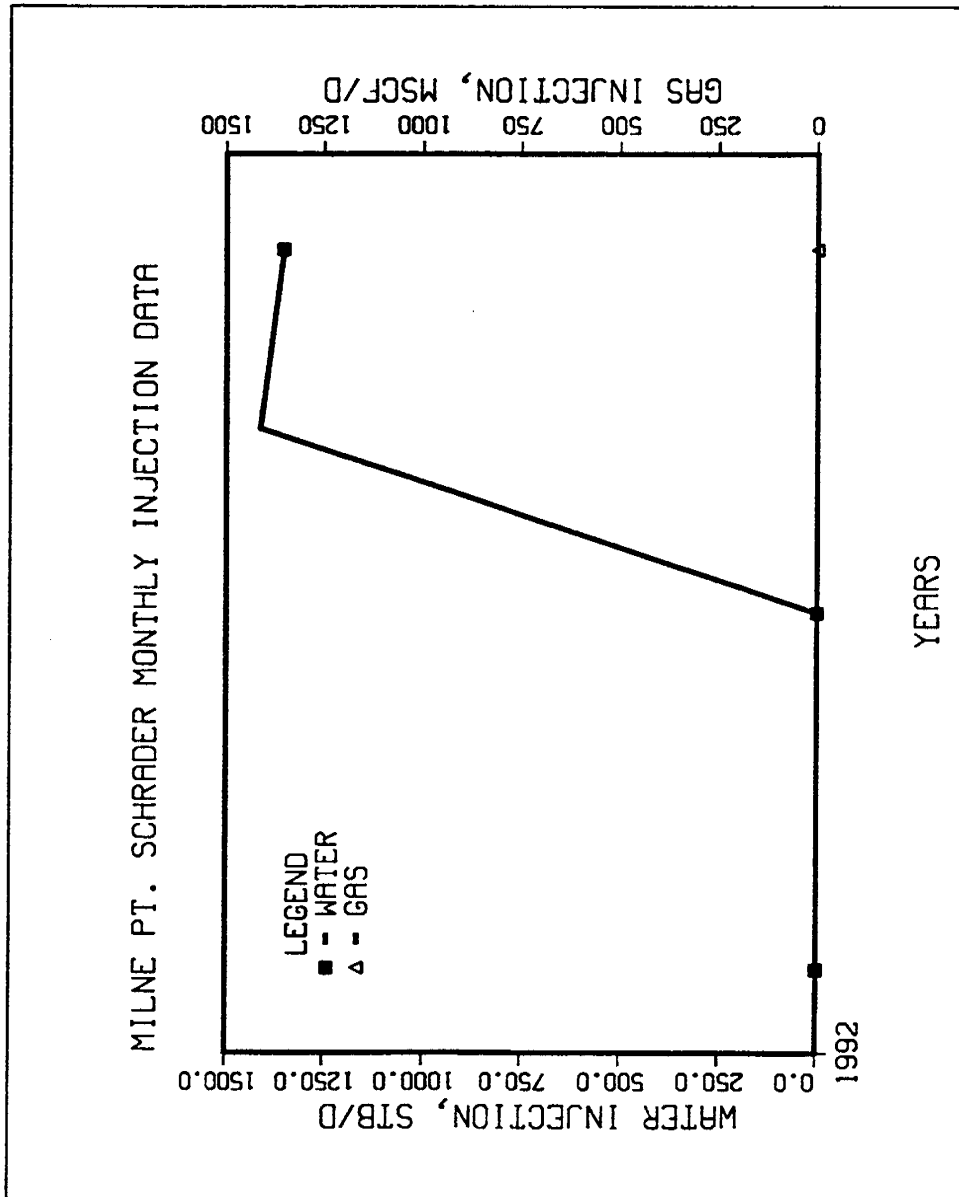


Figure XIV-16.

Table XIV-17.

Reservoir Heterogeneity Classification System for TORIS			
<b>1. Reservoir Identification</b>			
Reservoir Name: <u>West Sak</u>		Geologic Province: <u>Arctic Coastal Plain</u> Date: <u>7/10/92</u>	
Field Name: <u>West Sak</u>		Geologic Age: <u>Upper Cretaceous</u> Prepared By: <u>UAF/PDL</u>	
State: <u>AK</u>		Formation: <u>West Sak</u> Version: <u>1</u>	
<b>2. Depositional System</b> <input type="checkbox"/> 1 <input type="checkbox"/> 2 <input type="checkbox"/> 3 Degree of Confidence in Selection (1=Highest, 3= Lowest)			
Carbonate Reservoirs		Clastic Reservoirs	
<input type="checkbox"/> Lacustrine	<input type="checkbox"/> Reefs ___ Annular Reefs ___ Bioherms ___ Atolls	<input type="checkbox"/> Eolian ___ Ergs ___ Coastal Dunes	<input type="checkbox"/> Strandplain ___ Barrier Cores ___ Barrier Shorefaces
<input type="checkbox"/> Peritidal ___ Supratidal ___ Intertidal ___ Subtidal	<input type="checkbox"/> Slope/Basin ___ Debris Fans ___ Turbidite Fans ___ Mounds	<input type="checkbox"/> Lacustrine ___ Basin Margin ___ Basin Center	<input type="checkbox"/> Shelf (Accretionary Processes) ___ Sand Waves ___ Sand Ridges/Bars
<input type="checkbox"/> Shallow Shelf ___ Open Shelf ___ Restricted Shelf	<input type="checkbox"/> Basin ___ Drowned Shelf ___ Deep Basin	<input type="checkbox"/> Fluvial ___ Braided Streams ___ Meandering Streams	<input type="checkbox"/> Slope/Basin ___ Turbidite Fans ___ Debris Fans
<input type="checkbox"/> Shelf Margin ___ Rimmed Shelf ___ Ramp		<input checked="" type="checkbox"/> Delta ___ Wave-Dominated ___ Fluvial-Dominated ___ Tide-Dominated	<input type="checkbox"/> Basin ___ Pelagic
<b>3. Diagenetic Overprint</b> <input type="checkbox"/> 1 <input type="checkbox"/> 2 <input type="checkbox"/> 3 Degree of Confidence in Selection (1=Highest, 3= Lowest)			
Carbonate Reservoirs		Clastic Reservoirs	
<input type="checkbox"/> Compaction/Cementation	<input type="checkbox"/> Dolomitization	<input type="checkbox"/> Compaction/Cementation	<input checked="" type="checkbox"/> Authigenic Clay
<input type="checkbox"/> Grain Enhancement	<input type="checkbox"/> Massive Dissolution	<input type="checkbox"/> Intergranular Dissolution	<input type="checkbox"/> Chertification
<input type="checkbox"/> Dolomitization	<input type="checkbox"/> Silicification		
<b>4. Structural Compartmentalization</b> <input type="checkbox"/> 1 <input type="checkbox"/> 2 <input type="checkbox"/> 3 Degree of Confidence in Selection (1=Highest, 3= Lowest)			
<input type="checkbox"/> Natural Fracture Porosity	<input type="checkbox"/> Unstructured	<input checked="" type="checkbox"/> Faulted ___ Normal Fault ___ Reverse Fault ___ Strike-Slip Fault	<input type="checkbox"/> Fault/Fold ___ Normal Fault ___ Reverse Fault ___ Strike-Slip Fault
			<input type="checkbox"/> Folded
<b>5. Reservoir Heterogeneity Ternary Diagram</b>			
Predominant Element of Reservoir Heterogeneity: (Check Only One)		100% Depositional System	
<input type="checkbox"/> Depositional System	___		
<input type="checkbox"/> Diagenetic Overprint	___		
<input type="checkbox"/> Structural Compartmentalization	___		
<b>6. Trap Type</b> <input type="checkbox"/> Stratigraphic <input type="checkbox"/> Structural <input checked="" type="checkbox"/> Combination			
<b>7. Optional Comments (References, Details on Above Selections, Etc.)</b>			

**Table XIV-18.**

**TORIS DATA BASE  
FIELD: WEST SAK**

**Record 1:**

Field Code .....	N/A
STATE Postal Code .....	AK
Lithology Code (-1, 0 = Unknown; 1 = SS, 2 = LS; 3 = Dolo.) .....	1
Geologic Age Code AAPG .....	211
Field Name .....	West Sak
Reservoir Name .....	West Sak
Reference Number .....	N/A
Load Number .....	N/A
Formation Name .....	West Sak

**Record 2:**

( 1) Field Acres (Acres) .....	166400
( 2) Proven Acres (Acres) .....	N/A
( 3) Well Spacing (Acres) .....	N/A
( 4) Total Wells (Number) .....	N/A
( 5) Net Pay (Feet) .....	90
( 6) Gross Pay (Feet) .....	300
( 7) Porosity (%) .....	30
( 8) Initial Oil Saturation (%) .....	68.0
( 9) Current Oil Saturation (%) .....	64
(10) Initial Water Saturation (%) .....	32
(11) Current Water Saturation (%) .....	36
(12) Initial Gas Saturation (%) .....	0
(13) Current Gas Saturation (%) .....	0
(14) Initial Oil FVF (Res bbl/STB) .....	N/A
(15) Current Oil FVF (Res bbl/STB) .....	N/A
(16) True Vertical Depth (Feet)---Mid-Perforation .....	2500-4500
(17) Formation Temperature (°F) .....	70 (@ 3500 ft.)

**Record 3:**

(18) Current Formation Pressure (PSI) .....	1500 (@ 3500 ft.)
(19) Permeability (md) .....	75
(20) Geologic Age (AAPG) .....	211
(21) API Gravity (°API) .....	19
(22) Oil Viscosity (CP) :e Reservoir condition .....	1525.0
(23) Formation Salinity (ppm TDS) .....	6000 (@ 75°F)
(24) OOIP (BBL) .....	15-25 x 10 <sup>9</sup>
(25) Primary Recovery Factor (Fraction of OOIP) .....	N/A
(26) Cumulative Oil Production (BBL) .....	N/A

**Table XIV-18 (continued).**

(27)	Year For Cumulative Oil Production; EX/1986 .....	N/A
(28)	Technical Availability Date (Year); Ex/1990 .....	N/A
(29)	Primary Recovery (BBL/AC.FT.) .....	N/A
(30)	Primary Recovery (BBL) .....	N/A
(31)	Year For Primary Recovery .....	N/A
(32)	Current Producing GOR (SCF/BBL) .....	N/A
(33)	Initial Producing GOR (SCF/BBL) .....	N/A

Record 4:

(34)	Reservoir Acreage (Acres) .....	166400
(35)	Initial Formation Pressure (PSI) .....	N/A
(36)	Reservoir Dip (DEG) .....	1.5
(37)	Production Wells (Number) .....	N/A
(38)	Injection Wells (Number) .....	N/A
(39)	Swept Zone Oil Saturation: (%) (Residual to Water) .....	N/A
(40)	Injection Water Salinity (ppm TDS) .....	N/A
(41)	Clay Content (%) .....	17.5
(42)	Dykstra-Parsons Coefficient .....	N/A
(43)	Current Injection Rate (B/D/WELL) .....	N/A
(44)	Fractured-Fault (Y,N) (N = 0, Y = 1) .....	N/A
(45)	Shale Break or Laminations (Y,N) (N = 0, Y = 1) .....	0
(46)	Major Gas Cap (Y,N) (N = 0, Y = 1) .....	0
(47)	Field Multiplier (Number) .....	N/A
(48)	RRC District .....	N/A
(49)	Production Rate (MBBL/D); For the Year shown in element 28 ....	N/A
(50)	Recovery Efficiency-Waterflood (Factor) .....	N/A
(51)	Ultimate Recovery Factor (Fraction of OOIP) (Primary Plus Secondary) .....	N/A

Record 5:

(52)	Geologic Play Code (Table II) .....	-1
(53)	Depositional System Code (Table III) .....	152
(54)	Depositional System Degree of Confidence (1 = Highest, 2 = Moderate, 3 = Lowest) .....	N/A
(55)	Diagenetic Overprint Code (Table IV) .....	8
(56)	Diagenetic Overprint Degree of Confidence (1 = Highest, 2 = Moderate, 3 = Lowest) .....	N/A
(57)	Structural Compartmentalization (Table V) .....	31
(58)	Structural Compartmentalization Degree of Confidence (1 = Highest, 2 = Moderate, 3 = Lowest) .....	N/A
(59)	Predominant Element of Reservoir Heterogeneity (1 = Depositional System, 2 = Diagenetic Overprint, 3 = Structural Compartmentalization) .....	N/A
(60)	Trap Type (1 = Stratigraphic, 2 = Structural, 3 = Combination) ....	3
(61)	Geologic Province (Table VI) .....	058

Table XIV-19.

Reservoir Heterogeneity Classification System for TORIS		
<b>1. Reservoir Identification</b>		
Reservoir Play: _____		
Reservoir Name: <u>Ugnu</u>	Geologic Province: <u>Arctic Coastal Plain</u>	Date: <u>7/10/92</u>
Field Name: <u>Upper Ugnu</u>	Geologic Age: <u>Cretaceous/Upper</u>	Prepared By: <u>UAF/PDL</u>
State: <u>AK</u>	Formation: _____	Version: <u>1</u>
<b>2. Depositional System</b> <input checked="" type="checkbox"/> 1 <input type="checkbox"/> 2 <input type="checkbox"/> 3 Degree of Confidence in Selection (1=Highest, 3= Lowest)		
<p style="text-align: center;">Carbonate Reservoirs</p> <div style="display: flex; justify-content: space-between;"> <div style="width: 45%;"> <input type="checkbox"/> Lacustrine   <input type="checkbox"/> Peritidal            ___ Supratidal            ___ Intertidal            ___ Subtidal   <input type="checkbox"/> Shallow Shelf            ___ Open Shelf            ___ Restricted Shelf   <input type="checkbox"/> Shelf Margin            ___ Rimmed Shelf            ___ Ramp </div> <div style="width: 45%;"> <input type="checkbox"/> Reefs            ___ Princes Reefs            ___ Solerps            ___ Atolls   <input type="checkbox"/> Slope/Basin            ___ Carbon Fans            ___ Turbidite Fans   <input type="checkbox"/> Basin            ___ Mounds            ___ Drowned Shelf            ___ Deep Basin </div> </div>	<p style="text-align: center;">Clastic Reservoirs</p> <div style="display: flex; justify-content: space-between;"> <div style="width: 45%;"> <input type="checkbox"/> Eolian            ___ Ergs            ___ Coastal Dunes   <input type="checkbox"/> Lacustrine            ___ Basin Margin            ___ Basin Center   <input type="checkbox"/> Fluvial            ___ Braided Streams            ___ Meandering Streams   <input type="checkbox"/> Alluvial Fan            ___ Humid (Stream-Dominated)            ___ Arid/Semi-Arid            ___ Fan Deltas   <input checked="" type="checkbox"/> Delta            ___ Wave-Dominated            ___ Fluvial-Dominated            ___ Tide-Dominated </div> <div style="width: 45%;"> <input type="checkbox"/> Strandplain            ___ Barrier Cores            ___ Barrier Shoals            ___ Back Barriers            ___ Tidal Channels            ___ Washover Fan/Tidal Delta   <input type="checkbox"/> Shelf (Accretionary Processes)            ___ Sand Waves            ___ Sand Ridge/Bars   <input type="checkbox"/> Slope/Basin            ___ Turbidite Fans            ___ Carbon Fans   <input type="checkbox"/> Basin            ___ Pelagic </div> </div>	
<b>3. Diagenetic Overprint</b> <input type="checkbox"/> 1 <input checked="" type="checkbox"/> 2 <input type="checkbox"/> 3 Degree of Confidence in Selection (1=Highest, 3= Lowest)		
<p style="text-align: center;">Carbonate Reservoirs</p> <div style="display: flex; justify-content: space-between;"> <div style="width: 45%;"> <input type="checkbox"/> Compaction/Compaction  <input type="checkbox"/> Grain Enhancement  <input type="checkbox"/> Dolomitization </div> <div style="width: 45%;"> <input type="checkbox"/> Cementation (Evaporites)  <input type="checkbox"/> Massive Dissolution  <input type="checkbox"/> Silification </div> </div>	<p style="text-align: center;">Clastic Reservoirs</p> <div style="display: flex; justify-content: space-between;"> <div style="width: 45%;"> <input type="checkbox"/> Compaction/Compaction  <input type="checkbox"/> Intergranular Dissolution </div> <div style="width: 45%;"> <input checked="" type="checkbox"/> Authigenic Clay  <input type="checkbox"/> Chertification </div> </div>	
<b>4. Structural Compartmentalization</b> <input checked="" type="checkbox"/> 1 <input type="checkbox"/> 2 <input type="checkbox"/> 3 Degree of Confidence in Selection (1=Highest, 3= Lowest)		
<input type="checkbox"/> Natural Fracture Persesty  <input type="checkbox"/> L-structured	<input checked="" type="checkbox"/> Faulted ___ Normal Fault ___ Reverse Fault ___ Strike-Slip Fault	<input type="checkbox"/> Fault/Fold  <input type="checkbox"/> Folded ___ Normal Fault ___ Reverse Fault ___ Strike-Slip Fault
<b>5. Reservoir Heterogeneity Ternary Diagram</b>		
<p>Predominant Element of Reservoir Heterogeneity: (Check Only One)</p> <ul style="list-style-type: none"> <li>• Depositional System _____</li> <li>• Diagenetic Overprint _____</li> <li>• Structural Compartmentalization _____</li> </ul>		
<b>6. Trap Type</b> <input type="checkbox"/> Stratigraphic <input type="checkbox"/> Structural <input checked="" type="checkbox"/> Combination		
<b>7. Optional Comments (References, Details on Above Selections, Etc.)</b>		
<p>"Resource Description and Development Issues for the Ugnu Reservoir, North Slope Alaska," SPE 21779, R. J. Hallam, et al.</p>		

**Table XIV-20.**

**TORIS DATA BASE**  
**FIELD: UPPER UGNU (UGNU)**

**Record 1:**

Field Code .....	N/A
STATE Postal Code .....	AK
Lithology Code (-1, 0 = Unknown; 1 = SS, 2 = LS; 3 = Dolo.) .....	0
Geologic Age Code AAPG .....	211
Field Name .....	Upper Ugnu
Reservoir Name .....	Ugnu
Reference Number .....	N/A
Load Number .....	N/A
Formation Name .....	N/A

**Record 2:**

( 1) Field Acres (Acres) .....	64000
( 2) Proven Acres (Acres) .....	N/A
( 3) Well Spacing (Acres) .....	N/A
( 4) Total Wells (Number) .....	N/A
( 5) Net Pay (Feet) .....	65
( 6) Gross Pay (Feet) .....	112.5
( 7) Porosity (%) .....	32.5
( 8) Initial Oil Saturation (%) .....	69
( 9) Current Oil Saturation (%) .....	N/A
(10) Initial Water Saturation (%) .....	N/A
(11) Current Water Saturation (%) .....	N/A
(12) Initial Gas Saturation (%) .....	N/A
(13) Current Gas Saturation (%) .....	N/A
(14) Initial Oil FVF (Res bbl/STB) .....	1.0
(15) Current Oil FVF (Res bbl/STB) .....	1.0
(16) True Vertical Depth (Feet)---Mid-Perforation .....	2600
(17) Formation Temperature (°F) .....	5.5

**Record 3:**

(18) Current Formation Pressure (PSI) .....	1150
(19) Permeability (md) .....	1600
(20) Geologic Age (AAPG) .....	211
(21) API Gravity (°API) .....	10
(22) Oil Viscosity (CP) :e Reservoir condition .....	7,550,000
(23) Formation Salinity (ppm TDS) .....	N/A
(24) OOIP (BBL) .....	6.5 x 10 <sup>9</sup>
(25) Primary Recovery Factor (Fraction of OOIP) .....	N/A
(26) Cumulative Oil Production (BBL) .....	N/A

**Table XIV-20 (continued).**

(27)	Year For Cumulative Oil Production; EX/1986 .....	1992
(28)	Technical Availability Date (Year); Ex/1990 .....	N/A
(29)	Primary Recovery (BBL/AC.FT.) .....	N/A
(30)	Primary Recovery (BBL) .....	N/A
(31)	Year For Primary Recovery .....	N/A
(32)	Current Producing GOR (SCF/BBL) .....	75
(33)	Initial Producing GOR (SCF/BBL) .....	125

Record 4:

(34)	Reservoir Acreage (Acres) .....	N/A
(35)	Initial Formation Pressure (PSI) .....	1330
(36)	Reservoir Dip (DEG) .....	1.5
(37)	Production Wells (Number) .....	N/A
(38)	Injection Wells (Number) .....	N/A
(39)	Swept Zone Oil Saturation (%) (Residual to Water) .....	N/A
(40)	Injection Water Salinity (ppm TDS) .....	N/A
(41)	Clay Content (%) .....	6-47
(42)	Dykstra-Parsons Coefficient .....	N/A
(43)	Current Injection Rate (B/D/WELL) .....	N/A
(44)	Fractured-Fault (Y,N) (N = 0, Y = 1) .....	N/A
(45)	Shale Break or Laminations (Y,N) (N = 0, Y = 1) .....	0
(46)	Major Gas Cap (Y,N) (N = 0, Y = 1) .....	0
(47)	Field Multiplier (Number) .....	1
(48)	RRC District .....	N/A
(49)	Production Rate (MBBL/D); For the Year shown in element 28 ....	N/A
(50)	Recovery Efficiency-Waterflood (Factor) .....	N/A
(51)	Ultimate Recovery Factor (Fraction of OOIP) (Primary Plus Secondary) .....	N/A

Record 5:

(52)	Geologic Play Code (Table II) .....	-1
(53)	Depositional System Code (Table III) .....	151
(54)	Depositional System Degree of Confidence (1 = Highest, 2 = Moderate, 3 = Lowest) .....	1
(55)	Diagenetic Overprint Code (Table IV) .....	8
(56)	Diagenetic Overprint Degree of Confidence (1 = Highest, 2 = Moderate, 3 = Lowest) .....	2
(57)	Structural Compartmentalization (Table V) .....	31
(58)	Structural Compartmentalization Degree of Confidence (1 = Highest, 2 = Moderate, 3 = Lowest) .....	1
(59)	Predominant Element of Reservoir Heterogeneity (1 = Depositional System, 2 = Diagenetic Overprint, 3 = Structural Compartmentalization) .....	N/A
(60)	Trap Type (1 = Stratigraphic, 2 = Structural, 3 = Combination) ....	3
(61)	Geologic Province (Table VI) .....	058

Table XIV-21.

Reservoir Heterogeneity Classification System for TORIS		
<b>1. Reservoir Identification</b> Reservoir Play: _____ Reservoir Name: <u>Ugnu</u> Geologic Province: <u>Arctic Coastal Plain</u> Date: <u>7/10/92</u> Field Name: <u>Lower Ugnu</u> Geologic Age: <u>Cretaceous/Upper</u> Prepared By: <u>PDL/UAF</u> State: <u>AK</u> Formation: _____      Version: <u>1</u>		
<b>2. Depositional System</b> <input type="checkbox"/> 1 <input type="checkbox"/> 2 <input type="checkbox"/> 3      Degree of Confidence in Selection      (1=Highest, 3= Lowest)		
<b>Carbonate Reservoirs</b> <input type="checkbox"/> Lacustrine <input type="checkbox"/> Paritidal ___ Supratidal ___ Intertidal ___ Subtidal <input type="checkbox"/> Shallow Shelf ___ Open Shelf ___ Restricted Shelf <input type="checkbox"/> Shelf Margin ___ Rimmed Shelf ___ Ramp <input type="checkbox"/> Reefs ___ Pinnacle Reefs ___ Bioherms ___ Atolls <input type="checkbox"/> Slope/Basin ___ Debris Fans ___ Turbidite Fans ___ Mounds <input type="checkbox"/> Basin ___ Drowned Shelf ___ Deep Basin	<b>Clastic Reservoirs</b> <input type="checkbox"/> Eolian ___ Ergs ___ Coastal Dunes <input type="checkbox"/> Lacustrine ___ Basin Margin ___ Basin Center <input type="checkbox"/> Fluvial ___ Braided Streams ___ Meandering Streams <input type="checkbox"/> Alluvial Fan ___ Humid (Stream-Dominated) ___ Arid/Semi-Arid ___ Fan Deltas <input checked="" type="checkbox"/> Delta ___ Wave-Dominated ___ Fluvial-Dominated ___ Tide-Dominated <input type="checkbox"/> Strandplain ___ Barrier Cores ___ Barrier Shorefaces ___ Back Barriers ___ Tidal Channels ___ Washover Fan/Tidal Deltas <input type="checkbox"/> Shelf (Accretionary Processes) ___ Sand Waves ___ Sand Ridges/Bars <input type="checkbox"/> Slope/Basin ___ Turbidite Fans ___ Debris Fans <input type="checkbox"/> Basin ___ Pelagic	
<b>3. Diagenetic Overprint</b> <input type="checkbox"/> 1 <input type="checkbox"/> 2 <input type="checkbox"/> 3      Degree of Confidence in Selection      (1=Highest, 3= Lowest)		
<b>Carbonate Reservoirs</b> <input type="checkbox"/> Compaction/Cementation <input type="checkbox"/> Grain Enhancement <input type="checkbox"/> Dolomitization <input type="checkbox"/> Dolomitization (Evaporites) <input type="checkbox"/> Massive Dissolution <input type="checkbox"/> Silicification	<b>Clastic Reservoirs</b> <input type="checkbox"/> Compaction/Cementation <input type="checkbox"/> Intergranular Dissolution <input checked="" type="checkbox"/> Authigenic Clay <input type="checkbox"/> Chertification	
<b>4. Structural Compartmentalization</b> <input type="checkbox"/> 1 <input type="checkbox"/> 2 <input checked="" type="checkbox"/> 3      Degree of Confidence in Selection      (1=Highest, 3= Lowest)		
<input type="checkbox"/> Natural Fracture Porosity <input type="checkbox"/> Unstructured <input checked="" type="checkbox"/> Faulted <input type="checkbox"/> Fault/Fold <input type="checkbox"/> Folded X Normal Fault      ___ Normal Fault ___ Reverse Fault    ___ Reverse Fault ___ Strike-Slip Fault    ___ Strike-Slip Fault		
<b>5. Reservoir Heterogeneity Ternary Diagram</b> Predominant Element of Reservoir Heterogeneity: (Check Only One) • Depositional System      ___ • Diagenetic Overprint      ___ • Structural Compartmentalization      ___		
<b>6. Trap Type</b> <input type="checkbox"/> Stratigraphic <input type="checkbox"/> Structural <input checked="" type="checkbox"/> Combination		
<b>7. Optional Comments (References, Details on Above Selections, Etc.)</b> _____ _____ _____ _____		

**Table XIV-22.**

**TORIS DATA BASE**  
**FIELD: KUPARUK (LOWER UGNU)**

Record 1:

Field Code .....	N/A
STATE Postal Code .....	AK
Lithology Code (-1, 0 = Unknown; 1 = SS, 2 = LS; 3 = Dolo.) .....	1
Geologic Age Code AAPG .....	211
Field Name .....	Kuparuk
Reservoir Name .....	Ugnu
Reference Number .....	N/A
Load Number .....	N/A
Formation Name .....	Lower Ugnu

Record 2:

( 1) Field Acres (Acres) .....	76800
( 2) Proven Acres (Acres) .....	N/A
( 3) Well Spacing (Acres) .....	N/A
( 4) Total Wells (Number) .....	N/A
( 5) Net Pay (Feet) .....	65
( 6) Gross Pay (Feet) .....	112.5
( 7) Porosity (%) .....	32.5
( 8) Initial Oil Saturation (%) .....	69
( 9) Current Oil Saturation (%) .....	69
(10) Initial Water Saturation (%) .....	N/A
(11) Current Water Saturation (%) .....	N/A
(12) Initial Gas Saturation (%) .....	N/A
(13) Current Gas Saturation (%) .....	N/A
(14) Initial Oil FVF (Res bbl/STB) .....	1.0
(15) Current Oil FVF (Res bbl/STB) .....	1.0
(16) True Vertical Depth (Feet)----Mid-Perforation .....	2600
(17) Formation Temperature (°F) .....	55

Record 3:

(18) Current Formation Pressure (PSI) .....	1150
(19) Permeability (md) .....	1600
(20) Geologic Age (AAPG) .....	211
(21) API Gravity (°API) .....	10
(22) Oil Viscosity (CP) :e Reservoir condition .....	7,550,000
(23) Formation Salinity (ppm TDS) .....	18250
(24) OOIP (BBL) .....	6-11 x 10 <sup>9</sup>
(25) Primary Recovery Factor (Fraction of OOIP) .....	N/A
(26) Cumulative Oil Production (BBL) .....	N/A

**Table XIV-22 (continued).**

(27)	Year For Cumulative Oil Production; EX/1986 .....	1992
(28)	Technical Availability Date (Year); Ex/1990 .....	N/A
(29)	Primary Recovery (BBL/AC.FT.) .....	N/A
(30)	Primary Recovery (BBL) .....	N/A
(31)	Year For Primary Recovery .....	N/A
(32)	Current Producing GOR (SCF/BBL) .....	75
(33)	Initial Producing GOR (SCF/BBL) .....	N/A

Record 4:

(34)	Reservoir Acreage (Acres) .....	104800
(35)	Initial Formation Pressure (PSI) .....	N/A
(36)	Reservoir Dip (DEG) .....	2
(37)	Production Wells (Number) .....	N/A
(38)	Injection Wells (Number) .....	N/A
(39)	Swept Zone Oil Saturation (%) (Residual to Water) .....	N/A
(40)	Injection Water Salinity (ppm TDS) .....	N/A
(41)	Clay Content (%) .....	2.5
(42)	Dykstra-Parsons Coefficient .....	N/A
(43)	Current Injection Rate (B/D/WELL) .....	N/A
(44)	Fractured-Fault (Y,N) (N = 0, Y = 1) .....	N/A
(45)	Shale Break or Laminations (Y,N) (N = 0, Y = 1) .....	0
(46)	Major Gas Cap (Y,N) (N = 0, Y = 1) .....	0
(47)	Field Multiplier (Number) .....	1
(48)	RRC District .....	N/A
(49)	Production Rate (MBBL/D); For the Year shown in element 28 .....	N/A
(50)	Recovery Efficiency-Waterflood (Factor) .....	N/A
(51)	Ultimate Recovery Factor (Fraction of OOIP) (Primary Plus Secondary) .....	N/A

Record 5:

(52)	Geologic Play Code (Table II) .....	-1
(53)	Depositional System Code (Table III) .....	152
(54)	Depositional System Degree of Confidence (1 = Highest, 2 = Moderate, 3 = Lowest) .....	N/A
(55)	Diagenetic Overprint Code (Table IV) .....	8
(56)	Diagenetic Overprint Degree of Confidence (1 = Highest, 2 = Moderate, 3 = Lowest) .....	N/A
(57)	Structural Compartmentalization (Table V) .....	31
(58)	Structural Compartmentalization Degree of Confidence (1 = Highest, 2 = Moderate, 3 = Lowest) .....	N/A
(59)	Predominant Element of Reservoir Heterogeneity (1 = Depositional System, 2 = Diagenetic Overprint, 3 = Structural Compartmentalization) .....	N/A
(60)	Trap Type (1 = Stratigraphic, 2 = Structural, 3 = Combination) .....	3
(61)	Geologic Province (Table VI) .....	058

Table XIV-23.

Reservoir Heterogeneity Classification System for TORIS			
<b>1. Reservoir Identification</b>		Reservoir Play: _____	
Reservoir Name: <u>Middle Kenai B</u>	Geologic Province: <u>Cook Inlet Basin</u>	Date: <u>7/10/92</u>	
Field Name: <u>Trading Bay</u>	Geologic Age: _____	Prepared By: <u>UAF/PDL</u>	
State: <u>AK</u>	Formation: <u>Tyonek</u>	Version: <u>1</u>	
<b>2. Depositional System</b> <span style="float: right;">Degree of Confidence in Selection (1=Highest, 3= Lowest)</span>			
<b>Carbonate Reservoirs</b> <input type="checkbox"/> Lacustrine <input type="checkbox"/> Peritidal ___ Supratidal ___ Intertidal ___ Subtidal <input type="checkbox"/> Shallow Shelf ___ Open Shelf ___ Restricted Shelf <input type="checkbox"/> Shelf Margin ___ Rimmed Shelf ___ Ramp <input type="checkbox"/> Reefs ___ Pinnacle Reefs ___ Bioherms ___ Atolls <input type="checkbox"/> Slope/Basin ___ Debris Fans ___ Turbidite Fans ___ Mounds <input type="checkbox"/> Basin ___ Drowned Shelf ___ Deep Basin		<b>Clastic Reservoirs</b> <input type="checkbox"/> Eolian ___ Ergs ___ Coastal Dunes <input type="checkbox"/> Lacustrine ___ Basin Margin ___ Basin Center <input type="checkbox"/> Fluvial ___ Braided Streams ___ Meandering Streams <input type="checkbox"/> Alluvial Fan ___ Humid (Stream-Dominated) ___ Arid/Semi-Arid ___ Fan Deltas <input type="checkbox"/> Delta ___ Wave-Dominated ___ Fluvial-Dominated ___ Tide-Dominated <input type="checkbox"/> Strandplain ___ Barrier Cores ___ Barrier Shoetaces ___ Back Barriers ___ Tidal Channels ___ Washover Fan/Tidal Deltas <input type="checkbox"/> Shelf (Accretionary Processes) ___ Sand Waves ___ Sand Ridge/Bars <input type="checkbox"/> Slope/Basin ___ Turbidite Fans ___ Debris Fans <input type="checkbox"/> Basin ___ Pelagic	
<b>3. Diagenetic Overprint</b> <span style="float: right;">Degree of Confidence in Selection (1=Highest, 3= Lowest)</span>			
<b>Carbonate Reservoirs</b> <input type="checkbox"/> Compaction/Cementation <input type="checkbox"/> Grain Enhancement <input type="checkbox"/> Dolomitization <input type="checkbox"/> Dolomitization (Evaporites) <input type="checkbox"/> Massive Dissolution <input type="checkbox"/> Silicification		<b>Clastic Reservoirs</b> <input type="checkbox"/> Compaction/Cementation <input type="checkbox"/> Intergranular Dissolution <input type="checkbox"/> Authigenic Clay <input type="checkbox"/> Chertification	
<b>4. Structural Compartmentalization</b> <span style="float: right;">Degree of Confidence in Selection (1=Highest, 3= Lowest)</span>			
<input type="checkbox"/> Natural Fracture Porosity <input type="checkbox"/> Unstructured <input type="checkbox"/> Faulted ___ Normal Fault ___ Reverse Fault ___ Strike-Slip Fault <input type="checkbox"/> Fault/Fold <input type="checkbox"/> Folded ___ Normal Fault ___ Reverse Fault ___ Strike-Slip Fault			
<b>5. Reservoir Heterogeneity Ternary Diagram</b>			
Predominant Element of Reservoir Heterogeneity: (Check Only One)		100% Depositional System	
<input type="checkbox"/> Depositional System <input type="checkbox"/> Diagenetic Overprint <input type="checkbox"/> Structural Compartmentalization			
<b>6. Trap Type</b> <span style="float: right;">Degree of Confidence in Selection (1=Highest, 3= Lowest)</span>			
<input type="checkbox"/> Stratigraphic <input type="checkbox"/> Structural <input type="checkbox"/> Combination			
<b>7. Optional Comments (References, Details on Above Selections, Etc.)</b>			
_____ _____ _____			

**Table XIV-24.**

**TORIS DATA BASE**  
**FIELD: TRADING BAY (MIDDLE KENAI B)**

**Record 1:**

Field Code .....	N/A
STATE Postal Code .....	AK
Lithology Code (-1, 0 = Unknown; 1 = SS, 2 = LS; 3 = Dolo.) .....	-1
Geologic Age Code AAPG .....	-1
Field Name .....	Trading Bay
Reservoir Name .....	Middle Kenai B
Reference Number .....	N/A
Load Number .....	N/A
Formation Name .....	Tyonek

**Record 2:**

( 1) Field Acres (Acres) .....	N/A
( 2) Proven Acres (Acres) .....	N/A
( 3) Well Spacing (Acres) .....	N/A
( 4) Total Wells (Number) .....	8
( 5) Net Pay (Feet) .....	N/A
( 6) Gross Pay (Feet) .....	N/A
( 7) Porosity (%) .....	N/A
( 8) Initial Oil Saturation (%) .....	N/A
( 9) Current Oil Saturation (%) .....	N/A
(10) Initial Water Saturation (%) .....	N/A
(11) Current Water Saturation (%) .....	N/A
(12) Initial Gas Saturation (%) .....	N/A
(13) Current Gas Saturation (%) .....	N/A
(14) Initial Oil FVF (Res bbl/STB) .....	N/A
(15) Current Oil FVF (Res bbl/STB) .....	N/A
(16) True Vertical Depth (Feet)---Mid-Perforation .....	N/A
(17) Formation Temperature (°F) .....	N/A

**Record 3:**

(18) Current Formation Pressure (PSI) .....	N/A
(19) Permeability (md) .....	N/A
(20) Geologic Age (AAPG) .....	N/A
(21) API Gravity (°API) .....	20.0
(22) Oil Viscosity (CP) :e Reservoir condition .....	N/A
(23) Formation Salinity (ppm TDS) .....	N/A
(24) OOIP (BBL) .....	N/A
(25) Primary Recovery Factor (Fraction of OOIP) .....	N/A
(26) Cumulative Oil Production (BBL) .....	2,493,671

**Table XIV-24 (continued).**

(27)	Year For Cumulative Oil Production; EX/1986 .....	1990
(28)	Technical Availability Date (Year); Ex/1990 .....	N/A
(29)	Primary Recovery (BBL/AC.FT.) .....	N/A
(30)	Primary Recovery (BBL) .....	N/A
(31)	Year For Primary Recovery .....	N/A
(32)	Current Producing GOR (SCF/BBL) .....	406 (1990)
(33)	Initial Producing GOR (SCF/BBL) .....	N/A

Record 4:

(34)	Reservoir Acreage (Acres) .....	N/A
(35)	Initial Formation Pressure (PSI) .....	N/A
(36)	Reservoir Dip (DEG) .....	N/A
(37)	Production Wells (Number) .....	8
(38)	Injection Wells (Number) .....	0
(39)	Swept Zone Oil Saturation (%) (Residual to Water) .....	N/A
(40)	Injection Water Salinity (ppm TDS) .....	N/A
(41)	Clay Content (%) .....	N/A
(42)	Dykstra-Parsons Coefficient .....	N/A
(43)	Current Injection Rate (B/D/WELL) .....	N/A
(44)	Fractured-Fault (Y,N) (N = 0, Y = 1) .....	N/A
(45)	Shale Break or Laminations (Y,N) (N = 0, Y = 1) .....	N/A
(46)	Major Gas Cap (Y,N) (N = 0, Y = 1) .....	N/A
(47)	Field Multiplier (Number) .....	N/A
(48)	RRC District .....	N/A
(49)	Production Rate (MBBL/D); For the Year shown in element 28 .....	0.2835
(50)	Recovery Efficiency-Waterflood (Factor) .....	N/A
(51)	Ultimate Recovery Factor (Fraction of OOIP) (Primary Plus Secondary) .....	N/A

Record 5:

(52)	Geologic Play Code (Table II) .....	-1
(53)	Depositional System Code (Table III) .....	-1
(54)	Depositional System Degree of Confidence (1 = Highest, 2 = Moderate, 3 = Lowest) .....	N/A
(55)	Diagenetic Overprint Code (Table IV) .....	-1
(56)	Diagenetic Overprint Degree of Confidence (1 = Highest, 2 = Moderate, 3 = Lowest) .....	N/A
(57)	Structural Compartmentalization (Table V) .....	-1
(58)	Structural Compartmentalization Degree of Confidence (1 = Highest, 2 = Moderate, 3 = Lowest) .....	N/A
(59)	Predominant Element of Reservoir Heterogeneity (1 = Depositional System, 2 = Diagenetic Overprint, 3 = Structural Compartmentalization) .....	N/A
(60)	Trap Type (1 = Stratigraphic, 2 = Structural, 3 = Combination) .....	N/A
(61)	Geologic Province (Table VI) .....	067

Table XIV-25.

Reservoir Heterogeneity Classification System for TORIS		
<b>1. Reservoir Identification</b> Reservoir Play: _____		
Reservoir Name: <u>Middle Kenai C</u>	Geologic Province: <u>Cook Inlet Basin</u>	Date: <u>7/10/92</u>
Field Name: <u>Trading Bay</u>	Geologic Age: _____	Prepared By: <u>UAF/PDL</u>
State: <u>AK</u>	Formation: <u>Tyonek</u>	Version: <u>1</u>
<b>2. Depositional System</b> <input type="checkbox"/> 1 <input type="checkbox"/> 2 <input type="checkbox"/> 3      Degree of Confidence in Selection (1=Highest, 3= Lowest)		
<b>Carbonate Reservoirs</b>  <input type="checkbox"/> Lacustrine  <input type="checkbox"/> Peritidal ___ Subtidal ___ Intertidal ___ Subtidal  <input type="checkbox"/> Shallow Shelf ___ Open Shelf ___ Restricted Shelf  <input type="checkbox"/> Shelf Margin ___ Rimmed Shelf ___ Ramp  <input type="checkbox"/> Reefs ___ Pinnacle Reefs ___ Bioherms ___ Atolls  <input type="checkbox"/> Slope/Basin ___ Debris Fan ___ Turbidite Fans ___ Mounds  <input type="checkbox"/> Basin ___ Drowned Shelf ___ Deep Basin	<b>Clastic Reservoirs</b>  <input type="checkbox"/> Eolian ___ Ergs ___ Coastal Dunes  <input type="checkbox"/> Lacustrine ___ Basin Margin ___ Basin Center  <input type="checkbox"/> Fluvial ___ Braided Streams ___ Meandering Streams  <input type="checkbox"/> Alluvial Fan ___ Humid (Stream-Dominated) ___ Arid/Semi-Arid ___ Fan Deltas  <input type="checkbox"/> Delta ___ Wave-Dominated ___ Fluvial-Dominated ___ Tide-Dominated  <input type="checkbox"/> Strandplain ___ Barrier Cores ___ Barrier Shorefaces ___ Back Barriers ___ Tidal Channels ___ Washover Fan/Tidal Deltas  <input type="checkbox"/> Shelf (Accretionary Processes) ___ Sand Waves ___ Sand Ridges/Bars  <input type="checkbox"/> Slope/Basin ___ Turbidite Fans ___ Debris Fans  <input type="checkbox"/> Basin ___ Pelagic	
<b>3. Diagenetic Overprint</b> <input type="checkbox"/> 1 <input type="checkbox"/> 2 <input type="checkbox"/> 3      Degree of Confidence in Selection (1=Highest, 3= Lowest)		
<b>Carbonate Reservoirs</b>  <input type="checkbox"/> Compaction/Cementation <input type="checkbox"/> Grain Enhancement <input type="checkbox"/> Dolomitization  <input type="checkbox"/> Dolomitization (Evaporites) <input type="checkbox"/> Massive Dissolution <input type="checkbox"/> Silicification	<b>Clastic Reservoirs</b>  <input type="checkbox"/> Compaction/Cementation <input type="checkbox"/> Intergranular Dissolution  <input type="checkbox"/> Authigenic Clay <input type="checkbox"/> Chertification	
<b>4. Structural Compartmentalization</b> <input type="checkbox"/> 1 <input type="checkbox"/> 2 <input type="checkbox"/> 3      Degree of Confidence in Selection (1=Highest, 3= Lowest)		
<input type="checkbox"/> Natural Fracture Porosity  <input type="checkbox"/> Unstructured  <input type="checkbox"/> Faulted ___ Normal Fault ___ Reverse Fault ___ Strike-Slip Fault	<input type="checkbox"/> Fault/Fold  <input type="checkbox"/> Folded ___ Normal Fault ___ Reverse Fault ___ Strike-Slip Fault	
<b>5. Reservoir Heterogeneity Ternary Diagram</b> Predominant Element of Reservoir Heterogeneity: (Check Only One)		
<input type="checkbox"/> Depositional System  <input type="checkbox"/> Diagenetic Overprint  <input type="checkbox"/> Structural Compartmentalization		
<b>6. Trap Type</b> <input type="checkbox"/> Stratigraphic <input type="checkbox"/> Structural <input type="checkbox"/> Combination		
<b>7. Optional Comments (References, Details on Above Selections, Etc.)</b> _____ _____ _____		

**Table XIV-26.**

**TORIS DATA BASE**  
**FIELD: TRADING BAY (MIDDLE KENAI C)**

Record 1:

Field Code .....	N/A
STATE Postal Code .....	AK
Lithology Code (-1, 0 = Unknown; 1 = SS, 2 = LS; 3 = Dolo.) .....	-1
Geologic Age Code AAPG .....	-1
Field Name .....	Trading Bay
Reservoir Name .....	Middle Kenai C
Reference Number .....	N/A
Load Number .....	N/A
Formation Name .....	Tyonek

Record 2:

( 1) Field Acres (Acres) .....	N/A
( 2) Proven Acres (Acres) .....	N/A
( 3) Well Spacing (Acres) .....	N/A
( 4) Total Wells (Number) .....	6
( 5) Net Pay (Feet) .....	N/A
( 6) Gross Pay (Feet) .....	N/A
( 7) Porosity (%) .....	N/A
( 8) Initial Oil Saturation (%) .....	N/A
( 9) Current Oil Saturation (%) .....	N/A
(10) Initial Water Saturation (%) .....	N/A
(11) Current Water Saturation (%) .....	N/A
(12) Initial Gas Saturation (%) .....	N/A
(13) Current Gas Saturation (%) .....	N/A
(14) Initial Oil FVF (Res bbl/STB) .....	N/A
(15) Current Oil FVF (Res bbl/STB) .....	N/A
(16) True Vertical Depth (Feet)----Mid-Perforation .....	4400
(17) Formation Temperature (°F) .....	N/A

Record 3:

(18) Current Formation Pressure (PSI) .....	N/A
(19) Permeability (md) .....	N/A
(20) Geologic Age (AAPG) .....	N/A
(21) API Gravity (°API) .....	25.0
(22) Oil Viscosity (CP) :e Reservoir condition .....	N/A
(23) Formation Salinity (ppm TDS) .....	N/A
(24) OOIP (BBL) .....	N/A
(25) Primary Recovery Factor (Fraction of OOIP) .....	N/A
(26) Cumulative Oil Production (BBL) .....	18,983,423

**Table XIV-26 (continued).**

(27)	Year For Cumulative Oil Production; EX/1986 .....	1990
(28)	Technical Availability Date (Year); Ex/1990 .....	N/A
(29)	Primary Recovery (BBL/AC.FT.) .....	N/A
(30)	Primary Recovery (BBL) .....	N/A
(31)	Year For Primary Recovery .....	N/A
(32)	Current Producing GOR (SCF/BBL) .....	532 (1990)
(33)	Initial Producing GOR (SCF/BBL) .....	N/A

Record 4:

(34)	Reservoir Acreage (Acres) .....	N/A
(35)	Initial Formation Pressure (PSI) .....	2037
(36)	Reservoir Dip (DEG) .....	N/A
(37)	Production Wells (Number) .....	4
(38)	Injection Wells (Number) .....	2
(39)	Swept Zone Oil Saturation (%) (Residual to Water) .....	N/A
(40)	Injection Water Salinity (ppm TDS) .....	N/A
(41)	Clay Content (%) .....	N/A
(42)	Dykstra-Parsons Coefficient .....	N/A
(43)	Current Injection Rate (B/D/WELL) .....	N/A
(44)	Fractured-Fault (Y,N) (N = 0, Y = 1) .....	N/A
(45)	Shale Break or Laminations (Y,N) (N = 0, Y = 1) .....	N/A
(46)	Major Gas Cap (Y,N) (N = 0, Y = 1) .....	N/A
(47)	Field Multiplier (Number) .....	N/A
(48)	RRC District .....	N/A
(49)	Production Rate (MBBL/D); For the Year shown in element 28 .....	0.24
(50)	Recovery Efficiency-Waterflood (Factor) .....	N/A
(51)	Ultimate Recovery Factor (Fraction of OOIP) (Primary Plus Secondary) .....	N/A

Record 5:

(52)	Geologic Play Code (Table II) .....	-1
(53)	Depositional System Code (Table III) .....	-1
(54)	Depositional System Degree of Confidence (1 = Highest, 2 = Moderate, 3 = Lowest) .....	N/A
(55)	Diagenetic Overprint Code (Table IV) .....	-1
(56)	Diagenetic Overprint Degree of Confidence (1 = Highest, 2 = Moderate, 3 = Lowest) .....	N/A
(57)	Structural Compartmentalization (Table V) .....	-1
(58)	Structural Compartmentalization Degree of Confidence (1 = Highest, 2 = Moderate, 3 = Lowest) .....	N/A
(59)	Predominant Element of Reservoir Heterogeneity (1 = Depositional System, 2 = Diagenetic Overprint, 3 = Structural Compartmentalization) .....	N/A
(60)	Trap Type (1 = Stratigraphic, 2 = Structural, 3 = Combination) .....	N/A
(61)	Geologic Province (Table VI) .....	067

Table XIV-27.

Reservoir Heterogeneity Classification System for TORIS		
<b>1. Reservoir Identification</b> Reservoir Play: _____ Reservoir Name: <u>Middle Kenai D</u> Geologic Province: <u>Cook Inlet Basin</u> Date: <u>7/10/92</u> Field Name: <u>Trading Bay</u> Geologic Age: _____      Prepared By: <u>UAF/PDL</u> State: <u>AK</u> Formation: <u>Tyonek</u> Version: <u>1</u>		
<b>2. Depositional System</b> <input type="checkbox"/> 1 <input type="checkbox"/> 2 <input type="checkbox"/> 3      Degree of Confidence in Selection      (1=Highest, 3= Lowest)		
<b>Carbonate Reservoirs</b> <input type="checkbox"/> Lacustrine <input type="checkbox"/> Peritidal ___ Supratidal ___ Intertidal ___ Subtidal <input type="checkbox"/> Shallow Shelf ___ Open Shelf ___ Restricted Shelf <input type="checkbox"/> Shelf Margin ___ Rimmed Shelf ___ Ramp <input type="checkbox"/> Reefs ___ Pinnacle Reefs ___ Bioherms ___ Atolls <input type="checkbox"/> Slope/Basin ___ Debris Fans ___ Turbidite Fans ___ Mounds <input type="checkbox"/> Basin ___ Drowned Shelf ___ Deep Basin	<b>Clastic Reservoirs</b> <input type="checkbox"/> Eolian ___ Ergs ___ Coastal Dunes <input type="checkbox"/> Lacustrine ___ Basin Margin ___ Basin Center <input type="checkbox"/> Fluvial ___ Braided Streams ___ Meandering Streams <input type="checkbox"/> Alluvial Fan ___ Humid (Stream-Dominated) ___ Arid/Semi-Arid ___ Fan Deltas <input type="checkbox"/> Delta ___ Wave-Dominated ___ Fluvial-Dominated ___ Tide-Dominated <input type="checkbox"/> Strandplain ___ Barrier Cores ___ Barrier Shorefaces ___ Back Barriers ___ Tidal Channels ___ Washover Fan/Tidal Deltas <input type="checkbox"/> Shelf (Accretionary Processes) ___ Sand Waves ___ Sand Ridges/Bars <input type="checkbox"/> Slope/Basin ___ Turbidite Fans ___ Debris Fans <input type="checkbox"/> Basin ___ Pelagic	
<b>3. Diagenetic Overprint</b> <input type="checkbox"/> 1 <input type="checkbox"/> 2 <input type="checkbox"/> 3      Degree of Confidence in Selection      (1=Highest, 3= Lowest)		
<b>Carbonate Reservoirs</b> <input type="checkbox"/> Compaction/Cementation <input type="checkbox"/> Grain Enhancement <input type="checkbox"/> Dolomitization <input type="checkbox"/> Dolomitization (Evaporites) <input type="checkbox"/> Massive Dissolution <input type="checkbox"/> Silicification	<b>Clastic Reservoirs</b> <input type="checkbox"/> Compaction/Cementation <input type="checkbox"/> Intergranular Dissolution <input type="checkbox"/> Authigenic Clay <input type="checkbox"/> Chertification	
<b>4. Structural Compartmentalization</b> <input type="checkbox"/> 1 <input type="checkbox"/> 2 <input type="checkbox"/> 3      Degree of Confidence in Selection      (1=Highest, 3= Lowest)		
<input type="checkbox"/> Natural Fracture Porosity <input type="checkbox"/> Unstructured <input type="checkbox"/> Faulted <input type="checkbox"/> Fault/Fold <input type="checkbox"/> Folded ___ Normal Fault      ___ Normal Fault ___ Reverse Fault      ___ Reverse Fault ___ Strike-Slip Fault    ___ Strike-Slip Fault		
<b>5. Reservoir Heterogeneity Ternary Diagram</b> Predominant Element of Reservoir Heterogeneity: (Check Only One) • Depositional System      _____ • Diagenetic Overprint      _____ • Structural Compartmentalization      _____		
<b>6. Trap Type</b> <input type="checkbox"/> Stratigraphic <input type="checkbox"/> Structural <input type="checkbox"/> Combination		
<b>7. Optional Comments (References, Details on Above Selections, Etc.)</b> _____ _____ _____		

**Table XIV-28.**

**TORIS DATA BASE  
FIELD: TRADING BAY (MIDDLE KENAI D)**

Record 1:

Field Code .....	N/A
STATE Postal Code .....	AK
Lithology Code (-1, 0 = Unknown; 1 = SS, 2 = LS; 3 = Dolo.) .....	-1
Geologic Age Code AAPG .....	-1
Field Name .....	Trading Bay
Reservoir Name .....	Middle Kenai D
Reference Number .....	N/A
Load Number .....	N/A
Formation Name .....	Tyonek

Record 2:

( 1) Field Acres (Acres) .....	N/A
( 2) Proven Acres (Acres) .....	N/A
( 3) Well Spacing (Acres) .....	N/A
( 4) Total Wells (Number) .....	9
( 5) Net Pay (Feet) .....	100-1000
( 6) Gross Pay (Feet) .....	N/A
( 7) Porosity (%) .....	16.5-24
( 8) Initial Oil Saturation (%) .....	N/A
( 9) Current Oil Saturation (%) .....	N/A
(10) Initial Water Saturation (%) .....	N/A
(11) Current Water Saturation (%) .....	N/A
(12) Initial Gas Saturation (%) .....	N/A
(13) Current Gas Saturation (%) .....	N/A
(14) Initial Oil FVF (Res bbl/STB) .....	N/A
(15) Current Oil FVF (Res bbl/STB) .....	N/A
(16) True Vertical Depth (Feet)---Mid-Perforation .....	5628
(17) Formation Temperature (°F) .....	112

Record 3:

(18) Current Formation Pressure (PSI) .....	N/A
(19) Permeability (md) .....	250
(20) Geologic Age (AAPG) .....	N/A
(21) API Gravity (°API) .....	26.0
(22) Oil Viscosity (CP) :e Reservoir condition .....	N/A
(23) Formation Salinity (ppm TDS) .....	N/A
(24) OOIP (BBL) .....	N/A
(25) Primary Recovery Factor (Fraction of OOIP) .....	N/A
(26) Cumulative Oil Production (BBL) .....	27,167,836

**Table XIV-28 (continued).**

(27)	Year For Cumulative Oil Production; EX/1986 .....	1990
(28)	Technical Availability Date (Year); Ex/1990 .....	N/A
(29)	Primary Recovery (BBL/AC.FT.) .....	N/A
(30)	Primary Recovery (BBL) .....	N/A
(31)	Year For Primary Recovery .....	N/A
(32)	Current Producing GOR (SCF/BBL) .....	729
(33)	Initial Producing GOR (SCF/BBL) .....	268

Record 4:

(34)	Reservoir Acreage (Acres) .....	N/A
(35)	Initial Formation Pressure (PSI) .....	2637
(36)	Reservoir Dip (DEG) .....	N/A
(37)	Production Wells (Number) .....	7
(38)	Injection Wells (Number) .....	2
(39)	Swept Zone Oil Saturation (%) (Residual to Water) .....	N/A
(40)	Injection Water Salinity (ppm TDS) .....	N/A
(41)	Clay Content (%) .....	N/A
(42)	Dykstra-Parsons Coefficient .....	N/A
(43)	Current Injection Rate (B/D/WELL) .....	N/A
(44)	Fractured-Fault (Y,N) (N = 0, Y = 1) .....	N/A
(45)	Shale Break or Laminations (Y,N) (N = 0, Y = 1) .....	N/A
(46)	Major Gas Cap (Y,N) (N = 0, Y = 1) .....	N/A
(47)	Field Multiplier (Number) .....	N/A
(48)	RRC District .....	N/A
(49)	Production Rate (MBBL/D); For the Year shown in element 28 .....	0.21
(50)	Recovery Efficiency-Waterflood (Factor) .....	N/A
(51)	Ultimate Recovery Factor (Fraction of OOIP) (Primary Plus Secondary) .....	N/A

Record 5:

(52)	Geologic Play Code (Table II) .....	-1
(53)	Depositional System Code (Table III) .....	-1
(54)	Depositional System Degree of Confidence (1 = Highest, 2 = Moderate, 3 = Lowest) .....	N/A
(55)	Diagenetic Overprint Code (Table IV) .....	-1
(56)	Diagenetic Overprint Degree of Confidence (1 = Highest, 2 = Moderate, 3 = Lowest) .....	N/A
(57)	Structural Compartmentalization (Table V) .....	-1
(58)	Structural Compartmentalization Degree of Confidence (1 = Highest, 2 = Moderate, 3 = Lowest) .....	N/A
(59)	Predominant Element of Reservoir Heterogeneity (1 = Depositional System, 2 = Diagenetic Overprint, 3 = Structural Compartmentalization) .....	N/A
(60)	Trap Type (1 = Stratigraphic, 2 = Structural, 3 = Combination) .....	N/A
(61)	Geologic Province (Table VI) .....	067

Table XIV-29.

<b>Reservoir Heterogeneity Classification System for TORIS</b>		
<b>1. Reservoir Identification</b> Reservoir Play: _____		
Reservoir Name: <u>Middle Kenai E</u>	Geologic Province: <u>Cook Inlet Basin</u>	Date: <u>7/10/92</u>
Field Name: <u>Trading Bay</u>	Geologic Age: _____	Prepared By: <u>UAF/PDL</u>
State: <u>AK</u>	Formation: <u>Tyonek</u>	Version: <u>1</u>
<b>2. Depositional System</b> <input type="checkbox"/> 1 <input type="checkbox"/> 2 <input type="checkbox"/> 3    Degree of Confidence in Selection    (1=Highest, 3= Lowest)		
<p style="text-align: center;"><b>Carbonate Reservoirs</b></p> <div style="display: flex; justify-content: space-between;"> <div style="width: 45%;"> <input type="checkbox"/> Lacustrine   <input type="checkbox"/> Peritidal            ___ Supratidal            ___ Intertidal            ___ Subtidal   <input type="checkbox"/> Shallow Shelf            ___ Open Shelf            ___ Restricted Shelf   <input type="checkbox"/> Shelf Margin            ___ Rimmed Shelf            ___ Ramp </div> <div style="width: 45%;"> <input type="checkbox"/> Reefs            ___ Pinnacle Reefs            ___ Bioherms            ___ Atolls   <input type="checkbox"/> Slope/Basin            ___ Debris Fans            ___ Turbidite Fans            ___ Mounds   <input type="checkbox"/> Basin            ___ Drowned Shelf            ___ Deep Basin </div> </div>	<p style="text-align: center;"><b>Clastic Reservoirs</b></p> <div style="display: flex; justify-content: space-between;"> <div style="width: 45%;"> <input type="checkbox"/> Eolian            ___ Ergs            ___ Coastal Dunes   <input type="checkbox"/> Lacustrine            ___ Basin Margin            ___ Basin Center   <input type="checkbox"/> Fluvial            ___ Braided Streams            ___ Meandering Streams   <input type="checkbox"/> Alluvial Fan            ___ Humid (Stream-Dominated)            ___ Arid/Semi-Arid            ___ Fan Deltas   <input type="checkbox"/> Delta            ___ Wave-Dominated            ___ Fluvial-Dominated            ___ Tide-Dominated </div> <div style="width: 45%;"> <input type="checkbox"/> Strandplain            ___ Barrier Cores            ___ Barrier Shoreface            ___ Back Barriers            ___ Tidal Channels            ___ Washover Fan/Tidal Deltas   <input type="checkbox"/> Shelf (Accretionary Processes)            ___ Sand Waves            ___ Sand Ridge/Bars   <input type="checkbox"/> Slope-Basin            ___ Turbidite Fans            ___ Debris Fans   <input type="checkbox"/> Basin            ___ Pelagic </div> </div>	
<b>3. Diagenetic Overprint</b> <input type="checkbox"/> 1 <input type="checkbox"/> 2 <input type="checkbox"/> 3    Degree of Confidence in Selection    (1=Highest, 3= Lowest)		
<p style="text-align: center;"><b>Carbonate Reservoirs</b></p> <div style="display: flex; justify-content: space-between;"> <div style="width: 45%;"> <input type="checkbox"/> Compaction/Cementation  <input type="checkbox"/> Grain Enhancement  <input type="checkbox"/> Dolomitization </div> <div style="width: 45%;"> <input type="checkbox"/> Dolomitization (Evaporites)  <input type="checkbox"/> Massive Dissolution  <input type="checkbox"/> Silicification </div> </div>	<p style="text-align: center;"><b>Clastic Reservoirs</b></p> <div style="display: flex; justify-content: space-between;"> <div style="width: 45%;"> <input type="checkbox"/> Compaction/Cementation  <input type="checkbox"/> Intergranular Dissolution </div> <div style="width: 45%;"> <input type="checkbox"/> Authigenic Clay  <input type="checkbox"/> Chertification </div> </div>	
<b>4. Structural Compartmentalization</b> <input type="checkbox"/> 1 <input type="checkbox"/> 2 <input type="checkbox"/> 3    Degree of Confidence in Selection    (1=Highest, 3= Lowest)		
<div style="display: flex; justify-content: space-between;"> <div style="width: 20%;"> <input type="checkbox"/> Natural Fracture Porosity </div> <div style="width: 20%;"> <input type="checkbox"/> Unstructured </div> <div style="width: 20%;"> <input type="checkbox"/> Faulted            ___ Normal Fault            ___ Reverse Fault            ___ Strike-Slip Fault </div> <div style="width: 20%;"> <input type="checkbox"/> Fault/Fold            ___ Normal Fault            ___ Reverse Fault            ___ Strike-Slip Fault </div> <div style="width: 20%;"> <input type="checkbox"/> Folded </div> </div>		
<b>5. Reservoir Heterogeneity Ternary Diagram</b>		
<p style="text-align: center;">Predominant Element of Reservoir Heterogeneity: (Check Only One)</p> <ul style="list-style-type: none"> <li>• Depositional System      _____</li> <li>• Diagenetic Overprint      _____</li> <li>• Structural Compartmentalization      _____</li> </ul>		
<b>6. Trap Type</b> <input type="checkbox"/> Stratigraphic <input type="checkbox"/> Structural <input type="checkbox"/> Combination		
<b>7. Optional Comments (References, Details on Above Selections, Etc.)</b>		
<hr/> <hr/> <hr/>		

**Table XIV-30.**

**TORIS DATA BASE**  
**FIELD: TRADING BAY (MIDDLE KENAI E)**

Record 1:

Field Code .....	N/A
STATE Postal Code .....	AK
Lithology Code (-1, 0 = Unknown; 1 = SS, 2 = LS; 3 = Dolo.) .....	-1
Geologic Age Code AAPG .....	-1
Field Name .....	Trading Bay
Reservoir Name .....	Middle Kenai E
Reference Number .....	N/A
Load Number .....	N/A
Formation Name .....	Tyonek

Record 2:

( 1) Field Acres (Acres) .....	N/A
( 2) Proven Acres (Acres) .....	N/A
( 3) Well Spacing (Acres) .....	N/A
( 4) Total Wells (Number) .....	3
( 5) Net Pay (Feet) .....	N/A
( 6) Gross Pay (Feet) .....	N/A
( 7) Porosity (%) .....	N/A
( 8) Initial Oil Saturation (%) .....	N/A
( 9) Current Oil Saturation (%) .....	N/A
(10) Initial Water Saturation (%) .....	N/A
(11) Current Water Saturation (%) .....	N/A
(12) Initial Gas Saturation (%) .....	N/A
(13) Current Gas Saturation (%) .....	N/A
(14) Initial Oil FVF (Res bbl/STB) .....	N/A
(15) Current Oil FVF (Res bbl/STB) .....	N/A
(16) True Vertical Depth (Feet)---Mid-Perforation .....	N/A
(17) Formation Temperature (°F) .....	N/A

Record 3:

(18) Current Formation Pressure (PSI) .....	N/A
(19) Permeability (md) .....	N/A
(20) Geologic Age (AAPG) .....	N/A
(21) API Gravity (°API) .....	N/A
(22) Oil Viscosity (CP) :e Reservoir condition .....	N/A
(23) Formation Salinity (ppm TDS) .....	N/A
(24) OOIP (BBL) .....	N/A
(25) Primary Recovery Factor (Fraction of OOIP) .....	N/A
(26) Cumulative Oil Production (BBL) .....	7,617,531

**Table XIV-30 (continued).**

(27)	Year For Cumulative Oil Production; EX/1986 .....	1990
(28)	Technical Availability Date (Year); Ex/1990 .....	N/A
(29)	Primary Recovery (BBL/AC.FT.) .....	N/A
(30)	Primary Recovery (BBL) .....	N/A
(31)	Year For Primary Recovery .....	N/A
(32)	Current Producing GOR (SCF/BBL) .....	711
(33)	Initial Producing GOR (SCF/BBL) .....	N/A

Record 4:

(34)	Reservoir Acreage (Acres) .....	N/A
(35)	Initial Formation Pressure (PSI) .....	N/A
(36)	Reservoir Dip (DEG) .....	N/A
(37)	Production Wells (Number) .....	3
(38)	Injection Wells (Number) .....	N/A
(39)	Swept Zone Oil Saturation (%) (Residual to Water) .....	N/A
(40)	Injection Water Salinity (ppm TDS) .....	N/A
(41)	Clay Content (%) .....	N/A
(42)	Dykstra-Parsons Coefficient .....	N/A
(43)	Current Injection Rate (B/D/WELL) .....	N/A
(44)	Fractured-Fault (Y,N) (N = 0, Y = 1) .....	N/A
(45)	Shale Break or Laminations (Y,N) (N = 0, Y = 1) .....	N/A
(46)	Major Gas Cap (Y,N) (N = 0, Y = 1) .....	N/A
(47)	Field Multiplier (Number) .....	N/A
(48)	RRC District .....	N/A
(49)	Production Rate (MBBL/D); For the Year shown in element 28 .....	0.079
(50)	Recovery Efficiency-Waterflood (Factor) .....	N/A
(51)	Ultimate Recovery Factor (Fraction of OOIP) (Primary Plus Secondary) .....	N/A

Record 5:

(52)	Geologic Play Code (Table II) .....	-1
(53)	Depositional System Code (Table III) .....	-1
(54)	Depositional System Degree of Confidence (1 = Highest, 2 = Moderate, 3 = Lowest) .....	N/A
(55)	Diagenetic Overprint Code (Table IV) .....	-1
(56)	Diagenetic Overprint Degree of Confidence (1 = Highest, 2 = Moderate, 3 = Lowest) .....	N/A
(57)	Structural Compartmentalization (Table V) .....	-1
(58)	Structural Compartmentalization Degree of Confidence (1 = Highest, 2 = Moderate, 3 = Lowest) .....	N/A
(59)	Predominant Element of Reservoir Heterogeneity (1 = Depositional System, 2 = Diagenetic Overprint, 3 = Structural Compartmentalization) .....	N/A
(60)	Trap Type (1 = Stratigraphic, 2 = Structural, 3 = Combination) .....	N/A
(61)	Geologic Province (Table VI) .....	067

Table XIV-31.

Reservoir Heterogeneity Classification System for TORIS		
<b>1. Reservoir Identification</b> Reservoir Play: _____		
Reservoir Name: <u>HemLock</u>	Geologic Province: <u>Cook Inlet Basin</u>	Date: <u>7/10/92</u>
Field Name: <u>Trading Bay</u>	Geologic Age: _____	Prepared By: <u>UAF/PDL</u>
State: <u>AK</u>	Formation: <u>HemLock Cgl.</u>	Version: <u>1</u>
<b>2. Depositional System</b> <input type="checkbox"/> 1 <input type="checkbox"/> 2 <input type="checkbox"/> 3    Degree of Confidence in Selection    (1=Highest, 3= Lowest)		
<p style="text-align: center;">Carbonate Reservoirs</p> <div style="display: flex; justify-content: space-between;"> <div style="width: 45%;"> <input type="checkbox"/> Lacustrine   <input type="checkbox"/> Peritidal     ___ Supratidal     ___ Intertidal     ___ Subtidal   <input type="checkbox"/> Shallow Shelf     ___ Open Shelf     ___ Restricted Shelf   <input type="checkbox"/> Shelf Margin     ___ Rimmed Shelf     ___ Ramp         </div> <div style="width: 45%;"> <input type="checkbox"/> Reefs     ___ Pinnacle Reefs     ___ Bioherms     ___ Atolls   <input type="checkbox"/> Slope/Basin     ___ Debris Fans     ___ Turbidite Fans     ___ Mounds   <input type="checkbox"/> Basin     ___ Drowned Shelf     ___ Deep Basin         </div> </div>	<p style="text-align: center;">Clastic Reservoirs</p> <div style="display: flex; justify-content: space-between;"> <div style="width: 45%;"> <input type="checkbox"/> Eolian     ___ Ergs     ___ Coastal Dunes   <input type="checkbox"/> Lacustrine     ___ Basin Margin     ___ Basin Center   <input type="checkbox"/> Fluvial     ___ Braided Streams     ___ Meandering Streams   <input type="checkbox"/> Alluvial Fan     ___ Humid (Stream-Dominated)     ___ Arid/Semi-Arid     ___ Fan Deltas   <input type="checkbox"/> Delta     ___ Wave-Dominated     ___ Fluvial-Dominated     ___ Tide-Dominated         </div> <div style="width: 45%;"> <input type="checkbox"/> Strandplain     ___ Barrier Cores     ___ Barrier Shoelaces     ___ Back Barriers     ___ Tidal Channels     ___ Washover Fan/Tidal Deltas   <input type="checkbox"/> Shelf (Accretionary Processes)     ___ Sand Waves     ___ Sand Ridges/Bars   <input type="checkbox"/> Slope/Basin     ___ Turbidite Fans     ___ Debris Fans   <input type="checkbox"/> Basin     ___ Pelagic         </div> </div>	
<b>3. Diagenetic Overprint</b> <input type="checkbox"/> 1 <input type="checkbox"/> 2 <input type="checkbox"/> 3    Degree of Confidence in Selection    (1=Highest, 3= Lowest)		
<p style="text-align: center;">Carbonate Reservoirs</p> <div style="display: flex; justify-content: space-between;"> <div style="width: 45%;"> <input type="checkbox"/> Compaction/Cementation  <input type="checkbox"/> Grain Enhancement  <input type="checkbox"/> Dolomitization         </div> <div style="width: 45%;"> <input type="checkbox"/> Dolomitization (Evaporites)  <input type="checkbox"/> Massive Dissolution  <input type="checkbox"/> Silicification         </div> </div>	<p style="text-align: center;">Clastic Reservoirs</p> <div style="display: flex; justify-content: space-between;"> <div style="width: 45%;"> <input type="checkbox"/> Compaction/Cementation  <input type="checkbox"/> Intergranular Dissolution         </div> <div style="width: 45%;"> <input type="checkbox"/> Authigenic Clay  <input type="checkbox"/> Chertification         </div> </div>	
<b>4. Structural Compartmentalization</b> <input type="checkbox"/> 1 <input type="checkbox"/> 2 <input type="checkbox"/> 3    Degree of Confidence in Selection    (1=Highest, 3= Lowest)		
<div style="display: flex; justify-content: space-between;"> <div style="width: 30%;"> <input type="checkbox"/> Natural Fracture Porosity         </div> <div style="width: 30%;"> <input type="checkbox"/> Unstructured         </div> <div style="width: 30%;"> <input type="checkbox"/> Faulted     ___ Normal Fault     ___ Reverse Fault     ___ Strike-Slip Fault         </div> <div style="width: 30%;"> <input type="checkbox"/> Fault/Fold     ___ Normal Fault     ___ Reverse Fault     ___ Strike-Slip Fault         </div> <div style="width: 30%;"> <input type="checkbox"/> Folded         </div> </div>		
<b>5. Reservoir Heterogeneity Ternary Diagram</b>		
<p style="text-align: center;">Predominant Element of Reservoir Heterogeneity: (Check Only One)</p> <div style="display: flex; justify-content: space-between;"> <div style="width: 30%;"> <ul style="list-style-type: none"> <li><input type="checkbox"/> Depositional System</li> <li><input type="checkbox"/> Diagenetic Overprint</li> <li><input type="checkbox"/> Structural Compartmentalization</li> </ul> </div> <div style="width: 40%; text-align: center;"> </div> <div style="width: 30%;"></div> </div>		
<b>6. Trap Type</b> <input type="checkbox"/> Stratigraphic <input type="checkbox"/> Structural <input type="checkbox"/> Combination		
<b>7. Optional Comments (References, Details on Above Selections, Etc.)</b>		
<hr/> <hr/> <hr/>		

**Table XIV-32.**

**TORIS DATA BASE**  
**FIELD: TRADING BAY (HEMLOCK)**

Record 1:

Field Code .....	N/A
STATE Postal Code .....	AK
Lithology Code (-1, 0 = Unknown; 1 = SS, 2 = LS; 3 = Dolo.) .....	-1
Geologic Age Code AAPG .....	-1
Field Name .....	Trading Bay
Reservoir Name .....	Hemlock
Reference Number .....	N/A
Load Number .....	N/A
Formation Name .....	Hemlock Cgl.

Record 2:

( 1) Field Acres (Acres) .....	N/A
( 2) Proven Acres (Acres) .....	N/A
( 3) Well Spacing (Acres) .....	N/A
( 4) Total Wells (Number) .....	8
( 5) Net Pay (Feet) .....	300
( 6) Gross Pay (Feet) .....	N/A
( 7) Porosity (%) .....	14.6
( 8) Initial Oil Saturation (%) .....	N/A
( 9) Current Oil Saturation (%) .....	N/A
(10) Initial Water Saturation (%) .....	N/A
(11) Current Water Saturation (%) .....	N/A
(12) Initial Gas Saturation (%) .....	N/A
(13) Current Gas Saturation (%) .....	N/A
(14) Initial Oil FVF (Res bbl/STB) .....	N/A
(15) Current Oil FVF (Res bbl/STB) .....	N/A
(16) True Vertical Depth (Feet)---Mid-Perforation .....	6100
(17) Formation Temperature (°F) .....	136

Record 3:

(18) Current Formation Pressure (PSI) .....	N/A
(19) Permeability (md) .....	10
(20) Geologic Age (AAPG) .....	N/A
(21) API Gravity (°API) .....	28.0
(22) Oil Viscosity (CP) :e Reservoir condition .....	N/A
(23) Formation Salinity (ppm TDS) .....	N/A
(24) OOIP (BBL) .....	N/A
(25) Primary Recovery Factor (Fraction of OOIP) .....	N/A
(26) Cumulative Oil Production (BBL) .....	11,278,347

**Table XIV-32 (continued).**

(27)	Year For Cumulative Oil Production; EX/1986 .....	1990
(28)	Technical Availability Date (Year); Ex/1990 .....	N/A
(29)	Primary Recovery (BBL/AC.FT.) .....	N/A
(30)	Primary Recovery (BBL) .....	N/A
(31)	Year For Primary Recovery .....	N/A
(32)	Current Producing GOR (SCF/BBL) .....	1364
(33)	Initial Producing GOR (SCF/BBL) .....	318

Record 4:

(34)	Reservoir Acreage (Acres) .....	N/A
(35)	Initial Formation Pressure (PSI) .....	2802
(36)	Reservoir Dip (DEG) .....	N/A
(37)	Production Wells (Number) .....	8
(38)	Injection Wells (Number) .....	0
(39)	Swept Zone Oil Saturation (%) (Residual to Water) .....	N/A
(40)	Injection Water Salinity (ppm TDS) .....	N/A
(41)	Clay Content (%) .....	N/A
(42)	Dykstra-Parsons Coefficient .....	N/A
(43)	Current Injection Rate (B/D/WELL) .....	N/A
(44)	Fractured-Fault (Y,N) (N = 0, Y = 1) .....	N/A
(45)	Shale Break or Laminations (Y,N) (N = 0, Y = 1) .....	N/A
(46)	Major Gas Cap (Y,N) (N = 0, Y = 1) .....	N/A
(47)	Field Multiplier (Number) .....	N/A
(48)	RRC District .....	N/A
(49)	Production Rate (MBBL/D); For the Year shown in element 28 .....	0.3315
(50)	Recovery Efficiency-Waterflood (Factor) .....	N/A
(51)	Ultimate Recovery Factor (Fraction of OOIP) (Primary Plus Secondary) .....	N/A

Record 5:

(52)	Geologic Play Code (Table II) .....	-1
(53)	Depositional System Code (Table III) .....	-1
(54)	Depositional System Degree of Confidence (1 = Highest, 2 = Moderate, 3 = Lowest) .....	N/A
(55)	Diagenetic Overprint Code (Table IV) .....	-1
(56)	Diagenetic Overprint Degree of Confidence (1 = Highest, 2 = Moderate, 3 = Lowest) .....	N/A
(57)	Structural Compartmentalization (Table V) .....	-1
(58)	Structural Compartmentalization Degree of Confidence (1 = Highest, 2 = Moderate, 3 = Lowest) .....	N/A
(59)	Predominant Element of Reservoir Heterogeneity (1 = Depositional System, 2 = Diagenetic Overprint, 3 = Structural Compartmentalization) .....	N/A
(60)	Trap Type (1 = Stratigraphic, 2 = Structural, 3 = Combination) .....	N/A
(61)	Geologic Province (Table VI) .....	067

Table XIV-33.

Reservoir Heterogeneity Classification System for TORIS		
<b>1. Reservoir Identification</b> Reservoir Play: _____ Reservoir Name: <u>"G" &amp; Hemlock NE Commingle</u> Geologic Province: <u>Cook Inlet Basin</u> Date: <u>7/10/92</u> Field Name: <u>Trading Bay</u> Geologic Age: _____      Prepared By: <u>UAF/EDL</u> State: <u>AK</u> Formation: <u>Tyonek/Hemlock Cgl.</u> Version: <u>1</u>		
<b>2. Depositional System</b> <input type="checkbox"/> 1 <input type="checkbox"/> 2 <input type="checkbox"/> 3    Degree of Confidence in Selection (1=Highest, 3= Lowest)		
<b>Carbonate Reservoirs</b> <input type="checkbox"/> Lacustrine <input type="checkbox"/> Peritidal ___ Supratidal ___ Intertidal ___ Subtidal <input type="checkbox"/> Shallow Shelf ___ Open Shelf ___ Restricted Shelf <input type="checkbox"/> Shelf Margin ___ Rimmed Shelf ___ Ramp <input type="checkbox"/> Reefs ___ Pinnacle Reefs ___ Bioherms ___ Atolls <input type="checkbox"/> Slope/Basin ___ Debris Fans ___ Turbidite Fans ___ Mounds <input type="checkbox"/> Basin ___ Drowned Shelf ___ Deep Basin	<b>Clastic Reservoirs</b> <input type="checkbox"/> Eolian ___ Ergs ___ Coastal Dunes <input type="checkbox"/> Lacustrine ___ Basin Margin ___ Basin Center <input type="checkbox"/> Fluvial ___ Braided Streams ___ Meandering Streams <input type="checkbox"/> Alluvial Fan ___ Humid (Stream-Dominated) ___ Arid/Semi-Arid ___ Fan Deltas <input type="checkbox"/> Delta ___ Wave-Dominated ___ Fluvial-Dominated ___ Tide-Dominated <input type="checkbox"/> Strandplain ___ Barrier Cores ___ Barrier Shorefaces ___ Back Barriers ___ Tidal Channels ___ Washover Fan/Tidal Deltas <input type="checkbox"/> Shelf (Accretionary Processes) ___ Sand Waves ___ Sand Ridge/Bars <input type="checkbox"/> Slope/Basin ___ Turbidite Fans ___ Debris Fans <input type="checkbox"/> Basin ___ Pelagic	
<b>3. Diagenetic Overprint</b> <input type="checkbox"/> 1 <input type="checkbox"/> 2 <input type="checkbox"/> 3    Degree of Confidence in Selection (1=Highest, 3= Lowest)		
<b>Carbonate Reservoirs</b> <input type="checkbox"/> Compaction/Cementation <input type="checkbox"/> Grain Enhancement <input type="checkbox"/> Dolomitization <input type="checkbox"/> Dolomitization (Evaporites) <input type="checkbox"/> Massive Dissolution <input type="checkbox"/> Silicification	<b>Clastic Reservoirs</b> <input type="checkbox"/> Compaction/Cementation <input type="checkbox"/> Intergranular Dissolution <input type="checkbox"/> Authigenic Clay <input type="checkbox"/> Chertification	
<b>4. Structural Compartmentalization</b> <input type="checkbox"/> 1 <input type="checkbox"/> 2 <input type="checkbox"/> 3    Degree of Confidence in Selection (1=Highest, 3= Lowest)		
<input type="checkbox"/> Natural Fracture Porosity <input type="checkbox"/> Unstructured <input type="checkbox"/> Faulted ___ Normal Fault ___ Reverse Fault ___ Strike-Slip Fault <input type="checkbox"/> Fault/Fold <input type="checkbox"/> Folded ___ Normal Fault ___ Reverse Fault ___ Strike-Slip Fault		
<b>5. Reservoir Heterogeneity Ternary Diagram</b> Predominant Element of Reservoir Heterogeneity: (Check Only One) <input type="checkbox"/> Depositional System <input type="checkbox"/> Diagenetic Overprint <input type="checkbox"/> Structural Compartmentalization		
<b>6. Trap Type</b> <input type="checkbox"/> Stratigraphic <input type="checkbox"/> Structural <input type="checkbox"/> Combination		
<b>7. Optional Comments (References, Details on Above Selections, Etc.)</b> _____ _____ _____		

**Table XIV-34.**

**TORIS DATA BASE**  
**FIELD: TRADING BAY ("G" & HEMLOCK NE COMMINGLE)**

**Record 1:**

Field Code .....	N/A
STATE Postal Code .....	AK
Lithology Code (-1, 0 = Unknown; 1 = SS, 2 = LS; 3 = Dolo.) .....	-1
Geologic Age Code AAPG .....	-1
Field Name .....	Trading Bay
Reservoir Name .....	"G" & Hemlock NE Commingle
Reference Number .....	N/A
Load Number .....	N/A
Formation Name .....	Tyonek/Hemlock Cgl.

**Record 2:**

( 1) Field Acres (Acres) .....	N/A
( 2) Proven Acres (Acres) .....	N/A
( 3) Well Spacing (Acres) .....	N/A
( 4) Total Wells (Number) .....	5
( 5) Net Pay (Feet) .....	215
( 6) Gross Pay (Feet) .....	400
( 7) Porosity (%) .....	11.5
( 8) Initial Oil Saturation (%) .....	N/A
( 9) Current Oil Saturation (%) .....	N/A
(10) Initial Water Saturation (%) .....	36
(11) Current Water Saturation (%) .....	N/A
(12) Initial Gas Saturation (%) .....	N/A
(13) Current Gas Saturation (%) .....	N/A
(14) Initial Oil FVF (Res bbl/STB) .....	1.29
(15) Current Oil FVF (Res bbl/STB) .....	N/A
(16) True Vertical Depth (Feet)---Mid-Perforation .....	9800
(17) Formation Temperature (°F) .....	180

**Record 3:**

(18) Current Formation Pressure (PSI) .....	N/A
(19) Permeability (md) .....	12
(20) Geologic Age (AAPG) .....	N/A
(21) API Gravity (°API) .....	35.8-36.2
(22) Oil Viscosity (CP) @ Reservoir condition .....	1.036
(23) Formation Salinity (ppm TDS) .....	N/A
(24) OOIP (BBL) .....	N/A
(25) Primary Recovery Factor (Fraction of OOIP) .....	N/A
(26) Cumulative Oil Production (BBL) .....	23,439,105

**Table XIV-34 (continued).**

(27)	Year For Cumulative Oil Production; EX/1986 .....	1990
(28)	Technical Availability Date (Year); Ex/1990 .....	N/A
(29)	Primary Recovery (BBL/AC.FT.) .....	N/A
(30)	Primary Recovery (BBL) .....	N/A
(31)	Year For Primary Recovery .....	N/A
(32)	Current Producing GOR (SCF/BBL) .....	482 (1990)
(33)	Initial Producing GOR (SCF/BBL) .....	275

Record 4:

(34)	Reservoir Acreage (Acres) .....	N/A
(35)	Initial Formation Pressure (PSI) .....	4470
(36)	Reservoir Dip (DEG) .....	N/A
(37)	Production Wells (Number) .....	5
(38)	Injection Wells (Number) .....	0
(39)	Swept Zone Oil Saturation (%) (Residual to Water) .....	N/A
(40)	Injection Water Salinity (ppm TDS) .....	N/A
(41)	Clay Content (%) .....	N/A
(42)	Dykstra-Parsons Coefficient .....	N/A
(43)	Current Injection Rate (B/D/WELL) .....	N/A
(44)	Fractured-Fault (Y,N) (N = 0, Y = 1) .....	N/A
(45)	Shale Break or Laminations (Y,N) (N = 0, Y = 1) .....	N/A
(46)	Major Gas Cap (Y,N) (N = 0, Y = 1) .....	N/A
(47)	Field Multiplier (Number) .....	N/A
(48)	RRC District .....	N/A
(49)	Production Rate (MBBL/D); For the Year shown in element 28 ....	0.3138
(50)	Recovery Efficiency-Waterflood (Factor) .....	N/A
(51)	Ultimate Recovery Factor (Fraction of OOIP) (Primary Plus Secondary) .....	N/A

Record 5:

(52)	Geologic Play Code (Table II) .....	-1
(53)	Depositional System Code (Table III) .....	-1
(54)	Depositional System Degree of Confidence (1 = Highest, 2 = Moderate, 3 = Lowest) .....	N/A
(55)	Diagenetic Overprint Code (Table IV) .....	-1
(56)	Diagenetic Overprint Degree of Confidence (1 = Highest, 2 = Moderate, 3 = Lowest) .....	N/A
(57)	Structural Compartmentalization (Table V) .....	-1
(58)	Structural Compartmentalization Degree of Confidence (1 = Highest, 2 = Moderate, 3 = Lowest) .....	N/A
(59)	Predominant Element of Reservoir Heterogeneity (1 = Depositional System, 2 = Diagenetic Overprint, 3 = Structural Compartmentalization) .....	N/A
(60)	Trap Type (1 = Stratigraphic, 2 = Structural, 3 = Combination) ....	N/A
(61)	Geologic Province (Table VI) .....	067

Table XIV-35.

Reservoir Heterogeneity Classification System for TORIS		
<b>1. Reservoir Identification</b>		
Reservoir Name: <u>Undefined</u>	Geologic Province: <u>Cook Inlet Basin</u>	Date: <u>7/10/92</u>
Field Name: <u>Trading Bay</u>	Geologic Age: _____	Prepared By: <u>UAF/PDL</u>
State: <u>AK</u>	Formation: _____	Version: <u>1</u>
<b>2. Depositional System</b> <input type="checkbox"/> 1 <input type="checkbox"/> 2 <input type="checkbox"/> 3   Degree of Confidence in Selection   (1-Highest, 3= Lowest)		
<p style="text-align: center;">Carbonate Reservoirs</p> <div style="display: flex; justify-content: space-between;"> <div style="width: 45%;"> <input type="checkbox"/> Lacustrine   <input type="checkbox"/> Peritidal            ___ Subtidal            ___ Intertidal            ___ Subtidal   <input type="checkbox"/> Shallow Shelf            ___ Open Shelf            ___ Restricted Shelf   <input type="checkbox"/> Shelf Margin            ___ Rimmed Shelf            ___ Ramp </div> <div style="width: 45%;"> <input type="checkbox"/> Reefs            ___ Pinnacle Reefs            ___ Bioherms            ___ Atolls   <input type="checkbox"/> Slope/Basin            ___ Debris Fan            ___ Turbidite Fan   <input type="checkbox"/> Basin            ___ Mounds            ___ Drowned Shelf            ___ Deep Basin </div> </div>	<p style="text-align: center;">Clastic Reservoirs</p> <div style="display: flex; justify-content: space-between;"> <div style="width: 45%;"> <input type="checkbox"/> Eolian            ___ Ergs            ___ Coastal Dunes   <input type="checkbox"/> Lacustrine            ___ Basin Margin            ___ Basin Center   <input type="checkbox"/> Fluvial            ___ Braided Streams            ___ Meandering Streams   <input type="checkbox"/> Alluvial Fan            ___ Humid (Stream-Dominated)            ___ Arid/Semi-Arid            ___ Fan Deltas   <input type="checkbox"/> Delta            ___ Wave-Dominated            ___ Fluvial-Dominated            ___ Tide-Dominated </div> <div style="width: 45%;"> <input type="checkbox"/> Strandplain            ___ Barrier Cores            ___ Barrier Shorefaces            ___ Back Barriers            ___ Tidal Channels            ___ Washover Fan/Tidal Deltas   <input type="checkbox"/> Shelf (Accretionary Processes)            ___ Sand Waves            ___ Sand Ridges/Bars   <input type="checkbox"/> Slope/Basin            ___ Turbidite Fan            ___ Debris Fan   <input type="checkbox"/> Basin            ___ Pelagic </div> </div>	
<b>3. Diagenetic Overprint</b> <input type="checkbox"/> 1 <input type="checkbox"/> 2 <input type="checkbox"/> 3   Degree of Confidence in Selection   (1-Highest, 3= Lowest)		
<p style="text-align: center;">Carbonate Reservoirs</p> <div style="display: flex; justify-content: space-between;"> <div style="width: 45%;"> <input type="checkbox"/> Compaction/Cementation  <input type="checkbox"/> Grain Enhancement  <input type="checkbox"/> Dolomitization </div> <div style="width: 45%;"> <input type="checkbox"/> Dolomitization (Evaporate)  <input type="checkbox"/> Massive Dissolution  <input type="checkbox"/> Silicification </div> </div>	<p style="text-align: center;">Clastic Reservoirs</p> <div style="display: flex; justify-content: space-between;"> <div style="width: 45%;"> <input type="checkbox"/> Compaction/Cementation  <input type="checkbox"/> Intergranular Dissolution </div> <div style="width: 45%;"> <input type="checkbox"/> Authigenic Clay  <input type="checkbox"/> Chertification </div> </div>	
<b>4. Structural Compartmentalization</b> <input type="checkbox"/> 1 <input type="checkbox"/> 2 <input type="checkbox"/> 3   Degree of Confidence in Selection   (1-Highest, 3= Lowest)		
<input type="checkbox"/> Natural Fracture Porosity <input type="checkbox"/> Unstructured	<input type="checkbox"/> Faulted ___ Normal Fault ___ Reverse Fault ___ Strike-Slip Fault	<input type="checkbox"/> Fault/Fold <input type="checkbox"/> Folded ___ Normal Fault ___ Reverse Fault ___ Strike-Slip Fault
<b>5. Reservoir Heterogeneity Ternary Diagram</b>		
<p>Predominant Element of Reservoir Heterogeneity: (Check Only One)</p> <ul style="list-style-type: none"> <li>• Depositional System      ___</li> <li>• Diagenetic Overprint      ___</li> <li>• Structural Compartmentalization      ___</li> </ul>		
<b>6. Trap Type</b> <input type="checkbox"/> Stratigraphic <input type="checkbox"/> Structural <input type="checkbox"/> Combination		
<b>7. Optional Comments (References, Details on Above Selections, Etc.)</b>		
<hr/> <hr/> <hr/>		

**Table XIV-36.**

**TORIS DATA BASE**  
**FIELD: TRADING BAY (UNDEFINED)**

**Record 1:**

Field Code .....	N/A
STATE Postal Code .....	AK
Lithology Code (-1, 0 = Unknown; 1 = SS, 2 = LS; 3 = Dolo.) .....	-1
Geologic Age Code AAPG .....	-1
Field Name .....	Trading Bay
Reservoir Name .....	Undefined
Reference Number .....	N/A
Load Number .....	N/A
Formation Name .....	N/A

**Record 2:**

( 1) Field Acres (Acres) .....	N/A
( 2) Proven Acres (Acres) .....	N/A
( 3) Well Spacing (Acres) .....	N/A
( 4) Total Wells (Number) .....	2
( 5) Net Pay (Feet) .....	N/A
( 6) Gross Pay (Feet) .....	N/A
( 7) Porosity (%) .....	N/A
( 8) Initial Oil Saturation (%) .....	N/A
( 9) Current Oil Saturation (%) .....	N/A
(10) Initial Water Saturation (%) .....	N/A
(11) Current Water Saturation (%) .....	N/A
(12) Initial Gas Saturation (%) .....	N/A
(13) Current Gas Saturation (%) .....	N/A
(14) Initial Oil FVF (Res bbl/STB) .....	N/A
(15) Current Oil FVF (Res bbl/STB) .....	N/A
(16) True Vertical Depth (Feet)---Mid-Perforation .....	N/A
(17) Formation Temperature (°F) .....	N/A

**Record 3:**

(18) Current Formation Pressure (PSI) .....	N/A
(19) Permeability (md) .....	N/A
(20) Geologic Age (AAPG) .....	N/A
(21) API Gravity (°API) .....	23.0
(22) Oil Viscosity (CP) :e Reservoir condition .....	N/A
(23) Formation Salinity (ppm TDS) .....	N/A
(24) OOIP (BBL) .....	N/A
(25) Primary Recovery Factor (Fraction of OOIP) .....	N/A
(26) Cumulative Oil Production (BBL) .....	824,401

**Table XIV-36 (continued).**

(27)	Year For Cumulative Oil Production; EX/1986	1990
(28)	Technical Availability Date (Year); Ex/1990	N/A
(29)	Primary Recovery (BBL/AC.FT.)	N/A
(30)	Primary Recovery (BBL)	N/A
(31)	Year For Primary Recovery	N/A
(32)	Current Producing GOR (SCF/BBL)	183
(33)	Initial Producing GOR (SCF/BBL)	N/A

Record 4:

(34)	Reservoir Acreage (Acres)	N/A
(35)	Initial Formation Pressure (PSI)	N/A
(36)	Reservoir Dip (DEG)	N/A
(37)	Production Wells (Number)	2
(38)	Injection Wells (Number)	0
(39)	Swept Zone Oil Saturation (%) (Residual to Water)	N/A
(40)	Injection Water Salinity (ppm TDS)	N/A
(41)	Clay Content (%)	N/A
(42)	Dykstra-Parsons Coefficient	N/A
(43)	Current Injection Rate (B/D/WELL)	N/A
(44)	Fractured-Fault (Y,N) (N = 0, Y = 1)	N/A
(45)	Shale Break or Laminations (Y,N) (N = 0, Y = 1)	N/A
(46)	Major Gas Cap (Y,N) (N = 0, Y = 1)	N/A
(47)	Field Multiplier (Number)	N/A
(48)	RRC District	N/A
(49)	Production Rate (MBBL/D); For the Year shown in element 28	0.2846
(50)	Recovery Efficiency-Waterflood (Factor)	N/A
(51)	Ultimate Recovery Factor (Fraction of OOIP) (Primary Plus Secondary)	N/A

Record 5:

(52)	Geologic Play Code (Table II)	-1
(53)	Depositional System Code (Table III)	-1
(54)	Depositional System Degree of Confidence (1 = Highest, 2 = Moderate, 3 = Lowest)	N/A
(55)	Diagenetic Overprint Code (Table IV)	-1
(56)	Diagenetic Overprint Degree of Confidence (1 = Highest, 2 = Moderate, 3 = Lowest)	N/A
(57)	Structural Compartmentalization (Table V)	-1
(58)	Structural Compartmentalization Degree of Confidence (1 = Highest, 2 = Moderate, 3 = Lowest)	N/A
(59)	Predominant Element of Reservoir Heterogeneity (1 = Depositional System, 2 = Diagenetic Overprint, 3 = Structural Compartmentalization)	N/A
(60)	Trap Type (1 = Stratigraphic, 2 = Structural, 3 = Combination)	N/A
(61)	Geologic Province (Table VI)	067



**Table XIV-38.**

**TORIS DATA BASE**  
**FIELD: TRADING BAY (WEST FORELAND)**

Record 1:

Field Code .....	N/A
STATE Postal Code .....	AK
Lithology Code (-1, 0 = Unknown; 1 = SS, 2 = LS; 3 = Dolo.) .....	-1
Geologic Age Code AAPG .....	-1
Field Name .....	Trading Bay
Reservoir Name .....	West Foreland
Reference Number .....	N/A
Load Number .....	N/A
Formation Name .....	West Foreland

Record 2:

( 1) Field Acres (Acres) .....	N/A
( 2) Proven Acres (Acres) .....	N/A
( 3) Well Spacing (Acres) .....	N/A
( 4) Total Wells (Number) .....	1
( 5) Net Pay (Feet) .....	N/A
( 6) Gross Pay (Feet) .....	N/A
( 7) Porosity (%) .....	N/A
( 8) Initial Oil Saturation (%) .....	N/A
( 9) Current Oil Saturation (%) .....	N/A
(10) Initial Water Saturation (%) .....	N/A
(11) Current Water Saturation (%) .....	N/A
(12) Initial Gas Saturation (%) .....	N/A
(13) Current Gas Saturation (%) .....	N/A
(14) Initial Oil FVF (Res bbl/STB) .....	N/A
(15) Current Oil FVF (Res bbl/STB) .....	N/A
(16) True Vertical Depth (Feet)---Mid-Perforation .....	N/A
(17) Formation Temperature (°F) .....	N/A

Record 3:

(18) Current Formation Pressure (PSI) .....	N/A
(19) Permeability (md) .....	N/A
(20) Geologic Age (AAPG) .....	N/A
(21) API Gravity (°API) .....	N/A
(22) Oil Viscosity (CP) :e Reservoir condition .....	N/A
(23) Formation Salinity (ppm TDS) .....	N/A
(24) OOIP (BBL) .....	N/A
(25) Primary Recovery Factor (Fraction of OOIP) .....	N/A
(26) Cumulative Oil Production (BBL) .....	53,946

**Table XIV-38 (continued).**

(27)	Year For Cumulative Oil Production; EX/1986 .....	1990
(28)	Technical Availability Date (Year); Ex/1990 .....	N/A
(29)	Primary Recovery (BBL/AC.FT.) .....	N/A
(30)	Primary Recovery (BBL) .....	N/A
(31)	Year For Primary Recovery .....	N/A
(32)	Current Producing GOR (SCF/BBL) .....	N/A
(33)	Initial Producing GOR (SCF/BBL) .....	N/A

Record 4:

(34)	Reservoir Acreage (Acres) .....	N/A
(35)	Initial Formation Pressure (PSI) .....	N/A
(36)	Reservoir Dip (DEG) .....	N/A
(37)	Production Wells (Number) .....	1
(38)	Injection Wells (Number) .....	N/A
(39)	Swept Zone Oil Saturation (%) (Residual to Water) .....	N/A
(40)	Injection Water Salinity (ppm TDS) .....	N/A
(41)	Clay Content (%) .....	N/A
(42)	Dykstra-Parsons Coefficient .....	N/A
(43)	Current Injection Rate (B/D/WELL) .....	N/A
(44)	Fractured-Fault (Y,N) (N = 0, Y = 1) .....	N/A
(45)	Shale Break or Laminations (Y,N) (N = 0, Y = 1) .....	N/A
(46)	Major Gas Cap (Y,N) (N = 0, Y = 1) .....	N/A
(47)	Field Multiplier (Number) .....	N/A
(48)	RRC District .....	N/A
(49)	Production Rate (MBBL/D); For the Year shown in element 28 ....	0.0166
(50)	Recovery Efficiency-Waterflood (Factor) .....	N/A
(51)	Ultimate Recovery Factor (Fraction of OOIP) (Primary Plus Secondary) .....	N/A

Record 5:

(52)	Geologic Play Code (Table II) .....	-1
(53)	Depositional System Code (Table III) .....	-1
(54)	Depositional System Degree of Confidence (1 = Highest, 2 = Moderate, 3 = Lowest) .....	N/A
(55)	Diagenetic Overprint Code (Table IV) .....	-1
(56)	Diagenetic Overprint Degree of Confidence (1 = Highest, 2 = Moderate, 3 = Lowest) .....	N/A
(57)	Structural Compartmentalization (Table V) .....	-1
(58)	Structural Compartmentalization Degree of Confidence (1 = Highest, 2 = Moderate, 3 = Lowest) .....	N/A
(59)	Predominant Element of Reservoir Heterogeneity (1 = Depositional System, 2 = Diagenetic Overprint, 3 = Structural Compartmentalization) .....	N/A
(60)	Trap Type (1 = Stratigraphic, 2 = Structural, 3 = Combination) ....	N/A
(61)	Geologic Province (Table VI) .....	067

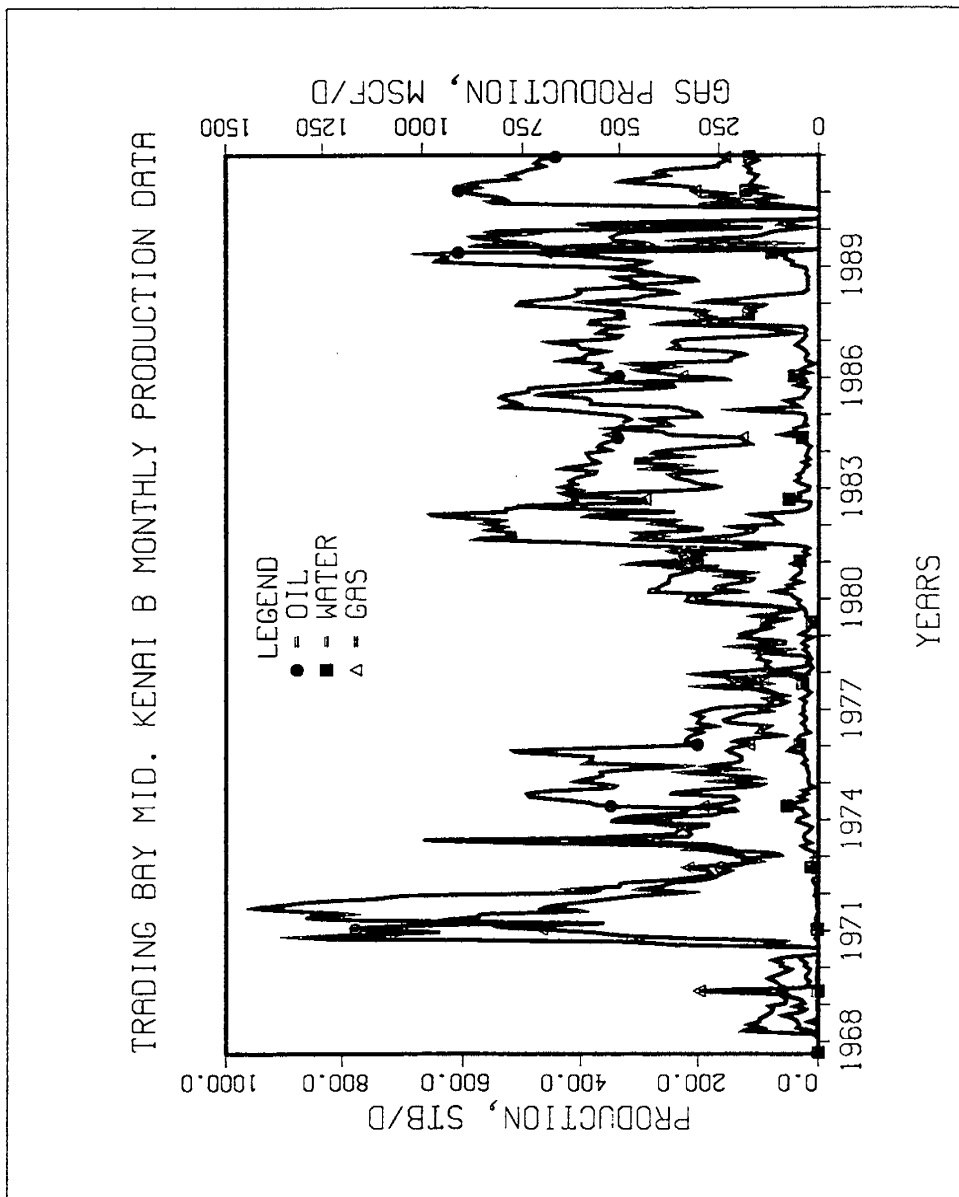


Figure XIV-17.

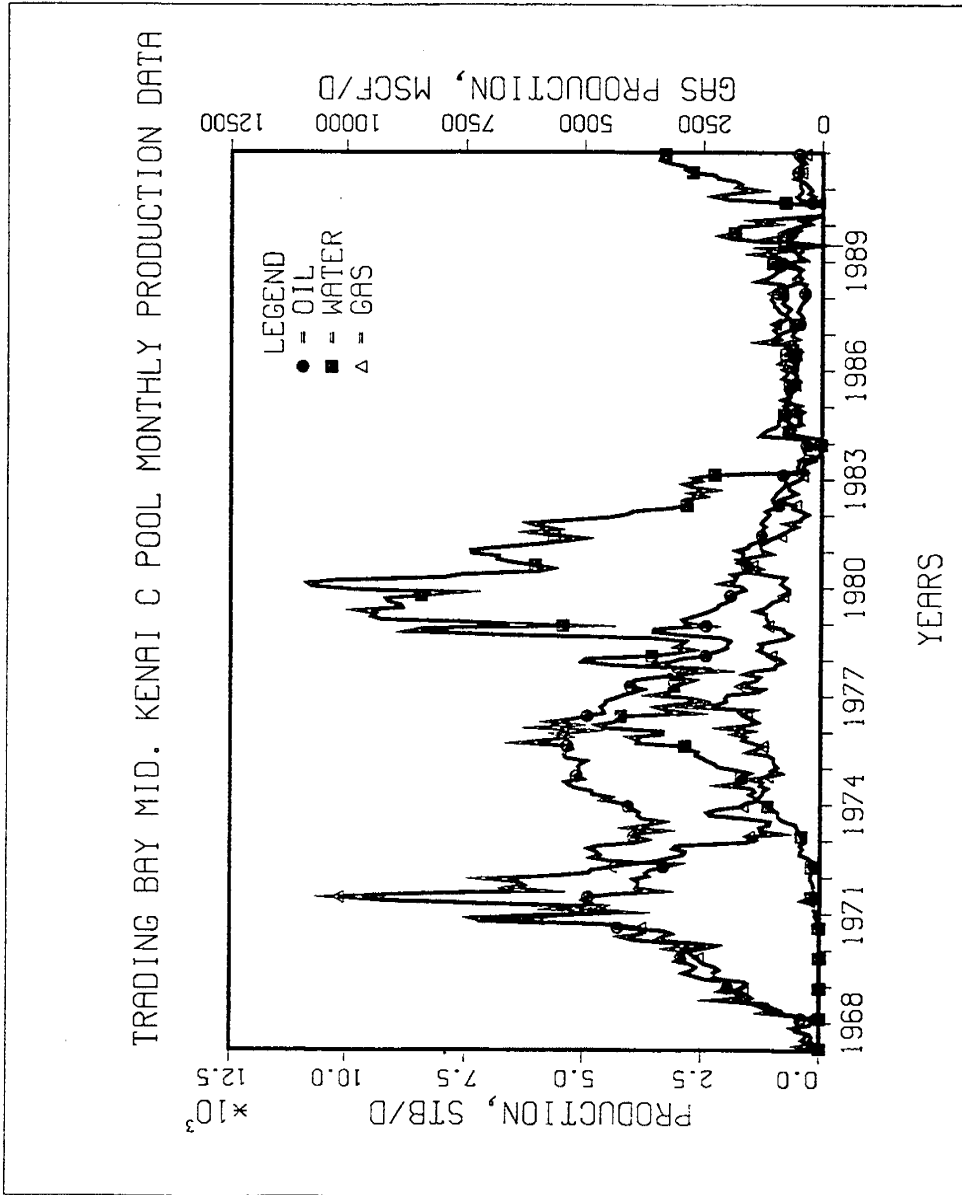


Figure XIV-18.

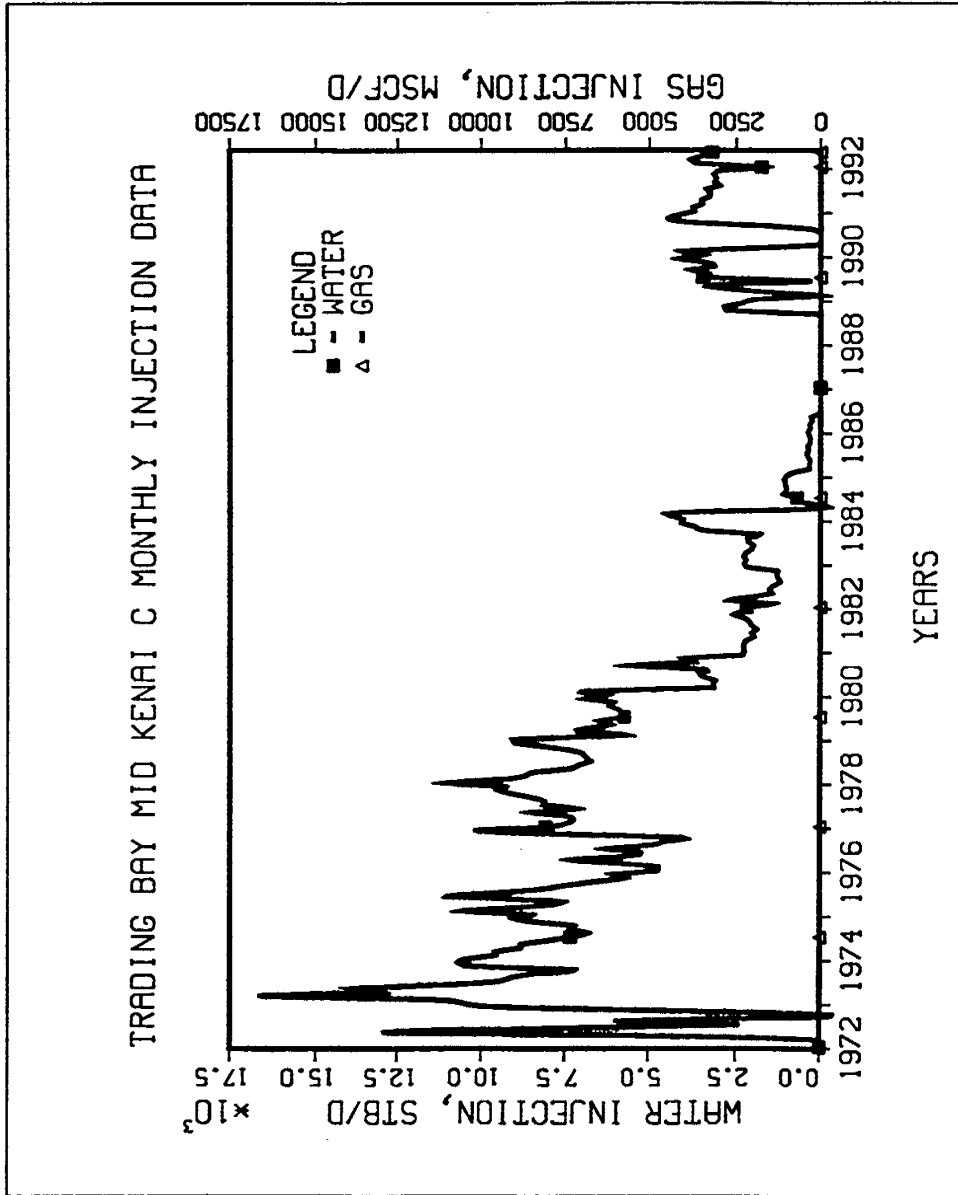


Figure XIV-19.

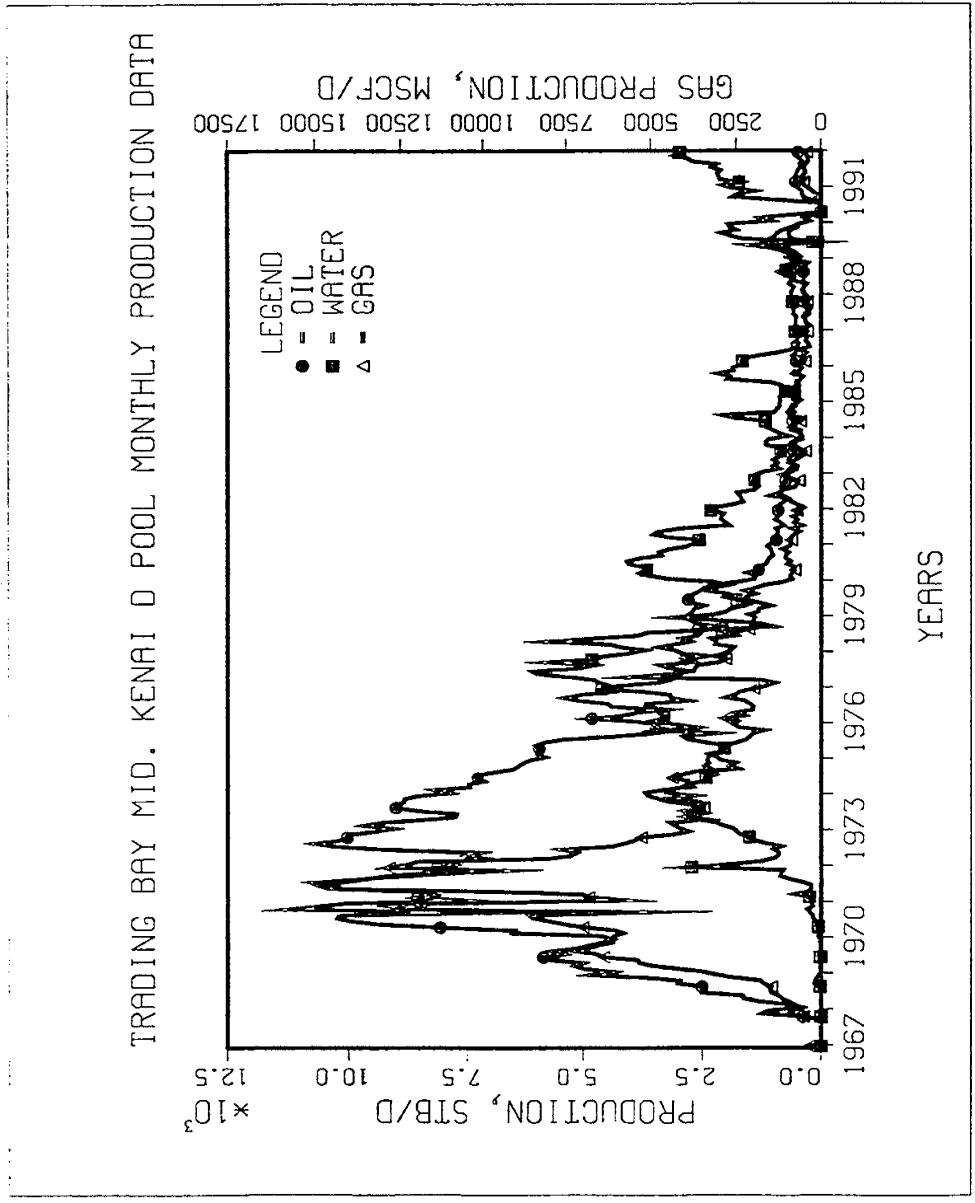


Figure XIV-20.

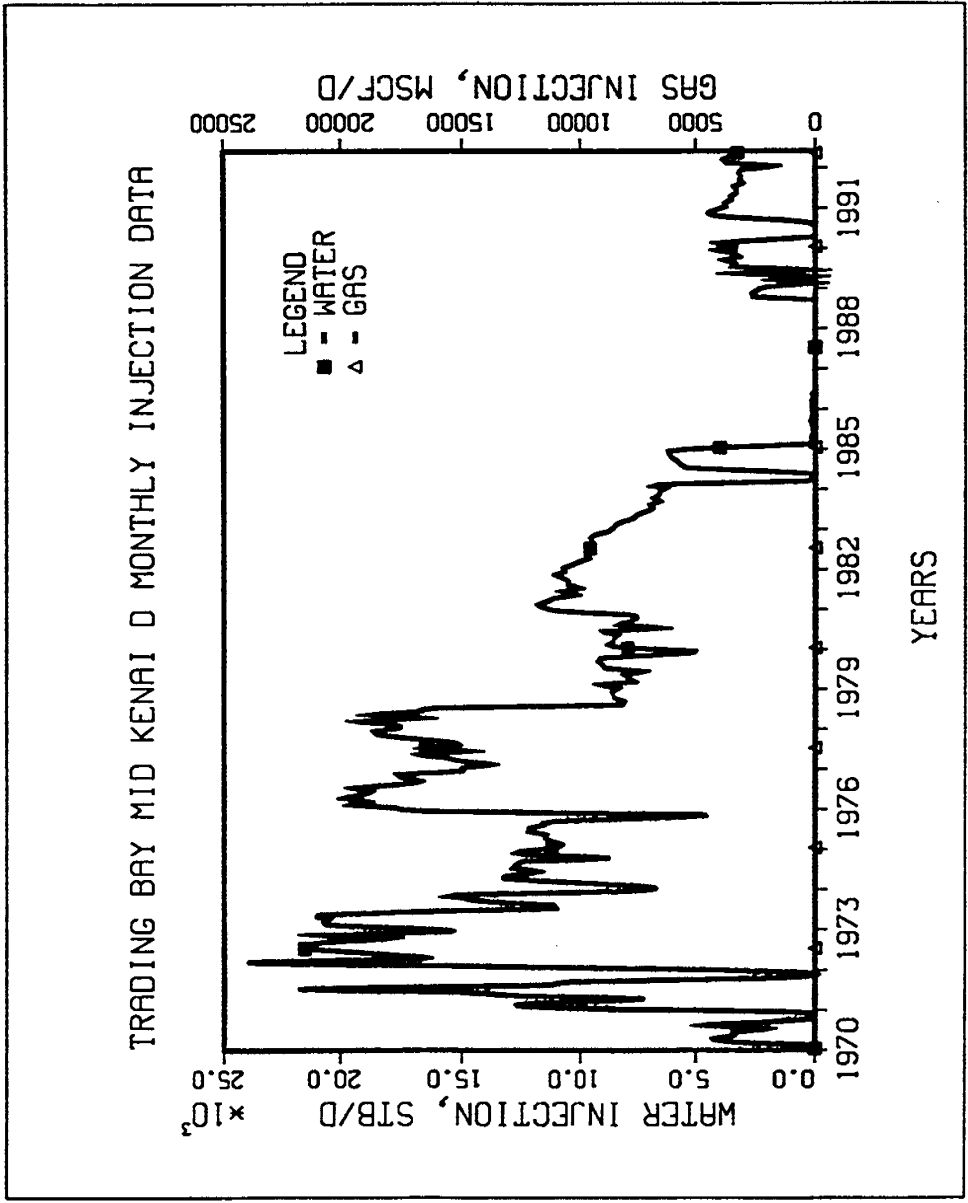


Figure XIV-21.

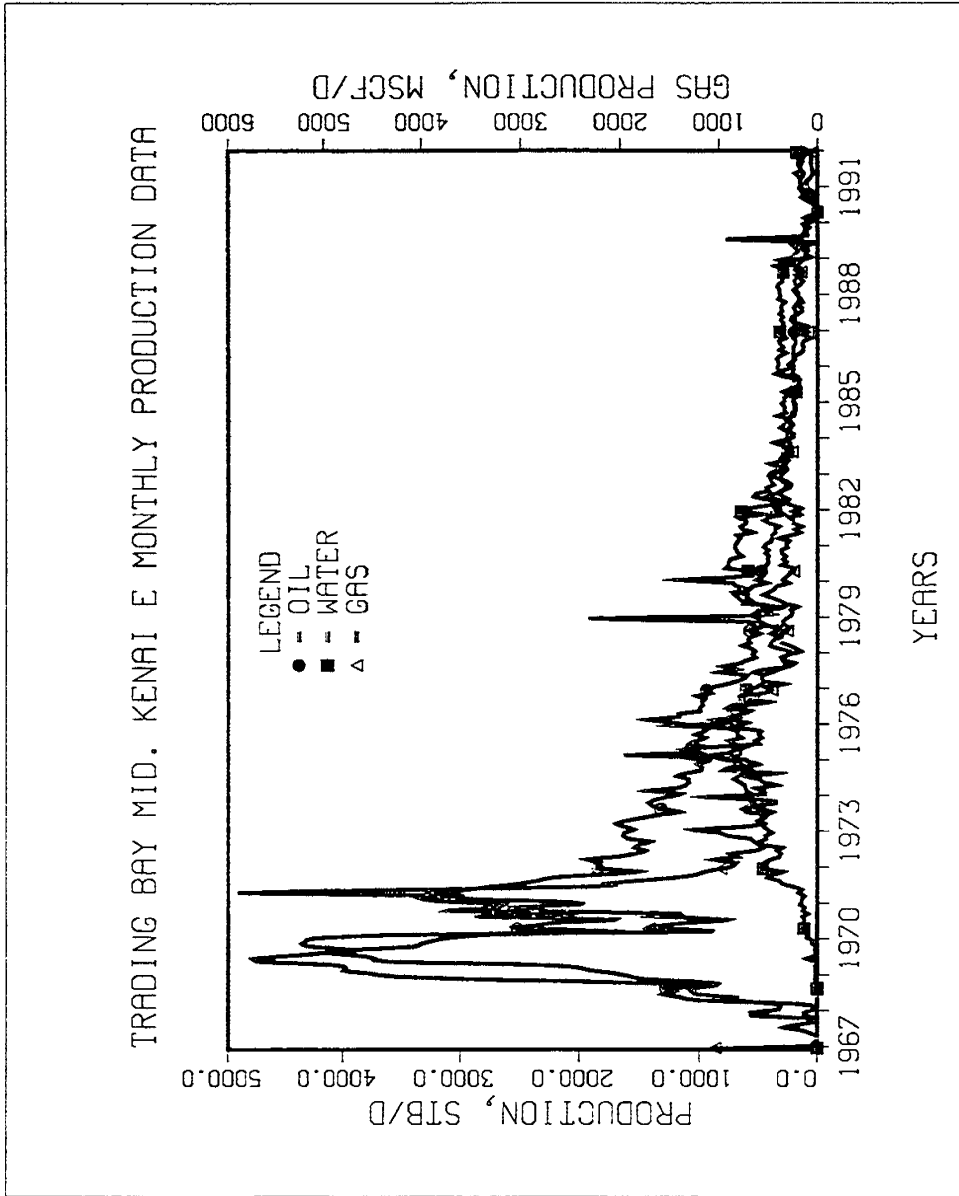


Figure XIV-22.

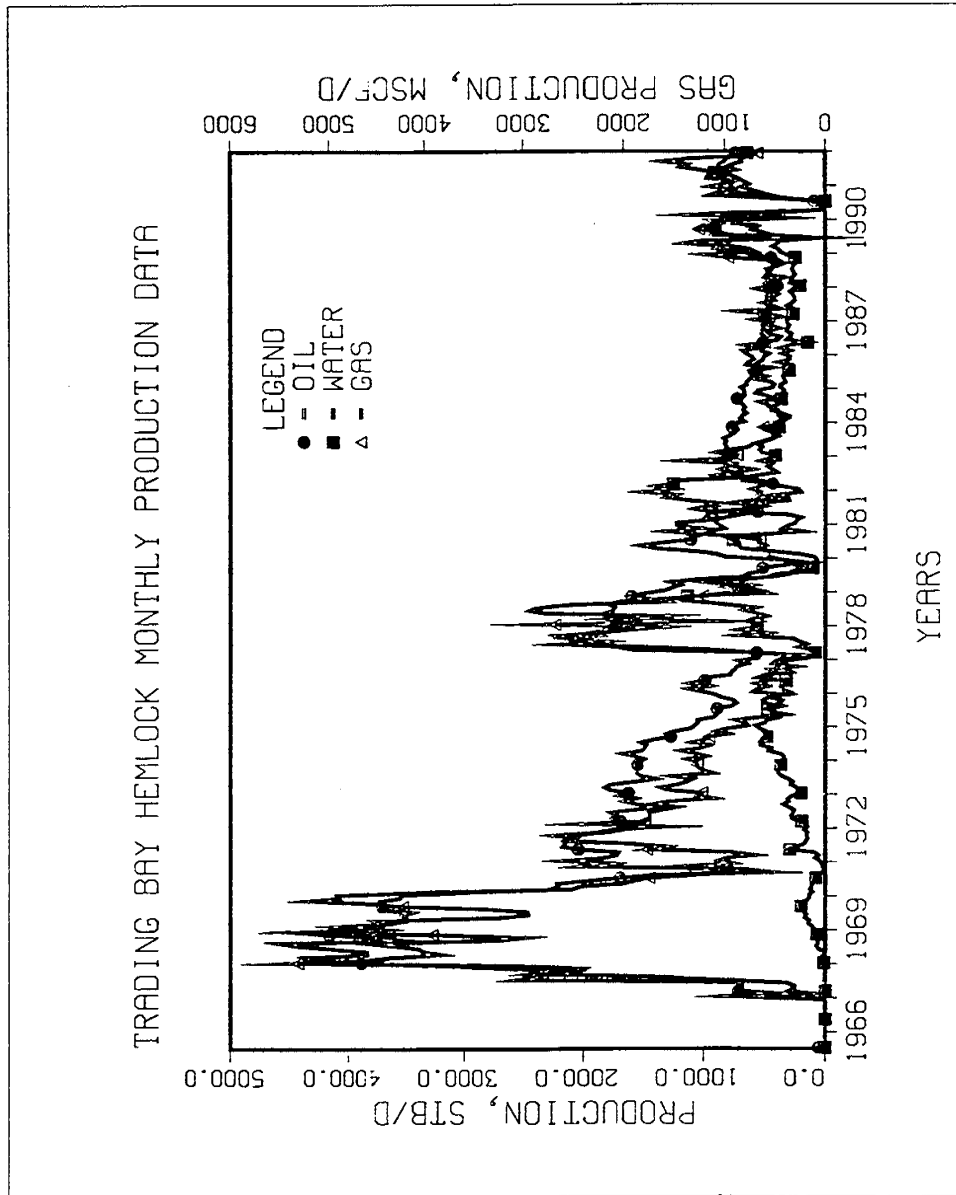


Figure XIV-23.

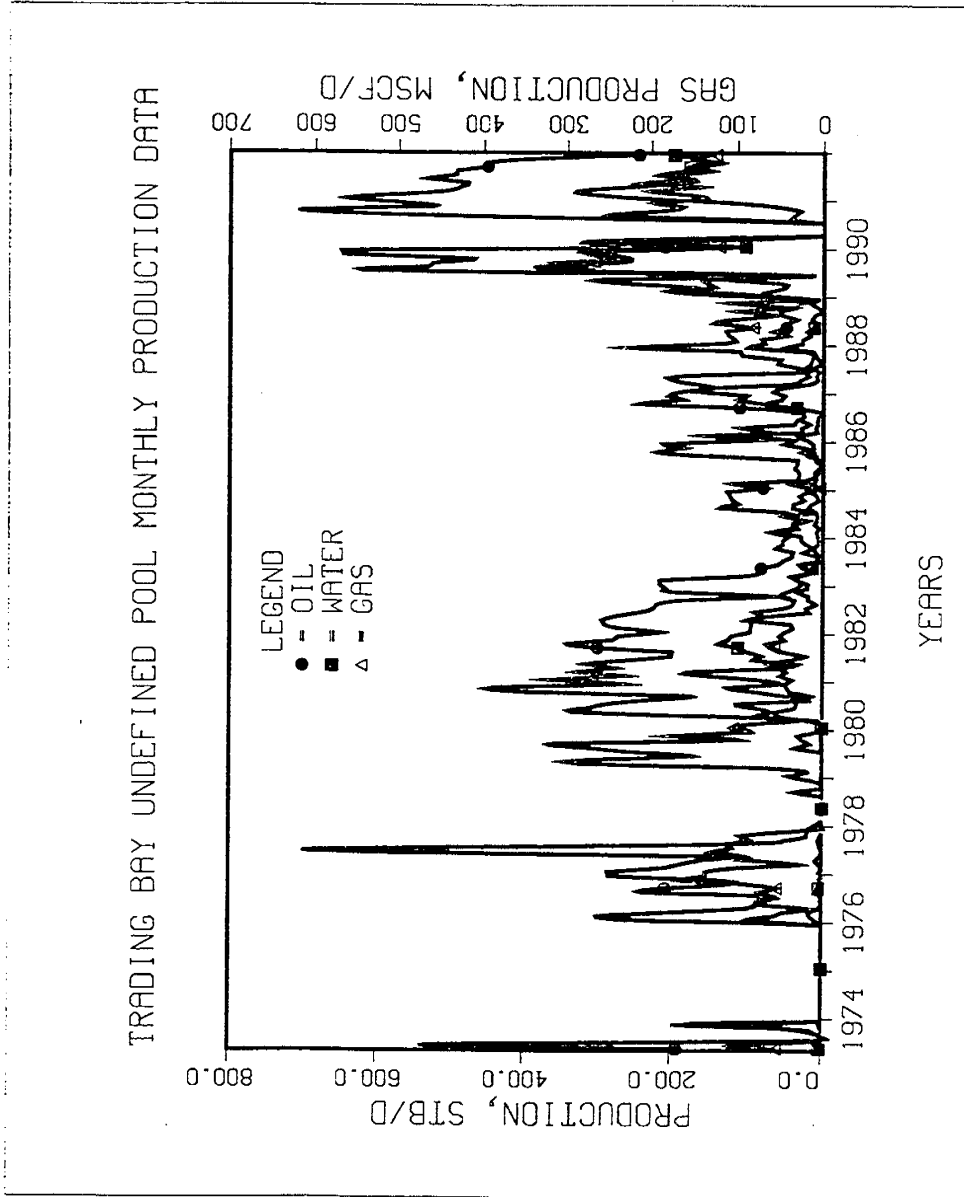


Figure XIV-24.



**Table XIV-40.**

**TORIS DATA BASE  
FIELD: NORTH TRADING BAY**

Record 1:

Field Code .....	N/A
STATE Postal Code .....	AK
Lithology Code (-1, 0 = Unknown; 1 = SS, 2 = LS; 3 = Dolo.) .....	1
Geologic Age Code AAPG .....	120
Field Name .....	North Trading Bay
Reservoir Name .....	G Zone/Hemlock
Reference Number .....	N/A
Load Number .....	N/A
Formation Name .....	G Zone/Hemlock

Record 2:

( 1) Field Acres (Acres) .....	500
( 2) Proven Acres (Acres) .....	500
( 3) Well Spacing (Acres) .....	40
( 4) Total Wells (Number) .....	17
( 5) Net Pay (Feet) .....	31
( 6) Gross Pay (Feet) .....	N/A
( 7) Porosity (%) .....	11
( 8) Initial Oil Saturation (%) .....	65
( 9) Current Oil Saturation (%) .....	N/A
(10) Initial Water Saturation (%) .....	35
(11) Current Water Saturation (%) .....	N/A
(12) Initial Gas Saturation (%) .....	0
(13) Current Gas Saturation (%) .....	N/A
(14) Initial Oil FVF (Res bbl/STB) .....	1.3
(15) Current Oil FVF (Res bbl/STB) .....	N/A
(16) True Vertical Depth (Feet)----Mid-Perforation .....	9,800
(17) Formation Temperature (°F) .....	180

Record 3:

(18) Current Formation Pressure (PSI) .....	3100
(19) Permeability (md) .....	20
(20) Geologic Age (AAPG) .....	120
(21) API Gravity (°API) .....	36
(22) Oil Viscosity (CP) :e Reservoir condition .....	0.86
(23) Formation Salinity (ppm TDS) .....	20,000
(24) OOIP (BBL) .....	N/A
(25) Primary Recovery Factor (Fraction of OOIP) .....	N/A
(26) Cumulative Oil Production (BBL) .....	23,690,000

**Table XIV-40 (continued).**

(27)	Year For Cumulative Oil Production; EX/1986 .....	1992
(28)	Technical Availability Date (Year); Ex/1990 .....	1992
(29)	Primary Recovery (BBL/AC.FT.) .....	N/A
(30)	Primary Recovery (BBL) .....	N/A
(31)	Year For Primary Recovery .....	N/A
(32)	Current Producing GOR (SCF/BBL) .....	N/A
(33)	Initial Producing GOR (SCF/BBL) .....	275

Record 4:

(34)	Reservoir Acreage (Acres) .....	500
(35)	Initial Formation Pressure (PSI) .....	4470
(36)	Reservoir Dip (DEG) .....	N/A
(37)	Production Wells (Number) .....	17
(38)	Injection Wells (Number) .....	2
(39)	Swept Zone Oil Saturation (%) (Residual to Water) .....	N/A
(40)	Injection Water Salinity (ppm TDS) .....	N/A
(41)	Clay Content (%) .....	N/A
(42)	Dykstra-Parsons Coefficient .....	N/A
(43)	Current Injection Rate (B/D/WELL) .....	N/A
(44)	Fractured-Fault (Y,N) (N = 0, Y = 1) .....	0
(45)	Shale Break or Laminations (Y,N) (N = 0, Y = 1) .....	1
(46)	Major Gas Cap (Y,N) (N = 0, Y = 1) .....	0
(47)	Field Multiplier (Number) .....	N/A
(48)	RRC District .....	N/A
(49)	Production Rate (MBBL/D); For the Year shown in element 28 .....	0
(50)	Recovery Efficiency-Waterflood (Factor) .....	N/A
(51)	Ultimate Recovery Factor (Fraction of OOIP) (Primary Plus Secondary) .....	N/A

Record 5:

(52)	Geologic Play Code (Table II) .....	-1
(53)	Depositional System Code (Table III) .....	130
(54)	Depositional System Degree of Confidence (1 = Highest, 2 = Moderate, 3 = Lowest) .....	1
(55)	Diagenetic Overprint Code (Table IV) .....	-1
(56)	Diagenetic Overprint Degree of Confidence (1 = Highest, 2 = Moderate, 3 = Lowest) .....	N/A
(57)	Structural Compartmentalization (Table V) .....	-1
(58)	Structural Compartmentalization Degree of Confidence (1 = Highest, 2 = Moderate, 3 = Lowest) .....	N/A
(59)	Predominant Element of Reservoir Heterogeneity (1 = Depositional System, 2 = Diagenetic Overprint, 3 = Structural Compartmentalization) .....	1
(60)	Trap Type (1 = Stratigraphic, 2 = Structural, 3 = Combination) .....	2
(61)	Geologic Province (Table VI) .....	067

Table XIV-41.

Reservoir Heterogeneity Classification System for TORIS		
<b>1. Reservoir Identification</b> Reservoir Play: _____		
Reservoir Name: <u>West Foreland</u>	Geologic Province: <u>Cook Inlet Basin</u>	Date: <u>7/10/92</u>
Field Name: <u>North Trading Bay</u>	Geologic Age: <u>Tertiary</u>	Prepared By: <u>UAF/PDL</u>
State: <u>AK</u>	Formation: <u>West Foreland</u>	Version: <u>1</u>
<b>2. Depositional System</b> <input type="checkbox"/> 1 <input type="checkbox"/> 2 <input type="checkbox"/> 3   Degree of Confidence in Selection    (1=Highest, 3= Lowest)		
<p style="text-align: center;">Carbonate Reservoirs</p> <div style="display: flex; justify-content: space-between;"> <div style="width: 45%;"> <input type="checkbox"/> Lacustrine   <input type="checkbox"/> Peritidal     ___ Supratidal     ___ Intertidal     ___ Subtidal   <input type="checkbox"/> Shallow Shelf     ___ Open Shelf     ___ Restricted Shelf   <input type="checkbox"/> Shelf Margin     ___ Rimmed Shelf     ___ Ramp </div> <div style="width: 45%;"> <input type="checkbox"/> Reefs     ___ Pinnacle Reefs     ___ Bioherms     ___ Atolls   <input type="checkbox"/> Slope/Basin     ___ Debris Fans     ___ Turbidite Fans     ___ Mounds   <input type="checkbox"/> Basin     ___ Crowded Shelf     ___ Deep Basin </div> </div>	<p style="text-align: center;">Clastic Reservoirs</p> <div style="display: flex; justify-content: space-between;"> <div style="width: 45%;"> <input type="checkbox"/> Eolian     ___ Ergs     ___ Coastal Dunes   <input type="checkbox"/> Lacustrine     ___ Basin Margin     ___ Basin Center   <input checked="" type="checkbox"/> Fluvial     ___ Braided Streams     ___ Meandering Streams   <input type="checkbox"/> Alluvial Fan     ___ Humid (Stream-Dominated)     ___ Arid/Semi-Arid     ___ Fan Deltas   <input type="checkbox"/> Delta     ___ Wave-Dominated     ___ Fluvial-Dominated     ___ Tide-Dominated </div> <div style="width: 45%;"> <input type="checkbox"/> Strandplain     ___ Barrier Cores     ___ Barrier Shoalaces     ___ Back Barriers     ___ Tidal Channels     ___ Washover Fan/Tidal Deltas   <input type="checkbox"/> Shelf (Accretionary Processes)     ___ Sand Waves     ___ Sand Ridge/Bars   <input type="checkbox"/> Slope/Basin     ___ Turbidite Fans     ___ Debris Fans   <input type="checkbox"/> Basin     ___ Pelagic </div> </div>	
<b>3. Diagenetic Overprint</b> <input type="checkbox"/> 1 <input type="checkbox"/> 2 <input type="checkbox"/> 3   Degree of Confidence in Selection    (1=Highest, 3= Lowest)		
<p style="text-align: center;">Carbonate Reservoirs</p> <div style="display: flex; justify-content: space-between;"> <div style="width: 45%;"> <input type="checkbox"/> Compaction/Cementation <input type="checkbox"/> Grain Enhancement <input type="checkbox"/> Dolomitization </div> <div style="width: 45%;"> <input type="checkbox"/> Dolomitization (Evaporites) <input type="checkbox"/> Massave Dissolution <input type="checkbox"/> Silicification </div> </div>	<p style="text-align: center;">Clastic Reservoirs</p> <div style="display: flex; justify-content: space-between;"> <div style="width: 45%;"> <input type="checkbox"/> Compaction/Cementation <input type="checkbox"/> Intergranular Dissolution </div> <div style="width: 45%;"> <input type="checkbox"/> Authigenic Clay <input type="checkbox"/> Chertification </div> </div>	
<b>4. Structural Compartmentalization</b> <input type="checkbox"/> 1 <input type="checkbox"/> 2 <input type="checkbox"/> 3   Degree of Confidence in Selection    (1=Highest, 3= Lowest)		
<input type="checkbox"/> Natural Fracture Porosity <input type="checkbox"/> Unstructured	<input type="checkbox"/> Faulted ___ Normal Fault ___ Reverse Fault ___ Strike-Slip Fault	<input type="checkbox"/> Fault/Fold <input type="checkbox"/> Folded ___ Normal Fault ___ Reverse Fault ___ Strike-Slip Fault
<b>5. Reservoir Heterogeneity Ternary Diagram</b>		
<p>Predominant Element of Reservoir Heterogeneity: (Check Only One)</p> <ul style="list-style-type: none"> <li>• Depositional System      <input checked="" type="checkbox"/> <u>X</u></li> <li>• Diagenetic Overprint      <input type="checkbox"/> _____</li> <li>• Structural Compartmentalization      <input type="checkbox"/> _____</li> </ul>		
<b>6. Trap Type</b> <input type="checkbox"/> Stratigraphic <input checked="" type="checkbox"/> Structural <input type="checkbox"/> Combination		
<b>7. Optional Comments (References, Details on Above Selections, Etc.)</b>		
<hr/> <hr/> <hr/>		

**Table XIV-42.**

**TORIS DATA BASE  
FIELD: NORTH TRADING BAY**

**Record 1:**

Field Code .....	N/A
STATE Postal Code .....	AK
Lithology Code (-1, 0 = Unknown; 1 = SS, 2 = LS; 3 = Dolo.) .....	-1
Geologic Age Code AAPG .....	120
Field Name .....	North Trading Bay
Reservoir Name .....	West Foreland
Reference Number .....	N/A
Load Number .....	N/A
Formation Name .....	West Foreland

**Record 2:**

( 1) Field Acres (Acres) .....	40
( 2) Proven Acres (Acres) .....	40
( 3) Well Spacing (Acres) .....	40
( 4) Total Wells (Number) .....	1
( 5) Net Pay (Feet) .....	70
( 6) Gross Pay (Feet) .....	N/A
( 7) Porosity (%) .....	12
( 8) Initial Oil Saturation (%) .....	65
( 9) Current Oil Saturation (%) .....	N/A
(10) Initial Water Saturation (%) .....	35
(11) Current Water Saturation (%) .....	N/A
(12) Initial Gas Saturation (%) .....	0
(13) Current Gas Saturation (%) .....	N/A
(14) Initial Oil FVF (Res bbl/STB) .....	1.30
(15) Current Oil FVF (Res bbl/STB) .....	N/A
(16) True Vertical Depth (Feet)----Mid-Perforation .....	10,700
(17) Formation Temperature (°F) .....	180

**Record 3:**

(18) Current Formation Pressure (PSI) .....	5400
(19) Permeability (md) .....	1
(20) Geologic Age (AAPG) .....	120
(21) API Gravity (°API) .....	34
(22) Oil Viscosity (CP) :e Reservoir condition .....	0.85
(23) Formation Salinity (ppm TDS) .....	11,000
(24) OOIP (BBL) .....	N/A
(25) Primary Recovery Factor (Fraction of OOIP) .....	N/A
(26) Cumulative Oil Production (BBL) .....	60,400,580

**Table XIV-42 (continued).**

(27)	Year For Cumulative Oil Production; EX/1986 .....	1992
(28)	Technical Availability Date (Year); Ex/1990 .....	1992
(29)	Primary Recovery (BBL/AC.FT.) .....	N/A
(30)	Primary Recovery (BBL) .....	N/A
(31)	Year For Primary Recovery .....	N/A
(32)	Current Producing GOR (SCF/BBL) .....	SHUT IN
(33)	Initial Producing GOR (SCF/BBL) .....	290

Record 4:

(34)	Reservoir Acreage (Acres) .....	40
(35)	Initial Formation Pressure (PSI) .....	6000
(36)	Reservoir Dip (DEG) .....	N/A
(37)	Production Wells (Number) .....	1
(38)	Injection Wells (Number) .....	N/A
(39)	Swept Zone Oil Saturation (%) (Residual to Water) .....	N/A
(40)	Injection Water Salinity (ppm TDS) .....	N/A
(41)	Clay Content (%) .....	N/A
(42)	Dykstra-Parsons Coefficient .....	N/A
(43)	Current Injection Rate (B/D/WELL) .....	N/A
(44)	Fractured-Fault (Y,N) (N = 0, Y = 1) .....	0
(45)	Shale Break or Laminations (Y,N) (N = 0, Y = 1) .....	1
(46)	Major Gas Cap (Y,N) (N = 0, Y = 1) .....	0
(47)	Field Multiplier (Number) .....	N/A
(48)	RRC District .....	N/A
(49)	Production Rate (MBBL/D); For the Year shown in element 28 ....	SHUT IN
(50)	Recovery Efficiency-Waterflood (Factor) .....	N/A
(51)	Ultimate Recovery Factor (Fraction of OOIP) (Primary Plus Secondary) .....	N/A

Record 5:

(52)	Geologic Play Code (Table II) .....	-1
(53)	Depositional System Code (Table III) .....	130
(54)	Depositional System Degree of Confidence (1 = Highest, 2 = Moderate, 3 = Lowest) .....	1
(55)	Diagenetic Overprint Code (Table IV) .....	-1
(56)	Diagenetic Overprint Degree of Confidence (1 = Highest, 2 = Moderate, 3 = Lowest) .....	N/A
(57)	Structural Compartmentalization (Table V) .....	-1
(58)	Structural Compartmentalization Degree of Confidence (1 = Highest, 2 = Moderate, 3 = Lowest) .....	N/A
(59)	Predominant Element of Reservoir Heterogeneity (1 = Depositional System, 2 = Diagenetic Overprint, 3 = Structural Compartmentalization) .....	1
(60)	Trap Type (1 = Stratigraphic, 2 = Structural, 3 = Combination) ....	2
(61)	Geologic Province (Table VI) .....	067

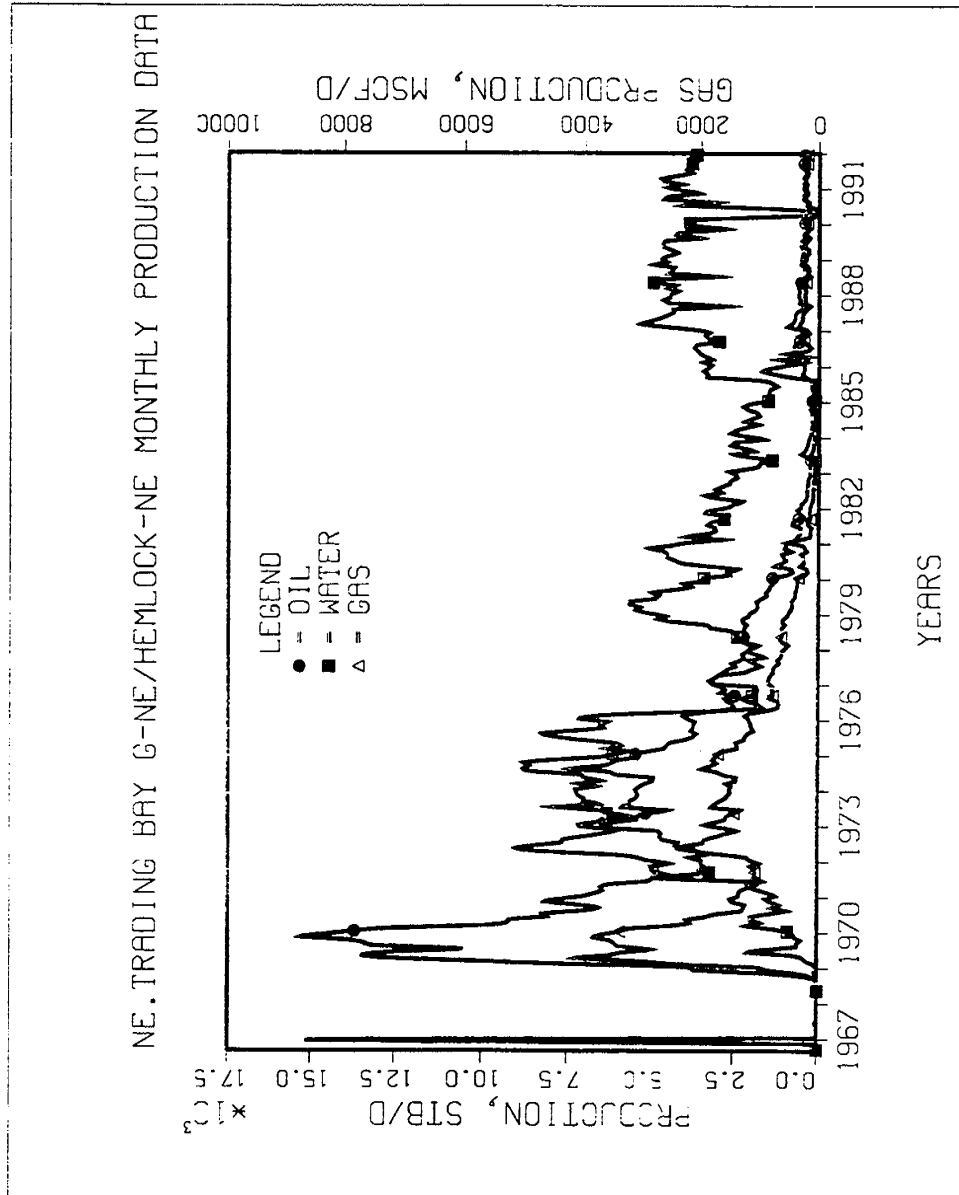


Figure XIV-25.

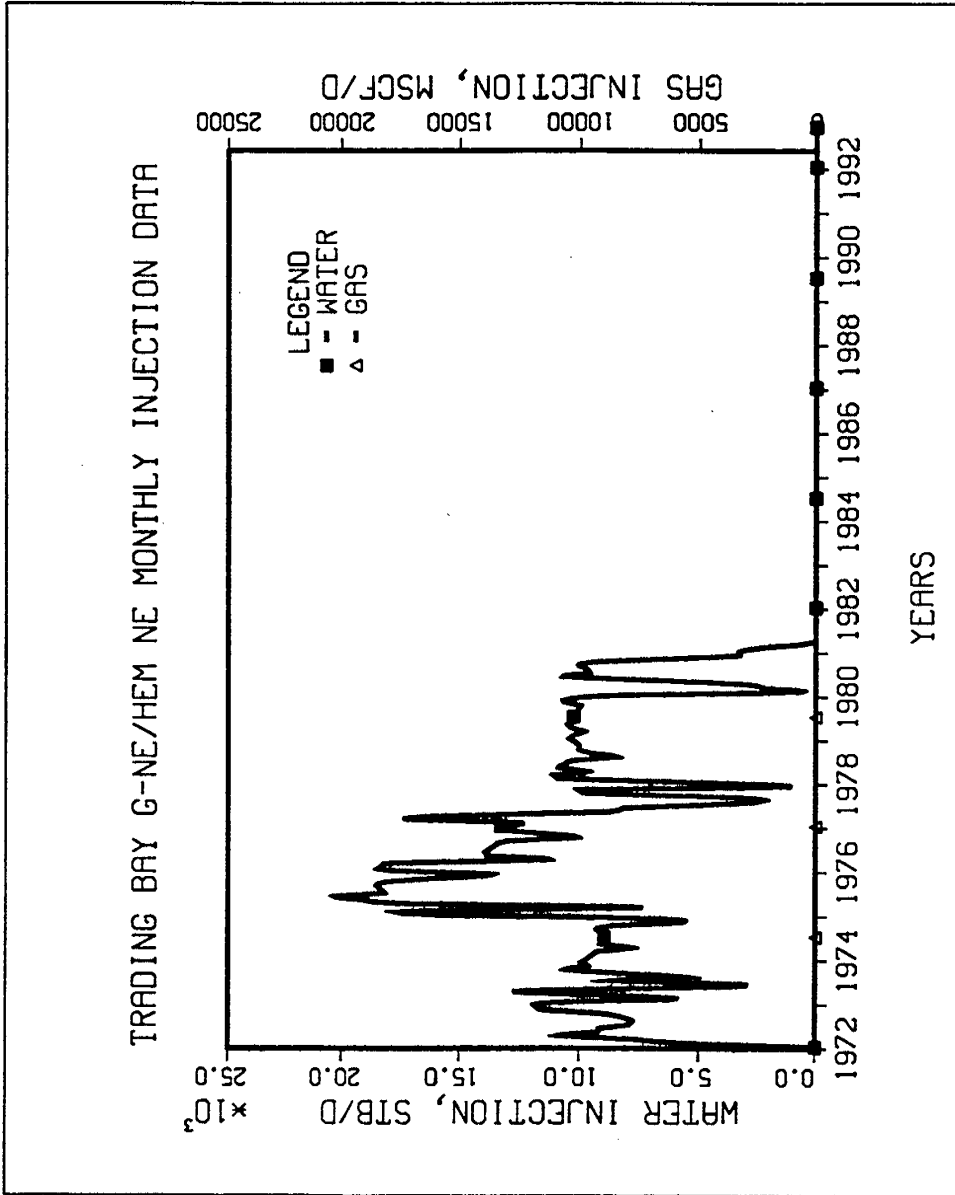


Figure XIV-26.

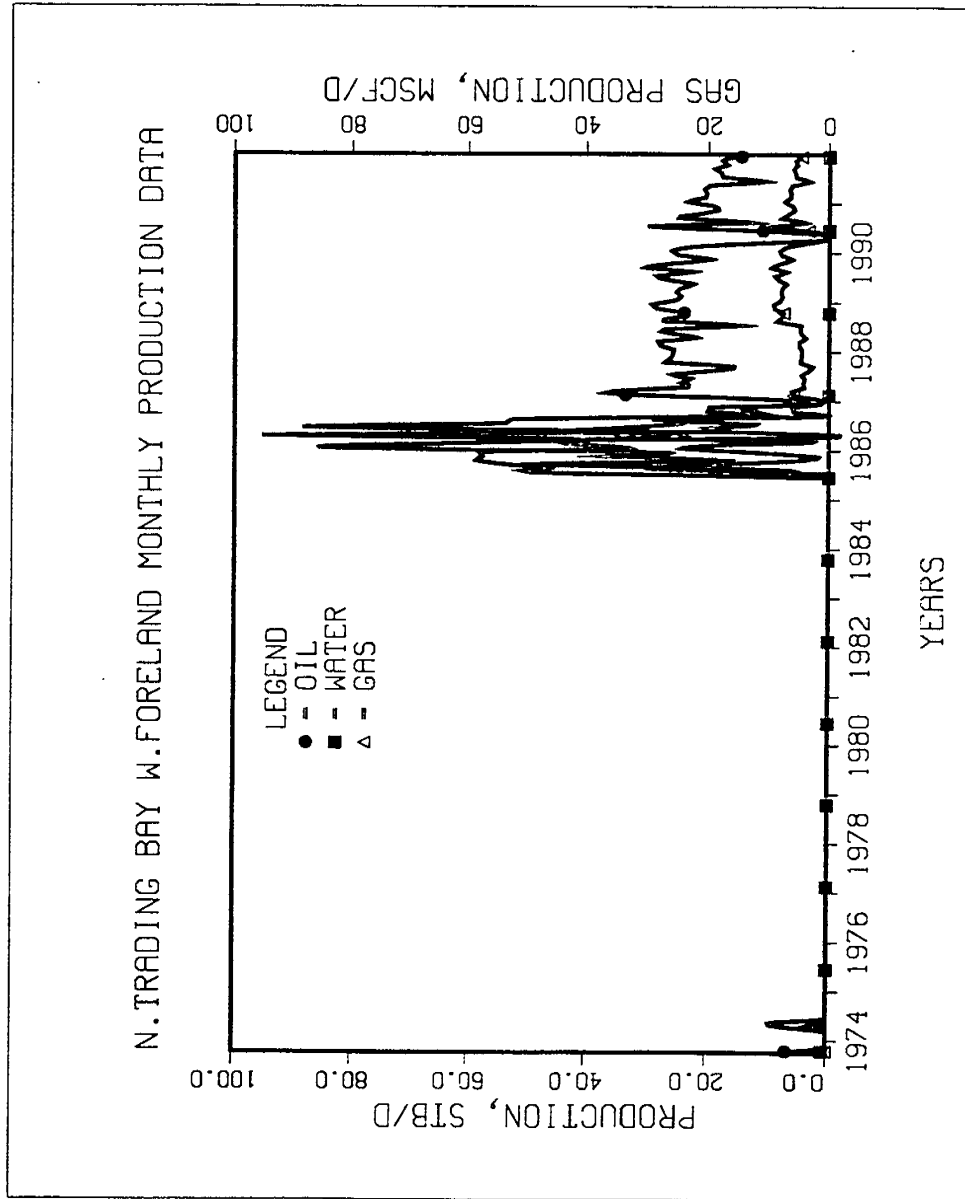


Figure XIV-27.

Table XIV-43.

Reservoir Heterogeneity Classification System for TORIS			
<b>1. Reservoir Identification</b>		Reservoir Play: _____	
Reservoir Name: <u>Hemlock</u>	Geologic Province: <u>Cook Inlet Basin</u>	Date: <u>7/10/92</u>	
Field Name: <u>McArthur River</u>	Geologic Age: <u>Oligocene</u>	Prepared By: <u>PDL/UAF</u>	
State: <u>AK</u>	Formation: <u>Hemlock Conglomerate</u>	Version: <u>1</u>	
<b>2. Depositional System</b> <input type="checkbox"/> 1 <input type="checkbox"/> 2 <input type="checkbox"/> 3    Degree of Confidence in Selection    (1=Highest, 3= Lowest)			
<p style="text-align: center;">Carbonate Reservoirs</p> <div style="display: flex; justify-content: space-between;"> <div style="width: 45%;"> <input type="checkbox"/> Lacustrine   <input type="checkbox"/> Peritidal            ___ Supratidal            ___ Intertidal            ___ Subtidal   <input type="checkbox"/> Shallow Shelf            ___ Open Shelf            ___ Restricted Shelf   <input type="checkbox"/> Shelf Margin            ___ Rimmed Shelf            ___ Ramp </div> <div style="width: 45%;"> <input type="checkbox"/> Reefs            ___ Pinnacle Reefs            ___ Bioherms            ___ Atolls   <input type="checkbox"/> Slope/Basin            ___ Debris Fans            ___ Turbidite Fans   <input type="checkbox"/> Basin            ___ Drowned Shelf            ___ Deep Basin </div> </div>		<p style="text-align: center;">Clastic Reservoirs</p> <div style="display: flex; justify-content: space-between;"> <div style="width: 45%;"> <input type="checkbox"/> Eolian            ___ Ergs            ___ Coastal Dunes   <input type="checkbox"/> Lacustrine            ___ Basin Margin            ___ Basin Center   <input type="checkbox"/> Fluvial            ___ Braided Streams            ___ Meandering Streams   <input type="checkbox"/> Alluvial Fan            ___ Humid (Stream-Dominated)            ___ Arid/Semi-Arid            ___ Fan Deltas   <input checked="" type="checkbox"/> Delta            ___ Wave-Dominated            ___ Fluvial-Dominated            ___ Tide-Dominated </div> <div style="width: 45%;"> <input type="checkbox"/> Strandplain            ___ Barrier Cores            ___ Barrier Shoetaces            ___ Back Barriers            ___ Tidal Channels            ___ Washover Fan/Tidal Deltas   <input type="checkbox"/> Shelf (Accretionary Processes)            ___ Sand Waves            ___ Sand Ridges/Bars   <input type="checkbox"/> Slope/Basin            ___ Turbidite Fans            ___ Debris Fans   <input type="checkbox"/> Basin            ___ Pelagic </div> </div>	
<b>3. Diagenetic Overprint</b> <input type="checkbox"/> 1 <input type="checkbox"/> 2 <input type="checkbox"/> 3    Degree of Confidence in Selection    (1=Highest, 3= Lowest)			
<p style="text-align: center;">Carbonate Reservoirs</p> <div style="display: flex; justify-content: space-between;"> <div style="width: 45%;"> <input type="checkbox"/> Compaction/Cementation  <input type="checkbox"/> Grain Enhancement  <input type="checkbox"/> Dolomitization </div> <div style="width: 45%;"> <input type="checkbox"/> Desilicification (Evaporites)  <input type="checkbox"/> Massive Dissolution  <input type="checkbox"/> Silicification </div> </div>		<p style="text-align: center;">Clastic Reservoirs</p> <div style="display: flex; justify-content: space-between;"> <div style="width: 45%;"> <input checked="" type="checkbox"/> Compaction/Cementation  <input type="checkbox"/> Intergranular Dissolution </div> <div style="width: 45%;"> <input type="checkbox"/> Authigenic Clay  <input type="checkbox"/> Chertification </div> </div>	
<b>4. Structural Compartmentalization</b> <input type="checkbox"/> 1 <input type="checkbox"/> 2 <input type="checkbox"/> 3    Degree of Confidence in Selection    (1=Highest, 3= Lowest)			
<div style="display: flex; justify-content: space-between;"> <div style="width: 20%;"> <input type="checkbox"/> Natural Fracture Perosity </div> <div style="width: 20%;"> <input type="checkbox"/> Unstructured </div> <div style="width: 20%;"> <input type="checkbox"/> Faulted            ___ Normal Fault            ___ Reverse Fault            ___ Strike-Slip Fault </div> <div style="width: 20%;"> <input checked="" type="checkbox"/> Fault/Fold            ___ Normal Fault            ___ Reverse Fault            ___ Strike-Slip Fault </div> <div style="width: 20%;"> <input type="checkbox"/> Folded </div> </div>			
<b>5. Reservoir Heterogeneity Ternary Diagram</b>			
<p style="text-align: center;">Predominant Element of Reservoir Heterogeneity: (Check Only One)</p> <ul style="list-style-type: none"> <li>• Depositional System      _____</li> <li>• Diagenetic Overprint      _____</li> <li>• Structural Compartmentalization      _____</li> </ul>			
<b>6. Trap Type</b> <input type="checkbox"/> Stratigraphic <input type="checkbox"/> Structural <input checked="" type="checkbox"/> Combination			
<b>7. Optional Comments (References, Details on Above Selections, Etc.)</b>			
_____ _____ _____ _____			

**Table XIV-44.**

**TORIS DATA BASE**  
**FIELD: MCARTHUR RIVER (HEMLOCK)**

Record 1:

Field Code .....	N/A
STATE Postal Code .....	AK
Lithology Code (-1, 0 = Unknown; 1 = SS, 2 = LS; 3 = Dolo.) .....	1
Geologic Age Code AAPG .....	123
Field Name .....	McArthur River
Reservoir Name .....	Hemlock
Reference Number .....	3078
Load Number .....	N/A
Formation Name .....	Hemlock Conglomerate

Record 2:

( 1) Field Acres (Acres) .....	12400.0
( 2) Proven Acres (Acres) .....	N/A
( 3) Well Spacing (Acres) .....	80
( 4) Total Wells (Number) .....	80.0
( 5) Net Pay (Feet) .....	290.0
( 6) Gross Pay (Feet) .....	475.0
( 7) Porosity (%) .....	10.5
( 8) Initial Oil Saturation (%) .....	65.0
( 9) Current Oil Saturation (%) .....	41.0
(10) Initial Water Saturation (%) .....	35.0
(11) Current Water Saturation (%) .....	59.0
(12) Initial Gas Saturation (%) .....	0
(13) Current Gas Saturation (%) .....	0
(14) Initial Oil FVF (Res bbl/STB) .....	1.25
(15) Current Oil FVF (Res bbl/STB) .....	1.26
(16) True Vertical Depth (Feet)---Mid-Perforation .....	9350.0
(17) Formation Temperature (°F) .....	180

Record 3:

(18) Current Formation Pressure (PSI) .....	3900
(19) Permeability (md) .....	53.0
(20) Geologic Age (AAPG) .....	123
(21) API Gravity (°API) .....	35.40
(22) Oil Viscosity (CP) :e Reservoir condition .....	1.19
(23) Formation Salinity (ppm TDS) .....	28200.0
(24) OOIP (BBL) .....	1.150 × 10 <sup>9</sup>
(25) Primary Recovery Factor (Fraction of OOIP) .....	.37 (1982)
(26) Cumulative Oil Production (BBL) .....	481 × 10 <sup>6</sup>

**Table XIV-44 (continued).**

(27)	Year For Cumulative Oil Production; EX/1986 .....	1990
(28)	Technical Availability Date (Year); Ex/1990 .....	N/A
(29)	Primary Recovery (BBL/AC.FT.) .....	N/A
(30)	Primary Recovery (BBL) .....	4.304 × 10 <sup>8</sup>
(31)	Year For Primary Recovery .....	1982
(32)	Current Producing GOR (SCF/BBL) .....	654.0
(33)	Initial Producing GOR (SCF/BBL) .....	404.0

Record 4:

(34)	Reservoir Acreage (Acres) .....	8260.0
(35)	Initial Formation Pressure (PSI) .....	4250.0
(36)	Reservoir Dip (DEG) .....	5.00
(37)	Production Wells (Number) .....	59.0
(38)	Injection Wells (Number) .....	21.0
(39)	Swept Zone Oil Saturation (%) (Residual to Water) .....	40.0
(40)	Injection Water Salinity (ppm TDS) .....	26400.0
(41)	Clay Content (%) .....	0.17
(42)	Dykstra-Parsons Coefficient .....	0.72
(43)	Current Injection Rate (B/D/WELL) .....	5900.0
(44)	Fractured-Fault (Y,N) (N = 0, Y = 1) .....	0
(45)	Shale Break or Laminations (Y,N) (N = 0, Y = 1) .....	0
(46)	Major Gas Cap (Y,N) (N = 0, Y = 1) .....	0
(47)	Field Multiplier (Number) .....	N/A
(48)	RRC District .....	N/A
(49)	Production Rate (MBBL/D); For the Year shown in element 28 ....	15.0
(50)	Recovery Efficiency-Waterflood (Factor) .....	N/A
(51)	Ultimate Recovery Factor (Fraction of OOIP) (Primary Plus Secondary) .....	N/A

Record 5:

(52)	Geologic Play Code (Table II) .....	-1
(53)	Depositional System Code (Table III) .....	-1
(54)	Depositional System Degree of Confidence (1 = Highest, 2 = Moderate, 3 = Lowest) .....	N/A
(55)	Diagenetic Overprint Code (Table IV) .....	-1
(56)	Diagenetic Overprint Degree of Confidence (1 = Highest, 2 = Moderate, 3 = Lowest) .....	N/A
(57)	Structural Compartmentalization (Table V) .....	-1
(58)	Structural Compartmentalization Degree of Confidence (1 = Highest, 2 = Moderate, 3 = Lowest) .....	N/A
(59)	Predominant Element of Reservoir Heterogeneity (1 = Depositional System, 2 = Diagenetic Overprint, 3 = Structural Compartmentalization) .....	N/A
(60)	Trap Type (1 = Stratigraphic, 2 = Structural, 3 = Combination) ....	N/A
(61)	Geologic Province (Table VI) .....	067



**Table XIV-46.**

**TORIS DATA BASE**

FIELD: MCARTHUR RIVER (TYONEK MIDDLE KENAI G ZONE)

Record 1:

Field Code .....	N/A
STATE Postal Code .....	AK
Lithology Code (-1, 0 = Unknown; 1 = SS, 2 = LS; 3 = Dolo.) .....	1
Geologic Age Code AAPG .....	123
Field Name .....	McArthur River
Reservoir Name .....	Tyonek Middle Kenai G Zone
Reference Number .....	3079
Load Number .....	N/A
Formation Name .....	Tyonek

Record 2:

( 1) Field Acres (Acres) .....	2400.0
( 2) Proven Acres (Acres) .....	N/A
( 3) Well Spacing (Acres) .....	160.0
( 4) Total Wells (Number) .....	20.0
( 5) Net Pay (Feet) .....	100.0
( 6) Gross Pay (Feet) .....	160.0
( 7) Porosity (%) .....	18.1
( 8) Initial Oil Saturation (%) .....	65.0
( 9) Current Oil Saturation (%) .....	N/A
(10) Initial Water Saturation (%) .....	35.0
(11) Current Water Saturation (%) .....	N/A
(12) Initial Gas Saturation (%) .....	N/A
(13) Current Gas Saturation (%) .....	N/A
(14) Initial Oil FVF (Res bbl/STB) .....	1.23
(15) Current Oil FVF (Res bbl/STB) .....	1.22
(16) True Vertical Depth (Feet)---Mid-Perforation .....	8850.0
(17) Formation Temperature (°F) .....	163.0

Record 3:

(18) Current Formation Pressure (PSI) .....	3000.0
(19) Permeability (md) .....	65.0
(20) Geologic Age (AAPG) .....	123
(21) API Gravity (°API) .....	35.60
(22) Oil Viscosity (CP) :e Reservoir condition .....	1.088
(23) Formation Salinity (ppm TDS) .....	26000.0
(24) OOIP (BBL) .....	130 × 10 <sup>6</sup>
(25) Primary Recovery Factor (Fraction of OOIP) .....	.04 (1982)
(26) Cumulative Oil Production (BBL) .....	39.07 × 10 <sup>6</sup>

**Table XIV-46 (continued).**

(27)	Year For Cumulative Oil Production; EX/1986 .....	1990
(28)	Technical Availability Date (Year); Ex/1990 .....	N/A
(29)	Primary Recovery (BBL/AC.FT.) .....	N/A
(30)	Primary Recovery (BBL) .....	N/A
(31)	Year For Primary Recovery .....	N/A
(32)	Current Producing GOR (SCF/BBL) .....	480.0
(33)	Initial Producing GOR (SCF/BBL) .....	297.0

Record 4:

(34)	Reservoir Acreage (Acres) .....	1752.0
(35)	Initial Formation Pressure (PSI) .....	4009.0
(36)	Reservoir Dip (DEG) .....	5.00
(37)	Production Wells (Number) .....	14.0
(38)	Injection Wells (Number) .....	6.0
(39)	Swept Zone Oil Saturation (%) (Residual to Water) .....	35.00
(40)	Injection Water Salinity (ppm TDS) .....	26400.0
(41)	Clay Content (%) .....	0.15
(42)	Dykstra-Parsons Coefficient .....	0.81
(43)	Current Injection Rate (B/D/WELL) .....	6500.0
(44)	Fractured-Fault (Y,N) (N = 0, Y = 1) .....	0
(45)	Shale Break or Laminations (Y,N) (N = 0, Y = 1) .....	0
(46)	Major Gas Cap (Y,N) (N = 0, Y = 1) .....	0
(47)	Field Multiplier (Number) .....	N/A
(48)	RRC District .....	N/A
(49)	Production Rate (MBBL/D); For the Year shown in element 28 .....	3.25
(50)	Recovery Efficiency-Waterflood (Factor) .....	N/A
(51)	Ultimate Recovery Factor (Fraction of OOIP) (Primary Plus Secondary) .....	N/A

Record 5:

(52)	Geologic Play Code (Table II) .....	-1
(53)	Depositional System Code (Table III) .....	-1
(54)	Depositional System Degree of Confidence (1 = Highest, 2 = Moderate, 3 = Lowest) .....	N/A
(55)	Diagenetic Overprint Code (Table IV) .....	-1
(56)	Diagenetic Overprint Degree of Confidence (1 = Highest, 2 = Moderate, 3 = Lowest) .....	N/A
(57)	Structural Compartmentalization (Table V) .....	-1
(58)	Structural Compartmentalization Degree of Confidence (1 = Highest, 2 = Moderate, 3 = Lowest) .....	N/A
(59)	Predominant Element of Reservoir Heterogeneity (1 = Depositional System, 2 = Diagenetic Overprint, 3 = Structural Compartmentalization) .....	N/A
(60)	Trap Type (1 = Stratigraphic, 2 = Structural, 3 = Combination) .....	N/A
(61)	Geologic Province (Table VI) .....	067

Table XIV-47.

Reservoir Heterogeneity Classification System for TORIS		
1. Reservoir Identification		
Reservoir Name: <u>West Foreland</u>	Geologic Province: <u>Cook Inlet Basin</u>	Date: <u>7/10/92</u>
Field Name: <u>McArthur River</u>	Geologic Age: <u>Eocene</u>	Prepared By: <u>UAF/PDL</u>
State: <u>AK</u>	Formation: <u>West Foreland</u>	Version: <u>1</u>
2. Depositional System <span style="float: right;">Degree of Confidence in Selection (1=Highest, 3= Lowest)</span>		
<input type="checkbox"/> 1 <input type="checkbox"/> 2 <input type="checkbox"/> 3		
<p style="text-align: center;">Carbonate Reservoirs</p> <div style="display: flex; justify-content: space-between;"> <div style="width: 45%;"> <input type="checkbox"/> Lacustrine   <input type="checkbox"/> Peritidal                ___ Subtidal                ___ Intertidal                ___ Subtidal   <input type="checkbox"/> Shallow Shelf                ___ Open Shelf                ___ Restricted Shelf   <input type="checkbox"/> Shelf Margin                ___ Rimmed Shelf                ___ Ramp         </div> <div style="width: 45%;"> <input type="checkbox"/> Reefs                ___ Pinnacle Reefs                ___ Bioherms                ___ Atolls   <input type="checkbox"/> Slope/Basin                ___ Carbon Fans                ___ Turbidite Fans                ___ Mounds   <input type="checkbox"/> Basin                ___ Drowned Shelf                ___ Deep Basin         </div> </div>	<p style="text-align: center;">Clastic Reservoirs</p> <div style="display: flex; justify-content: space-between;"> <div style="width: 45%;"> <input type="checkbox"/> Eolian                ___ Ergs                ___ Coastal Dunes   <input type="checkbox"/> Lacustrine                ___ Basin Margin                ___ Basin Center   <input checked="" type="checkbox"/> Fluvial                ___ Braided Streams                ___ Meandering Streams   <input type="checkbox"/> Alluvial Fan                ___ Humid (Stream-Dominated)                ___ Arid/Semi-Arid                ___ Fan Deltas   <input type="checkbox"/> Delta                ___ Wave-Dominated                ___ Fluvial-Dominated                ___ Tide-Dominated         </div> <div style="width: 45%;"> <input type="checkbox"/> Strandplain                ___ Barrier Cores                ___ Barrier Shoelaces                ___ Back Barriers                ___ Tidal Channels                ___ Washover Fan/Tidal Delta   <input type="checkbox"/> Shelf (Accretionary Processes)                ___ Sand Waves                ___ Sand Ridges/Bars   <input type="checkbox"/> Slope/Basin                ___ Turbidite Fans                ___ Carbon Fans   <input type="checkbox"/> Basin                ___ Pelagic         </div> </div>	
3. Diagenetic Overprint <span style="float: right;">Degree of Confidence in Selection (1=Highest, 3= Lowest)</span>		
<input type="checkbox"/> 1 <input type="checkbox"/> 2 <input type="checkbox"/> 3		
<p style="text-align: center;">Carbonate Reservoirs</p> <div style="display: flex; justify-content: space-between;"> <div style="width: 45%;"> <input type="checkbox"/> Compaction/Compaction  <input type="checkbox"/> Grain Enhancement  <input type="checkbox"/> Dolomitization         </div> <div style="width: 45%;"> <input type="checkbox"/> Diagenesis (Evaporites)  <input type="checkbox"/> Massive Dissolution  <input type="checkbox"/> Silicification         </div> </div>	<p style="text-align: center;">Clastic Reservoirs</p> <div style="display: flex; justify-content: space-between;"> <div style="width: 45%;"> <input checked="" type="checkbox"/> Compaction/Compaction  <input type="checkbox"/> Intergranular Dissolution         </div> <div style="width: 45%;"> <input type="checkbox"/> Authigenic Clay  <input type="checkbox"/> Cementation         </div> </div>	
4. Structural Compartmentalization <span style="float: right;">Degree of Confidence in Selection (1=Highest, 3= Lowest)</span>		
<input type="checkbox"/> 1 <input type="checkbox"/> 2 <input type="checkbox"/> 3		
<input type="checkbox"/> Natural Fracture Porosity	<input type="checkbox"/> Unstructured	<input type="checkbox"/> Faulted ___ Normal Fault ___ Reverse Fault ___ Strike-Slip Fault
<input checked="" type="checkbox"/> Fault/Fold ___ Normal Fault ___ Reverse Fault ___ Strike-Slip Fault		
5. Reservoir Heterogeneity Ternary Diagram		
<p>Predominant Element of Reservoir Heterogeneity: (Check Only One)</p> <ul style="list-style-type: none"> <li>• Depositional System <input type="checkbox"/></li> <li>• Diagenetic Overprint <input type="checkbox"/></li> <li>• Structural Compartmentalization <input type="checkbox"/></li> </ul>		
6. Trap Type <span style="float: right;">Degree of Confidence in Selection (1=Highest, 3= Lowest)</span>		
<input type="checkbox"/> 1 <input type="checkbox"/> 2 <input type="checkbox"/> 3		
<input type="checkbox"/> Stratigraphic	<input type="checkbox"/> Structural	<input checked="" type="checkbox"/> Combination
7. Optional Comments (References, Details on Above Selections, Etc.)		
<hr/> <hr/> <hr/>		

**Table XIV-48.**

**TORIS DATA BASE**  
**FIELD: MCARTHUR RIVER (WEST FORELAND)**

**Record 1:**

Field Code .....	N/A
STATE Postal Code .....	AK
Lithology Code (-1, 0 = Unknown; 1 = SS, 2 = LS; 3 = Dolo.) .....	1
Geologic Age Code AAPG .....	124
Field Name .....	McArthur River
Reservoir Name .....	West Foreland
Reference Number .....	3080
Load Number .....	N/A
Formation Name .....	West Foreland

**Record 2:**

( 1) Field Acres (Acres) .....	1515.0
( 2) Proven Acres (Acres) .....	N/A
( 3) Well Spacing (Acres) .....	160.00
( 4) Total Wells (Number) .....	7
( 5) Net Pay (Feet) .....	100.0
( 6) Gross Pay (Feet) .....	300.0
( 7) Porosity (%) .....	15.7
( 8) Initial Oil Saturation (%) .....	N/A
( 9) Current Oil Saturation (%) .....	31.59
(10) Initial Water Saturation (%) .....	51.83
(11) Current Water Saturation (%) .....	68.41
(12) Initial Gas Saturation (%) .....	N/A
(13) Current Gas Saturation (%) .....	0
(14) Initial Oil FVF (Res bbl/STB) .....	1.19
(15) Current Oil FVF (Res bbl/STB) .....	1.22
(16) True Vertical Depth (Feet)---Mid-Perforation .....	9650.0
(17) Formation Temperature (°F) .....	185.0

**Record 3:**

(18) Current Formation Pressure (PSI) .....	2800.0
(19) Permeability (md) .....	102.0
(20) Geologic Age (AAPG) .....	124
(21) API Gravity (°API) .....	32.9
(22) Oil Viscosity (CP) :e Reservoir condition .....	1.497 (@ 4457 psi)
(23) Formation Salinity (ppm TDS) .....	28.4
(24) OOIP (BBL) .....	75.0 × 10 <sup>6</sup>
(25) Primary Recovery Factor (Fraction of OOIP) .....	0.27 (1982)
(26) Cumulative Oil Production (BBL) .....	20 × 10 <sup>6</sup>

**Table XIV-48 (continued).**

(27)	Year For Cumulative Oil Production; EX/1986 .....	N/A
(28)	Technical Availability Date (Year); Ex/1990 .....	N/A
(29)	Primary Recovery (BBL/AC.FT.) .....	N/A
(30)	Primary Recovery (BBL) .....	16.7 x 10 <sup>6</sup>
(31)	Year For Primary Recovery .....	1982
(32)	Current Producing GOR (SCF/BBL) .....	498 (1990)
(33)	Initial Producing GOR (SCF/BBL) .....	271

Record 4:

(34)	Reservoir Acreage (Acres) .....	1515
(35)	Initial Formation Pressure (PSI) .....	4457
(36)	Reservoir Dip (DEG) .....	5.0
(37)	Production Wells (Number) .....	5.0
(38)	Injection Wells (Number) .....	2
(39)	Swept Zone Oil Saturation (%) (Residual to Water) .....	28.38
(40)	Injection Water Salinity (ppm TDS) .....	N/A
(41)	Clay Content (%) .....	N/A
(42)	Dykstra-Parsons Coefficient .....	0.50
(43)	Current Injection Rate (B/D/WELL) .....	1395.78
(44)	Fractured-Fault (Y,N) (N=0, Y=1) .....	0
(45)	Shale Break or Laminations (Y,N) (N=0, Y=1) .....	1
(46)	Major Gas Cap (Y,N) (N=0, Y=1) .....	0
(47)	Field Multiplier (Number) .....	N/A
(48)	RRC District .....	N/A
(49)	Production Rate (MBBL/D); For the Year shown in element 28 .....	1.2
(50)	Recovery Efficiency-Waterflood (Factor) .....	N/A
(51)	Ultimate Recovery Factor (Fraction of OOIP) (Primary Plus Secondary) .....	0.28

Record 5:

(52)	Geologic Play Code (Table II) .....	-1
(53)	Depositional System Code (Table III) .....	-1
(54)	Depositional System Degree of Confidence (1 = Highest, 2 = Moderate, 3 = Lowest) .....	N/A
(55)	Diagenetic Overprint Code (Table IV) .....	-1
(56)	Diagenetic Overprint Degree of Confidence (1 = Highest, 2 = Moderate, 3 = Lowest) .....	N/A
(57)	Structural Compartmentalization (Table V) .....	-1
(58)	Structural Compartmentalization Degree of Confidence (1 = Highest, 2 = Moderate, 3 = Lowest) .....	N/A
(59)	Predominant Element of Reservoir Heterogeneity (1 = Depositional System, 2 = Diagenetic Overprint, 3 = Structural Compartmentalization) .....	N/A
(60)	Trap Type (1 = Stratigraphic, 2 = Structural, 3 = Combination) .....	N/A
(61)	Geologic Province (Table VI) .....	067

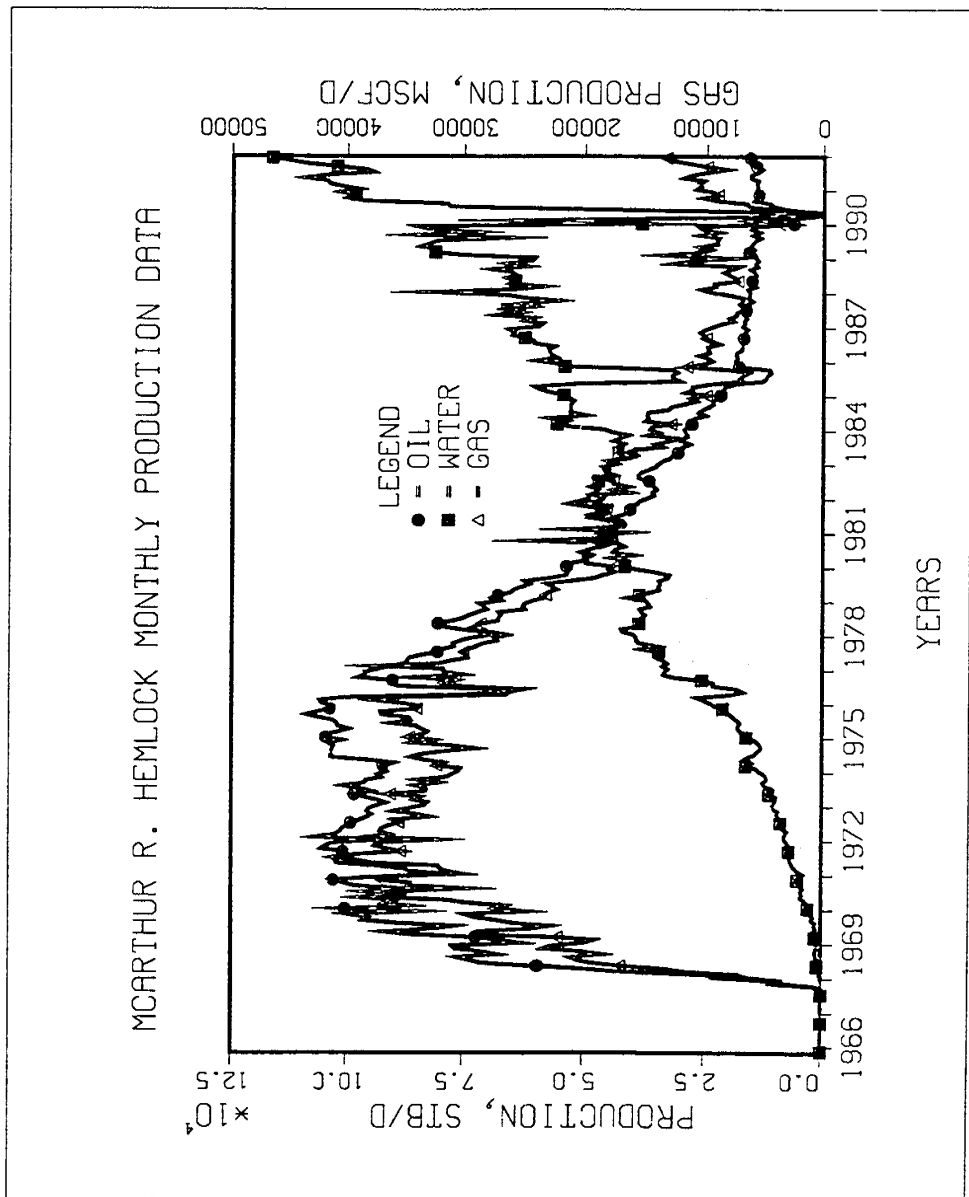


Figure XIV-28.

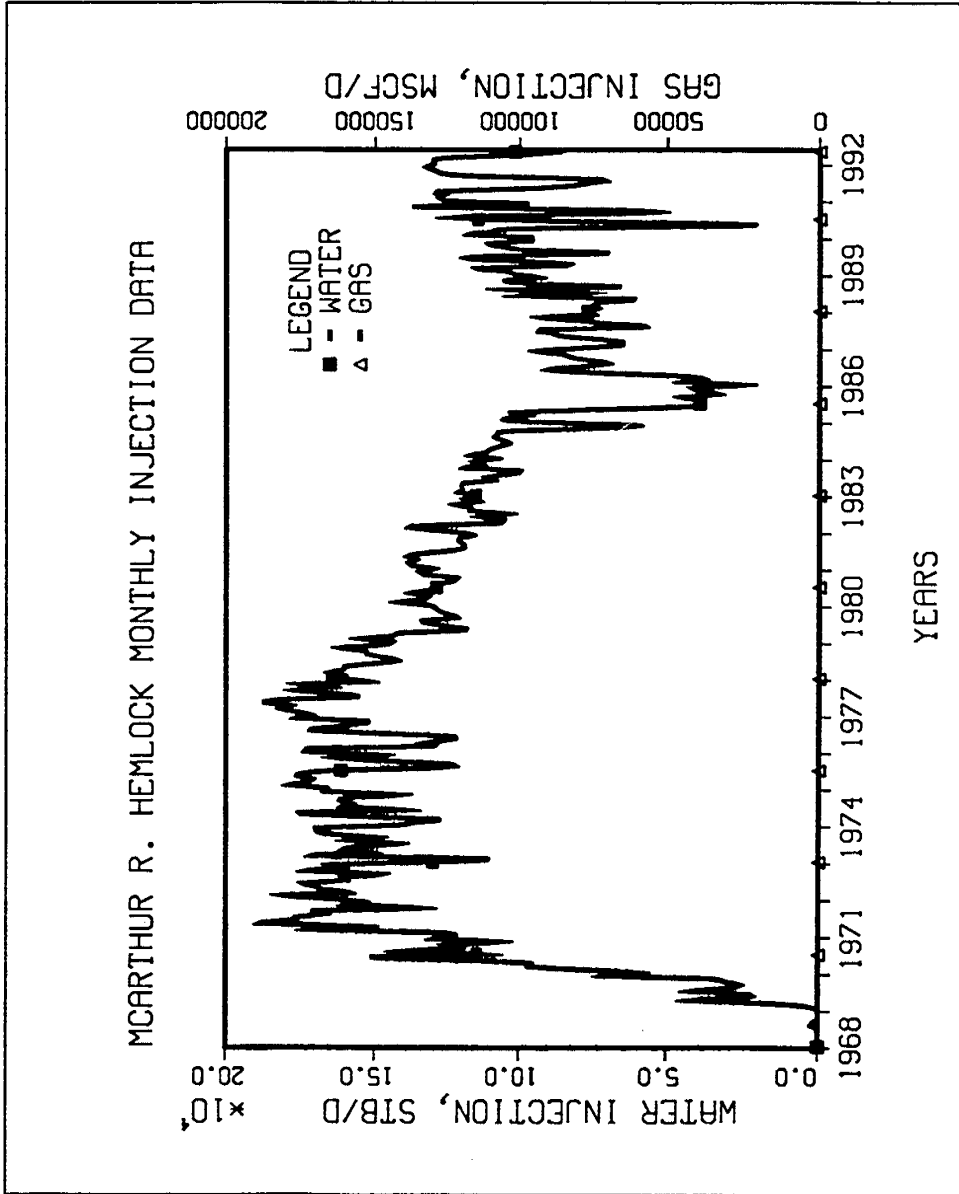


Figure XIV-29.

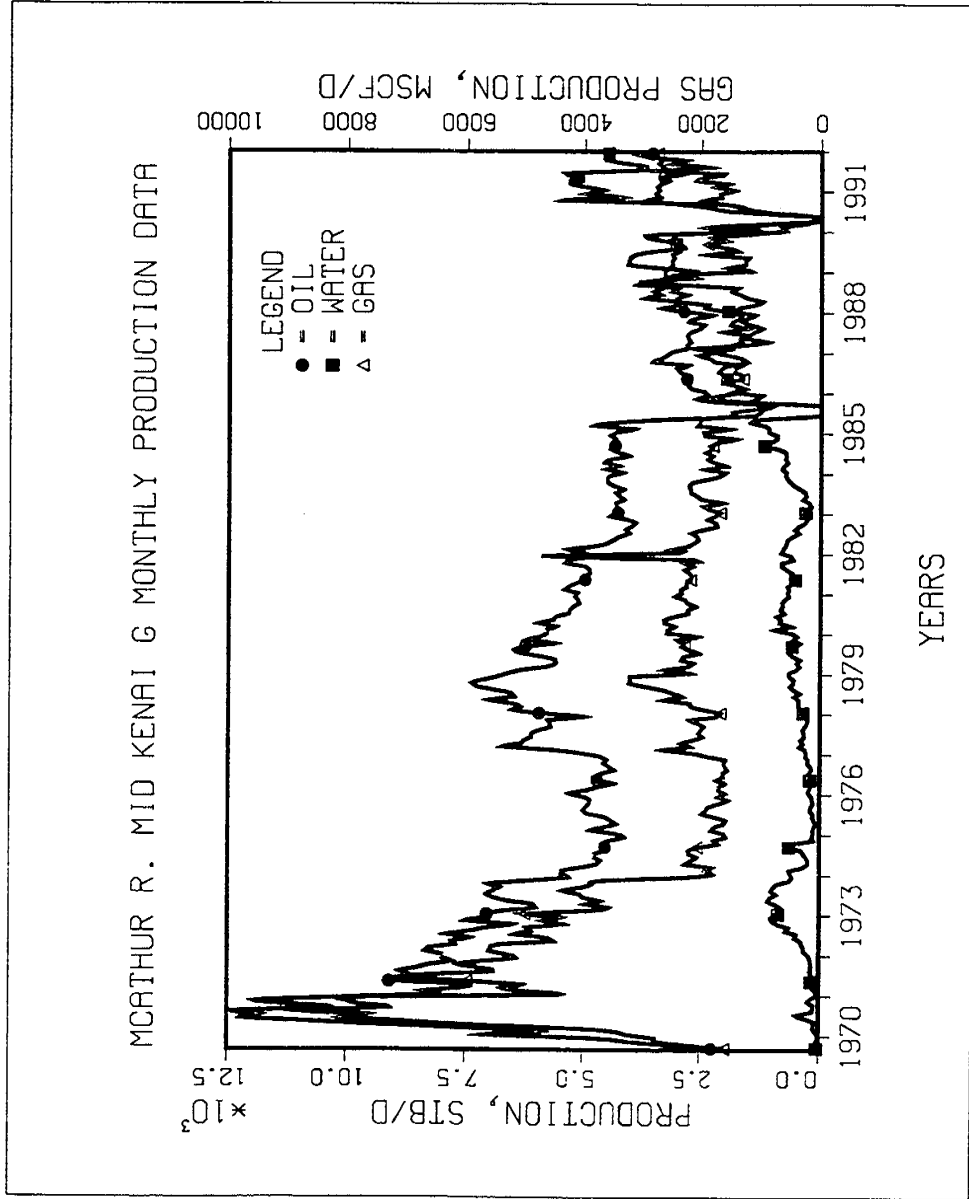


Figure XIV-30.

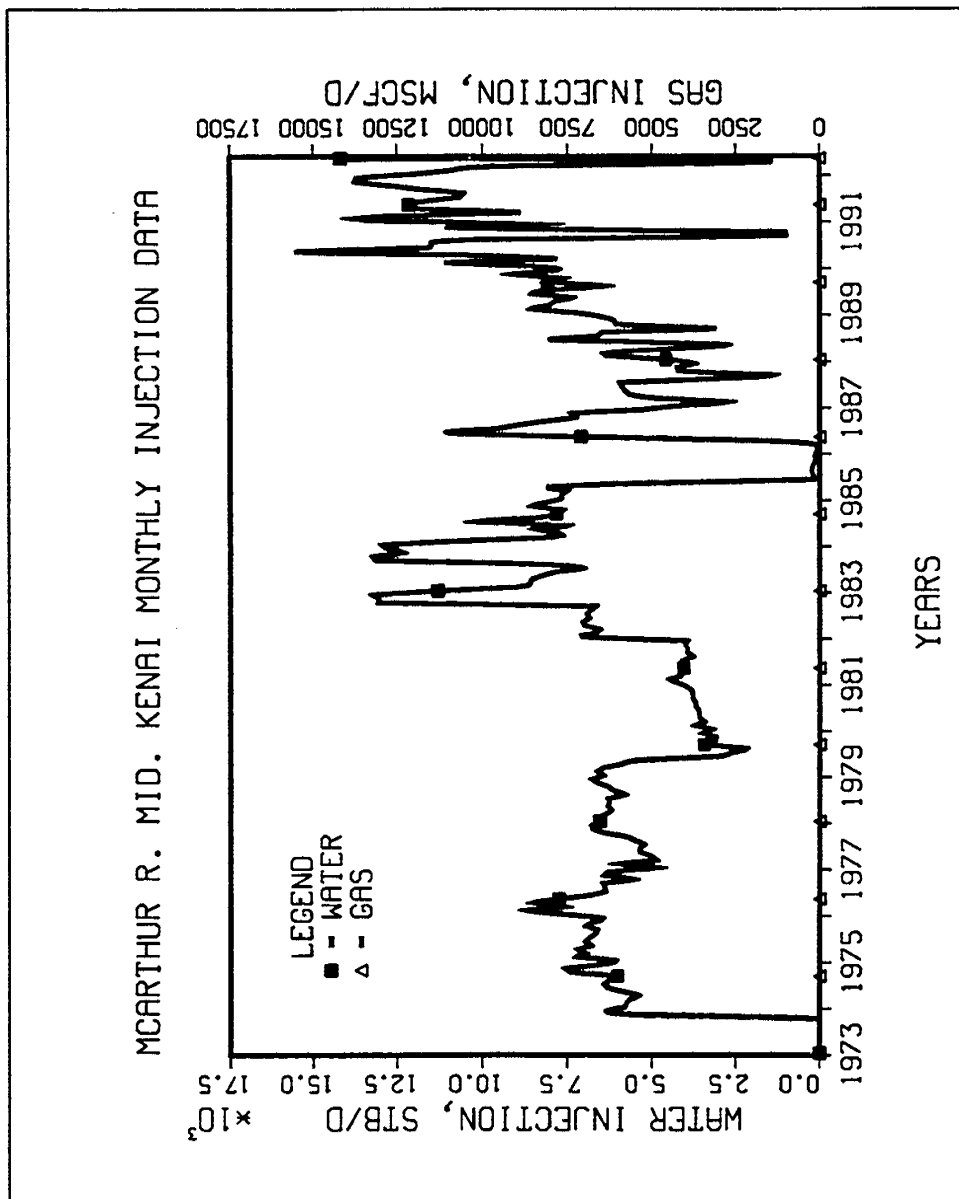


Figure XIV-31.

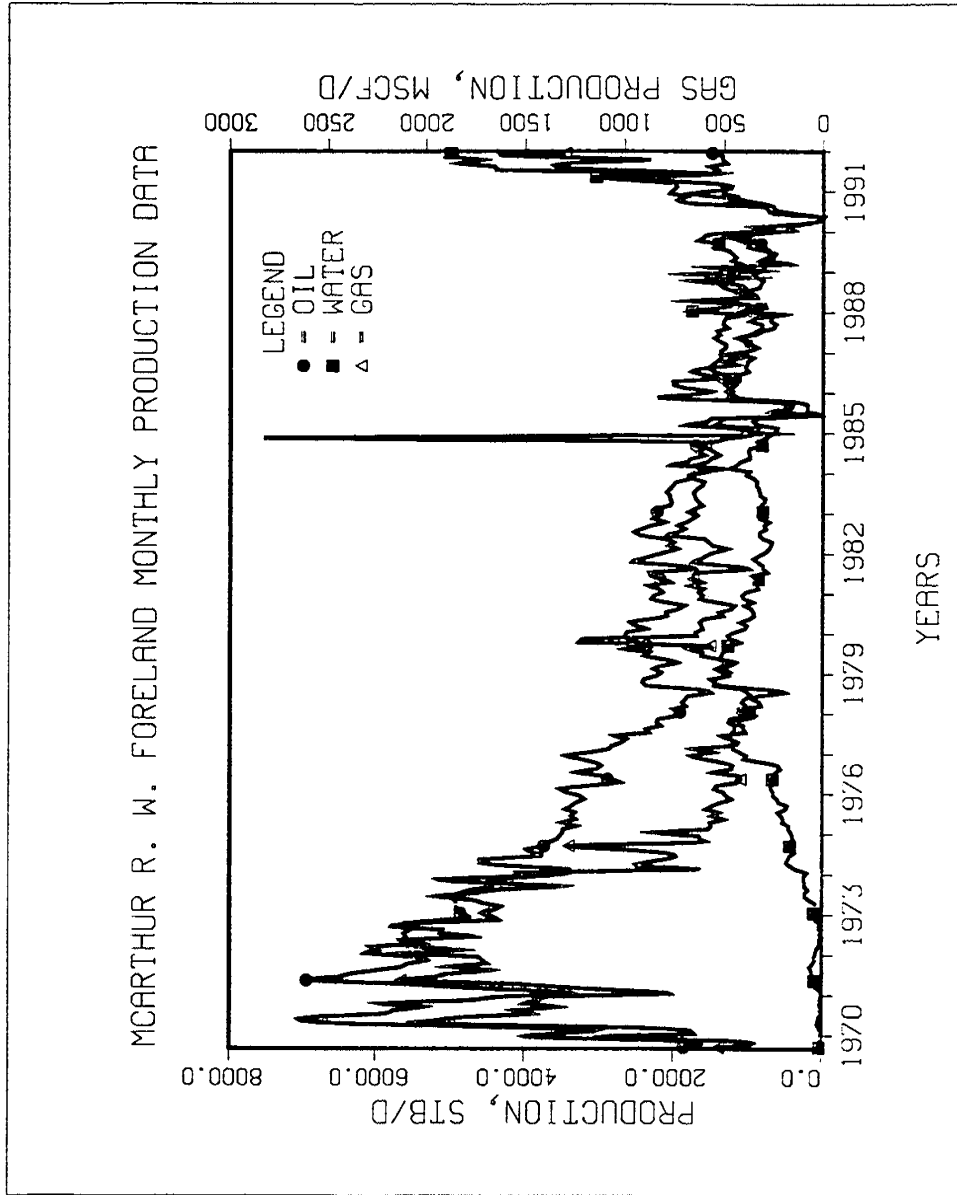


Figure XIV-32.

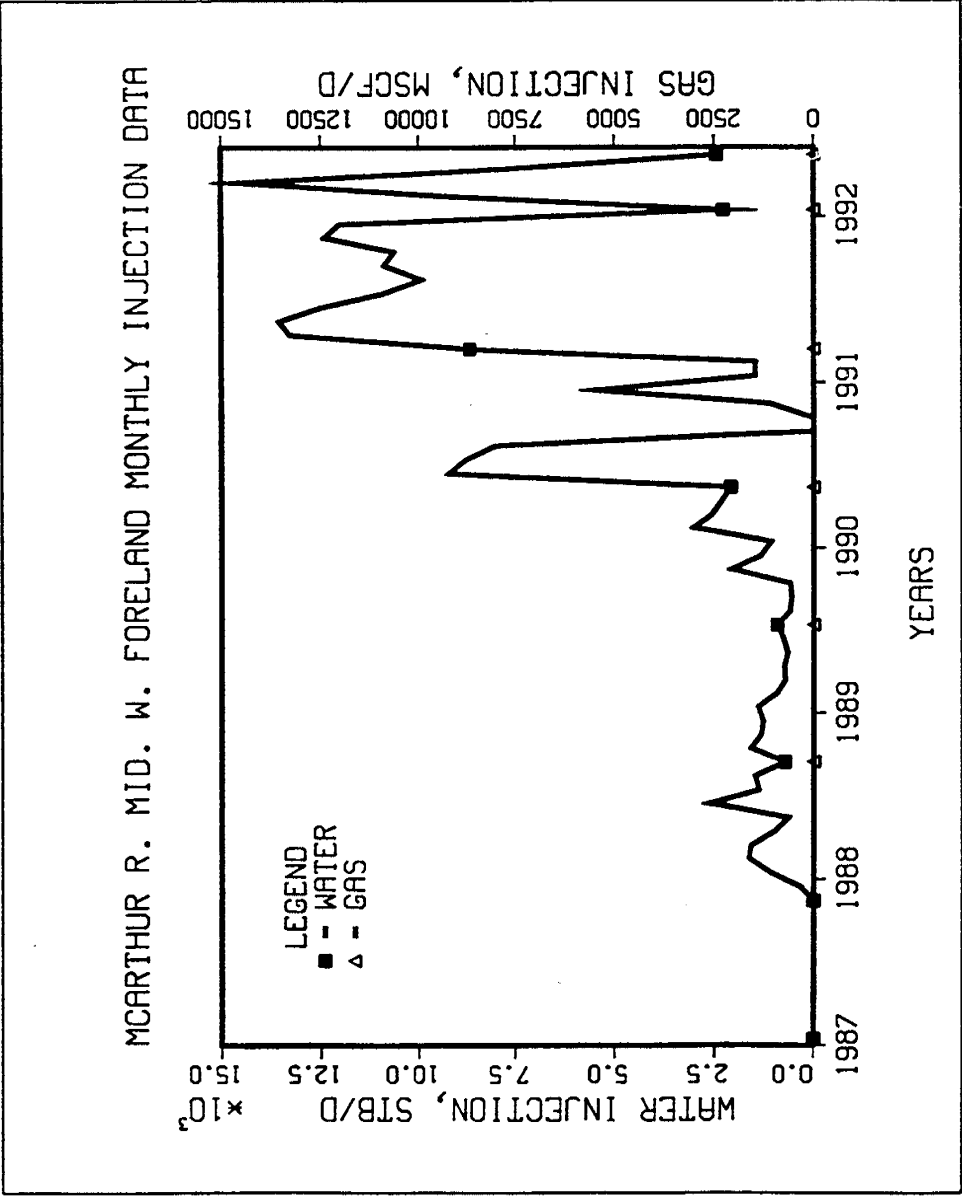


Figure XIV-33.



**Table XIV-50.**

**TORIS DATA BASE  
FIELD: GRANITE POINT**

Record 1:

Field Code .....	N/A
STATE Postal Code .....	AK
Lithology Code (-1, 0 = Unknown; 1 = SS, 2 = LS; 3 = Dolo.) .....	-1
Geologic Age Code AAPG .....	-1
Field Name .....	Granite Point
Reservoir Name .....	Middle Kenai
Reference Number .....	N/A
Load Number .....	N/A
Formation Name .....	Tyonek

Record 2:

( 1) Field Acres (Acres) .....	N/A
( 2) Proven Acres (Acres) .....	N/A
( 3) Well Spacing (Acres) .....	N/A
( 4) Total Wells (Number) .....	33
( 5) Net Pay (Feet) .....	250-600
( 6) Gross Pay (Feet) .....	N/A
( 7) Porosity (%) .....	14
( 8) Initial Oil Saturation (%) .....	N/A
( 9) Current Oil Saturation (%) .....	N/A
(10) Initial Water Saturation (%) .....	39
(11) Current Water Saturation (%) .....	N/A
(12) Initial Gas Saturation (%) .....	N/A
(13) Current Gas Saturation (%) .....	N/A
(14) Initial Oil FVF (Res bbl/STB) .....	N/A
(15) Current Oil FVF (Res bbl/STB) .....	N/A
(16) True Vertical Depth (Feet)---Mid-Perforation .....	8780
(17) Formation Temperature (°F) .....	135-170

Record 3:

(18) Current Formation Pressure (PSI) .....	N/A
(19) Permeability (md) .....	10
(20) Geologic Age (AAPG) .....	N/A
(21) API Gravity (°API) .....	41-44
(22) Oil Viscosity (CP) :e Reservoir condition .....	N/A
(23) Formation Salinity (ppm TDS) .....	N/A
(24) OOIP (BBL) .....	N/A
(25) Primary Recovery Factor (Fraction of OOIP) .....	N/A
(26) Cumulative Oil Production (BBL) .....	113,251,657

**Table XIV-50 (continued).**

(27)	Year For Cumulative Oil Production; EX/1986 .....	1990
(28)	Technical Availability Date (Year); Ex/1990 .....	N/A
(29)	Primary Recovery (BBL/AC.FT.) .....	N/A
(30)	Primary Recovery (BBL) .....	N/A
(31)	Year For Primary Recovery .....	N/A
(32)	Current Producing GOR (SCF/BBL) .....	754
(33)	Initial Producing GOR (SCF/BBL) .....	1110

Record 4:

(34)	Reservoir Acreage (Acres) .....	N/A
(35)	Initial Formation Pressure (PSI) .....	4251
(36)	Reservoir Dip (DEG) .....	N/A
(37)	Production Wells (Number) .....	24
(38)	Injection Wells (Number) .....	9
(39)	Swept Zone Oil Saturation (%) (Residual to Water) .....	N/A
(40)	Injection Water Salinity (ppm TDS) .....	N/A
(41)	Clay Content (%) .....	N/A
(42)	Dykstra-Parsons Coefficient .....	N/A
(43)	Current Injection Rate (B/D/WELL) .....	N/A
(44)	Fractured-Fault (Y,N) (N = 0, Y = 1) .....	N/A
(45)	Shale Break or Laminations (Y,N) (N = 0, Y = 1) .....	N/A
(46)	Major Gas Cap (Y,N) (N = 0, Y = 1) .....	N/A
(47)	Field Multiplier (Number) .....	N/A
(48)	RRC District .....	N/A
(49)	Production Rate (MBBL/D); For the Year shown in element 28 .....	4.0
(50)	Recovery Efficiency-Waterflood (Factor) .....	N/A
(51)	Ultimate Recovery Factor (Fraction of OOIP) (Primary Plus Secondary) .....	N/A

Record 5:

(52)	Geologic Play Code (Table II) .....	-1
(53)	Depositional System Code (Table III) .....	-1
(54)	Depositional System Degree of Confidence (1 = Highest, 2 = Moderate, 3 = Lowest) .....	N/A
(55)	Diagenetic Overprint Code (Table IV) .....	-1
(56)	Diagenetic Overprint Degree of Confidence (1 = Highest, 2 = Moderate, 3 = Lowest) .....	N/A
(57)	Structural Compartmentalization (Table V) .....	-1
(58)	Structural Compartmentalization Degree of Confidence (1 = Highest, 2 = Moderate, 3 = Lowest) .....	N/A
(59)	Predominant Element of Reservoir Heterogeneity (1 = Depositional System, 2 = Diagenetic Overprint, 3 = Structural Compartmentalization) .....	N/A
(60)	Trap Type (1 = Stratigraphic, 2 = Structural, 3 = Combination) .....	N/A
(61)	Geologic Province (Table VI) .....	067

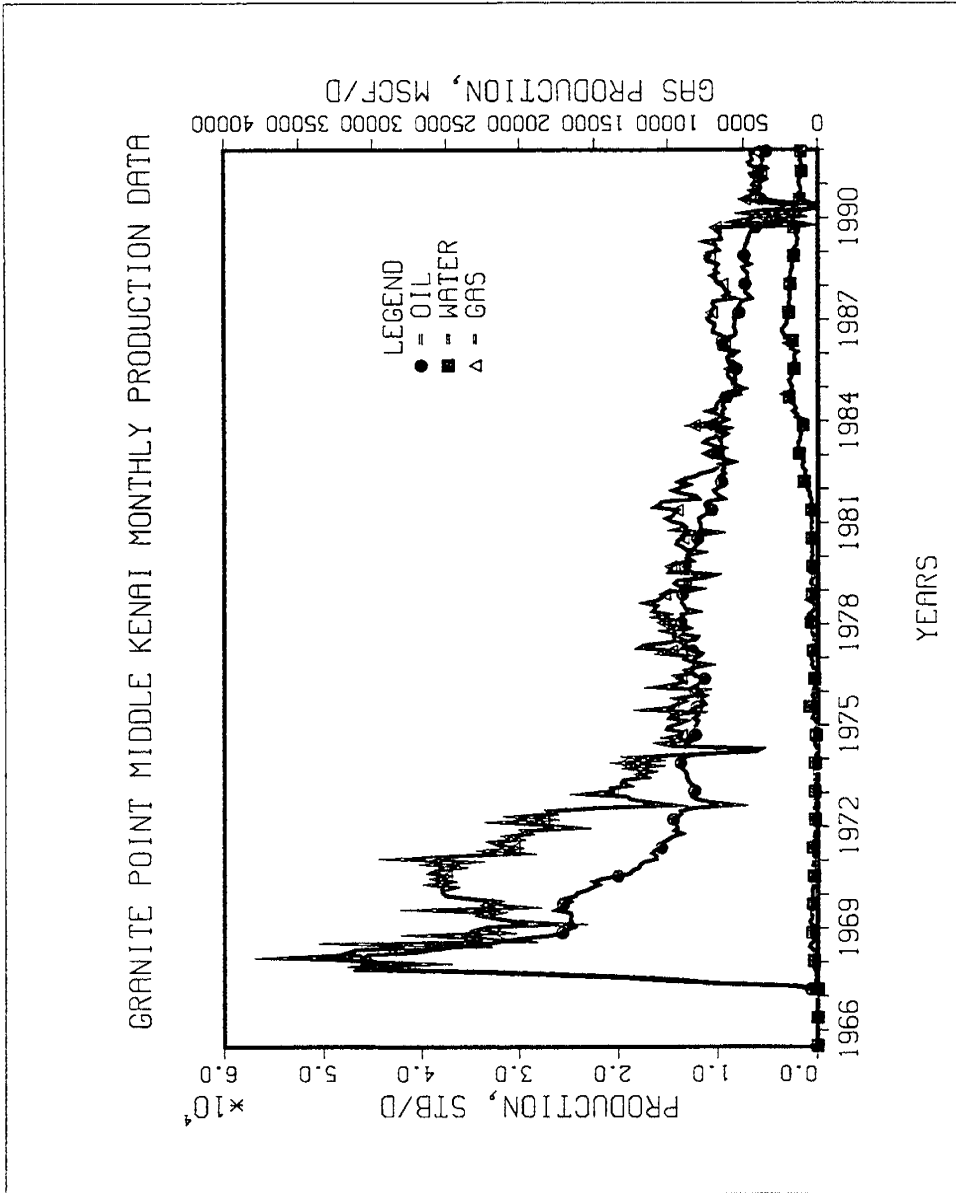


Figure XIV-34.

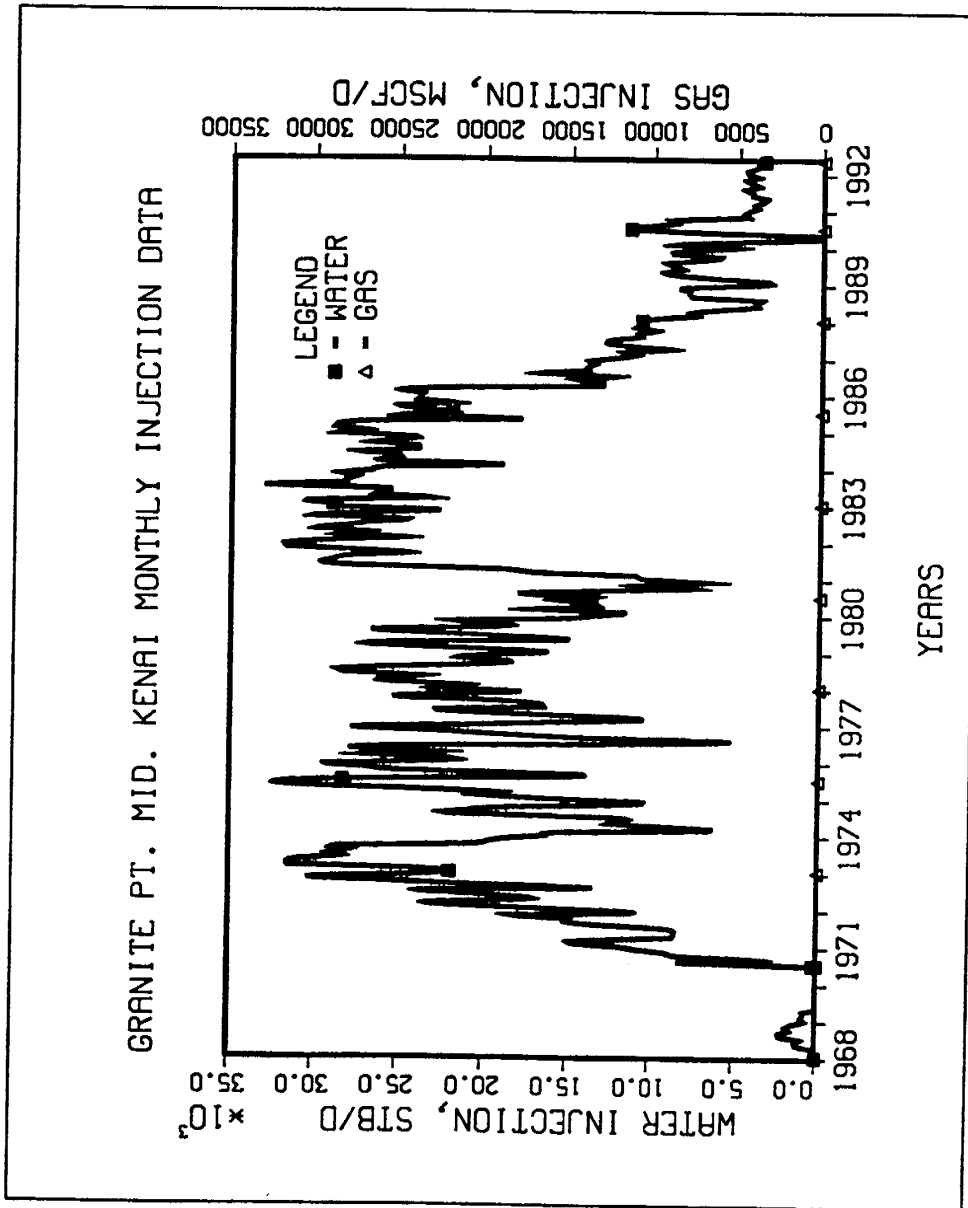


Figure XIV-35.

Table XIV-51.

Reservoir Heterogeneity Classification System for TORIS		
<b>1. Reservoir Identification</b> Reservoir Play: _____		
Reservoir Name: <u>Hemlock</u>	Geologic Province: <u>Cook Inlet Basin</u>	Date: <u>7/10/92</u>
Field Name: <u>Swanson River</u>	Geologic Age: <u>Eocene</u>	Prepared By: <u>UAE/PDL</u>
State: <u>AK</u>	Formation: <u>Hemlock Conglomerate</u>	Version: <u>1</u>
<b>2. Depositional System</b> <input type="checkbox"/> 1 <input type="checkbox"/> 2 <input type="checkbox"/> 3    Degree of Confidence in Selection    (1=Highest, 3= Lowest)		
<b>Carbonate Reservoirs</b> <input type="checkbox"/> Lacustrine <input type="checkbox"/> Peritidal ___ Supratidal ___ Intertidal ___ Subtidal <input type="checkbox"/> Shallow Shelf ___ Open Shelf ___ Restricted Shelf <input type="checkbox"/> Shelf Margin ___ Rimmed Shelf ___ Ramp <input type="checkbox"/> Reefs ___ Pinnacled Reefs ___ Bioherms ___ Atolls <input type="checkbox"/> Slope/Basin ___ Debris Fans ___ Turbidite Fans ___ Mounds <input type="checkbox"/> Basin ___ Drowned Shelf ___ Deep Basin	<b>Clastic Reservoirs</b> <input type="checkbox"/> Eolian ___ Ergs ___ Coastal Dunes <input type="checkbox"/> Lacustrine ___ Basin Margin ___ Basin Center <input type="checkbox"/> Fluvial ___ Braided Streams ___ Meandering Streams <input type="checkbox"/> Alluvial Fan ___ Humid (Stream-Dominated) ___ Arid/Semi-Arid ___ Fan Deltas <input checked="" type="checkbox"/> Delta ___ Wave-Dominated ___ Fluvial-Dominated ___ Tide-Dominated <input type="checkbox"/> Strandplain ___ Barrier Cores ___ Barrier Shoals ___ Back Barriers ___ Tidal Channels ___ Washover Fan/Tidal Deltas <input type="checkbox"/> Shelf (Accretionary Processes) ___ Sand Waves ___ Sand Ridges/Bars <input type="checkbox"/> Slope/Basin ___ Turbidite Fans ___ Debris Fans <input type="checkbox"/> Basin ___ Pelagic	
<b>3. Diagenetic Overprint</b> <input type="checkbox"/> 1 <input type="checkbox"/> 2 <input type="checkbox"/> 3    Degree of Confidence in Selection    (1=Highest, 3= Lowest)		
<b>Carbonate Reservoirs</b> <input type="checkbox"/> Compaction/Cementation <input type="checkbox"/> Grain Enhancement <input type="checkbox"/> Dolomitization <input type="checkbox"/> Dolomitization <input type="checkbox"/> Dolomitization	<b>Clastic Reservoirs</b> <input checked="" type="checkbox"/> Compaction/Cementation <input type="checkbox"/> Intragranular Dissolution <input type="checkbox"/> Diagenetic Overprint (Evaporites) <input type="checkbox"/> Massive Dissolution <input type="checkbox"/> Silicification <input type="checkbox"/> Authigenic Clay <input type="checkbox"/> Chertification	
<b>4. Structural Compartmentalization</b> <input type="checkbox"/> 1 <input type="checkbox"/> 2 <input type="checkbox"/> 3    Degree of Confidence in Selection    (1=Highest, 3= Lowest)		
<input type="checkbox"/> Natural Fracture Porosity <input type="checkbox"/> Unstructured <input type="checkbox"/> Faulted ___ Normal Fault ___ Reverse Fault ___ Strike-Slip Fault <input checked="" type="checkbox"/> Fault/Fold <input type="checkbox"/> Folded ___ Normal Fault ___ Reverse Fault ___ Strike-Slip Fault		
<b>5. Reservoir Heterogeneity Ternary Diagram</b> Predominant Element of Reservoir Heterogeneity: (Check Only One) <ul style="list-style-type: none"> <li>• Depositional System      <input type="checkbox"/></li> <li>• Diagenetic Overprint      <input type="checkbox"/></li> <li>• Structural Compartmentalization      <input type="checkbox"/></li> </ul> <div style="display: flex; justify-content: space-between; align-items: center;"> <div style="text-align: center;"> <p>100% Depositional System</p> <p>100% Diagenetic Overprint      100% Structural Compartmentalization</p> </div> </div>		
<b>6. Trap Type</b> <input type="checkbox"/> Stratigraphic <input type="checkbox"/> Structural <input checked="" type="checkbox"/> Combination		
<b>7. Optional Comments (References, Details on Above Selections, Etc.)</b> _____ _____ _____ _____		

**Table XIV-52.**

**TORIS DATA BASE  
FIELD: SWANSON RIVER**

**Record 1:**

Field Code .....	N/A
STATE Postal Code .....	AK
Lithology Code (-1, 0 = Unknown; 1 = SS, 2 = LS; 3 = Dolo.) .....	1
Geologic Age Code AAPG .....	124
Field Name .....	Swanson River
Reservoir Name .....	Hemlock
Reference Number .....	3149
Load Number .....	N/A
Formation Name .....	Hemlock Conglomerate

**Record 2:**

( 1) Field Acres (Acres) .....	3450
( 2) Proven Acres (Acres) .....	N/A
( 3) Well Spacing (Acres) .....	70
( 4) Total Wells (Number) .....	37
( 5) Net Pay (Feet) .....	70
( 6) Gross Pay (Feet) .....	117.60
( 7) Porosity (%) .....	20
( 8) Initial Oil Saturation (%) .....	60
( 9) Current Oil Saturation (%) .....	34
(10) Initial Water Saturation (%) .....	30
(11) Current Water Saturation (%) .....	66
(12) Initial Gas Saturation (%) .....	N/A
(13) Current Gas Saturation (%) .....	N/A
(14) Initial Oil FVF (Res bbl/STB) .....	1.2
(15) Current Oil FVF (Res bbl/STB) .....	1.28
(16) True Vertical Depth (Feet)---Mid-Perforation .....	N/A
(17) Formation Temperature (°F) .....	180

**Record 3:**

(18) Current Formation Pressure (PSI) .....	4100
(19) Permeability (md) .....	65
(20) Geologic Age (AAPG) .....	124
(21) API Gravity (°API) .....	30
(22) Oil Viscosity (CP) :e Reservoir condition .....	1.9
(23) Formation Salinity (ppm TDS) .....	N/A
(24) OOIP (BBL) .....	438.0 × 10 <sup>6</sup>
(25) Primary Recovery Factor (Fraction of OOIP) .....	0.39
(26) Cumulative Oil Production (BBL) .....	211 × 10 <sup>6</sup>

**Table XIV-52 (continued).**

(27)	Year For Cumulative Oil Production; EX/1986 .....	1991
(28)	Technical Availability Date (Year); Ex/1990 .....	N/A
(29)	Primary Recovery (BBL/AC.FT.) .....	N/A
(30)	Primary Recovery (BBL) .....	172 × 10 <sup>6</sup>
(31)	Year For Primary Recovery .....	N/A
(32)	Current Producing GOR (SCF/BBL) .....	9474
(33)	Initial Producing GOR (SCF/BBL) .....	175

Record 4:

(34)	Reservoir Acreage (Acres) .....	5450
(35)	Initial Formation Pressure (PSI) .....	5700
(36)	Reservoir Dip (DEG) .....	N/A
(37)	Production Wells (Number) .....	29
(38)	Injection Wells (Number) .....	8
(39)	Swept Zone Oil Saturation (%) (Residual to Water) .....	24.2
(40)	Injection Water Salinity (ppm TDS) .....	N/A
(41)	Clay Content (%) .....	N/A
(42)	Dykstra-Parsons Coefficient .....	0.5
(43)	Current Injection Rate (B/D/WELL) .....	1884.53
(44)	Fractured-Fault (Y,N) (N = 0, Y = 1) .....	1
(45)	Shale Break or Laminations (Y,N) (N = 0, Y = 1) .....	1
(46)	Major Gas Cap (Y,N) (N = 0, Y = 1) .....	1
(47)	Field Multiplier (Number) .....	N/A
(48)	RRC District .....	N/A
(49)	Production Rate (MBBL/D); For the Year shown in element 28 .....	6.2
(50)	Recovery Efficiency-Waterflood (Factor) .....	0.39
(51)	Ultimate Recovery Factor (Fraction of OOIP) (Primary Plus Secondary) .....	0.9

Record 5:

(52)	Geologic Play Code (Table II) .....	-1
(53)	Depositional System Code (Table III) .....	-1
(54)	Depositional System Degree of Confidence (1 = Highest, 2 = Moderate, 3 = Lowest) .....	N/A
(55)	Diagenetic Overprint Code (Table IV) .....	-1
(56)	Diagenetic Overprint Degree of Confidence (1 = Highest, 2 = Moderate, 3 = Lowest) .....	N/A
(57)	Structural Compartmentalization (Table V) .....	-1
(58)	Structural Compartmentalization Degree of Confidence (1 = Highest, 2 = Moderate, 3 = Lowest) .....	N/A
(59)	Predominant Element of Reservoir Heterogeneity (1 = Depositional System, 2 = Diagenetic Overprint, 3 = Structural Compartmentalization) .....	N/A
(60)	Trap Type (1 = Stratigraphic, 2 = Structural, 3 = Combination) .....	N/A
(61)	Geologic Province (Table VI) .....	-1

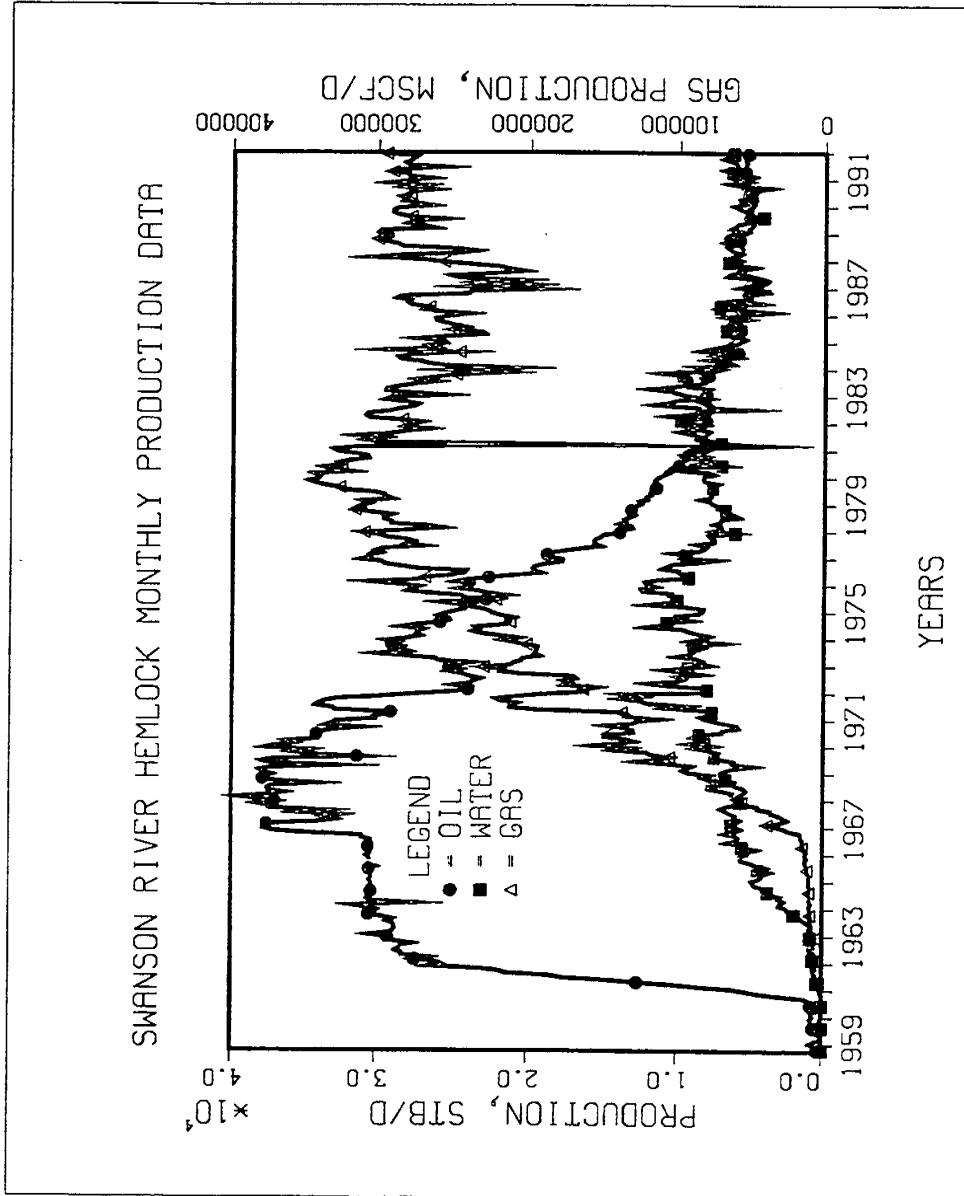


Figure XIV-36.

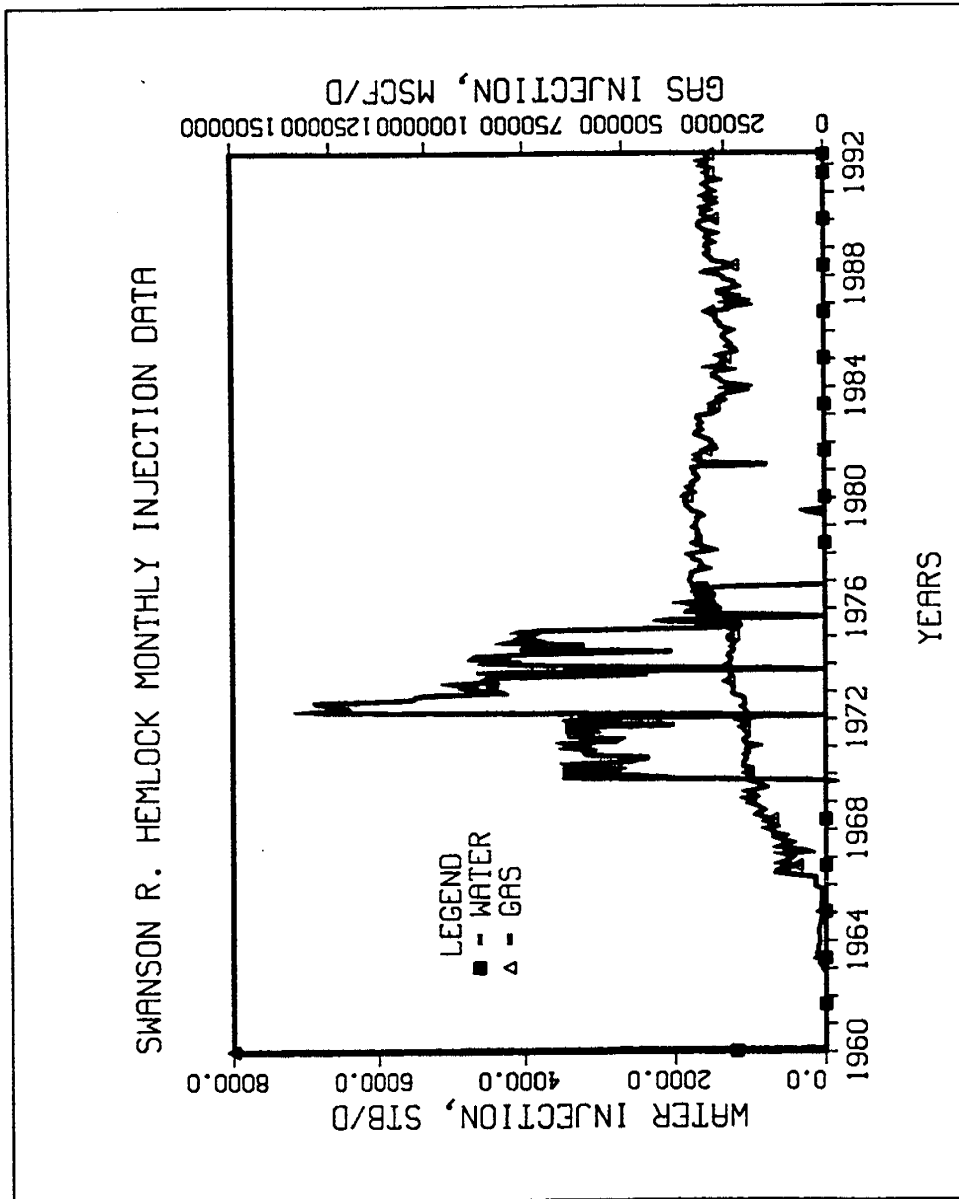


Figure XIV-37.



**Table XIV-54.**

**TORIS DATA BASE**  
**FIELD: MIDDLE GROUND SHOAL (A POOL)**

Record 1:

Field Code .....	N/A
STATE Postal Code .....	AK
Lithology Code (-1, 0 = Unknown; 1 = SS, 2 = LS; 3 = Dolo.) .....	-1
Geologic Age Code AAPG .....	-1
Field Name .....	Middle Ground Shoal
Reservoir Name .....	A Pool
Reference Number .....	N/A
Load Number .....	N/A
Formation Name .....	Tyonek

Record 2:

( 1) Field Acres (Acres) .....	N/A
( 2) Proven Acres (Acres) .....	N/A
( 3) Well Spacing (Acres) .....	N/A
( 4) Total Wells (Number) .....	2
( 5) Net Pay (Feet) .....	190
( 6) Gross Pay (Feet) .....	N/A
( 7) Porosity (%) .....	16
( 8) Initial Oil Saturation (%) .....	N/A
( 9) Current Oil Saturation (%) .....	N/A
(10) Initial Water Saturation (%) .....	0.40
(11) Current Water Saturation (%) .....	N/A
(12) Initial Gas Saturation (%) .....	N/A
(13) Current Gas Saturation (%) .....	N/A
(14) Initial Oil FVF (Res bbl/STB) .....	N/A
(15) Current Oil FVF (Res bbl/STB) .....	N/A
(16) True Vertical Depth (Feet)----Mid-Perforation .....	5500
(17) Formation Temperature (°F) .....	128

Record 3:

(18) Current Formation Pressure (PSI) .....	N/A
(19) Permeability (md) .....	15
(20) Geologic Age (AAPG) .....	N/A
(21) API Gravity (°API) .....	39
(22) Oil Viscosity (CP) :e Reservoir condition .....	N/A
(23) Formation Salinity (ppm TDS) .....	N/A
(24) OOIP (BBL) .....	N/A
(25) Primary Recovery Factor (Fraction of OOIP) .....	N/A
(26) Cumulative Oil Production (BBL) .....	2,025,453

**Table XIV-54 (continued).**

(27)	Year For Cumulative Oil Production; EX/1986 .....	1990
(28)	Technical Availability Date (Year); Ex/1990 .....	N/A
(29)	Primary Recovery (BBL/AC.FT.) .....	N/A
(30)	Primary Recovery (BBL) .....	N/A
(31)	Year For Primary Recovery .....	N/A
(32)	Current Producing GOR (SCF/BBL) .....	N/A
(33)	Initial Producing GOR (SCF/BBL) .....	1000

Record 4:

(34)	Reservoir Acreage (Acres) .....	N/A
(35)	Initial Formation Pressure (PSI) .....	2508
(36)	Reservoir Dip (DEG) .....	N/A
(37)	Production Wells (Number) .....	1
(38)	Injection Wells (Number) .....	1
(39)	Swept Zone Oil Saturation (%) (Residual to Water) .....	N/A
(40)	Injection Water Salinity (ppm TDS) .....	N/A
(41)	Clay Content (%) .....	N/A
(42)	Dykstra-Parsons Coefficient .....	N/A
(43)	Current Injection Rate (B/D/WELL) .....	N/A
(44)	Fractured-Fault (Y,N) (N = 0, Y = 1) .....	N/A
(45)	Shale Break or Laminations (Y,N) (N = 0, Y = 1) .....	N/A
(46)	Major Gas Cap (Y,N) (N = 0, Y = 1) .....	N/A
(47)	Field Multiplier (Number) .....	N/A
(48)	RRC District .....	N/A
(49)	Production Rate (MBBL/D); For the Year shown in element 28 .....	0.0064
(50)	Recovery Efficiency-Waterflood (Factor) .....	N/A
(51)	Ultimate Recovery Factor (Fraction of OOIP) (Primary Plus Secondary) .....	N/A

Record 5:

(52)	Geologic Play Code (Table II) .....	-1
(53)	Depositional System Code (Table III) .....	-1
(54)	Depositional System Degree of Confidence (1 = Highest, 2 = Moderate, 3 = Lowest) .....	N/A
(55)	Diagenetic Overprint Code (Table IV) .....	-1
(56)	Diagenetic Overprint Degree of Confidence (1 = Highest, 2 = Moderate, 3 = Lowest) .....	N/A
(57)	Structural Compartmentalization (Table V) .....	-1
(58)	Structural Compartmentalization Degree of Confidence (1 = Highest, 2 = Moderate, 3 = Lowest) .....	N/A
(59)	Predominant Element of Reservoir Heterogeneity (1 = Depositional System, 2 = Diagenetic Overprint, 3 = Structural Compartmentalization) .....	N/A
(60)	Trap Type (1 = Stratigraphic, 2 = Structural, 3 = Combination) .....	N/A
(61)	Geologic Province (Table VI) .....	067

Table XIV-55.

Reservoir Heterogeneity Classification System for TORIS			
<b>1. Reservoir Identification</b> Reservoir Play: _____			
Reservoir Name: <u>B. C. &amp; D. Pool</u>	Geologic Province: <u>Cook Inlet Basin</u>	Date: <u>7/10/92</u>	
Field Name: <u>Middle Ground Shoal</u>	Geologic Age: _____	Prepared By: <u>UAF/PDL</u>	
State: <u>AK</u>	Formation: <u>Tyonek</u>	Version: <u>1</u>	
<b>2. Depositional System</b> <input type="checkbox"/> 1 <input type="checkbox"/> 2 <input type="checkbox"/> 3    Degree of Confidence in Selection    (1=Highest, 3= Lowest)			
<p style="text-align: center;">Carbonate Reservoirs</p> <div style="display: flex; justify-content: space-between;"> <div style="width: 45%;"> <input type="checkbox"/> Lacustrine   <input type="checkbox"/> Peritidal            ___ Subtidal            ___ Intertidal            ___ Subtidal   <input type="checkbox"/> Shallow Shelf            ___ Open Shelf            ___ Restricted Shelf   <input type="checkbox"/> Shelf Margin            ___ Rimmed Shelf            ___ Ramp </div> <div style="width: 45%;"> <input type="checkbox"/> Reefs            ___ Pinnacle Reefs            ___ Bioherms            ___ Atolls   <input type="checkbox"/> Slope/Basin            ___ Debris Fans            ___ Turbidite Fans            ___ Mounds   <input type="checkbox"/> Basin            ___ Drowned Shelf            ___ Deep Basin </div> </div>		<p style="text-align: center;">Clastic Reservoirs</p> <div style="display: flex; justify-content: space-between;"> <div style="width: 45%;"> <input type="checkbox"/> Eolian            ___ Ergs            ___ Coastal Dunes   <input type="checkbox"/> Lacustrine            ___ Basin Margin            ___ Basin Center   <input type="checkbox"/> Fluvial            ___ Braided Streams            ___ Meandering Streams   <input type="checkbox"/> Alluvial Fan            ___ Humid (Stream-Dominated)            ___ Arid/Semi-Arid            ___ Fan Deltas   <input type="checkbox"/> Delta            ___ Wave-Dominated            ___ Fluvial-Dominated            ___ Tide-Dominated </div> <div style="width: 45%;"> <input type="checkbox"/> Strandplain            ___ Barrier Cores            ___ Barrier Shorefaces            ___ Back Barriers            ___ Tidal Channels            ___ Washover Fan/Tidal Deltas   <input type="checkbox"/> Shelf (Accretionary Processes)            ___ Sand Waves            ___ Sand Ridges/Bars   <input type="checkbox"/> Slope/Basin            ___ Turbidite Fans            ___ Debris Fans   <input type="checkbox"/> Basin            ___ Pelagic </div> </div>	
<b>3. Diagenetic Overprint</b> <input type="checkbox"/> 1 <input type="checkbox"/> 2 <input type="checkbox"/> 3    Degree of Confidence in Selection    (1=Highest, 3= Lowest)			
<p style="text-align: center;">Carbonate Reservoirs</p> <div style="display: flex; justify-content: space-between;"> <div style="width: 45%;"> <input type="checkbox"/> Compaction/Cementation  <input type="checkbox"/> Grain Enhancement  <input type="checkbox"/> Dolomitization </div> <div style="width: 45%;"> <input type="checkbox"/> Dolomitization (Exposures)  <input type="checkbox"/> Massive Dissolution  <input type="checkbox"/> Silicification </div> </div>		<p style="text-align: center;">Clastic Reservoirs</p> <div style="display: flex; justify-content: space-between;"> <div style="width: 45%;"> <input type="checkbox"/> Compaction/Cementation  <input type="checkbox"/> Intergranular Dissolution </div> <div style="width: 45%;"> <input type="checkbox"/> Authigenic Clay  <input type="checkbox"/> Chertification </div> </div>	
<b>4. Structural Compartmentalization</b> <input type="checkbox"/> 1 <input type="checkbox"/> 2 <input type="checkbox"/> 3    Degree of Confidence in Selection    (1=Highest, 3= Lowest)			
<div style="display: flex; justify-content: space-between;"> <div style="width: 20%;"> <input type="checkbox"/> Natural Fracture Porosity </div> <div style="width: 20%;"> <input type="checkbox"/> Unstructured </div> <div style="width: 20%;"> <input type="checkbox"/> Faulted            ___ Normal Fault            ___ Reverse Fault            ___ Strike-Slip Fault </div> <div style="width: 20%;"> <input type="checkbox"/> Fault/Fold            ___ Normal Fault            ___ Reverse Fault            ___ Strike-Slip Fault </div> <div style="width: 20%;"> <input type="checkbox"/> Folded </div> </div>			
<b>5. Reservoir Heterogeneity Ternary Diagram</b>			
Predominant Element of Reservoir Heterogeneity: (Check Only One)			
<input type="checkbox"/> Depositional System <input type="checkbox"/> Diagenetic Overprint <input type="checkbox"/> Structural Compartmentalization			
<b>6. Trap Type</b> <input type="checkbox"/> Stratigraphic <input type="checkbox"/> Structural <input type="checkbox"/> Combination			
<b>7. Optional Comments (References, Details on Above Selections, Etc.)</b>			
_____ _____ _____			

**Table XIV-56.**

**TORIS DATA BASE**  
**FIELD: MIDDLE GROUND SHOAL (B. C. & D. POOL)**

**Record 1:**

Field Code .....	N/A
STATE Postal Code .....	AK
Lithology Code (-1, 0 = Unknown; 1 = SS, 2 = LS; 3 = Dolo.) .....	-1
Geologic Age Code AAPG .....	-1
Field Name .....	Middle Ground Shoal
Reservoir Name .....	B. C. & D. Pool
Reference Number .....	N/A
Load Number .....	N/A
Formation Name .....	Tyonek

**Record 2:**

( 1) Field Acres (Acres) .....	N/A
( 2) Proven Acres (Acres) .....	N/A
( 3) Well Spacing (Acres) .....	N/A
( 4) Total Wells (Number) .....	8
( 5) Net Pay (Feet) .....	335
( 6) Gross Pay (Feet) .....	N/A
( 7) Porosity (%) .....	16
( 8) Initial Oil Saturation (%) .....	N/A
( 9) Current Oil Saturation (%) .....	N/A
(10) Initial Water Saturation (%) .....	0.40
(11) Current Water Saturation (%) .....	N/A
(12) Initial Gas Saturation (%) .....	N/A
(13) Current Gas Saturation (%) .....	N/A
(14) Initial Oil FVF (Res bbl/STB) .....	N/A
(15) Current Oil FVF (Res bbl/STB) .....	N/A
(16) True Vertical Depth (Feet)---Mid-Perforation .....	6000
(17) Formation Temperature (°F) .....	N/A

**Record 3:**

(18) Current Formation Pressure (PSI) .....	N/A
(19) Permeability (md) .....	15
(20) Geologic Age (AAPG) .....	N/A
(21) API Gravity (°API) .....	36-38
(22) Oil Viscosity (CP) :e Reservoir condition .....	N/A
(23) Formation Salinity (ppm TDS) .....	N/A
(24) OOIP (BBL) .....	N/A
(25) Primary Recovery Factor (Fraction of OOIP) .....	N/A
(26) Cumulative Oil Production (BBL) .....	11,190,946

**Table XIV-56 (continued).**

(27)	Year For Cumulative Oil Production; EX/1986 .....	1990
(28)	Technical Availability Date (Year); Ex/1990 .....	N/A
(29)	Primary Recovery (BBL/AC.FT.) .....	N/A
(30)	Primary Recovery (BBL) .....	N/A
(31)	Year For Primary Recovery .....	N/A
(32)	Current Producing GOR (SCF/BBL) .....	737
(33)	Initial Producing GOR (SCF/BBL) .....	650

Record 4:

(34)	Reservoir Acreage (Acres) .....	N/A
(35)	Initial Formation Pressure (PSI) .....	2768
(36)	Reservoir Dip (DEG) .....	N/A
(37)	Production Wells (Number) .....	5
(38)	Injection Wells (Number) .....	3
(39)	Swept Zone Oil Saturation (%) (Residual to Water) .....	N/A
(40)	Injection Water Salinity (ppm TDS) .....	N/A
(41)	Clay Content (%) .....	N/A
(42)	Dykstra-Parsons Coefficient .....	N/A
(43)	Current Injection Rate (B/D/WELL) .....	N/A
(44)	Fractured-Fault (Y,N) (N = 0, Y = 1) .....	N/A
(45)	Shale Break or Laminations (Y,N) (N = 0, Y = 1) .....	N/A
(46)	Major Gas Cap (Y,N) (N = 0, Y = 1) .....	N/A
(47)	Field Multiplier (Number) .....	N/A
(48)	RRC District .....	N/A
(49)	Production Rate (MBBL/D); For the Year shown in element 28 ....	0.465
(50)	Recovery Efficiency-Waterflood (Factor) .....	N/A
(51)	Ultimate Recovery Factor (Fraction of OOIP) (Primary Plus Secondary) .....	N/A

Record 5:

(52)	Geologic Play Code (Table II) .....	-1
(53)	Depositional System Code (Table III) .....	-1
(54)	Depositional System Degree of Confidence (1 = Highest, 2 = Moderate, 3 = Lowest) .....	N/A
(55)	Diagenetic Overprint Code (Table IV) .....	-1
(56)	Diagenetic Overprint Degree of Confidence (1 = Highest, 2 = Moderate, 3 = Lowest) .....	N/A
(57)	Structural Compartmentalization (Table V) .....	-1
(58)	Structural Compartmentalization Degree of Confidence (1 = Highest, 2 = Moderate, 3 = Lowest) .....	N/A
(59)	Predominant Element of Reservoir Heterogeneity (1 = Depositional System, 2 = Diagenetic Overprint, 3 = Structural Compartmentalization) .....	N/A
(60)	Trap Type (1 = Stratigraphic, 2 = Structural, 3 = Combination) ....	N/A
(61)	Geologic Province (Table VI) .....	067

Table XIV-57.

Reservoir Heterogeneity Classification System for TORIS			
<b>1. Reservoir Identification</b>			
Reservoir Play: _____			
Reservoir Name: <u>Tyonek-Hemlock</u>	Geologic Province: <u>Cook Inlet</u>	Date: <u>7/10/92</u>	
Field Name: <u>Middle Ground Shoal</u>	Geologic Age: <u>Paleocene</u>	Prepared By: <u>UAF/PDL</u>	
State: <u>AK</u>	Formation: <u>Tyonek-Hemlock</u>	Version: <u>1</u>	
<b>2. Depositional System</b> <input type="checkbox"/> 1 <input type="checkbox"/> 2 <input type="checkbox"/> 3    Degree of Confidence in Selection (1=Highest, 3= Lowest)			
<b>Carbonate Reservoirs</b>  <input type="checkbox"/> Lacustrine  <input type="checkbox"/> Peritidal ___ Supratidal ___ Intertidal ___ Subtidal  <input type="checkbox"/> Shallow Shelf ___ Open Shelf ___ Restricted Shelf  <input type="checkbox"/> Shelf Margin ___ Rimmed Shelf ___ Ramp  <input type="checkbox"/> Reefs ___ Pinnacle Reefs ___ Bioherms ___ Atolls <input type="checkbox"/> Slope/Basin ___ Debris Fans ___ Turbidite Fans ___ Mounds  <input type="checkbox"/> Basin ___ Drowned Shelf ___ Deep Basin		<b>Clastic Reservoirs</b>  <input type="checkbox"/> Eolian ___ Ergs ___ Coastal Dunes <input type="checkbox"/> Lacustrine ___ Basin Margin ___ Basin Center  <input type="checkbox"/> Fluvial ___ Braided Streams ___ Meandering Streams  <input type="checkbox"/> Alluvial Fan ___ Humid (Stream-Dominated) ___ Arid/Semi-Arid ___ Fan Deltas  <input type="checkbox"/> Delta ___ Wave-Dominated ___ Fluvial-Dominated ___ Tide-Dominated  <input checked="" type="checkbox"/> Strandplain ___ Barrier Cores ___ Barrier Shorelines ___ Back Barriers <input checked="" type="checkbox"/> Tidal Channels ___ Washover Fan/Tidal Deltas <input type="checkbox"/> Shelf (Accretionary Processes) ___ Sand Waves ___ Sand Ridge/Bars  <input type="checkbox"/> Slope/Basin ___ Turbidite Fans ___ Debris Fans  <input type="checkbox"/> Basin ___ Pelagic	
<b>3. Diagenetic Overprint</b> <input type="checkbox"/> 1 <input type="checkbox"/> 2 <input type="checkbox"/> 3    Degree of Confidence in Selection (1=Highest, 3= Lowest)			
<b>Carbonate Reservoirs</b>  <input type="checkbox"/> Compaction/Cementation <input type="checkbox"/> Dolomitization (Evaporites) <input type="checkbox"/> Grain Enhancement <input type="checkbox"/> Massive Dissolution <input type="checkbox"/> Dolomitization <input type="checkbox"/> Silicification		<b>Clastic Reservoirs</b>  <input checked="" type="checkbox"/> Compaction/Cementation <input type="checkbox"/> Authigenic Clay <input type="checkbox"/> Intergranular Dissolution <input type="checkbox"/> Cementation	
<b>4. Structural Compartmentalization</b> <input type="checkbox"/> 1 <input type="checkbox"/> 2 <input type="checkbox"/> 3    Degree of Confidence in Selection (1=Highest, 3= Lowest)			
<input type="checkbox"/> Natural Fracture Porosity <input type="checkbox"/> Unstructured		<input type="checkbox"/> Faulted ___ Normal Fault ___ Reverse Fault ___ Strike-Slip Fault  <input checked="" type="checkbox"/> Fault/Fold <input type="checkbox"/> Folded ___ Normal Fault ___ Reverse Fault ___ Strike-Slip Fault	
<b>5. Reservoir Heterogeneity Ternary Diagram</b>			
Predominant Element of Reservoir Heterogeneity: (Check Only One)  <input type="checkbox"/> Depositional System <input type="checkbox"/> Diagenetic Overprint <input type="checkbox"/> Structural Compartmentalization			
<b>6. Trap Type</b> <input type="checkbox"/> Stratigraphic <input type="checkbox"/> Structural <input checked="" type="checkbox"/> Combination			
<b>7. Optional Comments (References, Details on Above Selections, Etc.)</b>			
_____ _____ _____ _____			

**Table XIV-58.**

**TORIS DATA BASE**  
**FIELD: MIDDLE GROUND SHOAL**

Record 1:

Field Code .....	N/A
STATE Postal Code .....	AK
Lithology Code (-1, 0 = Unknown; 1 = SS, 2 = LS; 3 = Dolo.) .....	1
Geologic Age Code AAPG .....	125
Field Name .....	Middle Ground Shoal
Reservoir Name .....	Tyonek-Hemlock E. F. & G.
Reference Number .....	3430
Load Number .....	N/A
Formation Name .....	Tyonek-Hemlock

Record 2:

( 1) Field Acres (Acres) .....	8866.0
( 2) Proven Acres (Acres) .....	N/A
( 3) Well Spacing (Acres) .....	80
( 4) Total Wells (Number) .....	50
( 5) Net Pay (Feet) .....	500
( 6) Gross Pay (Feet) .....	1400
( 7) Porosity (%) .....	11
( 8) Initial Oil Saturation (%) .....	70
( 9) Current Oil Saturation (%) .....	51
(10) Initial Water Saturation (%) .....	30
(11) Current Water Saturation (%) .....	49
(12) Initial Gas Saturation (%) .....	0.0
(13) Current Gas Saturation (%) .....	0.0
(14) Initial Oil FVF (Res bbl/STB) .....	1.23
(15) Current Oil FVF (Res bbl/STB) .....	1.20
(16) True Vertical Depth (Feet)----Mid-Perforation .....	8500
(17) Formation Temperature (°F) .....	155

Record 3:

(18) Current Formation Pressure (PSI) .....	2352
(19) Permeability (md) .....	10
(20) Geologic Age (AAPG) .....	125
(21) API Gravity (°API) .....	36-38
(22) Oil Viscosity (CP) :e Reservoir condition .....	0.27
(23) Formation Salinity (ppm TDS) .....	1.28
(24) OOIP (BBL) .....	300 × 10 <sup>6</sup>
(25) Primary Recovery Factor (Fraction of OOIP) .....	0.5 (1982)
(26) Cumulative Oil Production (BBL) .....	150 × 10 <sup>6</sup>

**Table XIV-58 (continued).**

(27)	Year For Cumulative Oil Production; EX/1986 .....	1991
(28)	Technical Availability Date (Year); Ex/1990 .....	N/A
(29)	Primary Recovery (BBL/AC.FT.) .....	N/A
(30)	Primary Recovery (BBL) .....	80 x 10 <sup>6</sup>
(31)	Year For Primary Recovery .....	N/A
(32)	Current Producing GOR (SCF/BBL) .....	368 (1990)
(33)	Initial Producing GOR (SCF/BBL) .....	381

Record 4:

(34)	Reservoir Acreage (Acres) .....	1493
(35)	Initial Formation Pressure (PSI) .....	4220
(36)	Reservoir Dip (DEG) .....	N/A
(37)	Production Wells (Number) .....	36
(38)	Injection Wells (Number) .....	14
(39)	Swept Zone Oil Saturation (%) (Residual to Water) .....	31.98
(40)	Injection Water Salinity (ppm TDS) .....	30
(41)	Clay Content (%) .....	N/A
(42)	Dykstra-Parsons Coefficient .....	0.5
(43)	Current Injection Rate (B/D/WELL) .....	1171
(44)	Fractured-Fault (Y,N) (N = 0, Y = 1) .....	1
(45)	Shale Break or Laminations (Y,N) (N = 0, Y = 1) .....	1
(46)	Major Gas Cap (Y,N) (N = 0, Y = 1) .....	0
(47)	Field Multiplier (Number) .....	N/A
(48)	RRC District .....	N/A
(49)	Production Rate (MBBL/D); For the Year shown in element 28 .....	7
(50)	Recovery Efficiency-Waterflood (Factor) .....	0.68
(51)	Ultimate Recovery Factor (Fraction of OOIP) (Primary Plus Secondary) .....	N/A

Record 5:

(52)	Geologic Play Code (Table II) .....	-1
(53)	Depositional System Code (Table III) .....	-1
(54)	Depositional System Degree of Confidence (1 = Highest, 2 = Moderate, 3 = Lowest) .....	N/A
(55)	Diagenetic Overprint Code (Table IV) .....	-1
(56)	Diagenetic Overprint Degree of Confidence (1 = Highest, 2 = Moderate, 3 = Lowest) .....	N/A
(57)	Structural Compartmentalization (Table V) .....	-1
(58)	Structural Compartmentalization Degree of Confidence (1 = Highest, 2 = Moderate, 3 = Lowest) .....	N/A
(59)	Predominant Element of Reservoir Heterogeneity (1 = Depositional System, 2 = Diagenetic Overprint, 3 = Structural Compartmentalization) .....	N/A
(60)	Trap Type (1 = Stratigraphic, 2 = Structural, 3 = Combination) .....	N/A
(61)	Geologic Province (Table VI) .....	067

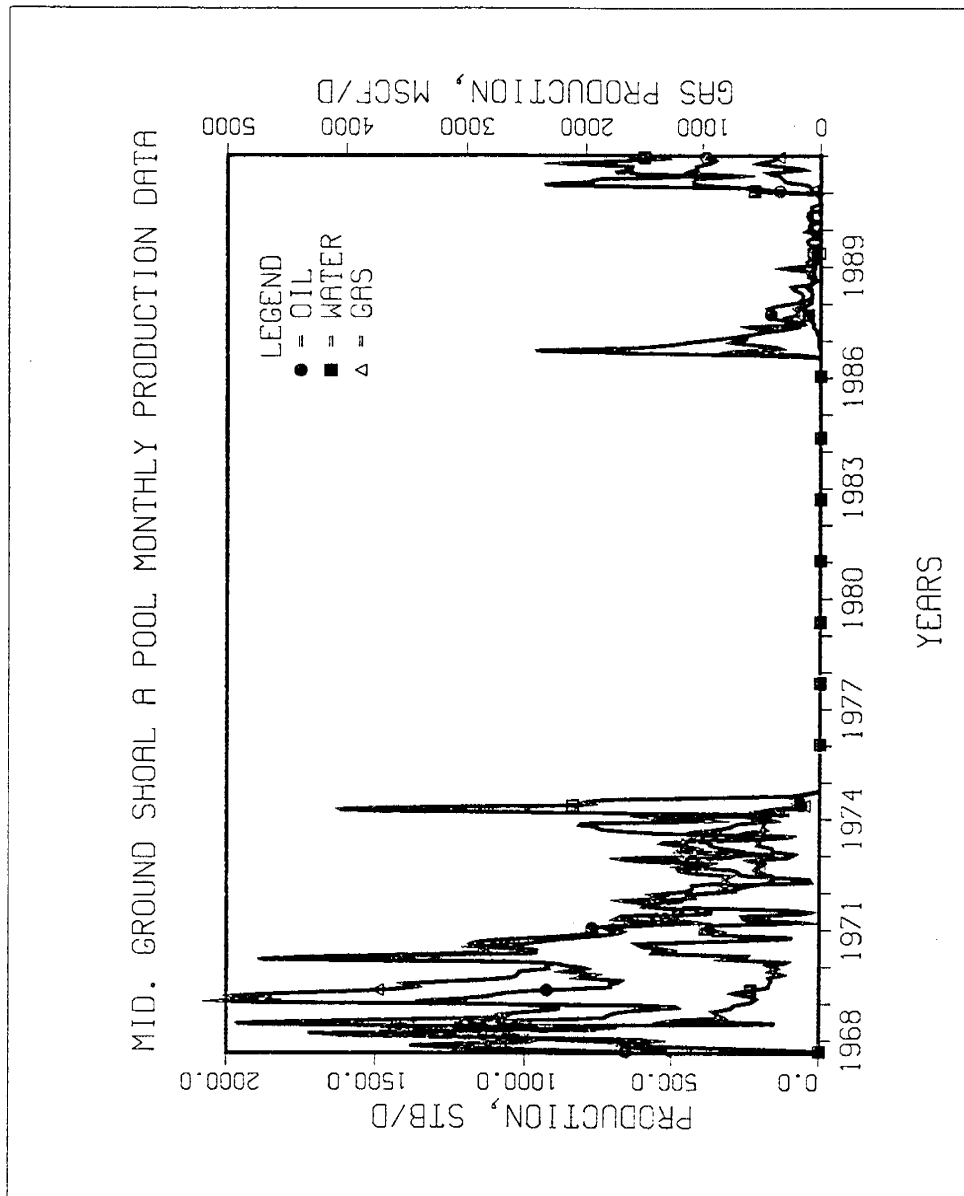


Figure XIV-38.

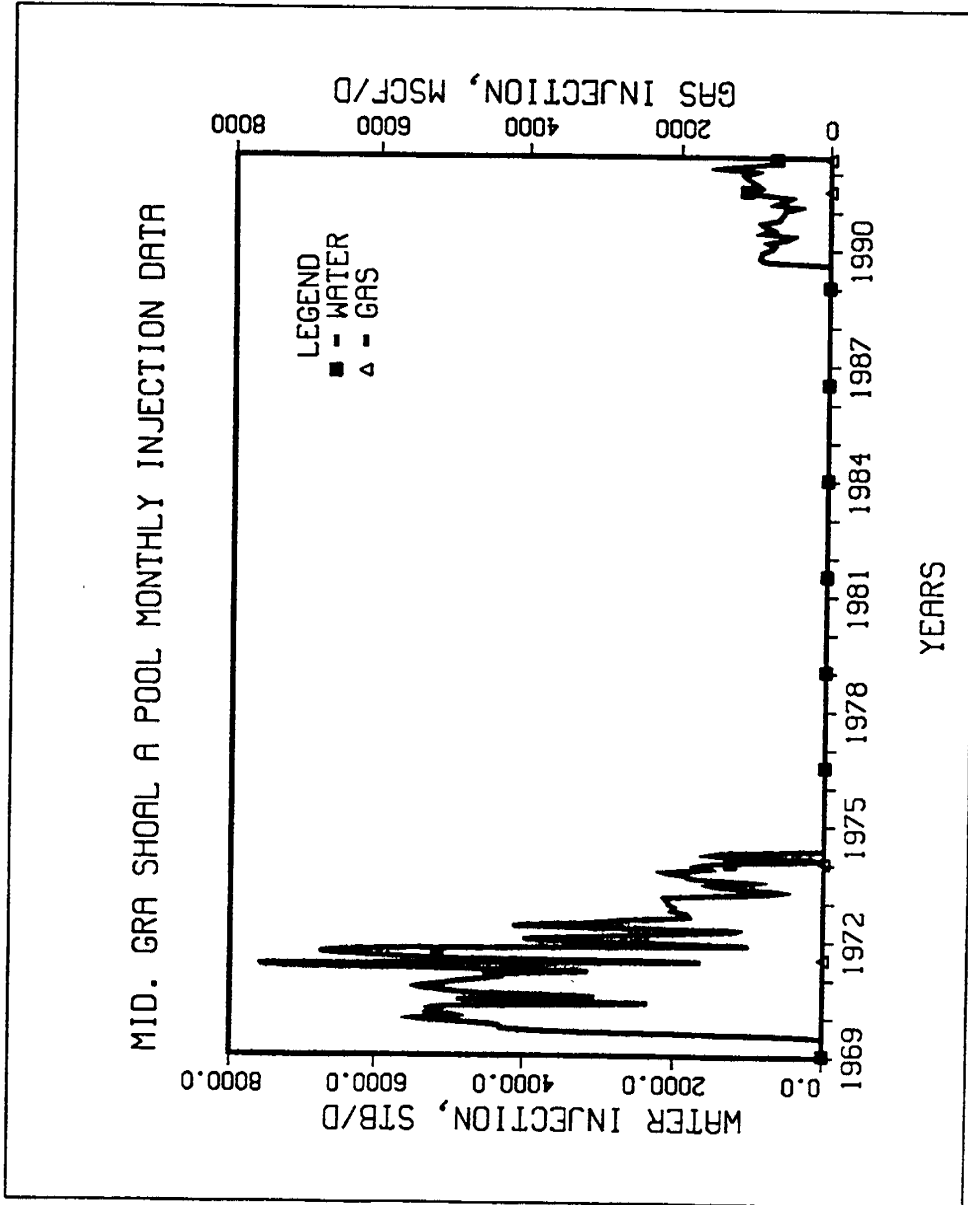


Figure XIV-39.

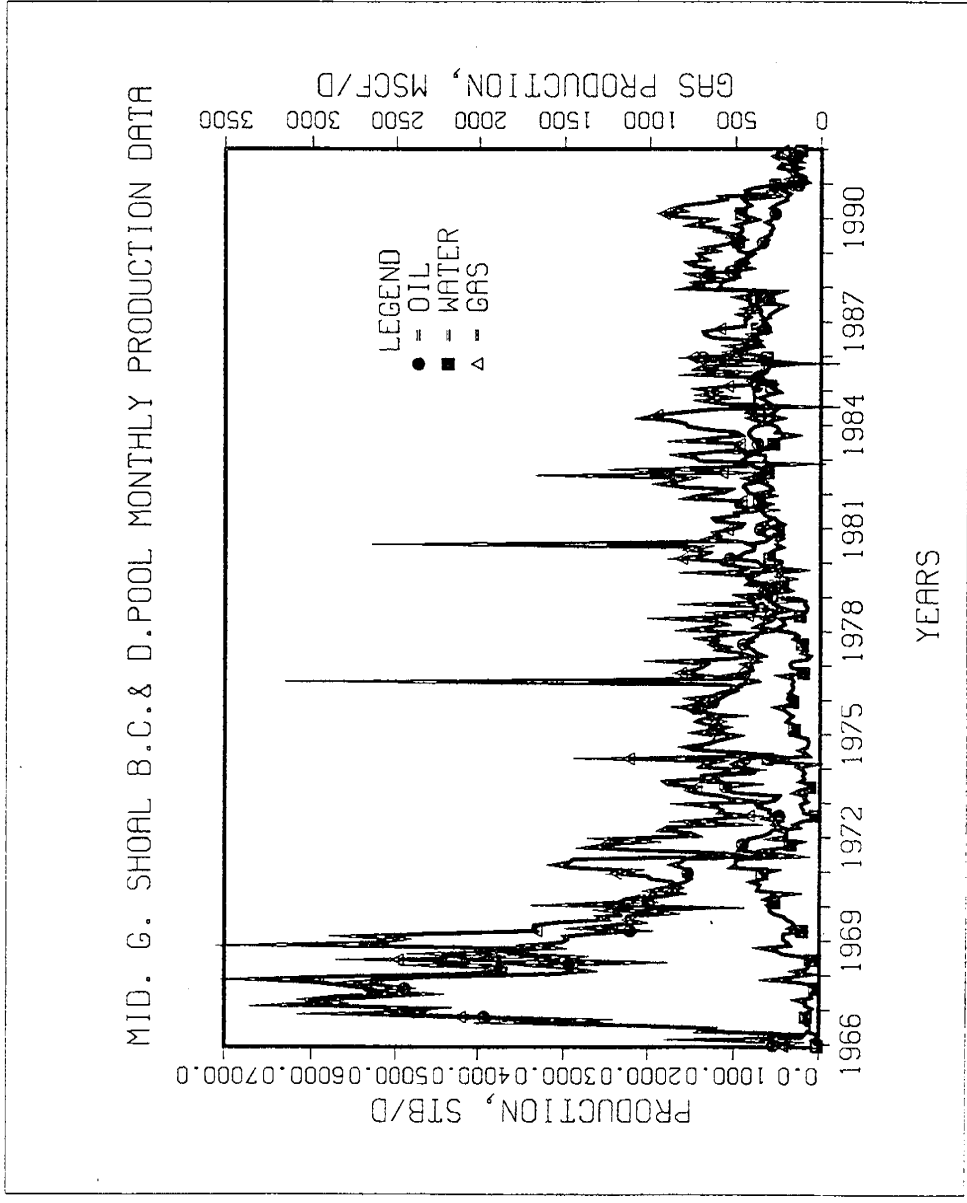


Figure XIV-40.

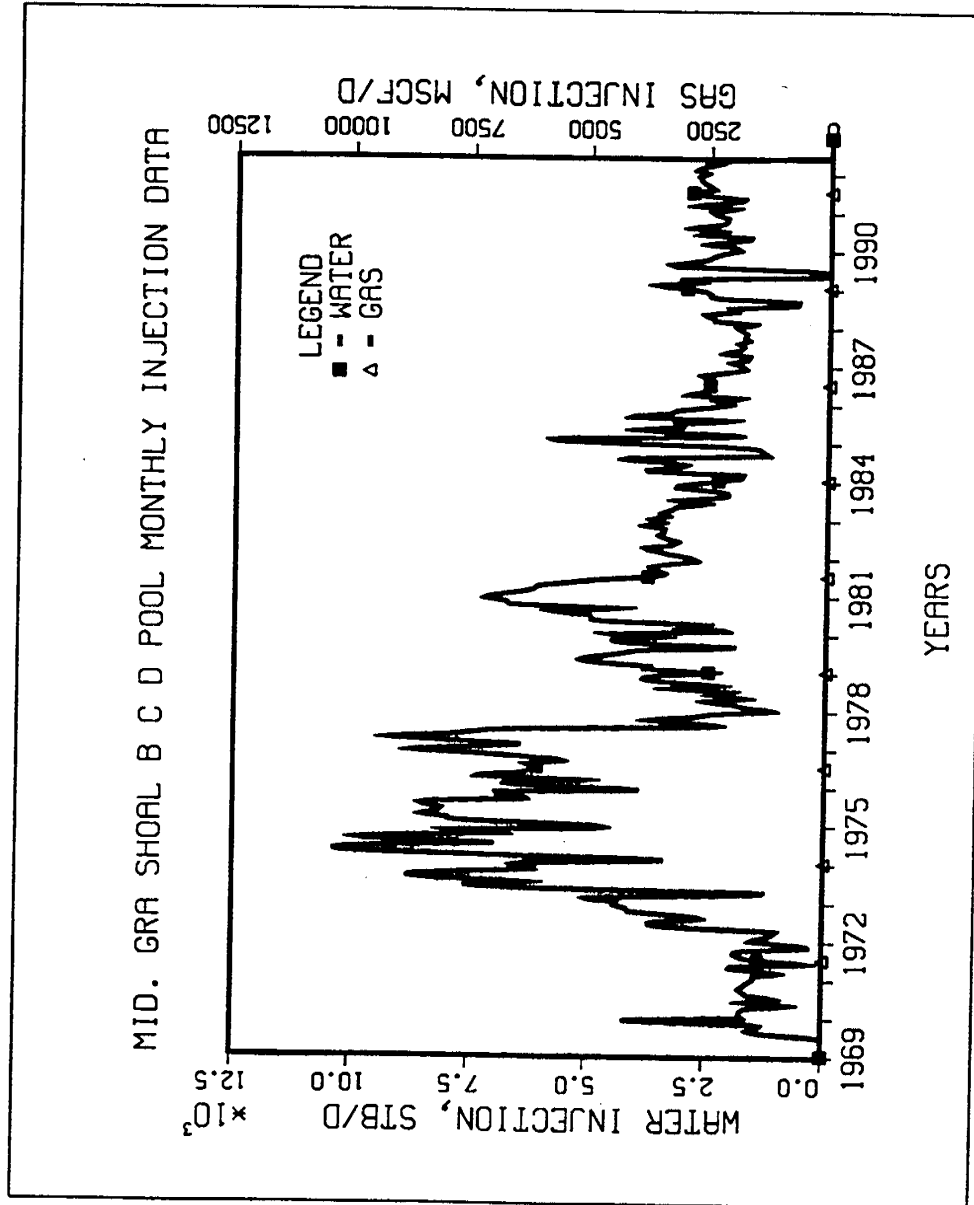


Figure XIV-41.

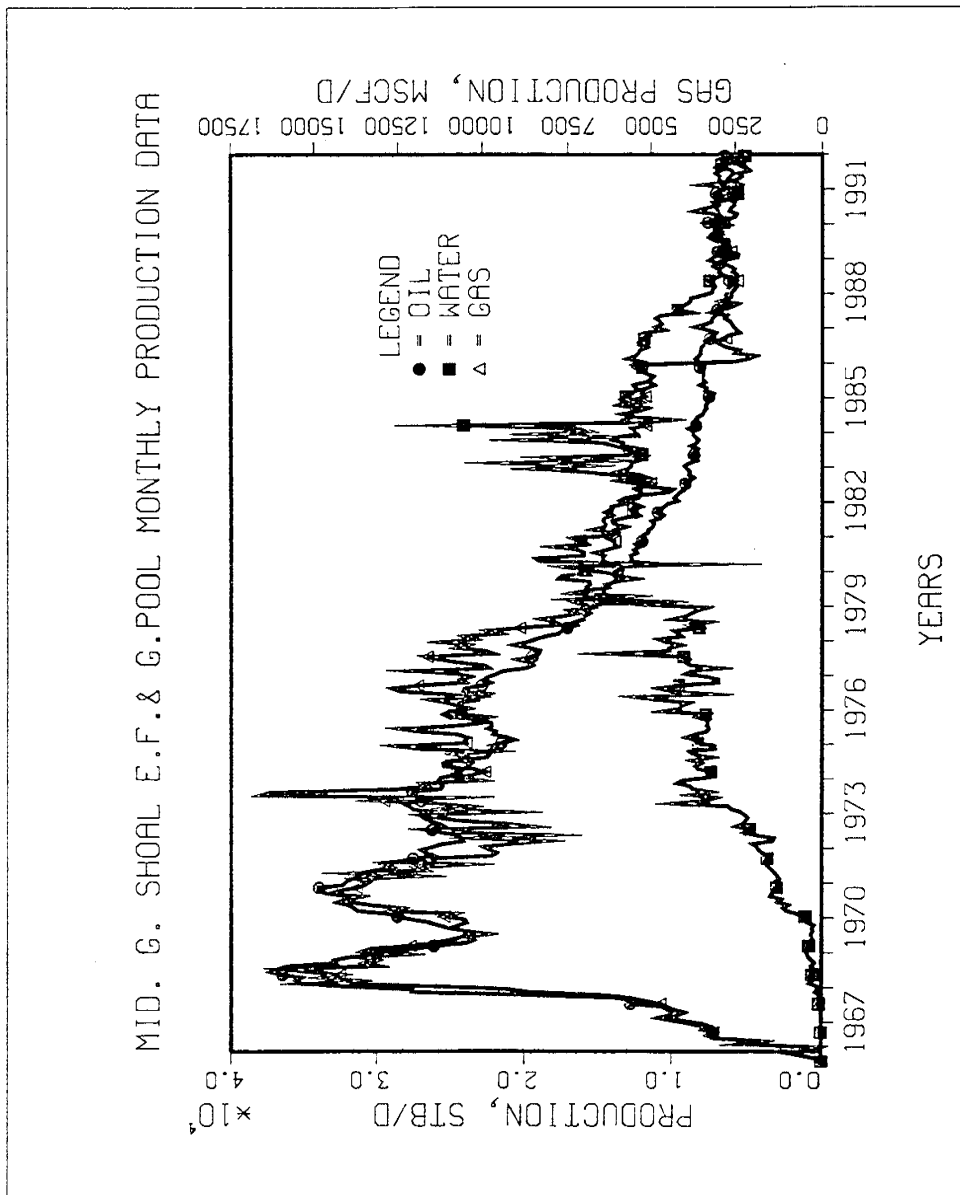


Figure XIV-42.

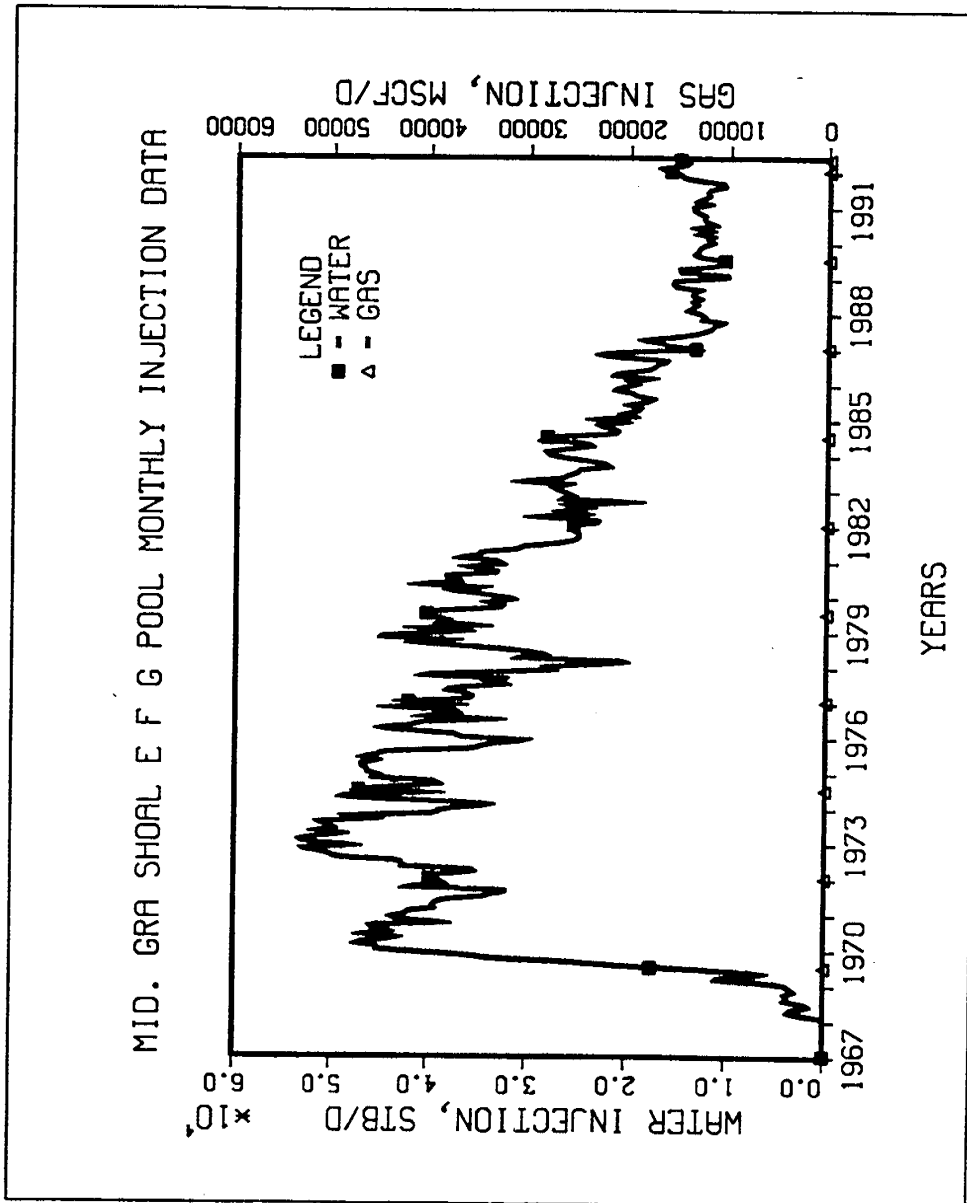


Figure XIV-43.

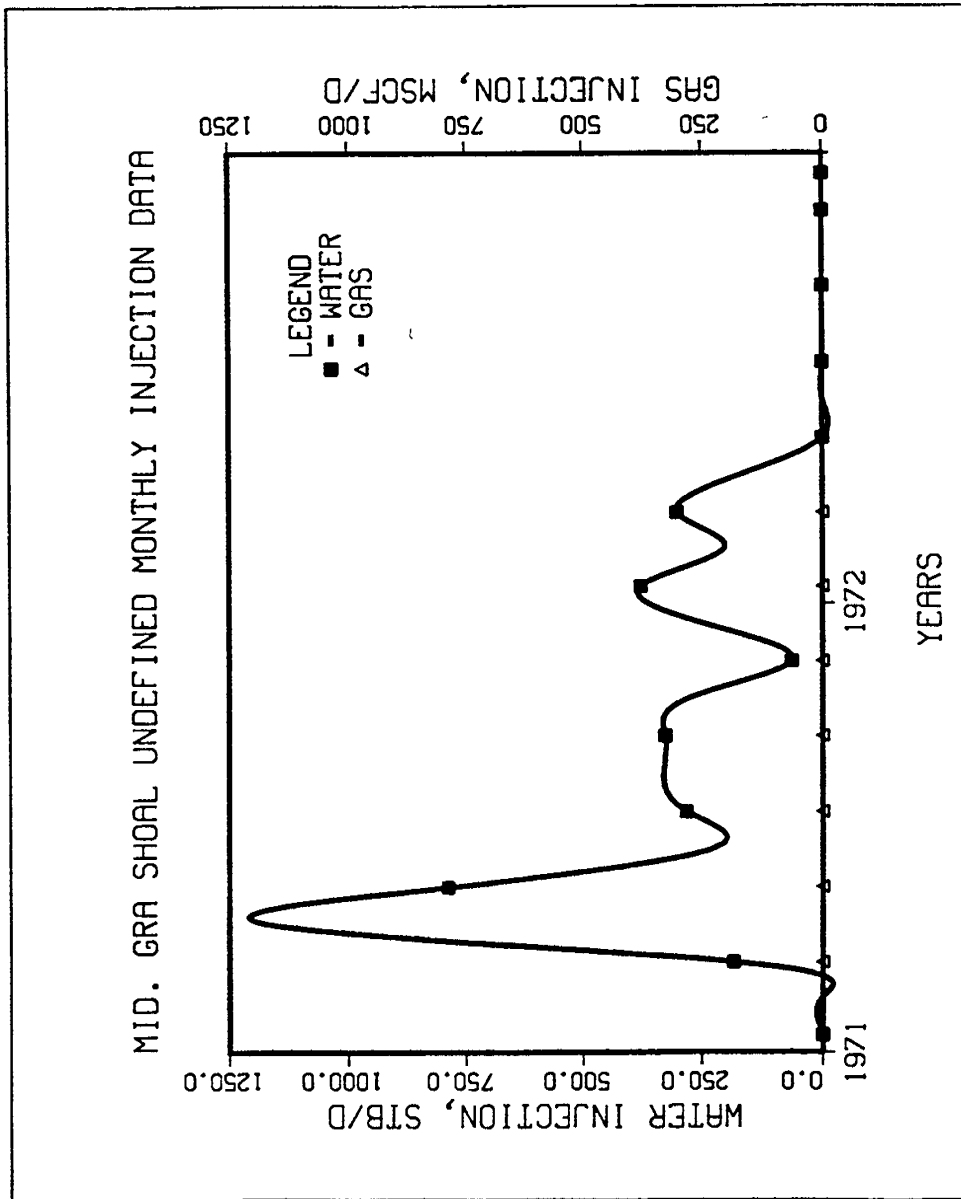


Figure XIV-44.



**Table XIV-60.**

**TORIS DATA BASE  
FIELD: BEAVER CREEK**

Record 1:

Field Code .....	N/A
STATE Postal Code .....	AK
Lithology Code (-1, 0 = Unknown; 1 = SS, 2 = LS; 3 = Dolo.) .....	-1
Geologic Age Code AAPG .....	-1
Field Name .....	Beaver Creek
Reservoir Name .....	Beaver Creek
Reference Number .....	N/A
Load Number .....	N/A
Formation Name .....	Lower Tyonek & Hemlock Conglomerate

Record 2:

( 1) Field Acres (Acres) .....	N/A
( 2) Proven Acres (Acres) .....	N/A
( 3) Well Spacing (Acres) .....	N/A
( 4) Total Wells (Number) .....	2
( 5) Net Pay (Feet) .....	100
( 6) Gross Pay (Feet) .....	N/A
( 7) Porosity (%) .....	N/A
( 8) Initial Oil Saturation (%) .....	N/A
( 9) Current Oil Saturation (%) .....	N/A
(10) Initial Water Saturation (%) .....	N/A
(11) Current Water Saturation (%) .....	N/A
(12) Initial Gas Saturation (%) .....	N/A
(13) Current Gas Saturation (%) .....	N/A
(14) Initial Oil FVF (Res bbl/STB) .....	N/A
(15) Current Oil FVF (Res bbl/STB) .....	N/A
(16) True Vertical Depth (Feet)----Mid-Perforation .....	14,800
(17) Formation Temperature (°F) .....	215

Record 3:

(18) Current Formation Pressure (PSI) .....	N/A
(19) Permeability (md) .....	N/A
(20) Geologic Age (AAPG) .....	N/A
(21) API Gravity (°API) .....	35
(22) Oil Viscosity (CP) :e Reservoir condition .....	N/A
(23) Formation Salinity (ppm TDS) .....	N/A
(24) OOIP (BBL) .....	N/A
(25) Primary Recovery Factor (Fraction of OOIP) .....	N/A
(26) Cumulative Oil Production (BBL) .....	4,100,188

**Table XIV-60 (continued).**

(27)	Year For Cumulative Oil Production; EX/1986 .....	1990
(28)	Technical Availability Date (Year); Ex/1990 .....	N/A
(29)	Primary Recovery (BBL/AC.FT.) .....	N/A
(30)	Primary Recovery (BBL) .....	N/A
(31)	Year For Primary Recovery .....	N/A
(32)	Current Producing GOR (SCF/BBL) .....	274 (1990)
(33)	Initial Producing GOR (SCF/BBL) .....	380

Record 4:

(34)	Reservoir Acreage (Acres) .....	N/A
(35)	Initial Formation Pressure (PSI) .....	7552
(36)	Reservoir Dip (DEG) .....	N/A
(37)	Production Wells (Number) .....	N/A
(38)	Injection Wells (Number) .....	N/A
(39)	Swept Zone Oil Saturation (%) (Residual to Water) .....	N/A
(40)	Injection Water Salinity (ppm TDS) .....	N/A
(41)	Clay Content (%) .....	N/A
(42)	Dykstra-Parsons Coefficient .....	N/A
(43)	Current Injection Rate (B/D/WELL) .....	N/A
(44)	Fractured-Fault (Y,N) (N = 0, Y = 1) .....	N/A
(45)	Shale Break or Laminations (Y,N) (N = 0, Y = 1) .....	N/A
(46)	Major Gas Cap (Y,N) (N = 0, Y = 1) .....	N/A
(47)	Field Multiplier (Number) .....	N/A
(48)	RRC District .....	N/A
(49)	Production Rate (MBBL/D); For the Year shown in element 28 .....	0.58
(50)	Recovery Efficiency-Waterflood (Factor) .....	N/A
(51)	Ultimate Recovery Factor (Fraction of OOIP) (Primary Plus Secondary) .....	N/A

Record 5:

(52)	Geologic Play Code (Table II) .....	-1
(53)	Depositional System Code (Table III) .....	-1
(54)	Depositional System Degree of Confidence (1 = Highest, 2 = Moderate, 3 = Lowest) .....	N/A
(55)	Diagenetic Overprint Code (Table IV) .....	-1
(56)	Diagenetic Overprint Degree of Confidence (1 = Highest, 2 = Moderate, 3 = Lowest) .....	N/A
(57)	Structural Compartmentalization (Table V) .....	-1
(58)	Structural Compartmentalization Degree of Confidence (1 = Highest, 2 = Moderate, 3 = Lowest) .....	N/A
(59)	Predominant Element of Reservoir Heterogeneity (1 = Depositional System, 2 = Diagenetic Overprint, 3 = Structural Compartmentalization) .....	N/A
(60)	Trap Type (1 = Stratigraphic, 2 = Structural, 3 = Combination) .....	N/A
(61)	Geologic Province (Table VI) .....	067

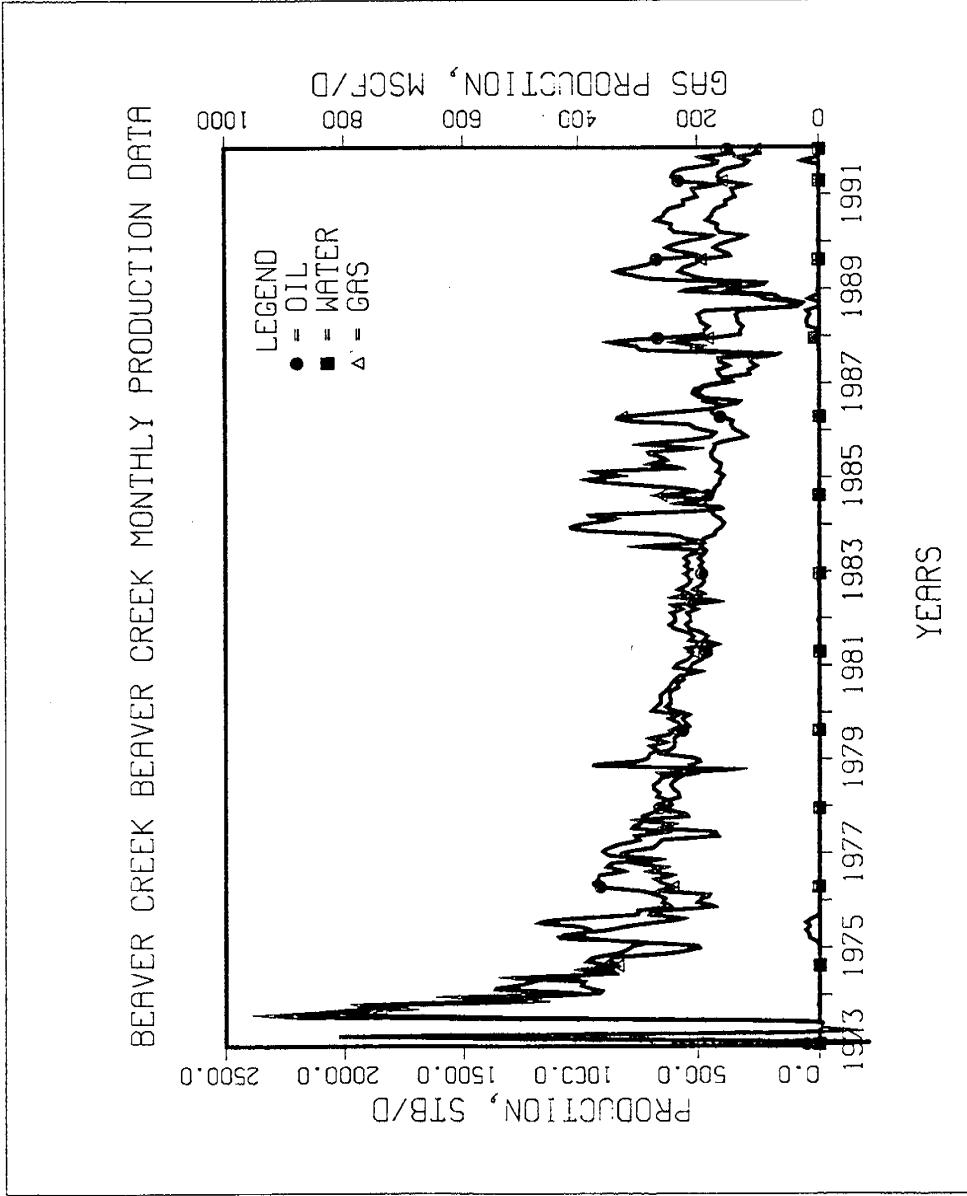


Figure XIV-45.

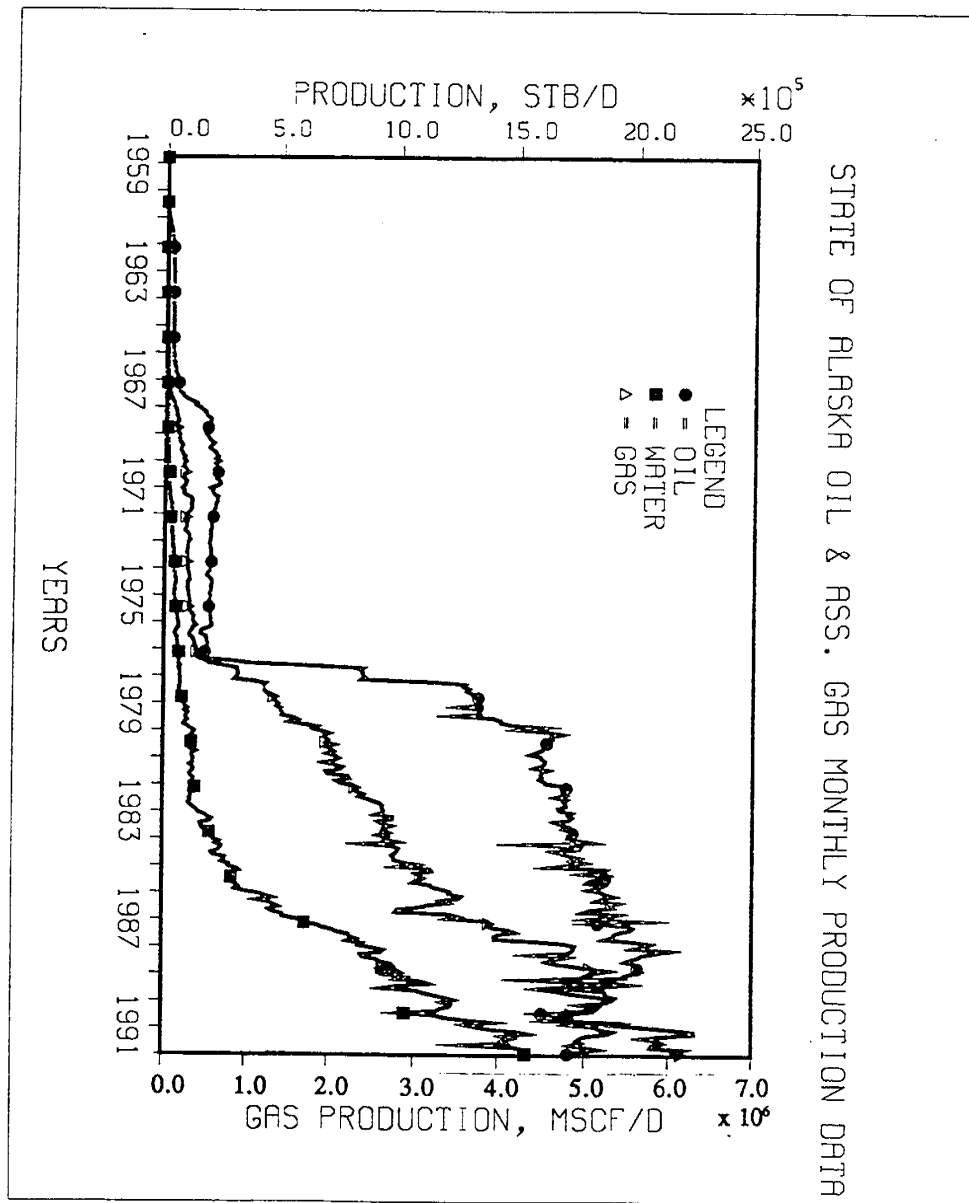


Figure XIV-46.



# APPENDIX A: PUBLISHED AAPG ABSTRACT FROM MOWATT ET AL.

---

---

The American Association of Petroleum Geologists Bulletin  
V. 75, No. 5 (March 1991), P. 515-700

---

## ASSOCIATION ROUND TABLE

---

1991 ANNUAL CONVENTION  
WITH DPA/EMD DIVISIONS AND SEPM, AN ASSOCIATED SOCIETY  
April 7-10, 1991, Dallas, Texas

MOWATT, THOMAS C., U.S. Bureau of Land Management, Anchorage, AK, and D. O. OGBE, V. A. KAMATH, and G. D. SHARMA, University of Alaska, Fairbanks, AK

Petrologic-Petrophysical Relationships, West Sak and Ugnu (Brookian), Northern Alaska

Petrographic-mineralogic analyses have been combined with petrophysical information derived from wireline logs, as part of an investigation of geological and engineering characteristics of the West Sak and Ugnu (Brookian) stratigraphic intervals in several wells in the central portion of the Alaskan Northslope.

The strata are semi- to unconsolidated clastics—sand, silt, clay in size—"cemented" by viscous (API gravity 8° to 22°) hydrocarbon material. This presents serious problems in terms of sample integrity during borehole recovery and subsequent storage, transportation, and sample preparation. Pressure changes from subsurface to surface conditions pose particular difficulties.

Textural relationships in thin section are often problematic with respect to original relationships in the undisturbed subsurface. In-situ analyses—e.g., wireline logs—represent the potentially most useful means of elucidating petrophysical-engineering properties of concern to drilling, completion, and production. Petrographic-mineralogic analysis of sample materials, as feasible, is essential for rigorous application of such in-situ techniques.

The present work confirms the heterogeneous nature of the West Sak and Ugnu intervals, with frequent, often substantial proportions of silt-clay size materials associated intimately within, and/or interbedded with, coarser grained reservoir intervals. Major intervals with moderate-good reservoir properties are recognized, as well as significant intervals ranging from relatively poor reservoir quality to good seal quality materials.

Hydrocarbon production will undoubtedly require enhanced recovery techniques, hence thorough, detailed reservoir/nonreservoir characterization will be imperative to achieve viable efficiency.



## CHAPTER XV: REFERENCES

---

- Adialalis, S.: "Investigation of Physical and Chemical Criteria as Related to the Prevention of Asphalt Deposition in Oil Well Tubings," M.Sc. Thesis, Petroleum Eng. Dept., Imperial College, University of London, London (Sept. 1982).
- Alaska Oil and Gas Conservation Commission Bulletin (July 1993).
- Alaska Oil and Gas Conservation Commission: "Statistical Report," Anchorage, AK (1985-1990).
- Bird, Kenneth J.: "Framework Geology of the North Slope of Alaska as Related to Oil-Source Rock Correlations," Alaskan North Slope Geology, Vol. 1, edited by Irv Taillair and Paul Weirner, published by the Pacific Section, Society of Economic Paleontologists and Mineralogists, Bakersfield, CA, and the Alaska Geological Society, Anchorage, AK (1987).
- Boussingault, M.: Memoire sur la Composition des Bitumes, Annales de Clinic Ser. 2, Vol. 64, p. 141 (1837).
- Bowsher, Arthur L.: "Sinclair Oil and Gas Company on the Alaskan North Slope," Alaskan North Slope Geology, Vol. 1, edited by Irv Tailleir and Paul Weimer, published by the Pacific Section, Society of Economic Paleontologists, Bakersfield, CA, and the Alaskan Geological Society, Anchorage, AK (1987).
- Burke, N.D., Hobbs, R.D., and Kashou, S.F.: "Measurement and Modeling of Asphaltene Precipitation from Live Reservoir Fluid Systems," SPE 18273, Presented at 63rd Ann. Tech. Conf. & Exh. of SPE, Houston, TX (Oct. 2-5, 1988).
- Carmen, G.J., and Hardwick, P.: "Geology and Regional Setting of Kuparuk Oil Field, Alaska," American Association of Petroleum Geologists Bulletin, Vol. 67, No. 6, pp. 1014-1031 (1983).
- Chilingar, G.V., and Yen, T.F.: Bitumens, Asphalts and Tar Sands, Elseviere Scientific Pub. Co., Amsterdam (1978).
- Clementz, D.M.: "Interaction of Petroleum Heavy Ends with Montmorillonite," Clay and Clay Minerals, Vol. 24, pp. 312-319 (1976).

- Coats, K.H.: "Equation of State PVT Program: Users' Manual," Scientific Software Intercomp, Denver, CO (1984).
- Collins, S.H., and Melrose, J.C.: "Adsorption of Asphaltenes and Water on Reservoir Rock Minerals," SPE 11800, SPE Intl. Symposium on Oilfield Chemistry, Denver, CO (June 1-3, 1983).
- Corbett, L.W., and Petrossi, U.: "Differences in Distillation and Solvent Separated Asphalt Residue," Ind. Eng. Chem. Prod. Res. Dev., Vol. 17 (1978).
- Crocker, M.E., and Marchin, L.M.: "Wettability and Adsorption Characteristics of Crude Oil Asphaltene and Polar Fractions," J. Pet. Tech., pp. 470-474 (April 1988).
- Curtis, M.I., and Huxley, D.B.: First Arctic Offshore Field, Endicott, on Decade Long Way to Production, Oil and Gas Journal, Vol. 83, No. 13, Pages 64-70 (1985).
- Danesh, A., Krinis, D., Henderson, G.D., and Peden, J.M.: "Asphaltene Deposition in Miscible Gas Flooding of Oil Reservoirs," Ind. Chem. Eng. Prod. Res. Dev., Vol. 66, No. 7, pp. 339-344 (1988).
- Dubey, S.T., and Waxman, M.H.: "Asphaltene Adsorption and Desorption From Mineral Surfaces," SPE 18462, SPE Intl. Symposium on Oilfield Chemistry, Houston, TX (Feb. 8-10, 1989).
- Dyes, A.B.: "Alternate Injection of HPG and Water - A Two Well Pilot," SPE 4082, proceedings of 1972 SPE Annual Meeting held in San Antonio, TX (Oct. 8-11, 1972).
- Eggert, J. Thomas: "Sandstone Petrology, Diagenesis and Reservoir Quality, Lower Cretaceous Kuparuk River Formation, Kuparuk River Field, North Slope, Alaska," Alaska North Slope Geology, Vol. 1, the Pacific Section Society of Economic Paleontologists and Mineralogists and the Alaska Geologists Society (Oct. 1987).
- Fussel, L.T.: "A Technique of Calculating Multiphase Equilibria," SPEJ. pp. 203-209 (Aug. 1979).
- Gambill, W.R.: "Determine Heat of vaporization," Chem. Eng., Vol. 64, No. 12, pp. 261-266 (Dec. 1957).

- Gaynor, G.C., and Scheihing, M.H.: "Shelf Depositional Environments and Reservoir Characteristics of the Kuparuk River Formation (Lower Cretaceous), Kuparuk Field, North Slope Alaska," Reservoir Geology, Research and Technical Services, ARCO Oil and Gas Co., 2300 West Plano Parkway, Plano, TX, 75075 (1989).
- Hansen, P.W.: "A CO<sub>2</sub> Tertiary Recovery Pilot-Little Creek Mississippi," SPE 6747, Presented at the SPE Annual Fall Tech. Conf. & Exhibition, Denver, CO (Oct. 9-12, 1977).
- Harvey, M.T., Jr., Shelton, L.J., and Kelm, C.H.: "Field Injectivity Experiences with Miscible Recovery Projects Using Alternate Rich Gas and Water Injection," J. Pet. Tech., pp. 1051-55 (Sept. 1977).
- Haskett, C.E., and Tartera, M.: "A Practical Solution to the Problem of Asphaltene Deposits - Hassi Messahoud Field, Algeria," J. Pet. Tech., pp. 387-391 (April 1965).
- Hirshberg, A., deJong, L.N.J., Schipper, B.A., and Meijer, J.G.: "Influence of Temperature and Pressure on Asphaltene Flocculation," Soc. Pet. Eng. J. No. 6, pp. 283-293 (1984).
- Jacobs, I.C., and Thorne, M.A.: "Asphaltene Precipitation During Acid Stimulation Treatments," SPE 14823, Seventh SPE Symposium on Formation Damage Control, Lafayette, LA (Feb. 26-27, 1986).
- Jacobs, I.C.: "Chemical Systems for the Control of Asphaltene Sludge During Oilwell Acidizing Treatments," SPE 18475, Presented at SPE Int. Symp. on Oilfield Chem. Houston, TX (Feb. 8-10, 1989).
- Jamison, H.C., Brockett, L.D., and McIntosh, R.A.: "Prudhoe Bay - A 10 Year Perspective," Giant Oil and Gas Fields of the Decade 1968-1978, Edited by M.T. Halbority, AAPG, Tulsa, OK (1980).
- Jiang, J.C., Patil, S.L., and Kamath, V.A.: "Study of Asphalt/Asphaltene Precipitation During Addition of Solvents to West Sak Crude," Division of Pet. Chem. Inc., ACS Meeting, Washington, D.C., Vol. 35, No. 3, pp. 522-530 (Aug. 26-31, 1990).
- Johnson, E.F., Bossler, D.P., and Naumann, V.O.: "Calculation of Relative Permeability from Displacement Experiments," Trans. AIME, Vol. 216, pp. 370-372 (1959).

- Jones, H.P., and Speers, R.G.: "Permo-Triassic Reservoirs of Prudhoe Bay Field, North Slope, Alaska," Memo 24, AAPG, pp. 23-50 (1976).
- Kamath, V.A., Islam, M.R., Patil, S.L., Jiang, J.C., and Kakade, M.G.: "The Role of Asphaltene Aggregation in Viscosity Variation of Reservoir Hydrocarbons and in Miscible Processes," Particle Tech. & Surface Phen. in Min. & Pet Plenum Publ. Corp. pp. 1-22 (1991).
- Kamath, V.A., Kakade, M.G., and Sharma, G.D.: "An Improved Molecular Thermodynamic Model of Asphaltene Equilibria," 23rd Annual Meeting of Fine Particle Society, Las Vegas, Nevada (July 14-17, 1992).
- Kawanaka, S., Park, S.J., and Mansoori, G.A.: "The Role of Asphaltene Deposition in EOR Gas Flooding: A Predictive Technique," SPE/DOE 17376, Presented at the SPE/DOE EOR Symp; Tulsa, OK (April 17-20, 1988).
- Kim, S.T., Boudh-Hir, M.D., and Mansoori, G.A.: "The Role of Asphaltene in Wettability Reversal," SPE 20700, Presented at 65th SPE Ann. Tech. Conf. and Exh. New Orleans, LA (Sept. 23-28, 1990).
- Kokal, S., Najman, J., Sayegh, S.G., and George, A.: "Asphaltene Precipitation During Enhanced Recovery of Heavy Oils by Gas injection," CIM/AOSTRA Paper 91-10 Presented at CIM/AOSTRA Tech. Conf., Banff, Canada (April 21-24, 1991).
- Lawton, Timothy F., Geehan, Gregory W., and Voorhees, Brent J.: "Lithofacies and Depositional Environments of the Ivishak formation, Prudhoe Bay field," Alaskan North Slope Geology, Vol. 1, The Pacific Section, Society of Economic Paleontologists and mineralogists and the Alaska Geological Society (Oct. 1987).
- Leontaritis, K.J., and Mansoori, G.A.: "Asphaltene Flocculation During Oil Recovery and Processing: A Thermodynamic Collodal Model," SPE 16258, proceedings of 1987 SPE Symposium on Oil Field Chemistry (1987).
- Leontaritis, K.J.: "Asphaltene Deposition: A Comprehensive Description of Problem Manifestations and Modeling Approaches," SPE 18892, Presented at SPE Prod. Op. Symp. Oklahoma City, OK (March 3-4, 1989).
- Lichaa, P.M.: "Asphaltene Deposition Problem in Venezuela Crudes - Usage of Asphaltene in Emulsion Stability Oil Sands," Soc. Pet. Eng. J., pp. 609-624 (1977).

- Long, R.B.: "The Concept of Asphaltene," The Advances in Chemistry Series No. 195, p. 17 (1981).
- Mansoori, G.A.: "Asphaltene Deposition: An Economic Challenge in Heavy Petroleum Crude Utilization and Processing," OPEC Review pp. 103-113 (Spring 1988).
- Masterson, W. Dallam, and Paris, Chester E.: "Depositional History and Reservoir Description of the Kuparuk River Formation, North Slope, Alaska," Alaskan North Slope Geology, Vol. 1, edited by Irv Taillair and Paul Weirner, published by the Pacific Section, Society of Economic Paleontologists and Mineralogists, Bakersfield, CA, and the Alaska Geological Society, Anchorage, AK (1987).
- McGowen, J.H., Bloch, S., and Hite, D.M.: "Depositional Facies, Diagenesis and Reservoir Quality of the Ivishak Sandstone (Sadlerochit Group), Prudhoe Bay field," Alaskan North Slope Geology, Vol. 1, the Pacific Section Society of Economic Paleontologists and Mineralogists and the Alaska Geologists Society (Oct. 1987).
- McKay, J.F., Amend, P.J., Cogswell, T.E., Harnsberger, P.M., Erickson, R.B., and Latham, D.R.: "Analytical Chemistry of Liquid Fuel Sources," Adv. in Chem. Series 170 Chap. 9, pp. 128-142 (1978).
- Mehta, V.: "Displacement of Endicott Crude by Enriched Gases in a Slim Tube," MS Thesis, The University of Alaska Fairbanks (1993).
- Melvin, J.: "Sedimentological Evolution of the Mississippian Kekiktuk Formation, Sagavanirktok Delta Area, North Slope, Alaska," in Alaskan North Slope Geology, Vol. 1, Page 60 (1987).
- Miller, M.A., and Ramey, H.J., Jr.: "Effect of Temperature on Oil/Water Relative Permeabilities of Unconsolidated and Consolidated Sands," SPE 12116, SPE Annual Tech. Conf. and Exhibition, San Francisco, CA (Oct. 5-8, 1983).
- Monger, T.G., and Trujillo, D.E.: "Organic Deposition During Carbon Dioxide and Rich-Gas Flooding," SPE 18063, SPE Annual Tech. Conf. and Exhibition, Houston, TX, (Oct. 2-5, 1988).
- Mowatt, T.C., Ogbe, D.O., Kamath, V.A., and Sharma, G.D.: "Petrologic-Petrophysical Relationships, West Sak and Ugnu (Brookian), Northern Alaska," abstract published in AAPG Bulletin, Vol. 75, No. 5, pp. 515-700 (March 1991).

- Novasad, Z., and Costain, T.G.: "Experimental and Modeling Studies of Asphaltene Equilibria for a Reservoir Under CO<sub>2</sub> Injection," SPE 20530 Presented at the 65th SPE Ann. Tech. Conf. & Exh., New Orleans, LA (Sept. 23-26, 1990).
- Payne, Janie H.: "Diagenetic Variations in the Permo-Triassic Ivishak Sandstone in the Prudhoe Bay field and central-northeastern National Petroleum Reserve in Alaska (NPRA)," Alaskan North Slope Geology, Vol. 1, The Pacific Section Society of Economic Paleontologists and Mineralogists and the Alaska Geological Society (Oct. 1987).
- Prekshot, G.W., Dehisle, N.G., Cottrell, C.E., and Katz, D.C.: "Asphaltene Substances in Crude Oils," Trans AIME No. 151, pp. 188-194 (1954).
- Rogacheva, O.V., Rimaev, R.N., Gubaidullin, V.A., and Khakinov, D.K.: "Investigation of the Surface Activity of the Asphaltene of Petroleum Residues," Colloid J. Vol. 42, p. 490 (1980).
- Roper, M.K.: "An Experimental Study of CO<sub>2</sub>/West-Sak-Crude-Oil Phase Behavior," MS Thesis, The University of Alaska Fairbanks (1989).
- Sampson, R.J.: Surface II Graphics System, Computer Sciences Section, Kansas Geological Survey, Lawrence, Kansas, Pages 91-98 (1984).
- Scott, R.L., and Magat, M.: "The Thermodynamics of High Polymer Solutions: I. The Free Energy of Mixing of Solvents and Polymers of Heterogeneous Distribution," J. Chem. Physics. 13(5), pp. 172-177 (May 1945).
- Selley, R.C.: Ancient Sedimentary Environments (2d Ed.): Ithaca, New York, Cornell University Press, Page 287 (1978).
- Siddiqui, N.: "Effect of Gas Solubility on Viscosity of West Sak Crude," MS Thesis, The University of Alaska Fairbanks (1989).
- Speight, J.G., and Moschopedis, S.C.: "On the Molecular Nature of Petroleum Asphaltenes," proceedings of American Chemical Society Meeting, Chemistry of Asphaltenes Symposium, Washington D.C., pp. 1-15 (1981).
- Stalkup, F.I.: "Carbon Dioxide Miscible Flooding, Past, Present and the Outlook for Future," Journal of Petroleum Technology, pp. 1102-12 (Aug. 1978).

- Stalkup, F.I.: Miscible Displacement, SPE Monograph (June 1983).
- Thomas, C.P., Doughty, T.C., Faulder, D.D., Harrison, W.E., Irving, J.S., Jamison, H.C., and White, G.J.: "Alaska Oil and Gas: Energy Wealth or Vanishing Opportunity," U.S. Department of Energy Report, DOE/ID/01570-H1 (1991).
- Thomas, C.P., Allaire, R.B., Doughty, T.C., Faulder, D.D., Irving, J.S., Jamison, H.C., White, G.J.: "Alaska North Slope National Energy Strategy Initiative, Analysis of Five Undeveloped Fields," U.S. Department of Energy, Bartlesville Project Office, Bartlesville, OK (1993).
- Tuttle, R.N.: "High Pour Point and Asphaltic Crude Oils and Condensates," J.P.T., p. 1192 (June 1983).
- Twu, C.H.: "An Internally Consistent Correlation for Predicting Critical Properties and Molecular Weights of Petroleum and Coal-Tar Liquids," Fluid Phase Equil. Vol. 16, pp. 137-150 (1984).
- Vail, P.R., Hardenbol, J., and Todd, R.G.: "Jurassic Unconformities, Chronostratigraphy, and Sea-Level Changes from Seismic Stratigraphy and Bio-Stratigraphy," in Schlee, J.S., ed., Interregional Unconformities and Hydrocarbon Accumulation: American Association of Petroleum Geologists Memoir 36, pp. 129-144 (1984).
- Van Poolen, H.K., and Hamilton, H.H.: "Prediction of Reservoir Fluid Recovery Sadlerochit Formation Prudhoe Bay Field," report published by Department of Natural Resources (Division of Oil and Gas), State of Alaska (1976).
- Van Poolen, H.K., and Associates: "In-Place Hydrocarbon Determination of Kuparuk River Formation," Report Prepared for the State of Alaska by H.K. Van Poolen and Associates, Inc. (1978).
- Wadman, D.H., Lamprecht, D.E., and Mrosovsky, I.: "Joint Geologic/Engineering Analysis of the Sadlerochit Reservoir, Prudhoe Bay Field," Society of Petroleum Engineers Journal of Petroleum Technology, pp. 933-940 (July 1979).

Werner, M.R.: "West Sak and Ugnu Sands: Low Gravity Oil Zones of the Kuparuk River Area," Alaskan North Slope Geology, Vol. 1, edited by Irv Tailleir and Paul Weiner, published by the Pacific Section, Society of Economic Paleontologists and mineralogists, Bakersfield, CA, and the Alaska Geological Society, Anchorage, AK (1987).

Woidneck, Keith, Behrman, Philip, Souls, Charles, and Wu, Juliet: "Reservoir Description of the Endicott Field, North Slope, Alaska," Alaska North Slope Geology, Vol. 1, the Pacific Section Society of Economic Paleontologists and Mineralogists and the Alaska Geological Society (Oct. 1987).

Yang, J.: "Effect of Asphaltene Deposition on Rock-Fluid Properties," M.S. Thesis, U. Alaska Fairbanks pp. 1-104 (Aug. 1992).

Yen, T.F.: "The Nature of Asphaltenes in Heavy Oils," Pan Pac. Synfuels Conf. 2, p. 547 (1982).

Zhang, M.: "Characterization and Description of Lower Ugnu and West Sak Reservoirs Using Well Logs," M.S. Thesis, presented to the Faculty of the University of Alaska, Fairbanks, AK (May 1990).

